BULLETIN OF THE EARTHQUAKE RESEARCH INSTITUTE,
TOKYO IMPERIAL UNIVERSITY. Vol. VII, Part 1. June, 1929

東京帝國大學
地震研究所彙報

第七號　第一册

昭和四年六月

目　次

論文及ビ報告

頁
1. 内部歪核による半無限固體の表面傾斜（英文）……妹澤克惟 1
2. 水中衝撃による淺海波の生成（英文）……妹澤克惟 15
3. 内部にある多重原によるレーレー波の生成（英文）……妹澤克惟・西村源六郎 41
4. 砂層の崩壞に關する實驗（第三報）（英文）……寺田寅彦・宮部直巳 65
5. 油壺灣内の海水の副振動に因る地殼の傾斜運動（英文）……高橋龍太郎 95
6. 水準測量に依りて見出されたる地塊運動に就いて（英文）……坪井忠二 103
7. 低氣壓の海水面に及ぼす影響に就て（英文）……山口生知 115
8. 丹後地震の餘震調査報告（第二報）（邦文）……那須信治 133
9. 地表面の高さ及び地變の量（邦文）……井上宇胤 153
10. 平常時における一建築物の振動測定（佛文）……石本巳四雄・高橋龍太郎 175
11. 丹後震災地一二等三角點移動檢測成果第二報告（邦文）……陸地測量部 185
12. 丹後地方震災地復舊一等三角測量記事（邦文）……陸地測量部 187

所　報

(The titles in occidental languages are given on the back cover.)

本彙報ハ年四回發行ス（第一號ヨリ第六號マデハ不定期ニ發行セリ）.

本彙報掲載ノ論文及ビ報告ノ内容ニ關シテハ著者ノミニ其責任アルモノトス.

本彙報ニ關スル照會通信ハ東京帝國大學地震研究所長へ宛テラレタシ.

The bulletin is published quarterly (Vols. I–VI were published at irregular intervals).

The authors of the papers alone are responsible for the statements and opinions contained in their respective papers.

All communications relating to this bulletin should be addressed to the Director of the Earthquake Research Institute, Tokyo Imperial University.

東京帝國大學
地震研究所彙報
第七號

---

1. *The Tilting of the Surface of a Semi-infinite Solid due to Internal Nuclei of Strain.*[1]

By **Katsutada SEZAWA,**

Earthquake Research Institute.

(Received March 20, 1929.)

1. The theory of the equilibrium of a semi-infinite solid due to the surface loading was already given by many investigators, each in a different method. Among these J. Boussinesq,[2] H. Hertz,[3] H. Nagaoka,[4] K. Terazawa[5] and H. Lamb[6] are, I think, most notable writers, by whom the problem has undergone a great development. The theory of the equilibrium of a similar solid due to internal nuclei of strain has not yet been studied as far as I am aware. The problem has attracted very little attention of the investigators probably because of the unknown state of the interior of the earth crust. Indeed, we cannot yet find out the complete nature of the internal state of the crust, especially that of the seismic focus together with the action of its motive force. This is the origin of the difficulties which arise when we attempt to imagine the mechanism of the earthquake occurrence. It is of very recent time that the deformation of the land surface was precisely[7]

---

[1] Some introductory notes have been published in *Proc. Imp. Acad.*, **4** (1928), 267.

[2] BOUSSINESQ, *Applications des Potentials....* (1885).

[3] H. HERTZ, *Ges. Werke,* **1** (1895).

[4] H. NAGAOKA, *Tokyo Math.-Phys. Soc. Proc.,* **6** (1912), 208.

[5] K. TERAZAWA, *Phil. Trans. Roy. Soc.* (A), **217** (1916), 35.

[6] H. LAMB, *Proc. Roy. Soc.* (A), **93** (1917), 293.

[7] M. ISHIMOTO, *Bull. Earthq. Res. Inst.,* **2** (1927), 1–12 & **4** (1928), 203–222; also *Jap. Journ. Astr.-Geophys.,* **6** (1928), 119–137.
Land Survey Department & our Institute, *Bull. Earthq. Res. Inst.,* **1** (1926), 65–68, **3** (1927), 167–170 & **4** (1928), 223–224, 225–226, 231–232.

observed with the view of drawing some conclusion on the configulation of the internal crust from the surface data. Though the question of the internal state yet involves a great deal of the obscurity under the present state of the knowledge, the distribution and time variation of the deformation of the surface are now going to be clear. A difficulty which attaches to this developed problem will be caused by the fact that there is no any reliable criterion of the judgment on the internal disturbances which correspond to the surface deformation. The present problem which deals with the deformation of the surface of a semi-infinite solid due to internal nuclei of strain may have some importance on such a difficult question, though in the present case the internal disturbance is assumed to be of the nucleous type for the sake of simplicity. In some future studies I will consider the sheet or the assemblage of nuclei to compare with the data of the actual observation.

It is important to notice that in some cases the origin of the disturbance is composed of two kinds of nuclei. One of them is the kind of the multiplet nuclei or compressional and dilatational type and the other is that corresponding to the distortional type. When these two types are combined suitably, we obtain the cases equivalent to the various deformations of a spherical origin. It will, however, be seen that the consideration of only one type is not violent in the present case, because the residence of only one type is a very possible problem in the sense of the theoretical treatment and also the independent calculation of that type can be used as an additive component of the deformation in general cases.

2. We shall take the free surface of the semi-infinite solid to be $z=0$ and also that the axis of z is directed downwards positively. Then the deformation due to the multiplet-nuclei resident at the point $(r=0,\ z=\xi)$ may be expressed by

$$\varDelta_0'=\left(\cos\theta\frac{\partial}{\partial x}+\sin\theta\frac{\partial}{\partial z}\right)^n\frac{1}{\sqrt{r^2+(z-\xi)^2}},\ \ldots\ldots\ldots\ldots\ (1)$$

and analogous expressions for the distortional strain. It is to be noticed that in the present case we consider the deformation corresponding to (1); in other words, we will treat of the effect of a number of the compressional and dilatational singularities accumulated at the point $(r=0,\ z=\xi)$.[8]

The type of dilatation in (1) has not been taken at our disposition.

---

[8] In my advanced paper, *l.c.* p. 1, I considered some additional displacement besides $\varDelta_0'$ to adjust certain conditions at $r=o$ and $z=\xi$. In the present problem the effect of $\varDelta_0'$ alone has been considered owing to the more theoretical reasoning.

This type is the only possible solution of the equations of equilibrium of an elastic body having a singularity at $r=0$ and $z=\xi$.

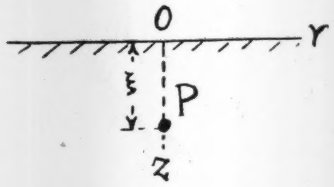

If we substitute in (1) from the expression

$$\frac{1}{\sqrt{r^2+z^2}}=\int_0^\infty e^{-fz} J_0(fr)\,df, \quad \ldots\ldots\ldots(2)$$

then, by means of the relation[9)]

$$\left.\begin{aligned}
&\frac{\partial^n}{\partial x^m \partial z^{n-m}}\int_0^\infty e^{-fz} J_0(fr)\,df\\
&=\frac{(-1)^n}{2^{m-1}}\Bigg\{\sum_{p=0}^{p=\frac{m-2}{2}}(-1)^p\frac{m!\,\cos(m-2p)\,\omega}{(m-p)!\,p!}\int_0^\infty e^{-fz} J_{m-2p}(fr)f^n\,df\\
&\qquad\qquad +(-1)^{\frac{m}{2}}\frac{m!}{(m/2)!^2}\int_0^\infty e^{-fz}\frac{J_0(fr)}{2}f^n\,df\Bigg\}, \quad [m=\text{even}]\\
&=\frac{(-1)^n}{2^{m-1}}\Bigg\{\sum_{p=0}^{p=\frac{m-1}{2}}(-1)^p\frac{m!\,\cos(m-2p)\,\omega}{(m-p)!\,p!}\int_0^\infty e^{-fz} J_{m-2p}(fr)\,f^n\,df, \quad [m=\text{odd}]
\end{aligned}\right\}(3)$$

we have

$$\begin{aligned}
\Delta_0' &= \sum_{m=0}^{m=n}\frac{(-1)^n\,n!\,\sin^{n-m}\theta\cos^m\theta}{2^{m-1}(n-m)!}\\
&\quad\times\Bigg\{\sum_{p=0}^{p=\frac{m-2}{2}}\frac{(-1)^p\cos(m-2p)\,\omega}{(m-p)!\,p!}\int_0^\infty e^{f(z-\xi)} J_{m-2p}(fr)\,f^n\,df\\
&\qquad\qquad +(-1)^{\frac{m}{2}}\frac{1}{(m/2!)^2}\int_0^\infty e^{f(z-\xi)}\frac{J_0(fr)}{2}f^n\,df\Bigg\}, \quad [m=\text{even}]\\
&= \sum_{m=0}^{m=n}\frac{(-1)^n\,n!\,\sin^{n-m}\theta\cos^m\theta}{2^{m-1}(n-m)!}\\
&\quad\times\sum_{p=0}^{p=\frac{m-1}{2}}\frac{(-1)^p\cos(m-2p)\,\omega}{(m-p)!\,p!}\int_0^\infty e^{f(z-\xi)} J_{m-2p}(fr)\,f^n\,df, \quad [m=\text{odd}]\\
&\qquad\ldots\ldots\ldots\ldots\ldots\ldots\ldots\ldots\ldots\ldots(4)
\end{aligned}$$

provided that ω is the azimuth in cylindrical coordinates.

Now, we consider the image at the point $r=0$, $z=-\xi$, where the nuclei of strain is of the form:

---

9) This relation has been obtained by modifying a formula in the paper, K. SEZAWA & G. NISHIMURA, "Generation of Rayleigh-waves due to Internal Multiplet Source," *l.c. poste,* 41.

$$\varDelta_0'' = -\left(\cos\theta\frac{\partial}{\partial x} + \sin\theta\frac{\partial}{\partial z}\right)^n \frac{1}{\sqrt{r^2+(z+\xi)^2}} \quad \ldots\ldots\ldots\ldots (5)$$

This expression is, too, transformed in a form similar to (4).

Superposition of $\varDelta_0''$ on $\varDelta_0'$ gives us

$$\varDelta_0 = \varDelta_0' + \varDelta_0'' = (-1)^n\, n!\sum_{m=0}^{m=n} \frac{\sin^{n-m}\theta\cos^m\theta}{2^{m-2}(n-m)!}$$

$$\times \sum_{p=0}^{p=q} \gamma\,(-1)^p \frac{\cos(m-2p)\,\omega}{(m-p)!\,p!} \int_0^\infty e^{-f\xi}\,\mathrm{sh}\, fz\, J_{m-2p}(fr)\, f^n\, df, \quad \ldots (6)$$

where q should be taken at $m/2$ or $(m-1)/2$ according as m is even or odd and it is to be remarked that γ is taken to be unity excepting the term, $p=m/2$, in which case $\gamma=1/2$.

3. In order to find the expressions of displacement on the surface, we shall solve the following equations.

When u, v, w, are radial azimuthal and axial components of displacement respectively and λ, μ are Lamé's elastic constants, the equations of equilibrium are expressed by

$$\left.\begin{aligned} &(\lambda+2\mu)\frac{\partial\varDelta_0}{\partial r} - \frac{2\mu}{r}\frac{\partial\varpi_z}{\partial\theta} + 2\mu\frac{\partial\varpi_\theta}{\partial z} = 0, \\ &(\lambda+2\mu)\frac{1}{r}\frac{\partial\varDelta_0}{\partial\theta} - 2\mu\frac{\partial\varpi_r}{\partial z} + 2\mu\frac{\partial\varpi_z}{\partial r} = 0, \\ &(\lambda+2\mu)\frac{\partial\varDelta_0}{\partial z} - \frac{2\mu}{r}\frac{\partial}{\partial z}(r\varpi_\theta) + \frac{2\mu}{r}\frac{\partial\varpi_r}{\partial\theta} = 0, \end{aligned}\right\} \quad \ldots\ldots\ldots\ldots (7)$$

where

$$\left.\begin{aligned} &\varDelta_0 = \frac{1}{r}\frac{\partial(ru)}{\partial r} + \frac{1}{r}\frac{\partial v}{\partial\theta} + \frac{\partial w}{\partial z}, & &2\varpi_r = \frac{1}{r}\frac{\partial w}{\partial\theta} - \frac{\partial v}{\partial z}, \\ &2\varpi_\theta = \frac{\partial u}{\partial z} - \frac{\partial w}{\partial r}, & &2\varpi_z = \frac{1}{r}\left(\frac{\partial(rv)}{\partial r} - \frac{\partial u}{\partial\theta}\right). \end{aligned}\right\} \quad \ldots\ldots (8)$$

These are particularly satisfied by the following system of solutions.[10]

$$\begin{aligned} &\varDelta_0 = \mathrm{sh}\, fz\, J_{m-2p}(fr)\cos(m-2p)\,\omega, \\ &u = -\left[\frac{\lambda+\mu}{2\mu} z\,\mathrm{ch}\, fz + \alpha\,\mathrm{sh}\, fz\right]\frac{\partial J_{m-2p}(fr)}{f\partial r}\cos(m-2p)\,\omega, \end{aligned}$$

---

10) These are easily obtained by the method as that of Prof. K. TERAZAWA, *l.c.* p. 1 or by the way which I have employed in Rayleigh-wave problem, *Proc. Imp. Acad.*, **4**, besides the addition of free displacement satisfying $\varDelta_0 = \varpi_r = \varpi_\theta = \varpi_z = 0$.

$$\left.\begin{aligned} v&=(m-2p)\left[\frac{\lambda+\mu}{2\mu}z\,\mathrm{ch}\,fz+\alpha\,\mathrm{sh}\,fz\right]\frac{J_{m-2p}(fr)}{fr}\sin(m-2p)\,\omega,\\ w&=-\left[\frac{\lambda+\mu}{2\mu}z\,\mathrm{sh}\,fz+\beta\,\mathrm{ch}\,fz\right]J_{m-2p}(fr)\cos(m-2p)\,\omega,\end{aligned}\right\}\quad\ldots\ldots(9)$$

provided

$$f(\alpha-\beta)=\frac{\lambda+3\mu}{2\mu}.\quad\ldots\ldots(10)$$

When the surface, $z=0$, is free from traction, we should have

$$\lambda\Delta_0+2\mu\frac{\partial w}{\partial z}=0,\qquad \frac{1}{r}\frac{\partial w}{\partial\theta}+\frac{\partial v}{\partial z}=0,\qquad \frac{\partial u}{\partial z}+\frac{\partial w}{\partial r}=0.\quad\ldots\ldots(11)$$

The first of these is satisfied identically in this case, while the second and the third give us

$$f(\alpha+\beta)+\frac{\lambda+\mu}{2\mu}=0.\quad\ldots\ldots(12)$$

Solving (10) and (12), we find

$$\alpha=\frac{1}{2f},\qquad \beta=-\frac{\lambda+2\mu}{2\mu f}.\quad\ldots\ldots(13)$$

Thus the expressions in (9) together with (13) give us the typical solutions appropriate to the present problem.

4. The expressions of displacement corresponding to Δ_0 in (6) are now given by

$$\left.\begin{aligned} u&=(-1)^{n+1}n!\sum_{m=0}^{m=n}\frac{\sin^{n-m}\theta\cos^{m}\theta}{2^{m-2}(n-m)!}\sum_{p=0}^{p=q}\gamma(-1)^{p}\frac{\cos(m-2p)\,\omega}{(m-p)!\,p!}\\ &\quad\times\int_0^\infty\left[\frac{\lambda+\mu}{2\mu}z\,\mathrm{ch}\,fz+\frac{1}{2f}\,\mathrm{sh}\,fz\right]e^{-f\xi}\,\frac{\partial J_{m-2p}(fr)}{\partial r}\,f^{n-1}\,df,\\ v&=(-1)^{n}n!\sum_{m=0}^{m=n}\frac{\sin^{n-m}\theta\cos^{m}\theta}{2^{m-2}(n-m)!}\sum_{p=0}^{p=q}\gamma(-1)^{p}\frac{(m-2p)\sin(m-2p)\,\omega}{(m-p)!\,p!}\\ &\quad\times\int_0^\infty\left[\frac{\lambda+\mu}{2\mu}z\,\mathrm{ch}\,fz+\frac{1}{2f}\,\mathrm{sh}\,fz\right]e^{-f\xi}\,\frac{J_{m-2p}(fr)}{r}\,f^{n-1}\,df,\\ w&=(-1)^{n+1}n!\sum_{m=0}^{m=n}\frac{\sin^{n-m}\theta\cos^{m}\theta}{2^{m-2}(n-m)!}\sum_{p=0}^{p=q}\gamma(-1)^{p}\frac{\cos(m-2p)\,\omega}{(m-p)!\,p!}\\ &\quad\times\int_0^\infty\left[\frac{\lambda+\mu}{2\mu}z\,\mathrm{sh}\,fz-\frac{\lambda+2\mu}{2\mu f}\,\mathrm{ch}\,fz\right]e^{-f\xi}J_{m-2p}(fr)f^{n}\,df.\end{aligned}\right\}\ldots(14)$$

We may remark that these expressions of displacement give us not only the dilatation Δ_0, but also the rotational components together with the component which is neither dilatational nor distortional. We may, however, show that the above gives us the only displacement which forms the expression of $\varDelta_0$ in (6) and satisfies the equations of equilibrium and of boundary conditions. It is also mentioned that the present problem treats of the case where the nuclei of strain are at the point $r=0$, $z=\xi$. Hence such a case that the nuclei themselves are shifted otherwise than the movements due to the type of the nuclei should be excluded from our consideration.

5. As a very simple example we take the case of a singlet-nucleous. Since $n=0$ in this case, we have

$$\varDelta=\frac{1}{R_1}=\frac{1}{\sqrt{r^2+(z-\xi)^2}}, \quad\text{.....................}(15)$$

where $\varDelta$ is written in place of $\varDelta_0'$ in (1) ; and

$$\left.\begin{aligned} u&=-2\int_0^\infty\left[\frac{\lambda+\mu}{2\mu}z\operatorname{ch}fz+\frac{1}{2f}\operatorname{sh}fz\right]e^{-f\xi}\frac{1}{f}\frac{\partial J_0(fr)}{\partial r}df,\\ v&=0,\\ w&=-2\int_0^\infty\left[\frac{\lambda+\mu}{2\mu}z\operatorname{sh}fz-\frac{\lambda+2\mu}{2\mu f}\operatorname{ch}fz\right]e^{-f\xi}J_0(fr)\,df. \end{aligned}\right\}\quad\text{........}(16)$$

When $z=0$, the inclination of the surface can be easily found to be

$$\frac{\partial w_0}{\partial r}=-\left(\frac{\lambda+2\mu}{\mu}\right)\frac{\sqrt{\xi^2+r^2}-\xi}{r\sqrt{\xi^2+r^2}}, \quad\text{.................}(17)$$

the distribution of which is shewn in the annexed drawing.

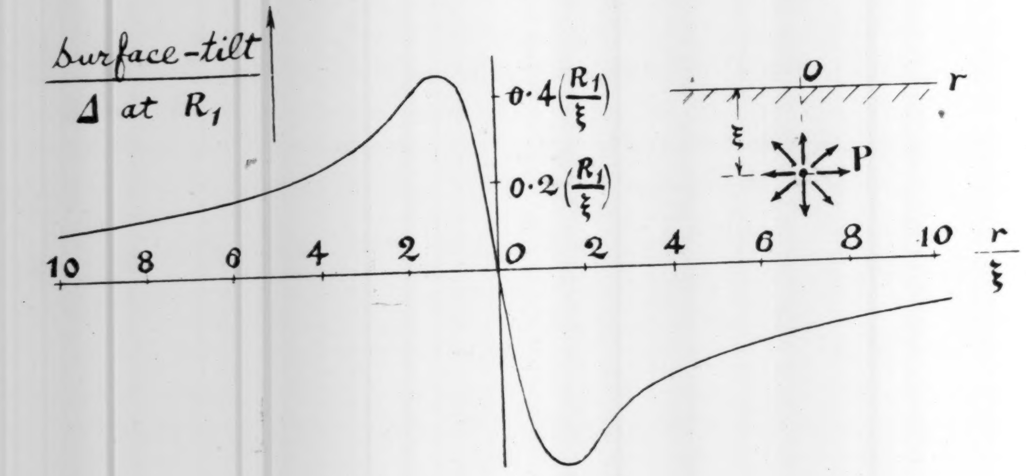

Fig. I.

6. Secondly, we put $n=1$, which gives us the problem of doublet-nuclei. The dilatation and the displacement can be expressed by

$$\Delta=\left(\cos\theta\frac{\partial}{\partial x}+\sin\theta\frac{\partial}{\partial z}\right)\frac{1}{\sqrt{r^2+(z-\xi)^2}},\quad\dots\dots\dots\dots\dots(18)$$

$$\left.\begin{aligned}
u&=2\int_0^\infty\left[\frac{\lambda+\mu}{2\mu}z\,\mathrm{ch}\,fz+\frac{1}{2f}\,\mathrm{sh}\,fz\right]e^{-f\xi}\left\{\cos\theta\cos\omega\frac{\partial J_1(fr)}{\partial r}\right.\\
&\qquad\qquad\left.-\sin\theta\frac{\partial J_0(fr)}{\partial r}\right\}df,\\
v&=-2\int_0^\infty\left[\frac{\lambda+\mu}{2\mu}z\,\mathrm{ch}\,fz+\frac{1}{2f}\,\mathrm{sh}\,fz\right]\cos\theta\sin\omega\, e^{-f\xi}\frac{J_1(fr)}{r}\,df,\\
w&=2\int_0^\infty\left[\frac{\lambda+\mu}{2\mu}z\,\mathrm{sh}\,fz-\frac{\lambda+2\mu}{2\mu f}\,\mathrm{ch}\,fz\right]e^{-f\xi}\Big\{\cos\theta\cos\omega J_1(fr)\\
&\qquad\qquad-\sin\theta J_0(fr)\Big\}f\,df.
\end{aligned}\right\}\quad\dots(19)$$

If we take, particularly, the case, $z=0$, we get

$$w_0=-\frac{\lambda+2\mu}{\mu}\left[\cos\theta\cos\omega\frac{\sqrt{\xi^2+r^2}-\xi}{r\sqrt{\xi^2+r^2}}-\sin\theta\frac{1}{\sqrt{\xi^2+r^2}}\right],\quad\dots\dots(20)$$

and

$$\left.\begin{aligned}
\frac{\partial w_0}{\partial r}&=\frac{\lambda+2\mu}{\mu}\left[\cos\theta\cos\omega\left\{\frac{1}{r^2}-\frac{\xi}{r^2\sqrt{\xi^2+r^2}}\right.\right.\\
&\qquad\left.\left.-\frac{r}{(\xi^2+r^2)^{\frac{3}{2}}}\right\}+\sin\theta\frac{r}{(\xi^2+r^2)^{\frac{3}{2}}}\right],\\
\frac{1}{r}\frac{\partial w_0}{\partial\omega}&=\frac{\lambda+2\mu}{\mu}\cos\theta\sin\omega\left\{\frac{1}{r^2}-\frac{\xi}{r^2\sqrt{\xi^2+r^2}}\right\}.
\end{aligned}\right\}\quad\dots\dots(21)$$

The distribution of $\dfrac{\partial w_0}{\partial r}$ at $\omega=0$ and of $\dfrac{1}{r}\dfrac{\partial w_0}{\partial\omega}$ at $\omega=\dfrac{\pi}{2}$ are plotted in Fig. II*a* and Fig. II*b*.

7. We proceed to the case in which $n=2$. The nuclei in the present example may be named quadruplet-nuclei. The dilatation and the displacement are expressed in the forms:

$$\Delta=\left(\cos\theta\frac{\partial}{\partial x}+\sin\theta\frac{\partial}{\partial z}\right)^2\frac{1}{\sqrt{r^2+(z-\xi)^2}},\quad\dots\dots\dots\dots\dots(22)$$

with

$$\begin{aligned}
u=-\int_0^\infty&\left[\frac{\lambda+\mu}{2\mu}z\,\mathrm{ch}\,fz+\frac{1}{2f}\,\mathrm{sh}\,fz\right]e^{-f\xi}\left\{\cos^2\theta\cos2\omega\frac{\partial J_2(fr)}{\partial r}\right.\\
&\left.-2\sin2\theta\cos\omega\frac{\partial J_1(fr)}{\partial r}-(\cos^2\theta-2\sin^2\theta)\frac{\partial J_0(fr)}{\partial r}\right\}f\,df,
\end{aligned}$$

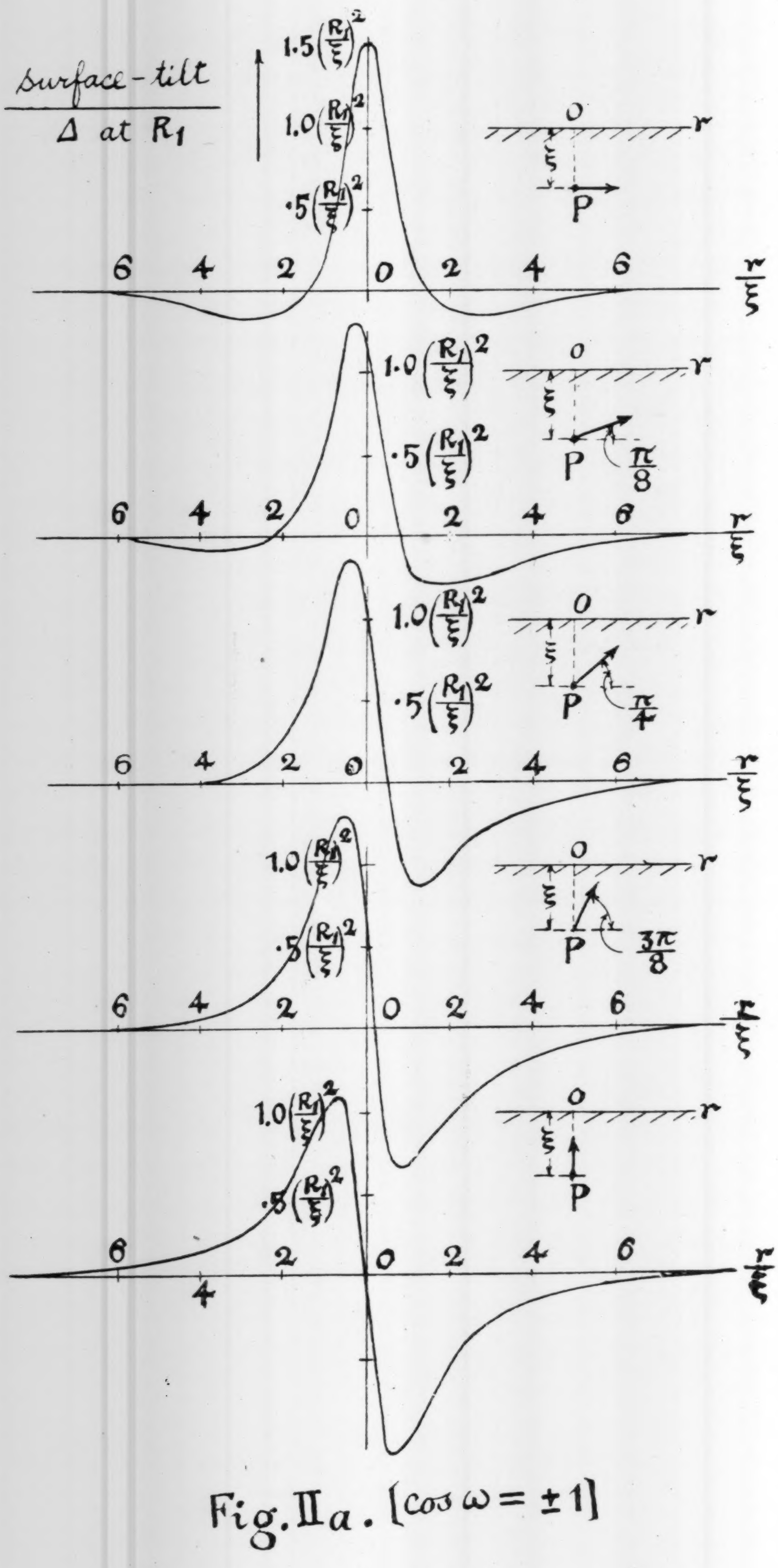

Fig. IIa. [cos ω = ±1]

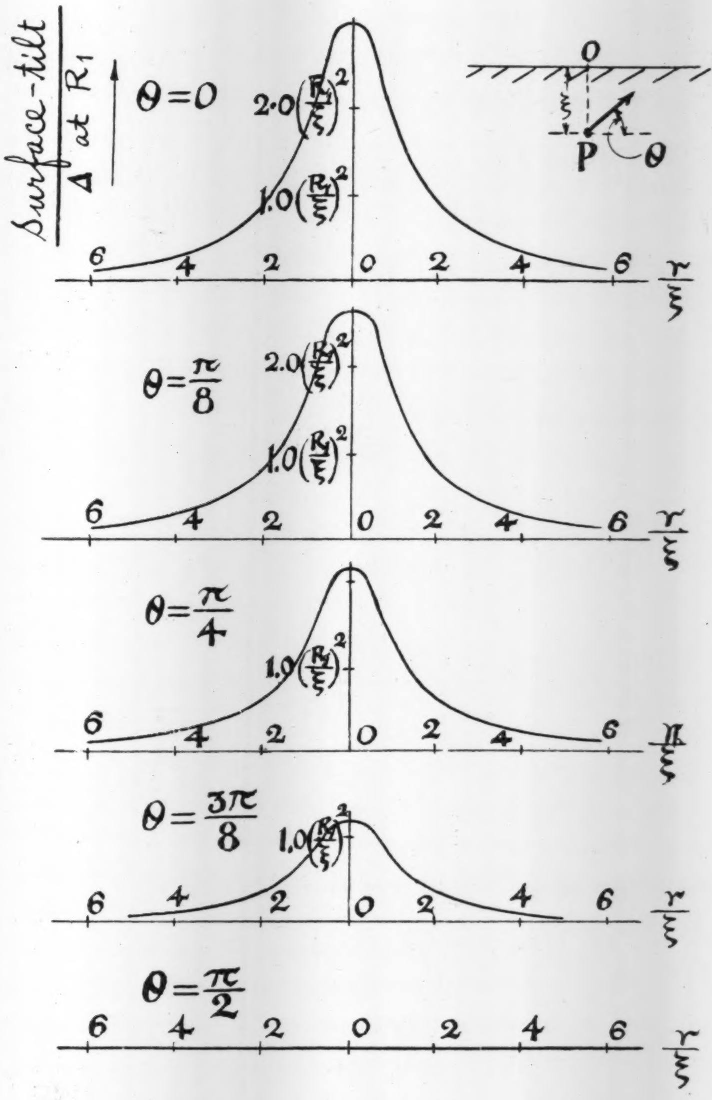

Fig. II$_f$. [$\cos\omega = 0$]

$$v=2\int_0^\infty\left[\frac{\lambda+\mu}{2\mu}z\,\mathrm{ch}\,fz+\frac{1}{2f}\,\mathrm{sh}\,fz\right]e^{-f\xi}\left\{\cos^2\theta\sin2\omega\,\frac{J_2(fr)}{r}\right.$$
$$\left.-\sin2\theta\sin\omega\,\frac{J_1(fr)}{r}\right\}fdf,$$

$$w=-\int_0^\infty\left[\frac{\lambda+2\mu}{2\mu}z\,\mathrm{sh}\,fz-\frac{\lambda+2\mu}{2\mu f}\,\mathrm{ch}\,fz\right]e^{-f\xi}\left\{\cos^2\theta\cos2\omega\,J_2(fr)\right.$$
$$\left.-2\sin2\theta\cos\omega\,J_1(fr)-(\cos^2\theta-2\sin^2\theta)J_0(fr)\right\}f^2df.$$

. . . . (23)

The evaluation of these integrals is very simple. Owing to the importance of the vertical displacement, we consider w only as in the preceding cases. We can readily write

$$w_0=\frac{\lambda+2\mu}{\mu}\Big[\cos^2\theta\cos 2\omega\Big\{\frac{1}{r^2}-\frac{\xi}{r^2\sqrt{\xi^2+r^2}}-\frac{\xi}{2\,(\xi^2+r^2)^{\frac{3}{2}}}\Big\}$$
$$-\sin 2\theta\cos\omega\,\frac{r}{(\xi^2+r^2)^{\frac{3}{2}}}-\Big(\frac{\cos^2\theta}{2}-\sin^2\theta\Big)\frac{\xi}{(\xi^2+r^2)^{\frac{3}{2}}}\Big], \quad\ldots\ldots(24)$$

so that we find

$$\left.\begin{aligned}
&\frac{\partial w_0}{\partial r}=\frac{\lambda+2\mu}{\mu}\Big[\cos^2\theta\cos 2\omega\Big\{-\frac{2}{r^3}+\frac{2\xi}{r^3\sqrt{\xi^2+r^2}}+\frac{\xi}{r\,(\xi^2+r^2)^{\frac{3}{2}}}+\frac{3\xi r}{2\,(\xi^2+r^2)^{\frac{5}{2}}}\Big\}\\
&\quad-\sin 2\theta\cos\omega\Big(\frac{1}{(\xi^2+r^2)^{\frac{3}{2}}}-\frac{3r^2}{(\xi^2+r^2)^{\frac{5}{2}}}\Big)+\Big(\frac{\cos^2\theta}{2}-\sin^2\theta\Big)\frac{3\xi r}{(\xi^2+r^2)^{\frac{5}{2}}}\Big],\\
&\text{and}\\
&\frac{1}{r}\frac{\partial w_0}{\partial\omega}=-\frac{\lambda+2\mu}{\mu}\Big[\cos^2\theta\sin 2\omega\Big\{\frac{2}{r^3}-\frac{2\xi}{r^3\sqrt{\xi^2+r^2}}-\frac{\xi}{r\,(\xi^2+r^2)^{\frac{3}{2}}}\Big\}\\
&\qquad\qquad-\sin 2\theta\sin\omega\frac{1}{(\xi^2+r^2)^{\frac{3}{2}}}\Big]
\end{aligned}\right\}\quad(25)$$

The distribution of $\frac{\partial w_0}{\partial r}$ at $\cos\omega=\pm 1$ and of $\frac{1}{r}\frac{\partial w_0}{\partial\omega}$ at $\cos\omega=0$ are illustrated in Fig. III*a* and Fig. III*b*.

8. Lastly it may be noticed that the evaluation of the definite integrals where the multiplet is of the general order, n, can be easily formulated[11] though the actual computation of the formulae is very difficult.

9. We may complete this investigation by a brief notice on the general results.

It has been shewn in Figs. I, II, III that the increase of the depth of the nuclei diminishes the surface deformation. When the dilatation at a certain radial distance from the focus is assigned, the tilting of the surface due to the singlet is inversely proportional to the depth of the focus; whilst that due to the doublet is proportional to its inverse square. In the case of a quadruplet the tilting decreases as the inverse cube of the focal depth. From these we may conclude that the surface deformation due to a multiplet of order n decreases inversely as $(n+1)$th power of the depth of origin.

---

[11] WATSON, *Theory of Bessel Functions* (1922), 384.

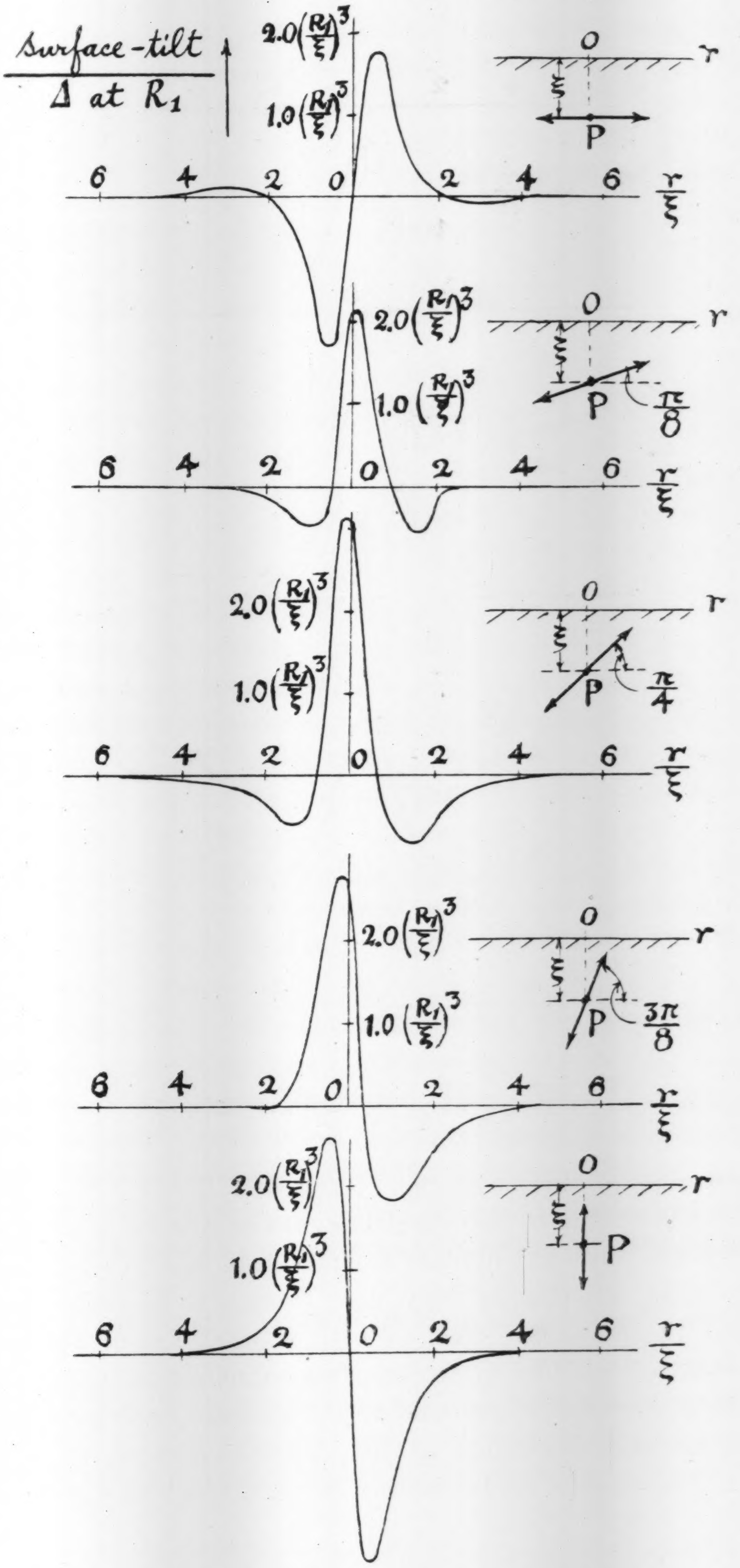

Fig. III$_a$. [$\cos\omega = \pm 1$]

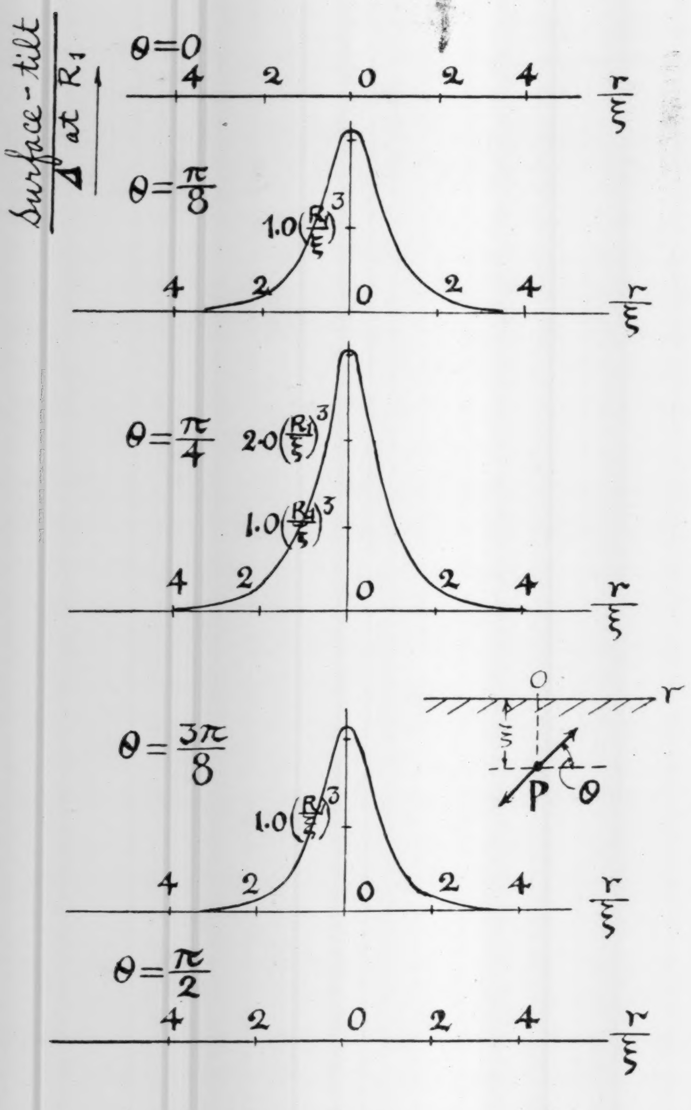

Fig. III$_b$. [$\cos\omega = 0$]

The interpretation of this is simple. Take first the deformation due to a singlet. The tilting due to this singlet occurs in a manner as expressed by (17) and Fig. I. Since the doublet is equivalent to a pair of singlets, both of contrary signs, residing at very near points, it is plain that at some distance from the focus the effect of both singlets are of the tendency of cancelling each other. The problem of the quadruplet gives us the case where a pair of doublets of the contrary signs take their positions at very near points, so that the effect of the doublet at a distance is further diminished. The similar explanation will be applied to higher multiplets.

Hence, the higher the order of multiplet becomes, the more limitedly the disturbance due to that nuclei is localised in the neighbourhood of the focus. It appears that, if the depth of the origin is determined otherwise and the limiting value of $\varDelta$ at a certain R_1 is specified, we may find the effective type of the nuclei from the surface data. Though it is impossible to anticipate the value of $\varDelta$ and R_1 in the present state of seismology, yet I think that we may realize our purpose to a certain extent by taking yielding strain of the crust and the approximate dimensions of the sliding fault as the rough estimation of $\varDelta$ and R_1.

Again, the preceding figures tell us the fact that the distribution of tilting of the surface is of a different form for each type of the multiplets. By this evidence together with the note already cited, we may probably confirm more closely the effective type of the internal multiplet. The preceding figures also shew that the extent of the deformation due to the higher multiplets is limited in a small portion of the epicentral region, while that due to the singlet is rather large. This fact can be interpreted in the same way as that on the depth of the focus. It is, however, remarked that even in the case of a singlet the principal portion of the tilting is accumulated in the epicentral area with the diameter of four or five times the depth of the focus.

In the present paper very particular cases of the tilting due to internal disturbances have been written. My intention is to study more general problems such as the tilting due to the nuclei of distortional type, the deformation due to the imbedded rigid body and that caused by the strain widely extending through the elastic body. These cases have been left for the future study.

In concluding this paper I am indebted to Profs. Nagaoka and Suyehiro who have some interests on this study and also to Mr. G. Nishimura who has assisted me in preparing this paper.

---

1. 內部歪核による半無限固體の表面傾斜

地震研究所　妹澤克惟

半無限固體の表面に壓力が加はる場合の研究は既に幾多の學者によつて發表されてゐるが、この固體の內部に壓力の原點がある問題は未だ見當らぬ樣に思はれる。私は以前から斯る問題の研究を目論んで居たが、極く簡單な部分が出來上つたので、ここに其をしるすことにした。もつと複雜で面白い部分は遺憾ながら後の機會に讓ることとした。

問題は內部の一點に力學的に最も可能な壓力の原點を置き、其爲めに表面上の點が如何に變動するかを計算したものである。尤も原點は單原や複原のみでなく多重原として考へた。

計算上注意すべき事項は、流體力學でよく行はれる樣に、原點の球狀解法を表面に適する圓壔狀解法に變更する事と別の論文にもある樣に多重原に適する一般解法を求める事などである。

計算の主要な結果として、內部の或場所の歪を一定に保つ時、內部に n 次の原點があるならば、表面の傾斜は原點の深さの $(n+1)$ 乘に反比例して少くなる理論、表面の變位部分は原點の上部の部分にのみ集中し而も高次のもの程、一層中央へ集まる事實、又、內部の型により表面の型も異なる事、而してこれ等の事柄と他の測定の助けとによつて、內部の變形傾向の大體が推定できる可能性などを擧げ得る。

2. *Formation of Shallow-water Waves due to Subaqueous Shocks.*

By **Katsutada SEZAWA,**

Earthquake Research Institute.

(Read Dec. 18, 1928 and Jan. 15, 1929.—Received March 20, 1929.)

In a recent paper[1] I have described the formation of deep-water waves due to subaqueous shocks. Since the publication of that paper, it occurred me that it is rather important to solve the problem of shallow-water waves due to bottom or subaqueous shocks, because the conspicuous phenomena[2] of tsunami will be observed in the shallow sea[3] or in the effectively shallow water in which the length of the waves is large compared with the depth of the sea. Although Drs. K. Sano and K. Hasegawa[4] have already studied such a problem, yet the nature of the transmission of disturbances from the bottom, which is given in their paper, is quite different from that in the present case. In my theory the compressional disturbances are transmitted radially from a source and when these disturbances make multiple-reflections at the bottom as well as at the surface in succession, a series of shallow-water waves are gradually developed by the surface conditions of the water.

The paper consists of four parts: the first part is on the formation of shallow-water waves where the effect of the inertia of the water on the compressional disturbances is negligible and the depth of the water is very small, the second part is on the same problem where the depth of the water is not restricted so small, and the third is on the shallow-water waves in which the effect of the inertia in the subaqueous region is not negligible, while the remaining part deals with the generation of waves from a subaqueous point at an intermediate depth of the water.

Part I. Waves due to Bottom Pressure.

The subaqueous motion at the initial stage is supposed to be free from the inertia of the water and the transmission of the bottom pressure is considered as taking place in three dimensions, r, ω, z, the origin of the coordinates being taken on the surface of the water and the axis of z normal to this free surface. The bottom of the shallow-water is expressed by $z=\xi$. The differential equation of the pressure-distribution is denoted by

---

[1] "Formation of Deep-water Waves due to Subaqueous Shocks," *Bull. Earthq. Res. Inst.*, **6** (1929).

[2] Prof. T. Iki, *Rep. Imp. Earthq. Inv. Comm.*, **11** (1897).

[3] Prof. A. Imamura, *Rep. Imp. Earthq. Inv. Comm.*, **29** (1899).

[4] K. Sano & K. Hasegawa, *Proc. Tokyo Math.-Phys. Soc.*, **II 8** (1915).

$$\frac{\partial^2 p_0}{\partial R^2}+\frac{2}{R}\frac{\partial p_0}{\partial R}=0, \qquad \text{(1)}$$

in which $R=\sqrt{(z-\xi)^2+r^2}$ and p_0 is the pressure at the point whose radial distance from P is R.

When the nucleous of the pressure is situated at the point $r=0$, $z=\xi$, the distribution of that pressure can be expressed by

$$p_0=\frac{e^{ipt}}{R}, \qquad \text{(2)}$$

where $2\pi/p$ is the period of the harmonic variation of the pressure.

Since we know the expression

$$\frac{1}{R}=\int_0^\infty e^{-fz}J_0(fr)\,df, \qquad \text{(3)}$$

we may transform (2) in a form suitable to the wave motion at the surface.

In the case of a bottom source of pressure, resident at the point $r=0$, $z=\xi$, it will be convenient to consider a series of the successive images at $z=-\xi$, 3ξ, -3ξ, 5ξ, -5ξ, ..., all in a vertical line $r=0$. The resulting pressure is, thus, written by

$$\begin{aligned} p_0=e^{ipt}\Big[&\int_0^\infty e^{f(z-\xi)}J_0(fr)\,df+\int_0^\infty e^{-f(z+\xi)}J_0(fr)\,df \\ &-\int_0^\infty e^{f(z-3\xi)}J_0(fr)\,df-\int_0^\infty e^{-f(z+3\xi)}J_0(fr)\,df \\ &+\int_0^\infty e^{f(z-5\xi)}J_0(fr)\,df+\int_0^\infty e^{-f(z+5\xi)}J_0(fr)\,df \\ &-\cdots\cdots\cdots\Big] \\ =2e^{ipt}&\int_0^\infty \operatorname{ch} fz\,\frac{e^{-f\xi}}{1+e^{-2f\xi}}J_0(fr)\,df. \qquad [z<\xi] \qquad \text{(4)} \end{aligned}$$

Now, for gravity waves, the velocity potential ϕ is subject to the equation

$$\frac{\partial^2\phi}{\partial r^2}+\frac{1}{r}\frac{\partial\phi}{\partial r}+\frac{\partial^2\phi}{\partial z^2}=0, \qquad \text{(5)}$$

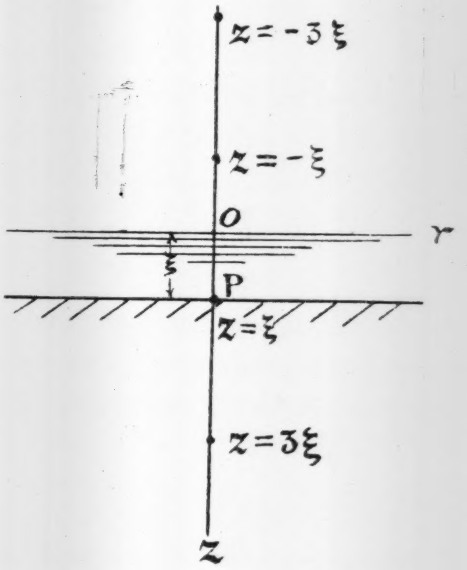

the solution of which is easily found to be

$$\phi=e^{ipt}C\operatorname{ch}f(z-\xi)J_0(fr).\qquad(6)$$

It is known that the components of displacement u and w in r and z directions are related with ϕ in the forms:

$$\frac{\partial u}{\partial t}=-\frac{\partial\phi}{\partial r},\qquad \frac{\partial w}{\partial t}=-\frac{\partial\phi}{\partial z},\qquad(7)$$

so that we find the solutions of displacement such that

$$\left.\begin{aligned}u&=-\frac{if}{p}e^{ipt}C\operatorname{ch}f(z-\xi)J_1(fr),\\ w&=\frac{if}{p}e^{ipt}C\operatorname{sh}f(z-\xi)J_0(fr),\end{aligned}\right\}\qquad(8)$$

with the condition that there is no vertical displacement at any point of the bottom of the sea.

As the pressure due to gravity waves satisfies the condition

$$\frac{p_1}{\rho}=\frac{\partial\phi}{\partial t}+gw\qquad(9)$$

at the surface $z=0$, we obtain

$$p_1=i\rho Ce^{ipt}\frac{p^2\operatorname{ch}f\xi-fg\operatorname{sh}f\xi}{p}J_0(fr).\qquad(10)$$

The surface $z=0$ being free from pressure, we can put

$$p_0+p_1=0\qquad(11)$$

at that surface. By the above relation we find

$$C=-2\int_0^\infty \frac{e^{-f\xi}}{(1+e^{-2f\xi})}\,\frac{p\,df}{i\rho\,(p^2\operatorname{ch} f\xi-fg\operatorname{sh} f\xi)}. \qquad (12)$$

Thus u and w in (8) can be written by

$$\left.\begin{aligned} u&=\frac{2e^{ipt}}{\rho}\int_0^\infty \frac{e^{-f\xi}\operatorname{ch} f\xi}{(1+e^{-2f\xi})(p^2\operatorname{ch} f\xi-fg\operatorname{sh} f\xi)}J_1(fr)f\,df,\\ w&=\frac{2e^{ipt}}{\rho}\int_0^\infty \frac{e^{-f\xi}\operatorname{sh} f\xi}{(1+e^{-2f\xi})(p^2\operatorname{ch} f\xi-fg\operatorname{sh} f\xi)}J_0(fr)f\,df.\end{aligned}\right\} \qquad (13)$$

These expressions can be applied to the waves for any depth of the water. When the depth ξ is so small that we may put

$$\operatorname{th} f\xi=f\xi, \qquad (14)$$

the equations in (13) are transformed into

$$\left.\begin{aligned} u&=\frac{2e^{ipt}}{\rho}\int_0^\infty [e^{-f\xi}-e^{-3f\xi}+e^{-5f\xi}-\ldots.]\,\frac{J_1(fr)f\,df}{(p^2-f^2g\xi)},\\ w&=\frac{2e^{ipt}}{\rho}\int_0^\infty [e^{-f\xi}-e^{-3f\xi}+e^{-5f\xi}-\ldots.]\,\frac{J_0(fr)f^2\xi\,df}{(p^2-f^2g\xi)}.\end{aligned}\right\} \qquad (15)$$

As we know the relations

$$\left.\begin{aligned} J_0(fr)&=\frac{2}{\pi}\int_0^\infty \sin(fr\operatorname{ch} k)\,dk\\ &=-\frac{i}{\pi}\int_0^\infty (e^{ifr\operatorname{ch} k}-e^{-ifr\operatorname{ch} k})\,dk,\\ J_1(fr)&=-\frac{2}{\pi}\int_0^\infty \cos(fr\operatorname{ch} k)\operatorname{ch} k\,dk\\ &=-\frac{1}{\pi}\int_0^\infty (e^{ifr\operatorname{ch} k}+e^{-ifr\operatorname{ch} k})\operatorname{ch} k\,dk,\end{aligned}\right\} \qquad (16)$$

the formlae (15) reduce to

$$\left.\begin{aligned} u&=-\frac{2e^{ipt}}{\pi\rho}\int_0^\infty \operatorname{ch} k\,dk\int_0^\infty \frac{(e^{-f\xi}-e^{-3f\xi}+\ldots.)(e^{ifr\operatorname{ch} k}+e^{-ifr\operatorname{ch} k})\,f\,df}{(p^2-f^2g\xi)},\\ w&=-\frac{2i\xi\,e^{ipt}}{\pi\rho}\int_0^\infty dk\int_0^\infty \frac{(e^{-f\xi}-e^{-3f\xi}+\ldots.)(e^{ifr\operatorname{ch} k}-e^{-ifr\operatorname{ch} k})\,f^2\,df}{(p^2-f^2g\xi)}.\end{aligned}\right\} \qquad (17)$$

To integrate the expressions of (17), we consider the integrals

$$\left.\begin{aligned} &\int \frac{e^{-mZ\xi}\,e^{iZr\operatorname{ch} k}}{p^2-Z^2g\xi}Z\,dZ,\\ &\int \frac{e^{-mZ\xi}\,e^{iZr\operatorname{ch} k}}{p^2-Z^2g\xi}Z^2\,dZ,\end{aligned}\right|$$

$$\left.\begin{array}{l}\displaystyle\int\frac{e^{-mZ\xi}\,e^{-iZr\,\mathrm{ch}\,k}}{p^2-Z^2\,g\xi}Z\,dZ,\\[2ex] \displaystyle\int\frac{e^{-mZ\xi}\,e^{-iZr\,\mathrm{ch}\,k}}{p^2-Z^2\,g\xi}Z^2\,dZ,\end{array}\right\}\cdots\cdots\cdots\cdots(18)$$

taken round some closed contrours. In the present case, the first two are taken round the contour of left-hand side of the following sketches and the remaining two integrals are taken round that of the right-hand side.

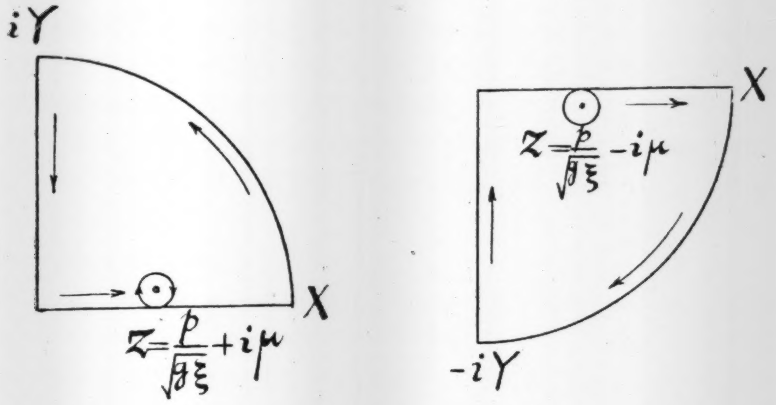
iY
X
$Z=\frac{p}{\sqrt{g\xi}}+i\mu$
X
$Z=\frac{p}{\sqrt{g\xi}}-i\mu$
$-iY$

$[\mu=0]$[5]

Making use of these contour integrations, we find

$$\left.\begin{array}{l}\displaystyle\int_0^\infty\frac{e^{-mf\xi+ifr\,\mathrm{ch}\,k}\,f\,df}{p^2-f^2\,g\xi}=-\frac{\pi i}{g\xi}e^{-\frac{m\xi p}{\sqrt{g\xi}}+\frac{ipr\,\mathrm{ch}\,k}{\sqrt{g\xi}}}-\int_0^\infty\frac{e^{-imf\xi-fr\,\mathrm{ch}\,k}\,f\,df}{p^2+f^2\,g\xi},\\[2ex] \displaystyle\int_0^\infty\frac{e^{-mf\xi+ifr\,\mathrm{ch}\,k}\,f^2\,df}{p^2-f^2\,g\xi}=-\frac{\pi i}{g\xi}\frac{p}{\sqrt{g\xi}}e^{-\frac{m\xi p}{\sqrt{g\xi}}+\frac{ipr\,\mathrm{ch}\,k}{\sqrt{g\xi}}}-i\int_0^\infty\frac{e^{-imf\xi-fr\,\mathrm{ch}\,k}\,f^2\,df}{p^2+f^2\,g\xi},\\[2ex] \displaystyle\int_0^\infty\frac{e^{-mf\xi-ifr\,\mathrm{ch}\,k}\,f\,df}{p^2-f^2\,g\xi}=\frac{\pi i}{g\xi}e^{-\frac{m\xi p}{\sqrt{g\xi}}-\frac{ipr\,\mathrm{ch}\,k}{\sqrt{g\xi}}}-\int_0^\infty\frac{e^{imf\xi-fr\,\mathrm{ch}\,k}\,f\,df}{p^2+f^2\,g\xi},\\[2ex] \displaystyle\int_0^\infty\frac{e^{-mf\xi-ifr\,\mathrm{ch}\,k}\,f^2\,df}{p^2-f^2\,g\xi}=\frac{\pi i}{g\xi}\frac{p}{\sqrt{g\xi}}e^{-\frac{m\xi p}{\sqrt{g\xi}}-\frac{ipr\,\mathrm{ch}\,k}{\sqrt{g\xi}}}+i\int_0^\infty\frac{e^{imf\xi-fr\,\mathrm{ch}\,k}\,f^2\,df}{p^2+f^2\,g\xi}.\end{array}\right\}\ldots(19)$$

The expressions in (17) therfore take the forms

$$\begin{aligned}u=-\frac{4e^{ipt}}{\rho g\xi}\int_0^\infty\mathrm{ch}\,k\Big[&\Big(e^{-p\sqrt{\frac{\xi}{g}}}-e^{-3p\sqrt{\frac{\xi}{g}}}+\ldots.\Big)\sin\frac{pr\,\mathrm{ch}\,k}{\sqrt{g\xi}}\\&-\frac{g\xi}{\pi}\int_0^\infty\frac{e^{-fr\,\mathrm{ch}\,k}(\cos f\xi-\cos 3f\xi+\ldots.)\,f\,df}{p^2+f^2\,g\xi}\Big]dk,\end{aligned}$$

---

[5] To make the problems determinate, we consider a frictional force which will be made zero after the several operations. This process is equivalent to shift the pole an infinitesimal distance in the direction of the imaginary part, viz. to make the contour integration around the pole through the complete circuit about the same point.

$$\left.\begin{aligned} w=-\frac{4e^{ipt}}{\rho g\xi}\int_0^\infty\Big[p\sqrt{\frac{\xi}{g}}\Big(e^{-p\sqrt{\frac{\xi}{g}}}-e^{-3p\sqrt{\frac{\xi}{g}}}\dots\Big)\cos\frac{pr\,\mathrm{ch}\,k}{\sqrt{g\xi}} \\ +\frac{g\xi^2}{\pi}\int_0^\infty\frac{e^{-fr\,\mathrm{ch}\,k}(\cos f\xi-\cos 3f\xi+\dots)\,f^2\,df}{p^2+f^2\,g\xi}\Big]dk. \end{aligned}\right\}\dots\dots(20)$$

Since the second terms of the above expressions of u and w vanish asymptotically as r is increased, we may disregard these terms in a restricted sense that we should hereafter treat of the waves transmitted for a certain distance.

Again, by means of the obvious formulae:

$$\left.\begin{aligned} \int_0^\infty \mathrm{ch}\,k\,\sin\frac{pr\,\mathrm{ch}\,k}{\sqrt{g\xi}}\,dk=-\frac{\pi}{2}\,Y_1\left(\frac{pr}{\sqrt{g\xi}}\right), \\ \int_0^\infty \cos\frac{pr\,\mathrm{ch}\,k}{\sqrt{g\xi}}\,dk=-\frac{\pi}{2}\,Y_0\left(\frac{pr}{\sqrt{g\xi}}\right), \end{aligned}\right\}\dots\dots\dots\dots(21)$$

we find easily

$$\left.\begin{aligned} u\sim\frac{2\pi e^{ipt}}{g\xi\rho}\,\frac{e^{-p\sqrt{\frac{\xi}{g}}}}{1+e^{-2p\sqrt{\frac{\xi}{g}}}}\,Y_1\left(\frac{pr}{\sqrt{g\xi}}\right), \\ w\sim\frac{2\pi e^{ipt}}{g\xi\rho}\,p\sqrt{\frac{\xi}{g}}\,\frac{e^{-p\sqrt{\frac{\xi}{g}}}}{1+e^{-2p\sqrt{\frac{\xi}{g}}}}\,Y_0\left(\frac{pr}{\sqrt{g\xi}}\right). \end{aligned}\right\}\dots\dots\dots\dots(22)$$

These expressions are suited for the transmission of a finite train of waves. To get the case of a train of an infinite length, it is convenient to superpose similar systems having Bessel's functions of the first kind and to take the mean value of them, since the composed systems can give us the progressive waves generated from the origin of the disturbance. It appears that, though conventional, this process is not unreasonable in physical mechanics. Thus the solutions are expressed by

$$\left.\begin{aligned} u\sim\frac{i\pi e^{ipt}}{g\xi\rho}\,\frac{e^{-p\sqrt{\frac{\xi}{g}}}}{1+e^{-2p\sqrt{\frac{\xi}{g}}}}\,H_1^{(2)}\left(\frac{pr}{\sqrt{g\xi}}\right), \\ w\sim\frac{i\pi e^{ipt}}{g\xi\rho}\,p\sqrt{\frac{\xi}{g}}\,\frac{e^{-p\sqrt{\frac{\xi}{g}}}}{1+e^{-2p\sqrt{\frac{\xi}{g}}}}\,H_0^{(2)}\left(\frac{pr}{\sqrt{g\xi}}\right), \end{aligned}\right\}\dots\dots\dots\dots(23)$$

corresponding to the pressure variation of the forms:

$$p_0=\frac{e^{ipt}}{\sqrt{r^2+(z-\xi)^2}}\dots\dots\dots\dots(24)$$

The velocity of propagation of waves is perfectly equal to that of the shallow-water waves, viz. $\sqrt{g\xi}$, while the motion of the water particle on the surface depends upon the initial pressure p_0, period of variation $T=2\pi/p$ and the depth of the sea ξ. Fig. I*a* and I*b* shew the horizontal and vertical components u, v of displacement on the surface due to the initial pressure $\rho g\xi$ at the radius R_1 in the immediate neighbourhood of the point P.

It may be mentioned that, though we have taken some special values of p_0 and R_1 in these figures, the sketches have yet their validity for the

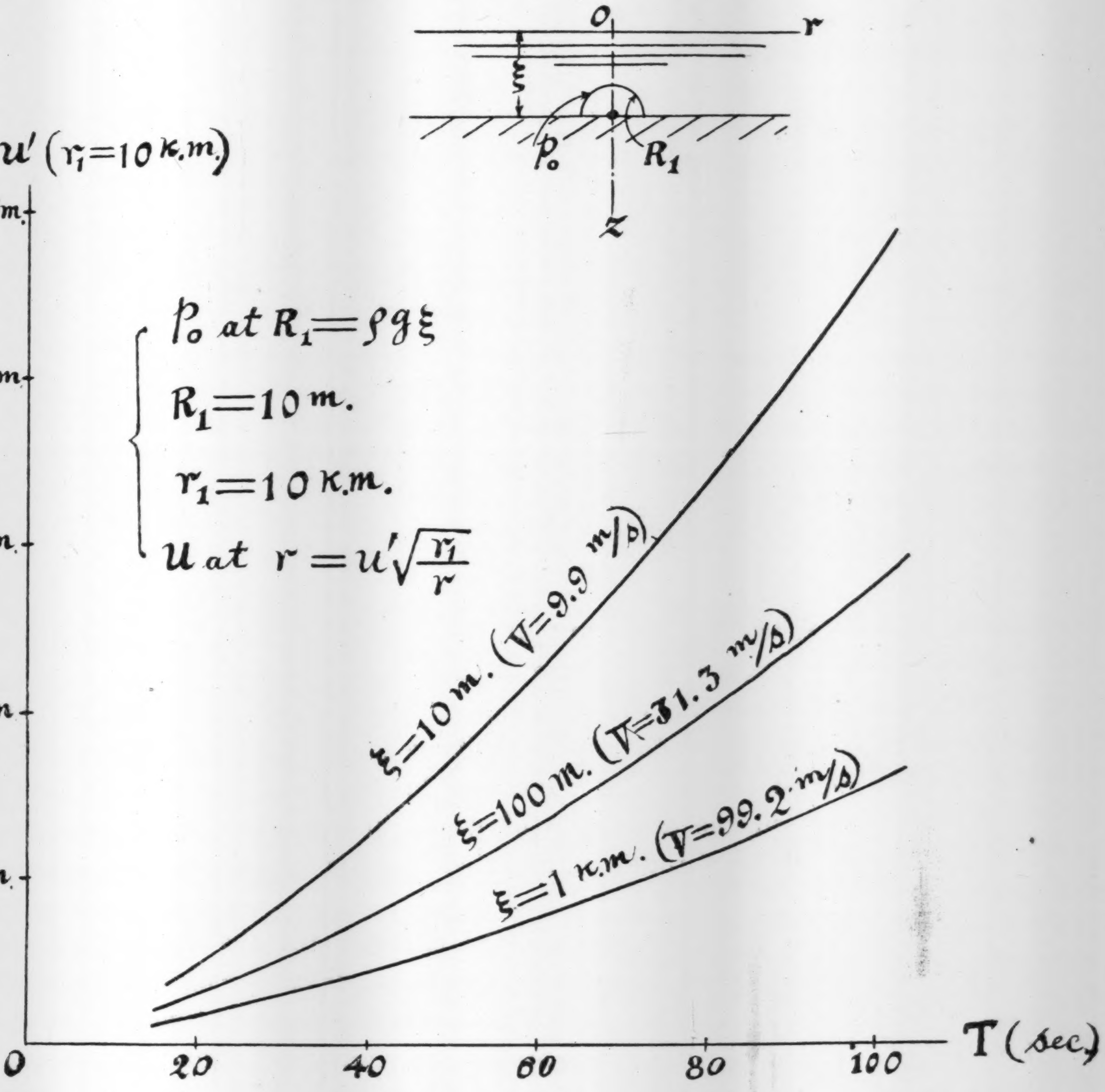

Fig. 1 *a*.

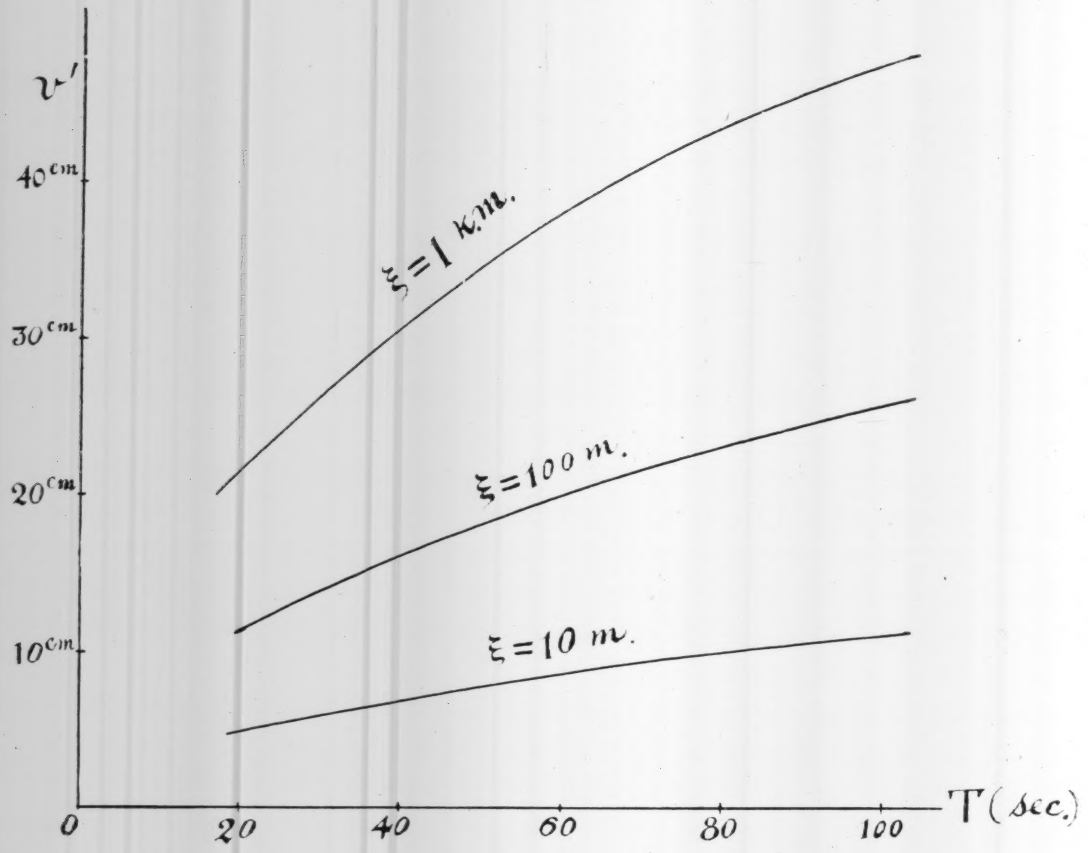

Fig. 1 b.

general cases. When the pressure at $R_2(=mR_1)$ is np_0, the values of u and v are then taken at n/m times of those above exemplified.

We can now estimate the rough magnitude of the pressure at the origin of shocks, provided that the amplitude of the generated waves and the effective period of the long waves are known from the surface data. There is no any sensible dispersion of waves in a shallow water, so that the postulation of amplitudes and period in this is not without significance.

We may now introduce some actual example for the verification of the present problem. The great Sanriku *tsunami* which damaged the north-east coast of our country in 1896 has already been investigated[6] fully by Prof. T. Iki and A. Imamura, besides the analytical study of Drs. K. Sano and K. Hasegawa. It is known that the origin of the shock was about 300 k.m. east of Sanriku, the depth of the water at the origin being 6 k.m., while the *tsunamis* observed at the coast (not bay or inlet) of Sanriku is one or two meters in height, having the effective period of 15 minutes. Assuming the depth of the water at the observing station to be so deep as 20 meters and making the correction of straight inclining bed, we find that the pressure change approximately equal to the hydrostatic height at the depth of 6 k.m. may have occurred within the region of 10 or 20 meters from the mathematical point of the origin. As it appears that the pressure change was not actually so large as the hydrostatic height of the sea, we cannot apply the relation of the forgoing sketches to the practical case. If the disturbed portion of the bed at the origin were known from some other relation, the actual change of the pressure at the central region of the shock would be easily obtained by means of the present calculation.

---

[6] T. IKI, A. IMAMURA, K. SANO and K. HASEGAWA, *ll. cc.*

Part II. Waves due to Bottom Pressure in a Shallow-sea of Moderate Depth.

If in the expressions of u and w which are given in (13) of the preceding part we suppose that the depth ξ is not necessarily small, there will be some difficulty in the evaluation of the definite integrals. The difficulty, however, can be evaded by the introduction of some complex contour integration.

Now we have, in place of the equations (17), the expressions

$$\left.\begin{aligned} u &= -\frac{2e^{ipt}}{\pi\rho}\int_0^\infty \operatorname{ch} k\,dk \int_0^\infty \frac{(e^{-f\xi}-e^{-3f\xi}+\dots.)\,(e^{ifr\operatorname{ch}k}+e^{-ifr\operatorname{ch}k})\,f\,df}{(p^2-fg\operatorname{th}f\xi)}, \\ w &= -\frac{2ie^{ipt}}{\pi\rho}\int_0^\infty dk \int_0^\infty \frac{(e^{-f\xi}-e^{-3f\xi}+\dots.)\,(e^{ifr\operatorname{ch}k}-e^{-ifr\operatorname{ch}k})\,f\,df}{(p^2\operatorname{cth}f\xi-fg)}. \end{aligned}\right\}\dots(25)$$

If we put $f\xi=j$, these are reduced to

$$\left.\begin{aligned} u &= -\frac{2e^{ipt}}{\pi\rho\xi^2}\int_0^\infty \operatorname{ch} k\,dk \int_0^\infty \frac{(e^{-j}-e^{-3j}+\dots.)\,\left(e^{\frac{ijr\operatorname{ch}k}{\xi}}+e^{-\frac{ijr\operatorname{ch}k}{\xi}}\right)j\,dj}{\left(p^2-\frac{jg}{\xi}\operatorname{th}j\right)}, \\ w &= -\frac{2ie^{ipt}}{\pi\rho\xi^2}\int_0^\infty dk \int_0^\infty \frac{(e^{-j}-e^{-3j}+\dots.)\,\left(e^{\frac{ijr\operatorname{ch}k}{\xi}}-e^{-\frac{ijr\operatorname{ch}k}{\xi}}\right)j\,dj}{\left(p^2\operatorname{cth}j-\frac{jg}{\xi}\right)}. \end{aligned}\right\}\dots(26)$$

To integrate the above expressions, we consider the integrals

$$\left.\begin{aligned}
&\int\frac{e^{-mZ+iZ\frac{r\,\mathrm{ch}\,k}{\xi}}}{p^2-Z\dfrac{g}{\xi}\,\mathrm{th}\,Z}\,ZdZ,\\
&\int\frac{e^{-mZ+iZ\frac{r\,\mathrm{ch}\,k}{\xi}}}{p^2\,\mathrm{cth}\,Z-Z\dfrac{g}{\xi}}\,ZdZ,\\
&\int\frac{e^{-mZ-iZ\frac{r\,\mathrm{ch}\,k}{\xi}}}{p^2-Z\dfrac{g}{\xi}\,\mathrm{th}\,Z}\,ZdZ,\\
&\int\frac{e^{-mZ-iZ\frac{r\,\mathrm{ch}\,k}{\xi}}}{p^2\,\mathrm{cth}\,Z-Z\dfrac{g}{\xi}}\,ZdZ,
\end{aligned}\right\}\quad\ldots\ldots\ldots\ldots\ldots\ldots(27)$$

taken round the contours in the drawings of this page. The beginning two integrals should be taken round the contour of the left-hand side, while the last two are on that of the right-hand side.

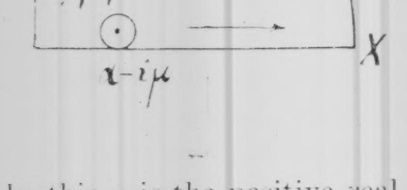

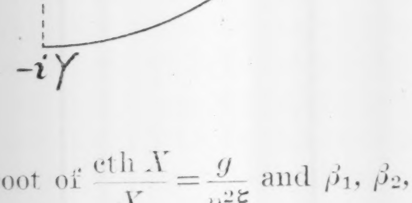

$$\begin{bmatrix}\mu=0\\ \mu'=0\end{bmatrix}$$ [7]

In this α is the positive real root of $\frac{\mathrm{cth}\,X}{X}=\frac{g}{p^2\xi}$ and $\beta_1,\beta_2,\beta_3,\ldots.$ are the real positive roots of $\frac{\mathrm{ct}\,Y}{Y}=-\frac{g}{p^2\xi}$. The contour integrations in question then give us

---

[7] μ and μ' have the similar quality as that given in the preceding part.

$$\left.\begin{aligned}
&\int_0^\infty \frac{e^{-mj}\left(e^{\frac{ijr\,\mathrm{ch}\,k}{\xi}}+e^{-\frac{ijr\,\mathrm{ch}\,k}{\xi}}\right)j\,dj}{p^2-\frac{jg}{\xi}\,\mathrm{th}\,j}=-\frac{4\pi\alpha^2e^{-m\alpha}\sin\frac{\alpha r\,\mathrm{ch}\,k}{\xi}}{p^2\left(\frac{p^2\xi}{g}-1\right)-\frac{g\alpha^2}{\xi}}\\
&\qquad -4\pi\sum_{n=1}^{\infty}\frac{\beta_n^2\,e^{-\beta_n\frac{r\,\mathrm{ch}\,k}{\xi}}\sin m\beta_n}{p^2\left(\frac{p^2\xi}{g}-1\right)+\frac{g}{\xi}\,\beta_n^2}-2\int_0^\infty\frac{e^{-j\frac{r\,\mathrm{ch}\,k}{\xi}}\cos mj\,.\,j\,dj}{p^2+\frac{g}{\xi}\,j\tan j},\\
&\int_0^\infty \frac{e^{-mj}\left(e^{\frac{ijr\,\mathrm{ch}\,k}{\xi}}-e^{-\frac{ijr\,\mathrm{ch}\,k}{\xi}}\right)j\,dj}{p^2\,\mathrm{cth}\,j-\frac{jg}{\xi}}=-\frac{4\pi\,\alpha\,e^{-m\alpha}\cos\frac{\alpha r\,\mathrm{ch}\,k}{\xi}}{p^2\left(\frac{g^2\alpha^2}{p^4\xi^2}-1\right)+\frac{g}{\xi}}\\
&\qquad -4\pi\sum_{n=1}^{\infty}\frac{\beta_n\,e^{-\beta_n\frac{r\,\mathrm{ch}\,k}{\xi}}\sin m\beta_n}{p^2\left(\frac{g^2\beta_n^2}{p^4\xi^2}+1\right)-\frac{g}{\xi}}-2i\int_0^\infty\frac{e^{-j\frac{r\,\mathrm{ch}\,k}{\xi}}\cos mj\,.\,j\,dj}{p^2\,\mathrm{ct}\,j+\frac{g}{\xi}}.
\end{aligned}\right\}\quad\ldots\ldots(28)$$

The expressions of (26) therefore take the forms

$$\left.\begin{aligned}
u=\frac{8e^{ipt}}{\rho\xi^2}\int_0^\infty \mathrm{ch}\,k\Bigg[&(e^{-\alpha}-e^{-3\alpha}+\ldots.)\,\frac{\alpha^2\sin\frac{\alpha r\,\mathrm{ch}\,\kappa}{\xi}}{p^2\left(\frac{p^2\xi}{g}-1\right)-\frac{g\alpha^2}{\xi}}\\
&+\sum_{n=1}^{\infty}\frac{\beta_n^2\,e^{-\beta_n\frac{r\,\mathrm{ch}\,k}{\xi}}(\sin\beta_n-\sin 3\beta_n+\ldots.)}{p^2\left(\frac{p^2\xi}{g}-1\right)+\frac{g}{\xi}\,\beta_n^2}\\
&+\frac{1}{2\pi}\int_0^\infty\frac{e^{-j\frac{r\,\mathrm{ch}\,k}{\xi}}(\cos j-\cos 3+\ldots.)\,j\,dj}{p^2+\frac{g}{\xi}\,j\tan j}\Bigg]dk,\\
w=-\frac{8e^{ipt}}{\rho\xi^2}\int_0^\infty\Bigg[&e^{-\alpha}-e^{-3\alpha}+\ldots.)\,\frac{\alpha\cos\frac{\alpha r\,\mathrm{ch}\,k}{\xi}}{\frac{g^2\alpha^2}{p^2\xi^2}-p^2+\frac{g}{\xi}}\\
&-i\sum_{n=1}^{\infty}\frac{\beta_n e^{-\beta_n\frac{r\,\mathrm{ch}\,k}{\xi}}(\sin\beta_n-\sin 3\beta_n+\ldots.)}{\frac{g^2\beta_n^2}{p^2\xi^2}+p^2-\frac{g}{\xi}}\\
&+\frac{1}{2\pi}\int_0^\infty\frac{e^{-j\frac{r\,\mathrm{ch}\,k}{\xi}}(\cos j-\cos 3j+\ldots.)\,j\,dj}{p^2\,\mathrm{ct}\,j+\frac{jg}{\xi}}\Bigg]dk.
\end{aligned}\right\}\quad\ldots\ldots(29)$$

It is easily seen as in the preceding case that all terms except the first of the expressions of u and w become insignificant as r is increased. Hence we find in virtue of this and the relations given in (21),

$$\left.\begin{aligned} u &\sim -\frac{4\pi e^{ipt}}{\rho\xi^2}\frac{\alpha^2}{p^2\left(\frac{p^2\xi}{g}-1\right)-\frac{g\alpha^2}{\xi}}\frac{e^{-\alpha}}{1+e^{-2\alpha}}Y_1\left(\frac{\alpha r}{\xi}\right), \\ w &\sim \frac{4\pi e^{ipt}}{\rho\xi^2}\frac{\alpha}{\frac{g^2\alpha^2}{p^2\xi^2}-p^2+\frac{g}{\xi}}\frac{e^{-\alpha}}{1+e^{-2\alpha}}Y_0\left(\frac{\alpha r}{\xi}\right). \end{aligned}\right\} \quad \ldots\ldots\ldots (30)$$

On half of the displacement represented by these formulae we can superpose half of another system of stationary waves to annul the standing oscillations at a large distance. We, thus, obtain

$$\left.\begin{aligned} u &\sim -\frac{2\pi i\, e^{ipt}}{\rho\xi^2}\frac{\alpha^2}{p^2\left(\frac{p^2\xi}{g}-1\right)-\frac{g\alpha^2}{\xi}}\frac{e^{-\alpha}}{1+e^{-2\alpha}}H_1^{(2)}\left(\frac{\alpha r}{\xi}\right), \\ w &\sim 2\pi i\,\frac{e^{ipt}}{\rho\xi^2}\frac{\alpha}{\frac{g^2\alpha^2}{p^2\xi^2}-p^2+\frac{g}{\xi}}\frac{e^{-\alpha}}{1+e^{-2\alpha}}H_0^{(2)}\left(\frac{\alpha r}{\xi}\right), \end{aligned}\right\} \quad \ldots\ldots\ldots (31)$$

corresponding to the pressure variation of the form:

$$p_0=\frac{e^{ipt}}{\sqrt{r^2+(z-\xi)^2}} \quad \ldots\ldots\ldots\ldots\ldots\ldots (24')$$

The expressions in (31) are valid for any depth of water provided that the shock is originated from a point of the bottom of the sea. The velocity of propagation is given by

$$\frac{p\xi}{\alpha} \quad \ldots\ldots\ldots\ldots\ldots\ldots\ldots\ldots (32)$$

We remark that, when the depth ξ is very small, we should put, in place of cth $\alpha/\alpha=g/p^2\xi$, the formula of the form:

$$\frac{1}{\alpha^2}=\frac{g}{p^2\xi}, \quad \ldots\ldots\ldots\ldots\ldots\ldots\ldots\ldots (33)$$

besides the relation

$$p=f\sqrt{g\xi}. \quad \ldots\ldots\ldots\ldots\ldots\ldots\ldots\ldots (34)$$

Putting (33) and (34) in (31), we get

$$\left.\begin{aligned} u &\approx \frac{i\pi e^{ipt}}{g\xi\rho}\,\frac{e^{-p\sqrt{\frac{\xi}{g}}}}{1+e^{-2p\sqrt{\frac{\xi}{g}}}}\,H_1^{(2)}\left(\frac{pr}{\sqrt{g\xi}}\right), \\ w &\approx \frac{i\pi e^{ipt}}{g\xi\rho}\,p\sqrt{\frac{\xi}{g}}\,\frac{e^{-p\sqrt{\frac{\xi}{g}}}}{1+e^{-2p\sqrt{\frac{\xi}{g}}}}\,H_0^{(2)}\left(\frac{pr}{\sqrt{g\xi}}\right), \end{aligned}\right\} \qquad (23')$$

which are the same forms as those in (23). Here we find that the method of derivation of the formulae in (23) is not violent.

Part III. The Effect of the Inertia of the Subaqueous Medium.

When the depth of the water is large compared with the wave length of the shock waves, it must be borne in mind that the effect of the inertia of the water on the compressional waves in the subaqueous stage cannot be neglected. In such a case we must first find the solution of the equation

$$\rho\frac{\partial^2\psi}{\partial t^2}=\kappa\left(\frac{\partial^2\psi}{\partial R^2}+\frac{2}{R}\frac{\partial\psi}{\partial R}\right), \qquad (35)$$

in which ψ is the dilatation of the water and κ is the volume elasticity of the water.

In the case of simple-harmonic disturbance, the expression of the shock waves is given by

$$\psi=e^{ipt}\frac{e^{-ihR}}{R}, \qquad (36)$$

provided

$$h^2=\frac{\rho p^2}{\kappa} \qquad (37)$$

The radial displacement near the source is written by

$$u_R=-\frac{1}{hR}\sin\,(pt-hR). \qquad (38)$$

Now we know Lamb's formula:

$$\frac{e^{-ihR}}{R}=\int_0^\infty\frac{e^{-\alpha z}}{\alpha}J_0(fr)\,f\,df, \qquad (39)$$

where $\alpha=\sqrt{f^2-h^2}$.

In the case of a source of disturbance at the point $r=0$, $z=\xi$, the expression of ψ is given by

$$\begin{aligned}\psi=e^{ipt}\Big[&\int_0^\infty\frac{e^{\alpha(z-\xi)}}{\alpha}J_0(fr)\,fdf+\int_0^\infty\frac{e^{-\alpha(z+\xi)}}{\alpha}J_0(fr)\,fdf\\&-\int_0^\infty\frac{e^{\alpha(z-3\xi)}}{\alpha}J_0(fr)\,fdf-\int_0^\infty\frac{e^{-\alpha(z+3\xi)}}{\alpha}J_0(fr)\,fdf\\&+\cdots\cdots\cdots\cdots\cdots\Big]\\=2e^{ipt}&\int_0^\infty\frac{\operatorname{ch}\alpha z}{\alpha}\,\frac{e^{-\alpha\xi}}{1+e^{-2\alpha\xi}}J_0(fr)\,fdf.\qquad[z<\xi]\end{aligned}\qquad\qquad(40)$$

The expressions of displacement are given by

$$\left.\begin{aligned}u_0&=-\frac{1}{h^2}\frac{\partial\psi}{\partial r}=2\frac{e^{ipt}}{h^2}\int_0^\infty\frac{\operatorname{ch}\alpha z}{\alpha}\,\frac{e^{-\alpha\xi}}{1+e^{-2\alpha\xi}}J_1(fr)\,f^2df,\\w_0&=-\frac{1}{h^2}\frac{\partial\psi}{\partial z}=-\frac{2e^{ipt}}{h^2}\int_0^\infty\operatorname{sh}\alpha z\,\frac{e^{-\alpha\xi}}{1+e^{-2\alpha\xi}}J_0(fr)\,fdf.\end{aligned}\right\}\qquad(41)$$

The pressure on the surface $z=0$ is expressed by

$$p_0=\kappa\psi=2\kappa e^{ipt}\int_0^\infty\frac{e^{-\alpha\xi}}{\alpha(1+e^{-2\alpha\xi})}J_0(fr)\,fdf.\qquad(42)$$

Now, for gravity waves, the similar process as in the preceding cases will give us the expression of the surface pressure in the forms:

$$p_1=i\rho C\,\frac{p^2\operatorname{ch}f\xi-fg\operatorname{sh}f\xi}{p}\,e^{ipt}J_0(fr).\qquad(43)$$

The condition that the surface pressure is nil, viz.

$$p_0+p_1=0\qquad(44)$$

is satisfied provided

$$C=-2\kappa\int_0^\infty\frac{fe^{-\alpha\xi}}{\alpha(1+e^{-2\alpha\xi})}\,\frac{pdf}{i\rho(p^2\operatorname{ch}f\xi-fg\operatorname{sh}f\xi)}\,.^{8)}\qquad(45)$$

Substituting this in the equations in (8), we find the values of the displacement $(u_1,\ w_1)$. The real displacement of the surface is, thus, expressed by

$$\left.\begin{aligned}u=u_0+u_1&=\frac{2\kappa e^{ipt}}{\rho}\int_0^\infty\left[\frac{\operatorname{ch}f\xi}{p^2\operatorname{ch}f\xi-fg\operatorname{sh}f\xi}+\frac{1}{p^2}\right]\frac{e^{-\alpha\xi}}{1+e^{-2\alpha\xi}}J_1(fr)\,\frac{f^2df}{\alpha},\\w=w_0+w_1&=\frac{2\kappa e^{ipt}}{\rho}\int_0^\infty\frac{\operatorname{sh}f\xi}{p^2\operatorname{ch}f\xi-fg\operatorname{sh}f\xi}\,\frac{e^{-\alpha\xi}}{1+e^{-2\alpha\xi}}J_0(fr)\,\frac{f^2\,df}{\alpha}.\end{aligned}\right\}\qquad(46)$$

In virtue of the formulae in (16) and from the assumption that ξ is small, these are transformed into

---

8) This expression is temporarily used for the sake of simplicity.

$$\left.\begin{aligned} u &= -\frac{2\kappa\, e^{ipt}}{\pi\rho}\int_0^\infty \mathrm{ch}\, k dk\int_0^\infty (e^{-f\xi}-e^{-3f\xi}+\ldots.)\,(e^{ifr\,\mathrm{ch}\,k} \\ &\qquad\qquad + e^{-ifr\,\mathrm{ch}\,k})\left[\frac{1}{p^2-f^2 g\xi}+\frac{1}{p^2}\right]\frac{f^2\,df}{\alpha}, \\ w &= -\frac{2\,\kappa\xi\, e^{ipt}}{\pi\rho}\int_0^\infty dk\int_0^\infty (e^{-f\xi}-e^{-3f\xi}+\ldots.)\,\frac{e^{ifr\,\mathrm{ch}\,\kappa}-e^{-ifr\,\mathrm{ch}\,k})}{(p^2-f^2 g\xi)}\,\frac{f^3\,df}{\alpha}. \end{aligned}\right\}\ldots(47)$$

To integrate these expressions, we consider the integrals,

$$\left.\begin{aligned} &\int\frac{e^{-m\sqrt{Z^2-h^2}\xi}\,e^{iZr\,\mathrm{ch}\,k}\,Z^2 dZ}{(p^2-Z^2 g\xi)\sqrt{Z^2-h^2}}, &&\text{(I)} \\ &\int\frac{e^{-m\sqrt{Z^2-h^2}\xi}\,e^{iZr\,\mathrm{ch}\,k}\,Z^3 dZ}{(p^2-Z^2 g\xi)\sqrt{Z^2-h^2}}, &&\text{(II)} \\ &\int\frac{e^{-m\sqrt{Z^2-h^2}\xi}\,e^{iZr\,\mathrm{ch}\,k}\,Z\cdot dZ}{\sqrt{Z^2-h^2}}, &&\text{(III)} \\ &\int\frac{e^{-m\sqrt{Z^2-h^2}\xi}\,e^{-iZr\,\mathrm{ch}\,k}\,Z^2 dZ}{(p^2-Z^2 g\xi)\sqrt{Z^2-h^2}}, &&\text{(IV)} \\ &\int\frac{e^{-m\sqrt{Z^2-h^2}\xi}\,e^{-iZr\,\mathrm{ch}\,k}\,Z^3 dZ}{(p^2-Z^2 g\xi)\sqrt{Z^2-h^2}}, &&\text{(V)} \\ &\int\frac{e^{-m\sqrt{Z^2-h^2}\xi}\,e^{-iZr\,\mathrm{ch}\,k}\,Z^2 dZ}{\sqrt{Z^2-h^2}}, &&\text{(VI)} \end{aligned}\right\}\ldots\ldots\ldots\ldots.(48)$$

taken round the contours in the drawings given in the next page, in which the numbers of the figures correspond to those in (48).

The contour integrations then give us

$$\left.\begin{aligned} \int_0^\infty \frac{e^{-m\sqrt{f^2-h^2}\,\xi\pm ifr\,\mathrm{ch}\,k}f^2df}{(p^2-f^2 g\xi)\sqrt{f^2-h^2}} &= \mp\frac{\pi}{g\xi}\,e^{-m\xi\sqrt{\frac{p^2}{g\xi}-h^2}\pm i\frac{pr\,\mathrm{ch}\,k}{\sqrt{g\xi}}}\,\frac{p}{\sqrt{p^2-h^2 g\xi}} \\ &\quad -2i\int_0^h\frac{\cos m\sqrt{h^2-f^2}\,\xi\; e^{\pm ifr\,\mathrm{ch}\,k}\,f^2 df}{(p^2-f^2 g\xi)\sqrt{h^2-f^2}}-\int_0^\infty\frac{e^{\mp im\sqrt{f^2+h^2}\,\xi-fr\,\mathrm{ch}\,k}\,f^2 df}{(p^2+f^2 g\xi)\sqrt{f^2+h^2}}, \\ \int_0^\infty \frac{e^{-m\sqrt{f^2-h^2}\,\xi\pm ifr\,\mathrm{ch}\,k}f^3df}{(p^2-f^2 g\xi)\sqrt{f^2-h^2}} &= \mp\frac{\pi i}{g\xi}\,e^{-m\xi\sqrt{\frac{p^2}{g\xi}-h^2}\pm i\frac{pr\,\mathrm{ch}\,k}{\sqrt{g\xi}}}\,\frac{p^2}{\sqrt{g\xi(p^2-h^2 g\xi)}} \\ &\quad -2i\int_0^h\frac{\cos m\sqrt{h^2-f^2}\,\xi\; e^{\pm ifr\,\mathrm{ch}\,k}\,f^3 df}{(p^2-f^2 g\xi)\sqrt{h^2-f^2}}\mp i\int_0^\infty\frac{e^{\mp im\sqrt{f^2+h^2}\,\xi-fr\,\mathrm{ch}\,k}\,f^3 df}{(p^2+f^2 g\xi)\sqrt{f^2+h^2)}}, \\ \int_0^\infty \frac{e^{-m\sqrt{f^2-h^2}\,\xi\pm ifr\,\mathrm{ch}\,k}\,f^2df}{\sqrt{f^2-h^2}} &= -2i\int_0^h\frac{\cos m\sqrt{h^2-f^2}\,\xi\; e^{\pm ifr\,\mathrm{ch}\,k}\,f^2 df}{\sqrt{h^2-f^2}} \\ &\quad -\int_0^\infty\frac{e^{\mp im\sqrt{f^2+h^2}\,\xi-fr\,\mathrm{ch}\,k}\,f^2 df}{\sqrt{f^2+h^2}}. \end{aligned}\right\}(49)$$

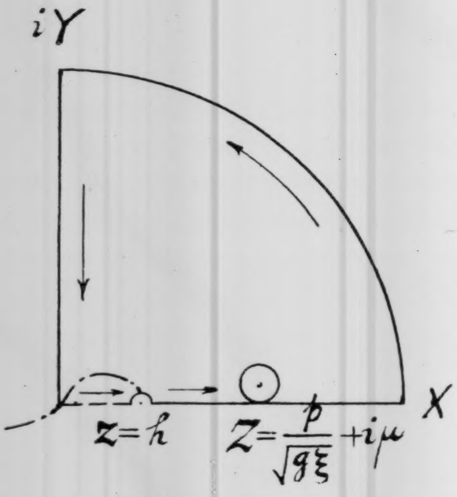
iY
X
z=h
$Z=\frac{p}{\sqrt{g\xi}}+i\mu$

(I) (II)

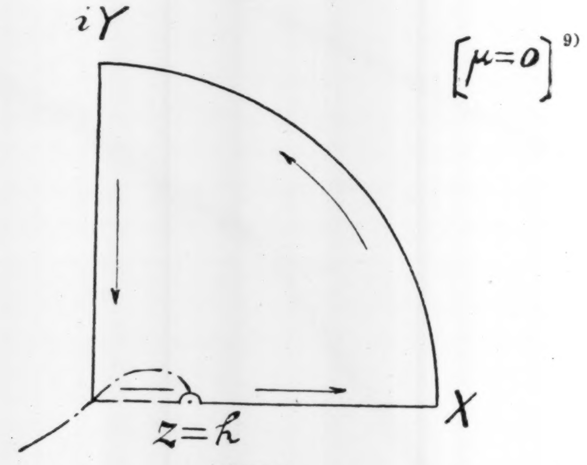

(III)

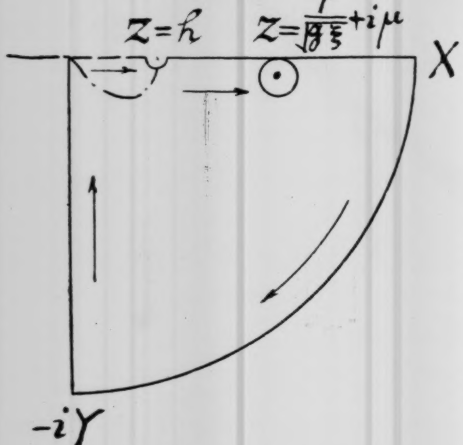
z=h
$Z=\frac{p}{\sqrt{g\xi}}+i\mu$
X
-iY

(IV) (V)

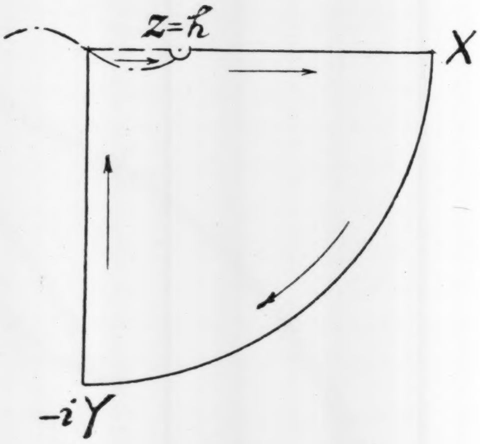

(VI)

Hence the expressions in (47) become

$$u=-\frac{4\kappa\, e^{ipt}}{\rho g\xi}\int_0^\infty \mathrm{ch}\, k\left[\left(e^{-\xi\sqrt{\frac{p^2}{g\xi}-h^2}}-e^{-3\xi\sqrt{\frac{p^2}{g\xi}-h^2}}+\ldots.\right)\frac{p}{\sqrt{p^2-h^2 g\xi}}\sin\frac{pr\,\mathrm{ch}\,k}{\sqrt{g\xi}}\right.$$
$$-\frac{2ig\xi}{\pi}\int_0^h\left(\cos\sqrt{h^2-f^2}\,\xi-\cos 3\sqrt{h^2-f^2}\,\xi\right.$$
$$\left.\left.-\cos 5\sqrt{h^2-f^2}\,\xi-\ldots.\right)\left(\frac{1}{p^2-f^2\, g\xi}+\frac{1}{p^2}\right)\frac{\cos fr\,\mathrm{ch}\, k.\, f^2\, df}{\sqrt{h^2-f^2}}\right|$$

---

9) μ is given for the same purpose as in the preceding cases.

$$\left.\begin{aligned}
&-\frac{g\xi}{\pi}\int_0^\infty e^{-fr\,\mathrm{ch}\,k}\,(\cos\sqrt{f^2+h^2}\,\xi-\cos 3\sqrt{f^2+h^2}\,\xi\\
&\qquad\qquad+\cos 5\sqrt{f^2+h^2}\,\xi-\ldots.)\left(\frac{1}{p^2+f^2\,g\xi}+\frac{1}{p^2}\right)\frac{f^2\,df}{\sqrt{f^2+h^2}}\Bigg]\,dk,\\
w=&-\frac{4\kappa\;e^{ipt}}{\rho g\xi}\int_0^\infty\Bigg[p\sqrt{\frac{\xi}{g}}\Bigg(e^{-\xi\sqrt{\frac{p2}{g\xi}-h2}}-e^{-3\xi\sqrt{\frac{p2}{g\xi}-h2}}\\
&\qquad\qquad+e^{-5\xi\sqrt{\frac{p2}{g\xi}-h2}}-\ldots.\Bigg)\frac{p}{\sqrt{p^2-h^2\,g\xi}}\cos\frac{pr\,\mathrm{ch}\,k}{\sqrt{g\xi}}\\
&+2\,\frac{g\,\xi^2}{\pi}\int_0^h(\cos\sqrt{h^2-f^2}\,\xi-\cos 3\sqrt{h^2-f^2}\,\xi+\ldots.)\frac{\sin fr\,\mathrm{ch}\,k\quad f^3\,df}{(p^2-f^2\,g\xi)\sqrt{h^2-f^2}}\\
&+\frac{g\xi^2}{\pi}\int_0^\infty \epsilon^{-fr\,\mathrm{ch}\,k}\,(\cos\sqrt{f^2+h^2}\,\xi-\cos 3\sqrt{f^2+h^2}\\
&\qquad\qquad+\cos 5\sqrt{f^2+h^2}\,\xi-\ldots.)\,\frac{f^3\,df}{(p^2+f^2g\xi)\sqrt{f^2+h^2}}\Bigg]\,dk.
\end{aligned}\right\}\quad(50)$$

Neglecting each third term in the expressions of u and w and substituting the relations in (16) and (21), we get

$$\left.\begin{aligned}
u\approx&\frac{2\pi\kappa\,e^{ipt}}{\rho g\xi}\Bigg[\frac{p}{\sqrt{p^2-h^2\,g\xi}}\,\frac{e^{-\xi\sqrt{\frac{p2}{g\xi}-h2}}}{1+e^{-2\xi\sqrt{\frac{p2}{g\xi}-h2}}}\,Y_1\left(\frac{pr}{\sqrt{g\xi}}\right)-2\,\frac{ig\xi}{\pi}\int_0^h(\cos\sqrt{h^2-f^2}\,\xi\\
&\qquad-\cos 3\sqrt{h^2-f^2}\,\xi+\ldots.)\left(\frac{1}{p^2-f^2\,g\xi}+\frac{1}{p^2}\right)\frac{f^2}{\sqrt{h^2-f^2}}\,J_1(fr)\,df\Bigg],\\
w\approx&\frac{2\pi\kappa\;e^{ipt}}{\rho g\xi}\Bigg[p\sqrt{\frac{\xi}{g}}\;\frac{p}{\sqrt{p^2-h^2\,g\xi}}\;\frac{e^{-\xi\sqrt{\frac{p2}{g\xi}-h2}}}{1+e^{-2\xi\sqrt{\frac{p2}{g\xi}-h2}}}\,Y_0\left(\frac{pr}{\sqrt{g\xi}}\right)\\
&\qquad-2\,\frac{ig\xi^2}{\pi}\int_0^h(\cos\sqrt{h^2-f^2}\,\xi-\cos 3\sqrt{h^2-f^2}\,\xi\\
&\qquad\qquad+\cos 3\sqrt{h^2-f^2}\,\xi-\ldots.)\frac{f^3}{(p^2-f^2g\xi)\sqrt{h^2-f^2}}\,J_0(fr)\,df\Bigg)\Bigg].
\end{aligned}\right\}\quad(51)$$

It appears that the second terms of the expressions of u and w will give some forerunners with the type of the pressure waves. We can, however, notice that they are negligibly small owing to the assumption of small $f\xi$ and the nature of h which is very near to zero in the case of water. It follows that, remembering $h^2=\dfrac{\rho p^2}{\kappa}$,

$$\left.\begin{aligned} u &\sim \frac{2\pi\kappa\, e^{ipt}}{\rho g\xi}\,\frac{1}{\sqrt{1-\dfrac{pg\xi}{\kappa}}}\,\frac{e^{-p\xi\sqrt{\frac{1}{g\xi}-\frac{\rho}{\kappa}}}}{1+e^{-2p\xi\sqrt{\frac{1}{g\xi}-\frac{\rho}{\kappa}}}}\,Y_1\left(\frac{pr}{\sqrt{g\xi}}\right), \\ w &\sim \frac{2\pi\kappa\, e^{ipt}}{\rho g\xi}\,p\sqrt{\frac{\xi}{g}}\,\frac{1}{\sqrt{1-\dfrac{\rho g\xi}{\kappa}}}\,\frac{e^{-p\xi\sqrt{\frac{1}{g\xi}-\frac{\rho}{\kappa}}}}{1+e^{-2p\xi\sqrt{\frac{1}{g\xi}-\frac{\rho}{\kappa}}}}\,Y_0\left(\frac{pr}{\sqrt{g\xi}}\right). \end{aligned}\right\}\cdots\cdots(52)$$

Adding free oscillations having Bessel's functions of other kinds and taking the half of them, we get

$$\left.\begin{aligned} u &\sim \frac{i\pi\kappa\, e^{ipt}}{\rho g\xi}\,\frac{1}{\sqrt{1-\dfrac{\rho g\xi}{\kappa}}}\,\frac{e^{-p\xi\sqrt{\frac{1}{g\xi}-\frac{\rho}{\kappa}}}}{1+e^{-2p\xi\sqrt{\frac{1}{g\xi}-\frac{\rho}{\kappa}}}}\,H_1^{(2)}\left(\frac{pr}{\sqrt{g\xi}}\right), \\ w &\sim \frac{i\pi\kappa\, e^{ipt}}{\rho g\xi}\,\frac{1}{\sqrt{1-\dfrac{\rho g\xi}{\kappa}}}\,p\sqrt{\frac{\xi}{g}}\,\frac{e^{-p\xi\sqrt{\frac{1}{g\xi}-\frac{\rho}{\kappa}}}}{1+e^{-2p\xi\sqrt{\frac{1}{g\xi}-\frac{\rho}{\kappa}}}}\,H_0^{(2)}\left(\frac{pr}{\sqrt{g\xi}}\right), \end{aligned}\right\}\cdots\cdots(53)$$

corresponding to the displacement near the origin, viz.

$$u_R = -\frac{e^{ipt}}{h^2}\frac{\partial}{\partial R}\frac{e^{-ihR}}{R}. \cdots\cdots\cdots\cdots\cdots\cdots(54)$$

As ρ/κ is very small compared with $1/g\xi$, we may write (53) in the following forms:

$$\left.\begin{aligned} u &\sim \frac{i\pi\kappa\, e^{ipt}}{\rho g\xi}\,\frac{e^{-p\sqrt{\frac{\xi}{g}}}}{1+e^{-2p\sqrt{\frac{\xi}{g}}}}\,H_1^{(2)}\left(\frac{pr}{\sqrt{g\xi}}\right), \\ w &\sim \frac{i\pi\kappa\, e^{ipt}}{\rho g\xi}\,p\sqrt{\frac{\xi}{g}}\,\frac{e^{-p\sqrt{\frac{\xi}{g}}}}{1+e^{-2p\sqrt{\frac{\xi}{g}}}}\,H_0^{(2)}\left(\frac{pr}{\sqrt{g\xi}}\right), \end{aligned}\right\}\cdots\cdots\cdots\cdots(55)$$

which are similar, excepting the factor κ, to the expressions of u and w in (23). The pressure distribution corresponding to (54), when h tends to zero, is given by

$$\kappa\psi = \frac{\kappa\, e^{ipt}}{\sqrt{r^2+(z-\xi)^2}}. \cdots\cdots\cdots\cdots\cdots\cdots(56)$$

We find that the equation in (55) are quite analogous to those in (23).

Figs. 2*a* and 2*b* are given for the illustration of the ratio of the amplitudes of the surface waves to those of the pressure waves near the origin.

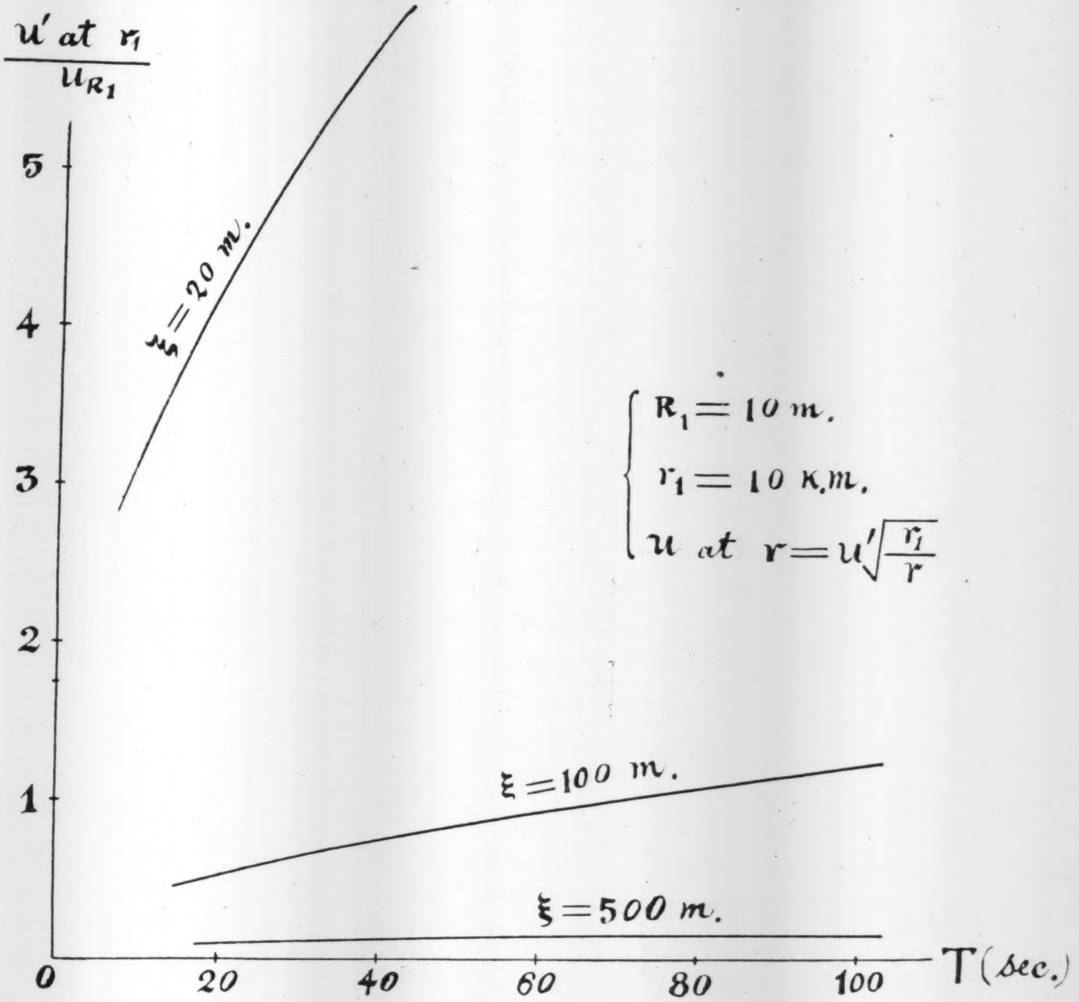

Fig. 2a.

It will be noticed that as T is decreased, the horizontal component of displacement becomes smaller and smaller, while the vertical component of displacement increases. This conforms with the evident fact that even in a shallow water the surface waves of very small length tend to manifest the nature of deep-sea waves.

Again, it will be seen that the surface displacements of the shallow-water waves at a certain distance are comparable with the displacement of the pressure waves in the neighbourhood of the origin and accordingly it will be impossible to imagine a great crustal deformation of the bottom of the sea occuring in a short interval of time unless we can observe the phenomena of *tsunami* with some violence. The case of Sagami Bay, where a depression of a kilometer or more has been observed after the great Kwanto earthquake in 1923, is a noteworthy example. It is said that the amplitude of *tsunami* experienced at the coast of Sagami Bay at the time of that earthquake are not more than a few meters. Though it is beyond our scope to determine clearly the duration of the deformation of the bed, yet we may add that the depression was made at least during several years.

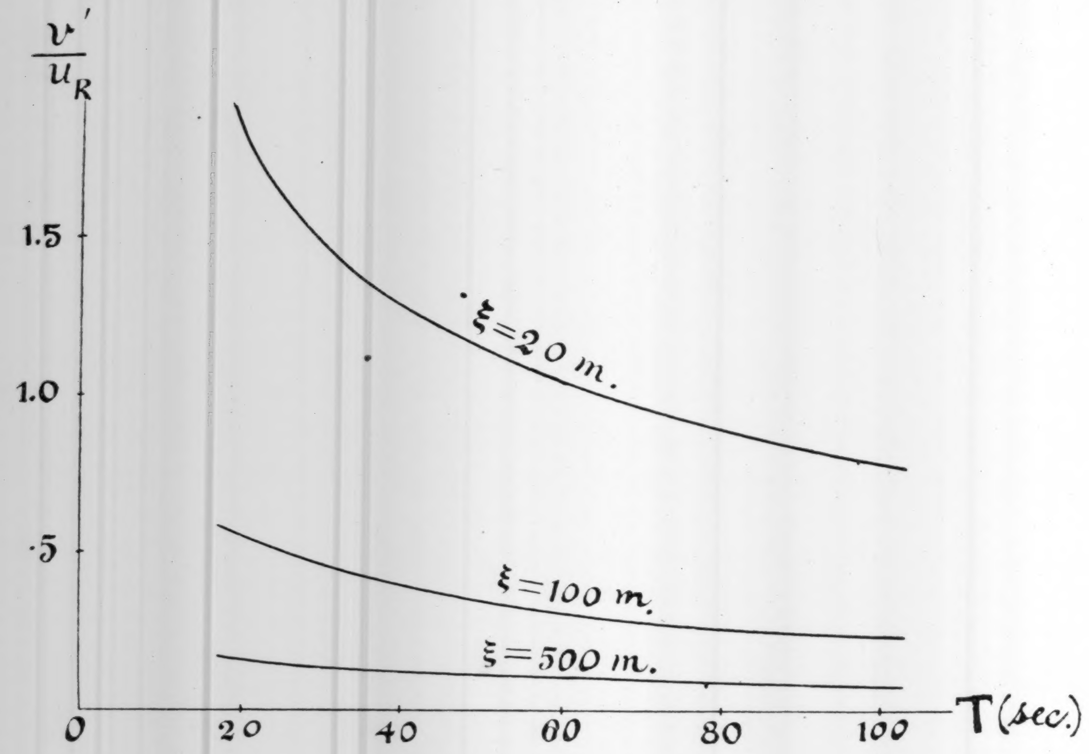

Fig. 2 b.

Part IV. Waves due to Subaqueous Pressure at an Intermediate Depth.

We have now to study the wave motion due to the subaqueous shocks which take place at an intermediate depth of the shallow water. Though it appears that this case has not much connections with the formation of *tsunami*, yet this problem is more important in the direction of the question that the nucleous of shocks may be embedded partially in the water bed or it may take its position in a subaqueous region very near the sea floor. Also the significance on the submarine explosion is too well-known to need the description here.

If the source of pressure is taken at the point $r=0$, $z=\xi$ and the depth of the shallow water is given by $z=\eta$, it will be easily seen that the images should be of two series of successive points.

$$\left.\begin{array}{llll} z=-\xi, & (2\eta+\xi),\ -(2\eta+\xi), & (4\eta+\xi),\ -(4\eta+\xi), & \ldots, \\ z=(2\eta-\xi), & -(2\eta-\xi),\ \ (4\eta-\xi), & (4\eta+\xi), & \ldots\ldots \end{array}\right\}[r=0] \quad (57)$$

The resulting pressure which is composed of the primary disturbance and those of all images is written in the form:

$$\begin{aligned} p_0=e^{ipt}\Big[&\int_0^\infty e^{f(z-\xi)} J_0(fr)\,df+\int_0^\infty e^{-f(z+\xi)} J_0(fr)\,df \\ &-\int_0^\infty e^{f(z-\overline{2\eta+\xi})} J_0(fr)\,df-\int_0^\infty e^{-f(z+\overline{2\eta+\xi})} J_0(fr)\,df \\ &+\int_0^\infty e^{f(z-\overline{4\eta+\xi})} J_0(fr)\,df+\int_0^\infty e^{-f(z+\overline{4\eta+\xi})} J_0(fr)\,df \\ &-\ldots\ldots\ldots\ldots\ldots\ldots\ldots\ldots\ldots\ldots\ldots\ldots \\ &-\int_0^\infty e^{-f(z+\overline{2\eta-\xi})} J_0(fr)\,df-\int_0^\infty e^{f(z-\overline{2\eta-\xi})} (fr)\,df \\ &+\int_0^\infty e^{-f(z+\overline{4\eta-\xi})} J_0(fr)\,df+\int_0^\infty e^{f(z-\overline{4\eta-\xi})} (fr)\,df \\ &-\int_0^\infty e^{-f(z+\overline{6\eta-\xi})} J_0(fr)\,df-\int_0^\infty e^{f(z-\overline{6\eta-\xi})} J_0(fr)\,df \\ &+\ldots\ldots\ldots\ldots\ldots\ldots\ldots\ldots\ldots\ldots\ldots\ldots\Big] \end{aligned}$$

$$=2e^{ipt}\int_0^\infty \mathrm{ch}\, fz\left\{\frac{e^{-f\xi}-e^{-f(2\eta-\xi)}}{1+e^{-2f\eta}}\right\} J_0(fr)\,df. \qquad [\xi<\eta,\quad z<\xi]\ldots\ldots(58)$$

If we put $\eta=\infty$ in (58), we obtain

$$p_0=2e^{ipt}\int_0^\infty \mathrm{ch}\, fz\; e^{-f\xi} J_0(fr)\,df, \quad \ldots\ldots\ldots\ldots\ldots\ldots(59)$$

which is the problem of the deep water waves due to subaqueous shocks.[10]

If we write $\eta=\xi$ in (58), we find

---

[10] "Formation of Deep-water Waves due to Subaqueous Shocks," *Bull. Earthq. Res. Inst.* **6**. In that paper the effect of the inertia of the water on the pressure waves has not been neglected.

$$p_0 = 4e^{ipt}\int_0^\infty \operatorname{ch} fz \, \frac{e^{-f\xi}}{1+e^{-2f\xi}} J_0(fr)\,df, \quad \ldots\ldots\ldots\ldots\ldots\ldots (60)$$

which is twice the value of p_0 given in (4) where the origin is situated at the bottom. Although it may seem to be paradoxical, a little consideration will enable us to understand that there is a clear distinction between two cases. The problem in (4) is the generation of the pressure waves from a semi-spherical origin at the bed, while that in (60) is the transmission from the source of a complete sphere whose centre resides very near the bed.

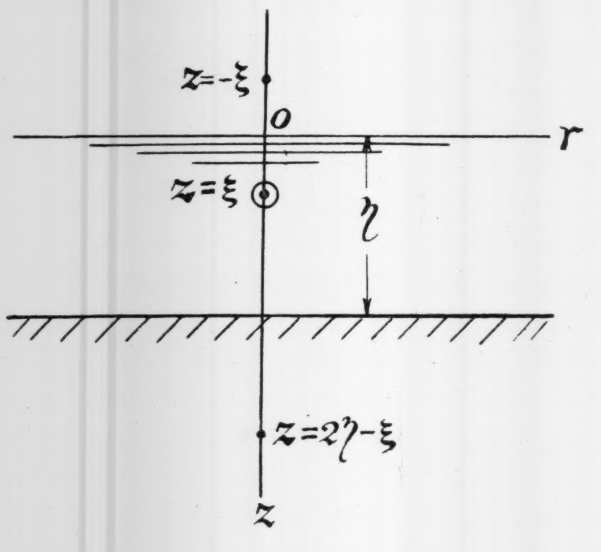

Pursuing the same line of argument as in Part I, we arrive at the expressions of displacement of the forms:

$$\left.\begin{aligned} u &= \frac{2e^{ipt}}{\rho}\int_0^\infty \frac{\{e^{-f\xi}-e^{-f(2\eta-\xi)}\}\operatorname{ch} f\eta}{(1+e^{-2f\eta})(p^2\operatorname{ch} f\eta - fg\operatorname{sh} f\eta)} J_1(fr)\,fdf, \\ w &= \frac{2e^{ipt}}{\rho}\int_0^\infty \frac{\{e^{-f\xi}-e^{-f(2\eta-\xi)}\}\operatorname{sh} f\eta}{(1+e^{-2f\eta})(p^2\operatorname{ch} f\eta - fg\operatorname{sh} f\xi)} J_0(fr)\,fdf, \end{aligned}\right\} \ldots\ldots\ldots (61)$$

for all values of ξ and η.

Now we write (61) in the forms:

$$\left.\begin{aligned} u = -\frac{2e^{ipt}}{\pi\rho}\int_0^\infty \operatorname{ch} k\,dk\int_0^\infty &(e^{-f\xi}-e^{-f\overline{2\eta+\xi}}+e^{-f\overline{4\eta+\xi}}-\ldots\ldots \\ &-e^{-\overline{2\eta-\xi}}+e^{-\overline{4\eta-\xi}}-\ldots\ldots)\frac{(e^{ifr\operatorname{ch}k}+e^{-ifr\operatorname{ch}k})}{p^2-fg\operatorname{th} f\eta}\,fdf, \\ w = -\frac{2ie^{ipt}}{\pi\rho}\int_0^\infty dk\int_0^\infty &(e^{-f\xi}-e^{-f\overline{2\eta+\xi}}+e^{-f\overline{4\eta+\xi}}-\ldots\ldots \\ &-e^{-\overline{2\eta-\xi}}+e^{-\overline{4\eta-\xi}}-\ldots\ldots)\frac{(e^{ifr\operatorname{ch}k}-e^{-ifr\operatorname{ch}k})}{p^2\operatorname{cth} f\eta-fg}\,fdf. \end{aligned}\right\} \ldots (62)$$

If we write $f\eta=j$, $\xi/\eta=q$, these reduce to

$$\left.\begin{aligned}
u&=-\frac{2e^{ipt}}{\pi\rho\eta^2}\int_0^\infty \operatorname{ch} k\,dk\int_0^\infty\left(e^{-qj}-e^{-\overline{2+q}\,j}+e^{-\overline{4+q}\,j}-\dots\right.\\
&\qquad\left.-e^{-\overline{2-q}\,j}+e^{-\overline{4-q}\,j}-\dots\right)\frac{e^{\frac{ijr\operatorname{ch}k}{\xi}}+e^{-\frac{ijr\operatorname{ch}k}{\xi}}}{p^2-j\dfrac{g}{\xi}\operatorname{th}j}\,j\,dj,\\
w&=-\frac{2\,e^{ipt}}{\pi\rho\eta^2}\int_0^\infty dk\int_0^\infty\left(e^{-qj}-e^{-\overline{2+q}\,j}+e^{-\overline{4+q}\,j}-\dots\right.\\
&\qquad\left.-e^{-\overline{2-q}\,j}+e^{-\overline{4-q}\,j}-\dots\right)\frac{e^{\frac{ijr\operatorname{ch}k}{\xi}}-e^{-\frac{ijr\operatorname{ch}k}{\xi}}}{p^2\operatorname{cth}j-\dfrac{jg}{\xi}}\,j\,dj.
\end{aligned}\right\}\dots(63)$$

When we apply the similar process as in Part II, we get finally

$$\left.\begin{aligned}
u&\sim-\frac{2\pi i\,e^{ipt}}{\rho\eta^2}\,\frac{\alpha^2}{p^2\left(\dfrac{p^2\eta}{g}-1\right)-\dfrac{g\alpha^2}{\eta}}\,\frac{e^{-\frac{\xi\alpha}{\eta}}-e^{-\left(2-\frac{\xi}{\eta}\right)\alpha}}{1+e^{-2\alpha}}H_1^{(2)}\left(\frac{\alpha r}{\eta}\right),\\
w&\sim\frac{2\pi i\,e^{ipt}}{\rho\eta^2}\,\frac{\alpha}{\dfrac{g^2\alpha^2}{p^2\eta^2}-p^2+\dfrac{g}{\eta}}\,\frac{e^{-\frac{\xi\alpha}{\eta}}-e^{-\left(2-\frac{\xi}{\eta}\right)\alpha}}{1+e^{-2\alpha}}H_0^{(2)}\left(\frac{\alpha r}{\eta}\right),
\end{aligned}\right\}\dots\dots(64)$$

corresponding to the pressure change of the form:

$$p_0=\frac{e^{ipt}}{\sqrt{r^2+(z-\xi)^2}}\dots\dots\dots\dots\dots\dots\dots(24'')$$

In the equations (64), α is the positive real root of

$$\frac{\operatorname{ct}X}{X}=\frac{g}{p^2\eta}\dots\dots\dots\dots\dots\dots\dots\dots(65)$$

If we put $\xi=\eta$ in (64), we have

$$\left.\begin{aligned}
u&\sim-\frac{4\pi i\,e^{ipt}}{\rho\xi^2}\,\frac{\alpha^2}{p^2\left(\dfrac{p^2\xi}{g}-1\right)-\dfrac{g\alpha^2}{\xi}}\,\frac{e^{-\alpha}}{1+e^{-2\alpha}}H_1^{(2)}\left(\frac{\alpha r}{\xi}\right),\\
w&\sim\frac{4\pi i\,e^{ipt}}{\rho\xi^2}\,\frac{\alpha}{\dfrac{g^2\alpha^2}{p^2\xi^2}-p^2-\dfrac{g}{\xi}}\,\frac{e^{-\alpha}}{1+e^{-2\alpha}}H_0^{(2)}\left(\frac{\alpha r}{\xi}\right),
\end{aligned}\right\}\dots\dots\dots(66)$$

each value of which is twice that in (31).[11] This is due to the same reasoning noticed in (60).

---

[11] *loc cit.* p. 26.

If we put $\eta = \infty$, then the root of (65) is infinity and

$$\frac{\alpha}{\eta} = \frac{p^2}{g}, \qquad \qquad (67)$$

so that the expressions in (64) become

$$\left.\begin{aligned} u &\sim \frac{2\pi i\, e^{ipt}}{\rho}\left(\frac{p}{g}\right)^2 e^{-\frac{p^2 \xi}{g}}\, H_1^{(2)}\left(\frac{p^2 r}{g}\right), \\ w &\sim \frac{2\pi i\, e^{ipt}}{\rho}\left(\frac{p}{g}\right)^2 e^{-\frac{p^2 \xi}{g}}\, H_0^{(2)}\left(\frac{p^2 r}{g}\right), \end{aligned}\right\} \qquad \qquad (68)$$

which are the same forms, except κ and the inertia of the water, as that of the deep-water waves[12] due to the subaqueous shocks. In this case the motion of the water particle is perfectly circular.

Concluding Remarks.

I would add that, though this paper had aimed previously at the study of the formation of the shallow-water waves due to a bottom disturbance, my attention was rather attracted in the course of the investigation to some other cases such as the generation of the waves in a sea of moderate depth and the similar problem in which the origin of the shocks resides midway between the bed and the surface of the water.

The mathematical analysis contained in this paper, especially the part of contour integration is somewhat complicated; this part has been studied in a strict manner as far as possible. Full discussions on the nature of the definite integrals or on the branches have not been given to avoid the mathematical complexity. In all cases of contour integration I have ventured to introduce the effect of the small frictional terms by means of which the problem becomes free from ambiguity.

It may, however, be questioned that the present problem which is much idealised can be applied to the practical problem of *tsunami.* As to the form of the disturbing origin which is a symmetrical point or a spherical type, I warrant that such a form is rather convenient to determine the nature of the problem in which the internal source excites the surface waves. It appears that, if we wish to solve from the first the shallow-water waves

---

12) Cf. "Formation of Deep-water Waves ....", *loc cit.*, p. 15. It is to be noticed that in that paper principal values have been taken and for the solutions two systems of standing oscillations have been simply superposed, while in the present case the criterion of small friction is introduced and for the solutions each half of two systems of oscillations has been adopted.

formed by the disturbance distributed in a large area of the bottom of the sea, we will meet with a great deal of the obscurity in finding the manner of the transmission of the pressure waves in the subaqueous region.

We may complete this investigation by a brief summary of the results.

It has been shewn that in the beginning part that the shallow water waves caused by the bottom disturbance in a very shallow-sea have horizontal displacements varying with the depth in the law as $e^{-p\sqrt{\frac{\xi}{g}}}\Big/(1-e^{-2p\sqrt{\frac{\xi}{g}}})\xi$ where ξ is the depth of the sea and $2\pi/p$ is the period of the harmonic disturbances, while their vertical displacement is $p\sqrt{\xi/g}$ times the horizontal displacement. The fact that, in such a restricted case, the horizontal displacement decreases and the vertical one increases when the period of the disturbance is increased. The velocity of the propagation is, of course, $\sqrt{g\xi}$. This result has the practical importance that, when the depth of the sea, the period of the waves and the amplitude at a certain epicentral distance are known, we can find the approximate magnitude of the disturbance at the origin. The inverse case in which, the deformation at the origin being observed, time interval of the deformation of the bed can be imagined, is rather important.

In the second part the formation of the surface waves due to bottom shocks in a water of moderate depth has been investigated. A further modification of the amplitude concerning the depth of the water has been discovered. The velocity of propagation in this case is not constant and hence the dispersion of waves is possible.

Part III deals with the effect of the inertia of the subaqueous medium on the propagation of the pressure waves. In this case the surface waves are modified with a more complex law; the velocity of propagation of the surface waves is not altered by this inertia.

Lastly, it has been shewn in Part IV that the waves due to a disturbance resident midway between the surface and the bed of the water have the displacements varying as some function of the depth of the disturbance and the bed, besides the periods of the shocks. When the disturbance is at the bed, the amplitudes of the surface waves become twice those given in Part II. The above fact is consistent because the problem in Part II treats of the case where the origin is supposed to be of a semi-spherical type.

In concluding this paper I should express my thanks to Professor Imamura for his kind advice and also to Mr. G. Nishimura for his laborious assistance in preparing this paper.

2. 水中衝撃による淺海波の生成

地震研究所 妹澤克惟

この論文は淺水底に衝撃が加はる時に起る波が、どれ位の勢力を持つものかを研究する事が最初の目的であつたが、計算を行ふにつれて、次第に複雑な場合にも氣がとられた。それは中位の深さの海底に震動が働く場合や、水中の壓力波動にきく水の慣性の影響及び衝撃が水面と水底の中間に働く場合などである。

計算の方法殊に複素積分の部分は出來る限り正確に行つた。しかし定積分の算出や分岐の吟味などは其議論に限りがないから極く實用的な部分に止めた。又定積分を行ふに當つて微少摩擦の考へは入れる事にした。

この論文では餘り理想的な場合を取扱つた爲めに、實際の樣に淺海底の廣汎な面積が震動原になる場合とはかけ離れて居る樣にも思へるが、然し水中での壓力波の傳はり方と其が表面波を誘起する時の諸性質は寧ろこの方法によつて初めて明瞭になる樣に思はれる。

論文の始めの方では極く淺い海の底に衝撃が働く時に誘起される表面波の事が論じてある。即ち水平の變位は $e^{-p\sqrt{\frac{\xi}{g}}}\Big/\Big(1+e^{-2p\sqrt{\frac{\xi}{g}}}\Big)\xi$ の法則に從ふ。こゝに ξ は淺海の深さ、$2\pi/p$ は震動の週期とする。上下の變位は水平の變位に $p\sqrt{\xi/g}$ をかけたもので表はされる。これによつて週期が減ずるに從つて、水平の變位は減じ、上下の變位は增加する事が認められる。波動速度は勿論 $\sqrt{g\xi}$ となる。この計算の結果を適當に利用するならば、海深と震動の效果的週期が知れ、且つ或距離での振幅が測定されて居る場合に震動原の動きの大さを推定する事が出來るし、又逆に海底の地變動が測定出來た時、其變動はどれ位の期間に行はれたかが想像される。

次の部は海深が勝手な深さを持つ時、水底の衝撃によつて起る表面波の研究である。水深による振幅の變更狀態は大分複雜である。又表面波の波動速度も波長によつて種々のものがあるから波の分散現象も起り、從て表面波の振幅から原點の模樣を推定する事が幾分困難となる。

其次には水中の壓力波が水の慣性に影響される樣な短波長の場合が論じてある。表面波の波動速度は殆ど影響されぬが其振幅は多少變更される。

最後の所では、震動原が水中の中間の所にある場合を示して置いた。振幅は水深と震動原の深さで變るが倚極端な場合、即ち震動原が水底に來た場合を研究して見ると、最初の部で見出されたものゝ二倍の振幅を與へる事である。しかし最初のものは原點が半球形をなして水底にある場合であり、この場合は球が水底に接して完全に存するものである事がわかれば、其理由は極めて簡單な事柄となる。

3. *Generation of Rayleigh-waves from an Internal Source of Multiplet-type.**

By **Katsutada SEZAWA** and **Genrokuro NISHIMURA**,

Earthquake Research Institute.

(Received March 20, 1929.)

In a previous paper,[1] one of the present authors had the occasion of studying the problem of the transmission of Rayleigh-waves from an internal source of a doublet-type. Very recently Mr. T. Sakai[2] and Dr. H. Nakano[3] have attacked independently similar problems probably without knowing the paper cited above,[4] though they have given more fully the detailed explanations on the evaluation of the integrals involved in them as H. Lamb[5] had done in his paper on the generation of Rayleigh-waves from an internal singlet. The present paper which was written, rather earlier than even those two other writers, as a continuation of the preceding paper,[6] deals with the more extended case where the source of waves is a multiplet, say n.

Very simple problem where the oscillations of mutiplet-type are transmitted through an elastic body extending to infinity in all directions has already been studied[7] and it was found that the waves generated from such an origin are of two kinds, i.e. dilatational waves and distortional waves. Since we have already seen that both kinds of waves are partitioned at the origin with the prescribed conditions of stresses or displacements there, we can treat of each kind of waves separately for any point outside the origin.

We shall take the free surface of the semi-infinite solid to be $z=0$ and also that the positive sense of the axis of z is directed downwards. In a three dimensional problem the primary waves generated from the multiplet-source ($r=0$, $z=\xi$) may be expressed by

---

* A brief note of this was published in *Proc. Imp. Acad.*, **7** (1929), No. 2, 75–77.

1) K. SEZAWA, *Bull. Earthq. Res. Inst.*, **6** (1929), 1–17.

2) T. SAKAI's paper read at the meeting of *Math.-Phys. Soc., Tokyo*, in Jan. 1929.

3) H. NAKANO's paper read at the meeting of *Meteorol. Soc., Tokyo*, in Feb. 1929.

4) K. SEZAWA, *l.c.*

5) H. LAMB, *Phil. Trans. Roy. Soc.*, **203** (1904).

6) K. SEZAWA, *l.c.*

7) K. SEZAWA, *Bull. Earthq. Res. Inst.*, **2** (1927), 13–20.

$$\Delta_0'=Ae^{i\sigma t}\left(\cos\theta\frac{\partial}{\partial x}+\sin\theta\frac{\partial}{\partial z}\right)\left(\cos\theta\frac{\partial}{\partial x}+\sin\theta\frac{\partial}{\partial z}\right)^{n-1}\frac{e^{-ih\sqrt{r^2+(z-\xi)^2}}}{\sqrt{r^2+(z-\xi)^2}}, \quad \text{..(1)}$$

$$\left.\begin{aligned}2\varpi_y'&=Be^{i\sigma t}\left(\sin\theta\frac{\partial}{\partial x}-\cos\theta\frac{\partial}{\partial z}\right)\left(\cos\theta\frac{\partial}{\partial x}+\sin\theta\frac{\partial}{\partial z}\right)^{n-1}\frac{e^{-ij\sqrt{r^2+(z-\xi)^2}}}{\sqrt{r^2+(z-\xi)^2}},\\ 2\varpi_1'&=Be^{i\sigma t}\frac{\partial}{\partial y}\left(\cos\theta\frac{\partial}{\partial x}+\sin\theta\frac{\partial}{\partial z}\right)^{n-1}\frac{e^{-ij\sqrt{r^2+(z-\xi)^2}}}{\sqrt{r^2+(z-\xi)^2}},\end{aligned}\right\} \text{..(2)}$$

in which $h^2=\rho\sigma^2/(\lambda+2\mu)$, $j^2=\rho\sigma^2/\mu$ and θ is the inclination of the axis of the multiplet, while Δ_0' is the dilatational waves, ϖ_1' is the rotation about the axis perpendicular to the axis of the multiplet in the plane of xz and ϖ_y' is the rotation about the axis perpendicular to xz-plane. The ratio[8] of A to B can be easily obtained in the case of polar coordinates by the conditions of stresses at the origin. Since such determination is not important in this problem as we have explained, we will consider independently the respective cases of the generation of the surface waves due to Δ_0' and due to the resultant of ϖ_y' and ϖ_1'. In the present case we will deal with the problem concerning to Δ_0'[9] given in (1).

Now we know the expression

$$\frac{e^{-ih\sqrt{r^2+z^2}}}{\sqrt{r^2+z^2}}=\int_0^\infty\frac{e^{-\alpha z}}{\alpha}J_0(kr)\,kdk, \quad \text{..................(3)}$$

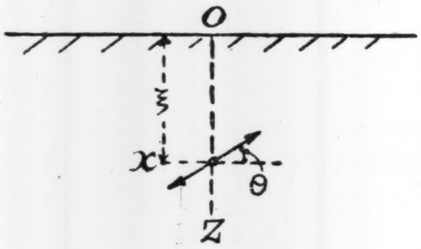

which is due to H. Lamb.[10] In this $\alpha=\sqrt{k^2-h^2}$ or $i\sqrt{h^2-k^2}$ according as $k^2\gtrless h^2$.

By the method of induction we can easily find the relations

$$\begin{aligned}&\frac{\partial^n}{\partial x^m\partial z^{n-m}}\int_0^\infty\frac{e^{-\alpha z}}{\alpha}J_0(kr)\,kdk\\ &=\frac{(-1)^n}{2^{m-1}}\Bigg\{\sum_{p=0}^{p=\frac{m-2}{2}}(-1)^p\frac{m!}{(m-p)!\,p!}\cos(m-2p)\,\omega\\ &\qquad\times\int_0^\infty e^{-\alpha z}J_{m-2p}(kr)\,\alpha^{n-m-1}k^{m+1}\,dk\\ &\quad+(-1)^{\frac{m}{2}}\frac{m!}{\left(\frac{m}{2}!\right)^2}\int_0^\infty e^{-\alpha z}\frac{J_0(kr)}{2}\alpha^{n-m-1}k^{m+1}\,dk\Bigg\}, \qquad [m:\text{even}]\end{aligned}$$

---

[8] K. SEZAWA, *l.c.* p. 41.

[9] Hereafter we shall omit the constant A for the sake of simplicity.

[10] H. LAMB, *Phil. Trans. Roy. Soc.*, **203** (1904).

$$=\frac{(-1)^n}{2^{m-1}}\sum_{p=0}^{p=\frac{m-1}{2}}(-1)^p\frac{m\,!}{(m-p)\,!\,p\,!}\cos(m-2p)\,\omega$$

$$\times\int_0^\infty e^{-\alpha z}J_{m-2p}(kr)\,\alpha^{n-m-1}k^{m+1}\,dk,\qquad[m:\text{odd}]$$

$$\dots\dots\dots\dots(4)$$

in which ω is the azimuth angle in cylindrical coordinates.

Thus, the primary waves can be expressed by

$$\Delta_0'=e^{i\sigma t}\sum_{m=0}^{m=n}\frac{(-1)^n}{2^{m-1}}\frac{n\,!}{(n-m)\,!\,m\,!}\sin^{n-m}\theta\cos^m\theta$$

$$\times\left\{\sum_{p=0}^{p=\frac{m-2}{2}}(-1)^p\frac{m\,!}{(m-p)\,!\,p\,!}\cos(m-2p)\,\omega\int_0^\infty e^{-\alpha z}J_{m-2p}(kr)\,\alpha^{n-m-1}k^{m+1}\,dk\right.$$

$$\left.+(-1)^{\frac{m}{2}}\frac{m\,!}{\left(\frac{m}{2}\,!\right)^2}\int_0^\infty e^{-\alpha z}\frac{J_0(kr)}{2}\,\alpha^{n-m-1}k^{m+1}\,dk\right\},\qquad[m:\text{even}]$$

$$=e^{i\sigma t}\sum_{m=0}^{m=n}\frac{(-1)^n}{2^{m-1}}\frac{n\,!}{(n-m)\,!\,m\,!}\sin^{n-m}\theta\cos^m\theta$$

$$\times\sum_{p=0}^{p=\frac{m-1}{2}}(-1)^p\frac{m\,!}{(m-p)\,!\,p\,!}\cos(m-2p)\,\omega$$

$$\times\int_0^\infty e^{-\alpha z}J_{m-2p}(kr)\,\alpha^{n-m-1}k^{m+1}\,dk.\qquad[m:\text{odd}]$$

$$\dots\dots\dots\dots(5)$$

It is convenient to consider the image at the point $r=0$, $z=-\xi$. The dilatation due to the image is expressed by

$$\Delta_0''=e^{i\sigma t}\left(\cos\theta\frac{\partial}{\partial x}+\sin\theta\frac{\partial}{\partial z}\right)^n\frac{e^{-ih\sqrt{r^2+(z+\xi)^2}}}{\sqrt{r^2+(z+\xi)^2}}\dots\dots\dots(6)$$

Superposing this on Δ_0' in (1) and applying the formulae in (4), we get

$$\Delta_0=\Delta_0'+\Delta_0''$$

$$=e^{i\sigma t}\sum_{m=0}^{m=n}\frac{(-1)^n}{2^{m-2}}\frac{n\,!}{(n-m)\,!\,m\,!}\sin^{n-m}\theta\cos^m\theta$$

$$\times\left\{\sum_{p=0}^{p=\frac{m-2}{2}}\frac{(-1)^p\,m\,!}{(m-p)\,!\,p\,!}\cos(m-2p)\,\omega\int_0^\infty \operatorname{ch}\alpha z\,e^{-\alpha\xi}J_{m-2p}(kr)\,\alpha^{n-m-1}k^{m+1}\,dk\right.$$

$$+(-1)^{\frac{m}{2}}\frac{m!}{\left(\frac{m}{2}!\right)^2}\int_0^\infty \mathrm{ch}\,\alpha z\, e^{-\alpha\xi}\frac{J_0(kr)}{2}\,\alpha^{n-m-1}\,k^{m+1}\,dk\Bigg\}, \qquad [m:\text{even}]$$

$$=e^{i\sigma t}\sum_{m=0}^{m=n}\frac{(-1)^n}{2^{m-2}}\frac{n!}{(n-m)!\,m!}\sin^{n-m}\theta\cos^m\theta$$

$$\times\sum_{p=0}^{p=\frac{m-1}{2}}(-1)^p\frac{m!}{(n-p)!p!}\cos(m-2p)\,\omega$$

$$\times\int_0^\infty \mathrm{ch}\,\alpha z\, e^{-\alpha\xi}\, J_{m-2p}(kr)\,\alpha^{n-m-1}\,k^{m+1}\,dk. \qquad [m:\text{odd}]$$

$$\dots\dots\dots\dots\dots\dots\dots\dots\dots(7)$$

The components of displacement in radial, azimuthal and vertical directions can be expressed by

$$u_0=-\frac{1}{h^2}\frac{\partial\Delta_0}{\partial r}$$

$$=-e^{i\sigma t}\sum_{m=0}^{m=n}\frac{(-1)^n}{2^{m-2}h^2}\frac{n!}{(n-m)!\,m!}\sin^{n-m}\theta\cos^m\theta$$

$$\times\Bigg\{\sum_{p=0}^{p=\frac{m-2}{2}}(-1)^p\frac{m!}{(m-p)\,!p\,!}\cos(m-2p)\,\omega$$

$$\times\int_0^\infty \mathrm{ch}\,\alpha z\, e^{-\alpha\xi}\frac{\partial J_{m-2p}(kr)}{\partial r}\,\alpha^{n-m-1}\,k^{m+1}\,dk$$

$$+(-1)^{\frac{m}{2}}\frac{m!}{\left(\frac{m}{2}!\right)^2}\int_0^\infty \mathrm{ch}\,\alpha z\, e^{-\alpha\xi}\frac{\partial J_0(kr)}{2\partial r}\,\alpha^{n-m-1}\,k^{m+1}\,dk\Bigg\}, \qquad [m:\text{even}]$$

$$=-e^{i\sigma t}\sum_{m=0}^{m=n}\frac{(-1)^n}{2^{m-2}h^2}\frac{n!}{(n-m)!\,m!}\sin^{n-m}\theta\cos^m\theta$$

$$\times\sum_{p=0}^{p=\frac{m-1}{2}}(-1)^p\frac{m!}{(m-p)!\,p!}\cos(m-2p)\,\omega$$

$$\times\int_0^\infty \mathrm{ch}\,\alpha z\, e^{-\alpha\xi}\frac{\partial J_{m-2p}(kr)}{\partial r}\,\alpha^{n-m-1}\,k^{m+1}\,dk, \qquad [m:\text{odd}]$$

$$v_0=-\frac{1}{h^2 r}\frac{\partial\Delta_0}{\partial\omega}$$

$$
\begin{aligned}
&= e^{i\sigma t}\sum_{m=0}^{m=n}\frac{(-1)^n}{2^{m-2}\,h^2}\frac{n!}{(n-m)!\,m!}\sin^{n-m}\theta\cos^m\theta \\
&\qquad\times\sum_{p=0}^{p=\frac{m-1}{2}}(-1)^p\frac{m!}{(m-p)!\,p!}(m-2p)\sin(m-2p)\,\omega \\
&\qquad\qquad\times\int_0^\infty \mathrm{ch}\,\alpha z\, e^{-\alpha\xi}\frac{J_{m-2p}(kr)}{r}\alpha^{n-m-1}\,k^{m+1}\,dk, \qquad [m:\text{even}] \\
&= e^{i\sigma t}\sum_{m=0}^{m=n}\frac{(-1)^n}{2^{m-2}\,h^2}\frac{n!}{(n-m)!\,m!}\sin^{n-m}\theta\cos^m\theta \\
&\qquad\times\sum_{p=0}^{p=\frac{m-1}{2}}(-1)^p\frac{m!}{(m-p)!\,p!}(m-2p)\sin(m-2p)\,\omega \\
&\qquad\qquad\times\int_0^\infty \mathrm{ch}\,\alpha z\, e^{-\alpha\xi}\frac{J_{m-2p}(kr)}{r}\alpha^{n-m-1}\,k^{m+1}\,dk, \qquad [m:\text{odd}]
\end{aligned}
$$

$$
\begin{aligned}
w_0 &= -\frac{1}{h^2}\frac{\partial\Delta_0}{\partial z} \\
&= -e^{i\sigma t}\sum_{m=0}^{m=n}\frac{(-1)^n}{2^{m-2}\,h^2}\frac{n!}{(n-m)!\,m!}\sin^{n-m}\theta\cos^m\theta \\
&\qquad\times\Bigg\{\sum_{p=0}^{p=\frac{m-2}{2}}(-1)^p\frac{m!}{(m-p)!\,p!}\cos(m-2p)\,\omega \\
&\qquad\qquad\times\int_0^\infty \mathrm{sh}\,\alpha z\, e^{-\alpha\xi}J_{m-2p}(kr)\,\alpha^{n-m}\,k^{m+1}\,dk \\
&\qquad+(-1)^{\frac{m}{2}}\frac{m!}{\left(\frac{m}{2}!\right)^2}\int_0^\infty \mathrm{sh}\,\alpha z\, e^{-\alpha\xi}\frac{J_0(kr)}{2}\alpha^{n-m}\,k^{m+1}\,dk\Bigg\}, \qquad [m:\text{even}] \\
&= -e^{i\sigma t}\sum_{m=0}^{m=n}\frac{(-1)^n}{2^{m-2}\,h^2}\frac{n!}{(n-m!)\,m!}\sin^{n-m}\theta\cos^m\theta \\
&\qquad\times\sum_{p=0}^{p=\frac{m-1}{2}}(-1)^p\frac{m!}{(m-p)!\,p!}\cos(m-2p)\,\omega \\
&\qquad\qquad\times\int_0^\infty \mathrm{sh}\,\alpha z\, e^{-\alpha\xi}J_{m-2p}(kr)\,\alpha^{n-m}\,k^{m+1}\,dk. \qquad [m:\text{odd}]
\end{aligned}
$$

..............................(8)

We may superpose on these some free waves[11] accumulated in the neighbourhood of the surface to annual the normal stress on that surface. The free waves are given by the solutions of the type, such that

---

[11] The free waves in this case are specified such that they give no any tangential stress, but they give some normal stress.

$$\left.\begin{aligned} u_1&=-\frac{\{(2k^2-j^2)-2\alpha\beta\}}{h^2(2k^2-j^2)}\frac{\partial J_{m-2p}(kr)}{\partial r}\cos(m-2p)\omega\, e^{i\sigma t},\\ v_1&=\frac{(m-2p)\{2k^2-j^2-2\alpha\beta\}}{h^2(2k^2-j^2)}\frac{J_{m-2p}(kr)}{r}\sin(m-2p)\omega\, e^{i\sigma t},\\ w_1&=-\frac{\alpha^2}{h^2(2k^2-j^2)}J_{m-2p}(kr)\cos(m-2p)\omega\, e^{i\sigma t},\end{aligned}\right\}[z=0]\;..\;(9)^{12)}$$

in which $\alpha^2=k^2-h^2$, $\beta^2=k^2-j^2$ and $j^2=\rho p^2/\mu$. The above solutions give no any tangential stress, but give us some normal stress on $z=0$.

The condition of no stress on the surface can be satisfied by summing up the solutions of the type (9) in the forms:

$$\begin{aligned} u_1=e^{i\sigma t}&\sum_{m=0}^{m=n}\frac{(-1)^n}{2^{m-2}h^2}\frac{n!}{(n-m)!\,m!}\sin^{n-m}\theta\cos^m\theta\\ &\times\left\{\sum_{p=0}^{p=\frac{m-2}{2}}\frac{(-1)^p m!}{(m-p)!\,p!}\cos(m-2p)\,\omega\right.\\ &\times\int_0^\infty\frac{(2k^2-j^2-2\alpha\beta)(2k^2-j^2)}{F(k)}e^{-\alpha\xi}\frac{\partial J_{m-2p}(kr)}{\partial r}\alpha^{n-m-1}k^{m+1}\,dk\\ &\left.+\frac{(-1)^{\frac{m}{2}}m!}{\left(\frac{m}{2}!\right)^2}\int_0^\infty\frac{(2k^2-j^2-2\alpha\beta)(2k^2-j^2)}{2F(k)}e^{-\alpha\xi}\frac{\partial J_0(kr)}{\partial r}\alpha^{n-m-1}k^{m+1}\,dk\right\},\\ &\hspace{20em}[\mathrm{m:even}]\\ =e^{i\sigma t}&\sum_{m=0}^{m=n}\frac{(-1)^n}{2^{m-2}h^2}\frac{n!}{(n-m)!\,m!}\sin^{n-m}\theta\cos^m\theta\\ &\times\sum_{p=0}^{p=\frac{m-1}{2}}(-1)^p\frac{m!}{(m-p)!\,p!}\cos(m-2p)\,\omega\\ &\times\int_0^\infty\frac{(2k^2-j^2-2\alpha\beta)(2k^2-j^2)}{F(k)}e^{-\alpha\xi}\frac{\partial J_{m-2p}(kr)}{\partial r}\alpha^{n-m-1}k^{m+1}\,dk,\ [m:\mathrm{odd}]\end{aligned}$$

$$\begin{aligned} v_1=-e^{i\sigma t}&\sum_{m=0}^{m=n}\frac{(-1)^n}{2^{m-2}h^2}\frac{n!}{(n-m)!\,m!}\sin^{n-m}\theta\cos^m\theta\\ &\times\sum_{m=0}^{p=\frac{m-2}{2}}(-1)^p\frac{m!}{(m-p)!\,p!}(m-2p)\sin(m-2p)\omega\end{aligned}$$

---

12) K. SEZAWA, *Bull. Earthq. Res. Inst.*, **6** (1929), 7–8.

$$\times\int_0^\infty \frac{(2k^2-j^2-2\alpha\beta)\,(2k^2-j^2)}{F\,(k)}\,e^{-\alpha\xi}\,\frac{J_{m-2p}\,(kr)}{r}\,\alpha^{n-m-1}\,k^{m+1}\,dk,\quad [m:\text{even}]$$

$$=-e^{i\sigma t}\sum_{m=0}^{m=n}\frac{(-1)^n}{2^{m-2}\,h^2}\,\frac{n\,!}{(n-m)\,!\;m\,!}\,\sin^{n-m}\theta\,\cos^m\theta$$

$$\times\sum_{p=0}^{p=\frac{m-1}{2}}(-1)^p\,\frac{m\,!}{(m-p)\,!\;p\,!}\,(m-2p)\,\sin\,(m-2)\,\omega$$

$$\times\int_0^\infty \frac{(2k^2-j^2-2\alpha\beta)\,(2k^2-j^2)}{F\,(k)}\,e^{-\alpha\xi}\,\frac{J_{m-2p}\,(kr)}{r}\,\alpha^{n-m-1}\,k^{m+1}\,dk,\quad [m:\text{odd}]$$

$$u_1=e^{i\sigma t}\sum_{m=0}^{m=n}\frac{(-1)^n}{2^{m-2}\,h^2}\,\frac{n\,!}{(n-m)\,!\;m\,!}\,\sin^{n-m}\theta\,\cos^m\theta$$

$$\times\Bigg\{\sum_{p=0}^{p=\frac{m-2}{2}}(-1)^p\,\frac{m\,!}{(m-p)\,!\,p\,!}\,\cos\,(m-2p)\,\omega$$

$$\times\int_0^\infty \frac{\alpha j^2\,(2k^2-j^2)}{F\,(k)}\,e^{-\alpha\xi}\,J_{m-2p}\,(kr)\,\alpha^{n-m-1}\,k^{m+1}\,dk$$

$$+\frac{(-1)^{\frac{m}{2}}\,m\,!}{\left(\frac{m}{2}\,!\right)^2}\int_0^\infty \frac{\alpha j^2\,(2k^2-j^2)}{2F\,(k)}\,e^{-\alpha\xi}\,J_0\,(kr)\,\alpha^{n-m-1}\,k^{m+1}\,dk\Bigg\},\qquad [m:\text{even}]$$

$$=e^{i\sigma t}\sum_{m=0}^{m=n}\frac{(-1)^n}{2^{m-2}\,h^2}\,\frac{n\,!}{(n-m)\,!\;m\,!}\,\sin^{n-m}\theta\,\cos^m\theta$$

$$\times\sum_{p=0}^{p=\frac{m-1}{2}}(-1)^p\,\frac{m\,!}{(m-p)\,!\;p\,!}\,\cos\,(m-2p)\,\omega$$

$$\times\int_0^\infty \frac{\alpha j^2\,(2k^2-j^2)}{F\,(k)}\,e^{-\alpha\xi}\,J_{m-2p}\,(kr)\,\alpha^{n-m-1}\,k^{m+1}\,dk,\qquad [m:\text{odd}]$$

$$\dots\dots\dots\dots\dots\dots\dots\dots\dots\dots\dots\dots\dots\;(10)$$

provided $$F\,(k)=(2k^2-j^2)^2-4k^2\,\alpha\beta.\qquad\dots\dots\dots\dots\dots\;(11)$$

The resultant displacements on $z=0$ are therefore written by

$$u=u_0+u_1$$

$$=e^{i\sigma t}\sum_{m=0}^{m=n}\frac{(-1)^n}{2^{m-2}\,h^2}\,\frac{n\,!}{(n-m)\,!\;m\,!}\,\sin^{n-m}\theta\,\cos^m\theta$$

$$\times\Bigg\{\sum_{p=0}^{p=\frac{m-2}{2}}(-1)^p\,\frac{m\,!}{(m-p)\,!\;p\,!}\,\cos\,(m-2p)\,\omega$$

$$\times \int_0^\infty \frac{2\beta j^2}{F(k)} e^{-\alpha\xi} \frac{\partial J_{m-2p}(kr)}{\partial r} \alpha^{n-m} k^{m+1} \, dk$$

$$+ \frac{(-1)^{\frac{m}{2}} m!}{\left(\frac{m}{2}!\right)^2} \int_0^\infty \frac{\beta j^2}{F(k)} e^{-\alpha\xi} \frac{\partial J_0(kr)}{\partial r} \alpha^{n-m} k^{m+1} \, dk \Big\}, \quad [m:\text{even}]$$

$$= e^{i\sigma t} \sum_{m=0}^{m=n} \frac{(-1)^n}{2^{m-2} h^2} \frac{n!}{(n-m)!\, m!} \sin^{n-m}\theta \cos^m\theta$$

$$\times \sum_{p=0}^{p=\frac{m-1}{2}} (-1)^p \frac{m!}{(m-p)!\, p!} \cos(m-2p)\,\omega$$

$$\times \int_0^\infty \frac{2\beta j^2}{F(k)} e^{-\alpha\xi} \frac{\partial J_{m-2p}(kr)}{\partial r} \alpha^{n-m} k^{m+1} \, dk, \qquad [m:\text{odd}]$$

$$v = v_0 + v_1$$

$$= -e^{i\sigma t} \sum_{m=0}^{m=n} \frac{(-1)^n}{2^{m-2} h^2} \frac{n!}{(n-m)!\, m} \sin^{n-m}\theta \cos^m\theta$$

$$\times \sum_{p=0}^{p=\frac{m-2}{2}} (-1)^p \frac{m!}{(m-p)!\, p!} (m-2p) \sin(m-2p)\,\omega$$

$$\times \int_0^\infty \frac{2\beta j^2}{F(k)} e^{-\alpha\xi} \frac{J_{m-2p}(kr)}{r} \alpha^{n-m} k^{m+1} \, dk, \qquad [m:\text{even}]$$

$$= -e^{i\sigma t} \sum_{m=0}^{m=n} \frac{(-1)^n}{2^{m-2} h^2} \frac{n!}{(n-m)!\, m!} \sin^{n-m}\theta \cos^m\theta$$

$$\times \sum_{p=0}^{p=\frac{m-1}{2}} (-1)^p \frac{m!}{(m-p)!\, p!} (m-2p) \sin(m-2p)\,\omega$$

$$\times \int_0^\infty \frac{2\beta j^2}{F(r)} e^{-\alpha\xi} \frac{J_{m-2p}(kr)}{r} \alpha^{n-m} k^{m+1} \, dk, \qquad [m:\text{odd}]$$

$$w = w_0 + w_1$$

$$= e^{i\sigma t} \sum_{m=0}^{m=n} \frac{(-1)^n}{2^{m-2} h^2} \frac{n!}{(n-m)!\, m!} \sin^{n-m}\theta \cos^m\theta$$

$$\times \Big\{ \sum_{p=0}^{p=\frac{m-1}{2}} (-1)^p \frac{m!}{(m-p)!\, p!} \cos(m-2p)\,\omega$$

$$\times \int_0^\infty \frac{\alpha j^2 (2k^2 - j^2)}{F(k)} e^{-\alpha\xi} J_{m-2p}(kr) \alpha^{n-m-1} k^{m+1} \, dk$$

$$+\frac{(-1)^{\frac{m}{2}}\,m!}{\left(\frac{m}{2}!\right)^2}\int_0^\infty \frac{\alpha j^2(2k^2-j^2)}{2F(k)}\,e^{-\alpha\xi}\,J_0(kr)\,\alpha^{n-m-1}\,k^{m+1}\,dk\Bigg\}, \quad [m:\text{even}]$$

$$=e\sum_{m=0}^{m=n}\frac{(-1)^n}{2^{m-2}\,h^2}\,\frac{n!}{(n-m)!\,m!}\sin^{n-m}\theta\cos^m\theta$$

$$\times\sum_{p=0}^{p=\frac{m-1}{2}}(-1)^p\,\frac{m!}{(m-p)!\,p!}\cos(m-2p)\,\omega$$

$$\times\int_0^\infty\frac{\alpha j^2(2k^2-j^2)}{F(k)}\,e^{-\alpha\xi}\,J_{m-2p}(kr)\,\alpha^{n-m-1}\,k^{m+1}\,dk. \quad [m:\text{odd}]$$

$$\dots\dots\dots\dots\dots\dots\dots\dots\dots(12)$$

Since we know the expressions

$$J_{m-2p}(kr)=\frac{2}{\pi}\int_0^\infty \sin\left(kr\,\mathrm{ch}\,f-\frac{m-2p}{2}\pi\right)\mathrm{ch}\,(m-2p)\,f\,df,^{13)} \quad \dots\dots(13)$$

we find the equations (12) are equivalent to

$$\left.\begin{aligned}
u&=e^{\sigma t}\,\frac{(-1)^n\,n!}{\pi h^2}\sum_{m=0}^{m=n}\frac{\sin^{n-m}\theta\cos^m\theta}{2^{m-3}(n-m)!}\,\frac{\partial\Phi_m}{\partial r},\\
v&=e^{\sigma t}\,\frac{(-1)^n\,n!}{\pi h^2}\sum_{m=0}^{m=n}\frac{\sin^{n-m}\theta\cos^m\theta}{2^{m-3}(n-m)!}\,\frac{1}{r}\,\frac{\partial\Phi_m}{\partial\omega},\\
w&=e^{\sigma t}\,\frac{(-1)^n\,n!}{\pi h^2}\sum_{m=0}^{m=n}\frac{\sin^{n-m}\theta\cos^m\theta}{2^{m-3}(n-m)!}\,\Psi_m,
\end{aligned}\right\}\dots\dots\dots\dots(14)$$

in which

$$\left.\begin{aligned}
\Phi_m&=i\,(-1)^{\frac{n}{2}+1}\sum_{p=0}^{p=q}\gamma\,\frac{\cos(m-2p)\,\omega}{(m-p)!\,p!}\int_0^\infty\cos(m-2p)\,f\,df\\
&\qquad\times\int_{-\infty}^\infty\frac{\beta j^2}{F(k)}\,e^{-\alpha\xi+ikr\,\mathrm{ch}\,f}\,\alpha^{n-m}\,\kappa^{m+1}\,d\kappa,\\
\Psi_m&=i\,(-1)^{\frac{n}{2}+1}\sum_{p=0}^{p=q}\gamma\,\frac{\cos(m-2p)\,\omega}{(m-p)!\,p!}\int_0^\infty\cos(m-2p)\,f\,df\\
&\qquad\times\int_{-\infty}^\infty\frac{j^2(2k^2-j^2)}{2F(k)}\,e^{-\alpha\xi+ikr\,\mathrm{ch}\,f}\,\alpha^{n-m}\,k^{m+1}\,dk,
\end{aligned}\right\}\dots(15)$$

where q should be taken at $m/2$ or $(m-1)/2$ according as m is even or odd

---

13) WATSON, *Theory of Bessel Functions* (1922), 180.

and it is to be remarked that γ is taken to be unity excepting the term, $p=m/2$, in which case $\gamma=1/2$.

The evaluation of the integrals of the forms:

$$\left.\begin{aligned}&\int_{-\infty}^{\infty}\frac{\beta j^2}{F(k)}\,e^{-\alpha\xi+ikr\,\mathrm{ch}\,f}\,\alpha^{n-m}\,k^{m+1}\,dk,\\&\int_{-\infty}^{\infty}\frac{j^2(2k^2-j^2)}{2F(k)}\,e^{-\alpha\xi+ikr\,\mathrm{ch}\,f}\,\alpha^{n-m}\,k^{m+1}\,dk,\end{aligned}\right\}\ldots\ldots\ldots\ldots(16)$$

can be performed after H. Lamb's method described in his paper[14] on Rayleigh-waves. We thus obtain

$$\left.\begin{aligned}&\int_{-\infty}^{\infty}\frac{\beta j^2}{F(\kappa)}\,e^{-\alpha\xi}\,e^{ikr\,\mathrm{ch}\,f}\,\alpha^{n-m}\,\kappa^{m+1}\,d\kappa\\&\qquad=\left.\begin{matrix}i\\-\end{matrix}\right\}4\pi\,\frac{\beta_1\,j^2}{F'(\kappa)}\,e^{-\alpha_1\xi}\left.\begin{matrix}\cos\\\sin\end{matrix}\right\}\kappa r\,\mathrm{ch}\,f\,\alpha_1^{n-m}\,\kappa^{m+1}\\&\qquad\qquad+\text{asymptotically vanishing term},\\&\int_{-\infty}^{\infty}\frac{j^2(2k^2-j^2)}{F(k)}\,e^{-\alpha\xi}\,e^{ikr\,\mathrm{ch}\,f}\,\alpha^{n-m}\,k^{m+1}\,dk\\&\qquad=\left.\begin{matrix}i\\-\end{matrix}\right\}4\pi\,\frac{j^2(2\kappa^2-j^2)}{F'(\kappa)}\,e^{-\alpha_1\xi}\left.\begin{matrix}\cos\\\sin\end{matrix}\right\}\kappa r\,\mathrm{ch}\,f\,\alpha_1^{n-m}\,\kappa^{m+1}\\&\qquad\qquad+\text{asymptotically vanishing term}.\end{aligned}\right\}\ldots(17)$$

In these, κ is the real positive root of $F(k)$ and α_1, β_1 are the corresponding values of α, β. (i is for even m and $-$ for odd m.)

The above evaluations, which are obtained directly from a simple process similar to that of H. Lamb, are sufficient for our purpose. Yet we shall here give the more close investigation of the evaluation to find the residual disturbance, though we owe to H. Lamb the method of investigations thoroughly as described above.

To integrate the left-hand sides of the expressions in (17), we consider the integrals

$$\left.\begin{aligned}&\int\frac{\sqrt{Z^2-j^2}\,j^2}{F(Z)}\,e^{-\sqrt{Z^2-h^2}\,\xi}\,e^{iZr\,\mathrm{ch}\,f}\,(\sqrt{Z^2-h^2})^{n-m}\,Z^{m+1}\,dZ,\\&\int\frac{j^2(2Z^2-j^2)}{F(Z)}\,e^{-\sqrt{Z^2-h^2}\,\xi}\,e^{iZr\,\mathrm{ch}\,f}\,(\sqrt{Z^2-h^2})^{n-m}\,Z^{m+1}\,dZ,\end{aligned}\right\}\ldots\ldots\ldots(18)$$

taken round the contour annexed in the next page. Though the part enclosed by $(-j\ \ -h)$ and two grooves directed towards infinitely belongs

---

[14] H. LAMB, *loc. cit.* p. 41.

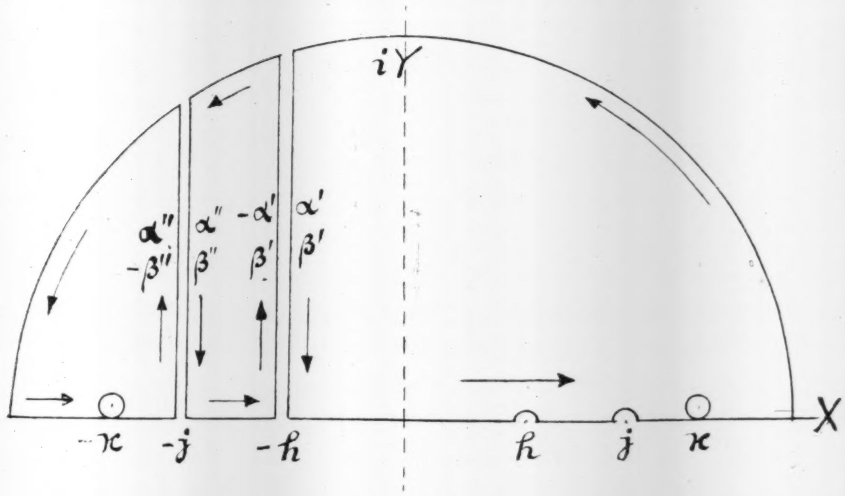

to a different sheet, we treat of that part independently and adding to the results of two other systems of contour integrations. Hence we find

$$\int_{-\infty}^{\infty}\frac{\beta j^2}{F(k)}\,e^{-\alpha\xi}\,e^{ikr\,\mathrm{ch}\,f}\,\alpha^{n-m}\,k^{m+1}\,dk=\overset{i}{-}\Big\}\frac{4\pi\beta_1 j^2}{F'(\kappa)}\,e^{-\alpha_1\xi}\begin{matrix}\cos\\ \sin\end{matrix}\Big\}(\kappa r\,\mathrm{ch}\,f)\,\alpha_1^{n-m}\,\kappa^{m+1}$$

$$+e^{-ijr\,\mathrm{ch}\,f}\int_0^{\infty}\Big\{\frac{j^2\beta''}{(2Z^2-j^2)^2-4Z^2\alpha''\beta''}$$

$$+\frac{j^2\beta''}{(2Z^2-j^2)^2+4Z^2\alpha''\beta''}\Big\}Z^{m+1}(Z^2-h^2)^{\frac{n-m}{2}}\,e^{-\sqrt{Z^2-h^2}\,\xi-Yr\,\mathrm{ch}\,f}\,idY$$

$$+e^{-ihr\,\mathrm{ch}\,f}\int_0^{\infty}\Big\{\frac{j^2\beta'}{(2Z^2-j^2)^2-4Z^2\alpha'\beta'}$$

$$-\frac{j^2\beta'}{(2Z^2-j^2)^2+4Z^2\alpha'\beta'}\Big\}Z^{m+1}(Z^2-h^2)^{\frac{n-m}{2}}\,e^{-\sqrt{Z^2-h^2}\,\xi-Yr\,\mathrm{ch}\,f}\,idY$$

$$=\overset{i}{-}\Big\}\frac{4\pi\beta_1 j^2}{F'(\kappa)}\,e^{-\alpha_1\xi}\begin{matrix}\cos\\ \sin\end{matrix}\Big\}(\kappa r\,\mathrm{ch}\,f)\,\alpha_1^{n-m}\,\kappa^{m+1}$$

$$+8ie^{-ijr\,\mathrm{ch}\,f}\int_0^{\infty}\frac{j^2\beta''(2Z^2-j^2)^2\,Z^{m+1}(Z^2-h^2)^{\frac{n-m}{2}}}{(2Z^2-j^2)^4-16Z^4\alpha''^2\beta''^2}\,e^{-\sqrt{Z^2-h^2}\,\xi-Yr\,\mathrm{ch}\,f}\,dY$$

$$+8ie^{-ihr\,\mathrm{ch}\,f}\int_0^{\infty}\frac{j^2\beta' Z^2\alpha'\beta'\,Z^{m+1}(Z^2-h^2)^{\frac{n-m}{2}}}{(2Z^2-j^2)^4-16Z^4\alpha'^2\beta'^2}\,e^{-\sqrt{Z^2-h^2}\,\xi-Yr\,\mathrm{ch}\,f}\,dY,$$

$$\int_{-\infty}^{\infty}\frac{j^2(2k^2-j^2)}{F(k)}\,e^{-\alpha\xi}\,e^{ikr\,\mathrm{ch}\,f}\,\alpha^{n-m}\,k^{m+1}\,dk$$

$$=\overset{i}{-}\Big\}\frac{4\pi i j^2(2\kappa^2-j^2)}{F'(\kappa)}\,e^{-\alpha_1\xi}\cos(\kappa r\,\mathrm{ch}\,f)\,\alpha_1^{n-m}\,\kappa^{m+1}$$

$$
\begin{aligned}
&+e^{-ijr\,\mathrm{ch}\,f}\int_0^\infty\left\{\frac{2k^2-j^2}{(2Z^2-j^2)^2-4Z^2\alpha''\beta''}\right.\\
&\qquad\left.-\frac{2k^2-j^2}{(2Z^2-j^2)^2+4Z^2\alpha''\beta''}\right\}j^2Z^{m+1}(Z^2-h^2)^{\frac{n-m}{2}}e^{-\sqrt{Z^2-h^2}\,\xi-Yr\,\mathrm{ch}\,f}\,idY\\
&+e^{-ihr\,\mathrm{ch}\,f}\int_0^\infty\left\{\frac{2k^2-j^2}{(2Z^2-j^2)^2-4Z^2\alpha'\beta'}\right.\\
&\qquad\left.-\frac{2k^2-j^2}{(2Z^2-j^2)^2+4Z^2\alpha'\beta'}\right\}j^2Z^{m+1}(Z^2-h^2)^{\frac{n-m}{2}}e^{-\sqrt{Z^2-h^2}\,\xi-Yr\,\mathrm{ch}\,f}\,idY\\
=&\left.\begin{matrix}i\\-\end{matrix}\right\}\frac{4\pi j^2(2\kappa^2-j^2)}{F'(\kappa)}e^{-\alpha_1\xi}\,\mathrm{ccs}\,(\kappa r\,\mathrm{ch}\,f)\,\alpha_1^{n-m}\,\kappa^{m+1}\\
&+8ie^{-ijr\,\mathrm{ch}\,f}\int_0^\infty\frac{(2k^2-j^2)Z^2\alpha''\beta''j^2Z^{m+1}(Z^2-h^2)^{\frac{n-m}{2}}}{(2Z^2-j^2)^4-16Z^4\alpha''^2\beta''^2}e^{-\sqrt{Z^2-h^2}-Yr\,\mathrm{ch}\,f}\,dY\\
&+8ie^{-ihr\,\mathrm{ch}\,f}\int_0^\infty\frac{(2k^2-j^2)Z^2\alpha'\beta'j^2Z^{m+1}(Z^2-h^2)^{\frac{n-m}{2}}}{(2Z^2-j^2)^4-16Z^4\alpha^{2'}\beta^{2'}}e^{-\sqrt{Z^2-h^2}-Yr\,\mathrm{ch}\,f}\,dY.
\end{aligned}
\qquad\ldots\ldots(19)
$$

In each first integral of the right-hand side of these we should put $Z=-j+iY$, and in each second, $Z=-h+iY$. Approximate evaluation of the above integrals can be easily performed. They give the expressions of residual disturbances whose velocities of propagation are limited to two kinds, one of them corresponding to that of dilatational waves and the other to that of distortional waves. It will be noticed that the terms corresponding to these waves quickly disappears in virtue of the factor $e^{-Yr\,\mathrm{ch}\,f}$, so that we disregard these terms hereafter for the investigation of Rayleigh-waves. Thus we arrive at

$$
\left.
\begin{aligned}
&\int_{-\infty}^{\infty}\frac{\beta j^2}{F(k)}e^{-\alpha\xi}e^{ikr\,\mathrm{ch}\,f}\alpha^{n-m}k^{m+1}\,dk\\
&\qquad=\left.\begin{matrix}i\\-\end{matrix}\right\}\frac{4\pi\beta_1j^2}{F'(\kappa)}e^{-\alpha_1\xi}\left.\begin{matrix}\cos\\ \sin\end{matrix}\right\}(\kappa r\,\mathrm{ch}\,f)\,\alpha_1^{n-m}\,\kappa^{m+1}\\
&\qquad\qquad+\text{asymptotically vanishing terms,}\\
&\int_{-\infty}^{\infty}\frac{j^2(2k^2-j^2)}{F(k)}e^{-\alpha\xi}e^{ikr\,\mathrm{ch}\,f}\alpha^{n-m}k^{m+1}\,dk\\
&\qquad=\left.\begin{matrix}i\\-\end{matrix}\right\}\frac{4\pi j^2(2\kappa^2-j^2)}{F'(\kappa)}e^{-\alpha_1\xi}\left.\begin{matrix}\cos\\ \sin\end{matrix}\right\}(\kappa r\,\mathrm{ch}\,f)\,\alpha_1^{n-m}\,\kappa^{m+1}\\
&\qquad\qquad+\text{asymptotically vanishing terms.}
\end{aligned}
\right\}\quad\ldots.(17')
$$

Now we return to the original problem. The expressions of Φ_m and Ψ_m which we have written in (15) thus take the forms:

$$\left.\begin{aligned}
\Phi_m &= i\,(-1)^{\frac{3m}{2}+1}\sum_{p=0}^{p=q}\gamma\,\frac{\cos\,(m-2p)\,\omega}{(m-p)\ \ p\,!}\\
&\quad\times\int_0^\infty \cos\,(m-2p)\,f\left[\left.\begin{matrix} i\\ -\end{matrix}\right\}\frac{4\pi\beta_1\,j^2}{F'(\kappa)}\,e^{-\alpha_1\xi}\left.\begin{matrix}\cos\\ \sin\end{matrix}\right\}(\kappa r\ \mathrm{ch}\,f)\,\alpha_1^{n-m}\,\kappa^{m+1}\right]df,\\
\Psi_m &= i\,(-1)^{\frac{3m}{2}+1}\sum_{p=0}^{p=q}\gamma\,\frac{\cos\,(m-2p)\,\omega}{(m-p)\,!\,p\,!}\\
&\times\int_0^\infty \cos\,(m-2p)\,f\left[\left.\begin{matrix} i\\ -\end{matrix}\right\}\frac{4\pi i j^2(2\kappa^2-j^2)}{2F'(\kappa)}\,e^{-\alpha_1\xi}\left.\begin{matrix}\cos\\ \sin\end{matrix}\right\}(\kappa r\ \mathrm{ch}\,f)\,\alpha_1^{n-m}\,\kappa^{m+1}\right]df.
\end{aligned}\right\}\quad(20)$$

In virtue of (13) and the equation

$$Y_{m-2p}(\kappa r) = -\frac{2}{\pi}\int_0^\infty \cos\left(\kappa r\ \mathrm{ch}\,f - \frac{m-2p}{2}\,\pi\right)\mathrm{ch}\,(m-2p)\,f\,df,^{15)}\quad \ldots\ldots(21)$$

we find

$$\begin{aligned}
\Phi_m &= -\ \frac{2\pi^2\beta_1\ {}^2}{F'(\kappa)}\,e^{-\alpha_1\xi}\,\alpha_1^{n-m}\,\kappa^{m+1}\\
&\qquad\times\sum_{p=0}^{p=q}\gamma\,(-1)^p\,\frac{\cos\,(m-2p)\,\omega}{(m-p)\,!\,p\,!}\,Y_{m-2p}(\kappa r), && [m\!:\!\text{even}]\\
&= +\frac{2\pi^2\beta_1\,j^2}{F'(\kappa)}\,e^{-\alpha_1\xi}\,\alpha_1^{n-m}\,\kappa^{m+1}\\
&\qquad\times\sum_{p=0}^{p=q}\gamma\,(-1)^p\,\frac{\cos\,(m-2p)\,\omega}{(m-p)\,!\,p\,!}\,Y_{m-2p}(\kappa r), && [m\!:\!\text{odd}]\\
\Psi_m &= -\ \frac{2\pi^2 j^2\,(2\kappa^2-j^2)}{2F'(\kappa)}\,e^{-\alpha_1\xi}\,\alpha_1^{n-m}\,\kappa^{m+1}\\
&\qquad\times\sum_{p=0}^{p=q}\gamma\,(-1)^p\,\frac{\cos\,(m-2p)\,\omega}{(m-p)\,!\,p\,!}\,Y_{m-2p}(\kappa r); && [m\!:\!\text{even}]\\
&= \frac{2\pi^2 j^2\,(2\kappa^2-j^2)}{2F'(\kappa)}\,e^{-\alpha_1\xi}\,\alpha_1^{n-m}\,\kappa^{m+1}\\
&\qquad+\sum_{p=0}^{p=q}\gamma\,(-1)^p\,\frac{\cos\,(m-2p)\,\omega}{(m-p)\,!\,p\,!}\,Y_{m-2p}(\kappa r). && [m\!:\!\text{odd}]
\end{aligned}$$

$$\ldots\ldots\ldots\ldots\ldots\ldots\ldots\ldots\ldots\ldots(22)$$

Substituting these values of Φ_m and Ψ_m in (14), we find

---

15) WATSON, *loc. cit.*, p. 180.

$$
\begin{aligned}
u &= \frac{2e^{i\sigma t}(-1)^n n!\,\pi}{h^2}\,\frac{\beta_1 j^2}{F'(\kappa)}\,e^{-\alpha_1 \xi}\sum_{m=0}^{m=n}(-1)^m \sin^{n-m}\theta\cos^m\theta\,\alpha_1{}^{n-m}\,\kappa^{m+1} \\
&\qquad\times\sum_{m=0}^{p=q}\gamma\,(-1)^p\frac{\cos(m-2p)\,\omega}{(m-p)!\,p!}\,\frac{\partial}{\partial r}\Big\{-Y_{m-2p}(\kappa r),\quad Y_{m-2p}(\kappa r)\Big\}, \\
v &= \frac{2e^{i\sigma t}(-1)^n n!\,\pi}{h^2}\,\frac{\beta_1 j^2}{F'(\kappa)}\,e^{-\alpha_1 \xi}\sum_{m=0}^{m=n}(-1)^m \sin^{n-m}\theta\cos^m\theta\,\alpha_1^{n-m}\,\kappa^{m+1} \\
&\qquad\times\sum_{p=0}^{p=q}\gamma\,(-1)^{p+1}\frac{(m-2p)\sin(m-2p)\,\omega}{(m-p)!\,p!\,r}\Big\{-Y_{m-2p}(\kappa r),\quad Y_{m-2p}(\kappa r)\Big\}, \\
w &= +\frac{2ie^{i\sigma t}(-1)^n n!\,\pi}{h^2}\,\frac{j^2(2\kappa^2-j^2)}{2F'(\kappa)}\sum_{m=0}^{m=n}(-1)^m \sin^{n-m}\theta\cos^m\theta\,\alpha_1^{n-m}\,\kappa^{m+1} \\
&\qquad\times\sum_{p=0}^{p=q}\gamma\,(-1)^p\frac{\cos(m-2p)\,\omega}{(m-p)!\,p!}\Big\{-Y_{m-2p}(\kappa r),\quad Y_{m-2p}(\kappa r)\Big\},
\end{aligned}
\qquad\qquad\ldots\ldots\ldots\ldots(23)
$$

where the first term in each bracket should be taken for even value of m and the second for odd value of m. These expressions are suitable to the transmission of waves of a finite extent of disturbances. To get progressive waves of an infinite train, we may combine two systems of different standing types. Though the method is somewhat conventional, it must be borne in mind that, as we know from Fourier's integral theorem, half the amplitude of the standing type is effective for the actual progressive waves. Thus, the final solutions, when r is large, can be expressed by

$$
\left.
\begin{aligned}
u &\sim \frac{ie^{i\sigma t}(-1)^n n!\,\pi}{h^2}\,\frac{\beta_1 j^2}{F'(\kappa)}\,e^{-\alpha_1 \xi} \\
&\quad\times\sum_{m=0}^{m=n}(-1)^m\frac{\sin^{n-m}\theta\cos^m\theta\,\alpha_1^{n-m}\,\kappa^{m+1}}{2^{m-3}(n-m)!} \\
&\quad\times\sum_{p=0}^{p=q}\gamma\,(-1)^p\frac{\cos(m-2p)\,\omega}{(m-p)!\,p!}\,\frac{\partial H^{(2)}_{m-2p}(\kappa r)}{\partial r}, \\
v &\sim \frac{ie^{i\sigma t}(-1)^n n!\,\pi}{h^2}\,\frac{\beta_1 j^2}{F'(\kappa)}\,e^{-\alpha_1 \xi} \\
&\quad\times\sum_{m=0}^{m=n}(-1)^m\frac{\sin^{n-m}\theta\cos^m\theta\,\alpha_1^{n-m}\,\kappa^{m+1}}{2^{m-3}(n-m)!} \\
&\quad\times\sum_{p=0}^{p=q}\gamma\,(-1)^{p+1}\frac{(m-2p)\sin(m-2p)\,\omega}{(m-p)!\,p!}\,\frac{H^{(2)}_{m-2p}(\kappa r)}{r},
\end{aligned}
\right\}\ldots.(24)
$$

$$\left.\begin{aligned} w \approx & -\frac{ie^{i\sigma t}(-1)^n n!\,\pi}{h^2}\frac{j^2(2\kappa^2-j^2)}{2F'(\kappa)} \\ & \times\sum_{m=0}^{m=n}(-1)^m\frac{\sin^{n-m}\theta\cos^m\theta\,\alpha_1^{n-m}\,\kappa^{m+1}}{2^{m-3}(n-m)!} \\ & \times\sum_{p=0}^{p=q}\gamma(-1)^p\frac{\cos(m-2p)\,\omega}{(m-p)!\,p!}H^{(2)}_{m-2p}(\kappa r), \end{aligned}\right\}$$

corresponding to the primary disturbance at $(r=0,\ z=\xi)$ in the form:

$$\varDelta_0'=e^{i\sigma t}\left(\cos\theta\frac{\partial}{\partial x}+\sin\theta\frac{\partial}{\partial z}\right)^n\frac{e^{-ih\sqrt{r^2+(z-\xi)^2}}}{\sqrt{r^2+(z-\xi)^2}}\ldots\ldots\ldots\ldots\ldots(1')$$

In the expressions in (24) q should be taken at $m/2$ or $(m-1)/2$ according as m is even or odd and γ is taken to be unity excepting the term $p=m/2$ in which case $\gamma=1/2$.

In a special case where $\theta=0$ and $n=1$, we have

$$\left.\begin{aligned} u &\approx e^{i\sigma t}\frac{4i\pi\cos\omega}{h^2}\frac{j^2\kappa^2\beta_1}{F'(\kappa)}\epsilon^{-\alpha_1\xi}\frac{\partial H_1^{(2)}(\kappa r)}{\partial r}, \\ v &\approx -e^{i\sigma t}\frac{4\pi\sin\omega}{h^2}\frac{j^2\kappa^2\beta_1}{F'(\kappa)}\epsilon^{-\alpha_1\xi}\frac{H_1^{(2)}(\kappa r)}{r}, \\ w &\approx -e^{i\sigma t}\frac{2\pi\cos\omega}{h^2}\frac{j^2\kappa^2(2\kappa^2-j^2)}{F'(\kappa)}\epsilon^{-\alpha_1\xi}H_1^{(2}(\kappa r), \end{aligned}\right\}\ldots\ldots\ldots\ldots(25)$$

which is the same form as what one[16] of the authors has already obtained in a preceding time, though the negative signs in u and v in this are introduced during the superposing operations.

If we take the case where θ is not zero but n is unity, the expressions of displacement are given by

$$\left.\begin{aligned} u &= -i\,e^{i\sigma t}\frac{4\pi}{h^2}\frac{\beta_1 j^2\kappa}{F'(\kappa)}e^{-\alpha_1\xi}\left\{\alpha_1\sin\theta\frac{\partial H_0^{(2)}(\kappa r)}{\partial r}\right. \\ &\qquad\qquad\left.-\kappa\cos\theta\cos\omega\frac{\partial H_1^{(2)}(\kappa r)}{\partial r}\right\}, \\ v &= -i\,e^{i\sigma t}\frac{4\pi}{h^2}\frac{\beta_1 j^2\kappa^2}{F'(\kappa)}e^{-\alpha_1\xi}\cos\theta\sin\omega\frac{H_1^{(2)}(\kappa r)}{r}, \\ w &= i\,e^{i\sigma t}\frac{2\pi}{h^2}\frac{j^2(2\kappa^2-j^2)\kappa}{F'(\kappa)}e^{-\alpha_1\xi}\left\{\alpha_1\sin\theta H_0^{(2)}(\kappa r)\right. \\ &\qquad\qquad\left.-\kappa\cos\theta\cos\omega H_1^{(2)}(\kappa r)\right\}, \end{aligned}\right\}\ldots\ldots\ldots(26)$$

---

16) K. SEZAWA, *loc. cit.* p. 41.

corresponding to the disturbance at the origin,

$$\varDelta_0'=e^{i\sigma t}\left(\sin\theta\frac{\partial}{\partial z}+\cos\theta\frac{\partial}{\partial x}\right)\frac{e^{-ih\sqrt{r^2+(z-\xi)^2}}}{\sqrt{r^2+(z-\xi)^2}}\qquad\qquad(27)$$

Let us next consider the case $n=2$. The displacements can be written at once in the forms:

$$\left.\begin{aligned}
u&=i\,e^{i\sigma t}\frac{2\pi}{h^2}\frac{\beta_1\,j^2\,\kappa}{F'(\kappa)}\,e^{-\alpha_1\xi}\left\{(2\alpha_1{}^2\sin^2\theta-\kappa^2\cos^2\theta)\frac{\partial H_0^{(2)}(\kappa r)}{\partial r}\right.\\
&\qquad\left.-4\alpha_1\kappa\sin\theta\cos\theta\cos\omega\frac{\partial H_1^{(2)}(\kappa r)}{\partial r}+\kappa^2\cos^2\theta\cos 2\omega\frac{\partial H_2^{(2)}(\kappa r)}{\partial r}\right\},\\
v&=i\,e^{i\sigma t}\frac{2\pi}{h^2}\frac{\beta_1\,j^2\,\kappa}{F'(\kappa)}\,e^{-\alpha_1\xi}\left\{4\alpha_1\sin\theta\cos\theta\sin\omega\frac{H_1^{(2)}(\kappa r)}{r}\right.\\
&\qquad\qquad\left.-\kappa\cos^2\theta\sin 2\omega\frac{H_2^{(2)}(\kappa r)}{r}\right\},\\
w&=-\,e^{i\sigma t}\frac{i\pi}{h^2}\frac{2(2\kappa^2-j^2)\kappa}{F'(\kappa)}\,e^{-\alpha_1\xi}\left\{(2\alpha_1{}^2\sin^2\theta-\kappa^2\cos^2\theta)H_0^{(2)}(\kappa r)\right.\\
&\qquad\left.-4\alpha_1\kappa\sin\theta\cos\theta\cos\omega\,H_1^{(2)}(\kappa r)+\kappa^2\cos^2\theta\cos 2\omega\,H_2^{(2)}(\kappa r)\right\},
\end{aligned}\right\}\qquad(28)$$

corresponding to

$$\varDelta_0'=e^{i\sigma t}\left(\sin\theta\frac{\partial}{\partial z}+\cos\theta\frac{\partial}{\partial x}\right)^2\frac{e^{-ih\sqrt{r^2+(s-\xi)^2}}}{\sqrt{r^2+(z-\xi)^2}}\qquad\qquad(29)$$

These two cases, where $n=1$ and 2, have been computed in all details and the results are illustrated in Fig. I—IV. In these U is the maximum displacement at the radial distance R from the focus and L is the wave length of the bodily waves in the interior of the solid. Some general notions on these result may be gathered. In the case of a doublet having the horizontal axis, there are maximum displacements of the type of Rayleigh-waves at the azimuth angle $\omega=0$ and π while at $\omega=\pi/2$ and $3\pi/2$ there are no such displacements but the prevalence of the horizontal movement at right angle to the direction of the propagation, indicating the appearance of Love-waves. This azimuthal component of displacement quickly disappears as the distance from the epicentre increases, in spite of the persistence of the nature of the vertical and the horizontal component of displacement in the radial plane. The above facts[17] have already been pointed out by one of the authors in the investigation of Rayleigh-waves due to an internal doublet-source. When the axis of the doublet is inclined, the amplitude of the surface waves is modified. The chief feature of this case is such that there is superposition of the movements of the type due to the horizontal doublet and those of the ordinary annular Rayleigh-waves. It is to be remarked that the displacements at $\omega=0$ and at $\omega=\pi$ is the same in their magnitudes in spite of the inclined axis of the doublet. If the axis of the doublet is vertical, the movements on the surface are completely symmetrical with respect to the vertical line passing through the origin.

---

[17] K. SEZAWA, *Bull. Earthq. Res. Inst.*, **6** (1929), 12.

If we proceed to the case due to a quadruplet, more complicated evidence will be observed. In this case the motion at all points of the surface represents no more the type of the pure Love-waves. This is interpreted by the fact that Bessel's functions of zero order are involved in the solutions of u and w. We observe that even at a certain inclination θ of the axis of the quadruplet the amounts of amplitudes at $\omega=0$ and π are the same; it will, however, be understood that this is not unreasonable when the analysis is closely examined.

The foregoing remarks are given for the sake of simplicity on such simple cases as the doublet- or quadruplet-nuclei. Some particular tendencies of them, the authors think, will exist even in more higher multiplets. The fact that the azimuthal component of displacement decreases more quickly than others is valid in any case. It also appears that the azimuthal distribution of the amplitudes (excluding the azimuthal component of the amplitude) is maintained for all radii, so that the disturbances having the azimuthal variation cannot be diffused in their wave fronts progressing outwards. It must be remarked, in addition, that the deeper the origin of the disturbances, the more quickly decrease the amplitudes of the surface waves. The rate of the decreasing amplitudes is proportional to $e^{-\alpha_1\xi}$ and therefore a small increase of the depth of the focus obliges much decrease of the surface displacement, as seen in the appended figures.

The present paper deals merely with the formation of Rayleigh-waves due to dilatational waves from a multiplet-source in the interior of the semi-infinite elastic solid body. This is equivalent to the problem of the generation of the surface waves due to the body waves from a multiplet composed of pure compressional and dilatational sources. The problems concerning distortional waves from multiplets of the type similar to the present case and of the pure distortional type will be left for the future study.

In concluding this paper the authors are indebted to Prof. K. Suyehiro who has allowed them to proceed with this problem.

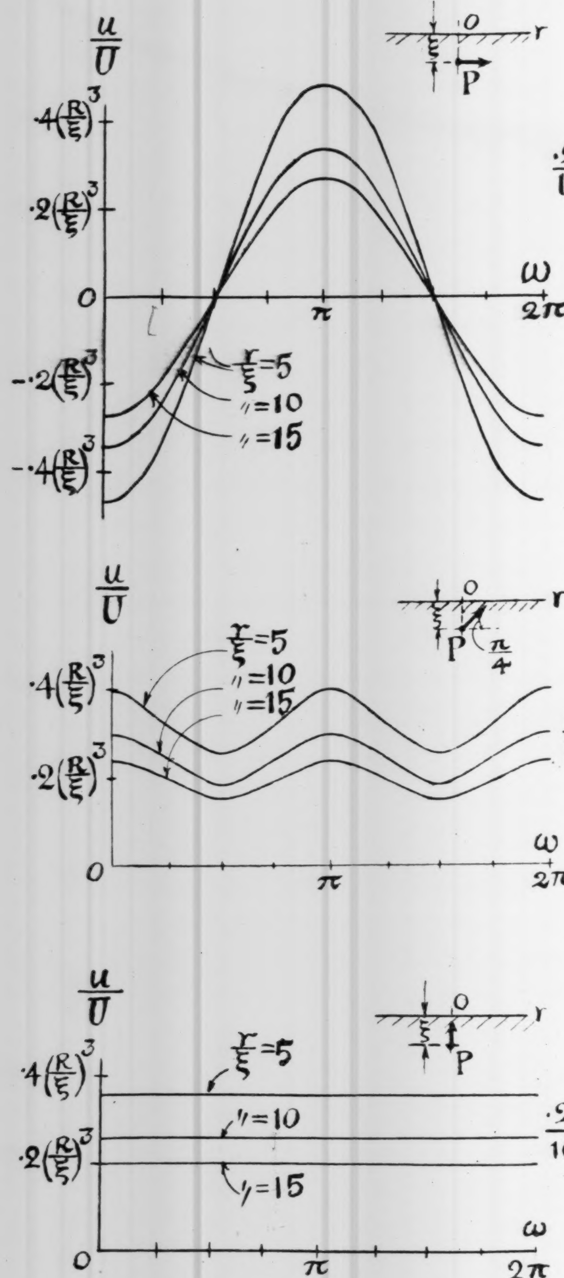

Fig: I$_a$. n=1, $\frac{\xi}{L}$=1.

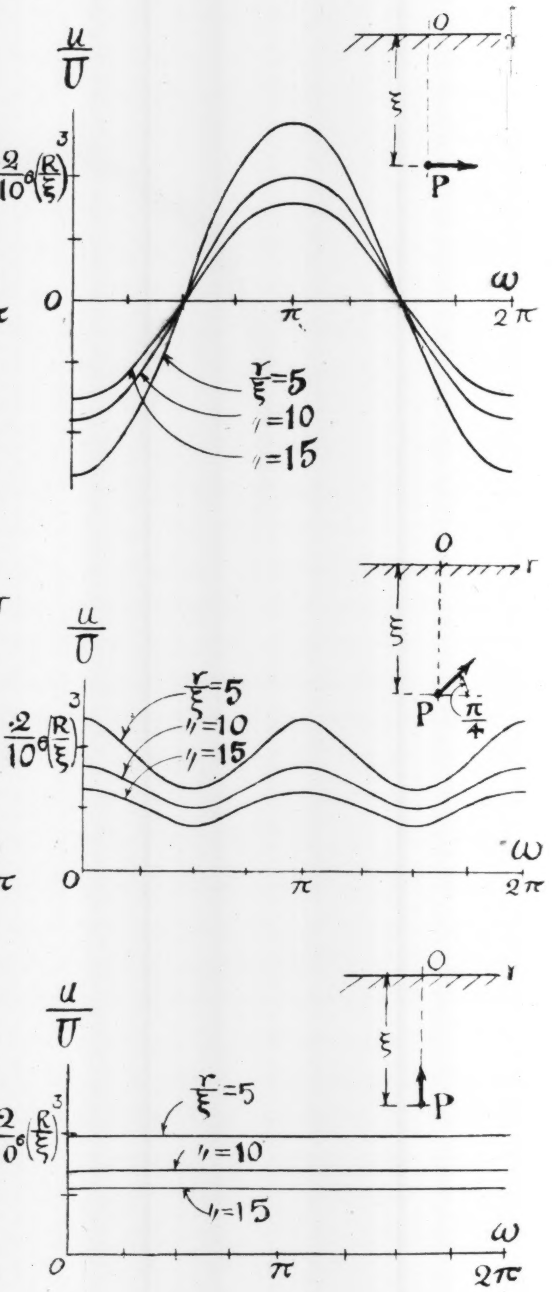

Fig. II$_a$. n=1, $\frac{\xi}{L}$=5.

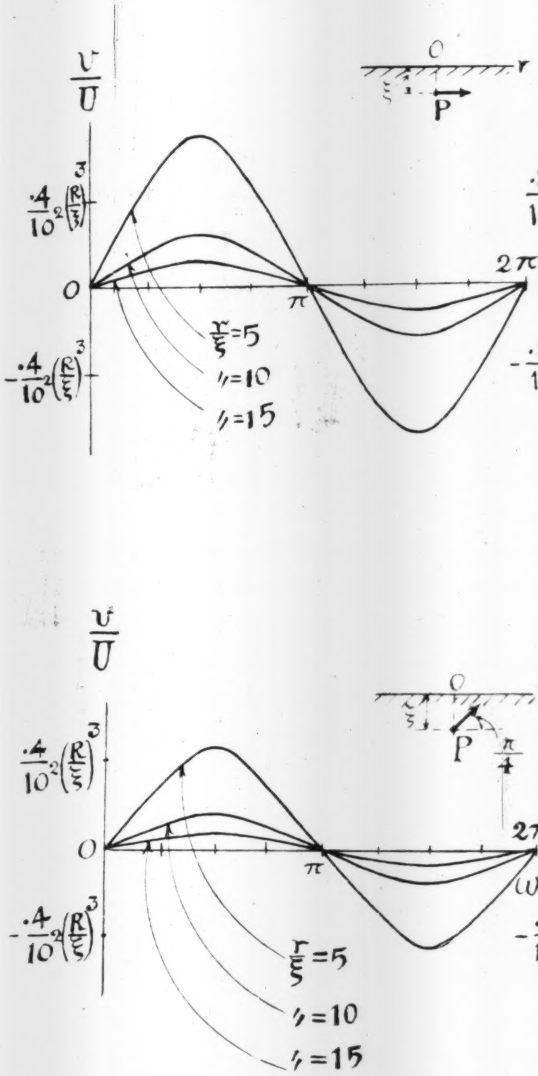

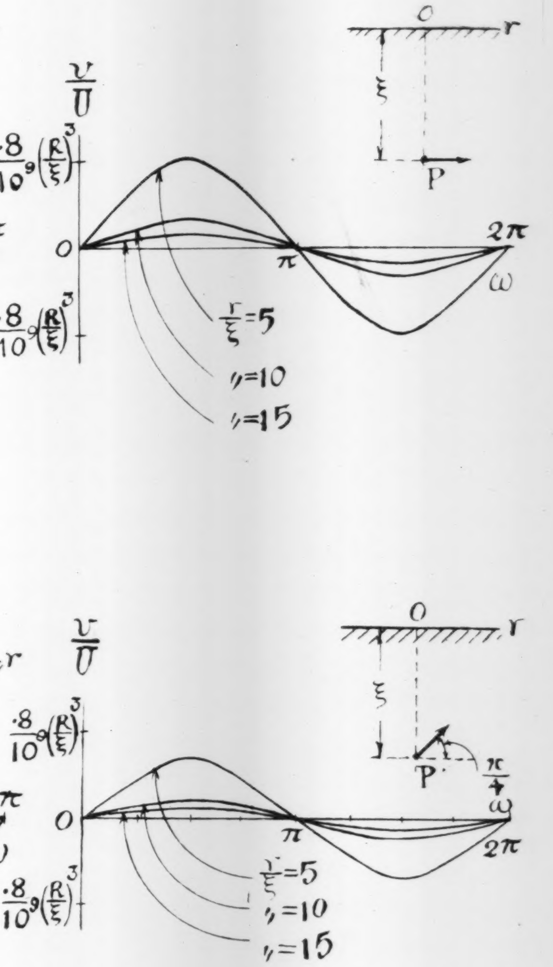

Fig. I_f. $n=1$, $\frac{\xi}{L}=1$.

Fig. II_f. $n=1$, $\frac{\xi}{L}=5$.

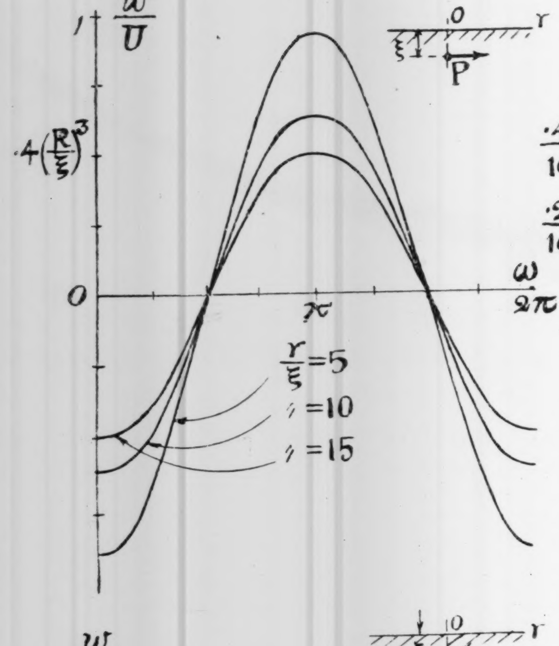

Fig. I_c. $n=1$, $\frac{\xi}{L}=1$.

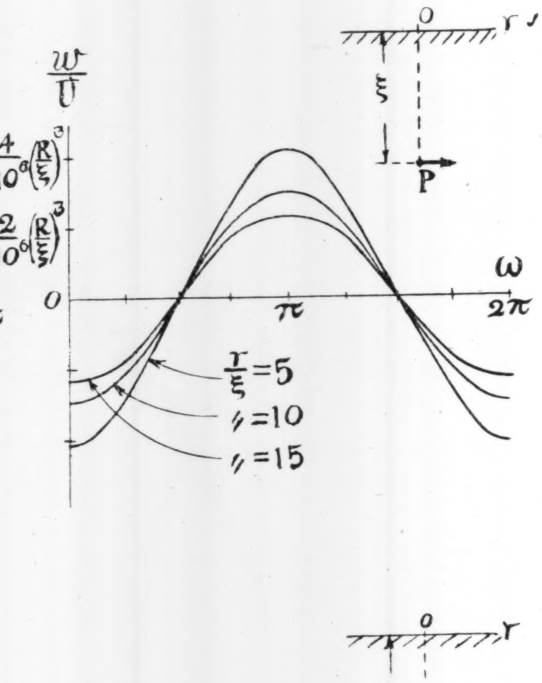

Fig. II_c. $n=1$, $\frac{\xi}{L}=5$.

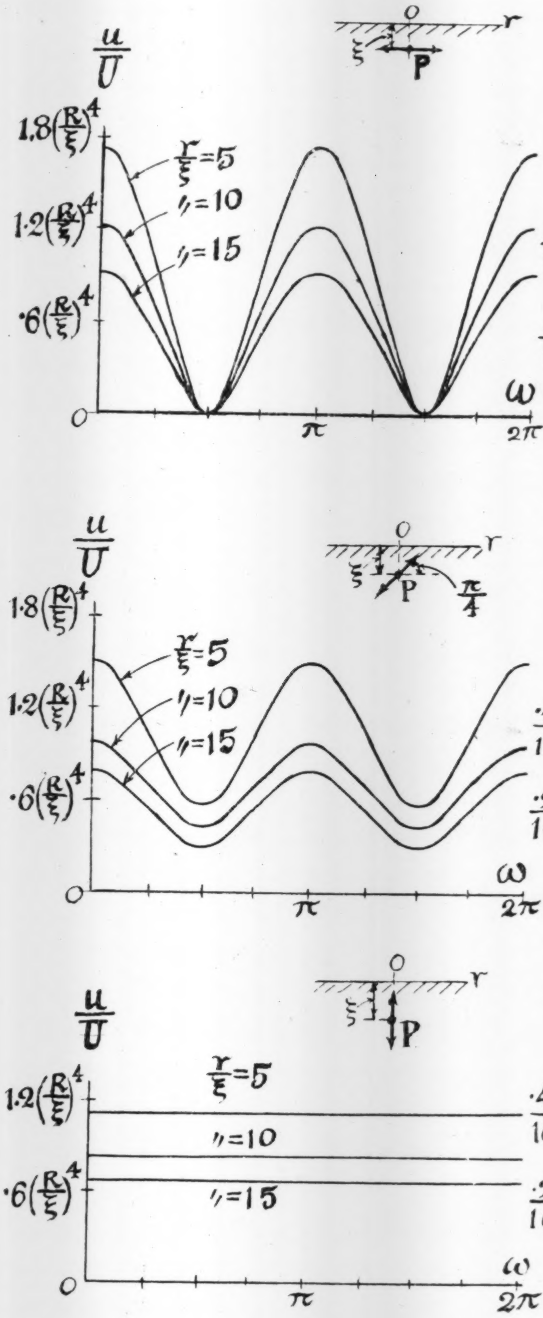

Fig. III_a. $n=2,\ \frac{\xi}{L}=1.$

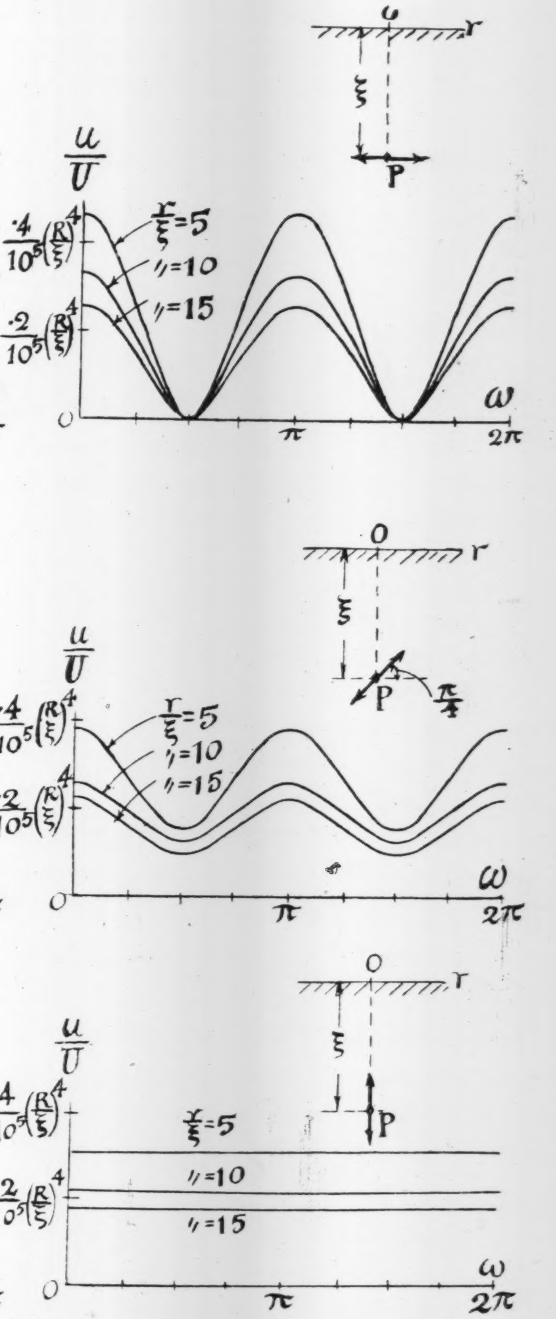

Fig. IV_a. $n=2,\ \frac{\xi}{L}=5.$

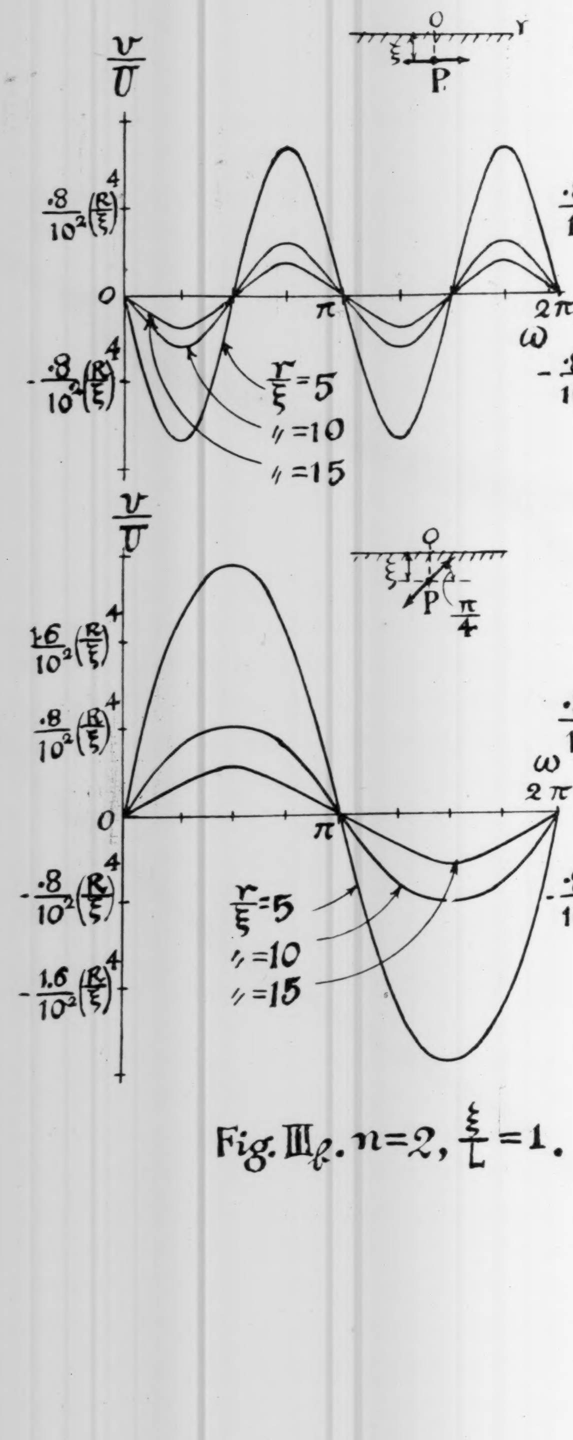

Fig. III$_b$. $n=2$, $\frac{\xi}{L}=1$.

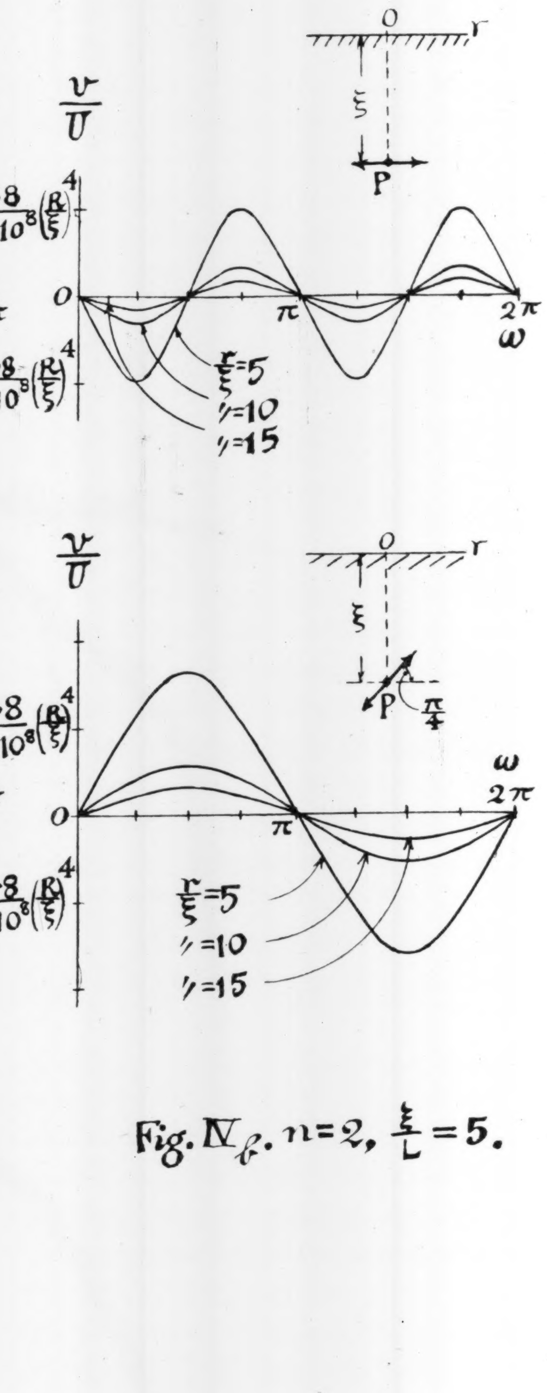

Fig. IV$_b$. $n=2$, $\frac{\xi}{L}=5$.

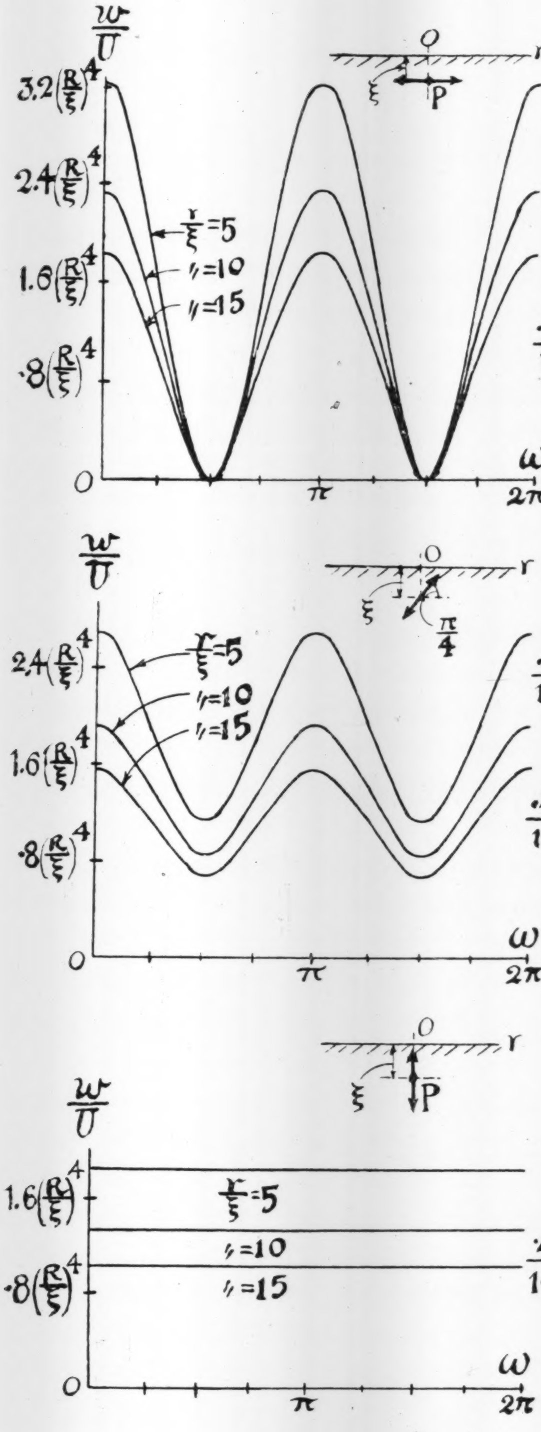

Fig. IIIc. $n=2$, $\frac{\xi}{L}=1$.

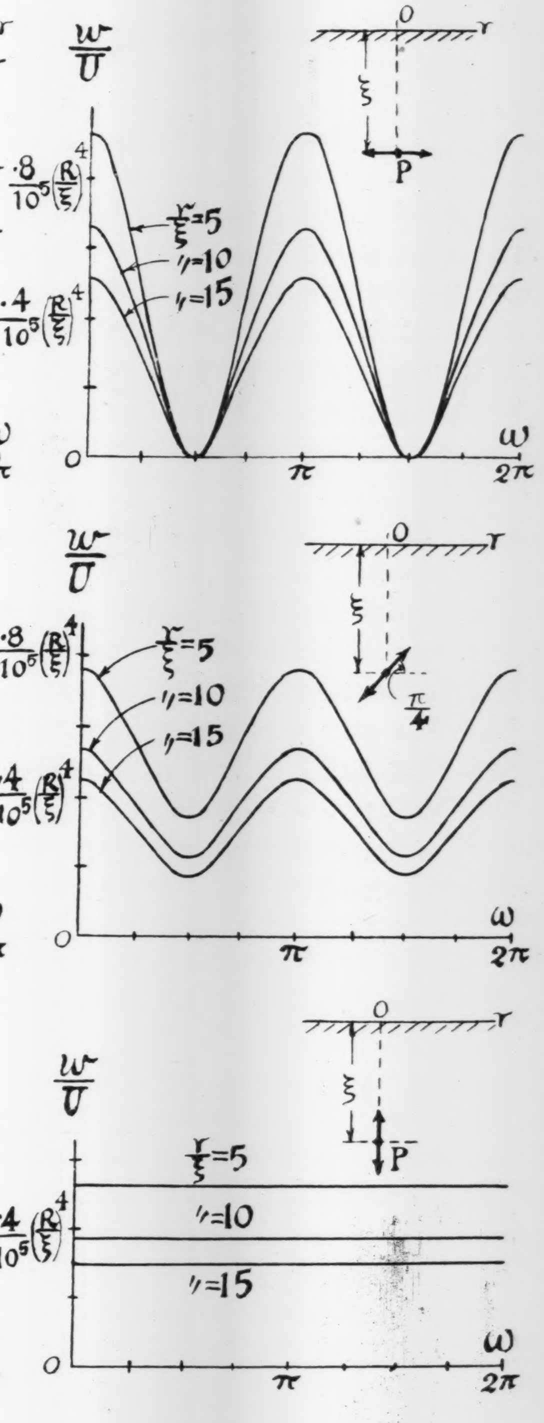

Fig. IVc. $n=2$, $\frac{\xi}{L}=5$.

3. 内部にある多重原によるレーレー波の生成

地震研究所 妹澤克惟
西村源六郎

この前の機會に著者の一人が半無限固體の內部にある二重原から出る波動によつてレーレー波が誘發される問題を論じて見たが、この論文はその繼續とも見るべきものであつて、こゝには內部の原點が多重點である場合の計算が示してある。しかしこの論文の方が遙に複雜である事は論をまたぬ。而も尙これに直接關聯する問題が殘つて居るが、其は次の時期に殘して置いた。

計算の方法は勝手な n 次の波動原を考へ、之から出る波動を圓壔函數形に變形し、且つ適當な自由波を附加して遠方へ送られるレーレー波を算出した。且つ表面波でなく固體の內部を直接に傳はる縱橫波の議論をも述べてある。

應用性のある結果を所々摘錄すれば

1. 前出の事ではあるが震央に近くラブ型波の大なる變位があるが震央から少し遠くなると次第に無くなる。
2. 普通のレーレー波に近い變位の部分は遠方まで送られる。
3. 震央の周圍にあつたレーレー波の振幅の方位的分布は其儘遠方へ送られる。
4. 震原の軸を含む垂直面が地表面を切る線上では震央の兩側に於て同振幅の表面波動が行はれると言ふ一見不思議な事柄がある。
5. 震原の深さが增すに從て深さの負價に比例する自然函數的にレーレー波の振幅の減ずる事は普通のレーレー波の場合に等しい。
6. 多重原の次數が增すに從ひ、誘發される表面波は多重原の次數以下に相當する種々の方位的分布を有するレーレー波の集まりから構成される。
7. 多重原の軸が垂直となれば表面波は單に零次のレーレー波のみとなる。

4. *Experimental Investigations of the Deformation of Sand Mass. Part III.*[*]

By **Torahiko TERADA** and **Naomi MIYABE.**

(Read March 19, 1929.—Received March 20, 1929.)

In the previous reports, the results of some preliminary experiments were described, in which a horizontal layer of sand contained in a rectangular vessel was subjected to a deformation such as to develop a series of step-faults, by horizontally receding or pressing one of the vertical side walls. Since the ordinary photographic camera was used in those experiments for photographing the successive stages of deformation, it was difficult, as already mentioned in the first report, to follow the process of deformation of a given sand layer by sufficiently close steps, with sufficiently small interval of time between the successive photograms. To avoid this difficulty, a kinematographical camera2) was employed for the further experiments which we are going to report in the following.

The other apparatuses used in the present experiments are the same as those described in the first report. The same two kinds of sand as described in the second report were used, i.e. the finer and the coarser, both in the two different states of packing, i.e. close and loose. The velocity of motion of the moving wall was chosen at 0.02 or 0.08 cm./sec. As far as the present results show, we can find no systematic difference of the results due to the difference of the velocity of this order, so that we will make no distinction between the two cases in the following description. The successive photograms were taken at a constant interval corresponding to each 2 mm. of the displacement of the moving wall.

An enlarged print was taken of each photographic film obtained and subjected to examinations in the manner which will be described below.

The two cases of receding and pressing the movable side wall were respectively repeated for the verification of the previous results. The following four cases were treated separately:

1. Finer sand, closely packed: F.C.
2. Finer sand, loosely packed: F.L.

---

[*] For the sake of future reference, the first report, this *Bull.*, 4 (1928), 33, and the second one, ibid., 6 (1929), 109, will be called Part I and II respectively.

1) Ica Kinamo was employed.

3. Coarser sand, closely packed: C.C.
4. Coarser sand, loosely packed: C.L.

For the sake of brevity we will denote these cases by the abbreviation given above to the right of the lines. For each of these cases, two or three series of the experiments were repeated for the purpose of control. The individual results of the repeated experiments for the same case varied quantitatively within a sensible range. This is unavoidable from the nature of the phenomena in which some instabitity plays an essential rôle and a slight heterogeneity in the state of packing or an accidental irregularity in the motion of the moving wall may bring about a finite difference in the results. In order to obtain any quantative average result, a great number of experiments must be repeated which would require a considerable expenditure of time and labour. Still, in the results of the present experiments, there are some essential features characteristic to different cases which may be distinctly observed in spite of these statistical variations. In the following we will take only one example for each of the above four cases and will describe those features regarded qualitatively invariant for the respective case considered.

(I) Receding Wall.

In the previous report of the experiments with the receding wall,[2] the form of the slip line was expressed by a simple algebraic curve which seemed to fit the observed curve, except near the upper and the lower ends. At the lower end of the curve the formula fails, as it makes the curve tangent to the bed plate, while the actual curve is by no means of such a form. The use of the formula was made merely with the purpose of comparing the relative inclination and curvature of different curves by comparing the coefficient k and the index n respectively.

For examining the results of the present experiments, we tried another method of reduction which seemed to suit our purpose better than the previous one.

In most cases, the slip line is nearly straight in its upper part down to about one half or more of its depth so that we may define a straight line touching or coinciding nearly with that part (Fig. 1, AB). On the other hand, a finite portion of the slip line at its lowest extremity may also generally be regarded as approximately straight so that we may always draw a definite tangent at this lower branch (Fig. 1, CD). It cannot be denied

---

2) We avoid the use of the words, "active" and "passive pressure" which are in common use among civil engineers.

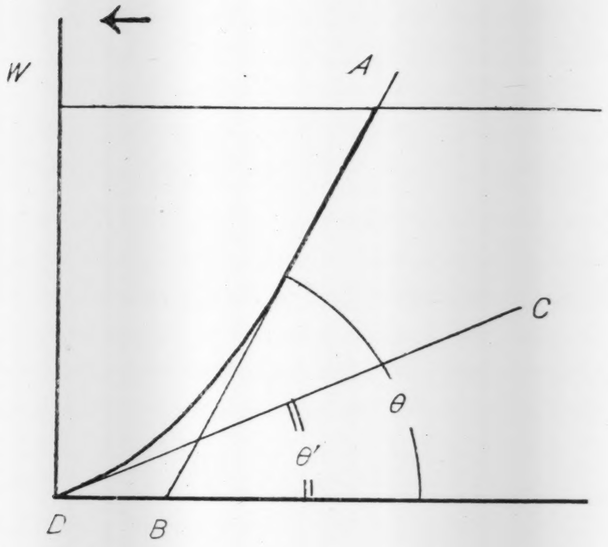

Fig. 1.

that in the case of the latter tangent, the error in determining its direction is sensibly larger than in the case of the upper tangent, but as we take a larger number of successive photograms, the general mode of its variation

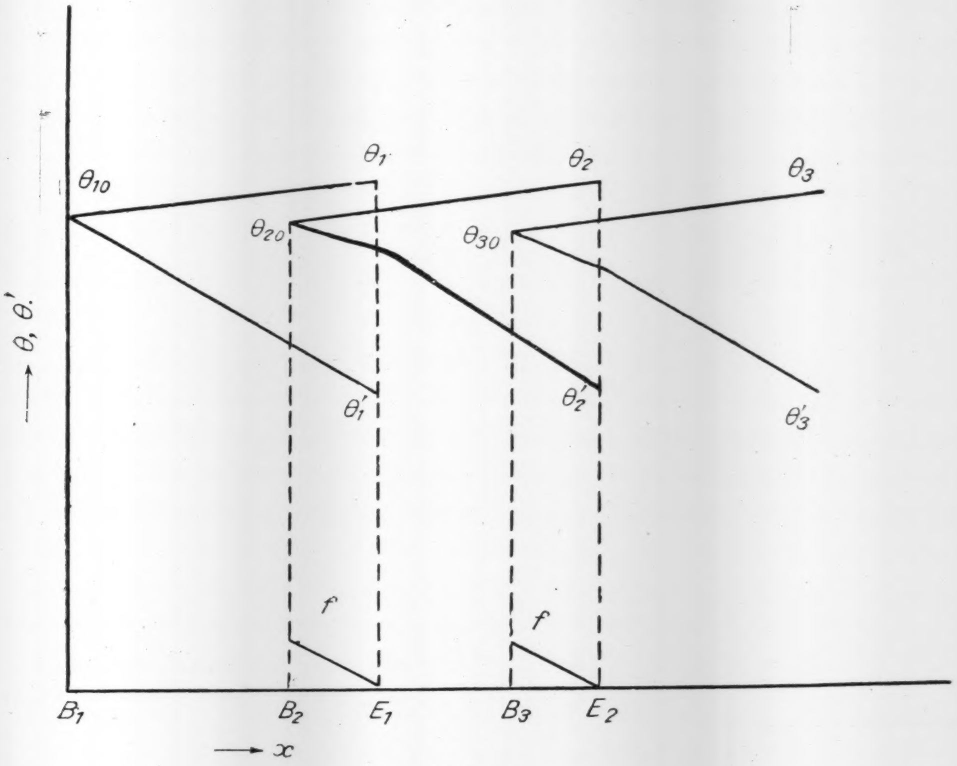

Fig. 2.

during the motion of the wall may be determined with a degree of accuracy just wanted for the present purpose. As shown in the figure the angle of inclination of the two tangent will be denoted by θ and θ' respectively.

The variation of the form of the slip line during the receding motion of the wall may then be conveniently illustrated by a digram in which the abscissa stands for the displacement, x, of the moving wall from its initial position at rest and the ordinates gives the value of θ and θ' respectively. Plotting the two angles in the same diagram we obtain two branches of curves, the upper one corresponding to the upper tangent and the lower to the lower (Fig. 2 is a schematical representation of such diagram).

As already mentioned in Part I, it may occur in some cases that two slip lines coexist and are simultaneously2) active. In such a case, two pairs

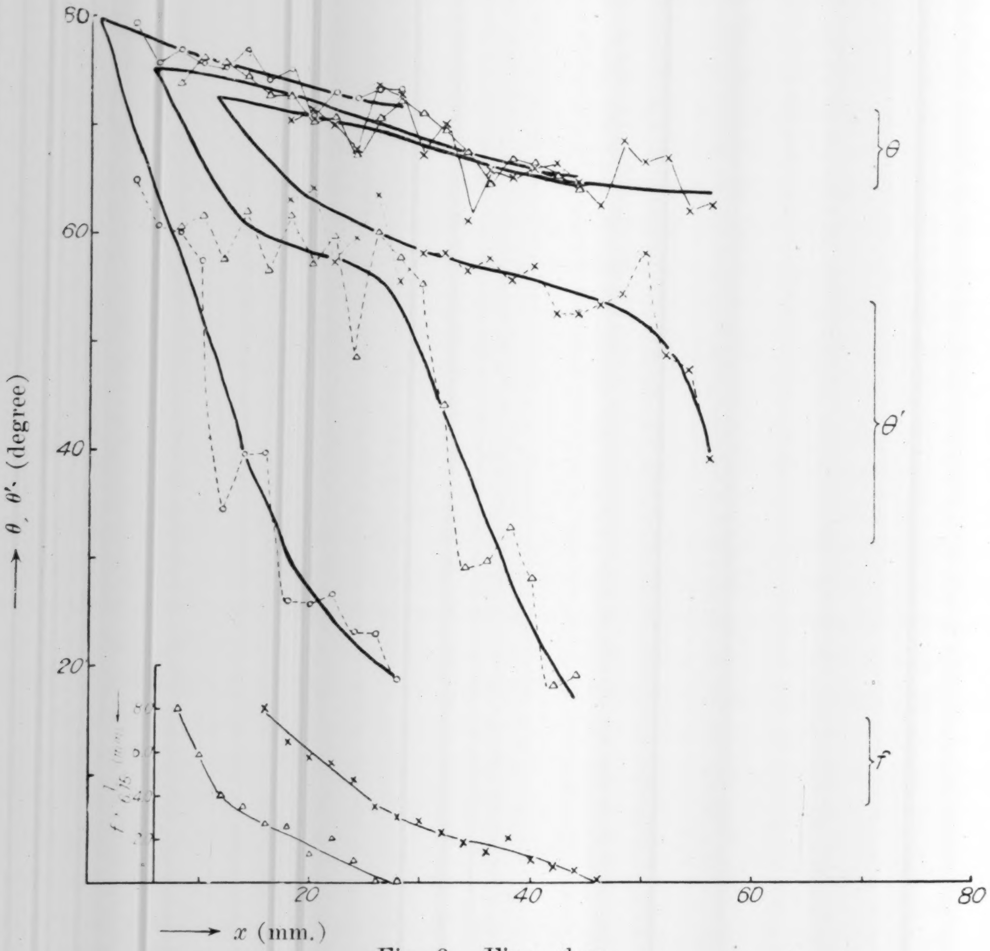

Fig. 3. Fine, close.

---

3) Or possibly alternatively with short irregular periods; at present, this point cannot be decided.

of θ and θ' (i.e., for example, θ_1, θ_1', θ_2 and θ_2'), are obtained as shown in Fig. 2 between $B_2 E_1$ or $B_3 E_2$. In some cases, especially in the case of close packing, the foot of the second (i.e. later developed) slip line does not pass the foot of the moving wall, but starts from a point of the wall at some height, say f, from the bottom (Fig. 15). In such a case, the variation of f with x will be given in the same diagram as f-curve below θ-and θ'-curves.

At the initial stage the slip line is approximately of a straight line so that θ-and θ'-curves intersect with each other at $x=0$,[4] whence the difference $\theta-\theta'$ increases with x showing the increasing curvature of the slip line. The angle between θ-and θ'-curves on the diagram is, therefore, a measure of the rate at which the curvature is increasing with x.

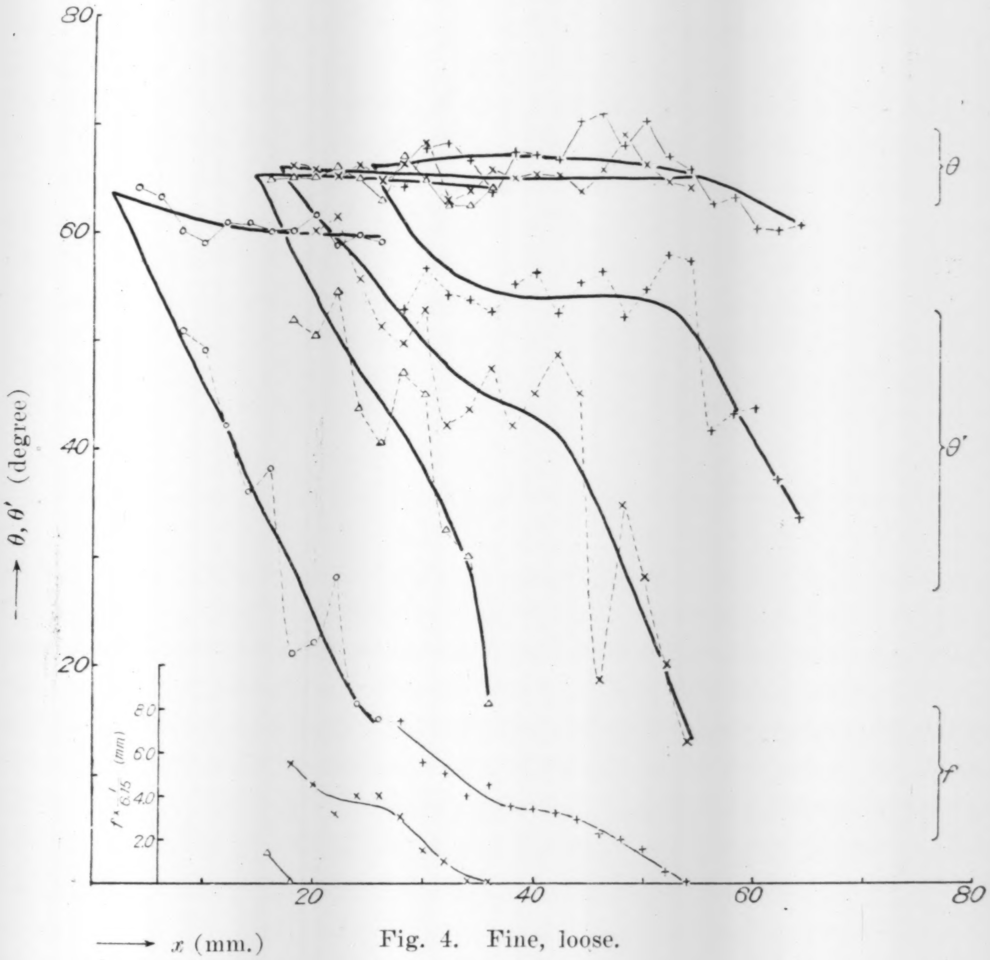

Fig. 4. Fine, loose.

---

[4] The theory of earth pressure gives $\theta=\theta'=\frac{\pi}{4}+\frac{\rho}{2}$ where ρ is the angle of friction.

With these explanations kept in mind, the different characteristics of the different cases will be easily understood from Figs. 3, 4, 5 and 6 which

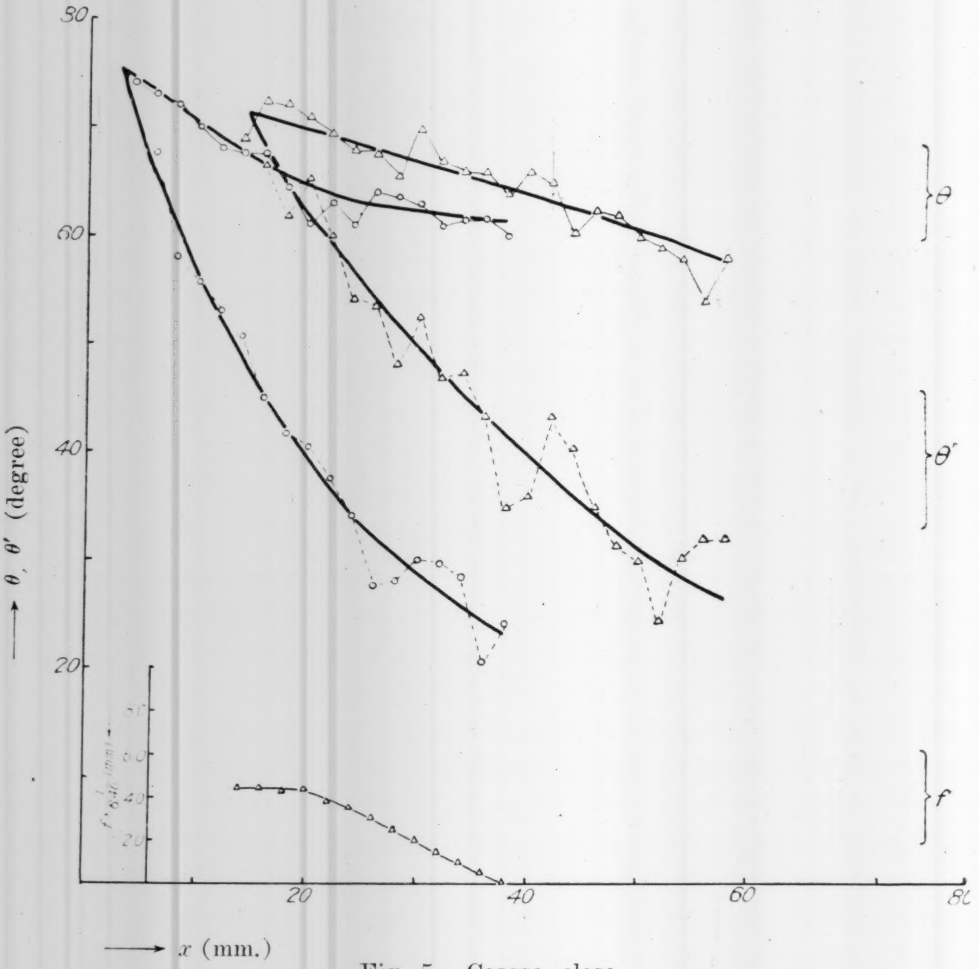

Fig. 5. Coarse, close.

respectively represent the above four cases. In these figures, the actually observed values of the angles are plotted by different marks corresponding to different slip lines and connected by thin full and dotted lines. Besides, the thick lines are drawn to show the gross features of the variations which are to be compared with Fig. 2 above explained.

From these figures, we may point out the following facts:

(1) In the case of close packing (Fig. 3 and 5), the initial value of $\theta=\theta'$ decreases successively for the successive slip lines, while in the case of loose packing it generally increases though not conspicuously. This fact may be understood if we assume that θ is generally greater for the closer packed state than for the looser one and that the sand mass initially in the

closest state is gradually loosened by the disturbance, whereas the loosest state may tend to settle down in some measure on account of the disturbance.

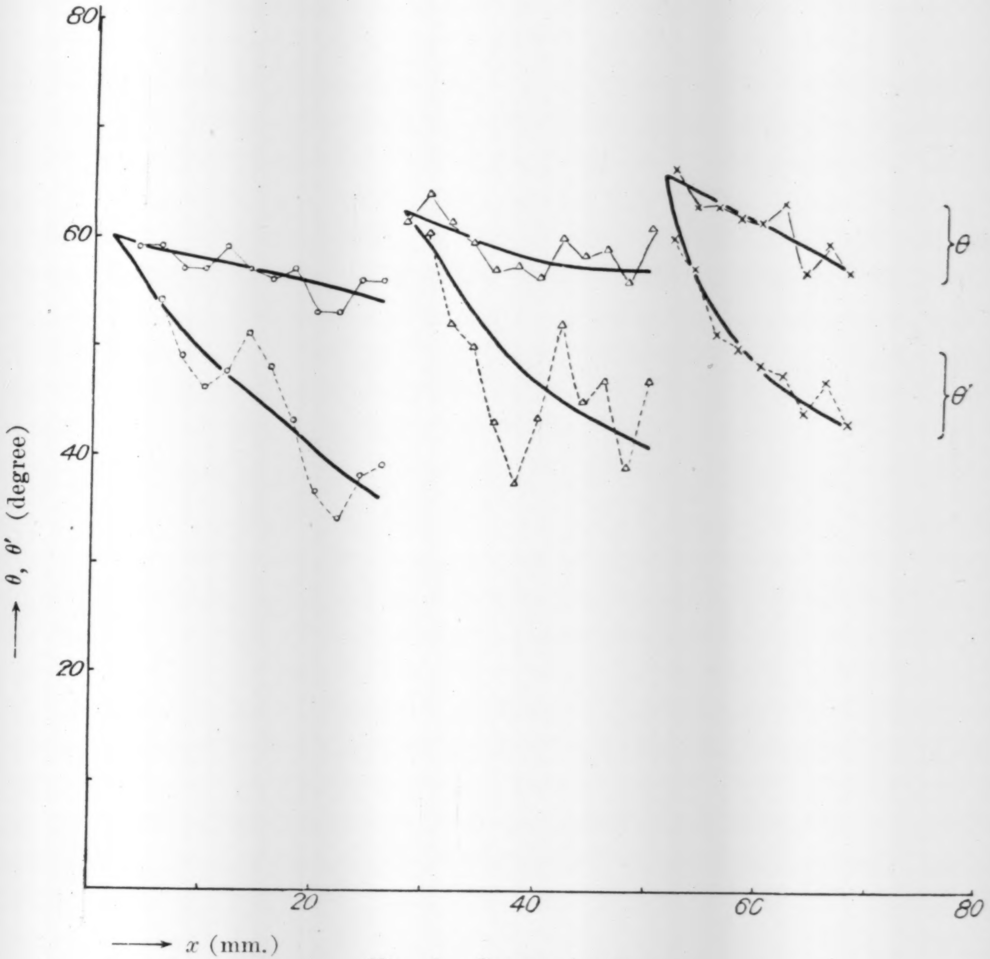

Fig. 6. Coarse, loose.

(2) The occurrence of a pair of simultaneously active slip lines is common in the three cases, F.C., F.L. and C.C., but absent in the case of C.L., i.e. the coarser sand in loosely packed state. As the development of a new slip line corresponds to the formation of a new crack in the case of an ordinary solid body, we may say that in the case of C.L. the sand between the wall and the existing first slip line behaves most "fluidous"[5] compared with the other cases, or on the other hand it may also be said to be greatest

---

[5] In other words, in C.L. state the entire mass is beset with an infinite number of infinitesimal slip lines, while, in the other cases, the shearing deformation has a tendency to be concentrated into a small number of slip lines with finite slips.

in strength, though it may sound paradoxical. The mechanism by which the simultaneous slip line may be produced will be discussed in a later section.

(3) In the case of the finer sand, i.e. F.C. and F.L. (Fig. 3 and 4), it will be generally seen that as long as the two slip lines are simultaneously active, the earlier, i.e. the lower nth. slip line is rapidly decreasing θ_n' and thus increasing $\theta_n-\theta_n'$, while $\theta_{n+1}-\theta_{n+1}'$ for the secondary or upper $(n+1)$th. simultaneous slip line varies only slowly with x. As soon as the primary slip line is stopped, the value of $d(\theta_{n+1}-\theta_{n+1}')/dx$ for the new slip line is suddenly increased nearly up to the amount formerly shown by the first slip line.

(4) In the case of C.C. (Fig. 5), the absolute value of $d\theta'/dx$ is generally small compared with the cases F.C. and F.L. and the coexisting two slip lines behave quite similar to each other.

(II) Pressing Wall.

Preliminary experiments of the case in which the movable side wall is horizontally pressed upon the vertical lateral side face of the sand layer have been described in Part II, in which the angles θ and ω (Fig. 7) giving the inclinations of the two slip lines ab and bc were measured and their variations were followed as functions of the displacement, x, of the moving wall. The same two angles were measured also in the present experiments and plotted in Figs. 8, 9, 10 and 11.

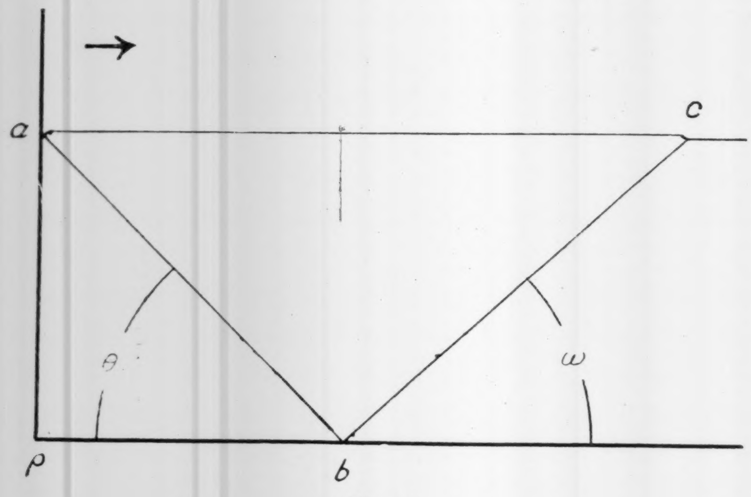

Fig. 7.

The line bc (Fig. 7) is sharply defined in photograms and there is no ambiguity in determining ω. On the other hand, the region near the line ab is really to be considered as run through by a bundle of slip lines, as

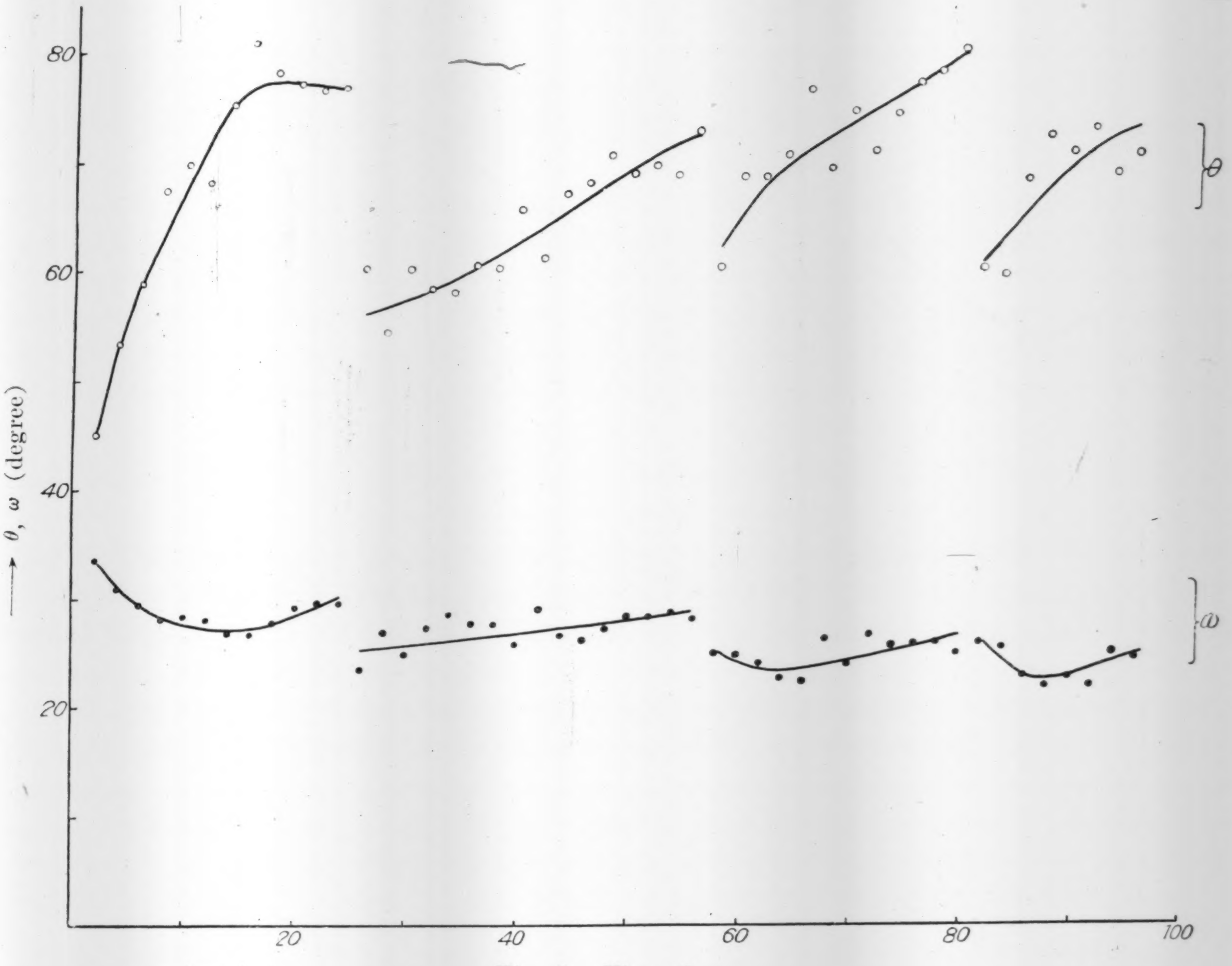

Fig. 8. Fine, close.

it is this portion which is undergoing the most conspicuous deformation, as already mentioned in Part II. Defining, however, the line *ab* as a straight line joining the foot of the line *bc* to the point *a*, the angle θ is determined and this line *ab* will nearly coincide with the boundary of the wedge-shaped sand mass *apb* moving with the moving wall, as if it were a rigid body fixed to the wall.

Fig. 12 is a schematical diagram showing the general feature of variation of θ and ω with x. When the wall begins to move on, i.e. at $x=0$, it seems that the initial values of θ and ω are nearly equal to each other. This fact is difficult to be directly verified from the photograms, but may be seen by the extrapolation of θ-and ω-curves. Besides, it is just what may be expected from the theory of plastic deformation[6] in general.

---

[6] See the discussion in the later section.

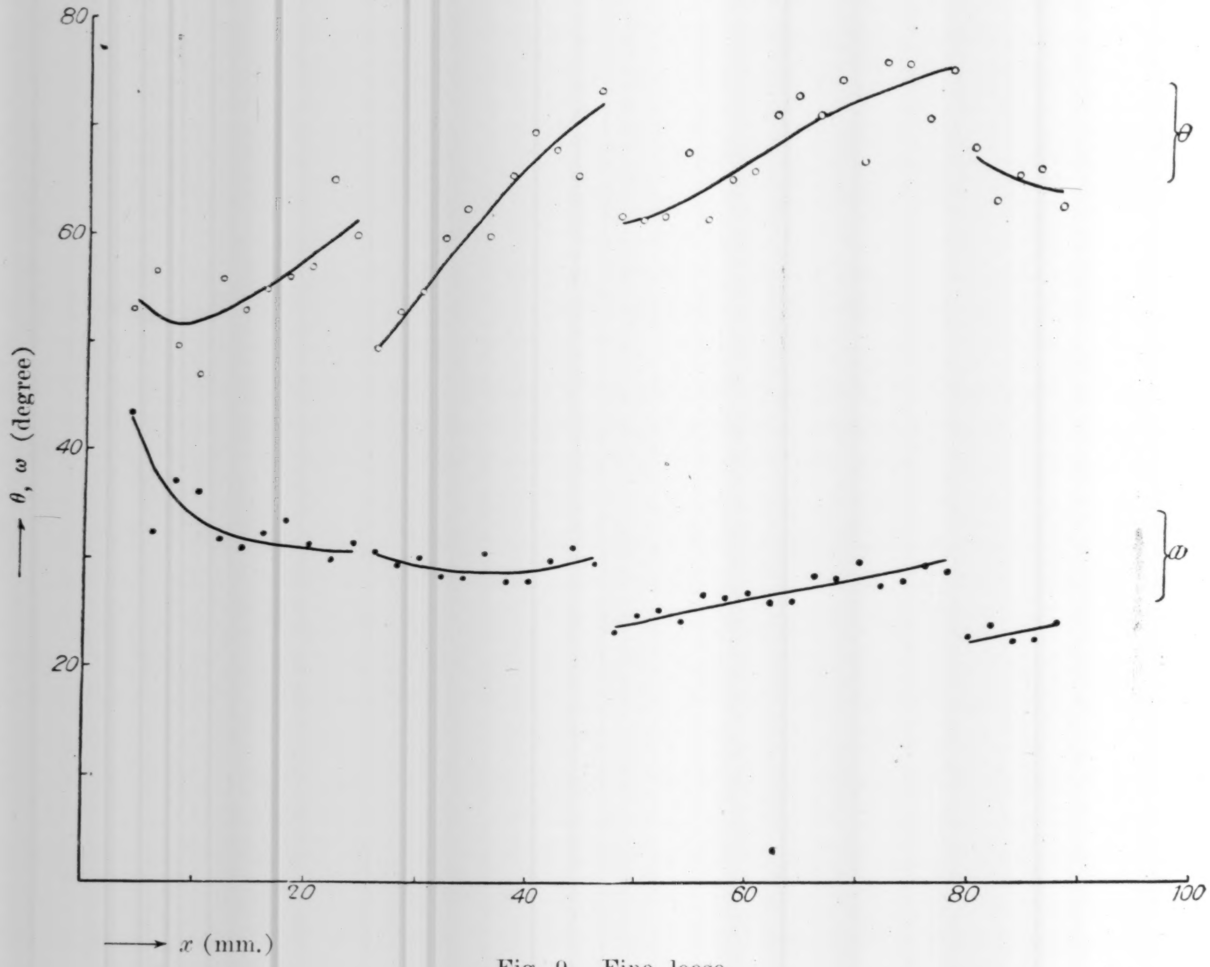

Fig. 9. Fine, loose.

At the first stage of the increase of x, ω decreases while θ increases. As x increases ω attains a minimum and, thence, $d\omega/dx$ changes its sign, while $d\theta/dx$ remains generally positive. As x increases further up to a critical point, $x=x_1$ say, θ has attained its greatest value θ_{m1} and the second slip line shoots forth, of which the initial values, θ_{02} and ω_{02} in Fig. 12, are generally less than the respective final values θ_{m1} and ω_{m1} for the first slip line. For the further increase of x, both the rates $d\theta/dx$ and $d\omega/dx$ are positive. At $x=x_2$, the discontinuity again occurs at which the greatest values θ_{m2} and ω_{m2} are reached and the third slip line appears with their initial inclinations θ_{03} and ω_{03} respectively less than θ_{m2} and ω_{m2}.

Referring to Fig. 8, 9, 10 and 11, it will be seen that the limiting values θ_0 and θ_m generally increase with the order numbers of the slip lines. On the other hand, the variation of ω_0 and ω_m with the number of the slip lines

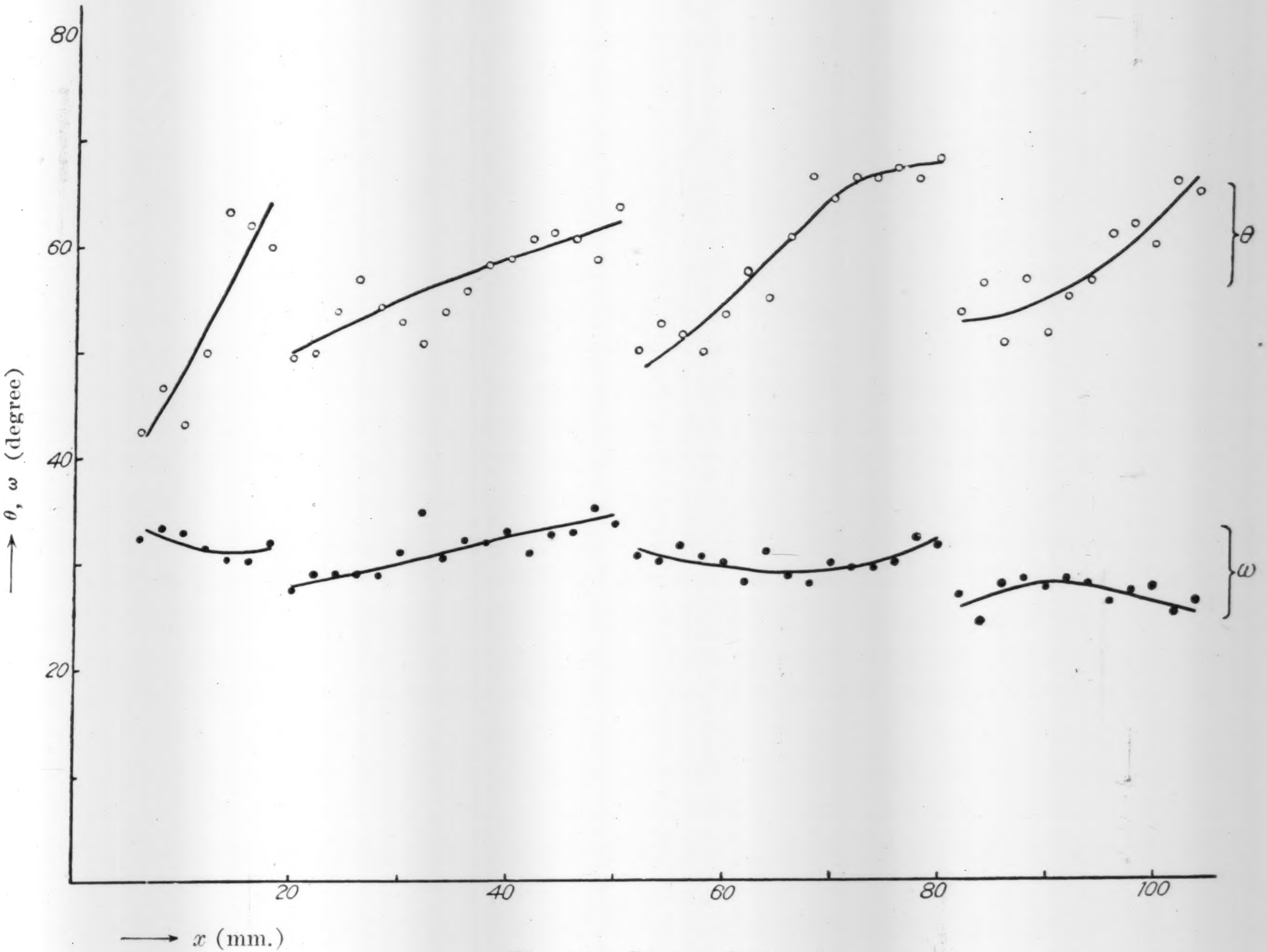

Fig. 10. Coarse, close.

is not remarkable, though a general tendency of gradual decrease may be perceived.

Thus, the qualitative characteristics of θ-and ω-curves are almost the same for the four different cases as far as above pointed out. Examining the four cases separately we may remark the following points.

(1) Comparing Fig. 8 with Fig. 10, or Fig. 9 with Fig. 11, it is interesting to observe that θ is generally greater for the finer sand than for the coarser one, while ω is smaller for F sand than for C sand. Moreover, the sum $\theta+\omega$ varies within a range nearly similar for all of the four states, i.e. not much dependent on the grain size and the state of packing. Fig. 13 shows the variations of $\theta+\omega$ for the four cases. This angle may also be considered to corresponds to the angle between the two intersecting slip planes in the lowest layer, which is a quantity defining the nature of a

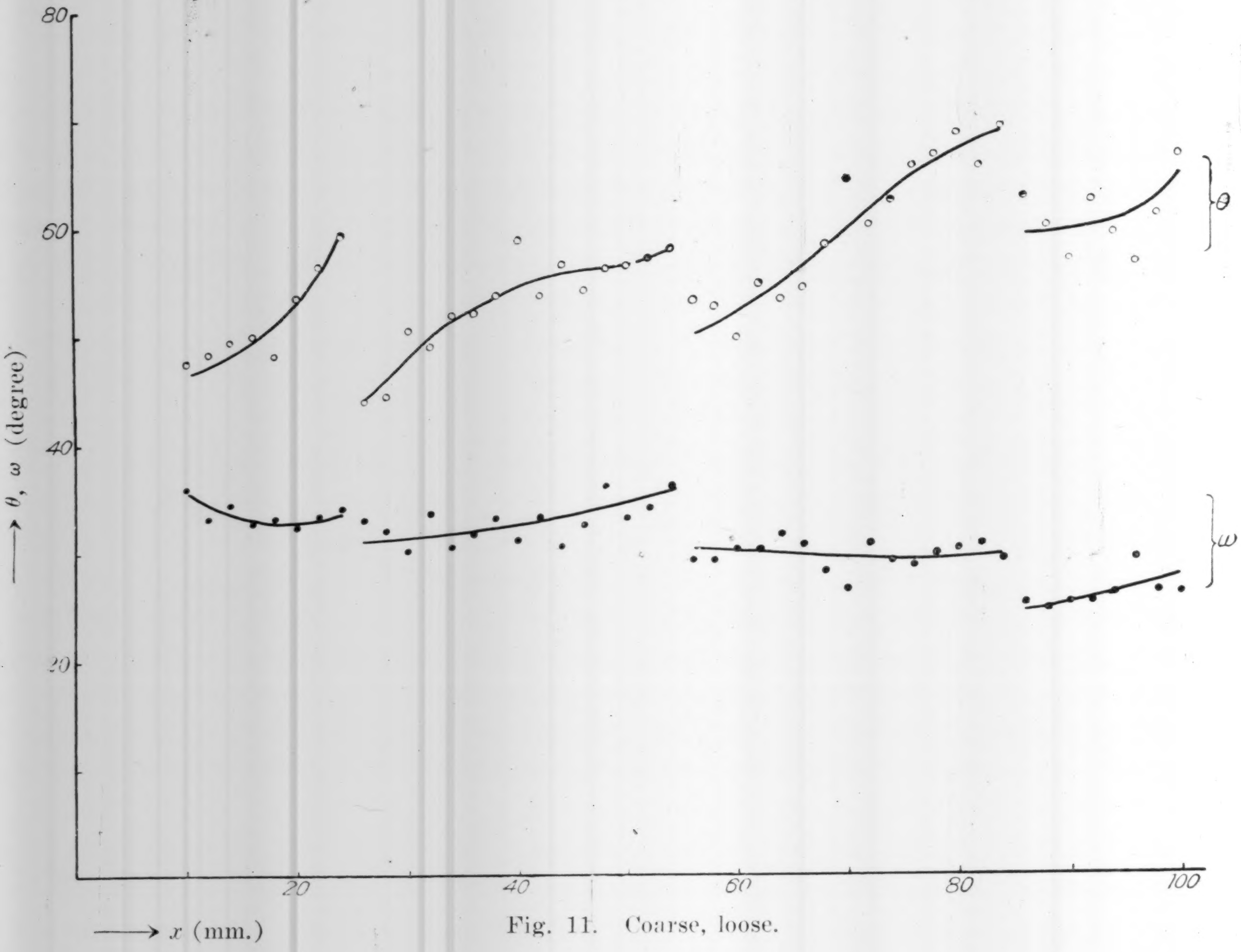

Fig. 11. Coarse, loose.

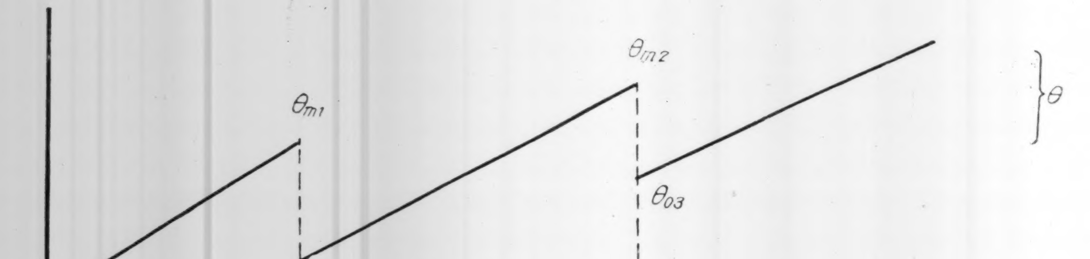
θ_{m1}
θ_{m2}
θ
θ_{03}
θ_{02}
$\theta_0 = \omega_0$
ω_{m1}
ω_{m2}
ω
ω_{02}
ω_{03}
→ θ, ω
x_1
x_2
→ x

Fig. 12.

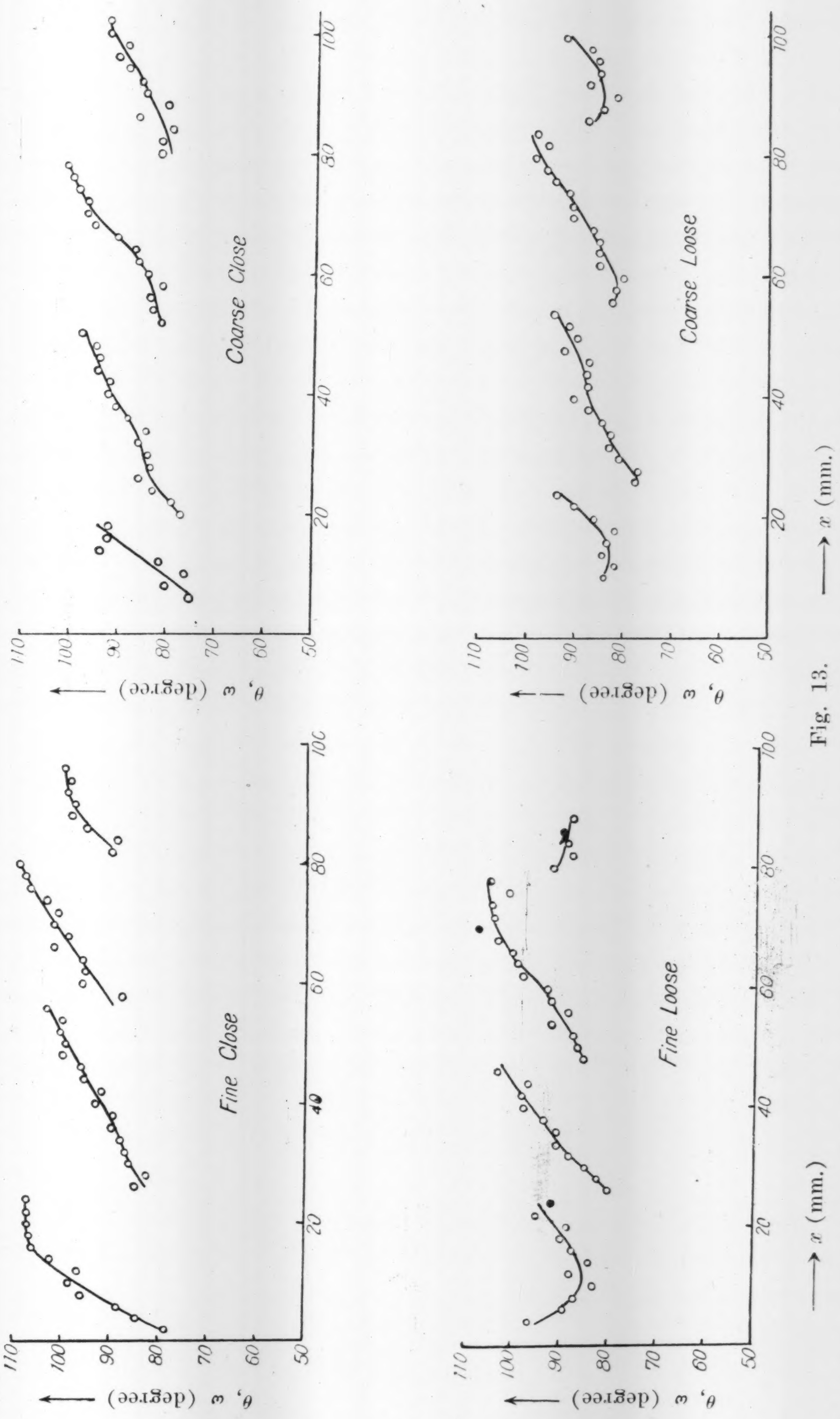
Fine Close
Coarse Close
Fine Loose
Coarse Loose
θ, ω (degree)
50
60
70
80
90
100
110
x (mm.)
20
40
60
80
100

Fig. 13.

plastic body. The physical meaning of the variation of $\theta+\omega$ will be explained later.

(2) Comparing again Fig. 8 with Fig. 9, or Fig. 10 with Fig. 11, it will be seen that the difference due to the state of packing expresses itself mainly in the mode of variation of θ and ω in the initial stage of the first slip plane. Thus, the initial value $\theta_0=\omega_0$ for $x=0$ is less for the closely packed state than for the loosely packed. Besides, as the consequence of the above fact, the initial value of $d\theta/dx$ is larger for C-state than for L-state, while the initial value of $|d\omega/dx|$ is greater for L-state than for C-state. According to the theory of plastic deformation, the initial angle $\theta_0=\omega_0$ corresponds, as will be explained later, to the angle between the slip plane and the major axis of the stress ellipse which decreases with the increasing angle of friction in the case of sand mass. As the value of this angle, ρ, for C-state is greater than that for L-state, the observed difference of θ_0 and ω_0 for the two states may easily be understood. It may be said, therefore, that the loosely packed sand is, at least apparently, transformed into a more closely packed state with the increases of x, which may mean that the disturbances due to the deformation is effective in rapidly settling down some of the most unstable state of packing.

(3) The difference between the initial values of $\theta_0=\omega_0$ for F-sand and C-sand is not conspicuous, for both the states of packing. This seems to imply that the angle ρ for the similar state of packing does not much depend on the grain size.

(III) Discussion.

In the previous reports, the preliminary results of the experiments were discussed in a provisory manner, merely with the purpose of facilitating the description of the general features of the phenomena observed. Though the results of the present experiments are still neither sufficiently systematic nor accurate to allow us any quantitative analysis, it seems proper to attempt at this stage a general review of the observed phenomena under the light of some mechanical considerations.

Since the classical treatise by Coulomb, numerous mechanical theories regarding the plastic deformation of sandy or earthy materials have already been developed, especially connected with the practical problem of earth pressure in civil engineerings and, consequently, these theories are little concerned with the further progress of deformation after the first slip has set in.

The same may be said with respect to the theory of plastic deformation of solid materials, in which the interest is similarly concentrated on the very initial stage of break-down. When the rupture has once commenced, the further mode of destruction is of little interest from the engineer's practical point of view. For the geologists and geophysicists, however, it is of prime importance to follow the entire history of the plastic earth crust through its incessant series of deformations, folding and faulting. For this reason model experiments of the kind as is here made have been repeatedly attempted in most various ways, chiefly by geologists such as Daubrée, Pfaff, Meunier, Paulke, Willis etc. In most of these cases, the physical conditions of the experiments are too much complicated to be subjected to a mechanical analysis. Our present investigations may, we hope, be regarded as taking something like a middle route between the widely diverging lines of research taken respectively by engineers and geologists, though it is only a first small step which has thus far been taken towards this direction.

The existing theories of earth pressure and plastic deformation[7)] are exclusively concerned with statical problems. Though our cases are also nearly statical, in the sense that the kinetic energy plays no important rôle, they are still much complicated by the fact that the stress distribution in the deforming mass varies continually with the progress of deformation which is in its turn governed by the said distribution. It seems, therefore, difficult to make any direct application of the elaborate analytical theories of Prandtl, Hencky, Reissner, Kármán, etc. to the present case. At the present stage, however, the consideration of the distribution of stress ellipses among the sand mass as indicated by the observed slip lines seems to be just suitable for the general discussion of the qualitative results as hitherto observed. In the following we will mainly follow the method given in H. Krey's "Erddruck, Erdwiderstand," third edition, 1926.

In a sand mass which is characterized by a given angle of friction, ρ, a limiting value, n, is determined of the ratio, $p/q=r$ say, of the major axis p to the minor axis q of the stress ellipse, to which the ellipsoid reduces in our present cases, by a relation

$$\operatorname{tg} \rho=\frac{n-1}{2\sqrt{n}}\,.$$

Thus, when the ratio r increases and reaches the critical value n, the slip will take place along a slip line (plane) making an angle κ with the major axis such that

---

7) A concise summary of these theories has recently be given by Nadai in Geiger and Scheel's "Handbuch der Physik." **4**, and also in his book "Der bildsame Zustand der Werkstoffe," 1927.

$$\operatorname{tg} \kappa = \frac{1}{\sqrt{n}} \cdot$$

Thence, if ρ is given for the given sand, we may at once find the general orientation of the stress ellipse along any observed slip line, though some complication will occur near the solid walls.

In the vicinity of a wall, the friction between the wall and sand must be taken into account in which case we may, after Krey, distinguish four cases, according as the modes of the relative motion of the sand and wall. In our present case we may simplify the matter by the assumption that the angle of friction between the sand and wall is equal to ρ, as is approximately true. In such a case, the angle between the sliding wall and the major axis of the ellipse is just equal to the angle κ above given. Besides, the slip line running into the sand mass from the wall will be inclined to the wall by an angle 2κ, which is bisected by the major axis of the ellipse. The direction of the stress acting upon the slip plane is naturally inclined by ρ to the normal of the plane. The two cases, therefore, chiefly come here under consideration, according to the relative sense of motion on the two sides of the slip line:

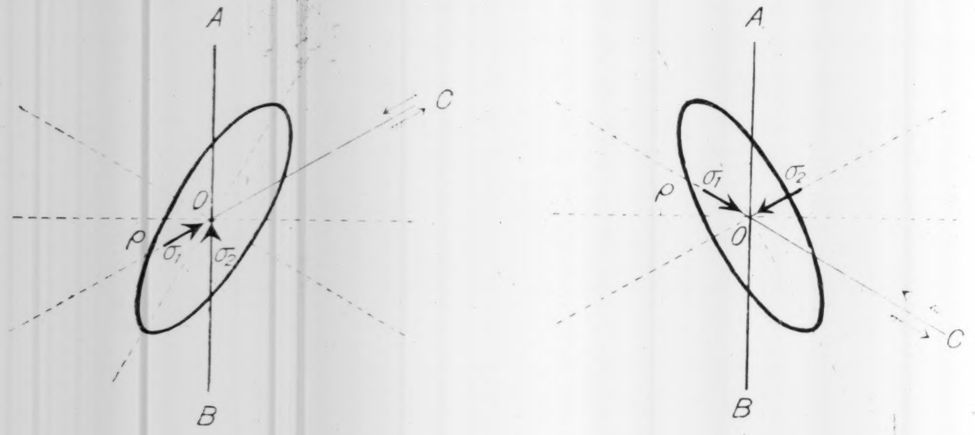

(a) (b)

Fig. 14.

(I) If, referring to Fig. 14*a*, the sand mass on the right side of the receding vertical wall AB is considered sliding down along it, the pressure from the wall, σ_1 in Fig., must be directed from left down to right up, inclined by ρ to the horizontal.

(II) On the other hand, if the sand is sliding up along the pressing wall, the case is such as shown in Fig. 14*b*.

In each of these two cases, there is another possible slip line shown by OC running into the sand mass. In the cases of our experiments, the relative motion of sand on both sides of this slip plane OC will be such as shown by the pair of winged arrows and the direction of the pressure upon the slip line will be represented by the thick arrow σ_2. The cases of Fig. 14*a* and *b* will correspond respectively to the cases of receding and pressing wall.

With the above considerations kept in mind, we will attempt some discussions of the results described in the foregoing, for the two cases separately.

(1) The case of receding wall.

Referring to Figs. 3, 4, 5 and 6, it was found that the slip line observed is generally curved and while the angle of inclination θ of the upper branch varies only slightly, the inclination θ' of the lower part rapidly decreases with the displacement x of the moving wall.

Assuming roughly $\rho=30°$,[8] corresponding to $n=3$ and $\kappa=30°$, the fact that $\theta \fallingdotseq 60°$ will mean that the major axis of the stress ellipse is directed nearly vertical in the region near the free surface of the sand layer remote from the moving wall (Fig. 15). On the other hand, if we find $\theta' \fallingdotseq 30$, it will show that the state of stress at the foot of the moving wall is just corresponding to the case represented by Fig. 14*a* above.

In the first outset of deformation, we may assume that the stress ellipse is everywhere nearly circular. With the infinitesimal receding motion of the wall, the horizontal diameter of the circular ellipse will be reduced by some amount, depending on the position of the point considered. In any case, we may expect the initial orientation of the major axis to be more or less vertical. With the increasing deformation and the beginning of slip along the wall, the condition near the moving wall will approach the state of Fig. 14*a*, while the region remote from the wall will preserve the initial state with the vertical ellipse, except the possible change due to the change in the value of ρ, i.e. of θ, which depends on the state of packing and therefore may be affected by the deformation. The observed decrease of θ with the increase of x in the case of the closely packed sand (Figs. 3 and 5) may chiefly be due to this latter cause. The assumption $\rho=30°$ will give the ultimate value of $\theta'=30°$ which is roughly verified by the experiments.

---

[8] The actual value of ρ determined from the natural slope varies within a range 30°–40°, according to the states of packing; the corresponding range for $\pi/4+\rho/2$ is 60°–65°. The actual effective range within the sand mass seems to be much greater.

Referring to Fig. 15, the region on the right side of the first slip line I, AD, is behaving nearly as a rigid or elastic body; in other words, the axial ratio r of the stress ellipse is less than the critical value $n=3$, while on the left side of AD the ratio is equal or greater than n. As the motion of the wall is continued, we may suppose that the axial ratio r in the region ADW (Fig. 15) is constantly tending to recover its initial value 1. This is facilitated by the fact that the slip line I once started to activity has a tendency to remain as such, because the value of ρ in the much disturbed layer along, and near, the line I will be decidedly decreased and, therefore, the shearing stress in the region to the left of AD may be gradually relieved, except near the moving vertical wall. Thus, we may expect that, somewhere in the midway between AD and WD, the ratio r may eventually fall back just below n. In this case the right side of this portion will regain the condition $r < n$ and become "solidified", so to speak, while on the left side, r will be everywhere $> n$. Thus, a new slip line, II in Fig. 15, will appear as a necessary consequence.

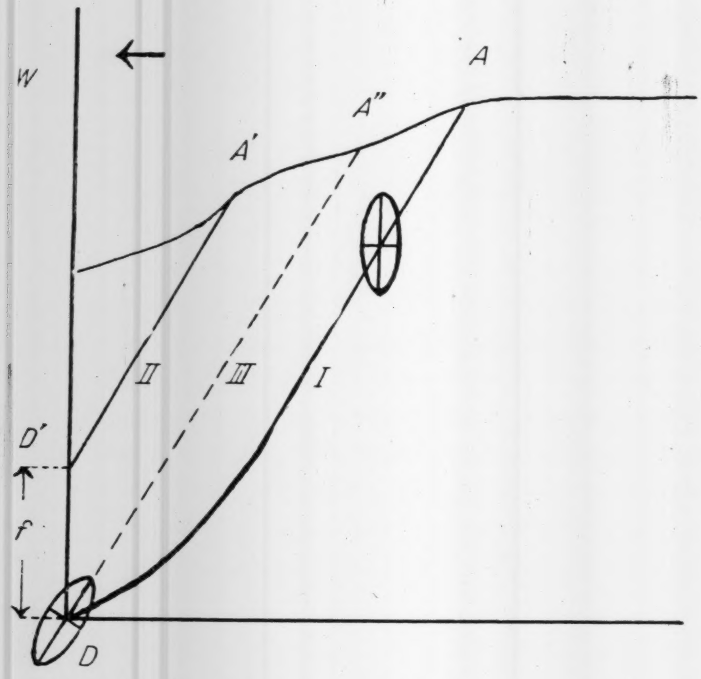

Fig. 15.

The fact that $d\theta/dx$ for this new slip line is small may be explained if we consider that at the foot of this secondary slip line, D′, the downward motion of sand must be continuous along the wall and thence just near the wall the condition of Fig. 14a is not quite fulfilled.

In Fig. 3, 4 and 5, the variation of the height f of the point D′ is plotted at the bottom of each diagram. It will be seen from the value of df/dx that the downward motion is decidedly slower than if the line A′D′ be fixed in space and the wall only be receding. The line A′D′ seems to retain its position rather relative to the sand mass ADD′A′ which is sliding as a whole along the slip line I.

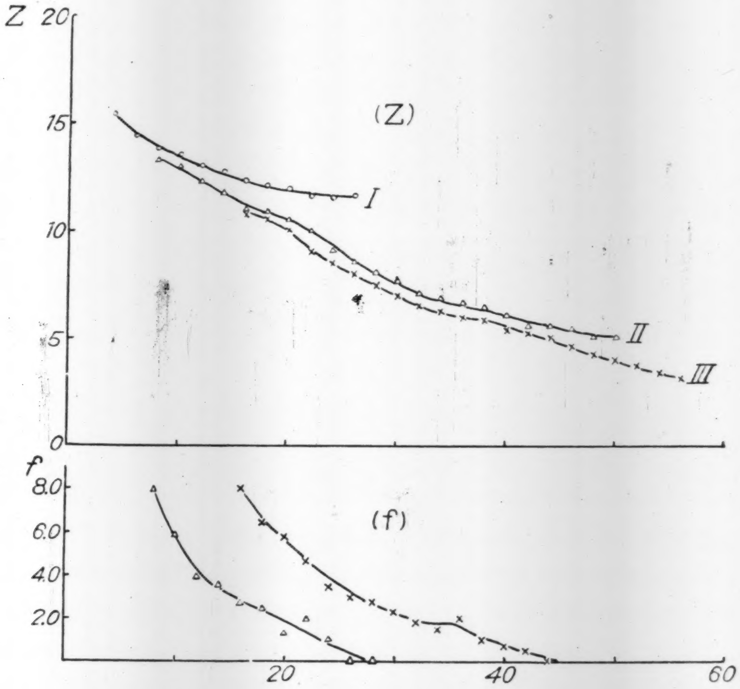

Fig. 16. Z is measured for the uppermost mark line;
I, in front of the first slip line,
II, „ second „ „ ,
III, „ third „ „ ,
Z and f are given in mm. measured on photograms which is 1/6.15 natural size.

Fig. 16 shows the variation of the height, f, of the foot, D′, of the second slip line, II, (Fig. 15), compared with the variation of the height, Z, of the horizontal mark line of white sand in the region between the two slip lines I and II. The two curves, f and Z, show a nearly similar trend. As Z is, however, measured at the middle point of the segment of the white mark line cut off between the two slip lines, it may be understood that f-curve must be a little steeper than Z-curve, if the second slip line is nearly fixed with respect to the sand mass gliding along I, though possessing a small relative downward velocity relative to it.

Referring again to Fig. 15, when the point D′ approaches D, its motion is slackened as may be seen from f-curve of Fig. 16. When D′ coincides with D, the first slip line I decreases in its activity and II is now ready to take the place of I.

In the case of the finer sand, it occurs sometimes that the second slip line takes from the beginning such a form as shown by III in Fig. 15, i.e. $f=0$. Even in such a case, the two slip lines I and III may be simultaneously active for a certain interval of time.

All these phenomena seem to be conveniently explained referring to the schematical diagram Fig. 17. Taking a horizontal layer of sand in its initial undisturbed state we denote the position of any elementary portion of sand by a *parameter* ξ which is the initial distance of the element from a fixed point remote from the moving wall. Let this parameter define the said element relative to the entire mass, regardless of its actual distance from the origin during the progress of deformation. Our ultimate problem will be to give the coordinates of the element as a function of ξ and t, which we will, however, not venture in the present paper.

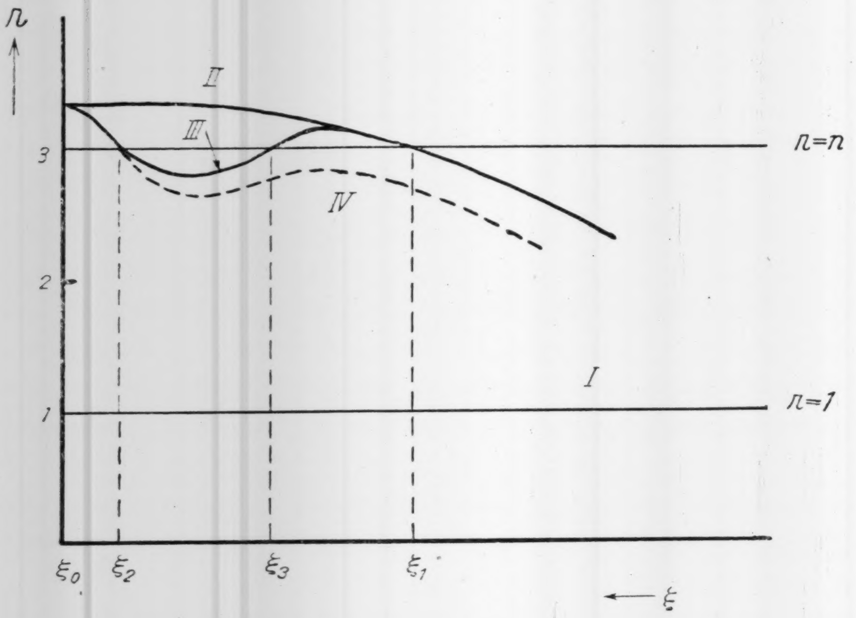

Fig. 17.

For every value of ξ we may consider associated a definite value of the axial ratio r of the stress ellipse which is a function of ξ and the time t, or the displacement of the moving wall x. Besides, if the height of the initial layer be taken as another parameter, η, we have

$$r = F(\xi, \eta, x).$$

The same may be said with regard to the angle of inclination of the major axis of the ellipse.

Referring to Fig. 17, we will consider the variation of r as the function of ξ only, taking as η constant. For a given postition x of the moving wall, we will have a corresponding (r, ξ) curve. In the initial undisturbed state r will be nearly equal to 1 for all values of ξ, so that (r, ξ) curve is given by the straight line I parallel to ξ-axis. When the receding wall is set in motion, (r, ξ) curve will tend to take such a form as shown by II. If this curve cuts the line $r = n$ at $\xi = \xi_1$, a discontinuous slip line will be developed at ξ_1 and the region between the wall, $\xi = \xi_0$ and ξ_1 will be subjected to plastic shearing, while the mass beyond this point will remain nearly rigid or elastic. By the later process of deformation (r, ξ) curve will be subjected to an irregular fluctuation due to the heterogeneity in sand and the irregularity of motion due to it. As the portion in the midway between ξ_0 and ξ_1 has a tendency to settle down, as already mentioned,[9] (r, ξ) curve may tend to assume such a form as shown by III (Fig. 17). Then, a new slip line will start at $\xi = \xi_2$ and the portion between ξ_2 and ξ_3 will behave nearly as rigid. Later, (r, ξ) will take a form such as shown by IV (Fig. 17) in which case the first slip line at ξ_1 will stop, and so on.

The hypothetical variation of (r, ξ) curve with the increase of x as above depicted is just what we may expect in the actual case, if we consider that by the initial displacement of the wall the horizontal component of stress is released by an amount the greater the nearer the moving wall, while on the other hand the moving sand has a tendency to recover the hydrostatic state as soon as the disturbance subsides. If we consider, moreover, the constraint introduced by the friction of the bed plate of the vessel, we may conclude that the point ξ_1 will appear the nearer the moving wall the lower the layer considered. This latter point will be probably important in ensuring the stability, i.e. the tendency to remain as such, of the slip line as a whole.

The theory of infinitesimal slip has really nothing to do with the development of a *stable* line of discontinuity with a *finite* slip as is here mainly in question, but gives only a swarm or net-work of mutually intersecting system of possible slip lines. In order to explain the actual phenomena as are here observed, it is, therefore, necessary to consider some process which may tend to concentrate the theoretical swarm of the in-

---

9) I.e., as an element with a given ξ is increasing its distance from the moving wall.

finitesimal slip lines into a definite slip line, or lines, with finite slips. The idea expressed in the above Fig. 17 seems to throw some light on this point. The said concentration implies the existence of some factor of instability which is afforded by the fact that ρ or n is sensibly reduced below its normal value in the region adjoining the slip plane. Referring to Fig. 17 we may say that at ξ_1 and ξ_2 the curve for n will not be given by the straight line I, but will show a sensible depression near these points; in other words, this region will approach the fluidous state compared with the other parts. The other parts will thus be partly relieved from the shearing stress and tend to reduce the ratio r; moreover, even a slight elevation of n-curve at these parts is probable, which will enhance the settling down of these parts.

In the case of the coarser sand in loose state, the said depression of n-curve near the slip line may be expected to be less accentuated than in the other three cases, since the initial state is already sufficiently loose and the corresponding n is near its lower limit.

Another condition for a stable finite slip line is that it will start from a singular point, i.e. a point at which the boundary condition is discontinuous. This fact has rarely been emphasized, but is of vital importance in the case of finite slip. At the foot of the wall, in the case of receding wall, both p and q tend to zero and r becomes indeterminate, or, in other words, the fluctuation of r is very large so that any slip line must pass this point.

(2) The case of pressing wall.

In the case of pressing wall, we have seen that the initial value of θ and ω are nearly equal. This seems to mean that the major axis of the stress ellipse is everywhere horizontal and $\theta=\omega=\rho$. This is just what we may expect from the theory of plastic deformation. The case is, indeed, somewhat analogous to a special case of the problems treated by Prandtl[10] and others with respect to the "special" plastic body, for which Mohr's "Grenzkurve" is a pair of straight lines parallel to σ-axis. It is, indeed, very interesting and instructive to compare the case of the photograms of slip bands developed in paraffin prism, as given in Nadai's book (p. 82 and 83) above cited, with the present case. In the present case of sand, Mohr's limiting curves is not parallel but inclined to σ axis by ρ, so that the orthogonal net of slip lines in the former case will appear transformed into another net with the angle of intersection equal to $\pi/2-\rho$. Another point of essential difference is that in the present case the bed plate of the vessel may play an important rôle, while in the case of the paraffin prism such a boundary condition is absent. Since, however, the bed plate is situated in the regions where the plastic limit is not attained, i.e. on one side in the region at rest and on the other in the part moving as a rigid wedge, the comparison with the pressed paraffin prism is not quite illegitimate and may be freely utilized in our discussion as long as the qualitative features are in question.

---

[10] For the literature see Nadai, *loc. cit.* For example, compare the case of a prismatic body pressed upon one of the lateral face, *ZS. f. angew. Math. Phys.*, **1** (1921), 15–20, Fig. 2 and 7.

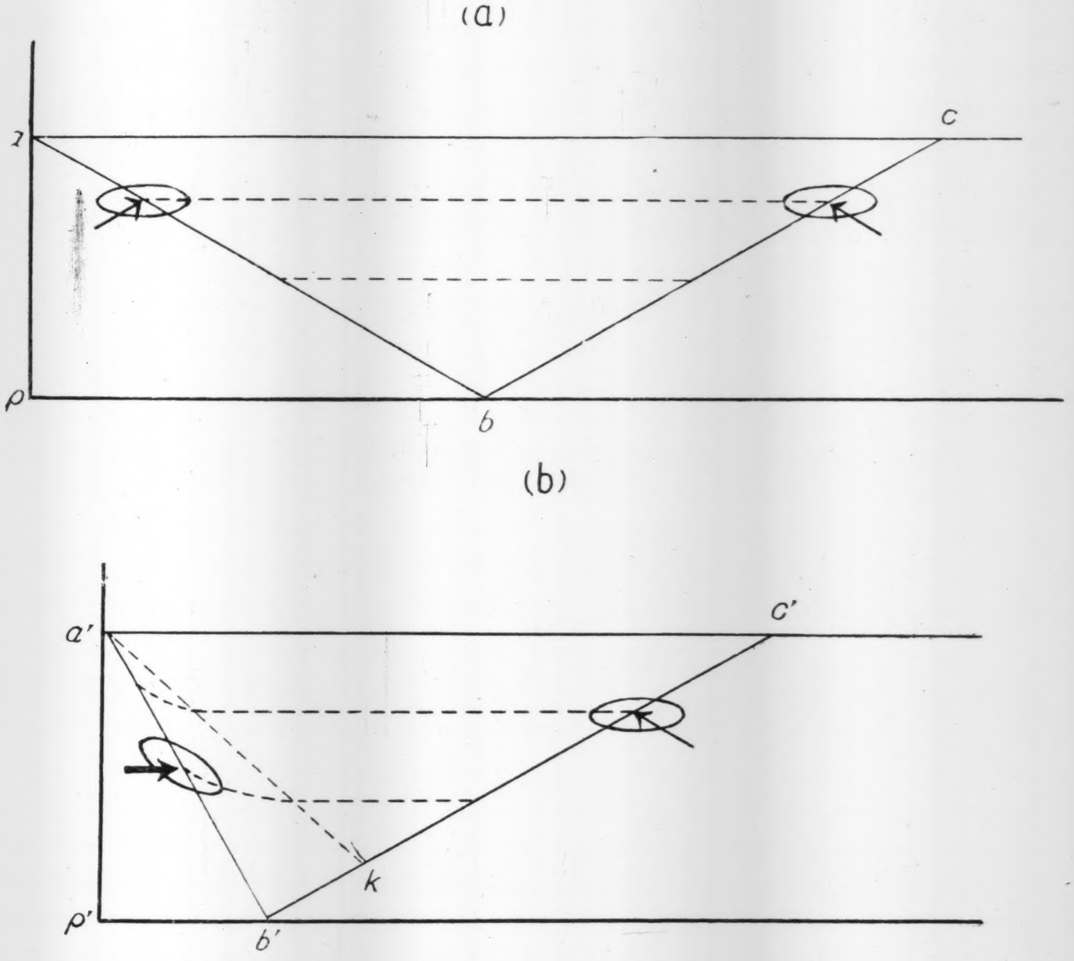

Fig. 18.

In the present case, a sensible slip may also take place between the moving wall and the sand particles, especially near the upper part. In this case, the state will approach that given by Fig. 14*b* and there θ will be again equal to ρ. This circumstance may be significant in starting the initial slip line from the top of the wall.

However, the fact that the portion $a'p'b'$ (Fig. 18*b*) is behaving approximately as a rigid body, while the angle θ is rapidly increasing with x, shows that the horizontal pressure from the wall is being applied as such upon the slip plane $a'b'$. This will mean that, in the case $\rho=30°$, the major axis of the ellipse at the slip line is inclined to the horizontal by 30° and thus $\theta=60°$. This gives the ultimate value of θ to which it approaches with the increasing rigidity of the portion $a'p'b'$. The trajectory of the major axis will be somewhat as shown by the dotted line in Fig. 18*b*.

The region on the right side of the line $a'b'$ is subjected to the most conspicuous deformation, as mentioned in Part II and there may be brought about a similar variation as illustrated in Fig. 17 and thereby give an opportunity for starting the second slip line somewhere about $a'k$ (Fig. 18*b*).

In Fig. 13, a characteristic variations have been shown of the sum $\theta+\omega$ which varies within nearly the same range of 20° for the different cases. This range may probably correspond to the range of the sectorial segment within which the theoretical slip lines consist of divergent straight lines and logarithmic spirals.[11] Such a segment could, indeed, be formed when the direction of pressure from the pressing wall relative to the moving sand mass deviates from the horizontal, as may be expected to be the case in our dynamical case. If such be actually the case, we may expect that the observed slip line will be curved in a form of logarithmic spiral somewhere near the bed plate. This cannot be verified directly from the photogram on account of the irregularity observed in this region probably due to the glass wall, but at least made probable by the curvature of the streaks on the photogram marked by the moving sand grains. As this range of θ is then determined by the value of ρ in the most disturbed state of sand, it is natural that the value $\theta+\omega$ is not much different for the different states.

It may be remarked that in the case of pressing wall, the top of the moving wall is the singular point, as mentioned above, from which the actual slip line must start.

Summarising, thus far, we have seen that the process of step-faulting seems to be determined chiefly by the following three conditions:

(a) The space variation, and its time variation, of the stress ellipse within the sand mass as determined by the motion of the prime mover, i.e. the moving wall, when the stable, existing slip planes are given as boundary conditions.

---

[11] See Prandtl, *loc. cit.*

(b) The existence of a critical value n of the axial ratio of the ellipse which is a function of the degree or rather the rate of deformation, its value decreasing with the increasing rate of deformation and tending to its maximum normal value when the rate of deformation falls under a certain value.

(c) Existence of a discontinuity of boundary condition, which determines the location of the slip plane.

Taking the existing slip line as if it were a rigid boundary, the condition (a) may probably be followed in some simple cases by treating the moving sand mass as a kind of special viscous fluid[12)] and thus anticipate in some measure the position of the next slip plane, taking (c) into consideration. The stability of the possible slip line will then be judged after (b) by a consideration similar to that described above referring to Fig. 17.

The above considerations may at least suggest a way of future formulation of the allied problem regarding the dynamics of moving granular mass.

The condition (b) will be rather accentuated if the cohesion between the sand grains comes into play beside the friction.

In the case of the earth crust the condition (b) may also be considered to hold, as it is known that the fragments of a fractured rock may again form a compact mass under a state in which the principal stresses are sufficiently large and the axial ratio of the ellipse is subjected to a suitable cycle of variation. Besides, a mode of variation of the plastic limit with the variation of the rate of deformation, similar to that considered above with respect to sand, may also be supposed in the case of the earth crust, since heat is generated by shearing and its rate of generation will increase with the rate of shearing, and the resulting temperature rise may tend to bring Mohr's curve nearer to σ-axis.

These considerations seem to justify the use of sand in the model experiments in preference to the other elastic or plastic materials such as mostly used by the previous investigators. In short, we may say that a sand mass is more dynamically similar to the earth crust than the other substance. The similitude holds also with regard to the effect of gravity playing an important part in both cases in determining the increase of the

---

12) The fact that a granular mass once set in deforming motion behaves more like a fluid than a plastic solid is well known, though the law of internal friction might differ considerably.

principal stresses with the depth, while in the laboratory experiments with elastic materials the gravity is utterly negligible. Both in the cases of sand and the earth crust, the absolute magnitude of stress is given by the gravity while the effect of the deforming mechanism is mainly to affect the shape of the stress ellipse.

Mohr's curve defining the plastic limit is of course different for the two cases compared. It must not, however, be overlooked that there is an essential point in which the two cases resemble to each other. Geotectonic features of the earth surface suggest that the earth crust is easily ruptured by tension. This is also natural, if we consider that the crust is run through by numerous cracks and fissures, as may be illustrated by Nasu's investigation, cited later, and also by Ch. Tsuboi's investigation[13] of the block structure of Tango Districts. Mohr's curve, therefore, may be assumed to lie almost exclusively on the negative side of σ, as in the case of sand mass. Ignoring, therefore, the quantitative difference for the present qualitative comparison, we may say that the sand model experiment in laboratory deals with the part of Mohr's diagram near the origin of (σ, τ) while the phenomena in the earth crust is related to the part of the same diagram very remote from τ-axis.

In passing, it may be remarked that the formation of the quasiperiodic series of slip planes in overstrained metallic crystals may be explained by a similar mechanism subjected to the three conditions (a) (b) and (c) above mentioned. When the average state of stress reaches the critical state, the actual stress at individual points will be subjected to natural fluctuation which will be quasiperiodic with respect to space and time. This fluctuation may become unstable on account of the circumstance analogous to (b) and the deformation will be concentrated to a finite number of slip bands while the remaining parts are released from strain. The periodic interval of the bands will probably be determined by the degree of heterogeneity in the molecular lattice and also by the irregularity of the boundary surface, which give the required singular points.

(IV) Geophysical Applications.

Some of the possible geophysical applications of the results of our present series of experiments have already been enumerated in the previous report, Part II.

Assuming the force applied to the earth crust on account of geological disturbances to be chiefly horizontal, we may predict in some measure the probable angle of inclination of the fault planes if we could assume the proper value of ρ or n, or the form of Mohr's curve, and vice versa. Or, in some case, we may perhaps judge whether it is the case of receding or pressing the prime mover, provided the latter, i.e. the virtual "moving wall" may be located from some other considerations. The same may also be judged from the observed order of sequence of seismic activity among a set of parallel earthquake zones, if such could be previously located by a large number of observations, as was made by Mr. N. Nasu[14)] in the case of Tango Districts. In his case, however, the intervals between the successive "slip planes" seem to be of an order of a few km., and, moreover, the angle between the intersecting slip planes is mostly near a right angle so that we may assume here the case of ordinary plastic deformation analogous to that of paraffin prism above cited. A more proper field of application of the present results seems to lie in the domain of geological phenomena of much larger scale. One of the most beautiful examples of a periodic series of fault lines may be seen in the geotectonic map of Korea given in Prof. Koto's[15)] classical paper on the orographical features of Korean Peninsula. Another remarkable example is afforded by Prof. Yamasaki's investigation[16)] on the typical block structure of Bôsô Districts. In most of these examples, the cases seem to correspond to our case of the receding wall, and they suggest that the boundary between the land mass and the oceanic bed is receding towards the ocean. This inference, if correct, may support

---

[13] CHUJI TSUBOI, *Proc. Imp. Acad.*, **4** (1928), 529; this Bull., **6** (1929), 71; also in the present Vol. of Bull.

---

14) N. Nasu, *Proc. Imp. Acad.*, **4** (1928), 378. After this paper was read in the Meeting of the Institute, Mr. Nasu informed me of an interesting fact that, in Kwanto region, there is a set of parallel seismic zones which become successively active, i.e. among which the activity is transferred from one zone to the next one and so on. In the same Meeting, he read a very interesting paper on the three-dimensional distribution of the epicentres in Tango Districts. The distribution along a system of intersecting "slip planes" is quite conspicuous. Under the light of the considerations given in our present paper, his results vividy reveal the actual mechanism of earthquakes in the said district, in such a manner that we may now clearly trace the space distribution of stress ellipses as well as that of the plastic properties of the crust in defferent regions. The location of the net-work of the slip planes agrees well with that which we may just expect from the results of triangulations published by the Land Survey Department (to be published later in this Bulletin). We will return to the subject in some future. In passing, it seems to the authors that the most *direct* way of answering the question of earthquake forewarning is to measure the state of *existing* strain of the crust by triangulations and levellings and review the results under the light of the theory of plasticity.

15) B. Koto., *Jour. Coll. Sci., Tokyo,* **19** (1903), Art. 1.

16) N. Yamasaki, *Report of E.I.C.*, **100** B (1925), 11; *Journ. Fac. Sci., Tokyo,* [ii] **2**, (1926), 77.

Wegener's view and also the authors' hypothesis[17] on the origin of the Japanese Arc.[18] In our present case, however, the friction of the bed plate of the containing vessel introduces a boundary condition which cannot generally hold in the case of the earth crust, as already emphatically stated in Part II. Further discussion of the geophysical application may, therefore, be postponed until the experiment with a viscous substratum which we are now planning, has made some progress.

SUMMARY.

(1) The experiments similar to those described in the previous two reports are repeated somewhat more systematically, using a kinematographical camera for following successive stages of deformation with a sufficiently close step.

(2) Two kinds of sand were investigated, each in two different states of packing, respectively for the cases of receding as well as pressing the side wall of the containing vessel.

(3) In general, the closest packing tends to be loosened, and the loosest state to be settled down, towards a certain normal middle state, during the course of deformation.

(4) The difference of grain size expresses itself mainly in the results of experiment as the effects of the corresponding difference in the mode of variation of packing during the course of deformation, but not as those due to any essential difference in the angle of friction.

(5) The tendency to form simultaneously active slip lines is most remarkable in the case of the finer sand, while it is absent in the case of the coaser sand in loose packing. It may be said that the latter is more fluidous while the former is more brittle.

(6) The results of the experiments thus far made are reviewed under the light of the mechanical theory of plastic deformation, by considering the distribution of the stress ellipse and its variation due to the deformation. The circumstances[19] determining the formation of step faults are enumerated, and a way is thereby suggested which may be taken for a future analytical formulation of the allied problems.

---

[17] T. TERADA, *Rep. E.I.C.*, **100** B (1925), 63; this *Bull.*, **5** (1928), 21.

[18] There are also some examples in which the case of pressing wall is applicable especially in cases of local disturbances; for example, the case of Tango Districts above cited in ft. nt. p. 91 and also the case of Kii districts recently investigated by Imamura *Proc. Imp. Acad.*, **5** (1929), 161.

[19] I.e., the conditions (a), (b) and (c) in p. 89.

(7) Some features of dynamical similitude between the experimental sand layer and the earth crust is pointed out with respect to the following relations:

(*a*) The stress ellipses are mainly determined by gravity in both cases. Elasticity is negligible.

(*b*) Mohr's diagrams are of qualitatively similar character for the two cases.

(*c*) The mode of variation of the plastic property as the function of the rate of deformation may probably be similar in either case. This mode is essential in determining the formation of step fault.

(8) Some geophysical applications are mentioned.

(9) Analogy of the case of slip bands in deformed metallic crystals is again cited.

4. 砂層の崩壊に關する實驗（第三報）

寺田寅彦
宮部直巳

前二回の報告に誌したと同様に、砂層の横壁を後退或は前進させて斷層を生ぜしめる實驗を、今度は活動寫眞器械を用ゐて、前よりは稍系統的に繰返した。其結果によつて從前の結果を確めると同時に、又、砂粒の大小及其の充塡粗密度の差異に因る異同を、前よりも詳しく又確に知る事が出來た。

Stress ellipse の考を用ゐて、此等の實驗の場合に於ける砂層の變形破壞の機巧を考察した結果として、砂の摩擦角が砂の充塡度により又其運動狀態によつて色々に變る事が、現在の場合に重要な決定因子であるといふ考へを確かめ、其考へから階段的斷層の發生する經路を幾分明にする事が出來た。

又、此等の考察の結果から、地殼と砂層との力學的肖似が偶然でなく本質的のものであるといふ事を一般 plastic deformation の理論に照して指摘した。

終りに、此等實驗の結果を地球物理學上の現象に應用するに際して注意すべき二三の點を擧げておいた。

5. *Tilting Motion of the Earth Crust caused by Secondary Undulations of Tides in a Bay.*

By **Ryûtarô TAKAHASI,**

Earthquake Research Institute.

(Read January 15, 1929.—Received March 20, 1929.)

In the last number of this Bulletin,[1] the present author gave some account of the tilting motion of the earth crust caused by tidal loading. The present paper is a continuation of that work and describes the results of observation of the tilting motion of the earth crust caused by seiches or secondary undulations of tides in a bay with some discussions.

Our knowledges about the mechanical behaviour of the earth crust seem to be still meagre except for those deduced from the observations of earthquakes and from the experiments on the elastic properties of the constituent rocks of the crust.

Observations regarding the movements of the crust in a larger scale, or of its mechanical behaviour under the action of a force of a longer period than those playing rôle in the cases cited above, have been quite limited and wanted.

Block movements of the crust in meizo-seismal regions were brought to light by the results of the precise levellings carried out after the destructive earthquake which occurred recently in our country. Land blocks consisting the earth crust were proved to be able to change their directions of tilting quite independently to each other as if there were no elastic connections between them.[2] On careful examinations, however, of the results of these precise levellings carried out over seismic regions, the land blocks seem to be subjected to bendings as well as to tiltings.

Bending of a land block and other movements of a medium scale taking place in a block as the results of the isostatic force or other local causes, have escaped the eyes of geophysicists and the most of them are left untouched.

One class of the motion of the crust belonging to this category may be that due to the tidal loadings. In the last paper of the present writer, he studied a case of the last mentioned subject and pointed out, firstly, that the rise of the sea surface of the Aburatubo Bay, Sagami, by 34 cm. produces a tilting of 0″·22 of the crust at a point 22·6 metres distant from the nearest beach line; and, secondly, that the value of the effective rigidity of the crust increases abruptly at the distance of about 150 m. from the observing station. Moreover, it was suggested that the minute indentations superposed on the record of the tilting caused by tides may probably be due to the secondary undulations or the seiches of the sea water which are predominant in the Aburatubo Bay.

---

[1] R. TAKAHASI, *Bull. Earthq. Res. Inst.*, **6** (1929), 85–108.

[2] C. TSUBOI, *ibid.*, **6** (1929), 71–83.

The present observation was undertaken to ascertain the last mentioned view and to know, if possible, how the elastic properties of the crust vary according to different periods of force which is being exerted on it. In the winter vacation of this year, the present author, with the kind assistance of Professor M. Ishimoto and Mr. N. Miyabe, made a series of simultaneous observations of the seiches in the Aburatubo Bay and of the tilting of the crust near the bay. The results obtained will be given in the following pages.

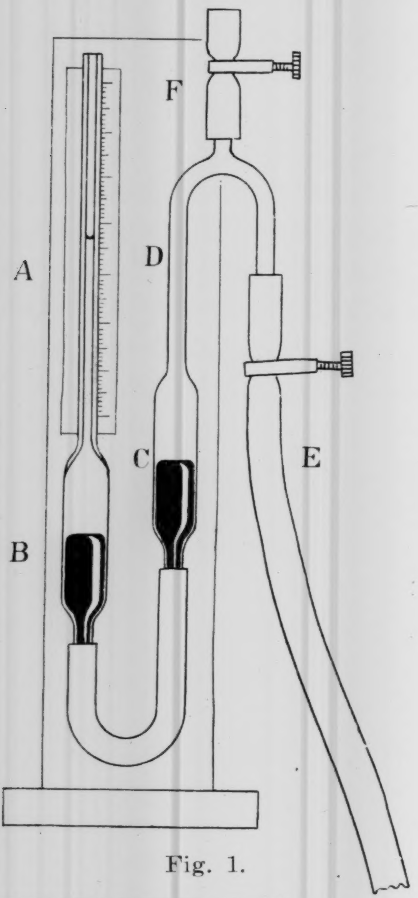

Fig. 1.

Apparatus.

The apparatus[3] used for the measurement of seiches in the present observation is shown diagramatically in Fig. 1. It consists essentially of two glass tubes *A-B* and *C-D* connected with each other by a piece of thick-walled rubber tube to form a U-tube. The tube *A-B* consists of a glass tube *B* 12 mm. in its inner diameter and 15 cm. long, and a capillary glass tube *A* with an inner diameter of 2 mm. and a length of 50 cm. connected with the upper part of *B*. The tube *A-B* is mounted on a stand with a scale behind the capillary part of the tube. The tube *C* is of equal diameter with *B* and is narrowed at the upper part *D*. The tube *C-D* is attached to the same stand with the tube *A-B* and its vertical position can be adjusted up and down parallel to the tube *A-B*. One end of a long piece of thick-walled rubber tube *E* is connected with *D* and the other end is immersed in the sea water. The lower part of both *B* and *C* tubes are filled with mercury. The upper part of *B* is filled with sea water of a quantity such that the meniscus of the water reaches the middle part of the capillary tube *A* when the mercury head is at the middle point of the tube *B*. The part *D* of the tube *C-D* and the rubber tube *E* are filled with sea water, this being effected by sacking through a short branch tube *F* by mouth. A stop.cock is provided to *E* to regulate and damp the quick oscillations of the sea water, thus facilitating the reading of the height of meniscus in the capillary tube *A*. The vertical position of the tube *C-D* is so adjusted that the mercury meniscuses in the tubes *B* and *C* will remain at their respective original positions in successive observations.

---

[3] Designed by Prof. M. ISHIMOTO.

Denoting by *A, B, C, D* and *E* the heights shown in Fig. 2, we have

$$A\rho+B\rho'+E\rho=D\rho+C\rho',$$
$$B+C=\text{const.}=L,$$
$$C+D=\text{const.}=K,$$
$$\frac{d\,(A+B)}{dB}=\frac{S}{s}$$

where ρ is the specific gravity of sea water,
ρ' the specific gravity of mercury,
s the cross-sectional area of the capillary tube,
S the cross-sectional area of the glass tube under the capillary tube.

From these equations we have

$$\frac{d}{dE}(A+B)=-\frac{(S/s)\,\rho}{(S/s)\,\rho+2(\rho'-\rho)}.$$

As can be seen by this equation, the magnification coefficient of this apparatus approaches to unity as the ratio S/s increases.

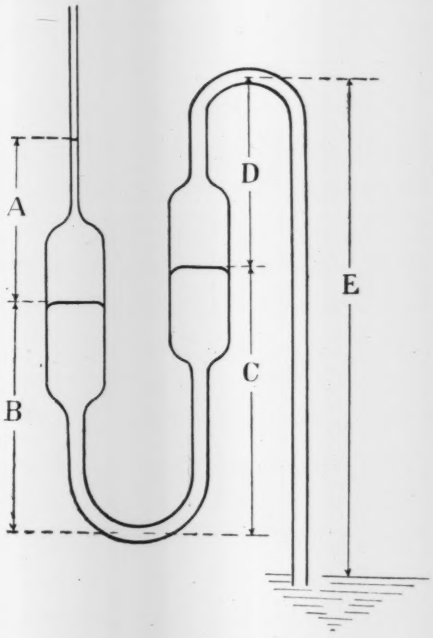

Fig. 2.

In the present observation of the seiches in the Aburatubo Bay, three of the apparatus of this type were used. In each of the apparatus, S was about 113 mm.^{2} and s $3{\cdot}1$ mm.^{2} Therefore, the ratio S/s was about 36. The calibration of the apparatuses made just before the observations gave the following respective constants:

Apparatus	No. 1	No. 2	No. 3
Magnification Coef.	0·557	0·663	0·586

The apparatus with which the simultaneous observations of the tilting of the earth crust were made was a pair of tiltmeters described in the last paper. As in the former observations the tiltmeters were installed in a horizontal cave on the hill side facing to the neck of the Aburatubo Bay. The position of the tilmeter is 22·6 m. distant from the nearest beach line and 8·7 metres high above the mean sea level. The sensibility of the tiltmeters was so adjusted in the present observation that they give 3 cm. deflection on the record when the crust is tilted by 1″. The recording drum was made to rotate once a day, the time marks being made automatically in every one hour by extinguishing the light source for two minutes interval.

Observation.

In each series of simultaneous observations of the seiches, the measuring apparatuses were installed at three points selected on the coast of the Aburatubo Bay or the Moroiso Bay, or sometimes of both, and observations

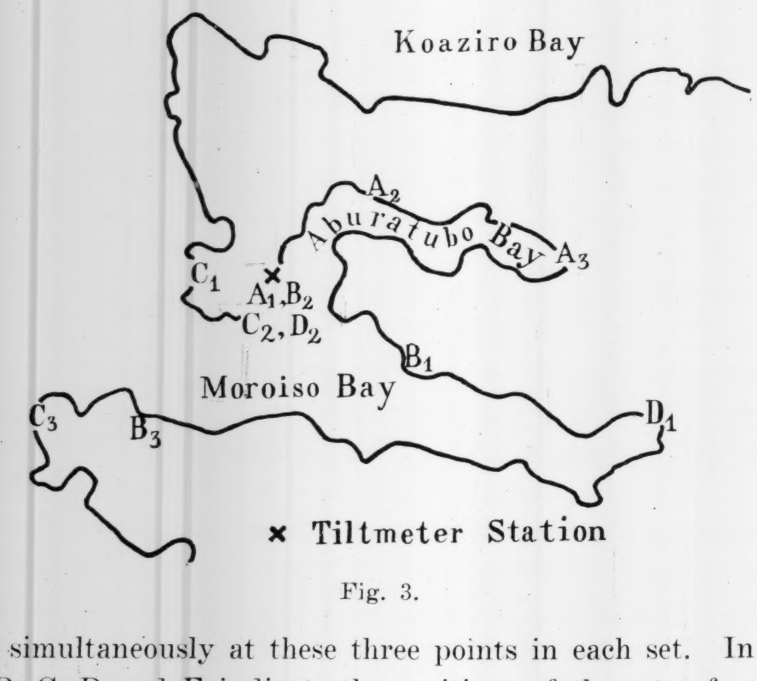

Fig. 3.

were made simultaneously at these three points in each set. In Fig. 3 the letters A, B, C, D and E indicate the positions of the sets of points where

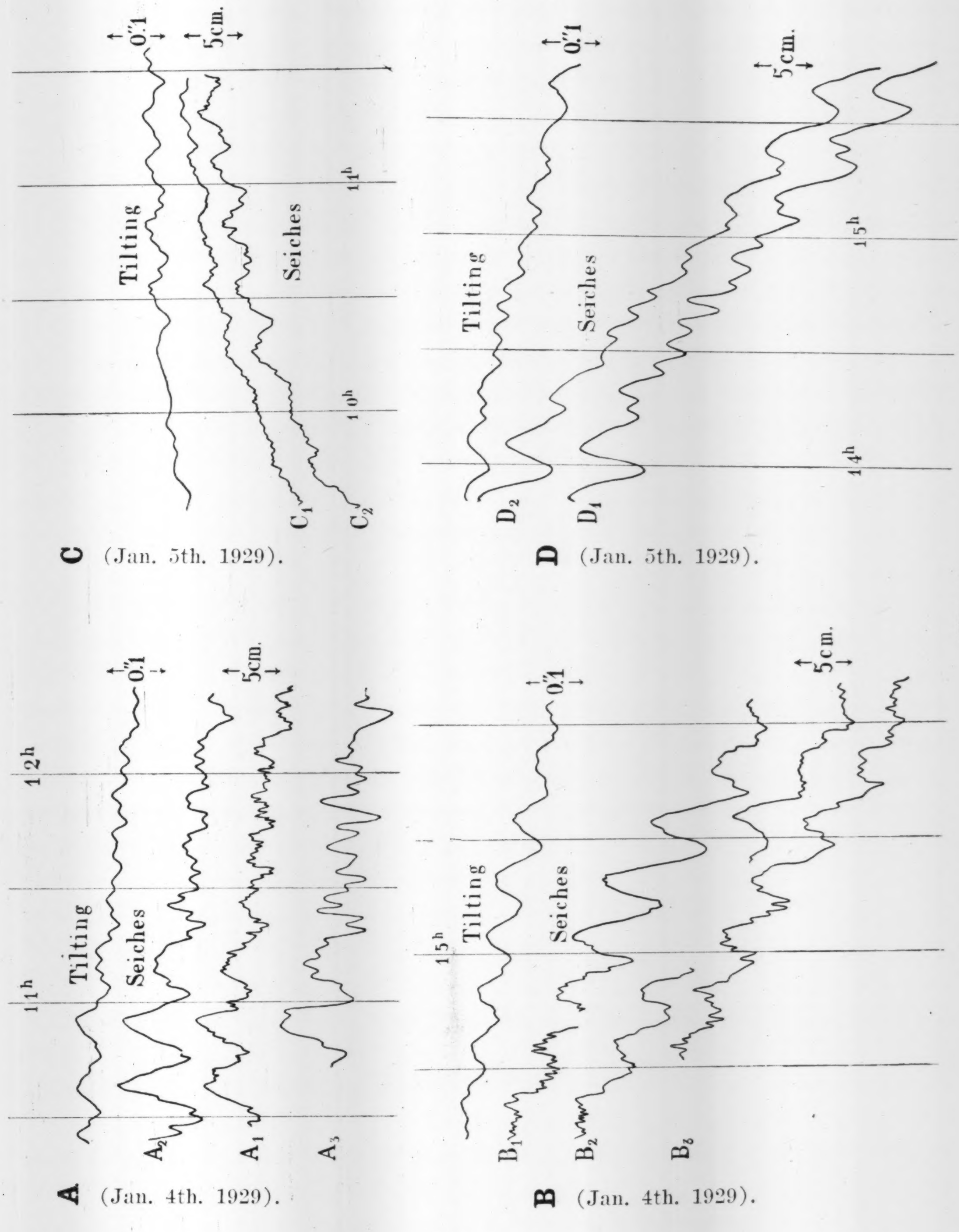

A (Jan. 4th. 1929).

B (Jan. 4th. 1929).

C (Jan. 5th. 1929).

D (Jan. 5th. 1929).

Fig. 4.

simultaneous observations were carried out and suffixes 1, 2 and 3 show the ordinal number of the appratus used at that point. Thus A_1 shows, for instance, that an observation was made at that point indicated by the letter using No. 1 apparatus, and that this observation was made simultaneously with those carried out at the points indicated by A_2 and A_3. The heights of the meniscus of the water in the capillary tube of the apparatus were measured at every thirty seconds, and the measurement was continued for two hours in each series of observations. The results of the observation are shown graphically in Fig. 4 together with the record obtained with the tiltmeters which is given at the top of each series.

From these results it has become clear that there is a foundamental oscillation of sea water with a period of 14–16 minutes having the node of the vertical displacements off the mouth of the Aburatubo Bay. Superposed on this oscillation there is another with which the sea water in the Aburatubo Bay oscillates in alternate phase with that in the Moroiso Bay. This mode of oscillation is of a period of about 7 minutes. Beside these two modes there seems to be still others (probably the third and higher harmonies) of periods less than 3·5 minutes.

The foundamental oscillation of the Aburatubo and Moroiso Bays was studied formerly by Professor K. Honda.[4] According to his results, the period of this oscillation is 13·8–15·0 minutes. It seems that the upheaval of the coast of the Aburatubo Bay connected with the Great Kwantô Earthquake has probably made the period of the seiches predominating in the bays a little longer. Comparison of the record obtained with the tiltmeter with the curves of the seiches observed at the coast nearest to the tiltmeter cave, shows that the indentations on the record of the tilting is quite similar to the curves of seiches proving that they are caused by the seiches in the bay. There seems to be neither lag nor advance in the phases of seiches relative to the corresponding tilting. The rise of the sea surface by 1 cm. produces the tilting of the crust of the amount of $0''\cdot0086$ which is 1·3 times as large as the corresponding tilting in the case of the tides.

Conclusion.

As was described in the last paper, the value of the effective rigidity of the earth crust undergoes a sharp increase at the distance of about 150 m. from the observing station. In other words, the load which is really effec-

---

4) *Publication Earthq. Inv. Comm.*, **26** (1908).
Journ. Coll. Sci., Tokyo, **24** (1908).

tive in producing the tilting of the observing station is that located within the distance of 150 m. from the station. This characteristic relation regarding the effective rigidity of the crust, which was found to hold in the case of tides, seems to hold also in this case of seiches. The record obtained by the tiltmeter is quite similar to the curve of the seiches observed at a point 22 m. distant from the station, but is not so to those observed at points distant more than 150 m. from the station. The ratio of the amount of tilting of the crust to the height of seiches is, as is said above, 1·3 times as large as the ratio taken in the case of the lunar semidiurnal tide. This unequality of the ratios may be approximately accounted for by assuming firstly that the effective rigidity of the crust is a function both of the distance between the load and the observing station and of the period with which the load varies, and secondly that the shorter the period of the variation of the load is, the more rapidly the amplitude of the tilting motion decays with the distance from the load. The absolute depression of the crust caused by the load of the seiches may be much smaller than that caused by the load of the lunar tides, even if the amplitudes of the loads were supposed to be the same in both cases. The tilting of the crust at the observing station can on the contrary be greater for the former case. The tilting caused by a load with a shorter period is not, however, always greater than that by a load of a longer period. Whether the load of a longer period will produce a greater tilting at a given station than that of a shorter period or will not, depends on the relative position of the station to the load, the period of variation of the load and also on the functional form accordingly to which the effective rigidity of the earth crust at that station varies with the distance.

In conclusion, the author wishes to express his most cordial thanks to Professor M. Ishimoto and Dr. N. Miyabe for their kind assistance and to Professors T. Terada and C. Tsuboi for their valuable discussions.

5. 油壺灣内の海水の副振動に因る地殼の傾斜運動

地震研究所　高橋龍太郎

概要

（1） 本論文は携持用檢潮器三臺と、一對の石本式傾斜計とを使用して、油壺灣内の副振動と、同灣の頸部に面する一地點に於ける地殼の傾斜變化とを同時に觀測し、以て兩者の關係を調査研究したものである。

（2） 檢潮器は第一圖に示せる如きものであつて、海面の昇降に伴ふ器内水銀面の昇降を、毛細管を利用して擴大し、海面昇降を約 0·6 倍にして讀取るものである。

（3） 檢潮器を油壺灣、諸磯灣の各所に据付けて副振動の同時觀測を行ひ、之を傾斜計の記錄と比較した。其の結果、傾斜計の記錄は傾斜計据付所脇に於ける副振動の記錄と全く相似であるが、傾斜計より 150 m 以上離れた場所に於ける副振動の記錄とは最早相似して居らぬ事が判明した。之に依つて見れば、地殼の有效剛性値は、太陰半日潮に對する場所と同じく、短週期の副振動に對しても亦觀測點より 150 m 以内の距離に於て急激なる増加を爲すものと思はれる。

（4） 油壺灣の入口に節を有する 14-16 分の週期の第一次振動に因る地殼の傾斜變化は、海面の上昇 1 cm に對して 0″·0086 の割合であつて、太陰の半日潮に對する値の約 1·3 倍となつてゐる。此の如く、海面變化に伴ふ傾斜の變化量の、海面變化に對する割合が兩者に於て其の値を異にする事實は、次の假定を作る事に依つて大體説明しうるのである。

（イ） 地殼の有效剛性値は觀測點と負荷との距離の函數なるのみならず、負荷の變化する週期の函數でもある事。

（ロ） 負荷變化の週期が少なる程､傾斜運動の振幅は觀測所海岸間の距離と共に速に減衰する事。

（5） 尙上記海水の第一次振動の外に油壺灣内の海水が、油壺灣に隣接する諸磯灣内の海水と交互に昇降する、約 7 分週期の振動も觀測された。

6. *Block Movements as Revealed by Means of Precise Levellings in Some Earthquake Districts of Japan.*

By **Chûji TSUBOI,**

Earthquake Research Institute.

(Read Dec. 18, 1928.—Received March 20, 1929.)

1. INTRODUCTION.

It is of prime importance for the research of the factor determining earthquake occurence to learn the modes of the existing secular movements of the earth crust. It is, and there are good many reasons to be, believed, that the earth crust is even at present subjected to a slow but continual movement as it has been in geologic ages. The cumulative or integrated effect of these movements in a locality may be seen in its topographic and other physiographical features. If we remember, however, that the phenomenon of earthquake is nothing but an accidental manifestation of the geologic movement in the course of its present activity, the quantitative evidence of its differential, but not of its integrated, effect is urgently wanted. Regarded as a physical phenomenon, this movement, however, is exceedingly slow in its rate of progress, thus for the present purpose is required an extremely delicate instrument to make the measurement with and a very long interval of time to make the measurement through. With this object in view, the revisions of the triangulations and precise levellings have been made by the Land Survey Department of the Imperial Army since some decades of years after some of the severe earthquakes and volcanic eruptions over their respective disturbed areas. That we have at present not a few data available for the enunciated investigations is to be counted into the credit of the pioneer students of earthquake who duly payed their attentions to this direction and arranged the scheme of revisions and also of the Land Survey Department of the Imperial Army which actually practised the revisions. The results of these revisions have already been published in a number of reports and the discussions are also made of these results from many divergent points of view. In all of these levelling surveys, sensible changes in heights of bench marks are found to have taken place during the intervals between the successive levellings in which the events of the earthquakes or volcanic eruptions are involved. The relations between these movements and the geological structures of the district concerned, however, seem to have been unduly left untouched except in the case of Echigo and Shinano levellings which was discussed by Prof. N. Yamasaki[1] from a geological point of view. He emphasised that the chronic tilting of land blocks is actually detected in this case, of which the meaning is readily understood by the geological features of the district. K. Mutô[2] of the Land Survey Department also discussed the tilting of land blocks in the Kwantô district. The present writer has recently made some similar but more detailed examinations on the earth movements in some earthquake and volcanic districts in this country which seem to have hitherto been left untouched from this interesting point of view. In the following pages, the results of these examinations will be given in due sequence.

2. SHIMABARA EARTHQUAKE DISTRICT.

In connection with the great earthquake which devastated the Shimabara district in the Central Kyûshû on Dec. 8th, 1922, the revision of the precise levellings was made in the district in the next year of the catastroph. The object of this work was to detect vertical movements of the crust in this district which might have taken place since the older observations were made in 1894 and 1897. The results of the postseismic levellings when compared with the older ones will give the vertical movements of the crust, most of which is presumably directly associated with the very earthquake. The results of comparisons of the levellings are contained in the paper by Prof. A. Imamura.[3]

These results were subjected to a quite similar process of examination as was adopted by the present author in his research on the postseismic block movements in the Tango earthquake district.[4] The process adopted is as follows. Firstly, every conspicuous turning point of the levelling routes with a sharp bent was marked by A, B, C, etc., as is shown in Pl. I. Secondly, every pair of the consecutive points was connected by a segment of straight line. Thirdly, the position of every bench mark between these

---

[1] N. YAMASAKI, *Proc. Imp. Acad.*, **4** (1928), 60.

[2] Read at the Monthly Meeting of this Institute, May 22nd, 1928. He pointed out for the first time, that the secular tiltings of land blocks are found by the comparison of two successive levellings.

[3] A. IMAMURA, *Bull. Imp. Earthq. Inv. Comm.*, **10** (1928), 63.

[4] C. TSUBOI, *Proc. Imp. Acad.*, **4** (1928), 529.
Bull. Earthq. Res. Inst., **6** (1929), 74.

two points was normally projected upon the segment which connects the two. Fourthly and finally, taking these projections along the horizontal axis, the vertical displacement Δh of a bench mark was represented by a point with its ordinate taken proportional to Δh. A few examples of the diagrams thus obtained are shown in Figs. 1 and 2. The positions of the bench marks may be identified by the reference to Pl. I. In making these diagrams, the zero of the ordinate is assumed arbitrarily. No loss in generality in the following discussions is, of course, introduced by this assumption.

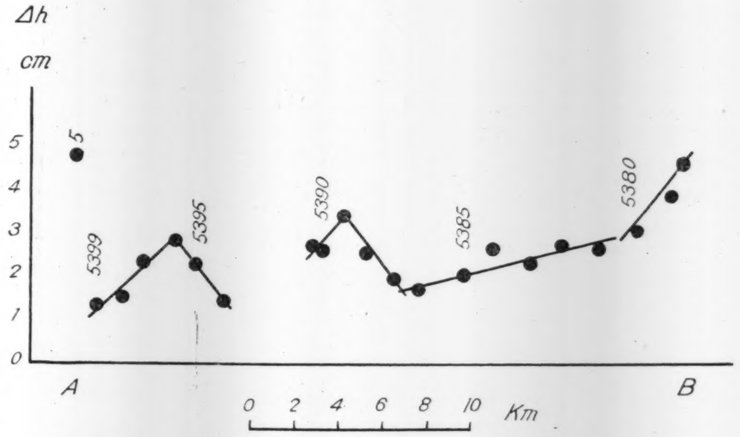

Fig. 1.

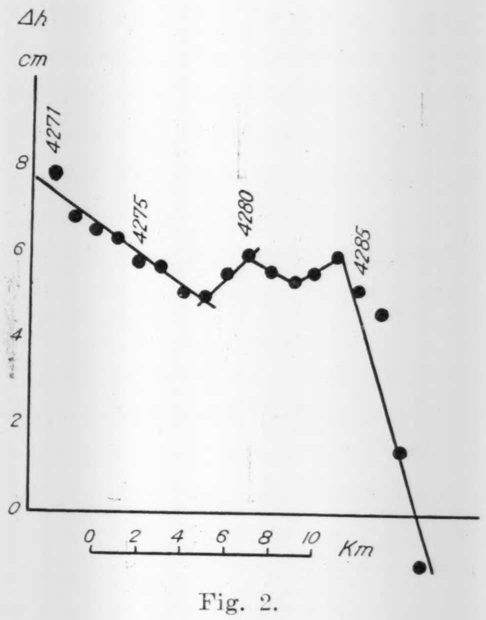

Fig. 2.

Remarkable features will be found in the manner of distribution of the points in the diagrams. These points illustrating the changes of heights of the bench marks lie neither on a smooth nor on an irregular curve but they lie on a number of broken segments of straight lines. These characteristic facts may well be elucidated by assuming that the earth crust in this district is made up of a number of descrete structural units, each of which behaves approximately as a rigid body as a whole. Each of these units is bordered by its neighbours along the boundary lines corresponding to the joints of segments of straight lines in the graphs. The geographical positions of the boundary lines of these units as revealed by the above analysis are indicated by thick lines in Pl. I, each coloured part between two of these lines correcponding to an elementaly unit of structure of the crust. The bench marks lying on one and the same unit are, thus, rigidly connected to each other, being only subjected to a common tilting, upheaval, depression of the unit as a whole.

On the other hand, it is accepted that the earth crust in some district is run through by a number of faults, being devided into what is called land blocks. That these geological land blocks actually correspond to what we have called the structural units in the above will be obvious, if we refer to the topography and the geology of this Shimabara district.

3. Sakurajima Volcanic District.

A great eruption took place on Jan. 12th, 1914 of the volcano Sakurajima in the Southern Kyûshû. In view of getting, if possible, some informations regarding the deformation of the earth crust caused by this eruption in the neighbourhood of the volcano, the revision of the precise levellings was made around the volcano. The results were compared with those of the older surveys which were done in 1891–1898. The descrepancies between the two levellings give the vertical movement of the crust probably associated with the eruption. A part of the levelling route which runs close to the volcano was again covered by another series of precise levellings in February of 1915. The difference of the second and the third levellings gives the vertical movement of the crust in the interval of about one year after the eruption.

The results of levellings are contained in the comprehensive work of Prof. F. Omori[5] on the eruption of this volcano. These results were examined just in the same manner as in the former cases. The graphs shown in Fig. 3 represent the vertical displacements of the bench marks in this district. In these graphs, the mark ○ corresponds to the difference in height

---

5) F. Omori, *Bull. Imp. Earthq. Inv. Comm.*, 8 (1914–1922), 50.

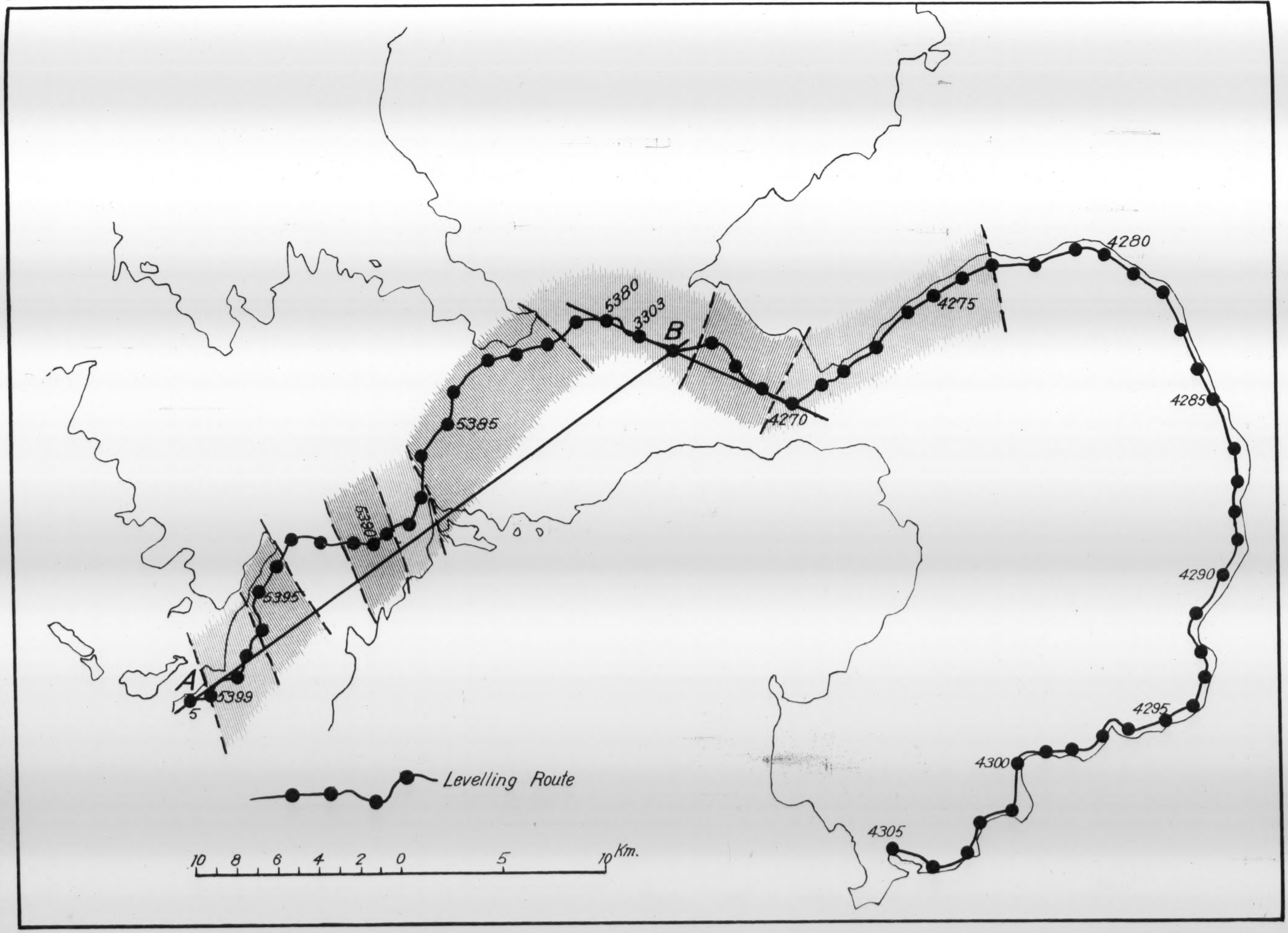
A
5
5399
5395
5390
5385
5380
3303
B
4270
4275
4280
4285
4290
4295
4300
4305
Levelling Route
10 8 6 4 2 0 5 10 Km.

Land Blocks in the Shimabara District.

(Facing p. 106)

（震研彙報第七號、圖版、坪井）

between the first and the second levellings while the mark • to that between the second and the third. In these graphs, the characteristic linear distribution of the points is also clearly seen as in the former cases. Moreover, a remarkable fact is found in these graphs that two series of graphs, though entirely different in their absolute magnitudes, are of quite similar form. The joints of the segments of straight lines occur at the same abscissa for both series of the graphs which correspond to different epochs of the levellings. This fact may be regarded as a sufficient support for the statement that the characteristic features in the distribution of the points are not due to a mere accidental play of chance nor due to errors in the observation of the surveys, but are due to some real physical causes, and that the boundary lines of the assumed land blocks which correspond to the joints of the segments have important significances connected with the geological structures of the district concerned.

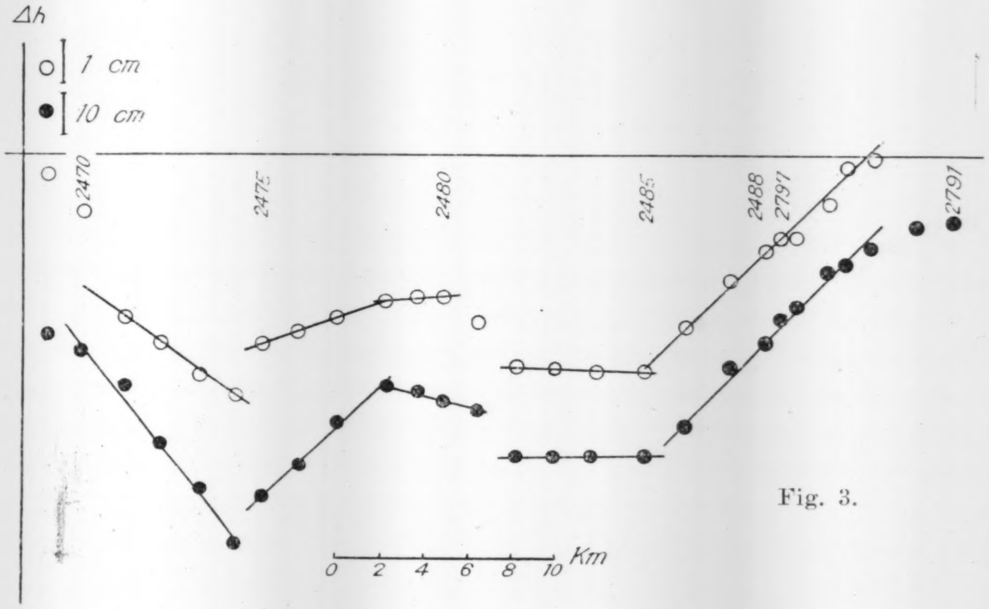

Fig. 3.

In discussing the results of these levellings, Prof. F. Omori pointed out the fact that there is a general depression of the crust which gradually decreases with the increasing distance from the centre of the volcano. In the great eruption of this volcano, an immence quantity of lava overflowed the crator which is estimated to be about 3×10^{15} gr. by Prof. B. Kotô.6) This immense mass will disturb the initial gravitational field in its neighbourhood and the plumb lines will be slightly directed towards this mass. The angle

---

6) B. Kotô, *Journ. Col. Sci. Tokyo Imp. Univ.*, **38** (1916), 107.

of deflection of the plumb line caused by this disturbance is given by

$$\alpha = \frac{km}{r^2 g},$$

where k is the gravitational constant
m the mass of the lava
r the distance from the mass
g the accerelation due to gravity.

In response to these deflections of plumb lines, the bench mark at x appears as if it has been subjected to a depression of amount Δh such that

$$\left| \Delta h \right| = \left| \int_{\infty}^{x} \frac{km}{r^2 g} dr \right| = \frac{km}{gx}$$

if the levelling is carried out along a route from an infinite distance up to the distance x from the lava mass. Roughly putting $k=6\times10^{-8}$, $m=3\times10^{15}$, $g=10^3$, we have the following relation between $|\Delta h|$ and x.

TABELE I.

x (cm.)	Δh (cm.)
10^1	18000
10^2	1800
10^3	180
10^4	18
10^5	1.8
10^6	0.18

As is seen in the above calculation, this amount is not large enough to account for the general "depression" actually observed around Sakurajima. It must be remembered, however, that here the mass which came out of the crator only is taken into consideration, but not the subterranean mass change which must have taken place with the eruption.

On the other hand, the effect of loading by the mass of lava may also yields the general depression. A part of the observed general depression in the neighbourhood of Sakurajima may indeed be due to this circumstance. Superposed on these general depression, we have seen that the individual tiltings of some land blocks took place.

In the present case, the bench marks are two-dimensionally distributed over the disturbed area, so that the magnitudes and directions of tilting of some of the land blocks can be calculated. Thus for instance, bench marks 2486, 2487, 2488, 2797, 2796, 2795, 2794, 2793, 2792, 2489, 2490, 2491 lie on one and the same land block. Given the co-ordinates of these bench marks and their respective vertical displacements, the magnitude and direction of tilting of the block were calculated by the method of least square. By this method, it was found that this block tilted down towards the direction N 72°50′ W by the amount of 9″. The vertical displacements of the bench marks calculated by this assumption are compared with the observed values in the following table.

TABELE II.

Bench Mark	Δh obs.	Δh calc.
	mm.	mm.
2486	−616	−580
2487	−485	−495
2488	−421	−411
2797	−369	−370
2796	−338	−358
2795	−260	−293
2794	−244	−261
2793	−206	−196
2792	−155	−108
2789	−348	−365
2490	−301	−308
2491	−306	−291

Good agreements between these values are seen proving the correctness of our present suppositions. Similarly, the directions and the magnitudes of inclinations of two other blocks were calculated, with the results shown in the following tables.

TABELE III.

Bench Mark	Δh obs.	Δh calc.
	mm.	mm.
2505	−174	−143
2504	−207	−200
2503	−242	−280
2502	−314	−302
2501	−379	−393
2499	−468	−430
2498	−401	−395
2497	−363	−351
2496	−344	−367

Direction of tilting .... N 30° 40′ W

Magnitude of tilting .... 10″

TABELE IV.

Bench Mark	Δh obs.	Δh calc.
	mm.	mm.
2463	-259	-270
2464	-291	-311
2465	-291	-380
2466	-302	-292
2469	-407	-370
2470	-446	-468
2471	-527	-563
2472	-658	-677
2473	-770	-756
2474	-894	-846

Direction of tilting	N 57° 40′ E
Magnitude of tilting	12″

In the Pl. II, the tilting of these land blocks are represented by the arrows drawn in the direction of depression with their lengths taken proportional to the amount of tilting. The three arrows are seen to converge towards a point somewhat to the north of the volcanic crator. The aggregates of land blocks subjected to a general depression may have behaved as shown in the accompanying diagramatic figure.

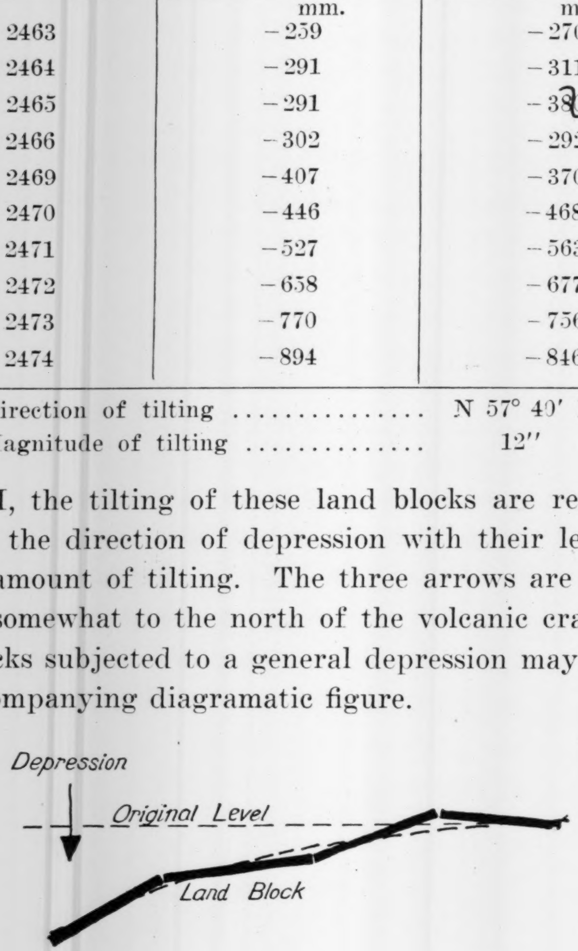

Fig. 4.

4. MINO OWARI EARTHQUAKE DISTRICT.

A great earthquake took place on Oct. 28th, 1891 in Mino Owari districts of Central Honshû. In this earthquake, a well-known great fault was formed whose trend is, according to Prof. K. Kotô, in good agreement with a line of geological significance. In this case also, a revision of levelling surveys was carried out over the disturbed area. The changes of heights of the crust in the interval of two levellings are graphically shown in Figs. 5 and 6, just in the same manner as in former cases. In this case also, some block movements are seen to have clearly taken place. (Pl. III).

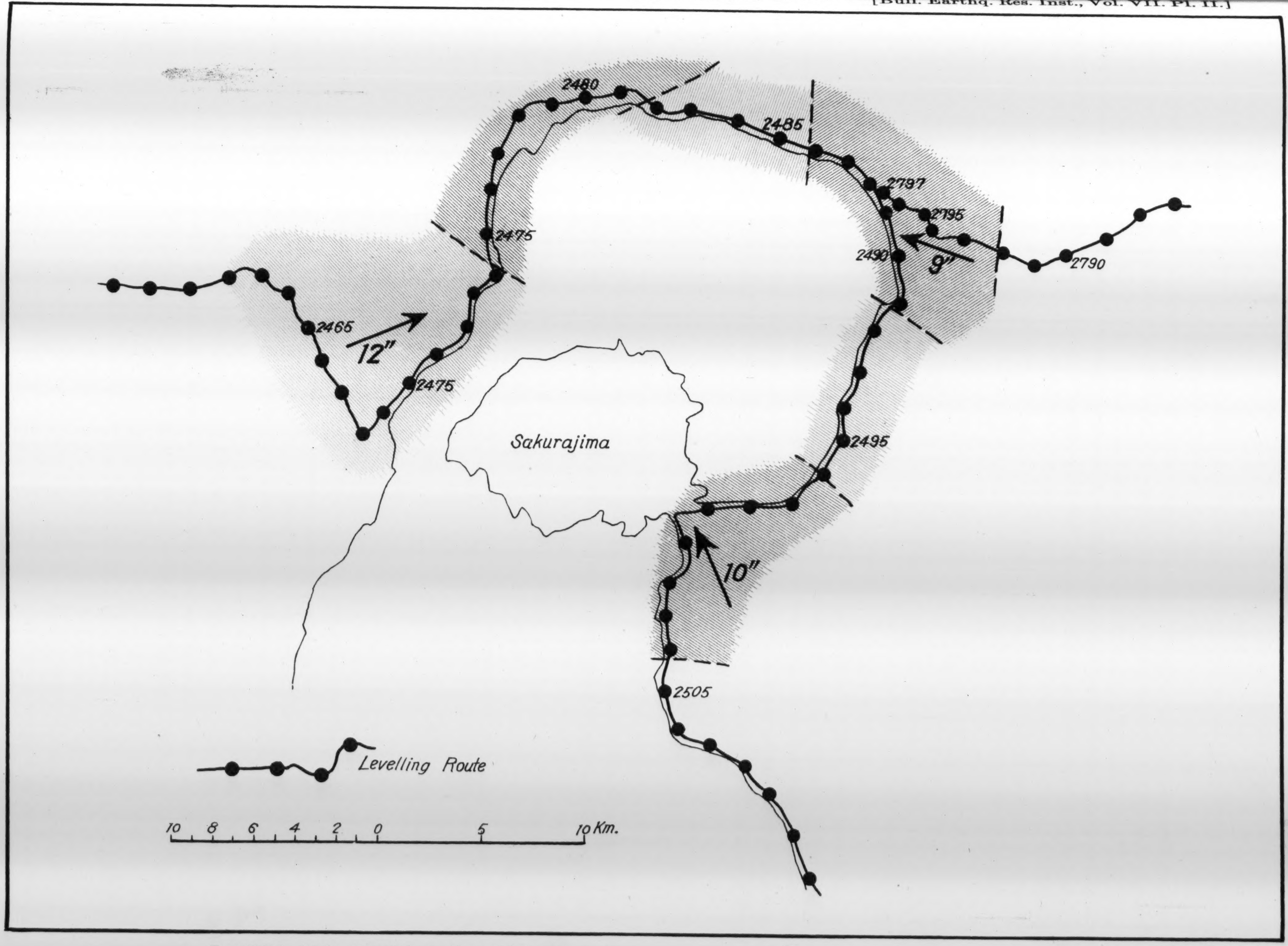
2480
2485
2797
2795
2790
2490
9"
2475
2465
12"
2475
Sakurajima
2495
10"
2505
Levelling Route
10 8 6 4 2 0 5 10 Km.

（震研彙報第七號・圖版、坪井）

Land Blocks in the Sakurajima District.

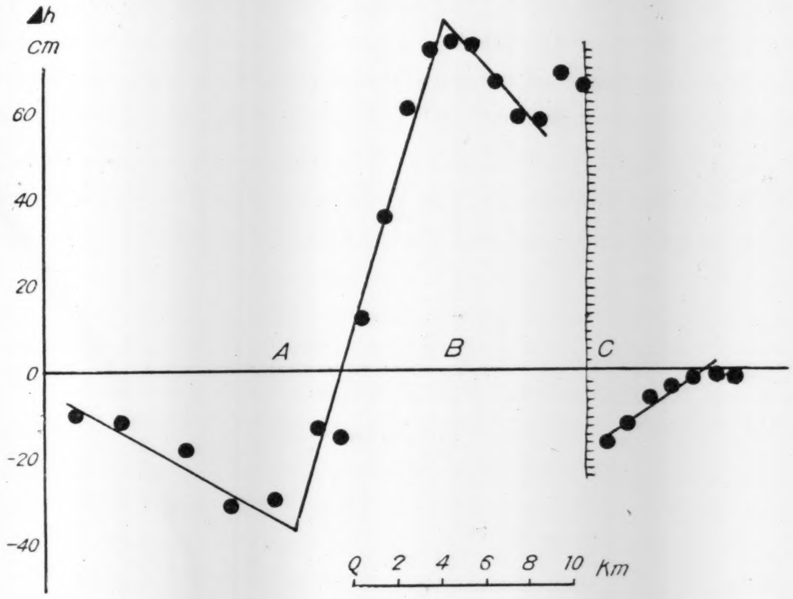

Fig. 5.

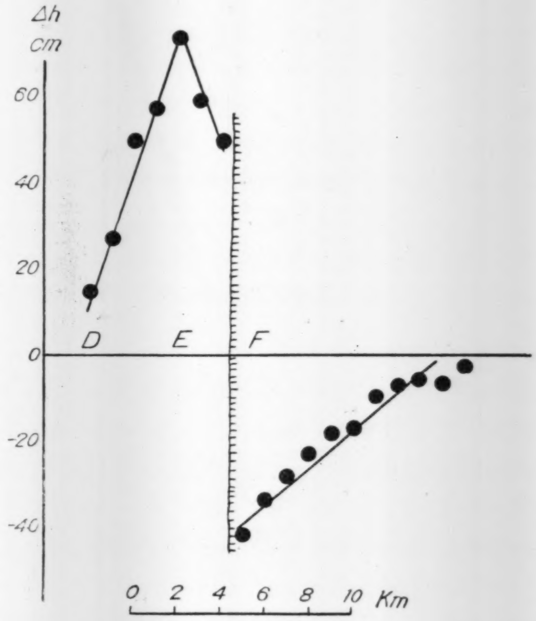

Fig. 6.

5. TAJIMA AND TANGO EARTHQUAKE DISTRICTS.

In an interval of about a couple of years, two great earthquakes took place in the Tango and Tajima districts. The Tajima earthquake took place on May 23rd, 1925, and the Tango earthquake on March 7th, 1927. Their epicentres were only 20 km. apart from each other. After these earthquakes, the revisions of precise levellings were extended to the areas affected by these earthquakes.[7] A part of the results of the investigation made have already been published.[8] The results of examination made for the Tajima district are seen in the following Fig.7. Here also the block movements are seen to have taken place. (Pl. IV).

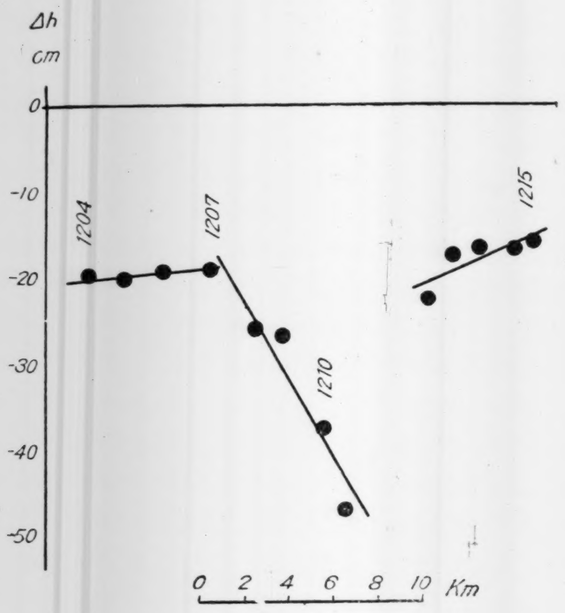

Fig. 7.

6. DISCUSSIONS.

After all, the present author believes to have succeeded in demonstrating the actual manifestation of the existing geological movements in some localities of this country. It has become clear that the land blocks still preserves their physical significance in geologically instantaneous and minute movements of so short a duration as may be counted in scale of years. Such being the structure, there seems many problems to be reviewed under a new postulate regarding the physical, especially mechanical, properties of the earth crust in somewhat a different manner from what has hitherto been accepted. Can any elastic stress of major scale due to some geological forces really exist in the earth crust with so much structural cosntituents? The

---

7) A. IMAMURA, *Bull. Imp. Earthq. Inv. Comm.*, **10** (1922–1928), 71.

8) C. TSUBOI, *Proc. Imp. Acad.*, 4 (1928), 529.
Bull. Earthq. Res. Inst., **6** (1929), 74.

（震研彙報第七號、圖版、坪井）

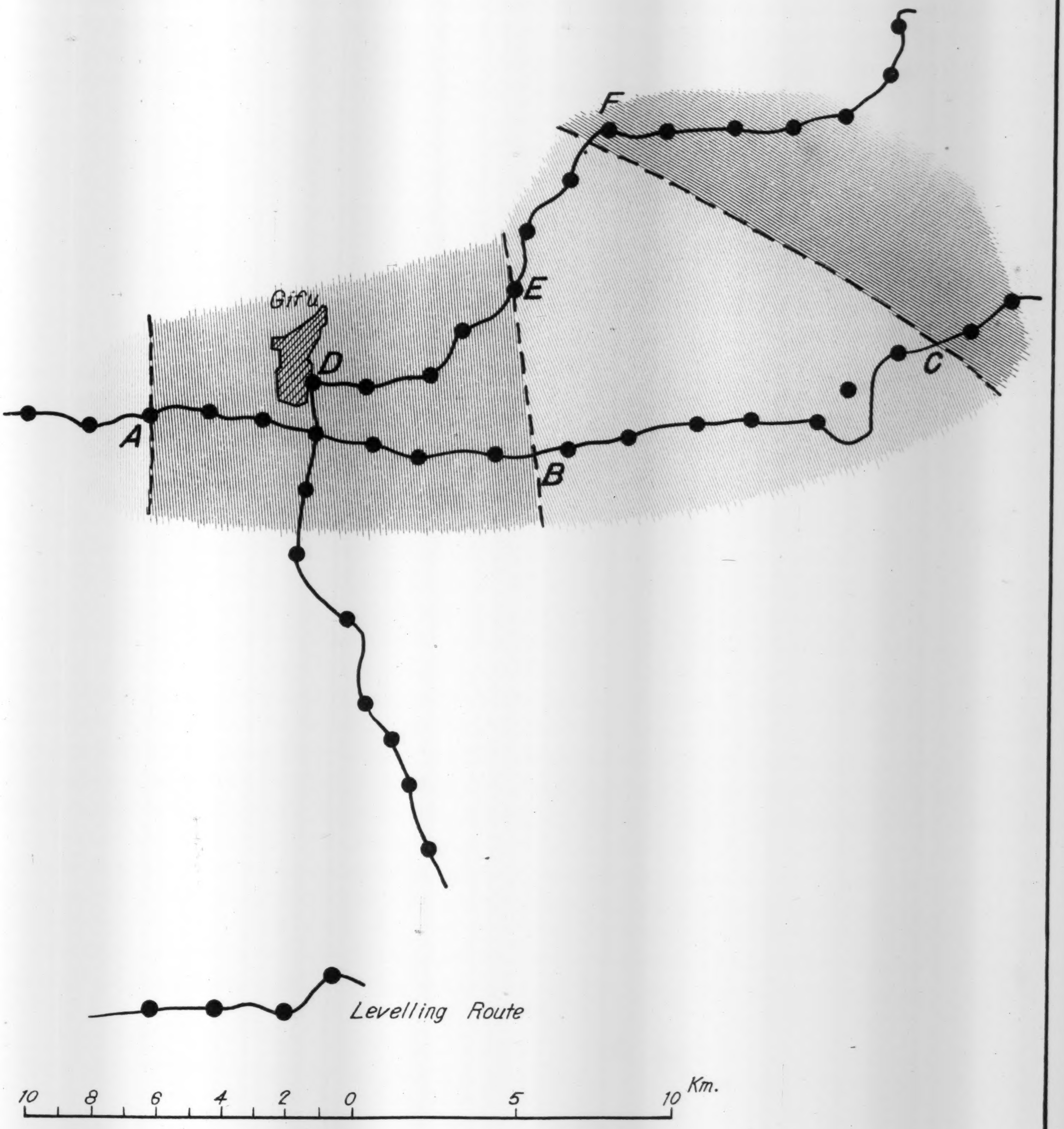
F
Gifu
E
D
A
B
C
Levelling Route
10 8 6 4 2 0 5 10 Km.

Land Blacks in the Mino-Owari District.

(Facing p. 112)

characteristic behaviour displayed by a medium with aggregate constituents is well-known. The most conspicuous example is furnished by the pile of sand. The experiments of T. Terada and N. Miyabe[9] regarding the deformation of sand pile afford us brilliant examples. If the physical properties of the earth crust are not entirely analogous with those of the sand pile, there seems no doubt that the statical elastic stress extending to infinity cannot exist in the earth crust. The earth crust may be regarded under a certain class of force as an aggregate of wooden blocks floating on a liquid in contact with each other by their lateral faces. Putting aside the problem regarding the position of the source of generation of the train of seismic disturbances, the whole system of the land blocks in the earthquake district must be subjected to a general slow displacement at the moment of the earthquake occurrence, each of the blocks being in mutual coupling with others. Let there be considered three land blocks A, B, and C in successive arrangement. Suppose they were disturbed by an earthquake and let the diplacement in the boundary A and B be small but discontinuous and that in the boundary of B and C large but continuous. In such cases, a passing field observation will only reveal the existence of the discontinuity of the displacement between A and B—what is called a fault. It has been usual in such cases to lay much stress on this visible discontinuity and to take this as a unique significant phenomenon concerning the earthquake. But how could we attribute the prime importance to the discontinuity between A and B if we could only know that the absolute displacement between B and C was far much larger? The *chaos* of the block movements as a whole, but not each of the differential movements at the boundary lines of the blocks appears to be the most characteristic and important phenomenon in the district of earthquake origin.

In conclusion, the present writer wishes to express his gratitudes to Professor Torahiko Terada for much suggestive instructions and helpful critisisms he has constantly given.

---

9) T. TERADA, and N. MIYABE, *Bull. Earthq. Res. Inst.*, **4** (1928), 33; **6** (1929), 109.

6. 水準測量に依りて見出されたる地塊運動に就いて

地震研究所 坪井忠二

地震發生の本源を考へるに就いては、現在地殼が如何なる變動をなしつつあるかと云ふ事を明にするのが肝要である。我が國に於いては、明治二十四年の濃尾地震以來、大地震、大噴火のあつた毎に該地方の三角測量や水準測量の改測が行はれて來た。此の論文は、夫等の改測によつて明にされた地殼の變動を詳しく調査したものであつて、夫等の改測の結果、所謂地塊運動が明に見出される事を强張したものである。尙之等の物理的の方法で求められた地塊が、地質構造から見た地塊と一致するものである事は、著者の前論文で指摘した所であるが、此の論文に於いても此の見解が確められた。地殼が此の樣な片々的な構造を持つて居るものとすれば、それに彈性的ストレスが存在し得るやと云ふ點に就いても疑問を生ずるのであるが、著者は寧ろ之を否定する樣に傾いて居る。地震の際に生ずる所謂斷層は、唯二地塊の運動が不連續であつたと云ふ所に過ぎず、其の附近には連續ながらもつと大なる變移もあり得るわけであるから、只肉眼の野外觀察で發見し得る斷層よりも、地震地方の地塊全體としての動きと云ふものの方がより重大な意義を持つて居るのであらうと考へられる。

（震研彙報第七號、圖版、坪井）

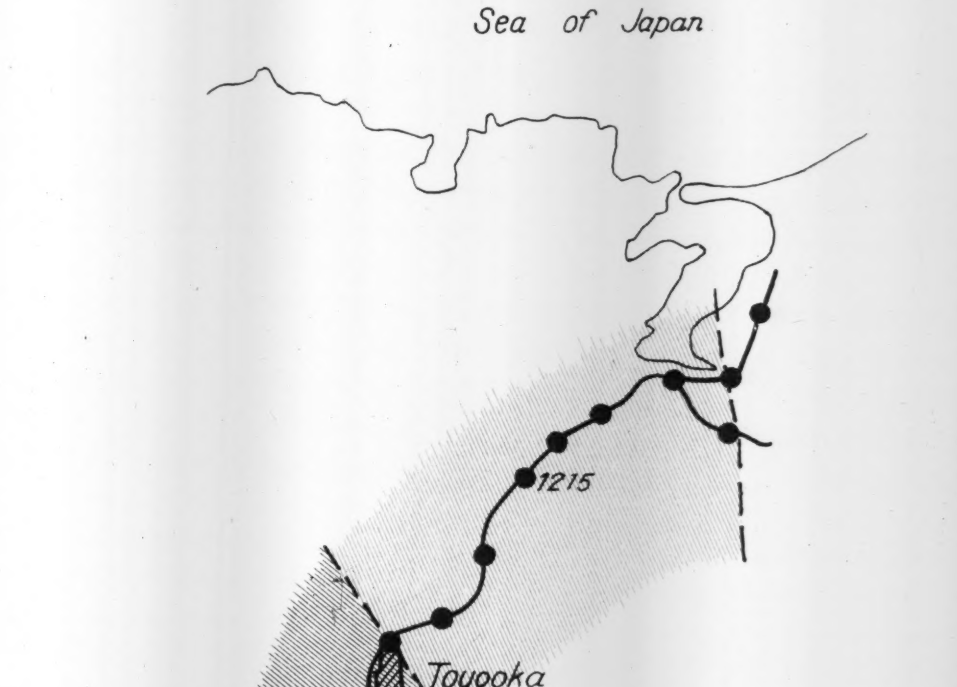
Sea of Japan
1215
Toyooka
1210
1206
Levelling Route
10
8
6
4
2
0
5
10 Km.

Land Blocks in the Tajima District.

（震研彙報第七號、圖版、坪井）

7. *On the Effect of Cyclones upon Sea Level.*

By **Seiti YAMAGUTI.**

(Read Jan. 15, 1929.—Received March 20, 1929.)

INTRODUCTION.

In a previous paper,[1] the report was given of the result of some investigations on the effect of cyclone frequenting our Pacific Coast, upon the height of the sea level at Aburatubo, Province of Sagami. The present paper may be regarded as a continuation of the above, dealing with the sea level at Aburatubo, as well as at three other stations: (1) Hososima, in Hyûga, (2) Hanasaki, in Province of Nemuro, Hokkaidô, and (3) Wazima, in Noto. The geographical situations of these stations may be seen from Fig. 1. of the paper given in Jap. J. Astr. Geophys., IV (1926), 1.

Instead of taking the monthly distribution of the frequency of cyclonic tracks visiting our coast as in the previous preliminary investigation, the daily variation of the distribution of the cyclones in the oceanic area was examined, taking the data from the Daily Weather Charts of the North Pacific Ocean, published by the Imperial Marine Observatory, Kôbe, Japan.

It was assumed that any elementary area of a cyclone on the ocean will contribute an elementary variation of the height of the sea level at the station considered, which is proportional to the area of the element and is a function of the distance of the element from the station. For the first approximation we may define the cyclonic area as bounded by an closed isobar with a certain pressure and regard all the elementary areas within the area equivalent, as regards their contribution to the sea level, whereas the area on the outside of the said boundary is of no effect. Again, the effect of the distance may be accounted for if we divide the ocean into successive zones by drawing concentric circles with the station as centre, and the cyclonic area as defined above be allotted with a proper weight according as the distance of the zone in which the cyclonic area lies.

The method of procedure adopted is as follows.

On the Daily Weather Chart, the oceanic area was divided into n equal sections by radii vector with the given station as the origin and with $\theta = n \times 15^\circ$, $n = 1, 2, 3, \ldots$, where the prime vector and the last radius were taken nearly tangential respectively to the coast lines on both sides of the station. The area was again divided into circular zones by seven concentric circles with radii of 300, 600, 900, ... 2100 km. respectively, except in the case of Wazima for which five circles were drawn (300–1500 km.). The area of each section thus divided by successive radii vector and concentric circles was taken as an unit area for measuring the cyclonic area, so that the nearer the area is situated to the station, the greater is the weight attached to that elementary area. The "*reduced*" *cyclonic area* as defined above, i.e. Σ (actual area)/(area of the section) $= \Gamma$, which has fallen within a circle of 900 km. radius, or 2100 km. radius was denoted by Γ_3, or Γ_7 respectively, the effect of the azimuth being assumed immaterial. The boundary of the cyclonic area was taken at the isobar with 756 mm. Hg. In order to take account of extremely deep depression, the areas within the isobars of 748 mm. Hg were alloted with the double weight.

---

[1] T. TERADA and S. YAMAGUTI, *Proc. Imp. Acad.*, **4** (1928), No. 8; *Bull. I.E.I.C.*, **11** (1928), No. 3.

To save the labour, use was made of a celluloid plate, upon which were drawn the radii vector and concentric circles above explained. This was applied on the Chart and the cyclonic area as above defined was counted. Thus the values of Γ_3 or Γ_7 for every day were read off with no great labour.

The data of the sea level for the said stations were kindly placed at my disposal by the Military Land Survey Department through the intervention of the Authorities of the Imperial Earthquake Investigation Committee, except the data for Hanasaki from December 16, 1924 to the end of the year 1927, which were kindly furnished by the Imperial Marine Observatory, Kôbe. The latter data are grouped according to the Moon's ages, namely each monthly mean covers an interval between the days next to the days of successive full moon.

According to the estimation of the Military Land Survey Department, the values of the sea level after the Great Earthquake of Sept. 1, 1923, were reduced by 1394 mm., assuming the upward displacement of the earth crust on that occasion to be of this amount.

The comparisons were made of the cyclonic area reduced as above, firstly with the monthly mean sea level, secondly with the daily mean sea level, and lastly with the yearly mean sea level, during a period of five years (1923–1927).

On the other hand, the comparison was also tried of the monthly mean value of Γ_7/Γ_3 with the corresponding value of $\Sigma|\Delta L|/\Sigma|\Delta b|$, corresponding to the method taken in the previous report,[2] for 1923 and 1924 in the case of Aburatubo and Hososima, and for 1923 alone in the case of Wazima and Hanasaki.

Method of Investigation.

a) On plotting the monthly mean sea level as ordinates against the month taken as abscissa, it may be seen at first glance that there exists a conspicuous annual fluctuation with a minimum in March or April and a maximum in September or October, which may be caused partly by the variation of the sea water temperature[3] and probably also by that of ocean current and some other meteorological effects.

It was considered suitable to apply at first some correction due to the systematic annual variation of sea level directly due to the annual variation of pressure, before entering into the investigation of the specific effect of the cyclonic area. On plotting the barometer-sea level diagram, however, we noticed that the barometric pressure has a complicated fluctuation with the irregular periods of about two months or more, besides the annual variation, it is not practicable to correct the deviation of sea level for the annual barometric variation. Hence, in order to eliminate the averaged systematic annual variation, regardless of its causes, and make the effect of the cyclones more prominent, it was preferred to take, for the comparison with the cyclonic data, the value of the deviation, $\varDelta L$ from the mean of each monthly value of sea level for 25 years (1900–1924). For Aburatubo, the mean for 24 years (1900–1923) was available.

As to the corresponding value of the cyclonic area, the value of the deviation, $\varDelta \varGamma_3$ from the mean monthly value of $\varGamma_3$ for the five years, 1923–1927, was subjected to examination.

For Aburatubo, the zone for $\varGamma_3$ (i.e. with 900 km. radius) extends to Hokkaidô and to Kyûsyû, while the region for $\varGamma_7$ reaches Saghalien toward N and Formosa toward S, the aperture of the entire sector, θ, being 210°. For Hososima, the prime vector touches the Kurile Islands Arc, and the last vector, the southern coast of China, making $\theta=195°$. For Hanasaki, the prime vector also touches the Kurile Islands, and the last vector was so chosen as to pass the south end of Kyûsyû, θ being 180°. For

---

2) Prof. TERADA and S. YAMAGUTI, *Proc. Imp. Aacd.*, **4** (1928), No. 8; $\varDelta L$ is the deviation of the sea level from the corresponding mean and $\varDelta b$ the deviation of the barometric pressure.

3) T. NOMITU and M. OKAMOTO, *Mem. Coll. Sci., Kyôto Imp. Univ.*, A. **10**, No. 3 (1927), 125.

Wazima, the prime vector is directed to Hokkaidô, and the last to the north end of Kyûsyû, θ being 150°. In this last case, the region for Γ_3 includes Japan Sea only, and that for Γ_5 includes the Chinese Waters besides the above. For all these stations, the area of the land which are occupied by the cyclone was put out of account.

Thus, firstly, the ΔL-curve and the $\Delta\Gamma_3$-curve were drawn with the months as the common abscissa as shown in Fig. 1. The two curves show in most cases some evident parallelism with each other, though some discrepancies are observed during some epoch at some stations. Next, a diagram was plotted for each station, in which the monthly values of ΔL and $\Delta\Gamma_3$ are taken respectively as the ordinate and abscissa, as shown in Fig. 2. The zero line of ΔL being transformed by an amount of 27, −8, 70 and 38 in millimeters for Aburatubo, Hososima, Hanasaki and Wazima respectively in order to make $\Sigma\Delta L=0$. It will be seen that the points plotted are rather

ΔL from 25 years' mean and $\Delta\Gamma_3$

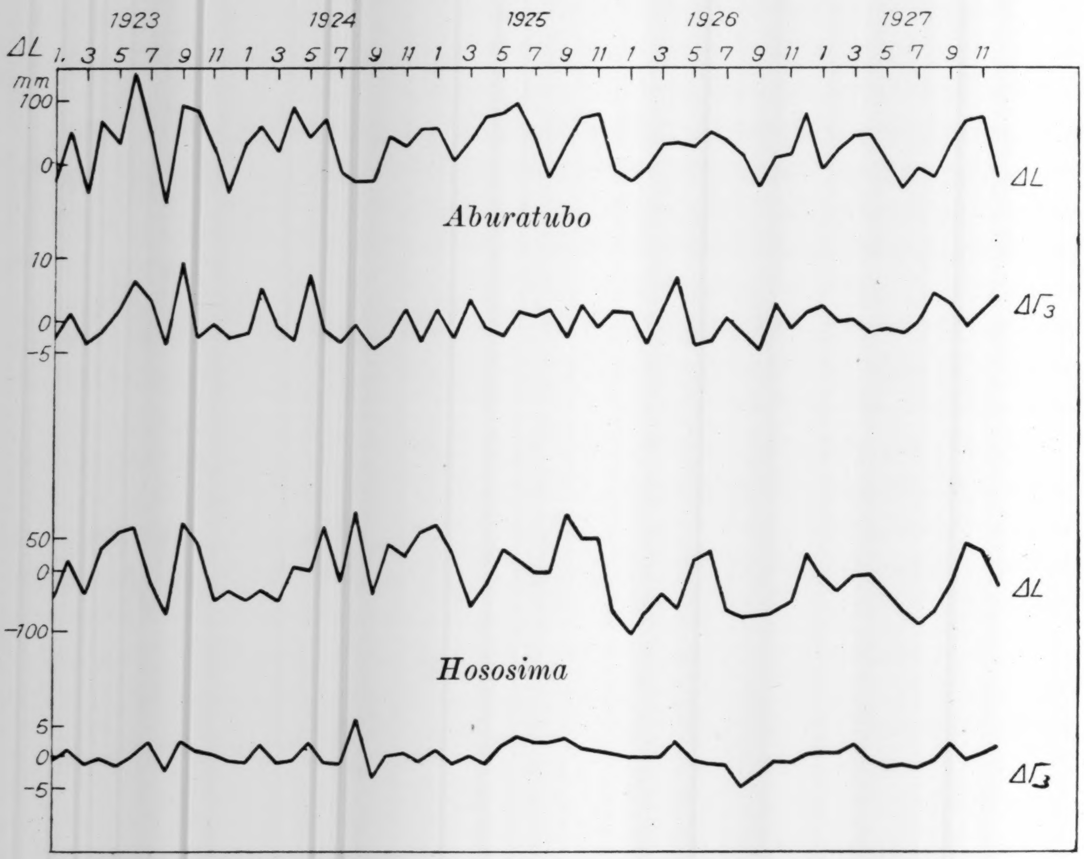

Fig. 1 *a*.

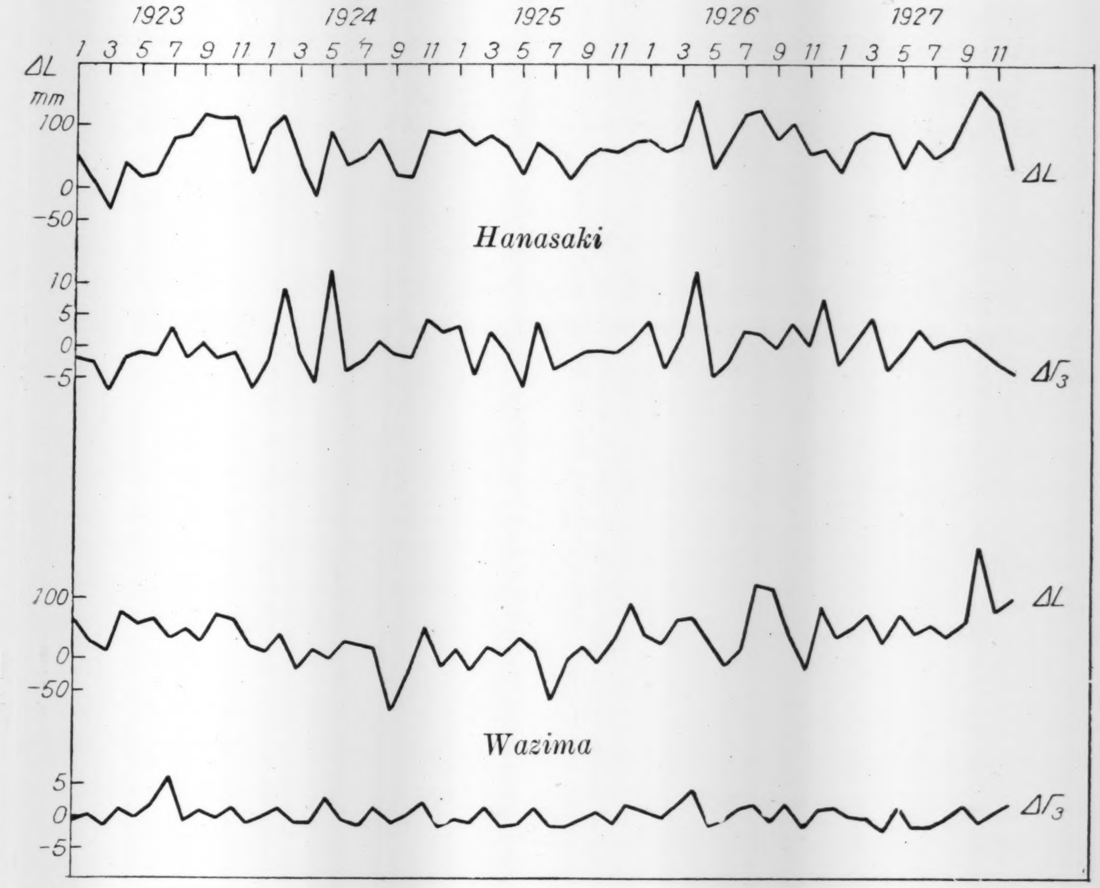

Fig. 1 *b.*

widely scattered; still, the points show a tendency to be distributed in an elliptic area of which the major axis is inclined to the axis of abscissa at an angle somewhat similar for different stations.

b) Next, with the purpose of finding out the *"cyclonic factor"*, i.e. a factor giving the normal ratio of $\Delta L'$ to $\Delta \Gamma_3'$, the relation between the *daily* values of the sea level and the area which we denote by, L' and Γ', were examined. On plotting the daily values of the sea level as ordinates against the dates taken as abscissa, the deviation from the straight line connecting the mean point of the four days at the beginning of the month to that of the four days at the end, was measured for every day and was denoted by $\Delta L'$, of which the positive value means the elevation of the sea level relative to the earth crust. Taking this value of $\Delta L'$, which is considered to be thus nearly freed from the astronomical tides with long period, and the *reduced area* Γ_3' as the ordinate and abscissa respectively, we

ΔL from 25 years' mean and $\Delta\Gamma_3$ from 5 years' mean.

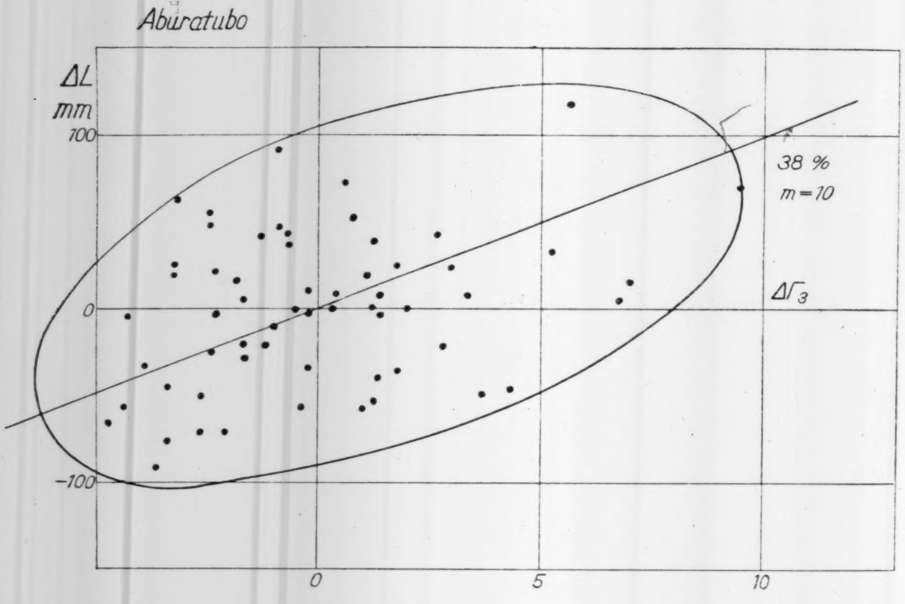

Fig. 2 *a*.

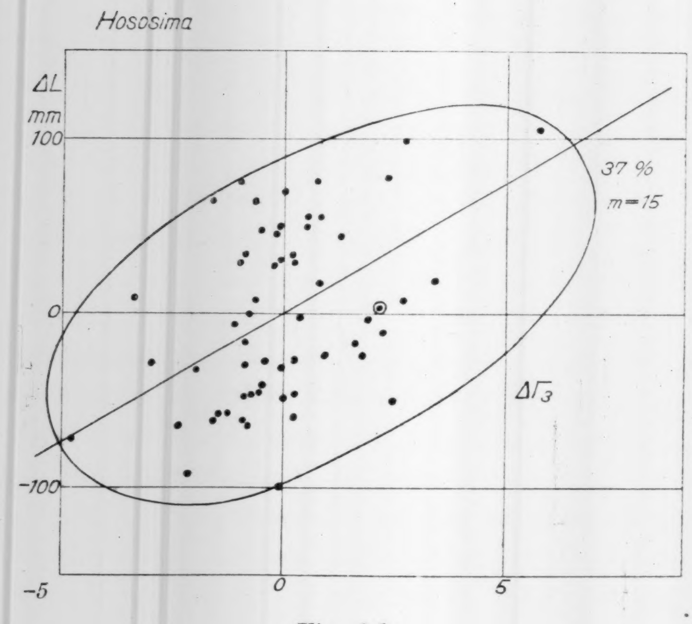

Fig. 2 *b*.

ΔL from 25 years' mean and $\Delta \Gamma_3$ from 5 years' mean

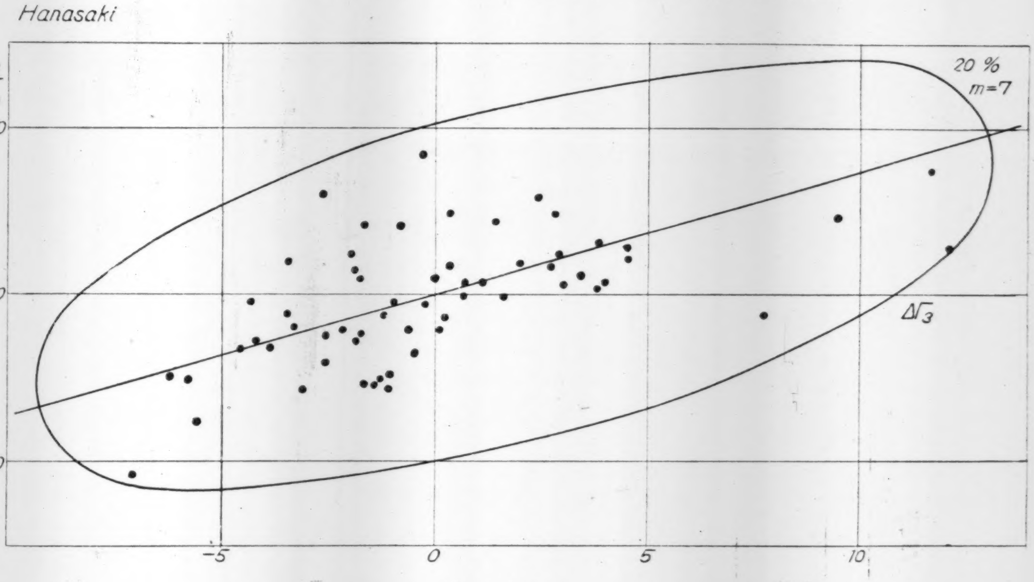

Fig. 2 *c*.

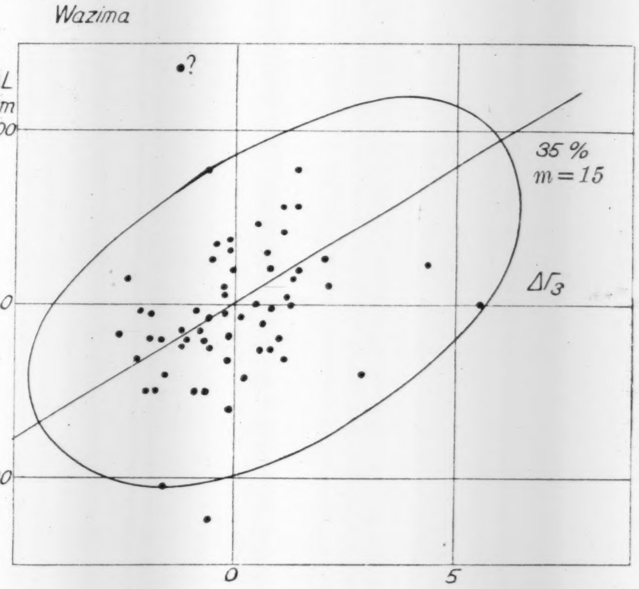

Fig. 2 *d*.

plotted the point for every day, making one diagram for each month of two years (1923, 1924). The diagrams thus obtained for each month show a pretty regularity in general, though a few diagrams show a rather wide scattering of the points.

Hence, only the mean for 12 months was taken combining all the points together. For this purpose, the mean of $\Delta L''$s falling within the range

Cyclonic factor

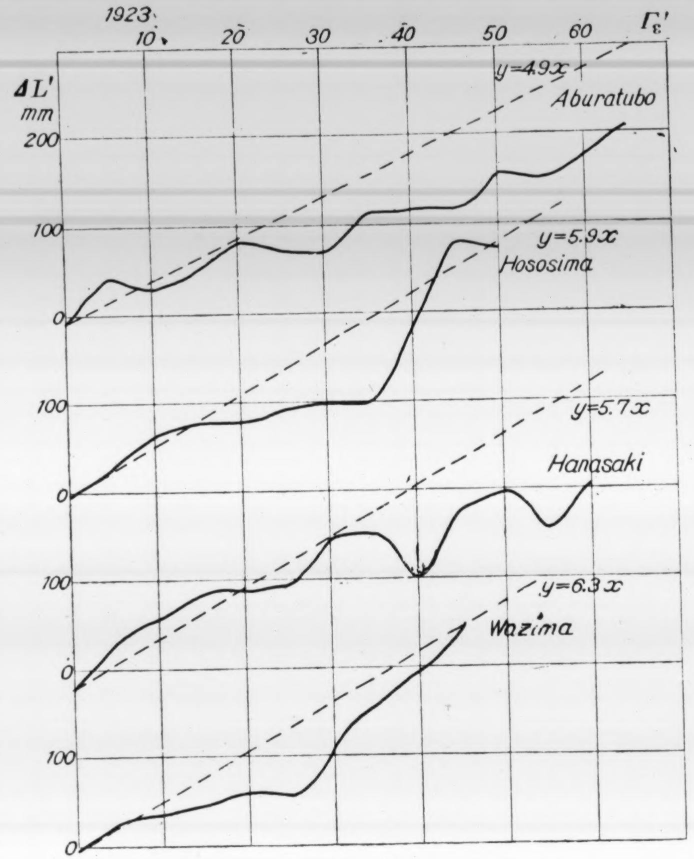

Fig. 3 *a*.

Cyclonic factor

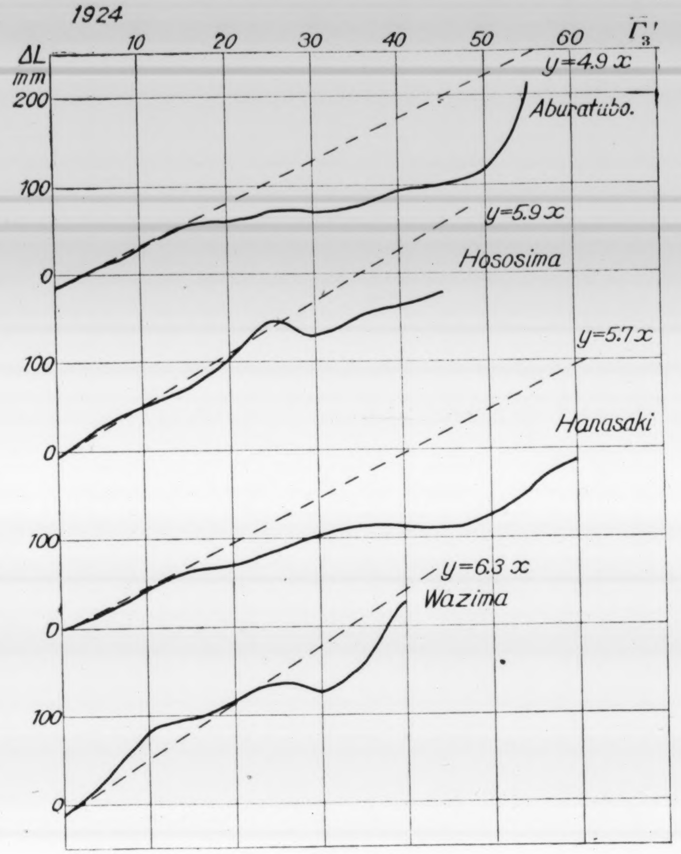

Fig. 3 *b*.

$\Gamma_3'=x-5$ to $x+5$ was assigned to correspond to the value of $\Gamma_3'=x$; only the mean of $\Delta L'$'s falling on the axis $\Gamma_3'=x=0$ was treated specially, namely taking their mean to correspond to $x=0$. The resulting diagrams are shown in Fig. 3, in which the straight lines are obtained from the weighted means

Yearly mean sea level and reduced cyclonic area.

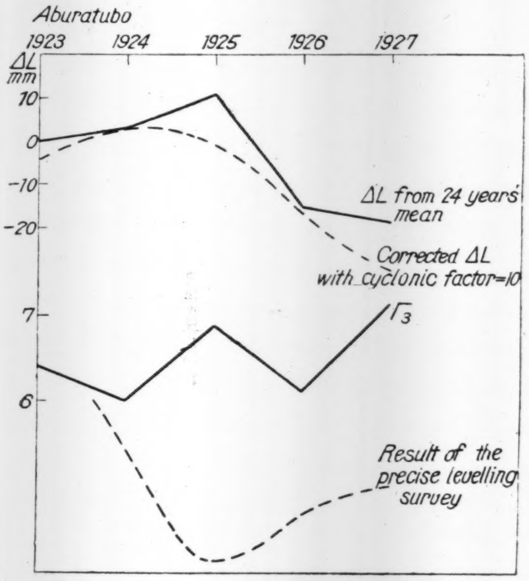

Fig. 4 *a*.

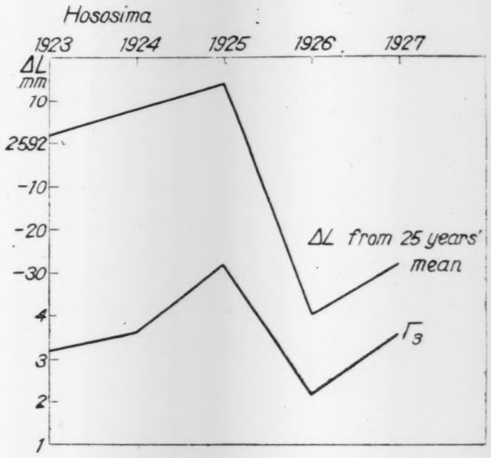

Fig. 4 *b*.

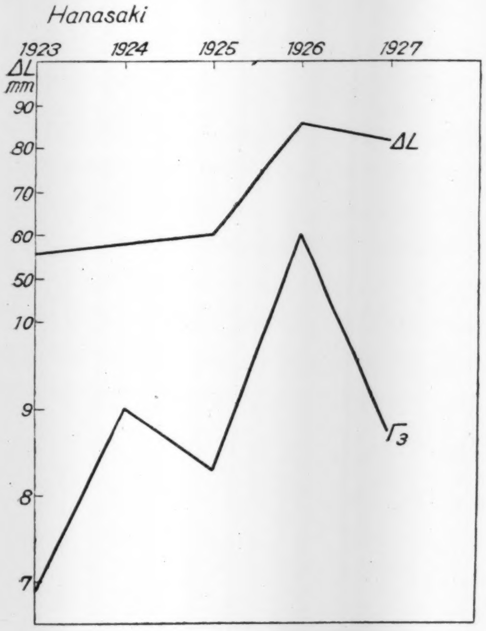

Fig. 4 *c*.

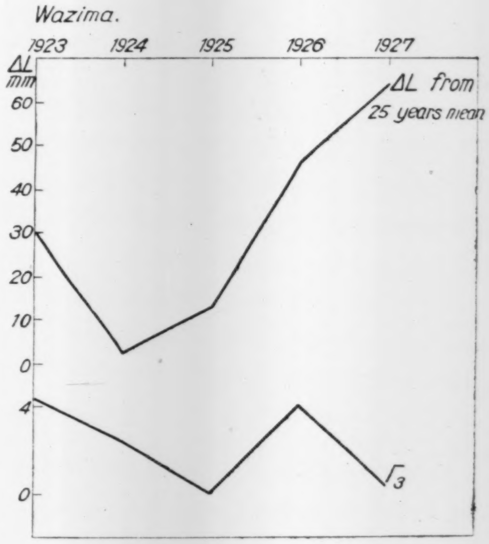

Fig. 4 *d*.

of $\varDelta L'$, by applying the method of least squares. From the inclination of these straight lines, the *"cyclonic factors"* are estimated to be 4.9, 5.9, 5.7 and 6.3 for Aburatubo, Hososima, Hanasaki and Wazima respectively.

c) The deviation of the yearly mean sea level from the mean value of 25 years (24 years for Aburatubo) was also compared with the corresponding mean value of Γ_3 as shown in Fig. 4. A general tendency to parallelism may scarcely be overlooked.

d) To verify the result given in the previous report, the value of $\Sigma|\varDelta L|/\Sigma|\varDelta b|$ above described was compared with the value of Γ_7/Γ_3 in the diagram shown in Fig. 5, in which a general correlation will be observed.

e) Lastly, picking up the most conspicuous cyclonic days, on which the values of the sea level have shown extremely large elevations, among 731 days of the years 1923 and 1924, the relation between the so-called *"barometric factor"* and the *"cyclonic factor"* was investigated.

For this purpose, the differences which we denote by $\varDelta b$, $\varDelta \Gamma_3''$ and $\varDelta L''$, of b, Γ and L respectively between the day before and the day in question, and also these differences between the day in question and the day after were estimated. From these data, the values of $\frac{\Sigma \varDelta L''}{\Sigma \varDelta b}$, $\frac{1}{n}\sum\frac{\varDelta L''}{\varDelta b}$ and $f=\frac{\Sigma \varDelta L''}{\Sigma \varDelta \Gamma_3''}$ were calculated. The results are shown in Table I.

TABLE I.

Stations	The Day before			The Day after		
	$\frac{\Sigma \varDelta L''}{\Sigma \varDelta b}$	$\frac{1}{n}\sum\frac{\varDelta L''}{\varDelta b}$	$f=\frac{\Sigma \varDelta L''}{\Sigma \varDelta \Gamma_3''}$	$\frac{\Sigma \varDelta L''}{\Sigma \varDelta b}$	$\frac{1}{n}\sum\frac{\varDelta L''}{\varDelta b}$	$f=\frac{\Sigma \varDelta L''}{\Sigma \varDelta \Gamma_3'}$
Aburatubo	15.7	30	5.0	12.0	14.1	3.8
Hososima	22.5	41	9.7	20.5	23.3	7.5
Hanasaki	12.3	15.3	5.4	14.2	16.8	6.8
Wazima	25.6	52	12.7	13.5	19.5	6.4

Discussion of Results.

We can see from Fig. 3, that the cyclonic effect upon the *daily* mean sea level is conspicuous. On the other hand, Fig. 2 which refers to the *monthly* mean sea level, shows some apparent discrepancy in some epochs for some stations. This apparent discrepancy may be due to the reason that in some month, for instance, such as August, 1923 for Aburatubo, the

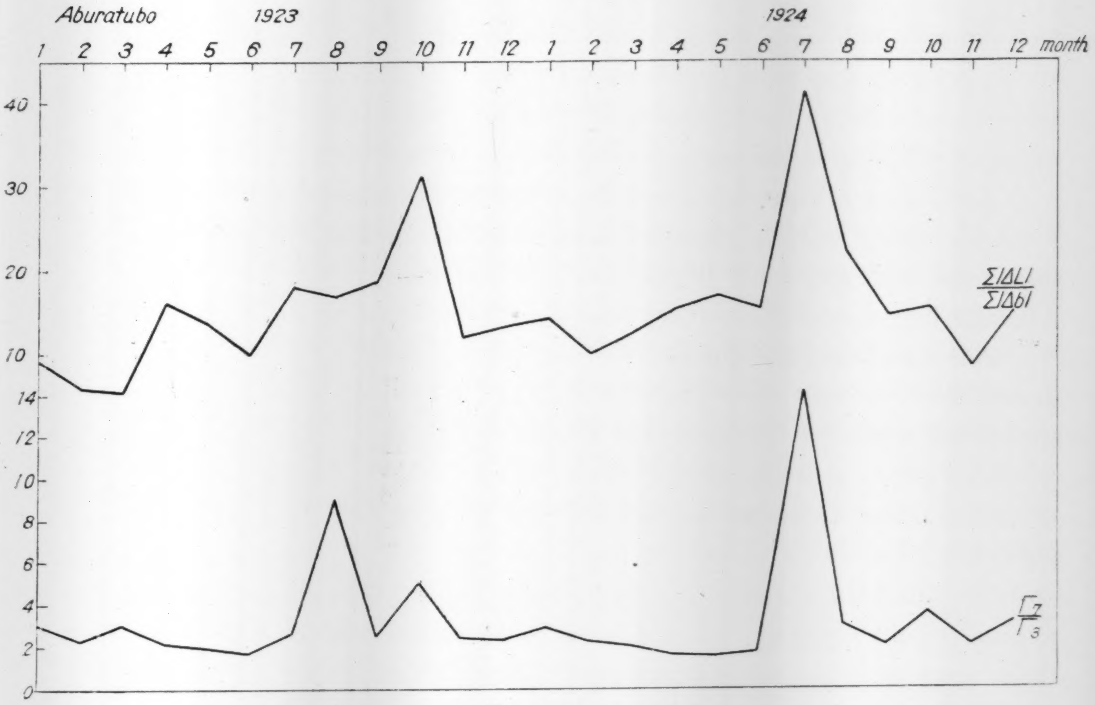

Fig. 5 *a*.

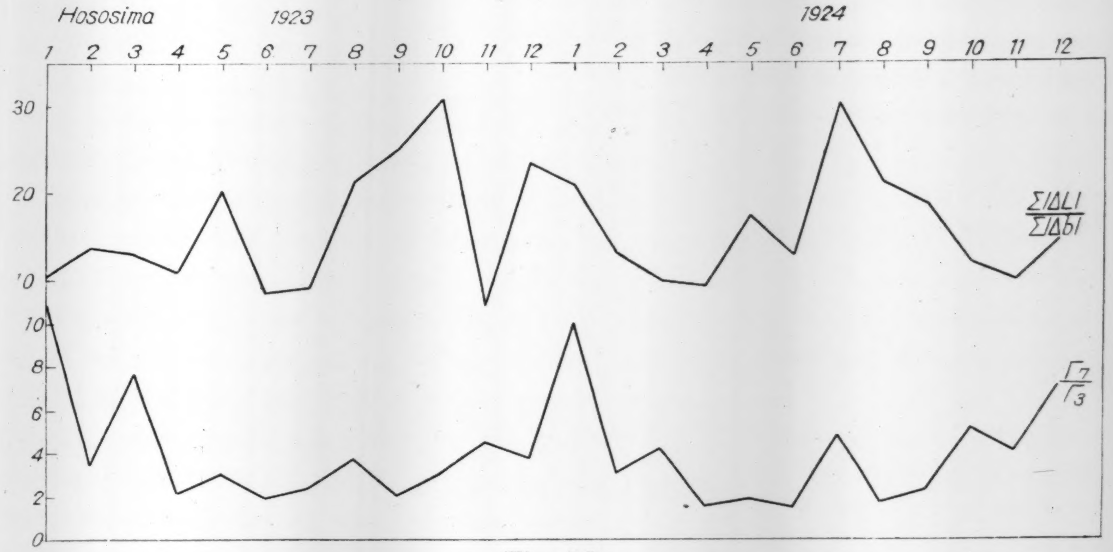

Fig. 5 *b*.

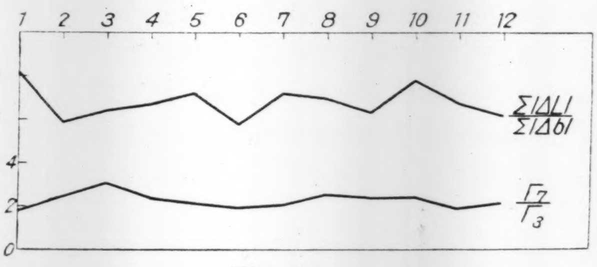

Fig. 5 *c*.

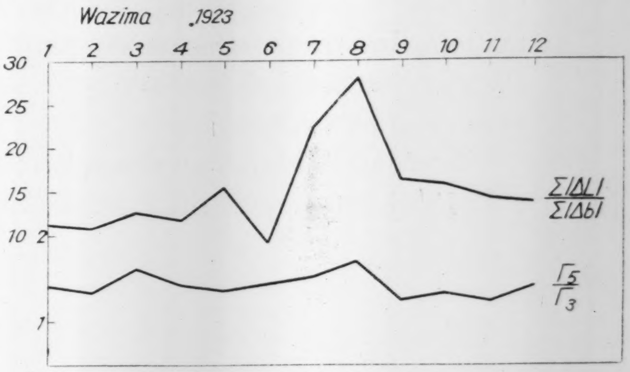

Fig. 5 *d*.

number of cyclonic days is exceptionally small and therefore the cyclonic effect is effaced by the predominant effects of the other meteorological disturbances, such as those caused by anti-cyclones, the winds, etc., when the mean of 30 days is taken.

Again, we also noticed, in the process of obtaining the "*cyclonic factor*" from the daily values, that the month in which the cyclonic days are predominant, for instance, September and October, 1923, for Aburatubo, the relation between the sea level and the cyclonic data was most conspicuous.

For Wazima, the parallelism of ΔL-curve to the $\Delta\Gamma_3$-curve is better generally in winter time than in summer, a fact of which may probably be connected with the frequency of winter cyclones passing over Japan Sea.

Moreover, we noticed for all the stations that, on calm days, the values of $\Delta L'$ are scattered widely above and below the origin along the axis of $\Gamma_3'=0$. This mean value i.e. the mean $\Delta L'$ for $\Gamma_3'=0$, is always negative and its absolute amount is small, being mostly less than 20 mm. for any month for all stations. The case with $\Gamma_3'=0$ includes those cases in which there may exist some sensible effect of anticyclone prevalent in the neighbouring sea. Hence, if this effect of anticyclone be conspicuous, we may expect the above mean $\Delta L'$ for $\Gamma_3'=0$ to be large. The fact that this is small, may therefore mean that the effect of anti-cyclone upon the mean sea level is comparatively small.

After all, we can draw an ellipse enclosing all the points of which the major axis is inclined by a certain angle to the axis $\Delta L=0$, as shown in Fig. 2. From the angle of inclination thus estimated, we may obtain a "*cyclonic factor*" with respect to the monthly value. The factors thus determined roughly are 10, 15, 7 and 15 for Aburatubo, Hososima, Hanasaki and Wazima respectively. Again, counting the number of points which fall in the second and the fourth quadrant of $\Delta\Gamma_3-\Delta L$ diagram shown in Fig. 2, we can find that the numbers of months in which the correlation is in opposite sense, are only 38, 37, 20 and 35 per cent. for Aburatubo, Hososima, Hanasaki and Wazima respectively.

Hanasaki, which shows the greatest value of the correlation coefficient is, in fact, mostly frequented by cyclones among those four stations. The existence of even this degree of correlation between the two quantities $\Delta\Gamma_3$ and ΔL, in spite of the numerous disturbances superposed owing to many other meteorological factors, will show how conspicuous is the effect of cyclone upon sea level.

Looking at Fig. 5, we recognize a fair correlation between $\Sigma|\Delta L|/\Sigma|\Delta b|$ and Γ_7/Γ_3 for each of the four stations, though there exist some exceptional months, for which the exact reason is not yet known. Again, the parallelism in the curves of the above quantities for 1923 is not generally so good as in the case of 1924, for Aburatubo and Hososima, while for the curve of ΔL and $\Delta\Gamma_3$, the contrary is the case. A plausible explanation may be sought in the fact that the amount of fluctuation of the barometric pressure over a wide area of the sea neighbouring the mareographic station may be considerably larger than at the land station of which the barometric data are taken, and that the effect upon the sea level of a cyclone which passed through the region nearer than 900 km. from the mareographic station is associated with the positive elevation of the sea level, while the effect of a cyclone which passes over remote part of the sea further than 1200 km. from the station may correspond to the depression of the sea level at the station. In general, it will be seen that when the fluctuation of the barometric factor is small, the fluctuation of the value Γ_7/Γ_3 is also small as shown in Fig. *5c*, for the case of Hanasaki.

From the Table I, we may be able to say the following:

If we define the "*barometric factor*" by the mean of $\Delta L''/\Delta b$, the value of the factor is more than twice or four times the theoretical value for the days when the cyclone is approaching, and less than twice the theoretical value when the cyclone is going away; this holds at least for the three stations, Aburatubo, Hososima and Wazima, excepting Hanasaki. In the case of Hanasaki, it is somewhat greater than the theoretical value and, moreover, it is less when the cyclone is approaching than when it is receding.

All these facts suggest some effect of wind accompanying the cyclone, keeping in mind that most cyclones frequenting our coast of Honsyû come from the south-western quarter of the North Pacific Ocean and proceed towards the north-eastern part, while in the case of those cyclones considered to affect the sea level of Hanasaki, the relations are otherwise, as the cyclones coming from NW are predominant.

A similar discrepancy may also be found with regard to the "*cyclonic factor*" of which the values found in Table I are somewhat greater, for all stations, than those derived from the daily values of $\Delta L'$ and Γ_3'.

Though the results shown in Fig. 4, are not yet conclusive and a more sufficient data based on many years' investigation are necessary in order to enable us to infer anything definite, we may at least be convinced that a certain physcial connection exists between the yearly mean sea level and the corresponding yearly mean "*reduced cyclonic area*" of the cyclones frequenting the sea area within 900 km. of the station. Especially for Hososima the parallelism is so good that the sea level curve may be reduced very flat if the proper correction due to the cyclone be applied.

For a trial, the yearly mean sea level of Aburatubo was corrected for the cyclonic effect with the cyclonic factor of 10, which is estimated from the inclination of the major axis in Fig. 2*a*, and the corrected height of the annual sea level is drawn with dotted curve in Fig. 4*a*. This corrected curve agrees, in character as well as in magnitude, with the variation of the height of the bench mark at Aburatubo deduced from the result of the precise levelling survey carried out by the Land Survey Department after the Great Earthquake of Sept. 1., 1923, the datum line at Hudisawa being assumed to be constant.

At any rate, it seems advisable in following the annual variation of the sea level as a means for inquiring after the true crustal deformation, to take account of the cyclonic factor as here investigated, which can not be generally negligible, though the other meteorological disturbances may be considered to cancel each other in a whole year.

The effect of cyclone seems to become faint when its centr recedes to a certain distance remoter than 1000 km. from the station. It may be suspected that beyond this range the effect may change its sign, though a further research is wanted to ascertain this point.

As Wazima is situated on the Japan Sea coast, a special consideration will be made with respect to this station. The mean velocity of water current entering the Japan Sea basin through the Straits of Tusima was calculated, which may occur when a cyclone is raging on the Japan Sea and consequently its mean level is raised by a certain amount. The velocity is given by

$$V=\frac{A\,.\,dh}{S\,.\,t},$$

where A is the surface area of the Japan Sea, dh the elevation of the sea level, S the sectional area of the straits, and t the time. We get $V=0.070$ metre/sec., the values of A and S, being estimated from the hydrographical chart, and dh and t assumed as follows:

$$\mathrm{A}=1.46\times10^{12}\ \mathrm{m.}^2;\ S=2.41\times10^{7}\ \mathrm{m.}^2;\ dh=0.1\ \mathrm{m.};\ t=24\ \text{hours.}$$

This value of current velocity is by no means abnormal, and may be admitted by sea men.

Our original purpose of the present series of investigation regarding the meteorological disturbances was, however, otherwise than dealing with these oceanographical problems. Returning now to our proper problem, it was wanted to eliminate the effect of barometric pressure, winds and the other meteorological factors from the observed variation of the sea level and to detect any possible vertical movement of the earth crust which was suspected to have occurred on the occasion of the recent Great Earthquake of Sept. 1, 1923. In the present paper, the new correction due to the specific effect of cyclone was investigated, besides the corrections due to the pressure and gradient⁴⁾ (winds) which were already applied to the daily values of the sea level for the four stations, Aburatubo, Hososima, Hanasaki and Wazima for 1923, and for the first two stations, also for 1924. For Aburatubo, the corrections due to the cyclone as well as those due to the pressure and gradient were applied for the two years, 1923 and 1924. As it was found, however, that the corrections due to the pressure and gradient are generally small and affect the general feature of the sea level curve to a small extent, it is considered convenient for the present purpose to apply the cyclonic correction only, to save the labour in the case when the data for a long range of years is to be examined. Thus, we took also a series of data for the five years, 1923–1927, for which only the correction due to the cyclone was applied, and thus corrected values of the monthly mean sea level were plotted against the month, the datum line being brought down by an amount of 1000 mm. in order to make $+\Delta L$ represent an elevation of the sea level.

Comparing the two curves with and without the barometric and gradient correction for the two years (1923, 1924), they show scarcely any essential difference in the general character of the curve, as already mentioned above. The monthly values corrected for the cyclonic factor$=10$ show still a systematic annual fluctuation. To eliminate the latter, the deviation from the five year mean of each month was taken and plotted in the diagram shown in Fig. 6.

The days, on which a remarkable earthquake has happened near the station, (within the region of Kwantô District), are marked in the figure along with the curve by $\otimes$ and $\times$, corresponding to the strong and the weak shock respectively. The data for the earthquakes were taken from the Monthly Summary Report of the Central Meteorological Observatory in Japan. It appears that the strong shocks have a tendency to occur after the minimum point, or in ascending stage of the curve and the weak shocks, in descending stage, as far as may be judged from the scanty data.

It appears also that the graph shows a sensible downward displacement⁵⁾

---

4) T. TERADA and S. YAMAGUTI, *Jap. J. Astr. Geophys.*, **4**, No. 1 (1926).

5) *I.e.* on the assumption that the amount of the elevation of the crust immediately after the Earthquake as given by the Land Survey Department, and employed here in transferring the datum line, is correct.

ΔL from 5 years' mean, corrected by cyclonic factor, $(f=10)$

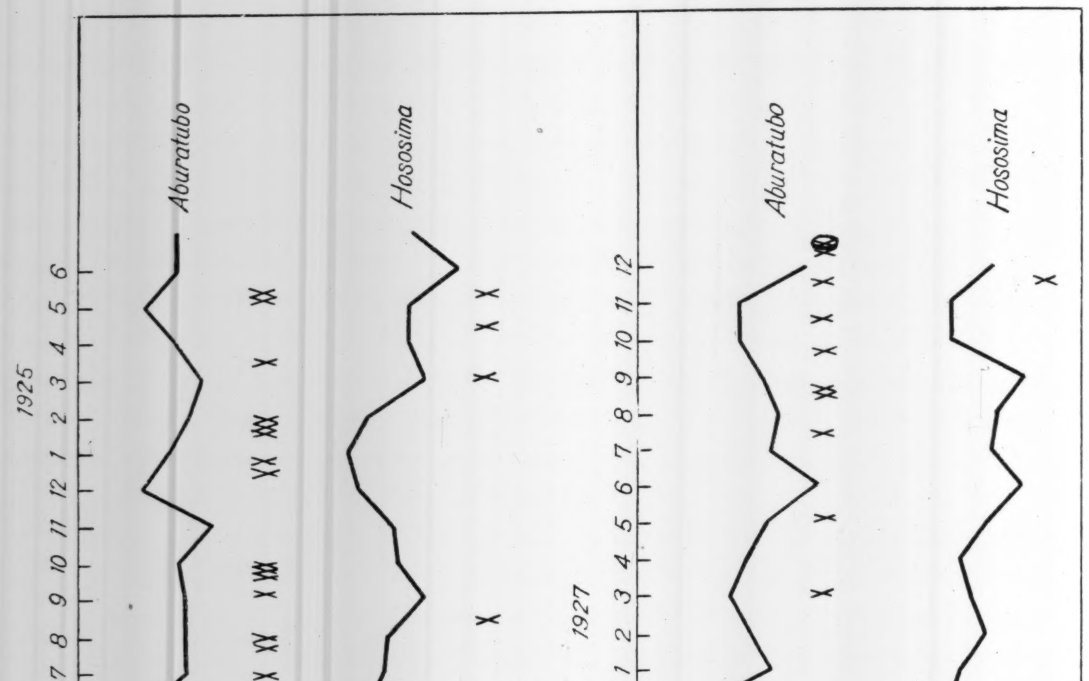

Fig. 6.

of the crust for a certain interval of time after the Great Earthquake of Sept. 1, 1923. The crust seems to have gradually returned to its original height at about Sept., 1924, and the upward motion is seen to have continued to the end of the investigating year, 1927. These points are worth notice and may stimulate a further research on this line.

The data for Hososima were also taken and corrected with the cyclonic factor=15 above obtained, and similarly treated for the sake of comparison, the datum line being brought down by an amount of 2800 mm. in order to make $+\Delta L$ represent an elevation of the sea level, as shown in Fig. 6.

Comparing these two curves for Aburatubo and Hososima, it will be seen that the parallelism is good for some months, which may probably be due to the effect of Ocean current, "*Kurosio,*" upon sea level, as suggested by Prof. T. Terada.

There remains still many factors governing the height of the sea level which must be investigated before we may detect any actual deformation of the earth crust from the mareographic data. It is only a step toward this direction which has been here taken. The investigations are being continued and the further results will be reported in a future communication.

In conclusion, I wish to express my best thanks to Prof. T. Terada under whose supervision the entire work has been carried out and who has given me many useful suggestions throughout the course of my investigation.

---

7. 低氣壓の海水面に及ぼす影響に就て

山口生知

日本近海に現れたる低氣壓の痕跡の數と相模の國油壺に於ける海水面との間に密接なる關係あることは既に寺田博士及び山口生知の名を以て、震災豫防調査會紀要第十一卷第三號に於て報告したり。今回の研究は其繼續作業にして低氣壓の海水面に及ぼす影響を今少しく數量的に見出さんとし即ち低氣壓係數を見出さんとして次の如き方法に依り調査を進めたるものなり。即ち神戸海洋氣象臺發行の日々の天氣圖上に於て問題の地點を中心とし半徑三百キロメートル、六百キロメートル、九百キロメートル、二千百キロメートルを有する七つの同心圓を畫き又一方十五度づゝの動徑を引きたり。最初の動徑及び最後の動徑は問題の地點より兩方面に於ける海岸線に接する樣にひけり、斯くて之等の同心圓と動徑とに依つて圍まれたる扇形の面積を單位の面積と定め日本近海に現れたる低氣壓の海洋上に於ける面積の毎日の價を計算せり。此面積を基とし日々の平均海面、月々の平均海面及び一年間の平均海面等に及ぼす低氣壓の影響を大正十二年より昭和二年迄の五ヶ年間に亘り調査したるに何れも著しき影響ある事を見出したり。されば本來の目的即ち大正十二年九月關東

大地震の前後に於て地盤の上下したるや否やを平均海水面を基準として推定する爲には觀測中より種々の氣象の影響を取去る可き問題に立歸り月々の價より見出したる低氣壓係數を以て月々の平均海面に低氣壓に依る修正を加ふる事を試みたり、其結果月々の平均水面曲線は甚しく上下したる個所消え失せ餘程平坦となり大地震直後地盤は少しく降下しそれより次第に復舊を續け一ヶ年後即ち大正十三年九月に元の高さとなり、以後昭和二年終迄靜に上昇を續けつゝある如き形勢を窺ふ事を得。以上は油壷に就ての調査なるが日向の國細島に就ても全く同樣の調査を行ひたる結果の月々の平均海面曲線を比較し見るに尙未だ海流の影響の如きもの殘存する狀況見え其方の研究は目下繼續中なり。尙此外能登の國輪島及北海道根室の國花咲に於ても同樣の調査を行ひたるに何れも海水面に及ぼす低氣壓の影響の著しき事を見出せり。

8. 丹後地震の餘震調査報告

（第二報）

囑託　那須信治

（昭和四年三月二十日受理）

緒言

前回の報告中には丹後地方の餘震觀測は烈震直後に始り今猶ほ繼續中であると記して置いたが昨年六月下旬限り、舞鶴、城崎、間人の三觀測所を撤廢して一先づ調査を打切ることとなつた。而して其後と言へ共該地方の觀測が全然廢止されたのではなくて現今に至る迄河邊村一ケ所だけは觀測を繼續してゐる。それは同村に設置されてある傾斜計による傾斜變化の觀測の補助機關として殘在されてゐるのである。前號の彙報には主として烈震直後より同年の八月下旬に至る間に起つた餘震に就いて報告して置いたが更に第二報として同年九月より翌年昭和三年六月下旬に至る期間に起つた餘震の觀測調査の結果を茲に報告する次第である。

餘震の回數

昭和二年九月一日より翌三年七月末日に至る間少くも一ケ所に於て觀測された餘震の回數は百三十三回である。その内七十二の餘震に就いてはその震原を推定し得たのである。

之を觀測開始の當初より通算すれば一千三百三十八回の餘震が少くも一ケ所以上で觀測され、その内四百八十二の餘震の震原を決定し得た事になる。

餘震の震央の分布

丹後地方の餘震の震央は主として郷村斷層の西部及山田斷層の東南部に分布され、その分布の狀態は極めて稠密である。是れに反し奥丹後半島内に於ては震央の分布は極めて粗であることは第一報に既に報告して置いた。

烈震後約一ケ年を經たる後に於ても矢張り震央の分布は同樣であることは第一圖に依つて判ること丶思ふ。同圖中大小の黑點の區別は第一報中に用ゐたのと同じであ

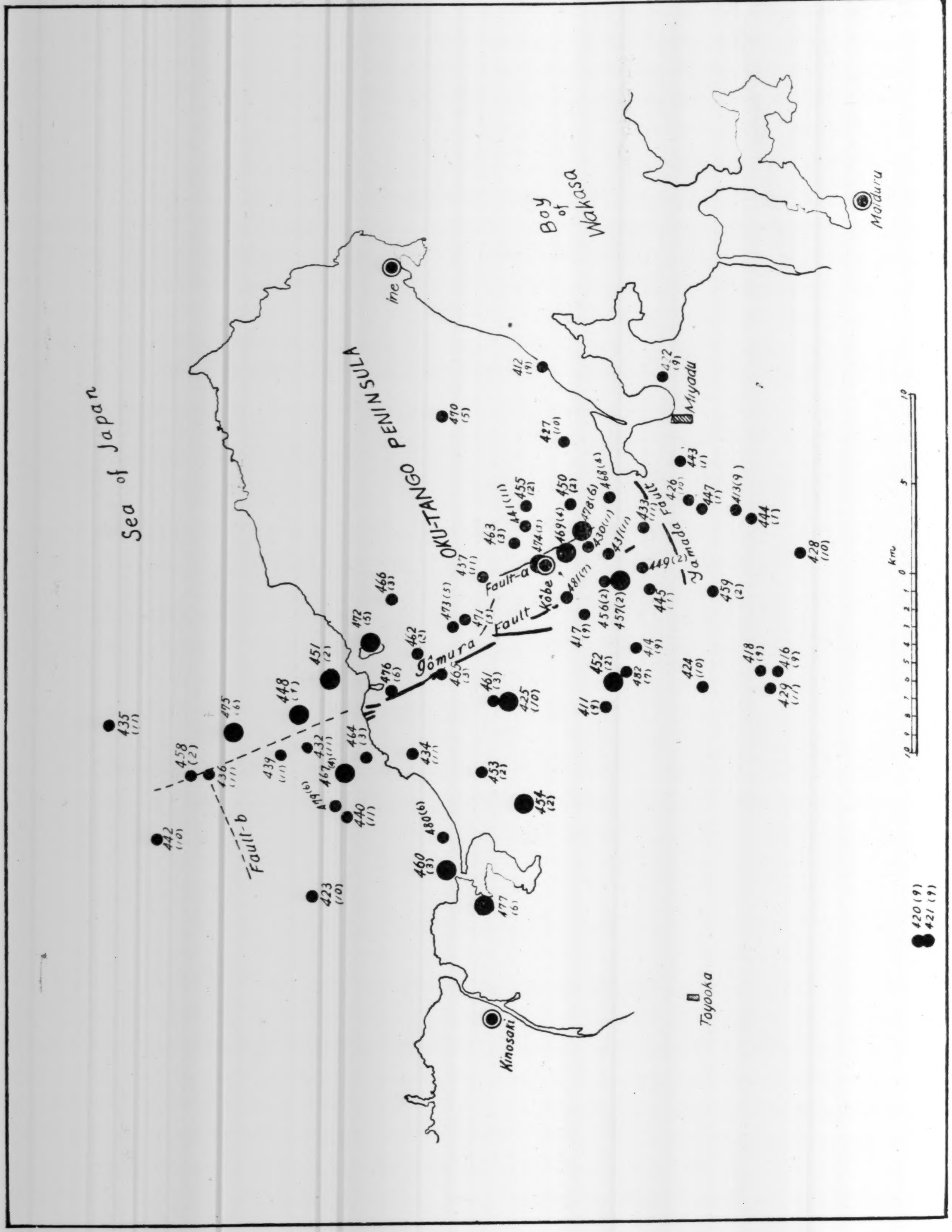
Sea of Japan
OKU-TANGO PENINSULA
Boy of Wakasa
Ine
Maiduru
Miyadu
Kinosaki
Toyooka
Gōmura Fault
Fault-a
Fault-b
Kōbe
Yamada Fault
km
10 5 0 5 10
420 (9)
421 (9)

第一圖 昭和二年九月一日より同三年七月三十一日に至る間に於ける餘震分布を示す。

Fig. 1. Map showing the distribution of aftershoks for Sept. 1, 1927–July 31, 1928.

る。即ち黑點の大なる方は少くとも一ケ所に於て最大振幅100ミクロン以上の記錄を殘した餘震に關し、小點はそれ以下の最大振幅の記錄を殘した餘震に關係してゐる。以下震原の立體的配列を示す場合にもこの區別は同じとす。震央に附してある番號は附表中震央欄に掲げた番號である。又圖中の震央番號の下方に括弧をして中に數字の記してあるのは餘震の起つた月を一見して知り得るに便ならしめるためである。例―(11) は昭和二年十一月、(3) は昭和三年三月。第一圖中河邊村附近に餘震が數回發生した事が注目されることゝ思ふ。これに附いては次に述べることとす。

餘震の震原の立體的配列

第一報告中には震原の立體的配列を調べるために郷村斷層の西側に三箇、山田斷層東南部に四箇の地塊を假定してそれ等の地塊內に含まれてゐる餘震の震原を二樣に投影したのであつた。即ち郷村斷層帶の西側にある三地塊に就いては該斷層帶に垂直な平面に投影し（この場を (A) と名付けておいた）又同じ地塊內の震原を郷村斷層帶を含んで垂直な平面上へも投影した（この場合を (B) と名付けておいた）。山田斷層以南の地塊では、地塊によつて斷層線の交角の二等分線を含む垂直面に或は宮津附近に存在する若狹灣沿岸に極めて特異に見得られる放射線的配列をなす斷層を含む垂直面に投影し（この場合は上と反し (A) と名付けて置いた）、又この斷層線に垂直な平面上へも投影した（この場合 (B) と名付けて置いた）。この方法を矢張其後に起つた餘震の震原の配列を調べるために用ふることとし餘震の分布の最稠密な地塊に就いて述べて見ようと思ふ。最も稠密に分布されてゐるのは郷村斷層の西部にあつて一は日本海底を表面とせる地塊及山田斷層の直ぐ北に接してゐる地塊である。前者は第一、後者は第三地塊と夫々名付けておいたものである。先づ後者の地塊から記すこととす。

第三地塊　此の地塊の表面は東は郷村斷層南に山田斷層は依つて境されてゐる。

(A) 郷村斷層に直角なる垂直面に投影せし場合。（第二圖及第一報中第九圖參照）

投影された震原の分布狀態は一見して二線上に密集して位置してゐることが誰にでも氣附かれることゝ思ふ。座標の原點より右の部分は郷村斷層以東の地塊內の餘震の震原の配列を示したのである。座標の原點を通過する線は明かに郷村斷層の傾斜面の投影を示し右にある今一つの線は河邊村の東方に郷村斷層に平行な斷層の存在してゐることを示してゐるのである。後者の斷層に丁度相當して斷層が實在してゐることは

Fig. 1. Map showing the distribution of aftershoks for Sept. 1, 1927-July 31, 1928.

津屋所員の奥丹後半島の地質構造調査報告（地震研究所彙報第四卷百五十八頁）の附圖を見れば明白な事實である。即ちこの斷層面に沿つて發生した餘震の震原を立體的に配列することに依つてこの斷層は全く鄉村斷層と平行な傾斜面を有することが判明

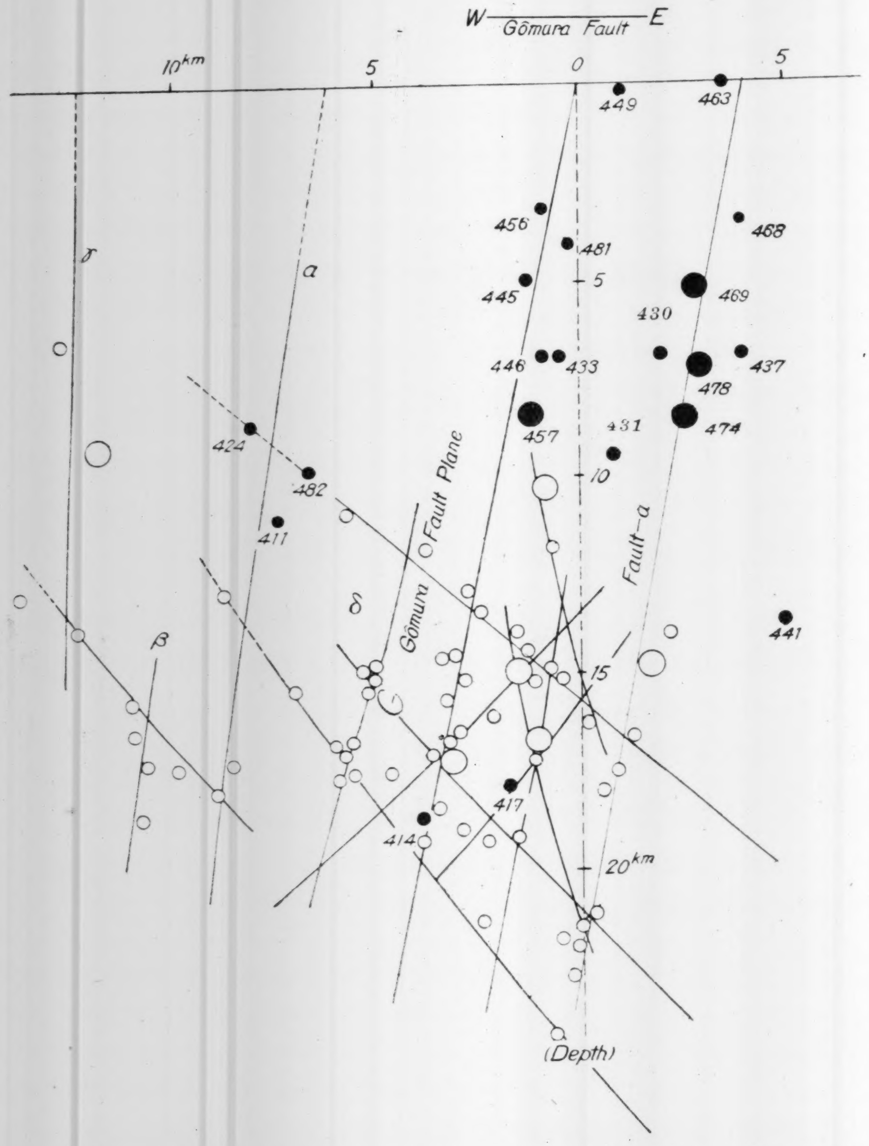

第二圖　第三地塊及其近傍に發生したる餘震の震原を鄉村斷層帶に垂直なる平面上に投影せし場合を示す（白圓點は昭和二年三月十二日―同八月三十一日の期間の餘震、黑圓點は同年九月一日―翌三年七月三十一日期間餘震に關す。）

Fig. 2. Seismic foci in block No. 3 and in its littoral, projected on the vertical plane normal to the Gômura fault. (Blank circles denote the occurrences during the period March 12–Aug. 31, 1927: Black circles to those during the period Sept. 1–July, 1928).

したのである。兩斷層面は西南或は南南西へ約七十度の伏角を有すと判定し得るのである。

尙餘震の活動區域は前回報告せし場合は主として十粁以上の深さに限られてゐると云つたが地震活動の末期には比較的淺い場所に活動區域が限られてゐるのは注目に値することである。すべての大地震の餘震が地震活動の末期に比較的地表近くに發するものとは一概に云ひ得ない、又斯く斷定すべき資料もないのであるが丹後地震の餘震に就いては以上の事柄は事實として差支ない。

（B） 鄕村斷層を含み垂直なる平面に同地塊內の餘震の震原を投影せし場合。第三圖及第一報中第十圖参照。

圖中座標の原點は山田斷層の位置を示してゐる。同圖には河邊村の東方に存在する斷層面に發生した餘震の震原も同じ投影面に投影してある。震原の配列の模樣を見ると餘震は主として互に平行な二平面上に發した事が判る。座標の原點を通り第三象限內に引かれた一線は山田斷層面の投影を示してゐることは明かである。他の一線は該斷層の南に一つの平行なる斷層の存在することを暗示してゐるのである。

前述の（A）の方法では餘震の大部分が河邊村及鄕村の兩斷層の傾斜面上に發した事を知り得たのであるがこの方法に依るとそれ等の餘震が山田斷層の上にも發生した事が判るのである。即鄕村、河邊村の平行なる兩斷層面と山田斷層の斷層面との交線に沿つて餘震が發生した事が二樣の投影によつて判明するのである。即斷層面と斷層面との交線に沿つて地塊內の弱點が存在し且つ餘震の活動がこの線に沿つて比較的永い時日を經過した後までもなほ繼續された事は尤らしく考へられる。次に日本海々底下に發せし餘震の震原の配列に就いて述べる。

第一報中には第一地塊の名稱のもとに鄕村斷層帶が日本海の海底に表はれてゐると假定しこの斷層帶によつて地塊の表面の東部境界線が作られてゐる地塊を擧げて置いた。次に述べるのはこの地塊內部に其後發生した餘震の配列を調べた結果である。前述の地塊同樣二種の投影の結果に就いて述べよう。

（A） 鄕村斷層に垂直なる平面に投影せる場合。 第四圖及第一報中第十四圖參照。

第四圖に示されてゐる震原の配列の模樣は西南或は西南西に約八十度の伏角を以て傾斜せる二平面上に餘震が主として發した事を示してゐる。また之等と或る角度を以て交る數ケの平面上にも數回餘震が發生した事も示されてある。座標の原點を通過する直線は即ち鄕村斷層の傾斜面の投影に相當する事は誰しも一見して判ることゝ思

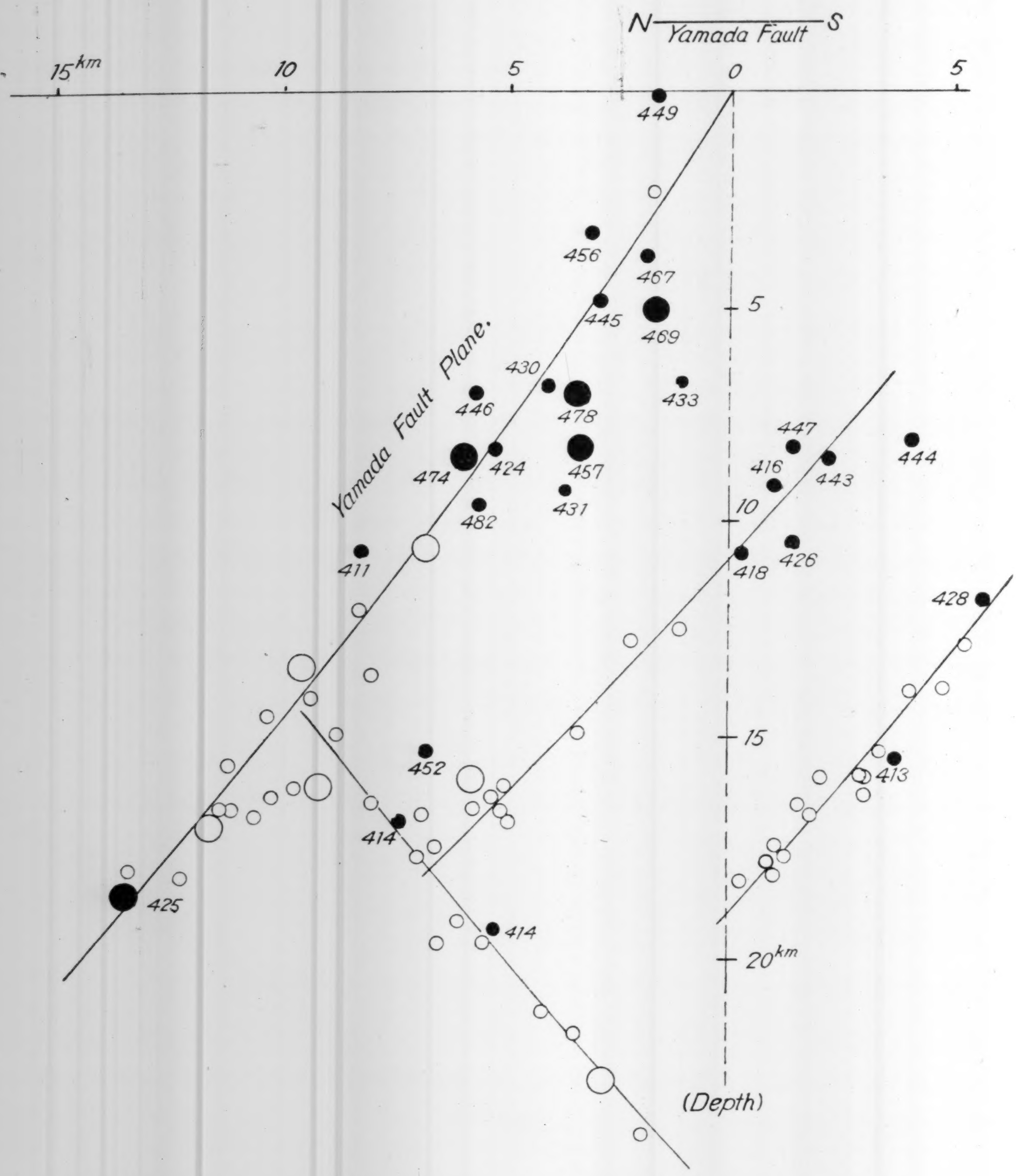

第三圖　第三地塊及其の近傍に於て發生したる餘震の震原を郷村斷層帶に垂直なる平面上に投影せし場合を示す

Fig. 3. Seismic foci in Block No. 3 and in its littoral part projected on the vertical plane passing through the Gômura fault zone.

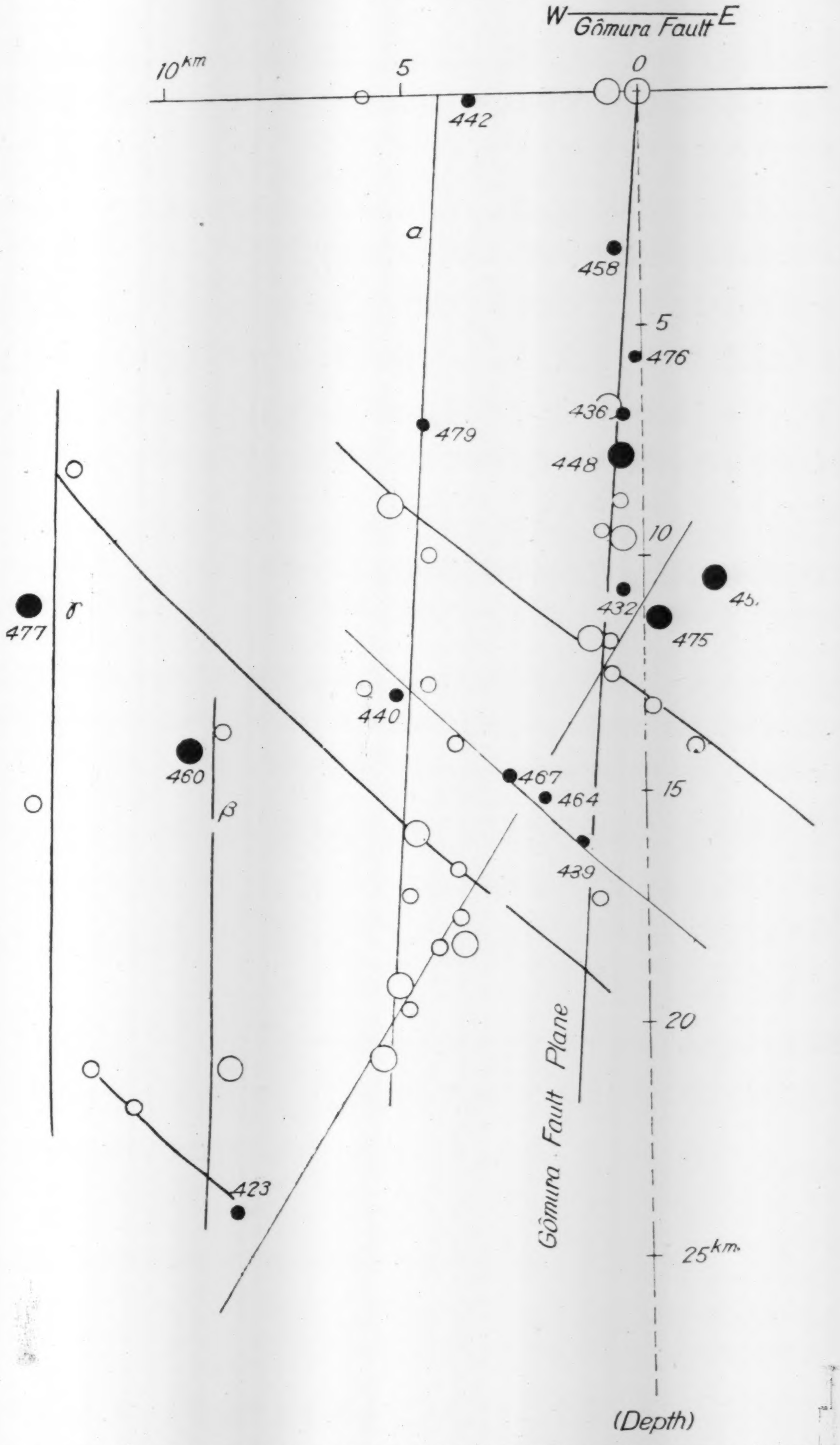
W Gômura Fault E
10km
5
0
442
a
458
5
476
436
479
448
10
432
45.
475
477
γ
440
460
β
467
464
15
439
20
Gômura Fault Plane
423
25km.
(Depth)

第四圖　第一地塊內に發生したる餘震の震原を郷村斷層に垂直なる面上に投影せし場合を示す

Fig. 4. Seismic foci in Black No. 1 projected on the vertical plane normal to the Gômura fault zone.

ふ。この線の左に即實際上では西側に約四粁の距離を距てゝ全くこれと平行な他の一平面がある。又同平面上で比較的地表に近い所に餘震が發生してゐる事から推察するにこの斷層面は海底面上に表はれてゐるのであらう。試みに海軍水路部の海面深度調査の結果（地震研究所彙報、第四卷、米村末喜氏報告中附圖第五十六）を參照して見よう。此の報告によれば網野、磯、埼穴、江鹽海岸の北方に於て稍複雜な海底變化のあることを知るのである。この變化の內網野北方の海底中の變化は鄕村斷層の延長附近に表はれた變動であらうが磯、埼穴、江鹽海岸の北方の變化はその位置より察すればこゝに述べた鄕村斷層とは違つた斷層の地表に現はれた附近の海底變化ではなからうか。斯く考へるときは海底變動のあること及餘震の震原の配列よりこの位置に一つの斷層の存在することは疑ひないことである。

(B)　鄕村斷層を含む垂直平面に餘震の震原を投影せし場合。

震原の配列は主として b を以て示された平面外に餘震が發生した事を示してゐる。この平面の地表面と交はる線は鄕村斷層に直角な斷層線であるべきである。これは丁度多田所員の調査された結果に一致してゐるやうである。同氏の推定せる位置とこの圖に示されてゐる b 斷層の斷層線の表はれるべき位置とは大差がない。この斷層面は南東或は南南東約四十五度の伏角を有するものと判定し得られる。

尙ほ木津村附近に存在する舊斷層の傾斜面はこれとは反對に北西或は北々西に傾斜してゐることは震原の配列から想像されることであるがこの斷層面上では餘震は比較的深い所に發生してゐる。

以上は餘震の比較的多數に發生した地塊に就いて述べたのであるが其他の地塊に就いて夫々の投影を行つて見ると第一報告中に揭載した斷層面の何れかの上に震原が位置してゐることを認め得るのである。玆では第一報告中の圖を再び揭載することを省略す。

以上述べ來つた餘震の震原の配列より次の數項を擧げて本調査報告の結論として置く。

（一）　鄕村斷層の傾斜面は西或は西南西に七十度乃至八十度の傾斜を有し傾斜面は地殼をその表面より地下少くも二十粁に達する深さまで切斷してゐる。

（二）　山田斷層は北西或は北々西に約六十度の伏角を有す。斷層面は同じく地下二十粁以上の深さにまで達してゐる。

（三）　餘震の立體的分布より今回の大地震を伴つた地塊運動を推定し得る可能性が

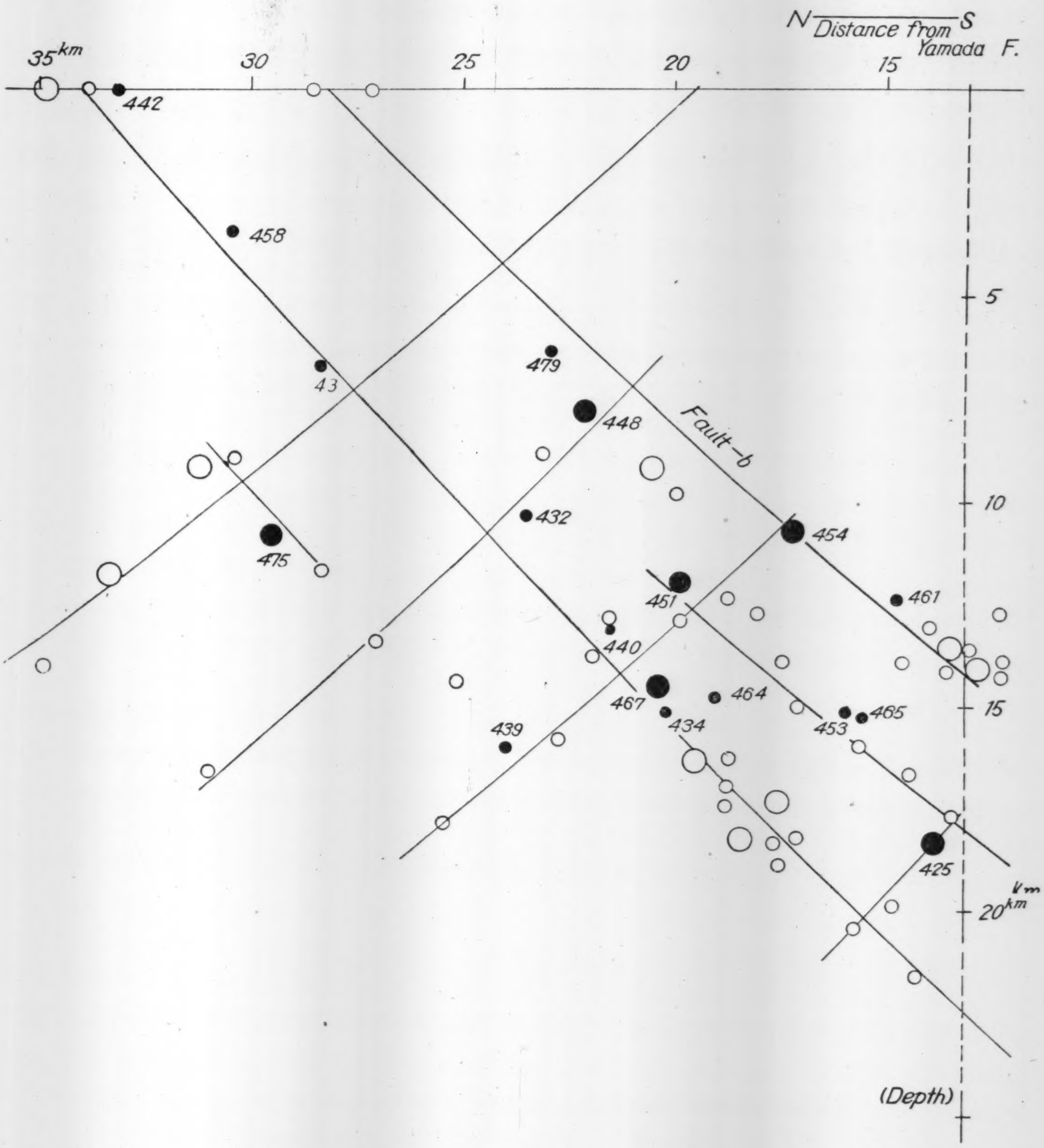

第五圖　第一地塊内に發生したる餘震の震原を鄉村斷層帶を含み垂直なる平面上に投影したるものを示す

Fig. 5. Seismic foci in the Block No. 1 projected on the vertical plane passing through the Gômura fault zone.

ある。これに就いて少しく次に述べて見やう。こゝでは鄉村斷層の西側に存在する地塊及その運動に就いて述べることゝす。此の目的のためには鄉村斷層以西の餘震の震原の二樣に投影された結果を綜合して考察せなければならぬ。

先づ最初は鄉村斷層帶を含み垂直なる平面上に震原を投影した場合に就いて述べよ

う。此の場合には同斷層の西側に南北に連る數箇の地塊（第一報告中、第一、第二、第三と名付けて置いもの）及それ以西の地塊內に發生した餘震の震原を同時に上述の平面上に投影する方が便利である。（第三圖、第五圖參照）第三圖及第五圖で示されてゐる震原の配列より推定される斷層面の位置を記入したのが第六圖である。この第六圖中太い點線を以て示されてゐる三角形の部分に就いて說明を試よう。この部分には大地震直後よりこの調査の終りに至るまで一回の餘震の震原も投影されなかつた事は實に興味ある事である。この三角形で示されてゐる部分に相當する斷面を有する地塊を想像することが出來る。即その地塊は東側は鄕村斷層、南側は山田斷層、北側は前述の　　と記しておいた斷層の夫々の傾斜面によつて區劃されてゐる地塊である。鄕村斷層以西に頻發した餘震はすべてこの地塊（最初は假りに一箇の地塊と考へる）の境界面上か或はこの地塊の外部にある裂罅面に發したのである。

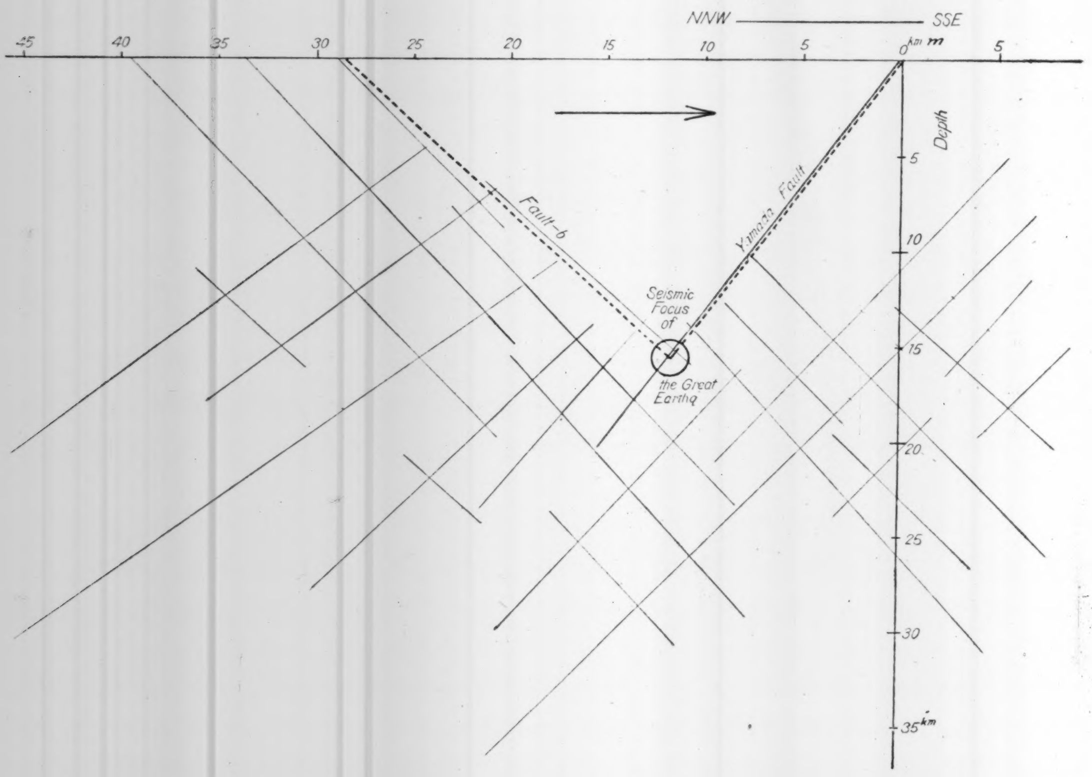
NNW — SSE
45
40
35
30
25
20
15
10
5
0 km m
5
Depth
5
10
15
20
25
30
35 km
Fault-b
Yamada Fault
Seismic Focus of the Great Earthq

第六圖　鄕村斷層西部及山田斷層南部に存在する斷層面を鄕村斷層帶を含み垂直なる平面上に投影せし場合を示す（各細線は餘震の發生したる斷層面の投影を示す。）

Fig. 6. The fault planes lying to the west of the Gômura fault and to the south of the Yamada fault projected on the vertical plane passing through the surface trace of the former fault. (Each thin tine shows the projection of the fault plane in which aftershocks, originated.)

大地震後に於て新斷層附近の各地塊の稍々著しい運動が夫々或る方向に行はれた事は想像に難くないが陸地測量部の丹後大地震後に行はれた測量の結果によつて此等地塊の運動が最も明瞭に示されてゐる。（地震研究所彙報、第四卷、第五卷、陸地測量部報告參照）。而して單に地塊の區劃を決定するといふ目的のためには垂直移動の測定が水平移動のそれよりも有效なものである事は記すまでもない事である。即ち數箇の地塊を通過する水準測量線が地塊の境界を横斷するときはその横斷する點を境として兩側の各數箇の測點の垂直移動量、或は移動の向きに不連續的の差異があることは明かな事である。それ故に地塊の表面の區劃は水準測量の結果によつて十分決定し得るもその劃區をなす境界面即ち斷層面の決定は餘震の配列によつて定めなければならない。若し餘震の配列より推定されたる斷層面の地表に現はれたる線を境としてその兩側の地表に於て垂直變動に不連續的の變化が測定されたならばこの斷層面を以て地塊の境界面と決定して差支ないのである。此の點に關して以下少しく述べて見よう。

先づ地塊の表面區劃に就いて述べて見たい。所員坪井忠二氏が丹後大地震後に行はれたる水準測量の結果を整理せられた結果（坪井忠二: On the Postseismic Block Movements in the Tango Earthquake District., Proc. Imp. Acad., IV (1928), No. 9）を見ると明瞭に地塊の表面區劃が指摘されてゐるかの感がある。同所員の論文第三圖中、郷村斷層線以西のものが現在の目的に必要である。即網野-久美濱及峰山-久美濱に至る各測量線上に於て地塊の境界を通過したる點を求めればよいのである。

前者の測量線は郷村斷層（含まず）以西に於てはを三度地塊の境界を横斷し、後者の測量線は四度地塊の境界を横斷してゐることが明瞭に坪井所員の前述の圖中に示されてゐる。今假りに網野-久美濱間にある地塊の境界を東より西に順次に α, β, γ と名付け峰山-久美濱間にあるそれ等を $\delta, \alpha', \beta', \gamma'$ とする。（δ に就きては後に述べる）。

(α, α'), (β, β'), (γ, γ') を夫々結ぶ線が地塊の境界線となることは相像し得るのである。郷村斷層より α に至る間と δ より α' に至る間の垂直變動は常に同方向に且つ略ぼ等量に行はれた事が測定された理由のもとに斯く想像し得るのである、又 $\alpha\beta$, $\alpha'\beta'$ の兩區間の垂直變動も同樣である。α の位置は郷村斷層より西に約六粁、木津村の西にある地點、α' は同斷層の西約七粁、五箇村の內、大呂附近のやうである。$\alpha\alpha'$ 線を含む斷層の面を餘震の配列から求めると第二圖及第四圖中の α でその面の投影を示されてゐる面となる。又同時に南方への同斷層面の延長は第七圖中の α' で略ぼその存在を知ることが出來る。即ち地塊の表面の區劃とその區劃をなす斷層面が決定さ

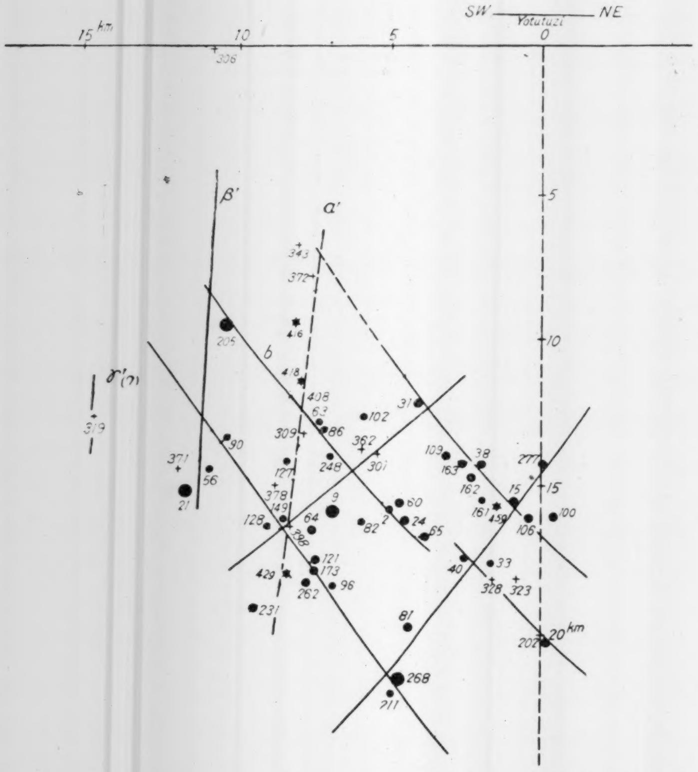

第七圖　山田斷層以南にある第四地塊內の餘震の震原を同地塊の表面の北及東側の境界をなす線の二等分線を含み垂直なる面（この面は鄉村斷層帶に略ぼ直角となる）に投影せし結果を示す。

（α′ 及 β′ を以て示されたる斷層面が山田斷層以南へも延長せることに注意すべし。）

Fig. 7. Seismic foci in the block No. 4 lying to the south of the Yamada Fault, projected on the vertical plane bisecting the angle between the northern and the eastern boundaries of the surface of the block; the vertical plane is nearly normal to the Gômura fault zone.

(Note: the fault planes which are indicated with α′ and β′ extend further to the south of the Yamada fault.)

れたのであるから鄉村斷層の直ぐ西側に存在してゐる地塊の形狀は判然と決定し得たのである。この地塊の垂直斷面は前述の三角形であることは疑ふ餘地はないが地表での形は北部の東西の幅員は南部でのそれよりも小であるらしい。即ち梯形の大なる底邊を山田斷層上に小なる邊を前述のb斷層線上に橫たへてゐるのである。それは第四圖中のα線の橫軸を切る點が鄉村斷層の西約四粁の點にあり、第二圖中の α′ 線が橫軸を切る點が同じく約七粁の所にあることから考へられることである。

次にββ′の境界線は佐濃谷を縱走する斷層線であらう。この斷層線を含む斷層面の投影は第二圖中の β 及第四圖中の β′ 及第七圖中の β によつて與へられてゐる。故

にこの斷層面即地塊の境界面の實在してゐることは先づ間違ひない事である。此の地塊も前同樣三角形の垂直斷面を有するのであるが地表での幅員は南部より北部に至るまで大體同じで約四粁である。

次に $\gamma\gamma'$ を結ぶ線は川上谷を縱走する斷層線であらう。この $\gamma\gamma'$ 線を含む斷層面を餘震の配列から求めると第二圖中の γ 線、第圖四中に γ 線がこの斷層面の投影を與へてゐることから先づ實在するとして差ない。

郷村斷層以西に三つの斷層面を決定し得たから同斷層の西側に存在する三箇の地塊をその形狀に至るまで十分に推定し得るのである。この三箇の地塊は何れも楔狀であるが尚ほ詳細に觀察すると郷村斷層及 $\alpha\alpha'$ で兩側が境されてゐる地塊は更に分割されてゐる。その分割されてゐる地點を求めるに第二圖中の δ 線の存在することから郷村及 $\alpha\alpha'$ 斷層の中間に今一つの斷層を相像し得るのである。この斷層の存在することは水準測量の結果よりも求め得るのである。前述の δ 點はこの斷層線上の點であらう。

以上の三つの地塊の大地震の際に於ける運動を想像するに先づ地殼の破綻は郷村斷層（舊郷村斷層の意味）の面に沿つて起つた事は大地震の地震波の初動の方向の分布より判定し得ることであるが、その破綻の後か或は同時であつたかは多少問題であるが恐らく少時間の後に舊山田及 b の斷層の傾斜面に沿ふ最も抵抗の少い方向に裂罅を新しく生じ上述の三箇の楔狀の地塊は北方より作用せる歪力のために滑動を始め山田斷層以南の地塊の抵抗を受けながら同斷層の傾斜面に沿つて上方に且つ南々東に全體として移動したのであらう。その内最も烈しい運動をしたのは郷村斷層の直ぐ西側に横たはつてゐる地塊である。この地塊の表面上の災害が最も激甚であつた。又大地震後四月一日に至る間の郷村斷層以西の餘震の震央の分布（第一報告中第三、四圖）を見るとこの地塊の東西の幅に相當する帶狀の部分に限られてゐるやうである。これには何か理由のあることと思ふ。この地塊の運動によつて地塊の外部に於てはほゞこの地塊の東西の幅に相當する部分が最も激しい衝動を受けそこに裂罅が新しく生じて餘震が發生したと考へるのである。

これ等の外方に生じたる裂罅は其後に於ても極めて活潑に發生を續けた。又この地塊の西側にある殘りの二箇の地塊の運動に伴つて餘震が發した事は第一報告中の震央分布圖（第六・七・八圖等參照）に示されてゐる震央の分布が次第に西方へも擴つてゐることから云ひ得るのである。而しこゝで一言して置きたい事は以上の三箇の地塊の境界面即郷村斷層、$\alpha\alpha'$ を含む斷層面（$\alpha\alpha'\alpha''$ 面とす）及 $\beta\beta'$ を含む面（$\beta\beta'\beta''$ 面）、

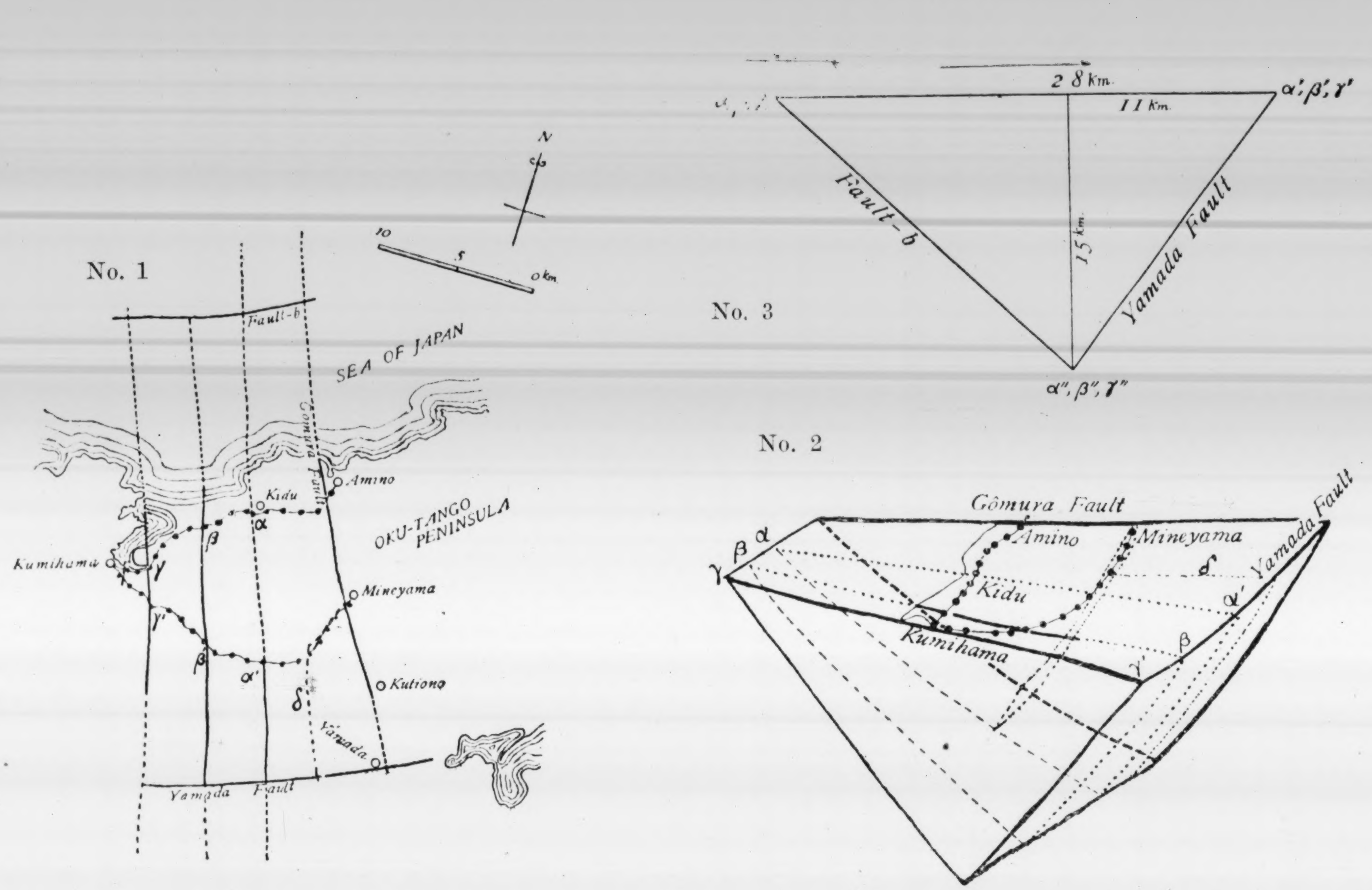
No. 1
N
10
5
0 km
Fault-b
SEA OF JAPAN
Gômura Fault
Amino
Kidu
OKU-TANGO PENINSULA
Kumihama
Mineyama
Kutiona
Yamada
Yamada Fault
α
β
γ
α'
β'
γ'
δ
No. 3
2 8 Km
11 Km
15 Km
α', β', γ'
α'', β'', γ''
Fault-b
Yamada Fault
No. 2
Gômura Fault
Amino
Mineyama
Kidu
Kumihama
Yamada Fault
γ β α
δ
α'
β
γ'

第八圖　今回の大地震の餘震の震原の立體的配列により決定せられたる郷村斷層の西側に存在する楔狀の地塊：（其一）地塊の表面區劃・（其二）地塊の形狀（其三）；垂直斷面を示す。

Fig. 8. Shows the wedge shaped land blocks lying on the west side of the Gômura fault zone, as revealed from the stereo material distribution of the afterhocks of the present destructive earthquake: No. 1. Surface boundaries of the blocks; No. 2, shape of the blocks; No. 3. vertical section.

$\gamma\gamma'$ を含む面（$\gamma\gamma'\gamma''$ 面）の夫々の面上の三角形に相當する部分には一回の餘震も起つてゐないのである。餘震の配列から求めたこれ等の地塊の境界面は以上の三角形の面の延長である。又第一、第二、第三地塊等の區別は單に震原の配列を求める爲め便宜上の區分に過ぎなかつた事が全般の結果を綜合して判明したのである。

郷村斷層の以西に横たはる三箇の地塊の形狀を模型圖によつて示してあるのが第八圖である。

餘震の觀測は重要である事は論を俟たないが大地震後に於ける地變の有樣殊に地塊の境界面等に餘震が發する關係上より地塊の區劃を決定し得るからこの方面に於て立體的の震原の配列が缺く可からざる調査方法となり得る可能性をこの調査によつて見出したのである。

終りに臨み永らく觀測を繼續するに就いて多大の支出を惜まれなかつた地震研究所所長末廣先生に厚く御禮を申上げる。又觀測當初より不斷懇切なる指導を賜つた今村先生に厚く感謝の意を表す。又永い間、直接觀測に從事された舞鶴桂林寺の兒玉至玄氏、赤石屋旅館主坂本誠一氏、河邊村助役吉岡利一郎氏、伊根村小學校林田信丸氏、間人小學校 増井梅雄氏 並に地震學教室在勤の脇元、高橋、加藤 和田、新井の諸氏の御盡力に對しても厚く感謝の意を表する次第である。

（昭•四•二•二二）

丹後地震の餘震觀測表（自昭和二年九月一日至三年七月三十一日）

List of the Aftershocks of the Tango Earthquake (For Sept. 1, 1927–July 31, 1928)

初微 (Pre. tr.) = **初期微動繼續時間** (Duration of Preliminary Tremor)

初動 (Init. Mot.) = (Initial Motion)

最大動 (Max. 2A) = **最大全振幅** (Maximum Double Amplitude)

E.W. = **東西動** (East West Component)： （＋）**東へ** (towrds E.)
－ **西へ** (towards W.)

N.S. = **南北動** (North South Component)： （＋）**北へ** (towards N.)
－ **南へ** (towards S.)

發現日時 Time of Occurrence			舞鶴 (Maiduru)					城崎 (Kinosaki)					伊根 (Ine)					摘要 Remark	震央 Epi-centre	震原の深さ Focal depth
			初微 Pre. tr.	初動 Init. Mot.		最大動 Max. 2A		初微 Pre. tr.	初動 Init. Mot.		最大動 Max. 2A		初微 Pre. tr.	初動 Init. Mot.		最大動 Max. 2A				
				E.W.	N.S.	E.W.	N.S.		E.W.	N.S.	E.W.	N.S.		E.W.	N.S.	E.W.	N.S.			
1927	d	h m	s	μ	μ	μ	μ	s	μ	μ	μ	μ	s	μ	μ	μ	μ			km
Sept.	1	4 58	—	—	—	—	—	2.5	—	—	55	50	3.6	—	—	32	60	Miyadu; pre. tr. = 2.4ˢ	411	10.8
		6 59	—	—	—	—	—	2.7	—	—	25	20	4.2	—	—	10	15		—	—
	5	22 58	—	—	—	—	—	2.7	—	—	4	4	—	—	—	—	—		—	—
	6	6 14	—	—	—	—	—	—	—	—	15	15	—	—	—	—	—		—	—
		16 47	—	—	—	—	—	2.7	—	—	8	10	4.0	—	—	—	—		—	—
	7	6 07	—	—	—	—	—	1.2	− 5	− 3	30	45	—	—	—	—	—		—	—
		11 58	—	—	—	—	—	1.5	—	—	20	17	—	—	—	—	—		—	—
	13	9 06	—	—	—	—	—	—	—	—	5	7	—	—	—	—	—		—	—
	14	14 14	2.5	—	—	10	10	—	—	—	10	10	1.6	—	—	4	4	Miyadu; pre. tr. = 2.4ˢ	412	4.0
	17	4 07	3.0	—	—	7	7	4.2	—	—	9	12	3.8	—	—	3	5		413	16.0
	18	7 17	4.1	—	—	5	5	3.4	—	—	10	10	3.9	—	—	8	8		414	19.4
		21 33	—	—	—	—	—	2.7	—	—	10	8	3.7	—	—	5	8		—	—
	19	21 22	—	—	—	—	—	2.3	—	—	15	15	—	—	—	—	—		—	—
	23	2 17	4.4	—	—	3	3	4.4	—	—	10	10	3.6	—	—	3	3		415	25.0
		5 11	3.5	− 3	− 3	10	10	3.2	− 8	+10	28	35	4.0	—	—	—	10	Toyooka; pre. tr. = 2.4ˢ	416	7.6
		5 12	3.9	—	—	7	7	3.5	—	—	8	8	3.4	—	—	—	5		417	17.7
		5 18	3.5	—	—	8	10	3.2	—	—	10	12	3.9	—	—	7	5		418	11.5
		21 54	5.0	—	—	4	4	3.0	—	—	15	13	4.8	—	—	3	3		419	21.0
	25	5 59	5.0	—	—	4	4	2.7	—	—	5	6	5.8	—	—	4	4		420	—
		6 09	5.0	—	—	7	7	2.7	—	—	7	7	5.8	—	—	5	5		421	—
	27	7 56	3.1	—	—	5	5	4.5	—	—	5	8	—	—	—	—	—		—	—
		8 38	2.0	—	—	3	3	4.5	—	—	5	1	2.1	—	—	2	2	Toyooka; pre. tr. = 3.9ˢ	422	8.0
Oct.	3	8 29	6.3	—	—	10	10	3.3	—	—	20	25	5.2	—	—	15	10	Toyooka; pre. tr. = 4.1ˢ	423	24.6
	14	12 37	3.6	—	—	3	3	2.8	—	—	10	12	3.7	—	—	5	5		424	8.6
	17	11 10	—	—	—	—	—	2.7	—	—	20	30	4.3	—	—	3	3	{Toyooka; pre. tr. = 3.7ˢ	—	—
	22	3 57	4.4	—	—	10	10	3.6	—	—	150	90	3.6	—	—	8	6	{Miyadu; pre. tr. = 3.1ˢ	425	18.7
	24	7 57	3.0	—	—	4	4	4.0	—	—	5	5	2.9	—	—	4	5	Miyadu; pre. tr. = 1.5ˢ	426	11.0
	28	0 24	2.7	—	—	8	14	4.2	—	—	5	5	1.8	—	—	10	18	Miyadu; pre. tr. = 0.8ˢ	427	—
		2 53	4.0	—	—	3	3	—	—	—	—	—	5.5	—	—	2	3		—	—
	29	7 46	2.8	—	—	—	5	3.9	—	—	5	3	3.6	—	—	25	22		428	12.0
Nov.	6	8 23	—	—	—	—	—	—	—	—	—	—	3.7	—	—	10	10		—	—
	9	11 43	3.0	—	—	3	3	—	—	—	—	—	—	—	—	—	—		—	—
	10	11 47	4.0	—	—	4	3	3.5	—	—	8	8	4.3	—	—	3	2	Toyooka; pre. tr. = 3.1ˢ	429	18.0
	11	9 24	2.9	—	—	10	10	—	—	—	—	—	2.3	—	—	10	18	{Toyooka; pre. tr. = 3.1ˢ	430	7.0
	12	0 02	3.9	—	—	2	2	2.8	—	—	10	10	2.9	—	—	4	6	{Miyadu; pre. tr. = 1.5ˢ	431	9.4

	4 18	2.6	—	—	5	5	3·1	—	—	5	3	—	—	—	—	—		—	—
	4 49	3·1	—	—	3	3	2.6	—	—	7	7	—	—	—	—	—		—	—
16	20 29	5.4	—	—	9	7	2.6	+15	+ 6	90	45	3.3	—	—	25	38	Toyooka; pre. tr.=3.4^s	432	10.6
22	15 31	2·7	—	—	5	5	—	—	—	—	—	—	—	—	—	—	Miyadu; pre. tr.=1.1^s	433	7.0
25	19 09	—	—	—	—	—	3.7	—	—	5	5	—	—	—	—	—		—	—
26	20 10	5.3	—	—	15	15	2.7	—	—	45	25	3.9	—	—	10	10	Toyooka; pre. tr.=1.1^s	434	15.0
27	0 15	5.3	—	—	4	4	2.7	—	—	8	5	—	—	—	—	—		—	—
28	6 28	—	—	—	—	—	2.6	—	—	5	5	—	—	—	—	—		—	—
	9 20	—	—	—	—	—	2.1	—	—	14	—	—	—	—	—	—		—	—
Dec. 2	16 00	—	—	—	—	—	2·7	—	—	4	3	—	—	—	—	—		—	—
4	9 56	5.6	—	—	5	5	—	—	—	—	—	3.7	—	—	15	20	Miyadu; pre. tr.=3.5^s Toyooka; pre. tr.=3.4^s	435	0
	12 34	5·0	—	—	5	5	—	—	—	—	—	3.9	—	—	17	15	Toyooka; pre. tr.=3.3^s	436	7.0
	18 28	3.1	—	—	3	3	—	—	—	—	—	2.4	—	—	30	20	Miyadu, pre. tr.=1.8^s Toyooka; pre. tr.=3.3^s	437	7.6
7	10 17	—	—	—	—	—	2.7	—	—	3	3	—	—	—	—	—		—	—
8	1 17	3.4	—	—	9	15	—	—	—	—	—	3.5	—	—	30	37	Toyooka; pre. tr.=3.3^s Miyadu; pre. tr.=2.3^s	438	19.8
11	5 17	—	—	—	—	—	—	—	—	6	7	—	—	—	—	—		—	—
	11 20	—	—	—	—	—	2.7	—	—	8	8	—	—	—	—	—		—	—
	16 27	—	—	—	—	—	2.8	—	—	10	5	—	—	—	—	—		—	—
13	14 55	—	—	—	—	—	2·8	—	—	9	6	—	—	—	—	—		—	—
16	6 29	—	—	—	—	—	1.9	+ 5	− 3	20	20	—	—	—	—	—		—	—
	16 27	—	—	—	—	—	2.8	—	—	9	9	—	—	—	—	—			

													河邊 (Kôbe)						
													初徵 Pre. tr.	初動 Init. Mot.		最大動 Max. 2A			
														E.W.	N.S.	E.W.	N.S.		
													s	μ	μ	μ	μ		
18	0 10	—	—	—	—	—	2.7	—	—	3	5							—	—
22	20 42	—	—	—	—	—	3.5	—	—	15	17	Toyooka; pre. tr.=3.7^s	2.9	—	—	20	30	439	16.4
28	12 35	5.5	—	—	5	5	2.3	—	—	32	17	Toyooka; pre. tr.=2.9^s	2.5	—	—	18	18	440	13.0
29	16 42	2·7	—	—	3	3	—	—	—	—	—		—	—	—	—	—	—	—
	20 42	3.5	—	—	5	5	3.7	—	—	10	10		2.6	—	—	8	10	441	14.0
	23 15	—	—	—	—	—	—	—	—	3	3		—	—	—	—	—	—	—
	22 15	—	—	—	2	2	—	—	—	—	—		—	—	—	—	—	—	—
30	13 52	6.1	—	—	3	5	2.9	—	—	20	27	Toyooka; pre. tr.=2.8^s	3.0	—	—	10	8	442	0

發現日時 Time of Occurrence		舞鶴 (Maiduru)					城崎 (Kinosaki)					河邊 (Kôbe)					間人 (Taiza)					震央 Epi-centre	震原の深さ Focal depth
		初微 Pre. tr.	初動 Init. Mot.		最大動 Max. 2A		初微 Pre. tr.	初動 Init. Mot.		最大動 Max. 2A		初微 Pre. tr.	初動 Init. Mot.		最大動 Max. 2A		初微 Pre. tr.	初動 Init. Mot.		最大動 Max. 2A			
			E.W.	N.S.	E.W.	N.S.		E.W.	N.S.	E.W.	N.S.		E.W.	N.S.	E.W.	N.S.		E.W.	N.S.	E.W.	N.S.		
1928 d	h m	s	μ	μ	μ	μ	s	μ	μ	μ	μ	s	μ	μ	μ	μ							km
Jan. 3	16 54	—	—	—	—	—	—	—	—	—	—	3.2	—	—	10	10						—	—
4	1 34	2.4	—	—	30	10	4.1	—	—	20	33	1.6	—	—	72	30						443	10.0
	18 43	—	—	—	—	—	—	—	—	—	—	1.3	—	—	40	20						—	—
5	11 19	—	—	—	—	—	—	—	—	—	—	1.6	—		10	5						—	—
10	12 32	2.4	—	—	175	200	3.8	—	—	270	100	1.6	−15	+30	1500	400	{Toyooka; pre. tr. = 3.4s {Miyadu; pre. tr. = 2.1s					444	8.0
14	6 40	—	—	—	—	—	—	—	—	—	—	3.0	—	—	75	25						—	—
15	22 27	—	—	—	—	—	—	—	—	—	—	1.0	—	—	10	13						—	—
19	22 36	—	—	—	—	—	2·4	—	—	12	15	2.2	—	—	42	20						—	—
25	7 10	3.1	—	—	5	3	3.2	—	—	8	10	0.8	—	—	13	10						445	5.0
	20 21	3.4	—	—	5	5	3.2	—	—	8	10	0.9	—	—	22	19						446	7.0
29	14 54	—	—	—	—	—	—	—	—	—	—	3.0	—	—	10	12	1.5	—	—	20	22	—	—
31	5 01	2.5	—	—	10	13	3.8	—	—	8	10	1.4	—	—	20	20	3.0	—	—	10	12	447	8.0
	18 14	5.1	—	—	7	7	2.8	—	—	5	47	2.3	—	—	80	50	1.7	—	—	60	55	448	9.7
Feb. 6	9 21	3.0	—	—	5	7	—	—	—	—	—	0.5	—	—	30	40	2.3	—	—	20	10	449	.0
8	13 40	3.1	—	—	5	7	—	—	—	—	—	1.4	—	—	10	13	2.4	—	—	8	10	450	11.0
12	21 27	5.0	—	—	5	3	3.0	—	—	20	18	2.2	—	—	30	30	1.6	−10	+20	180	80	451	12.0
14	20 48	4.0	—	—	14	17	2.8	—	—	20	20	1.6	−30	+40	240	75	2.7	—	—	40	30	452	12.0
18	18 49	5.2	—	—	3	4	2.6	—	—	50	38	2.3	—	—	20	20	2.4	—	—	10	8	453	15.5
	18 49	3.8	—	—	20	30	2.0	—	—	100	110	2.1	—	—	540	170	2.6	−10	−10	350	620	454	11.5
19	5 27	3.2	—	—	8	7	—	—	—	—	—	1.2	—	—	30	25	2.0	—	—	15	13	455	9.5
20	3 43	3.6	—	—	5	5	—	—	—	—	—	0.5	—	—	35	38	2.3	—	—	30	35	456	3.0
23	7 30	—	—	—	—	—	3.2	—	—	18	10	1.0	—	—	270	30	2.2	—	—	25	30	457	8.0
26	7 33	—	—	—	—	—	2.6	—	—	10	12	2.7	—	—	5	7	1.4	—	—	20	15	458	3.0
29	10 38	3.2	—	—	5	8	3.6	—	—	15	10	2.0	—	—	40	35	3.3	—	—	30	20	459	15.3
March 1	22 34	5.5	—	—	5	5	2.0	—	—	220	150	2.7	—	—	100	30	2.9	—	—	60	100	460	14.3
4	22 54	—	—	—	—	—	2.6	—	—	13	17	1.8	—	—	20	20	2.2	—	—	5	5	461	12.5
5	17 59	—	—	—	—	—	2.6	—	—	10	15	1.2	—	—	20	20	1.2	—	—	10	10	462	5.5
6	5 55	—	—	—	—	—	—	—	—	—	—	—	—	—	—	—	2.2	—	—	15	16	—	—
11	21 03	—	—	—	—	—	—	—	—	—	—	—	—	—	—	—	1.8	+20	−30	330	160	—	—
13	3 21	—	—	—	—	—	—	—	—	—	—	—	—	—	—	—	1.8	—	—	20	20	—	—
	22 49	—	—	—	—	—	—	—	—	—	—	—	—	—	—	—	1.5	—	—	20	20	—	—
14	19 18	—	—	—	—	—	—	—	—	—	—	2.1	—	—	15	20	2.9	—	—	50	50	—	—
18	20 04	—	—	—	—	—	—	—	—	—	—	2.2	—	—	35	42	1.9	—	—	60	60	—	—
23	12 43	3.0	−5	+2	47	37	3.2	—	—	15	15	—	—	—	—	—	1.6	—	—	23	15	463	0
	13 39	2.7	—	—	5	3	—	—	—	—	—	—	—	—	—	—	—	—	—	—	—	—	—

		18 01	—	—	—	—	—	2.7	—	—	10	10	2.5	—	—	20	18	2.2	—	—	5	5	464	15.0
	27	4 16	—	—	—	—	—	3.0	—	—	72	43	—	—	—	—	—	2.6	—	—	60	40	—	—
		8 06	—	—	—	—	—	3.0	—	—	10	15	2.1	—	—	20	30	2.2	—	—	15	18	465	15.2
		23 10	—	—	—	—	—	3.3	—	—	40	30	1.7	—	—	70	50	1.5	—	—	170	100	466	11.3
April	6	1 49	5.4	—	—	5	5	2.6	—	—	100	—	—	—	—	—	—	2.3	—	—	150	130	467	15.0
		1 49	—	—	—	—	—	—	—	—	—	—	—	—	—	—	—	1.6	—	—	10	15	—	—
	9	9 01	2.6	—	—	5	3	3.5	—	—	5	5	0.8	—	—	10	18	—	—	—	—	—	468	4.0
	17	11 26	3.1	-10	+2	50	20	—	—	—	—	—	0.6	—	—	530	180	0.9	—	—	233	125	469	5.0
	22	3 20	3.0	—	—	5	5	—	—	—	—	—	1.5	—	—	50	20	1.8	—	—	20	17	470	7.0
	23	16 41	—	—	—	—	—	1.4	—	—	70	70	—	—	—	—	—	—	—	—	—	—	—	—
	30	1 34	—	—	—	—	—	—	—	—	—	—	—	—	—	—	—	2.4	—	—	10	10	—	—
May	5	6 41	4.0	—	—	3	3	2.9	—	—	22	10	—	—	—	—	—	1.6	+10	-2	20	20	471	9.0
		6 41	4.7	—	—	8	8	2.4	—	—	80	45	—	—	—	—	—	2.0	+5	-10	130	90	472	15.4
	16	0 36	—	—	—	—	—	2.4	—	—	7	7	—	—	—	—	—	—	—	—	—	—	—	—
	22	6 25	—	—	—	—	—	3.0	—	—	10	15	1.1	—	—	—	—	—	—	—	—	—	—	—
	28	3 25	—	—	—	—	—	2.9	—	—	15	12	1.0	—	—	50	40	1.6	—	—	10	15	473	9.0
	29	0 14	3.3	—	—	10	10	—	—	—	—	—	2.4	-30	-10	100	50	2.0	—	—	30	50	474	8.4
June	1	8 04	3.0	—	—	50	35	3.0	—	—	50	35	—	—	—	57	70	1.8	+10	-6	160	95	475	12.0
		8 34	—	—	—	—	—	—	—	—	—	—	—	—	—	—	—	2.4	—	—	50	30	—	—
	7	6 31	—	—	—	—	—	2.6	—	—	18	15	1.5	—	—	32	36	1.3	—	—	44	33	476	7.0
	8	14 20	—	—	—	—	—	—	—	—	—	—	—	—	—	—	—	2.3	—	—	46	30	—	—
	9	23 52	5.5	—	—	—	10	1.5	-30	-10	1200	1010	—	—	—	—	—	2.9	—	—	225	85	477	10.8
	15	0 06	—	—	—	—	—	—	—	—	—	—	—	—	—	—	—	6.3	—	—	6	7	—	—
	16	12 06	3.0	—	—	10	15	3.5	—	—	10	15	0.9	+60	+30	580	540	2.2	—	—	24	50	478	7.4
	20	17 26	5.4	—	—	3	3						2.3	—	—	10	10	1.8	—	—	92	50	479	7.4
		17 29	5.2	—	—	5	5						2.0	—	—	25	55	2.2	+48	-45	370	220	480	7.0
	24	0 11	—	—	—	—	—						—	—	—	—	—	1.2	—	—	12	20	—	—
July	2	21 31	—	—	—	—	—						—	—	—	—	—	2.1	—	—	13	40	—	—
	4	6 22	—	—	—	—	—						—	—	—	—	—	2.4	—	—	14	20	—	—
	9	0 19	3.3	—	—	5	5						0.5	—	—	40	50	2.0	—	—	30	27	481	4.0
			舞鶴 (Maiduru)					河邊 (Kobe)					間人 (Taiza)										震央 Epi-centre	震原の深さ Focal depth
			初微 Pre. tr.	初動 Init. Mot.		最大動 Max. 2A		初微 Pre. tr.	初動 Init. Mot.		最大動 Max. 2A		初微 Pre. tr.	初動 Init. Mot.		最大動 Max. 2A								
				E.W.	N.S.	E.W.	N.S.		E.W.	N.S.	E.W	N.S.		E.W.	N.S.	E.W.	N.S.							
	10	3 02	—	—	—	—	—	—	—	—	—	—	1.8	—	—	50	55						—	—
		5 38	—	—	—	—	—	—	—	—	—	—	1.8	—	—	10	10						—	—
	14	15 01	3.9	—	—	10	8	1.5	—	—	100	75	2.7	—	—	—	40						482	11.0
	16	44 17	—	—	—	—	—	—	—	—	—	—	3.6	—	—	8	10						—	—

8. *Further Study of the Aftershocks of the Tango Earthquake.*

By **Nobuji NASU,**

Seismological Institute, Tokyo Imperial University.

It was already reported by the writer in No. 6 of this Bulletin that,

1) The distribution of the foci of aftershocks of the Tango earthquake was extremely dense towards the west of the Gômura fault and also towards the south of the Yamada fault, whilst in the east of the former fault it was very rare.

2) The distribution of the seismic foci projected on the vertical plane which is normal or parallel to the principal fault shows the arrangement of the fault planes which lie hidden under the surface of the earth.

Further observation has led the writer to a conclusion that

1) Most of the aftershocks of later occurrences originated at shallow places and conspicuously on the principal fault plane or on the line of intersection of two principal fault planes.

2) As to the Gômura fault, it has been made clear that the fault plane pierces deep into the earth crust to a depth at least greater than 20 km., dipping towards WSW at 70°–80°.

3) As to the Yamada fault, it may be inferred that the fault plane dips towards NW at about 60°, the plane reaches to a depth greater than 20 km.

4) In the land mass which lies in the western side of the Gômura fault zone and whose vertical section may be shown by means of the thick dotted line of a triangular shape, drawn in Fig. 6, when the land mass is projected on the vertical plane which passes through the Gômura fault zone, there occurred none of the aftershocks during our seismic observation. It may be inferred that this land mass as a whole uplifted and shifted towards SSE at the time of the present destructive earthquake. Three wedge shaped land blocks which lie on the west side of the Gômura fault zone have been revealed from the stereometrical distributions of the seismic foci of aftershocks. (See Fig. 8.) We may idealize the mechanism by which the present destructive earthquake occurred as follows. At first, the land mass crushed along the fault plane along which the new Gômura fault appeared and afterwards the land mass llying on the west side of this fault yielded to release itself along two directions of least resistance, i.e., along the old Yamada fault plane and the fault-b (see Fig. 6), in virtue of the stress applied on it from NW to SE. It may be said that the present great earthquake originated on the point of intersection of the above mentioned three old fault planes.

9. 地表面の高さ及び地變の量

井上宇胤

（昭和四年二月十九日發表－昭和四年三月二十日受理）

（1） 我が地球表面の高度分布は數人の學者に依つて統計されて居りまして、其中のトラベルトに依つて作られた高さの頻數曲線に依りますと約百米の高さの所と四千七百米の深さの所に頻數の極大の所がありまして、それ等は夫々シアルとシマの面をあらはすのであらうと云はれて居ります。私は頻數の極大の所は全體としては以上の二ケ所でありませうが、も少し小さい範圍に於て細かく見たならば、或は小さな頻數の極大の所が幾つか出て來て、夫々何か特別な面をあらはしはしないだらうかと思ひまして、日本の陸地の高さをしらべる事に致しました。

（2） さて海底ですと餘り浸蝕作用が働きませんが、陸地ですと假りに現在の地形圖から夫々の高さの面積をはかつてその分布を見ましても浸蝕作用の影響が多分に這入つて居りまして、地表面の比較的なまの樣子を知る事が出來ません。所が一般に侵蝕作用の程度は山の峯よりも谷の方が遙かに甚しいのですから、谷を埋めて了つた地形圖をこしらへたならば、幾らかでもそれによる高さの差異を取り除く事が出來るかも知れません。此の地形圖は所謂切峯面1)であつて地理學者間にしばしば用ひられてゐるものです。

辻村助教授2)に依ると日本の山地の樣に最近に隆起した所では、切峯面を作ると大體準平原が隆起した當時の樣子を知る事が出來やしないかとのことです。それで此の切峯面上の高さの分布を見る事に致しましたが、一般に平野は谷にあたりますし、火山地方は各火山體が孤立して居りまして臺地性の地形をあらはして居りませんので、

1） 今村學郎　地理學評論第一卷 759-781.
岡山俊雄　地理學評論第四卷 （昭和三年）
辻村太郎　地理學評論第二卷 （大正十五年）
辻村太郎　地形學　93-94.
辻村太郎　日本地形誌　118.
多田文雄　地震研究所彙報第五號。
渡邊 光　地理學評論第五卷　8.

2） 辻村太郎　日本地形誌　119.
辻村太郎　地理學評論第二卷 （大正十五年）

共に切峯面を作る趣意に合はないかと思はれますので此等は拔かす事にしまして、主な山脈だけをしらべて見ました。切峯面を作るのに陸地測量部の五萬分の一の地形圖を用ひましたので、日本と云つても朝鮮、臺灣はのぞいた本州、四國、九州、北海道でして、切峯面は五萬分の一の地形圖を等分する便宜上4.5〜4.6粁の正方形の網目內に於ける最高の地點を取つて作る事にいたしましたが、切峯面を作る時の過程は大分粗雜なものですから、それで夫々の高さの部分の面積をはかるよりも簡便法として各網目の面積は一定ですから、その內の最高地點の高さに就いて或る版圍內に這入る頻數を求め、切峯面上の面積を代表させる事に致しましたが、それは問題になる土地が廣ければ先づさしつかへ無からうかと思ひます。

(3)　それで以上の樣な取扱をした山脈を北から示せば次の樣なものです。

1. 北見山脈　2. 日高山脈　3. 北上山脈　4. 阿武隈山脈　5. 關東山脈　6. 飛驒山脈　7. 木曾山脈　8. 赤石山脈　9. 紀伊山脈　10. 中國山脈　11. 四國山脈　12. 九州山脈

各山脈の高さの頻數は五十米每に數へる事にしまして、それを次々に四つづつ平均を取つてなだらかにした値を第一圖乃至第七圖に圖示してあります。此等の圖を見ると各山脈每に頻數の極大の高さが一つ或は數個ありまして、それ等の高さは山脈相互間に可成り一致して居りますし、此等の高さの次々の差は第一表に示す樣に主として三百米乃至五百米であります。

第一表　(TABLE 1)

山脈名	頻數極大の高さ間の差（米單位）			
關東山脈	350,	400,	400,	300
飛驒山脈	225,	350,	425,	500
木曾山脈	400,	300,	350,	500
赤石山脈	600,	400,	300	
紀伊山脈	350,	300		
九州山脈	400			

さて偶然な事件が統計の仕方にしたがつて外觀上色々な週期を持つ事がありますが、[3] それであるとしますと此の場合では頻數極大の高さの次々の差即ち週期は六百

---

[3] T. TERADA & N. MIYABE, *Bull. Earthq. Res. Inst.*, **4**.

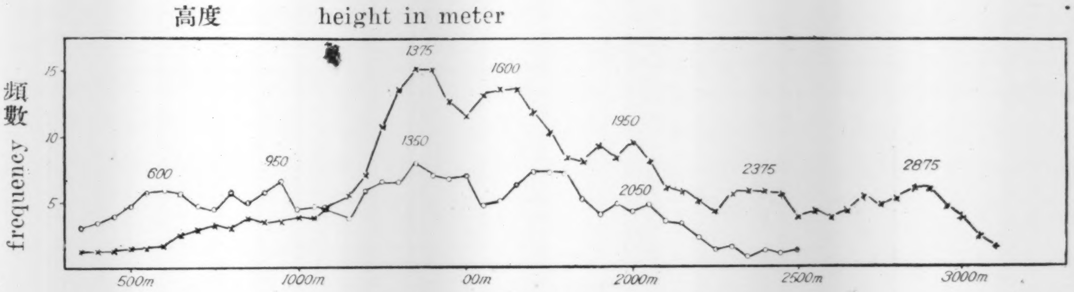

第一圖　本邦の山脈の高度分布
×····飛驒山脈 the Hida mountains
○····關東山脈 ,, Kwanto ,,

Fig. 1. Statistical Distribution of the Altitudes of Mountain Ranges in Japan.

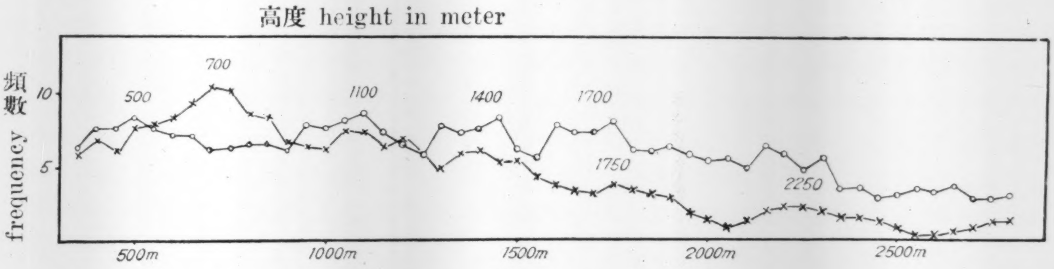

第二圖　同　上
×····木曾山脈 the Kiso mountains
○····赤石山脈 ,, Akaisi ,,

Fig. 2. Ditto.

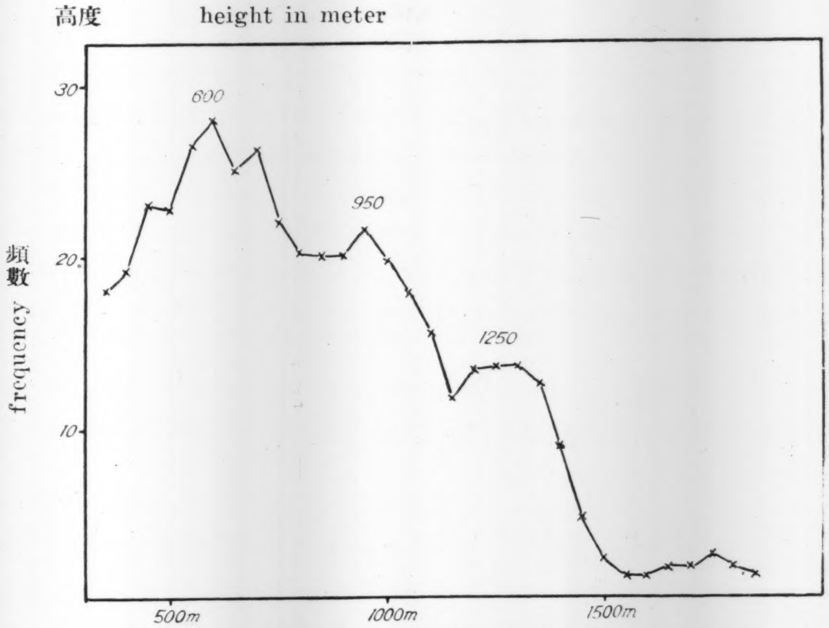

第三圖　紀伊山脈の高度分布

Fig. 3. Ditto of the Kii mountains.

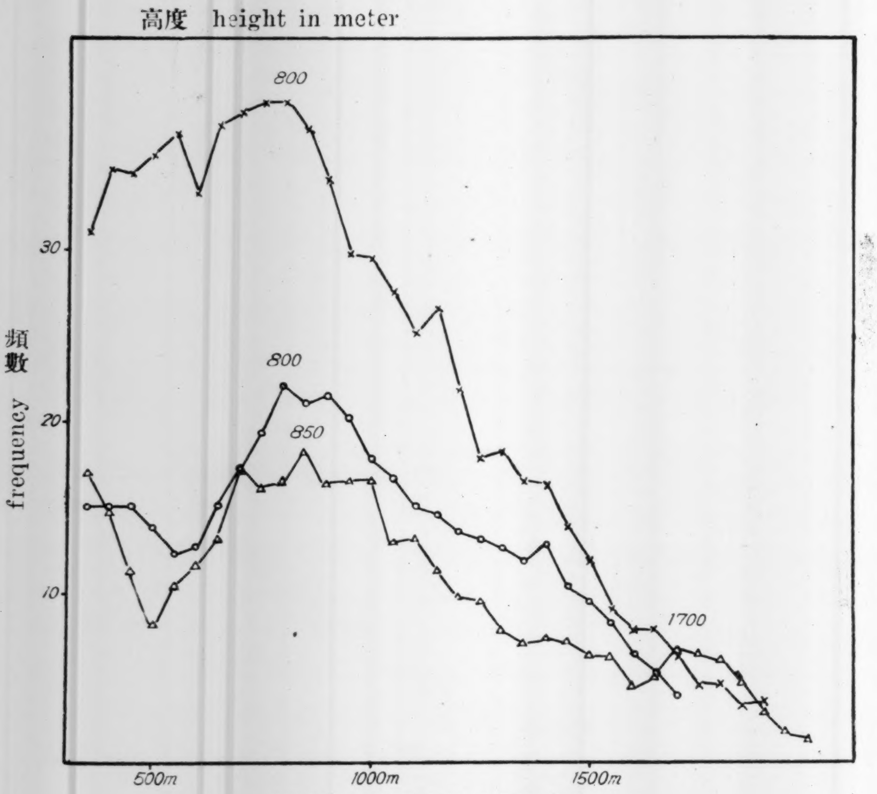

第四圖 本邦山脈の高度分布

×····四國山脈 the Shikoku mountains
○····九州山脈 ,, Kyûsyu ,,
△····日高山脈 ,, Hidaka ,,

Fig. 4. Ditto.

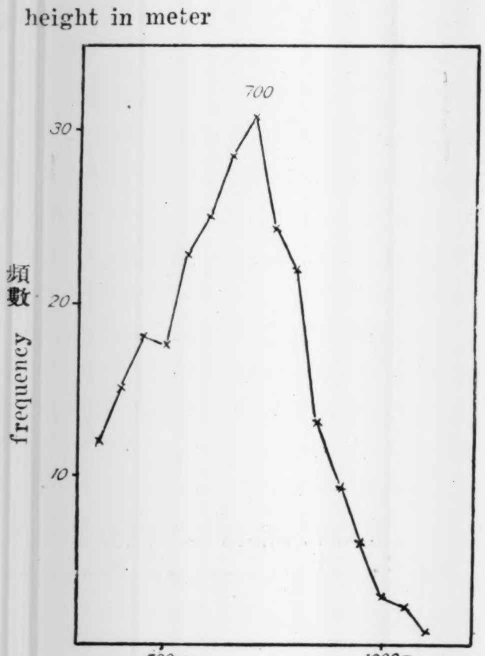

第五圖 阿武隈山脈の高度分布

Fig. 5. Ditto of the Abukuma mountains.

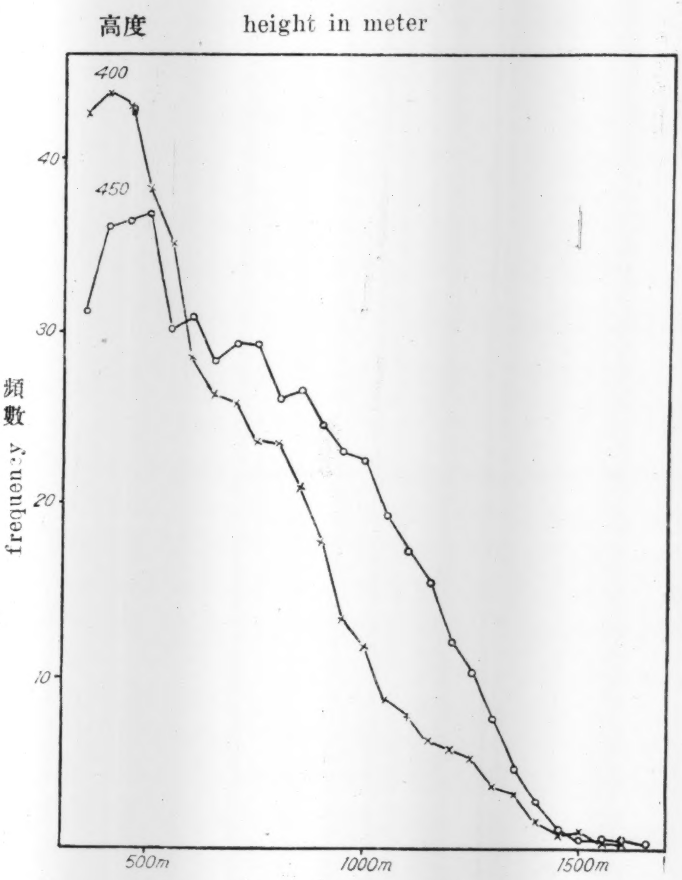

第六圖　本邦の山脈の高度分布
×····北見山脈 the Kitami mountains
○····北上山脈 „ Kitakami „
Fig. 6. Ditto.

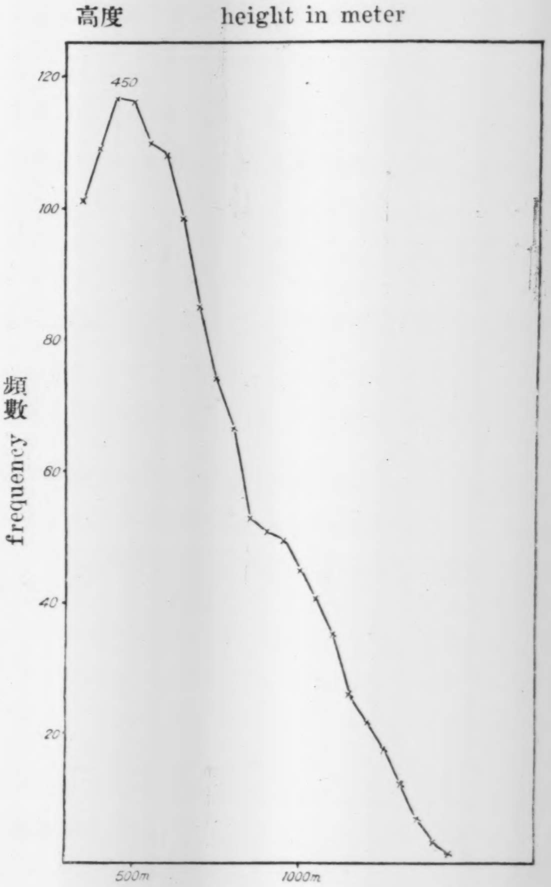

第七圖　中國山脈の高度分布
Fig. 7. Ditto. the Tyûgoku mountains.

米程になるべきですが、實際は上記の如く三百米乃至五百米であるから偶然のものではなからうと思はれます。尙偶然に出て來た事でないためしの爲に紀伊山脈に於て第八圖の樣に一つ置の網目內の最高の點を取つて a, b 二組のものを作り、夫々の頻數を取つて四つづつ平均した値を第九圖に掲げてあります。此に依ると、兩方が可成よく一致してをりまして、二組の偶然の事件とは思はれません。尙各山脈每に隣りの山脈や平野との境界を人爲的にもうけましたので、高さの低い方の頻數は不確かに成りますので二百五十米以下はすててあります。次に全體の山脈を通じての頻數曲線は同樣に滑かにして第十圖に示してあります。

(4) 以上の結果に依りますと日本の山脈には比較的平坦な高原性の部があり、其等が幾つかの段に成つてる時は三百米乃至五百米位の差があるものと思はれます。山脈に

a	b	a	b	a
b	a	b	a	b
a	b	a	b	a
b	a	b	a	b

第 八 圖

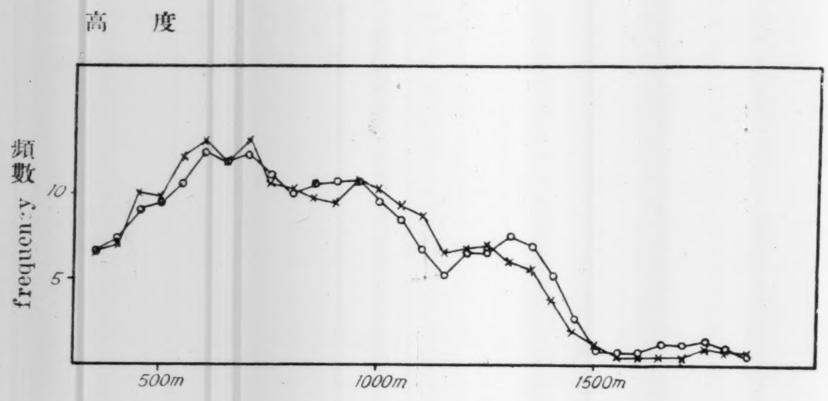

第九圖 紀伊山脈の高度分布
×····a 組 ○····b 組

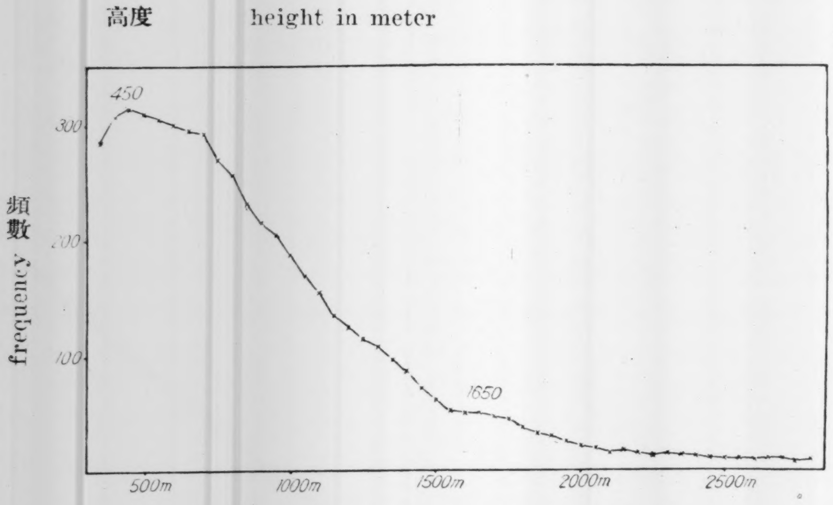

第十圖 日本群島の主要山脈全體の高度分布

Fig. 10. Statistical Distribution of the Height all of the Main Mountains in Japan.

此れに類した臺地面或は平頂峯 (flat-topped crest) がある事は地理學者の間に認められて居る様でして、辻村太郎著地形學の九十一頁に『或る山脈に於て山頂の高さは或る一定の規則に支配される様に見える。即ち相隣れる峯は略同じ高さを有し又最高の峯は殆同一平面內にあるやうに見える。』と出て居ります。尙同氏著日本地形誌の百二十四頁に W. Penck は獨逸のシユワルツワルト山地の一部に於て平坦な削剝面である所謂山麓面が幾段もあつて山麓階をなしてる事を研究された事が出て居りますし、百二十三頁には『Davis が說明してゐる地形輪廻に於ても、異る時期の隆起準平原が一地域に共存する可能性は考へられてゐる。形成の時期を同じくしない準平原が繼次的に發育して、山地の中央部に最も古い準平原遺物が存在し、此れを圍んで山地の緣邊部の低位置を占めた新しい侵蝕面が順次に配列してゐる場合が豫想される。而して其の實例は Appalachian Mountains に於て Davis 及びHayes, Campbell が觀察し、最近には Knopp が此れに就て詳細な研究を行つたのである。』と出て居ります。渡邊光氏[4] に依れば A. Winkler がアルプスの東南隅にあるコールアルプと云ふ山塊に於て研究した所に依ると次の様な四つの平坦面があり古期中新世以後の四回の隆起を示すとの事であります。

1. コール面	1900〜2000 m
2. ウヲルシエネツク面	1440〜1660 m
3. グラシツテン面	1200 m
4. ワイテンフエルド、トラキツテン面	900〜1000 m

尙此等の平坦面の次々の高さは三百米乃至五百米程度のものです。脇水鐵五郎博士[5] に依ると『飛驒山脈中の各部最高地點の高低の差は僅に二百米內外に過ぎない――海拔二千八百乃至三千米に對する二百米――之は水蝕基點からの距離の長短、岩質の硬軟等を考の中に入れたる數字としては餘りにその小なるに驚かざるを得ないのである。』との事です。

(5) 昔し準平原面であつたと思はれる平坦面が現在以上の頻數極大の高さに近い所に存在する場合が幾つかあります。例へば辻村太郎著地形學に依りますと、

1. 中國山脈中の岡山市の北部に當り高梁川、旭川の流域に於て約四百米乃至五百米の高さに準平原面と認むべき平坦面があります。(七十五頁)又所々に九百米乃至千

---

4) 渡邊光 地理學評論第五卷 87-91.

5) 脇水鐵五郎 學藝第四百九十一號

米の所に平坦面があつて隆起準平原面を示すのでは無いかとの事であります。（七十六頁乃至七十七頁）尙同氏著日本地形誌に依ると秋吉のカルスト臺地は四百米の高度を有する石灰岩準平原であります。（四十六頁）

2. 奈良の東方笠置山地、鈴鹿山脈及三河の臺地に於て五百米內外の高さに隆起準平原面の斷片がある。（八十四頁）

3. 北上山地に於ては廣く隆起した準平原面の殘りが千米內外の所にある。（八十四頁）

4. 紀伊山脈の大臺原山は高野山などゝ共に恐く前輪廻に於ける準平原面の存在を暗示するものらしく現在の高さは千三百米乃至千六百米の間にある。（八十三頁）

5. 赤石山脈の釜無山附近には二千米の高さに舊準平原面の殘部がある。

6. 外國の例であるがKarpatenには昔の準平原面の殘りが二千米附近の所にある。（二百六頁）

7. イタリアの北部を占めて居るアペニン山脈にはボログナの地方に於て隆起した準平原面が七百米乃至八百米の高さの所にある。（三百三十六頁）

尙同氏著日本地形誌によると九州山地の西部に於ては七百米乃至千米の高度に立派な準平原遺物が殘存して居ります。（五十四頁）

又山崎直方教授及び多田文男助教授[6]に依れば

1. 丹波高原は準平原の隆起して第二輪廻に在るものであるが西部綾部附近に於ては五百米程の邱稜地をなし三國嶽附近に於ては七百米乃至九百米の高原を成す。（九十三頁）

2. 屛風山脈と伊吹山脈は準平原の隆起した山地であるがその山頂部は平坦面をなし海拔千三百米の較々等高なる峯線を有す。（九十三頁）

3. 琵琶湖の北部の中央高原地帶及び乘鞍嶽傾斜地塊には八百米程の隆起準平原面をあらはす高原性の地域がある。（九十四頁乃至九十五頁）

尙多田助教授[7]に依れば奧丹後半島の中央部には四百米乃至六百米邊に隆起準平原面がある。以上の隆起準平原面の平坦面の高さの中九州山脈と紀伊山脈と中國山脈の分は夫々の山脈の頻數極大の部に相當して居りますが、其他の例も前掲の諸山脈の高度分布に於ける頻數極大の部即ち約五百米內外九百米內外千三百米內外千七百米內外

---

6) 山崎直方、多田文男　地震研究所彙報第二號
7) 多田文雄　地震研究所彙報第五號

及び二千米内外の高さとよく一致して居る事は面白い事です。

(6) 次にアルプス山脈の様な甚しい褶曲を受けてる地方に於ては高度分布がどうなつてるかと思ひましたが、地形圖がありませんので Stielers Handatlas の第十六、十七、十八、三十一圖に出て居る九十二萬五千分の一の圖に三角點の高さが十粁乃至廿粁に一つ位の割に出て居りますので此の高さを取つて五十米毎の頻數を求めて見たのが第十一圖に出て居ります。やはり四つづゝ滑かにしてありますが此れを見ると日本の山脈と殆ど同じ様な所に頻數極大の高さの所が幾つかありまして其等の次々の高さの差はやはり三百米乃至五百米程です。

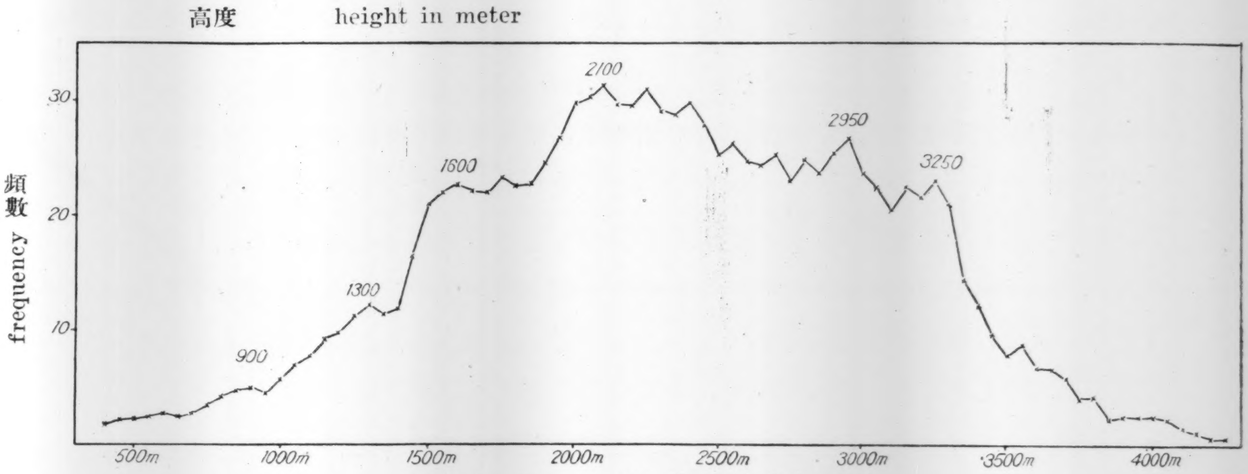

第十一圖　アルプス山脈の高度分

Fig 11. Statistical Distribution of the Height of the Alps.

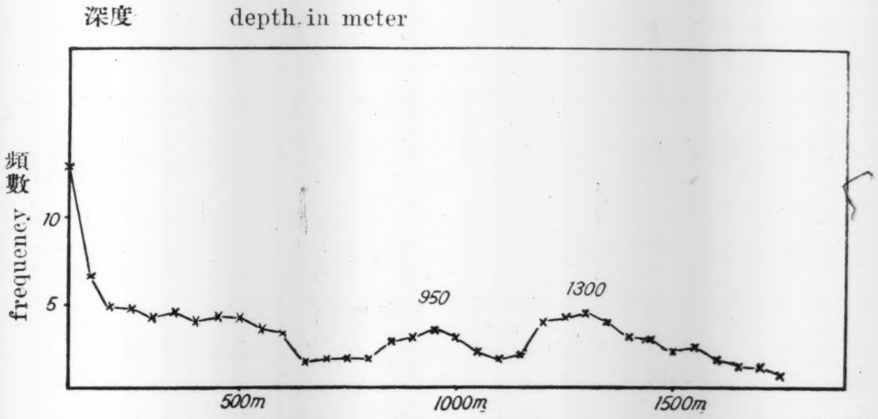

第十二圖　相模灘の深度分布

Fig. 12. Statistical Distribution of the Depth of the Bay of Sagami.

（7）陸地に近い海の部分例へば大陸棚や大陸坂の一部は陸地と同様な性質を持つて居るかも知れませんので雜用海圖第八十號によりまして相模灘を五粁平方づゝの網目に分けてその中で一番淺い所を取つてその深さの五十米毎の頻數を求めて見たのが第十二圖に示してあります。圖では四つづゝ平均した値が示してありますが此れを見ると山脈と同樣な三百米乃至五百米位の差のある頻數極大の深さの所がありまして陸地と同じ樣な性質を示して居りますが、此れは山崎直方博士[8]の認められた二段の海底斷層の存在と關聯して居るものと思はれます。

（8）次に火山の高さに就いてしらべて見ませう。所で1910年の有珠山の破裂の際に新しい山が出來ましたが、約百日間に百五十五米上昇して海面上約二百九十三米そびえる樣に成り、その附近の一番高い二つの小火口丘（約二百九十五米づゝ）と同じ高さに成つたので大森博士[9]は水壓的に釣合つてるのであらうと考へられました。それで火山は一般に conical or domed shape の孤立體であるし、以上の樣な事もありますので火山の頭がどこまでそびえるか、どの位の高さのものが一番多いかをしらべて見る事に致しました。先づ渡邊光、今泉政吉[10]兩氏の論文に依りまして日本のコニーデ全部とトロイデ全部の高さの五十米毎の頻數を別々に取つて四つゞつ平均したものを第十三圖及十四圖に示して置きましたが、此れを見ると山脈の高さの頻數曲線に見られた樣な頻數極大の高さが、幾つかありますが其等の高さの差は八百米乃至九百米でありまして山脈の場合の二倍程に成つて居ります。

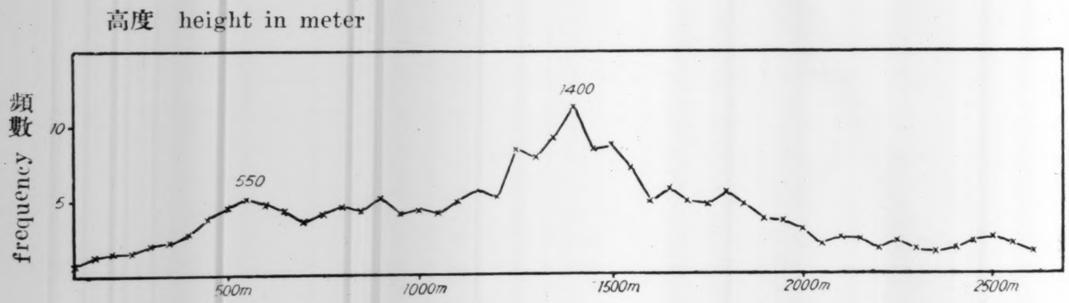

第十三圖　日本群島のコニーデの高度頻數

Fig. 13. Statistical Frequency of the Height of the Conides in Japan.

---

8) **山崎直方　震災豫防調査會報告** 100, B.
9) F. Omori, *Bull. Imp. E.I.C.*, **4**, No. 1.
10) **渡邊光、今泉政吉　地理學評論第三卷（昭和二年）**

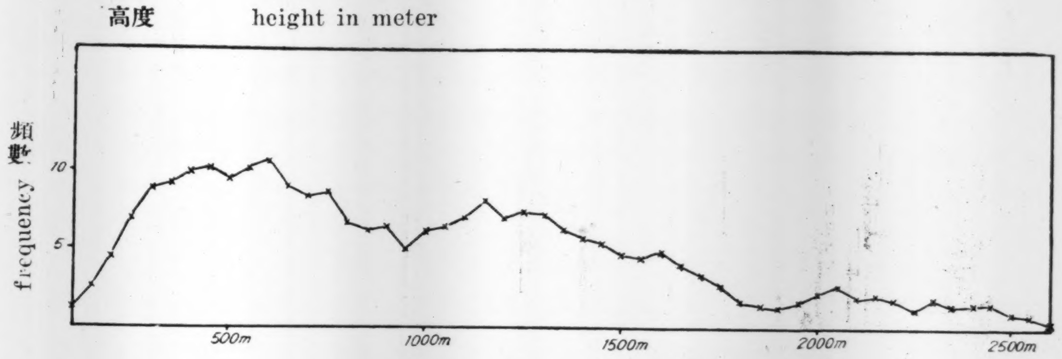

第十四圖 本邦のトロイデの高度頻數

Fig. 14. Statistical Distribution of the Height of the Thoroides in Japan.

次に K. Schneider[11] に依りまして世界中の活休火山の高さの頻數を取りましたのを第十五圖に示してあります。圖では同樣に滑かにした値が示されてありますが、數が少いので不明瞭ですが、それでも日本の山脈の場合と同じ樣に三百米乃至五百米位毎に頻數極大の所がある樣です。

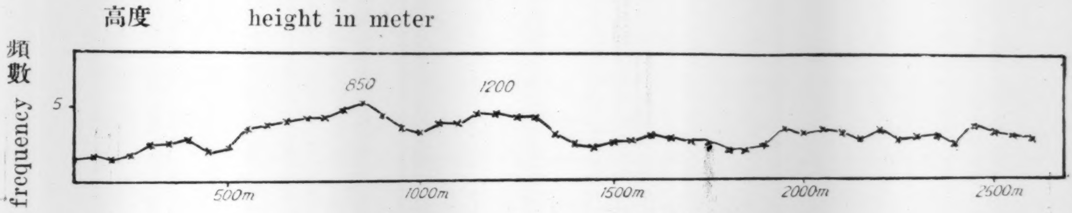

第十五圖 世界の活休火山の高度の頻數

Fig. 15. Statistical Frequency of the Height of the Volcanoes in the World.

(9) 以上の樣に山脈も淺海底も三百米乃至五百米程の段々に成つて居りますし、日本の山脈は最近の地質時代に準平原面が隆起したものであると云はれて居りますから、最近の時代の地變の量や地層の厚さにも關係して來るかも知れませんので兩方とも出來るだけ調べて見ました。先づ地變の量から申しますと日本の樣な地變の甚しい所では地殼は早さこそ間歇的に變動があるが絶へず變位してる事はよく知られて居る事であります。さて今日行はれてゐる其等の變位の量は一般に可成り小さいものですがそれが最近の地質年代にわたつて積分されたと思はれるものにはよく三百米乃至五百米程の變位が見られます。例へば、辻村太郎著地形學の七十五頁に依ると岡山市の

---

[11] K. SCHNEIDER, *Die Vulkanischen Erscheinungen der Erde.*

北部高梁川、旭川の流域に於ける準平原面と認むべき平坦面は第三紀中に約四百米隆起し更に其一部に堆積せる津山附近の第三紀層と共に百米の隆起を附加して現今の位置に來たと云ふ。

多田助教授のお話によると六甲山の南東に二段の斷層があり、各々四百米位の落差を有してるとの事であり、又紀伊半島に於ては伊賀上野の斷層が四百米乃至五百米の落差を有し、其の北方の鷲峯山の斷層は四百米、南方の斷層は四百米乃至五百米の落差を有してるとの事です。辻村助教授12)に依れば越中國泊町以南に於ける飛驒山脈の山麓部には二段になつてる階段斷層があり東部で上部に成つてるのを黒菱山斷層崖と云ひ西部のを棚山斷層崖と云ひ此れは二百米乃至三百米の落差を有するらしい。山崎教授、多田助教授13)に依ると琵琶湖附近に於て第一期に完成せられた準平原面は三百米乃至五百米の高度に達し云々。第三期の比較的靜止時代の後に全地域に亘つて急速なる隆起が行はれた。隆起の全量は三百米乃至五百米の範圍内に存するものと信ぜられる。寺田博士14)に依ると四國の Eohypsen を書いて見ると中央の部が五百米程陷沒した様である。此の際の地變の機巧は山崩れの場合と全く同一であらうと想像されるとの事であります。

辻村太郎著地形學三百三十六頁には能登邑知潟附近の地溝の北と南には百米と五百米の落差を有する斷層崖がある事が出て居りますし、三百四十三頁に依れば丹那盆地の附近には二百米の落差を有する斷層崖があるとの事です。尙同氏著日本地形誌百廿二頁には『山地高度の急變と斷層線との關係は阿寺斷層崖を挾む阿寺山脈と南部の山地との間に極めて明瞭に現れてゐる。田中薫理學士の研究によると北部の山地は高度千五百米以上に達し、南部の山地では千米を超過するものが稀である。また那岐山斷層崖を境として北部の山地は千米以上の高度を有し、南部の山地の高度は五百米内外に過ぎない。』と出て居ります。多田助教授15)に依ると奧丹後半島の中央部ではもとの準平原面が四百米以上隆起したとの事です。

次に外國の例を參考の爲掲げて見ますと、W. M. Davis 9(1に依ると Fuiji の數群の珊瑚礁は地質的年代にわたり相互に規則正しく上昇下降を繰り返してゐて、あたかも背斜が其處を通過してゐるかの様であり、此の背斜の波長は六十哩か八十哩位であ

---

12) 辻村太郎　地理學評論第二卷（大正十五年）
13) 山崎直方、多田文男　*loc. cit.*
14) 寺田寅彦　地震研究所彙報第四號
15) 多田文男　*loc. cit.*
16) W. M. DAVIS, *Americian Journ. of Science*, (Nov. 1927).

りその波丈は a few thousand feet であるとの事です。次に E. Kayser[17] の本に Alb. Heim がロイス谷、リンス谷、ライン谷の段丘の高さをはかつたのが出て居りますが、次に示す様に其等の次々の高さの差は主として三百米乃至五百米程です。

ロイス谷の段丘の高度	4.	1900〜2200 m
	3.	1400〜1600 m
	2.	900〜1200 m
	1.	600〜 900 m
リンス谷の段丘の高さ（現在の谷からの高さ）	4.	2800〜3000 m
	3.	2400〜2500 m
	2.	1800〜2000 m
	1.	1000〜1300 m
ライン谷の段丘の高さ	4.	2400 m
	3.	2000〜2100 m
	2.	1800〜1900 m
	1.	1300〜1500 m

尙前に述べた A. Winkler に依るとコールアルプでは古期中新世以後に四回の三百米乃至五百米位づつの隆起がありました。

(10) 次に地層の厚さですが、地質的な時間のとぎれが無く同じ様な狀態で比較的連續的に堆積したもので且その後の變質を餘り受けてゐないものとして第三紀の各 beds or formations の厚さをしらべる事にいたしました，此れに依ると以下に示す様に二百米乃至五百米程のものが頻繁にある事になつて居りまして堆積作用が行はれる間土地は細かな變動を考へなければ、まず二百米乃至五百米内外の間比較的連續して移動しては平靜に成ると云ふ様な地變をしてゐた事を示すのではなからうかと思はれます。勿論地層の厚さは場所により隨分差異がありますので、成可くよく發達してる所がよいのです。又各 beds 或は formations の境に就いては地質學者間に議論のあるものが多い事と思ひますが、此處ではほんの統計的に以上の様な傾向がある事が分れば、それで充分なのです。

飯塚保三郎氏[18] に依ると、

山形縣大石田油田第三紀層	下部	凝灰岩及頁岩層	約 2000 m
		黑色頁岩層	約 200 m
	中部	灰色頁岩層	180 m
		砂質頁岩層	170 m
		頁岩質砂岩層	250 m

---

17) E. Kayser, *Lehrb. d. Geologie*, **1**, 538.

18) 飯塚保三郎 山形縣大石田油田（大日本帝國油田第二十八區）地質及地質圖説明圖

上部	砂岩層	300 m
最上部	下部含炭層	240 m
	粗鬆砂岩層	200 m
	上部含炭層	700 m

早坂一郎博士19) によると、

常盤地方の新世界（青木助教授）

I.	白水統	厚さ約百七十乃至四十五米
II.	盤城統	厚さ二百九十及至九十米
III.	淺貝統	約二百九十及至四十米
IV.	龜の尾統	八百七十及至三百米

—— 著しい不整合 ——

V. 常盤統

北樺太の古第三紊 (Tichonovich)

I. 中新統下部 約百八十米弱

—— 不整合 ——

II. 中新統中部 約千三百米

III. 中新統上部 約五百五十米

IV. 鮮新統下部 約二百米

—— 斷絶 ——

V. 鮮新統上部 約五百五十米

—— 不整合 ——

VI. 鮮新世以後 Post-Pliocene の地層。

次に長尾巧氏20) によると、

高島炭田古第三紀層

芦屋層群	伊王島累層	純海水性	約 400 m
	沖の島累層	〃 〃	150 m+
高島層群	端島累層	主要夾炭層	250〜300 m
	二子島累層	一部海水性 一部は半鹹水性	300 m
	赤崎層	大部分陸性堆積物	300 m+

杵島炭田古第三紀層

---

19) 早坂一郎 日本地史の研究 194-196 & 187-189.

20) 長尾巧 地學雜誌第三十八卷（大正十五年）及第三十九卷（昭和二年）

佐世保層群		大部分淡水性	700 m?
芦屋層群	畑津頁岩	瀉湖性	200 m?
	畑津砂岩		200 m?
	行合野砂岩	海岸性沈積物なるも純海性	270 m
	佐里砂岩		
	杵島層	瀉湖性	180 m
相知層群	芳谷累管	淡水性	200〜250 m
	嚴木層	頻海性沈積物	270〜400 m
三池古第三紀層			
萬田層群		砂岩	300 m+
大牟田層群		砂岩	240 m
崎戸、松島炭田古第三紀層			
西彼杵層群	大島累層		250〜350 m?
	蠣の浦累層		50〜 80 m
	板の浦累層		100 m
松島層群			250 m+
寺島累層			300 m+

尙一寸外國の例を參照しますと、

E. Kayser[21] によると、

Tertiärs im Elsass

Rupelian	Blaue Mergel	290 m
	Bunte Mergel	400〜420 m
	Buntstreifige Mergel	bis 250 m
Sannoisian	Grüne u. Schwarze Mergel	bis 250 m

T. O. Bosworth[22] 等に依るとペルーの第三紀層の一部として、

The Negritos Formation at Negritos

Clavilithes Series	e. Parinas Sandstone	300 m
	d. Pale Shales	600 m
	c. Shales with Pebble Seams	450 m
Turritella Series	b, Shales with Pebble Seams	450 m
	a. Shales Unexposed	450 m+

(11) 以上は先づ地質年代にわたつて積分されたと思はれる量に就いてしらべたのですが、此度は現在の地殼の變動量に就いてしらべて見ませう。陸地測量部に依つて

---

[21] E. KAYSER, *Lehrb. d. Geologie*, **4**, 308.

[22] T. O. BOSWORTH & others, *Geology of the Tertiary and Quaternary Period in the North West part of Peru etc.*)

行はれた關東震災地の上下移動の中三角點に於けるものは此の邊の切峯面上の地點の移動を示すものであらうと思ひますが、以上の研究に於て日本の山脈の切峯面は三百米乃至五百米毎に平坦な所がある事になつて居りますので、此の際の上下移動量も此の切峯面の段々の色々な場所で統計的に差異があるかと思ひまして、各三角點の上下移動量の絶對値とその三角點の高さとを對比して見る事に致しました。それは第十六圖に示してあります。やはり高さで五十米毎の組の平均を四つづつ平均してあります

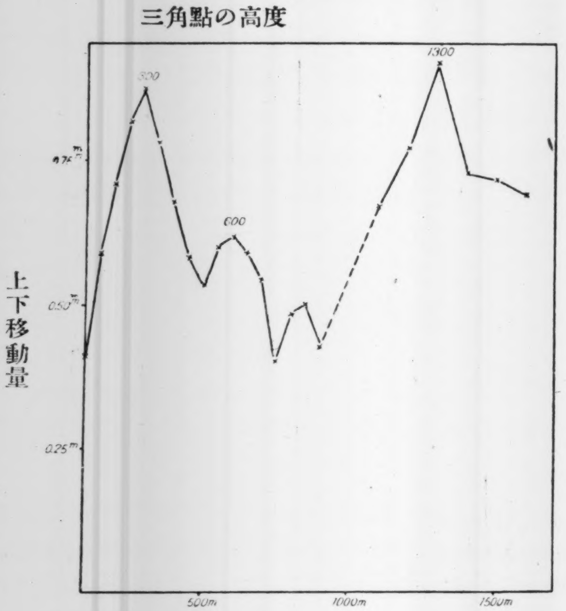

第十六圖　關東震災地三角點の上下移動の絶對値

が、千米以上は數が少いので百米毎のを二つづつ平均してあります。此れによると、三百米位の週期の小さな fluctuation と共に千米週期の 0.5 m 程の二倍振幅を有する fluctuation がある樣ですが、平均値のまはりの移動量の散らばり方の probable error と同程度の事なので疑はしい事です。尙房總半島だけの三角點の上下變位量（此の時は皆上昇して居ります）とその高さとを對比したのが第十七圖に出て居りますが、此れに依ると、房總半島に於て幾つかの谷に依つて分たれて居る約三百米の臺地面の變動量が一番大きく殆ど一樣であつた事を示して居ります。陸地測量部[23]の報告した圖にある此の地域の上下變動量の等變動量線が極めてよく此の部の地形の等高線と一致するのは其の爲です。渡邊光氏[24]は此の部の陸地測量部の報告した垂直移動に對し『加

23） 陸地測量部　地震研究所彙報第一號
24） 渡邊光　地理學評論第五卷（昭和四年）

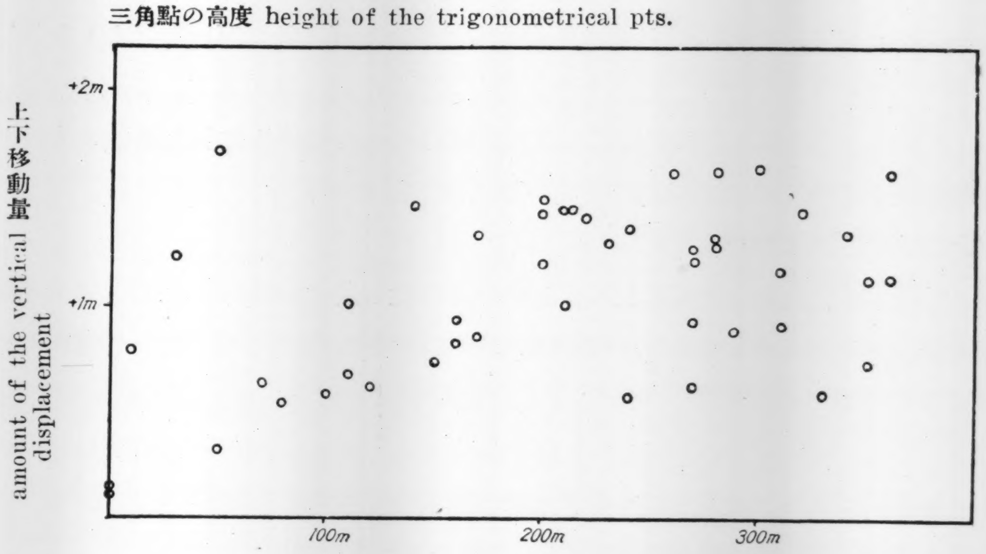

第十七圖 關東震災地三角點の上下移動量房總半島の部

茂川地溝に相當する部分がその南北の地域に比して隆起の少なかつたことが分り、地塊運動狀の水準變化が行はれたとも見られる』と云つてをられます。尙此の房總半島の臺地は第三紀層でありまして、熊谷直一氏[1]によりますと、此の邊の重力の gradient の樣子では此等の臺地は重力が大きいらしいのです。著者には此の臺地は山脈或は火山の段々の一つに相當してをつて此れが一樣に上昇しやうとするが、その表面にのつてる傾斜地塊がそれに從つて傾斜するので、表面では幾つかの傾斜地塊の傾斜運動の集合である事になるのではないかと思はれます。

(12) 次に本邦の各山脈の高度分布に就いて、山脈相互間の比較をして見ますと、三百米乃至五百米毎の高原性の部のある事が明かである山脈は關東山脈、飛驒山脈、木曾山脈、赤石山脈、紀伊山脈等本州の中央部にある山脈であり、此等の地方は現在一番高い位置を占め一番隆起が甚だしかつたのか或は他の部よりも遲く隆起したのかも知れませんが、最近の時代にも隆起して浸蝕の復活が行はれて居る樣です。例へば辻村太郎著地形學に依ると

1. 中央線上野原、四方津、與瀨驛附近に於て相模川沿岸の高い段丘を認める事が出來る。回春せる川は元の谷の中央に新なる狹い谷を掘り下げ、其の兩岸の崖には岩石を露出し、明かに土地の隆起が行はれたことを語る。(五十二頁)

2. 一般に關東平野を圍む山地より注ぐ多くの川は最近の時代に於て復活をした。

---

[1] 熊谷直一 地球第八卷(大正十五年)

荒川の上流は秩父盆地の入口に於ても内部に於ても低い段丘を作り、長瀞の如き若い谷の形を時に示す。利根川の上流渡良瀬川は大間々の邊に於て厚い礫層よりなる扇狀地を刻んで高い段丘を作り、更に上流赤城山麓沼田の町の邊に及ぶ。（五十三頁）

3. 天龍川の上流飯田伊那間に於ける段丘群は日本に於ける最も大規模のものである。最初著しき堆積によりて生じた廣い谷底は三百米の下方まで侵蝕され、二三段或は其れ以上の段丘を形成した。（五十三頁）

4. 天龍川は花崗岩の地域に於て天龍峽附近の最も若き峽谷を形成し、順次下流に結晶片岩、古代地層の區域を貫いて深五百米以上の狹い深谷を刻んだ。谷壁に於て小支流は多少半懸谷の狀をなして急に合し、近き時代に於ける侵蝕の復活を示す。（五十九頁）

5. 黑部川は立山、後立山間に深奥な峽谷を穿つてゐる。（二百三十九頁）

6. 木曾川は釜戸驛の北部に於ては花崗岩よりなる、平坦な臺地面以下三百米以上の深さを有する壯絕な谷を刻み、川は其の底を急駛する。（六十頁）

尙渡邊光氏[26]に依ると富山灣沿岸の黑部川、片貝川、早月川、上市川、常願寺川、神通川等の諸川の兩岸には隆起三角洲があつて飛驒山脈の隆起と富山灣の沈降を示すとの事です。次に北見山脈、北上山脈、中國山脈の高度分布が似て居りますが、此等の山地は低く大變侵蝕を受けて居る地方であり、最近の時代には中國山脈の樣に一部分沈降してる所もあります。

日高山脈、四國山脈、九州山脈、阿武隈山脈（此れは多少異なつてるが一共にして置く）は高度分布がよく似て居り八百米内外の高原性の部を持つて居りますが、此等の地方には可成の深い谷があつたり日高山脈[27]の樣に新しい河岸段丘が見られたりしていくらか若さを持つて居ります。

(13) 以上の結果の內山脈や相模灣底や火山の高度分布に三百乃至五百米每の頻數極大の部が見られる事と最近の地質時代に於ける地變の量に三百及至五百米程のものが多く第三紀層の各層の厚さに二百乃至五百米程のものが多い事は同一原因で說明せらるべきものであるかどうか分りませんが、少くとも其の一部は次の樣な機巧ではなからうかと思はれます。

1. 寺田教授[28]の硏究せられた砂崩れに依つて生ずる階段斷層と類似の現象であつ

---

26) 渡邊光 地理學評論第五卷（昭和四年）
27) 山崎直方、佐藤傳藏 大日本地誌卷九
28) T. Terada & N. Miyabc, *.Bull. Earthq Research Inst.*, **4.**

て、段々の高さをきめるものの一つは層の厚さでありませう。

2. 三百米乃至五百米位づつの隆起が繰り返してあつて、その間の平靜な時期に侵蝕が働いて段丘の樣なものが大規模に出來たのかも知れぬ。此は A. Winkler がコールアルプの四つの平坦面の成生を説明する際に四回の隆起を考へたのと同じ考へでありますし、W. Penck もその山麓階の成生を説明する際に隆起速度の變化が何回も繰返したと考へて居ります。此の三百乃至五百米毎の隆起をさせる原因は何に求むべきか明かでありませんが、或は

a. 侵蝕輪廻の途中に於てたえずみだされる isostatic equilibrium を回復する際に一樣に移動しないで數百米づつ飛び飛びに移動するのに依るのか、

b. 地下の岩漿溜內の岩漿の冷却作用や分體作用の現象中に生ずる蒸氣壓の變化と地殼との張合に求める事が出來るかも知れません。

理由は別として何回もの隆起が繰返された爲に所謂山麓面の樣なものが出來たとしましても辻村太郎著日本地形誌第百二十四頁に出て居ります樣に、隆起する地域の面積が隆起の量に對して十分に大きくないと、前の侵蝕面は後の侵蝕によつて全く破壞されて痕跡を止めないことになるのです。

尙同著書の百二十六乃至百二十七頁には『北海道では山麓面の著しい發達が行はれて居るらしい。四國山地や赤石山地の一部には不明瞭ながら山麓面の一部が殘存してゐることが略ぼ確實である。九州山地の內部には比較的に廣い區域に亘つて山麓面遺物が存在してゐて、高度五百米附近の所に多數の小起伏面形成が分布してゐる。』とあります。

(14) 兎に角地變の量は其に關係する時間の長さや地殼のひろがりなどに關するものでありまして、數十年數百年毎に繰返して居る大地震のときの變動量は數米數十米の程度（陸地內の事でして海底變化は數百米にも達する事がありませう）のものでせうが、最近の地質時代を幾つかに分けた位の時間に關係ある地變は以上にしらべた樣に三百乃至五百米程度のものでせう。但し其れだけの量だけ一時に變位したのでは無く、細かな移動が侵蝕作用に重要な關係のある樣な時間に對しては連續的と見てよい程度に何回も繰返して數百米にも達したのでせう。

(15) 結論。

さて以上の結果をまとめて見ますと、

1. 本邦の各山脈の切峯面上の高度分布を見ると一つ或は數個の高原性の部があり、數個ある時には次々の高さの差が三百乃至五百米であります。且此等の高原性の一部

は隆起準平原面の平坦部に相當するらしい。又數個の高原性の部がある山地は本州の中央部で且最高の地域を占め、最近の時代にも隆起して居ります。

2. アルプス山脈や相模灣底の高度分布にも高原性の部があり其等の次々の高さの差は同様に三百乃至五百米の程度であります。

3. 本邦の火山及び世界の活休火山の高度を見ますと頻繁に存在する高さがあり、その次々の差は前者では八百乃至九百米程であり後者には三百及至四百米程度のものがあるらしい。

4. 主として日本の最近の地質時代に於ける隆起や斷層作用の量には三百乃至五百米のものが多い。

5. 主として本邦の第三紀層の各層の厚さには二百乃至五百米程度のものが多い。

6. 關東震災地の上下變動量の絕對値は高さ三百米と千三百米の臺地性の部（兩部の高度差は千米です）が大きく且丁度房總半島の臺地は此の三百米の臺地性の部に相當して居つたらしいが、此れは疑はしい。

7. 以上の 1. 4. 5. 等の說明として寺田教授の研究せられた砂崩れと類似の機巧も考へられますが、著者としては、最近の地質時代に何回も三百乃至五百米程度の隆起が繰返されたのによると思ひます。此の様な隆起はイソスタシーの問題に關することか岩漿溜中の蒸氣壓に關係ある事かも知れぬ。

(16) 終りに臨み懇篤なる御注意を賜はつた寺田教授、藤原教授、石本教授に厚く御禮申し上げます。又色々御世話になつた多田助教授、津屋助手、岸上助手、杉山友紀雇員に厚く御禮申し上げます。

---

9. *Statistical Regularities regarding the Altitudes of Mountain Ranges and the Amounts of Dislocations of the Earth's Surface.*

By **Win INOUYE.**

The present author investigated the statistical distribution of the altitudes of mountain ranges and the amounts of dislocations of the earth's surface and found some regularities existing among them. A brief summary of the results obtained is given in the following lines with some discussions.

1. There are at least one or several well defined frequency maxima

in the areal frequency distribution of the height of the summit level of each of the main mountain ranges in Japan, showing that there exited, in geological ages, plateau-like flat surfaces or flat crests which are now eroded and destroyed. Some of the frequency maxima may correspond to peneplain remnants. The mountain ranges lying in the central part of the main island of Japan and forming the highest region of it show several marked flat-topped crests under the treatment used in the present investigation. In such a case when there are several plateaus or crests, the differences in heights of the successive crests fall within a constant range 300–500 m.

2. Among the heights of the volcanoes, belonging to conides and thoroides, in Japan, there exist several predominant values; the same can be said with volcanoes, active and dormant, in the world. The differences between any two successive predominating heights of the volcanoes in Japan are all 800–900 m., and those of the volcanoes in the world are estimated approximately to be 300–500 m.

3. It was found that the Alps, one of the most distorted district in the world, yield also a number of frequency maxima under the treatment of the present investigation. It was also the same with the statistical distribution of the depth of the Bay of Sagami, Japan. The differences of the levels of the predominating heights were 300–500 m. in both cases, which is of the same order of magnitude as those in the cases cited above.

4. The amounts of warpipngs and thrusts of the faults formed in the recent geological ages, most of those here taken being observed in Japan, fall most frequently in the range 300–500 m.

5. Of the geological formations or beds belonging to the tertiary period, those with the thickness of 200–500 m. seem to prevail in Japan.

6. The facts described in 1,4 and 5 may be taken as a phenomenon analogous to that of the formation of step-faults in a pile of sand as investigated by Prof. T. Terada and N. Miyabe. The present author is, however, inclined to understand them as the result of repeated upwarpings of the amount of 300–500 m. which occurred in the recent geological time.

These upwarpings may have some connections with isostatic adjustments of the earth's crust, or with the variation of the vapour pressure during the differentiation and the cooling of the magma under the crust.

10. Mesures des mouvements d'un bâtiment dans des conditions tranquilles

par

Mishio ISHIMOTO et Ryûtarô TAKAHASI.

(Reçu le 20 Mars 1929.)

1. INTRODUCTION.

Quand on veut étudier la résistance d'un bâtiment rapportée à la force sismique, on utilise le calcul sur les propriétés élastiques d'une substance sous l'action de la force oscillatoire. Si l'on adopte cette conception, la période élastique d'un bâtiment joue un rôle important sur le mesure de sa résistence. Bien que la valeur de la période du mouvement sismique, étant de l'ordre de la seconde, soit généralement assez grande par rapport à celle du bâtiment, il y aura tout d'abord très grand danger dans le cas où la période élastique du bâtiment a une valeur comparable à celle du mouvement sismique. Par conséquent, on ne peut négliger l'observation de la période élastique du bâtiment surtout dans les pays fréquentés par des tremblements de terre catastrophiques.

Bien que les observations sur la période élastique des bâtiments aient déjà été exécutées par plusieurs investigateurs,1) il y a certains résultats que l'on ne peut pas accepter comme étant d'origine élastique. Le regretté Prof. F. Omori2) a exécuté plusieurs observations sur un bâtiment (Maru-no-uti Building) de 7 étages au cours de sa construction. Cependant comme il n'a employé qu'un seul sismographe, il est difficile d'en conclure que toutes les oscillations enregistrées représentent celles d'origine élastique. Le Prof. K. Suyehiro3) a exécuté des observations en employant une paire de microsismographes comportant un tube en U rempli de mercure. Il a trouvé ainsi une sorte d'oscillation prédominante dans les enregistrements obtenus: et il l'a expliquée comme le résultat des mouvements en bloc d'un bâtiment. Ce mode de mouvement a été considéré comme cellui qui est contrôlé par des perturbations exterieures, c'est-à-dire les ondes superficielles du terrain. On a comparé ce fait au phénomène analogue d'un

---

1) T. TANIGUTI, *Kentikuzassi,* No. 480 (1926), 272.

2) F. OMORI, *Seismological Notes* (Imp. Earthq. Inv. Comm.), **3** (1922), 28.

3) K. SUYEHIRO, *Journ. Inst. Jap. Arch.*, No. 484 (1926).

bateau sur la mer, lequel oscille suivant le mouvement des vagues. De plus, il a constanté aussi l'existence de différences de phases dans certaines périodes d'oscillation et les oscillations correspondants sont considérées comme étant d'origine élastique.

Après la constatation de ce phénomène, la méthode des observations simultanées a été employées par plusieurs investigateurs. Monsieur T. Saida[4] a installé deux sismographes dans le Maru-no-uti Building et il a aussi prouvé que ce bâtiment posséde deux modes de mouvement, c'est-à-dire le mouvement en bloc et les mouvements d'origine élastique: mais ces observations ont été faites en tirant profit des mouvements sismiques. De plus le Prof. A. Imamura[5] a exécuté dernièrement plusieurs observations simultanées en disposant trois sismographes au Palais de la Diète, en cours de construction.

L'observation par le sismographe est possible dans le cas d'un bâtiment d'une certaine hauteur, surtout quand on profite des secousses sismiques; mais pour un bâtiment de hauteur faible en conditions tranquilles, on a besoin d'employer un appareil de plus grande amplification. Nous avons, à cet effet, construit deux sortes de sismographes pour la composante horizontale et la composante verticale et exécuté des observations simultanées pour examiner la caractéristique des mouvements du bâtiment de notre Institut.

2. Construction des microsismographes.

Il existe plusieurs types de microsismographes inventés par des sismologues de différents pays. Etant donné que certains bâtiments ont une période d'oscillation de 0,6s–0,8s, on a besoin d'avoir un microsismographe dont la période dépasse une seconde.[6] Quant à l'amplitude d'oscillation d'un bâtiment, on observe qu'elle reste de l'ordre d'un micron et on est obligé d'employer un appareil pouvant amplifier plusieurs milliers de fois les oscillations. Voici un tableau fournant les périodes et les amplifications de microsismographes connus.

---

[4] pas encore publié.

[5] A. Imamura, *Bull. Earthq. Res. Inst.*, **5** (1928), 143.

[6] Parmi les mouvements oscillatoires du terrain, bein qu'on distingue des ondes de période 3,0s–4,0s, celles-ci ne sont pas de nature à provoquer la vibration des bâtiments.

Noms		Périodes	Amplifications
WIECHERT	(horizontal)	0,62 s	2000-16000
	(vertical)		" "
GALITZINE	(horizontal)	0,5 s	500
	(vertical)	0,2 s	400
SHIDA	(horizontal)	0,6 s (?)	50000
SCHWEYDAR	(horizontal)	0,07 s	16000
ISHIMOTO	(horizontal)	1,5 s	3200
	(vertical)	1,0 s	3200

Pour avoir une période d'une seconde, nous avons employé un système de pendule inversé pour la composante horizontale: le poids de 3 kg. se trouve au bout d'une tige tenue verticalement avec une lame d'acier. (Fig. 1A). On règle la période du pendule en faisant varier l'épaisseur

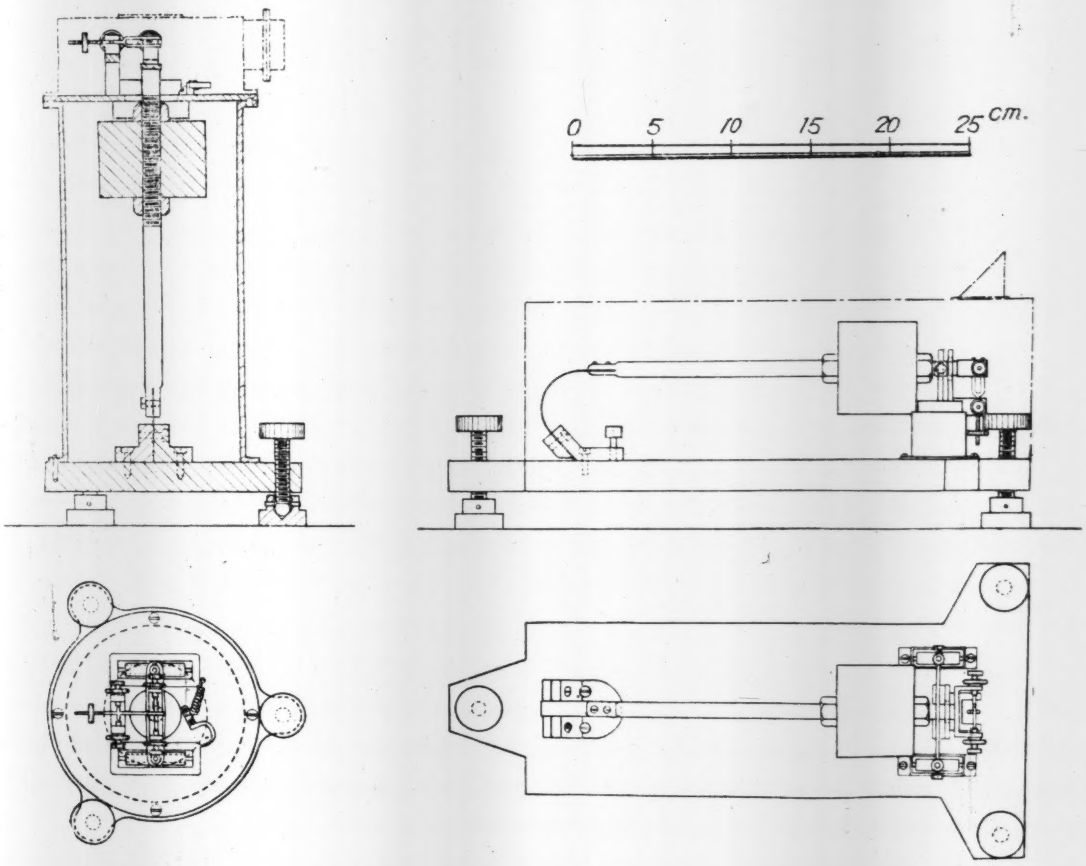

A B

Fig. 1.

et la longueur de la lame d'acier. Il n'est pas difficile d'obtenir une période de 2 secondes avec les dimensions représentées dans la figure 1: cependant le pendule devient instable sous une petite augmentation de l'amplitude et nous avons adopté une période de 1,5 s dans toutes les observations. Quant au procédé d'amplification (environs 3200), nous avons simplement employé une tige (1,79 mm. de diamètre) qui tourne d'un angle correspondant aux mouvements relatifs du poids. Un miroir attaché à la tige réfléchit le faisceau lumineux et les mouvements sont enregistrés optiquement sur une pellicule photographique enroulée à la surface d'un tambour tournant. La surface portante de la tige est constitutée par de l'agate; mais on a besoin d'un fin réglage de la vis de portée pour donner une rotation favorable à la tige. La transformation du mouvement du poids en la rotation de la tige est réalisée par un aimant qui ne permet aucun glissement, sans introduire de pression à la portée de la tige. Afin d'amortir l'oscillation propre du pendule, nous avons muni ce dernier de deux plaques plongeant dans deux cuvettes remplis d'huile. Les courants d'air provoquant des perturbations au mouvement de pendule, nous avons mis tout l'appareil dans un bâti étanche à l'air. La partie sismographique de cet arrangement communique avec la partie photographique au moyen d'une fenêtre fermé par une lame de verre. La distance entre le miroir et la pellicule photographique est de 1 mètre.

La construction d'un microsismographe pour la composante verticale est représentée par la figure 1 B. Nous avons un poids de 1 kg. et la période propre d'oscillation est de 1 seconde. Les dispositifs d'amplification et d'amortissement sont analogues à ceux qu'on voit dans le microsismographe pour la composante horizntale.

Nous avons fait une expérience avant d'exécution de nos observation, afin d'avoir la preuve que les deux microsismographes pouvent donner un même enregistrement. Les deux microsismographes (composante horizontale) sont installés côte à côte en un certain lieu du bâtiment et les deux enregistrements ont été pris en même temps sur un tambour tournant. La figure 2 (Pl. V) montre qu'il n'y a aucune différence entre les deux et nous pouvons accorder une certaine confiance à la construction du microsismographe. La même expérience a été exécutée avec les deux microsismographes de la composante verticale et nous avons obtenu une preuve qu'ils donnent aussi le même enregistrement.

Les expériences que nous avons faites nous ont permis de constater qu'il est possible de dégager certaines différences de mouvements en comparant les deux enregistrements obtenus par deux microsismographes.

3. OBSERVATIONS FAITES AVEC DEUX MICROSISMOGRAPHES POUR LA COMPOSANTE HORIZONTALE.

Nous avons exécuté une série d'observations simultanées en employant deux microsismographes de la composante horizontale installés en deux positions du bâtiment de notre Institut. (Fig. 3). Ce bâtiment est constitué par trois étages (33,6 m. × 14,5 m. × 12,3 m.) avec une cave supplémentaire sous l'étage principal du sous-sol. Il est construit en béton et carcasses en fer avec des précautions spéciales destinées à lui assurer une grande résistance contre les mouvements sismiques.

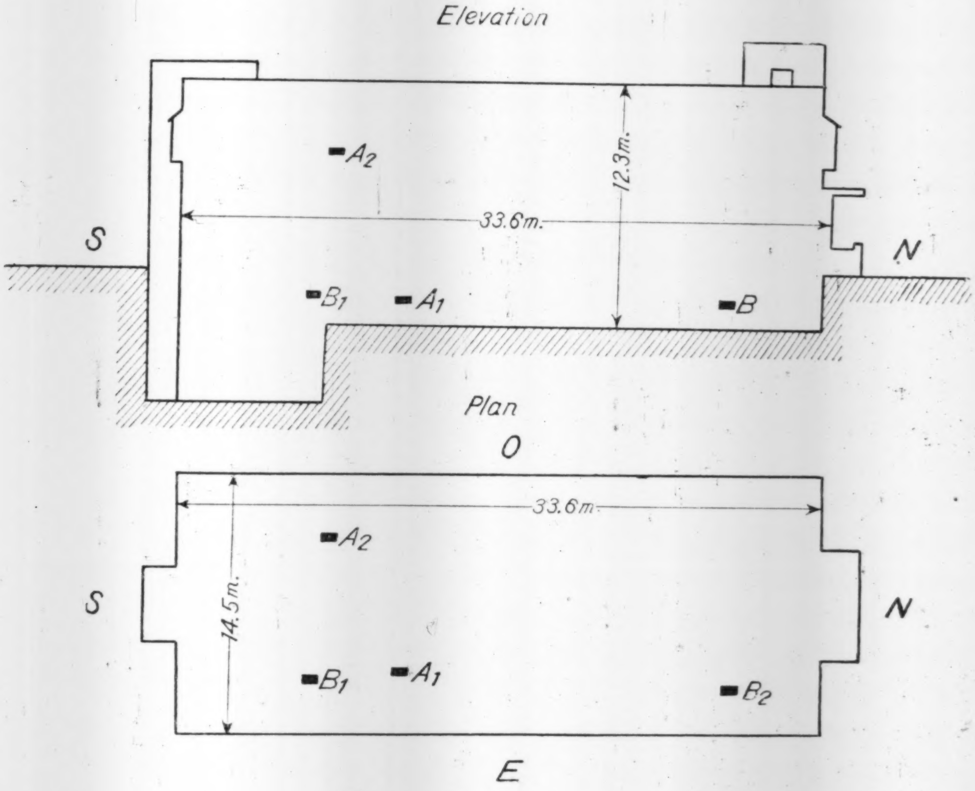

Fig. 3.

Nous avons posé deux microsismographes sur des tablettes de béton solidement fixées aux murs. Pour l'observation nous avons employé l'appareil d'une seule composante; il était donc necessaire d'avoir une pair d'observations (composantes NS et EO) pour déterminer le mouvement relatif de deux positions. Deux tambours rotatoires employés pour l'enregistrement photographique ont une vitesse superficielle de 1,33 cm/s qui nous permet aisément de dégager une oscillation de période égale ou superieure à 0,1 s.

Comme sources lumineuses nous avons pris deux lampes électriques connectées en série afin d'avoir des interruptions simultanées du courant électrique: les interruptions sont données constamment par un pendule de torsion toutes les 6,62 secondes et à volonté au moyen d'un interrupteur.

Nous constatons d'abord dans les enregistrements obtenus par les observations simultanées que deux positions du bâtiment donnent le même mouvement. Ce mode de mouvement correspond à celui qui été indiqué par le Prof. K. Suyehiro, que le bâtiment oscille en bloc. La période d'oscillation de ce mode de mouvement se trouve avoir pour valeur 0,3s–0,4s et le mouvement se présente sous une form sinusoïdale simple et son amplitude mesure généralement de 1 à 2 microns. Il nous semble que le mouvement en bloc du bâtiment doive être considéré comme un mouvement de translation de bâtiment; mais pour déterminer la réalité, il faut faire une observation utilisant le microsismographe de la composante verticale.

D'après une comparaison minutieuse, cependant, nous pouvons quelquefois mettre en évidence certaines différences de mouvement entre B_1 et B_2 à la composante EO. A la partie anormale où nous remarquons les différence de la phase et de l'amplitude d'oscillation, nous relevons la période 0,1s–0,2s et l'amplitude 0,3–0,2 micron. Ce fait nous amène à constater qu'il y a un cas où les deux points considérés exécutent des mouvements différents. Nous aurons, en effet, deux sortes d'explications: l'une est que le bâtiment tourne rigidement autour d'un axe vertical. Nous ne pouvons pas conclure pour le moment que ce mouvement résulte des propriétés élastiques du bâtiment ou est dû au mouvement en bloc du bâtiment; car la différence entre les deux est une quantité qui reste d'un ordre secondaire. La deuxième explication est qu'il existe un mouvement élastique de rotation rapporté à un axe median du bâtiment dirigé suivant la direction NS. En utilisant seulement deux microsismographes de la composante horizontale, il est impossible de distinguer le veritable mouvement et c'est cela que nous sommes obligé de faire une observation, comme nous verrons plus loin, en employant deux microsismographes de la composante verticale.

Considérant que l'oscillation d'un bâtiment est en rapport avec des mouvements irréguliers d'ondes superficielles qui existent toujour sur le terrain, nous avons exécuté une série d'observations simultanées sur le terrain et dans le bâtiment. Nous avons placé un des deux microsismographes (composante horizontale) à une position sur le terrain située à 10 mètres de distance du bâtiment et l'autre à la position A_1 (Fig. 3) dans la cave. D'après les enregistrements obtenus, nous constations l'existence d'une petite période de vibrations (presque 0,1s) sur le terrain, qui disparait dans le bâtiment. De plus quand des ondes dont la période est 0,3s–0,4s apparaissent successivement sur le terrain, le bâtiment oscille à peu près de la même façon suivant des mouvement sinusoïdaux. (Fig. 4. Pl. V). Ce mouvement en bloc du bâtiment est considéré comme un phénomène de résonance dont la période propre d'oscillation dépend d'une part de la propriété élastique du terrain et d'autre part de la masse du bâtiment: Mais il nous semble que même la période de résonance variera avec la valeur de l'amplitude d'oscillation. Le phénomène de résonance s'observe à peu près de la même maniere pour les deux composantes (EO et NS).

Ce phénomène d'oscillation propre d'un bâtiment est considéré comme correspondant à celui d'un système oscillatoire sous l'action d'impulsions irrégulières dont les phénomène des seiches peut être signalé comme un bel exemple dans la nature. D'autre part le Prof. T. Terada[7] a montré ce phénomène dans le laboratoire en plaçant un petit bloc de bois à la surface d'une nappe d'agar-agar. Pour mettre le mécanisme en évidence il[8] a ainsi executé une expérience sur le mouvement d'un pendule frappé successivement par la chute de grenailles. De toute façon, ce que nous avons observé au moyen de deux microsismographes pour la composante horizontale est pricipalement l'oscillation en bloc du bâtiment tandis qu'il était difficile de constater l'oscillation élastique du bâtiment: ceci tient probablement à la condition de résistance et aux dimensions de ce bâtiment.

4. OBSERVATIONS AVEC DEUX MICROSISMOGRAPHES POUR LA COMPOSANTE VERTICALE.

Observant que le mouvement du bâtiment n'est pas déterminable uniquement avec des microsismographes de la composante horizontale, nous avons ensuite essayé les observations utilisant deux microsismographes de la composante verticale. Pour dégager le mouvement roulant, c'est-à-dire la rotation rapportée à l'axe NS du bâtiment, nous avons mis deux microsismographes en deux positions C_1 et C_2 (Fig. 5) et obtenu des enregistrements simultanés. Nous ne remarquons aucune différence entre les deux enregistrements sur C_1 et C_2 pour toutes les ondes. Si le mouvement roulant du bâtiment existeit, les mouvements verticaux de C_1 et C_2 devraient être en sens contraires. De ce que nous n'observons rien de tel, nous concluons que le mouvement du bâtiment doit être considéré comme un mouvement de translation au moins dans la direction EO.

---

7) T. TERADA et C. TSUBOI, *Bulletin Earthq. Res. Inst.*, **3** (1927), 65.
8) T. TERADA et U. NAKAYA, *Bulletin Earthq. Res. Inst.*, **5** (1928), 93.

Par la suite, exécutant des observations simultanées aux deux positions D_1 et D_2, nous avons trouvé que certaines oscillations (0,1s–0,2s de période) donnent des différences de phase et d'amplitude, bien que les oscillations de période 0,3s–0,4s ne donnent pas de différence dans le mouvement. Ce fait correspond au cas de nos observations aux positions B_1 et B_2 (Fig. 3) sur la composante EO avec deux microsismographes de la composante horizontale. Pour expliquer ce phénomène, il est nécessaire de connaître la vitesse des ondes superficielles du terrain: cette dernière a été observée d'après la propagation des ondes de choc produites par la chute d'un corps. Il n'est pas certain que la vitesse des ondes produites de cette manière puisse être utilisée pour notre cas, mais la différence ne sera pas sensible quoique nous prenions la valeur 300 m/s pour la vitesse des ondes superficielles.

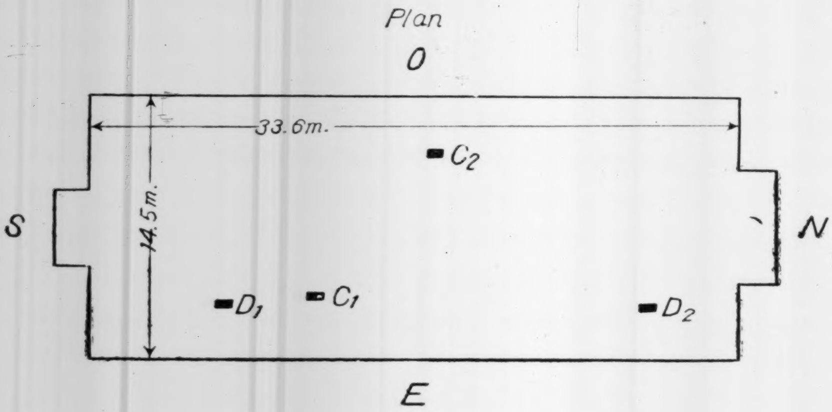

Fig. 5.

D'après cette supposition, ½ ou ¼ de la longueur d'une onde superficielle dont la période est 0,1s–0,2,s devient comparable à la longueur du bâtiment (33 m.) et le mouvement en bloc du batiment est considéré comme dû au mouvement local du terrain. Ce phénomène peut s'exprimer autrement: nous dirons que le bâtiment s'incline comme s'il faisait partie du terrain, suivant la pente des ondes. Naturellement, on ne sait pas si les ondes dont la période est de l'ordre de 0,1s–0,2s correspond aux vibrations élastiques du batiment; pourtant si nous observons que le rapport entre les amplitudes horizontales et verticales d'oscillation reste une valeur constante (à peu près 1), nous pouvons supposer que les mouvements d'une position dans le bâtiment représent ceux des ondes superficielles.

Ensuite pour observer le mouvement d'un point (C_1) dans le bâtiment nous avons installé deux microsismographes des composantes horizontale (NS) et verticale, en faisant enregistrer les deux mouvements sur un même tambour. La composition de ces deux mouvements représente une ellipse dont le grand axe est généralement dirigé suivant la direction du N-haut au S-bas et quelquefois suivant la direction du S-haut au N-bas. La translation entre les deux ellipses, est représentée par le mouvement circulaire dont la période est 0,1s–0,2s. Un phénomène analogue a été déjà étudié par le Prof. F. Omori(9) et récemment par M. K. Wadati(10) sur l'oscillation pulsatoire du terrain (3,0s–4,0s de période) ; mais cette fois la composition est faite avec deux composantes horizontales. Un point interessant est que l'on peut constater le même évidence parmi des ondes dont l'amplitude demeure de l'ordre d'un micron. Quant aux ondes superficielles du terrain, on considère que leur origine vient des automobiles, des tramways, etc. qui par leur passage produisent des impulsions sur terrain.

5. Remarques.

Nous avons constaté qu'il existe un mode de vibration en bloc du bâtiment qui n'est pas d'origine élastique. Le mouvement en bloc du bâtiment existera même au moment du tremblement du terre, et il devient peut être le mouvement principal d'oscillation du bâtiment; cependant il est certain qu'il ne peut pas provoquer de déformation élastique du bâtiment. Pour un tel phénomène on doit faire la discussion du couplage entre le bâtiment et le terrain.

Pour la suite de nos observations, nous nous proposons de construire, un appareil qui peut produire des ondes superficielles, et étudier d'une part la nature des ondes et d'autre part l'oscillation des bâtiments sous l'influence des ondes produites.

Pour terminer, nous tenons à exprimer nos vifs remercîments à Monsieur le Professeur K. Suyehiro, directeur de notre Institut, dont les suggestions et les encouragements nous ont été infiniment précieux.

Institut de Recherches sur les Tremblements de terre,
Université Impériale de Tôkyô.

---

9) F. Omori, *Bull. Imp. Earthq. Comm.*, **3** (1909), 1.
10) K. Wadati, *Kisyô-syûsi*, [2], **4** (1926), 1.

10. 平常時における一建築物の振動測定（梗概）

地震研究所 石本巳四雄
高橋龍太郎

1. 地震動に對する建築物の强度を論ずる場合においては、弾性體としての建築物の固有振動周期が問題となるのであるが、彈性振動を純粋に測定する事は多少の困難を伴ふのである。それは建築物振動の中には建築物が一塊となつて動搖する現象も含まれて居るからであつて、彈性振動と此の振動との間に確然たる區別を設けて測定しなければならないからである。

2. 平常時に存在する微動を利用して建築物の振動を測定する爲めに、第一圖に示した水平動、上下動微動計が製作せられたが、倍率は約 3200, 周期は 1.5 秒（水平動）及び 1.0 秒（上下動）を有してゐる。而して各成分の微動計において何れも同一記錄を與へるや否やを驗するために一個所に二臺の微動計が並置せられ、同一振動が記錄せられた。此の記錄は第二圖に示す如きものであつて此の程度において相當信用が置けるのである。

3. 水平動微動計二臺を地震研究所内二個所に据付けて爲した觀測結果は大部分の振動（周期約 0.3 秒）に對して建物が一塊となつて水平的に動搖するのが明白となつたのである。然し乍ら其の間に交つて建物の垂直軸の周圍に回轉する運動樣式も見出されるのである。（周期約 0.15 秒）又地表の一點と建築物内一點とに微動計を据付けて觀測した記錄（第四圖）からは、地表の波動が比較的不規則であるにも拘らず、其の運動に從つて建物が一塊としての共鳴的振動をなす現象が見出せるのである。

4. 水平動のみでは決定し兼ねる建物の振動樣式を上下動を用ひて測定した結果は、大部分の振動（周期約 0.3 秒）に對して建物は單純な上下、水平振動である事が云へるのである。但し地表波の周期が小であつて、其の波長が建物の大さと接近する場合においては、此の波の傾斜運動に從つて建物が傾斜運動をなす事實も見出せる。何れにもせよ平常時における此の建物の振動中には彈性振動と目されるものは見出し難いのである。

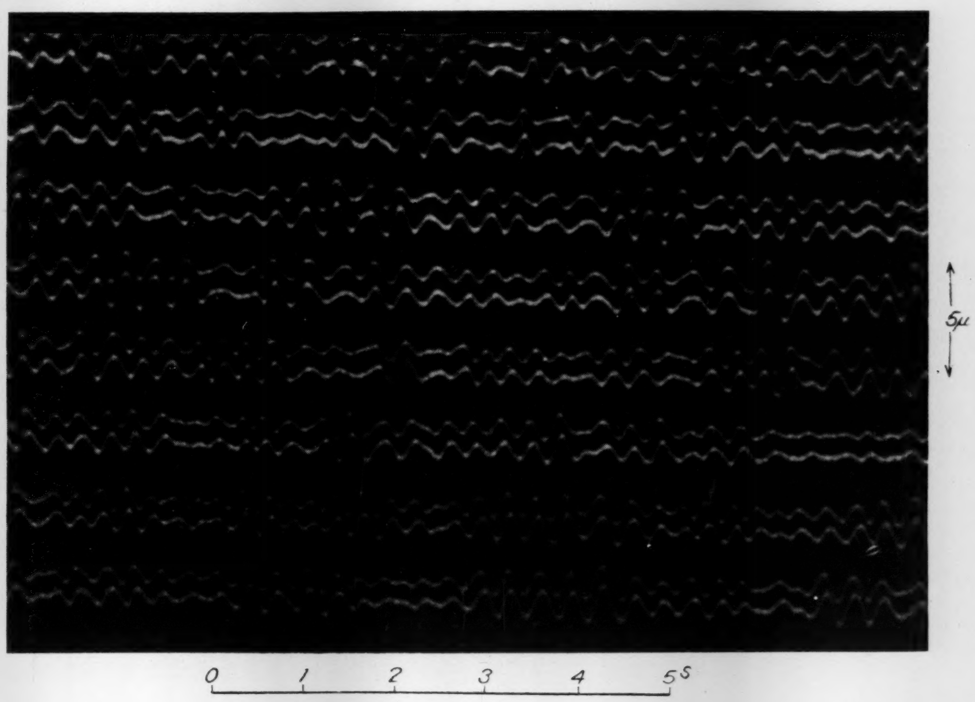

Fig. 2.

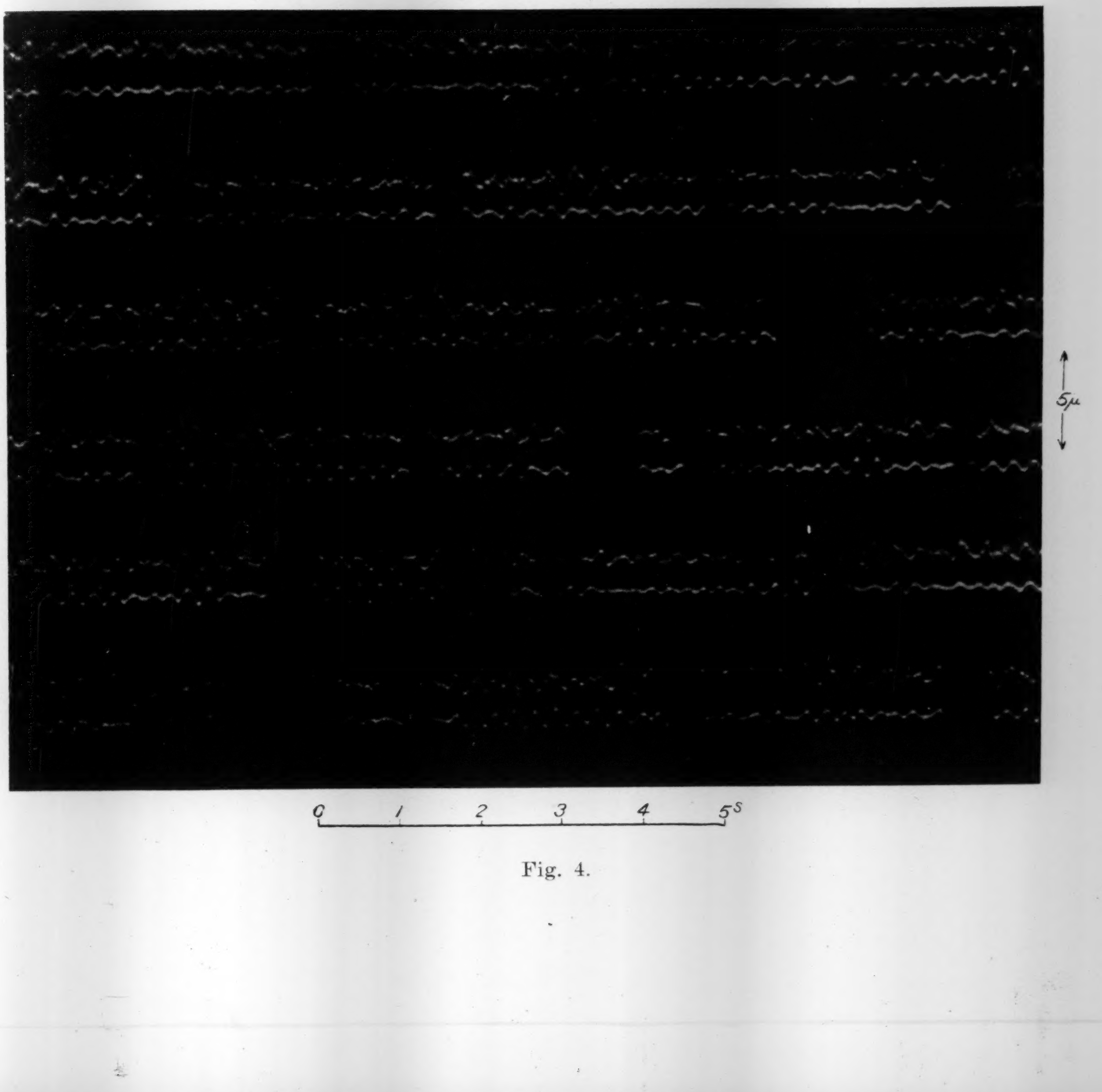

Fig. 4.

（震研彙報、第七號、圖版、石本、高橋）

11. 丹後震災地一二等三角點移動檢測成果第二報告

陸地測量部

1. 本圖は昭和二年東京帝國大學地震研究所の委託に依り一・二等三角測量を實施せる丹後震災地に於ける其後の移動を陸地測量部に於て施行せる復舊三角測量（昭和三年四月下旬より同年九月上旬に至る）の一部の結果と比較せるものにして其計算に於ては條件式等を全く一致せしめたり。

2. 本計算には一等三角點笠形山及此れより六甲山に至る方向並に笠形山、床之尾山間の距離を不動と假定し昭和二年十一月測量の觀測値を用ひ床之尾山及烏ケ岳の變動を計算し之に依りて得たる床之尾山、烏ケ岳の位置を基礎とし震災後の結果を求めたり。

3. 本測量にありては器材、方法等は全く地震研究所委託の場合と同一にして其一中數方向に對する諒必誤差は次の如し。

一中數方向に對する諒必誤差　　0.221 秒

---

11. Horizontal Displacements of the Primary and Secondary Triangulation Points, observed after the Earthquake of March 7, 1927, in Tango Districts. The Second Report.

By **Hitoshi OMURA,** Major General,

The Land Survey Department.

1. The map shows the relative horizontal displacements of the triangulation points obtained by the comparison of the results of the pre- and post-seismic measurments, comprizing the results of the later surveys (from Apr. to Sept. 1928) carried out since the previous reports in this Bull., Vol. IV. The same method of reduction is used for all the cases.

2. The coordinates of Kasagatayama, the direction Kasagatayama-Rokkôzan and the distance Kasagatayama-Tokonôyama are assumed unchanged; thence, using the results of the measurements of Nov. 1927, the displacements of Tokonôyama and Karasugadake were obtained. The positions of the last two stations thus obtained are taken as the basis of the present reduction.

3. The instruments and the methods of observations used in the later measurements are the same in the previous ones. The probable error for the mean value of the observed angles is 0″.221 for the last measurement.

Map showing the Horizontal Displacement of the Primary and Secondary Triangulation Points. observed after the Earthquake of March 7, 1927, in Tango Districts.

(Comprizing the Results of the Latest Fourth Surveys.)

丹後震災地一二等三角點移動要圖（第四回測量）

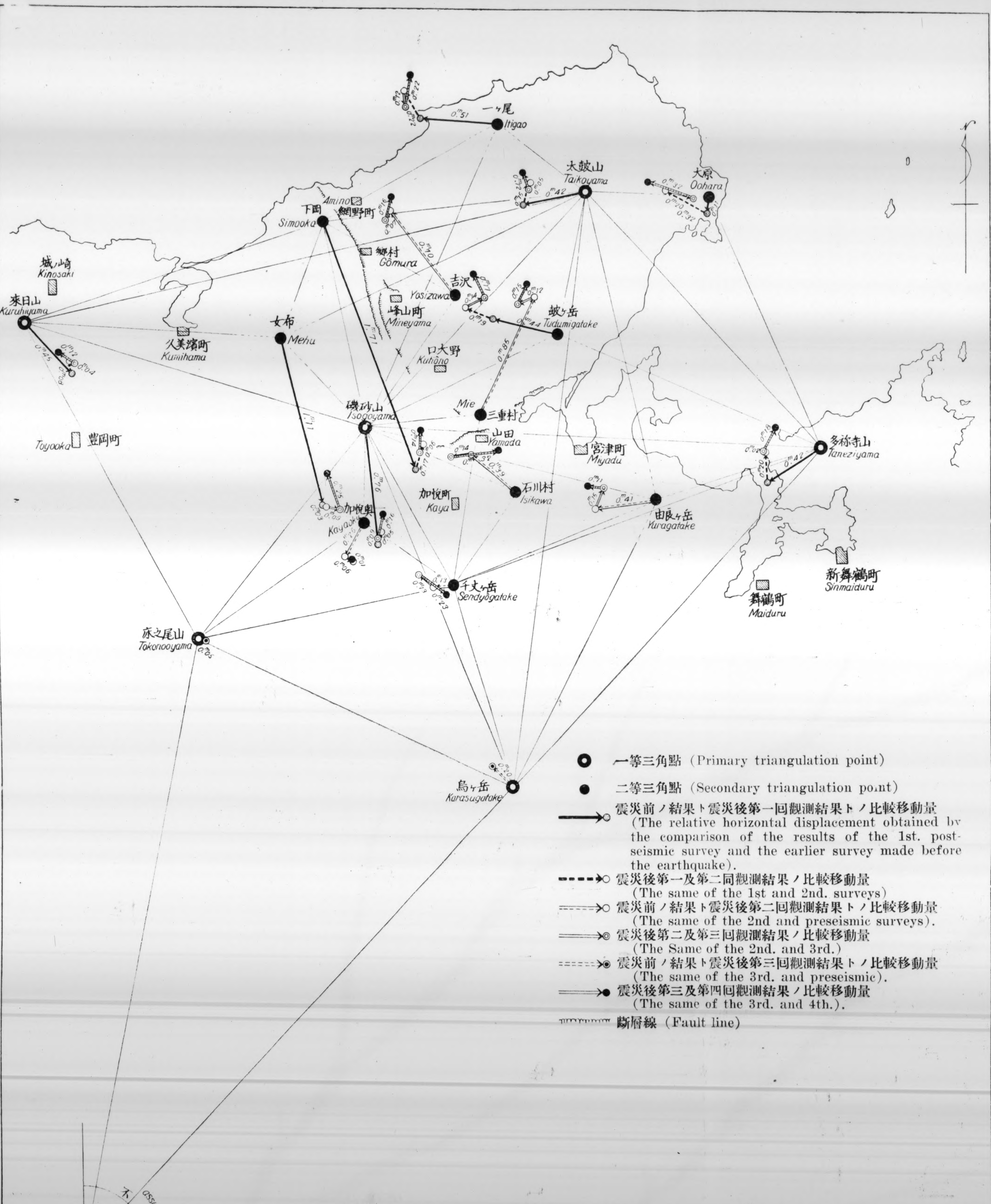
一ヶ尾
Itigao
太鼓山
Taikoyama
大原
Oohara
下岡
Simooka
Amino
網野町
鄕村
Gômura
城ノ崎
Kinosaki
來日山
Kuruhiyama
吉沢
Yosizawa
峰山町
Mineyama
皷ヶ岳
Tudumigatake
女布
Mehu
久美濱町
Kumihama
口大野
Kutiôno
Mie
三重村
磯砂山
Isogoyama
山田
Yamada
宮津町
Miyadu
多祢寺山
Taneziyama
豊岡町
Toyooka
加悦町
Kaya
石川村
Isikawa
由良ヶ岳
Yuragatake
加悦奥
Kayaoku
千丈ヶ岳
Sendyôgatake
新舞鶴町
Sinmaiduru
舞鶴町
Maiduru
床之尾山
Tokonooyama
烏ヶ岳
Karasugatake
笠形山
Kasagatayama
不變
assumed unchanged
六甲山方向
to Rokkôzan
N
一等三角點 (Primary triangulation point)
二等三角點 (Secondary triangulation point)
震災前ノ結果ト震災後第一回觀測結果トノ比較移動量 (The relative horizontal displacement obtained by the comparison of the results of the 1st. post-seismic survey and the earlier survey made before the earthquake).
震災後第一及第二同觀測結果ノ比較移動量 (The same of the 1st and 2nd. surveys)
震災前ノ結果ト震災後第二回觀測結果トノ比較移動量 (The same of the 2nd and preseismic surveys).
震災後第二及第三回觀測結果ノ比較移動量 (The Same of the 2nd. and 3rd.)
震災前ノ結果ト震災後第三回觀測結果トノ比較移動量 (The same of the 3rd. and preseismic).
震災後第三及第四回觀測結果ノ比較移動量 (The same of the 3rd. and 4th.).
斷層線 (Fault line)
Scale for the Map
0
5
10
15
20 KM
Scale for the Displacement
0
0.5
1
1.5
2 M

（震研彙報、第七號、圖版、陸地測量部）

12.　丹後地方震災地復舊一等三角測量記事

昭和四年三月

陸地測量部

大正十二年の關東地方大震は同地方一體に亘り複雜なる隆起沈下及び水平移動を來し復舊測量の結果概ね其眞相を捕捉し之が整理中に屬す。然るに間もなく山陰地方に在りても大正十四年五月但馬に昭和二年三月北丹地方に夫々稀有の激震あり。幾多の被害と共に斷層其他の地塊運動を招來せり。

當部は東京帝國大學の委託に應じて前記地方に於て震災直後の地塊移動を檢すべく昭和二年內に於て小範圍乍ら概ね三回の三角及水準測量を實施し當時其成果を提供せり。

然れども當部本然の復舊作業としては前例に鑑み成るべく廣地域に亘り寧ろ地震による地殼變動の靜止を待て實行すべく昭和二年覘標を建設し昭和三年之が觀測を實施し今や其第一次として一等三角測量作業の計算を完了せり本記事は該成果の大綱を錄するものにして復舊測定の必要を認むると同時に地震現象及經年の變化による三角點變移の狀態を知悉し得べく就中往年濃尾地方に起りたる大震の影響をも併せて觀察し得るものゝ如し。

一、作業區域竝ニ作業量

復舊一等三角測量地域は激震地を中心とし京都府、福井縣、滋賀縣、三重縣、兵庫縣、鳥取縣、岡山縣の一府六縣に跨り廣袤實に九九四方里、本點十八點、補點七點とす。而して是等諸點は嘗て明治十八年乃至二十二年の間に觀測を行ひ、其標石は概ね完全に維持保存せられ異狀を認めず今其點名所在地及舊觀測年次を示すこと別表第一及附圖の如し。

二、觀測作業

觀測は獨國 Carl Bamberg 製二十七糎測微經緯儀を用ひ本點は各方向共十二測回（二十四視準）補點は六測回（十二視準）の角觀測法（輪郭誤差を消去する爲め各測回

毎に輪郭を變換す）に據り視準點は全部回照器又は回光燈を用ひ其成果の組合せは朝、夕、夜の觀測の平均（濛氣差に依る水平角の影響を減少する爲め）を採用するに努めたり。

以上は陸地測量部の一等三角測量に於て採用せるものにして最良なる角觀測法とす。

三、計算及成果

今回測量したる一等三角網は從來三丹三角網、丹伯三角網、播讃三角網に屬し各三角網毎に平均しありしも是等諸點のみを以て獨立の一網とし先づ甲、乙二種の計算を實施せり。

甲、明治十八年乃至二十二年に於ける舊觀測値を用ひて之が平均計算をなし比良ヶ岳、野坂岳（此兩一等三角點は饗庭野基線網の第三增大邊の兩端を占む）の舊成果を既知件とし各點の距離、平面直角縱横線竝に經緯度を算出す。

乙、昭和三年に於ける新觀測値を用ひて甲と全く同一方法を以て平均計算を行ひ氷ノ山、笠形山を不動と假定し甲の成果に一致せしめ之に依り各點の距離、平面直角縱横線竝に經緯度を算出す。

甲、乙兩計算に依り求めたる經緯度を比較し各點の移動量竝に移動方向を算出す其結果は附圖第一及別表第二に示すが如し又各邊長は附圖第二に示す如く變化せり。

以上の計算に於て氷ノ山、笠形山を不動と假定したる根據次の如し。

甲、乙兩平均計算の結果各三角形の內角を比較するに附圖第三に示す如く其變動の最小なるは床之尾山、氷ノ山、笠形山の三角形にして此三角形に隣れる三角形中變動の最小なるは氷ノ山、笠形山、白旗山の三角形なり仍て此共通邊を不動と假定す。

附圖第一に依り田君谷山、氷ノ山、笠形山、御岳山，比良ヶ岳、野坂岳は移動量少く之を不動と假定するも實用上支障なきを知る仍て是等諸點を不動とし其內部の計算を復行し之を實用上の成果とせり但し其外方に於て伊吹山、御在所山は著大なる移動を示せり之れ其一部は不動の假定に幾分不合理あるに因るとするも大部は明治二十四年の濃尾地震其他の影響を受けたるものと認むるを得べく尙ほ廣き地域を改測するに非れば改算し得べからざるを以て今日之が實用上の成果を求めず。

四、精度

附圖第三は甲、乙兩計算結果の比較にして觀測誤差を含むこと勿論なり而して其精度は次の如し。

區分	舊觀測	新觀測
$m=\pm\sqrt{\dfrac{[Pvv]}{r}}$ ＝テ算出セルモノ	二秒六〇六	一秒六九〇
$M=\pm\sqrt{\dfrac{\Sigma\Delta^2}{3n}}$ ＝テ算出セルモノ	〇秒五五四	〇秒一〇三

但シ P ハ重量、v ハ剩餘、r ハ規約方程式ノ數

Δ ハ三角形ノ閉塞誤差、n ハ三角形ノ總數

TABLE I.

別表第一

等級	點名	所在地	舊觀測年
本點	御在所山	三重縣三重郡菰野村字御在所山	明治十八年
〃	伊吹山	滋賀縣坂田郡伊吹村大字上野字伊吹山	明治十八年
〃	比良ケ岳	〃 滋賀郡木戸村大字木戸字寄人山	明治十八年
〃	野坂岳	福井縣敦賀郡粟野村大字野坂字眞田峯	明治十八年
〃	鷲峯山	京都府綴喜郡宇治田原村大字奥山田字直谷	明治十九年
〃	多禰寺山	〃 加佐郡西大浦村大字多禰寺	明治十九年
〃	磯砂山	〃 中郡五箇村大字五箇字磯砂山	明治二十一年
〃	烏ケ岳	〃 何鹿郡佐賀村大字印内字大谷	明治二十一年
〃	御岳山	兵庫縣多紀郡畑村大字火打岩字畑山	明治十九年
〃	六甲山	〃 有馬郡有馬町字六甲山	明治十九年
〃	笠形山	〃 多可郡野間谷村大字大屋字笠形山	明治二十一年
〃	床之尾山	〃 出石郡合橋村大字畑字床之尾山	明治二十一年
〃	來日山	〃 城崎郡內川村大字來日字嶽	明治二十一年
〃	田君谷山	〃 美方郡溫泉町大字竹田字德原	明治二十一年
〃	氷ノ山	〃 〃 熊次村大字福定字四箇山	明治二十一年
〃	白旗山	〃 赤穗郡赤松村大字赤松字白旗城	明治二十一年
〃	瀧山	岡山縣勝田郡北吉野村大字瀧本字大屹	明治二十一年
〃	高鞍山	鳥取縣岩美郡中ノ鄉村大字覺寺字カリヨウ	明治二十一年
補點	木地山	滋賀縣高島郡朽木村大字麻生字廻戸	明治十九年
〃	久須夜ケ岳	福井縣遠敷郡內外海村大字堅海字久須夜	明治十九年
〃	太鼓山	京都府與謝郡野間村大字野中字住山	明治二十一年
〃	長老ケ岳	〃 北桑田郡大野村大字三埜字西谷	明治十九年
〃	蘇武瀧山	兵庫縣美方郡村岡町大字村岡字空山	明治二十一年
〃	石戸山	〃 氷上郡久下村大字金谷字コケモンジ	明治二十二年
〃	粟鹿山	〃 朝來郡粟鹿村字朝來山	明治二十二年

TABLE II.

別表第二

No.	Station	Latitude and Longitude		dB'' or dL''	dB^{m} or dL^{m}	$\sqrt{dB^2+dL^2}$	Azimuth
		Recent	Earlier				
數號	測站	新經緯度	舊經緯度				方位角
		° ′ ″	° ′ ″	″	m	m	° ′
1	氷ノ山 Hyônoyama	assumed as fixed 不動ト假定	35 21 2.8090 134 30 59.7128	——	——	——	——
2	笠形山 Kasagatayama	同上	35 3 39.4103 134 50 14 9468	——	——	——	——
3	來日山 Kuruhizan	35 36 31.6706 134 47 17.6068	35 36 31.6770 134 47 17.6026	−0.0064 +0.0042	−0.197 +0.106	0.224	151 43
4	野坂岳 Nosakadake	35 35 11.2966 136 1 38.8508	35 35 11.3018 136 1 38.8451	−0.0052 +0.0057	−0.160 +0.143	0 215	138 13
5	田君谷山 Takimitaniyama	35 35 8.3572 134 27 10.2931	35 35 8.3520 134 27 10.2908	+0.0052 +0.0023	+0.160 +0.058	0.170	19 56
6	磯砂山 Isanagosan	35 32 43.3244 135 2 27.2378	35 32 43.3401 135 2 27.2371	−0.0157 +0.0007	−0.484 +0.018	0.484	177 52
7	多禰寺山 Taneziyama	———	———	+0.0084 −0.0081	+0.259 −0.204	0.330	321 46
8	高龒山 Takatunboyama	35 31 4 8300 134 15 15.7420	35 31 4.8238 134 15 15.7420	+0.0062 0.0000	+0.191 0.000	0.191	0 0
9	床之尾山 Tokonooyama	35 35 7.3644 134 55 7.1095	35 35 7.3646 134 55 7.1108	−0.0002 −0.0013	−0.006 −0.033	0.033	259 42
10	伊吹山 Ibukiyama	35 24 52.7213 136 24 33.3044	35 24 52.7324 136 24 33.3367	−0.0111 −0.0323	−0.342 −0.815	0.884	247 14
11	烏ヶ岳 Karasugadake	35 19 52.0067 135 9 6.2257	35 19 52.0012 135 9 6.2292	+0.0055 −0.0035	+0.169 −0.088	0.190	332 30
12	比良ヶ岳 Hiragadake	35 12 22.8016 135 53 18.9236	35 12 22.8010 135 53 18.9328	+0.0006 −0.0092	+0.018 −0.233	0.234	274 25
13	瀧山 Takiyama	35 9 51.4345 134 9 12.7421	35 9 51.4348 134 9 12.7452	−0.0003 −0.0031	−0.009 −0.078	0.079	263 25
14	御岳山 Mitakesan	35 7 26.5968 135 14 51.7299	35 7 26.5936 135 14 51.7310	+0.0032 −0.0011	+0.099 −0.028	0.103	344 12
15	御在所山 Gozaisyoyama	35 1 2.0100 136 25 17.6360	35 1 1.9900 136 25 17.6840	+0.0200 −0.0480	+0.616 −1.217	1.364	296 51
16	白旗山 Sirahatayama	34 54 17.9222 134 23 0.6131	34 54 17.9222 134 23 0.6228	0.0000 −0.0097	0.000 −0.246	0.246	270 0
17	鷲峯山 Wasiminesan	34 49 52.0784 135 55 4.6208	34 49 52.0722 135 55 4.6390	+0.0062 −0.0182	+0.191 −0.462	0.500	292 28
18	六甲山 Rokkôzan	34 46 28.8120 135 15 59.5277	34 46 28.8109 135 15 59.5332	+0.0011 −0.0045	+0.034 −0.114	0.119	286 36
19	太鼓山 Taikoyama	———	———	+0.0110 −0.0188	+0.339 −0.473	0.582	305 38
20	久須夜ヶ岳 Kusuyogadake	35 33 15.4034 135 44 11.7476	35 33 15.3978 135 44 11.7390	+0.0056 +0.0086	+0.173 +0.217	0.278	51 26
21	蘇武瀧山 Sobutakiyama	35 28 3.4530 134 38 26.5964	35 28 3.4520 134 38 26.5933	+0.0010 +0.0031	+0.031 +0.078	0.084	68 20
22	木地山 Kidiyama	35 23 18.9689 135 48 46.6141	35 23 18.9556 135 48 46.6133	+0.0133 +0.0008	+0.410 +0.020	0.410	2 48
23	長老ヶ岳 Tyôrogadake	35 18 0.1832 135 28 36.5188	35 18 0.1826 135 28 36.5204	+0.0006 −0.0016	+0.018 −0.040	0.044	294 14
24	粟鹿山 Awagayama	35 16 10.5388 134 55 5.5344	35 16 10.5364 134 55 5.5358	+0.0024 −0.0014	+0.074 −0.035	0.082	334 41
25	石戸山 Isidoyama	35 6 16.9699 135 2 6.4273	35 6 16.9691 135 2 6.4257	+0.0008 +0.0016	+0.025 +0.041	0.048	58 38

12. Revision of the Primary Trigonometrical Survey in Tango Earthquake Districts.

Land Survey Department, Imperial Japanese Army.

(Publ. March 1929.)

Some results of the trigonometrical revision works carried out in Tango Districts after the recent destructive earthquake have already been published in this Bulletin, Vol. IV. Later, in 1928, a more extensive revision was carried out, comprising 18 primary and 7 suppdementary trigonometrical points which were all well preserved since the earlier survey in 1885–89. The comparison of the results of the two surveys gives the deformation of the triangulation net as shown in the Table and Figs.

The observed data of the earlier survey were recalculated treating the entire net here concerned as a single system, taking the positions of Hiragadake and Nozakadake as the basis. For the recent survey, the coordinates of Kasagatayama and Hyônoyama were assumed unchanged.

The probable errors of measurements are as follows:

	Earlier Survey	Recent Survey
$m=\pm\sqrt{\frac{[Pvv]}{r}}$	$2''.606$	$1''.690$
$M=\pm\sqrt{\frac{\Sigma\Delta^2}{3n}}$	$0''.554$	$0''.103$

where P is the weight, v the residual, r the number of equations, $\varDelta$ the closing error of triangle and n the number of triangles.

[Land Survey Dept.]

Map showing the Horizontal Displacements of the Primary Trigonometric

丹後震災地一等三角點移動

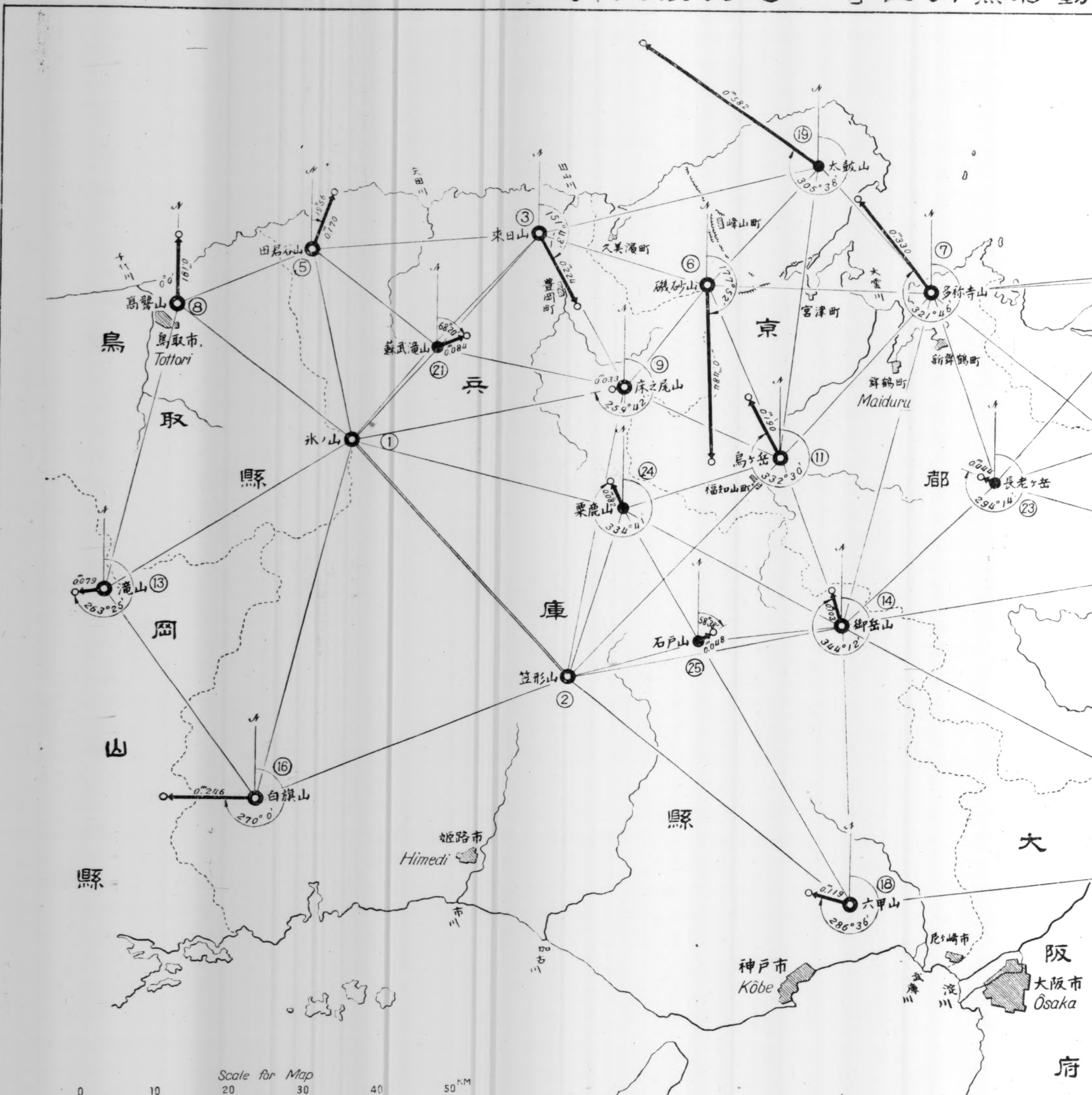

N
0.582
⑲
太鼓山
305°38'
⑦
多祢寺山
0.330
321°46'
③
來日山
151°43'
0.224
⑤
田倉山
0.170
153°6'
⑧
高鷲山
0.181
0°0'
鳥取市
Tottori
⑥
磯砂山
177°52'
0.884
⑨
床之尾山
0.033
254°42'
㉑
蘇武滝山
68°20'
0.084
①
氷ノ山
⑪
烏ヶ岳
0.190
332°30'
福知山町
⑳
長老ヶ岳
0.044
294°14'
㉓
㉔
栗鹿山
0.082
334°41'
⑬
滝山
0.079
263°25'
⑭
御岳山
0.103
344°12'
㉕
石戸山
58°36'
0.048
②
笠形山
⑯
白旗山
0.246
270°0'
⑱
六甲山
0.119
286°36'
姫路市
Himedi
神戸市
Kôbe
大阪市
Ôsaka
尼ヶ崎市
舞鶴町
Maiduru
新舞鶴町
宮津町
峰山町
久美濱町
豐岡町
鳥
取
縣
岡
山
縣
兵
庫
縣
京
都
大
阪
府
市川
加古川
武庫川
淀川
Scale for Map
0 10 20 30 40 50 KM
Scale for Displacement
0 0.5 1 M

trical Points in Tango Districts.

動要圖

附圖第一

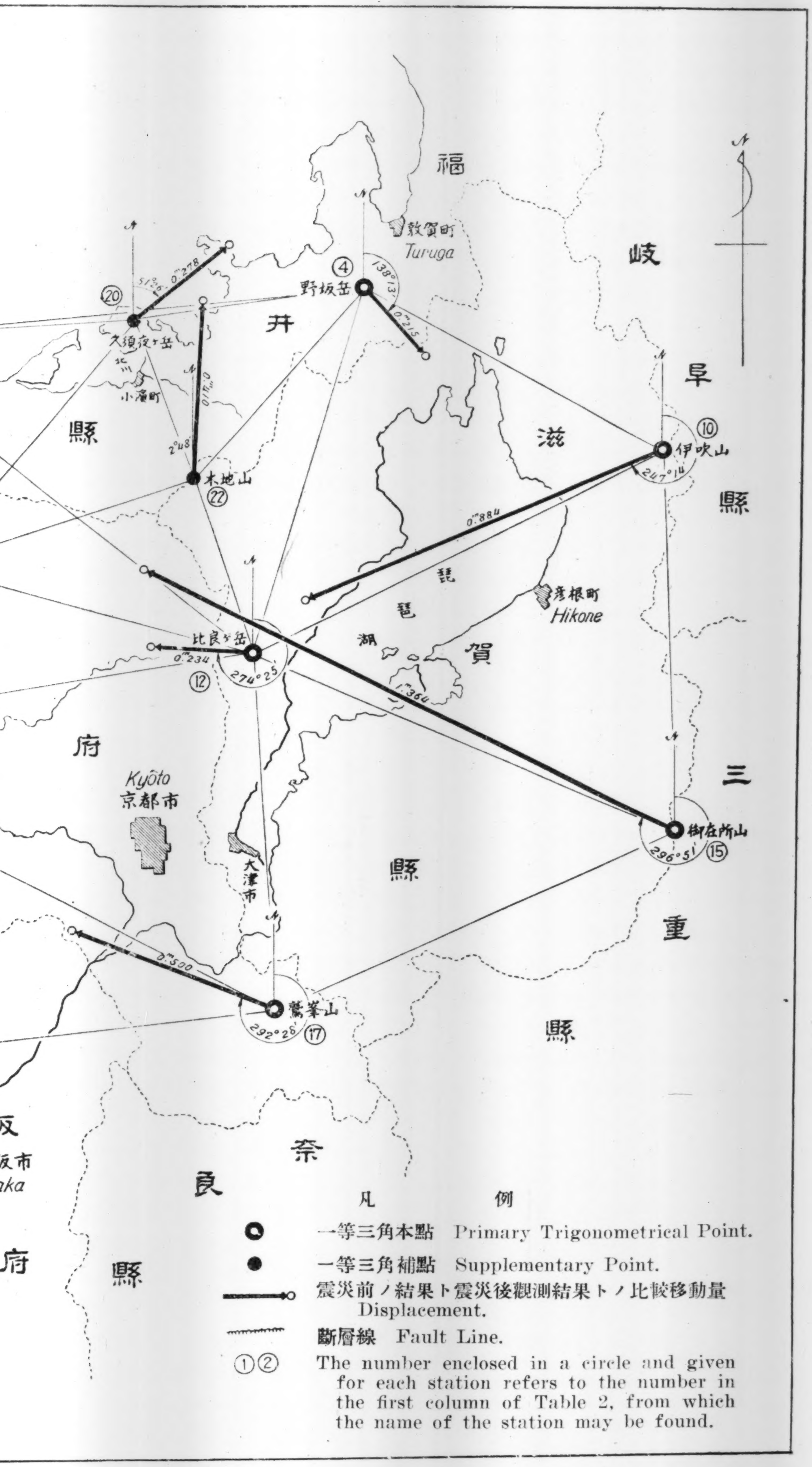
福
敦賀町
Turuga
岐
阜
④
野坂岳
138°13'
0".215
⑳
51°36'
0".278
久須夜ヶ岳
小濱町
井
縣
0".110
2°48'
木地山
㉒
滋
⑩
伊吹山
247°14'
0".884
縣
琵
琶
湖
彦根町
Hikone
賀
比良ヶ岳
0".234
⑫
274°25'
1".364
府
Kyōto
京都市
三
御在所山
296°51'
⑮
大津市
縣
重
0".500
鷲峯山
292°28'
⑰
縣
阪
阪市
aka
奈
良
府
縣
凡例
一等三角本點 Primary Trigonometrical Point.
一等三角補點 Supplementary Point.
震災前ノ結果ト震災後觀測結果トノ比較移動量 Displacement.
斷層線 Fault Line.
①②
The number enclosed in a circle and given for each station refers to the number in the first column of Table 2, from which the name of the station may be found.

附圖第二

Changes in Lengths of the Sides of Triangles.

一等本点三角網ニ於ケル邊長ノ變化

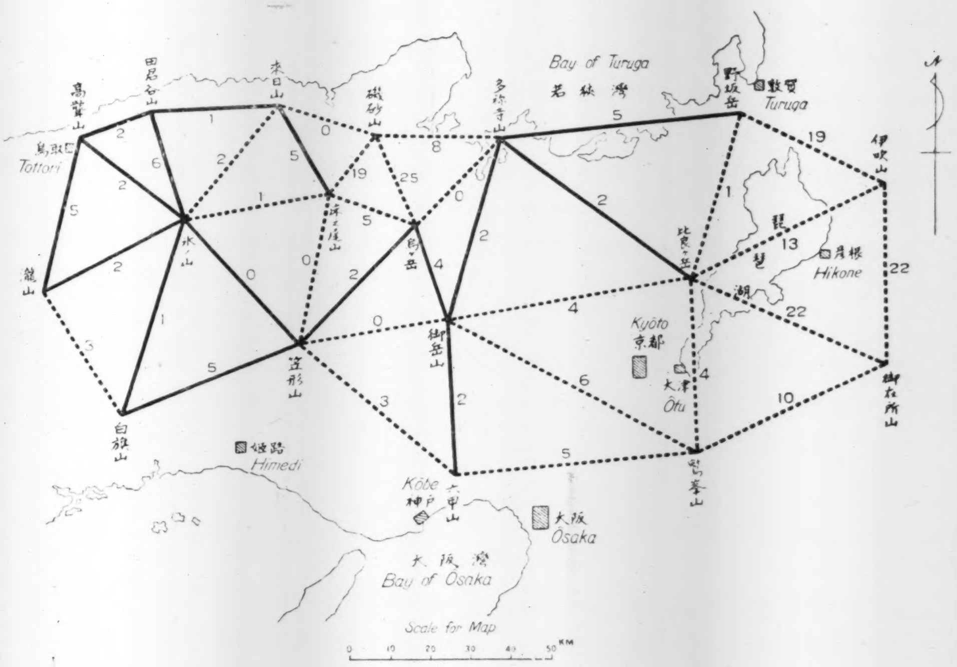
高鉢山
田君谷山
来日山
磯砂山
多祢寺山
Bay of Turuga
若狭灣
野坂岳
敦賀
Turuga
伊吹山
鳥取
Tottori
瀧山
氷ノ山
床ノ尾山
烏ヶ岳
比良ヶ岳
琵琶湖
彦根
Hikone
笠形山
御岳山
Kyōto
京都
大津
Ôtu
御在所山
白旗山
姫路
Himedi
Kōbe
神戸
六甲山
鷲峯山
大阪
Ôsaka
大阪灣
Bay of Ôsaka
Scale for Map
0
10
20
30
40
50
KM
N
2
1
6
2
5
0
8
5
19
25
1
2
5
0
2
1
2
19
5
2
0
0
4
2
13
22
22
4
0
1
5
3
2
6
4
10
5

凡例

━━━━━ 伸長シタル邊 (Side elongated)

┅┅┅┅┅ 短縮シタル邊 (Side contracted)

數字ハ邊長ノ $\frac{1}{1,000,000}$ ヲ單位トセル伸長(短縮)ノ割合

(The number given along the side is the amount of change in millionth of the total length.)

（震研彙報、第七號、圖版、陸地測量部）

附圖第三

Changes in Angles of Triangles.

一等本点三角網ニ於ケル角ノ變化

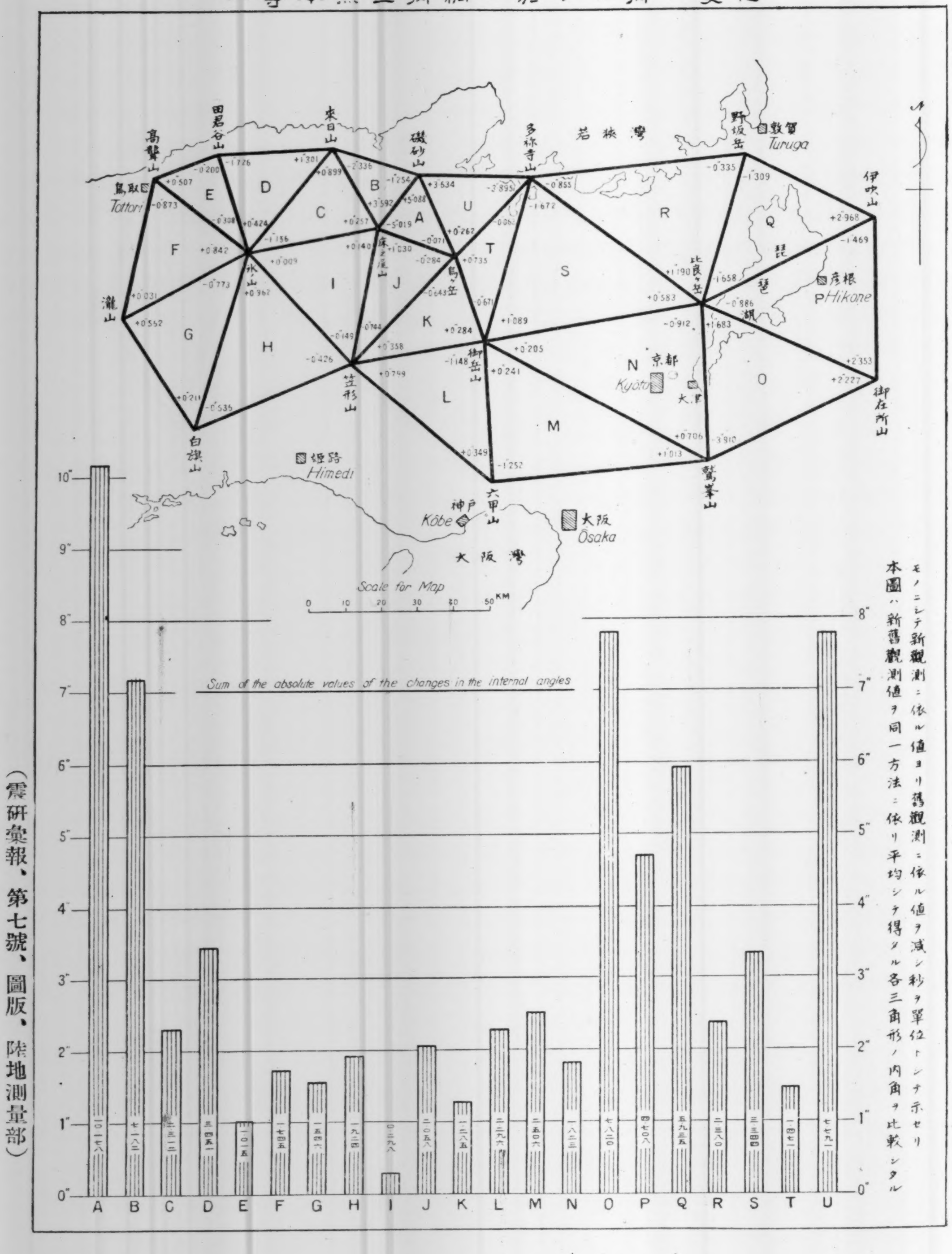
高鷲山
田君谷山
來日山
磯砂山
多祢寺山
若狭灣
野坂岳
敦賀
Turuga
伊吹山
鳥取
Tottori
瀧山
氷ノ山
床ノ尾山
鳥ヶ岳
比良ヶ岳
琵琶湖
彦根
Hikone
笠形山
御岳山
京都
Kyōto
大津
御在所山
白旗山
姫路
Himedi
六甲山
神戸
Kōbe
大阪
Ōsaka
大阪灣
鷲峯山
A B C D E F G H I J K L M N O P Q R S T U
+0.507
-0.200
-1.726
+1.301
+0.899
-2.336
-1.254
+3.634
-3.895
-0.855
-0.335
-1.309
-0.873
-0.308
+0.424
-1.156
+0.257
+3.592
+5.088
-5.019
+0.262
-0.063
-1.672
+2.968
-1.469
+0.842
+0.009
+0.140
+1.030
-0.071
-0.284
+0.735
+1.190
-1.658
+0.031
-0.773
+0.962
-0.643
-0.671
+0.583
-0.886
+0.552
-0.744
-0.149
+0.284
+1.089
-0.912
+1.683
-0.426
+0.358
-1.148
+0.205
+0.241
+2.353
+2.227
+0.211
-0.535
+0.799
+0.349
-1.252
+0.706
-3.910
+1.013
Scale for Map
0 10 20 30 40 50 KM
Sum of the absolute values of the changes in the internal angles
0" 1" 2" 3" 4" 5" 6" 7" 8" 9" 10"
一〇・一七八
七・一八二
二・三一二
三・四五一
一・〇一五
一・七四五
一・五四六
一・九二四
〇・二九八
二・〇五八
一・二八五
二・二九六
二・五〇六
一・八二三
七・八二〇
四・七〇八
五・九三五
二・三八〇
三・三四四
一・四七一
七・七九一

本圖ハ新舊觀測値ヲ同一方法ニ依リ平均シテ得タル各三角形ノ内角ヲ比較シタルモノニシテ新觀測ニ依ル値ヨリ舊觀測ニ依ル値ヲ減シ秒ヲ單位トシテ示セリ

（震研彙報、第七號、圖版、陸地測量部）

——所報——

○ 談話會記事

第卅四回談話會（昭和四年一月十五日）

1. 水底衝擊ニヨル淺海波ノ生成（第二報）	所員	妹澤克惟
1. 海上ビルデング新築鐵骨架構振動觀測	囑託	齊田時太郎 武藤清
1. 近海ノ低氣壓ト海水面トノ關係（前回ノ續）	囑託	山口生知
1. 油壺灣内ノ副振動ニ依ル地表傾斜運動	所員	高橋龍太郎

第卅五回談話會（昭和四年二月十九日）

1. 神戸海洋氣象臺及中央氣象臺リーフラー時計ノレートニ就テ		關口鯉吉 谷本誠
1. 内部ノ多量源ニヨル「レーレー」波ノ成生 附、内部ノ歪核ニヨル半無限固體ノ表面傾斜（第三報）	所員 所員	妹澤克惟 西村源六郎
1. 伊豆神津島火山ノ地質構造ト其岩石ニ就テ	所員	津屋弘逵
1. 地表面ノ高サ及地變ノ量	所員	井上宇胤
1. 大陸移動ノ原因	所員	長岡半太郎
1. 丹後震災地ニ於ケル其後ノ水平異動ニ就テ	陸地測量部三角科長	靑柳和夫
1. 重力狀況ノ變動ニ就テ	所員	坪井忠二

第卅六回談話會（昭和四年三月十九日）

1. 複式振子微動計ノ設計報告	囑託	那須信治
1. 丹後地震餘震觀測調査報告	囑託	那須信治
1. 丹後震災地ヲ中心トスル地方ノ三角點檢測ノ結果ニ就テ	陸地測量部三角科長	靑柳和夫
1. 砂層ノ崩壞ニ關スル實驗（第三報）	所員 所員	寺田寅彦 宮部直巳
1. 鍛冶屋澤ノ山崩ニ就テ	所員	藤原咲平
1. 裂罅ノ一種ニ就テ	所員	藤原咲平
1. 世界大地震地帶ト地殼ノ地質時代ノ變化	所員	長岡半太郎
1. 再ビ地震動ノ前驅部分ニ就テ	所員	松澤武雄 鈴木武夫

第卅七回談話會（昭和四年四月十六日）

1. 重力狀況ノ變動ニ就テ（第二報）	所員	坪井忠二
1. 昭和二年度ニ於ケル關東地震ノ統計的調査第二報（大森公式ニ於ケルkハ震原ノ深サト震央距離トノ函數ナルコト）	所員 所員 囑託	今村明恒 岸上冬彦 小平孝雄
1. 紀伊半島地塊最近三十年間ノ傾斜運動ハ地震力蓄積ノ發現ナランカ	所員	今村明恒

1. 火山ノ形（第二報）	所員	寺田寅彦
1. 過去ノ地殼裂ケ目並ニ地球表面ノ縮少	所員	長岡半太郎

第卅八回談話會（昭和四年五月廿一日）

1. 昭和三年五月二十一日千葉縣下ニ起レル地震ノ走時ノ研究	囑託	河角廣
1. 地球回轉速度ノ變化ト地震火山現象ノ關係	所員	長岡半太郎
1. 丹後震災地ニ於ケル復舊二等三角測量ノ成果ニ就テ	陸地測量部三角科長	青柳和夫

第卅九回談話會（昭和四年六月十八日）

1. 熔岩ノ流出スル時ニ受クルラシキ濾過作用ニ就テ	所員	坪井誠太郎
1. 地球自轉速度ノ變化ト緯度變位ノ噴火地震ニヨル影響	所員	長岡半太郎
1. 任意ノ衝擊ニヨツテ起ル週期的レーレー波	所員	妹澤克惟
1. 丹後震災地附近ニ於ケル地殼ノ變動	所員 所員	寺田寅彦 宮部直巳

○ 出張

昭和四年四月一日學術上取調ノタメ宮城縣下へ出張	所員	津屋弘逵
昭和四年四月一日地震事項調查ノタメ和歌山縣下へ出張	所員	今村明恒
昭和四年四月五日地震計及受信器修理ノタメ千葉縣下へ出張	囑託	波江野清藏
昭和四年四月二十七日學術上取調ノタメ大坂、徳島、高知ノ一府二縣下へ出張	囑託	那須信治
昭和四年六月四日學術上取調ノタメ岩手縣下へ出張	所員	坪井忠二
昭和四年六月十九日噴火事項調查ノタメ北海道へ出張	所員	多田文男
同	所員	坪井忠二
同	所員	津屋弘逵
同	所員	高橋龍太郎
同	所員	岸上冬彦

昭和四年七月二日印刷
昭和四年七月五日發行

編纂兼發行者　東京帝國大學地震研究所

東京市神田區美土代町二丁目一番地
印刷者　島連太郎

東京市神田區美土代町二丁目一番地
印刷所　三秀舎

東京市神田區南神保町十六番地
賣捌所　岩波書店

BULLETIN OF

THE EARTHQUAKE RESEARCH INSTITUTE

TOKYO IMPERIAL UNIVERSITY

Vol. VII, PART 1. June, 1929.

Contents

Papers and Reports

Page

1. K. Sezawa, The Tilting of the Surface of a Semi-infinite Solid due to Internal Nuclei of Strain. (in English) 1
2. K. Sezawa, Formation of Shallow-water Waves due to Subaqueous Shocks. (in English) 15
3. K. Sezawa and G. Nishimura, Generation of Rayleigh-waves from an Internal Source of Multiplet-type. (in English) 41
4. T. Terada and N. Miyabe, Experimental Investigation of the Deformation of Sand Mass. Part III. (in English) 65
5. R. Takahasi, Tilting Motion of the Earth Crust caused by Secondary Undulations of Tides in a Bay. (in English) 95
6. C. Tsuboi, Block Movements as Revealed by Means of Precise Levellings in Some Earthquake Districts of Japan. (in English) 103
7. S. Yamaguti, On the Effect of Cyclones upon Sea Level. (in English) 115
8. N. Nasu, Further Study of the Aftershocks of the Tango Earthquake. (in Japanese) 133
9. W. Inouye, Statistical Regularities regarding the Altitudes of Mountain Ranges and the Amounts of Dislocations of the Earth's Surface. (in Japanese) 153
10. M. Ishimoto et R. Takahasi, Mesures des mouvements d'un bâtiment dans des conditions tranquilles. (en français) 175
11. H. Omura, Horizontal Displacements of the Primary and Secondary Triangulation Points, observed after the Earthquake of March 7, 1927, in Tango Districts. The Second Report. (in Japanese) 185
12. Land Survey Department, Revision of the Primary Trigonometrical Survey in Tango Earthquake Districts. (in Japanese) 187

Institute Notes

(For the papers written in Japanese or in occidental languages, the abstracts are given in occidental languages or in Japanese respectively)

BULLETIN OF THE EARTHQUAKE RESEARCH INSTITUTE,
TOKYO IMPERIAL UNIVERSITY. Vol. VII, Part 2. September, 1929.

東京帝國大學

地震研究所彙報

第七號　第二册

昭和四年九月

目次

論文及報告

頁
13. 任意の衝擊によつて起る週期的レーレー波（英文）……妹澤克惟 193
14. 火山の形（英文）……寺田寅彦 207
15. 關西地方の地殼變形並に現在地形との關係（英文）……寺田寅彦・宮部直巳 223
16. 地震動の前驅部分に就いて（英文）……松澤武雄・山田國親・鈴木武夫 241
17. 太平洋に於ける激震帶の移動（獨文）……宮部直巳 261
18. 神津島火山（英文）……津屋弘逵 269
19. 茅ケ岳火山（英文）……市來政兼 335
20. 丹後地方震災地復舊二等三角測量記事（邦文）……陸地測量部 381

所報

(The titles in occidental languages are given on the back cover.)

本彙報ハ年四回發行ス（第一號ヨリ第六號マデハ不定期ニ發行セリ）.

本彙報掲載ノ論文及ビ報告ノ內容ニ關シテハ著者ノミニ其責任アルモノトス.

本彙報ニ關スル照會通信ハ東京帝國大學地震研究所長へ宛テラレタシ.

The bulletin is published quarterly (Vols. I–VI were published at irregular intervals).

The authors of the papers alone are responsible for the statements and opinions contained in their respective papers.

All communications relating to this bulletin should be addressed to the Director of the Earthquake Research Institute, Tokyo Imperial University.

13. *Periodic Rayleigh-waves caused by an Arbitrary Disturbance.*

By **Katsutada SEZAWA,**

Earthquake Research Institute.

(Read June 18, 1929.—Received June 19, 1929.)

A few years ago I studied an important problem[1] of the dispersion of Rayleigh-waves on the surface of a stratified elastic body. The problem gave merely the theory of the dispersion of an aggregate of trains of harmonic waves of an infinite extent, but did not involve the propagation of a train of waves of a finite extent. Although some cases of the transmission of a train of Rayleigh-waves of a limited extent in a dispersive medium have already been given in one of my papers,[2] yet the law of dispersion which was assumed in that paper was very simple and hence the results are far from being fulfilled in the actual waves at the ground.

It has in recent times been questioned by many seismologists that the regularity of the periods of the pulsatory motion of the ground may depend on the time intervals of the disturbances or on the restitutive nature of the ground itself. Prof. B. Gutenberg[3] and others pointed out that the continuous actions of the breach and the frost are the causal disturbances of the unceasing pulsations. Dr. K. Wadati ascribed in a former time the periodic pulsatory motion of the land surface to the effect of the free oscillations of the upper layer of that ground, though he does not seem now to care for such a problem. These theories will apparently account for the periodic motion of all the pulsation and, indeed, for each of the original disturbances the idea of Prof. Gutenberg seems to be most excellent; yet the explanation of the ordinary pulsatory motion can be made in another way. We know that the continuous periodic pulsation can be observed even beyond a certain distance from the shore or even at a season which is free from the frost. The superficial layer as in Dr. Wadati's sense is effective for the periodic oscillations under the condition that the rigidity of the bottom medium is extremely great in comparison with that of the layer, so that the arbitrary disturbance can be multiply reflected at the upper as well as at the lower boundaries and therefore the apparently periodic motion will be felt at the surface. This phenomena which takes place at such an extreme case is no more than the free oscillations of the vertical type of the layer and gives no explanation to the periodic waves propagated on the surface of the body.

---

[1] "Dispersion of Elastic Waves propagated on the Surface of Stratified Bodies & etc.", *Bull. Earthq. Res. Inst.*, **3** (1927), 1–18.

[2] "On the Propagation of the Leading and Trailing Parts of a Train of Elastic Waves," *Bull. Earthq. Res. Inst.*, **4** (1928), 107–122.

[3] B. GUTENBERG, *Zeits. f. Geophys.* **3** (1927) and a number of his other papers.

To understand such a nature of the propagated waves, it seems to be best to take some dispersive character of the waves caused by the outer disturbances. The postulation of the superficial layer is not meaningless in the direction that the dispersive character of the waves depends on such a layer. The formulation of the dispersion of waves propagated in a solid body is seriously complicated. Even if we could assume the law of the dispersion, such law would not apply with exactness to the solid of a certain geometrical form, as in the case of a stratified body. The difficulties, however, can be avoided by assuming that in the case of the surface waves the velocity of the phase of the harmonic waves is equivalent to that of Rayleigh-waves on a stratified body and that other treatments are quite analogous to those of the ordinary surface waves. This attempt is, of course, a first approximation; but, as far as the neighbourhood of the upper surface is concerned, the method seems to be rather correct than otherwise methods are employed.

Apart from the above problem, there is another fact to be noticed. The long trailing train of waves of the harmonic type which follows the main tremors may have some connection with the preceding problem. Though the periods of the oscillations are quite different from those of the ordinary pulsations, the character may be thought to be entirely similar; and it may be assumed in this case that the effective layer to cause the dispersion is of a larger scale, besides the path of the transmission of the waves which is long enough to excite the secondary or the sub-secondary trailing trains of waves.

The formula of the phase velocity which may be imagined from the results of my calculation in a preceding paper[1] is too complicated due to the inflexion nature of the velocity curves to apply the method of integration on such a complex formula. Owing to this reason, we shall assume that the velocity of the propagation of the phase of waves depends on the wave-length to the degree of the square. The more complicated cases will be left to some other occasion.

---

[1] *Loc cit.*, 193.

1. We may first consider the two-dimensional problem of Rayleigh-type waves. The axis of x being taken on the undisturbed surface, the axis of z is drawn vertically downwards. If we assume the effective elastic constants λ', μ' to be functions of the wave length such that

$$\left.\begin{aligned}\lambda'&=\lambda\left\{1+c_1\frac{L}{H}+\left(c_2\frac{L}{H}\right)^2\right\},\\ \mu'&=\mu\left\{1+c_1\frac{L}{H}+\left(c_2\frac{L}{H}\right)^2\right\},\end{aligned}\right\}\qquad\qquad(1)$$

in which L, H are the wave length and the effective depth of the layer and c_1, c_2 are dispersion constants, then the equations of motion of a semi-infinite body may be written in the forms:

$$\left.\begin{aligned}\rho\frac{\partial^2 u}{\partial t^2}&=(\lambda+2\mu)\left\{1+c_1\frac{L}{H}+\left(c_2\frac{L}{H}\right)^2\right\}\frac{\partial\Delta}{\partial x}\\ &\qquad+2\mu\left\{1+c_1\frac{L}{H}+\left(c_2\frac{L}{H}\right)^2\right\}\frac{\partial\varpi}{\partial z},\\ \rho\frac{\partial^2 w}{\partial t^2}&=(\lambda+2\mu)\left\{1+c_1\frac{L}{H}+\left(c_2\frac{L}{H}\right)^2\right\}\frac{\partial\Delta}{\partial z}\\ &\qquad-2\mu\left\{1+c_1\frac{L}{H}+\left(c_2\frac{L}{H}\right)^2\right\}\frac{\partial\varpi}{\partial x},\end{aligned}\right\}\qquad(2)$$

where

$$\Delta=\frac{\partial u}{\partial x}+\frac{\partial w}{\partial z}, \qquad 2\varpi=\frac{\partial u}{\partial z}-\frac{\partial w}{\partial x},\qquad\qquad(3)$$

and u, w are the components of displacement in x- and z-directions.

From (2) and (3), we get

$$\left.\begin{aligned}\Delta&=A_1e^{-\alpha z+ikx}\begin{matrix}\cos\\ \sin\end{matrix}\Big\}pt,\\ 2\varpi&=-iB_1e^{-\beta z+ikx}\begin{matrix}\cos\\ \sin\end{matrix}\Big\}pt,\end{aligned}\right\}\qquad\qquad(4)$$

in which

$$k^2-h^2=\alpha^2, \qquad k^2-j^2=\beta^2,\qquad\qquad(5)$$

$$\left.\begin{aligned}h^2&=\frac{\rho p^2}{\lambda+2\mu}\bigg/\left(1+\frac{2\pi c_1}{kH}+\frac{4\pi^2 c_2^2}{k^2H^2}\right),\\ j^2&=\frac{\rho p^2}{\mu}\bigg/\left(1+\frac{2\pi c_1}{kH}+\frac{4\pi^2 c_2}{k^2H^2}\right),\end{aligned}\right\}\qquad\qquad(6)$$

where $2\pi/k$ is taken in place of L.

The displacements corresponding to (4) can be easily written by

$$\left.\begin{aligned} u&=-i\left(\frac{kA_1}{h^2}e^{-\alpha z}+\frac{\beta B_1}{j^2}e^{-\beta z}\right)e^{ikx}\begin{matrix}\cos\\ \sin\end{matrix}\Big\}pt,\\ w&=\left(\frac{\alpha A_1}{h^2}e^{-\alpha z}+\frac{kB_1}{j^2}e^{-\beta z}\right)e^{ikx}\begin{matrix}\cos\\ \sin\end{matrix}\Big\}pt,\end{aligned}\right\}\dots\dots\dots\dots\dots(7)$$

At the surface, $z=0$, we should have

$$\lambda'\Delta+2\mu'\frac{\partial w}{\partial z}=0,\qquad \frac{\partial u}{\partial z}+\frac{\partial w}{\partial x}=0,\dots\dots\dots\dots\dots\dots(8)$$

from which we get

$$\frac{B_1}{j^2}\Big/\frac{A_1}{h^2}=\frac{-2k\alpha}{2k^2-j^2},\dots\dots\dots\dots\dots\dots\dots\dots(9)$$

and

$$(2k^2-j^2)^2-4k^2\alpha\beta=0.\dots\dots\dots\dots\dots\dots\dots\dots(10)$$

The typical solutions at $z=0$ are thus written by

$$\left.\begin{aligned} u&=-i\,\mathrm{ccs}\left\{\frac{jV_2}{\kappa}\sqrt{k^2+\frac{2\pi c_1}{H}k+\left(\frac{2\pi c_2}{H}\right)^2}\,t\right\}\frac{\kappa(2\kappa^2-j^2-2\alpha_1\beta_1)}{j^2\alpha_1}e^{ikx},\\ w&=\cos\left\{\frac{jV_2}{\kappa}\sqrt{k^2+\frac{2\pi c_1}{H}k+\left(\frac{2\pi c_2}{H}\right)^2}\,t\right\}e^{ikx},\end{aligned}\right\}\dots(11)^{4)}$$

where κ is the real positive root of the equation (10) and α_1, β_1 are the corresponding values of α, β, while V_2 is the velocity of the propagation of certain distortional waves of the form $\sqrt{\mu/\rho}$.

To generalise (10), we use Fourier's double integral theorem, the generalised forms of u, w being as follows:

$$\begin{aligned} u=&\frac{iq}{2\pi}\int_{-\infty}^{\infty}\cos\left\{l\sqrt{k^2+mk+n^2}\,t\right\}dk\int_{-\infty}^{\infty}f(\sigma)\,e^{ik(x-\sigma)}\,d\sigma\\ &+\frac{iq}{2\pi}\int_{-\infty}^{\infty}\frac{\sin\{l\sqrt{k^2+mk+n^2}\,t\}\,dk}{l\sqrt{k^2+mk+n^2}}\int_{-\infty}^{\infty}F(\sigma)\,e^{ik(x-\sigma)}\,d\sigma,\dots\dots(12)\end{aligned}$$

$$\begin{aligned} w=&\frac{1}{2\pi}\int_{-\infty}^{\infty}\cos\left\{l\sqrt{k^2+mk+n^2}\,t\right\}dk\int_{-\infty}^{\infty}f(\sigma)\,e^{ik(x-\sigma)}\,d\sigma\\ &+\frac{1}{2\pi}\int_{-\infty}^{\infty}\frac{\sin\{l\sqrt{k^2+mk+n^2}\,t\}\,dk}{l\sqrt{k^2+mk+n^2}}\int_{-\infty}^{\infty}F(\sigma)\,e^{ik(x-\sigma)}\,d\sigma,\dots\dots(13)\end{aligned}$$

for the initial conditions that $w=f(x)$ and $\partial w/\partial t=F(x)$ at $z=0$.

---

4) These expressions are most suitable for the condition that the surface is always free from the stress.

In (12) and (13) we have used the notations such that

$$\left.\begin{aligned} &q=\frac{\kappa\,(2\kappa^2-j^2-2\alpha_1\beta_1)}{j^2\alpha_1} \qquad (=\text{constant for any } p),\\ &l=\frac{jV_2}{\kappa}, \qquad m=\frac{2\pi c_1}{H}, \qquad n=\frac{2\pi c_2}{H}. \end{aligned}\right\}\quad\ldots\ldots(14)$$

If the intial disturbance is given by

$$f(x)=\frac{A}{a}\,e^{-\frac{x^2}{a^2}}, \qquad F(x)=\frac{B}{b}\,e^{-\frac{x^2}{b^2}}, \quad\ldots\ldots\ldots\ldots(15)$$

then, by means of the formula

$$\int_{-\infty}^{\infty} e^{-\frac{\sigma^2}{c^2}}\,e^{-ik\sigma}\,d\sigma=\sqrt{\pi}\,c\,e^{-\frac{c^2k^2}{4}}, \quad\ldots\ldots\ldots\ldots(16)$$

we get

$$\begin{aligned} u=&\frac{iAq}{2\sqrt{\pi}}\frac{\partial}{\partial t}\int_{-\infty}^{\infty}\left(1-\frac{a^2k^2}{4}+\ldots\right)\frac{\sin l\sqrt{k^2+mk+n^2t}}{l\sqrt{k^2+mk+n^2}}\,e^{ikx}\,dk\\ &+\frac{iBq}{2\sqrt{\pi}}\int_{-\infty}^{\infty}\left(1-\frac{b^2k^2}{4}+\ldots\right)\frac{\sin l\sqrt{k^2+mk+n^2t}}{l\sqrt{k^2+mk+n^2}}\,e^{ikx}\,dk, \quad\ldots(17)\\ w=&\frac{A}{2\sqrt{\pi}}\frac{\partial}{\partial t}\int_{-\infty}^{\infty}\left(1-\frac{a^2k^2}{4}+\ldots\right)\frac{\sin l\sqrt{k^2+mk+n^2t}}{l\sqrt{k^2+mk+n^2}}\,e^{ikx}\,dk\\ &+\frac{B}{2\sqrt{\pi}}\int_{-\infty}^{\infty}\left(1-\frac{b^2k^2}{4}+\ldots\right)\frac{\sin l\sqrt{k^2+mk+n^2t}}{l\sqrt{k^2+mk+n^2}}\,e^{ikx}\,dk. \quad\ldots(18) \end{aligned}$$

When the disturbance is very sharp and is concentrated in the neighbourhood of the origin, a and b will be negligibly small and therefore it will be sufficient to take each first term of the brackets. Taking, thus, such an extreme case and putting $k+m/2=k'$ and $n^2-m^2/4=n'^2$, we obtain

$$\left.\begin{aligned} u=&\frac{iAq}{2\sqrt{\pi}}\frac{\partial}{\partial t}\int_{-\infty}^{\infty}\frac{\sin l\sqrt{k'^2+n'^2}\,t}{i\sqrt{k'^2+n'^2}}\,e^{i\left(k'-\frac{m}{2}\right)x}\,dk'\\ &+\frac{iB}{2\sqrt{\pi}}\int_{-\infty}^{\infty}\frac{\sin l\sqrt{k'^2+n'^2}\,t}{l\sqrt{k'^2+n'^2}}\,e^{i\left(k'-\frac{m}{2}\right)x}\,dk',\\ w=&\frac{A}{2\sqrt{\pi}}\frac{\partial}{\partial t}\int_{-\infty}^{\infty}\frac{\sin l\sqrt{k'^2+n'^2}\,t}{l\sqrt{k'^2+n'^2}}\,e^{i\left(k'-\frac{m}{2}\right)x}\,dk'\\ &+\frac{B}{2\sqrt{\pi}}\int_{-\infty}^{\infty}\frac{\sin l\sqrt{k'^2+n'^2}\,t}{l\sqrt{k'^2+n'^2}}\,e^{i\left(k'-\frac{m}{2}\right)x}\,dk'. \end{aligned}\right\}\quad\ldots\ldots(19)$$

These may be transformed to

$$\left.\begin{aligned} u&=\frac{iAq\,e^{-\frac{imx}{2}}}{\sqrt{\pi}}\frac{\partial}{\partial t}\int_0^\infty\frac{\sin l\sqrt{k'^2+n'^2}\,t}{l\sqrt{k'^2+n'^2}}\cos k'xdk'\\ &\qquad+\frac{iBq\,e^{-\frac{imx}{2}}}{\sqrt{\pi}}\int_0^\infty\frac{\sin l\sqrt{k'^2+n'^2}\,t}{l\sqrt{k'^2+n'^2}}\cos k'xdk'.\\ w&=\frac{Ae^{-\frac{imx}{2}}}{\sqrt{\pi}}\frac{\partial}{\partial t}\int_0^\infty\frac{\sin l\sqrt{k'^2+n'^2}\,t}{l\sqrt{k'^2+n'^2}}\cos k'xdk'\\ &\qquad+\frac{Be^{-\frac{imx}{2}}}{\sqrt{\pi}}\int_0^\infty\frac{\sin\sqrt{k'^2+n'^2}\,t}{l\sqrt{k'^2+n'^2}}\cos k'xdk'. \end{aligned}\right\}\quad\ldots.(20)$$

But we know the expressions

$$\left.\begin{aligned} \int_0^\infty\frac{\sin l\sqrt{k'^2+n'^2}\,t}{\sqrt{k'^2+n'^2}}\cos k'xdk'&=\frac{\pi}{2}J_0(n'\sqrt{l^2t^2-x^2}), &&[x^2<l^2t^2]\\ &=0. &&[x^2>l^2t^2] \end{aligned}\right\}\ldots(21)^{5)}$$

Hence, taking the real part, we have

$$\begin{aligned} u=&-\frac{A\pi^{\frac{3}{2}}}{H}\sqrt{c_2^2-\frac{c_1^2}{4}}\,\frac{\frac{jV_2}{\kappa}t}{\sqrt{\left(\frac{jV_2}{\kappa}\right)^2t^2-x^2}}\,\frac{\kappa(2\kappa^2-j^2-2\alpha_1\beta_1)}{j^2\alpha_1}\sin\frac{2\pi c_1x}{H}\\ &\qquad\times J_1\left\{\frac{2\pi}{H}\sqrt{\left(c_2^2-\frac{c_1^2}{4}\right)\left\{\left(\frac{jV_2}{\kappa}\right)^2t^2-x^2\right\}}\right\}\\ &+\frac{B\sqrt{\pi}}{2}\,\frac{\kappa}{jV_2}\,\frac{\kappa(2\kappa^2-j^2-2\alpha_1\beta_1)}{j^2\alpha_1}\sin\frac{2\pi c_1x}{H}\\ &\qquad\times J_0\left\{\frac{2\pi}{H}\sqrt{\left(c_2^2-\frac{c_1^2}{4}\right)\left\{\left(\frac{jV_2}{\kappa}\right)^2t^2-x^2\right\}}\right\},\quad\left[\left(\frac{x}{t}\right)^2<\left(\frac{jV_2}{\kappa}\right)^2\right]\\ =&\,0, \qquad\qquad\left[\left(\frac{x}{t}\right)^2>\left(\frac{jV_2}{\kappa}\right)^2\right] \end{aligned}$$

$$\begin{aligned} w=&-\frac{A\pi^{\frac{3}{2}}}{H}\sqrt{c_2^2-\frac{c_1^2}{4}}\,\frac{\frac{jV_2}{\kappa}t}{\sqrt{\left(\frac{jV_2}{\kappa}\right)^2t^2-x^2}}\cos\frac{2\pi c_1x}{H}\\ &\qquad\times J_1\left\{\frac{2\pi}{H}\sqrt{\left(c_2^2-\frac{c_1^2}{4}\right)\left\{\left(\frac{jV_2}{\kappa}\right)^2t^2-x^2\right\}}\right\} \end{aligned}$$

---

5) H. LAMB, *Proc. Math. Soc.*, London, [2], **7** (1907), 122; and also S. SANO, *Bull. Centr. Meteor. Obs.*, Japan, **2** (1913), 13.

$$+\frac{B\sqrt{\pi}}{2}\,\frac{\kappa}{jV_2}\cos\frac{2\pi c_1 x}{H}$$

$$\times J_0\left\{\frac{2\pi}{H}\sqrt{\left(c_2^2-\frac{c_1^2}{4}\right)\left\{\left(\frac{jV_2}{\kappa}\right)^2 t^2-x^2\right\}}\right\},\qquad \left[\left(\frac{x}{t}\right)^2<\left(\frac{jV_2}{\kappa}\right)^2\right]$$

$$=0. \qquad \left[\left(\frac{x}{t}\right)^2>\left(\frac{jV_2}{\kappa}\right)^2\right]$$

$$\ldots\ldots\ldots\ldots\ldots\ldots\ldots\ldots\ldots\ldots (22)$$

Since jV_2/κ is the velocity of propagation of the ordinary Rayleigh-waves transmitted on the surface of a semi-infinite elastic body whose elastic constants are λ and μ, these results shew that the leading-part of a train of waves is transmitted with the velocity of Rayleigh-waves. It appears, moreover, that, in spite of the concentrated and impulsive type of the original disturbance, the propagated waves are of the harmonic type with gradually increasing periods and decreasing amplitudes. This fact is in agreement with the nature of the trailing waves which follow the main shock of the earthquake movements.

It is easily seen from the forms of the equations (22) that, though the period increases with successive oscillations in a train, each period is of a certain order of length depending on the values of H, c_1 and c_2. This fact well accounts for the curious nature that the the pulsatory motions with a certain range of periods will frequently be obserbed at a given station.

It is also to be remarked that the factors $\left.\begin{matrix}\cos\\ \sin\end{matrix}\right\}\frac{2\pi c_1 x}{H}$ in the expression of (22) give us the abnormal regions of the earthquake movements at certain periodic distances from the epicentre. This depends on c_1, H and the epicentral distance x. Such a special nature disappears when c_1 is nil.

The above investigation is taken substantially from the forms of the

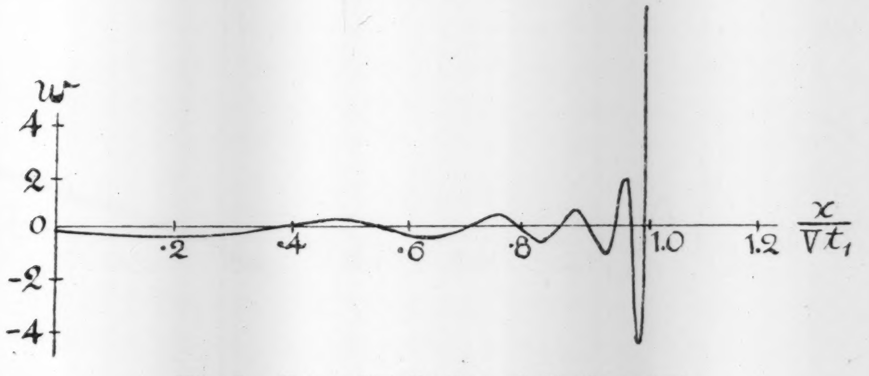

Fig. 1. Space-distribution of displacement at $t=t_1$ (Two-dimensions).

equations (22). To understand the nature more concretely, a few drawings have been illustrated: they will probably admit of a variety of

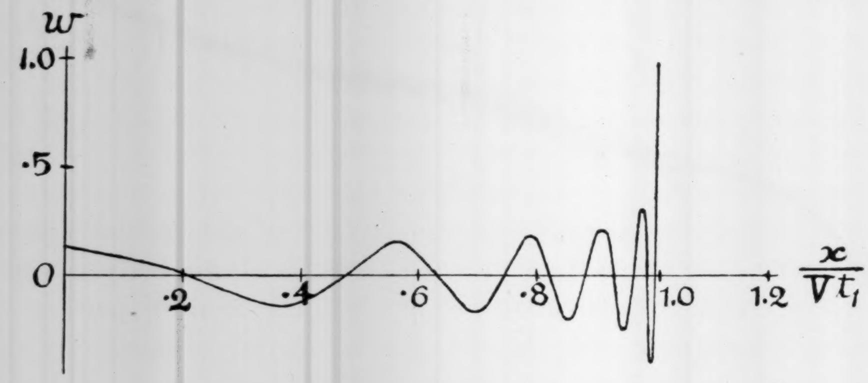

Fig. 2. Space-distribution of displacement at $t=t_1$ (Two-dimensions).

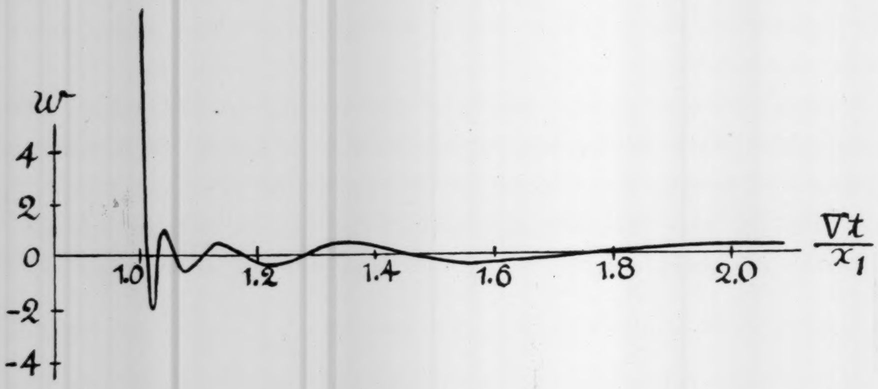

Fig. 3. Time-variation of displacement at $x=x_1$ (Two-dimensions).

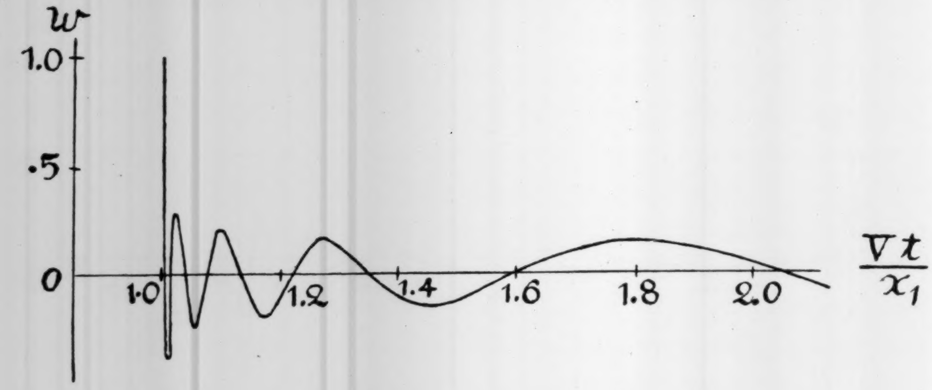

Fig. 4. Time-variation of displacement at $x=x_1$ (Two-dimensions).

interpretations. Fig. 1 is the distribution of the displacements in space at the time t_1 due to the initial surface displacement at $x=0$, while Fig. 2 is the similar distribution due to the initial surface velocity at the origin. Fig. 3 is the time variation of the displacement at the point x_1 due to the initial surface displacement at $x=0$, and Fig. 4 gives us the like problem due to the initial surface velocity at the origin. In these figures V is the velocity of certain Rayleigh-waves, i.e. $\frac{jV_2}{\kappa}$.

2. Secondly, we shall introduce the three-dimensional problem, which can be treated by a similar method as in the preceding section. The axis of r is taken on the free surface and u, w are the radial and the vertical components of displacement. The equatians of motion can be expressed by

$$\left.\begin{aligned}\rho\frac{\partial^2 u}{\partial t^2}=(\lambda+2\mu)\left\{1+c_1\frac{L}{H}+\left(c_2\frac{L}{H}\right)^2\right\}\frac{\partial\varDelta}{\partial r}&\\ +2\mu\left\{1+c_1\frac{L}{H}+\left(c_2\frac{L}{H}\right)^2\right\}\frac{\partial\varpi}{\partial z}=0&\\ \rho\frac{\partial^2 w}{\partial t^2}=(\lambda+2\mu)\left\{1+c_1\frac{L}{H}+\left(c_2\frac{L}{H}\right)^2\right\}\frac{\partial\varDelta}{\partial z}&\\ +2\mu\left\{1+c_1\frac{L}{H}+\left(c_2\frac{L}{H}\right)^2\right\}\frac{1}{r}\frac{\partial}{\partial r}(r\varpi)=0,&\end{aligned}\right\}\dots\dots(23)$$

where

$$\varDelta=\frac{\partial u}{\partial r}+\frac{u}{r}+\frac{\partial w}{\partial z},\qquad 2\varpi=\frac{\partial u}{\partial z}-\frac{\partial w}{\partial r}\dots\dots\dots\dots(24)$$

From (23) and (24), we obtain

$$\left.\begin{aligned}\varDelta&=A_1e^{-\alpha z}J_0(kr)\begin{matrix}\cos\\ \sin\end{matrix}\Big\}pt,\\ 2\varpi&=B_1e^{-\beta z}J_1(kr)\begin{matrix}\cos\\ \sin\end{matrix}\Big\}pt,\end{aligned}\right\}\dots\dots\dots\dots(25)$$

where

$$k^2=\alpha^2+h^2=\beta^2+j^2,\dots\dots\dots\dots(26)$$

and h^2 and j^2 have the same meanings as those in (6).

The displacements corresponding to (25) can be expressed by

$$\left.\begin{aligned}u&=\left(\frac{kA_1}{h^2}e^{-\alpha z}+\frac{\beta B_1}{j^2}e^{-\beta z}\right)J_1(kr)\begin{matrix}\cos\\ \sin\end{matrix}\Big\}pt,\\ w&=\left(\frac{\alpha A_1}{h^2}e^{-\alpha z}+\frac{kB_1}{j^2}e^{-\beta z}\right)J_0(kr)\begin{matrix}\cos\\ \sin\end{matrix}\Big\}pt.\end{aligned}\right\}\dots\dots\dots\dots(27)$$

As the boundary conditions we put

$$z=0, \qquad \lambda'\Delta+2\mu'\frac{\partial w}{\partial z}=0, \qquad \frac{\partial u}{\partial z}+\frac{\partial w}{\partial r}=0, \ldots\ldots\ldots\ldots (28)$$

from which we get

$$\frac{B_1}{j^2}\Big/\frac{A_1}{h^2}=-\frac{2k\alpha}{2k^2-j^2}, \ldots\ldots\ldots\ldots\ldots\ldots\ldots\ldots (9')$$

$$(2k^2-j^2)^2-4k^2\alpha\beta=0. \ldots\ldots\ldots\ldots\ldots\ldots\ldots (10')$$

The typical solutions at $z=0$ are written by

$$\left.\begin{aligned} u&=-\cos\left\{\frac{jV_2}{\kappa}\sqrt{k^2+\frac{2\pi c_1}{H}k+\left(\frac{2\pi c_2}{H}\right)^2}\,t\right\}\frac{\kappa\,(2\kappa^2-j^2-2\alpha_1\beta_1)}{j^2\alpha_1}J_1(kr),\\ w&=\cos\left\{\frac{jV_2}{\kappa}\sqrt{k^2+\frac{2\pi c_1}{H}k+\left(\frac{2\pi c_2}{H}\right)^2}\,t\right\}J_0(kr). \end{aligned}\right\} (29)^{5)}$$

Generalising these by means of Fourier's double integral, we find

$$\begin{aligned} u=&-q\int_0^\infty\cos\left\{l\sqrt{k^2+mk+n^2}\,t\right\}J_1(kr)\,kdk\int_0^\infty f(\sigma)\,J_0(k\sigma)\,\sigma d\sigma\\ &-q\int_0^\infty\frac{\sin\{l\sqrt{k^2+mk+n^2}\,t\}}{l\sqrt{k^2+mk+n^2}}J_1(kr)\,kdk\int_0^\infty F(\sigma)\,J_0(k\sigma)\,\sigma d\sigma, \ldots\ldots (30) \end{aligned}$$

$$\begin{aligned} w=&\int_0^\infty\cos\left\{l\sqrt{k^2+mk+n^2}\,t\right\}J_0(kr)\,kdk\int_0^\infty f(\sigma)\,J_0(k\sigma)\,\sigma d\sigma\\ &+\int_0^\infty\frac{\sin\{l\sqrt{k^2+mk+n^2}\,t\}}{l\sqrt{k^2+mk+n^2}}J_0(kr)\,kdk\int_0^\infty F(\sigma)\,J_0(k\sigma)\,\sigma d\sigma, \ldots\ldots\ldots (31) \end{aligned}$$

for the initial conditions that $w=f(r)$ and $\partial w/\partial t=F(r)$ at $z=0$.

If the initial disturbance is given by

$$f(r)=\frac{A}{a^2}e^{-\frac{r^2}{a^2}}, \qquad F(r)=\frac{B}{b^2}e^{-\frac{r^2}{b^2}}, \ldots\ldots\ldots\ldots\ldots\ldots (32)$$

then, by means of the formula

$$\int_0^\infty e^{-\frac{r^2}{c^2}}J_0(k\sigma)\,\sigma d\sigma=\frac{c^2}{2}e^{-\frac{k^2c^2}{4}}, \qquad \ldots\ldots\ldots\ldots\ldots (33)$$

we obtain

$$u=-\frac{Aq}{2}\frac{\partial}{\partial t}\int_0^\infty\left(1-\frac{a^2k^2}{4}+\ldots\right)\frac{\sin l\sqrt{k^2+mk+n^2}t}{l\sqrt{k^2+mk+n^2}}J_1(kr)\,kdk$$

---

5) These expressions are most suitable for the condition that the surface is always free from the stress.

$$-\frac{B}{2}\int_0^\infty\left(1-\frac{b^2k^2}{4}+\ldots\right)\frac{\sin l\sqrt{k^2+mk+n^2}\,t}{l\sqrt{k^2+mk+n^2}}J_1(kr)\,kdk,\qquad\ldots\ldots\ldots(34)$$

$$w=\frac{A}{2}\frac{\partial}{\partial i}\int_0^\infty\left(1-\frac{a^2k^2}{4}+\ldots\right)\frac{\sin l\sqrt{k^2+mk+n^2}\,t}{l\sqrt{k^2+mk+n^2}}J_0(kr)\,kdk$$

$$+\frac{B}{2}\int_0^\infty\left(1-\frac{b^2k^2}{4}+\ldots\right)\frac{\sin l\sqrt{k^2+mk+n^2}\,t}{l\sqrt{k^2+mk+n^2}}J_0(kr)\,kdk.\qquad\ldots\ldots\ldots(35)$$

Assuming that the initial disturbance is of the sharp nature and also that $c_1=0$ specially, we find the vertical displacement of the form:

$$w=\frac{A}{2}\frac{\partial}{\partial t}\int_0^\infty\frac{\sin l\sqrt{k^2+n^2}\,t}{l\sqrt{k^2+n^2}}J_0(kr)\,kdk$$

$$+\frac{B}{2}\int_0^\infty\frac{\sin l\sqrt{k^2+n^2}\,t}{l\sqrt{k^2+n^2}}J_0(kr)\,kdk.\qquad\ldots\ldots\ldots\ldots\ldots\ldots(36)$$

If we put $k^2+n^2=k'^2$, then

$$w=\frac{A}{2l}\frac{\partial}{\partial t}\int_n^\infty\sin lk'tJ_0\left(\sqrt{k'^2-n^2}\,r\right)dk'$$

$$+\frac{B}{2l}\int_n^\infty\sin lk'tJ_0\left(\sqrt{k'^2-n^2}\,r\right)dk'.\qquad\ldots\ldots\ldots\ldots\ldots\ldots(37)$$

Now we know

$$\int_n^\infty\sin lk'tJ_0\left(\sqrt{k'^2-n^2}\,r\right)dk'$$

$$=\int_{nr}^\infty\sin\frac{lt}{r}(k'r)\,J_0\left(\sqrt{(k'r)^2-(nr)^2}\right)\frac{d\,(k'r)}{r}$$

$$\left.\begin{aligned}&=\frac{\cos\sqrt{\left(\frac{lt}{r}\right)^2-1}\;nr}{r\sqrt{\left(\frac{lt}{r}\right)^2-1}}, &&[(lt)^2>r^2]\\ &=0. &&[(it)^2<r^2]\end{aligned}\right\}\qquad\ldots\ldots\ldots\ldots(38)^{6)}$$

Hence we have

$$w=\frac{A}{2}\left(\frac{\kappa}{jV_2}\right)\frac{\partial}{\partial t}\frac{\cos\frac{2\pi\,c_2\,x}{\mathrm{H}}\sqrt{\left(\frac{jV_2}{\kappa}\right)^2t^2-r^2}}{\sqrt{\left(\frac{jV_2}{\kappa}\right)^2t^2-r^2}}$$

---

6) H. LAMB and S. SANO, *loc cit.*, 198.

$$\left.\begin{array}{ll} +\dfrac{B}{2}\left(\dfrac{\kappa}{jV_2}\right)\dfrac{\cos\dfrac{2\pi\, c_2\, x}{H}\sqrt{\left(\dfrac{jV_2}{\kappa}\right)^2 t^2-r^2}}{\sqrt{\left(\dfrac{jV_2}{\kappa}\right)^2 t^2-r^2}}, & \left[r^2<\left(\dfrac{jV_2}{\kappa}\right)^2 t^2\right] \\ =0. & \left[r^2>\left(\dfrac{jV_2}{\kappa}\right)^2 t^2\right] \end{array}\right\} \quad \ldots (39)$$

In this case, too, the leading part of the group is transmitted with the velocity jV_2/κ and the train which is caused by a single disturbance is also of a harmonic type with the amplitudes more quickly disappearing than in the case of a two-dimension. The nature of the successive periods and other characters are the same as those of the two-dimensional problem.

The annexed figures are illustrated as examples of the propagation in

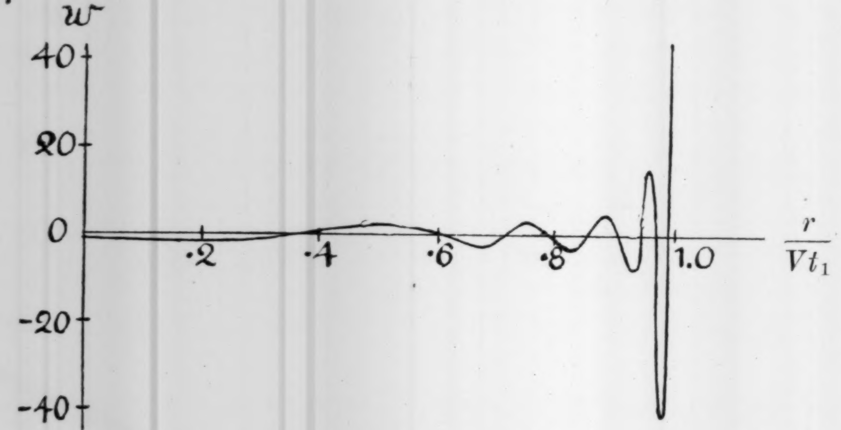

Fig. 5. Space-distribution of displacement at $t=t_1$ (Three-dimensions).

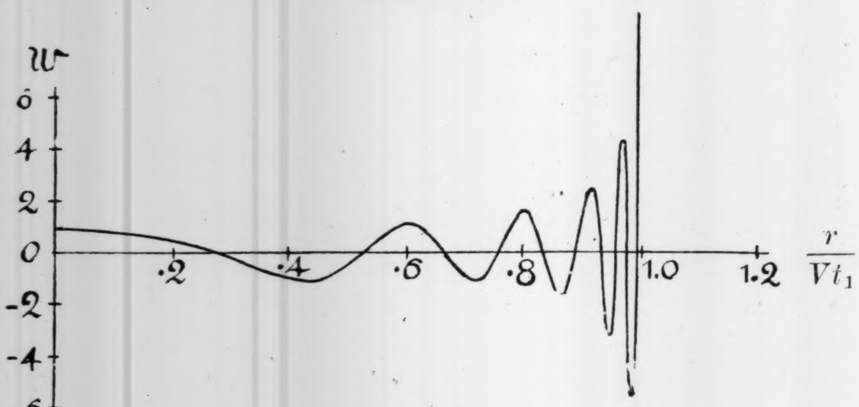

Fig. 6. Space-distribution of displacement at $t=t_1$ (Three-dimensions).

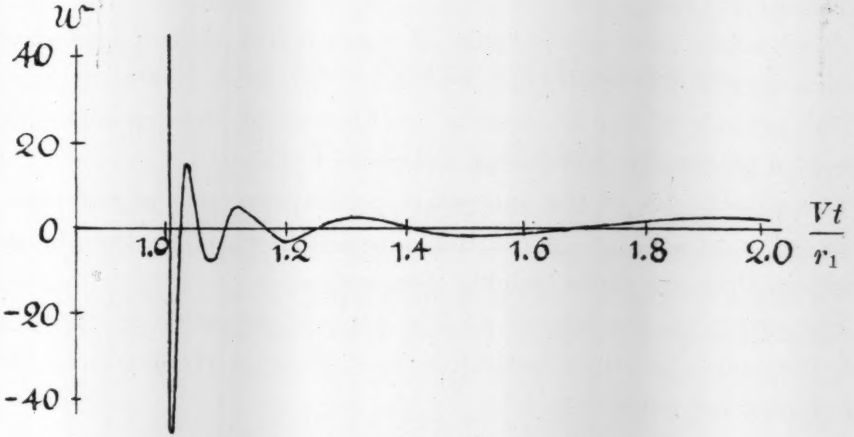

Fig. 7. Time-variation of displacement at $r=r_1$ (Three-dimensions).

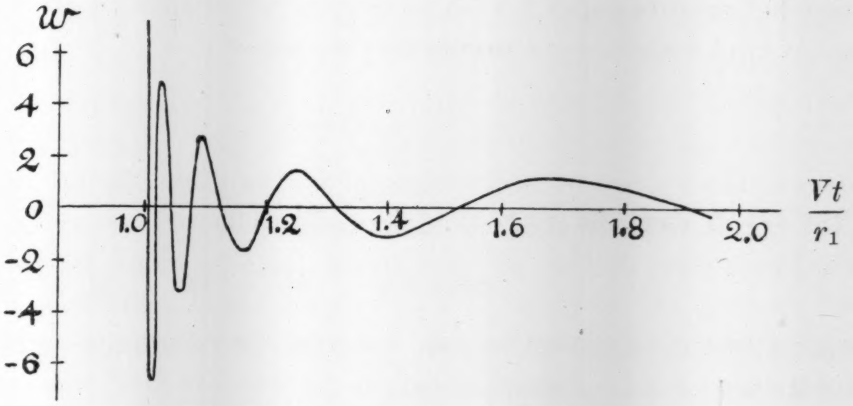

Fig. 8. Time-variation of displacement at $r=r_1$ (Three-dimensions).

three dimensions. Fig. 5 is the distribution of the displacements in space at the time t_1 due to the initial displacement at the origin, while Fig. 6 is the similar distribution due to the initial surface velocity. Fig. 7 is the time variation of the displacement at a certain point r_1 due to the initial surface displacement and Fig. 8 is that due to the initial surface velocity at the origin. In these V is written for jV_2/κ.

SUMMARY.

The principal results which have some importance on the seismology are enumerated as follows:

1. In spite of the application of a single disturbance at the origin of a semi-infinite body of a certain dispersive nature, the generated surface waves

are of a harmonic type.

2. The leading part of the train of these waves is propagated with the velocity of a special Rayleigh-type waves.

3. The periods of the successive oscillations of the harmonic displacements are of a gradually increasing nature.

4. The amplitudes of the successive oscillations are, in the case of two dimensions, of a gradually decreasing character, while in the three-dimensional problem they are more quickly decreasing.

5. The order of the length of the periods depends on the dispersive nature of the body, i.e. the elasticities, the effective thickness of the layer and some dispersive constants.

6. In certain dispersive waves there are abnormal regions of the earthquake movements at certain periodic distances from the epicentre.

In concluding this paper I wish to express my thanks to Mr. G. Nishimura for his kind assistance in preparing this paper.

13. 任意の衝擊によつて起る週期的レーレー波

地震研究所　妹澤克惟

半無限固體に或法則に從ふ波動分散性がある時、この固體面に勝手な擊力を加へても、週期的に繰替す調和波動が傳播されるといふ事柄がわかつた。

計算の方法は運動方程式の解を境界條件に適合させ、且つフーリエの積分によつて勝手な初動に對する一般化を行つただけに過ぎぬが、其結果は地震學上重要な種々の意味を持つ。地表面の微動や地震の主要動に續く振動などはこの問題に關聯して居る樣に思はれる。

研究の主な結果を摘錄すれば

1. 或波動分散性を有する半無限體上の一點に瞬時的外力を加へても發生する表面波動は調和波動となる。
2. この調和波動は群をなし、其首部は或レーレー波の速度を以て傳播される。
3. この調和波動の次々の週期は次第に長くなる傾向を持つ。
4. この調和波動の次々の振幅は二次元の問題では次第に減少し、三次元の場合には更に著しく減少して行く。
5. この調和波動の各週期の實際の長さは分散恒數及び彈性係數によつて決定される。
6. 或分散性波動では衝點から週期的の距離に異常震域が見出される。

14. *On the Form of Volcanos.*

By **Torahiko TERADA.**

(Read April 16, 1929.—Received June 20, 1929.)

(1) A volcano, in a purely mechanical point of view of a civil engineer, is a more or less irregular conical heap of rocky mass resting upon the ground, which we call the earth crust, and it may be his proper concern to inquire if the ground could endure or eventually yield to the superincumbent load of this gigantic masonry of the nature.

On the other hand, it is a noteworthy fact that the most volcanos, at least of this country, are surrounded by a conspicuous zone of depression of the surface crust. If such a tendency is universal, we are lead to the following alternatives, i.e. either the volcanic eruption is liable to occur in the zone of depression, or it is generally followed by a depression of the surrounding region. Nor is it improbable that both the factors may be cooperating in determining the characteristic topographical feature mentioned. For answering this question, many investigations will be wanted from geological, topographical, geophysical as well as mechanical sides. It is the last mentioned stand point which is taken by the present author in the following note. He will be much obliged by any criticism and information, especially from the side of geologists.

An actual example of the volcanic eruption which was accompanied with a general depression of the neighbouring region is afforded by the eruption of Sakurazima in 1914.[1] The very fact that this volcano is surrounded by a remarkable circumferential zone of depression below the sea level, taken together with the recent revelation of the existing activity makes us suspect that the mountain might have been repeating the similar process of eruption and depression through the geological ages since its first birth.

On the other hand, the heights of the most volcanos appear to be of the same order of magnitude, even when the differences are taken between the levels of the summits and the bottoms of the circumferential zones of depression (see Table I, 8th. column). As it seems difficult to assume that a single volcano may appear isostatically compensated,[2] the above fact may more plausibly be assumed as indicating an upper limit of the height of any volcano which may be sustained by the underlying crust.

---

[1] F. OMORI, *Bull. E.I.C.*, 8, No. 2 (1926), No. 4 (1920). CH. TSUBOI, *Bull. E.R.I.*, 7 (1926), 103.

The elasto-statical problem regarding the stability of a mountain has been already treated by such authorities as G. H. Darwin and A. E. H. Love. Prof. Nagaoka also treated some cases of the problem and compared his results with experiments.[3] It seems, therefore, interesting to regard the matter from a somewhat different side, i.e. with reference to the recent theories of plastic deformations, or those of the earth pressure. In a previous paper, the author pointed out some essential analogies between the sandy or earthy mass and the earth crust with regard to the plastic deformation of these matters, so that it will not be without some interest to treat a volcano as a load upon a sandy material.

(2) In order to examine and compare the geometrical forms of different volcanos with regard to the above point of view, it is necessary to take a procedure which may reduce the actual irregular form of a volcano and its surrounding region into its simplest essential outline. The method adopted here for this purpose is as follows.

The topographical maps in 1/50,000 scale, issued by the Military Land Survey Department, were utilized for the material of the investigation. On the summit of the volcano to be examined a point was chosen such that it may suitably represent the vertex of the ideal conical mountain. From this point, straight lines were drawn radiating towards the sixteen directions. The profile curve of the vertical section for each of these directions was constructed and thence the mean profile of these sixteen sections was calculated and plotted in a diagram as shown in Fig. 1. In carrying out the above method, the height for every kilometre of the distance from the vertex was read off from the map, and after obtaining the mean profile it was smoothed by calculating the means for the successive 5 km. intervals.[4]

---

[2] In the case of a perfect compensation, the depression of the circumferential zone will be comparatively larger than the elevation of the summit. Such a form of volcano, however, has rarely been observed. An example which may suggest an approach to such a case is given by Lake Tôya (Fig. 7). At the centre of this lake an island is situated concentrically, of which the summit is of nearly equal height as the surrounding region, whereas the surrounding lake bottom is below the sea level.

[3] His paper was communicated to the Colloquium Meeting of the Inst.; not yet published.

[4] The laborious works of map-reading and calculation were mostly made by late Mr. S. Higasi, to whom the author feels much obliged. The later part of the works was carried out by Mr. Kawasima to whom the best thanks of the author are due.

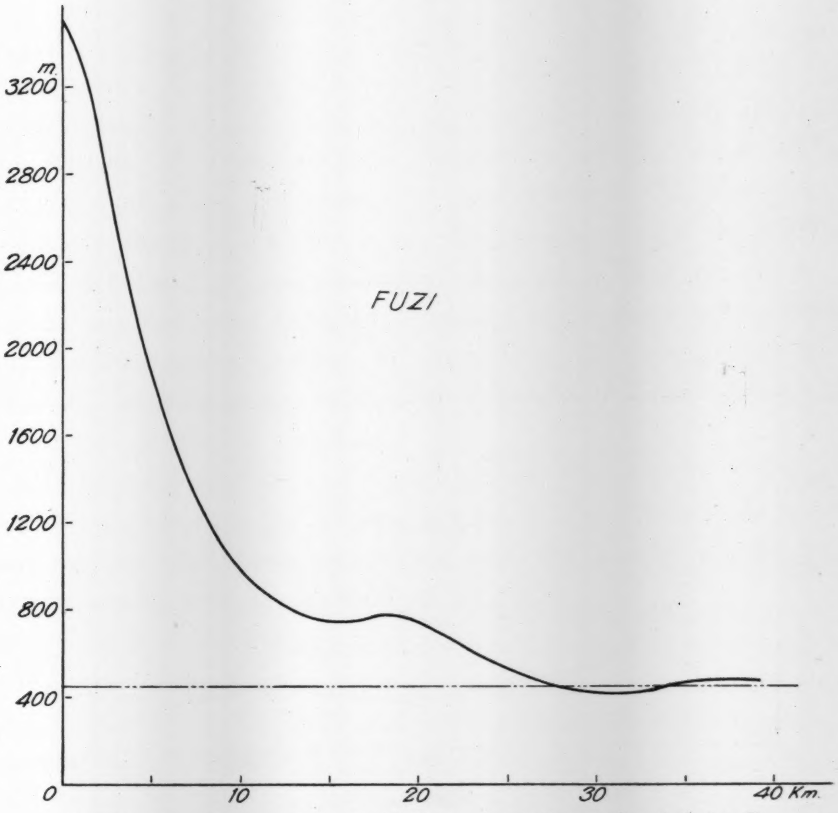

Fig. 1_1. Horizontal chain line gives the mean height Z_m.

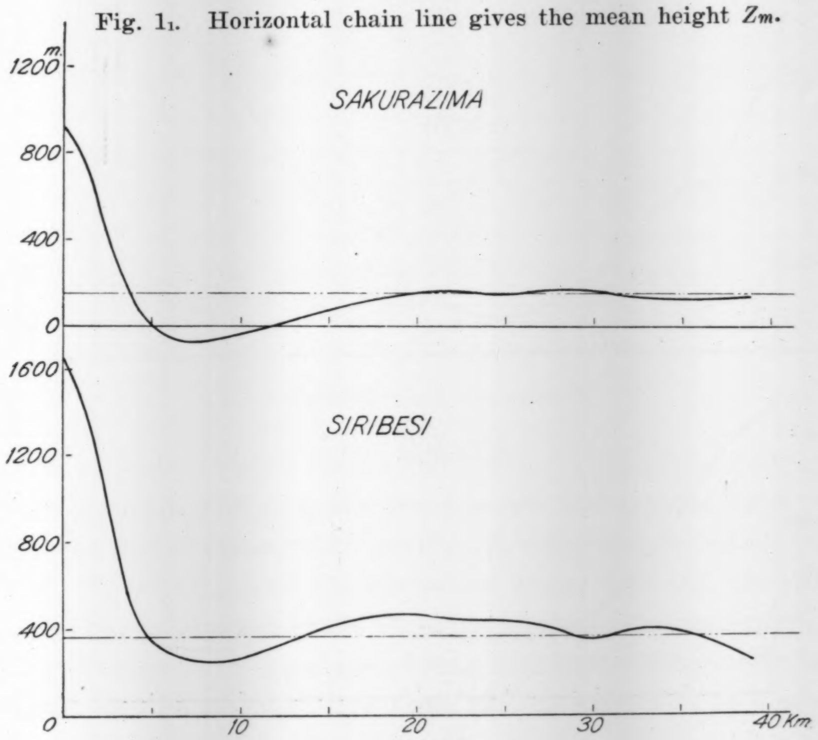

Fig. 1_2.

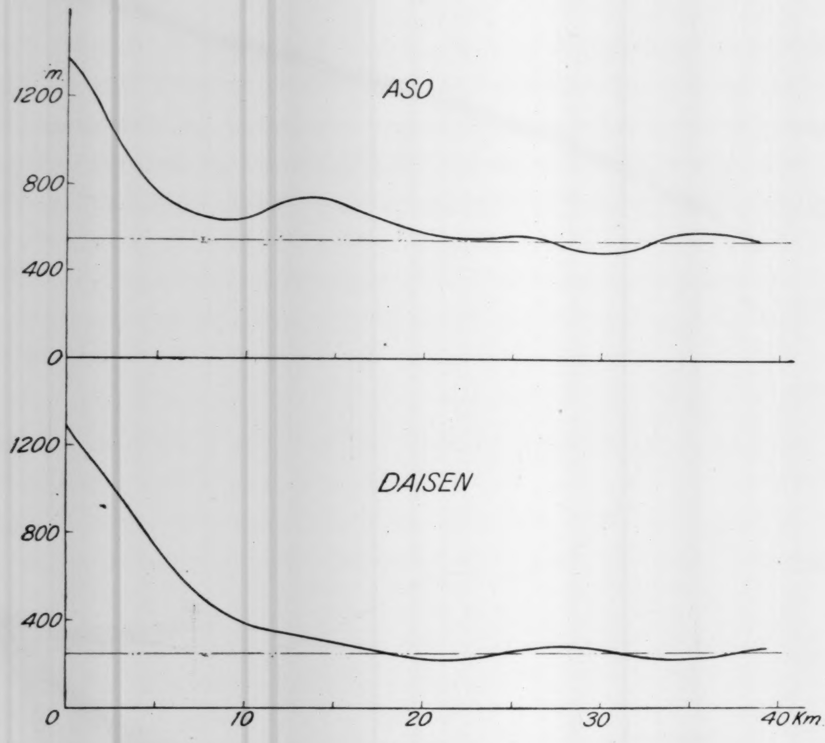
m.
1200
800
400
0
ASO
1200
800
400
DAISEN
0
10
20
30
40 Km.

Fig. 1_3.

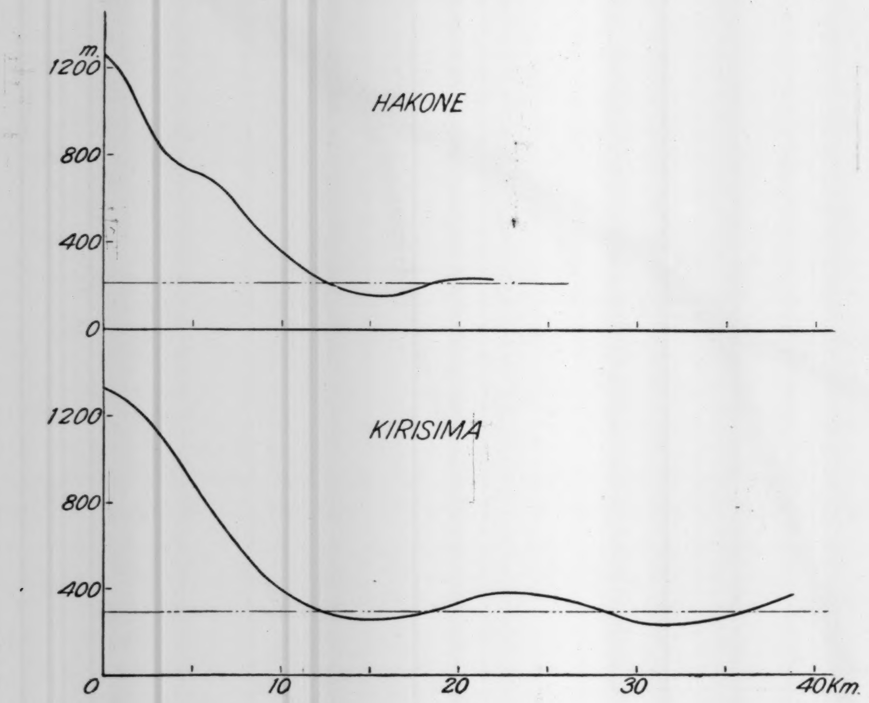
m.
1200
800
400
0
HAKONE
1200
800
400
KIRISIMA
0
10
20
30
40 Km.

Fig. 1_4.

By the above method, any irregularities which may be expressed as a periodic function of the azimuth are nearly eliminated and the zonal term will be made apparent. It may happen that the volcano is actually situated near the bottom of a conspicuous depression of the crust which existed before or formed after the genesis of the volcano. If, however, the mean profile show a marked narrow zone of depression just at the foot of the cone, while the land beyond it is generally of a uniform level, it will be plausible to assume some kind of genetical connection between the depression and the mountain, instead of regarding the phenomena as due to a mere chance; especially so, when the different volcanos have this characteristic form of profile in common.

It will be noticed that the irregularities due to the differences of the geological structure and the degree of erosion in different azimuth are also smoothed out by the above procedure and the purely mechanical feature, if such may exist, will be exposed in daylight.

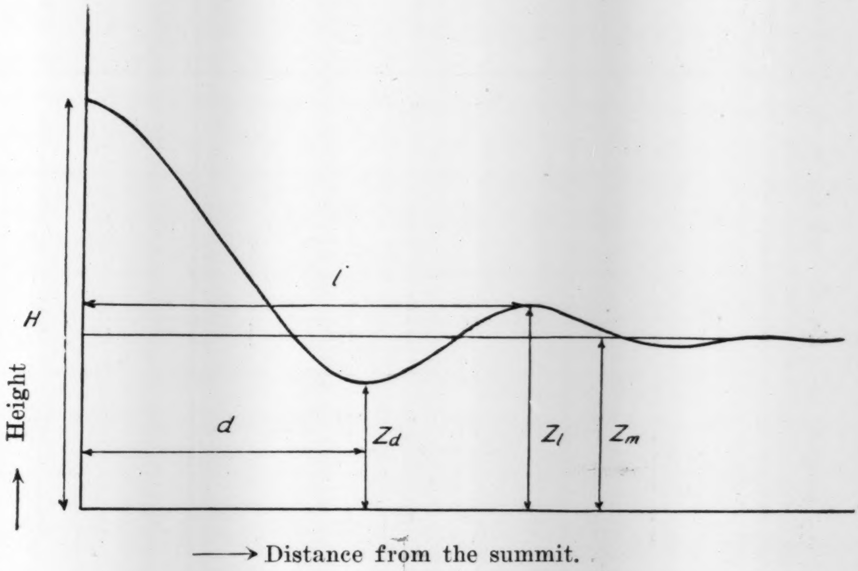

Fig. 2.

After examining Fig. 1, we may assume the typical form of a volcano to be represented schematically by Fig. 2, referring to which we define the heights H, Z_d, Z_l, Z_m and the distances d and l as the quantities suitable for specifying the characteristic features of the individual cases. Z_m is the mean height taken over the region lying within the zone 25–40 km. from the summit and may be assumed free from the disturbance due to the mountain, if such may exist near the foot.

TABLE I.

Heights H''', Z_a, Z_l and Z_m in m.; distance d and l in km.

Volcano	H'''	d	l	Z_a	Z_l	Z_m	$H'''-Z_a$	Z_l-Z_a	$H'''-Z_m$	Z_l-Z_n	$\frac{H'''-Z_a}{d}$	$\frac{Z_l-Z_a}{H'''-Z_a}$	$\frac{Z_l-Z_m}{H'''-Z_m}$
Huzi* (a)	3516	16	18·5	720	790	458	2796	70	3058	332	175	0·022	0·109
„ (b)	„	31·5	36·5	400	500	„	3116	100	„	42	99	0·032	0·014
Siribesi	1653	8	19	240	480	364	1413	240	1287	116	177	0·170	0·090
Sakurazima	913	7	21	−80	180	151	993	260	762	29	142	0·262	0·038
Kirisima	1329	15	22	260	390	294	1069	130	1035	96	71	0·122	0·093
Aso	1377	9	13·5	620	760	546	759	140	831	214	84	0·185	0·258
Daisen	1169	21	27·5	220	280	250	949	60	919	30	45	0·063	0·033
Hakone	1274	16	20	160	230	217	1114	70	1057	13	70	0·063	0·012
Akagi	1313	13	(20)	540	(540)	—	773	(70)	(628)	—	59	(0·091)	—
Haruna	1154	12	(21)	400	(590)	—	754	(70)	(359)	—	63	(0·093)	—

* For Huzi the two depressions are taken, one (a) at the Five-Lakes Zone and the other (b) at the base of the mountain.

Referring to Table I, it will be seen that Z_m varies from 150 m., for Sakurazima, to 550 m., for Aso, generally increasing with the distance from the sea coast. Again, it will be noticed that generally $Z_l > Z_m$, while Z_a is sometimes $>$ and sometimes $< Z_m$.

Instead of taking the actual height of the summit, H, for the comparison intended, the mean height H''' was taken of the heights at the three distances 0, 0.5 and 1 km. from the summit, in order to smooth out the minor accidental irregularity near the summit. The values of H''' are given in Table I. It may be observed that H''' shows a tendency to increase with Z_m, though no simple quantitative relation cannot be established from the scanty data. It may again be remarked that Huzi appears exceptional in its height whether we take H''' or $H'''-Z_a$ for comparison.

(3) Suppose now that the volcano was heaped up on a flat ground with the height Z_m, until the substratum failed and the depression took place. In some cases, the entire cone may be depressd as shown by I in Fig. 3. Or, the depression may take place as shown by II in the same figure. Sakurazima and Huzi may be taken respectively as the representatives of the cases I and II.

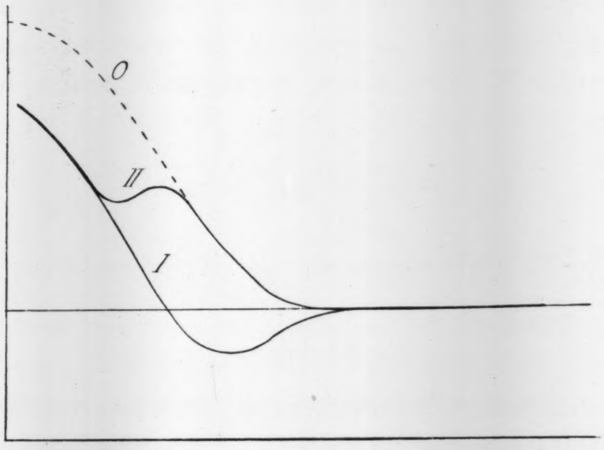

Fig. 3.

In any case, we may roughly assume $H'''-Z_a$ as giving the limiting height of the volcano.[5] Table I will show that this height varies within a range of about 800–1400 m. excepting Huzi which appears abnormal in any respect.

The plastic problem for the case when a semi-infinite body is subjected

---

5) This assumption may be justified if we realize that the actual slope near the foot of a volcano is very small.

to a uniform surface loading over a circular area was treated by Hencky.[6] If σ_s be the maximum pressure sustained and σ_c is the strength for compression we have

$$\sigma_s = 3{\cdot}33\ \sigma_c.$$

In the case of the two dimensional problem treated by Prandtl,[7]

$$\sigma_s = 2{\cdot}57\ \sigma_c.$$

In the present case, the pressure at the base of the mountain is not uniform, but must decrease with the increasing distance from the centre. We assume, however, the uniformity of the pressure for the present, which may be allowed if only the order of magnitude of the strength is in question. For the same reason, we take roughly

$$\sigma_s = 3\ \sigma_c$$

in the round number.

Taking the mountain as a cone with the height h cm. the mean pressure σ at the base is $h\rho/3$ gr./cm^2., where ρ is the density. Assuming $\rho=3$, we obtain simply $\sigma = h$. If σ be given in kg/cm^2. and h in km., we have $\sigma = 100h$. Hence,

$$\sigma_c = \frac{\sigma_s}{3} = \frac{\sigma}{3} \fallingdotseq 33\ h\ \ \mathrm{kg/cm^2}.$$

Assuming $h = H''' - Z_a$, its value is mostly of the order of 1 km. Thus we have

$$\sigma_c \fallingdotseq 33\ \ \mathrm{kg/cm^2}.$$

According to the data adopted commonly, σ_c for compression test of different rocks such as granite, marble, sandstone, etc. varies within a range 2000–3000 kg/cm^2. On the other hand, the corresponding value of σ_c for the surface loading of a loose sand layer was determined roughly by pressing upon a circular area of 5 cm. diameter and found to be of the order of about 0.05 kg/cm^2. Thence, we may say that the strength of the surface crust of the earth is of the order of 1/100 that of a compact rock piece and 1000 times that of a loose sand layer regarded as a kind of soft rock.

(4) Reissner[8] treated the problem of surface loading of a sand layer, for the case when one side of a straight line upon the surface is loaded

---

6) H. HENCKY, *ZS. f. angew. Math. u. Mech.*, **3** (1923), 241.

7) L. PRANDTL, *ibid.*, **1** (1921), 15.

8) REISSNER, *Proc. 1st. Intern. Congr. f. Appl. Mech.*, 1924, 297.

uniformly by p_1 while the other side is counterpoised by another uniform pressure p_2 $(< p_1)$ such that the yielding is just prevented. For the condition of equilibrium, he obtained

$$\frac{p_2}{p_1}=\frac{1-\sin\rho}{1+\sin\rho}\,e^{-\pi\,\mathrm{tg}\,\rho},$$

where ρ is the angle of repose of the sand mass. Fig. 4 shows an approximate form of the curve given by $y=p_2/p_1$, $x=\rho$.

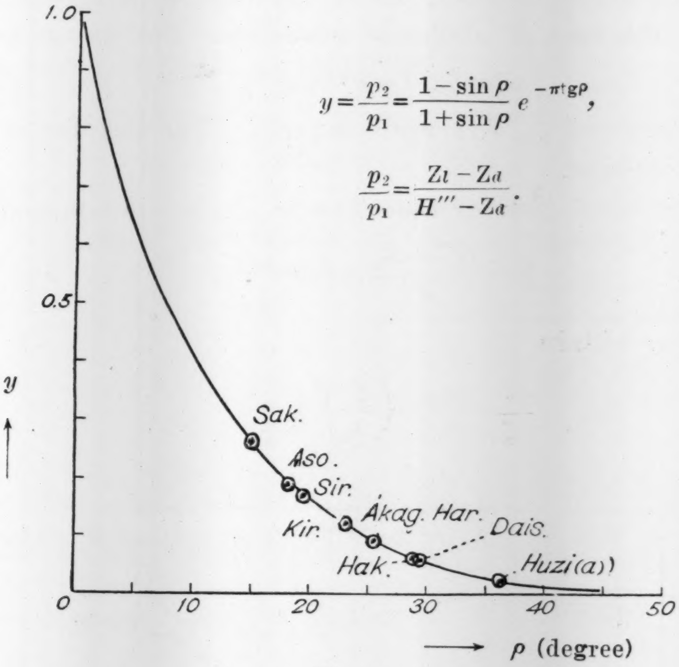

Fig. 4.

Suppose that the earth crust, considered as a sandy mass, has yielded under the load of volcano and is just sustained in equilibrium by the load of the surrounding region upheaved as the result of the deformation. In that case we may assume very roughly

$$\frac{p_2}{p_1}=\frac{Z_l-Z_a}{H'''-Z_a}.$$

The values of this ratio for different mountains are given in Table I. From these values of the ratio we may find the corresponding values of ρ from the curve in Fig. 4, or we may arrange the different volcanos upon the curve of the Figure. It will be seen that for Sakurazima, Siribesiyama, Kirisima and Aso, the values of ρ are generally much smaller than for the ordinary sand mass.

If we take

$$\frac{p_2}{p_1}=\frac{Z_l-Z_m}{H'''-Z_m},$$

the results are somewhat modified though not essentially. At any rate, it may be of some interest that the ratio of the pressures turns out to be of a right order of magnitude.

(5) According to the above hypothesis, Z_l-Z_a, which we denote by ζ, gives a measure of the plastic depression. A question may arise whether the depression occurred suddenly as in the case of a brittle material, or gradually as in the case of a plastic substance. Let us assume

$$\zeta=\zeta_0\,(1-e^{-\lambda t})\,e^{-kt},$$

where t is the time and ζ_0, λ, k are constants. The last factor is taken to account for the erosion.

On the other hand, put for the measure of the mountain slope

$$\xi=\frac{H'''-Z_a}{d}=\xi_0\,e^{-kt}.$$

Eliminating t, we obtain

$$\frac{\zeta}{\zeta_0}=\left\{1-\left(\frac{\xi}{\xi_0}\right)^{\mu}\right\}\frac{\xi}{\xi_0},$$

where $\mu=\lambda/k$.

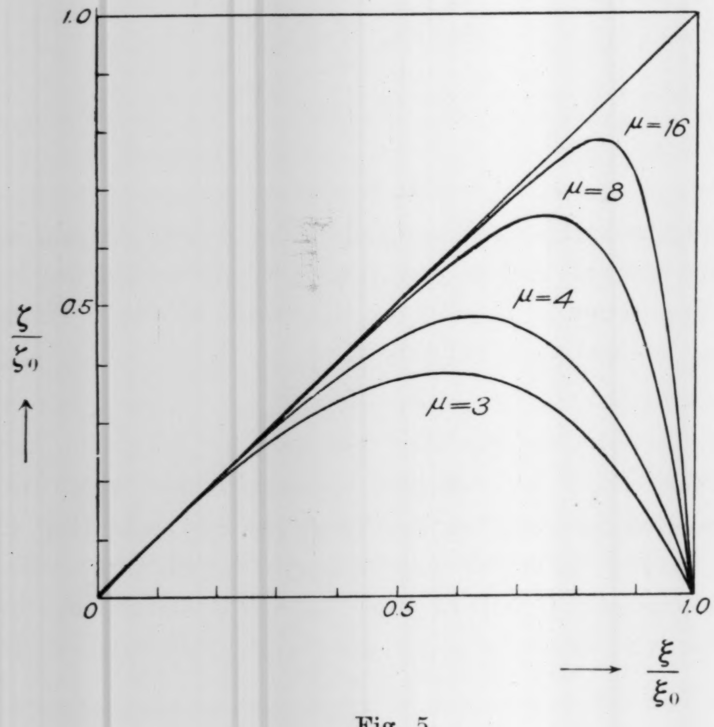

Fig. 5.

Fig. 5 shows (ζ/ζ_0)-(ξ/ξ_0) curve for different values of μ. In comparing this with Fig. 6 in which the actual relations between ζ and ξ are plotted, we may assume the value of ξ for Huzi(a) and Siribesiyama to be very near the maximum possible value ξ_0. In that case, we may infer that μ is rather large. This will mean that the depression took place rather rapidly compared with the progress of erosion. It may also appear that the Lake Zone of Mt. Huzi has not yet completed its depressing movement in these days and may still be depressed by a sensible amount in an indefinite future.

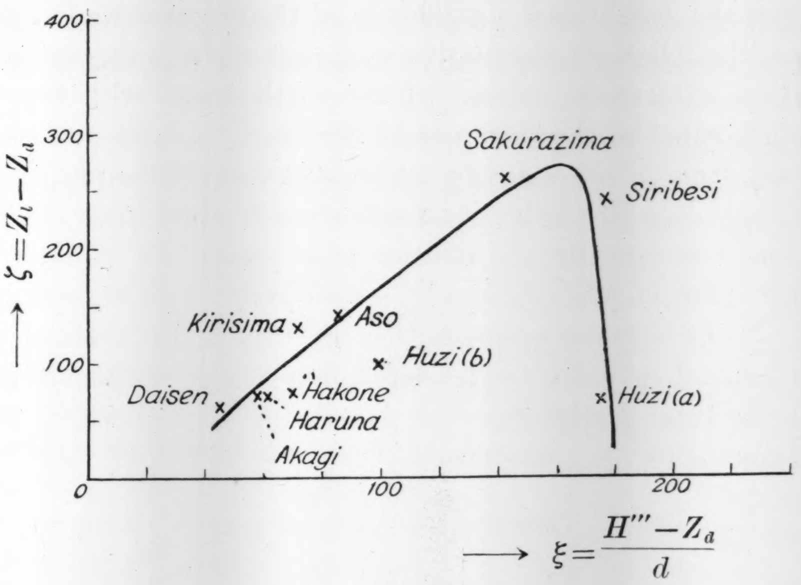

Fig. 6.

Apart from such a hypothesis, it will be noticed that Huzi is an exceptional phenomenon even with respect to the above relation between ζ and ξ.

(6) The exceptional height of Huzi may also be explained by assuming that the strength of the crust varies widely with the geological ages and that the age of Huzi is decidedly different from the ages of the other volcanos here compared. Huzi is, indeed, considered by many geologists as a young volcano. The assumption that in the age when the volcanic activity was at its height, the strength of the crust was much smaller than in the later period, is also plausible.

In the above the slope ξ was taken as a measure of the age of the mountain which is given by

$$t = \log \frac{\xi_0}{\xi}.$$

It appears (Fig. 6), therefore, according to this hypothetical measure, that Huzi (a), i.e. its Lake Zone, and Siribesiyama are the youngest. Daisen appears oldest.[9] Aso and Kirisima may be said to be of a middle age, while Sakurazima appears a little younger.

(7) For the geophysical significance of the circumferential depression of a volcano, the following alternative may perhaps be suggested. Suppose that a vertical cylindrical column of the earth crust, with the radius r_1 and the height equal to the thickness of the crust, is subjected to a change of density say from ρ to $\rho-\Delta_1\rho$, by a chemical transformation or any other cause. In expanding, the cylindrical column will press upon the surrounding crust and consequently the density of a concentric cylinder with the internal and external radii r_1 and r_2 respectively, will be change from ρ to $\rho+\Delta_2\rho$. If the isostatic compensation be effected, the ratio of the elevation of the central cylinder to the depression of the surrounding one will be equal to the ratio $\Delta_1\rho$ to $\Delta_2\rho$.

It r_1 expands to r_1+s, we have

$$\Delta_1\rho=\frac{2s}{r_1},$$

$$\Delta_2\rho=\frac{2r_1s}{r_2^2-r_1^2},$$

$$\frac{\Delta_1\rho}{\Delta_2\rho}=\left(\frac{r_2}{r_1}\right)^2-1.$$

We may take $r_1=\alpha d$ where $\alpha<1$ and $r_2=\beta h$ where $\beta>1$. On the other hand, we may assume roughly

$$\frac{\Delta_1\rho}{\Delta_2\rho}=\frac{H'''-Z_m}{Z_m-Z_d}.$$

Hence, we must have

$$\frac{H'''-Z_m}{Z_m-Z_d}=\left(\frac{\beta l}{\alpha d}\right)^2-1.$$

The assumption is, however, not valid even qualiltatively, since Z_m-Z_d is negative for the most volcanos. Even if we take Z_l-Z_d, which is positive, instead of Z_m-Z_d, the relation as above deduced does not hold in the least.

(8) If in the above assumption we take s negative, then Δ's will

---

9) Daisen belongs to the toroide-type, according to Schneider's classification, while the others are conides. In the present discussion, however, the difference of the type may be put out of account when only the order of magnitude of a physical constant of rock material is concerned.

become also negative. Such a case may possibly occur, in which case we will expect a central depression surrounded by a zone of elevation. It may, therefore, be suspected that some of the lakes such as Towada or Tazawa might have been produced by a similar process. The mean profile of the region with the lake as the centre was constructed in the same manner as in the case of volcanos. The results are shown in Fig. 7. It will be seen that the profile curves may be compared with the inverted profiles of some volcanos, the circumferential elevation of the formers corresponding to the zonal depressions of the latters. The zones of elevation in these examples seems, however, to be of too wide extents to be explained by the above assumption. It seems improbable that the general elevation is merely a secondary phenomenon caused by the central depression as the primary one. Here, the alternative hypotheses examined in the cases of volcanos seem to fail. There remains a possibility that a

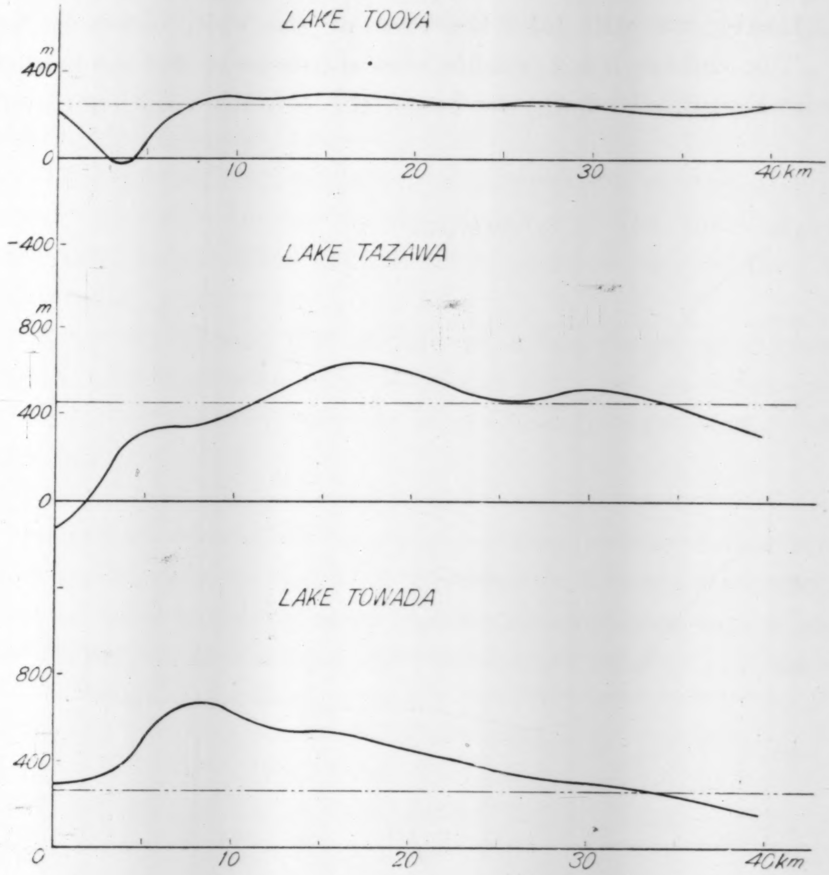

Fig. 7_1. —-·-— Mean Height Z_m.

local transformation of an extended magma field, resulting in a considerable change in the density of a nuclear spot may be associated with a density change in opposite sense in the surrounding region of wide extent.

It will of course be premature to try to decide among these various possibilities on the basis of the simple mechanical considerations as above expounded. The discussions may, however, at least be of some use in suggesting a further line of investigation regarding the allied problems.

(9) Lastly, we will take the case of the twin volcanos Akagi and Haruna. The similar mean profile was constructed for each of the pair, as given in Fig. 8. In both the cases, the ground rises continually from about 15 km. from the centre, i.e. the summit, to a distance greater than 40 km. This means that the volcano is situated at the bottom of a conspicuous depression area of large extent. Drawing the dotted line in the Figure as an ideal profile of the general depression, the difference of the curves in full line and dotted line is found to show the characteristic form given by Fig. 2. Estimating the values of d, l, Z_a and Z_l from this difference curve, as given in Table I enclosed in bracket, the position of the mountain in Fig. 6 was found. It will be seen that the "age" turns out

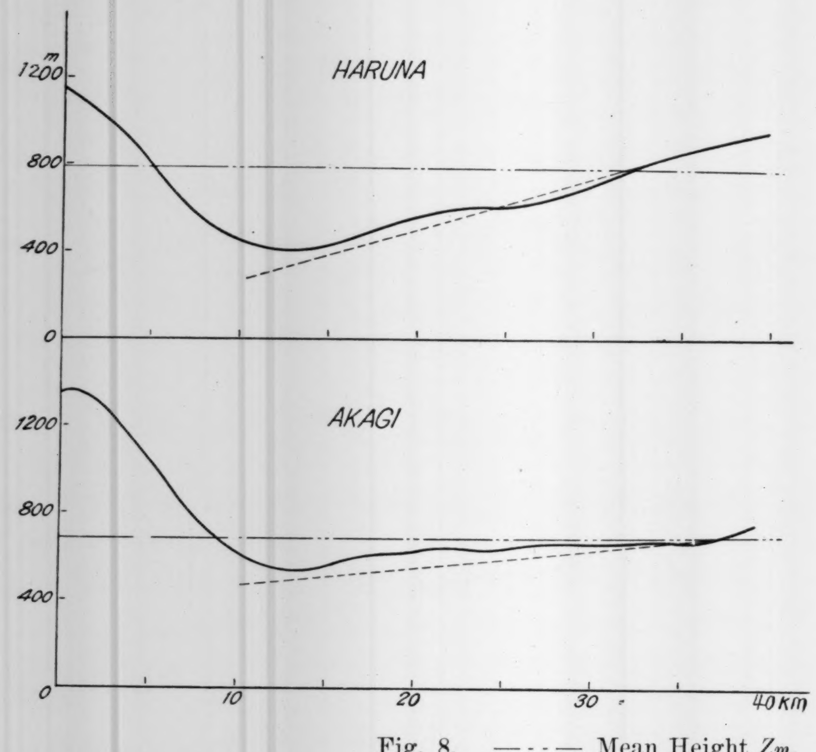

Fig. 8. —·—·— Mean Height Z_m.

rather old. The values of ρ in Fig. 4 fall also near those for Daisen and Hakone.

Compare again the profiles of these two mountains with the inverted profiles of the lakes given in Fig. 7. An essential similarity of feature can scarcely be overlooked. It strongly suggests the presence of some magmatic process which operated in opposite senses may give rise to such a pair of profiles which are mutually in inverted sense as in the case of a mirror image. This again leads to the consideration expounded at the end of § (8), regarding to a special type of magmatic differentiation.

(10) From all what has been said in the preceding paragraphs, we are lead to the following summary:

(A) The circumferential zone of depression at the foot of some valcanos may probably be due to the yielding of the earth crust by the load of the mountain. This suggest us a possible way of the "hardness test" of the earth crust.

(B) Some volcano in the middle of a large area of depression, on the one hand, and some lake situated at the centre of an extensive area of elevation, on the other hand, seem to be genetically correlated to each other in opposite senses.

The theoretical discussions above given may appear rather speculative and grossly qualitative for some of the readers, but may contain, I hope, some germs of what might in some future be developed into a more comprehensive theory of the crustal deformation at large.

---

14. 火山の形

寺田寅彦

火山を取巻く凹地帯は、火山の荷重によつてプラスティックな地盤が陷沒したものと假定すれば、地盤の堅さがどの位になるかといふことを、Hencky の理論を應用して計算すると、普通岩石試片と土壤の類との中間の強さが算出される。又砂の場合の Reissner の理論を應用すると、其の摩擦角の範圍は色々の山について 15°-35° 位となる。

15. Deformation of the Earth Crust in Kwansai Districts and its Relation to the Orographic Feature.

By **Torahiko TERADA** and **Naomi MIYABE.**

(Read June 18, 1929.—Received June 20, 1929.)

After the recent destructive earthquake in the Tango district, an extensive revision of the trigonometrical survey was executed by the Military Land Survey Department, not only over the very region severely disturbed by the earthquake but also over a much wider area including those districts which may probably be assumed to have been intact from the disturbance of the earthquake. A part of the results of the survey has already been published and the present authors¹⁾ inferred from it a rather remarkable relation between the "divergence" of the surface displacement and the post-seismic vertical displacement. The rest of the results of the survey works comprising the entire area revised was published later in Vol. VII of this Bulletin. This latter provides us with an invaluable material not only for visualizing the actual mode of deformation in the district in question, but also for subjecting the different theoretical considerations regarding various geotectonic problems in general to a crucial test, based on the direct measurements of the strain of the crust. The deformation of the crust deduced from the results of the present survey is probably composed of the two parts, i.e. one due to the cumulative effect of the secular or chronic deformation²⁾ and the other due to the immediate effect of the earthquake. The relative magnitudes of the two effects are at present difficult to determine. For the problem with which we are going to deal in the following, this point may, however, be put aside as immaterial for the present.

In the present communication, we will confine our attention to the general essential features of the deformations prevailing over the entire area covered by the recent triangulations, referring exclusively to the data for the primary trigonometrical points. The minor details, which may be revealed

---

1) T. TERADA and N. MIYABE, *Proc. Imp. Acad.*, 4 (1928), 211, 215, 218.

2) The existence of sensible chronic deformations of the crust was confirmed by N. YAMASAKI, *Proc. Imp. Acad.*, 4 (1928), 60 and also by A. IMAMURA, *ibid.*, 4 (1928), 58; 5 (1929), 161.

from the analysis of the data for the secondary points will be reserved for a future study.

The data published by the Land Survey Department give the horizontal component of displacement for each of 25 primary and supplementary trigonometrical points. From these data we can calculate the horizontal strain components for each of the triangles, on the assumption that the strain is uniform within each triangle and thence deduce the magnitudes and directions of the principal strains and also the divergence, rotation and shear respectively, if desired.

Let u, v be the component displacements of a trigonometrical point with respect to an arbitrary system of coordinates x, y and

$$2\frac{\partial u}{\partial x}=\gamma_{xx}, \qquad 2\frac{\partial v}{\partial y}=\gamma_{yy}, \qquad \frac{\partial u}{\partial y}+\frac{\partial v}{\partial x}=\gamma_{xy}.$$

The values of the principal strains will be given by the roots of the equation,

$$\begin{vmatrix} \gamma_{xx}-\gamma & \gamma_{xy} \\ \gamma_{xy} & \gamma_{yy}-\gamma \end{vmatrix}=0,$$

and the angle θ, which is made by the axes of the principal strains with x axis, by

$$\operatorname{tg}\theta=-\frac{\gamma_{xx}-\gamma}{\gamma_{xy}}.$$

Assuming the displacement components to be linear functions of x, y within each triangle formed by three stations P', P'', P''' of which the coordinates are

$$x'\ y' \qquad x''\ y'' \qquad x'''\ y''',$$

and the displacements

$$u'\ v' \qquad u''\ v'' \qquad u'''\ v'''.$$

We can substitute these values into

$$u= a_1x+b_1y+c_1,$$
$$v= a_2x+b_2y+c_2,$$

and determine the six constants a's, b's and c's respectively. Then

$$\gamma_{xx}=2a_1, \qquad \gamma_{yy}=2b_2, \qquad \gamma_{xy}=a_2+b_1$$

and

$$\gamma_{\substack{1\\2}}=a_1+b_2\pm\sqrt{a_1^2+a_2^2+b_1^2+b_2^2+2(a_2b_1-a_1b_2)},$$

$$\operatorname{tg} \theta_{\substack{1\\2}} = \frac{\gamma_{\substack{1\\2}} - 2a_1}{a_2 + b_1} = \frac{a_2 + b_1}{\gamma_{\substack{1\\2}} - 2b_2},$$

whence

$$\begin{aligned} &\text{Divergence} \quad \Delta = a_1 + b_2, \\ &\text{Rotation} \quad = \tfrac{1}{2}(a_2 - b_1), \\ &\text{Shear} \quad = \tfrac{1}{2}(a_2 + b_1). \end{aligned}$$

For the actual calculations, one of *P*'s may conveniently be taken for the origin.

The calculation was carried out only roughly, mainly by means of a graphical method, for the present preliminary investigation.[3] The results are shown by Figs. 1–4.

Fig. 1 shows the distribution of the triangular nets taken into account. The value of the divergence for each triangle is inscribed at the centre of the triangle. Contour lines, corresponding to the supposed lines of equal divergence, are drawn tentatively to visualize the general feature of the deformation. It needs not be remarked that these lines may be modified in details, if we take account of the data for the secondary triangular points.

Fig. 2 shows the magnitudes and directions of the principal axes of the strain ellipse for each of the triangles taken.

Figs. 3 and 4 show respectively the geographical distributions of the rotation and shear.

Examining these figures, we may remark the following:

(1) The largest strains are not confined to the region disturbed by the recent Tango Earthquake, but extended further towards E, i.e. from Oku-Tango Peninsula to the Lake Biwa and probably further eastwards. It is interesting to observe that this zone of the maximum deformation, if prolonged, seems to pass through the epicentres of Nôbi Earthquake of 1891, Anegawa Earthquake of 1909 and Ooigawa Earthquake of 1917, and still further to point to the epicentre of the Great Kwantô Earthquake of 1923, —a conspicuous zone already pointed out by the authors in a previous paper[4] on the secular fluctuation in position of the macroseismic zone of the earth.

(2) The strain is generally small in magnitude and mainly similar in type on the southern side of a line connecting the points A and B in Fig. 1. The small magnitude may partly be due to the fact that the two stations

---

[3] Mr. Ch. Tsuboi made numerical calculations for the divergence, the result of which he kindly placed at our disposal for the verification.

[4] T. Terada and N. Miyabe, *Proc. Imp. Acad.*, **3** (1927), 275; *Bull. E.R.I.*, **6** (1929), 333.

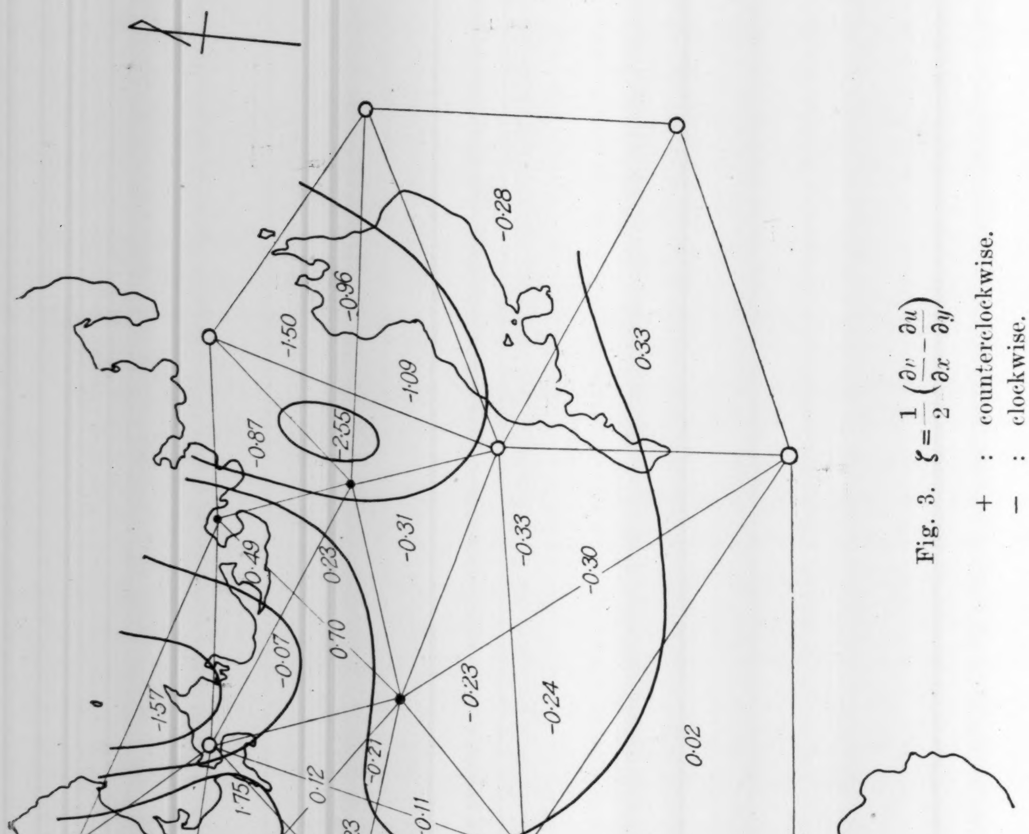
-0·28
0·33
-0·96
-1·50
-1·09
-0·87
-2·55
-0·31
-0·33
-0·30
0·49
0·23
0·70
-0·07
-1·57
-0·23
-0·24
0·02
-0·21
0·12
1·75
-0·11
2·24
1·10
0·23
0·33
0·45
0·01
1·14
-0·54
0·25
-1·21
0·17
0·04
-0·45
0·03
0·25
-0·35
-0·59
-0·44
-0·29
-0·20
-0·07
-0·33
-0·38
-0·26
-0·25

Fig. 3. $\zeta = \frac{1}{2}\left(\frac{\partial v}{\partial x} - \frac{\partial u}{\partial y}\right)$

+ : counterclockwise.

− : clockwise.

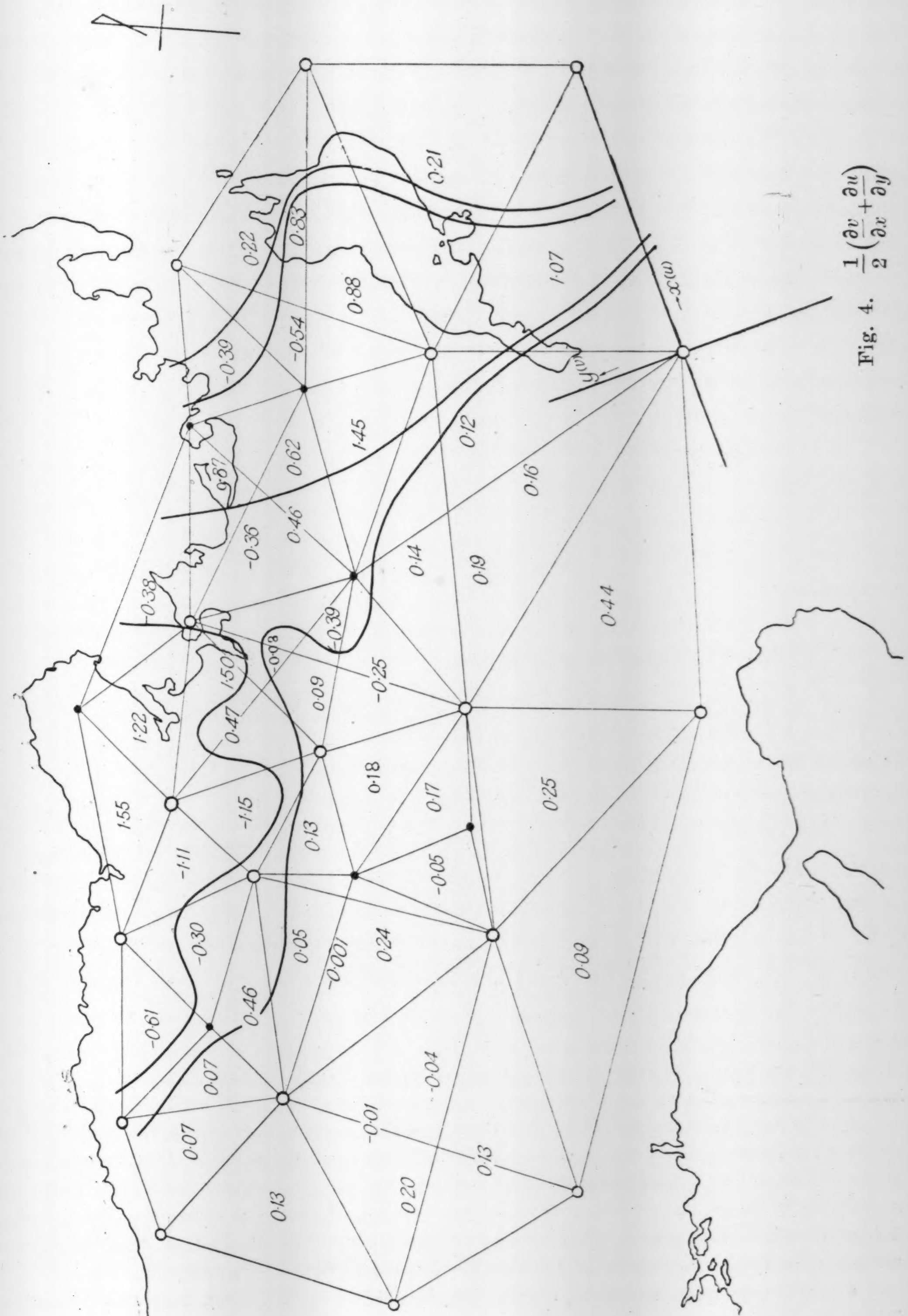
0·21
0·83
0·22
1·07
0·88
-0·54
-0·39
1·45
0·12
0·62
0·87
0·16
-0·36
0·46
0·14
0·19
-0·38
0·44
-0·39
-0·08
-0·25
1·50
0·09
1·22
0·47
0·18
0·17
0·25
1·55
-1·15
0·13
-1·11
-0·05
0·05
-0·001
0·24
-0·30
0·09
-0·61
0·46
0·07
-0·04
0·07
-0·01
0·13
0·20
0·13
−x(ω)
y(ω)

Fig. 4. $\frac{1}{2}\left(\frac{\partial v}{\partial x}+\frac{\partial u}{\partial y}\right)$

assumed immovable are situated within this area. Still, the uniformity of the size and shape of the strain ellipse in this region may be taken as an evidence of the fact that this region has been comparatively free from any conspicuous crustal deformation.[5]

(3) The magnitude and type of the strain show generally a zonal distribution parallel to a line connecting the points A and B in Fig. 1, which seems to be interrupted along a line connecting C and D. It may be pointed out that the line CD corresponds to a conspicuous zone on the geological map of the region, which is marked by the exposure of the parallel bands of diorite.

(4) In Fig. 2, we may divide the area of the map into a number of regions according to the type of the strain ellipse; thus, provisionally as follows:

I*a*: Elongation in N-S direction,
I*b*: ,, ,, all ,, ,
I*c* : The same as I*a*.

In short, we may regard I*a*, I*b* and I*c* as a zone with conspicuous N-S elongations

II*a*: Contraction in N-S direction.
II*b*: The same in less amount,
III: Strain generally small and mainly elongation in N-S direction.
IV: Large contraction in all directions.

It must be remarked that the striking contrast between the two regions I*a* and II*a*, or between I*c* and IV may be brought about by some anomalously large displacements of a few number of the trigonometrical stations lying between the two regions. It will be, however, interesting to regard the strain as continuous as in the case of an ordinary elastic body and compare the type of the strain with some well known cases of elastic deformations. For example, we may point out that the relation between the two regions I and II show some qualitative similarity with the case of flexural stretching of a curved rod.[6]

(5) Examining Fig. 3, we may notice that in the above mentioned

---

[5] It may be expected from the theory of fluctuation that the greater the average strain of a district, the greater the spatial fluctuation of the strain. On the other hand, it seems difficult to reduce the distribution of strains on the northern side of AB into such a state as it is on the southern side, by any choice of the base stations assumed fixed. The assumption made seems, therefore, approximately correct, though we must admit some margin of error in the values of the specific displacements, divergence, etc.

[6] For example, see TH. WYSS, Die Kraftfelder in festen elastischen Körpern, Tafel 13, Abb. 166.

zone of maximum disturbance, i.e. on the northern side of the line AB (Fig. 1), the sense of rotation is alternatively clockwise and counterclockwise when we proceed along the E-W direction. Such an alternation of the sense of rotation in the neighbouring regions was also found by Prof. Fujiwhara[7] in the case of the Kwantô District. On the other hand, it is interesting to note that the Oku-Tango Peninsula shows apparently a large counterclockwise rotation with regard to the main land, as the general trend of the coast line of this peninsula suggests that it might have been formed by a counterclockwise rotation of the whole peninsula from an initial position, in which the present NW coast of the block might have formed a prolongation of the general coast line to the west of it. Assuming a continuous rotation of 10^{-5} radians per 40 years, which is the observed rate, it will take about two million years to produce a total rotation of 30 degrees, a quite short interval of time on the geological point of view.[8]

(6) Drawing, in Fig. 4, the contour lines with the equal magnitudes

---

[7] S. FUJIWHARA and T. TAKAYAMA, *Bull. E.R.I.*, **6** (1929), 149, Pl. 7. The present case may probably be regarded as an example of the "chain of vortices" in Fujiwhara's sense.

[8] According to the estimation from He-contents of minerals, the age of the Pliocene is given as 1.5 million years which is considered an under-estimation. An estimation from Pb-contents gives 35 million years for the late Oligocene in U.S.A. See A. HOLMES, "The Age of the Earth," 1927, O. HAHN, "Was lehrt uns die Radioaktivität über die Geschichte der Erde," etc. The presence of fossil remains of some kinds of elephants and rhinoceros in this country shows that the interruption of the land connection between the continent and Japan took place in comparatively recent ages. Lately, Prof. H. Yabe inferred from his investigation on the reliefs of the sea-beds in different parts of this country, that very late in the geological history the connection between Formosa and the continent was broken by a considerable submergence of the connecting bridge, (Records of Oceanographic Works in Japan, **1**, 1929, 97 and *Proc. Imp. Acad.* **5**, 1929, 179). A similar submergence was also observed in other parts of Japan. It seems possible that such a remarkable submergence might have been connected with a considerable horizontal straining of the crust and therefore that a local differential movement might have caused a rotation of some marginal land block by a sensible angle. In the present authors' opinion, the fact of the submergence is easily reconcilable with the theory of horizontal drift of the Japanese Arc, if we may assume that the submergence was caused here by the decrease of the thickness of the crust by stretching rather than due to the change of density which cannot account for a level change of such an order as is here concerned, unless we resort to some physico-chemical change of crust materials. With regard to this point, see p. 235 of the text. It may depend upon the type of the strain whether the crust is merely decreased in its thickness, or is decreased in density associated with volcanic activity. On the other hand, if the angular velocity be fluctuating at random, its probable amount will be proportional to the square root of time. The above estimation of time must therefore he regarded as a kind of lowest limit.

of shear,[9] we may notice again an interruption of the zone of maximum shear at its middle part. It is rather remarkable that the mountainous district to the north of Kyôto, on the western side of the Lake Biwa, reveals a conspicuous amount of shear, in spite of the fact that no epicentre of sensible recent destructive earthquakes has yet been located in this region. On the other hand, the zone of the maximum shear here revealed seems to coincide nearly with the "zone of deep-seated earthquakes" pointed out by Mr. K. Wadati, Fig. 5.[10] The same zone, as already remarked, coincides

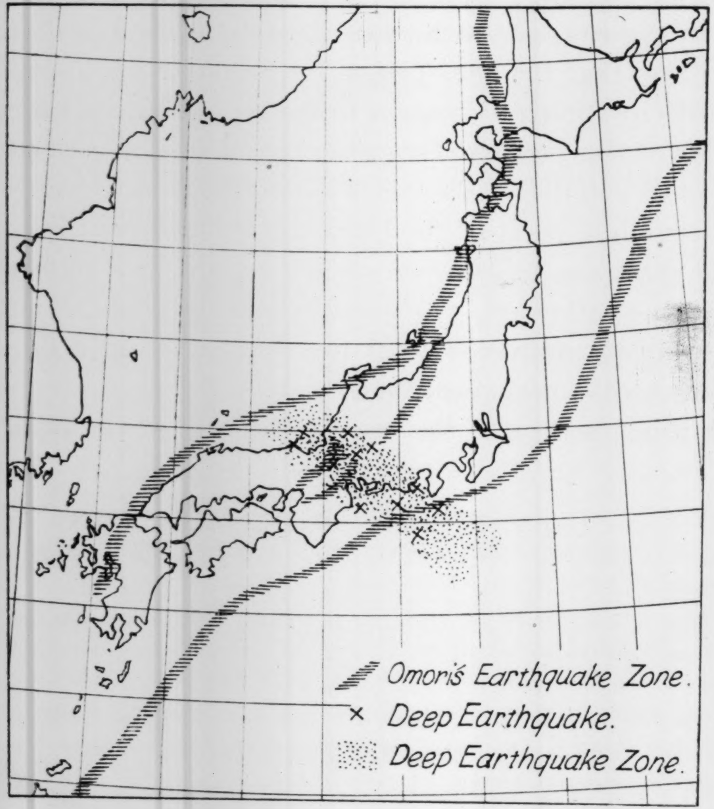

Fig. 5. (Reproduced from Wadati's paper.)

---

[9] The algebraic sign of the shear depends on the choice of the axes of reference, which is shown in Fig. 4. The direction of shear may roughly be estimated from the form of the strain ellipses in Fig. 2. The fact that the direction of the shear is rather irregularly distributed among the zone of the maximum shear is rather immaterial for the present discussions, since on account of the "chain of vortices" above mentioned, the local distribution may be subjected to an irregular fluctuation, as may be illustrated by the sand grains on the slip plane of a disturbed sand mass. At present, we refrain from drawing any conclusion on the average sense of the shear in the zone in question.

[10] K. Wadati, *Journ. Met. Soc. Jap.*, [ii], **5** (1927), 119; *Geophys. Mag.*, **1**, No. 4 (1928), 162.

nearly, or with a little inclination, with the line connecting the epicentres of some recent destructive earthquakes with rather shallow origins. It seems, therefore, that this very zone forms, as it were, the trace of a slip plane of the plastic deformation of the crust going on at the present half century. Our previous investigation[11] on the fluctuation of the position of the macroseismic zone suggests that this very zone of the maximum shear may gradually shift its position in the course of two or three centuries.

Our experimental studies[12] on the formation of slip planes in sand mass decidedly speaks in favour of such a conjecture.

(7) A comparison of Fig. 1 with the topographical map of the area investigated suggests a remarkable relation between the divergence Δ of the displacement above obtained and the height of the land above sea level. To demonstrate this relation, the following procedure was taken. The two lines EF and GH were drawn (not shown in Fig. 1) such that they run across the alternate zones with positive and negative Δ. The values of Δ along these lines are shown in Fig. 6 by the échelon curves, as the value of Δ is assumed constant within each triangle. The step-like curve is smoothed by a hypothetical curve to visualize the general feature of the distribution. On the other hand, the mean profile curve of the three vertical sections EF, E′F′, E″F″ was constructed from a rough topographical map and compared with the Δ-curve. The similar profile curve was also obtained for the section GH. A glance at this figure will show an infallible resemblance in the general features of the two curves compared.

Fig. 7 is given to show the above relation between the distribution of Δ and the gross topographical feature over the entire area in question.

The above result seems to shed a considerable light on the geophysical significance of the superficial topography of the earth crust. In our previous papers, the horizontal divergence in the vicinity of Oku-Tango Peninsula, obtained from the pre-and post-seismic triangulations, was compared with the *post-seismic* vertical movement of the same region. From the result of this comparison, it was made probable that the vertical movement is due to the process of the isostatic compensation caused by the change in density of the crust connected with the horizontal deformation observed. In the present case, the integral horizontal strain which has been effected during the recent forty years is compared with the existing topographical feature of the land, which must have been produced as the result of a complicated

---

[11] *loc. cit.*

[12] T. Terada and N. Miyabe, *Bull. E.R.I.*, **4** (1928), 33; **6** (1929), 109; **7** (1929), 65.

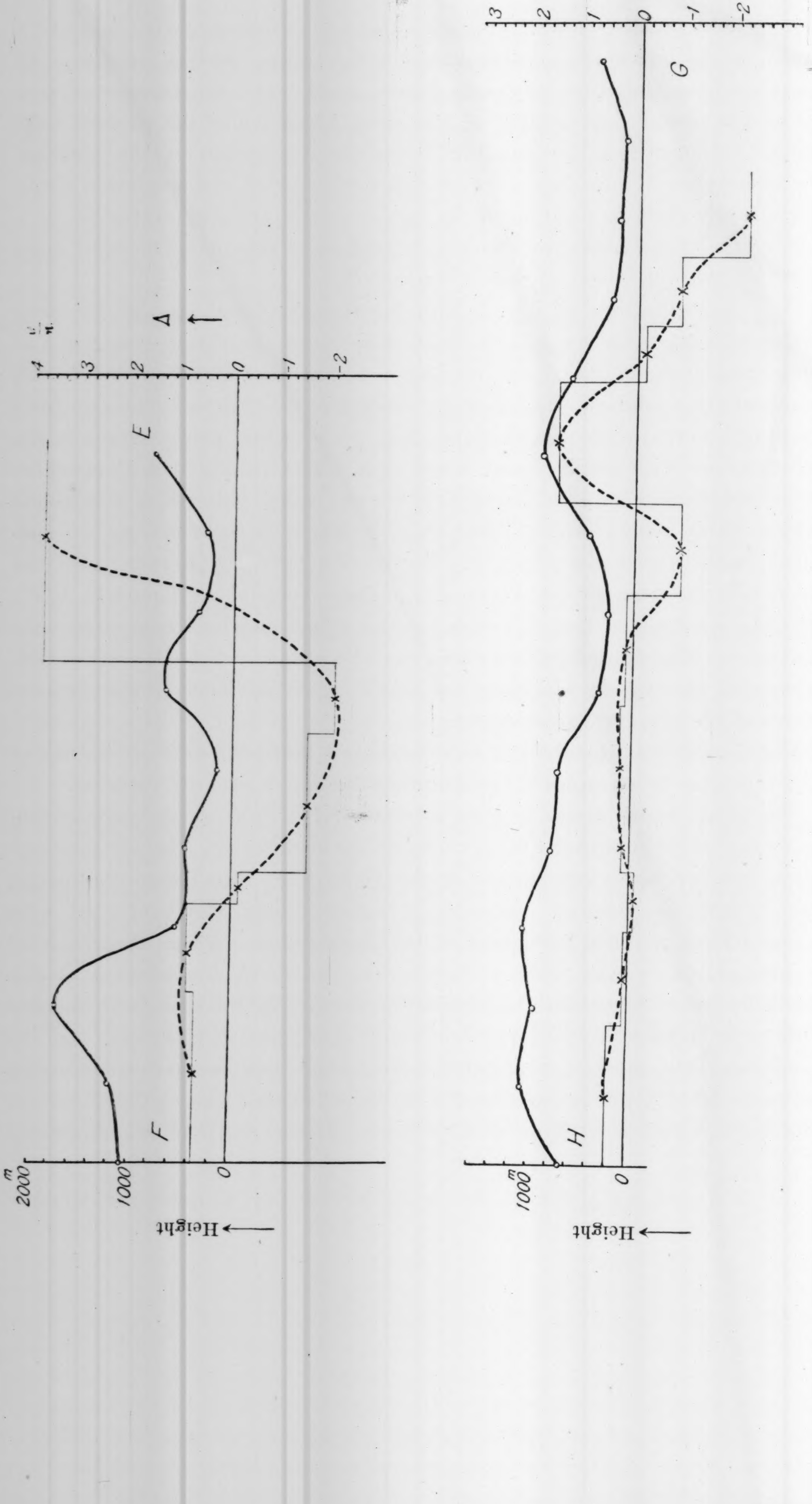

Fig. 6. ×: divergence; ○: height.

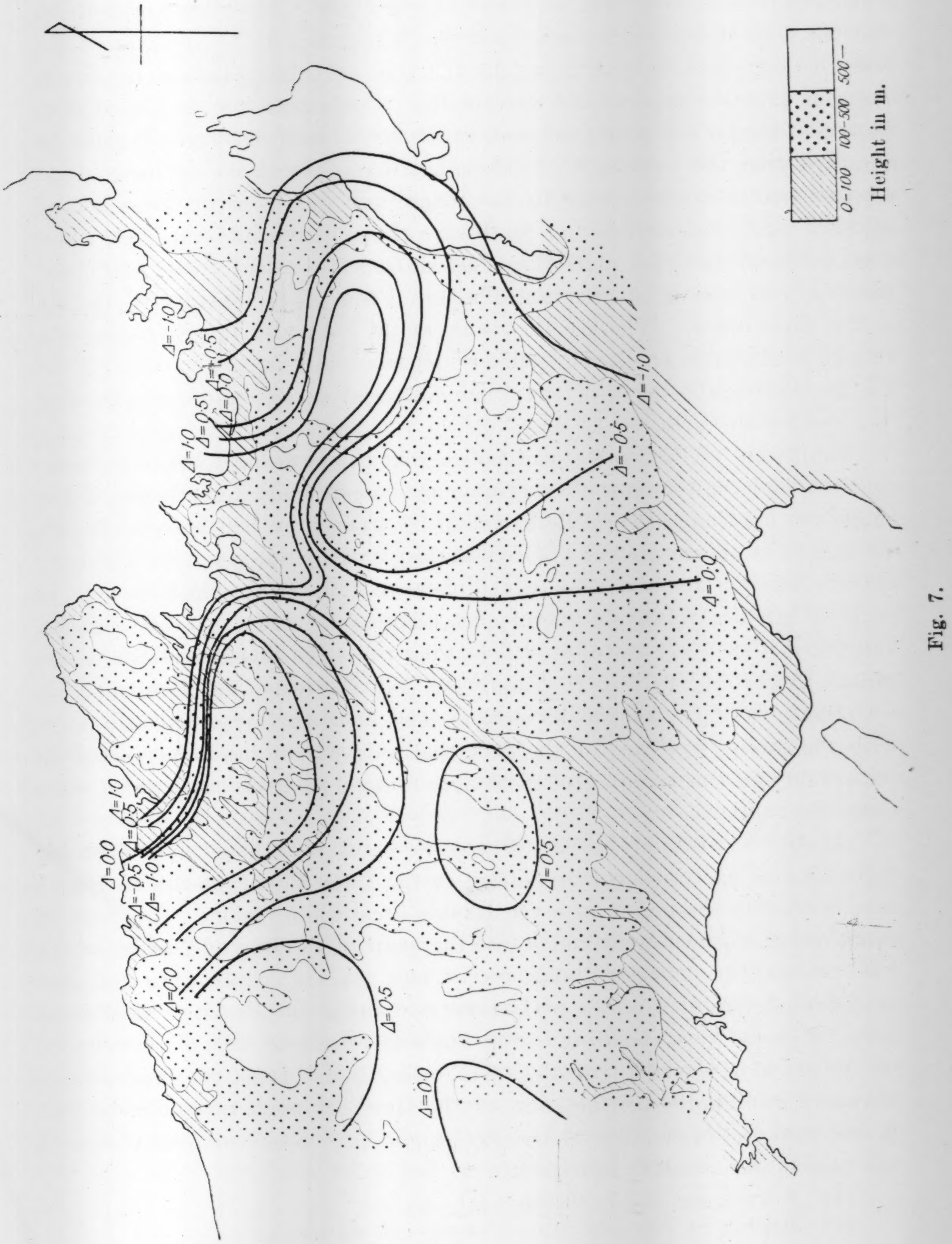
Δ=-1·0
Δ=+0·5
Δ=-0·5
Δ=0·0
Δ=1·0
Δ=-1·0
Δ=-0·5
Δ=0·0
Δ=1·0
Δ=0·5
Δ=-1·0
Δ=-0·5
Δ=0·0
Δ=0·0
Δ=0·5
Δ=0·5
Δ=0·0
0–100
100–500
500–
Height in m.

Fig. 7.

geological process continued since the remotest past. It appears, therefore, that the present topography was built up in the main by the process of the isostatic compensation determined by the type of deformation of the crust, and also that the type of the deformation which gave rise to the present feature of the land is continued even in the recent half century. It must be admitted that the process of deformation must have been subjected to a sensible fluctuation not only in the magnitude but even in the sense of motion. Still, it is interesting to observe that (i) the integral effect since a certain geological age, (ii) the effect during the recent forty years and (iii) the post-seismic effect revealed within a few years are directed largely in the same sense. Whether the same would hold also in other districts, or not, is of course another question which may only be answered after the similar thorough revision of the trigonometrical survey has been extended to a much wider area.

Returning to Fig. 7, we may notice that the agreement between the Δ-contours and the topographic feature may become more remarkable, if the height of Oku-Tango Peninsula be raised by a few hundred metres. Hence, assuming the correctness of our hypothesis, we may suppose that the horizontal dilatation and the consequent upheaval of the peninsula have been in progress since a relatively recent past, compared with the other regions, and the motion of upheaval is still lagging after the increase of the divergence. According to Mr. F. Tada[13] of our Institute, the results of his investigations of the coastal terraces as well as of the river beds afford us with the strong evidence of the fact that this region has been rising up remarkably in the recent geological age, though probably with some occasional fluctuations.

Again, it will not be superfluous to point out that the remarkable depression of the crust corresponding to the Lake Biwa appears in Fig. 1 associated with the region of a remarkable areal compression. This zone of compression is probably extended into the heart of the Bay of Wakasa which was presumably depressed in a recent age. A map[14] showing the geographical distribution of the prehistoric remains in the Province of Wakasa gives two zones corresponding to two kinds of remains. One of these zones, on the sea side, running parallel to the other which is on the land side, is abruptly interrupted on the coast of the Bay. It may, therefore, be suggested that the depression of the bay might have been completed even in the time of our remotest ancestors.

---

13) F. TADA, *Bull. E.R.I.*, 5 (1928), 111.

14) 若越小誌 (A Provincial History of Wakasa and Etizen.)

On the other hand, Prof. Fujiwhara and Mr. Takayama[15] calculated the "convergence" or the negative divergence of the Kwantô District from the similar data for this district. Glancing at the diagram given in Pl. VII of their paper, it is interesting to observe that the contour line corresponding to the relative number 20 of the convergence coincides very nearly with the general coast line surrounding the Bay of Sagami. The area with the larger convergence lies on the sea, whereas the area with the less convergence or negative convergence corresponds to the land area. It must be remarked that the sense at least of the correlation between the divergence and the topographical feature is just the same as in the case of the region here investigated.

In the above we have simply assumed that the divergence of the horizontal displacement corresponds to the variation of the density of the crust. It is, however, necessary to discuss this point in more details. In order to explain the present topography as the result of the density variation of the crust, we must indeed assume a considerable change of the density. For example, assuming a crust of 100 km. thickness, the vertical movement of 1 km. will require a density change of 1/1000, even if the Poisson ratio be zero. Moreover, the deformation is probably not elastic but mainly plastic. Beyond a certain amount of compression or dilatation, the effect of the divergence will be counteracted by the effect of the lateral elongation or contraction. This is evident, if we consider that, when the density change is zero, the change of thickness of the crust will vary with $-\Delta$. Therefore, in order to account for the required change of density, we must resort to some other effect than to the purely mechanical one. We may quote here as a probable factor the change of specific volume accompanying some allotropic transformation of the crustal substances as brought about by the change of prevailing pressure, which we may assume as a definite function of Δ.

A glance at a geological map of Japan will reveal a very conspicuous fact that the patches of area coloured brown, marking "volcanic ash and mud lava," appear always upon the region coloured yellow denoted as "Tertiary." This simple broad fact may signify that the Tertiary and post-Tertiary upheaval of the land was concomitant with an extensive display of volcanic activity. It seems[16] that, in the beginning of the Tertiary, the Northern Arc of Japan which had been largely submerged in the preceding age, was subjected to an upward motion, meanwhile the

---

15) S. FUJIWHARA and T. TAKAYAMA, *loc. cit.*

16) 日本帝國地質圖說明書（明治二十三年）

volcanic activity broke out with an unusual intensity which was continued up to the beginning of the Quaternary. It seems, therefore, that during the Tertiary Age the Northern Arc was subjected to a considerable divergence.

Similarly, the Palæozoic area richly spotted with the plutonic rocks, granite, porphyry, etc. seems to be a facsimile of the relation quite similar to the above, but referring to a much remoter past.

According to Mr. Tsuya[17] of our Institute, who carried out a thorough geological investigation of Oku-Tango Peninsula in question, a submarine eruption of andesite took place in the early Tertiary; then after an episode with a submergence of several hundred metres, the land was upheaved by a considerable amount to the present height. The upheaval was followed by conspicuous faulting movements accompanied with volcanic activities.

These considerations may suggest an interesting future problem of studying the relation between the activity fluctuation of some volcano, such as Sakurazima or Usu, and the divergence of the surrounding district, which may be obtained by repeated triangulations of a wide area including the district in question.

Thus far, we have tacitly assumed that the horizontal displacement of a trigonometrical point deduced from the results of the repeated triangulations is actually produced by a purely horizontal translation of the point. It is, however, necessary to consider the effect of the tilting of the land mass upon which the point stand, especially because the point is usually situated upon some mountain peak.

Let h be the height of the point above the crustal surface, which is tilted by a small angle θ. Then, the horizontal displacement will be $h\theta$. Assume $h=1$ km. in round number. As for the greatest possible amount of tilting for the present case we may consult the result of the precision levelling published in Vol. III of this Bulletin. Taking the section of the levelling route between B.M. 1229 and 1235, we find a level difference of about 1.2 m. per 8 km. distance. This makes $\theta=15\times10^{-4}$ in radian and $h\theta=0.15$ m. which is by no means small. On the other hand, the relative horizontal displacements among the neighbouring trigonometrical points, as obtained from the result of the trigonometrical survey, are generally of the order of several cm. at most. It follows that at least a sensible part of the observed displacement may be due to the effect of tilting. This may seem to vitiate our present results utterly. The difficulty is, however, apparent, as will be seen, if we consider the mechanism by which the tilting of the crustal surface is made possible.

---

17) H. TSUYA, *Bull. E.R.I.*, 4 (1928), 139.

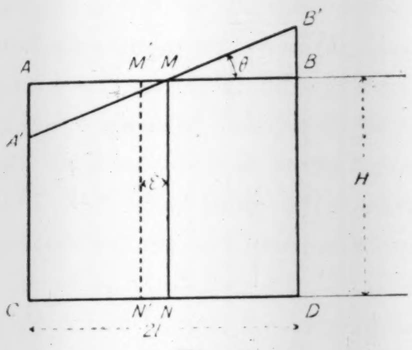

Fig. 8.

Referring to Fig. 8, suppose ABCD as a vertical section of a strip of block extending indefinitely in the direction perpendicular to to the plane of the figure. Suppose that the surface AB is tilted by θ and takes a new position A′B′, while the other boundaries of the block are fixed. Such a deformation is only possible by a compression of the part AMNC and an expansion of MBDN. The average compression or expansion is $l\theta/2H$.

On the other hand, if there is no tilting, but a horizontal displacement of MN by $MM'=\varepsilon$ towards the left, the amount of compression and expansion will be ε/l.

Equating, for a trial, the two values of the specific volume change with each other, we have

$$\frac{\varepsilon}{l}=\frac{l\theta}{2H} \quad \text{or} \quad \theta=\frac{2\varepsilon H}{l^2}.$$

In the case of the ordinary block tilting, the depth to which the sensible change of density is thereby brought about, is quite unknown, but it may be plausible to assume that H will be of the same order of magnitude as l. This may be expected from the theories and experiments regarding the plastic deformation of materials, especially those regarding the hardness test. Putting $2H=\alpha l$, where $\alpha\approx 1$, we have $\theta=\alpha\varepsilon/l$. Thus, the tilting by an amount θ is *equivalent* to a purely horizontal displacement of $\alpha\varepsilon/l$, as far as the compression and expansion of the crust is concerned.

Unfortunately, it is not feasible for the present to analyse the effect of tilting from that of the pure horizontal displacement, as it is necessary for this purpose to be able to avail of the ample data of the precise levellings repeated along a sufficiently dense network of the levelling routes, such that the complete mozaics of the block structure are covered by the net. The ambguity, however, is immaterial as far as the essential points of the result of the present investigation is concerned, i.e., our inference regarding the relations between Δ and topography.

If, however, the effect of tilting be predominating, the meaning of the strain ellipse, rotation, shear, etc. obtained in the above manner may be interpreted in a manner more or less different from usual. For the present, it will be plausible to take the *virtual* horizontal strain as something real, follow up the inferences to be drawn therefrom and seek after the crucial evidences from the other sides.

It may be remarked in passing that the assumption above made on the tilting of mountain may be an over-estimation. When the plane surface AB (Fig. 8) is tilted to such a position as A′B′, the tilted surface can probably no more remain as a plane, but may be deformed into an échelon form, as may be abundantly illustrated by similar examples observed in the case of land-slides or in our model experiments with sand mass.[18] This effect will reduce the apparent horizontal displacement due to the tilting by more or less amount, depending on the mode of the échelon formation. For a further inquiry after this problem, however, we must wait until more abundant data has been accumulated.[19]

From what we have seen in the above discussions, it seems that the study of the actual mode of strain going on in the earth crust, based on the results of repeated triangulation is the most *direct* way of obtaining, if possible at all, the clue for the so-called earthquake forewarning, though the present authors are at a loss to realize the exact meaning of this words.

Finally, we must express our most sincere feelings of gratitude for the invaluable contributions to the science of earthquakes made by the Authorities of the Land Survey Department, in providing seismologists and geophysicists with such precious data that we are now able on account of them to study the actual modes of deformation of the earth crust with nearly equal ease as we are dealing with a handy test piece of metal in the laboratory. As a Chino-Japanese adage says, "Procuring Rô Land, we long for Syoku." Nothing is more desirable on behalf of the Science of Earthquake than a further extension of the similar survey work by the hands of the same Authorities.

SUMMARY.

(1) From the result of the revision of the primary trigonometrical survey in the Kwansai Districts, the apparent horizontal strain components were calculated, for each mesh of the primary triangulation network, whence the divergence, rotation and shear as well as the magnitudes and directions of the principal axes of the strain were deduced for each triangle and the geographical distributions of these quantities were investigated.

(2) A remarkable correlation is found which exists between the divergence of the horizontal displacements effected during the past forty

---

18) *Loc. cit.*

19) Prof. NAGAOKA remarked, after this paper was read, that a deformation of the mountain body itself due to the shock, may also contribute to the observed horizontal displacement.

years and the present topographical relief of the districts, the positive divergence corresponding to the mountainous region. This result taken together with that of a previous investigation of the authors seems to throw a new light on the geophysical significance of the topographical feature of the surface crust at large.

(3) The zone of maximum strains revealed by the present analysis coincides, on one hand, nearly with a zone of macroseismic activity for the recent half century and, on the other hand, with a remarkable zone of deep-seated earthquakes, recently pointed out by K. Wadati.

(4) The effect is discussed of the tilting of a land block on the apparent horizontal displacement of the trigonometrical station which is situated on a mountain peak lying on the block, and it is shown that the tilting and a horizontal tilting may be regarded as equivalent when the compression and dilatation of the crust is in question.

(5) Some suggestions are given under the light of the present result, regarding the genetical factors which might have been essential in determining the present topographical and geological structures of Japan.

In conclusion, the present authors wish to express their best thanks to Prof. S. Tsuboi, Dr. F. Tada and Dr. H. Tsuya for many valuable informations and also to Assist. Prof. Ch. Tsuboi for his kindness in checking our calculation.

---

15. 關西地方の地殼變形並に現在地形との關係

寺　田　寅　彦
宮　部　直　巳

陸地測量部によつて行はれた關西地方復舊一等三角測量の結果から、各點水平移動の divergence, rotation, shear 及 strain ellipse の主軸の大さと方向を算出し其の地理的分布を調べた結果として次のやうなことが云はれる。

（1） 過去四十年間の水平移動のダイヴアーヂエンスと現在の陸地の高さとは正の相關がある。此事は地形といふものゝ地球物理學的の意義の解釋上參考になる。

（2） 變形の量の最大な地域を連れる一つの地帶は和達清夫氏の深層地震帶と略一致し、又最近數十年間に於ける大地震の或ものを連れる線とも近接する。

（3） 以上の結果から考へて、日本陸地の生成の機巧に關する想像說を述べておいた。

（震研彙報第七號，圖版、寺田、宮部）

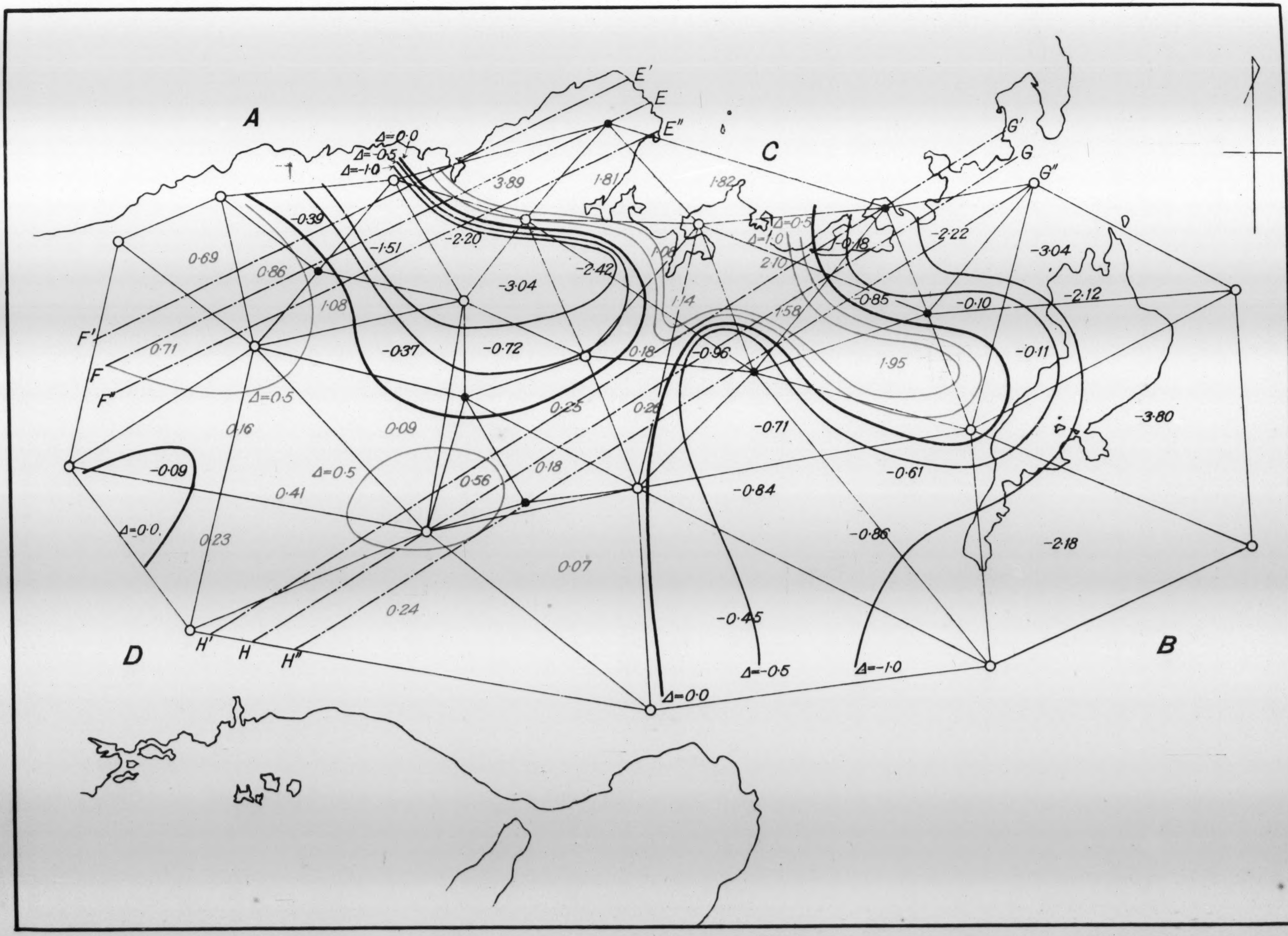
A
B
C
D
E'
E
E"
F'
F
F"
G'
G
G"
H'
H
H"
Δ=0·0
Δ=-0·5
Δ=-1·0
Δ=0·5
Δ=-0·5
Δ=-1·0
Δ=0·5
Δ=0·5
Δ=0·0.
Δ=0·0
Δ=-0·5
Δ=-1·0
3·89
1·81
1·82
-0·39
-1·51
-2·20
-2·42
-3·04
1·06
2·10
1·14
1·58
-0·18
-2·22
-3·04
-0·85
-0·10
-2·12
0·69
0·86
1·08
0·71
-0·37
-0·72
0·18
-0·96
1·95
-0·11
-3·80
0·16
0·09
0·25
0·28
-0·71
-0·61
-0·09
0·41
0·56
0·18
-0·84
0·23
0·07
-0·86
-2·18
0·24
-0·45

Fig. 1.

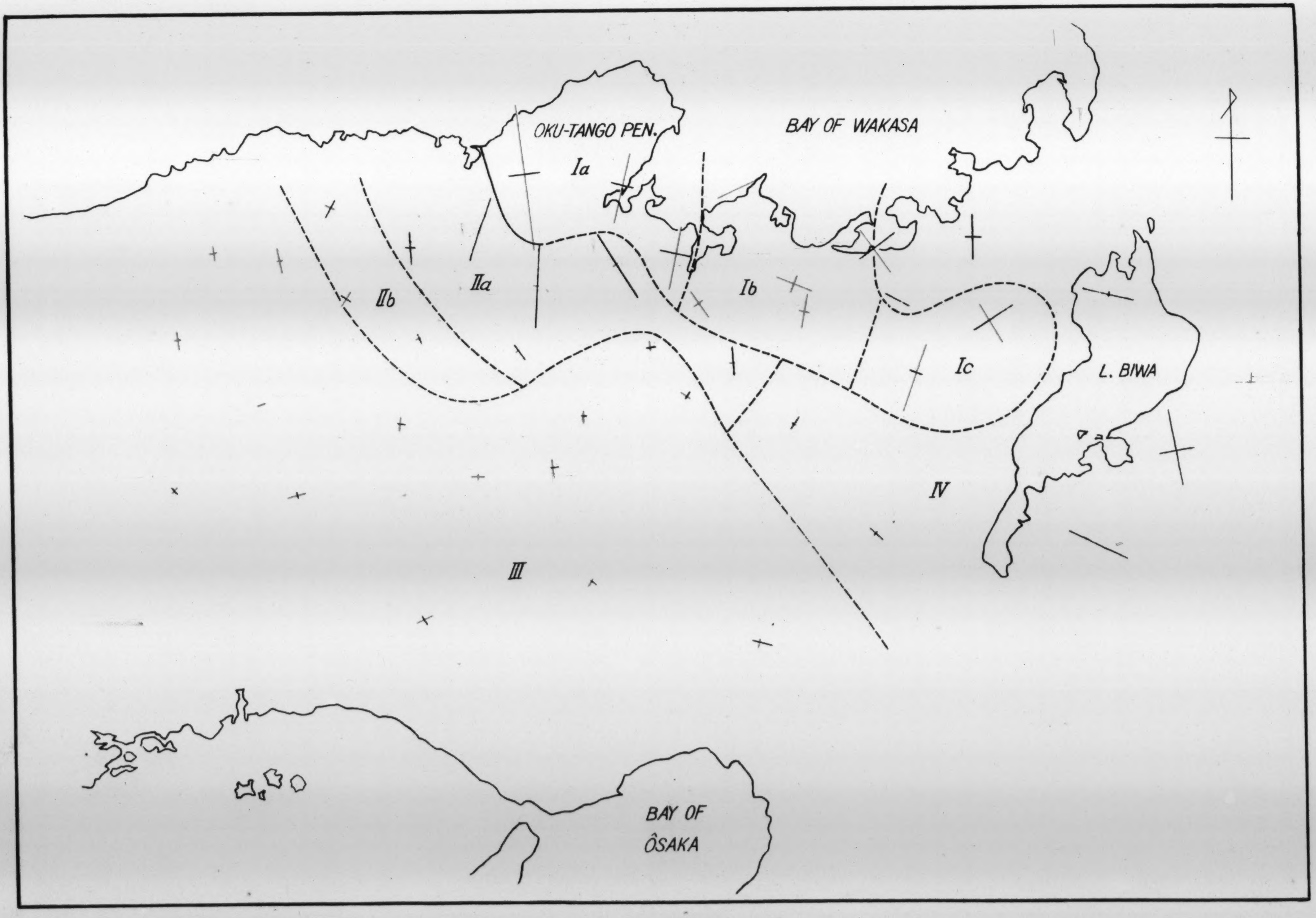
OKU-TANGO PEN.
BAY OF WAKASA
Ia
Ib
Ic
IIa
IIb
III
IV
L. BIWA
BAY OF ÔSAKA

Fig. 2.

（震研彙報第七號、圖版、寺田、宮部）

16. *On the Forerunners of Earthquake-motions.*

(The Second Paper.)

By **Takeo MATUZAWA, Kunitika YAMADA**
and **Takeo SUZUKI.**

(Read March 19,—Received June 12, 1929.)

I. INTRODUCTION.

One of us[1] and others have shown that seismograms of certain earthquakes recorded at Hongô (Tôkyô) or Kamakura indicate a typical forerunning part which may be attributed to a certain kind of local geological structure characteristic to the Kwantô District.

In the course of further study of that case, the present authors' attention was directed to existence of other set of forerunning waves with somewhat more general character. In this paper, these phases of waves will mainly be treated.

II. OBSERVED FACTS WITH REGARD TO THE FORERUNNING PART OF EARTHQUAKE-MOTIONS.

For explaining the existence of certain phases other than those such as P^*, $\overline{P}$, etc., it will be convenient to show examples of seismograms which reveal such phases clearly. In the following, some examples will be shown.

No. 1. Earthquake of Jan. 18, 1927. This earthquake occurred far off the coast of Kinkwazan, and the position of its epicentre is estimated as $\lambda=142°14'$ and $\varphi=38°40'$. The time of commencement observed at Hongô, Tôkyô, was 6h 59m 88s. (l.m.t. $\lambda=135°$E). The epicentral distance from Hongô was 388 km. A set of seismograms recorded at Hongô will be reproduced in Pl. XII, Fig. 1. Phase P^* and $\overline{P}$ are clearly identified on the seismograms at the exact position expected. From the fact that phase $\overline{P}$ appeared clearly, it will be inferred that the waves were generated in the uppermost layer. Closer examination will reveal a phase marked P_2' somewhat well defined and further P_2 though less defined. The $P-P_2'$ duration is about 3.1 sec. and the $P-P_2$ is 1.5 sec. in this case. The phase denoted by P_2 seems to correspond to the phase denoted by "2" in the former paper.[1] Seismograms recorded at Kiyosumi-yama, Yuigahama and Misaki were also available and the P_2' phase was identified as shown in Table I.

---

[1] T. MATUZAWA, K. HASEGAWA and S. HAENO, *Bull. Earthq. Res. Inst.*, 4 (1928), 85–106.

TABLE I.

	Tôkyô	Kiyosumi	Yuigahama	Misaki
Epicentral dist. in km.	388	424	434	448
Duration from commencement to phases concerned	$P-P_2=1{\cdot}5$ $P-P_2'=3{\cdot}1$	3·6	3·5	3·8

No. 2. Earthquake of June 1, 1928. This earthquake occurred far off the coast of Miyako and the position of its epicentre is estimated as $\lambda=143^\circ.3$ and $\varphi=39^\circ.8$. The time of commencement observed at Hongô was 22h 13m 31s or so (l.m.t. $\lambda=135^\circ$E.) The epicentral distance from Hongô was 553 km. A seismogram recorded at Hongô is reproduced in Pl. XIII, Fig. 2. Phase P^* and $\overline{P}$ are also clearly identified. Thus, in this case also, the waves might have been generated in the uppermost layer. Further, phase P_2' is seen as before. The P_2 phase cannot be defined in this case, perhaps owing to the smallness of the motion and the lack of quick movements. This point will be taken up later in the section of discussion. Some other seismographs in our institute recorded other incidence of a phase 5.7 seconds after the commencement of phase P. In Fig. 2 it is difficult to identify this phase. But it is inevitable that a phase recorded by a seismograph is sometimes obscure in other records, because each seismograph has its own resolving power for incident waves similarly as spectrographs in spectroscopy.

From seismograms available we have obtained some values as shown in the following table.

TABLE II.

	Tôgane	Hongô	Titibu	Kiyosumi	Misaki	Yuigahama
Epicentral distance	542	553	563	588	612	601
Duration from comm.	5·0	3·2; 5·7 $P-S^*=72{\cdot}5$	2·8	6·3	3·3 5·9	4·4

---

1) **T. MATUZAWA**, et. al., *loc. cit.*, 241.

No. 3. Earthquake of Aug. 27, 1928. The epicentre of this earthquake is estimated as $\lambda=141^\circ 07'$ and $\varphi=36^\circ 34'$ in the Pacific. The depth of its origin is inferred to be situated in the uppermost layer by studying its seismograms within our reach and its time-distance curve. From reported time of commencement and duration of preliminary tremor the time distance curve has been constructed as shown in Fig. 3. The fact that most stations took the S^* phase for the commencement of the principal portion and at certain stations the $\bar{S}$ phase was interpreted as such may tell that the depth of its origin was in the uppermost layer as discussed in the former paper by one of us.[2]

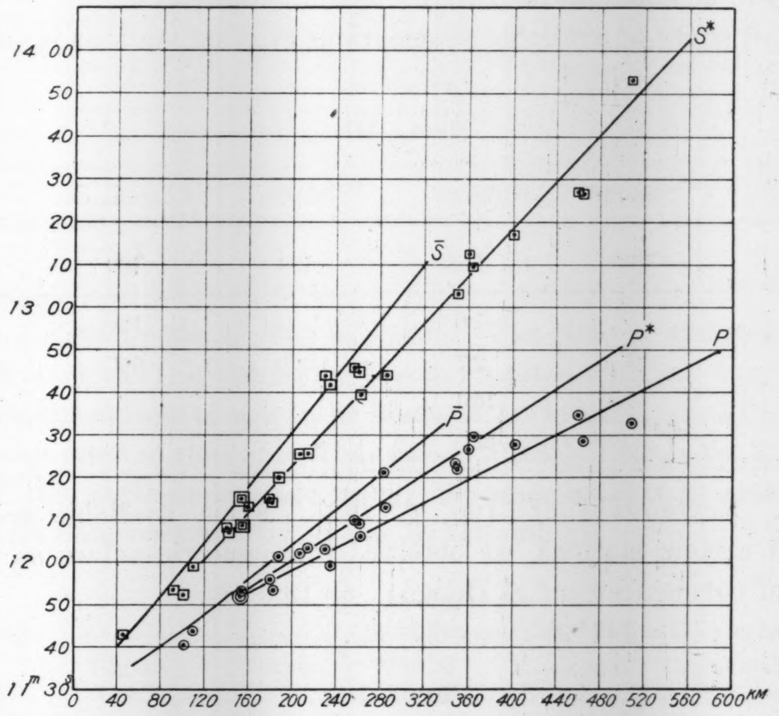

Fig. 3. Time-distance curve of earthquake on Aug. 27, 1928. ($\lambda=141^\circ 07'$, $\varphi=36^\circ 34'$.) ◎, ▣; determined by us.

One of seismograms obtained at Hongô is reproduced in Pl. XIII, Fig. 4. In the figure phase S^* and $\bar{S}$ are clearly identified. In the forerunning portion two distinct incidences marked as P_2' and P_2 can be seen. In this case it is somewhat difficult to interpret each incidence exactly. As the epicentral distance from Hongô is 155 km. or so, it is not easy to say with exact certainty, though inevitable from the present state of accuracy of observation, whether the very commencement is the P or P* phase, for at such an epicentral distance the first incidence may be phase P or P* according to circumstances. In this case, if the first incidence is P*, then the phase marked P_2' may be the $\overline{P}$ phase. Nevertheless the phase marked P_2 may be the same as that discussed before. It is worth noticing that the epicentre of this earthquake was in the region excluded in the former paper[1] (Fig. 7) from places producing earthquakes showing phase "2" distinctly. This point will be taken up later in discussion.

---

[2] T. Matuzawa, *Bull. Earthq. Res. Inst*, **6** (1929), 177–204.

Result of study of available seismograms at other stations is summarised as follows.

TABLE III.

	Tôgane	Tôkyô	Titibu	Yuigahama	Misaki
Δ km.	133	155	194	199	207
$P-P_2$		1·6		1·5	
$P-P_2'$	2·4	2·7	2·5	6·3	2·3 ; 4·5
$P-S^*$		16·1			
$P-\overline{S}$		22·5			

No. 4. Earthquake of Aug. 6, 1927. From available seismograms recorded at certain stations, we obtained seismometric values as follows:

Time of commencement at Hongô; 6h 13m 38s.

Epicentre; $\lambda=141°25'$, $\varphi=37°32'$.

TABLE IV.

Station	Δ km.	$P-P_2'$	$P-P^*$	$P-\overline{P}$	$P-S$	$P-S^*$	$P-\overline{S}$
Hongô	250	2·8	5·3	13·5	26·0	32·0	43·0
Titibu	268	4·3	6·4	13·4	28·5	36·5	48·–
Kiyosumi	286	4·0	7·2		29·8	42·6	
Yuigahama	297	4·0	7·9	15·4	28·6	40·0	59·–

In this case also, phases marked with * or – were clearly observed. Therefore, the origin of the disturbance may have been in the uppermost layer at least in the sense as discussed in the former paper by one of us.[3] The P_2' phase was also clearly identified.

---

1) T. MATUZAWA, et. al., *loc. cit.*, 241.

3) T. MATUZAWA, *Bull. Earthq. Res. Inst.*, **5** (1928), 1–29.

No. 5. Earthquake of Aug. 19, 1927. This was an earthquake with considerable intensity and studied by Dr. K. Wadati[4] as a "deep sea earthquake." The data of time of commencement and those of the P–S duration reported from some stations were somewhat inconsistent to determine an exact position of its epicentre. Here it will be tentatively assumed as $\lambda=141°03'$ and $\varphi=34°13'$, according to "Kisyô Yôran." Then with respect to the forerunning phase, we obtained the following values.

TABLE V.

	Koyosumi	Yuigahama	Tôkyô	Titibu
Δ km.	144	199	216	272
$P\text{–}P_2'$	2·1	3·3	2·9	3·0
$P\text{–}P_3'$	4·8			

No. 6. Earthquake of May 27, 1928. The time of commencement observed at Hongô was 18h 51m 36.9s. From reported data and our own seismometric data, the epicentre was to be taken as $\lambda=142°30'$, $\varphi=40°00'$. Hence the position is close to that of earthquake on June 1, 1928, (No. 2.) Characteristics of this earthquake were nearly the same as that in many respects. Seismometric data obtained by us are as follows.

TABLE VI.

Station	Tôgane	Tôkyô	Titibu	Kiyosumi	Yuigahama	Misaki
Δ km.	530	534	576	576	580	596
$P\text{–}P_2'$	3·9	2·9	3·1	3·6	3·6	3·5
$P\text{–}P_3'$		5·1	5·3			5·6
$P\text{–}P^*$	11·6	13·0	12·6	13·7		
$P\text{–}\bar{P}$		25·1				
P–S	48·5	54·–	47·0	28·5		
$P\text{–}P^*$	68·6	70·7	70·0	80·2		

No. 7. Earthquake of May 19, 1928. This earthquake occurred off the Pacific coast of the Kasima Province and its epicentre was estimated as $\lambda=141°01'$ and $\varphi=36°30'$. This position is not far distant from the

---

4) K. WADATI, *Journ. Meteor. Soc. Japan,* [ii] **6** (1928), No. 1.

epicentre of the earthquake of Aug. 27, 1928 already shown as No. 3. The time of commencement observed at Hongô was 18h 32m 32.6s.

Seismometric values with respect to forerunning phases are shown as follows.

TABLE VII.

Station	Tôgane	Tôkyô	Yuigahama	Kiyosumi	Titibu	Misaki
Δ km.	123	142	188	168	182	196
$P-P_2$	1·4	1·5				
$P-P_2'$		2·3	3·9	2·4	2·0	2·6

In this case also as in the case shown in No. 3 the phase defined as P_2 was clearly observed at Tôgane and Tôkyô.

No. 8. The great Tango earthquake on March 7, 1927. A seismometric study of this earthquake by one of the present authors was already published.[3] As widely known this was a very large earthquake so that very sensitive instruments were not available. Especially in the EW component at Hongô (most stations in the Kwantô District were under a similar condition) the movement of the earth crust was so large that certain phases of wave trains were masked by the instrumental vibration and analysis of them was difficult. And yet as the NS component was not so large as the EW, certain characteristics were revealed. Thus seismometric data concerning the forerunning phase determined by us are as follows.

TABLE VIII.

Station	Yuigahama	Misaki	Tôkyô	Kiyosumi
Δ km.	405	415	427	470
$P-P_2'$	4·2	3·6	5·0	3·8

According to Dr. S. I. Kunitomi's investigation,[5] he observed a typical incidence few seconds after the commencement of motion at certain stations as shown in the following table denoted by P$-$iP after his notation.

---

[3] T. MATUZAWA, *loc. cit.*, 244.

[5] S. I. KUNITOMI, *Journ. Meteor. Soc. Japan*, [ii] **5** (1927), No. 8.

TABLE IX.

Station	Δ km	P–iP	Station	Δ km	P–iP
Toyooka	24·6	1·9	Nagoya	176	2·7
Kanazawa	175·7	2·2	Husiki	223	3·1
Kyôto	92·5	2·2	Tadotu	193	2·3
Sumoto	148	2·3	Kôti	267	4·7
Kôbe	106	1·9	Tokusima	179	2·5
Hukui	125·7	1·5	Hamada	280	2·8
Hikone	116	2·7	Hirosima	231	2·4
Gihu	157·2	2·5	Nagano	306	2·3
Yagi	140·5	2·2	Matuyama	285	2·8
Sakai	163	2·4	Sionomisaki	255	3·0
Takayama	209	2·5	Kumagai	399	4·7
Wakayama	160	2·9	Hamamatu	267	4·9
Okayama	149	2·5	Tôkyô	431	5·2

From our view point, this P$-$iP difference seems to be the same as our $P-P_2'$ (refer to Fig. 9.)

No. 9. Earthquake of Dec. 31, 1927. In the cases above shown, the origin of earthquakes was inferred to be in the uppermost layer, that is, very shallow. On the other hand, for elucidation of mechanism of occurrence of such phases, it is necessary to study earthquakes of different epicentral distances as well as of different depth.

The P$-$S duration reported from meteorological stations is shown in the table. (Table X.) The epicentral distance is calculated taking the epicentre as $\lambda=139°35'$, $\varphi=36°07'$ which was determined by us using the method proposed by Dr. R. Takahasi.[6] The time of commencement at Hongô was 14h 51m 06.9s. on Dec. 31, 1927.

---

[6] R. TAKAHASI, *Bull. Earthq. Res. Inst.*, **6 (1929), 231–244.**

TABLE X.

Station	Δ km.	P–S s	Station	Δ km.	P–S s	Station	Δ km.	P–S s
Mito	87	16·4	Takayama	209	25·5	Sendai	264	30·3
Kumagai	17	14·5	Takada	159	23·1	Isinomaki	300	34·0
Maebasi	56	16·0	Tu	318	29·4	Miyako	443	44·0
Tukuba	48	16·0	Utunomiya	56	14·0			
Yokohama	70	18·8	Kôhu	104	15·0	Titibu	46	14·9
Kakioka	55	16·3	Husiki	240	25·9	Hongô	49	16·2
Niigata	208	28·0	Nagoya	263	21·9	Tukuba	50	16·2
Nagano	140	19·7	Onahama	150	20·9	Yuigahama	89	16·8
Mera	129	18·5	Hukui	303	35·2	Misaki	107	17·2
Tyôsi	120	23·4	Gihu	266	25·2	Kiyosumi	119	18·3
Numadu	130	17·4	Hikone	315	30·0			

(The last 6 cases were determined by us.)

A diagram showing the relation between the epicentral distance and the P—S duration is constructed as shown in Fig. 5. From the figure it may be seen that the P—S duration at the epicentre is expected to be 14 seconds or so. Thus, taking into account the stratified structure of the superficial portion of the earth crust and assuming those values obtained in our former paper, the depth of the origin in estimated at 140 km. in round numbers. A set of seismograms obtained at Hongô is shown in Pl. XIV, Fig. 6. As apparent from the figure, in this case also we can define some step-wise incidences of waves marked such as “P_2” “P_2'” and “P_3'”. From seismograms within our reach recorded at other stations, we measured several values as shown below.

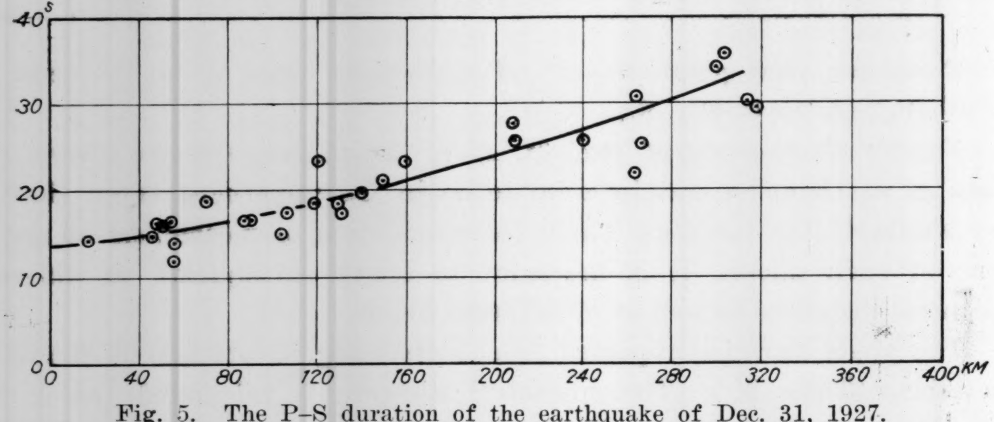

Fig. 5. The P–S duration of the earthquake of Dec. 31, 1927.

TABLE XI.

Station	Δ km.	P–P$_2$	P–P$_2'$	P–P$_3'$	P–S
Titibu	46	1·4	2·1		14·9
Hongô	49	1·2	2·4	5·6	16·2
Tukuba	50	1·0			16·2
Yuigahama	89	1·6	2·5	5·0	16·8
Misaki	107			7·5	17·2
Kiyosumi	119	1·6	2·2		18·3

No. 10. Earthquake of March 29, 1928.[7] This earthquake occurred at a certain place in the Pacific close to the Huzi volcanic zone. Unfortunately, however, the epicentre was too far from the main island of Japan, where observatories are mainly distributed, to determine the exact position. For the sake of reference, reported values of the time of commencement and the duration of the preliminary tremor observed at meteorological stations will be shown.

TABLE XII.

Station	Δ		Time of comm.			Dur. of P.T.	
	1	2	h	m	s	m	s
Sakai	605	798				1	11·6
Miyadu	488	701	14	07	22·8	1	03·6
Tukuba	488	688			33·0		
Matumoto	466	685					58·–
Yagi	376	587			1·0	1	10·8
Hatizyô	173	344			2·–		50·–
Sionomisaki	288	480			4·2		49·4
Gihu	402	625			8·1		52·5
Numazu	347	561			12·7	1	01·2
Mera	347	544			13·3		58·5
Wakayama	372	570			14·0	1	00·–
Muroto	410	573			14·5		57·2
Uwazima	546	688			14·8	1	06·3

(to be continued.)

---

[7] This earthquake was investigated by Dr. K. Wadati as an extremely deep-seated one. *Jour. Meteor. Soc. Japan,* [ii] **6** (1928), No. 5.

TABLE XII. (continued.)

Station	Δ		Time of Comm.			Dur. of P.T.	
	1	2	h	m	s	m	s
Nagoya	368	590	14	07	15·8		51·6
Kyôto	427	629			16·1		57·7
Sumoto	402	600			16·1		56·4
Kôbe	415	616			16·7		57·3
Oosaka	394	600			17·3		58·8
Ibukiyama	432	650			17·3		54·0
Yokohama	393	597			17·9		56·1
Tôkyô	423	625			18·3		59·8
Hongô	425	627			19·8		57·7
Hikone	410	629			19·7		57·6
Tadotu	483	660			21·–	1	03·–
Kumagai	377	671			21·4	1	01·4
Kôti	466	629			21·6		58·9
Utunomiya	504	710			23·9	1	06·8
Tyôsi	466	650			24·3	1	01·5
Kakioka	491	688			24·6	1	01·6
Mito	512	708			26·–	1	05·0
Toyooka	495	710			26·5	1	03·7
Maebasi	472	683			2 71		59·6
Husiki	542	766			28·2	1	09·2
Nagano	516	735			28·7	1	04·7
Oiwake	478	697			28·8		54·0
Okayama	500	688			30·0	1	03·0
Hirosima	592	765			33·2	1	11·5
Takayama	474	694			33·8		50·2
Hukui	487	710			34·8	1	02·6
Takada	559	778			36·0	1	06·1
Hamada	643	816			36·2	1	08·9
Matuyama	542	703			36·3	1	07·1
Miyazaki	632	727			36·4	1	09·7
Ooita	623	756			38·2	1	06·8
Aidu	623	829			42·–	1	13·6
Hukusima	775	858			42·–	1	16·8

(to be continued.)

TABLE XII. (continued.)

Station	Δ		Time of Comm.			Dur. of P.T.	
	1	2	h	m	s	m	s
Onahama	585	780	14	07	45·3	1	08·2
Unzendake	738	853			46·6	1	20·8
Isinomaki	747	943			49·7	1	21·6
Nagasaki	776	887			50·0	1	22·7
Hukuoka	742	875			50·4	1	07·5
Miyako	890	1088		08	00·0	1	27·-
Midusawa	814	1018			00·0	1	27·-
Husan	904	1060			1·-	1	38·-
Simonoseki	705	850			3·-	1	16·-
Akita	892	1062			3·8	1	32·7
Iduhara	850	986			4·2	1	33·-
etc.							

The epicentral distance in column "1" was calculated from an epicentre taken as $\lambda=138°22'$E, $\varphi=32°00'$N and that in "2" from that taken as $\lambda=138°58'$E, $\varphi=30°05'$N. In this case the reported data are somewhat inconsistent mutually. Both epicentres taken above render the fluctuation of reported values from the mean smaller than other assumptions. If the epicentre is taken as "1" the depth of origin of this earthquake must be very deep (above a few hundreds of kilometres) as Mr. K. Wadati[7] stated. On the other hand, if the second position is taken, it is not so extraordinary as the case "1". And yet its origin will be far deep-seated than ordinary inland earthquakes. Seismograms obtained at Hongô are shown in Pl. XV–XVI, Fig. 7 and Fig. 8. If this earthquake was of a shallow origin, certain phases such as P^*, $\overline{P}$, S^* or $\overline{S}$ would be observed. Nevertheless, the preliminary portion is far simple, as apparent from the figures, compared with ordinary cases. And yet, phase P_2' is quite clearly identified in Fig. 7. In this figure the commencement of phase P is somewhat vague, but in Fig. 8 it will clearly be defined, especially in the vertical component. From seismograms at some other stations within our reach the following values were obtained.

---

7) K. WADATI, *loc. cit.*, 249.

TABLE XIII.

Station		Tôkyô	Titibu	Yuigahama	Misaki	Kiyosumi	Tôgane
Δ	1	425	446	378	369	378	433
	2	627	648	581	570	572	618
$P-P_2'$		3·7	4·3	3·0	4·5	4·1	4·9
$P-P_3'$		8·9					8·2
P–S		57·7	59·5	55·1	54·6	56	57·6

No. 11. Earthquake of Nov. 11, 1927. The epicentre of this earthquake was estimated as $\lambda=138°00'E$, $\varphi=36°03'N$ from the time of commencement and the duration of the preliminary tremor reported from meteorological stations. The data adopted from "Kisyô Yôran" are shown below.

TABLE XIV.

Station	Δ	Time of Comm.			Dur. of P.T.
		h	m	s	s
Onahama	278	4	48	11·4	36·5
Tu	202			52·1	33·8
Maebasi	104			49·3	31·6
Iida	62			52·2	32·0
Nagano	70			53·2	23·8
Takada	118			54·0	25·1
Gihu	133			54·9	26·1
Nagoya	144			55·2	24·7
Kumagai	126			55·5	26·3
Husiki	119			56·8	22·7
Tukuba	190			57·3	32·0
Numadu	131			58·9	27·9
Matumoto	22			59·–	18·0
Kakioka	196			59·5	32·6
Hikone	181		49	01·2	27·5
Yagi	264			01·5	
Kôhu	70			02·–	30·–
Miyadu	260			02·7	

(to be continued.)

TABLE XIV. (continued.)

Station	Δ	Time of comm.			Dur. of P.T.
		h	m	s	s
Tôkyô	166	4	49	02·9	29·7
Kanazawa	134			04·–	25·–
Mito	225			04·–	28·7
Toyooka	292			05·0	
Kôbe	297			06·6	
Kyôto	233			07·1	34·5
Mera	202			07·9	28·2
Wakayama	328			08·0	
Oosaka	275			08·4	35·4
Tyôsi	256			09·3	34·5
Niigata	229			10·0	17·0
Oiwake	59				24·0
Sumoto	340			11·6	39·8
Sendai	353			14·2	
Sionomisaki	350			18·0	43·2
Isinomaki	395			18·8	42·0
Tokusima	385			20·5	43·2
Mizusawa	441			21·–	47·–
Okayama	400			23·0	38·0
Akita	448			23·6	48·5
Morioka	494			26·9	53·5
Kôti	490			27·2	52·0
Ibukiyama	160			31·2	
Miyazaki	766			54·6	86·3
Ooita	667			56·0	
Sapporo	832		50	04·5	80·6
etc.					

From these data it may be seen that the origin of this earthquake was very deep-seated. Owing to the limited accuracy of the data the position is not determined very exactly, but the depth of the origin seems to be about 200 km. in round numbers.

In this case also, certain forerunning phases were observed as shown below.

TABLE XV.

Station	Δ km.	P–P_2	P–P_2'
Titibu	100	1·2	2·6
Tôkyô	166		2·0
Yuigahama	164	1·3	3·4

No. 12. Earthquake of Dec. 10, 1927. The epicentre was determined as $\lambda=138°56'$E, $\varphi=38°00'$N from the data shown below, which was adopted from "Kisyô Yôran."

TABLE XVI.

Station	Δ km.	Time of comm.			Dur. of P.T.
		h	m	s	s
Aidu	122				27·6
Tukuba	230				28·0
Niigata	22	11	44	47·5	19·0
Hukusima	147			51·–	20·6
Takada	114			51·6	21·1
Utunomiya	186			52·7	24·7
Sendai	180			54·8	23·3
Yamagata	136			55·9	19·1
Maebasi	180			56·1	24·4
Takayama	250			56·4	32·0
Nagano	160			56·9	22·2
Kumagai	213			57·8	25·5
Kakioka	232			58·0	25·2
Oiwake	188			58·0	31·5
Hamamatu	380			58·0	
Akita	218			59·4	25·8
Midusawa	235		45	00·–	26·–
Mito	231			00·–	25·2
Onahama	217			00·9	23·8
Isinomaki	220			02·6	24·5
Morioka	275			03·8	30·3
Tôkyô	273			05·2	31·1
Tyôsi	312			06·3	28·9

(to be continued.)

TABLE XVI. (continued.)

Station	Δ km.	Time of comm.			Dur. of P.T.	
		h	m	s	m	s
Yokohama	294	11	45	06·7		31·5
Numadu	325			09·1		37·5
Matumoto	212					28·0
Kôhu	266			10·5		
Miyako	323			12·0		33·0
Gihu	344			13·1		45·5
Hikone	383			20·8		44·1
Ibukiyama	361			20·8		40·8
Nagoya	362			21·8		46·0
Hakodate	447			22·0		
Kyôto	434			25·0		54·5
Toyooka	450			26·3		52·4
Husiki	210					31·8
Obihiro	658			40·0		59·0
Sionomisaki	575			40·6	1	04·8
Sapporo	600			41·6		
Kusiro	720		46	00·0	1	02·7
Mera	350		45	11·5		36·0

From these data, the depth of the origin is estimated as about 100 km. in round numbers. Results of our own observations are as follows.

TABLE XVII.

Station	Δ km.	$P-P_2'$	P–S	Remarks
		s	s	
Titibu	230	2·1	27·1	In the record at Kiyosumiyama time marks were not printed. Therefore the P–S duration 34s was determined by interpolation.
Tôkyô (Hongô)	273	4·5	28·7	
Yuigahama	300	4·3	31·2	
Kiyosumiyama	342	5	34	

DISCUSSION.

From examples shown above, in the forerunning portion of earthquake motions some kinds of incidence of train of waves other than the P^* or $\overline{P}$ phase are defined with considerable certainty.

One evidence that these phases are not due to mistake of identification of the P* or $\overline{\text{P}}$ phase is that these phases are found even in the case of extremely deep-seated earthquakes, the origin of which is plausibly inferred to lie below the lower boundary of the second layer.

If this phenomenon is a real entity and not an apparent matter due to certain errors, it is desirable to make clear the mechanism of production of such phases. Generally speaking, the characteristic features of the seismigram will, on one part, be due to the mechanism of occurrence of an earthquake and, on the other part, to the mechanism of propagation of disturbances. For interpretation of seismograms, it is necessary at first

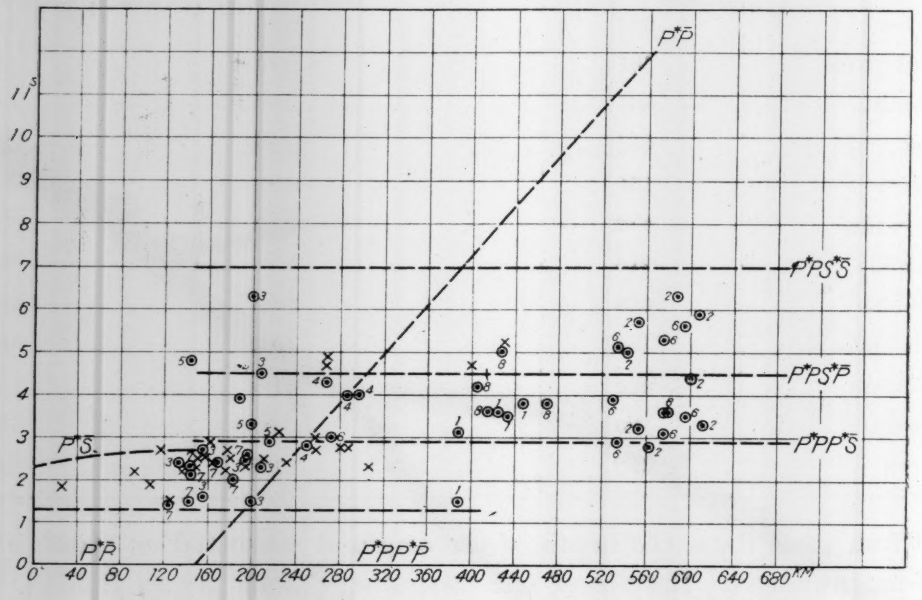

Fig. 9. Interval from the commencement to each phase.

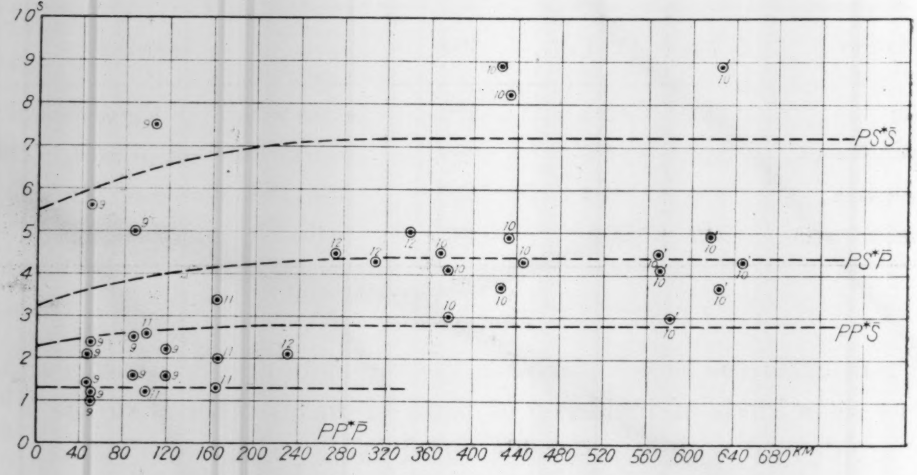

Fig. 10. Interval from the commencement to each phase.

to distinguish these two effects. Thus, in our cases we shall study this point at first.

The data concerning shallow-seated earthquakes (from No. 1 to No. 8 in the foregoing section) are plotted in Fig. 9 and those of deep-seated ones (from No. 9 to No. 12) in Fig. 10.

The fact that these phases occur in different cases in almost similar positions in seismograms may be a strong support to infer that these phases are due to the mechanism of propagation and not to that of generation of earthquakes.

Even if such a case is taken for granted, there may be several ways of elucidation. Some one may attribute this to a mosaic structure of earth's crust. A principal difficulty in this way of explanation is in the typical polarisation of waves, that is, in the observed waves the vertical component of movement at the commencement is generally far distinct compared with the horizontal. Thus a case of apparent earlier commencement of the vertical motion than the horizontal occurs very frequently owing to insufficient sensitivity of the horizontal component of a seismograph. This point was correctly discussed by Visser[8] and Berlage and their way of explanation was similar to that proposed in our former paper.[1]

Now we shall try to explain this phenomenon in a similar way discussed in that paper. The mode of the superficial stratification of the earth's crust will be assumed as determined by one of us,[2,3] and shown in the following table.

TABLE XVIII.

	Thickness	Vel. of dil. waves.	Vel. of dis. waves.
The first layer	20 km.	5·0 km/sec.	3·15 km/sec.
The second layer	30	6·2	3·7
Immediately below the lower boundary of the second layer	50 from the surface.	7·5	4·5

For the sake of simplicity, we will denote the dilatational wave in the first layer by $\overline{P}$, that in the second layer by P^* and that in the lower medium simply by P. With regard to the distortional wave, similar notations such as S, S* and $\overline{\mathrm{S}}$ will be used.

---

[8] S. W. VISSER and H. P. BERLAGE, JUN, *Beitr. z. Geophys.* **19** (1928), 147–152.

[1] T. MATUZAWA, et. al., *loc. cit.*, 241.

[2,3] T. MATUZAWA, *loc. cit.*, 243–244.

At first we shall treat the case when the source of disturbance is in the first layer. As an examplel its depth will be taken 15 km. deep. Results of calculation are shown in Fig. 11.

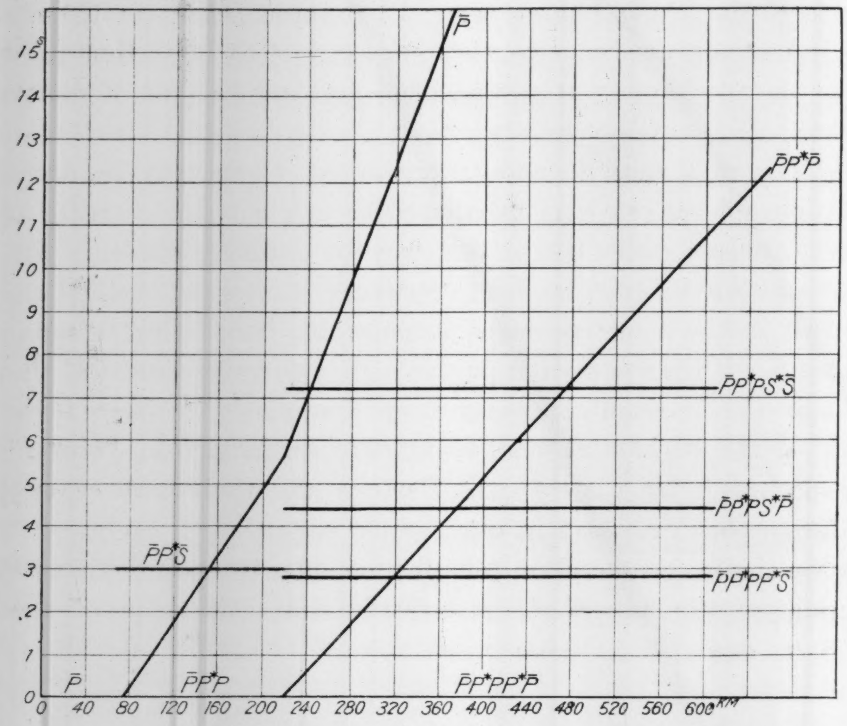

Fig. 11. Interval from the commencement to each phase.

In the figure, intervals of time from the first incidence of a certain phase to that of other kinds of phases are shown as ordinate and the abscissa represents the epicentral distance. For instance, at a place 120 km. from the epicentre the first incidence is that of waves tentatively denoted by $\overline{\mathrm{P}}$ P* $\overline{\mathrm{P}}$ (a disturbance which is started in the first layer as dilatational waves, refracted into the second layer as dilatational and again into the first layer as dilatational waves.) After 1.7 sec. the $\overline{\mathrm{P}}$ phase may set in and after 3 sec. from the commencement the $\overline{\mathrm{P}}$ P* $\overline{\mathrm{S}}$ phase will arrive. Transformation of the dilatatinal wave into the distortional wave or *vice versa* will occur every time when waves are refracted or reflected at a boundary. Thus, there will take place a lot of varieties of waves. Indeed, such will be the case in the real earthquakes. Comparative simple appearance of seismograms due to deep-seated earthquakes is perhaps due to this cause. But here our attention will only be paid to the case of transformation of types at the later stage of propagation. Otherwise, the interval of phases will be affected very much according to the difference of depth of disturbance and of the epicentral distance. On the other hand, our each observed case has much mutual similarity and generality.

In the next place, the case when the source of disturbance is in the depth of 40 km. from the surface, that is, in the second layer, will be treated. The results are shown in Fig. 9 with broken lines. The line at 1.3 sec. is drawn in addition as a local character of the Kwantô district.[1] By this local effect certain phases must undergo some corrections, as far as they concern with observations in the Kwantô District, but the amount is about 0.3 sec. or so even at the greatest.

From the figure, the observed values seem to be somewhat well explained at least qualitatively, considering the practical difficulty of exact identification of incidence of waves. The observed values plotted in Fig. 9 concern with such earthquakes that show the $\overline{\mathrm{P}}$ phase. On the other hand, the curves have been drawn according to the calculation on an assumption that the origin of disturbance is in the middle layer. Therefore, it may seem erroneous to compare them. These earthquakes here shown, however, were all of considerable magnitude. Therefore, if the idea of generation of seismic waves discussed in a paper by one of us[3] is allowed, this way of comparison may be justified. Indeed, some of them may rather be compared with Fig. 11.

In the next place, we shall try the case of deep-seated earthquakes. For example, the depth of the source of disturbance will be assumed as 100 km. from the surface. Our cases depend mainly on the mode of stratification of the superficial earth's crust and less on the position of origin of disturbance. The curves showing the results of calculation are shown in Fig. 10. Comparison with the observed data will make clear that the general features of the observed phenomena are considerably well explained by the assumption.

If it is taken for granted that this observed phenomenon is due to the superficial stratification of the earth's crust, it may naturally be inferred that the practical difficulty of identification of incidence of certain phases is greatly due to the wave length. If the wave length is too large compared with the thickness of stratification it will be practically difficult to distinguish the transformed waves from another. When the epicentral dis-

---

1) T. MATUZAWA, et. al., *loc. cit.*, 241.

3) T. MATUZAWA, *loc. cit.*, 244.

tance is large, it is generally observed that waves with long wave length survive from certain causes. Thus, in the case of distant earthquakes the identification of phases especially with short duration becomes difficult.

The distribution of earthquakes showing the characteristic forerunner with 1.3 sec. duration at certain stations in the Kwantô District was shown in Fig. 7 of our former paper, "On the forerunners of earthquake motions of certain earthquakes, this Bull. **4** (1928) 93." Its explanation then given must undergo now some modification. Indeed, as apparent from Fig. 9 and Fig. 10 even in the case of distant earthquakes (for example, earthquake No. 1) it was clearly observed. Therefore it is inferred that if the movement is sufficiently quick that phase will generally be observed despite of the position of its epicentre. Thus, the typical distribution of earthquakes explained in the former paper is considered to be due to the typical character of earthquakes habitual to each locality. (Of course it does not mean the step-wise occurrence of movements, but the character of waves.) Deep-seated earthquakes contain generally quick movements, and show clearly the typical forerunner.

The P_2' wave discussed in this paper seems to correspond to the P_x wave by Prof. V. Conrad9) in the case of "Schwadorfer Beben."

---

16. Disin-dô no Sakigake no Bubun ni Tuite.

1. Disin-dô no Hazimari no Bubun ni P^* ya $\overline{P}$ to tigatta Nami no Atumari ga kubetu dekiru Baai ga ooi.
2. Sorera no Nami no Seisitu wa mae no Ronbun "Aru Disin no Sindô no Sakigake no Bubun ni tuite, Ihô, Maki no **4** (1928), 85–106" ni nobeta Baai to yoku nite iru.
3. Kono Gensyô no okoru Setumei to sitewa Ue no Ronbun no Baai to dôyô na Kangae ni yori, tada Nami no tutawaru Hayasa ya Tikaku no Kôzô wa Tyosya no Hitori2,3) (Matuzawa) ga mae ni motometa mono wo tukatte kanari na Teido ni setumei dekiru koto wo simesita.
4. Kono Gensyô ni tomonau ikutukano Tyûi mo nobetearu.

---

9) V. Conrad, *Beitr. z. Geophys.*, **20** (1928), 259.
2, 3) T. Matuzawa, *loc. cit.*, 243–244.

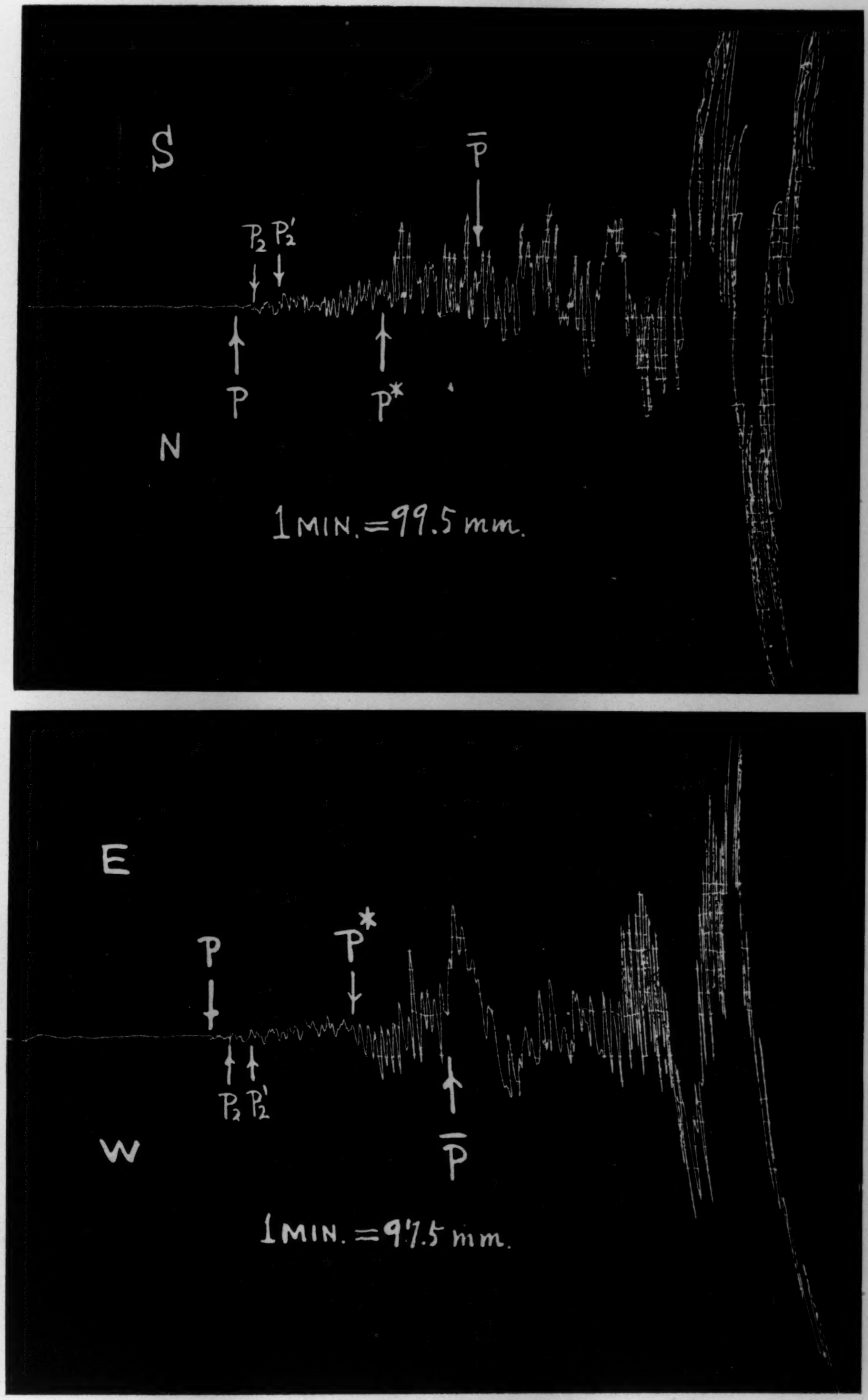

Fig. 1. Earthquake of Jan. 18, 1927.
$\lambda = 142°14'$E, $\varphi = 38°40'$N.
Magnification, 300.

（震研彙報、第七號、圖版、松澤、山田、鈴木）

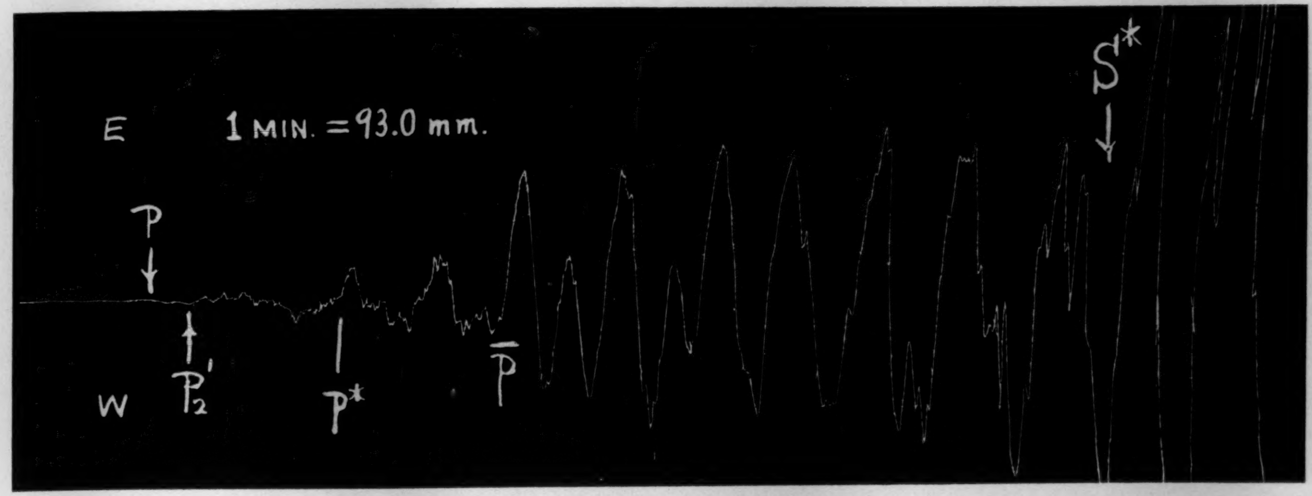

Fig. 2. Earthquake of June 1, 1928.
λ = 143°.3 φ = 39°.8. Recorded at Hongô.
Magnification, 300.

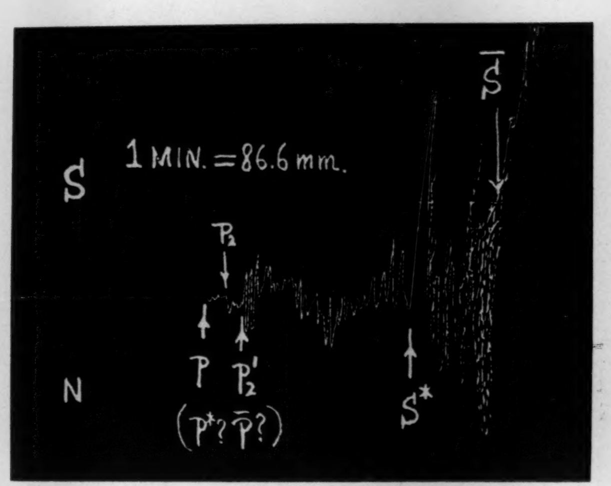

Fig. 4. Earthquake of Aug. 27, 1928.
λ = 141°07′, φ = 36°34′.
Recorded at Hongô.
Magnification, 300.

（震研彙報、第七號、圖版、松澤、山田、鈴木）

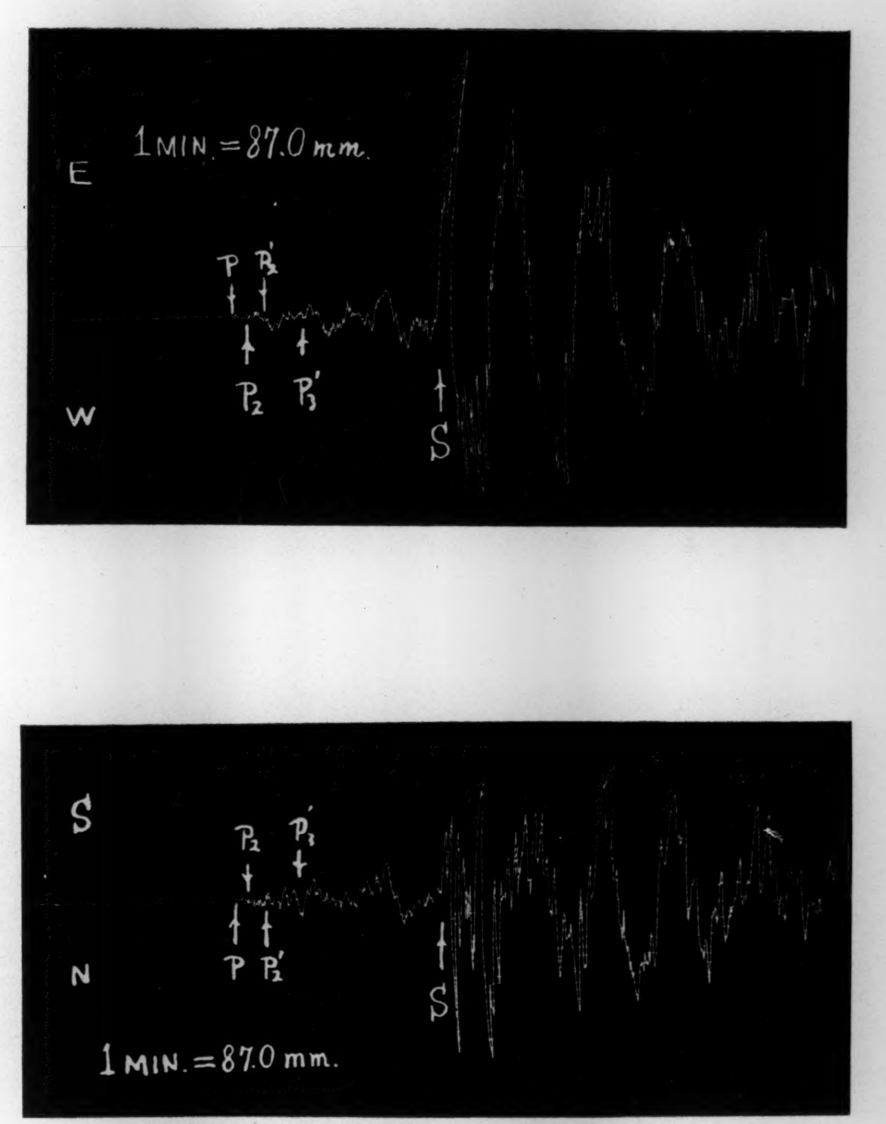

Fig. 6. Earthquake of Dec. 31, 1927.
Recorded at Hongô.

（震研彙報、第七號、圖版、松澤、山田、鈴木）

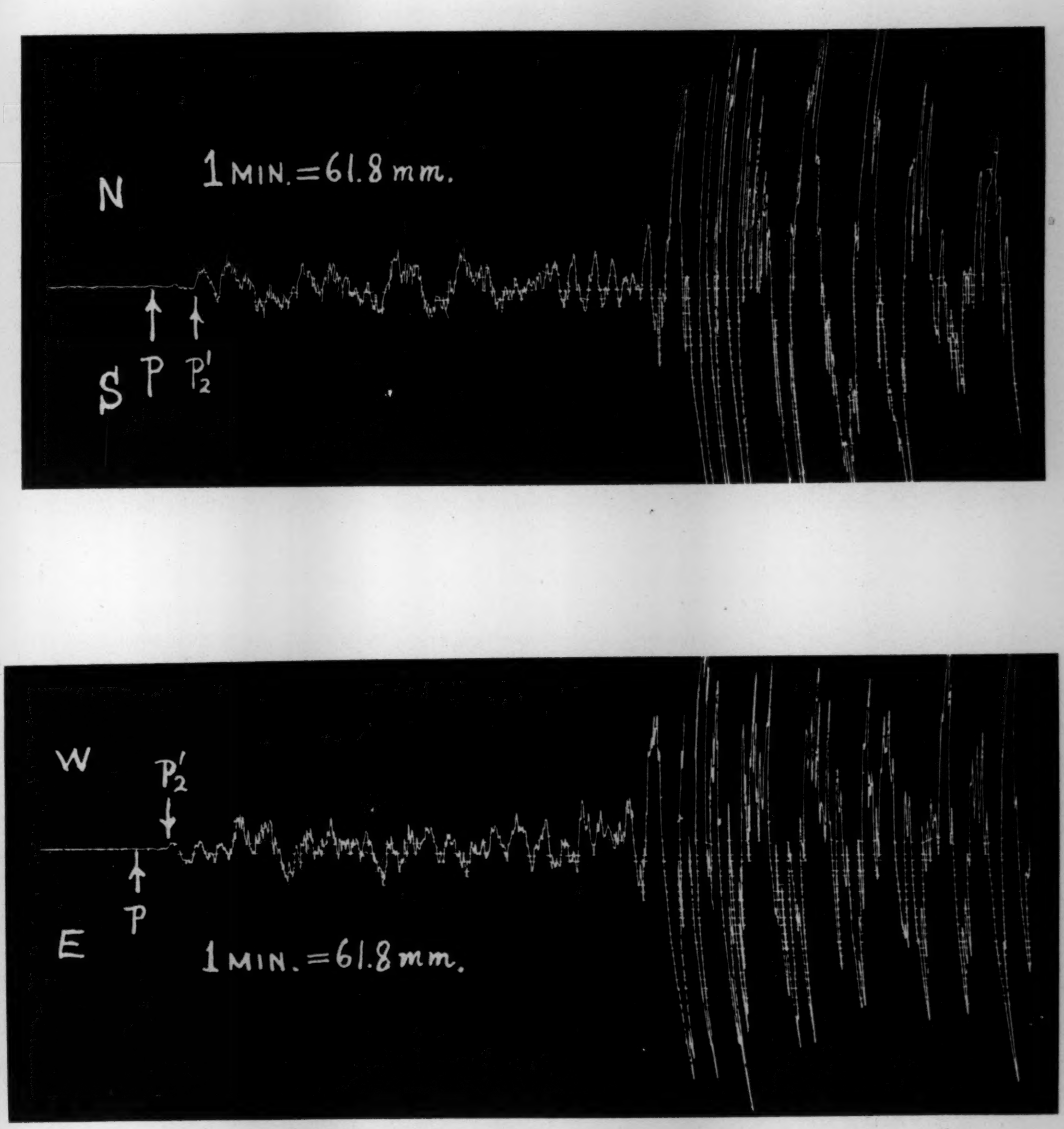

Fig. 7. Earthquake of March 29, 1928.
Recorded at Hongô.

（震研彙報、第七號、圖版、松澤、山田、鈴木）

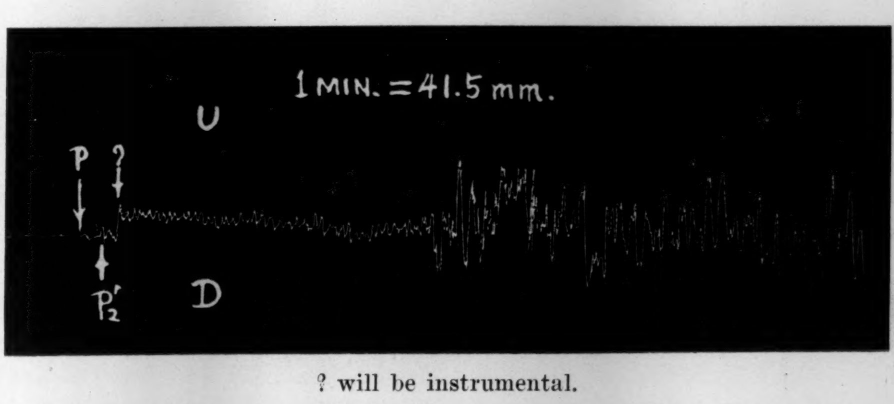

? will be instrumental.

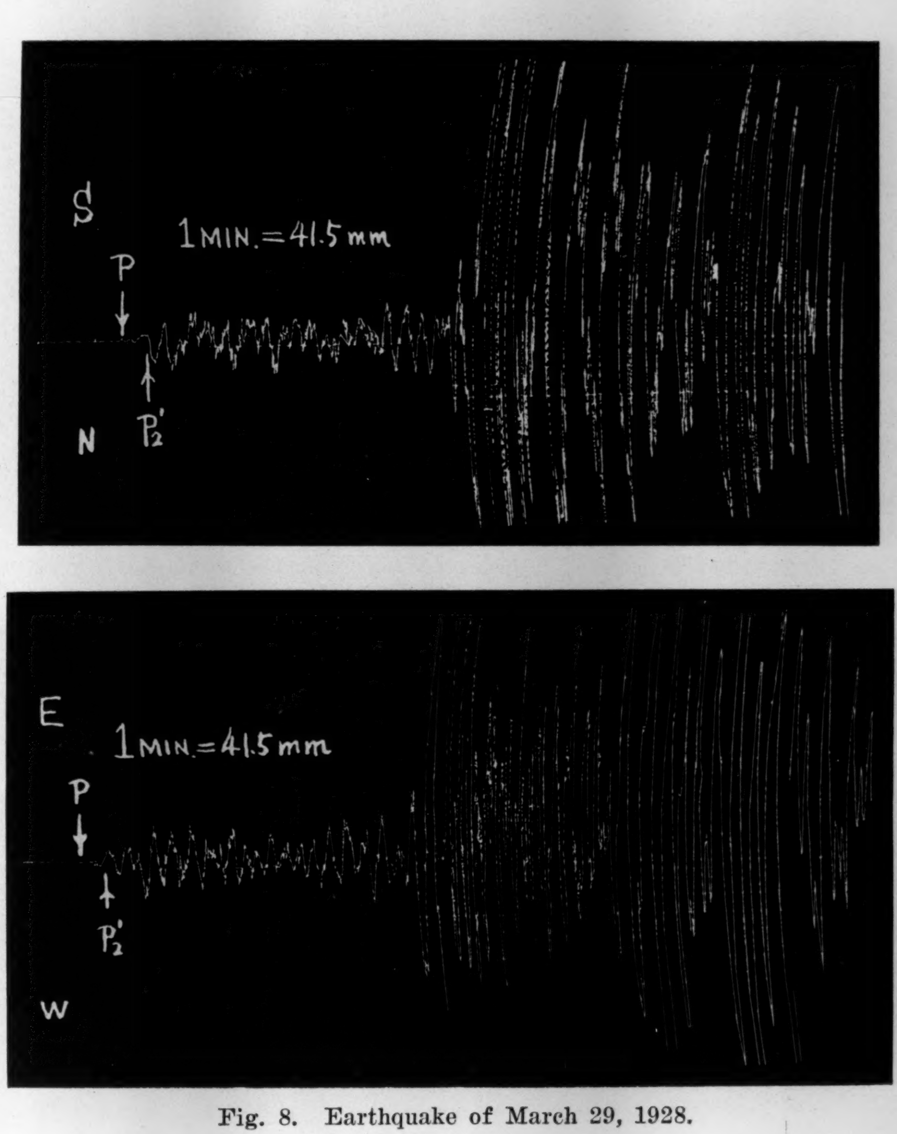

Fig. 8. Earthquake of March 29, 1928.
Recorded at Hongô.

（震研彙報、第七號、圖版、松澤、山田、鈴木）

17. *Die Schwankungen der Makroseismischen Tätigkeitszonen um den Pazifischen Ozean.*1)

von **Naomi MIYABE.**

(Vorgelegt am 20 Nov., 1928.—Eingegangen am 20 Juni, 1929.)

Seit Beginn dieses Jahrhunderts, hat der weit verbreitete Gebrauch der modernen verbesserten Instrumenten es möglich gemacht viele starke Erdbeben, deren Epizentren im Ozean liegen, in verschiedenen Orten zu registieren, häufiger als es früher möglich war. In der Untersuchung über die örtlichen Schwankungen der markroseismischen Tätigkeit in den Kontinenten, worüber Prof. Terada und der Verfasser2) schon berichtet haben, sind solche Erdbeden allerdings nicht mitgezählt worden.

Die Epizentren der Erdbeben im pazifischen Ozean, mit welchen der Verfasser sich hier beschäftigen will, sind, wie schon wohl bekannt, in einer etwas ringförmigen Zone verteilt. Es lässt sich aber zeigen, dasz diese Zone sich in ihrer Lage und Gestalt im Laufe der Zeit einigermaszen verändert hat. Zum Beispiel, änderte sich die Lage und Gestalt dieser Zone im Jahre 1917, für welche die Epizentren der dazwischen ausgebrochenen Erdbeben durch die unten zuerwähnenden Koordinaten a und ψ in Tabelle I

TABELLE I. (1917).

Datum Mon.	Tag.	a	ψ
VI	24	19°·5	280°·2
V	24	22·0	270·0
V	1	29·5	275·4
VI	13	30·0	273·5
VII	29	36·0	188·5
V	9	37·5	161·5
I	30	56·0	101·4
V	31	56·0	76·3

TABELLE II. (1922).

Datum Mon.	Tag.	a	ψ
I	1	19°·5	278°·5
V	12	24·0	147·5
X	24	51·5	111·0
III	4	56·0	106·5
VII	2	56·5	74·0
I	31	63·5	47·2
VI	12	74·5	25·0
I	17	72·0	358·0 (– 2·0)
I	6	76·5	341·0 (–19·0)

---

1) Ein kurzer zusammenfassender Bericht ist schon in *Proc. Imp. Acad.*, **5** (1929), 243 erschienen.

2) T. TERADA und N. MIYABE, *Bull. Earthq. Res. Inst.*, **6** (1929), 333.

bestimmt werden, im Jahre 1922 in einen anderen, für welche die Koordinaten der in diesem Zeitraum ausgebrochenen Erdbeben in Tabelle II angegeben sind. Die in den Tabellen angegebenen Koordinaten a und ψ werden zwar in folgender Weise eingeführt. Seien φ und λ die gewöhnliche geographische Breite und Länge eines Epizentrums. Ein neues sphärisches Koordinatensystem wird so gewählt dasz die Koordinaten des Pols des neuen Systems nach dem älteren Koordinatensystem durch $\varphi=0$, $\lambda=180°$ gegeben sind. Dann lauten die Transformationsgleichungen

$$\cos a = \cos\varphi \cos\lambda_1{}^{3)}, \tag{1}$$

$$\cos\psi = \cos\varphi \frac{\sin\lambda_1}{\sin a}, \tag{2}$$

worin a und ψ die Koordinaten des Epizentrums nach dem neuen System bezeichnen. Der Äquator und die 180° Meridianlinie des älteren Systems sind danach beim neuen System die aufeinander senkrechtfallenden Meridianlinien. Die aus den oben gezeigten Tabellen ersichtliche Tatsache reizt uns noch etwas in den systematischen Versuchen über solchen statistischen Probleme fortzuschreiten.

Die dafür gebrauchte statistische Materiale nimmt der Verfasser aus dem "Rika Nenpyô" (1929) heraus, in welchem die seismologische Kolonne von Prof. A. Imamura verfasst worden sind. Bei der ersten statistischen Behandlung dieser Materiale, sind φ und λ durch die Gleichungen (1) und (2) in das neuen Koordinatensystem transformiert, und alle Azimute um den neuen Pol sind in Oktanten geteilt. Für jede dieser Oktanten und für jeden fünf-jährigen Zeitraum, werden die mittleren Werte von a und ψ berechnet, und in Abb. 1 graphisch dargestellt. Dadurch wird die Schwankungen der seismischen Tätigkeitszone etwas klärer zutage gebracht und man sieht dasz die ringförmige Zone merklich in 4te, 5te und 6te Oktanten[4] schwankt, dasz heiszt, im westlichen Bereiche des pazifischen Ozeans. Hier ist es auch bemerkbar dasz es scheint, in diesen Oktanten, die Lage der Tätigkeitszone sich im Zeitraum 1911–1925 allmählich westwärts gewandert zu haben.

Die Häufigkeitsverhältnisse der Erdbeben in diesen Oktanten sind in Tabelle III angegeben. Das Häufigkeitsmaximum, wie man in der Tabelle III ansieht, wanderte also vom 6ten Oktanten im Zeitraume 1906–1910 zum

---

3) $\lambda_1 = 180° - |\lambda|$, worin λ die Länge eines Epizentrums bezeichnet.

4) Die Oktanten sind in folgender Weise genannt worden; der zwischen $\psi=0$ und $\psi=45°$ liegende Bereich ist 1, der zwischen $\psi=45°$ und $\psi=90°$ liegende Bereich ist 2, u.s.w., worin $\psi=0$ mit dem gewöhnlichen Aquator übereinstimmt.

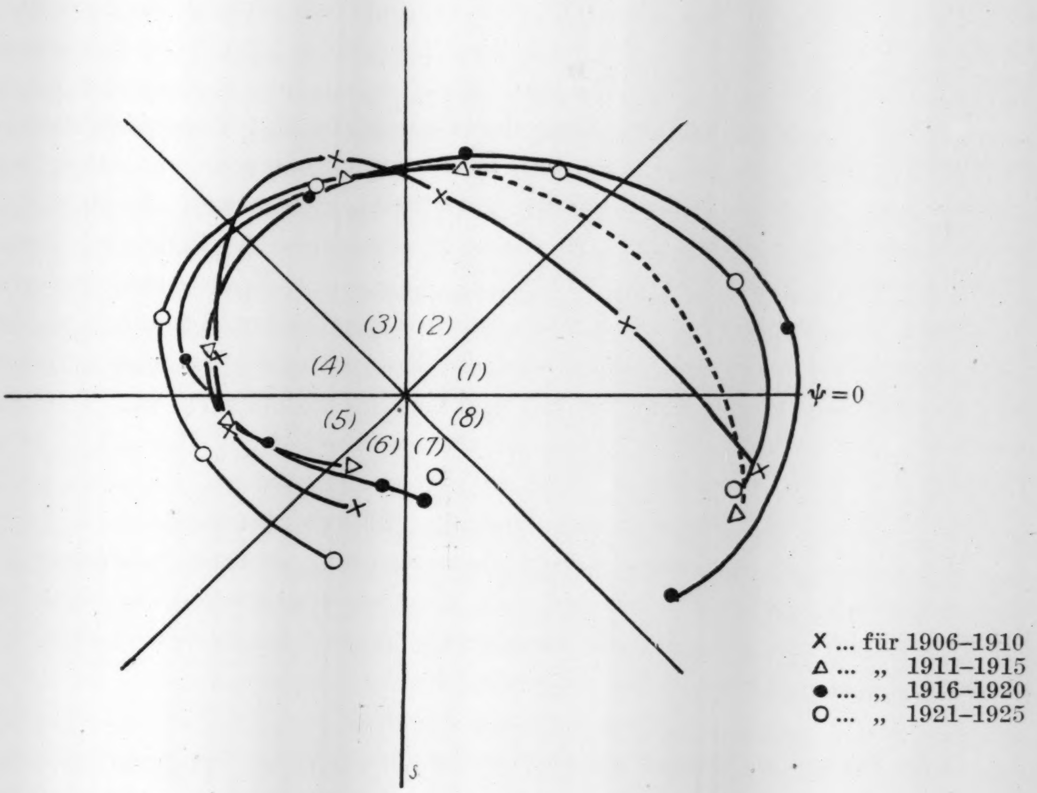

Abb. 1.

4ten Oktanten in 1911–1915, zum 5ten Oktanten in 1916–1920, und zuletzt in 1921–1925 zum 4ten Oktanten.

TABELLE III.

Zeitraum	Oktanten								
	1	2	3	4	5	6	7	8	Summe
1906–1910	3	1	3	4	3	8	0	1	23
1911–1915	0	3	4	7	1	1	0	2	18
1916–1920	1	1	7	8	12	3	6	2	40
1921–1925	3	3	9	10	6	6	2	6	4
1906–1925	7	8	23	29	22	18	8	11	126

Die Ergebnisse dieses vorläufigen Versuches kann folgendermaszen kurz zusammengefasst werden; (i) Es gibt eine merkwürdige Schwankung der makroseismischen Tätigkeitszone um den pazifischen Ozean, die (a) durch die treffende Transformation des Koordinatensystems und (b) durch die zeitliche und räumliche Gruppierung der Erdbeben etwas klärer erkennbar gemacht worden kann. (ii) Was die Häufigkeitsschwankung anbetrifft, zeigt die obere Tabelle dasz das Häufigkeitsmaximum vom 6ten Oktanten in 1906–1910 zum 4ten in 1921–1925 wanderte.

Betrachtet man die Verteilung der Epizentren der Erdbeben um den pazifischen Ozean, so kann man mit Recht annehmen dasz die makroseismische Zone in zwei Hauptbereiche geteilt ist, das heiszt, die nord-und südwest-pazifischen Bereiche. In dem nordpazifischen Bereiche, dessen Raum zwischen $\psi=0$ und $\psi=170°$ fällt, liegen die Epizentren, in erster Näherung, in einem kleinen Kreise um den pazifischen Ozean. In dem südwestpazifischen Bereiche, aber, sind die Epizentren in einer geradlinigen oder groszkreisförmigen Zone verteilt und sie sind südostwärts von Nordwest erstreckt, der gröszte Teil davon in der Südhalbkugel liegend. Diese Teilung der makroseismischen Zone scheint einigermaszen mit dem geologischen Makrostrukturen auf der Erdrinde übereinzustimmen.[5]

Die Erdbeben in jedem diesen Bereiche sind deshalb besonders für sich statistisch untersucht worden. In dem nordpazifischen Bereiche, die Schwankungen des Pols der als kreisförmig angenommene makroseismische Zone wird statistisch nach der folgenden Formel bestimmt

$$a=a_0+x\cos\psi+y\sin\psi.^{6)} \qquad (3)$$

Diese Formel ist formell genau dieselbe wie diejenige für geographischen Polschwankungen, in der jedoch a und ψ in der Statt von φ und λ stehen. Von dieser Gleichung, sind x und y, die Schwankungskomponenten,[7] für

TABELLE IV.

Zeitraum	Schwank. Komp.	
	x	y
1906–1908	$-0{\cdot}169$	$0{\cdot}035$
1909–1911	$0{\cdot}225$	$-0{\cdot}021$
1912–1914	$0{\cdot}137$	$0{\cdot}044$
1915–1917	$0{\cdot}415$	$-0{\cdot}126$
1918–1920	$0{\cdot}478$	$-0{\cdot}303$
1921–1923	$0{\cdot}343$	$-0{\cdot}083$
1924–1926	$0{\cdot}004_5$	$0{\cdot}038$
1927–1928	$0{\cdot}380$	$-0{\cdot}177$

---

[5] Z. B. A. WEGENER, *"Entstehung der Kontinente und Ozeane"* 3 Aufl. (1922), etc.

[6] In dieser Gleichung, a_0 bezeichnet den mittelere Wert von a im 1906–1928.

[7] In diesem Falle, wird ein dreijähriger Zeitraum anstatt des fünfjährigen wie im vorigen Falle, genommen.

jeden dreijährigen Zeitraum nach der Methode der kleinsten Quadraten berechnet worden. Die Werte x und y sind in der Tabelle IV angegeben. Die so bestimmten mitteleren Werte von x und y sind mit den gewöhnlichen Polschwankungsgröszen x' und y' verglichen worden, die von der Commission der Internationalen Polschwankungsuntersuchung (1899.9–1912.0), nach Prof. Wanach (1912.1–1922.7), und Prof. Kimura (1918-Gegenwart) angegeben worden sind.[8] Die Werte x' und y' sind auch aus dem "Rika Nenpyô" genommen und für jeden den Komponenten x und y entsprechenden dreijährigen Zeitraum auf die Mittelwerte gebracht worden. Die zwischen beiden Schwankungskomponenten existierenden

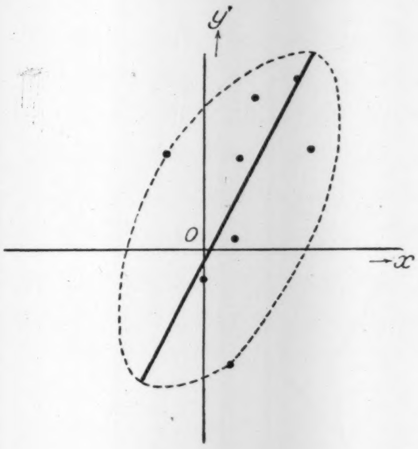

Abb. 2*a*.

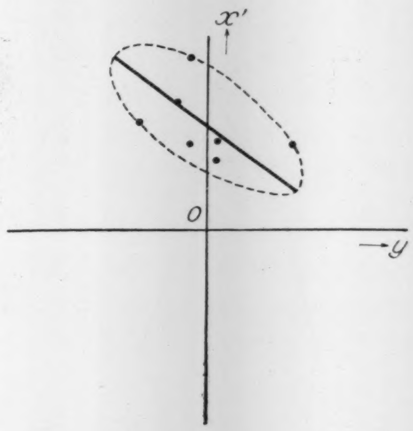

Abb. 2*b*.

Korrelationen sind in Abb. 2*a* und 2*b* dargestellt. In Abb. 2*a*, entsprechen die Ordinaten und Abscissen bezw. y' und x, während in Abb. 2*b*, die Ordinaten x' und Abscissen y angegeben. In den Abbildungen, erscheinen die Punkten resp. in einer Ellipse eingeschlossen, und die längere Achse[9] der Ellipse deutet ein lineares Verhältnis zwischen x und y' in Abb. 2*a* und auch diejenige zwischen y und x' in Abb. 2*b* an. In Abb. 3, sind die Veränderungen der Komponenten der beiden Polschwankungen nach der Zeit gezeigt worden. In Abb. 3 und auch in Abb. 2*a* ,*b*, erscheint die Korrelation positiv zwischen x und y', während sie negativ zwischen x' und y ist. Die lineare Korrelation gilt allerdings nicht streng, sondern lässt sich nur qualitativ anerkennen. In Bezug auf dasselbe Problem, hat bereits Prof. Omori[10]

---

[8] Hierzu lautet die Polschwankungsgleichung: $\varphi=\varphi_0+x'\cos\lambda+y'\sin\lambda$.

[9] Die kurzeren Achsen bedeuten die Abweichungen von den durch die längeren Achsen angedeuteten linearen Verhältnisse.

[10] F. Omori, *Bull. E.I.C.*, **49** (1904), 9. (Japanisch).

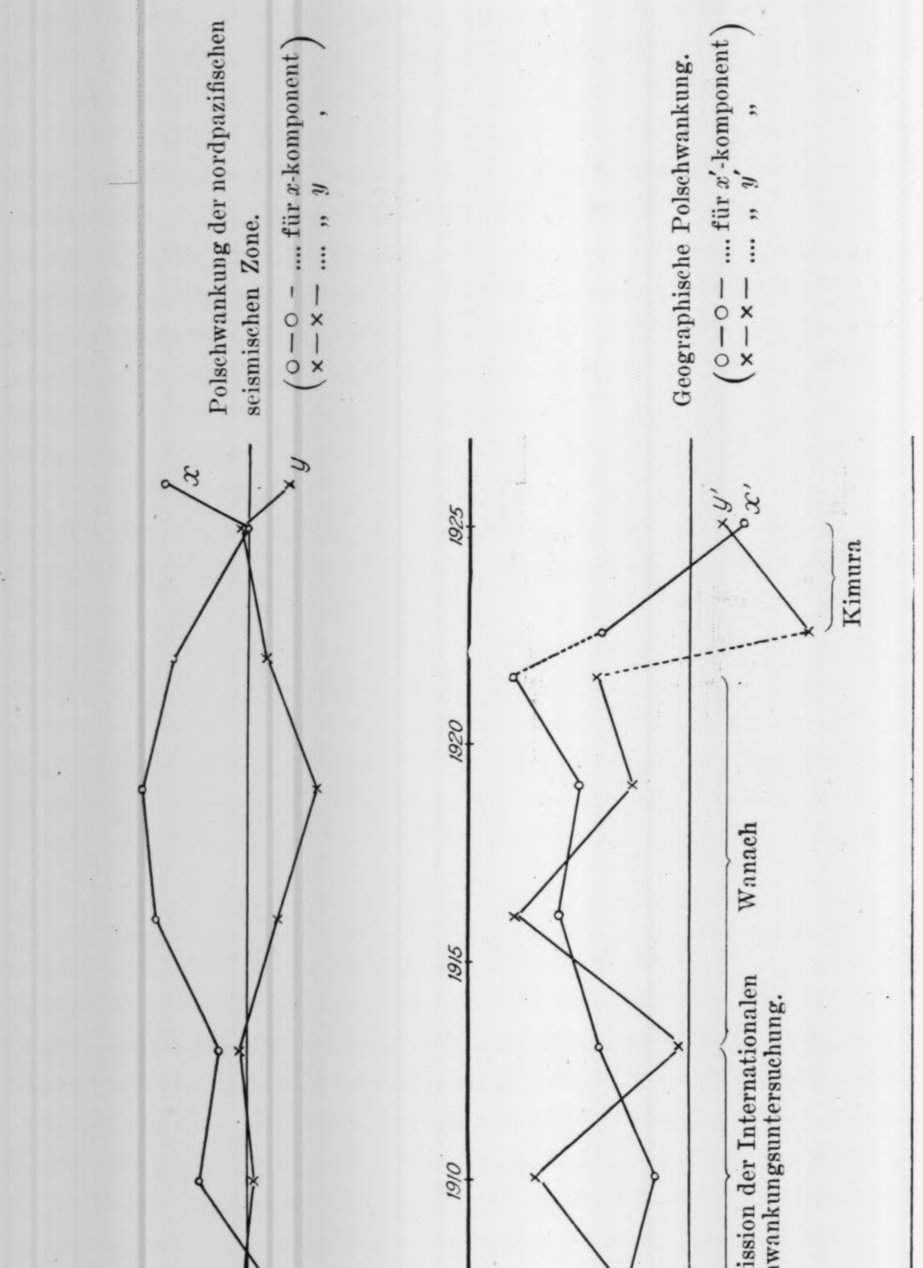
Polschwankung der nordpazifischen seismischen Zone.
(○—○ – .... für x-komponent)
(×—×— .... „ y ,)
Geographische Polschwankung.
(○—○— .... für x'-komponent)
(×—×— .... „ y' „)
x
y
x'
y'
1910
1915
1920
1925
1.0
0.0
−1.0
0.1
0.0
−0.1
Commission der Internationalen Polschwankungsuntersuchung.
Wanach
Kimura

Abb. 3.

einige Versuche ausgeführt. Er schlieszt dasz die starke Beben in solchen Zeiten ausbrechen wo der geographische Pol, in seiner Wanderung, seine extreme Lage erreicht.

So wird es auch nicht allzu entfernt von der Wahrheit sein, wenn man schlieszt dasz die durch den Verfasser eingeführten Schwankungsgröszen x und y mit der geographischen Polschwankung einigermaszen verwandt sind.

Eine dergleiche qualitative Verwandtschaft erhält man auch bezüglich der Sonnenflecken. Die Maxima und Minima der Sonnenflecken sind, in den letzten Zeiten, nach dem "Rika Nenpyô," bezw. in 1906.4, 1917.6 (Max.) und in 1913.6, 1923.6 (Min.) eingetroffen. Hierzu berücksichtigen wir die Tabelle IV oder Abb. 3, und da läszt es sich zeigen dasz die Zeiten der Maxima und Minima der Sonnenflecken näherungsweise mit den Maxima und Minima der Schwankungskomponenten x und y übereinstimmen.

Die Tätigkeitsschwankung der anderen makroseismischen Zone, d.h., diejenige der südpazifischen Zone scheint in folgender Weise mit der nordpazifischen seismischen Tätigkeit verbunden zu sein. Nach der Teilung der seismischen Tätigkeitsbereiche, sind die mittleren Lagen der Epizentren in den beiden Bereichen im jeden dreijährigen Zeitraum berechnet. Abb. 4 stellt diese Ergebnisse dar.

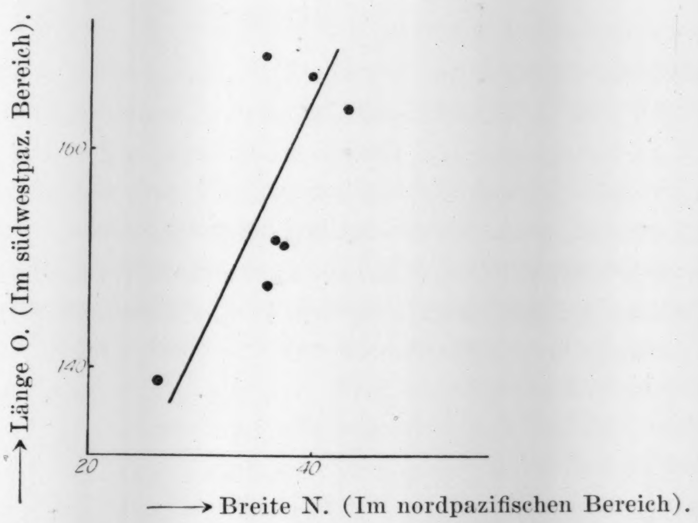

Abb. 4.

In der Abbildung, entsprechen die Ordinaten den mittleren Breiten der Epizentren der nordpazifischen Beben, und die Abscissen den mitteren

Längen der Epizentren der südwestpazifischen Beben. Danach sieht man eine ähnliche qualitative Verwandtschaft indem sich die Nordwärtswanderung der Tätigkeitszone im nordpazifischen Ozean mit der Ostwärtswanderung der Tätigkeitszone im südwestpazifischen Ozean zusammenhängt. Dieses Häufigkeitsverhältnis in dieser beiden seismischen Tätigkeitszonen läszt sich noch nicht sicherlich bestätigen, denn die gesammte Zahl der berücksichtigten Erdbeben ist noch nicht genügend grosz.

Zusammenfassend, darf es gesagt werden dasz es eine merkliche Schwankung oder Wanderung der makroseismischen Tätigkeitszone um den pazifischen Ozean gibt. Die Wanderung des Pols der Tätigkeitszone ist einigermaszen verwandt mit der geographische Polschwankung. Dieselbe qualitative Verwandtschaft erhält man auch bezüglich der Sonnenflecken.

Zum Schlusz, Herrn Professor T. Terada bin ich für seine Anregung und Ratschläge besondere Danke verpflichtet.

---

17. 太平洋に於ける激震帯の移動

地震研究所 宮部直巳

地震の統計的研究の斷片である。

1906-1925 の間に起つた太平洋附近の海底地震の中、理科年表の激震の表に記載されてゐるものを拾ひ出して之を統計的に取扱つた。震源の位置を示すのに、φ 及び λ によらず、$\varphi=0$, $\lambda=180°$ なる點を極とする新らしい座標によつてあらはした。

是等の地震の震源は、概れ、太平洋を環る帯狀の地帯に入れられる。この帯狀地帯、所謂地震帯は、時と共に多少の移動をなすことが認められる。その傾向は太平洋の西側の部分に於いて稍著しく目立つて見える。又、是等の移動は、極の移動等の他の地球物理學的現象とも多少關聯する樣であるが、以上の統計に用ひた材料の數が極めて尠いため決然たる判斷を下すことは出來ない。

18. *Volcanoes of Kôzu-shima.*

By **Hiromichi TSUYA,**

Earthquake Research Institute.

(Read Feb. 19, 1929.—Received March 20, 1929.)

CONTENTS.

Chapter I. Introduction.
Chapter II. Morphological and Structural Features.
Chapter III. Petrography.
Chapter IV. Petrology.
Chapter V. Comparison of Certain Aspects of Volcanoes in the Seven Izu Islands.
Chapter VI. Geological Relations of the Izu Seven Islands to the Izu Peninsula.

Chapter I. Introduction.

The present study is the result of the writer's geological investigation of the insular volcano Kôzu-shima, in the Seven Izu Islands, conducted under the auspices of the Earthquake Research Institute of the Tokyo Imperial University.

The writer made his first visit to the island in August, 1925, when he was a third year student of geology in the University. In the summer of 1928, he made again a field observation. The laboratory study has been done partly in the Geological Institute and partly in the Earthquake Research Institute.

The chief objects of this paper are: first, to describe the geologic structure and the building materials of the island based on the writer's own observation; second, to show relations, geological as well as petrological, of the island to the neighbouring district.

Here the writer expresses his many thanks to Prof. Dr. S. Tsuboi for cordial guidance which he has received constantly and also for revision of his manuscript. He also wishes his hearty acknowledgement to Prof. Dr. B. Koto, Prof. Dr. T. Kato, and Prof. T. Tsujimura for their much valuable suggestions. For the chemical analyses of the rocks collected during his field work the writer is indebted to Mr. S. Tanaka, an analyst of the Earth-

quake Research Institute, whose accurate work has thrown much light on the chemical side of the present study. He also thanks to Mr. K. Yasumuro, a cartographer of the Institute, for the preparation of the geologic map annexed to this paper.

Geographical Sketch.—Kôzu-shima is a member of Izu Shichito, or the Seven Izu Islands (all volcanic), and lies about 60 km. south of Shimoda, a well known harbour at the southern end of the Izu peninsula. The highest point of the island, 574.2 m. above the sea level, is situated at 34°12′58″N. lat. and 139°9′12″E. long. The island is guard-shaped and its length from north to south is about 6 km. and its maximum breadth is about 4 km.[1] There are two islet groups belonging to Kôzu-shima, viz. Tadanae-jima (about 1 km. off the shore of Sanuka-saki, the southeastern headland of the main island) and Ombashi-jima (about 4 km. southwest of the main island).

The whole island is thickly covered with vegetation except on Tenjô-san, the largest volcano on the island; but on the wave-cut sea cliffs around the island and the precipitous cliffs along the river-valleys the rocky structure is well exposed. The southwest upland called Membô is the unique arable land on the island. On the low, steep mountains in the northern half grow wild camellia trees from which is obtained superior camellia oil.

For lack of reliable documents it is not known when the island became inhabited for the first time. In ancient times the island together with other members of the Seven Izu Islands was a place of banishment. At present the island is populated over two thousands. The people there live mainly on fishing, while firming and collection of utilizable seaweeds are in women's hands.

Previous Work.—N. Fukuchi,[2] who studied the island of Nii-jima

---

[1] The island is in its size next to Nii-jima or the fifth of the Seven Izu Islands, each of which having the following dimensions:

	Islands	Due N-S km.	Due E-W km.	Circum. km.	Area sq. km.	Height m. above the sea level
1.	Ô-shima	15	8·5	50	103·8	755
2.	Hachijô-jima	14	7·5	39	71	854·3
	Ko-shima	3	1·5	8	3	616·8
3.	Miyake-jima	7	6	30	56	813·8
4.	Nii-jima	11	2·5	27	23	428·5
	Shikine-jima	2·5	2·5	10·5	4	105
5.	Kôzu-shima	6	4	23	17	574·2
6.	Mikura-jima	5	5	16	16·5	850·8
7.	To-shima	2·3	2·5	7·5	4	507·5

[2] N. FUKUCHI, "Geology of Nii-jima," *Report Earthq. Invest. Com.*, **39** (1902), 4–40, (in Japanese).

which stands in a kindred relation with Kôzu-shima, referred briefly to the geology of Kôzu-shima. According to him, Kôzu-shima is built up of liparitic lavas and the "Shiromama"[3] bed similar to that on Nii-jima. He considered Tenjô-san as a distinct volcano.

In July, 1906, when a great landslide occurred on Kôzu-shima, T. Kato[4] examined in some detail the geological structure and gave a full account of the landslide. On the same occasion S. Noda[5] also visited the island and made a geological investigation.

T. Tsujimura,[6] in his morphological work of Kôzu-shima and Nii-jima in 1918, remarked that these two islands are far too young in their morphological aspects to match the Tertiary volcanoes on the Izu peninsula with which they had used to be correlated.

The sequences of the geological elements of the island, as determined by Kato, Noda, and Tsujimura, are shown in the following table:

Kato	Noda	Tsujimura
1. Alluvium	1. Alluvium	1. Tenjô-san lava (Kuroshima tholoid)
2. Younger tuff-bed (coastal terrace)	2. Tuff-bed	2. Pumice (Shiroshima and Kushigamine homates) "Shiromama" bed
3. Tenjô-san lava (Tenjô-san Takôdo-yama)	3. Tenjô-san lava	3. Massive lavas (tholoids at the northern part)
4. Tachimoto lava (Nachi-san)	4. Upper pumice-bed (Takôdo-yama Chichibu-yama)	4. Older pumice-bed
5. Earlier pumice-bed (Chichibu-yama)	5. Tachimoto lava	5. Oldest liparites
6. Basal lavas.	6. Lower pumice-bed	
	7. Basal lavas	

In 1909, I. Friedländer[7] made some volcanological observations of the Seven Izu Islands, including Kôzu-shima. He recognized there three extinct volcanoes, Chichibu-yama, Takôdo-yama, and Tenjô-san. The rocks collected by him were described later (1914) by C. Bacher.8) According to Bacher, the specimens from Tenjô-san are of "Liparitglas," and those from the southeastern coast are of "Dacitobsidiane."

---

[3] The name "Shiromama" was given originally by N. Fukuchi to the liparitic tuff-bed on Nii-jima, being introduced from mama, a term for the sea-cliff cut into the tuff-bed.

[4] T. Kato, "Landslips in the Kôzu-shima, Izu," *Report Earthq. Invest. Com.*, **63** (1909), 23–32, (in Japanese).

[5] S. Noda, "Geology of Kôzu-shima," *Report Geological Survey*, **2** (1906), 29–38, (in Japanese).

[6] T. Tsujimura, "On the Topography of Kôzu-shima and Nii-jima Islands (Izu)", *Report Earthq. Invest. Com.*, **89** (1918), 57–96, (in Japanese).

[7] I. Friedländer, "Über einige japanische Vulkane," *Mitteilungen der Deutschen Gesellschaft für Natur- und Völkerkunde Ostasiens*, **12** (1909–1910), 66–67.

F. Omori and S. Nakamura9) compiled the historic records of volcanic eruptions in Japan. They interpreted an eruption on August, 838 recorded in a history without mentioning of the spot of the eruption as that occurred on the island.

S. Tsuboi,10) in his work on Volcano Ô-shima, discussed the relation between the basaltic and rhyolitic rocks of the Seven Izu Islands. As to their age relation, he endorsed the Tsujimura's view. He divided the insular volcanoes of Izu into two groups, basaltic Ô-shima group and rhyolitic Nii-jima group, according to the nature of the building materials.

The island has no record of earthquake damage, except one that due to an earthquake in 1899 in the sea between the Zenizu rock and the Inamba islets, 43 km. southwest and 72 km. southeast respectively, of Kôzu-shima. According to Fukuchi,11) who visited Kôzu-shima on that occasion, falling of tombstones and small landslidings were the only effects due to the earthquake. Even the great Kwantô earthquake on Sept. 1st, 1923 which occurred in the sea of Sagami and devastated the larger part of Tokyo was only felt feebly on the island, though Tokyo and Kôzu-shima lie at about the same distance on the opposite side of the probable epicenter of the earthquake.

Chapter II. Morphological and Structural Features.

General Characteristics of the Volcanic Products.—The island is characterized, in common with the other of the Seven Izu Islands, by the absence of the fossiliferous beds. Its building materials are lavas and ejecta of liparitic nature.

The lava-flows are generally thick, sometimes attaining hundred meters

---

8) C. BACHER, *Über die Laven der kleineren Izu Inseln, Ein Beitrag zur Petrographie Japans.* (Munchen, 1914), 16–18.

9) F. OMORI and S. NAKAMURA, "Historical Sketches of the Volcanic Eruptions in Japan," *Report Earthq. Invest. Com.*, **86** (1915), 106–108, (in Japanese).

10) S. TSUBOI, "Volcano Ō-shima, Izu," *Jour. Col. Sci., Tokyo Imp. Univ.*, Art. 6, **43** (1920), 128–133.

11) N. FUKUCHI, "On the Earthquake of Nov. 5th, 1900, off the southern coast of Izu," *Report Earthq. Invest. Com.*, **38** (1902), 39–53, (in Japanese).

in thickness. As is usually the case with extrusive rocks of acid composition, those on Kôzu-shima are glassy, with extremely diversified appearance. They vary from white to black, phyric to aphyric, dense to highly vesicular. These varieties pass to one another through intermediate ones, even within a single mass of lava. Spherulitic structure due to small spherulitic growths is seen in almost all the lavas. Some of the lavas have flow-structure marked by straight, tortuous, or convoluted lamination resulted from (a) the alternation of thin layers of obsidian and pumice; (b) the banding of the lavas of different shades of color; and (c) the arrangement of spherulites in line. The weathered surface of these laminated lavas show ridges and furrows due to different resistance to weathering. The lava exposed on the northern coast of the Membô upland exhibits the most striking flow-structure consisting of beautiful color bands.

Fragmentary materials constitute some portions of the island, either as tuff-beds made up of fine ashes or as agglomerate-beds composed of blocks mingled with bread-crust bombs, thread-lace scoria, lapilli, and ashes. Most of the ejected fragments are white juvenile pumices of all grades in size. Mingled with these are found fragments of preexisting rocks. They are stony, vitreous, or pumiceous, according to the nature of the preexisting rocks from whose shattered portions they came on the subsequent eruptions. Accessory or accidental blocks of quartz-porphyry, hornblende-andesite, two-pyroxene-andesite, and porphyritic hornblende-diorite are sporadically found imbedded in the beds, but no fragment of sedimentary rocks has ever been found.

The beds show some signs of stratification, often very finely laminated; nevertheless they have probably been accumulated under subaerial condition. They yield yet no organic remain with the exception of small pieces of carbonized wood, so that it is not certain in what geological age they were formed. There is, however, little doubt about that at least the youngest lava (Tenjô-san lava) on the island is not so old as the lavas of the similar character on the Izu peninsula.

General Features.—Kôzu-shima is not very simple in its morphological features. The mountains are generally flat-topped or dome-shaped rather than conical. Although the present surficial features are the result of counteraction of repeated vulcanicity and erosion, the initial structure of the volcanoes and the nature of the building materials are important factors for the development of the present features.

The order of succession of the volcanic product was determined by geologic structures, but partly by the morphological features effected by denudation. The volcanic sequence, from younger to older is:

(1) Tenjô-san lava (lava of the fourth period).
(2) Cinder-cone ejecta (Shiroshima and Kushigamine cinder-cones).
(3) "Shiromama" ejecta-bed.
(4) Jôgoro-yama, Kaminari-yama, Anagi-yama, and Kôbe-yama lavas (lavas of the third period).
(5) Nachi-san and Takôdo-yama lavas (lavas of the second period).
(6) Chichibu-yama ejecta-bed.
(7) Lavas of the first period.

(1) Tenjô-san Lava.—This lava is the latest one on the island forming the Tenjô-san volcano.

Tenjô-san is a cupola-shaped volcano, its side sloping at an angle of about 35°, and is superior in bulk as well as in height to any of the other volcanoes on the island. It rises to a height of 574.2 m. above the sea level, but to a height varying from 180 m. to 400 m. above the ground around. The base of the volcano is 2.2 km. long and 1.7 km. broad, its circumference being 6.4 km., while the top area is elliptical, 2 km. long and 1 km. broad, with the circumference of about 4.5 km. At the summit is an area of 1.3 sq. km. with the general feature of the so-called "Blockmeer." There the surface of the lava, being cracked and broken in blocks (Pl. XVII, Fig. 1), is dotted with such irregular eminences of broken lava rising to a height from 20 m. to 50 m. as long extended hills with sharp or rounded edge, conical protuberances, dome-shaped swellings, and ring-walls with various diameters. Accordingly, the intervening spaces are also irregular in shape as well as in height. Some of these spaces are hollow, occasionally filled with water, like crater having a shape of inverted cone. Some others are depressed in crescentic form and look like atrio with flat bottoms. Such depressed spaces are covered with white, sandy detritus accumulated like a snow-drift or sand-dune.

The irregularity of the lava surface is liable to be created whenever viscous lava is extruded. When a viscous lava is dammed up to form the so-called "Staukuppe," concentric folding of the lava surface may be formed around the crater. Tsujimura remarked such a case on the summit of Tenjô-san, saying that the small eminences on the summit are arranged in two or three concentric lines.

The northern half of the summit is almost barren; while the southern half is grown with both tiny bushes and short grasses.

The northern and southwestern flanks show the natural slope of talus formed of broken lava detached from the massive lava above. The upper parts of these flanks are scarcely clothed by herbage, the rocky skin being excavated to show frequent scars and slips. The ravines there are spoon-shaped and become narrower as well as shallower downwards.

The southern and eastern flanks have been remarkably demolished and show there steep slope (about 40°). The southern flank fronting the sea of Takô rests on the erosible "Shiromama" bed and looks down directly the sea. Accordingly, the talus which developed primarily there just as now observed on the southwestern flank was largely destroyed at its foot by the sea-waves (Pl. XVII, Fig. 2). The lower steep slope is furrowed by trenches and the sharp ridges between the trenches are the parts left behind denudation of the primary talus. On that side, therefore, the steep slope rises to an altitude of 400 m. above the sea level and thence upward a vertical lava cliff, 100 m. in height, stands high forming an abrupt escarpment. The eastern flank of Tenjô-san shows (Pl. XVII, Fig. 3), in the same manner, vertical escarpment of the upper half and deeply dissected talus of the lower. The foot of the flank has not been attacked by the sea-waves, but there cutting-back at the heads of gorges traversing the hill around is effective for the destruction of the talus.

As understood from its topographical feature, the volcano is built up of a single lava, about 200 m. thick, rising from the foundation formed of the ejecta of both Shiroshima and Kushigamine cinder-cones and also of "Shiromama" (p. 277). Inner structure of the lava is distinctly visible on the cliff around. The southern cliff fronting the sea of Takô reveals the lava drawn lines by the flow-banding seemingly dipping to the west. The southern half of the eastern flank shows the lava having flow-structure descending to the south, while the northern half to the north. The lava exposed on the northern flank shows onion-banding which is a characteristic of the so-called "Staukuppe."

From the structure described, it is inferred that the lava was extruded, in a very viscous condition, through an orifice which might be somewhat northsided, probably from a crater adjoining to that of the Shiroshima cinder-cone. The lava was mainly spread to the south, though not distant, because of falling of the ground beneath to that direction; while it was dammed up to the north, resulting in the characteristic structure of the "Staukuppe."

The lava displays vesicular structure at the surface, yet it has not been weathered out in soil, showing very fresh appearance. There can be little doubt about that the last great volcanic activity on that island was the effusion of the Tenjô-san lava.

(2) Cinder-cone Ejecta.—This ejecta form the Shiroshima and Kushigamine cinder-cones.

Shiroshima cinder-cone occupies only a small portion of the northwestern flank of Tenjô-san (Pl. XVII, Fig. 4). It is a snow-white cone composed throughout of liparitic ejecta, resting on the erosion surface of the Nachi-san lava either directly or with the Chichibu-yama ejecta-bed (cf. p. 279) between. Thus, its height above the base is about 250 m., though about 510 m. above the sea level. The eastern half of the cone was destroyed when the Tenjô-san lava was extruded out of the neighbouring vent. At the summit there is a crescentic crater (Pl. XVIII, Fig. 1), a quarter segment of a circular one whose diameter would be about 300 m. if the cone had been a complete form. The northwestern flank of the cone is the only part preserved. It is 20–25° in slope and convex outwards. Neither valleys nor gulches have been excavated on that flank.

The inner structure of the cone is exposed on the rocky cliff at the valley-head of the Kawara, a temporary river which rises at the northwestern flank of Tenjô-san and flows into the sea at Mae-hama. On the cliff is seen the stratified bed of the cone, half-destroyed by the extrusion of the Tenjô-san lava which at that place makes a bluff of 200 m. high. The bed dips apparently southward with an angle of about 40°. Near the upper end of the cliff, that is, near the crater-lip of the cone the bed becomes apparently horizontal. At the northwestern foot of the cone is exposed the bed dipping divergently according to the nature of the underlying ground, though generally about 20° away from the crater. About there, loose materials of liparitic nature, ashes, sands, and lapilli, are finely stratified, occasionally being alternated as much as five times in the thickness of one meter. Pisolitic concretions of ash, 0.5–10 mm. in diameter, are found abundantly.

As above-mentioned the bed exhibits generally the "quaquaversal dip," in other words, it dips away on all sides from the crater and forms a typical cinder-cone. In front of the cliff of the Nachi-san lava facing the valley of the Kawara, the bed of the cone dips in a high angle (70°) off the cliff. Accordingly, it is inferred that the cliff of the Nachi-san lava was already present at the time when the cinder-cone was formed. From its morphological aspect and also from the nature of its products, the cone is supposed to owe its formation to some eruption of comparatively recent date, though earlier than the extrusion of the Tenjô-san lava.

On the eastern side of Tenjô-san is seen another diminutive cone called Kushigamine (Pl. XVIII, Fig. 2). Its height above the surrounding ground is not more than 50 m., while that above the sea level matches the height of

Shiroshima. The diameters of the base and the top of the cone are 500 m. and 200 m. respectively. The northern flank of the cone shows a smooth natural slope, about 30°, being scarcely furrowed by mountain torrents; while its foot is about to be destructed, since the Jôgoro-yama lava beneath has been penetrated by deep gorges. On the other hand, denudation has acted with greater effect on the southern side where a deep gorge has been excavated up to the summit of the cone. Fine stratification of the building materials is seen on the valley-wall. The western side is covered with the Tenjô-san lava. At the contact with the overlying Tenjô-san lava, the white ash of the cone is stained and becomes hard.

The building materials of the cone are the same as those of the Shiroshima. The stratified bed dips away on all sides from the center. In the bed are found pisolitic concretions.

(3) "Shiromama" Ejecta-bed.—''Shiromama'' ejecta-bed is a formation of rudely stratified ejecta which covers the decomposition surface of the older volcanic products, both lavas and ejecta (Pl. XVIII, Fig. 3). Its distribution is mainly confined to the low ground near the sea-shore. It makes a cliff of about 20 m. in height fronting the sea and is suggestive of a coastal terrace-deposit (Pl. XVIII, Fig. 4). Inlets are apt to be formed at the places (Takô-hama, Mae-hama, Sawajiri-hama, and Naga-hama) where the bed is developed, since the bed is loose and erosible. The bed is traced landwards along the valley of the Kawara, but soon is kept out of sight by the fluviatile deposit of the valley. It is also found on the flat land at the pass between Takôdo-yama and Chichibu-yama. There the bed rests unconformably on the Chichibu-yama ejecta-bed whose surface has been decomposed in black soil.

The stratification of the bed is visible only from a distance, larger fragments being rudely conglomerated in some horizons (Pl. XVIII, Fig. 3). The building materials are volcanic ashes, sands, lapilli, and blocks of liparitic nature. They are pumiceous, glassy, or felsitic. Besides these are found blocks of hornblende-andesite and quartz-porphyry. Pieces of carbonized wood are often met with in the lower horizons of the bed. No other organic remain has ever been discovered. Accordingly, it is inferred that the deposition of the volcanic fragments was subaerial. In addition, the deposit is of neither fluviatile nor submarine, if not at its very base which is now largely invisible.

The deposition of the ''Shiromama'' ejecta must have preceded the formation of the Shiroshima and Kushigamine cinder-cones, though both are of successive eruptions. The juvenile ejecta in the bed are identical in petrographic characters with those of the cinder-cones. Probably, the cinder cones were formed by eruptions with decreasing vulcanicity, following the paroxysmal eruptions by which the "Shiromama" ejecta-bed was formed.

(4) Jôgoro-yama, Kaminari-yama, Anagi-yama, and Kôbe-yama Lavas.—The four mountains along the northern sea-coast, viz. Jôgoro-yama, Kaminari-yama, Anagi-yama, and Kôbe-yama are capped with the lavas resting on the Chichibu-yama ejecta-bed. Of the four just-mentioned mountains, the first one is partially covered with the Kushigamine ejecta, though the others are bare (Pl. XIX, Fig. 1).

The Jôgoro-yama lava is the same as the Kaminari-yama lava, both having been primarily connected, but subsequently separated by the erosion. The inner structur of the lava is exposed on the valley-walls which bound the mountains on the west, and also on the steep and rocky declivities by which Jôgoro-yama and Kaminari-yama rise up to the height of 460 m. and 300 m. respectively from the eastern seashore.

The Anagi-yama lava forms the top of the dome-shaped Anagi-yama, a mountain situated between Kaminari-yama and Kôbe-yama, attaining about 100 m. in thickness. It has a horseshoe-shaped depression on the summit. The pumiceous surface of the lava is bare, though the just-mentioned depression is piled deep with huge blocks of the lava. This lava is probably of contemporaneous extrusion, with that of the Jôgoro-yama lava if the two were not extruded from a single vent.

At the northwestern corner of the island rises a dome-shaped hill called Kôbe-yama, one of the most remarkable and perfect volcanoes on the island (Pl. XIX, Fig. 2). It slopes on the west, east, and south sides at an angle of 40°, while the northern flank is somewhat greater in inclination. The steep slopes (Pl. XIX, Fig. 3) show the talus formed of broken lava. The Kôbe-yama lava is about 100 m. in thickness. Its surface is pumiceous, variegated, and cracked into irregular patterns. Thus, the summit of the hill is uneven field of block lava, small eminences and hollows lying scattered as on the summit of Tenjô-san. At the center of the summit is a crater-like depression breached towards the northwest and southeast. From the inside of the depression run down steep-sided valleys through the V-shaped clefts on the rim. The height of the rim around the central depression is nearly 50 m. and on the northern side of the depression towers up precipitous cliff of uncovered lava. The bottom of the depression is piled up with huge blocks of the lava detached from the cliffs around. The depression may have been resulted from breaking-down of the upper surface of the lava.

(5) Nachi-san and Takôdo-yama Lavas.—The lavas are represented by the biotite-plagioliparites of Nachi-san and Takôdo-yama.

The lava exposed on the cliffs which bound the west side of Nachi-san (Pl. XIX, Fig. 4), a mountain forming the basement of the Shiroshima cinder-cone, is about 100 m. in thickness and is sandwiched in between the lower and upper parts of the Chichibu-yama ejecta-bed.

The Takôdo-yama lava forms the top of Takôdo-yama which stands to the southwest of Tenjô-san. Takôdo-yama is a dome-shaped hill (Pl. XX, Fig. 1), 304 m. high above the sea level or 150 m. above the foundation. A pointed eminence on its central summit gives the hill, when viewed from the western side, something of the shape of a peach. On the other hand, its singular shape which attracts attention from a distance to the southeast is compared to a mortar placed bottom upward. The lateral slope has an inclination of about 35°. The summit is elongated in the E-W direction and flattened, being covered thickly with black soil. About a dozen radial valleys are furrowed on the flank around the hill, all having their sources near the summit and on the valley-walls is exposed the lava. The lava occupies only the upper half of the hill and forms a lava-flow of about 130 m. in thickness. It rests on the Chichibu-yama ejecta-bed. High above the pass, Akabane-toge, from the village to the shore of the bay of Takô and within 15 m. of the pass stands an outcrop of the Chichibu-yama ejecta-bed (Pl. XXI, Fig. 1) directly covered with the Takôdo-yama lava.

From the structures described above, it is suggested that the Nachi-san and Takôdo-yama lavas were extruded in the same period with the deposition of the Chichibu-yama ejecta-bed, or a little later.

(6) Chichibu-yama Ejecta-bed.—Covering the erosion surface of the lavas of the first period, the Chichibu-yama ejecta-bed is widely distributed over the island, partially covered with the succeeding formations (Pl. XX, Fig. 2). It forms notched irregular hills of rather low latitude, Chichibu-yama, Takô-yama, and Takane-yama, etc.

Chichibu-yama is the most distinguished mountain consisting of the ejecta. It is situated at the northeastern corner of the Membô upland (Pl. XX, Fig. 3). The land rises gradually to the summit of Chichibu-yama, 282.9 m. high above the sea level, with an inclination from 5° at the skirt to 10° near the summit. The eastern flank of the mountain descends abruptly to the bay of Miura, showing slope as steep as 70° in its lower part and about 50° in the upper. The northern flank is also steep in slope and is incised by a number of empty valleys. On these steep slopes is exposed the horizontal bed of the ejecta. A distant view of the mountain is suggestive to a single volcano, but actually the mountain has been resulted from erosion acting on the horizontal ejecta-bed.

The thickness of the bed varies from a few to 150 m. as is estimated at Chichibu-yama. This is largely due to the subsequent erosion acting on the loose deposit of the ejecta. The center of ejection is entirely obliterated owing to the advanced erosion. Nothing can be inferred as to the position of the centre from the stratification of the bed, since the bed is generally horizontal (Pl. XX, Fig. 4), except at the places where it covers the uneven surface of the underlying lavas. Occasionally, the bed shows false-bedding and unconformity due to temporary erosion. The surface of the underlying lavas exhibits subaerial decomposition, the black soil being sharply contiguous to the overlying white ejecta-bed. Accordingly, it is inferred that the deposition of the ejecta took place on land.

The building materials of the bed are volcanic ashes, sands, lapilli, and blocks (Pl. XXI, Fig. 1), most of them being juvenile in origin. Among them, pumiceous lapilli are exceedingly abundant. Blocks, 5–20 cm. in diameter, of glassy, spherulitic, and felsitic lavas are intercalated in some definite horizons or are scattered through the finer ejecta. Being intermingled with these, are found rather small blocks of quartz-porphyry, hornblende-andesite, porphyritic hornblende-diorite, and two-pyroxene-andesite. Fragments of carbonized wood are also found.

The doposition of the Chichibu-yama ejecta-bed was nearly contemporaneous with the extrusion of the Nachi-san and Takôdo-yama lavas.

(7) Lavas of the First Period.—As far as the visible part of the island is concerned, the liparitic lavas exposed on the sea cliffs around are the oldest and form the foundation of the island (Pl. XXI, Figs. 2, 3). They are of various types which may be grouped as follows:

α-Lava (Potash-liparite).
β-Lava (Hypersthene-plagioliparite).
γ-Lava (Hornblende-bearing hypersthene-plagioliparite).
δ-Lava (Hornblende-plagioliparite).
ε-Lava (Biotite-plagioliparite).

The order of extrusion of these lavas is difficult to be determined.

Chapter III. Petrography.

According to T. Kato,[12] the lavas of Kôzu-shima are: basal lavas, Tachimoto lava, and Tenjô-san lava, enumerating in the order of extrusion, from older to younger. Among the basal lavas he distinguished four varieties, viz. obsidian, agglomerate lava, lava of Kohama type, and spherulitic lava. In his petrographic descriptions he mentioned of orthoclase, plagioclase, and biotite as essential minerals found in all these lavas. Beyond these sporadic occurrence of hypersthene in the basal lavas was remarked.

---

[12] T. KATO, *loc. cit.*

Bacher,[13] on the other hand, described four rock specimens collected by Friedländer, two from Tenjô-san and two from the southeastern coast.

These descriptions, however, are fragmentary and not sufficiently detailed. Here more systematic descriptions of the rocks of Kôzu-shima are given in the order as follows:

I. Lava of the Fourth Period.
  1) Biotite-plagioliparite .... Tenjô-san lava

II. Shiroshima and Kushigamine Ejecta.
  2) Biotite-plagioliparite .... Juvenile ejecta

III. "Shiromama" Ejecta.
  3) Biotite-plagioliparite .... Do

IV. Lavas of the Third Period.
  4) Biotite-plagioliparite .... { Jôgoro-yama lava, Anagi-yama lava, Kôbe-yama lava

V. Lavas of the Second Period.
  5) Biotite-plagioliparite .... { Nachi-san lava, Takôdo-yama lava

VI. Chichibu-yama Ejecta.
  6) Biotite-plagioliparite .... Juvenile ejecta
  7) Liparite
  8) Quartz-porphyry
  9) Porphyritic hornblende-diorite
  10) Hornblende-andesite
  11) Two-pyroxene-andesite
  } ... Accessory ejecta (7–11)

VII. Lavas of the First Period.
  12) Biotite-plagioliparite .... ε-Lava
  13) Hornblende-plagioliparite .... δ-Lava
  14) Hornblende-bearing hypersthene-plagioliparite .... γ-Lava
  15) Hypersthene-plagioliparite .... β-Lava
    (Basic xenoliths)
  16) Potash-liparite .... α-Lava

---

13) C. Bacher, *loc. cit.*

I. Lava of the Fourth Period.

1) Biotite-plagioliparite....Tenjô-san lava. (Pl. XXII, Fig. 1.).

Mode of Occurrence.—This occurs as a massive lava forming the latest volcano, Tenjô-san, on the island.

Megascopic Characters.—The rock is generally pumiceous and highly vesicular. It is commonly white; while in many places, especially at the northwestern part of the summit, it is stained throughout with varying shades of a yellow, citron, brown, or scarlet color. These varying shades of color may be attributed to the effects of the exhalations which were probably evolved through crevices from the interior of the lava. Moderate phenocrysts of plagioclase, quartz, and biotite are scattered through the vitreous groundmass.

Microscopic Characters.—Microscopically the most conspicuous phenocrysts are of plagioclase. They are euhedral or subhedral and about 1 mm. in average diameter. Sometimes the mineral is zonally built, showing inner calcic zone coated with outer less calcic one. From the optical constant on cleavage flakes as determined by Tsuboi's method,[14] the outer shell (n_{1D}=1.533(5)) of the zonal plagioclase was identified as a sodic oligoclase $Ab_{88}An_{12}$, and the core part (n_{1D}=1.535) as a little less sodic one $Ab_{85}An_{15}$. Small inclusions of colorless glass are often arranged in concentric zones. The phenocrysts of sanidine are of very rare occurrence.

Quartz is angular or subangular. Apart from the irregular outline, the mineral does not shows no special features to be remarked here.

Biotite occurs as flakes, up to 1 mm. long. It is of greenish-brown color with the refractive index: $\gamma_D=1.665$. Accompanying with this are found often flakes of reddish-brown biotite of another type. The latter is very high in refraction, $\gamma_D>1.700$, higher than any biotite yet recorded.[15]

---

[14] S. TSUBOI, "A Dispersion Method of Discriminating Rock-Constituents and its Use in Petrogenic Investigation," *Jour. Fac Sci., Imp. Univ. Tokyo*, Part 5, **1** (1926); *Miner. Mag.* (*London*), **20** (1923), 93–107.

[15] N. Fukuchi, describing two kinds of biotite in the biotite-liparite of Nii-jima, pointed out their dissimilarity to each other, one being of reddish-brown color and larger in optic axial angle than the other greenish-brown biotite, though both shows similar crystal form and equally strong pleochroism. According to him, the greenish-brown biotite is a decomposition product of the reddish-brown one. The specimens collected by the writer on Nii-jima contain biotites showing $\gamma_L>1.700$. See N. FUKUCHI, *op. cit.*, *Report Earthq. Invest. Com.*, **39** (1902), 18–19, (in Japanese).

A. L. Day noticed a biotite in a 1915 lava (quartz-bearing andesite) of the Lassen Volcano, California, which showed γ varying from 1.680 to 1.700. See A. L. DAY, "The Volcanic Activity and Hot Springs of Lassen Peak," *Carnegie Institution of Washington*, **360** (1925), 49.

As will be shown in the next chapter, these flakes are of the thermally decomposed biotite.[16]

The groundmass of the Tenjô-san lava is colorless and entirely glassy. Flow structure is well marked. Dusty substances of brown color to which the various colors of the hand-specimens are due, are scattered through the groundmass. The refractive index of the glass is 1.490 for Na light.

Chemical Composition.—A specimen of uniformly pumiceous white rock having phenocrysts of feldspar, quartz, and biotite, from the north-western part of the summit of Tenjô-san was analysed by S. Tanaka of our Institute, with the result shown under the column I of Table I.

TABLE I.

Wt. %	I	II
SiO_2	76·60	76·05
Al_2O_3	13·22	12·44
Fe_2O_3	0·27	0·84
FeO	0·43	0·22
MgO	0·19	0·17
CaO	0·75	0·87
Na_2O	4·62	4·31
K_2O	1·61	2·88
H_2O +	1·50	1·66
−	0·11	0·11
TiO_2	—	0·12
P_2O_5	—	tr.
MnO	0·16	0·07
Total	99·46	99·74

Norms	I	II
Quartz	41·6	37·9
Orthoclase	9·4	17·2
Albite	38·8	36·1
Anorthite	3·6	4·2
Corundum	2·5	0·7
Hypersthene	1·2	0·5
Ilmenite	—	0·1
Magnetite	0·2	0·4
Hematite	—	0·5

Ratios	I	II
Sal/Fem	67·6	59·3
Q/F	0·8	0·6
$\frac{K_2O' + Na_2O'}{CaO'}$	7·0	6·6
$\frac{K_2O'}{Na_2O'}$	0·3	0·4

For comparison, the chemical composition of the Mukô-yama lava (biotite-liparite) of Nii-jima, by the same analyst, is shown under the column II of the table. The Tenjô-san lava is lower in ferriferous oxides and potash, but a little higher in lime than the Mukô-yama lava. Moreover, in the former ferrous oxide dominates over the ferric one, as contrasted with the inverse relation in the latter. The normative quartz of the Tenjô-san lava is present in much greater amount than that of Mukô-yama lava, in correspondence with the reverse relation of the normative orthoclase. Thus, the norms, also shown in that table, place the Tenjô-san lava in Tordrillose (I. 3. 1. 4) and the Mukô-yama lava in Alsbachose (I. 3(4). (1)2. 4), according to the C. I. P. W. quantitative system of classification. As compared with the type liparite, these rocks are quite different, Na_2O being much higher and K_2O much lower, differences that are in accord with the dominant sodic plagioclase in these rocks. Indeed, so small is the percentage of the potash-feldspar, if present, that the rocks deserve the name of dacite rather than that of liparite, according to the current classification. But the chemical composition and microscopic characters of the rock of Tenjô-san reveal much of the characteristic feature of liparite. Accordingly, the name "plagioliparite," a name proposed by Koto, should be applied to this rock, as has been given to the liparitic rocks with dominant plagioclase among the Tertiary volcanics in our country. On the same reason all the rocks, except for the potash-liparite, of Kôzu-shima may be called plagioliparite.

---

[16] Cf. p. 307 of this paper. From the thermal study of biotite, it is inferred that reddening, increasing of optic axial angle, and rising of refractive indices of biotite is carried out during a process of thermal decomposition acting on a common biotite.

II. Shiroshima and Kushigamine Ejecta.

2) Biotite-plagioliparite....Juvenile ejecta.

Pumiceous ejecta of this rock forms the entire masses of the Shiroshima and Kushigamine cinder-cones. In the rock the phenocrystic plagioclase was identified as an oligoclase $Ab_{88}An_{12}$ ($n_{1D}=1.533$). Biotite has the refractive index: $\gamma_D=1.666$.

III. "Shiromama" Ejecta.

3) Biotite-plagioliparite....Juvenile ejecta

This occurs as the fragmentary products (volcanic ashes, lapilli, and bombs) forming the greater part of the "Shiromama" bed. Mingled with pumice, dense ejecta and bread-crust bombs, though of very rare occurrence, are also imbedded. The outer crust of the bread-crust bomb is rather dense, while the core part is highly vesiculated, there the glass being drawn out into fine thread-lace with silky luster.

The ejecta contain megacrysts of plagioclase, quartz, and biotite. The composition of the plagioclase is $Ab_{86}An_{14}$ ($n_{1D}=1.534$). The refractive index γ_{1D} of the biotite is 1.664. A specimen of bread-crust bomb from the bed on the shore of Mae-hama contained reddish-brown biotite with the refractive index: $1.680<\gamma_D<1.695$.

Besides the juvenile ejecta, the accessory ones of hornblende-andesite and quartz-porphyry are found in the bed. They are identical in petrographic characters with those found in the Chichibu-yama ejecta-bed and will be described later.

The juvenile ejecta from the "Shiromama" bed and the cinder-cones are identical in the composition of the phenocrystic plagioclase and the refractive indices of biotite with the lava from Tenjô-san. Field relations also show that the ejection of these ejecta and the extrusion of the Tenjô-san lava took place in the same general period of volcanic activity on the island.

IV. Lavas of the Third Period.

4) *Biotite-plagioliparite*....
- *Kôbe-yama lava.* Pl. XXII, Fig. 2).
- *Anagi-yama lava.*
- *Jôgoro-yama lava.*

Mode of Occurrence.—This occurs as the dome-shaped masses, about 100 m. thick, of Kôbe-yama and Anagi-yama and also as a lava-flow, 150 m. thick, forming the flat-topped mountains—Jôgoro-yama and Kaminari-yama.

The Kôbe-yama lava rather resembles in its petrographic characters the Tenjô-san lava. The hand-specimen of the lava is pumiceous and finely vesiculated. The phenocrysts of plagioclase, quartz, and biotite are scattered through the vitreous groundmass. Occasionally, the rock is stained throughout with varying shades of color. The phenocrystic plagioclase shows indistinct zoning with less or more calcic material alternating, though generally the outer zone is less calcic than the neighbouring inner zone. The outer shell was identified as a sodic oligoclase $Ab_{88}An_{12}$ (n_{1_D}=1.533(5)). Biotite occurs as brownish flakes with the refractive index: γ_D=1.664, 1 mm. long, and is often contorted. The groundmass is entirely colorless glass having n_D=1.490.

V. Lavas of the Second Period.

5) *Biotite-plagioliparite*....
- *Takôdo-yama lava.* (Pl. XXII, Fig. 3).
- *Nachi-san lava.* (Pl. XXII, Fig. 4).

Mode of Occurrence.—This occurs as a massive lava, about 130 m. thick, forming the upper portion of Takôdo-yama and also as an extensive lava-flow, the best exposure of which is seen on the 100 m. cliff at Tachimoto near the head of the valley of the Kawara (Pl. XIX, Fig. 4).

Megascopic Characters.—A specimen from an outcrop near the summit of Takôdo-yama is pumiceous through which are scattered megacrysts of plagioclase, quartz, and biotite. On the other hand, a specimen from the foot of the hill is compact and of ash-gray color. It is strongly porphyritic, with numerous phenocrysts of plagioclase and quartz, with subsidiary amount of biotite. The hand-specimen of the Nachi-san lava often exhibits spherulitic growths of the groundmass. In a dense one a distinct flow-banding is shown by alternating lamination of various shades of color.

Microscopic Characters.—The thin section of a compact specimen from the Takôdo-yama lava shows phenocrysts of plagioclase, quartz, and biotite in a devitrified groundmass. The phenocrystic plagioclase is euhedral, commonly twinned, and indistinctly zoned. It is a calcic oligoclase $Ab_{73}An_{27}$ ($n_{1D}=1.541$). Biotite is frequently bordered with a resorption-rim. Unaltered flake of the mineral has the refractive index: $\gamma_D=1.656$. The groundmass is composed of interlocking mosaic of quartz and feldspar, with a few glass base. The groundmass glass of a pumiceous specimen has the refractive index: $n_D=1.4985$.

The thin section of the Nachi-san lava shows phenocrysts of plagioclase, quartz, and biotite in either finely crystallized or entirely vitreous groundmass. The phenocrystic plagioclase, up to 1 mm. by 2 mm. in size, is poorly built in zones. It was identified as an oligoclase $Ab_{82}An_{18}$ ($n_{1D}=1.537$). When it shows zoning, the inner zones are more calcic than the outer zones. Biotite is of brown color with refractive index: $\gamma_D=1.660(5)$, but one separated from a rather pumiceous specimen is reddish-brown in color and is very high in refraction, $\gamma_D>1.700$, showing distinct biaxiality.

VI. Chichibu-yama Ejecta.

6) Biotite-plagioliparite....Juvenile ejecta.

The juvenile ejecta are naturally greater in quantity than the others and are largely of pumice, mingled with a small amount of other varieties of the same lava. They are of every conceivable size from what may be called volcanic ashes to volcanic bombs as large as human's head and are essentially composed of plagioclase, quartz, biotite, and glass. Ashes are generally snow-white, but often of chocolate color. The composition of the phenocrystic plagioclase is $Ab_{80}An_{20}$($n_{1D}=1.539$). The refractive index of the biotite is: $\gamma_D=1.651$.

7) Liparite.

Mingled with the juvenile ejecta are found numerous fragments of preexisting rocks. Among them, liparite is about 3 cm. in diameter, yellowish gray in color, and fine-grained. Thin section of the block shows a brecciated structure, microscopic rock fragments, 1.5 mm. in diameter, being cemented with minute interlocking mosaic of orthoclase and quartz. Every one of the microscopic rock fragments shows a porphyritic texture with phenocrysts of orthoclase scattered through a trachytic groundmass. In the groundmass are arranged small prismoids of orthoclase lengthways in the direction of flow.

8). . *Quartz-porphyry.*

Angular or subangular blocks, up to 5 cm. in diameter, of acidic nature, but more crystalline than the juvenile ejecta are frequently imbedded. Megascopically they are of pale gray color and porphyritic with phenocrysts of quartz and feldspar, up to 5 mm. in diameter, scattered through an fine-grained aphanitic groundmass. Under the microscope the phenocrysts are orthoclase and quartz. Orthoclase, far inferior in quantity to quartz, shows somewhat rounded outline and is often altered to sericite. The groundmass consists entirely of quartz and orthoclase forming an interlocking mosaic.

9) Porphyritic hornblende-diorite. (Pl. XXIII, Fig. 1).

Angular blocks, about 5 cm. in diameter, of this rock were found in the ejecta-bed. The hand-specimens are holocrystalline, medium-grained, and of dull gray color with a tinge of green. Megacrysts, up to 3 mm. in diameter, of plagioclase and hornblende are respectively light pink and dark green in color. In thin section the rock is of hypidiomorphic texture, consisting essentially of plagioclase and hornblende, with some interstitial quartz. Plagioclase was identified as an andesine $Ab_{65}An_{35}$ (n_{1D}=1.545). It shows commonly the twin-lamellation according to the albite law, often accompanied with Carlsbad or pericline twin. Hornblende is of green color and shows very slight pleochroism: X or Y—pale green and Z—deep green. It exhibits twinning parallel to (100). The refractive index of the mineral is: n_{1D}=1.646, and the extinction angle is: $c \wedge Z' = 17°30'$. Quartz occurs less abundantly, filling the interstices. As accessory minerals, there occur magnetite and apatite.

10) Hornblende-andesite. (Pl. XXIII, Fig. 2).

This rock are frequently found everywhere in the ejecta-bed as angular or subangular blocks of 5 cm. across. Mingled with other ejected blocks, juvenile as well as either accessory or accidental, these blocks occasionally form agglomerate or rather breccia interstratified in the finer ejecta. Megascopically the rock is of medium gray color, with a tinge of brown, compact, and distinctly porphyritic with phenocrysts, 1–2 mm. in diameter, of plagioclase and hornblende, scattered through a dense aphanitic groundmass.

The thin section of this rock shows numerous phenocrysts of plagioclase and hornblende. Plagioclase is euhedral and commonly twinned according to the albite and Carlsbad laws, but rarely to the pericline law. It is often zoned, more calcic and less calcic layers alternating or otherwise the less calcic crust surrounding the more calcic core. The least calcic part was identified as an andesine $Ab_{59}An_{41}$ with $n_{1_D}=1.548$. But none of the plagioclase phenocrysts is as calcic as $Ab_{55}An_{45}$ ($n_{1_D}=1.551$). The mineral is optically positive. Hornblende is idiomorphic, of prismoid, and often twinned parallel to (100). It is light green and exhibits a slight pleochroism: X—pale green, Y—medium green, and Z—deep grass green. Occasionally, the mineral has more or less completely altered either to chlorite, often accompanied with epidote, or to red-brown iron-oxide. Unaltered flake has the refractive index: $n_{1_D}=1.655$. In some sections a few phenocrysts of quartz are found. The groundmass is various in structure. The cryptocrystalline groundmass is the commonest one and consists of granular crystal-aggregate, often accompanied with microspherulites. The trachytic groundmass is composed of slender feldpar laths, isometric crystals of magnetite, and devitrified glass with specks of alteration products.

11) Two-pyroxene-andesite. (Pl. XXIII, Fig. 3).

At the headland between the bays of Miura and Takô, was found a block, 8 cm. in diameter, of this rock. It is of dark gray color, compact, and strongly porphyritic with numerous phenocrysts of plagioclase, 1–3 mm. long, scattered through a very dense, fine-grained aphanitic groundmass.

Under the microscope the phenocrystic plagioclase is euhedral, of rather equant habit, and twinned according to the albite and Carlsbad laws. It is not zonally built and was identified as a labradorite $Ab_{27}An_{73}$ with $n_{1_D}=1.568$. Inclusions, most of which are of brown glass, are often arranged in zones. Augite is light greenish and euhedral, ranging up to 1 mm. by 1.5 mm. in size. Two or more individuals of this mineral occasionally form a grouped phenocryst. The mineral is often twinned parallel to (100). On the cleavage flake the refractive index is: $n_{1_D}=1.691$. Hypersthene is subordinate in amount. It exhibits a slight pleochroism: X—light green, Y—light brown, and Z—green. The groundmass consists of plagioclase prismoids, 0.1 mm. long, minute augite grains, and isometric magnetite, with a small amount of brown glass.

VII. Lavas of the First Period.

12) Biotite-plagioliparite....ε-Lava. (Pl. XXIII, Fig. 4).

Mode of Occurrence.—This forms two distinct lava-flows (ε_1-lava and ε_2-lava) exposed on the sea cliff running around the southeastern shore of the island. The ε_1-lava extends from Sanuka-saki to Kannon-ura and is exposed on the 150 m. sea cliff. On the southeastern side of Tenjô-san it crops out 300 m. up and is overlain by the Tenjô-san lava. But the greater part of the lava is unconformably covered with the Chichibu-yama ejectabed, though the latter is but barely left from erosion. A noticeable feature of the lava is that it consists of distinct layers: pumiceous in the upper part, glassy in the middle, and felsitic in the lowermost layer which is just above the sea level. Forming the headland between the bays of Miura and Takô, another lava (ε_2-lava) is exposed on the sea cliff. West side of the headland, on the point north of the bay of Miura it is in contact with the hypersthene-plagioliparite of the Membô upland, though it is veiled by the debris in the valley that open to the bay which of the two has been extruded first.

Megascopic Characters.—Megascopically three principal varieties of the biotite-plagioliparite from the ε_1-lava may be distinguished. Felsitic variety is white or pale gray in color and very compact. Phenocrysts of plagioclase are scattered through the aphanitic groundmass, but those of biotite are little or entirely absent. Glassy variety is a jet-black obsidian. A splinter from it shows a conchoidal fracture and has a sharp knife-edge. A thin piece is translucent, darkening as it becomes thick. In the obsidian, phenocrysts of plagioclase are fairly abundant, while a few crystals of biotite are looked through the black glass. Frequently, the obsidian is traversed by numerous perlitic cracks and the hand-specimen is easily crumbled into pieces. Pumiceous variety is white and vesicular. The specimens from the ε_2-lava are rather pumiceous and strongly porphyritic, with numerous phenocrysts of plagioclase, quartz, and biotite.

Microscopic Characters.—In thin section of a felsitic specimen of the ε_1-lava there are a few phenocrysts of plagioclase and biotite scattered through a largely devitrified groundmass. The phenocrystic plagioclase is commonly twinned and zonally built, though very faint. The extreme margin of the crystal was identified as an oligoclase $Ab_{75}An_{25}$ with $n_{1D}=1.541$, and slightly more calcic core part, $Ab_{71}An_{29}$ with $n_{1D}=1.541$. Biotite is greenish brown with $\gamma_D=1.661$. Sometimes it has been decomposed into grains of magnetite. No phenocryst of quartz is to be seen. The groundmass is largely microcryptocrystalline, though glassy base has been left in lenticular patches arranged lengthways in the direction of flow. It occasionally exhibits microspherulitic crystallization.

A thin section of the obsidian is colorless glass in which are poorly found phenocrysts of plagioclase and biotite. The refractive index of the glass is:

n_D=1.484. An obsidian from the southeastern foot of Tenjô-san is traversed with numerous perlitic cracks and contains abundant phenocrysts of plagioclase, quartz, and biotite. The groundmass shows perfectly clear glass crowded thickly with incipient crystallizations such as crystallites, trichites, margarites, etc. (Pl. XXIII, Fig. 4). Sometimes devitrified aureole, brown in color, is seen around the phenocrysts. The refractive index of this glass is: n_D=1.494, far higher than that of the just-mentioned obsidian.

The white pumiceous specimen is nothing but highly vesicular form of the former ones. As to the specimen, the only point of interest is that the refractive index of the glass is higher than those of the obsidian glasses, giving n_D=1.498(5). From this it is inferred that volatile substances that have been preserved in larger amount in obsidian glass than in pumice lower the refractive index of the glass.

The thin section of the ε_2-lava shows phenocrysts of sanidine, plagioclase, quartz, and biotite. Sanidine is negligible in amount. Plagioclase exhibits slight zonal structure, though not striking enough to be optically analysed. Thus, the mineral was identified as an oligoclase $Ab_{82}An_{18}$ (n_{1D}=1.538). Small inclusions of apatite, magnetite, and of a few biotite flakes are seen. The phenocrystic biotite is brown in color, frequently with a tinge of either red or green. Contortion of the flakes is frequent. The refractive index is: γ_D=1.661. In some specimens, however, are found a few flakes of reddish-brown biotite which differ optically from the just-mentioned one. Basal section of this biotite shows low but distinct biaxiality, with the refractive index: γ_D=1.684, far higher than the above one. As already remarked this biotite has possibly been derived, through a thermal decomposition, from the normal biotite (γ_D=1.661).

Tadanae-jima islets are formed of the same lava as that of Sanukasaki (ε_1-lava).

Ombashi-jima islet-group consists of two larger islets, Ombashi-jima and Sappan-jima, with many stacks ("Ne") and reefs ("Asara") around them. The islets are formed of felsitic lava with a marked flow structure. The rock is entirely devoid of phenocrysts and the whole mass is hyaline or cryptocrystalline with very poor crystals of plagioclase and seemingly of biotite (Pl. XXIV, Fig. 1.) Jet-black obsidian occasionally is sandwiched in between the felsitic part. Chemical composition of a felsitic specimen from Sappan-jima is shown in Table II (Analyst S. Tanaka).

TABLE II.

	Wt. %
SiO_2	74·93
Al_2O_3	13·52
Fe_2O_3	0·76
FeO	0·72
MgO	0·32
CaO	0·93
Na_2O	4·50
K_2O	3·39
H_2O +	0·46
−	0·33
TiO_2	0·13
P_2O_5	0·08
MnO	0·08
Total	100·15

Norm	
Quartz	33·2
Orthoclase	20·0
Albite	38·2
Anorthite	3·9
Corundum	0·9
Hypersthene	1·3
Magnetite	1·2
Ilmenite	0·3
Apatite	0·3

Ratios	
Sal/Fem	31·0
Q/F	0·5
$\frac{K_2O' + Na_2O'}{CaO'}$	6·7
$\frac{K_2O'}{Na_2O'}$	0·5

13) *Hornblende-plagioliparite*....δ-Lava. (Pl. XXIV, Fig. 2).

Mode of Occurrence.—This constitutes a lava-flow, about 150 m. in average thickness, and forms the western part of the basement of the island. On the 60 m. cliff around the northwestern foot of Kôbe-yama, a glassy lava, rich in spherulite, is seen, being overlain by the Chichibu-yama ejecta-bed. From this place to the shore of Mae-hama the lava continues and exposes on the sea cliff. Platy banding is a characteristic feature of this lava.

Megascopic Characters.—This rock exhibits diverse megascopic appearances, pumiceous, glassy, and felsitic. Pumiceous portion is megascopically of porphyritic texture, megacrysts of plagioclase, quartz, and hornblende being scattered through a white glass base. Sometimes, the alternating laminae of vitreous and felsitic materials are developed, showing viscous flowage of the lava. Much more frequently, however, are found spherulites either scattered or arranged in parallel lines through a vitreous base. These spherulites attain occasionally a diameter of 3 cm., but far often they are 2–5 mm. in diameter.

Microscopic Characters.—Under the microscope are found phenocrysts of feldspar, quartz, and hornblende. Of the feldspar sanidine is far less in amount than plagioclase.

Phenocrystic plagioclase is euhedral and of prismoid, 3–5 mm. long, with the usual twin-lamellation. The indices of refraction of the mineral are: $\alpha_D<1.544<\beta_D 1.548<\gamma_D$ or $n_{1D}=1.541$. Thus the plagioclase was identified as an oligoclase $Ab_{74}An_{26}$. Sometimes it exhibits indistinct zonal structure, the outermost part being slightly more sodic ($Ab_{76}An_{24}$, $n_{1D}=1.540$) .

Quartz is abundant, its amount being competed with that of the plagioclase. It is rounded, angular, but rarely euhedral. The euhedral one is dihexagonal and six-sided, often being indented to result in inlets of the groundmass. Minute inclusions are commonly visible in the mineral.

Hornblende occurs as idiomorphic prismoids of about 3 mm. in length. It is usually of pale green or of greenish brown and is moderately pleochroic, giving pale green (X), greenish brown (Y), and greenish brown (Z) colors respectively for the three directions of absorption. Basal section shows a set of prismatic cleavage, so characteristic of the mineral. Lamellar twinning is often developed. The refractive index is: $n_{1D}=1.644$. The extinction ngle $c \wedge Z'$ is about 11°. As inclusions are found plagioclose, magnetite, but rarely glass. The mineral is generally fresh and has suffered no resorption, while that in the felsitic variety has undergone some alteration.

Much less commonly are found biotite flakes, of very small size, scattered through the groundmass.

In accordance with the diverse megascopic appearances of the rock, the groundmass exhibits various textures and structures. The vesicular structure is commonly of the pumiceous specimen. The groundmass in which neither microlite nor crystallite is visible is but a vesicular form of natural glass. The vesicles are drawn out in the direction of flow. The vitreous but non-vesicular groundmass is a common structure assumed by obsidian. The colorless glass traversed with or without perlitic cracks is crowded with minute laths of crystallites arranged lengthways in the direction of flow. Occasionally, they are crowded in bands exhibiting megascopic lamellation of the rock. In a specimen from Mae-hama are scattered through the groundmass a number of crystallites of a colorless mineral forked in swallow tail. The cryptocrystalline groundmass is of the felsitic variety. It consists in the interlocking masaic of minute crystals of quartz and feldspar. In the devitrified groundmass of a specimen from the shore of the bay of Nagumi was found secondary diaspore filling the interstices. It is blue in color and strongly pleochroic, varying from deep blue to light blue or to almost colorless.

The spherulitic structure is exhibited by the groundmass in which spherulites, about 0.05 mm. in diameter, composed of radiating crystals with negative character of the principal zone are imbedded. These microspherulites are often enclosed in some larger spherulites, 2–5 mm. in diameter, scattered through the groundmass when develop but poorly, otherwise arranged in straight or tortuous layers. In thin section the larger spherulites are made up of radiating but markedly branching fibres which may possibly be the so-called trichites. Phenocrysts of quartz and feldpar are often enclosed in these spherulites and have served as the nucli for the radial development of the spherulites. The spherulites sometimes show concentric zones, along with the radial structure, the more crystalline zones alternating with the less crystalline ones. Thus, largely devitrified spherulites show between crossed nicols optically positive character. In the groundmass with spherulitic crystallization minute lods of crystallites are distributed equally in both the spherulites and the main groundmass and are arranged lengthways in the direction of flow. Accordingly, it is inferred that the spherulites, microscopic as well as macroscopic, were formed after the extrusion of the lava. There is no mistake about that the spherulites came into existence after the flowage of the lava and could not be due to liquid immiscible in the magma.[17]

Chemical Composition.—An uniformly pumiceous specimen from Naga-hama was chemically analysed by S. Tanaka, the result being as shown in Table III.

TABLE III.

Wt. %		Norm	
SiO_2	75·10	Quartz	41·2
Al_2O_3	13·36	Orthoclase	8·9
Fe_2O_3	0·30	Albite	35·1
FeO	0·74	Anorthite	6·9
MgO	0·27	Corundum	2·3
CaO	1·43	Hypersthene	0·6
Na_2O	4·21	Magnetite	0·2
K_2O	1·58		
H_2O +	2·27	Ratios	
−	0·17	Sal/Fem	168·0
TiO_2	—	Q/F	0·9
P_2O_5	—	$\frac{K_2O' + Na_2O'}{CaO'}$	3·3
MnO	0·10		
Total	99·53	$\frac{K_2O'}{Na_2O'}$	0·2

According to the C. I. P. W. quantitative system of classification, the rock resembles very closely the hypersthene-plagioliparite (cf. p. 296), both falling in Alsbachose (I. 3. 2. 4), though the latter is almost in quardofelic.

---

[17] J. W. GREIG: "Liquid Silicate Immiscibility," *Amer. Jour. Sci.*, **15** (1928), 375–402.

14) Hornblende-bearing hypersthene-plagioliparite....γ-Lava. (Pl. XXIV, Fig. 3).

Mode of Occurrence.—This is exposed along the coast of Ushi-hana at the northeastern corner of the island, forming a lava-flow of about 170 m. in thickness. Its surface is likewise pumiceous, while the lower portion is compact and shows magnificient columnar structure. The lava is covered with the Chichibu-yama ejecta-bed which is in turn overlain by the Jôgoro-yama lava.

Megascopic Characters.—Megascopic appearance is quite various. The chief variation is from a dense rock with abundant megacrysts, up to 2 mm. long, of plagioclase and quartz scattered through the aphanitic groundmass, to a glassy one.

Microscopic Characters.—Microscopically the rock contains phenocrysts of plagioclase, quartz, hypersthene, and hornblende.

Plagioclase is euhedral or subhedral, and of prismoid. Multiple twinning according to the albite law, often combined with the Carlsbad twinning is commonly developed. Zonal structure is very faintly exhibited. The mineral was identified as an oligoclase $Ab_{72}An_{28}$, with $n_{1D}=1.542$.

Hypersthene is euhedral (laths up to 1 mm. long), pale brownish, and pleochroic, viz. Z—light greenish, Y—brownish, and X—pale brownish. Conoscopically two forms of the mineral are distinguished. One has the optical plane parallel to the elongation direction (c-axis) and the other transverse to it. The former is the normal form and is by far the more of the two. The normal form exhibits more prismatic cleavage but less pleochroism than the other. The transverse cleavage are equally developed. Two or more individuals of this mineral occasionally form a grouped crystal associated with those of the plagioclase.

Quartz occurs in somewhat rounded crystals broken by irregular fractures. Hornblende is negligible in amount. It is euhedral (0.1–0.2 mm. long) and light green in color. Twinning lamellae are often exhibited.

The groundmass is various, from extremely hyaline one to more or less crystalline. The dense specimen from the lower portion of the lava has a groundmass consisted of minute mosaic of feldspar and quartz, sometimes with the spherulitic crystallization. Besides, slender flakes of biotite are rarely found.

15) Hypersthene-plagioliparite....β-Lava. (Pl. XXIV, Fig. 4).

Mode of Occurrence.—This forms a lava-flow, about 100 m. thick constituting the rectangular table-land at the southeastern part of the island.

Where the lava cut back into sea cliff, a distinct flow line dipping northeast is exhibited. The flow banding is often contorted as shown by color differences between the bands, which vary from faint to quite pronounced. Small outcrops of the same rock are also found at Yoko-kawa and Tadanuke, on the middle course of the Kawara.

Megascopic Characters.—Megascopically the rock is various, as it exhibits every gradation between the pumiceous and stony characters. Specimens from the upper portion of the lava-flow are highly pumiceous, while those from the interior are dense. Sometimes it is strongly variegated with the colors of white, gray, brown, and black. Megacrysts of plagioclase, and quartz lie in a glassy or vesicular groundmass. Spherulites are frequently scattered through the vitreous matrix.

Microscopic Characters.—The thin section shows numerous phenocrysts, of staut prismoid, 0.5 to 1 mm. long, of plagioclase. The plagioclase is oligoclase-andesine $Ab_{68}An_{32}$, with $n_{1D}=1.544$ and the extreme margin an oligoclase $Ab_{77}An_{23}$, with $n_{1D}=1.539(8)$, the lowest refractive index measured. Twinning is commonly of the albite law showing rather narrow twin-lamellation. As inclusions occur euhedral hypersthene, minute grains of magnetite, and slender prisms of apatite, along with small patches of colorless glass crowded with microlites.

Phenocrystic quartz is always present in less amount than plagioclase. It is subhedral or anhedral, with rounded or irregular outlines, but exceptionally occurs in bipyramidal crystals. The mineral contains inclusions, mostly of glass thickly crowded with microlites.

Hypersthene is euhedral, yellowish brown, moderately pleochroic: X—yellowish brown, Y—pale brown, Z—yellowish green. The refractive index is: $n_{1D}=1.700(5)$. The optical plane is parallel to the elongation direction of the crystal. It is practically free from inclusions, except a rare small grains of magnetite.

In very rare instances, minute flakes of biotite are recognized.

The groundmass is very glassy, of various colors, and is generally crowded with microlites which are arranged in the sinuous flow lines. Sometimes the groundmass shows a vesicular structure, the vesicles being elongated in the direction of flow.

Chemical Composition.—An analysis, by S. Tanaka, of a specimen from Himmashi-hana gave the result shown in Table IV, there being also given the ratios, according to the C. I. P. W. quantitative system of classification, which place the rock in Alsbachose (I. 3′. 2.4).

TABLE IV.

	Wt. %	Norm	
SiO_2	75·35	Quartz	37·1
Al_2O_3	13·49	Orthoclase	15·0
Fe_2O_3	0·95	Albite	36·1
FeO	0·55	Anorthite	7·2
MgO	0·36	Corundum	1·0
CaO	1·61	Hypersthene	0·9
Na_2O	4·28	Ilmenite	0·5
K_2O	2·52	Magnetite	1·2
H_2O +	0·61	Hematite	0·2
–	0·06		
TiO_2	0·20	Ratios	
P_2O_5	—	Sal/Fem	36·0
MnO	0·08	Q/F	0·6
Total	100·06	$\frac{K_2O'+Na_2O'}{CaO'}$	3·3
		$\frac{K_2O'}{Na_2O'}$	0·4

Basic Xenoliths. (Pl. XXV, Figs. 1, 2).

Mode of Occurrence.—The basic xenoliths lie scattered in the hypersthene-plagioliparite exposed along the shore from Himmashi-hana to Ichinokubi on the southwestern coast of the island. There the agglomeratic appearance of the lava is due to these xenoliths. Many of the xenoliths are quite angular, while some are well rounded, their size ranging from a few cm. to 15 cm. in diameter. The liparite surrounding these xenoliths is very vitreous.

Megascopic Characters.—The xenoliths are dark or almost black in color, often with a tinge of brown or dark green. In most hand-specimens no phenocryst is observed, but in a specimen are found glistening black prismoids of hornblende, about 3 mm. in length.

Microscopic Characters.—One specimen, that which was chemically analysed, is composed almost wholly of plagioclase, hornblende, augite, and magnetite, with a little glass. It is not strongly porphyritic, while all the plagioclase crystals are idiomorphic against the other essential minerals.

Plagioclase is dominantly lath-shaped and about 0.5 mm. long. With the refractive index, $n_{1D}=1.561(5)$ this plagioclase was identified as an intermediate labradorite $Ab_{37}An_{63}$. Zonal structure due to chemical difference is very faintly exhibited. The mineral is twinned, either multiply or simply, according to the albite law.

Hornblende is euhedral or subhedral, and equant in habit. The cleavage is perfectly developed, the transverse section of the mineral exhibiting the characteristic cleavage lines intersecting at an angle of 124°. The mineral is brown in color and strongly pleochroic, its axial colors being: X—light brown with a tinge of green, Y—yellowish green, and Z—brown. The refractive index is: $n_{1_D}=1.682$. The extinction angle is: $c \wedge Z' = 7°$.

In less amount than the hornblende are present equant grains of light greenish augite, much of it are subhedral or anhedral individuals of about 0.5 mm. in diameter. The mineral is scarcely pleochroic, varying from light green to almost colorless. The extinction angle of the mineral is: $c \wedge Z' = 53°$ and the refractive index is: $n_{1_D}=1.696(5)$. It is often surrounded with the reaction-rim of hornblende.

Isometric crystals of magnetite, 0.05–0.2 mm. in diameter, are present in moderate amount. There is some ill-defined, colorless glass interstitial between the crystals.

Chemical Composition.—A specimen from Himmashi-hana was analysed by S. Tanaka, with the result shown under the column I of Table V. It is there compared with the olivine-basalt from Udone-shima (col. II. Dittrich, Analyst), an islet to the north of Nii-jima. The close correspondence between these analyses is well brought by the calculation of the norms which are also shown in the same table.

TABLE V.

Wt. %	I	II
SiO_2	50·74	50·79
Al_2O_3	18·59	16·16
Fe_2O_3	9·23	6·96
FeO	1·01	3·51
MgO	5·37	7·63
CaO	10·21	10·03
Na_2O	2·35	2·58
K_2O	0·57	0·55
H_2O +	0·74	0·31
−	0·16	0·07
TiO_2	0·98	1·01
P_2O_5	0·06	—
MnO	0·16	—
Total	100·14	100·05

Norms	I	II
Quartz	6·5	4·4
Orthoclase	3·0	3·3
Albite	19·9	22·0
Anorthite	38·4	32·0
Diopside	9·1	13·8
Hypersthene	9·4	12·7
Magnetite	0·3	8·4
Ilmenite	1·8	1·9
Hematite	8·6	1·2

Ratios	I	II
Sal/Fem	2·3	1·6
Q/F	0·1	0·1
$\frac{K_2O' + Na_2O'}{CaO'}$	0·3	0·4
$\frac{K_2O'}{Na_2O'}$	0·1	0·1

According to the C. I. P. W. quantitative system of classification, the xenolith analysed belongs to Hessose (II. 4(5). 4. 4(5)), and the basalt to Auvergnose ((II)III. ′5. 4. 4(5)). The close correspondence between the xenolith and the basalt is a fact of some interest in view of the origin of the xenolith, since the similar xenolith is found in the biotite-liparite exposed at Awai-ura, northeastern shore of Nii-jima and only 1 km. to the south of Udone-shima.

The xenoliths from Nii-jima occur as ellipsoidal patches, up to 20 cm. in average diameter, arranged in the direction of flow of the Awai-ura lava.[18] A specimen collected by the writer is megascopically almost black in color and somewhat vesicular, the vesicles being filled with the white pumiceous lava. Plagioclase phenocrysts are rarely seen with the naked eyes. Under the microscope the essential constituent minerals are plagioclase, augite, and magnetite. Among them, plagioclase and augite occur as phenocrysts. The plagioclase phenocrysts were identified as a calcic bytownite $Ab_{15}An_{85}$ with $n_{1D}=1.572$. Zoning due to chemical difference of the mineral is scarcely visible, while a distinct zone of less calcic plagioclase frames not infrequently the thinnest margin of the phenocrysts. Phenocrystic augite is of very rare occurrence. It is rimmed with narrow zone of hornblende. The groundmass is composed of plagioclase, augite, hornblende, magnetite, and a little interstitial glass. Plagioclase was identified as an andesine $Ab_{54}An_{46}$, with the refractive index $n_{1D}=1.552$. Hornblende is strongly pleochroic, exhibiting the axial colors: Z—reddish brown, Y—brown, and X—yellow, with absorption $Z>X$. The refractive index is: $n_{1D}=1.713$. The mineral occurs not only as euhedral crystals but also as reaction-rim surrounding augite crystals in the groundmass.

Another specimen of xenolith from Kôzu-shima is somewhat different from the above-mentioned one, though identical in mineral constitution. It is almost black in color, having a number of megacrysts of hornblende. In thin section plagioclase, 0.05–0.5 mm. across, is multiply twinned and often exhibits very faint zoning. With the refractive index $n_{1D}=1.566(7)$, it was identified as a labradorite-bytownite $Ab_{29}An_{71}$. The slender laths of plagioclase are enclosed ophitically in both hornblende and augite. The hornblende crystals are of prismoids, 0.5–2 mm. in length, and greenish brown in color. They are moderately pleochroic, showing axial colors: Z—greenish brown, Y—brown, and X—light green, with absorption $Z>X$. Extinction angle is: $c \wedge Z'=15°$. The refractive index is: $n_{1D}=1.672(5)$. The augite crystals are mostly subhedral, equant in habit and light-greenish. The refractive index is: $n_{1D}=1.694(5)$. The crystals are surrounded with the

---

18) N. FUKUCHI, *op. cit.*, *Report Earthq. Invest. Com.*, **39** (1902), 8–10, (in Japanese). Fukuchi described these xenoliths under the name "diorite-porphyrite."

reaction-rim of green hornblende. The interstitial glass is light brown in color and is highly vesiculated.

The xenoliths described here are somewhat similar in microscopic structure to a secretionary patch discovered by Koto[19] among the ejecta of Volcano Sakura-jima, exhibiting what Lacroix terms "structure enchevetree." But it is difficult to conceive of the formation of such secretionary patches, chemically almost equivalent to a basalt, in the rhyolitic magma. They are probably of preexisting rock caught by the liparitic lavas either before or during the outpouring.

16) Potash-liparite....a-Lava. (Pl. XXV, Fig. 3).

Mode of Occurrence.—This is exposed at Ôyase on the northern coast, forming an outcrop, 5 m. high above the sea level and 250 m. long along the shore. Whether the rock occurs in an extensive lava-flow, could not be decided from the exposure. The decomposed surface of this rock is covered with the Chichibu-yama ejecta-bed overlain by the Anagi-yama lava. The rock has undergone a certain amount of alteration by the attack of the sea water.

Megascopic Characters.—Megascopically the rock is pale gray in color, of non-vesicular, and porphyritic, having only phenocrysts of orthoclase scattered through an aphanitic groundmass.

Microscopic Characters.—Phenocrystic feldspar is generally euhedral to subhedral. It is low both in refractive indices, $n_{1D}=1.520$, and in double refraction. It is optically negative and shows very small optic angle. The mineral, accordingly, was identified as sanidine. Twinning according to the Carlsbad law is frequently exhibited. Occasionally, the mineral has been altered into kaoline which causes the cloudiness of the mineral.

No mafic mineral is detected, though red iron oxide and epidote, possibly secondary products derived from mafic mineral, are frequently seen.

Rounded phenocrysts of quartz are of very rare occurrence.

The groundmass is hypocrystalline, consisting of sanidine and devitrified glass. Slender prisms of sanidine, commonly twinned according to the Carlsbad law, exhibit trachytic arrangement. The devitrified base consists of quartz and feldspar in a granular mixture and is disseminated with minute grains of magnetite and secondary pyrite. Microscopic veins of secondary quartz traverse the groundmass.

Chemical Composition.—The result of chemical analysis by S. Tanaka

---

19) B. Koto, "The Great Eruption of Sakura-jima in 1914," *Jour. Col. Sci., Imp. Univ. Tokyo,* Art. 3, **38** (1916), 213.

is shown in Table VI, col. I, there being also given other two analyses of the similar rock from Manzô-yama, Izu.[20]

TABLE VI.

Wt. %

	I	II	III
SiO_2	71·64	70·85	70·75
Al_2O_3	14·13	14·03	12·44
Fe_2O_3	0·34	1·76	2·66
FeO	0·50	0·67	0·79
MgO	0·08	tr.	0·08
CaO	0·17	0·10	0·39
Na_2O	0·50	0·13	0·39
K_2O	10·77	11·36	11·51
H_2O +	0·80	0·66	0·84
−	0·23	0·26	
TiO_2	0·55	0·32	0·53
P_2O_5	0·08	tr.	0·10
MnO	tr.	0·23	0·09
Total	99·79	100·27	100·57

I. Potash-liparite, Kôzu-shima. S. Tanaka, Analyst.
II. Potash-liparite, Manzô-yama, Izu. S. Tanaka, Analyst.
III. Ditto, Manzô-yama, Izu. K. Yokoyama, Analyst.

The potash-liparite of Kôzu-shima resembles, in microscopical and chemical characters, the rock of Manzô-yama, east of Shimoda at the southern end of the Izu peninsula. Under the name "potash-rhyolite" the rock of Manzô-yama has been described by S. Kozu. Column III of the above table shows the chemical composition of the rock originally defined by Kozu. As shown in the table, two analyses, one by Tanaka and the other by Yokoyama, of the rock of Manzô-yama are not seriously inconsistent with each other, and moreover they closely agree with the composition of the potash-liparite of Kôzu-shima. The amount of K_2O is more than 10%, while that of Na_2O is less than 0.5% inclusive.

The norms and ratios calculated, according to the C. I. P. W. quantitative system of classification, are shown in Table VII. These potash-liparites belong to Lebachose (I. 4. 1. 1.).

---

[20] S. KOZU, "Preliminary Notes on Some Igneous Rocks of Japan," V. *Jour. Geol.*, **20** (1912), 1.

TABLE VII.

Norms	I	II	III
Quartz	27·6	26·5	25·2
Orthoclase	63·3	66·7	67·8
Albite	4·2	1·0	—
Anorthite	—	0.5	—
Corundum	1·6	1·3	—
Acmite	—	—	2·8
Diopside	—	—	0·7
Hypersthene	1·6	0·4	—
Ilmenite	1·0	0·6	1·1
Magnetite	—	1·1	0·6
Hematite	0·3	0·9	1·1
Apatite	0·3	—	0·3

Ratios	I	II	III
Sal/Fem	25·1	30·7	14·1
Q/F	0·4	0·4	0·4
$\frac{K_2O'+Na_2O'}{CaO'}$	∞	61·0	∞
$\frac{K_2O'}{Na_2O'}$	14·2	60·0	∞

Chapter IV. Petrology of Kôzu-shima.

In this chapter it is intended to treat the petrology of Kôzu-shima, making the best use of the results of the petrographic investigation.

For this purpose, the method of the optical analyses of rocks recently proposed by S. Tsuboi,[19] was applied to the study of Kôzu-shima rocks.

The rocks of Kôzu-shima contain mostly phenocrysts embedded in the glassy groundmass. The phenocrysts are the ready-made crystals immersed in the magma at the time of eruption. The minerals of the phenocrysts are quartz, orthoclase, plagioclase, hypersthene, hornblende, and biotite. The common accessories are zircon, magnetite, and apatite. Here attention will be mainly confined to the crystallization of the essential minerals.

Hypersthene and Hornblende.—Among the lavas of the first period, β-and δ-lavas carry as phenocrysts hypersthene and hornblende respectively, and γ-lava both of these minerals. Hypersthene and hornblende are not closely associated with each other, while both are respectively in close associa-

---

19) S. TSUBOI, "The Optical Analysis of Volcanic Rocks as a Means of studying their Genetical Relationship," *Bull. Earthq. Reser. Inst., Tokyo Imp. Univ.*, **4** (1928), 131.

tion with plagioclase. There is nothing to show which of the plagioclase and either hypersthene or hornblende began to crystallize first. There is also no evidence for the discontinuous reaction relation between pyroxene and hornblende. In the rocks, in which either hornblende or hypersthene occurs as phenocrysts, are found very minute flakes of biotite. Although little can be said with certainty in the present case whatever of reaction relation or of concomitant crystallization of biotite and either hypersthene or hornblende, there are some reasons for considering that the magmas were saturated with neither hornblende nor hypersthene, but with biotite when the lavas were extruded. The reasons for this will be stated later.

Plagioclase.—The plagioclase forms a perfectly continuous series of mix-crystal of two components—albite ($NaAlSi_3O_8$) and anorthite ($CaAl_2Si_2O_8$)—which are reciprocally miscible each other (solid solution Type I of Bakhius Roozeboom). It follows, therefore, that the plagioclase crystals separated at any temperature are always richer in the higher melting component (anorthite) than the liquid with which they are in equilibrium. If the cooling is so slow that perfect equilibrium is maintained between the crystals and liquid, the ready-made crystals are continuously made over to the homogeneous crystals with composition richer in the lower melting component (albite) as the temperature continues to fall. But this process is specially difficult of attainment in shallow-seated magmas from which volcanic rock are derived. When the equilibrium is not fully attained, that is, cooling is too rapid for the interchange of materials between the ready-made crystals and the liquid, the crystals are zonally built, their core part containing too much the higher melting component.

The rocks of Kôzu-shima, with the exception of the potash-liparite, contain dominant phenocrysts of plagioclase. The crystals are commonly more or less zoned, showing a chemical change from the more calcic inner zones to the less calcic outer zones. Sometimes the zoned crystals change their compositions continuously from the core to the margin. The repeated zonal structure in which reversed order of zones happens may be explained by undercooling and recurrence of equilibrium introduced at the time when the zoned crystals are forming. When a crystal shows numerous zones, each visible zone has a width ranging from 0.01 mm. to 0.1 mm. The inner zone is occasionally encroached upon, showing indentation or is woven irregular figures by the substance of the near-by outer zone.

TABLE VIII.

Lavas	Ab(max.)	Ab(min.)
β-Lava	77	68
γ-Lava	72	—
δ-Lava	76	74
ε_1-Lava	75	71
ε_2-Lava	82	—
Takôdo-yama lava	73	—
Nachi-san lava	82	79
Jôgoro-yama lava	82	—
Anagi-yama lava	83	—
Kôbe-yama lava	88	86
Tenjô-san lava	88	85

As a whole, cooling of the magma from which the various rocks have been derived was not so slow as to form homogeneous phenocrysts of plagioclase, but stepwise, rapid and slow cooling alternating, to show partial remaking of the ready-made crystals by reaction with the liquid. In the above table are shown the compositions of the plagioclase phenocrysts.

The compositions of the plagioclases were determined by using the diagram for determining plagioclases proposed by S. Tsuboi.(20) The cleavage flakes of plagioclase are immersed in sequence in liquids whose refractive indices and dispersions have been determined with the Abbe's refractometer. The smaller refractive index n_{1_D} on cleavage flakes parallel to M(010) or to P(001) is compared with the refractive index of the liquid used under the microscope. Then the refractive index of the plagioclase can easily be determined by Tsuboi's dispersion method.

From the table we see that the plagioclase phenocrysts are nearly within the limit of oligoclase-plagioclase ($Ab_{70}An_{30}$—$Ab_{90}An_{10}$) and their compositions have been but slightly affected by zoning. But the plagioclase phenocrysts in various lavas are not uniformly sodic, those in the later lavas being generally more sodic. Accordingly, it is inferred that the plagioclase phenocrysts in various lavas have separated out of the magma effected by either:

---

20) S. TSUBOI, "A Dispersion Method Discriminating Rock-Constituents and its Use in Petrogenic Investigation," *Jour. Fac. Sci., Tokyo Imp. Univ., Sec. II*, **2** (1926), 5.

1. local grouping of the ready-made crystals under uniform rate of cooling, while the temperature falling is slight, or

2. somewhat long extended cooling within the period of forming the various lavas, or

3. local diversity of rate of cooling.

Local grouping of the phenocrysts in the rhyolitic magma is not likely to take place, if the magma is really of such a high viscosity as may be postulated from the artificial siliceous melt. Now if we assume for a while that the phenocrysts were freely movable through the magma, there must have been an opportunity for either sinking or floating of them according to the relative densities of the crystals and the magma under plutonic condition. The specific gravity of oligoclase-plagioclase at room temperature and under normal atmospheric pressure is far high in comparison with that of rhyolitic glass, as seen in the following table.

TABLE IX.

Glass	Sp. Gr.	n_D	Crystal	Sp. Gr.	n_{1D}
1. Liparite	2·33	1·500	5. Ab	2·605	1·534
2. Dacite	2·51	1·510			
3. Obsidian	2·106	1·485	6. Ab_2An_1	2·660	1·549
4. Miharaite	2·84–7	1·593–6	7. Ab_1An_5	2·733	1·577

1., 2. Average liparite and average dacite; See W. O. GEORGE, "The Relation of the Physical Properties of Natural Glasses to their Chemical Composition," *Jour. Geol.*, **32** (1924), 353–372.

3. Obsidian glass of Kôzu-shima.

4. Hyaline part of miharaite; See S. TSUBOI, "Volcano O-shima, Izu," *Jour. Col. Sci., Imp. Univ. Tokyo*, Art. 6, **43** (1920), 84.

5–7. Albite, oligoclase-andesine, and bytownite; See E. S. LARSON, "Relation between the Refractive Index and Density of Some Crystallized Silicates and Their Glasses," *Amer. Jour. Sci.*, **28** (1909), 263–274.

As a basis for comparing the specific gravity at high temperature and at high pressure of solid crystals with that of liquid magma in which the crystals are immersed, the specific gravity at ordinary temperature and at normal atmospheric pressure are quite unreliable. But as has been suggested by Daly,[21] the difference of density between the magma and the crystals would but slightly be affected through the pressure. Assuming, on the other hand, the high coefficients of cubic expansion of sodic plagioclase, the difference of density between the rhyolitic magma and the crystals may become smaller as the temperature is raised. But water and mineralizers in depth would increase by far such difference calculated for one atmosphere and ordinary temperature. Thus, there is reason for supposing that the sodic plagioclase crystals would sink due to gravitation in the rhyolitic magma even under plutonic condition. The existence of basic seggregations in granites does not necessarily show that these seggregated minerals were floating in the granitic magmas.

---

[21] R. A. DALY, "Mechanics of Igneous Intrusion," *Amer. Jour. Sci.*, **15** (1903), 269; **16** (1903), 107.

From what has been said, the diversity of composition of the phenocrystic plagioclases in various lavas may or may not be explained by only effect of sinking of the ready-made plagioclase crystals in the magma.

Plagioclase phenocrysts always associate with the mafic minerals, showing simultaneous crystallization with the latter. They frequently enclose mafic minerals arranged in zones in accord with the zonal structure of the plagioclase.

Quartz.— Quartz in the rocks of Kôzu-shima has the high temperature crystal form traversed with numerous microscopic cracks due to high-low inversion. The biotite-plagioliparite of Sanuka-saki (ε_1-lava) is devoid of quartz phenocrysts, while it contains plagioclase and a little biotite. But in other parts of the same lava quartz is present along with plagioclase and biotite. Generally quartz crystals are scarce where the lava is poor in plagioclase phenocrysts. In the felsitic rock of Ombashi-jima neither quartz nor plagioclase is found. In this respect it is to be noted that quartz is heavier than liparitic magma. The specific gravity of the mineral is 2.649 at 20°C. and under 1 atmospheric pressure. At 900°C. and under 1 atmospheric pressure it is 2.529.[22] On comparing the density of quartz at 900°C. with that, at ordinary temperature, of the liparitic magma, it is remarkable that the mineral is heavier than the magma. Therefore the difference will be increased when the magma is under plutonic conditions. (cf. Table IX, p. 304). Local diversity of the amount of this mineral in the liparites may be explained by local sinking of the mineral. The potash-liparite is almost devoid of the phenocrysts of quartz. The similar rock from Manzô-yama in the Izu peninsula (p. 300) is partly devoid of the mineral but partly enriched with conspicuous phenocrysts of quartz. This diversity may be ascribed to the local sinking of the phenocrysts.

---

[22] A. L. DAY, R. B. SOSMAN, and J. C. HOSTETTER, "The Determination of Mineral and Rock Densities at High Temperatures," *Amer. Jour. Sci.*, **37** (1915), 16.

There is no indication in the rocks of Kôzu-shima, which of quartz and other minerals began to crystallize first.

Biotite.—The molecular constitution of biotite is extremely complex, though it is generally accepted that the mineral is an alumino-silicate of both alkali and either iron or magnesia or of both, along with hydroxyl. In all probability, the mineral forms a mix-crystal series and its crystallization must be spread over an interval of temperature, falling at least partly on that of plagioclase. Then the composition of the mineral has to change, along with the change of plagioclase, to cooling within a range of temperature. Thus, the paragenic relations of plagioclase and biotite have already been ascertained by studying these minerals in some genetically related rocks, the change of their compositions being confirmed by variation of their optical constants. For the purpose, the refractive indices of biotites in the rocks of Kôzu-shima were measured for Na light. They are shown in Table X, there being accompanied with the compositions of the phenocrystic plagioclases in the corresponding rocks.

Table X.

Lava	Plagioclase	Biotite (γ_D)
ε_1-Lava	$Ab_{75}An_{25}$	1·661
ε_2-Lava	$Ab_{82}An_{18}$	1·661
Takôdo-yama lava	$Ab_{73}An_{27}$	1·656
Nachi-san lava	$Ab_{82}An_{18}$	1·661
Jôgoro-yama lava	$Ab_{82}An_{18}$	n. d.
Anagi-yama lava	$Ab_{82}An_{18}$	n. d.
Kôbe-yama lava	$Ab_{88}An_{12}$	1·664
Tenjô-san lava	$Ab_{88}An_{12}$	1·665

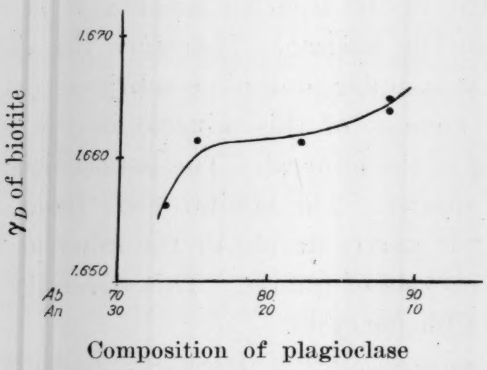

Fig. 1. The paragenic relation between plagioclase and biotite.

From the data given in Table X, the paragenesis diagram of Fig. 1 is constructed. As seen in the figure, the biotites become high in some extent in their refractive indices as the associating plagioclases become rich in albite. This is just what might be expected if the biotite forms a mix-crystal series and if its refractive indices become higher as the biotite grows rich in the lower melting component of the series. Chemical analyses of a number of biotite show that magnesia is in antipathetic relation with iron oxides, addition of the former to the biotite reducing the latter still further, and that magnesia-rich biotites are more common in basic rocks than in acidic ones.[23] On the other hand, the more the rocks become acidic, the higher the refractive indices of the biotites are. Accordingly, it is inferred that the addition of iron oxides raises effectively the refractive indices of biotite.

Besides the biotites cited in Table X, the Tenjô-san lava occasionally contains biotite with the refractive index: $\gamma_D > 1.700$. The ε_2-lava, Nachi-san

TABLE XI.

T (in C.)	γ_D	2E	Type
23	1·665	37° 38′	meroxene
120	1·665		
160	1·665		
220	1·669		
260	1·669		
290	1·671	46° 26′	meroxene
320	1·671		meroxene
360	1·678		meroxene
420	1·684		meroxene
450	1·684		
490	1·690		
530	1·699		
720	n. d.	50° 58′	meroxene
760	n. d.		
800	n. d.		
900	n. d.	60° 18′	
1000	n. d.		

---

[23] GERDA SCHAUBERGER, "Biotit in tertiären Eruptivgesteinen Böhmens," *Centralblatt für Mineralogie, Geologie und Paläontologie*, Abt. A, (1927), 89–105.

lava, and Jôgoro-yama lava also contain biotites, unusually high in the refractive indices. From the thermal study on biotite flakes collected from the Tenjô-san lava, it was confirmed that increase of the refractive indices might be due to a thermal decomposition to which the normal biotite was subjected.

The greenish-brown biotite, whose refractive index is: γ_D=1.665, collected from the Tenjô-san lava was heated by means of an electric resistance furnace, the temperature being measured with a Pt.-Pt.Rh. thermo-couple connected to a millivoltmeter. The biotite flakes were heated an hour at a constant temperature and then they were dropped to quench into water by cutting the suspension wire of the substance heated. The treatment was done at various temperatures from 120°C. to 1000°C., and the refractive indices for Na light of the heated biotites were determined by the immersion method. The results obtained are tabulated above and are graphically represented in Fig. 2.

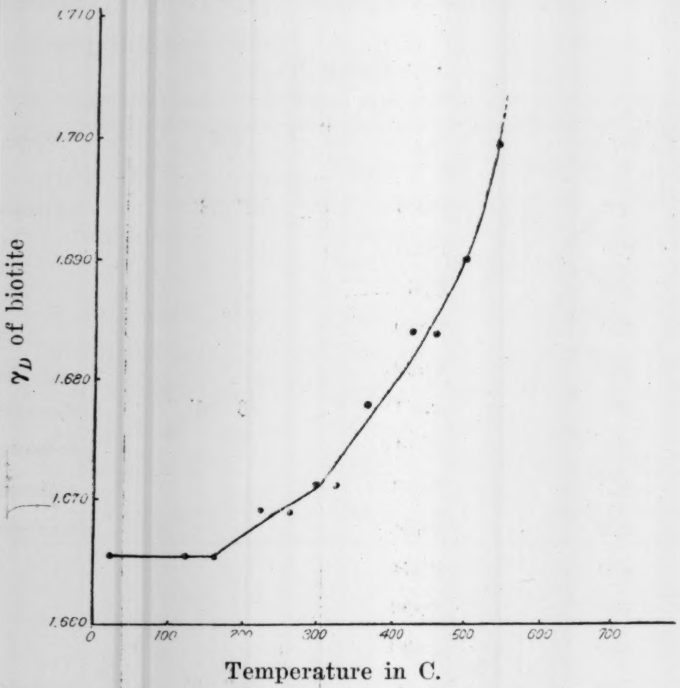

Fig. 2. The thermal change of biotite.

On heating, the biotite shows already a slight heat effect just above 200°C. and the refractive indices become higher and higher as the heating temperature increases, attaining γ_D=1.699 at 530°C. The biotite heated at 720°C. and upwards shows γ_D decidedly higher than the refractive index of methylen iodide (n=1.741–50)). Macroscopically, it is noticed that the heated biotite intensifies its luster, becoming golden-colored at temperatures above 500°C., while at first it is almost black. Under the microscope the biotites heated at higher temperatures are more red in color than those at lower temperatures. The optic axial angles increase as the heating temperature is raised, though their systematic variation is left uninquired, their optical orientation being unaltered.

The unusual yellowish-brown biotite found in the Tenjô-san lava resembles in its characters, macroscopical as well as microscopical, the product obtained by heating above 720°C. the greenish-brown biotite found in the same lava. It may, therefore, be presumed that the unusual biotite is not magmatic in origin, but a secondary product due to a thermal action, probably volcanic, on the greenish-brown biotite which is uniformly distributed in the lava. In this connection it is also remarkable that the unusual biotite is mainly confined to the portion where the lava is highly vesicular.

The thermal studies on biotites have been done by S. Kozu[24] and by A. L. Day and others.[25] The results obtained by these authors are qualitatively in accord with the writer's ones. While Kozu has done the heat treatment of biotite in a neutral air, his results are in accord with those obtained by heating biotites in the air. It is, therefore, inferred that the change of biotite due to heating does not mean simple oxidation of the biotite. According to Day, the transformation of the biotite in the lava of Lassen Volcano is due to decomposition which occurs in two ways; one by the loss of the volatile matter, the other by oxidation.

From the experimental data above given, it is probable that heat generated by the volcanic gases escaping from the lava surface will have far-reaching effect upon forming the unusual biotites.

The biotites in the rocks of Kôzu-shima are higher, whatever the just-mentioned unusual biotite may be, in their refractive indices than those of the other localities. This fact may probably mean higher content of iron oxides. They are generally fresh, without suffering magmatic resorption, but in devitrified rocks they are often partly resorbed. Some specimens stained with various shades of color, of the Tenjô-san lava contain biotite crystals which have been completely decomposed, probably due to volcanic emanation. These altered biotite must be carefully excluded for petrogenic discussion.

---

24) S. Kozu, "The Influence of Heat on the Refractive Indices and Optic Axial Angle of Biotite," *Chikyu* (*the Globe*), **9** (1928), 330–338 (in Japanese).

25) A. L. Day and E. T. Allen, *op. cit.*, *Publ. Carnegie Inst. Wash.*, **360** (1925), 49.

Groundmass.—By sudden chilling of the lavic magma at the time of extrusion, the magma in which the ready-made crystals had been immersed consolidated as the groundmass. The groundmass of the rocks of Kôzu-shima has consolidated to result in very poor crystallization. Excepting the fugitive substances, therefore, the groundmass is just the same in composition at one stage of the cooling magma. The composition of the groundmass may be various in different rocks, since the phenocrysts with which the magma was in equilibrium at the time of extrusion are not always same both in composition as well as in kind. The variation of the chemical composition of the groundmass must correspond to the variation of its optical constants. The refractive indices of the groundmasses of various rocks are given in Table XII, with the compositions of the phenocrystic plagioclases in parallel col.

TABLE XII.

Lava	n_D	Plagioclase
β-Lava	1·497	$Ab_{77}An_{23}$
γ-Lava	1·499 (5)	$Ab_{72}An_{28}$
δ-Lava	1·497	$Ab_{76}An_{24}$
ε_1 Lava	1·498	$Ab_{75}An_{25}$
ε_2-Lava	1·494	$Ab_{82}An_{18}$
Takôdo-yama lava	1·498 (5)	$Ab_{73}An_{27}$
Nachi-san lava	1·494	$Ab_{82}An_{18}$
Jôgoro-yama lava	1·493 (5)	$Ab_{82}An_{18}$
Anagi-yama lava	1·491 (5)	$Ab_{82}An_{18}$
Kôbe-yama lava	1·490	$Ab_{88}An_{12}$
Tenjô-san lava	1·490	$Ab_{88}An_{12}$

All the refractive indices in the table were measured on glasses of pumiceous specimens. Obsidian glass has a refractive index different from that of pumice, even though both are of a single lava. The obsidian glass from Sanuka-saki (ε_1-lava) shows $n_D = 1.484$, a value far lower than the pumice ($n_D = 1.498$) from the same lava. Accordingly, it is inferred that volatile substances which have been occluded in obsidian are in larger quantity than those in pumice. The specific gravity of the obsidian is 2.106 at 28°C. (cf. p. 304), white that of the pumice is 2.394 at 28°C.26) There-

---

26) A perlite from Shimoda in Izu peninsula: n_D of the groundmass glass = 1.493, sp. gr. of the glass at 28°C. = 2.269, the phenocrystic plagioclase $Ab_{88}An_{12}$.

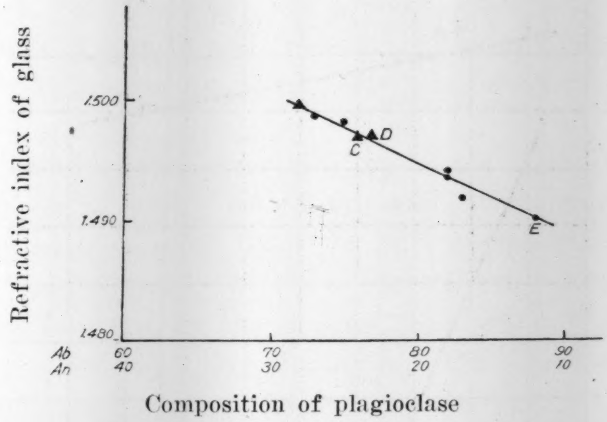

Fig. 3. Relation between the refractive index of natural glasses and the composition of plagioclases in the rocks of Kozu-shima.
● Biotite-plagioliparites.
▲ Hypersthene- and hornblende-plagioliparites.

fore, it is not correct to apply to natural magma the relative densities of crystals to the magma derived from dry melt.

From the data given in Table XII, the diagram of Fig. 3 is constructed. The figure shows a linear relation of the refractive index of groundmasses and the composition of accompanying plagioclases. The refractive index of the groundmass glass lowers as the accompanying phenocrystic plagioclase becomes richer in albite. According to W. O. George, the natural glass with higher refractive index is poorer in silica and alkalies, richer in lime and the ferromagnesion oxides. If so, the relation shows that a magma in equilibrium with more sodic plagioclase is more acidic than another one in equilibrium with less sodic plagioclase.

Chemical Composition.—The bulk composition of volcanic rock is the mixture of quenched magma (groundmass) and phenocrysts suspending in the magma.[27] The net composition of the magma is, therefore, obtained by estimating and eliminating the approximate amount of the phenocrysts in the rock. As the rocks of Kôzu-shima are rather poor in phenocrysts, the variation diagram of their bulk compositions must be only slightly shifted from the variation diagram of their groundmasses only. The bulk compositions of the rocks of Kôzu-shima described in the preceding chapter are plotted in Fig. 4. The phenocrystic minerals which seem to scatter the indicative points of the variation diagram of the rocks are quartz and feldspar, but ferromagnesian minerals (hypersthene, hornblende, and

---

27) S. Tsuboi, "The Genetical Interpretation of Extrusive Rocks," *Jour. Fac. Sci., Imp. Univ., Tokyo, Sec. II,* **1** (1925), 77–86.

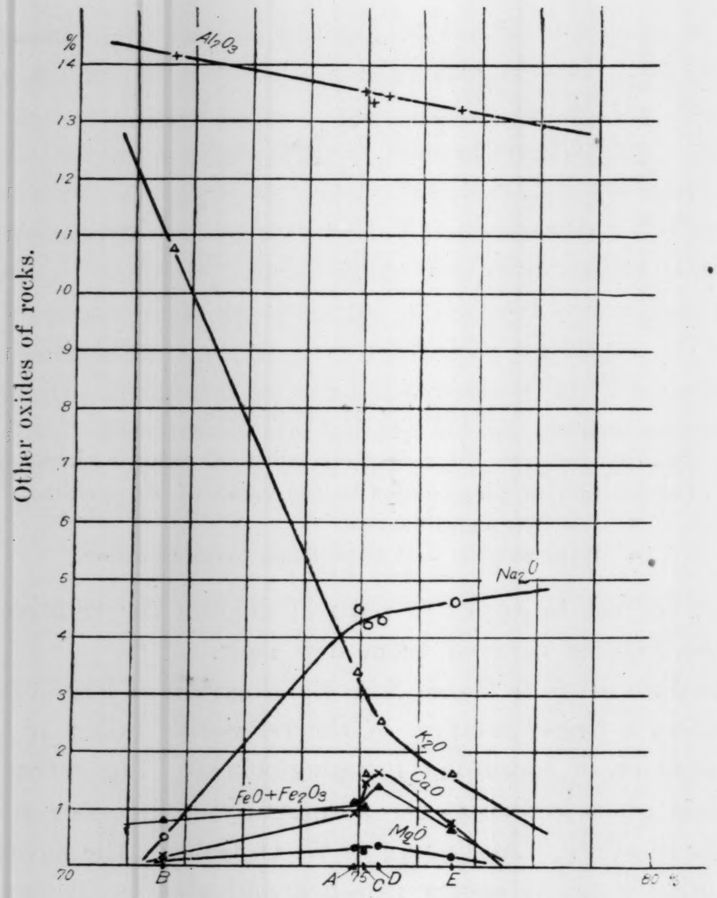

Fig. 4. Curves showing the variations in the composition of the rocks of Kôzu-shima.

TABLE XIII.

Rock	Orthoclase	Plagioclase	Quartz
Potash-liparite (α-Lava)	5%	—	—
Hypersthene-plagioliparite (β-Lava)	—	10% ($Ab_{77}An_{23}$)	5%
Hornblende-plagioliparite (δ-Lava)	—	5% ($Ab_{76}An_{24}$)	1%
Aphanitic rock (Ombashi-jima lava)	—	—	—
Biotite-plagioliparite (Tenjô-san lava)	—	5% ($Ab_{88}An_{12}$)	3%

biotite) may be neglected for the present consideration. The approximate percentages of quartz and feldspar in the analysed specimens were estimated under the microscope, the results being shown in the above table. (Table XIII).

Orthoclase, albite, and anorthite have the forms respectively of $KAlSi_3O_8$, $NaAlSi_3O_8$, and $CaAl_2Si_2O_8$, and the composition of these phenocrysts may be eliminated from the bulk compositions. The diagram thus plotted is approximately to show the variation of the groundmass, that is, variation followed by the magma from which the rocks of Kôzu-shima have been derived. By eliminating the dominant phenocrystic minerals, however, the variation diagram of the bulk compositions is but slightly modified. Accordingly, there is no serious error in regarding the variation diagram, Fig. 4, of the bulk compositions as that of the groundmasses. In the figure the amount of Al_2O_3 varies in nearly rectilinear relation with that of SiO_2, while other oxides do not show such relation. The indicative points of each oxide, however, are not irregularly scattered, showing a serial variation. It should be noted that K_2O and Na_2O show an antipathetic variation. There is a distinct tendency for one of these to be low where the other is high.

Differentiation.—The magma from which the rocks of Kôzu-shima have been derived may be regarded as corresponding in essentials to the later stage of crystallization, though it must be left for further study whether the magma is a salic differentiate derived from a basaltic magma by crystallization following the course of the so-called gabbro-granite differentiation or not The groundmass of the volcanic rock represents the residual liquid in which the phenocrysts have suspended. Then, on the assumption that the various rocks of Kôzu-shima have been derived from a common magma, we must search for the sort of material from which differentiation starts and the process of differentiation by which the variation of the succeeding magmas represented by the groundmasses has been brought about. From the variation diagram of the groundmasses, therefore, it is possible to deduce what sort of material would have been separated from a magma to change the composition in such a manner as shown in the variation diagram. If we assume that the diagram in Fig. 4 shows approximately the variation of the groundmasses, there are theoretically two possibilities to produce a change of the required kind: first, change from B to E by subtraction of potash-rich material, and second, change from E to B by subtraction of soda-rich material. But the first possibility is actually improbable. No evidence bearing upon such differentiation was found. As a simple graphic construction will show, the change from E to B is able to accomplish by separation of sodic plagioclase and quartz. These minerals are really the dominant phenocrysts suspended in the liquids E, D, and C. In this case, however, the course of differentiation and the order of extrusion become reverse. Moreover, the rock represented by E contains the phenocrysts of plagioclase and biotite which are of the most advanced stage as shown in Fig. 3. Accordingly, the change of the magma from E to B in the way as above-mentioned is also improbable; indeed the variation can not be explained by only one course of crystallization which changes the magma from B to E or from E to B.

Unfortunately, no silicate system which demonstrates the course of crystallization of liparitic magma has ever been investigated. But if we assume that the liparitic magma is a residual liquid at the later stage of crystallization of the basaltic magma, whatever of the course of the crystallization-differentiation, SiO_2 may be the principal constituent present in addition to feldspar. Therefore, the quaternary mixtures of quartz, orthoclase, albite, and anorthite may be considered here. To point the course of crystallization, it is possible to make some very useful deductions from theoretical considerations on the ternary mixture, orthoclase, albite, and anorthite. Although the equilibrium relations between the three feldspars, $KAlSi_3O_8$, $NaAlSi_3O_8$ and $CaAl_2Si_2O_8$, is yet problematical, the ternary diagram of feldspars, Fig. 5, deduced by Bowen[28] may be useful in the present connection.

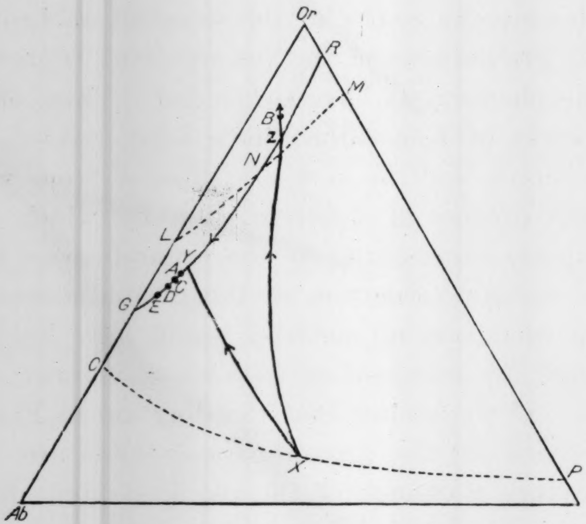

Fig. 5. Ternary diagram of the system, orthoclase-anorthite-albite (after N. L. Bowen).

---

28) N. L. BOWEN, The Evolution of the Igneous Rocks, (Princeton, 1928), 231.

In the figure the general relations between the three feldspars are represented. The curve GNR is the boundary between the fields of orthoclase and plagioclase. Orthoclase and albite have a eutectic point G with solid solutions on both sides; while orthoclase and anorthite is to be regarded as having a reaction relation at R. The curves OXP and LNM indicate the limits of solid solutions, orthoclase in plagioclase and plagioclase in orthoclase. The incongruent melting of orthoclase need not be considered on the crystallization of a liquid with excess silica. Now, we may take the mixture X which has the composition, orthoclase 10, albite 45, anorthite 45. The mixture crystallizes following the curve XY, if the opportunity for reaction of the separating crystals with the liquid is highly limited since early stage of crystallization. The liparitic magma may be expected in the later stage of crystallization following such a course. When the point Y is reached rather sodic plagioclase is jointed by orthoclase and the liquid changes the composition along the boundary curve towards G. On the other hand, the liquid X crystallizes following the course XZ, if perfect equilibrium prevails at least at the earlier stages. The point Z lies on the boundary curve between N and R where plagioclase reacts with the liquid to produce orthoclase. If the reaction can take place freely the liquid Z will move along the boundary curve towards E. But if reaction is prevented for any reason, the liquid Z will pass into the orthoclase field with separation of orthoclase only.

We may illustrate the variation of the rocks of Kôzu-shima with the aid of the diagram whose theoretical considerations have been outlined above. The potash-liparite (B in Fig. 4) and the plagioliparites (A, C, D, and E in Fig. 4) must have been derived by crystallization-differentiation following different courses, even if they are comagmatic in origin. The liquid X in Fig. 5, whose composition might be either andesitic or basaltic, began to crystallize with separation of plagioclase. As a result of crystal fractionation (either local grouping of the crystals or any method of prevention of reaction between the crystals and the liquid), the liquid followed the course XY. At Y orthoclase began to crystallize along with plagioclase and the liquid changed along YG. Through the course the separating plagioclase became richer in albite. In the actual rock series quartz and biotite show simultaneous crystallization with feldspar, and yet these crystal phases can not be represented in the simple ternary diagram. When the liquid became the composition A, a portion of the liquid free from phenocrysts was extruded as the aphanitic lava whose actual composition is represented at A in Fig. 4. When the liquid became the composition E, it was extruded as the Tenjô-san lava whose actual composition is represented at E in Fig. 4. In the liquid were suspended a little phenocrysts of orthoclase, quartz, plagioclase and biotite. As shown in the paragenesis diagram, Fig. 1, plagioclase and biotite changed their compositions as the crystallization advanced. The plagioclase and biotite suspended in E are of the most advance stage. The rocks represented by C and D in Fig. 4 are of such compositions of the liquid and such stages of crystallization as those represented by the corresponding points in Fig. 5. The rocks C and D contain conspicuous, though sporadical, phenocrysts respectively of hornblende and hypersthene. But there are reasons for believing that these minerals are not ones with which the liquids were saturated, at least when the lavic magmas were about to be extruded. The refractive index of the groundmass glass of the biotite-plagioliparite varies, as has been plotted in Fig. 3, in approximately linear relation with the composition of the plagioclase suspended in the glass. On the other hand, Fig. 1 illustrates a distinct paragenic relation of plagioclase and biotite. Since abrupt change of composition of liquid may be expected whenever a new crystal phase begins to crystallize, it seems probable that, if the liquid were saturated with either hypersthene or hornblende, the liquid (groundmass) might have shown some aberration from the relation shown in Fig. 3. But actually the groundmasses of the hypersthene- and hornblende-plagioliparites fall just on the line in Fig. 3, the plagioclases in these rocks being more sodic ($Ab_{77}An_{23}$) than the least sodic plagioclase ($Ab_{73}An_{27}$) in a biotite-plagioliparite. A deduction from this relation is that the groundmasses of the hypersthene- and hornblende-plagioliparites may have been saturated with biotite. In this connection, it should be noted first, that these two rocks carry minute flakes of biotite, and second, that the hypersthene-plagioliparite carries xenoliths of basaltic nature in which augite has been subjected to reaction with the liparite magma and transformed partly to green hornblende (cf. p. 296). From the behavior of the xenolith it is inferred that, whereas the conspicuous mafic mineral is hypersthene, the groundmass of the hypersthene-plagioliparite has been saturated with biotite, and that, by interaction with this liquid, the augite crystals in the xenolith have been partly converted into hornblende without changing far into biotite. The hypersthene- and hornblende-plagioliparites might be extruded from a portion of the magma where the cooling was a little more rapid than the portion wherefrom the biotite-plagioliparites came. As the results the serial variation of the liquid compositions and the actual relations of the phenocrysts and the groundmasses may be expected.

The variation of the liquid, from which the plagioliparites have been derived, is of only a short interval of the course of crystallization corresponding to AE in the ternary diagram. By simple graphic construction it is ascertained that to change the composition A to the composition B in the variation diagram, Fig. 4, quartz, orthoclase, sodic plagioclase, and some mafic minerals are to be subtracted. All of these minerals are present more or less in the actual rocks. The relative amount of these minerals is dependent on the relative movement of different kinds of the crystals. It was already mentioned that quartz and sodic plagioclase might be rather heavier than the residual liquid even in the plutonic condition.

The potash-liparite represented at B in Fig 4 has been produced by crystallization which might start on X in Fig. 5, but followed a different course XZ. When the liquid reached the point, Z, orthoclase began to crystalize along with plagioclase. But further reaction was prevented and the liquid B was reached with separation of orthoclase only. Accordingly, the liquid is very rich in potash but very poor in soda. The liquid corresponds to the potash-liparite whose actual composition is represented at B in Fig. 4.

From what has been stated, the curves in Fig. 4 can not be considered as the real liquid line of descent for the rocks of Kôzu-shima. They correspond to the curves obtained by plotting, after the method of the ordinary variation diagram, the change of the various oxides at B, A, C, D, and E in the ternary diagram.

Summary.—As the results of this investigation, the petrology of Kôzu-shima is summarised as follows:

All the rocks of the island have been developed from a common magma by fractional crystallization. The magma continued to crystallize following different courses. By low crystal fractionation (high reaction), potash-rich liquid from which the potash-liparite has come was formed. On the other hand, by high crystal fractionation (low reaction) the sodi-potassic liquid from which the plagioliparites have come was formed. Variation within the plagioliparites may be elucidated by the simultaneous separation of feldspar, quartz, and some mafic minerals. The hypersthene- and hornblende-plagioliparites were extruded from a portion where rather rapid cooling limited the opportunity for reaction in such a manner that either hypersthene or hornblende has been left as relict mineral. Among the mafic minerals (hypersthene, hornblende, and biotite), there is indication neither of reaction relations, nor of their simultaneous crystallization. The plagioclase and biotite show a regular paragenic relation, indicating the concomitant crystallization. The plagioliparites are not balanced in proportion of orthoclase and plagioclase, orthoclase being much less in amount than plagioclase. The relative amount of these minerals may be due to their relative movement in the liquid. The variation of the rocks of Kôzu-shima may be explained by fractional crystallization which starts on a common magma. The courses of crystallization correspond fairly well with those expected in the ternary mixtures, orthoclase, albite, and anorthite. The deduced courses of fractionation explain the variation, microscopical as well as chemical of the rocks of Kôzu-shima. Thus, the rock sequence in the order of differentiation:

Original magma → potash-liparite.
→ { aphanitic liparite → biotite-plagioliparites.
hypersthene-plagioliparite.
hornblende-plagioliparite. }

Chapter V. Comparison of Certain Aspects of Volcanoes in the Seven Izu Islands.

General Remark.—The "fossa magna," a well known volcano-tectonic zone, traverses central Japan from the Japan Sea coast to the Pacific in the direction of S. 10° E. and in this zone are arranged many volcanoes, one of which being the celebrated Volcano Fuji. This zone extends far away in the Pacific Ocean where it forms a submarine ridge which descends on its east side abruptly to a trench of over 8000 m. in depth. All of the Izu insular volcanoes rest on this submarine ridge and are considered to belong to the so-called Fuji Volcanic Zone which is represented by the volcano-tectonic zone.

In examining the bathymetric map of the Bay of Sagami, we can readily find out a subsidiary but sharply defined submarine ridge which is above the afore-mentioned one and runs from N. 40° E. to S. 40° W. Being separated by the shallow sea, 100 m. or thereabout in depth, Nii-jima, Shikine-jima, and Kôzu-shima rest on this ridge whose southwestern extension reaches as far as the Zenizu rocks, while other members of the Seven Izu Islands—Ô-shima, Miyake-jima, Mikura-jima, To-shima, and Hachijô-jima are arranged in the direction of the main submarine ridge, that is in the so-called Fuji Volcanic Zone. Being annexed to the main trend, the southwesterly trend is structurally expressive, since it is not only indicated by other several submarine ridges parallel to the Nii-jima—Kôzu-shima ridge, but also by distribution of acidic rocks in the southern part of the neighbouring Izu peninsula.

Thus the insular volcanoes are naturally divided into two groups, Nii-jima group and Ô-shima group, as already remarked by the previous writers.

Kôzu-shima and Nii-jima.—Nii-jima was studied in detail geologically as well as petrographically, by Fukuchi.[29] According to him, the rocks of the island are divided into the following kinds, with the exception of the loose products:

Pyroxene-liparite.	(1)	Enstatite-liparite	a. Nebu-saki type
	(2)	Augite-liparite	b. Nishino-ura type
Amphibole-liparite	(3)	Pyroxene-amphibole-liparite	c. Dômaru type
			d. Wakada type
	(4)	Hornblende-liparite	e. Jinai-shima type
Mica-liparite	(5)	Pyroxene-biotite-liparite ..	f. Atomizuno-sawa type
	(6)	Biotite-liparite	g. Habushi-ura type
			h. Awai-ura type
			j. Mukô-yama type

He systematized these lavas in the order of their extrusion from earliest one to later as follows:

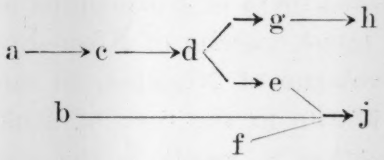

The writer landed twice the island and collected the rock. After careful observation, the writer can not agree with Fukuchi as to the order of extrusion of these rocks, but he thinks for certain that the biotite-liparites are younger in eruption than all the other. The collected samples were studied under the microscope. The petrographic description of these rocks, however, is out of the scope of this paper. For the purpose of petrogenic discussion, the refractive indices of the essential minerals were determined as shown in the following table.

---

29) N. Fukuchi, *op. cit.*

TABLE XIV.

Type	Plagioclase	Augite (n_{1D})	Hornblende (n_{1D})	Biotite (γ_D)
a	n. d.	—	—	—
b	$Ab_{72}An_{28}$	1·698	—	—
c	$Ab_{76}An_{24}$	1·696	1·645	—
d	$Ab_{78}An_{22}$	n. d.	1·642	—
e	$Ab_{66}An_{34}$	—	1·649	—
f	n. d.	n. d.	—	n. d.
g	$Ab_{84}An_{16}$	—	—	1·664
h	$Ab_{84}An_{16}$	—	—	1·678
j	$Ab_{82}An_{18}$	—	—	1·700<

In comparing with the paragenic relations of the minerals in the rocks of Kôzu-shima, the above table shows that the rocks of Kôzu-shima are genetically related with those of Nii-jima. In the rocks of Nii-jima, the plagioclase phenocrysts more calcic in composition than $Ab_{78}An_{22}$ are always in accompany with either pyroxene or hornblende, while the corresponding plagioclase phenocrysts in some rocks of Kôzu-shima are attended by biotite. The rock of Tenjô-san, the latest volcano of Kôzu-shima, resembles the rock of Mukô-yama, the latest volcano of Nii-jima, in microscopical as well as chemical properties. The biotite in the rock of Mukô-yama has been subjected to thermal decomposition to result in the similar product as some biotite flakes in the rock of Tenjô-san. The biotite in the rock (h) of Nii-jima also shows the same decomposition.

TABLE XV.

Rock	Plagioclase	Augite (n_{1D})	Hornblende (n_{1D})	Biotite (γ_D)
Kôzu-shima				
Xenolith a)	$Ab_{28}An_{72}$	1·694	1·672	—
b)	$Ab_{37}An_{63}$	1·696	1·682	—
Hypersthene-plagioliparite	$Ab_{77}An_{23}$	—	—	—
Nii-jima				
Xenolith phenocryst	$Ab_{16}An_{84}$	n. d.	—	—
groundmass	$Ab_{54}An_{46}$	1·695	1·713	—
Biotite-liparite	$Ab_{84}An_{16}$	—	—	1·678

The biotite-liparite of Awai-ura type (h) of Nii-jima carries basic xenoliths similar in mineral constitution to the xenoliths found in the hypersthene-plagioliparite (β-lava) of Kôzu-shima. A short petrographic description of these xenoliths was already given (cf. p. 298). In Table XV are summarized the refractive indices of the constituent minerals of the xenoliths, together with the rocks in which these xenoliths are carried.

The xenoliths, either of Kôzu-shima or of Nii-jima are not the dark patches or seggregations in the liparites as usually found in granites. Whether they are in direct genetical relation with liparites, is a matter of great importance, since these xenoliths and the basaltic rocks of the Ô-shima group including the basaltic ejecta of Nii-jima show not only petrogenic relations between the constituent minerals, but also chemical resemblance (cf. p. 297). If such a xenolith were a seggregated clot in the liparite, therefore, it would afford a strong evidence for concluding that the both extreme types of rocks in the Izu insular volcanoes are in intimate genetical relation. In any case, however, the fact that the xenoliths, which are correlative with the basaltic rocks of the Ô-shima group, have been enclosed in the liparites is an evidence for believing that the liparitic lavas are as young as the basaltic ones in the Izu insular volcanoes.

Nii-jima Group and Ô-shima Group.—As to the age relation between the liparitic and basaltic volcanoes in the Izu islands, two opinions have been raised among geologists. Fukuchi,(30) Kato,(31) and Kozu(32) considered that the liparitic vulcanisms are older than the basaltic ones, the former being correlated to the latest Tertiary vulcanism in the southern part of the Izu peninsula. Studying the geology of Nii-jima, Fukuchi reached the conclusions that the liparitic islands (Nii-jima, Shikine-jima, and Kôzu-shima) are to be geologically correlated to the Tertiary volcanoes (liparites and allied rocks) in the southern part of the Izu peninsula, both being situated structurally on the west of the Fuji Volcanic Zone to which the basaltic volcanoes both in the islands and in the peninsula belong, and that the liparitic insular volcanoes are to the basaltic ones what the Tertiary volcanoes in the southern part of the peninsula are to the volcanoes, Fuji, Hakone, Amagi, etc. in their aspects, morphological as well as geological.

---

30) N. Fukuchi, *Report Earthq. Invest. Com.*, **39** (1902), 4–40, (in Japanese).

31) T. Kato, *Ibid.*, **63** (1909), 23–32, (in Japanese).

32) S. Kozu, "Geology of the Southern Part of the Izu Peninsula," *Report Geological Survey*, **38** (1913), 1–38, (in Japanese).

Tsujimura[33] and Tsuboi[34] raised an objection to the views of the previous writers respectively from morphological and geological standpoints of view. Giving some critical review on the previous works, Tsuboi expressed in his "Volcano Ô-shima" the opinions that the Izu insular volcanoes are to be divided into Ô-shima group and Nii-jima group, and that all the volcanoes of these two groups are very young, the basaltic Ô-shima, Miyake-jima, and Hachijô-jima on the one hand and liparitic Nii-jima and Kôzu-shima on the other having displayed volcanic activity in historic times.

The idea that the liparitic volcanoes are as young as the recent basaltic ones seems to be heterodoxical to those who follow the doctorine that the former represents in our country of the pre-andesitic vulcanism of the Tertiary period. But the writer's personal observations both in Nii-jima and in the Izu peninsula were nothing but indorsing the views proposed by Tsujimura and also by Tsuboi.

Being very close to the basaltic Udone-shima (1 km. to the south), the liparitic lava at the northern end of Nii-jima is capped by a basaltic ejecta-bed. This relation between a liparitic lava and a basaltic ejecta-bed induced Fukuchi to conclude that all the liparites and allied rocks are older than the basaltic rocks of the Ô-shima group. The basaltic ejecta resemble petrographically the rocks of the near-by basaltic insular volcanoes. In the basaltic ejecta-bed, moreover, are found not only numerous blocks of liparite, but also basaltic blocks in which liparitic fragments are caught. It is, therefore, certain that the basaltic ejecta are of younger date than the underlying liparite. Nevertheless, the biotite-liparites which are of the latest vulcanism on Nii-jima are on no occasion covered by the basaltic ejecta-bed and, on the contrary, the biotite-liparite of Awai-ura type (h) rests on the bed, catching numerous basic xenoliths. As already mentioned, the basic xenoliths are not seggregated clots in liparite, being correlative petrographically and chemically to the basaltic rocks of the Ô-shima group. Accordingly, the presence of these xenoliths is a strong evidence for believing that some of the liparitic lavas are as young as the basaltic ones. The basaltic blocks are moreover imbedded in the liparitic ejecta-bed ("Shiromama" bed) of Nii-jima.

From what has been stated, it is an indisputable fact that in the insular volcanoes the liparitic rocks erupted, alternately with the basaltic ones, still in very recent times. To say nothing of the basaltic vulcanism of Ô-shima, Miyake-jima, etc., the liparitic vulcanism of Kôzu-shima and

---

33) T. TSUJIMURA, *Report Earthq. Invest. Com.*, **89** (1918), 57–96, (in Japanese).

34) S. TSUBOI, *Jour. Col. Sci. Tokyo Imp. Univ.*, Art. 6, **43** (1920), 125–141.

Nii-jima is also recorded in some reliable annals of the ancients.[35] The basaltic Ô-shima, Miyake-jima, and Hachijô-jima have many historic records of outburst whose latest ones being in 1923, 1847, and 1605 respectively. On the other hand, either one of the liparitic volcanoes, Kôzu-shima and Nii-jima has only one historic record of eruption, namely Kôzu-shima in 838 and Nii-jima in 886. Whether these liparitic eruptions were in such a nature that new lavas were extruded in quantity sufficient to form distinct volcanoes, the historic records are too unsatisfactorily detailed. But both islands bear no trace of recent explosion, either volcanic or phreatic; and on the contrary, Tenjô-san and Mukô-yama volcanoes respectively in Kôzu-shima and Nii-jima have very young morphological features, so young that they may well date from historic times. Thus, the liparitic volcanoes in the Izu islands are in all probability as young as the basaltic ones, being one of the leading examples of the recent liparitic volcanoes in the world.[36]

The insular volcanoes of Ô-shima group and Nii-jima group, besides being situated close together, have thus displayed volcanic activity alternately. It is, therefore, of no little importance to see whether the rocks of the two groups are genetically related with each other.

As far as the bulk composition is concerned, the rocks of the two groups have gone to the opposite extremities, the Ô-shima group being of extremely basic and the Nii-jima group highly acidic, and there is none which has an intermediate chemical composition between the two extremities. The rocks of the Ô-shima group are all basaltic in both chemical and normative mineral compositions, while the amount of SiO_2 in them is in excess to form the highest silicates, the excess silica being left as occult quartz in the norms. But actually these rocks are characterized by such califemic minerals as hypersthene and either olivine or augite. The plagioclase phenocrysts, modal as well as normative, are represented by bytownite. On the contrary,

---

[35] Zoku-Nihon-kôki (續日本後記), Sandai-jitsuroku (三代實錄), Nihon-kiryaku (日本紀略), and Fusô-ryakki (扶桑記略). See F. OMORI and S. NAKAMURA, *op. cit.*,

[36] According to I. Friedländer (''Vulkaninseln Griechenlands,'' *Zeitschrift für Vulkanologie*, 8 (1924)), recent acidic volcanoes in the world are:

Kôzu-shima	Liparit
Nii-jima	Ditto
Lassen Peak	Ditto (Dacit?), seit 1913, Kalifornien
Guadajara	Ditto, noch etlich Fumarolen, Mexiko
Monte Pelato	Ditto, Lipari
Phyriplaka und Trachylas	Ditto, Milos (Vulkaninseln Griechenlands)

To these we may add the volcano Esan (Atsusa-nupri) in Hokkaido, which is built up of augite-plagioliparite or rhyodacite.

Table XVI.

	I	II	III	IV	V	VI	VII	VIII	IX	X	XI	XII	XIII
SiO_2	53·10	51·45	54·55	53·35	49·91	50·79	50·74	71·64	74·93	75·35	75·10	76·60	76·05
Al_2O_3	14·73	16·84	16·26	15·62	18·13	16·61	18·59	14·13	13·52	13·49	13·36	13·22	12·44
Fe_2O_3	3·38	1·49	4·07	4·21	3·87	6·96	9·23	0·34	0·76	0·95	0·30	0·27	0·84
FeO	9·42	10·95	8·02	8·21	5·48	3·51	1·01	0·50	0·72	0·55	0·74	0·43	0·22
MgO	4·97	4·48	3·66	4·44	6·16	7·63	5·37	0·08	0·32	0·36	0·27	0·19	0·17
CaO	9·09	10·71	8·91	9·68	9·90	10·03	10·21	0·17	0·93	1·61	1·43	0·75	0·87
Na_2O	2·09	1·23	2·44	2·18	2·33	2·58	2·35	0·50	4·50	4·28	4·21	4·62	4·31
K_2O	0·44	0·37	0·32	0·84	0·37	0·55	0·57	10·77	3·39	2·52	1·58	1·61	2·88
$H_2O +$	1·22	0·72	0·05	0·06	1·90	0·07	0·74	0·23	0·46	0·06	0·17	0·11	1·66
$-$			0·24	0·34	0·88	0·31	0·16	0·80	0·33	0·61	2·27	1·50	0·11
TiO_2	1·03	1·27	1·19	1·18	0·87	1·01	0·98	0·55	0·13	0·20	—	—	0·12
P_2O_5	0·11	0·26	—	—	—	—	0·06	0·08	0·08	—	—	—	tr.
MnO	0·34	0·19	—	—	—	—	0·16	tr.	0·08	0·08	0·10	0·16	0·07
ZrO_2	0·04	—	—	—	—	—	—	—	—	—	—	—	
CO_2	—	—	0·24	tr.	tr.	0·19	—	—	—	—	—	—	
Total	99·87	99·96	99·95	100·02	99·90	100·24	100·14	99·79	100·15	100·06	99·53	99·46	99·74

Q	9·6	8·8	13·4	9·6	4·3	4·4	6·5	27·6	33·2	37·1	41·2	41·6	37·9
Or	2·8	2·2	1·7	5·0	2·2	3·3	3·0	63·3	20·0	15·0	8·9	9·4	17·2
Ab	17·8	10·5	20·4	18·3	19·9	22·0	19·9	4·2	38·2	36·1	35·1	38·8	36·1
An	29·2	39·2	32·0	30·4	37·8	32·0	38·4	—	3·9	7·2	6·9	3·6	4·2
C	—	—	—	—	—	—	—	1·6	0·9	1·0	2·3	2·5	0·7
Di	12·4	10·3	8·0	14·6	9·1	13·8	9·1	—	—	—	—	—	—
Hy	19·7	23·2	14·6	13·4	16·4	12·7	9·4	1·6	1·3	0·9	0·6	1·2	0·5
Mt	4·9	2·1	5·8	6·0	5·6	8·4	0·3	—	1·2	1·2	0·2	0·2	0·4
Il	2·0	2·4	2·3	2·3	1·7	1·9	1·8	1·0	0·3	0·5	—	—	0·1
Ap	0·3	0·6	—	—	—	—	—	0·3	0·3	—	—	—	—
Hm	—	—	—	—	—	1·2	8·6	0·3	—	2·0	—	—	0·5

Ô-shima Group.
Ô-shima I. The somma lava (basaltic bandaite).
II. The central cone lava (miharaite).
Miyake-jima III. A specimen from the summit (augite-andesite).
IV. The lava of 1874 (olivine-bearing feldspar-basalt).
To-shima V. A specimen from 60 m. down the top (olivine-bearing feldspar-basalt).
Udone-shima VI. Locality not mentioned (olivine-bearing feldspar-basalt).

Nii-jima Group.
Kôzu-shima VII. Basic xenolith in the plagioliparite.
VIII. α-Lava (potash-liparite).
IX. Ombashi-jima lava (aphanitic rock).
X. β-Lava (hypersthene-plagioliparite).
XI. δ-Lava (hornblende-plagioliparite).
XII. Tenjô-san lava (biotite-plagioliparite).
Nii-jima XIII. Mukô-yama lava (biotite-plagioliparite).

the rocks of Nii-jima group are extremely high in SiO_2 and low in femic oxides. Hypersthene is the only califemic mineral in the norms calculated from the chemical compositions, though the rocks actually diversified by the presence of biotite, hornblende, and pyroxene. Excepting the potash-liparite, the amount of Na_2O is always larger than that of K_2O and dominant feldspar, normative as well as modal, is oligoclase. The chemical composition along with the normative mineral compositions of the rocks of the two groups are shown in Table XVI. As seen from the table, of the genetical relation

TABLE XVII.

Rock	Plagioclase	Augite (n_{1D})	Hypersthene (n_{1D})
	$Ab_{77}An_{23}$	—	1·700 (5)
Xa	$Ab_{28}An_{72}$	1·694	—
Xb	$Ab_{37}An_{63}$	1·696	—
11	$Ab_{27}An_{73}$	1·691 (5)	n. d.
b	$Ab_{72}An_{28}$	1·698	—
Xn	$Ab_{16}An_{84}$	n. d.	—
(groundmass)	$Ab_{54}An_{46}$	1·695	—
En	$Ab_{27}An_{73}$	1·692	—
A	$Ab_{15}An_{85}$	1·686 (5)	n. d.
66	$Ab_{25}An_{75}$	1·691 (5)	—
10	$Ab_{32}An_{68}$	1·696	—
12	$Ab_{25}An_{75}$	1·691 (5)	—
M	$Ab_{25}An_{75}$	1·691	n. d.
H	$Ab_{25}An_{75}$	1·692	—

Nii-jima Group.
  Kôzu-shima
    Xa } Xenoliths in the Hypersthene-
    Xb } plagioliparite (β-lava).
    11 Two-pyroxene-andesite (ejecta in the Chichibu-yama ejecta-bed).
  Nii-jima
    b Augite-liparite (lava of Nishino-ura type).
    Xn Xenolith in the lava of Awai-ura type.
    En Olivine-augite-andesite (ejecta in the basaltic ejecta-bed).

Ô-shima Group.
  Ô-shima
    A Hypersthene-bearing olivine-bytownite-basalt (somma lava).
  Miyake-jima
    66 Olivine-augite-andesite (central cone lava).
    10 Augite-andesite (lava at Tsubota).
    12 Ditto (Benkene lava).
  Mikura-jima
    M Pyroxene-andesite (lava at the landing place).
  Hachijô-jima
    H Pyroxene-andesite (lava, locality uncertain).

between the two groups nothing can be drawn from the chemical relation, the only fact being that they are of calci-alkalic suit.

Some rocks of the two groups have in common, plagioclase and one or both of hypersthene and augite as phenocrystic minerals. These minerals, therefore, are useful for the petrogenic discussion. In Table XVII are shown the compositions of the plagioclase phenocrysts and the refractive indices of the associating pyroxene phenocrysts, following S. Tsuboi's optical analysis.

The above table shows distinctly that the monoclinic pyroxenes in association with less calcic plagioclases have higher refractive indices. Thus, the paragenic relations between these porphyritic minerals can well be likened to those of rocks of a distinct lineage. Here, however, it is confronted with a certain difficulty to conclude that the two groups are genetically related with each other, being wanted in an intermediate rock type which may link the one group to the other. In addition, when two or more mafic minerals are present in a rock, the paragenic relation between the mafic minerals and the associating plagioclases becomes complex. To judge whether some of such rocks are genetically related with each other, therefore, requires further investigation.

In concluding this chapter, the rocks of the Izu insular volcanoes are divided into two groups, Ô-shima group and Nii-jima group, and it is beyond question that all the liparitic rocks of the Nii-jima group are not older than the basaltic rocks of the Ô-shima group, but both kinds of rock have been extruded alternately, no matter what their genetical relations may be. Even if the rocks of the two groups are comagmatic in origin, they have been too widely differentiated to be put easily in direct relation.

Chapter VI. Geological Relations of the Seven Izu Islands to the Izu Peninsula.

For the discussion on the volcanologic history of the Seven Izu Islands, it is desirable to know the geology of the near-by Izu peninsula, because it is reasonably expected that the southern part of the peninsula has some geological connection with the Izu islands.

Geology of the Izu Peninsula.—The references to the geology of the Izu peninsula are to be found in a paper By H. Ishiwara[37] and that by S.

---

[37] H. Ishiwara, "Geology of the Volcanoes of Izu Peninsula," *Report Earthq. Invest. Com.*, **17** (1898), 3–49, (in Japanese).

Kozu.[38] The geology of the Volcano Amagi was specially studied by J. Suzuki.[39]

In the winter of 1925–6, the writer made a short visit to the vicinity of Shimoda. But it is not the writer's intention in this paper to discuss the geology of the whole of the peninsula, nor to give detailed description of the rocks. The present aim is limited to find anything pertaining to the geology of the Izu islands.

The southern part of the peninsula is largely built up of volcanic rocks accompanying tuffs, agglomerates, and breccias. As far as the writer's observations go, these rocks are in sequence: propylite, tuffite, potash-liparite, plagioliparite, dacite, and pyroxene-andesite. The propylite occupies a considerable portion and is covered unconformably by the tuffite. The propylite is an altered andesite, though its characters, macroscopical as well as microscopical, are quite multifarious. Sometimes it is hardly distinguished from the fresh andesite.[40]

Throughout the greater part of the district of Shimoda, the sedimentary rocks are of volcanic origin, occupying a considerable portion of the area. They often exhibit a distinct bedding, owing to the alternation of layers of coarser and finer materials. Fine tuff and tufaceous sandstone alternate with andesite-agglomerate and tuff-breccia. Sometimes the white tuff is coarsely mottled with black patches of andesite, occasionally along with fragments of pitchstone, perlite, and obsidian. Besides, andesite sheets are sandwiched in between these beds, and also andesite dikes run through the latter. A large outcrop of liparitic perlite is found in the tuff-breccia at Hayashiyama, 2 km. to the west of Shimoda. Thus, these tufaceous beds are of both andesitic and either liparitic or dacitic materials, these materials being often commingled with each other. In places the beds are fossiliferous, containing several marine fauna,[41] though not sufficiently well preserved to be identified. As the rocks become more calcareous, so do the fossils

---

38) S. KOZU, "Geology of the Southern Part of Izu Peninsula," *Report Geological Survey*, **38** (1913), 1–19, (in Japanese).

39) J. SUZUKI, "Geology of Volcano Amagi," *Jour. Geol. Soc. Tokyo*, **28** (1922), 431–448, (in Japanese).

40) For the sequence of the formations of the peninsula, the conceptions of the previous writers diverge. According to Kozu the geological sequence of the southern part of the peninsula is: plagioliparite, potash-liparite, propylite, liparite, Tertiary sediments, dacite, and pyroxene-andesite; all volcanic rocks accompanying their own tuffs and breccias or agglomerates.

41) According to Ishiwara these fossils are of the uppermost pliocene. See ISHIWARA, *op. cit.*, *Report Earthq. Invest. Com.*, **17** (1898), 14–17, (in Japanese).

become more numerous. Stratigraphical relations of the beds are so complicated that their detailed account may take too many pages. As far as the writer's observations go, the liparitic and dacitic lavas overlie the propylite or the more or less altered andesite, yet they are of the same general period as the corresponding tuffs which alternate with the andesite agglomerate and the andesite tuff. Accordingly, some andesites are of the same age with either the liparites or the dacites, but eruption of the andesitic rocks was further continued after that of the liparitic and dacitic rocks had ceased. Namely, eruptions of the acidic rocks and basic rocks were not followed in regular sequence, but first andesite; next andesite, dacite, and liparite; and finally andesite. The eruption of the andesite was continued up to the Quaternary period when the volcanoes of central type, Amagi, Hakone, etc. were formed.

Volcanic Rocks of the Izu Peninsula.—Detailed, petrographical descriptions of the rocks of the peninsula may be out of place here, but a few remarks are necessary for the discussion on the rocks of the Izu islands. Volcanic rocks in various kinds are represented in the peninsula, and by studying the rocks, the petrological relations to the Izu islands may be understood. The propylite is, for a while, to be put aside, since it has been

TABLE XVIII.

Rock	Plagioclase	Augite (n_{1D})	Hornblende (n_{1D})	Bietite (γ_D)
1	$Ab_{88}An_{12}$	—	—	1·665 (5)
2	$Ab_{62}An_{38}$	—	1·666	—
3	$Ab_{41}An_{59}$	1·691	—	—
4 a)	$Ab_{28}An_{72}$	1·689	—	—
b)	$Ab_{48}An_{52}$	1·690	—	—
c)	$Ab_{56}An_{44}$	1·691	—	—
5 a)	$Ab_{25}An_{75}$	1·689	—	—
b)	$Ab_{25}An_{75}$	1·690	—	—

1—Plagioliparite (lava of Mikura-yama at the boundary of Asahi-mura and Chikuma-mura, 4 km. to the west of Shimoda).

2—Dacite (lava of Takane-san, 3.5 km. to the northwest of Shimoda).

3—Auganite (lava-sheet at Susaki, 3 km. to the southeast of Shimoda).

4—Andesites (lavas of the Volcano Amagi), a) Asama-yama lava; b) Tôgasa-yama lava; c) Io-yama lava.

5—Andesites (lavas of the Volcano Hakone), a) Myôjô-yama lava; b) Myôjin-yama lava.

subjected to more or less the so-called propylitization whose origin is another important problem. The refractive indices of the essential mafic minerals and the composition of the associating plagioclases in the rocks of the peninsula are given in Table XVIII.

The plagioclases and pyroxene in the andesitic rocks of the peninsula show a regular paragenic relation; while the same relation between the plagioclases and mafic minerals in the liparite and dacite remains uncertain for absence of mafic minerals common to these rocks. The genetical relation, which may be suggested by paragenic relations of porphyritic minerals, between the andesitic rocks and the liparitic rocks of the peninsula is to be left for further study. Then, the question that is just to be solved is whether the liparitic rocks and the andesitic rocks of the peninsula are genetically related with the corresponding rocks of the Izu islands.

From the data given in Table XVII (p. 326) and XVIII (p. 329), the paragenic relations between plagioclase and pyroxene in the rocks of both the peninsula and the islands are graphically represented below.

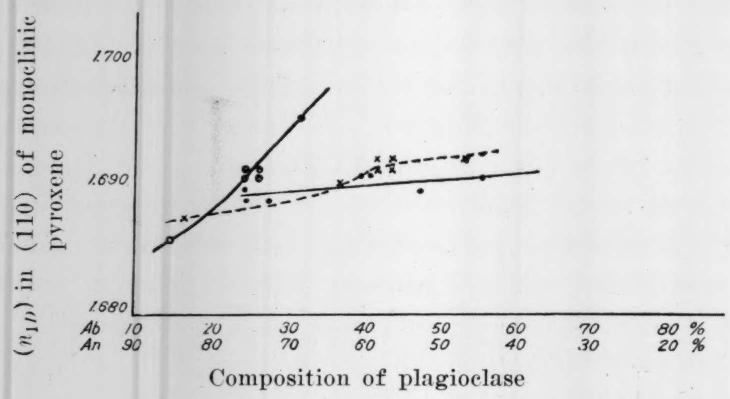

Fig. 6. The actual paragenic relations of plagioclases and monoclinic pyroxenes in the rocks of Izu islands (thick line), Izu peninsula (thin line), and Tokachi in Hokkaido (broken line).

As seen from the figure, the paragenic relation in the basaltic rocks of the insular volcanoes is not represented on the same curve as that of the corresponding relation in the andesitic rocks of the peninsula. Accordingly, andesitic or basaltic rocks of both regions seem to be of two distinct genetical lineages. But it must be in mind that a rock series which shows a definite paragenic relation is of a genetical lineage, yet all the rocks of comagmatic origin do not always show a definite paragenic relation, that is to say, even if a number of rocks are of comagmatic origin, some of these rocks may belong to a different genetical lineage. If the magma had cooled uniformly in its every portion, the volcanic rocks resulted from quenching of the magma at various stages of cooling would be enlisted in a definite genetical lineage. But the rate of cooling is not, in all probability, uniform through the magma and, therefore, the rocks resulted from a portion of the magma may be different in genetical lineage from those resulted from another portion of the same magma. From the figure we can suggest that the basaltic rocks of the insular volcanoes, among which Ô-shima and Miyake-jima are yet active, were derived from a portion of the magma where the cooling might be slower than another portion, wherefrom the andesitic rocks of the peninsula had come in the Diluvio-Tertiary period. On the same figure may be plotted the augite-liparites of Nii-jima, but it is not certain with which of the two lineages of andesitic rocks they are genetically related.

The liparitic rocks of the peninsula and those of the islands are genetically related with each other, the biotite-plagioliparite from Mikura-yama (No. 1, Table XVIII, p. 329) comes just on the curve showing the paragenic relation between plagioclases and biotites in the liparites of Kôzu-shima (cf. Fig. 1, p. 306). But, at present, data on this subject are too poor to give decisive conclusion.

If the suggestion, by means of the optical analyses of the rock minerals, that the andesitic rocks of the peninsula and those of the islands are different in genetical lineage is not erroneous, it may be expected that the chemical characters of these rocks will show some particular relations. The bulk compositions and any classification based upon them have, as they are, not any petrological problem to be discussed, but in order to see whether the rocks of one region have distinct chemical characteristics, it will be permissible to use the bulk composition.

The refractive indices and the chemical compositions of the rock minerals have to be mutually related, though the actual interdependence must be determined by means of quantitative chemical analyses of the optically analysed minerals.

The relations between the compositions of the normative plagioclases and those of the normative mafic minerals may or may not reflect the paragenic relations of the modal minerals in the same rocks. In order to ascertain this expectation, the normative mineral compositions of the rocks of the region now concerned were calculated (Table XVI, p. 324). According to the normative representation of the C. I. P. W. quantitative system, composition of plagioclase depends upon the relative amount of lime and soda combined with alminium silicate to form anorthite and albite respectively; and normative pyroxene is silicate of ferrous oxide and magnesia, together with or without lime left after forming the plagioclase.

The refractive indices of ferromagnesian minerals seem to change effectively according to the relative amount of ferrous oxide and magnesia held in them. Therefore, the relation between the ferro-magnesian ratio of normative pyroxenes and the compositions of normative plagioclases may be parallel to the relation between the refractive indices of modal pyroxenes and the composition of modal plagioclases.

In Figure 7, the composition of normative plagioclase is denoted by the Ab% on the abscissa; and the molecular ratio of FeO (+MnO) and MgO combined to form normative pyroxene is denoted by the ordinate.

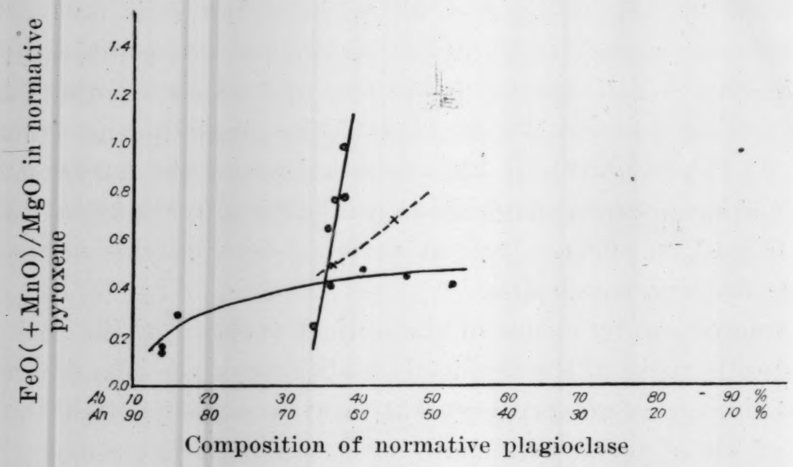

Fig. 7. The relations of the normative plagioclases and ferromagnesian ratios in the normative pyroxenes in the rocks of Izu islands (thick line), Izu peninsula (thin line), and Tokachi in Hokkaido (broken line).

As seen from the figure, the ratio FeO(+MnO) : MgO in the normative pyroxene increases as the normative plagioclase grows rich in albite. The rocks of a distinct genetical lineage are arranged on a distinct curve. Thus, as in the paragenic relation of the optically analysed porphyritic minerals, so in chemical relation deduced from the bulk compositions of the rock, the basaltic rocks of the Izu insular volcanoes are different in lineage from the andesitic rocks of the Izu peninsula. For the comparison, the chemical relation of the normative minerals of the andesitic rocks of Volcano Tokachi in Hokkaido is also shown in the figure. The actual paragenic relation of the porphyritic minerals in the rocks is given in Fig. 6 (p. 330).[42] In the rocks of the volcano, we see that the curve showing the paragenic relation of the porphyritic minerals is in the similitude of the curve showing the chemical relation of the normative minerals. Comparing the figures, therefore, we may assume that the compositions of the porphyritic minerals run parallel with the compositions of the rocks. The refractive indices of pyroxene seem to change effectively in proportion to the ferro-magnesian ratio in the mineral. But this assumption is yet not well grounded, since in actual cases the rock-forming minerals are complex in their constitutions. Especially that is the case in biotite and hornblende, so that the liparitic rocks in which these minerals are widely diffused, must be kept from the present discussion.

---

[42] F. Tada and H. Tsuya, "The Eruption of the Tokachi-dake Volcano, Hokkaido, on May 24th, 1626," *Bull. Earthq. Research Inst., Tokyo Imp. Univ.*, **2** (1927), 84, (in Japanese).

The variation diagram do not show the above-mentioned particular relations between the rocks of the peninsula and those of the islands. Throughout the whole period (Tertiary and subsequent ages), the sequence of eruption of the liparitic rocks are from less silicic to more silicic, at the same time potash being richer in earlier rocks while soda in later ones. The basaltic rocks have changed from those of intermediate acidity of the peninsula to more basic ones of the islands. Moreover, the variation diagram constructed from the chemical analyses of the rocks of both the peninsula and the islands does not show any distinct serial relation.[43] But the chemical compositions have some common characteristics that are good for distinguishing these rocks from those of other districts. The rocks of the Izu region are always higher in CaO and lower in alkalies, while the other oxides are present respectively in slightly varied amounts. The same thing is also said when the Niggli's projection diagram is constructed and compared with the type-diagram of calc-alkali rocks.[44]

Very little can be said now concerning the process of differentiation through which the various rocks of the Izu region have been derived. If we assume for a moment that all the rocks are of comagmatic origin, the processes of differentiation must have been followed on condition, though tentative, that

1) the andesitic rocks of the Izu peninsula and the basaltic rocks of the Izu islands are of respective distinct genetical lineage;
2) the andesitic rocks of the peninsula were extruded from a portion

---

43) It seems more reasonable that if a magma is subjected to the crystallization-differentiation, the resulting various rocks are to be arranged in a variation diagram which shows neither linear nor smoothed serial relations.

44) Conrad R. Burri, *Min. Pet. Mitt.*, **6** (1925), 1.

of the magma where the rate of cooling was more rapid than another portion wherefrom the basaltic rocks of the islands have been erupted; and

3) the liparitic rocks of the Izu islands are genetically related with the similar rocks of the peninsula and these rocks have been erupted, alternately with the andesitic rocks since the Tertiary period.

The general rock sequence in the order of extrusion may be systematized in the following scheme:

Izu peninsula	Izu islands
Propylite → andesite → basaltic andesite	Basaltic andesite
Potash-liparite → dacite → plagioliparite	Potash-liparite → plagioliparite

18. 神津島火山

地震研究所　津屋弘逵

神津島は伊豆七島の一であつて、大島の南西六十粁の距離にある。本島は流紋岩火山の重疊せる火山島であつて、その火山は大島の如き玄武岩火山と著しい對照をなしてゐる。故に先づその地形及び地質構造を明かにし、岩石をその產状、肉眼的及び顯微鏡的性質等によつて類別記載した。次に岩石の顯微鏡的研究より知り得た事實に基いて岩漿分化の過程を論究し、進んで隣接諸島及び伊豆半島の火山岩と比較し、神津島火山の地質學的、岩石學的位置を知る手掛りを述べた。

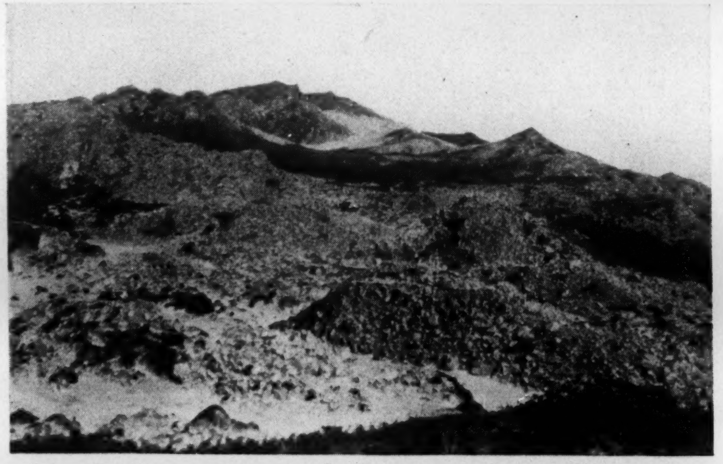

Fig. 1. The surface of the Tenjô-san lava, viewed southwards from the highest point. See p. 274.

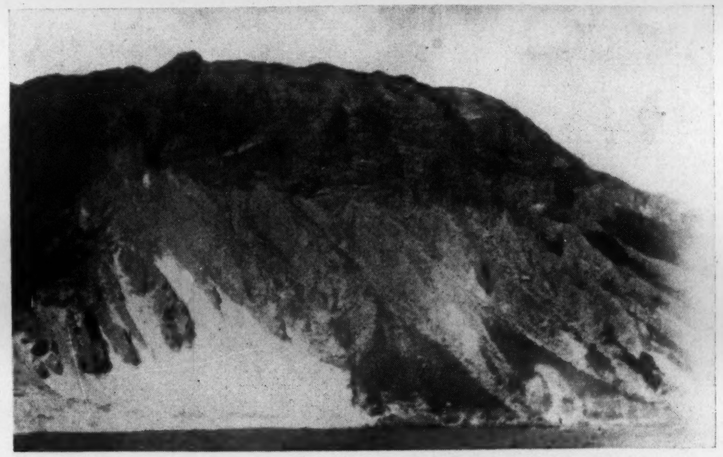

Fig. 2. The southeastern lava cliff of Tenjô-san with talus at its foot, viewed northwards from Takô-wan. See p. 275.

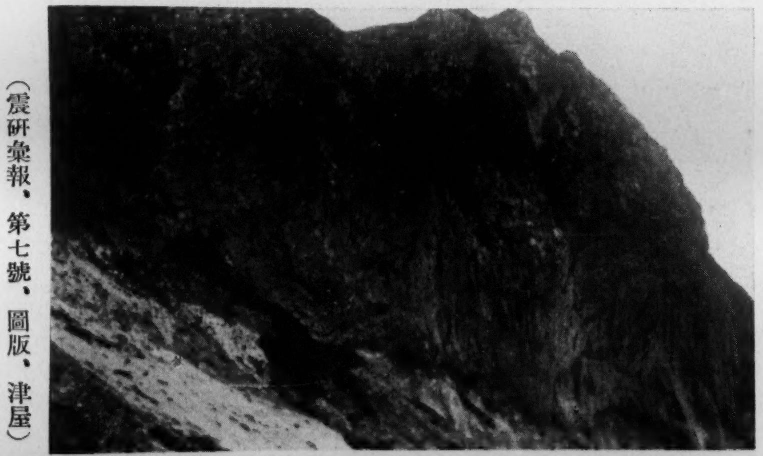

Fig. 3. The eastern lava cliff of Tenjô-san, with the Kushigamine ejecta below, viewed westwards. See p. 275.

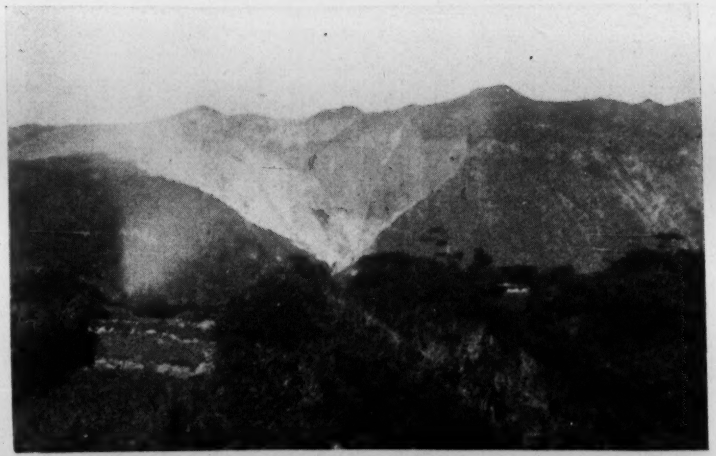

Fig. 4. A distant view of the Shiroshima cinder-cone, with the Tenjô-san lava in the right, viewed eastwards from Takane-san. See p. 276.

（震研彙報、第七號、圖版、津屋）

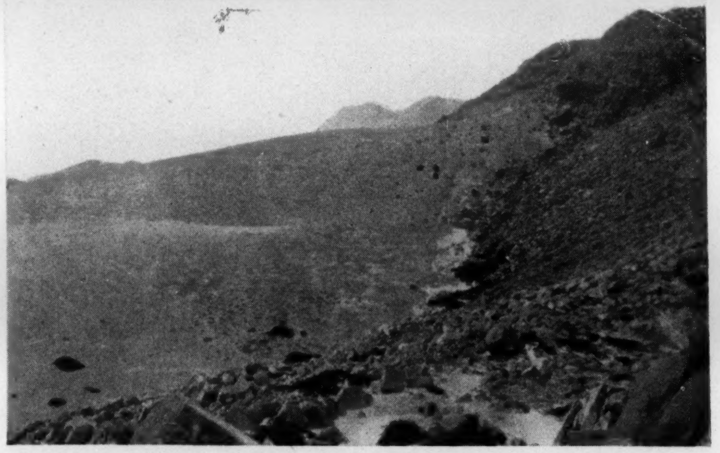

Fig. 1. The crescentic crater of the Shiroshima cinder-cone, viewed northwestwards from the highest point of Tenjô-san. See p. 276.

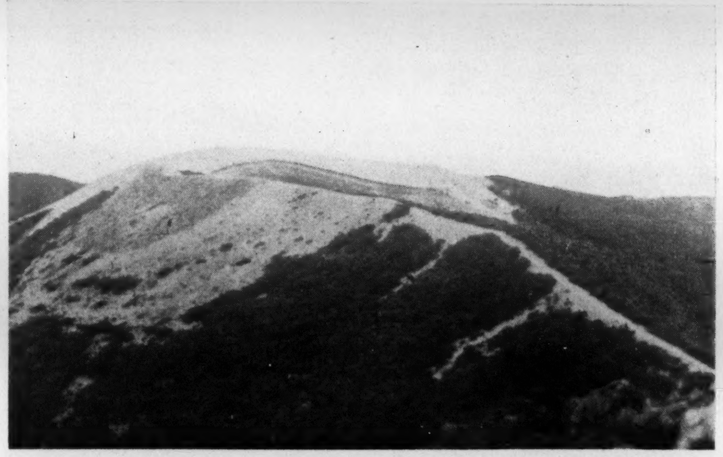

Fig. 2. The Kushigamine cinder-cone, viewed eastwards from Tenjô-san. See p. 276.

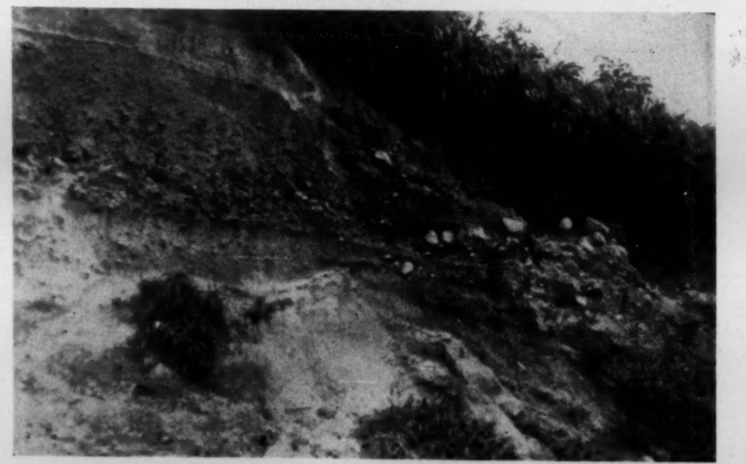

Fig. 3. The "Shiromama" ejecta-bed in the left and fluvial gravel in the right, at the northern shore of Mae-hama. See p. 277.

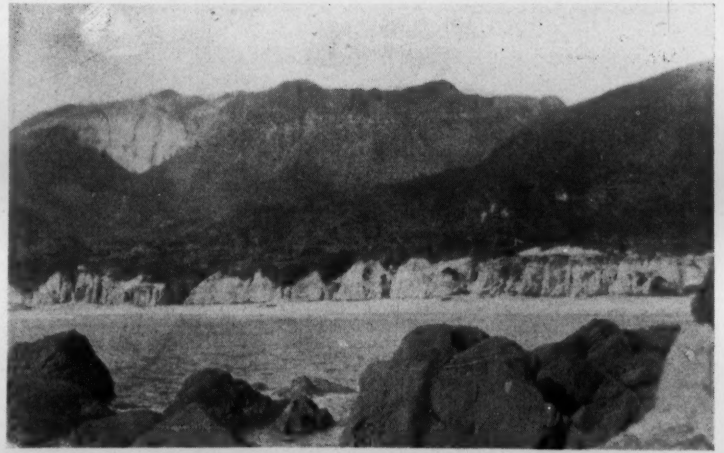

Fig. 4. The "Shiromama" ejecta-bed along the shore of Mae-hama. See p. 277.

（震研彙報、第七號、圖版、津屋）

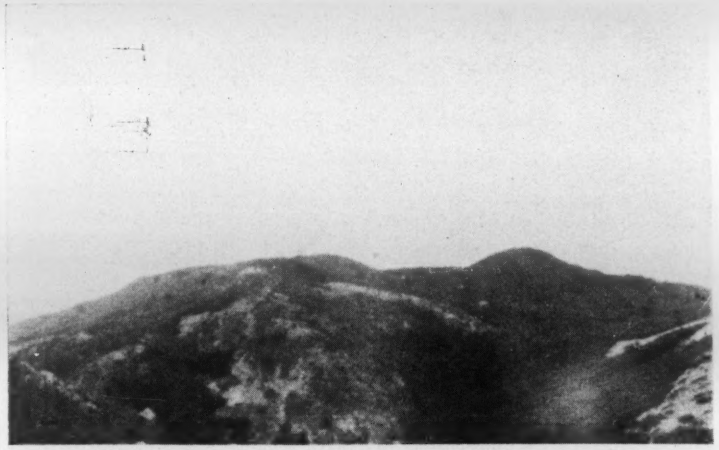

Fig. 1. The summit of Jôgoro-yama, and the northern foot of Kushigamine in the right, viewed northeastwards from Tenjô-san. See p. 278.

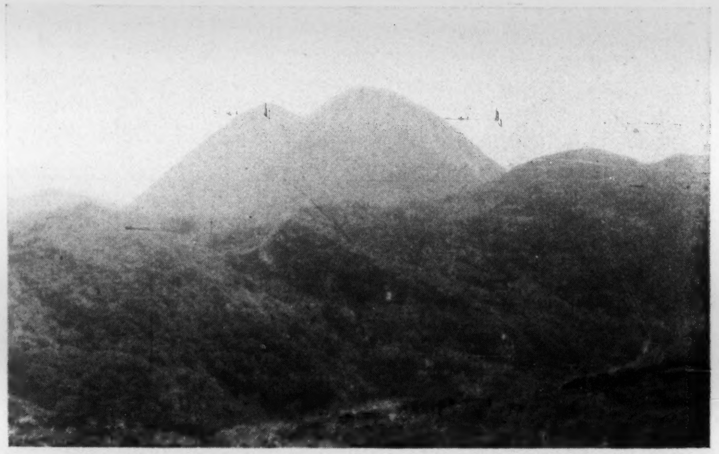

Fig. 2. Kôbe-yama, viewed northwestwards from Jôgoro-yama. See p. 278.

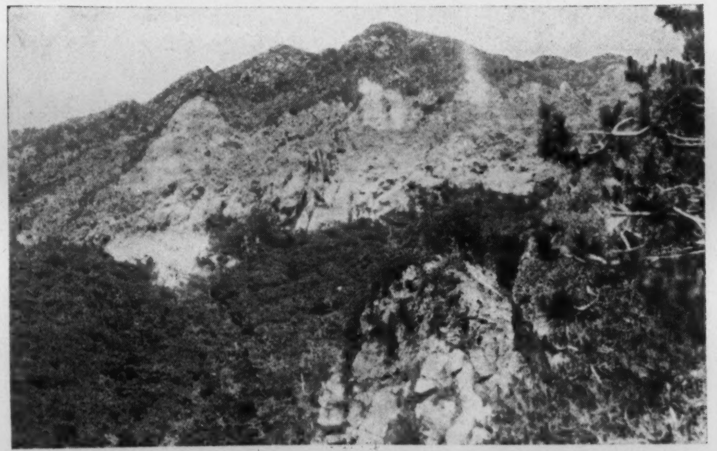

Fig. 3. The western flank of Kôbe-yama, broken lava near the summit and the ejecta-bed below. See p. 278.

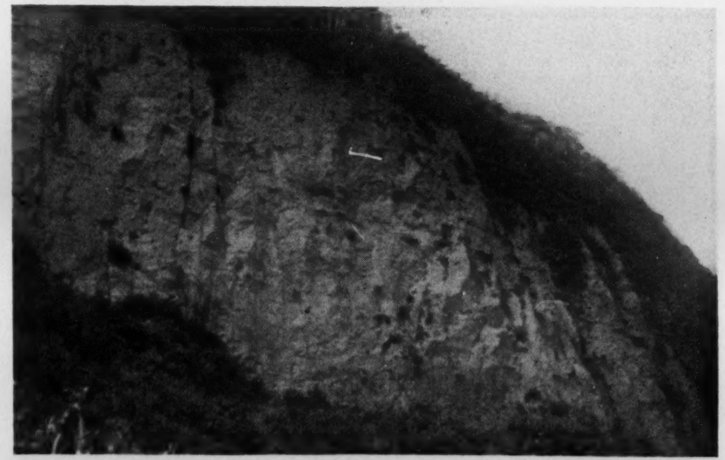

Fig. 4. The Nachi-san lava, a lava cliff fronting the valley of the Kawara, at Tachimoto. See p. 279.

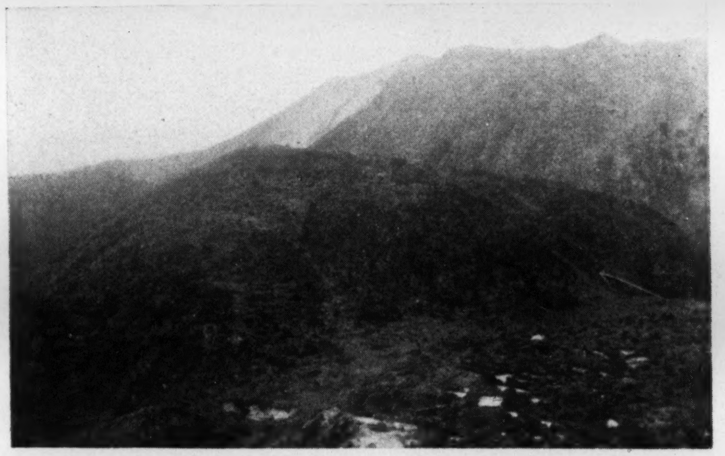

Fig. 1. Takôdo-yama, with Tenjô-san, viewed eastwards from Chichibu-yama. See p. 279.

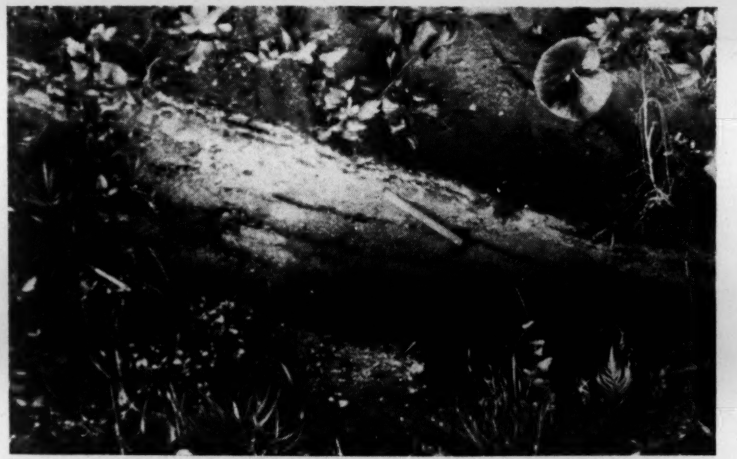

Fig. 2. The Chichibu-yama ejecta-bed below and the "Shiromama" bed above, a view illustrating unconformity of the two formations, at Tachimoto. See p. 279.

Fig. 3. General view of Chichibu-yama, as seen from the sea of the shore of Naga-hama. See p. 279.

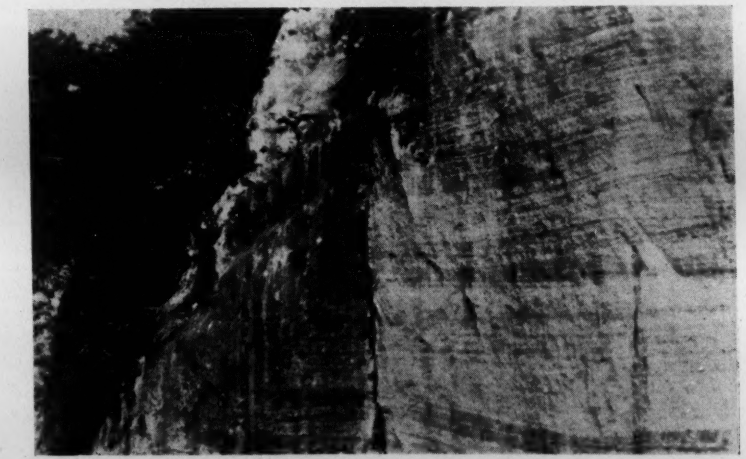

Fig. 4. The Chichibu-yama ejecta-bed at Yokokawa. See p. 280.

（震研彙報、第七號、圖版、津屋）

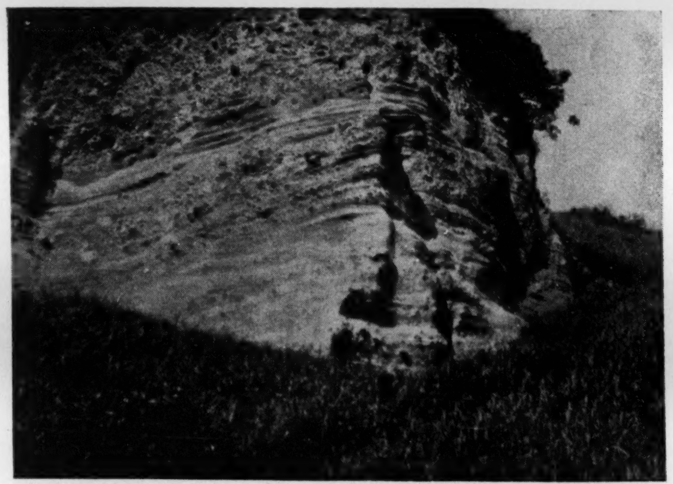

Fig. 1. The Chichibu-yama ejecta-bed near the pass between Chichibu-yama and Takôdo-yama. See p. 280.

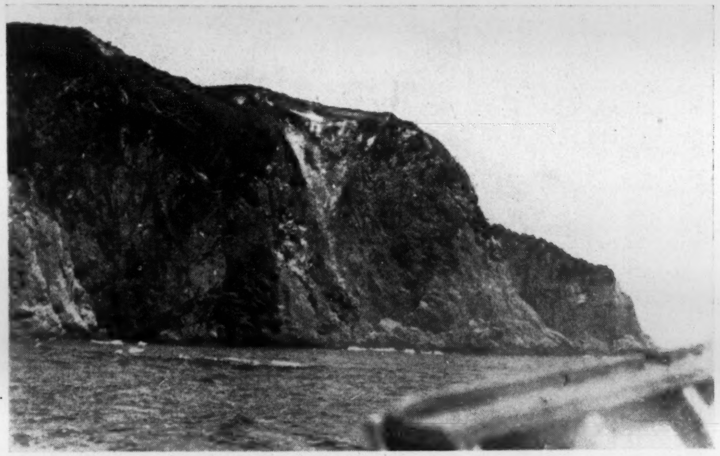

Fig. 2. Ditto, above the β-lava, near Kinnaga-hana, southwestern coast. See p. 280.

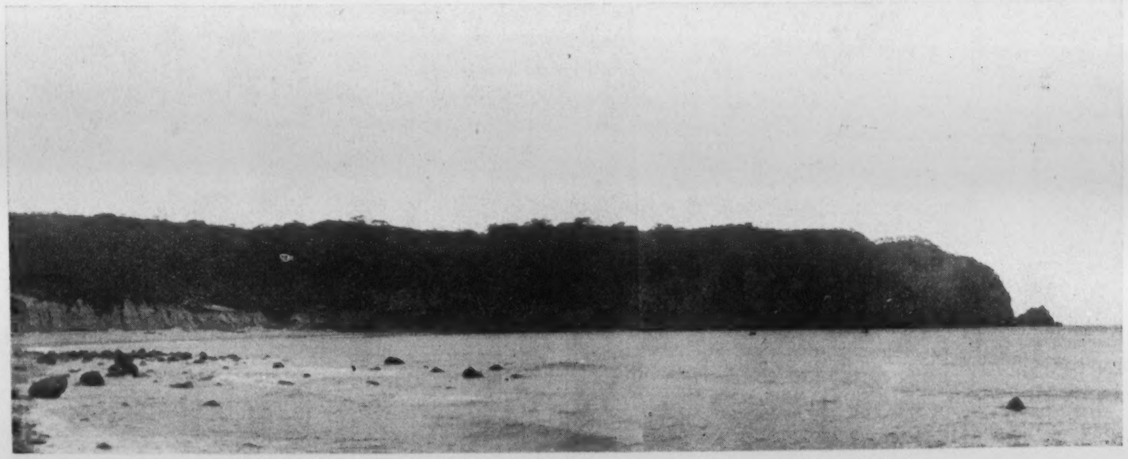

Fig. 3. The lava forming the table land of Membô, and the "Shiromama" bed along the shore of Mae-hama in the left. See p. 280.

（震研彙報、第七號、圖版、津屋）

Microphotographs of the Rocks of Kôzu-shima.

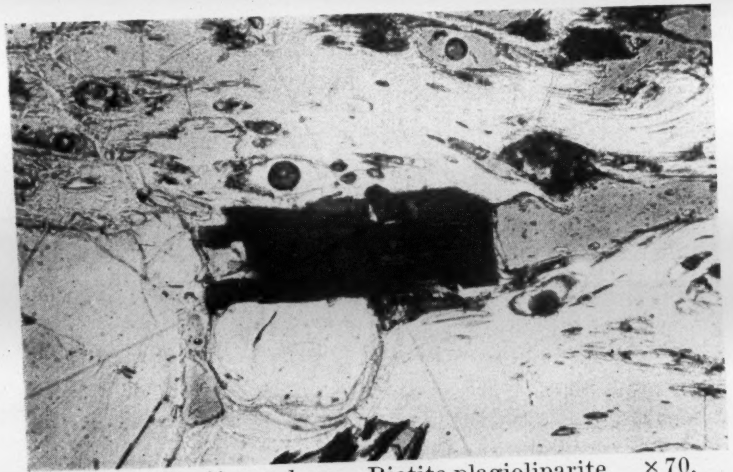

Fig. 1. Tenjô-san lava. Biotite-plagioliparite. ×70. See p. 282.

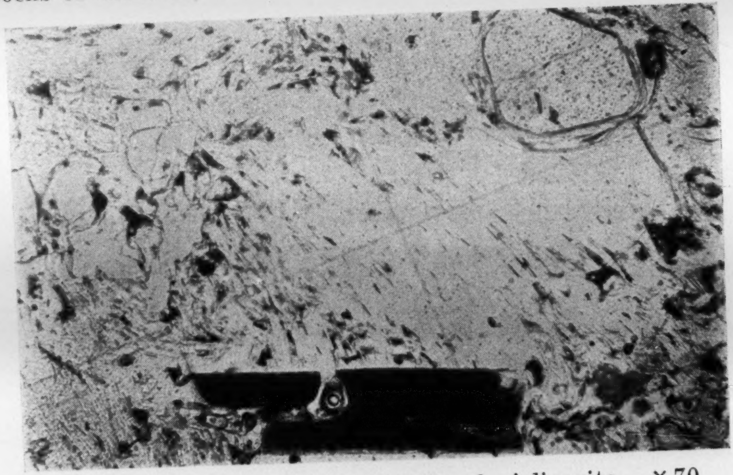

Fig. 2. Kôbe-yama lava. Biotite-plagioliparite. ×70. See p. 285.

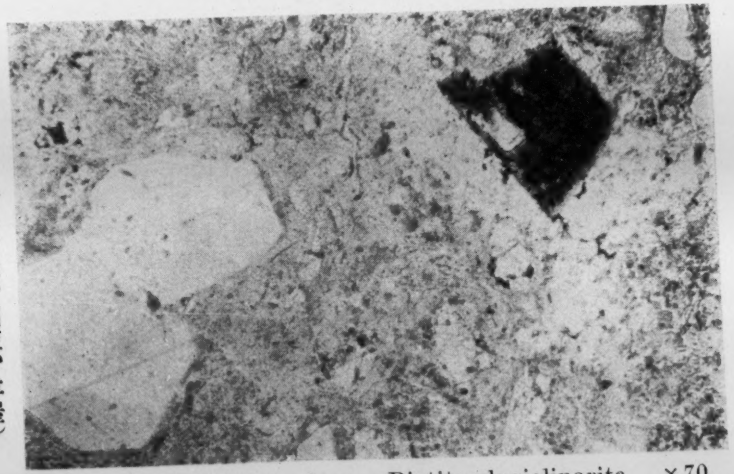

Fig. 3. Takôdo-yama lava. Biotite-plagioliparite. ×70. See p. 285.

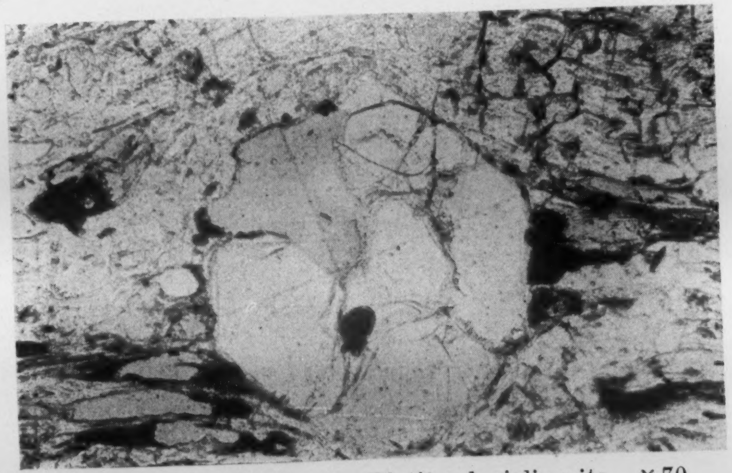

Fig. 4. Nachi-san lava. Biotite-plagioliparite. ×70. See p. 285.

（震研彙報、第七號、圖版、津屋）

Microphotographs of the Rocks of Kôzu-shima.

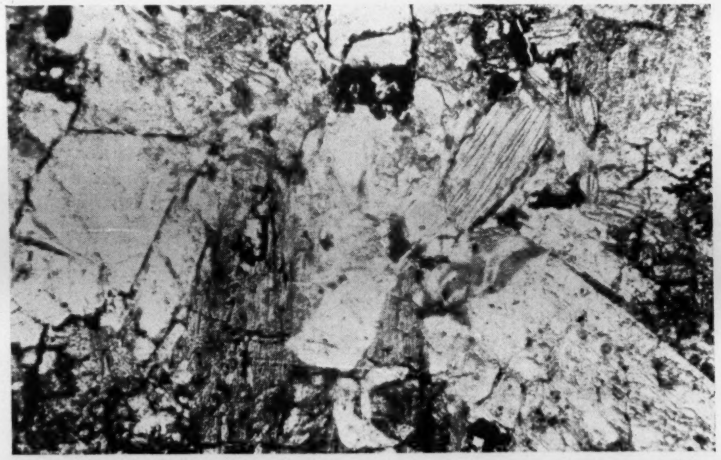

Fig. 1. An ejected block in the Chichibu-yama ejecta-bed. Porphyritic hornblende-diorite. ×70. See p. 287.

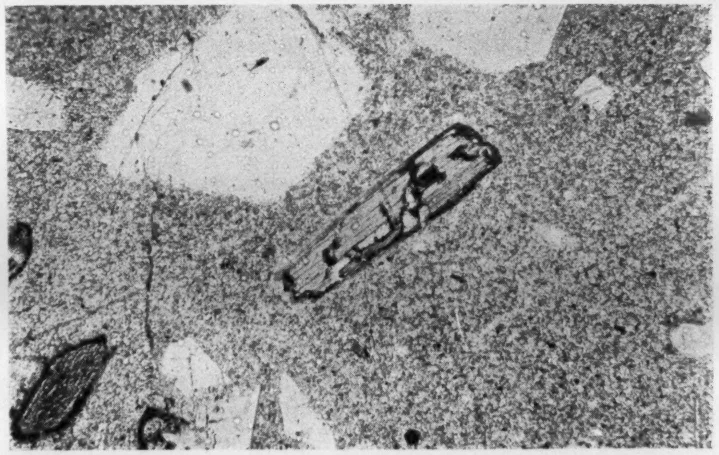

Fig. 2. An ejected block in the Chichibu-yama ejecta-bed. Hornblende-andesite. ×70. See p. 287.

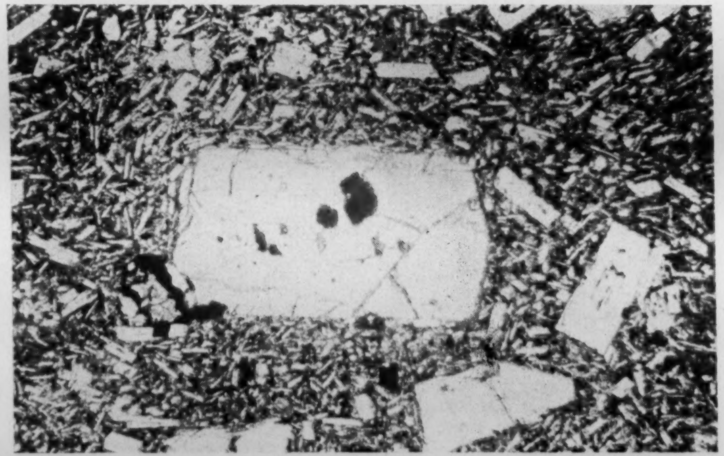

Fig. 3. An ejected block in the Chichibu-yama ejecta-bed. Two pyroxene-andesite. ×70. See p. 288.

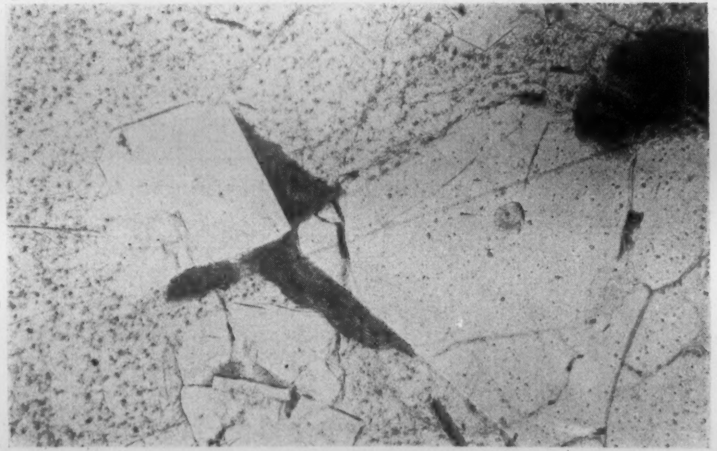

Fig. 4. ϵ-Lava of the first period. Biotite-plagioliparite. ×70. See p. 288.

（震研彙報、第七號、圖版、津屋）

Microphotographs of the Rocks of Kôzu-shima.

Fig. 1. Ombashi-jima lava. An aphanitic rock. ×70. See p. 290.

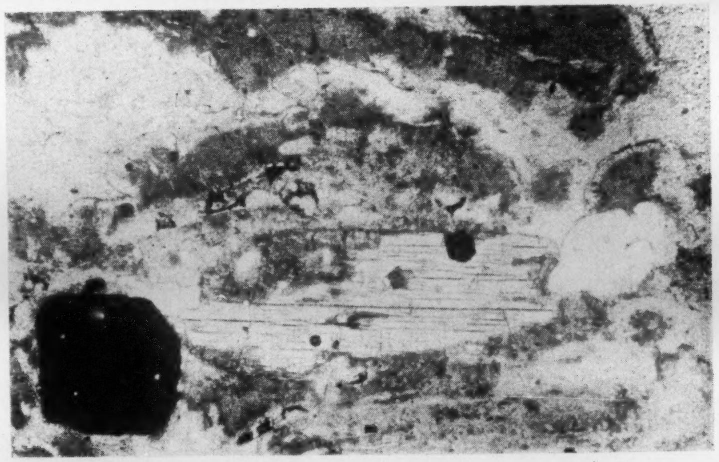

Fig. 2. δ-Lava of the first period. Hornblende-plagioliparite. ×70. See p. 291.

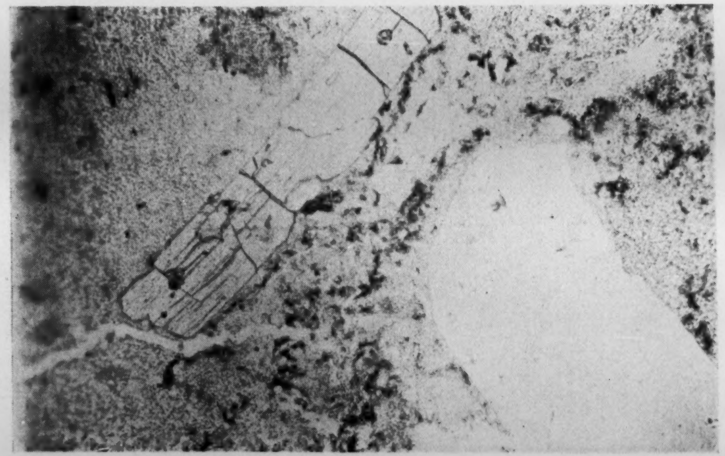

Fig. 3. γ-Lava of the first period. Hornblende-bearing hypersthene-plagioliparite. ×70. See p. 294.

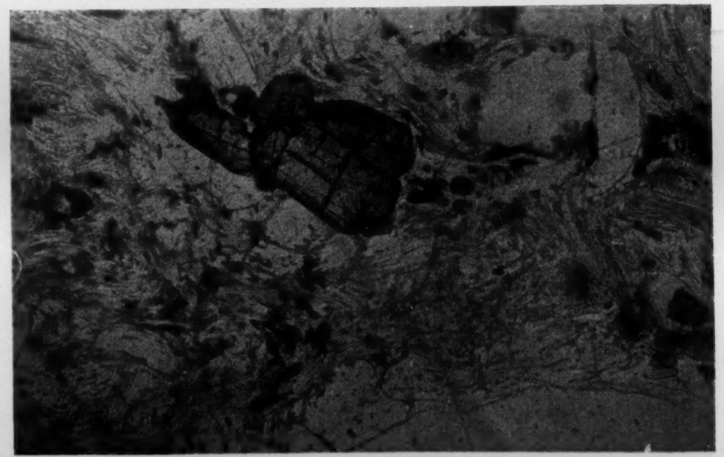

Fig. 4. β-Lava of the first period. Hypersthene-plagioliparite. ×70. See p. 294.

（震研彙報、第七號、圖版、津屋）

Microphotographs of the Rocks of Kôzu-shima.

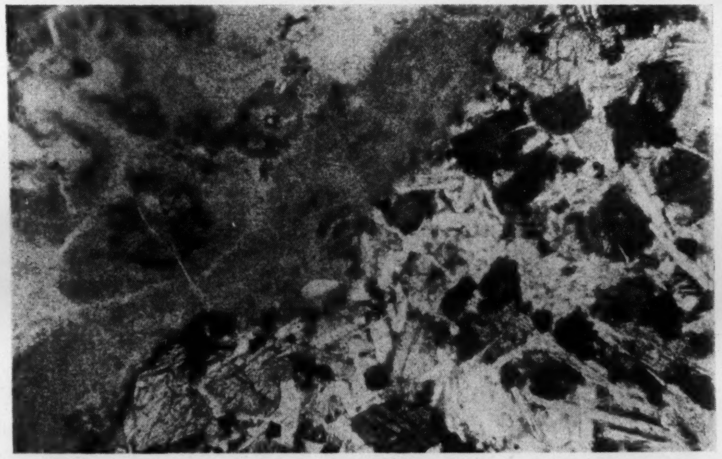

Fig. 1. Basic xenolith in the hypersthene-plagioliparite (β-lava). Augite-hornblende-labradorite rock. × 70. See p. 296.

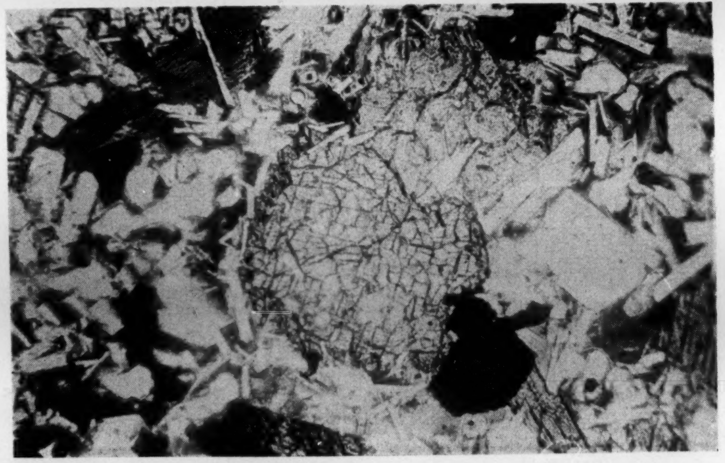

Fig. 2. Basic xenolith in the hypersthene-plagioliparite (β-lava). Augite-hornblende-labradorite rock. × 70. See p. 296.

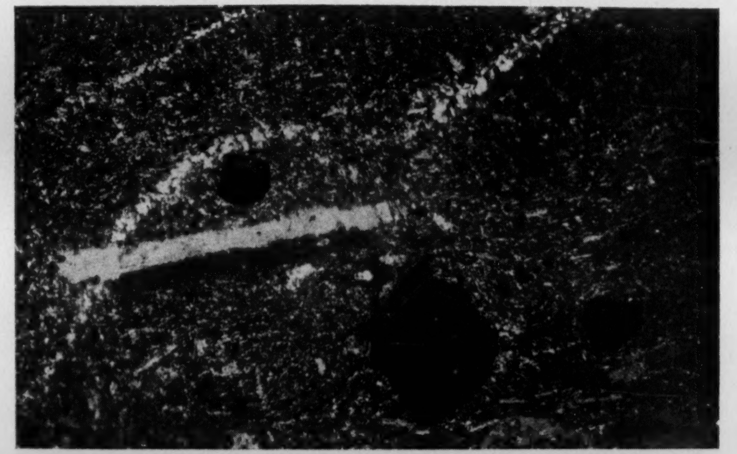

Fig. 3. α-Lava of the first period. Potash-liparite. × 70. See p. 299.

（震研彙報、第七號、圖版、津屋）

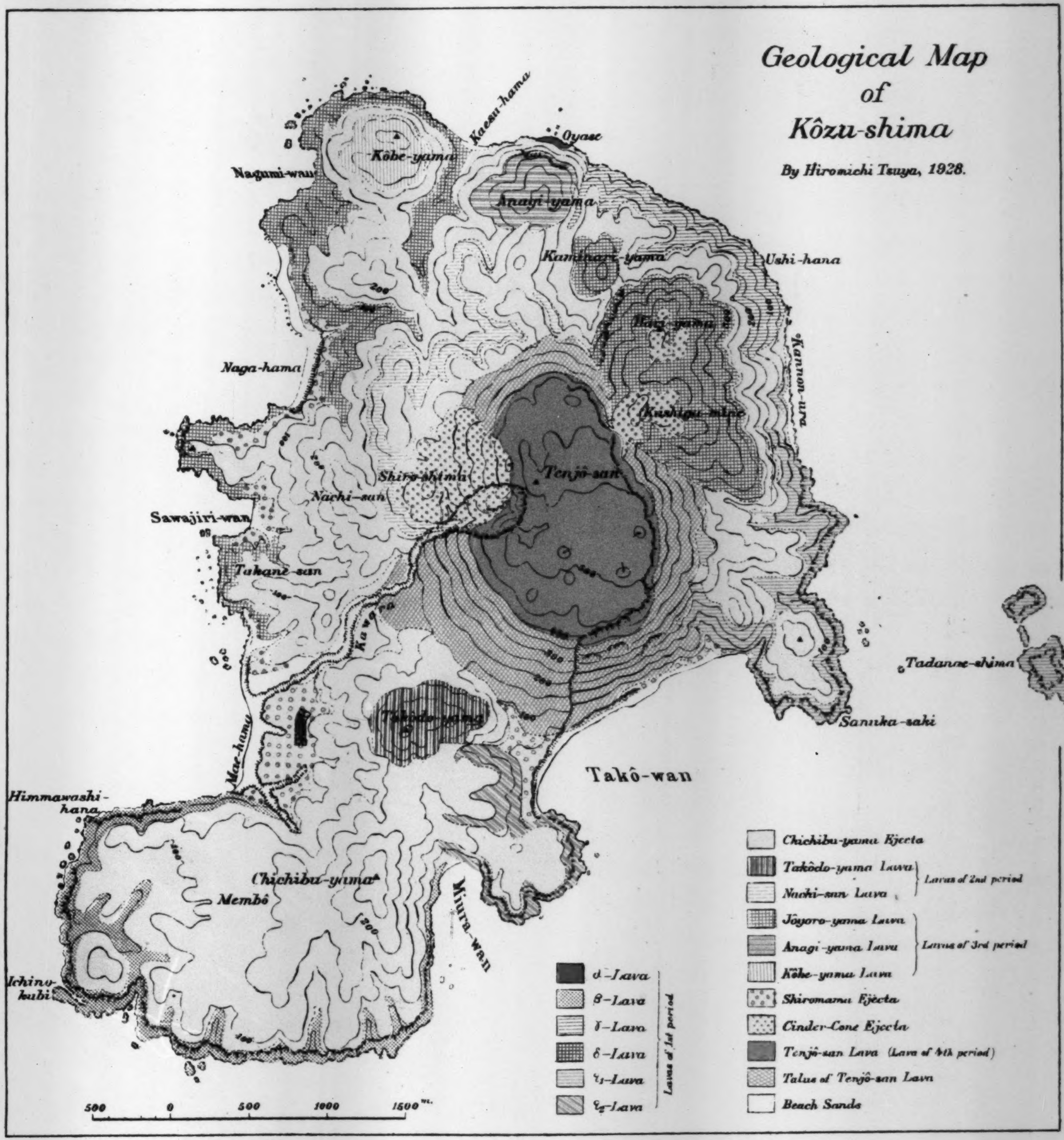

Geological Map of Kôzu-shima

By Hiromichi Tsuya, 1928.

Kôbe-yama
Kaesu-hama
Oyase
Nagumi-wan
Anagi-yama
Kaminari-yama
Ushi-hana
Naga-hama
Kannon-ura
Kushigu-mine
Tenjô-san
Shiro-shima
Nachi-san
Sawajiri-wan
Takane-san
Tadanae-shima
Takôdo-yama
Sanuka-saki
Mae-hama
Takô-wan
Himmawashi-hana
Chichibu-yama
Membô
Miura-wan
Ichino-kubi
500 0 500 1000 1500 m.
α-Lava
β-Lava
γ-Lava
δ-Lava
ε1-Lava
ε2-Lava
Lavas of 1st period
Chichibu-yama Ejecta
Takôdo-yama Lava
Nachi-san Lava
Lavas of 2nd period
Jôyoro-yama Lava
Anagi-yama Lava
Kôbe-yama Lava
Lavas of 3rd period
Shiromama Ejecta
Cinder-Cone Ejecta
Tenjô-san Lava (Lava of 4th period)
Talus of Tenjô-san Lava
Beach Sands

（震研彙報、第七號、圖版、津屋）

19. *Volcano Kayagatake.*

By **Masakane ICHIKI**,*

Geological Institute, Imperial University of Tokyo.

(Read Dec. 18, 1928.—Received March 20, 1929.)

Introduction.

The present paper embodies the result of the geological and petrological investigation of the Kayagatake volcano conducted under the auspice of the Earthquake Research Institute of the University of Tokyo.

The preliminary field survey was done in the spring of 1926 and the detailed mapping was performed during seven weeks in the summer of the same year. In 1928, a short trip was again done. Laboratory work has been carried out in the author's third year course in the university. The chief object of the present research has been to determine the genetical relation between the acidic and basic effusive rocks which constitute the volcano, following the investigation method proposed by Dr. S. Tsuboi.[1)]

As a result of the investigation some interesting facts were revealed which have important significance in petrogenesis and the geologic history of the volcanic region here concerned.

The author expresses in this occasion his heartiful thanks to Dr. T. Kato and Dr. Y. Ozawa for their kind directions and especially to Dr. S. Tsuboi for his kindness in reviewing the manuscript and for valuable suggestions and encouragement without which the present work would not have been accomplished. The author's gratitudes are also offered to other members of the Geological Institute for their help in the preparation of the present work.

---

* It is with deep sorrow to record here the death of Mr. Masakane Ichiki, *Rigakushi*, which occurred on April 24th, 1929. Mr. Ichiki was born in Kagoshima on February 26th, 1905, and since 1926, as a student and as a postgraduate of geology in the Tokyo Imperial University, was engaged, at the suggestion of the undersigned, in the study of Volcano Kayagatake. The results of his researches, carried out with unusual enthusiasm, are embodied in this paper. I should like to express my thanks to Messrs. H. Tsuya, H. Ôtani and K. Yasumuro for the assistance given to me in giving the paper its present form.—Seitaro Tsuboi.

1) S. Tsuboi, *Jour Fac. Sci. Imp. Univ. Tokyo*, Sect. II, **1**, Part 2.
„ *Jour. Fac. Sci. Imp. Univ. Tokyo*, Sect. II, **1**, Part 5, 160–180.

Previous Works.

The volcano Kayagatake is an extinct-volcano lying between the two grand conides, Fuji-yama and Yatsugatake, and extends over 35°40′–35°50.3′ N. lat. and 138°25′–138°36′ E. long.

The present area was firstly surveyed by Dr. T. Suzuki,2) was published in 1879, a brief note on the geology and topography. He pointed out that there are two young volcanoes arranged in E.W. direction: Kurofuji, the eastern one, and Kayagatake, of which he considered the former is younger than the latter.

In 1898, Professor N. Yamasaki3) described the volcanic rocks in this region in some details, and distinguished three kinds of extrusive rocks: green hornblende andesite, brown hornblende andesite and two pyroxene andesite.

In 1908, the volcano was again studied by Tetsunosuke Katô4) in greater details. The geologic map annexed to the present paper owes much to his work, although corrections were made in some essential points. The result of his research may be summarized as follows. In the Tertiary period, an andesite volcano, Yumihariyama5) was formed at the northern margin of a hypothetical lake of Kôfu whose level, he considered, was in the height of 1000 m. above sea-level at that time. After a long time interval, during which the lake level became as low as 800 m. above sea-level, a dacite volcano, Kurofuji was formed. Immediately succeeding it, another one appeared on the western flank of the preceding volcano. The extrusive rocks of the volcano Kayagatake were classified by T. Katô into four types, all of which he considered to have been derived from a common original magma by means of "gravitational differentiation." The profile of the volcano drawn by him is reproduced in this place (Fig. 1).

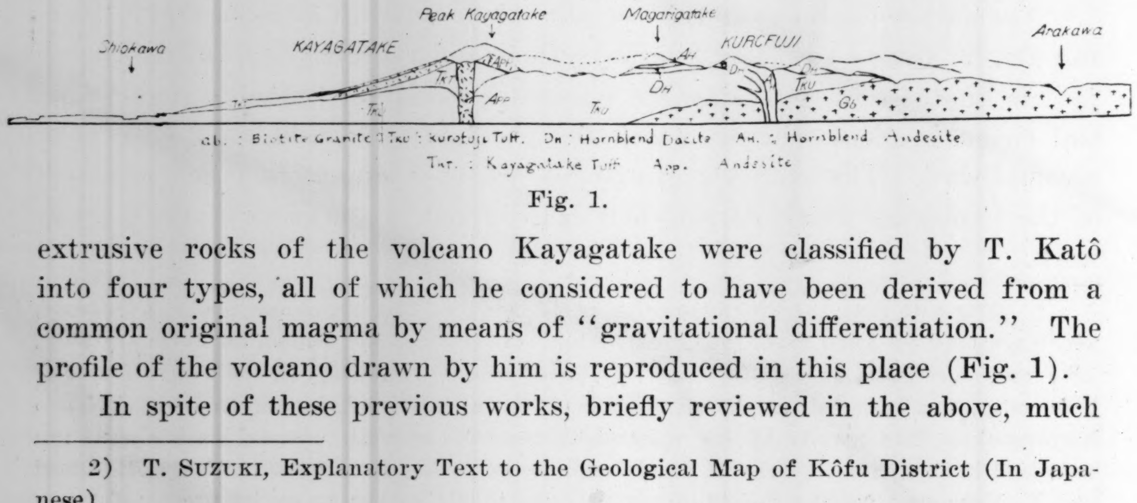
Peak Kayagatake
Magarigatake
Shiokawa
KAYAGATAKE
KUROFUJI
Arakawa
TKT
TAp
App
TKU
AH
DH
Gb
Gb. : Biotite Granite TKU : Kurofuji Tuff. DH : Hornblend Dacite AH. : Hornblend Andesite
TKT. : Kayagatake Tuff App. Andesite

Fig. 1.

In spite of these previous works, briefly reviewed in the above, much

---

2) T. Suzuki, Explanatory Text to the Geological Map of Kôfu District (In Japanese).

3) N. Yamasaki, Report of the Geological Investigation of the Yatsugatake Volcanic Group. (In Japanese).

4) T. Katô, Note on the Volcano Kayagatake, 1908, (MS.)

5) 弓張山

has been still left to be studied of this volcano, especially in the field of petrography and petrology. Therefore the chief effort of the present writer has been directed to the genetical interpretation of different rock-types although the geological history of the present field has not been neglected.

Part I. Morphology and Geology.

CHAPTER I. BASEMENT OF THE VOLCANO.

The present area lies immediate east of the great tectonic line[6] traversing the central part of Japan and is situated between the volcano Yatsugatake[7] and a flat basin of Kôfu.[8] Altitude of land increases eastward culminating at a prominent peak called Kimbuzan[9] (2966 m.). From the peak a long spur stretched to southwest. At the terminal of this spur stands the volcano now under consideration. On the both sides of the main ridge, run other two spurs parallel to the former, of which the northern one separates the present volcanic field from that of Yatsugatake, while the southeastern one bounds the northern margin of Kôfu basin.

Between the above three ridges flow two rivers taking nearly parallel courses. But the both rivers turn their direction to S.S.E. in their lower courses. The eastern one called Arakawa[10] excavates a deep canyon, Shôsenkyô[11] which is renowned on account of the beautiful scenery.

The morphology above described has some relation to the structure of the region. Along the course of Shiokawa[12] a remarkable fault with length of about 13 km. is seen, the fault-plane of which is observed at two places; Hishi[13] (2. b.) and Yudo[14] (2. c.) where the sedimentary rocks constructing the basement of the volcano, are intensely folded and finally brecciated. Moreover, the strike of the formation is curved in opposite directions on both sides of the fault as if the northwestern block displaced relatively southwestwards. Parallel to the fault above mentioned, a marked line passing Mitake[15] is recognized on the geological map. It is highly probable that the line indicates some tectonic line, although fault-plane has not yet been observed. These faults are covered by tuff breccia of the young volcano under consideration showing that the block movement preceded the appearance of the volcano.

Besides the above two lines there run other faults in the meridional direction; one of which follows the course of the Kiyokawa while the other passes Takanari[16] (4. e). The age of the faulting could not have

---

6) Nirazaki-Shizuoka-Line. 7) 八ヶ嶽 8) 甲府盆地 9) 金峯山 10) 荒川
11) 昇仙峡 12) 鹽川 13) 比志 14) 湯戸 15) 御嶽 16) 高成

been strictly determined, but it is clearly later than the effusion of paleo-andesite because the latter is cut by the fault. It is ascertained also that the fault along the Kiyokawa moved even after the formation of Kayagatake, for the eastern half of Kayagatake is sharply cut and the fault scarp is preserved along the western bank of the Kiyokawa. A minor fault found on the western cliff of Tachiokayama and gassing springs at Urushido affirm the above consideration.

Curiously there is no observable fissure indicating the general direction of the volcanic zone which trends N.N.W. to S.S.E. Moreover there is no regularity in the distribution of volcanic vents. It is already known that fissures relating the formation of volcanoes have not necessarily direct connection with surface faults, the former lying in a deep part of the earth crust;17) a remarkable example of which is seen in Great Britain.18)

The basement of the volcano consists chiefly of the rocks of Kobotoke Series, biotite granite and two pyroxene andesite with its tuff breccia.

Kobotoke Series. Kobotoke Series is composed of alternation of sandstone and clay slate accompanying negligible amount of quartzite and schalstein. The general strike is almost uniform throughout the present area ranging N 55°W to N 65°W with steep dip varying from 60° to north to almost vertical. The sedimentary rocks are considered to belong to the Kobotoke Series from their lithological characters as has already been suggested by Tetsunosuke Katô. Its geological age is unknown though it has been considered to be the Paleozoic.19) It is intruded by biotite granite in several localities where the rock is converted into hornfels which contains contact minerals such as biotite, muscovite, cordierite and rarely garnet according to T. Katô.

Biotite granite. Biotite granite is exposed extensively in the north-eastern part of the field including the elegant peak, Kimbu-zan, Mizugaki-yama,20) etc. A local exposure of the granite is found at Rakanji-yama21) (Index map 4. e) and along the northern margin of Kôfu basin. The granite is usually coarse grained, uniform in petrographic character throughout the present area, although porphyritic and aplitic facies are locally observed. Typical aplite is found at the river bank of the Kiyokawa in the neighbour-

---

17) R. DALY, *Igneous Rocks and Their Origin*, 252.

18) A. GEIKIE, *Ancient Volcanoes of Great Britain*, **2**. The same fact is also recognized in the Katmai Region, Alaska. (C. N. FENNER, *Jour. Geol.* (1920), 574).

19) Recently some authors consider it to be the Cretaceous.

20) 瑞牆山 21) 羅漢寺山

hood of Shimokawakubo (4. e.),[22] where it traverses dark coloured slate in various directions. It is noticeable that the granite contacts with slate in various manners. For example, the granite contacts with slate without change in its petrographic character on road side at Shimofukuzawa;[23] while it forms injection gneiss at a place, about 500 m. north of the former locality. In some cases the granite becomes fine grained variety at the contact, while it becomes porphyritic in the other.

Two pyroxene andesite. (Paleo-andesite.) The oldest volcanic rock found in the present field is two pyroxene andesite which is effused from numerous vents irregularly distributed in the district. The total number of the vents is at least eight among which Mizugamoriyama[24] is prominent. Tuff breccia of the same rock is widely distributed in the southeastern part of the field where it covers the eroded surface of biotite granite. The very contact of the two rocks is clearly observed on a roadside at the vicinity of Shishidaira[25] (4. e.). Besides small blocks of andesite (rarely over 20 cm. in diameter), large blocks of biotite granite are found in the lower part of the tuff breccia. The existence of the granite blocks in the bed and its horizontal stratification well developed in the vicinity of Kirisashi[26] suggest that the tuff breccia has been at least partly transported by running water and deposited in subaqueous condition. Lava flows of the andesite are preserved only as fragments, and numerous dykes are exposed on account of advanced dissection.

The rock is grey to greyish black, very compact. It carries minute phenocrysts of plagioclase ($Ab_{40}An_{60}$), augite and hypersthene, but lacks entirely olivine. The groundmass is andesitic in texture including magnetite and plagioclase. The uniformity in petrographic character of the specimens from different localities is noticeable. The two pyroxene andesite is easily discriminated from the younger volcanic rocks even in the field.

A flow of the paleo-andesite is covered by dacite of Kurofuji at Yokoiwa about 3 km. east to Iwanoshita[27] (2/3 c.) and the former does not cover the latter. Therefore it is beyond all doubts that the effusion of the andesite preceded the appearance of the young volcano.

Tetsunosuke Katô who found *Sequoia* sp. in the tuff breccia considered the formation to belong to the Tertiary. But the data are too insufficient to determine the age of the activity of the andesite. It may be said, however, that there was more or less long time interval between the effusion of

---

22) 下川窪 23) 下福澤 24) 水ヶ森山 25) 獅子平 26) 切差
27) 岩ノ下

the andesite and the appearance of the young volcano, because a block movement took place between the two volcanic activities. Difference in type of activity and the state of dissection of the volcanic bodies also affirm what has been just said.

There is also a long interval between the intrusion of granite and the the activity of paleo-andesite for the latter lies directly upon the eroded surface of the former as was already described.

History before the appearance of the volcano.

The northern part of the present region where the young Tertiary is well developed has been studied in detail by F. Homma[28] who states that there were twice igneous activities during the deposition of the Tertiary formation,[29] and that quartz diorite exposed in the middle part of ''fossa magna'' intrudes the upper Miocene. It is thought that the granite exposed in the present area is also younger than the Miocene, because it appears to be the northern extension of quartz diorite which intrudes Misaka Series at Misaka mountain range. The transition from the quartz diorite to the granite is well seen along the course of the Fuefukigawa.[30] In this part, it is affirmed that there is no distinct boundary between the two rocks.

The vast exposure of the young granite shows how erosion had advanced before the activity of paleo-andesite. The activity began in severe explosion effusing enormous quantity of tuff and fragments of andesite, which partly accumulated under the water. After the activity of the old volcanoes had ceased and the erosion had more or less advanced, the region suffered a disturbance which formed the four faults above mentioned. The above description is condensed in the following table.

	Formation	Crustal Movement	Igneous Activity
Quaternary		Block movement	Activity of the young volcano
Tertiary	Yumihari S.		Activity of two pyroxene andesite (Paleo-andesite)
	(Misaka S.)		Intrusion of granite
Paleozoic?	Kobotoke S.		

---

[28] F. HOMMA, ''On the Geologic Structure of the Central Part of the Nagano Prefecture,'' *Jour. Geol. Soc. Tokyo*, **24**, No. 403, p. 146.

[29] The formation belongs the burdigalien stage according to Prof. Yabe. (*Jour. Geol. Soc. Tokyo*, **27**, 389.)

[30] 笛吹川

CHAPTER II. GEOLOGY AND MORPHOLOGY OF THE VOLCANO.

General Outline.

There are two eminent conides arranged in E.W. direction. The eastern one dissected intensely is called Kurofuji,[31] while the western standing on the shoulder of the former is named Kayagatake[32] which is comparatively young in dissection having smooth and gentle piano on its southwestern slope.

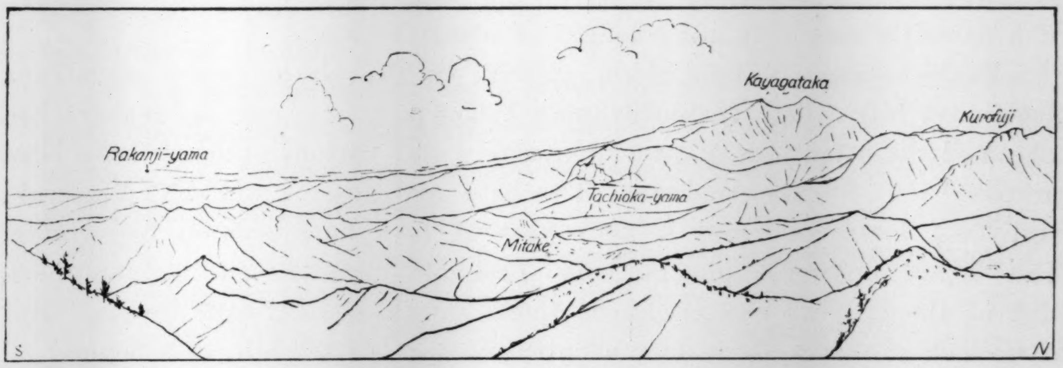

Fig. 2. General view of the volcano sketched by the author at Yumihari pass.

These two conides are distinctly divided by a wide valley through which a stream called Kiyokawa[33] flows. On the western bank and along the course of the Kiyokawa there is a cliff reminding us a fault scarp.

There are many other elevations which are not so eminent as the above two conides; among which the most distinct are Tachiokayama[34] and Magozaemon.[35]

Judging from the high grade of dissection and lack of post magmatic phenomena such as fumaroles and hot springs, it is evident that long time has elapsed since the last activity of the volcano. We have no historical record of the eruption of the volcano, but landslide is not infrequent on account of loose materials constituting the volcanic body.

Structure of Kurofuji.

On account of advanced dissection, it is not difficult to study the inner structure of the volcanic body. It has one chief vent and two subordinate orifices.

The chief vent is situated at the eastern margin of the field covered by

---

31) 黒富士 32) 茅ヶ嶽 33) 清川 34) 太刀岡山 35) 孫左衛門

younger volcanic material, within the distance of 500 m. from an exposure of granite which constructs the basement of the volcano.

Radial dykes of the chief vent. The most notable feature of the principal vent is the existence of radial dykes diverging from the core to east and south. There are four; among which a dyke stretched S.E. is about 2.5 km. in length with mean breadth of 100 m. Its southeastern part is traversed by a deep ravine and here we can observe that the dyke intrudes thick accumulation of tuff breccia from the chief vent.

A less eminent dyke lying immediately north of the present one has a curious elevation in the middle part of its body which appears to be a core of a parasitic cone. It has a length of about 1.7 km.

Tachiokayama. About 4 km. S.S.W. to the above center elevates a prominent hill called Tachiokayama (1295.3 m.). Its curious feature has attracted the attentions of previous writers and various opinions have been proposed. T. Suzuki considered it to be a central cone while N. Yamasaki and Tets. Katô described it as a part of lava flow isolated by erosion. The latter opinion appears very probable because on the southern cliff of the hill, we can recognize thick flow overlying tuff breccia. But if we look at the exposure at southwestern slope of the hill, it is beyond all doubts that the solid rock constructing the curious hill extrudes the surrounding layer of tuff breccia. On the bottom of a ravine formed at the northern foot of the hill, angular blocks of shale and granite are abundantly discovered. These facts show clearly that the isolated hill also represents

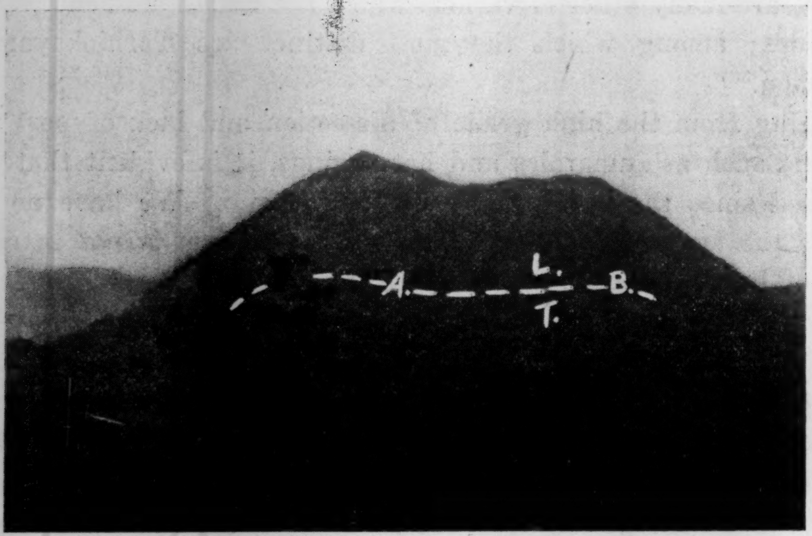

Fig. 3. Tachiokayama viewed from south. L.: Extrusive rock; T: Tuff breccia; A-B: The boundary between L and T.

an independent orifice from which viscous lava was extruded resulting in the formation of a dome-shaped mountain.

The constituting material is dacite of light grey colour.

Magozaemon. About 5 km. west of the main conduit and on the northern slope of Kayagatake, we can recognize another center from which dacite was extruded. Its base has elliptic form whose major axis is 2.5 km. Eastern side of the stock is narrowed and takes the form of a typical dyke in which sporadical occurrence of large hornblende is seen.

Lava flows. Upper part of the conide is chiefly constructed of thick flows of dacite which sometimes reach 100 m. in thickness. These lavas form small mesas inclining slightly to the direction of the chief vent, the feeder of the flows.

It is a remarkable fact that it is extremely rare to see two or more flows piled up, though such occurrence is said to be common in other stratified conides. The following photograph shows a typical example of thick flow of dacite lying upon tuff breccia.

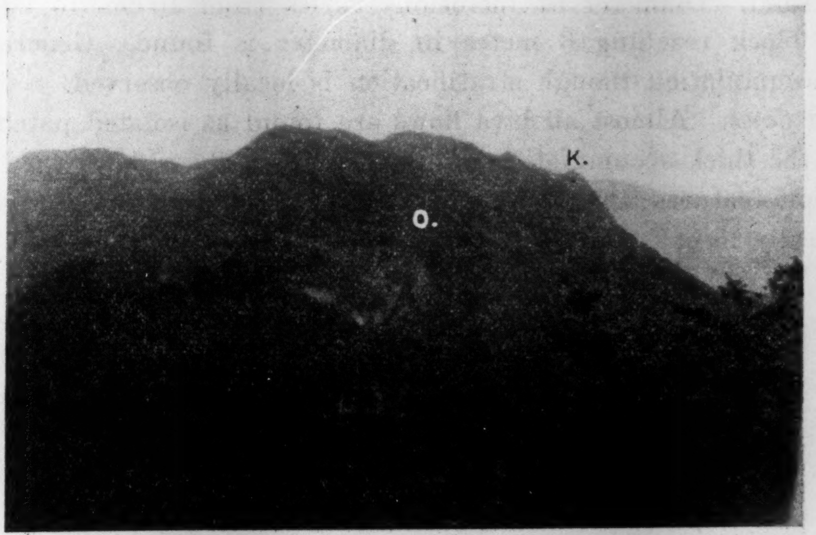

Fig. 4. The southward stretched crest of Kurofuji, O: Onigawa, K: Kurofuji proper Note thick flow of dacite lying on tuff breccia of the same rock.

The flow exposed on the scarp on the left bank of the Kiyokawa to the west of Tachiokayama is also considered to be a lava that came from the eastern side of the Kiyokawa before the excavation of the wide valley dividing the volcano. As the rock closely resembles dacite of Tachiokayama and the lava dips westward, the writer inclined to consider that the above vent is the feeder of the flow.

From the position of center of volcanic activity, direction of dykes and inclination of lava flows, it is not difficult to reconstruct the original feature of the volcano, now entirely demolished.

The following is the idealized section in N.S. direction.

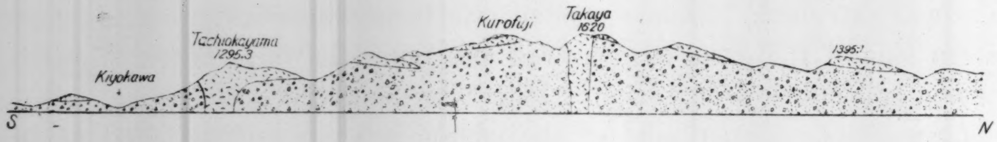

Fig. 5.

Building Materials.

Tuff breccia. Tuff breccia is the most important material of the constituents of Kurofuji and is found in almost every part excepting the upper ridges where it is capped with the flow. The tuff breccia is composed of abundant blocks of dacite which are cemented with light greyish tuff and volcanic sand. Diameter of inclusions varies from 10 cm. to 20 cm., but rarely a block reaching 3 metre in diameter is found. Generally it is chaotic accumulation though stratification is locally observed.

Lava flows. Almost all lava flows are found as isolated patches which lie upon the thick accumulation of tuff breccia. These flows vary much in macroscopic features; their colour varying from light grey to reddish brown, but generally light coloured. Microscopically, however, these are classified

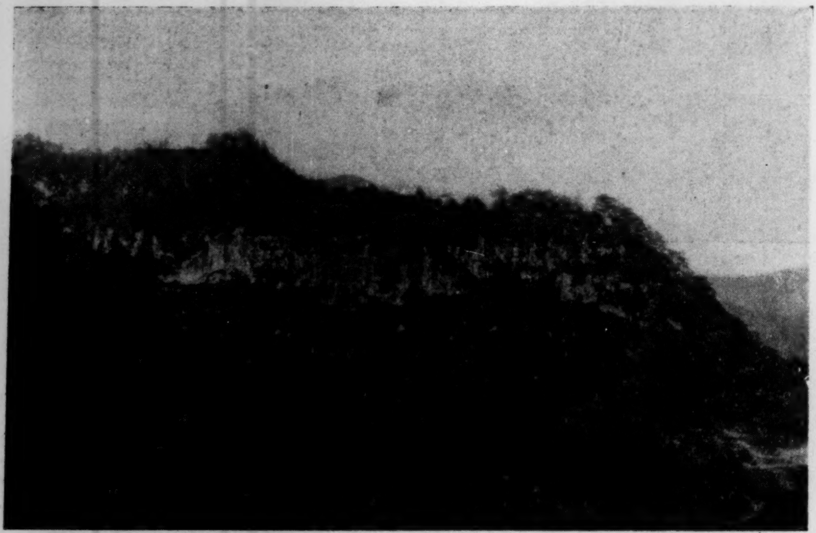

Fig. 6. The cliff of flow-breccia lying upon tuff breccia in the neighbourhood of Mitake.

into three principal varieties: olivine-bearing two pyroxene dacite, green-hornblende dacite, and brown-hornblende dacite. Petrography of these rocks is given in Part II. (See p. 349).

Flow breccia. Usually flow breccia constructs long precipitous cliff on which sometimes develops distinct columnar joint, and is called by the name "Yokoiwa" (horizontal rock).

It includes abundant blocks of dacite which are cemented by more or less slaggy variety of dacite. The most typical one is seen at Iwanoshita36) and Mitake. At the latter places a silicified trunk has been found immediately beneath the flow breccia.

Structure of Kayagatake.

The magnificient scarp cutting meridionally the central part of the volcanic body shows natural profile of the volcano. The following figure is an idealized sketch of that part.

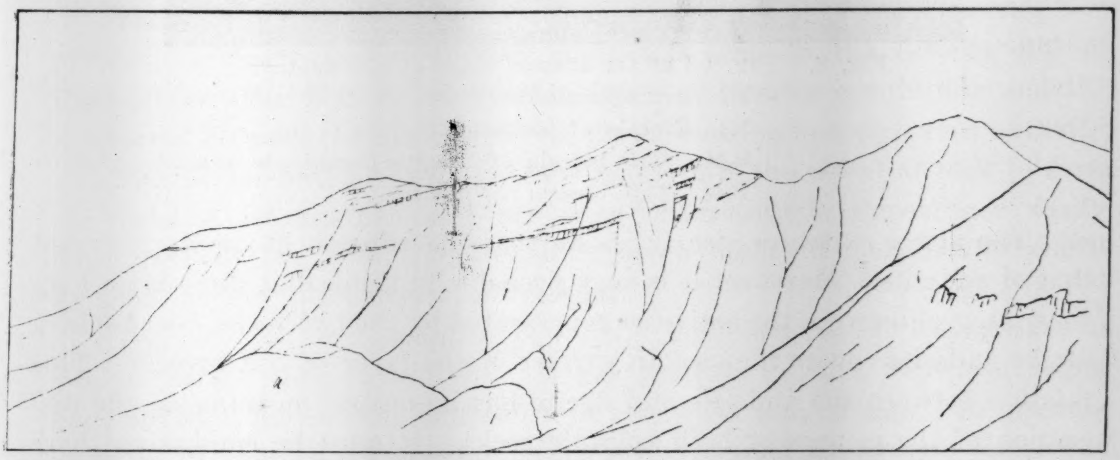

Fig. 7. The steep escarpment of Kayagatake; viewed from the top of Magarigatake. The inner structure of Kayagatake is well exposed on the surface of the cliff.

On the surface of the slope one can recognize at least eight flows which intercalate thin layers of tuff breccia. Structure of the same type is observed on the side of all ridges radiating from the highest peak, Kanagatake,37) showing that center of activity which supplied abundant flows is that peak. This is also confirmed by the fact that the peak consists of massive andesite which cuts surrounding tuff in steep angle.

In Fig. 7, the lower half of the slope consists of dacite, while the materials of Kayagatake form the upper portion of the scarp. The very

---

36) 岩ノ下 37) 金ヶ獄

contact of the both material is seen on the terminal of a short spur stretched eastward from the highest peak. It is shown in the following photograph (Fig. 8).

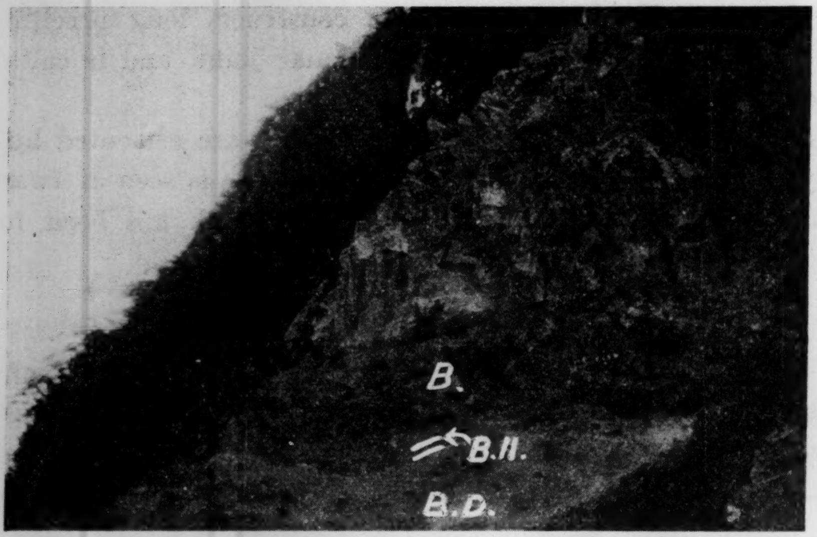

Fig. 8. The end of the eastern ridge of Kanagatake.
L: Lava of andesite.
B: Breccia of andesite.
B.H.: Tuff breccia of basaltic-hornblende andesite.
B.D.: Tuff breccia of dacite

The above exposure clearly shows that the effusion of dacite preceded that of andesite. Moreover it is very probable to think that there is no long time interval between the activities represented by the two rocks, because lava of the andesite covers the smooth surface of the layer of tuff breccia. This relation between the andesite and dacite has important meaning on the discussion of the genesis of both volcanic rocks. It must be emphasized here that the reversal order or effusion has not been recognized in the present field.

There are three small knobs in the valley head of the Kiyokawa. They all consist of hornblende andesite, and are considered to be dykes or small stocks belonging to Kayagatake. One of them, called Yoroi-iwa[38] pierces the tuff breccia with almost vertical contact plane. Two small knobs lying on the northwestern skirt of Kayagatake consist of basic pyroxene andesite. These are considered to be parasitic cones by N. Yamasaki, but Tetsu. Katô described them as erosion relics of a lava flowed from upper part of the volcano. Although sure geologic data are lacking, the former opinion is more probable, considering the morphology of those knobs and petrography of the constituting rocks.

---

38) 鎧岩

Building Materials of Kayagatake.

In contrast to Kurofuji where tuff breccia far surpasses lava in quantity, alternation of flows and tuff composes the essential portion of Kayagatake.

Lava flows. Lavas of Kayagatake chiefly consist of olivine-bearing two pyroxene andesite. The earliest material effused at the volcano is basaltic-hornblende andesite. Not only it is found as flows and dykes but also the andesite is widely distributed as ejectamenta. It is covered by green-hornblende andesite at Tochikubo,(39) the location of a crater according to Tetsunosuke Katô. The rock resembles dacite in macroscopic appearance, but is easily discriminated under the microscope.

The two rocks mentioned above must be genetically related since the green hornblende and basaltic hornblende occurs, in one case side by side in one and the same specimen.

The hornblende andesites are always covered by olivine-bearing two pyroxene andesite and their very contact is seen on the eastern cliff of Kayagatake (See Fig. 8) where thin layer of basaltic-hornblende andesite is inserted between the dacite and the olivine-bearing two pyroxene andesite.

The olivine-bearing two pyroxene andesite is the essential rock to form the volcano Kayagatake and has very characteristic appearance easily recognized in the field. It has dark green spots of porphyritic augite without distinct phenocrysts of feldspar.

Tuff breccia and younger deposits. Tuff breccia of Kayagatake is less important than lava flows. It has reddish to dark brownish colour and includes hornblende andesites in one case and slaggy two proxene andesite in another. These inclusions are cemented by greyish white tuff and volcanic sand. In some cases we can find many pisolites in the tuff of Kayagatake.

A curious formation found in the vicinity of Yemido(40) has many peculiar characters which are recognized neither in the material of Kurofuji nor in that of Kayagatake. Usually it forms precipitous cliff on which is seen no stratification, and large blocks of andesite reaching a metre in diameter are abundantly contained in it. Intermingled with them, small blocks of slate, schist, sandstone and granite are found. These inclusions show that the formation is derived from the upper course of the Shiokawa where the sedimentary rocks are exposed. It may not be a fluvial deposit

---

39) 栃窪　　40) 絵見堂

because inclusions are all angular, but may be of the same origin with "Shichiri-iwa"[41] extensively developed in the northern part of Nirazaki. It covers the tuff breccia of Kayagatake and is covered in turn by terrace deposit. The formation must be very young as it includes a wooden piece with iron mails.

Western and southwestern flank of the volcano is covered by orderless accumulation of andesite whose section is observed on the bank of the Shiokawa. In addition to the blocks of andesite numerous trunks are embedded in that accumulation. One of these trunks reaches 2 metres in length. This is covered by terrace deposit.

Terraces are well developed in the neighbourhood of Wakamiko.[42] Five steps are recognized on the western bank of the Shiokawa, while on the opposite side only two are clearly observed (Fig. 9).

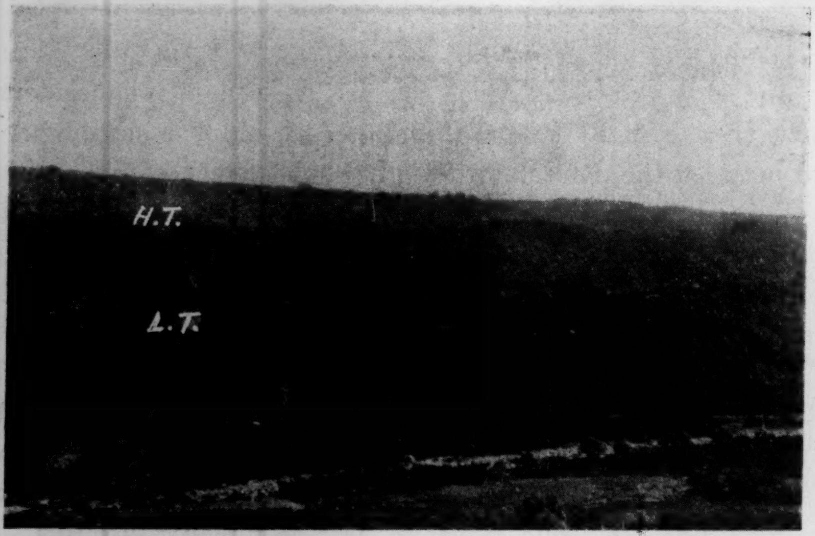

Fig. 9. Terraces found at the northwestern foot of Kayagatake.
H.T.: Higher terrace. L.T.: Lower terrace.

The thickness of the terrace deposit reaches 10 meter and includes well rounded pebbles of andesites, graywacke, chert, sandstone and granite.

The history of the volcano and the order of effusion of extruded materials are given in the following table.

---

[41] 七里岩 [42] 若神子

History of Kayagatake
- Block movement
- Effusion of dacites (Kurofuji)
  - Olivine-bearing dacite
    - Construction of 1) Tachiokayama 2) Magozaemon
  - Brown-hornblende dacite
    - Construction of Kurofuji
  - Green-hornblende dacite
    - Construction of Takaya and intrusion of radial dykes
- Effusion of andesites (Kayagatake)
  - Basaltic-hornblende andesite
    - Construction of Gakisan and Yoroi-iwa
  - Green-hornblende andesite
    - Construction of Nabeyama
  - Olivine-bearing two pyroxene andesite
    - Construction of the essential part of Kayagatake
- Block movement
  - Construction of the escarpment along the Kiyokawa
- Degradation and deposition of younger formations.
  - Formation of terraces, mud flows and torrential fans.

Part II. Petrography and Petrology.

CHAPTER I. DACITES.

Constituent Minerals.

General remarks.—As previously mentioned dacites are found as tuff breccia, flow breccia, lava flows and stocks in the volcano Kurofuji. Usually it is of light grey colour and is strongly porphyritic, carrying large phenocrysts of plagioclase. Other phenocrysts observable by naked eyes are hornblende, pyroxene, olivine and quartz. But the latter three are present in negligible quantity.

Under the microscope, we can recognize three kinds of hornblende and two kinds of pyroxene. The groundmass shows various texture such as trachytic, cryptocrystalline and vitrophyric. The constituent minerals of the groundmass are plagioclase, pyroxene and magnetite. Rarely large automorphic apatite is seen among microlites. Zeolite is found filling miarolitic cavities in some kinds of lava. It must be noted here that biotite is found neither as phenocryst nor in the groundmass.

Quartz.—Quartz is found as phenocrysts in almost all the rocks extruded at Kurofuji, but the quantity is extremely variable, some specimens lacking entirely of the mineral.

It is highly corroded, although the original bipyramidal form is more or less preserved. Every stage of corrosion may be traced when a large number of slices are observed. In other cases the quartz is surrounded by a chain of monoclinic pyroxene, the relic of quartz being left in the middle part (Fig. 10). The interstices between the quartz and the surrounding pyroxene are filled with low double refracting mineral which is determined to be zeolite.

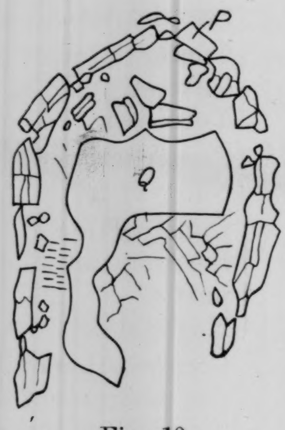

Fig. 10.

Large phenocrysts of quartz have irregular cracks. Occasionally flakes of quartz with sharp edge can be found. Commonly it shows optical anomaly, probably due to strain produced by the transition from the higher form to the lower one. It is almost free from inclusions and is not included in other minerals.

Quartz is rarely found in the groundmass of the dacite. When it occurs, it fills interstice between other microlites.

Plagioclase.—Plagioclase forms the most prominent phenocrysts in the dacite. Usually it has large size reaching ¾ cm. in diameter. Frequently the mineral forms grouped phenocrysts.

Under the microscope, the polysynthetic twinning of albite type is prominent, often accompanying Carlsbad and pericline twins; the last being the most rare. The crystals are strongly zoned. The mode of the change of chemical composition in successive zones is not regular though the innermost is the most calcic and the outermost is the most sodic. The mode of arrangement of zones is entirely different from that of the plagioclase in the andesite of Kayagatake. Reversal order of zoning is frequently observed. The range in chemical composition of porphyritic plagioclase in one specimen reaches 18% An.

Another noticeable fact is that the plagioclase found in lavas of relatively earlier stage of eruption includes some flakes of plagioclase of different nature from that common in the dacite (Pl. XXVIII, Figs. 5, 6). As this has an important bearing on the genesis of the dacite it will be described in detail in a later paragraph.

The chemical composition of the plagioclases measured by means of Tsuboi's method[43] varies more or less in different specimens as is shown in the following table.

Locality	Specimen	Calcic part	Sodic part	Composition range in An %
Myôjinbara	N_1	$Ab_{55}An_{45}$	$Ab_{61}An_{39}$	6
Tachiokayama	K_{48}	$Ab_{56}An_{44}$	$Ab_{63}An_{37}$	7
Magozaemon	NK_{98}	$Ab_{47}An_{53}$	$Ab_{65}An_{35}$	18
Shimokurobera	G_{41}	$Ab_{52}An_{48}$	$Ab_{65}An_{35}$	13
,,	K_{172}	$Ab_{45}An_{55}$	$Ab_{52}An_{48}$	7
Magarigatake	J_6	$Ab_{56}An_{44}$	$Ab_{67}An_{33}$	11

Plagioclases are chiefly andesine though in some specimens acidic labradorite is found.

The plagioclase of the groundmass has prismatic form; it is simply twined. Zonal structure is not recognized. Its refractive indices in one specimen show the composition to be $Ab_{73}An_{27}$.

Hornblende.—Hornblende is next in abundance as phenocrysts in dacite. We have three varieties of the mineral (1) basaltic hornblende[44] (2), brown hornblende (3), and green hornblende.

Basaltic hornblende. Optical properties of the mineral are as follows: $n_{1(D)}=1.702\pm0.001$, $n_{2(D)}=1.749\pm0.001$: $2V \fallingdotseq 0$: Pleochroism is noticeably strong; X=pale yellowish brown, Y=brown, Z=dark brown. $Z' \wedge c$ (in cleavage flakes) $=1^\circ-2^\circ$.

In a thin slice, the basaltic hornblende is attached to augite in such a manner as is shown in Fig. 12. The boundary between the two crystals is very sharp and there is an indentation which appears to show that the hornblende is formed from augite by the reaction of magma with the augite crystal. Usually it is opacitized; in some cases, however, the original crystal is found in patches (*H* in Fig. 12).

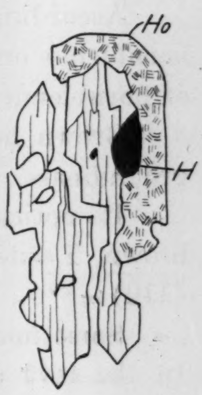

Fig. 12.

Green hornblende.—Of mafic minerals found in the dacite, green hornblende is the most abundant. They occur in euhedral form but are usually opacitized.

---

[43] S. Tsuboi, "A Dispersion Method of Determining Plagioclases in Cleavage Flakes," *Min. Mag.*, **20** (1923), 108.

[44] Determined from its optical properties.

The extinction angle in cleavage flakes is somewhat variable, but does not widely deviate from 15°. Preochroism is as follows; Z'=light green, X'=light yellowish green. Absorption is not strong: $Z>Y>X$. Indices of refraction in cleavage flakes in one specimen: $n_1=1.662$, $n_2=1.676$.

In some slices green hornblende forms a corona around augite as is shown in the following figure.

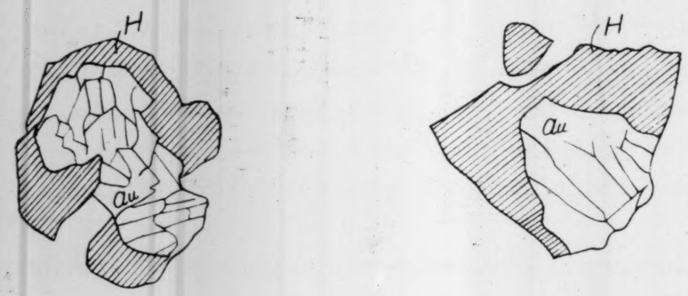

Fig. 13.

The relation between the green hornblende and basaltic one is peculiar and deserves a special description.

Not only these two minerals occur in one specimen but the two construct one and the same crystal (See Pl. XXVIII. Fig. 2). A large phenocryst of green hornblende includes abundant patches which have all the characteristics of basaltic hornblende though their chemical composition has not been determined. The brown patches have the same orientation with the host. Accordingly it is very probable that the basaltic hornblende was partly replaced by green hornblende.

According to Lark and Kôzu, green hornblende changes into basaltic hornblende on heating. It is difficult to explain the present peculiar feature of hornblende by that theory.

Brown hornblende.—Brown hornblende occurs in dacite with vitreous groundmass. Opacitization is extremely rare.

Its optical properties are as follows, $n_{1(D)}=1.679$, $n_{2(D)}=1.692$, Z=deep brown, Y=deep greenish brown, X=greenish brown. $Z>Y>X$, $Z'\wedge c$ in $(110)\fallingdotseq 8°$.

Sometimes hornblende occurs as a reaction rim around hypersthene. In the lava constructing the peak Kurofuji brown hornblende occurs in association with basaltic hornblende. In other cases brown hornblende is partly replaced by green one in the same manner as basaltic hornblende.

From the above observation are determined the following orders of crystallization.

1. Hypersthene → brown hornblende → green hornblende.
2. Augite → basaltic hornblende → green hornblende.
3. Augite → basaltic hornblende.

Locality	Specimen	n1 (D)	n2 (D)
Tachiokayama	K_{48}*	1·668±0·001	1·684±0·001
Ôtoge	K_{49}*	1·668± „	1·684± „
Shimokurobera	K_{172}**	1·662± „	1·676± „
„	G_{41}**	1·672± „	1·686± „
Kurofuji	K_{60}***	1·672± „	1·688± „
Magarigatake	J_6***	1·679± „	1·692± „

* Olivine-bearing two pyroxene dacite.
** Green-hornblende dacite.
*** Brown-hornblende dacite.

Opacitization of hornblende.—Remarkable feature of hornblende found in the dacite is its opacitization. It is a noticeable fact that the more the groundmass is vitreous, the less remarkable is the opacitization.[45]

In olivine-bearing dacite the decomposition of hornblende is almost complete, the hornblende occurring frequently as ghost. Rarely, however, the original mineral, basaltic hornblende is preserved. The decomposition products are magnetite, augite and plagioclase.

In green-hornblende dacite, the opacitization is not so advanced as in the former case. But every stage of decomposition may be traced. (See Pl. XXVIII. Fig. 4). The opacitized margin does not show the original crystal outline, dispersing gradually into the groundmass. The decomposition products are magnetite, plagioclase, augite and hypersthene.

The opacitization is rarely found in vitreous types as has been mentioned. In some cases the decomposition begins not from the periphery of a crystal but along the cleavage of it. This fact was taken by H. S. Washington as an evidence of his theory which opposes the resorption theory suggested by Zirkel[46] and others.

---

45) This is a general rule according to H. S. Washington. (*Jour. Geol.*, **4** (1896), 264). He attributes the decomposition of hornblende to its highly complex chemical character and its instability under condition of high temperature and diminished pressure. It is also promoted by the dissociation of a volatile substance from the crystal.

46) *Lehrbuch der Mineralogie*, **1**, 716.

Pyroxene.—There are two varieties of pyroxene, each of which has been formed in two generations.

Monoclinic pyroxene.—Augite is abundantly observed in the earlier products of effusion but is rare in the later lavas. The augite is always fresh and has usually idiomorphic form. Twinning of the usual type is frequent. It is pale greenish to green with no pleochroism. Its indices of refraction are shown in the following table.

Locality	Specimen	n_1 (D)	n_2 (D)
Myôjinbara	N_1	1·690±0·001	1·703±0·001
Tachiokayama	K_{48}	1·690± „	1·708± „
„	N_4	1·704± „	1·714± „
Shimokurobara	G_{41}	1·690± „	1·708± „
„	K_{172}	1·690± „	1·708± „

There is no essential difference in indices of refraction excepting N_4.

Augite in the groundmass has not been determined exactly on account of the minuteness of the crystal. It has almost similar mineralogical character as the porphyritic one.

Rhombic pyroxene.—Porphyritic crystal of hypersthene occurs almost in the same quantity as augite in the earlier product of effusion. It has also idiomorphic, especially so the minute crystal. Sometimes it is more or less irregularly formed and at the same time is surrounded by monoclinic pyroxene. It has distinct pleochroism, from light reddish brown to pale green. Index of refraction n_1 in cleavage flakes is 1.692, showing the chemical composition $(MgSiO_3)_{72}$ $(FeSiO_3)_{28}$.

Olivine.—Under the microscope it is observed that the olivine in the dacite is highly corroded and is frequently enclosed by aggregate of minute crystals which have characteristic pleochroism of hypersthene. In some slices the crystal in the aggregate is so large as to allow exact determination. In this case its general feature resembles that of the opacitized margin of hornblende, but the colona consists of hypersthene. Rarely the olivine is surrounded by a zone of minute grains of augite. The olivine is rich in irregular cracks along which colourless crystal is stained in yellowish green.

The principal refractive indices measured in sodium light by the immersion method are as follows.

Locality	Specimen	$N_{min} \doteqdot \alpha_{(D)}$	$\beta_{(D)}$	$N_{max} \doteqdot \gamma_{(D)}$
Mvôjinbara	N_1	1·663	1·677	1·706
Tachiokayama	K_{48}	1·662	1·688	1·706
Magozaemon	K_{98}	1·665	1·692	1·708

It is seen that there is a marked variation in the value β which is the most accurately determinable in the measurement.

Other minute constituents.—Magnetite, apatite and zircon are other minerals scattered through the groundmass of the dacite. Of these magnetite is the most abundant. Apatite occurs in large size. It is colourless; includes some opaque material which is arranged parallel to c axis. Zircon is extremely rare and is very minute in size. Zeolite is another mineral which is frequently found filling miarolitic cavities. It was determined carefully to be heulandite by Tetsunosuke Katô.

In the following three principal types of the dacite will be petrographically described.

OLIVINE-BEARING TWO PYROXENE ANDESINE DACITE.

(Pl. XXVIII. Fig. 1)

Locality.—The rock is found at Tachiokayama, Magozaemon and Kamiashizawa. The writer takes the specimen collected at the western foot of Tachiokayama as a representative.

Megascopic characters.—It is of light grey color; carries marked phenocrysts of plagioclase which reaches ¾ cm. in diameter. The other phenocrysts observable by naked eyes are of pyroxene, quartz and olivine in the order of abundance.

Microscopic characters.—Microscopically, porphyritic minerals are plagioclase, ,monoclinic pyroxene, rhombic pyroxene and magnetite are the hornblende.

The groundmass is percrystalline and more or less trachytic in texture. Plagioclase, monolinic pyroxene, rhombic pyroxene and magnetite are the chief constituents of the groundmass.

The porphyritic plagioclase has marked zonal structure and is twinned after the albite law. It includes flakes of plagioclase which is different in character from the surrounding one. The indices of refraction of the porphyritic plagioclase show that its composition ranges from $Ab_{63}An_{37}$ to $Ab_{58}An_{42}$. While the chemical composition of one of those inclusions is

$Ab_{24}An_{76}$.[47] Frequently it is found in grouped crystal. No alteration of the plagioclase is observed.

The quartz occurs in dihexahedral form which is usually highly corroded. It frequently shows optical anomaly. It is free from inclusion.

The olivine is more or less abundantly found in the specimen. It is always corroded and is enclosed by minute crystals of hypersthene. Sometimes the thickness of such colona reaches 0.06 mm. The indices of refraction is as follows: $\alpha=1.662$, $\beta=1.688$, $\gamma=1.706$. From the optical data, the composition was found as $(Mg_2SiO_4)_{81}$ $(Fe_2SiO_4)_{19}$.[48]

The augite commonly occurs in subhedral to euhedral crystal. It is pale geen, and has no pleochroism. It is twinned in the albite law but exhibits no zonal structure. No alteration is seen. It frequently includes magnetite and rarely minute grains of hypersthene. Extinction angle in cleavage flakes amounts to 36° − 37°; the indices of refraction are $1.7025 < n_1 < 1.7063$, $n_2 = 1.714 \pm 0.001$. From these data we can determine its probable chemical composition: $CaFe(SiO_3)_{2(40)}$, $CaMgSi_2O_{6(53)}$, $MgSiO_{3(7)}$.[49]

The hypersthene is not so abundant as augite. It builds idiomorphic crystal. It has sometimes a reaction rim of augite. Pleochroism is distinct, pale red to light green. The refractive indices were not determined.

The basaltic hornblende is almost wholly opacitized, flaky one being left as a remnant of the original mineral. The decomposition products are augite and magnetite.

As stated above, the groundmass is almost holocrystalline. The plagioclase in the groundmass is simply twinned. The index of refraction measured by the immersion method is $\alpha \fallingdotseq 1.540$, showing the chemical composition to be $An_{27}Ab_{73}$, that is basic oligoclase.

Some varieties. There are some varieties of the dacite belonging to this type. The dacite constructing Magozaemon closely resembles the above described one, but has a little glass base between the microlites in the groundmass.

At the eastern end of the stock, sporadic phenocrysts of basaltic hornblende reaching 1 cm. in length are observed. The dacite exposed on the opposite escarpment of Tachiokayama is dense and has a greenish black

---

47) The value was calculated by Dr. S. Tsuboi by means of a graphical method specially deviced by him, using the optical data such as the extinction angle, the optical orientation, etc. measured on a thin slice.

48) E. ERNST, *Neus Jahr. für Min. etc.*, **52**, Beilage Bd. Abt. A. 1 Heft.

49) T. TOMITA, "Diagrams for Determining Pyroxenes," *Jour. Geol. Soc., Tokyo,* **31**, Nos. 373–374.

colour. The chemical composition of porphyritic plagioclases ranges from $Ab_{55}An_{45}$ to $Ab_{41}An_{59}$. It is rich in coloured minerals such as olivine and pyroxene.

GREEN-HORNBLENDE ANDESINE DACITE.

(Pl. XXVIII. Figs. 3, 4)

Mode of occurrence.—It mainly forms the radial dykes and the stock standing at the northern part of volcano.

Megascopic characters.—It is of light grey colour and is compact. Megascopically recognizable minerals are plagioclase and hornblende. The type specimen collected at the eastern end of the dyke stretching to Shimokurobera was chemically analyzed by Mr. S. Tanaka (See p. 370).

Microscopic characters.—The rock contains abundant phenocrysts of plagioclase, hornblende with subordinate amount of augite and hypersthene. The texture of the groundmass is typically pilotaxitic and is composed of plagioclase, quartz, pyroxene, magnetite and apatite.

The plagioclase is the most abundant porphyritic mineral in the rock. Sometimes they are found as grouped phenocrysts; in other cases they occur in tabular form. With albite lamellation is frequently associated twinning after the pericline or the Carlsbad law. The crystal is strongly zoned showing change of chemical composition from the most calcic variety in the center to the most sodic one at the margin. The zoning, however. is not gradual nor simple, but shows alternation of sodic and calcic ones. The refractive indices measured by the dispersion method show their composition to be $Ab_{54}An_{46}$ to $Ab_{49}An_{51}$. Inclusions in plagioclase are scarcely found. They are augite, plagioclase and glass.

The hornblende occurs in subhedral form which is characterized by opacitized margin. Colour of the hornblende is sometimes irregularly distributed. Occasionally zonal structure is faintly observable. The pleochroism is as follows: X=yellowish green, Y=brownish green, Z=green. Absorption is not strong: $Z>Y>X$. $c \wedge Z'=15°$ in (110). The refractive index $n_1=1.662$. From the refractive index and the extinction angle, molecular ratio is found[50] as $(FeSiO_3:CaFeSi_2O_6)_{33}:(NaFeSi_2O_6+Fe_2O_3)_{29}:(MgSiO_3CaMgSi_2O_6)_{38}$. Every stage of opacitization is observable. The alteration products are magnetite, plagioclase, augite and hypersthene.

The augite is usually euhedral but is sometimes anhedral. As a rule it is light greenish without pleochroism. Twinning of common type is frequently observed. It is very fresh. The refractive indices are as fol-

---

50) T. TOMITA, *Jour. Geol. Soc., Tokyo,* **31**, Nos. 375, 415.

lows: $n_1=1.689\pm0.001$, $n_2=1.707\pm0.001$, $c\wedge Z'$ in (110) $=37°$. These data show the chemical composition: $CaMgSi_2O_{6(70)}:CaFeSi_2O_{6(30)}:MgSiO_{3(0)}$.

The hypersthene forms an idiomorphic crystal in which the pinacoidal faces are more prominent than the prisms. Decomposition into yellowish bastite is occasionally found. The refractive index in (110) is as follows: $n_1=1.6921\pm0.001$. It shows the probable chemical composition to be $MgSiO_{3(72)}:FeSiO_{3(28)}$.

The groundmass is holocrystalline. The chief constituents are plagioclase ($Ab_{58}An_{42}$), quartz, augite, hypersthene, magnetite and apatite. Some of the pyroxenes of the groundmass appear to have been derived by the decomposition of hornblende. Miarolitic cavities are scarce in this variety of dacite.

Some varieties.—There is some diversity in macroscopic feature of this rock type, although microscopically the divergence is not great.

The dacite exposed on the western shoulder of the main part of Kurofuji is of extremely dark colour and is very compact. Under the microscope, however, it is almost analogous to that described above.

The dacite forming the dyke exposed on the west bank of a stream at a distance of 500 m. from Shimokurobera is slaggy carrying large phenocrysts of quartz. Microscope shows that plagioclase, green hornblende and quartz are scattered among cryptocrystalline groundmass which is almost wholly composed by plagioclase with a small amount of quartz. Augite and hypersthene occur in negligible quantity.

BROWN-HORNBLENDE ANDESINE DACITE.

(Pl. XXVIII. Fig. 2.)

Mode of occurrence.—Brown-hornblende andesine dacite is found as mesas or buttes constructing the upper part of Kurofuji. As a representative of that type a specimen collected at the top of Magarigatake will be described.

Megascopic characters.—This rock type is greyish white and is more or less slaggy. Megascopically recognizable minerals are plagioclase, hornblende and quartz, of which the first is the most abundant. The hornblende occurs in black needles whose maximum length is about ½ cm.

Microscopic characters.—The plagioclase is subhedral to euhedral and is of tabular habit. The crystal is strongly zoned as in the case of green-hornblende dacite. It is generally free from inclusion, though magnetite grains and apatite needles are occasionally found. It is extremely fresh. Chemical composition ranges from $Ab_{67}An_{33}$ to $Ab_{57}An_{43}$.

The hornblende is in idiomorphic prisms. It is remarkable that no opacitized margin is recognized in the slice. Pleochroism is as follows: Z=deep brown, Y=greenish brown, X=light greenish brown. Absorption: $Z>Y>X$. Extinction angle in (110) is nearly 18°; $n_1=1.679$, $n_2=1.692$. It has noticeably high double refraction. The probable chemical composition is $(MgSiO_3:CaMgSi_2O_6)_{48}:(FeSiO_3:CaFeSi_2O_6)_{25}:(NaFeSi_2O_6+Fe_2O_3)_{27}$.[51)]

The hypersthene occurs always in small size and is frequently enveloped by brown hornblende.

The quartz is occasionally found in large size; the outline being highly rounded with inlet of the groundmass. It is cracked.

The groundmass is entirely different from that of the preceding type. It is typically vitrophyric accompanying abundant vesicles. The glass base carrying abundant trichites and spherulite is almost colourless. Perlitic fissure is also recognized. The development of fluidal structure is not distinct. The refractive index of the glass is 1.505. It is decidedly lower than that of the glass in the Hawaiian lava which varies from 1.603 to 1.605.[52)]

Some varieties.—The rock constructing the main ridge of Kurofuji has a megascopic feature different from the type above described. It is of brownish colour; carries abundant, but small phenocrysts of plagioclase ($Ab_{47}An_{53}$ to $Ab_{51}An_{49}$). Under the microscope it is found that the dacite carries basaltic hornblende besides the brown one in dirty vitrophyric groundmass.

Another variety is found on the top of Yeboshidake and at other places. The variety is dark grey, and is compact. The porphyritic plagioclase is medium andesine ($n_1 \fallingdotseq 1.548$ $Ab_{60}An_{40}$). The hornblende is more or less opacitized. X=light greenish yellow, Y=yellowish brown, Z=greenish brown. The groundmass is greyish and shows distinct fluidal structure. The index of refraction of glass is 1.518, i.e. slightly higher than in the type specimen.

---

51) T. Tomita, *loc. cit.*

52) H. S. Washington, "Petrology of Hawaiian Islands," *Am. Jour. Sci.* [4], **6** (1923).

CHAPTER II. ANDESITES.

General remarks.—Andesite is abundantly extruded from the vent of Kayagatake. Flowing down to every direction, it built up the typical conide Kayagatake.

It is easily distinguished from the dacite above described by its dark colour, the presence of phenocrysts of augite which appear as black spots in the field.

The chief constituents found as phenocrysts are plagioclase, olivine, rhombic pyroxene and augite. In the earlier product of extrusion, sporadic occurrence of hornblende is observed.

The phenocrysts above enumerated are scattered in hyalopilitic groundmass which consists of plagioclase, hypersthene, augite, magnetite and a little glass. Zeolite is found in miarolitic cavity.

Before describing the various types belonging to this rock the essential minerals will be described.

Plagioclase.—The plagioclase of the andesite is of decidedly basic composition. It does not form a grouped phenocryst as that in the dacite and always occurs in prismatic form without terminal faces. There is a fact that the plagioclase crystals are always cracked. The plagioclase shows albite lamellation often combined with pericline and Carlsbad twinning. Zonary arrangement is commonly observed but is not so distinct as in the plagioclase of dacite. Moreover the mode of zoning is quite different from that in the dacite. Every zone is extremely narrow. Sometimes the transition is quite gradual. In a thin slice, the difference of extinction angle between the innermost part and the outer shell reaches 27°.

Locality	Specimen	Calcic part	Sodic part	Composition range in An %
Gakisan	K_{101}*	$Ab_{23}An_{77}$	$Ab_{30}An_{70}$	7
Kanagatake	M_2*	$Ab_{40}An_{60}$	$Ab_{47}An_{53}$	7
Tochikubo	A_3*	$Ab_{34}An_{66}$	$Ab_{40}An_{60}$	6
Nabeyama	K_1**	$Ab_{47}An_{53}$	$An_{47}An_{53}$	0
Kayagatake	Ky***	$Ab_{45}An_{65}$	$Ab_{52}An_{48}$	17
Kayagatake	Kn***	$Ab_{45}An_{65}$	$Ab_{40}An_{60}$	5
Gyôninyama	K_{144}***	$Ab_{27}An_{73}$	$Ab_{34}An_{66}$	7
Yudo	B_5***	$Ab_{30}An_{70}$	$Ab_{50}An_{50}$	20

* Basaltic-hornblende andesite.
** Green-hornblende andesite.
*** Olivine-bearing two pyroxene andesite.

The chemical composition of the plagioclase obtained by means of Tsuboi's diagram varies in wide range as is shown in the foregoing table.

It appears that there is no regularity in the relation between the variation in the anorthite content and the order of effusion of lava flows.

Olivine.—Olivine is universally distributed in the rocks of Kayagatake but is always so small in size that it is only detected by close examination of specimens. Under the microscope, the olivine is highly corroded. The mineral is colourless; rarely pale yellowish green in thin slice. Alteration is common producing brown margin, probably due to the separation of iron oxide. Neither the serpentinization nor the formation of iddingsite is observed.

The refractive indices of the olivine are shown in the following table.

Locality	Specimen	$N_{min} \doteqdot \alpha_{(D)}$	$\beta_{(D)}$	$N_{max} \doteqdot \gamma_{(D)}$
Gyôninyama	K_{144}	1·664	1·690	1·709
Kanagatake	Kn	1·672	1·698	1·707
Kayagatake	K_{28}	—	1·699	—

Hypersthene.—Commonly hypersthene is found in automorphic form. In some cases zonal or hourglass structure is recognized. n_2 in cleavage flakes is 1.692. Therefore the chemical composition of the hypersthene is $(MgSiO_3)_{72}$ $(FeSiO_3)_{28}$.[53]

Augite.—Augite is the most predominant and largest phenocryst in the andesite under consideration. Curiously it scarcely has its original form, being highly corroded. The corrosion is entirely different from that which is usual in olivine, and is the result of mechanical crushing, as is shown by the fact that the margin of the crystal is frequently brecciated. The brecciated margin graduates into the aggregate of minute grains of augite scattered abundantly in the groundmass of rock. This feature has an important meaning in the genesis of the dacite of Kurofuji.

Augite is of pale greenish colour in thin slice. In rare cases pleochroism is reconizable Z'=green, X'=yellowish green, in cleavage flakes. Zonal or hourglass structure is distinctly observed in some slices. Extinction angle varies from 45° to 50° in section cut almost parallel to the optical plane. The refractive indices measured on cleavage flakes are shown in the following table.

---

53) T. Tomita, *loc. cit.*

Locality	Specimen	n_1 (D)	n_2 (D)	$c \wedge Z'_{(110)}$
Gakisan	K_{101}	1·693	1·706	36°
Kayagatake	Ky	1·693	1·714	38°
Kanagatake	Kn	1·693	1·713	—
Kayagatake	K_{28}	1·693	1·714	37°
Gyôninyama	K_{144}	1·696	1·714	38°
Yudo	B_4	1·706	1·714	37°

The augite is decidedly fresh. The inclusions are plagioclase, hypersthene and magnetite.

Hornblende.—Hornblende is sporadically found in flows and ejectamenta of earlier effusion and in some dykes of Kayagatake. There are two varieties of that mineral.

Basaltic hornblende. There is no marked difference between the basaltic hornblende in the andesite and that of the dacite. In one slice a remarkable zoning of the hornblende is observed. (Pl. XXIX. Fig. 2). Inner reddish brown part is surrounded by a broad zone of yellowish brown colour. extinction angle is very small: $c \wedge Z \fallingdotseq 4°$ in section cut nearly parallel to (010). Pleochroism is strong: Z=brownish red, Y=reddish brown, X=light brownish yellow. Absorption: $Z>Y>X$. There are two modes of opacitization. In one case the alteration occurs as follows:

Hornblende → Augite + Hypersthene
+ Plagioclase + Magnetite
+ Hematite.

Zonal arrangement of these minerals is frequently observed. (See the accompanying diagram.) The outermost shell is composed of pyroxene, the adjacent inner zone is of plagioclase. In direct contact with hornblende is formed a zone of magnetite. The transition from one zone to another is not abrupt. Refractive indices of the hornblende are $n_1=1.702$, $n_2=1.749$ in cleavage flakes, $c \wedge Z' \fallingdotseq 0°$ in 110. Optic angle appears to be very small as in biotite.

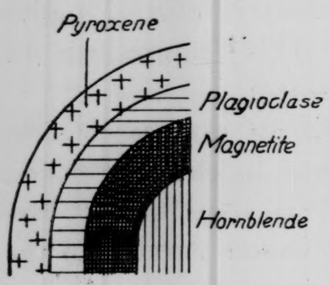

Fig. 11.

Green hornblende. Green hornblende occurs somewhat in large size. It has marked pleochroism. X=pale greenish, Y=green, Z=dark green. Absorption is not strong: $Z>Y>X$. $c \wedge Z=18.5°$ in 010. The refractive indices are as follows: $n_1=1.662$, $n_2=1.688$ in cleavage flakes. Inclusions in the green hornblende are not abundant; they are magnetite, hypersthene and glass which fills minute interstitial spaces.

Other minute constituents.—Other minute constituents are magnetite and zeolite. Magnetite is anhedral and is very small rarely reaching 0.3 mm. in diameter. In spite of its abundance in the groundmass, phenocrysts of plagioclase are almost free from magnetite inclusions. This fact is noticeable in contrast to that phenocrysts of pyroxene include abundant grains of magnetite. It is possible that the magnetite separates from pyroxene after the crystallization of the latter mineral.

Zeolite occurs chiefly in basaltic-hornblende andesite filling mialoritic cavities. Apatite and zircon are not found in this rock.

BASALTIC-HORNBLENDE BYTOWNITE ANDESITE.

(Pl. XXIX. Fig. 2.)

Locality.—Basaltic-hornblende bytownite andesite occurs in dykes and stocks in the neighbourhood of the conduite, Kanagatake. It is also found as flows at the western ridge of Kanagatake. Ejected fragments in the early stage of activity chiefly belong to the type under consideration. The specimen here described was collected at Gakisan.

Megascopic characters.—The rock type is of dark brownish colour and is compact. It is fine grained. Porphyritic minerals recognizable by naked eyes are plagioclase, pyroxene and hornblende. Sometimes hornblende occurs sporadically in large size reaching 1.5 cm. in length.

Microscopic characters.—It is sempatic and docrystalline.

The plagioclase has prismatic form and is generally subhedral. It exhibits complicate twinning of albite type, accompanying twinning of Carlsbad and pericline types. It shows faint zonal structure. Anorthite content determined by optical method is various. It belongs to bytownite; the variation of chemical composition being as follows: $Ab_{30}An_{70}$–$Ab_{23}An_{77}$.

The basaltic hornblende is pleochroic and shows marked zoning which is composed of light coloured outer shell and deep coloured inner core; the boundary is very distinct. Opacitization is remarkable. In some cases, the opacitized margin graduates into groundmass. It is beyond all doubts that some of the grains of pyroxene, plagioclase and magnetite scattered abundantly in the groundmass were resulted from the disintegration of the hornblende.

The porphyritic augite is commonly well shaped. It is of light green colour, usually having no pleochroism. Twin lamellation is common, and marked zoning is frequently observed. The refractive indices measured by immersion method are: $n_{1(D)} = 1.693$, $n_{2(D)} = 1.706$. $c \wedge Z' \ (110) \fallingdotseq 36.5^\circ$.

The hypersthene is not abundant in the described slice. It also forms idiomorphic crystal and is of pale greenish colour with distinct pleochroism. In some slices, the hypersthene is entirely absent.

Zeolite is found abundantly in some slices.

The groundmass is typically hyalopilitic in texture. It accompanies minute residium of glassy matter which has brownish colour. The component minerals are andesine, monoclinic pyroxene, rhombic pyroxene and magnetite. The andesine has the chemical composition: $Ab_{55}An_{45}$. Microlite of pyroxene is usually stained into reddish brown, especially in the neighbourhood of basaltic hornblende.

Some inclusions in the rock.—The basaltic-hornblende bytownite andesite includes some inclusions. One of them is slate which is large in size, sometimes reaching 2–3 m. in diameter. It is found on the eastern cliff of Kanagatake. Under the microscope, it has marked schistosity carrying minute grains of quartz, plagioclase and cordierite.

Another variety of the inclusion is microhyperite. It is equigranular and has typicl dioritic structure. The constituents are labradorite (maximum symmetrical extinction angle is 40°), augite and hypersthene. Minute grains of magnetite are also observed. The hypersthene is a highly pleochroic variety.54)

GREEN-HORNBLENDE LABRADORITE ANDESITE.

(Pl. XXIX. Fig. 1.)

Locality—It is also found in the neighbourhood of the center of eruption. At Tochikubo, the green-hornblende labradorite andesite appears to cover the basaltic-hornblende bytownite andesite. At the eastern foot of the steep cliff of Kayagatake, a lava flow is detected, while at the eastern ridge of Kanagatake the rock occurs as a narrow dyke. It is also found at the saddle between Kanagatake and Kayagatake where it appears to cover the basaltic-hornblende andesite, although the very contact is not observed. The type specimen was collected at Tochikubo.55)

---

54) Its optical plane is perpendicular to c axis. Accordingly it belongs to clinohypersthene.

55) 栃窪

Megascopic characters.—It is of light grey colour, very compact. Porphyritic plagioclase is so minute, that it is not taken as phenocryst in macroscopic observation. On the contrary, green hornblende occurs sporadically in large size often reaching 1 cm. in length.

Microscopic characters.—Under the microscope, it is almost holocrystalline and is sempatic to dopatic.

The plagioclase shows maximum extinction angle of 35° showing that it belongs to acidic labradorite. The refractive index for the faster light in cleavage flakes is 1.556, showing molecular ratio $Ab_{47}An_{53}$.

Monoclinic pyroxene is not abundant. It is in euhedral crystal indicating that it is a crystallizing mineral. Hypersthene is weakly pleochroic. The optical properties of the green hornblende are as follows: pleochroism is distinct; Z=brownish green, $Y=X$=light yellowish green. Absorption $Z>Y=X$. Maximum extinction angle in longitudinal section is 11°.

Minerals composing the groundmass are chiefly plagioclase and magnetite accompanying negligible amount of pyroxene.

It must be remarked in this place that basaltic hornblende and green hornblende coexist side by side in one and the same specimen which is collected at the eastern foot of the cliff of Kanagatake. The same occurrence is also found in the basaltic-hornblende andesite constituting the western ridge of Kanagatake.

This fact appears not to correspond to the experimental result which shows a mineral having the same optical properties as basaltic hornblende is formed by heating green hornblende. (See p. 352).

OLIVINE-BEARING PYROXENE LABRADORITE ANDESITE.

(Pl. XXIX. Fig. 3.)

Locality and general remarks.—This is the youngest effusive rock found in the volcanic group, and is the most abundant, constructing the main part of the younger conide.

There are some varieties in this type among which we can enumerate olivine-bearing augite andesite, olivine-bearing two pyroxene andesite and two pyroxene andesite. They are almost analogous in general characters except in the proportion of the quantity of the essential minerals. Accordingly the writer will describe the first one as representative of this type, which was chemically analyzed. (See p. 370).

Megascopic characters.—The rock type is dark brown and is strongly porphyritic. The most notable phenocrysts are of augite which appear as dark spots with diameter reaching ½ cm. Minute but abundant phenocrysts of plagioclase and small crystals of olivine are also observable by naked eyes.

Microscopic characters.—The rock is percrystalline and dosemic.

The plagioclase is rich in crack as is described in the preceding paragraph. Zonal structure is noticeably developed. Molecular ratio varies from $Ab_{27}An_{73}$ to $Ab_{34}An_{66}$ showing, that the plagioclase is basic labradorite. Inclusions in the plagioclase are extremely rare. They are of magnetite and pyroxene. No alteration is observed.

The olivine occurs in highly corroded form, always being small in size. It is colourless but stained into reddish brown from the periphery of the crystal or along cracks which is remarkably developed in that mineral. The refractive indices measured in sodium light by immersion method are as follows: $N_{min} \fallingdotseq \alpha = 1.664$, $\beta = 1.690$, $N_{max} \fallingdotseq \gamma = 1.709$. From the value of β, molecular ratio is $(Mg_2SiO_4)_{80}$ $(Fe_2SiO_4)_{20}$.

The augite in the andesite is usually corroded and highly cracked. The refractive indices are as follows: $n_1 = 1.696$, $n_2 = 1.714$ in cleavage flakes, $c \wedge Z$ $(110) = 38.5°$. Molecular ratio is calculated as $(CaMgSi_2O_6)_{52}$ $(CaFeSi_2O_6)_{40}$ $(MgSiO_3)_8$. Inclusions in augite are of plagioclase and magnetite.

The groundmass is chiefly composed of abundant crystals of plagioclase $Ab_{52}An_{48}$ which is simply twinned or shows no twinning. They are closely packed together, the rock almost lacking glass base. Some of the grains of plagioclase and of augite appear to be derived by brecciation of porphyritic minerals. Small anhedral grains of magnetite are also found abundantly.

Some varieties.

(1) Olivine-bearing two pyroxene labradorite andesite. (Pl. XXIX. Fig. 4.) This variety is found as lava flows which construct the higher part of the peak, Kayagatake. It is dark reddish brown and is more or less slaggy. Porphyritic augite which is so distinct in the specimen described in the above is rare in this variety.

Under the microscope, it is sempatic and docrystalline. Phenocrystic hypersthene is more abundant than augite. The augite has marked zonal structure; n_1 in cleavage flakes varying from 1.692 to 1.693. $c \wedge Z'$ $(110) = 39° - 39.5°$.

The groundmass is more or less rich in glass which is dirty including abundant dusty material. Rarely we can observe brown transparent part where refractive index is determined to be 1.533. It is decidedly higher than that of the glass in the dacite of Kurofuji which is 1.505.

(2) Two pyroxene labradorite andesite. (Pl. XXIX. Fig. 5). It is found at the southern extremity of the southern ridge of Kayagatake. It is characterized by the absence of olivine and its texture resembling that of basaltic-hornblende bytownite andesite. It is sempatic; carries no glass residue. Porphyritic plagioclase has chemical composition, $Ab_{47}An_{53}$.

(3) Cumulophyric olivine-bearing two pyroxene andesite. It is found on the top of Kanagatake, the conduit. The peculiarity of this rock exists in its texture (See Pl. XXIX. Fig. 6). It is equigranular and appears like a plutonic rock. Close examination, however, shows that narrow interstices of crystals are filled with brown glass. Porphyritic pyroxene is highly corroded accompanying granulated margin. Some of the minerals are entirely granulated leaving no original form.

CHAPTER III. PETROGRAPHIC AND CHEMICAL COMPARISON OF DACITES AND ANDESITES.

Before proceeding to the discussion of genetical relationship between the various rock types found at the volcano, it will be convenient to compare the main types in this place.

The following table shows the mineral constituents in various specimens taken from different lavas.

It is a noticeable fact that there is no marked difference in mineral composition between both principal types. However, if we compare the

	Rocks / Essential Minerals	Andesites					Dacites				
		K_{144}	Ky	Kn	A_{11}	K_{101}	N_1	48	98	172	J_6
Porphyritic Minerals	Olivine	+	+	+			+	+	+		
	Rhombic Pyroxene		+	+	+	+	+	+	+	+	+
	Monoclinic Pyroxene	+	+	+	+	+	+	+	+	+	
	Basaltic Hornblende					+	?	?	+		
	Brown Hornblende										+
	Green Hornblende				+	+				+	
	Biotite										
	Quartz						+		+		+
	Plagioclase	+	+	+	+	+	+	+	+	+	+
Minerals in Groundmass	Olivine						+	+	+	+	+
	Rhombic Pyroxene		+	+	+	+	+	+	+	+	
	Monoclinic Pyroxene	+	+	+	+	+					
	Basaltic Hornblende										
	Brown Hornblende										
	Green Hornblende										
	Biotite										
	Quartz									?	
	Plagioclase	+	+	+	+	+	+	+	+	+	+

optical properties of plagioclases in these rock types, the contrast of the two without an intermediate type is easily recognized.

As these facts have important meaning on genetical consideration, it will be treated more in detail in the following chapter.

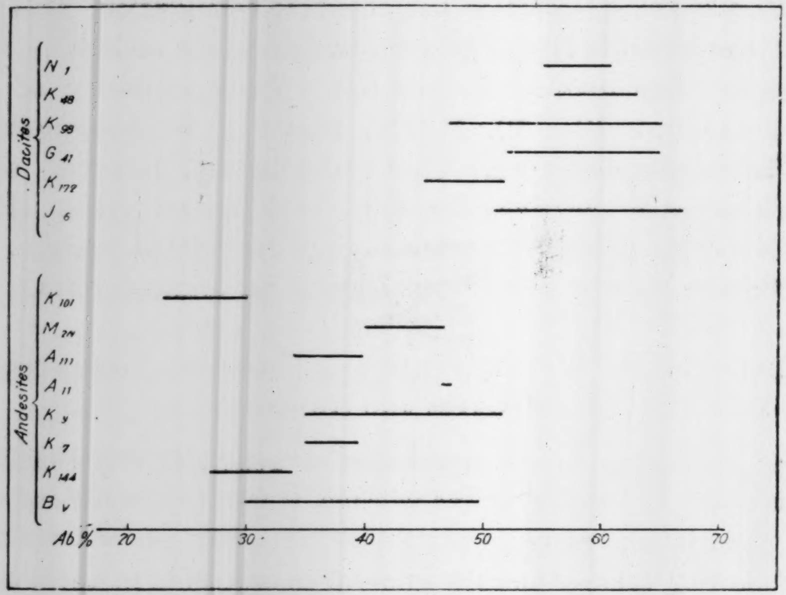

Fig. 12. Diagram showing molecular ratio of plagioclase.
(The arrangement is roughly followed to the order of effusion; the upper one being older than the lower.)

The relation between the refractive indices of mafic minerals and the chemical composition of associating plagioclase is seen from the following diagrams.

The diagrams show that indices of refraction of olivine as well as of augite are lower distinctly in the dacite. At first sight the above relation

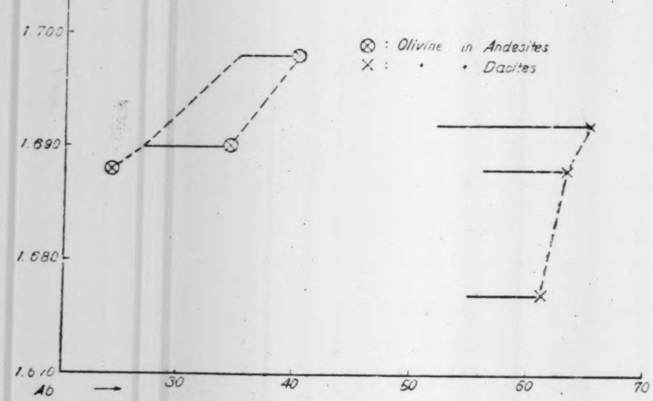

Fig. 13. Paragenesis diagram of olivine and plagioclase.

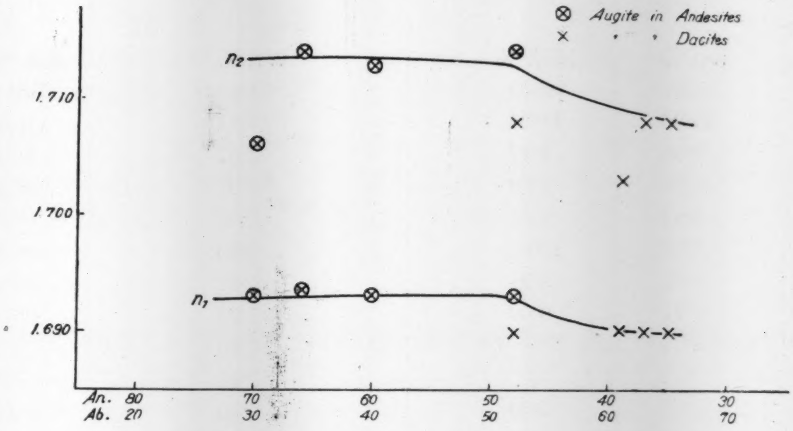

Fig. 14. Paragenesis diagram of augite and plagioclase.

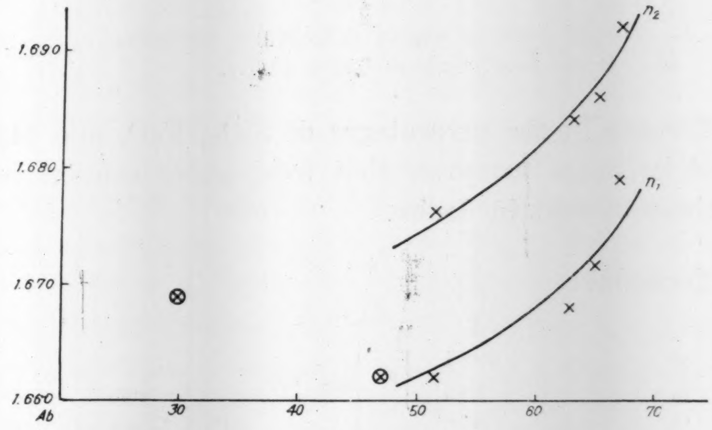

Fig. 15. Paragenesis diagram of hornblende and plagioclase.

appears to be incomprehensive, for in usual case, indices of refraction of mafic minerals increase as albite content of plagioclase increases. However, as will be shown in the later chapter, it is only apparently so.

In Fig. 15 there is some regularity that hornblende associating with sodic plagioclase has higher refractive indices than that with calcic plagioclase.

Two specimens are chemically analyzed by Mr. Tanaka of the Earthquake Research Institute through the kindness of Professor Tsuboi, to both of whom the writer is much indebted.

One of the specimens analyzed as the representative of the dacite is green-hornblende dacite whose petrographic description is given in p. 357. Another one which represents andesites at Kayagatake is olivine-bearing augite labradorite andesite (p. 365).

	I		II	
	Wt. %	Mol. %	Wt. %	Mol. %
SiO_2	52·35	58·55	64·41	70·18
Al_2O_3	18·86	12·73	17·11	11·09
Fe_2O_3	3·68	1·37	2·57	1·03
FeO	5·29	4·39	2·62	2·40
MgO	4·42	7·21	2·02	2·30
CaO	8·32	10·02	5·80	6·79
Na_2O	3·62	3·94	3·57	3·79
K_2O	0·97	0·69	1·23	0·86
H_2O+	1·03		0·45	
H_2O-	0·75		0·11	
Ti O_2	1·05	0·89	0·56	0·47
P_2O_5	0·27	0·17	0·13	0·06
MnO	0·10	0·09	0·07	0·07
Sum	100·71		100·65	

I: Olivine-bearing augite labradorite andesite.
II: Green-hornblende andesine dacite.

Wide difference in the percentages of SiO_2, FeO, and MgO is noticeable. It must be noted moreover that total water content in andesite is about three times of that in dacite.

Osann's formulae:

	I	II
s	59·61	70·71
A	4·63	4·65
C	8·10	6·44
F	14·98	7·15
a	3·34	5·10
c	5·85	7·06
f	10·81	7·84
n	8·51	8·20
k	1·01	1·36

Norms:

		II
Quartz	3·18	25·68
Orthoclase	5·56	7·23
Albite	30·39	29·87
Anorthite	32·54	27·87
Diopside	5·59	0·68
Hypersthene	13·42	6·52
Magnetite	5·34	3·71
Ilmenite	1·82	0·98
Apatite	0·93	0·47

Ratios:

$\frac{Sal}{Fem}$	2·64	7·27
$\frac{Q}{F}$	0·05	0·40
$\frac{Na_2O'+K_2O'}{CaO'}$	0·55	0·70
$\frac{K_2O'}{Na_2O'}$	0·17	0·23

According to C. I. P. W. quantitative system No. 1 belongs to Hessose (II.′ 4. 4′.5) while No. 2 to Yellowstonose (I′. 3′. 4′.4).

Wolff's formula:

	I	II
L	67·64	62·96
M	26·28	12·10
Q	+ 4·60	+24·38
A	4·18	4·65
C	8·55	6·44
F	11·77	5·02
K_2O	0·69	0·86
Na_2O	3·49	3·79

$$\text{I}\quad \frac{C}{2}=4{\cdot}275,\qquad A=4{\cdot}18,\qquad \frac{C}{2}>A.$$

$$\text{II}\quad \frac{C}{2}=3{\cdot}22,\qquad A=4{\cdot}65,\qquad \frac{C}{2}<A.$$

According to Wolff No. 1 belongs to Alboranit (Feld; Q H D), while No. 2 to Dazit (Feld; Q Eb).

CHAPTER IV. MAGMATIC DIFFERENTIATION.

The Principle of Differentiation.

Magma is a mixed solution of silicates with some volatile substances. Since igneous rocks are derivatives from the magma under different conditions, it is reasonable to base our consideration of magma on experimental data about simple systems of silicate solutions.[56)]

If we assume that the original magma is basaltic, two courses are considered to produce acidic rock from the original magma. In order to illustrate this the course of crystallization will be traced on the following equilibrium diagram (Fig. 16).

Suppose, for convenience, the composition of original magma is x.

[56)] S. TSUBOI, *Tôyô-Gakugei Zasshi*, **42**, No. 3, 41.

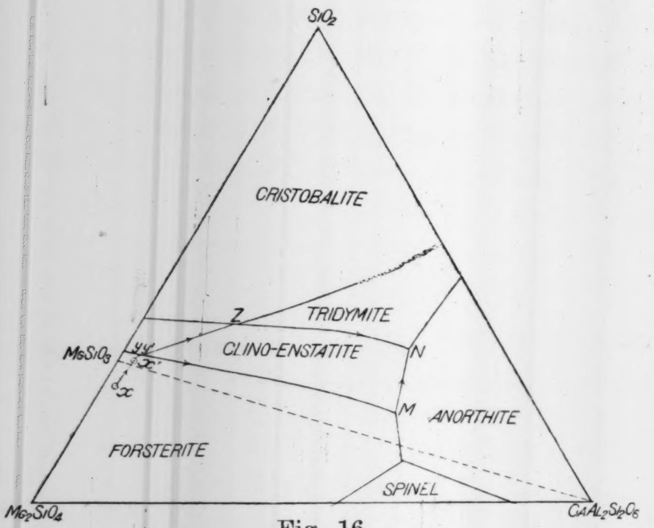

Fig. 16.

If the magma cools with perfect equilibrium, forsterite begins to crystallize out at *x* which lies on the melting surface of the forsterite. As the cooling proceeds the residual liquid changes its composition along the straight line *xy*. When cooled to *y* clinoenstatite appears. At the same time forsterite begins to redissolve. When the temperature M is reached anorthite crystallizes out and finally is formed an aggregate of forsterite, clinoenstatite and anorthite. If sinking of forsterite crystals occur, the upper layer of the melt becomes more acidic in bulk composition than *x*. It is represented by such a point as *x'* in the diagram. Then the crystallization will not complete at M; thus clinoenstatite and anorthite continues to separate from the liquid which changes its composition along the line MN. At last it is cooled to N where tridymite separates and is obtained a mass of pyroxene, anorthite and tridymite. The order of crystallization is forsterite→clinoenstatite→anorthite→tridymite.

If, in some stage of crystallization, for example at *y'*, the residual liquid is "squeezed out" the course of change of the composition of the residual liquid will be quite different from that in the former case. It crosses the pyroxene field along the line *y'Z*, departing from the normal course *yM*. When the temperature *Z* is reached, cristobalite separates. Thereafter the composition of residual liquid changes along *ZN*. At *N* anorthite separates and the whole solidifies as mixture of solid phases, clinoenstatite, anorthite and tridymite. The order of crystallization is forsterite→clinoenstatite→cristobalite→tridymite→anorthite.

It must be noted here that free silica separates in earlier stage and that it appears in high temperature form.

N. L. Bowen remarking the importance of the above two processes in magmatic differentiation says; "The sinking of crystals and the squeezing out of residual liquid are considered the all-important instrument of differentiation."(57)

It is necessary, in the first place, to investigate which one of these processes is the most important at the volcano Kayagatake.

Sinking of Crystals.

A favourable condition for sinking of crystals in a magma is its slow cooling. Experimental researches on thermal properties of plagioclase(58) show that its mode of zoning is an indication of the thermal condition of the magma from which the mineral crystallizes.

The phenocryst of plagioclase found in lavas of Kayagatake has remarkable zonal structure as was already stated; range of variation of chemical composition in one specimen reaches 18 percent of anorthite molecule. Moreover microscope shows that the mode of arrangement of zones of the plagioclase in dacite is different from that in andesite. These facts indicate not only that the magma in the reservoir from which dacite lavas were derived cooled moderately but also the magma cooled in different rate of cooling from that which derived andesites.

There is another fact which shows that the rate of cooling was not slow and sinking of crystals was prevented, viz. that the same sample carries mafic minerals of different stages of crystallization. If the rate of cooling is slow and sinking of crystals occur, minerals crystallized in earlier stage will sink in the lower part of magma basin and the upper part will be occupied only by minerals of later stage. Accordingly extruded lava which represents the upper part of magma basin can hardly carry mafic minerals of different stages.

Those evidences described above are almost sufficient to show that the dacite was not derived by sinking of crystals from the original magma.

Separation of Crystals and Liquid.

Failing to explain the genesis of dacite by gravitational differentiation, we must seek other process to produce the acidic rock. In this case, the second course of crystallization in the above ternary diagram gives important suggestion to the origin of the dacite.

---

57) N. L. Bowen, *Jour. Geol.*, (1915), Suppl. 80.

58) A. L. Day and E. T. Allen, The isomorphism and thermal properties of the feldspar.

In the discussion with the diagram, the writer remarked that the course of crystallization of a liquid separated by ''squeezing out'' is different from that of the original liquid. The most important point is that the separation of free silica takes place in earlier stage prior to that of anorthite.

Now, in the dacite of Kurofuji, crystallization of quartz took place prior to that of oligoclase and has the form of high quartz.

This close analogy in separation of free silica is so important that it can not be considered merely as apparent. It seems most reasonable to think that the same process as ''squeezing out'' occurred in the natural magma.

The above consideration is supported by many evidences among which the following may be mentioned.

1) Existence of olivine in the dacite: If a magma is transported from one place to another, it is expected that the magma will accompany some of the minerals which have been in equilibrium with the magma. Such example has already been described by J. W. Judd in western Isle of Scotland.[59]

It has been previously described that olivine is found in the dacite of Kurofuji, especially in the earlier lava of that volcano.

Existence of olivine in so acidic a rock as the dacite can be explained neither by gravitational effect nor by special rate of cooling of the original magma. It is highly probable that the olivine is xenocryst which is transported by the magma. An angular fragment of olivine armoured by pyroxene is a strong evidence to support such consideration.

Comparing refractive indices of the olivine in dacite with those of olivine in andesite, it is found that the former are lower than the latter. Apparently this is against the general rule that olivine increases its indices of refraction as the associating plagioclase decreases its anorthite content. The anomaly, I think, is due to that the olivine in the dacite ceased to react with the liquid in earlier stage than that of the andesite, the corona of hypersthene being immediately formed to surround the olivine.

2) Inclusion of plagioclase in the porphyritic feldspar of the dacite: The second evidence to show the transportation of minerals is the inclusion of plagioclase found in the porphyritic feldspar of dacite, although such example is rare. In some cases, these broken inclusions are surrounded by

---

59) J. W. JUDD, ''The Phopylites of the Western Isl. of Scotland, and their Relation to the Andesites and Diorites of District,'' *Quart. Jour. Geol. Soc.*, (1890), 379.

radial aggregate of feldspar. It is to be noted here, that the enclosed plagioclase has abundant cracks, and has a zonal structure, just as the plagioclase in the andesite. The extinction angle of the inclusion is much different from that of the surrounding crystal. The chemical composition of the core calculated by specially devised method by Prof. S. Tsuboi is $Ab_{24}An_{76}$; decidedly basic variety. These evidences are sufficient to show that the inclusion is a fragment of plagioclase of exotic origin.

3) Evidences of accumulation of porphyritic minerals: It must be noted in this connection, that almost all the phenocrysts of the andesites of Kayagatake have marked cataclastic structure. (See Pl. XXIX. Fig. 3). The cracks are developed only in phenocrysts and the groundmass is free from them. Accordingly it is apparent that they are formed before the consolidation of the flow, but it is difficult to ascertain if these cracks were formed in intratelluric stage or at the time of effusion.

However there are some evidences which appear to show the crashing was performed in intratelluric stage on account of accumulation of porphyritic minerals.

The most remarkable evidence which shows such process is in the texture of an andesite collected at Kanagatake. It is equigranular and appears to be a plutonic rock. However we can find brown glass filling among the crystals which are highly corroded and accompany granulated margins; moreover some of them are entirely granulated leaving no original outline.

Besides the above, there is a notable fact that cracks of many crystals of the plagioclase are more abundant in inner part; and in some instances highly brecciated inner part is enveloped by a crackless zone.

Considering these facts we are led to the conclusion that crystals were accumulated by some mechanical processes which resulted in squeezing out of the magma, as has been suggested by G. Barrow.[60]

4) Chemical consideration: I have treated in the above pages, the problem chiefly from petrological and petrographical side. But chemical consideration must not be neglected.

It is natural to expect from the above theory that bulk composition of the Kurofuji dacite may represent the composition of groundmass of some acidic basalt, while that of the andesite of Kayagatake represents the chemical composition of phenocrysts in it.

The following table gives a valuable base. This was taken from the

---

60) G. Barrow, "On Certain Gneisses with Rounded-grained Oligoclase and their Relation to Pegmatites," *Geol. Mag.*, (1892), 64–65.

results of chemical analyses performed by Lagorio and by Siemiradjki according J. H. L. Vogt.[61]

Percentage of SiO_2

	Phenocryst of Plagioclase	Groundmass	Difference
	53·95	65·05	12·10
	55·64	68·71	13·07
	51·17	66·98	15·81
	52·01	69·41	17·40
	52·45	68·74	16·29
	55·42	70·19	14·77
	55·60	66·89	11·29
	58·01	67·56	9·55
mean	54·28	67·94	13·79

The difference in percentage of silica may be somewhat reduced if the mafic phenocrysts were taken.

These differences approach to that between the bulk composition of the dacites and the andesites now under consideration; the latter being 12.06. It is more interesting if we compare the above differences with that of the augite andesite and glassy andesite which are considered to have been separated by the process ''squeezing out.'' In one case described by J. W. Judd,[62] the difference is 13.94.

Thus petrological and petrographical as well as chemical considerations led to the same conclusion that the magma which produced the dacites of Kurofuji was separated from the original basaltic magma in early stage of its crystallization.

After the separation into the two magmas, differentiation of less importance has proceeded independently in each magma reservoir. In the following paragraph, I will briefly describe that process.

Differentiation in the both Magma Chambers.

In magma reservoir of acidic magma, high temperature quartz crystallized out, probably taking a similar course of crystallization as was shown in the ternary system, anorthite-forsterite-silica. At the same time, pyroxene reacting with liquid formed green hornblende which partly changed into basaltic hornblende.[63] While olivine transported with the magma was soon armoured by hypersthene and was left as a relic among minerals of later stage. Pressure of gases evolved as a result of crystallization rapidly increased and at last the pressure overwhelmed the resistance of the upper crust causing intense eruption.[64] This is the eruption which effused abundant ejecta constructing the lower portion of the volcano Kurofuji and flow of olivine-bearing dacite.

---

[61] J. H. L. VOGT, ''Physikalische-chemische Gesetz der Kristallizationsfolge in Eruptivgestein,'' *T. M. P. M.* [2], **24**, 492.

[62] J. W. JUDD, *loc. cit.*, 379.

[63] S. KÔZU, *Sci. Rep. Tôhoku Imp. Univ.*, [3], **3** (1927), 143–159.

After a repose of short time interval, the second eruption began extruding brown hornblende dacite. It is probable that there was sufficient time interval between the first and the second eruptions to produce abundant hornblende in place of pyroxenes as well as olivine.

In the other magma basin where crystals had accumulated, the differentiation was also caused by cooling at the upper part where cooling was rapid, and the crystallization of hornblende began producing enormous quantity of gases which caused the first eruption of the konide Kayagatake. Ejecta and lava of basaltic hornblende andesite are considered to be the material effused in this stage of eruption. The effusion of basaltic hornblende andesite is succeeded by olivine-bearing two pyroxene labradorite andesite which probably represents the lower part of the magma reservoir. Here we see a fact that in the volcano Kurofuji which is constructed of acidic rocks, the order of effusion of volcanic rock is from basic to acidic, while at Kayagatake the order is the reverse.

The course of differentiation is shown in the following diagram.

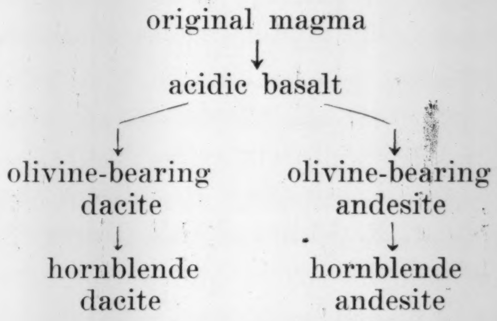

Geological Meaning of the Differentiation.

The conception of "squeezing out" has been introduced to the petrologic interpretation by G. Barrow,[65] J. W. Judd,[66] and A. Geikie according to Judd and its important significance in petrology has been recognized by A. Harker[67] and N. L. Bowen.[68] It was also suggested by Osann and Teall according to F. F. Grout.[69]

---

[64] G. W. Morey, *Jour. Amer. Chem. Soc.*, **36**, Feb., 1914, 226.
A. L. Day & E. T. Allen, "Volcanic Activity and Hot Springs of Lassen Peak."

[65] *loc. cit.*

[66] *loc. cit.*

As was already stated, it is evident that in the present case the separation of crystals and liquid was caused by squeezing out of residual liquid. This process was due probably to some crustal movement.

It must be noted here that the above conclusion well accords with the geologic history of the district.

According to Prof. Yabe,[70] the region was compared from west by movement of Akaishi block in late Tertiary. Although we have no evidence to affirm if the movement directly affected the differentiation, it is noticeable that the region where the volcano stands has been compressed.

Recently Prof. Fujiwara explanating the arrangement of volcanoes in Japan from geophysical point of view says that the central part of Fuji zone that is "fossa magna" was compressed from the northeastern direction.[71] Almost the same view was also proposed by Assist. Prof. F. Homma.[72] It appears to me that such coincidence of conclusions from different points of view is too remarkable to be overlooked as merely accidental.

It is well known that liparitic rocks and pyroxene andesites occur in close association in the volcanoes in Japan.[73] It may be dangerous to apply the same mechanism as the above to other regions but the fact that acidic effusives chiefly effused in Tertiary age when crustal movement was intense in Japan, seems to suggest that similar modes of differentiation occured at least in some other districts.

It is said that the order of effusion in the plutonic rocks shows decreasing basicity.[74] In the effusive rocks, however, the law can not be applied as was noted by Richthofen. It follows the law of increasing divergence according to J. P. Iddings,[75] A. Harker[76] and others. It is interesting that the order is also applicable in the volcano Kayagatake where the differentiation was accelerated by crustal movement.

---

[67] Natural History of Igneous Rocks, 325.

[68] "The Later Stage of the Evolution of Igneous Rocks," *Jour. Geol.*, **23** (1915), Suppl. to No. 8.

[69] F. F. GROUT, *Jour. Geol.*, (1920), 259.

[70] H. YABE, *Gendai-no-Kagaku*, **6**, No. 3, 20 (in Japanese).

[71] S. FUJIWARA, *Geographical Review of Japan*, **1**, No. 8, 2.

[72] F. HOMMA, *loc. cit.*, 147 and 152.

[73] B. KOTÔ, "On the Volcanoes of Japan," *Jour. Geol. Soc., Tokyô.*, **23**.
J. P. IDDINGS, Igneous Rock, **2**, 612.

[74] A. HARKER, Natural History of Igneous Rocks.

[75] J. P. IDDINGS, The Problems of Volcanism, 257.

[76] A. HARKER, Natural History of Igneous Rocks, 115.

Conclusion.

Lastly important results obtained in the present work will be summalized.

1) There is no direct connection between the surface faults and the arrangement in their vents though the latter roughly strike N.W.–S.E. the general direction of the volcanic zone.

2) The eruption began in the extrusion of dacite which has constructed a stratified conide Kurofuji. Piercing the western shoulder of Kurofuji, appeared a new conide, Kayagatake, whose chief constituent is olivine-bearing two pyroxene andesite. At present, both is highly dissected especially in the upper part of the volcanoes. No crater is preserved; stock is revealed as a remnant of the center of activity. No record of the eruption in historic time, nor any post volcanic action such as hot spring and fumaroles is found.

3) The various rocks constituting the volcanic group are classified largely in two types andesite and dacite. Then the andesite is subdivided into basaltic-hornblende labradorite andesite, green-hornblende labradorite andesite, and olivine-bearing two pyroxene labradorite andesite. The dacite is also divided into three types: olivine-bearing andesine dacite, green-hornblende andesine dacite, and brown-hornblende andesine dacite.

The order of effusion is olivine-bearing andesine dacite → brown-hornblende andesine dacite → green-hornblende andesine dacite → basaltic-hornblende labradorite andesite → green-hornblnde labradorite andesite → olivine-bearing two pyroxene labradorite andesite.

4) The dacites and the andesites were derived from the same basaltic magma. In some stage of cooling of the original magma, probably when the plagioclase reached the chemical composition $Ab_{24}An_{76}$ (or in more earlier stage), residual liquid was separated by the process "squeezing out." Hereafter differentiation proceeded independently in each magma reservoir. The dacites was derived from the liquid part, while andesite effused from the other chamber where crystals had been accumulated.

5) Sqeezing out of the residual liquid was a result of the compression of the magma chamber due to crustal movement. Thus an important relation between the magmatic differentiation and the crustal movement of the district has been found to exist.

19. 茅ケ岳火山

東京帝國大學理學部地質學教室
市來政兼

本報文の題目たる茅ケ岳火山は富士と八ケ岳との中間、北緯 35° 40-50.3′ 東徑 138° 25-36′ に位す。此の火山の地質學的並に岩石學的調査により得られたる結果の要點を摘錄すれば下の如し。

（1） 本火山群の火口は配置上地表の斷層と直接の關係認められざれども、火山帶の一般走向なる北西一南東の方向に排列す。

（2） 火山活動は先づ石英安山岩の噴出を以て始り、是は黑富士火山を構成せり。ついで其の西肩を破り安山岩より成る茅ケ岳を生ぜり。兩火山共今は著しく開析せられ其の原形を失ひ、又何等後火山作用に屬する現象を示さず。

（3） 火山を構成する岩石は下の如く分類せらる。

石英安山岩
- (a) 含橄欖石・中性長石・石英安山岩
- (b) 褐色角閃石・中性長石・石英安山岩
- (c) 綠色角閃石・中性長石・石英安山岩

安山岩
- (d) 玄武角閃石・曹灰長石・安山岩
- (e) 綠色角閃石・曹灰長石・安山岩
- (f) 含橄欖石・複輝石・曹灰長石・安山岩

其の噴出順序は (a)→(b)→(c)→(d)→(e)→(f) なり。

（4） 是等の岩石を生ぜし母岩漿は玄武岩漿にして、其の結晶作用の途中、是より晶出しつゝありし斜長石の成分が凡 $Ab_{24}An_{76}$ に達せる時（或は其以前）、殘液が他の部より分離して別の岩漿溜を成し、以後兩岩漿溜に於て各獨立に岩漿分化作用進み、本來の岩漿溜より安山岩を、分離せる岩漿溜より石英安山岩を生ぜしものと考へらる。

（5） 斯くの如く岩漿の結晶作用の途中に於て其の殘液が分離せるは地殼運動の結果なりと考へらる。

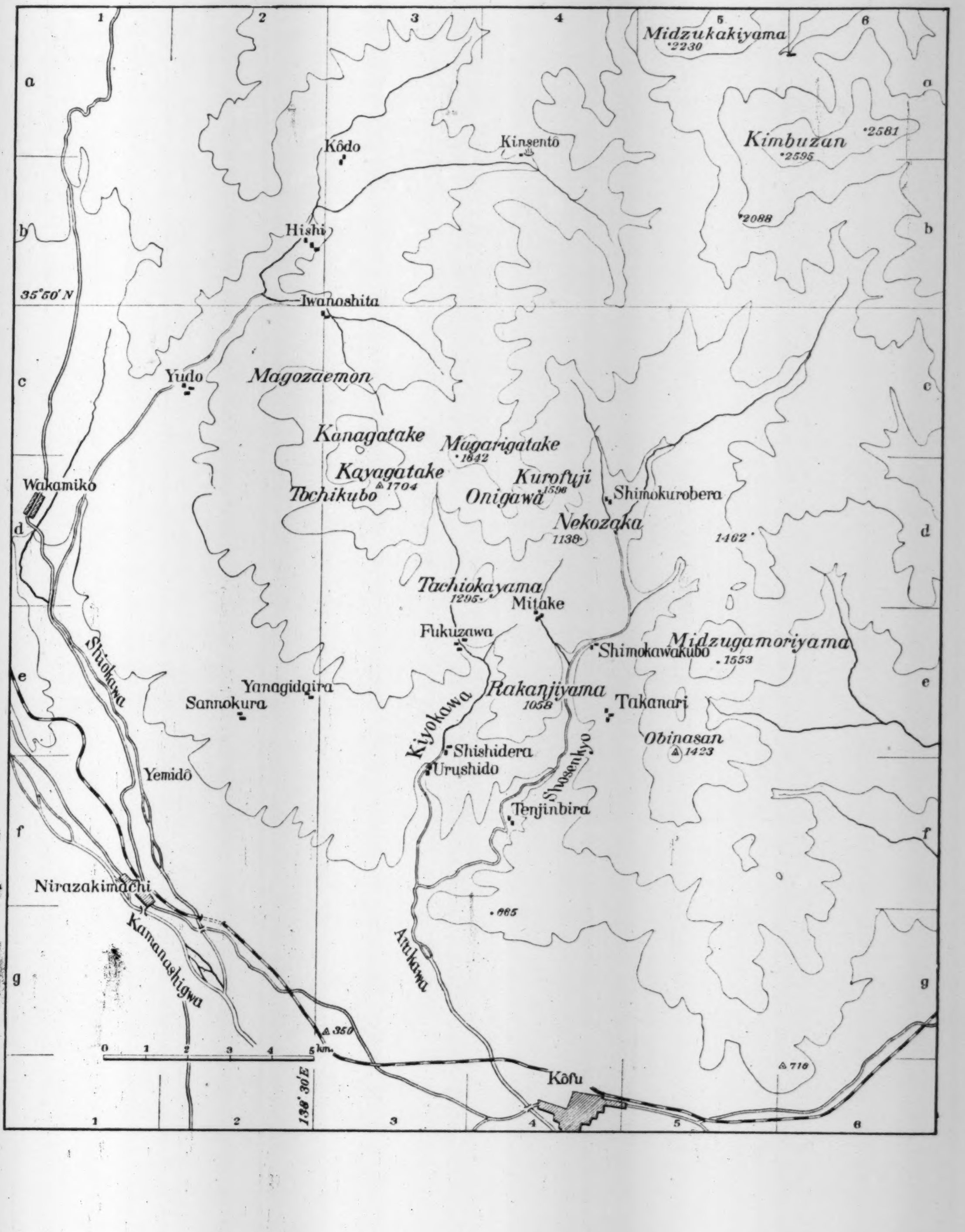
Midzukakiyama
2230
Kimbuzan
2581
2595
2088
Kinsentō
Kôdo
Hishi
Iwanoshita
35°50′ N
Yudo
Magozaemon
Kanagatake
Magarigatake
1642
Kayagatake
Tochikubo
1704
Kurofuji
1596
Onigawa
Shimokurobera
Nekozaka
1138
1462
Wakamiko
Tachiokayama
1295
Mitake
Fukuzawa
Shimokawakubo
Midzugamoriyama
1553
Shiokawa
Yanagidaira
Sannokura
Rakanjiyama
1058
Takanari
Kiyokawa
Obinasan
1423
Shishidera
Urushido
Yemidō
Shosenkyo
Tenjinbira
Nirazakimachi
Kamanashigwa
865
Arakawa
350
0 1 2 3 4 5 km.
138° 30′ E
Kōfu
716
1 2 3 4 5 6
a b c d e f g

（震研彙報、第七號、圖版、市來）

Plate XXVIII.

(Microphotographs)

Dacites of Kurofuji.

Fig. 1.—Olivine-bearing two pyroxene andesine dacite. (×10), (crossed nicols) ol: olivine, Au: augite Q: quartz. Collected at western foot of Tachiokayama (See pp. 355–357).

Fig. 2.—Brown-hornblende andesine dacite. (×28) H: brown hornblende, G: glassy groundmass. Collected at the southeastern terminal of Kurofuji. (See pp. 358–359).

Fig. 3.—Green-hornblende andesine dacite. (×28) H: green hornblende. Note the zoning of plagioclase. Collected from the longest dyke diverging from the vent.

Fig. 4.—Green-hornblende andesine dacite. (×28). Note the opacitization of green hornblende. Collected at Shimokurobera, from central portion of a dyke. (See pp. 357–358).

Fig. 5. Phenocryst of andesine growing upon a nucleus which is a fragment of basic plagioclase. (crossed nicols, ×28).

Fig. 6.—The same as the above. (See p. 374).

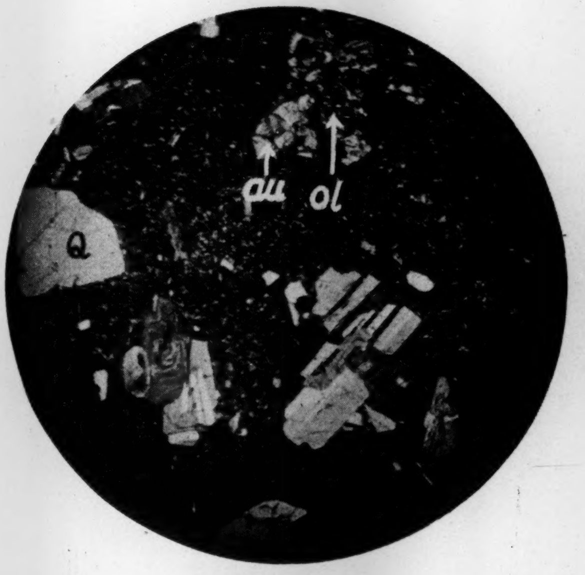

Fig. 1.

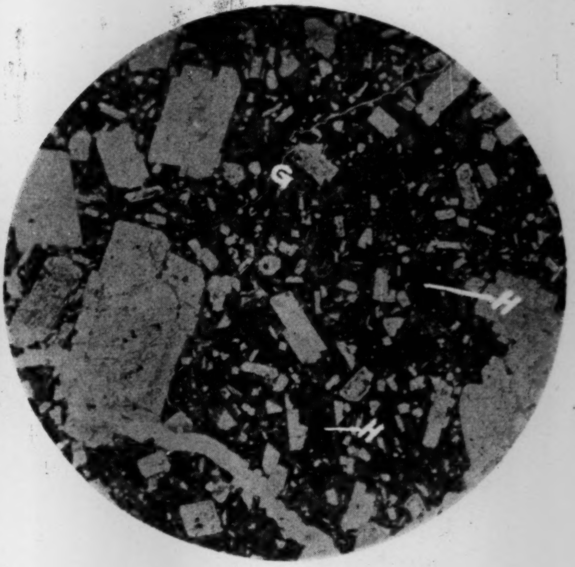

Fig. 2.

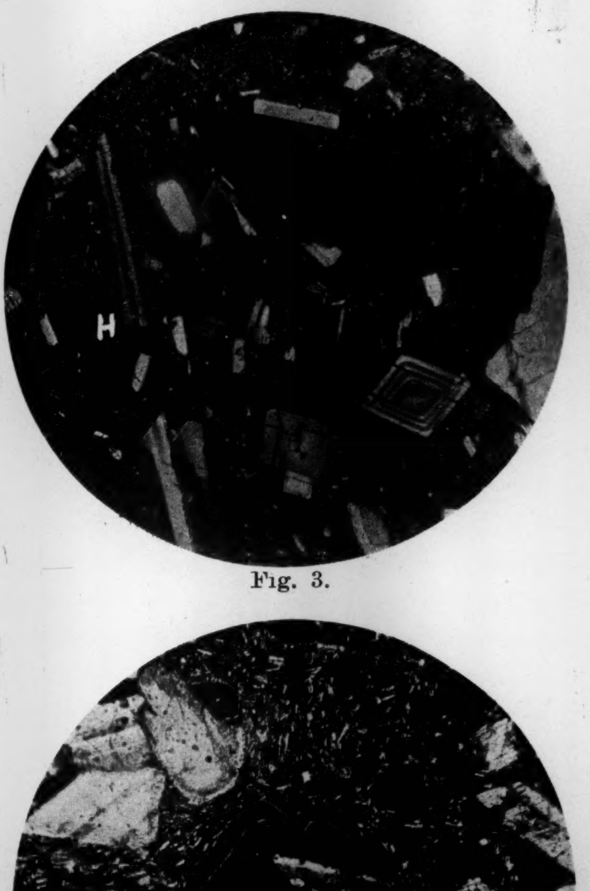

Fig. 3.

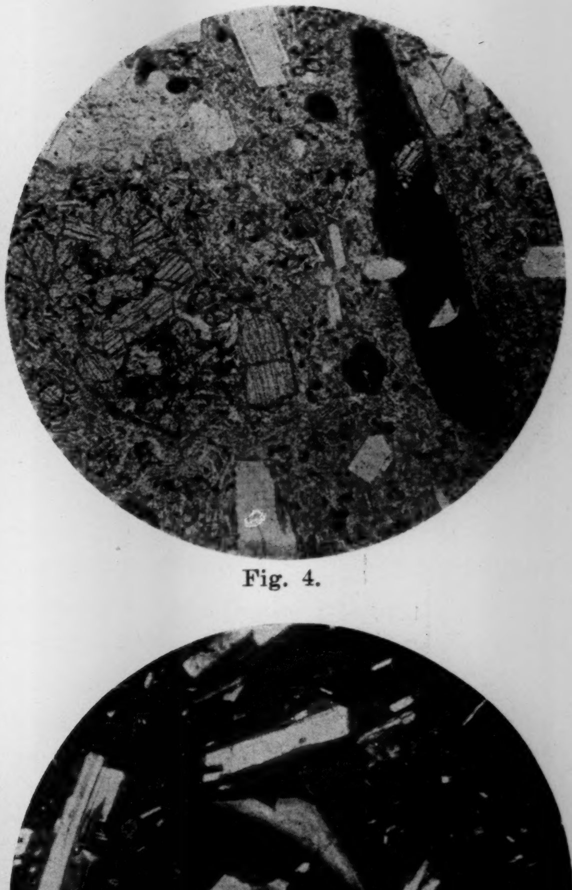

Fig. 4.

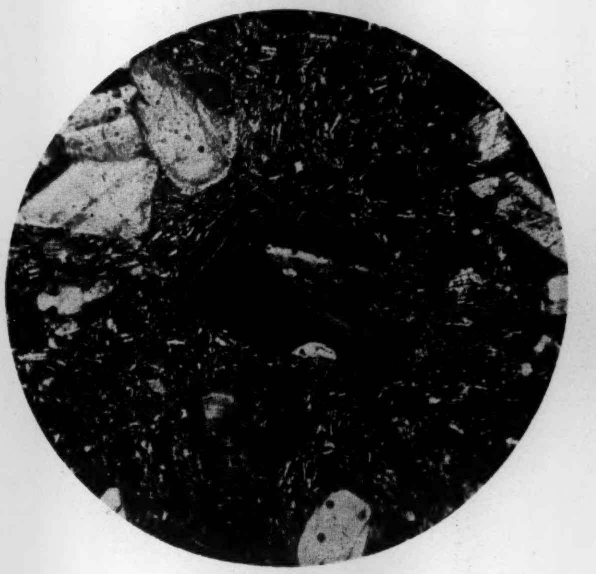

Fig. 5.

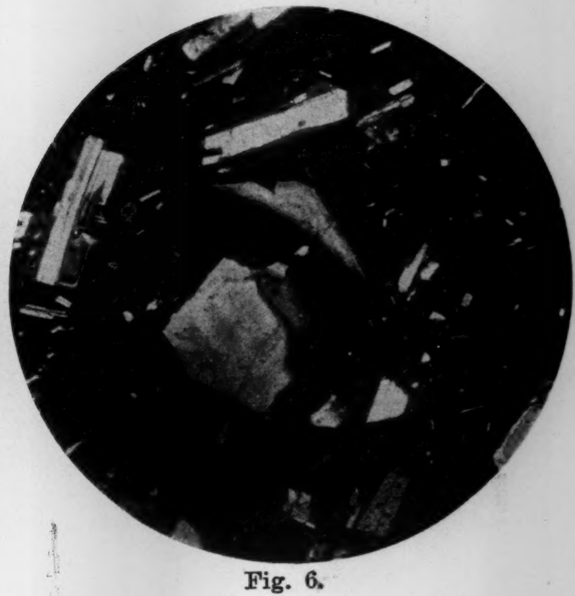

Fig. 6.

（震研彙報、第七號、圖版、市來）

Plate XXIX.

(Microphotographs)

Andesites of Kayagatake.

Fig. 1.—Green-hornblende labradorite andesite. (×10) H: green hornblende. Note sporadic occurrence of the hornblende. Loc., Tochikubo. (See p. 364).

Fig. 2.—Basaltic-hornblende bytownite andesite. (×33). Note the zonal structure of basaltic hornblende. Loc., Gakisan. (See p. 362).

Fig. 3.—Olivine-bearing augite labradorite andesite. (×33) Au: augite, Ol: olivine. Note cataclastic structure of porphyritic minerals. (See p. 365). Loc., Gyônin-yama (stock).

Fig. 4.—Olivine-bearing two pyroxene labradorite andesite. Collected at the top of Kayagatake (flow). See p. 366.

Fig. 5.—Two pyroxene labradorite andesite. (×33 crossed nicols). Collected at the southern terminal of a ridge of Kayagatake. (See p. 367).

Fig. 6.—Cumulophyric olivine-bearing two pyroxene labradorite andesite. (×33, crossed nicols) Au: augite. Augite and hypersthene are corroded; plagioclase is brecciated. Collected at the top of Kanagatake. (See p. 367).

[M. Ichiki] [Bull. Earthq. Res. Inst., Vol. VII, Pl. XXIX.]

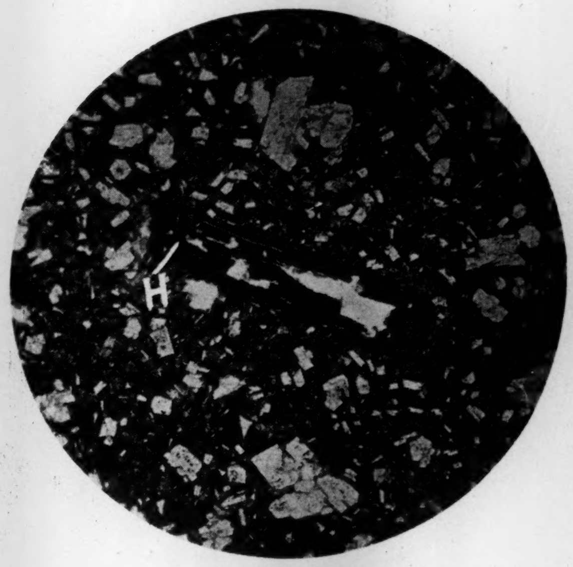

Fig. 1.

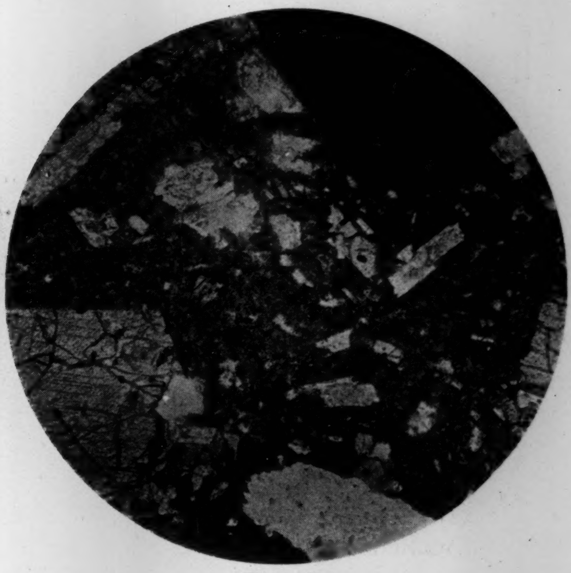

Fig. 2.

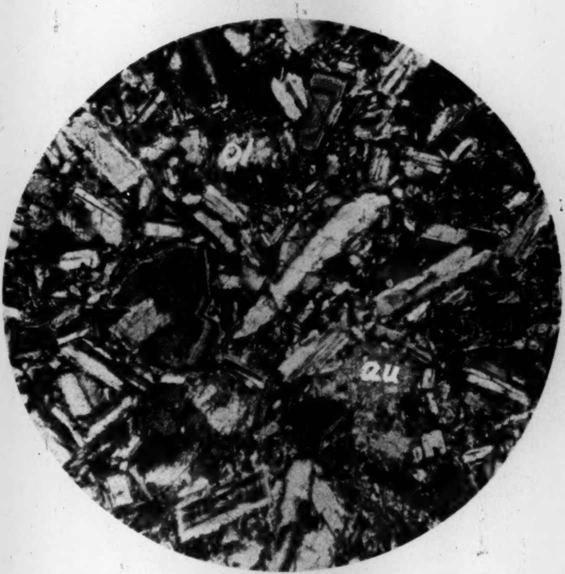

Fig. 3.

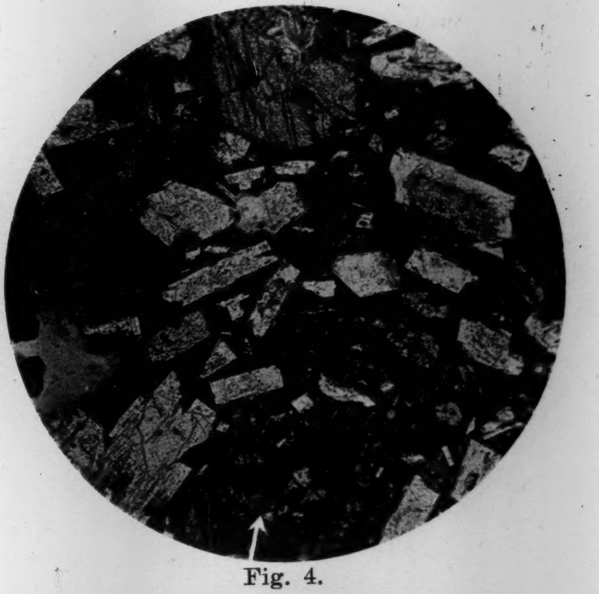

Fig. 4.

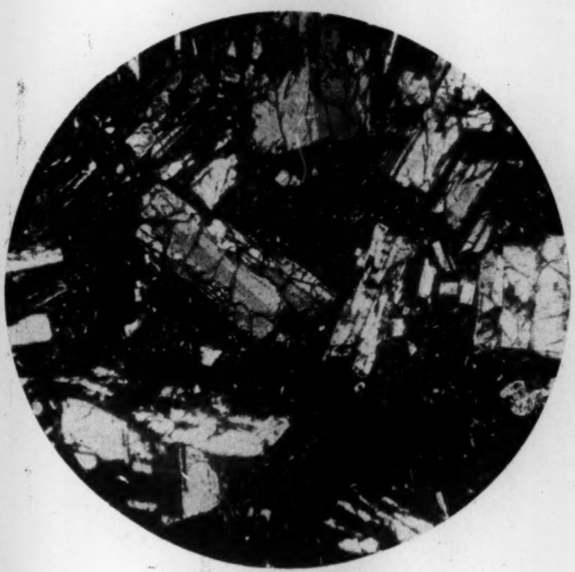

Fig. 5.

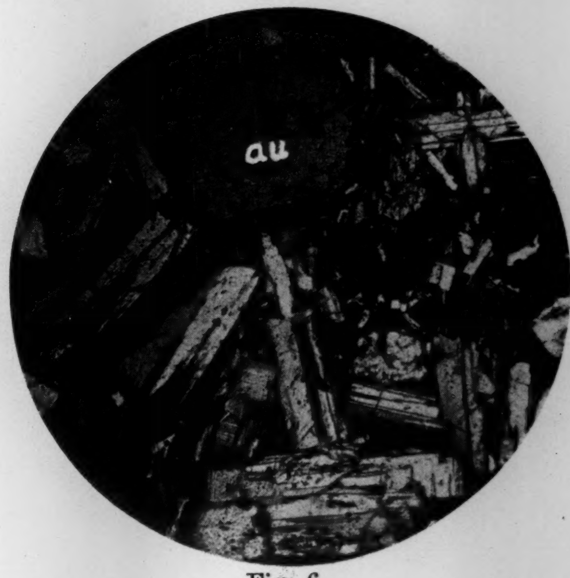

Fig. 6.

（研震彙報、第七號、圖版、市來）

[M. Ichiki]

GEOLOGIC MAP OF VOLCANO KAYAGATAKE, KAI

1926—1928

[Bull. Earthq. Res. Inst., Vol. VII, Pl. XXX.]

（震研彙報第七號、圖版、市來）

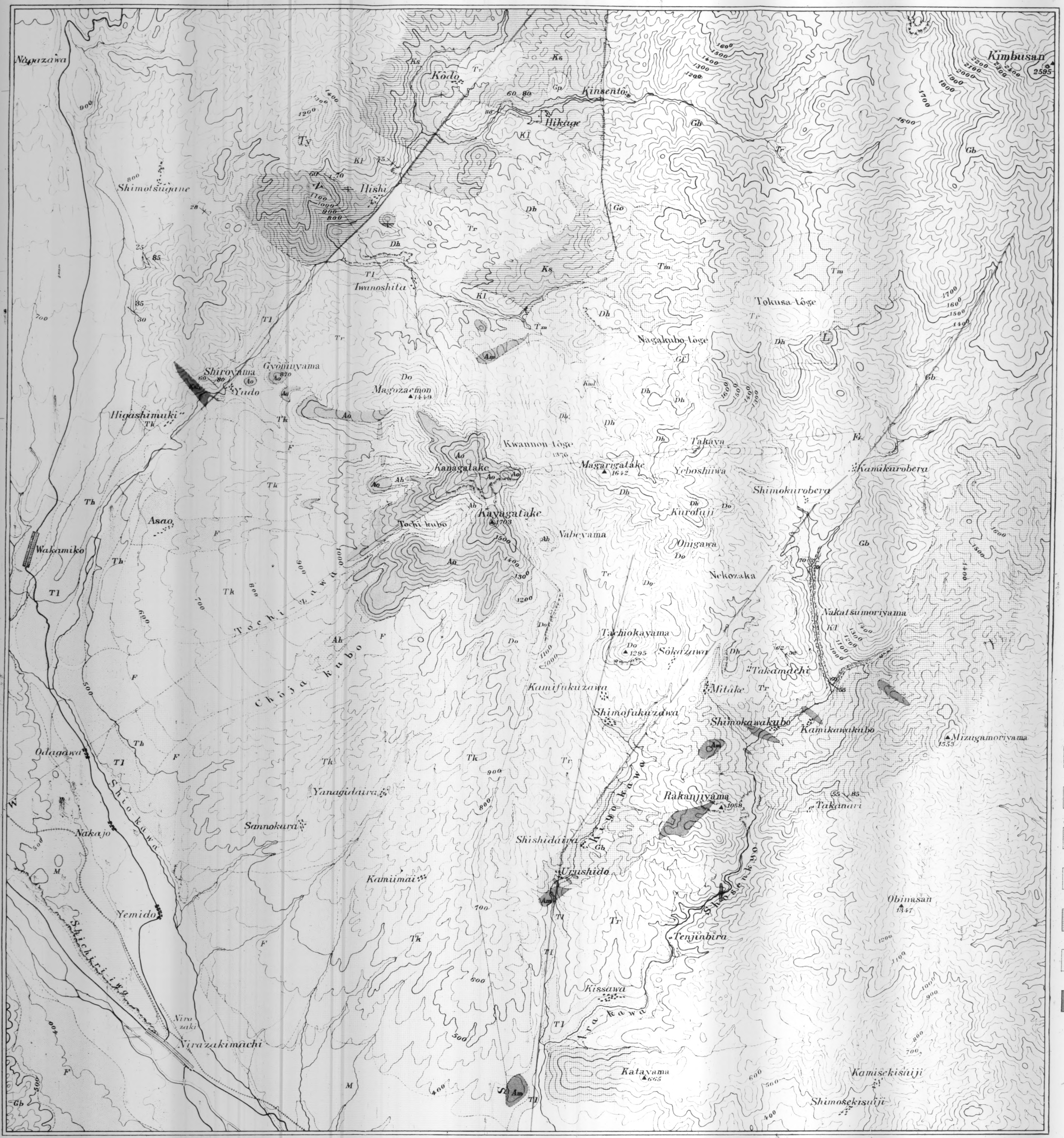
Nagazawa
Kodo
Kinsentō
Hikage
Kimbusan
2595
Shimotsugane
Ilishi
Iwanoshita
Tokusa tōge
Nagakubo tōge
Shiroyama
Gyōnin yama
Yado
Higashimuki
Magozaemon
1449
Kwannon tōge
Kanagatake
Magarigatake
1642
Takaya
Yeboshiiwa
Shimokurobera
Kamikurobera
Kayagatake
1703
Tochi kubo
Asao
Nabeyama
Kurofuji
Onigawa
Wakamiko
Nekozaka
Tochisawa
Chōja kubo
Tachiokayama
1295
Sōkazawa
Takamachi
Nakatsumoriyama
Mitake
Kamifukuzawa
Shimofukuzawa
Shimokawakubo
Kamikawakubo
Mizugamoriyama
1555
Odagawa
Shiokawa
Rakanjiyama
1058
Takanari
Yanagidaira
Sannokara
Nakajo
Shishidaira
Kiyokawa
Urushida
Kamiimai
Yemido
Obinasan
1347
Tenjinbira
Shichirigiwa
Nirazaki
Nirazakimachi
Kissawa
Arakawa
Katayama
Kamisekisuiji
Shimosekisuiji
Ty
Tk
Th
Tl
F
M
Gb
Go
Gp
Gf
Ks
Kl
Kml
Tr
Tm
Dh
Do
Ao
Ah
Am
L

Legend

R	Recent river bed
F	Torrential fan
Th	High-terrace deposit
Tl	Low-terrace deposit
M	Mud-flow
Ty	Tuff-breccia of Yatsugatake
Ao	Olivine-bearing pyroxene andesite
Ah	Hornblende labradorite andesite
Tk	Tuff-breccia of Kayagatake
Dh	Hornblende dacite
Do	Olivine-bearing dacite
Tr	Tuff-breccia of Kurofuji
Am	Lavas and stocks of two pyroxene andesite
Tm	Tuff-breccia of two pyroxene andesite
L	Lamprophyre
Gp	Granite porphyry
Go	Porphyritic granite
Gf	Fine-grained granite
Gb	Coarse grained granite
Kms	Metamorphosed sandstone
Kml	Metamorphosed clayslate
Ks	Sandstone of Kobotoke series
Kl	Clayslate of Kobotoke series
Ksh	Schalstein of Kobotoke series
⟋	Dip and strike
⟋	Fault

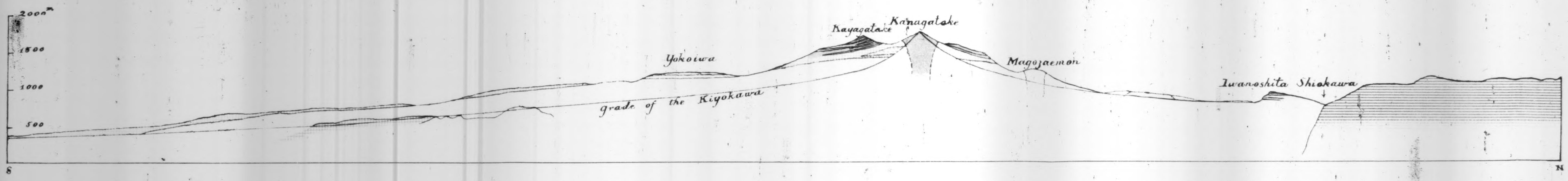
2000m
1500
1000
500
Kayagatake
Kanagatake
Yokoiwa
Magozaemon
grade of the Kiyokawa
Iwanoshita
Shiokawa
S
N

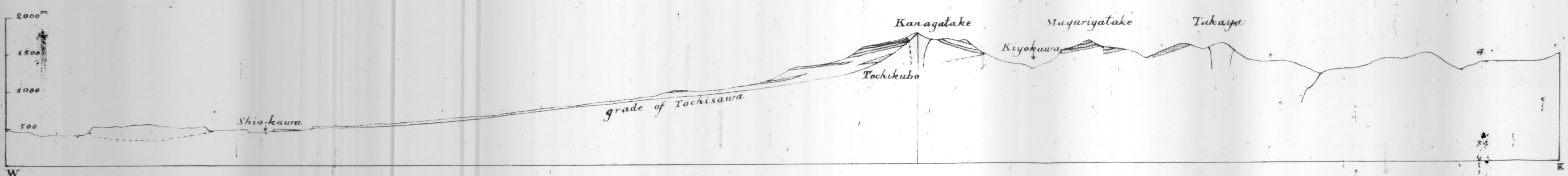
2000m
1500
1000
500
Kanagatake
Magarigatake
Takaya
Kiyokawa
Tochikubo
grade of Tochisawa
Shiokawa
W.
E.

Legend

☐	Mud-flow
▨	Olivine-bearing two pyroxene andesite
▨	Hornblende andesite
▨	Tuff-breccia of Kayagatake
☐	Green-hornblende dacite
▨	Brown-hornblende dacite
▨	Olivine-bearing two pyroxene dacite
▨	Tuff-breccia of Kurofuji
▨	Tuff-breccia and lava of paleo-andesite
▨	Biotite granite
▨	Kobotoke series

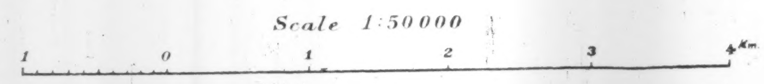
Scale 1:50000
1
0
1
2
3
4Km

20.　丹後地方震災地復舊二等三角測量記事

昭和四年五月

陸地測量部

丹後地方震災地に於ける復舊測量中一等三角測量に依る土地變動の狀況は過般既に之を發表せしが今や昭和三年度に於て實施せる二等三角測量作業の計算を完了せるを以て茲に其の成果の概要を記述せんとす。

思ふに一等三角測量に於ては震災地を中心とし稍々廣き地域に於て互に比較的隔離せる地點の變動狀態を知悉し得たるものなるが本二等三角測量の成果に依りて更に震災地中心に近き地方に於ける土地の稍々細部に渉る變動狀態を觀察し得るものと信ず。

一、作業區域並に作業量

復舊二等三角測量地域は昭和二年度に於て實施せる東京帝國大學委託三角測量の成果に鑑み其の豫想變動範圍を局限し激震地を中心とする京都府、兵庫縣及福井縣の一部に跨り面積二四三方里二等三角點五十二點とす此等の諸點は嘗て明治二十一年乃至二十四年の間に觀測を行はれたるものにして其の標石は概ね完全に維持保存せられ異狀を認めず今其の點名、所在地及觀測年次を示すこと別表第一及附圖の如し。

二、作業の概況

標石中心上に制規の覘標（尋常方錐形）を建設し（中には視通の關係上器械高五米に高めたるものあり）獨國 Carl Bamberg 製二十一糎測微經緯儀を用ひ六測回（十二視準）の方向觀測法に據り視準點は通常覘標中心を以てせるも特に距離遠大なるものに對しては回照器を使用せり。

三、計算及成果

丹後地方震災地復舊一等三角網甲、乙二種の成果を與件とし A, B 二種の計算を實施せり。（一等三角測量記事參照）

A. 一等三角點甲成果（明治十八年乃至二十二年に於ける舊觀測値を用ひて三角網平均計算を行ひ饗庭野基線網の第三增大邊なる比良ケ岳、野坂岳の舊成果を已知件とし各點の距離、平面直角縱橫線並に經緯度を算出せるもの）を與件として明治二十一年乃至二十四年に於ける舊觀測値を用ひて一點或は二點每に縱橫線平均法に依り逐次各點ノ距離、平面直角縱橫線並に經緯度を計算す。

B. 一等三角點乙成果（昭和三年度に於ける新觀測値を用ひて甲と全く同一方法を以て三角網の平均計算を行ひ氷ノ山、笠形山を不動と假定し甲の成果に一致せしめ此れに依りて各點の距離、平面直角縱橫線並に經緯度を算出せるもの）を與件とし昭和三年度實施せる新觀測値を用ひAと同一なる平均計劃に基き各點の距離、平面直角縱橫線並に經緯度を計算す。

斯くしてA, B兩計算に依り求めたる經緯度を比較し各點の移動量並に移動方向を算出す其の結果は別表第二及附圖に示すが如し。

此外實用上の成果としては移動量少なく此れを不動と假定するも實際に於て支障なき一等三角點田君谷山、氷ノ山、笠形山、御岳山、比良ケ岳及野坂岳を不動として計算せる一等三角網の成果を與件として昭和三年度施行せる新觀測値を用ひ（精度の向上に資する爲め舊觀測に比し觀測方向を增加し或は平均方向を變換する等の手段を講ず）計算を復行せるものを以てせり。

四、精　　度

甲乙兩計算の結果に對する精度を比較せん爲め其の中等誤差を記すれば次の如し。

區　分		舊觀測	新觀測	摘要
平均計算の中等誤差	$m=\sqrt{\frac{[VV]}{q-r}}$	一^{秒}四二	○^{秒}七七	五十二點の中數
一點の坐標に對する平均誤差	$M=\sqrt{\mu_I^2+\mu_{II}^2}$	○.^{米}○七七	○.^{米}○四○	同

但し　V は方向改正數及與點よりの標定誤差を以てし

q は誤差方程式の數

r は未知數の總數とす

$\mu_I=\frac{m}{\sqrt{P_I}}$　　$\mu_{II}=\frac{m}{\sqrt{P_{II}}}$ より成り P は重量を示す

TABLE I.

別表第一（其ノ一）

等級	點名	所在地	舊觀測年
一等本點	磯砂山	京都府中郡五箇村大字五箇字磯砂山	明治二十一年
〃	多禰寺	〃　加佐郡西大浦村大字多禰寺	明治十九年
〃	烏ヶ岳	〃　何鹿郡佐賀村大字印內字大谷	明治二十一年
〃	氷ノ山	兵庫縣美方郡熊次村大字福定字四箇山	明治二十一年
〃	笠形山	〃　多可郡野間谷村大字大谷字笠形山	明治二十一年
〃	來日山	〃　城崎郡內川村大字來日字嶽	明治二十一年
〃	床之尾山	〃　出石郡合橋村大字畑字床之尾山	明治二十一年
〃	御岳山	〃　多紀郡畑村大字火打岩字畑山	明治十九年
一等補點	太皷山	京都府與謝郡野間村大字野中字住山	明治二十一年
〃	長老ヶ岳	〃　北桑田郡大野村大字三埜字西谷	明治十九年
〃	蘇武瀧山	兵庫縣美方郡村岡町大字村岡字空山	明治二十一年
〃	粟鹿山	〃　朝來郡粟鹿村字朝來山	明治二十二年
二等點	野村	京都府與謝郡筒川村大字野村	明治二十二年
〃	一ヶ尾	〃　竹野郡八木村大字矢畑字市ヶ尾	明治二十二年
〃	大原	〃　與謝郡朝妻村大字新井字蝙蝠	明治二十二年
〃	雄島	〃　加佐郡東大浦村大字野原字大島	明治二十二年
〃	下岡	〃　竹野郡網野町大字下岡字落合	明治二十二年
〃	湊	〃　熊野郡湊村大字湊宮字大谷小峠	明治二十二年
〃	吉澤	〃　竹野郡吉野村大字吉澤字經塚	明治二十二年
〃	皷ヶ岳	〃　與謝郡府中村大字成相寺小字皷ケダキ	明治二十二年
〃	女布	〃　熊野郡下佐濃村大字女布字女布谷	明治二十二年
〃	黑崎	〃　與謝郡栗田村大字田井字黑崎	明治二十二年
〃	三谷	〃　熊野郡久美谷村大字三谷字二又谷	明治二十二年
〃	三重村	〃　中郡三重村大字三重字水戸谷	明治二十二年
〃	大山	〃　加佐郡東大浦村大字大山字森ノ上	明治二十二年
〃	石川村	〃　與謝郡石川村字金割谷	明治二十二年
〃	由良ヶ谷	〃　加佐郡由良村大字由良字由良ヶ岳	明治二十二年
〃	加悅奧	〃　與謝郡加悅町大字加悅奧字後山	明治二十二年
〃	泉源寺	〃　加佐郡志樂村大字泉源寺字倉谷	明治二十二年
〃	餘內村	〃　〃　餘內村大字上安字暮谷	明治二十二年
〃	千丈ヶ岳	〃　〃　河守上村大字佛性寺字及ビ谷	明治二十二年
〃	岡田中村	〃　〃　岡田中村大字河原字內森	明治二十二年
〃	養老ヶ岳	〃　〃　與保呂村大字與保呂字大瀧	明治二十二年
〃	小佐	〃　養父郡八鹿町大字小佐字大谷	明治二十四年

(to be continued.)

TABLE I. (continued.)

別表第一（其ノ二）

等級	點名	所在地	舊觀測年
二等點	八部ヶ岳	京都府加佐郡河守上村大字二俣字向山	明治二十二年
〃	登尾峠	〃 天田郡三岳村大字上佐々木字長谷	明治二十二年
〃	久田美	〃 加佐郡岡田下村大字久田美字肥莇	明治二十二年
〃	睦寄	〃 何鹿郡奥上林村大字睦寄字君尾	明治二十二年
〃	直見	〃 天田郡上夜久野村大字直見字二又	明治二十二年
〃	東八田村	〃 何鹿郡東八田村大字於與岐字大谷川	明治二十二年
〃	上川口村	〃 天田郡上川口村大字上大內字西山	明治二十二年
〃	星原	〃 何鹿郡物部村大字白道路字高浪	明治二十二年
〃	釜輪	〃 〃 山家村大字釜輪字古峠	明治二十二年
〃	小田	〃 天田郡上川口村大字上小田字蛇ヶ谷	明治二十二年
〃	上川合	〃 〃 川合村大字上川合字稲葉	明治二十二年
〃	三峠山	〃 船井郡質美村字一ノ谷	明治二十二年
〃	細谷	〃 天田郡菟原村大字菟原下字細谷	明治二十二年
〃	鷲尾深山	〃 船井郡梅田村大字上大久保字南山	明治二十二年
〃	觀音山	兵庫縣城崎郡奥佐津村大字九斗字觀浦	明治二十四年
〃	九斗山	〃 〃 餘部村大字餘部字ライシ	明治二十四年
〃	本見塚	〃 〃 奥佐津村大字本見塚字小判谷	明治二十四年
〃	境	〃 〃 〃 大字三川字桑垣	明治二十四年
〃	資母村	〃 出石郡資母村大字高龍寺字土谷	明治二十二年
〃	八條村	〃 城崎郡八條村大字九日市上町字西光寺谷	明治二十二年
〃	大岡寺	〃 〃 八代村大字大岡字イゼノヲク	明治二十四年
〃	古寺	〃 出石郡出石町大字寺町字カゴ谷	明治二十二年
〃	伊佐村	〃 養父郡伊佐村大字淺間字堂ノ奥	明治二十二年
〃	奥米地	〃 〃 養父市場村大字奥米地字高地	明治二十二年
〃	廣谷	〃 〃 廣谷町大字十二所字新宮	明治二十四年
〃	下竹田	〃 氷上郡竹田村大字下竹田字西谷	明治二十二年
〃	尾ノ寺山	〃 〃 前山村大字上鴨阪字奥谷	明治二十二年
〃	妙高山	〃 〃 鴨庄村大字多利字妙高	明治二十二年
〃	東三松村	福井縣大飯郡青鄉村大字東三松字嶽山	明治二十一年
〃	納田終村	〃 遠敷郡奥名田村大字納田終	明治二十一年

別表第二（其の一） TABLE II.

	Station	Latitude and Longitude						Difference of Latitude and Longitude		Displacement		
		Recent			Earlier					Amount	Azimuth	
等級	點名	新經緯度			舊經緯度			新舊經緯度差		移動量	移動方位角	
		°	′	″	°	′	″	″	m	m	°	′
II	石川村 Isikawamura	35 135	30 9	24·9380 18·6518	35 135	30 9	24·9242 18·6680	+0·0138 −0·0162	+0·425 −0·408	0·589	316	10
〃	由良ヶ岳 Yuragadake		—			—		+0·0096 −0·0156	+0·296 −0·393	0·492	306	59
〃	加悦奥 Kayaoku	35 135	29 3	20·0849 10·5810	35 135	29 3	20·0852 10·5870	−0·0003 −0·0060	−0·009 −0·151	0·151	266	35
〃	泉源寺 Sengenzi		—			—		+0·0086 −0·0087	+0·265 −0·219	0·344	320	26
〃	古寺 Hurudera	35 134	28 53	24·6054 52·5552	35 134	28 53	24·6109 52·5526	−0·0055 +0·0026	−0·169 +0·066	0·182	158	40
〃	東三松村 Higasi-Mimatumura		—			—		+0·0079 −0·0014	+0·243 −0·035	0·245	351	48
〃	餘內村 Amautimura		—			—		+0·0044 −0·0096	+0·136 −0·242	0·278	299	20
〃	千丈ヶ岳 Sendyôgadake	35 135	27 6	1·0136 34·0160	35 135	27 6	1·0054 34·0232	+0·0082 −0·0072	+0·253 −0·182	0·312	324	16
〃	伊佐村 Izamura	35 134	26 48	51·7352 29·8102	35 134	26 48	51·7401 29·8094	−0·0049 +0·0008	−0·151 +0·020	0·152	172	27
〃	岡田中村 Okada-Nakamura		—			—		+0·0104 −0·0108	+0·320 −0·272	0·420	319	38
〃	養老ヶ岳 Yorôgadake		—			—		+0·0050 −0·0046	+0·154 −0·116	0·193	323	1
〃	小佐 Osa	35 134	25 43	12·0650 50·3092	35 134	25 43	12·0672 50·3092	−0·0022 0·0000	−0·068 0·000	0·068	180	0
〃	八部ヶ岳 Yabegadake	35 135	24 9	20·9115 47·4731	35 135	24 9	20·9012 47·4780	+0·0103 −0·0049	+0·317 −0·124	0·340	338	38
〃	登尾峠 Noboriotôge	35 135	23 1	58·0196 43·9493	35 135	23 1	58·0182 43·9542	+0·0014 −0·0049	+0·043 −0·124	0·131	289	8
〃	久田美 Kutami		—			—		+0·0068 −0·0040	+0·210 −0·101	0·233	334	19
〃	睦寄 Mutuyori		—			—		+0·0050 −0·0044	+0·154 −0·111	0·190	324	13
〃	納田終村 Notaoemura		—			—		+0·0086 0·0000	+0·265 0·000	0·265	0	0
〃	直見 Naomi	35 134	22 57	21·4937 29·6380	35 134	22 57	21·4925 29·6398	+0·0012 −0·0018	+0·037 −0·045	0·058	309	26
〃	奥米地 Okumêdi	35 134	22 50	20·8466 20·6904	35 134	22 50	20·8440 20·6924	+0·0026 −0·0020	+0·080 −0·050	0·094	328	0
〃	廣谷 Hirotani	35 134	22 45	18·8810 20·7631	35 134	22 45	18·8821 20·7591	−0·0011 +0·0040	−0·034 +0·101	0·107	108	36
〃	東八田村 Higasi-Hattamura		—			—		+0·0044 −0·0019	+0·136 −0·048	0·144	340	34

(to be continued.)

別表第二（其の二） TABLE II. (continued.)

	Station	Latitude and Longitude						Difference of Latitude and Longitude		Displacement		
		Recent			Earlier					Amount	Azimuth	
等級	點名	新經緯度			舊經緯度			新舊經緯度差		移動量	移動方位角	
		°	′	″	°	′	″	″	m	m	°	′
II	上川口村 Kami-Kagumura	35 135	20 4	35·0904 38·5990	35 135	20 4	35·0883 38·6052	+0·0021 −0·0062	+0·065 −0·157	0·170	292	29
〃	星原 Hosibara	—			—			+0·0041 −0·0026	+0·126 −0·066	0·142	332	21
〃	釜輪 Kamanowa	35 135	18 21	35·4158 12·9357	35 135	18 21	35·4142 12·9351	+0·0016 +0·0006	+0·049 +0·015	0·051	17	1
〃	小田 Oda	35 135	18 3	3·7886 12·2566	35 135	18 3	3·7874 12·2588	+0·0012 −0·0022	+0·037 −0·056	0·067	303	27
〃	上川合 Kami-Kawai	35 135	15 15	46·0629 55·0636	35 135	15 15	46·0616 55·0631	+0·0013 +0·0005	+0·040 +0·013	0·042	18	0
〃	下竹田 Simo-Takeda	35 135	15 7	27·1562 53·1231	35 135	15 7	27·1552 53·1268	+0·0010 −0·0037	+0·031 −0·094	0·099	288	15
〃	三峠山 Mitôgeyama	35 135	14 22	41·8826 10·2981	35 135	14 22	41·8805 10·2984	+0·0021 −0·0003	+0·065 −0·008	0·066	352	59
〃	尾ノ寺山 Onoderayama	35 135	13 4	11·7710 17·2474	35 135	13 4	11·7676 17·2450	+0·0034 +0·0024	+0·105 +0·061	0·121	30	9
〃	細谷 Hosodani	35 135	12 14	5·8436 26·2642	35 135	12 14	5·8391 26·2629	+0·0045 +0·0013	+0·139 +0·033	0·143	13	21
〃	妙高山 Myôkôzan	35 135	10 9	10·0864 49·1386	35 135	10 9	10·0832 49·1400	+0·0032 −0·0014	+0·099 −0·035	0·105	340	32
〃	鷲尾深山 Wasiomiyama	35 135	9 18	44·1784 34·2720	35 135	9 18	44·1730 34·2712	+0·0054 +0·0008	+0·166 +0·020	0·167	6	52
I	氷ノ山 Hyônoyama	不動と假定			35 134	21 30	2·8090 59·7128	—	—	—	—	
〃	笠形山 Kasagatayama	同上			35 134	3 50	39·4103 14·9468	—	—	—	—	
〃	來日山 Kurihizan	35 134	36 47	31·6706 17·6068	35 134	36 47	31·6770 17·6026	−0·0064 +0·0042	−0·197 +0·106	0·224	151	43
〃	磯砂山 Isanagosan	35 135	32 2	43·3244 27·2378	35 135	32 2	43·3401 27·2371	−0·0157 +0·0007	−0·484 +0·018	0·484	177	52
〃	多禰寺山 Taneziyama	—			—			+0·0084 −0·0081	+0·259 −0·204	0·330	321	46
〃	床ノ尾山 Tokonooyama	35 134	35 55	7·3644 7·1095	35 134	35 55	7·3646 7·1108	−0·0002 −0·0013	−0·006 −0·033	0·033	259	42
〃	烏ヶ岳 Karasugadake	35 135	19 9	52·0067 6·2257	35 135	19 9	52·0012 6·2292	+0·0055 −0·0035	+0·169 +0·088	0·190	332	30
〃	御岳山 Mitakesan	35 135	7 14	26·5968 51·7299	35 135	7 14	26·5936 51·7310	+0·0032 −0·0011	+0·099 −0·028	0·103	344	12
〃	太皷山 Taikoyama	—			—			+0·0110 −0·0188	+0·339 −0·473	0·582	305	38
〃	蘇武瀧山 Sobutakiyama	35 134	28 38	3·4530 26·5964	35 134	28 38	3·4520 26·5933	+0·0010 +0·0031	+0·031 +0·078	0·084	68	20
〃	長老ヶ岳 Tyôrôgadake	35 135	18 28	0·1832 36·5188	35 135	18 28	0·1826 36·5204	+0·0006 −0·0016	+0·018 −0·040	0·044	294	14

(to be continued.)

別表第二(其の三) TABLE II. (continued.)

	Station	Latitude and Longitude						Difference of Latitude and Longitude		Displacement		
		Recent			Earlier					Amount	Azimuth	
等級	點名	新經緯度			舊經緯度			新舊經緯度差		移動量	移動方位角	
		°	′	″	°	′	″	″	m	m	°	′
I	粟鹿山 Awagayama	35 134	16 55	10·5388 5·5344	35 134	16 55	10·5364 5·5358	+0·0024 −0·0014	+0·074 −0·035	0·082	334	41
II	野村 Nomura	—			—			+0·0122 −0·0172	+0·376 −0·432	0·573	311	2
〃	一ケ尾 Itigao	—			—			+0·0203 −0·0346	+0·626 −0·869	1·071	305	46
〃	大原 Oohara	—			—			+0·0106 −0·0234	+0·327 −0·588	0·673	299	5
〃	雄島 Osima	—			—			+0·0131 −0·0114	+0·404 −0·287	0·496	324	37
〃	下岡 Simooka	—			—			−0·0366 +0·0211	−1·128 +0·531	1·247	154	48
〃	觀音山 Kwannonzan	35 134	38 40	21·6898 37·3823	35 134	38 40	21·6920 37·3832	−0·0022 −0·0009	−0·068 −0·023	0·072	198	41
〃	湊 Minato	35 134	37 52	44·2630 23·9285	35 134	37 52	44·2748 23·9254	−0·0118 +0·0031	−0·364 +0·078	0·372	167	54
〃	吉澤 Yoshizawa	35 135	37 6	44·0865 30·3238	35 135	37 6	44·0604 30·3534	+0·0261 −0·0296	+0·804 −0·745	1·096	317	11
〃	九斗山 Kutoyama	35 134	36 34	56·9911 27·6402	35 134	36 34	56·9926 27·6334	−0·0015 +0·0068	−0·046 +0·171	0·177	105	3
〃	皷ケ岳 Tutumigadake	35 135	36 11	11·9554 2·4762	35 135	36 11	11·9384 2·4970	+0·0170 −0·0208	+0·524 −0·524	0·741	315	0
〃	女布 Nyoô	35 134	36 58	10·7704 38·6756	35 134	36 58	10·7966 38·6784	−0·0262 −0·0028	−0·807 −0·070	0·810	184	57
〃	本見塚 Motomiduka	35 134	35 42	41·8638 32·3326	35 134	35 42	41·8687 32·3359	−0·0049 −0·0033	−0·151 −0·083	0·172	208	48
〃	黑崎 Kurosaki	—			—			+0·0158 −0·0221	+0·487 −0·556	0·739	311	13
〃	境 Sakai	35 134	33 38	36·2798 5·2578	35 134	33 38	36·2768 5·2644	+0·0030 −0·0086	+0·092 −0·217	0·236	292	59
〃	三谷 Mitani	35 134	33 54	30·8114 8·0916	35 134	33 54	30·8214 8·0866	−0·0100 +0·0050	−0·308 +0·126	0·333	157	45
〃	三重村 Miemura	35 135	33 7	8·2760 48·9568	35 135	33 7	8·2462 48·9522	+0·0298 +0·0046	+0·918 +0·116	0·925	7	12
〃	大山 Ooyama	—			—			+0·0079 −0·0055	+0·243 −0·139	0·280	330	14
〃	資母村 Sibomura	35 134	31 58	11·3047 25·9332	35 134	31 58	11·3106 25·9326	−0·0059 +0·0006	−0·182 +0·015	0·183	175	17
〃	八條村 Hatidyômura	35 134	31 48	8·7138 52·6261	35 134	31 48	8·7218 52·6260	−0·0080 +0·0001	−0·247 +0·003	0·247	179	18
〃	大岡寺 Ôokadera	35 134	30 43	30·7063 1·5890	35 134	30 43	30·7153 1·5944	−0·0090 −0·0054	−0·277 −0·136	0·309	206	9

20. *Revision of the Secondary Trigonometrical Survey in the Tango District.*

Land Survey Department, I. J. A.

(Publ. May, 1929.)

The result of revision of the primary trigonometrical survey in Tango and the other districts was already published in Vol. VII, part 1 of this Bulletin. The results of the survey which was carried out later with respect to the secondary trigonometrical points are now given in the Tables and the annexed Plate.

The assumption regarding the two fixed stations is the same as in the previous case.

The probable errors of the results of calculations are as follows:

	Earlier Survey	Recent Survey
$m=\sqrt{\frac{[vv]}{q-r}}$	1·″42	0·″77
$M=\sqrt{\mu_I^2+\mu_{II}^2}$	0·077m	0·040m

where v is the residual, q the number of equations, r the number of unknown quantities and

$$\mu_I=\frac{m}{\sqrt{P_I}} \qquad \mu_{II}=\frac{m}{\sqrt{P_{II}}},$$

P's being the weights.

[Land Survey Dept.]

Map Showing the Horizontal Displacements of the Se

丹後震災地一二等

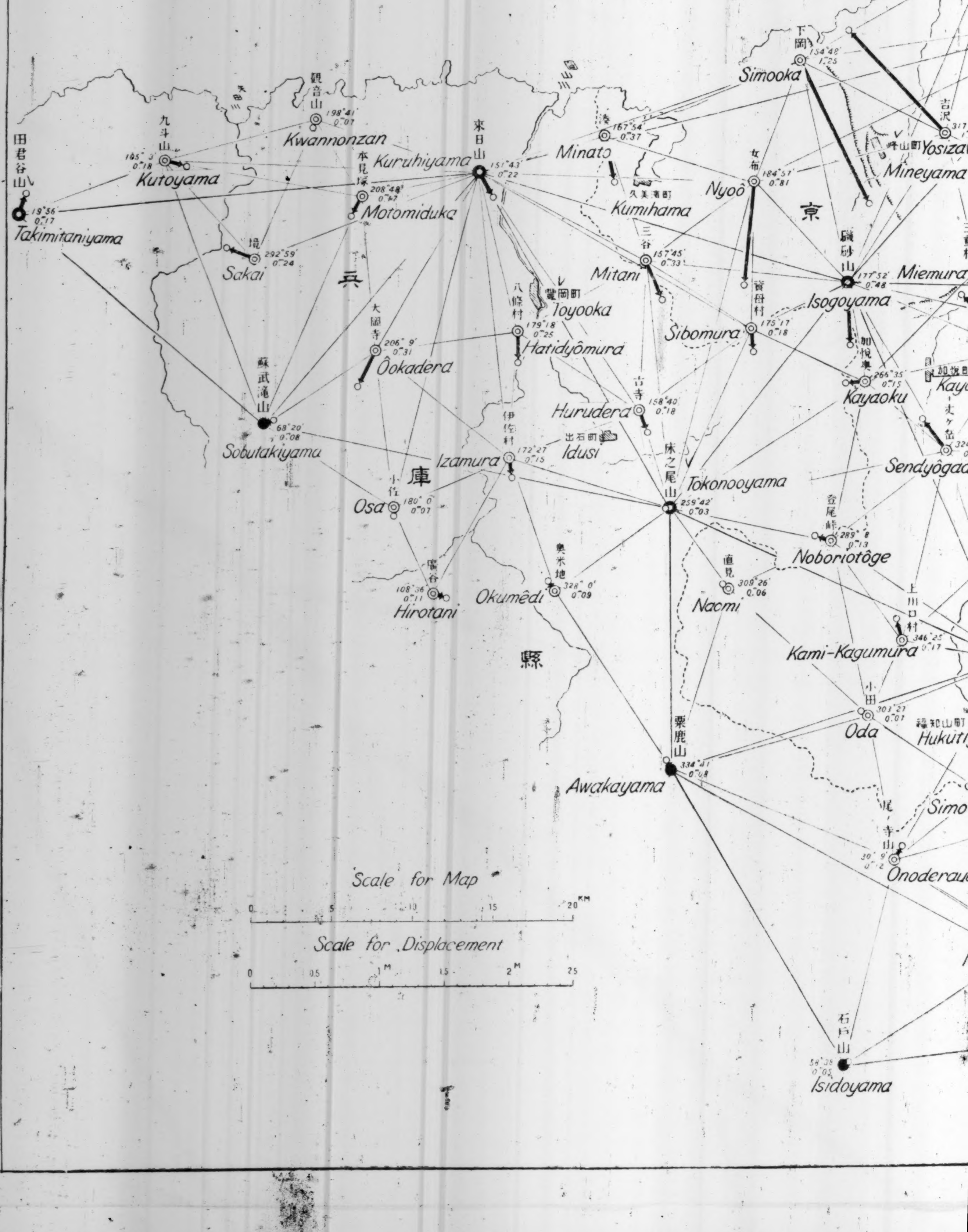
田君谷山
Takimitaniyama
19°56'
0.17
九斗山
Kutoyama
165°3'
0.18
観音山
Kwannonzan
198°41'
0.07
本見塚
Motomiduka
208°48'
0.47
来日山
Kuruhiyama
151°43'
0.22
境
Sakai
292°59'
0.24
兵
庫
縣
大岡寺
Ôokadera
206°9'
0.31
蘇武滝山
Sobutakiyama
68°20'
0.08
伊佐村
Izamura
172°27'
0.15
小佐
Osa
180°0'
0.07
廣谷
Hirotani
108°36'
0.11
奥米地
Okumêdi
328°0'
0.09
八條村
Hatidyômura
179°18'
0.25
豊岡町
Toyooka
出石町
Idusi
湊
Minato
167°54'
0.37
久美濱町
Kumihama
三谷
Mitani
157°45'
0.33
古寺
Hurudera
158°40'
0.18
床之尾山
Tokonooyama
259°42'
0.03
粟鹿山
Awakayama
334°41'
0.08
直見
Nacmi
309°26'
0.06
下岡
Simooka
154°48'
1.25
女布
Nyoô
184°51'
0.81
資母村
Sibomura
175°17'
0.18
磯砂山
Isogoyama
177°52'
0.48
京
加悦奥
Kayaoku
266°35'
0.15
登尾峠
Noboriotôge
289°8'
0.13
上川口村
Kami-Kagumura
346°25'
0.17
小田
Oda
301°21'
0.07
福知山町
Hukuti
Simo
尾寺山
Onoderau
30°9'
0.12
石戸山
Isidoyama
58°35'
0.05
Sendyôgad
加悦町
Kayo
丈ケ岳
Miemura
吉沢
Yosiza
峰山町
Mineyama
Scale for Map
0 5 10 15 20 KM
Scale for Displacement
0 0.5 1M 1.5 2M 2.5

（震研彙報第七號、圖版、陸地測量部）

Secondary Triangulation Points in Tango Districts.

等三角點移動要圖

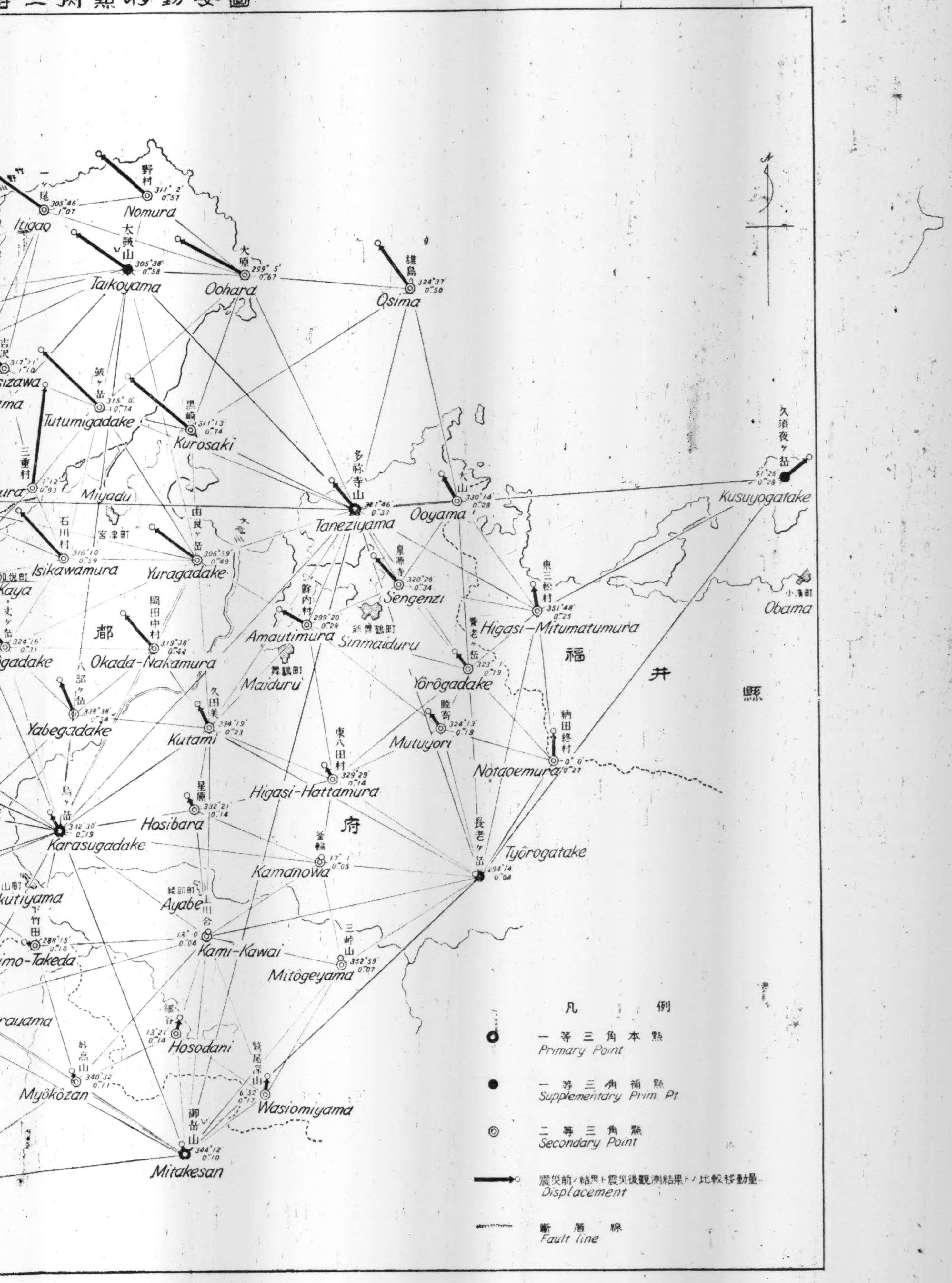
野村 311° 2' 0".57 Nomura
一ヶ尾 305°46' 1".07 Itigao
大皷山 305°38' 0".58 Taikoyama
大原 299° 5' 0".67 Oohara
雄島 324°37' 0".50 Osima
吉沢 317°11' 1".10 sizawa
ma
皷ヶ岳 315° 0' 0".74 Tutumigadake
黒崎 311°13' 0".74 Kurosaki
三重村 7°12' 0".93 ura
Miyadu
多禰寺山 321°46' 0".33 Taneziyama
大山 330°14' 0".28 Ooyama
久須夜ヶ岳 51°26' 0".28 Kusuyogatake
石川村 316°10' 0".59 Isikawamura
宮津町
由良ヶ岳 306°59' 0".49 Yuragadake
大雲川
泉源寺 320°26' 0".34 Sengenzi
東三松村 351°48' 0".25 Higasi-Mitumatumura
小濱町 Obama
加悦町 Kaya
丈ヶ岳 324°16' 0".31 gadake
岡田中村 319°38' 0".42 Okada-Nakamura
郡
餘内村 299°20' 0".28 Amautimura
新舞鶴町 Sinmaiduru
舞鶴町 Maiduru
養老ヶ岳 323° 1' 0".19 Yôrôgadake
福
井
縣
八部ヶ岳 338°38' 0".34 Yabegadake
久田美 334°19' 0".23 Kutami
睦寄 324°13' 0".19 Mutuyori
納田終村 0° 0' 0".21 Notaoemura
東八田村 329°29' 0".14 Higasi-Hattamura
星原 332°21' 0".14 Hosibara
烏ヶ岳 312°30' 0".19 Karasugadake
府
釜輪 17° 1' 0".05 Kamanowa
長老ヶ岳 294°14' 0".04 Tyôrogatake
山町 kutiyama
綾部町 Ayabe
上川合 18° 0' 0".04 Kami-Kawai
下竹田 288°15' 0".10 imo-Takeda
三峠山 352°59' 0".07 Mitogeyama
rauama
細谷 13°21' 0".14 Hosodani
妙高山 340°32' 0".11 Myôkôzan
鷲尾宮山 6°52' 0".17 Wasiomiyama
御岳山 344°12' 0".10 Mitakesan
N
凡例
一等三角本點 Primary Point
一等三角補點 Supplementary Prim. Pt
二等三角點 Secondary Point
震災前ノ結果ト震災後觀測結果トノ比較移動量 Displacement
斷層線 Fault line

——所　報——

○ 談話會記事

第四十回談話會（昭和四年七月九日）

1. 地殼カラ地殼ノ移動從テ地殼ニ働ク歪力ヲ判斷スルコトノ可能ニ就テ	所員 所員	藤原咲平 高山威雄
1. 紅海附近ノ構造	所員	藤原咲平
1. 地殼ノ長時期ニ亙ル變動ト地軸ノ移動	所員	長岡半太郎
1. 筑波山ニ於ケル土地ノ傾斜觀測報告	所員	井上宇胤 杉山友紀
1. 駒ケ岳調査概要報告		
内容		
1. 噴火ノ經過	所員	多田文男
1. 火口ノ狀態	所員	津屋弘逵
1. 空中電氣及地電流	理學士	中田金市
1. 微動計ニヨル觀測	所員	岸上冬彦
1. 水準測量及重力偏差計ニヨル觀測	所員	坪井忠二
1. 傾斜計ニヨル觀測	所員	高橋龍太郎

○ 出　張

昭和四年七月十五日傾斜計撤去ノタメ京都府下峰山町ヘ出張ノ序ヲ以テ同府下宮津町及河邊村ヘ出張	理學士	波江野清藏
昭和四年七月十七日噴火事項調査ノタメ北海道ヘ出張	所員	宮部直巳
昭和四年七月二十二日噴火事項調査ノタメ北海道札幌市ヨリ同道茅部郡ヘ出張	所員	石本巳四雄
昭和四年七月廿七日地震事項調査ノタメ神奈川縣下ヘ出張	所員	津屋弘逵
昭和四年七月廿七日地震事項調査ノタメ神奈川縣下ヘ出張	囑託	那須信治
昭和四年七月廿八日噴火事項調査ノタメ北海道札幌ヘ出張ノ序ヲ以テ同道茅部郡ヘ出張	所員	坪井誠太郎
昭和四年七月卅日時報受信器修理ノタメ神奈川縣下ヘ出張	理學士	波江野清藏
昭和四年八月六日行幸ニ付打合ノタメ神奈川縣下ヘ出張	所員	石本巳四雄
昭和四年八月十五日行幸ニ付準備ノタメ神奈川縣下ヘ出張	所員	石本巳四雄

昭和四年八月十九日地震事項調査ノタメ神奈川縣下へ出張	所員 津屋弘逵
昭和四年八月十九日地震事項調査ノタメ神奈川縣下へ出張	囑託 那須信治

昭和四年九月二十八日印刷
昭和四年九月三十日發行

編纂兼發行者　東京帝國大學地震研究所

東京市神田區美土代町二丁目一番地
印刷者　島連太郎

東京市神田區美土代町二丁目一番地
印刷所　三秀舍

東京市神田區南神保町十六番地
賣捌所　岩波書店

BULLETIN OF

THE EARTHQUAKE RESEARCH INSTITUTE

TOKYO IMPERIAL UNIVERSITY.

Vol. VII, Part 2. September, 1929.

Contents.

Papers and Reports.

Page

13. K. Sezawa, Periodic Rayleigh-waves caused by an Arbitrary Disturbance. (in English) 193

14. T. Terada, On the Form of Volcanos. (in English) 207

15. T. Terada and N. Miyabe, Deformation of the Earth Crust in Kwansai Districts and its Relation to the Orographic Feature. (in English) 223

16. T. Matuzawa, K. Yamada and T. Suzuki, On the Forerunners of Earthquake-motions (The Second Paper). (in English) 241

17. N. Miyabe, Die Schwankungen der Makroseismischen Tätigkeitszonen um den Pazifischen Ozean. (in deutsch) 261

18. H. Tsuya, Volcanoes of Kôzu-shima. (in English) 269

19. M. Ichiki, Volcano Kayagatake. (in English) 335

20. Land Survey Department, Revision of the Secondary Trigonometrical Survey in the Tango District. (in Japanese) 381

Institute Notes.

(For the papers written in Japanese or in occidental languages, the abstracts are given in occidental languages or in Japanese respectively.)

BULLETIN OF THE EARTHQUAKE RESEARCH INSTITUTE,
TOKYO IMPERIAL UNIVERSITY. Vol. VII, Part 3. December, 1929.

東京帝國大學
地震研究所彙報

第七號　第三册

昭和四年十二月

目次

論文及報告

頁
21. 固體のダイレテーションとロテーションとに無關係な變位に就いて（英文）……妹澤克惟・西村源六郎 389
22. 內部の層原によるレーレー波の生成（英文）……妹澤克惟 417
23. 球面上に於けるラブ波の傳播とこれに關聯する一二の問題（英文）……妹澤克惟 437
24. 重力ポテンシヤルの空間二次微分係數の時間的變動に就いて（英文）……坪井忠二 457
25. 振動分解器による地震の性質の研究（英文）……末廣恭二 467
26. 水成岩層の地震波傳播に及ぼす影響（邦文）……今村明恒・岸上冬彦・小平孝雄 471
27. 地震波によりて誘起せられたる土地の固有振動に就いて（邦文）……今村明恒 489
28. 關東地方改測水準測量結果に就ての研究（邦文）……武藤勝彦・熱海景良 495
29. 地形から地殼の移動從て地殼に働く歪力を判斷することの可能度に就いて（邦文）……藤原咲平・高山威雄 523
30. 川の流路の變遷によつて知り得たる伊賀國島ヶ原地塊の運動（邦文）……多田文男 531
31. 昭和四年一月二日の日本海海水面の異常（邦文）……山口生知 555
32. 自動車、汽車の振動測定を目的とする加速度計（第一部、水平動測定）（邦文）……石本巳四雄・高橋龍太郎 571
33. 丹後震災地一等水準測量第三回及第四回檢測成果比較要圖……陸地測量部 587

所報

(The titles in occidental languages are given on the back cover.)

本彙報ハ年四回發行ス. 但シ本號ニ限リ三冊ノミトス. （第一號ヨリ第六號マデハ不定期ニ發行セリ.）

本彙報掲載ノ論文及ビ報告ノ內容ニ關シテハ著者ノミニ其責任アルモノトス.

本彙報ニ關スル照會通信ハ東京帝國大學地震研究所長ヘ宛テラレタシ.

The bulletin is published quarterly, excepting this volume which consists of three parts. (Vols. I–VI were published at irregular intervals.)

The authors of the papers alone are responsible for the statements and opinions contained in their respective papers.

All communications relating to this bulletin should be addressed to the Director of the Earthquake Research Institute, Tokyo Imperial University.

21. *The Displacement independent of the Dilatation and the Rotation in a Solid Body.*

By **Katsutada SEZAWA** and **Genrokuro NISHIMURA**,

Earthquake Research Institute.

(Received Sept. 20, 1929.)

1. Very recently Professor Terada and Dr. Miyabe[1] pointed out that the deformation of the earth crust can be composed of the dilatation, the rotation and the shear. As they dealt with the actual problem of the earth crust and they seem to have given no definite specification on the nature of the solid body, whether the body is elastic or plastic, we cannot give any authentic discussion on the above problem. Even though the body may be assumed to be plastic in the sense of St. Venant[2] and Th. v. Kármán,[3] yet the natures of the dilatation, the rotation and others, we think, are not essentially different from those in the case of the elastic deformation. Leaving the problem of the difference between the elasticity and the plasticity, besides the discussion on the plastic deformation, for the present, we shall first consider the deformation of the elastic body.

It is of recent time[4] that the dilatation, rotation, and other components in elastic solid bodies are theoretically analysed with the view of arriving at the complete solutions of the mathematical equations of the equilibrium of the bodies. This problem has attracted very little attention of the investigators probably because of the existence of the other methods of solving the equations without such an analytical consideration.

According to our analytical investigation, the idea of expressing the deformation of a solid body by means of the dilatation, the rotation and the shear is not completely theoretical. The idea of expressing the displacement by means of the components of the dilatation, the rotation and the shear is due to Stokes and others. This idea seems to represent the method of expressing the infinitesimal displacement of a material point, but not involve any view on the essential nature of the deformable body, such as the consideration of the total dilatation. Thus the thought of taking the dilatation, the rotation and the shear in the analysis of a body seems to be violent. Our investigation shews that the deformation of a solid body should be composed of the dilatation, the rotation and another component which is neither dilatational nor rotational. The last of these is not such a meaningless component as to give the bodily movement to the solid; but it plays its important *role* in giving the strain or the stress to the solid both in normal and tangential directions. It has also been cleared that the dilatation and the rotation are by no means of different types. The component of the displacement which gives the dilatation is of the same form as that which gives the rotation; the ratio of the magnitudes of both components is invariable when the elasticities of the material and the type of the solution are specified. These will be seen presently at th part of th mathmatical investigation. The proposed fact[5] that the deformation of the land surface involves the rotational component is also self-evident.

---

[1] T. TERADA & N. MIYABE, 39th Colloq. Meeting of the Institute (June 18, 1929). The paper will perhaps appear in *Bull. Earthq. Res. Inst.*, 7 (1929) Part 2, which is now going to be published.

[2] ST. VENANT, C. R. (1868–1872).

[3] HAAR U. TH. V. KÁRMÁN, *Enc. d. Math. Wiss.*, 4 (1914).

[4] K. SEZAWA & B. MIYAZAKI. *Journ. Soc. Mech. Eng., Tokyo*, 31 (1928), 625–634.
K. SEZAWA & G. NISHIMURA, *Bull. Earthq. Res. Inst.*, 6 (1929), 47–62.
G. NISHIMURA, *Journ. Soc. Ord.-Expl.*, 23 (1929).

I. The Problems of a Spherical Heterogeneity in a Stressed Body.[6]

2. The equations of motion of elastic bodies in spherical coordinates, where the azimuthal component of the motion is omitted, are expressed by

$$(\lambda+2\mu)\frac{\partial \Delta}{\partial r}-\frac{2\mu}{r}\frac{\partial \varpi}{\partial \theta}-\frac{2\mu}{r}\varpi\cot\theta=0, \quad \ldots\ldots\ldots\ldots\ldots\ldots (1)$$

$$\frac{\lambda+2\mu}{r}\frac{\partial \Delta}{\partial \theta}+2\mu\frac{\partial \varpi}{\partial r}+2\mu\frac{\varpi}{r}=0 \quad \ldots\ldots\ldots\ldots\ldots\ldots (2)$$

where u, v are radial and colatitudinal components of displacement, and

$$\Delta=\frac{\partial u}{\partial r}+\frac{2u}{r}-\frac{1}{r}\frac{\partial v}{\partial \theta}+\frac{v}{r}\cot\theta, \quad \ldots\ldots\ldots\ldots\ldots\ldots (3)$$

$$2\varpi=\frac{\partial v}{\partial r}+\frac{v}{r}-\frac{1}{r}\frac{\partial u}{\partial \theta}. \quad \ldots\ldots\ldots\ldots\ldots\ldots (4)$$

Eliminating u and v in (1), (2) by means of (3) and (4), we get

$$\frac{\partial^2 \Delta}{\partial r^2}+\frac{2}{r}\frac{\partial \Delta}{\partial r}+\frac{1}{r^2}\frac{\partial^2 \Delta}{\partial \theta^2}+\frac{1}{r^2}\frac{\partial \Delta}{\partial \theta}\cot\theta=0, \quad \ldots\ldots\ldots\ldots (5)$$

---

[5] S. FUJIWHARA & T. TAKAYAMA, *Bull. Earthq. Res. Inst.*, **6** (1929), 174.

[6] K. SEZAWA & MIYAZAKI, *loc. cit.*, 389.

$$\frac{\partial^2 \varpi}{\partial r^2}+\frac{2}{r}\frac{\partial \varpi}{\partial r}+\frac{1}{r^2}\frac{\partial^2 \varpi}{\partial \theta^2}+\frac{1}{r^2}\frac{\partial \varpi}{\partial \theta}\cot\theta-\frac{\varpi}{r^2}(1+\cot^2\theta)=0. \;\ldots\ldots (6)$$

Solving (5) and (6), we obtain

$$\left.\begin{aligned} \Delta &= \left(A_n r^n+\frac{B_n}{r^{n+1}}\right)P_n(\cos\theta), \;\ldots\ldots (7) \\ 2\varpi &= \left(A_n' r^n+\frac{B_n'}{r^{n+1}}\right)\frac{dP_n(\cos\theta)}{d\theta} \;\ldots\ldots (8) \end{aligned}\right\}[n=0,\,1,\,2,\ldots]$$

Displacement (u_1, v_1) answering to Δ in (7) and satisfying $\varpi=0$ in (8) is denoted by

$$\left.\begin{aligned} u_1 &= \left[\frac{A_n(n+2)}{2(2n+3)}r^{n+1}+\frac{B_n(n-1)}{2(2n-1)r^n}\right]P_n(\cos\theta), \\ v_1 &= \left[\frac{A_n}{2(2n+3)}r^{n+1}-\frac{B_n}{2(2n-1)r^n}\right]\frac{dP_n(\cos\theta)}{d\theta}, \end{aligned}\right\}\ldots\ldots\ldots\ldots (9)$$

in which $n=0, 1, 2, \ldots$ for A_n and $n=1, 2, 3, \ldots$ for B_n.

Displacement (u_2, v_2) derived from the value of ϖ in (8) under the condition, $\Delta=0$, is expressed by

$$\left.\begin{aligned} u_2 &= \left[\frac{A_n' n(n+1)}{2(2n+3)}r^{n+1}-B_n'\frac{n(n+1)}{2(2n-1)r^n}\right]P_n(\cos\theta), \\ v_2 &= \left[\frac{A_n'(n+2)}{2(2n+3)}r^{n+1}+\frac{B_n'(n-2)}{2(2n-1)r^n}\right]\frac{dP_n(\cos\theta)}{d\theta}. \end{aligned}\right\}[n=1,2,\ldots]\ldots (10)$$

Displacement (u_3, v_3) which satisfies $\Delta=0$, $\varpi=0$ is expressed by

$$\left.\begin{aligned} u_3 &= \left[A_n'' n r^{n-1}-\frac{B_n''(n+1)}{r^{n+2}}\right]P_n(\cos\theta), \\ v_3 &= \left[A_n'' r^{n-1}+\frac{B_n''}{r^{n+2}}\right]\frac{dP_n(\cos\theta)}{d\theta}. \end{aligned}\right\}[n=0,\,1,\,2,\ldots]\ldots\ldots (11)$$

Now A_n and A_n' or B_n and B_n' are not independent. When we refer to the equation (1) or (2), we find that there is a fixed relation between A_n and A_n' or between B_n and B_n', the relation being expressed by

$$A_n'=-\frac{\lambda+2\mu}{\mu(n+1)}A_n; \qquad B_n'=\frac{\lambda+2\mu}{\mu n}B_n. \;\ldots\ldots\ldots\ldots (12)$$

From the above treatment, it will be seen that there are two kinds of constants, one of which corresponds to (A_n, A_n') or (B_n, B_n') and the other to A_n'' or B_n''. The practical examples can be solved definitely by these two kinds of the arbitrary constants. It will also be remarked that the form of the displacement (u_1, v_1) and that of (u_2, v_2) are completely of the same types, while that of (u_3, v_3) is of a different type. We may thus conclude that the first of two kinds of displacements gives the dilatation as well as the rotation, the proportion of the dilatational displacement to the rotational one being determined by the elastic constants and the order of the harmonics of the straining; while the second kind gives only the displacement which is neither dilatational nor rotational. Thus the decomposition of the actual deformation into the dilatation and the rotation is only significant in the sense that we may determine what order of the harmonics of the straining is prevalent in this deformation. The straining, however, corresponding to (u_3, v_3) is to be let behind in this case. It will not be useless to tabulate the principal natures thus obtained in the forms:

Kind of displacement	Types of solutions	Physical meaning	Arbitrary constants	
1st kind	$r^{n+1}\times\ldots,\ \frac{1}{r^n}\times\ldots,$	dilatation	$A_n,\quad B_n$	$A_n'=\frac{-(\lambda+2\mu)}{\mu(n+1)}A_n,$ $B_n'=\frac{(\lambda+2\mu)}{\mu n}B_n$
		rotation	$A_n',\quad B_n'$	
2nd kind	$r^{n-1}\times\ldots,\ \frac{1}{r^{n+2}}\times\ldots,$	indil. and irrot.	$A_n'',\ B_n''$	

3. We will now shew an example applied to a practical problem of the equilibrium of a solid body. Let us suppose that an elastic solid body has a spherical cavity of the radius a and the body is subjected to an uniform tension T or compression T, then the boundary conditions are expressed by

$$\widehat{rr}=0, \qquad \widehat{r\theta}=0 \qquad \text{on } r=a, \tag{13}$$

$$\widehat{rr}=T\cos^2\theta, \qquad \widehat{\theta\theta}=T\sin^2\theta \qquad \text{at } r=\infty. \tag{14}$$

By applying the general solutions in (9), (10), (11), we get the distribution of the stress components in all the point of the body as in the following forms:

$$\left.\begin{aligned}
\widehat{rr}&=T\left[\frac{1}{3}\left(1-\frac{a^3}{r^3}\right)+\left\{\frac{2}{3}-\frac{10(9\lambda+10\mu)}{3(9\lambda+14\mu)}\frac{a^3}{r^3}+\frac{24(\lambda+\mu)}{(9\lambda+14\mu)}\frac{a^5}{r^5}\right\}P_2(\cos\theta)\right],\\
\widehat{\theta\theta}&=T\left[\left\{\frac{2}{3}+\frac{(9\lambda+34\mu)}{6(9\lambda+14\mu)}\frac{a^3}{r^3}+\frac{2(\lambda+\mu)}{(9\lambda+14\mu)}\frac{a^5}{r^5}\right\}\right.\\
&\qquad\left.-\left\{\frac{2}{3}-\frac{10\mu}{3(9\lambda+14\mu)}\frac{a^3}{r^3}+\frac{14(\lambda+\mu)}{(9\lambda+14\mu)}\frac{a^5}{r^5}\right\}P_2(\cos\theta)\right],
\end{aligned}\right\} \tag{15}$$

$$\left.\begin{aligned}\widehat{\phi\phi}&=T\left[\left\{\frac{3\lambda-2\mu}{2\,(9\lambda+14\mu)}\frac{a^3}{r^3}-\frac{2\,(\lambda+\mu)}{(9\lambda+14\mu)}\frac{a^5}{r^5}\right\}\right.\\&\qquad\left.+\left\{\frac{10\mu}{(9\lambda+14\mu)}\frac{a^3}{r^3}-\frac{10\,(\lambda+\mu)}{(9\lambda+14\mu)}\frac{a^5}{r^5}\right\}P_2\,(\cos\theta)\right],\\\widehat{r\theta}&=T\left\{\frac{1}{3}+\frac{(15\lambda+10\mu)}{3\,(9\lambda+14\mu)}\frac{a^3}{r^3}-\frac{8\,(\lambda+\mu)}{(9\lambda+14\mu)}\frac{a^5}{r^5}\right\}\frac{dP_2(\cos\theta)}{d\theta}.\end{aligned}\right\}$$

At the point $r=a,\ \theta=\pi/2$, we have

$$\widehat{\theta\theta}=\frac{39\lambda+54\mu}{2\,(9\lambda+14\mu)}T,\qquad\ldots\ldots\ldots\ldots\ldots\ldots\ldots\ldots(16)$$

and, if $\lambda=\mu$, this becomes

$$\widehat{\theta\theta}=2.02T\,;\qquad\ldots\ldots\ldots\ldots\ldots\ldots\ldots\ldots(17)$$

while, if $\lambda=\infty$, $\widehat{\theta\theta}$ takes the value

$$\widehat{\theta\theta}=2.17T.\qquad\ldots\ldots\ldots\ldots\ldots\ldots\ldots\ldots(18)$$

This shews that, when there is a spherical cavity in a solid body, the stress $\widehat{\theta\theta}$ at the boundary of the cavity is about twice the magnitude of the applied traction. As to the maximum shear stress, the induction of such high stress at some portion of the solid due to the cavity is also easily calculated. Though this solutions have been obtained by one of us, the similar results obtained by other methods are frequently used in the discussion of the failure of bodies due to the statical loads and alternating stresses.

4. We may take another example for the confirmation of the applicability of the present problem. Suppose that the elastic body, which is stressed in one direction, has an imbedded spherical grain in itself. Then, taking the external and internal solutions, we get finally, when $r<a$,

$$\left.\begin{aligned}\widehat{rr}'&=T\left[\frac{(\lambda+2\mu)}{(3\lambda+2\mu)}\frac{(3\lambda'+2\mu')}{(3\lambda'+2\mu'+4\mu)}+4\mu'\frac{D_1}{D}P_2(\cos\theta)\right],\\\widehat{\theta\theta}'&=T\left[\frac{(\lambda+2\mu)}{(3\lambda+2\mu)}\frac{(3\lambda'+2\mu')}{(3\lambda'+2\mu'+4\mu)}+2\mu\frac{D_1}{D}-4\mu'\frac{D_1}{D}P_2(\cos\theta)\right],\\\widehat{\phi\phi}'&=T\left[\frac{(\lambda+2\mu)}{(3\lambda+2\mu)}\frac{(3\lambda'+2\mu')}{(3\lambda'+2\mu'+4\mu)}+2\mu'\frac{D_1}{D}\right],\\\widehat{r\theta}'&=T\left[2\mu'\frac{D_1}{D}\frac{dP_2(\cos\theta)}{d\theta}\right].\end{aligned}\right\}\ldots(19)$$

and when $r>a$,

$$\left.\begin{aligned}
\widehat{rr}&=T\left[\frac{1}{3}+\frac{4\mu}{3\lambda+2\mu}\,\frac{3(\lambda'-\lambda)+2(\mu'-\mu)}{9\lambda'+6\mu'+12\mu}\,\frac{a^3}{r^3}\right.\\
&\qquad\left.+\left(\frac{2}{3}+\frac{9\lambda+10\mu}{3}\,\frac{D_2}{D}\,\frac{a^3}{r^3}+24\mu\frac{D_3}{D}\,\frac{a^5}{r^5}\right)P_2(\cos\theta)\right],\\
\widehat{\theta\theta}&=T\left[\frac{2}{3}-\left(\frac{2\mu}{3\lambda+2\mu}\,\frac{3(\lambda'-\lambda)+2(\mu'-\mu)}{9\lambda'+6\mu'+12\mu}+\frac{\mu}{3}\,\frac{D_2}{D}\right)\frac{a^3}{r^3}\right.\\
&\qquad\left.+2\mu\frac{D_3}{D}\,\frac{a^5}{r^5}-\left(\frac{2}{3}+\frac{\mu}{3}\,\frac{D_2}{D}\,\frac{a^3}{r^3}+14\mu\frac{D_3}{D}\,\frac{a^5}{r^5}\right)P_2(\cos\theta)\right],\\
\widehat{\phi\phi}&=T\left[\left(\frac{\mu}{3}\,\frac{D_2}{D}-\frac{2\mu}{3\lambda+2\mu}\,\frac{3(\lambda'-\lambda)+2(\mu'-\mu)}{9\lambda'+6\mu'+12\mu}\right)\frac{a^3}{r^3}\right.\\
&\qquad\left.-2\mu\frac{D_3}{D}\,\frac{a^5}{r^5}-\left(\mu\frac{D_2}{D}\,\frac{a^3}{r^3}+10\mu\frac{D_3}{D}\,\frac{a^5}{r^5}\right)P_2(\cos\theta)\right],\\
\widehat{r\theta}&=T\left[\left(\frac{1}{3}-\frac{3\lambda+2\mu}{6}\,\frac{D_2}{D}\,\frac{a^3}{r^3}-8\mu\frac{D_3}{D}\,\frac{a^5}{r^5}\right)\frac{dP_2(\cos\theta)}{d\theta}\right].
\end{aligned}\right\}\qquad(20)$$

where **λ**, μ are elastic constants of the external medium and **λ**′, μ' are those of the internal grain, while

$$D=\begin{vmatrix}
\frac{\lambda'}{7}, & 4\mu', & -\frac{9\lambda+10\mu}{3}, & -24\mu\\
-\frac{8\lambda'+7\mu'}{21}, & 2\mu', & \frac{3\lambda+2\mu}{6}, & 8\mu\\
-\frac{\lambda'}{7\mu'}, & 2, & \frac{3\lambda+5\mu}{6\mu}, & 3\\
-\frac{5\lambda'+7\mu'}{42\mu'}, & 1, & \frac{1}{6}, & -1
\end{vmatrix},\qquad
D_2=\begin{vmatrix}
\frac{\lambda'}{7}, & 4\mu', & \frac{2}{3}, & -24\mu\\
-\frac{8\lambda'+7\mu'}{21}, & 2\mu', & \frac{1}{3}, & 8\mu\\
-\frac{\lambda'}{7\mu'}, & 2, & \frac{1}{3\mu}, & 3\\
-\frac{5\lambda'+7\mu'}{42\mu'}, & 1, & \frac{1}{6\mu}, & -1
\end{vmatrix},$$

$$D_1=\begin{vmatrix}
\frac{\lambda'}{7}, & \frac{2}{3}, & -\frac{9\lambda+10\mu}{3}, & -24\mu\\
-\frac{8\lambda'+7\mu'}{21}, & \frac{1}{3}, & \frac{3\lambda+2\mu}{6}, & 8\mu\\
-\frac{\lambda'}{7\mu'}, & \frac{1}{3\mu}, & \frac{3\lambda+5\mu}{6\mu}, & 3\\
-\frac{5\lambda'+7\mu'}{42\mu'}, & \frac{1}{6\mu}, & \frac{1}{6}, & -1
\end{vmatrix},\qquad
D_3=\begin{vmatrix}
\frac{\lambda'}{7}, & 4\mu', & -\frac{9\lambda+10\mu}{3}, & \frac{2}{3}\\
-\frac{8\lambda'+7\mu'}{21}, & 2\mu', & \frac{3\lambda+2\mu}{6}, & \frac{1}{3}\\
-\frac{\lambda'}{7\mu'}, & 2, & \frac{3\lambda+5\mu}{6\mu}, & \frac{1}{3\mu}\\
-\frac{5\lambda'+7\mu'}{42\mu}, & 1, & \frac{1}{6}, & \frac{1}{6\mu}
\end{vmatrix}.$$

$$\cdots\cdots\cdots\cdots\cdots\cdots\cdots\cdots\cdots\cdots(21)$$

The distribution of stresses, $\widehat{\theta\theta}'$ and $\widehat{\theta\theta}$, in the section $\theta=\frac{\pi}{2}$ for the two cases; (1) $\lambda=\mu,\ \lambda'=\mu',\ \frac{\mu'}{\mu}=\frac{1}{2}$ and (2) $\lambda=\mu,\ \lambda'=\mu',\ \frac{\mu'}{\mu}=2$ are illustrated in Fig. 1 and Fig. 2.

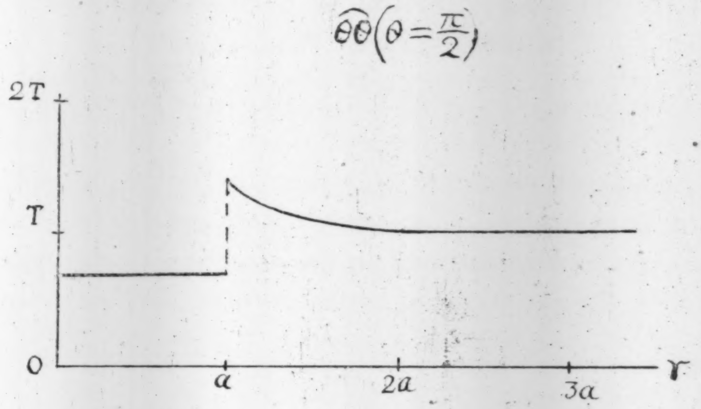

Fig. 1. $\left(\lambda=\mu,\quad \lambda'=\mu',\quad \frac{\mu'}{\mu}=\frac{1}{2}.\right)$

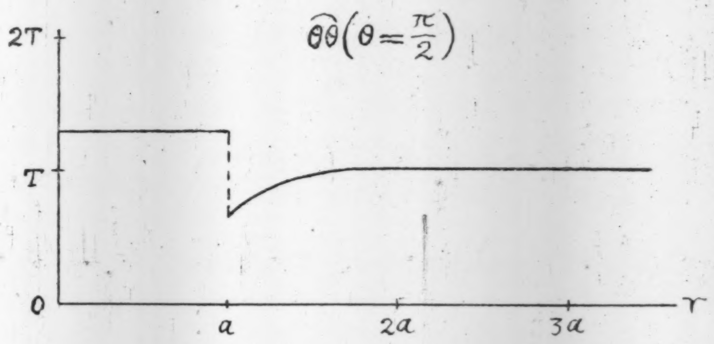

Fig. 2. $\left(\lambda=\mu,\quad \lambda'=\mu',\quad \frac{\mu'}{\mu}=2.\right)$

It is to be noticed that the stresses in the imbedded sphere are independent of the radial distance from the centre of th sphere. It is equally important fact that, when the internal grain is soft compared with the external medium, the stresses are accumulated at the neighbourhood of the external solid and the stresses in the grain is diminished more than the uniform stress, while in the case of a rigid grain imbedded in a soft medium, the stresses are accumulated in the imbedded grain and the stresses at the boundary region of the external solid is the more lessened than the uniform mean stress. The mean of the stresses in the plane surface $\theta=\pi/2$ is, of course, equal to the uniform traction.

The recent problem of block movements in the earth crust of our country will probably be nothing but the effect of such heterogeneity of physical constants on the stresses or the displacements.

II. The Equilibrium of a Spherical Body under Normal Pressures.[7]

5. The problem of the solid earth which is subjected to the normal boundary pressure of any distribution, when the curvature of the surface is taken into consideration, can be solved in the following manner.

Let r, θ, ϕ be spherical polar coordinates, and let us denote u, v, w as the components of the displacement in the direction of the radius, colatitude and azimuth, then the equations of equilibrium of the body can be expressed by

$$\left.\begin{aligned}
&(\lambda+2\mu)\frac{\partial\Delta}{\partial r}-\frac{2\mu}{r\sin\theta}\frac{\partial(\varpi_\phi\sin\theta)}{\partial\theta}+\frac{2\mu}{r\sin\theta}\frac{\partial\varpi_\theta}{\partial\phi}=0,\\
&(\lambda+2\mu)\frac{1}{r}\frac{\partial\Delta}{\partial\theta}-\frac{2\mu}{r\sin\theta}\frac{\partial\varpi_r}{\partial\phi}+\frac{2\mu}{r}\frac{\partial(\varpi_\phi r)}{\partial r}=0,\\
&(\lambda+2\mu)\frac{1}{r\sin\theta}\frac{\partial\Delta}{\partial\phi}-\frac{2\mu}{r}\frac{\partial(\varpi_\theta r)}{\partial r}+\frac{2\mu}{r}\frac{\partial\varpi_r}{\partial\theta}=0,
\end{aligned}\right\}\cdots\cdots\cdots(22)$$

where

$$\left.\begin{aligned}
\Delta&=\frac{1}{r^2\sin\theta}\left[\frac{\partial(ur^2\sin\theta)}{\partial r}+\frac{\partial(vr\sin\theta)}{\partial\theta}+\frac{\partial(wr)}{\partial\phi}\right],\\
2\varpi_r&=\frac{1}{r^2\sin\theta}\left[\frac{\partial}{\partial\theta}(wr\sin\theta)-\frac{\partial}{\partial\phi}(vr)\right],\\
2\varpi_\theta&=\frac{1}{r\sin\theta}\left[\frac{\partial u}{\partial\phi}-\frac{\partial(wr\sin\theta)}{\partial r}\right],\\
2\varpi_\phi&=\frac{1}{r}\left[\frac{\partial(vr)}{\partial r}-\frac{\partial u}{\partial\theta}\right].
\end{aligned}\right\}\cdots\cdots\cdots(23)$$

The elimination of u, v, w among (22) and (23) gives us that

$$\left.\begin{aligned}
&\frac{1}{r^2}\frac{\partial}{\partial r}\left(r^2\frac{\partial\Delta}{\partial r}\right)+\frac{1}{r^2\sin\theta}\frac{\partial}{\partial\theta}\left(\sin\theta\frac{\partial\Delta}{\partial\theta}\right)+\frac{1}{r^2\sin^2\theta}\frac{\partial^2\Delta}{\partial\phi^2}=0,\\
&\frac{\partial^2\varpi_r}{\partial r^2}+\frac{4}{r}\frac{\partial\varpi_r}{\partial r}+\frac{2}{r^2}\varpi_r+\frac{1}{r^2\sin\theta}\frac{\partial}{\partial\theta}\left(\sin\theta\frac{\partial\varpi_r}{\partial\theta}\right)+\frac{1}{r^2\sin^2\theta}\frac{\partial^2\varpi_r}{\partial\phi^2}=0,\\
&\frac{1}{r}\frac{\partial^2(\varpi_\theta r)}{\partial r^2}+\frac{1}{r^2\sin^2\theta}\frac{\partial^2\varpi_\theta}{\partial\phi^2}-\frac{1}{r^2\sin^2\theta}\frac{\partial^2(\varpi_\phi\sin\theta)}{\partial\phi\,\partial\theta}-\frac{1}{r}\frac{\partial^2\varpi_r}{\partial r\,\partial\theta}=0,\\
&\frac{1}{r}\frac{\partial^2(\varpi_\phi r)}{\partial r^2}+\frac{1}{r^2}\frac{\partial}{\partial\theta}\frac{1}{\sin\theta}\frac{\partial(\varpi_\phi\sin\theta)}{\partial\theta}-\frac{1}{r^2}\frac{\partial}{\partial\theta}\frac{1}{\sin\theta}\frac{\partial\varpi_\theta}{\partial\phi}\\
&\qquad\qquad\qquad\qquad\qquad\qquad-\frac{1}{r\sin\theta}\frac{\partial^2\varpi_r}{\partial r\partial\phi}=0.
\end{aligned}\right\}\cdots(24)$$

---

7) K. SEZAWA & G. NISHIMURA, *loc. cit.*, 389.

These gives us

$$\left.\begin{aligned}
\Delta&=\left(A_{mn}r^{n}+\frac{A'_{mn}}{r^{n+1}}\right)P_n^m(\cos\theta)\left.\begin{matrix}\cos\\ \sin\end{matrix}\right\}m\phi,\\
2\varpi_r&=\left(B_{mn}r^{n-1}+\frac{B'_{mn}}{r^{n+2}}\right)P_n^m(\cos\theta)\left.\begin{matrix}\sin\\ -\cos\end{matrix}\right\}m\phi,\\
2\varpi_\theta&=\Bigg[\left(D_{mn}r^{n}+\frac{D'_{mn}m}{r^{n+1}}\right)\frac{P_n^m(\cos\theta)}{\sin\theta}\\
&\qquad+\left(\frac{B_{mn}}{n}r^{n-1}-\frac{B'_{mn}}{(n+1)\,r^{n+2}}\right)\frac{dP_n^m(\cos\theta)}{d\theta}\Bigg]\left.\begin{matrix}\sin\\ -\cos\end{matrix}\right\}m\phi,\\
2\varpi_\phi&=\Bigg[\left(D_{mn}r^{n}+\frac{D'_{mn}}{r^{n+1}}\right)\frac{dP_n^m(\cos\theta)}{d\theta}\\
&\qquad+\left(\frac{B_{mn}}{n}r^{n-1}-\frac{B'_{mn}}{(n+1)\,r^{n+2}}\right)\frac{P_n^m(\cos\theta)}{\sin\theta}\Bigg]\left.\begin{matrix}\cos\\ \sin\end{matrix}\right\}m\phi.
\end{aligned}\right\}\quad\ldots(25)$$

in which A_{mn}, A'_{mn}, B_{mn}, B'_{mn}, C_{mn}, C'_{mn} are arbitrary constants.

Displacement (u_1, v_1, w_1) answering to Δ in (25) and satisfying $\varpi_r=\varpi_\theta=\varpi_\phi=0$ is expressed by

$$\left.\begin{aligned}
u_1&=\left[\frac{A_{mn}(n+2)}{2(2n+3)}r^{n+1}+\frac{A'_{mn}(n-1)}{2(2n-1)\,r^{n}}\right]P_n^m(\cos\theta)\left.\begin{matrix}\cos\\ \sin\end{matrix}\right\}m\phi,\\
v_1&=\left[\frac{A_{mn}}{2(2n+3)}r^{n+1}-\frac{A'_{mn}}{2(2n-1)\,r^{n}}\right]\frac{dP_n^m(\cos\theta)}{d\theta}\left.\begin{matrix}\cos\\ \sin\end{matrix}\right\}m\phi,\\
w_1&=-\left[\frac{A_{mn}m}{2(2n+3)}r^{n+1}-\frac{A'_{mn}}{2(2n-1)\,r^{n}}\right]\frac{P_n^m(\cos\theta)}{\sin\theta}\left.\begin{matrix}\sin\\ -\cos\end{matrix}\right\}m\phi.
\end{aligned}\right\}\quad\ldots.(26)$$

Displacement (u_2, v_2, w_2) answering to ϖ_r together with the second terms in the expression of ϖ_θ, ϖ_ϕ, all given in (25) under the condition that $\Delta=0$, is expressed by

$$\left.\begin{aligned}
u_2&=0,\\
v_2&=\left[\frac{mB_{mn}}{n(n+1)}r^{n}+\frac{mB_{mn}}{n(n+1)\,r^{n+1}}\right]\frac{P_n^m(\cos\theta)}{\sin\theta}\left.\begin{matrix}\cos\\ \sin\end{matrix}\right\}m\phi,\\
w_2&=-\left[\frac{B_{mn}}{n(n+1)}r^{n}+\frac{B'_{mn}}{n(n+1)\,r^{n+1}}\right]\frac{dP_n^m(\cos\theta)}{d\theta}\left.\begin{matrix}\sin\\ -\cos\end{matrix}\right\}m\phi.
\end{aligned}\right\}\quad\ldots.(27)$$

Displacement (u_4, v_4, w_4) derived from the values of the first terms of ϖ_θ, ϖ_ϕ, in (25) fulfilling the conditions, $\Delta=\varpi_r=0$ is written by

$$\left.\begin{aligned} u_4&=\left[\frac{D_{mn}\,n\,(n+1)}{2\,(2n+3)}\,r^{n+1}+\frac{D'_{mn}\,n\,(n+1)}{2\,(2n-1)\,r^n}\right]P_n^m(\cos\theta)\left.\begin{matrix}\cos\\ \sin\end{matrix}\right\}m\phi,\\ v_4&=\left[\frac{D_{mn}\,(n+3)}{2\,(2n+3)}\,r^{n+1}+\frac{D'_{mn}\,(n-2)}{2\,(2n-1)\,r^n}\right]\frac{1}{m}\cdot\frac{dP_n^m(\cos\theta)}{d\theta}\left.\begin{matrix}\cos\\ \sin\end{matrix}\right\}m\phi,\\ w_4&=-\left[\frac{D_{mn}\,m\,(n+3)}{2\,(2n+3)}\,r^{n+1}+\frac{D'_{mn}\,m\,(n-2)}{2\,(2n-1)\,r^n}\right]\frac{P_n^m(\cos\theta)}{\sin\theta}\left.\begin{matrix}\sin\\ -\cos\end{matrix}\right\}m\phi. \end{aligned}\right\}\quad(28)$$

Displacement (u_3, v_3, w_3) which satisfies $\Delta=\varpi_r=\varpi_\theta=\varpi_\phi=0$, is expressed by

$$\left.\begin{aligned} u_3&=\left[C_{mn}\,n\,r^{n-1}-\frac{C'_{mn}(n+1)}{r^{n+2}}\right]P_n^m(\cos\theta)\begin{bmatrix}\cos\\ \sin\end{bmatrix}m\phi,\\ v_3&=\left[C_{mn}\,r^{n-1}+\frac{C'_{mn}}{r^{n+2}}\right]\frac{dP_n^m(\cos\theta)}{d\theta}\left.\begin{matrix}\cos\\ \sin\end{matrix}\right\}m\phi,\\ w_3&=-m\left[C_{mn}\,r^{n-1}+\frac{C'_{mn}}{r^{n+2}}\right]\frac{P_n^m(\cos\theta)}{\sin\theta}\left.\begin{matrix}\sin\\ -\cos\end{matrix}\right\}m\phi. \end{aligned}\right\}\quad\ldots\ldots\ldots(29)$$

In the above solutions, the displacement (u_2, v_2, w_2) in (27) is without significance for the problem of normal pressure, so that this displacement may be excluded from the present study. It is the only proper term when the sphere is subjected to the distortional stress at the surface.

Now A_{mn} and D_{mn} or A'_{mn} and D'_{mn} are not independent of each other. When we refer to the equation (22), we find that there is a fixed relation between A_{mn} and D_{mn} or A'_{mn} and D'_{mn}, the relations being expressed by

$$\frac{D_{mn}}{A_{mn}}=-\frac{\lambda+2\mu}{\mu\,(n+1)};\quad \frac{D'_{mn}}{A'_{mn}}=\frac{\lambda+2\mu}{\mu n}\quad\ldots\ldots\ldots\ldots\ldots\ldots(30)$$

Proceeding in the same manner as in the preceding part we may write down the principal items in the following table:

Kind of displacement	Types of solutions	Physical meaning	Arbitray constants	
1st kind	$r^{n+1}\times\ldots,\ \frac{1}{r^n}\times\ldots,$	dilatation	$A_{mn},\ A'_{mn}$	$D_{mn}=-\frac{\lambda+2\mu}{\mu(n+1)}A_{mn},$
		rotation	$D_{mn},\ D'_{mn}$	$D'_{mn}=\frac{(\lambda+2\mu)}{\mu n}A'_{mn}$
2nd kind	$r^{n-1}\times\ldots,\ \frac{1}{r^{n+2}}\times\ldots,$	indil. and irrot.	$C_{mn},\ C'_{mn}$	

Examples of application have been omitted in this paper, as they have already appeared in the Bulletin VI.

III. Spheroidal Problems of Elasticity solved in Curvilinear Coordinates.

6. The equations of motion of elastic bodies in spheroidal coordinates, when the azimuthal component of the motion is omitted, are expressed by

$$\left.\begin{aligned}(\lambda+2\mu)\,h_1\frac{\partial\varDelta}{\partial\xi}-2\mu\,h_2\,h_3\frac{\partial}{\partial\eta}\left(\frac{\varpi}{h_3}\right)=0,\\ (\lambda+2\mu)\,h_2\frac{\partial\varDelta}{\partial\eta}+2\mu\,h_1\,h_3\frac{\partial}{\partial\xi}\left(\frac{\varpi}{h_3}\right)=0,\end{aligned}\right\}\quad\ldots\ldots\ldots\ldots\ldots(31)$$

in which

$$\left.\begin{aligned}\varDelta=h_1h_2h_3\left[\frac{\partial}{\partial\xi}\left(\frac{u}{h_2\,h_3}\right)+\frac{\partial}{\partial\eta}\left(\frac{v}{h_1\,h_2}\right)\right],\\ 2\varpi=h_1h_2\left[\frac{\partial}{\partial\xi}\left(\frac{v}{h_2}\right)-\frac{\partial}{\partial y}\left(\frac{u}{h_1}\right)\right],\end{aligned}\right\}\quad\ldots\ldots\ldots\ldots\ldots(32)$$

and

$$\frac{1}{h_1{}^2}=\frac{1}{h_2{}^2}=c^2(\mathrm{ch}^2\,\xi-\cos^2\,\eta),\qquad\frac{1}{h_3{}^2}=c^2\,\mathrm{sh}^2\,\xi\,\sin^2\eta,\quad\ldots\ldots\ldots(33)$$

in the case of a prolate-spheroidal coordinates (ξ,η) connected with Cartesian coordinates in the form:

$$z+\sqrt{x^2+y^2}=c\cosh\,(\xi+i\eta),\quad\ldots\ldots\ldots\ldots\ldots\ldots\ldots\ldots(34)$$

or in real forms,

$$\frac{x^2+y^2}{c^2\,\mathrm{sh}^2\,\xi}+\frac{z^2}{c^2\,\mathrm{ch}^2\,\xi}=1,\quad\frac{z^2}{c^2\cos^2\eta}-\frac{x^2+y^2}{c^2\sin^2\eta}=1.\quad\ldots\ldots\ldots\ldots(35)$$

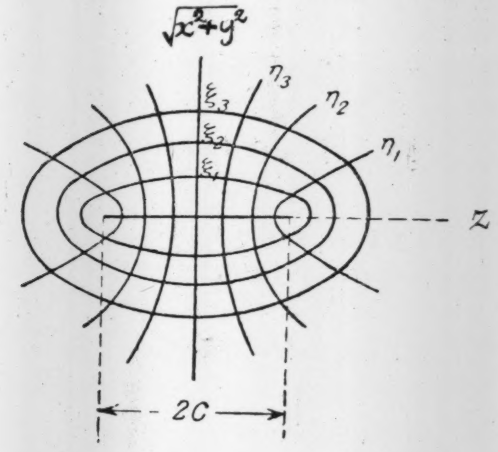

In equations (32) u, v are the displacement in the direction of ξ and η and $2c$ is the length of the major axis of the spheroid.

Eliminating u, v between (31) and (32), we obtain

$$\left.\begin{aligned}&\frac{\partial^2 \varDelta}{\partial \xi^2}+\operatorname{cth}\xi\,\frac{\partial \varDelta}{\partial \xi}+\frac{\partial^2 \varDelta}{\partial \eta^2}+\cot\eta\,\frac{\partial \varDelta}{\partial \eta}=0,\\&\frac{\partial^2 \varpi}{\partial \xi^2}+\operatorname{cth}\xi\,\frac{\partial \varpi}{\partial \xi}-\frac{\varpi}{\operatorname{sh}^2\xi}+\frac{\partial^2 \varpi}{\partial \eta^2}+\cot\eta\,\frac{\partial \varpi}{\partial \eta}-\frac{\varpi}{\sin^2\eta}=0.\end{aligned}\right\}\quad\ldots\ldots\ldots(36)$$

Solving (36), we find

$$\varDelta=\{A_n P_n(\operatorname{ch}\xi)+B_n Q_n(\operatorname{ch}\xi)\}P_n(\cos\eta),\qquad [n=0,\,1,\,2\,..]\quad\ldots.(37)$$

$$2\varpi=\left\{A_n'\,\frac{dP_n(\operatorname{ch}\xi)}{d\xi}+B_n'\,\frac{dQ_n(\operatorname{ch}\xi)}{d\xi}\right\}\frac{dP_n(\cos\eta)}{d\eta}.\qquad [n=1,\,2,\,3\,..]\quad\ldots.(38)$$

Displacement (u_1, v_1) answering to $\varDelta$ in (37) and fulfilling the condition that $\varpi=0$ is expressed by

$$\begin{aligned}u_1=\frac{c}{\sqrt{\operatorname{ch}^2\xi-\cos^2\eta}}&\left.\begin{aligned}\Bigg[&\frac{(n+1)(n+2)}{2(2n+1)(2n+3)^2}\left(A_n\frac{dP_{n+2}(\operatorname{ch}\xi)}{d\xi}\right.\\&\qquad\left.+B_n\frac{dQ_{n+2}(\operatorname{ch}\xi)}{d\xi}\right)P_n(\cos\eta)\\&+\frac{(n+1)(n+2)}{2(2n+1)(2n+3)^2}\left(A_n\frac{dP_n(\operatorname{ch}\xi)}{d\xi}\right.\\&\qquad\left.+B_n\frac{dQ_n(\operatorname{ch}\xi)}{d\xi}\right)P_{n+2}(\cos\eta)\end{aligned}\right\}[n=0,\,1,\,2,\,..]\\&\left.\begin{aligned}&-\frac{n(n-1)}{2(2n-1)^2(2n+1)}\left(A_n\frac{dP_{n-2}(\operatorname{ch}\xi)}{d\xi}\right.\\&\qquad\left.+B_n\frac{dQ_{n-2}(\operatorname{ch}\xi)}{d\xi}\right)P_n(\cos\eta)\\&-\frac{n(n-1)}{2(2n-1)^2(2n+1)}\left(A_n\frac{dP_n(\operatorname{ch}\xi)}{d\xi}\right.\\&\qquad\left.+B_n\frac{dQ_n(\operatorname{ch}\xi)}{d\xi}\right)P_{n-2}(\cos\eta)\Bigg],\end{aligned}\right\}[n=2,\,3,\,..]\end{aligned}$$

$$v_1=\frac{c}{\sqrt{\operatorname{ch}^2\xi-\cos^2\eta}}\left.\begin{aligned}\Bigg[&\frac{(n+1)(n+2)}{2(2n+1)(2n+3)^2}\Big(A_nP_{n+2}(\operatorname{ch}\xi)\\&\qquad+B_nQ_{n+2}(\operatorname{ch}\xi)\Big)\frac{dP_n(\cos\eta)}{d\eta}\\&+\frac{(n+1)(n+2)}{2(2n+1)(2n+3)^2}\Big(A_nP_n(\operatorname{ch}\xi)\\&\qquad+B_nQ_n(\operatorname{ch}\xi)\Big)\frac{dP_{n+2}(\cos\eta)}{d\eta}\end{aligned}\right\}[n=0,\,1,\,2,\,..]$$

$$\left.\begin{aligned} &-\frac{n\,(n-1)}{2\,(2n-1)^2(2n+1)}\Big(A_n P_{n-2}(\mathrm{ch}\,\xi) \\ &\qquad\qquad + B_n Q_{n-2}\,(\mathrm{ch}\,\xi)\Big)\frac{dP_n\,(\cos\eta)}{d\eta} \\ &-\frac{n\,(n-1)}{2\,(2n-1)^2(2n+1)}\Big(A_n\,P_n\,(\mathrm{ch}\,\xi) \\ &\qquad\qquad + B_n\,Q_n\,(\mathrm{ch}\,\xi)\Big)\frac{dP_{n-2}\,(\cos\eta)}{d\eta}\Bigg]. \end{aligned}\right\}[n=2,\,3,\,.\,.] \qquad \ldots\ldots(39)$$

Displacement $(u_2,\ v_2)$ corresponding to ϖ in (38) under the condition that $\varDelta=0$ is expressed by

$$u_2=\frac{cn\,(n+1)}{\sqrt{\mathrm{ch}^2\,\xi-\cos^2\eta}}\left[\left.\begin{aligned} &\frac{n\,(n+1)}{2\,(2n+1)(2n+3)^2}\Big(A_n{}'\,\frac{dP_{n+2}\,(\mathrm{ch}\,\xi)}{d\xi} \\ &\qquad\qquad + B_n{}'\,\frac{dQ_{n+2}\,(\mathrm{ch}\,\xi)}{d\xi}\Big)\,P_n\,(\cos\eta) \\ &+\frac{(n+2)\,(n+3)}{2\,(2n+1)(2n+3)^2}\Big(A_n{}'\,\frac{dP_n\,(\mathrm{ch}\,\xi)}{d\zeta} \\ &\qquad\qquad + B_n{}'\,\frac{dQ_n\,(\mathrm{ch}\,\xi)}{d\xi}\Big)\,P_{n+2}\,(\cos\eta) \end{aligned}\right\}[n=0,\,1,\,2,\,.\,.]\right. ,$$

$$\left.\begin{aligned} &-\frac{n\,(n+1)}{2\,(2n-1)^2(2n+1)}\Big(A_n{}'\,\frac{dP_{n-2}\,(\mathrm{ch}\,\xi)}{d\xi} \\ &\qquad\qquad + B_n{}'\,\frac{dQ_{n-2}\,(\mathrm{ch}\,\xi)}{d\xi}\Big)\,P_n\,(\cos\eta) \\ &-\frac{(n-1)\,(n-2)}{2\,(2n-1)^2(2n+1)}\Big(A_n{}'\,\frac{dP_n\,(\mathrm{ch}\,\xi)}{d\xi} \\ &\qquad\qquad + B_n{}'\,\frac{Q_n\,(\mathrm{ch}\,\xi)}{d\xi}\Big)\,P_{n-2}\,(\cos\eta)\Bigg], \end{aligned}\right\}[n=2,\,3,\,.\,.]$$

$$v_2=\frac{cn\,(n+1)}{\sqrt{\mathrm{ch}^2\,\xi-\cos^2\eta}}\left[\left.\begin{aligned} &\frac{(n+2)\,(n+3)}{2\,(2n+1)(2n+3)^2}\Big(A_n{}'\,P_{n+2}\,(\mathrm{ch}\,\xi) \\ &\qquad\qquad + B_n{}'\,Q_{n+2}\,(\mathrm{ch}\,\xi)\Big)\frac{dP_n\,(\cos\eta)}{d\eta} \\ &+\frac{n\,(n+1)}{2\,(2n+1)(2n+3)^2}A_n{}'\,P_n\,(\mathrm{ch}\,\xi) \\ &\qquad\qquad + B_n{}'\,Q_n\,(\mathrm{ch}\,\xi)\Big)\frac{dP_{n+2}\,(\cos\eta)}{d\zeta} \end{aligned}\right\}[n=0,\,1,\,2,\,.\,.]\right.$$

$$\left.\begin{aligned} &-\frac{(n-1)(n-2)}{2(2n-1)^2(2n+1)}\Big(A_n' P_{n-2}(\mathrm{ch}\,\xi) \\ &\qquad\qquad + B^{n\prime} Q^{n-2}(\mathrm{ch}\,\xi)\Big)\frac{dP_n(\cos\eta)}{d\eta} \\ &-\frac{n(n+1)}{2(2n-1)^2(2n+1)}\Big(A_n' P_n(\mathrm{ch}\,\xi) \\ &\qquad\qquad + B_n' Q_n(\mathrm{ch}\,\xi)\Big)\frac{dP_{n-2}(\cos\eta)}{d\eta}\Bigg]. \end{aligned}\right\} [n=2,\ 3,\ldots] \qquad \ldots\ldots(40)$$

Displacement (u_3, v_3) which satisfies $\varDelta=0$, $\varpi=0$ can be written in the forms:

$$\left.\begin{aligned} u_3 &= \frac{c}{\sqrt{\mathrm{ch}^2\,\xi-\cos^2\eta}}\left[A_n'' \frac{dP_n(\mathrm{ch}\,\xi)}{d\xi} + B_n'' \frac{dQ_n(\mathrm{ch}\,\xi)}{d\xi}\right] P_n(\cos\eta), \\ v_3 &= \frac{c}{\sqrt{\mathrm{ch}^2\,\xi-\cos^2\eta}}\left[A_n'' P_n(\mathrm{ch}\,\xi) + B_n'' Q_n(\mathrm{ch}\,\xi)\right]\frac{dP_n(\cos\eta)}{d\eta}. \end{aligned}\right\} [n=0,\ 1,\ 2,\ldots] \qquad \ldots\ldots(41)$$

Now A_n and A_n' or B_n and B_n' are not independent and there is a fixed relation between A_n and A_n' or B_n and B_n', the relations, which are obtained from (31), being expressed by

$$A_n' = -\frac{\lambda+2\mu}{\mu n(n+1)} A_n; \quad B_n' = -\frac{\lambda+2\mu}{\mu n(n+1)} B_n. \qquad \ldots\ldots(42)$$

The tabulated elements of the nature of the solutions are as follows:

Kind of displacement	Types of solutions	Physical meaning	Arbitrary constants	
1st kind	$P_{n+2},\ P_n,\ P_{n-2}\ldots$	dilatation	$A_n,\ B_n$	$\left.\begin{matrix} A_n' \\ B_n' \end{matrix}\right\} = -\dfrac{\lambda+2\mu}{\mu n(n+1)}\left\{\begin{matrix} A_n \\ B_n. \end{matrix}\right.$
	$Q_{n+2},\ Q_n,\ Q_{n-2}\ldots$	rotation	$A_n',\ B_n'$	
2nd kind	$P_n,\ Q_n$	indil. and irrot.	$A_n'',\ B_n''$	

7. In the case of the oblate spheroid, we should write

$$\frac{1}{h_1{}^2}=\frac{1}{h_2{}^2}=c^2\,(\mathrm{ch}^2\,\xi-\sin^2\eta)\,;\qquad \frac{1}{h_3{}^2}=c^2\,\mathrm{ch}^2\,\xi\,\sin^2\eta,\,\ldots\ldots\ldots(43)$$

where $2c$ is the magnitude of the major axis.

From (31) and (43), we obtain

$$\left.\begin{aligned}&\frac{\partial^2\varDelta}{\partial\xi^2}+\mathrm{th}\,\xi\,\frac{\partial\varDelta}{\partial\xi}+\frac{\partial^2\varDelta}{\partial\eta^2}+\cot\eta\,\frac{\partial\varDelta}{\partial\eta}=0,\\&\frac{\partial^2\varpi}{\partial\xi^2}+\mathrm{th}\,\xi\,\frac{\partial\varpi}{\partial\xi}+\frac{\varpi}{\mathrm{ch}^2\,\xi}+\frac{\partial^2\varpi}{\partial\eta^2}+\cot\eta\,\frac{\partial\varpi}{\partial\eta}-\frac{\varpi}{\sin^2\eta}=0,\end{aligned}\right\}\,\ldots\ldots\ldots(44)$$

the solutions of which are

$$\varDelta=\{A_n\,P_n\,(i\,\mathrm{sh}\,\xi)+B_n\,Q_n\,(i\,\mathrm{sh}\,\xi)\}\,P_n\,(\cos\eta),\,\ldots\ldots\ldots\ldots\ldots(45)$$

$$2\varpi=\left\{A_n{}'\,\frac{dP_n(i\,\mathrm{sh}\,\xi)}{d\xi}+B_n{}'\,\frac{dQ_n(i\,\mathrm{sh}\,\xi)}{d\xi}\right\}\frac{dP_n\,(\cos\eta)}{d\eta}.\,\ldots\ldots\ldots\ldots(46)$$

The corresponding displacements are of the similar forms except the negative signs of $(u_1,\,v_1)$, $(u_2,\,v_2)$ and also the argument of the function of the type $P_n(i\,\mathrm{sh}\,\xi)$. The other explanations have been omitted for the sake of simplicity.

IV. The Problem of an Elastic Cylinder.[8]

8. The equations of motion of an elastic body in cylindrical coordinates are expressed by

$$\left.\begin{aligned}&(\lambda+2\mu)\,\frac{\partial\varDelta}{\partial r}-\frac{2\mu}{r}\,\frac{\partial\varpi_z}{\partial\theta}+2\mu\,\frac{\partial\varpi_\theta}{\partial z}=0,\\&(\lambda+2\mu)\,\frac{\partial\varDelta}{r\partial\theta}-2\mu\,\frac{\partial\varpi_r}{\partial z}+2\mu\,\frac{\partial\varpi_z}{\partial r}=0,\\&(\lambda+2\mu)\,\frac{\partial\varDelta}{\partial z}-\frac{2\mu}{r}\,\frac{\partial}{\partial r}\,(r\varpi_\theta)+\frac{2\mu}{r}\,\frac{\partial\varpi_r}{\partial\theta}=0,\end{aligned}\right\}\,\ldots\ldots\ldots\ldots(47)$$

where

$$\left.\begin{aligned}\varDelta&=\frac{1}{r}\,\frac{\partial}{\partial r}\,(ru)+\frac{1}{r}\,\frac{\partial v}{\partial\theta}+\frac{\partial w}{\partial z},\\2\varpi_r&=\frac{1}{r}\,\frac{\partial w}{\partial\theta}-\frac{\partial v}{\partial z},\\2\varpi_\theta&=\frac{\partial u}{\partial z}-\frac{\partial w}{\partial r},\\2\varpi_z&=\frac{1}{r}\,\frac{\partial\,(rv)}{\partial r}-\frac{1}{r}\,\frac{\partial u}{\partial\theta},\end{aligned}\right\}\,\ldots\ldots\ldots\ldots\ldots(48)$$

---

[8] G. Nishimura, *Journ. Soc. Ord. and Expl.*, **23** (1929).

in which u, v, w are the components of displacement in r-, θ-, z-directions.

Eliminating u, v, w in (47) and (48), we get

$$\left.\begin{aligned}
&\frac{\partial^2 \Delta}{\partial r^2}+\frac{1}{r}\frac{\partial \Delta}{\partial r}+\frac{1}{r^2}\frac{\partial^2 \Delta}{\partial \theta^2}+\frac{\partial^2 \Delta}{\partial z^2}=0,\\
&\frac{\partial^2 \varpi_r}{\partial r^2}+\frac{3}{r}\frac{\partial \varpi_r}{\partial r}+\frac{\varpi_r}{r^2}+\frac{1}{r^2}\frac{\partial^2 \varpi_r}{\partial \theta^2}+\frac{\partial^2 \varpi_r}{\partial z^2}+\frac{2}{r}\frac{\partial \varpi_\theta}{\partial z}=0,\\
&\frac{\partial^2 \varpi_\theta}{\partial r^2}+\frac{1}{r}\frac{\partial \varpi_\theta}{\partial r}-\frac{\varpi_\theta}{r}+\frac{1}{r^2}\frac{\partial^2 \varpi_\theta}{\partial \theta^2}+\frac{\partial^2 \varpi_\theta}{\partial z^2}+\frac{2}{r^2}\frac{\partial \varpi_r}{\partial \theta}=0,\\
&\frac{\partial^2 \varpi_z}{\partial r^2}+\frac{1}{r}\frac{\partial \varpi_z}{\partial r}+\frac{1}{r^2}\frac{\partial^2 \varpi_z}{\partial \theta^2}+\frac{\partial^2 \varpi_z}{\partial z^2}=0.
\end{aligned}\right\}\quad\ldots\ldots\ldots(49)$$

The solutions of these can be expressed by

$$\begin{aligned}
\Delta&=\Big\{A_{mk}\,I_m(kr)+A'_{mk}\,K_m(kr)\Big\}\begin{matrix}\sin\\\cos\end{matrix}\Big\}kz\ \begin{matrix}\sin\\\cos\end{matrix}\Big\}m\theta,\\
2\varpi_r&=\Big\{B_{mk}\frac{1}{k}\frac{\partial I_m(kr)}{r}+C_{mk}\frac{I_m(kr)}{r}\\
&\qquad+B'_{mk}\frac{1}{k}\frac{\partial K_m(kr)}{\partial r}+C'_{mk}\frac{K_m(kr)}{\partial r}\Big\}\begin{matrix}-\cos\\\cos\end{matrix}\Big\}kz\ \begin{matrix}-\cos\\\sin\end{matrix}\Big\}m\theta,\\
2\varpi_\theta&=\Big\{B_{mk}\frac{m}{k}\frac{I_m(kr)}{r}+C_{mk}\frac{1}{m}\frac{\partial I_m(kr)}{\partial r}\\
&\qquad+B'_{mk}\frac{m}{k}\frac{K_m(kr)}{r}+C'_{mk}\frac{1}{m}\frac{\partial K_m(kr)}{\partial r}\Big\}\begin{matrix}-\cos\\\sin\end{matrix}\Big\}kz\ \begin{matrix}\sin\\\cos\end{matrix}\Big\}m\theta,\\
2\varpi_z&=\Big\{B_{mn}\,I_m(kr)+B'_{mk}\,K_m(kr)\Big\}\begin{matrix}\sin\\\cos\end{matrix}\Big\}kz\ \begin{matrix}-\cos\\\sin\end{matrix}\Big\}m\theta.
\end{aligned}$$

$$\ldots\ldots\ldots\ldots\ldots\ldots\ldots\ldots\ldots\ldots(50)$$

Displacement (u_1, v_1, w_1) which gives Δ in (50) and satisfies $\varpi_r=\varpi_\theta=\varpi_z=0$ are expressed by

$$\left.\begin{aligned}
u_1&=\frac{1}{2k^2}\Big\{A_{mk}\frac{\partial}{\partial r}\Big(r\,\frac{\partial I_m(kr)}{\partial r}\Big)\\
&\qquad+A'_{mk}\frac{\partial}{\partial r}\Big(r\,\frac{\partial K_m(kr)}{\partial r}\Big)\Big\}\begin{matrix}\sin\\\cos\end{matrix}\Big\}kz\ \begin{matrix}\sin\\\cos\end{matrix}\Big\}m\theta,\\
v_1&=-\frac{m}{2k^2}\Big\{A_{mk}\frac{\partial I_m(kr)}{\partial r}+A'_{mk}\frac{\partial K_m(kr)}{\partial r}\Big\}\begin{matrix}\sin\\\cos\end{matrix}\Big\}kz\ \begin{matrix}-\cos\\\sin\end{matrix}\Big\}m\theta,\\
w_1&=-\frac{1}{2k}\Big\{A_{mk}\,r\,\frac{\partial I_m(kr)}{\partial r}+A'_{mk}\,r\,\frac{\partial K_m(kr)}{\partial r}\Big\}\begin{matrix}-\cos\\\sin\end{matrix}\Big\}kz\ \begin{matrix}\sin\\\cos\end{matrix}\Big\}m\theta.
\end{aligned}\right\}\ldots(51)$$

Displacement which satisfies ϖ_z and 1st and 3rd terms of ϖ_r and ϖ_θ

in (50), with the condition that $\varDelta=0$ is written by

$$\left.\begin{aligned} u_2&=-\frac{m}{k^2}\left\{B_{mk}\frac{{}_m(kr)}{r}+B'_{mk}\frac{K_m(kr)}{r}\right\}\begin{matrix}\sin\\ \cos\end{matrix}\Big\}kz\ \begin{matrix}\sin\\ \cos\end{matrix}\Big\}m\theta,\\ v_2&=\frac{1}{k}\left\{B_{mk}\frac{\partial I_m(kr)}{\partial r}+B'_{mk}\frac{\partial K_m(kr)}{\partial r}\right\}\begin{matrix}\sin\\ \cos\end{matrix}\Big\}kz\ \begin{matrix}-\cos\\ \sin\end{matrix}\Big\}m\theta,\\ w_2&=0.\end{aligned}\right\}\quad\ldots\ldots(52)$$

Displacement (u_3, v_3, w_3) satisfying the 2nd and 4th terms of ϖ_r, ϖ_θ in (50) and fulfilling the condition $\varDelta=\varpi_z=0$ is expressed by

$$\begin{aligned} u_3&=-\frac{1}{mk}\left\{C_{mk}\frac{\partial}{\partial r}\left(r\frac{\partial I_m(kr)}{\partial r}\right)+C'_{mk}\frac{\partial}{\partial r}\left(r\frac{\partial K_m(kr)}{\partial r}\right)\right\}\begin{matrix}\sin\\ \cos\end{matrix}\Big\}kz\ \begin{matrix}\sin\\ \cos\end{matrix}\Big\}m\theta,\\ v_3&=\frac{1}{k}\left\{C_{mk}\frac{\partial I_m(kr)}{\partial r}+C'_{mk}\frac{\partial K_m(kr)}{\partial r}\right\}\begin{matrix}\sin\\ \cos\end{matrix}\Big\}kz\ \begin{matrix}-\cos\\ \sin\end{matrix}\Big\}m\theta,\\ w_3&=-\frac{1}{2m}\left\{C_{mk}\,r\frac{\partial I_m(kr)}{\partial r}+C'_{mk}\,r\frac{\partial K_m(kr)}{\partial r}\right\}\begin{matrix}-\cos\\ \sin\end{matrix}\Big\}kz\ \begin{matrix}\sin\\ \cos\end{matrix}\Big\}m\theta.\end{aligned}$$

$$\ldots\ldots\ldots\ldots\ldots\ldots\ldots\ldots\ldots(53)$$

Displacement (u_4, v_4, w_4) which answers to $\varDelta=\varpi_r=\varpi_\theta=\varpi_z=0$ is expressed by

$$\left.\begin{aligned} u_4&=-\frac{1}{k}\left\{E_{mk}\frac{\partial I_m(kr)}{\partial r}+E'_{mk}\frac{\partial K_m(kr)}{\partial r}\right\}\begin{matrix}\sin\\ \cos\end{matrix}\Big\}kz\ \begin{matrix}\sin\\ \cos\end{matrix}\Big\}m\theta,\\ v_4&=\frac{m}{k}\left\{E_{n\,k}\frac{I_m(kr)}{r}+E'_{mk}\frac{K_m(kr)}{r}\right\}\begin{matrix}\sin\\ \cos\end{matrix}\Big\}kz\ \begin{matrix}-\cos\\ \sin\end{matrix}\Big\}m\theta,\\ w_4&=\left\{E_{mk}I_m(kr)+E'_{mk}K_m(kr)\right\}\begin{matrix}-\cos\\ \sin\end{matrix}\Big\}kz\ \begin{matrix}\sin\\ \cos\end{matrix}\Big\}m\theta.\end{aligned}\right\}\ldots\ldots(54)$$

In the above equations, the displacement (u_2, v_2, w_2) in (52) has no significance for the extensional and flexural problems, but they are useful for the torsion problem. Now, taking the case of the extensional or flexural problem, it will be easily seen that A_{mk} and C_{mk} or A'_{mk} and C'_{mk} are not independent. There are the following connections:

$$\frac{C_{mk}}{A_{mk}}=-\frac{(\lambda+2\mu)\,m}{\mu k},\quad \frac{C'_{mk}}{A'_{mk}}=-\frac{(\lambda+2\mu)\,m}{\mu k}\ldots\ldots\ldots\ldots(55)$$

Thus, in this case, we have only two types of solutions, one of which corresponds to (u_1, v_1, w_1) and (u_3, v_3, w_3), while the other to (u_4, v_4, w_4). The tabulated summary is as follows:

Kind of displacement	Types of solutions	Physical meaning	Arbitrary constants
1st kind	$r\frac{\partial I_m(kr)}{\partial r},..$	dilatation rotation	$\frac{C_{mk}}{A_{mk}}=-\frac{(\lambda+2\mu)m}{\mu k}$, $\frac{C'_{mk}}{A'_{mk}}=-\frac{(\lambda+2\mu)m}{\mu k}$.
2nd kind	$I_m(kr),..$	indilatational irrotational	E_{mk}, E'_{mk}

The similar process can be applied to Boussinesq's problem on the equilibrium of a semi-infinite solid body under the normal traction or shearing stress on the free surface and we may find that the displacements consist of two kinds as already cited in the forgoing parts. The problem itself is too well-known to study here in any analytical manner.

V. Résumé on the Elastic Deformation.

9. We have now ascertained that the deformation of a solid body should be composed of the dilatation, the rotation and another component which is neither dilatational nor distortional and also that the dilatational component and the distortional component are not independent but they are connected both in types and in magnitudes. Thus, to get an analytical result from the data of the land survey, the mere consideration of the dilatation, the rotation and the shear is not sufficient and also the classification of the deformations into the dilatation and the rotation has not so much meaning. Such classification would be equivalent to seek the order of the harmonics of the deformation of the first kind. It is also theoretically useless to take up only the resulting rotation (or only the resulting dilatation) of the movement of the earthcrust, excepting the case where the rotation or the dilatation is thought to be a type of the nuclei of the strain. In general, it would be reasonable to take the stress components or the ordinary strain components in the analysis of the observed data of the deformation of the land surface. It would be rather better at least to consider the displacements only relative to some assigned axes.

VI. The Components of Displacement in Inelastic Deformation.

10. The most theoretical definition of the plastic deformation is such that, i) the stresses of all kinds acting at any element of the material should be in equilibrium, ii) the stresses are connected with the displacement of the material in certain laws of stress-strain relations and of compatibility, iii) the maximum shear stress at any point should not exceed a given limit,[9] iv) the time variation fo the deformation due to the stresses, the duration of the acting force and etc. obey definite rules, v) the material in a plastic state sometimes flows as if it were an imcompressible matter.

Among these, the criterions i), iii) and v) are generally taken up by the recent students in applied mechanics. We think that the criterion v) is not so important as to consider it to be a necessary condition. Such a criterion is probably based upon the fact that the behaviour of the plastic material resembles that of the incompressible fluid. We believe that the plastic material may be compressible or incompressible. Even the elastic solid can be treated as compressible or incompressible. Thus, in this part, the material is considered to be compressible in general and to be incompressible in some particular cases.

Again, the condition iv) would be the most important nature in the plastic deformation. In spite of its importance in geophysical problems, this nature is in many cases diregarded by the students due to no importance in the problems of the engineering and also due to the complicated behaviour which is yet unknown. A special case of this, however, attracted the keen attention of the theoreticians[10] of some classical manner, though they do not seem to care for the other conditions. In the present case we will not take this criterion iv) under the assumption that the behaviour of the plastic materials during relatively short intervals of time is only considered.

We have taken into account of the condition ii) which seems to be often disregarded by the recent investigators.

11. Now, we take a particular case of a plane polar coordinates, which will shew the nature of the displacement in a somewhat simple manner.

For the sake of simplicity, take the equation of the equilibrium of an inelastic body in polar coordinates in the forms:

$$\text{i)}\quad \begin{aligned} &\frac{\partial \widehat{rr}}{\partial r}+\frac{1}{r}\frac{\partial \widehat{r\theta}}{\partial \theta}+\frac{\widehat{rr}-\widehat{\theta\theta}}{r}=0, \quad\ldots\ldots\ldots\ldots\ldots\ldots\ldots\ldots (56)\\ &\frac{\partial \widehat{r\theta}}{\partial r}+\frac{1}{r}\frac{\partial \widehat{\theta\theta}}{\partial \theta}+\frac{2\widehat{r\theta}}{r}=0, \quad\ldots\ldots\ldots\ldots\ldots\ldots\ldots\ldots (57)\end{aligned}$$

where $\widehat{rr}$, $\widehat{\theta\theta}$, $\widehat{r\theta}$ are normal and tangential stresses in r-, θ- and $r\theta$-directions.

---

[9] O. Mohr, *V. D. I.* (1900), (1901).
Th. v. Kármán, *V. D. I.*, (1911), 1749.

[10] L. Bolzmann, *Ann. d. Phys.*, Erg.-Bd., 7 (1876), 625.
H. Shôji, *Sci. Rep. Tohoku Imp. Univ.*, 18 (1929), No. 1, 1–10.

The condition of the maximum shear stress is expressed in the manner of St. Venant[12] as in the forms:

iii)
$$\widehat{r\theta}^2+\left(\frac{\widehat{rr}-\widehat{\theta\theta}}{2}\right)^2\leq K^2, \tag{58}$$

in which K is a constant.

The stress-displacement relation is of the form:

ii)
$$\frac{\widehat{r\theta}}{\dfrac{\partial v}{\partial r}-\dfrac{v}{r}+\dfrac{1}{r}\dfrac{\partial u}{\partial\theta}}=\frac{\widehat{rr}-\widehat{\theta\theta}}{2\left(\dfrac{\partial u}{\partial r}-\dfrac{1}{r}\dfrac{\partial v}{\partial\theta}-\dfrac{u}{r}\right)}, \tag{59}$$

where u, v[12] are the displacement of a material point in r- and θ-directions, though it may be better to take u, v as velocity components in the sense of Tresca.[13]

The condition v) may temporarily be expressed by

v)
$$\frac{1}{r}\frac{\partial}{\partial r}(ur)+\frac{1}{r}\frac{\partial v}{\partial\theta}=0. \tag{60}$$

From five equations (56), (57), (58), (59), (60), we can determine the values of $\widehat{rr}$, $\widehat{\theta\theta}$, $\widehat{r\theta}$, u and v. The equations actually used by the plasticians are only three of them, i.e. (56), (57) and (58).

As the equation (60) is not important and the equation (59) is ambiguous, we can write in place of (59) and (60) the equivalent equations of the following forms, which involve more or less the idea of v. Mises[14] and which are more improved than those of v. Mises.

v)
$$\frac{\lambda_1}{2(\lambda_1+\mu_1)}=\sigma_1 \quad \text{or equivalent formulae.}^{15)} \tag{61}$$

ii)′
$$\delta\widehat{rr}=\lambda_1\,\delta\Delta+2\mu_1\,\delta\frac{\partial u}{\partial r}, \tag{62}$$

ii)″
$$\delta\widehat{\theta\theta}=\lambda_1\,\delta\Delta+2\mu_1\,\delta\left(\frac{1}{r}\frac{\partial v}{\partial\theta}+\frac{u}{r}\right), \tag{63}$$

---

11) ST. VENANT, *loc. cit.*, 389.

12) (u, v) may be taken to be the displacement in the present case, but not to be the velocity of the point. Though the students in Europe seem to take u, v as the velocity components, yet we think that they should be taken as the displacements, as far as the statical case is taken up and Boltmann's idea is neglected.

13) TRESCA, *C. R.* (1867).

14) R. v. MISES, *Nachr. Ges. Wiss., Göttingen* (1913).

15) The meaning of the equivalent formulae is that λ_1 and μ_1 are known functions of the strain.

ii)‴ $$\delta\widehat{r\theta}=\mu_1\,\delta\left(\frac{\partial v}{\partial r}-\frac{v}{r}+\frac{1}{r}\frac{\partial u}{\partial\theta}\right), \qquad\qquad (64)$$

where λ_1 (or μ_1) is a given function of a certain typical strain; and

$$\Delta=\frac{1}{r}\frac{\partial}{\partial r}(ur)+\frac{1}{r}\frac{\partial v}{\partial\theta}. \qquad\qquad (65)$$

Here we shall understand that, in place of (59) and (60), four equations (61), (62), (63), (64) having two quantities λ_1 and μ_1 are introduced. λ_1 and μ_1 should not be invariables like Lame's constants; they may take various values for different magnitudes of the strains or the stresses. This nature will perhaps be suited to the deformation in which the stresses and the strains are not related linearly. The equation (61) expresses the degree of the compressibility and it will not be much erroneous that we take σ_1 is constant for the ordinary plastic state of a given material. It is not, however, constant in a large range[16] of plasticity where the hydrostatis pressure changes to many thousand atmosphere. If the material is practically incompressible at the plastic region, we may take $\lambda_1=\infty$ or $\sigma_1=\frac{1}{2}$. If the material fulfills Poisson's condition at the plastic state, we have $\lambda_1=\mu_1$ or $\sigma_1=\frac{1}{4}$. Thus the condition of the incompressibility is satisfied if we take $\sigma_1=\frac{1}{2}$ in (61). This nature can be easily comprehended if we know the fact that $\lambda_1\Delta$ has a finite value even in an incompressible material.

Again, the introduction of (62), (63), (64) will enable us to consider the equation of compatibility even for a complex case of stress-strain relation.

Now we have found seven equations (56), (57), (58), (61), (62), (63), (64) to determine seven unknown values $\widehat{rr}$, $\widehat{\theta\theta}$, $\widehat{r\theta}$, u, v, limiting value of λ_1 and that of μ_1.[17] The problem is, thus, reduced to be determinate and soluble in an easy manner.

To solve the equations of the example, we put first (62), (63), (64) in (56), (57). Then we obtain

$$(\lambda_1+2\mu_1)\frac{\partial\Delta}{\partial r}-\frac{2\mu_1}{r}\frac{\partial\varpi}{\partial\theta}=0, \qquad\qquad (66)$$

$$(\lambda_1+2\mu_1)\frac{1}{r}\frac{\partial\Delta}{\partial\theta}+2\mu_1\frac{\partial\varpi}{\partial r}=0, \qquad\qquad (67)$$

---

[16] P. W. BRIDGMAN, *Proc. Amer. Acad.*, 58 (1923), 166.

[17] The meaning of the limiting value of λ_1 or μ_1 is such that at such value of λ_1 or μ_1 (both are functions of the strain) the plastic deformation takes place owing to Mohr's condition of the maximum shearing stress.

where

$$\Delta=\frac{1}{r}\frac{\partial(ru)}{\partial r}+\frac{1}{r}\frac{\partial v}{\partial\theta},\qquad 2\varpi=\frac{1}{r}\frac{\partial(rv)}{\partial r}-\frac{1}{r}\frac{\partial u}{\alpha\theta}\;\ldots\ldots\ldots(68)$$

In these equations, λ_1 and μ_1 are constants to express the tangent of the neighbourhood of a certain point of a properly described stress-strain curve.

From (66), (67) we obtain

$$\left.\begin{aligned}\frac{\partial^2\Delta}{\partial r^2}+\frac{1}{r}\frac{\partial\Delta}{\partial r}+\frac{1}{r^2}\frac{\partial^2\Delta}{\partial\theta^2}=0,\\ \frac{\partial^2\varpi}{\partial r^2}+\frac{1}{r}\frac{\partial\varpi}{\partial r}+\frac{1}{r^2}\frac{\partial^2\varpi}{\partial\theta^2}=0.\end{aligned}\right\}\;\ldots\ldots\ldots\ldots\ldots\ldots(69)$$

The solutions of these can be expressed by

$$\left.\begin{aligned}\Delta&=\left(A_n r^n+B_n\frac{1}{r^n}\right)\begin{matrix}\sin\\ \cos\end{matrix}\Big\}n\theta,\\ 2\varpi&=\left(A_n' r^n+B_n'\frac{1}{r^n}\right)\begin{matrix}\cos\\ -\sin\end{matrix}\Big\}n\theta,\end{aligned}\right\}[n>1]\;\ldots\ldots\ldots\ldots(70)$$

and

$$\left.\begin{aligned}\Delta&=A_0\log r,\\ 2\varpi&=A_0'\log r.\end{aligned}\right\}[n=0]\;\ldots\ldots\ldots\ldots\ldots\ldots\ldots(70')$$

The displacements satisfying Δ in (70) and fulfilling the condition $\varpi=0$ are expressed by

$$\left.\begin{aligned}u_1&=\left[\frac{(n+2)}{4(n+1)}A_n r^{n+1}+\frac{(n-2)}{4(n-1)}\frac{B_n}{r^n}\right]\begin{matrix}\sin\\ \cos\end{matrix}\Big\}n\theta,\\ v_1&=\left[\frac{n}{4(n+1)}A_n r^{n+1}-\frac{n}{4(n-1)}\frac{B_n}{r^{n-1}}\right]\begin{matrix}\cos\\ -\sin\end{matrix}\Big\}n\theta.\end{aligned}\right\}\begin{bmatrix}n>1\text{ for }A_n\\ n>2\text{ for }B_n\end{bmatrix}\;..(71)$$

$$\left.\begin{aligned}u_1&=\frac{(\log r+1)}{2}B_1\begin{matrix}\cos\\ \sin\end{matrix}\Big\}\theta,\\ v_1&=\frac{\log r}{2}B_1\begin{matrix}\cos\\ -\sin\end{matrix}\Big\}\theta,\end{aligned}\right\}[n=1\text{ for }B_1]\;\ldots\ldots\ldots\ldots(71')$$

$$\left.\begin{aligned}u_0&=A_0\frac{r}{2}\left(\log r-\frac{1}{2}\right),\\ v_0&=0.\end{aligned}\right\}[n=0]\;\ldots\ldots\ldots\ldots\ldots\ldots(71'')$$

The displacements corresponding to ϖ in (70) with the condition, $\Delta=0$, are writted by

$$\left.\begin{aligned} u_2&=\left[\frac{n}{4(n+1)}\,A_n'\,r^{n+1}-\frac{n}{4(n+1)}\,\frac{B_n'}{r^{n-1}}\right]\left.\begin{matrix}\sin\\ \cos\end{matrix}\right\}n\theta,\\ v_2&=\left[\frac{(n+2)}{4(n+1)}\,A_n'\,r^{n+1}+\frac{(n-2)}{4(n-1)}\,\frac{B_n'}{r^{n-1}}\right]\left.\begin{matrix}\cos\\ -\sin\end{matrix}\right\}n\theta,\end{aligned}\right\}\begin{bmatrix}n>1 \text{ for } A_n'\\ n>2 \text{ for } B_n'\end{bmatrix}\ldots\ldots(72)$$

$$\left.\begin{aligned} u_1'&=\frac{\log r}{2}\,B_1'\left.\begin{matrix}\sin\\ \cos\end{matrix}\right\}\theta,\\ v_1'&=\frac{(\log r+1)}{2}\,B_1'\left.\begin{matrix}\cos\\ -\sin\end{matrix}\right\}\theta.\end{aligned}\right\}[n=1 \text{ for } B_1']\ldots\ldots\ldots\ldots(72')$$

$$\left.\begin{aligned} u_0'&=0,\\ v_0'&=B_0'\,\frac{r}{2}\left(\log r-\frac{1}{2}\right).\end{aligned}\right\}[n=0]\ldots\ldots\ldots\ldots\ldots\ldots(72'')$$

The displacements satisfying $\varDelta=\varpi=0$ are denoted by

$$\left.\begin{aligned} u_3&=\left(A_n''\,r^{n-1}+\frac{B_n''}{r^{n+1}}\right)\left.\begin{matrix}\sin\\ \cos\end{matrix}\right\}n\theta,\\ v_3&=\left(A_n''\,r^{n-1}-\frac{B_n''}{r^{n+1}}\right)\left.\begin{matrix}\cos\\ -\sin\end{matrix}\right\}n\theta.\end{aligned}\right\}[n>0]\ldots\ldots\ldots\ldots(73)$$

It is worth noticing that the displacements belonging to the system of (71) and those attached to the system of (72) are not independent; they are connected by the formulae of the types:

$$A_n'=-\frac{\lambda_1+2\mu_1}{\mu_1}\,A_n,\qquad B_n'=\frac{\lambda_1+2\mu_1}{\mu_1}\,B_n,\ \ldots\ldots\ldots\ldots(74)$$

while the solutions in (73) give quite independent displacements which are free from the dilatation and the rotation.

Now suppose that λ_1 is the function of $\varDelta$ such that

$$\lambda_1=f(\varDelta),\ \ldots\ldots\ldots\ldots\ldots\ldots\ldots\ldots(75)$$

then, by means of (61), we find

$$\mu_1=\frac{1-2\sigma_1}{2\sigma_1}\,f(\varDelta),\ \ldots\ldots\ldots\ldots\ldots\ldots\ldots(76)$$

so that, from (62), (63), (64), we get

$$\left.\begin{aligned}\widehat{rr}&=\int_0^{\varDelta_1}f(\varDelta)\left\{1+\frac{1-2\sigma_1}{\sigma_1}\,\frac{\partial\dfrac{\partial u}{\partial r}}{\partial\varDelta}\right\}d\varDelta,\\ \widehat{\theta\theta}&=\int_0^{\varDelta_1}f(\varDelta)\left\{1+\frac{1-2\sigma_1}{\sigma_1}\,\frac{\partial\left(\dfrac{1}{r}\dfrac{\partial u}{\partial\theta}+\dfrac{u}{r}\right)}{\partial\varDelta}\right\}d\varDelta,\end{aligned}\right\}\ldots\ldots\ldots\ldots(77)$$

$$\left.\widehat{r\theta}=\int_0^{\Delta_1}\frac{1-2\sigma_1}{2\sigma_1}f(\Delta)\frac{\partial\left(\frac{\partial v}{\partial r}-\frac{v}{r}+\frac{1}{r}\frac{\partial u}{\partial \theta}\right)}{\partial \Delta}d\Delta,\quad\right|$$

where $\frac{\partial u}{\partial r}$, $\frac{1}{r}\frac{\partial v}{\partial \theta}+\frac{u}{r}$, $\frac{\partial v}{\partial r}-\frac{v}{r}+\frac{1}{r}\frac{\partial u}{\partial \theta}$ are the known functions of Δ having the paramater $f(\Delta)$. When we apply the boundary conditions of stresses to represent A_n'' or B_n'' in terms of A_n or B_n, the parameter $f(\Delta)$ will necessarily be induced.

Now, the limit of the integration Δ_1 at various positions can be determined for the plastic state by means of the equation (58). i.e.

$$\widehat{r\theta}^2+\left(\frac{\widehat{rr}-\widehat{\theta\theta}}{2}\right)^2=K^2. \qquad\qquad (58')$$

When the left-hand side of this equation becomes independent of r and θ, the derived relation has its applicability to all the positions; but, if it were not so, the problem becomes somewhat complicated and we must need some special consideration from the start.

Again, we have seen in this section that the displacements in an inelastic deformation are composed of two kinds, one of which is dilatational–distortional and the other is free from the dilatation and the rotation. This nature is quite similar to the case of an elastic deformation.

The application of the present theory to actual examples has been left to the future occasion, as our present intention is not to find the solutions of a plastic problem, but is to find a component of the displacement which is neither dilatational nor distortional.

12. Although we have treated in the preceding section some special case of the equations of the inelastic deformation, we can generalise the problem to more extended cases without any difficulty. Thus, in the case of the plane Cartesian coordinates, we get

$$\left.\begin{aligned}\frac{\partial X_x}{\partial x}+\frac{\partial X_y}{\partial y}=0,\\ \frac{\partial X_y}{\partial x}+\frac{\partial Y_y}{\partial y}=0,\end{aligned}\right\} \qquad\qquad (83)$$

$$\left(\frac{X_x-Y_y}{2}\right)^2+X_y^2\leqq K^2,\text{[18]} \qquad\qquad (84)$$

---

[18] The extended expressions of this equation of the limitation may be obtained in the manner of HENCKY, *Zeits. f. A. M. M.* **4** (1924), 323 & *V. D. I.* **69** (1925) 695.

$$\frac{\lambda_1}{2\,(\lambda_1+\mu_1)}=\sigma_1 \qquad \text{.........................}(85)$$

$$\left.\begin{aligned} \delta X_x &= \lambda_1\,\delta\Delta+2\mu_1\,\delta\,\frac{\partial u}{\partial x}, \\ \delta Y_y &= \lambda_1\,\delta\Delta+2\mu_1\,\delta\,\frac{\partial v}{\partial y}, \\ \delta X_y &= \mu_1\,\delta\left(\frac{\partial v}{\partial x}+\frac{\partial u}{\partial y}\right), \end{aligned}\right\} \qquad \text{.....................}(86)$$

where $\Delta=\frac{\partial u}{\partial x}+\frac{\partial v}{\partial y}$, and u, v are the components of displacement in x- and y-directions.

In a similar manner we can arrive at the equations in the cases of spherical, cylindrical and other coordinates.

VII. Some Notes on the Prevailing Theory of the Plasticity, with a Reference to the Study on the Distribution of the Cracks in a Body.

13. The present paper has aimed at the discovery of a component of the displacement which is neither dilatational nor distortional. The problem, however, is concerned with the deformation of the earthcrust, so that it will not be without significance to give some discussions on the theory of plasticity.

The theory of plasticity now prevailing among the students in applied mechanics should be discussed. In the first place, the equations[19] actually used in the calculations are limited only to those of the stress-equilibrium and that of the limiting value of the maximum shear stress. A little consideration will enable us to know that the conditions of the compatibility through the displacements of the material points are most important[20] excepting very simple cases as the deformation of simple bars. In our present idea these conditions have been taken into consideration. In the second place, the theory of plasticity developed by the european students in the engineering side does not involve the nature of the time effect on the behaviour of the plastic deformation, which shall not be left in the geophysical problems. As this effect will perhaps act during such a long time as many thousand years, we have neglected such behaviour in the present paper.

---

[19] C. Carathéodory & E. Schmidt, *Zeits. f. A. M. and M.*, 3 (1923), 468.
L. Prandtl, *Proc. 1. Int. Nat. Congr. Appl. Mech.* (1924), 43.
Th. v. Kármán, *Verh. 2. Int. Kong. f. Tech.-Mech.* (1927), 23.

[20] W. Jennne, *Z. A. M. M.*, 8 (1928), 18–44.

14. Next, we have to draw the attention of those who apply the plastic theory on the problem of the earth pressure or the movement of the earthcrust. The students seem to explain frequently the figures and the positions of the cracks only by the theory of the plasticity and they always assert that the theory of the elasticity can never explain the figures and the positions of the cracks or slip surface. We can not think that their idea would be true. Though the equation of the limiting value of the maximum shear stress gives us the extent of the proportionality of stress and the region of the plastic part, we can not yet determine the figure and the position of the sharp cracks as observed in a finite scale. Such indeterminateness can be clearly known from the mathematical equations of the plasticity. The observed figures and the position of the cracks are often produced by the boundary conditions either in plastic or in elastic state of the materials.

We think that these cracks are not formed by the general movements of the plastic body, but these are produced in an early stage of the deformation, which is principally of the elastic nature, at some heavy stressed portion[21] of the material. Thus the creation of the cracks or the slip surfaces may rather take place in an elastic body. Indeed, the theoretical plasticians in England seem to consider the deformed plastic body as an elactic body having an accumulation of cracks as well as the dead spaces of elastic regions.

The problem of so-called block movements, which are advocated by Japanese seismologists of the recent time in the manner of the physiographists, involves yet many doubtful points from the true sense of the plastic theory as well as from some other theoretical considerations.

VIII. Concluding Remarks.

15. We have now found some facts which may be important on the geophysical problem as well as on the applied mechanics. Although the general theory was considered by means of somewhat restricted examples, yet we may say that the theory would never lose its applicability to all cases of the problem. This can be clearly known in the light of other problems of mechanics in which the similar examples contribute very often to the determination of the general nature. To our dissatisfaction the various cases of the inelastic deformation could not be solved owing to the lack of time. These will be shortly published in conclusive forms.

---

[21] K. Suyehiro, *Engineering*, (Sept. 1, 1911).
C. E. Inglis, *Trans. Inst. Nav. Arch., London*, **60** (1913), 219.
A. A. Griffith, *Phil. Trans. Ray, Soc.*, **221** (1921), 163–198.
R. V. Southwell & H. J. *Gough, Phil. Mag.*, [7] **1** (1926), 71–96.
I. Nakayama, *Journ. Soc. Mech. Eng., Tokyo*, **29** (1926).

The principal results of the present investigation are as follows:

1. The deformation of an elastic solid body in equilibrium is composed of the dilatation, the rotation and another component which is neither dilatational nor rotational and which is an important component in affording the stresses or the strains.

2. The dilatational and the rotational components of displacement are not independent; the ratio of the constant factors belonging to these is determined only by the elastic constants of the material and the order of the harmonics of the straining. The component which is not dilatational nor rotational has an independent arbitrary constant factor.

3. The types of the solutions of the dilatational and the rotational components resemble one another, while that of the third component takes a different form.

4. By applying the present method of calculation to various cases of examples, we find easily the solutions of the various problems. Especially the solution of the heterogeneous distributions of the material in the displacements and stresses gives us the fact that the so-called block-movement may be nothing else the effect of such a heterogeneity of physical constants on the movements of the material points.

5. In an inelestic solid body, the similar nature as in the elastic body manifests itself. The method of the addition of all components to obtain a complete solution in this case is somewhat complicated.

6. A new idea of investigating the problem of the plasticity is obtained. The defect of the prevailing theory of plasticity, in which the condition of the compatibility is neglected, can be replaced by some improved theory.

7. The unnecessary condition of the incompressibility of the plastic material may be replaced by another controllable equation indicating the state of the material.

8. It is pointed out that the position and the number of the cracks in a strained material cannot be explained by the prevailing plastic theory to the same degree as the ordinary application of the elastic theory and that the above question can be solved even in the theory of elasticity by considering the effect of all the boundary conditions as in the manner of the students in England.

9. It is also added that the so-called block-movement advocated by the

seismologists cannot be explained by the plastic theory; rather it involves a great deal of doubtful points when it is considered from the true theory of inelasticity as well as from some other theoretical points.

---

21. 固體のダイレテーションとロテーションとに無關係な變位に就いて

地震研究所 妹澤克惟
西村源六郎

全く普遍的ではないが、成るべく理想的な數種の計算によつて、變形固體にダイレテーション及びロテーションに無關係な變位が存在する事を示し、併せて不完全な彈性變形の事にも言ひ及ぼした。不完全な彈性變形の計算は種々面白い場合があるが、時日の都合で餘り研究が進まなかつた。全體として主要な結果を摘錄すれば、

1. 固體が靜的變形を行ふ時、ダイレテーションにもロテーションにも無關係な變位が存在する。而もこの變位が固體の應力や歪みを與へる事には重要な役目をするものである。
2. ダイレテーションの變位とロテーションの變位とは互に無關係でなく、各の係數の間には固體の彈性恒數や變形次數によつて定まる關係が存在する。然るにダイレテーションとロテーションに無關係な變位の係數は全く獨立のものである。
3. ダイレテーションに相當する變位とロテーションに相當する變位とは其解が類似型をして居るが、ダイレテーションとロテーションとに無關係な變位は別の型を持つ。
4. この論文の計算法を多くの例題にあてはめて、種々の場合の解が容易に得られた。中でも材料の異質混合の場合は、所謂地塊運動の如きものが、材料の斯樣な分布によつて說明してもよい事を我々に敎へて吳れる。
5. 不完全な彈性體の場合にも彈性體の場合と殆んど同樣な數學的性質がある事がわかる。但しこの場合は充分な解を得る爲め各分變位を加へ合せる事が大分複雜となる。
6. この論文ではプラスチツク體の新しい研究方法を示してあるが、殊に現在流行して居る解法には鈌けて居る所の變位の融通を考慮した方法を與へて置いた。
7. 以前のプラスチツク力學に存在する材料の非壓縮性といふ條件は餘り意味がないから、之等の性質に相當の自由を許す別の條件で上述の條件に代つて置き換へた。
8. 歪み材料の切れ目の位置や數は現在流體するプラスチツク論では、彈性力學を普通の方法で均一材料に應用するのと同樣の程度に役に立たぬ事を示し、又之等は英國の學者がやつて居る樣に種々の境界條件を充分に考慮して所々高歪になつた場所を求める方法によれば彈性力學の方法でも可なりの程度まで解決出來るものである事を指摘した。
9. 地震學者が近來唱へる地塊運動なるものは純粹のプラスチツク論に照す時は說明出來るどころか反つ都合が惡く、倘又別の見地からしても可なり怪しいものである事を附加へて置いた。

22. *Generation of Rayleigh-waves from a Sheet of Internal Sources.*

By **Katsutada SEZAWA,**

Earthquake Research Institute.

(Received Sept. 20, 1929.)

1. In this paper I am going to show how Rayleigh-waves are generated from a splitting or a sliding surface in the interior of a semi-infinite solid body. The theory is based upon the conception that the splitting or the sliding surface is equivalent to a sheet of internal nuclei of disturbances. Although the ordinary treatment of the elastic waves under the assumption that they are transmitted from a point source can never violate the general mechanism of the generation of the waves and rather such a treatment gives us the rigorous and incomplex confirmation of the problem, yet this established manner of the treatment acquires frequently various objections from the side of the practical seismologists. To answer to the consideration of these practicians I have introduced the thought of a sheet of internal sources, which may, from the practical point of view, resemble the splitting or the sliding surface in the solid body.

An assigned distribution of energy at the surface of the crack may be obtained by applying the various strengths of the intensity to each elementary source which forms the sheet.

It may be questioned whether the waves in the neighbourhood of each source are transmitted with the velocity which is proper to the generation of the waves from a point source. A little consideration will enable us to know that the velocity at every point about the crack is not to be constant. It depends on the conditions at the boundary of the crack. A special case of this will be seen in one[1] of my papers where the propagation of elastic waves from a small elliptic or a spheroidal source of some regular form is investigated.

In the present case the crack is supposed to be so long compared with the wave length that the general form of the crack has no much effect on the motion of the solid body in the neighbourhood of the aperture. The criterion of the sheet of the sources seems to be based upon a most suitable reasoning.

---

[1] K. SEZAWA, "Propagation of Elastic Waves from an Elliptic or a Spheroidal Origin," *Bull. Earthq. Res. Inst.*, **2** (1927), 29–48.

I. Two-dimensional Propagation.

2. We shall take the free surface of a semi-infinite solid to be $z=0$ and also that the positive sense of the axis of z is directed downwards. Let the sheet of the sources lie in a straight line making an angle θ with the horizontal line and suppose that the dilatational disturbance at the depth ξ is to be

$$-ie^{i\sigma t}H_0^{(2)}\{h\sqrt{(x-\xi\cot\theta)^2+(z-\xi)^2}\}f(\xi), \qquad\ldots\ldots\ldots\ldots(1)$$

where $h^2=\dfrac{\rho\sigma^2}{\lambda+2\mu}$, ρ is the density of the solid and λ, μ are Lame's elastic constants.

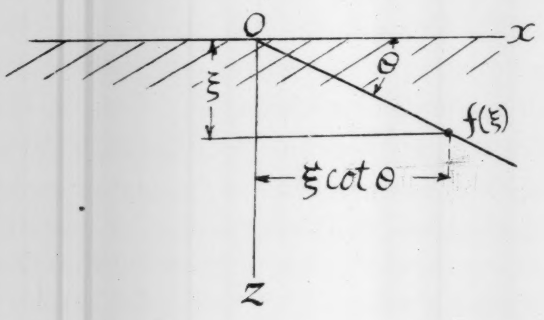

The expression (1) gives us an element of the sources in a splitting line denoted by

$$z=x\tan\theta. \qquad\ldots\ldots\ldots\ldots(2)$$

The generated dilatational waves are then given by

$$\Delta_0'=\frac{e^{i\sigma t}}{\pi}\int_0^\infty f(\xi)\,d\xi\operatorname{cosec}\theta\int_{-\infty}^\infty\frac{e^{\alpha(z-\xi)+ik(x-\xi\cot\theta)}}{\alpha}\,dk. \qquad\ldots\ldots\ldots\ldots(3)$$

In this expression use has been made of

$$H_0^{(2)}(h\sqrt{x^2+z^2})=\frac{i}{\pi}\int_{-\infty}^\infty\frac{e^{-\alpha z+ikx}}{\alpha}\,dk,^{2)} \qquad\ldots\ldots\ldots\ldots(4)$$

where $\alpha^2=k^2-h^2$.

Superposing the effect Δ_0'' of the reflection at the free surface, we obtain

---

2) H. LAMB, *Phil. Trans. Roy, Soc.*, **203** (1904).

$$\varDelta_0=\varDelta_0'+\varDelta_0''=\frac{2e^{i\sigma t}}{\pi}\int_0^\infty f(\xi)\,d\xi\,\operatorname{cosec}\theta\int_{-\infty}^{\infty}\frac{\operatorname{ch}\alpha z\;e^{-\alpha\xi+ik(x-\xi\cot\theta)}}{\alpha}\,dk.\,\ldots\,(5)$$

The corresponding components of displacement in x- and z-directions are written in the forms:

$$\left.\begin{aligned}u_0&=-\frac{1}{h^2}\frac{\partial\varDelta_0}{\partial x}\\&=-2\frac{ie^{i\sigma t}}{\pi h^2}\int_0^\infty f(\xi)\,d\xi\,\operatorname{cosec}\theta\int_{-\infty}^{\infty}\frac{\operatorname{ch}\alpha z\;e^{-\alpha\xi+ik(x-\xi\cot\theta)}}{\alpha}\,k\,dk,\\w_0&=-\frac{1}{h^2}\frac{\partial\varDelta_0}{\partial z}\\&=-2\frac{e^{i\sigma t}}{\pi h^2}\int_0^\infty f(\xi)\,d\xi\,\operatorname{cosec}\theta\int_{-\infty}^{\infty}\operatorname{sh}\alpha z\;e^{-\alpha\xi+ik(x-\xi\cot\theta)}\,dk.\end{aligned}\right\}\ldots.(6)$$

These waves give no tangential stress on $z=0$, but they give us a certain normal stress. We may superpose on these some free waves (without tangential stress) accumulated in the neighbourhood of the surface to annul the normal stress on that surface. The free waves are expressed by

$$\left.\begin{aligned}u_1&=\frac{2i\,e^{i\sigma t}}{\pi h_2}\int_0^\infty f(\xi)\,d\xi\,\operatorname{cosec}\theta\int_{-\infty}^{\infty}\frac{(2k^2-j^2-2\alpha\beta)(2k^2-j^2)}{\alpha F(k)}\\&\qquad\qquad\times e^{-\alpha\xi+ik(x-\xi\cos\theta)}\,k\,dk,\\w_1&=\frac{2e^{i\sigma t}}{\pi h^2}\int_0^\infty f(\xi)\,d\xi\,\operatorname{cosec}\theta\int_{-\infty}^{\infty}\frac{j^2(2k^2-j^2)}{F(k)}\,e^{-\alpha\xi+ik(x-\xi\cot\theta)}\,dk,\end{aligned}\right\}\ldots..(7)$$

provided

$$F(k)=(2k^2-j^2)^2-4k^2\alpha\beta,\,\ldots\ldots\ldots\ldots\ldots\ldots\ldots(8)$$

$$\alpha^2=k^2-h^2,\quad\beta^2=k^2-j^2,\quad j^2=\frac{\rho\sigma^2}{\mu}.\,\ldots\ldots\ldots\ldots\ldots(9)$$

The resultant displacement on $z=0$ is thus written by

$$\left.\begin{aligned}u=u_0+u_1&=\frac{4ie^{i\sigma t}}{\pi h^2}\int_0^\infty f(\xi)\,d\xi\,\operatorname{cosec}\theta\int_{-\infty}^{\infty}\frac{\beta kj^2\,e^{-\alpha\xi+ik(x-\xi\cot\theta)}}{F(k)}\,dk,\\w=w_0+w_1&=\frac{2e^{i\sigma t}}{\pi h^2}\int_0^\infty f(\xi)\,d\xi\,\operatorname{cosec}\theta\int_{-\infty}^{\infty}\frac{(2k^2-j^2)\,j^2\,e^{-\alpha\xi+ik(x-\xi\cot\theta)}}{F(k)}\,dk.\end{aligned}\right\}..(10)$$

Now we know that

$$\left.\begin{aligned}&\int_{-\infty}^{\infty}\frac{\beta j^2k\,e^{-\alpha\xi+ik(x-\xi\cot\theta)}}{F(k)}\,dk\sim\frac{4\pi i\beta_1j^2\kappa}{F'(\kappa)}\,e^{-\alpha_1\xi}\cos\kappa(x-\xi\cot\theta),\\&\int_{-\infty}^{\infty}\frac{j^2(2k^2-j^2)\,e^{-\alpha\xi+ik(x-\xi\cot\theta)}}{F(k)}\,dk\sim-\frac{4\pi j^2(2\kappa^2-j^2)}{F'(\kappa)}\,e^{-\alpha_1\xi}\sin\kappa(x-\xi\cot\theta),\end{aligned}\right\}$$

$$\ldots\ldots\ldots\ldots\ldots\ldots(11)$$

where κ is the real, positive root of $F(k)=0$ and α_1, β_1 are the corresponding values of α, β. These lead us to the results that

$$\left.\begin{aligned} u &\approx -\frac{16e^{i\sigma t}\beta_1 j^2\kappa}{h^2F'(\kappa)}\operatorname{cosec}\theta\int_0^\infty f(\xi)\,e^{-\alpha_1\xi}\cos\kappa\,(x-\xi\cot\theta)\,d\xi,\\ w &\approx -\frac{8e^{i\sigma t}j^2(2\kappa^2-j^2)}{h^2F'(\kappa)}\operatorname{cosec}\theta\int_0^\infty f(\xi)\,e^{-\alpha_1\xi}\sin\kappa\,(x-\xi\cot\theta)\,d\xi.\end{aligned}\right\}\quad ..(12)$$

These expressions are suitable to the transmission of waves of a finite extent of a harmonic train. To get the progressive waves of an infinite train, we must remember that the above expressions give a combination of two systems of progressive waves. The analysed waves are thus given by

$$\left.\begin{aligned} u &\approx -\frac{8\beta_1 j^2\kappa}{h^2F'(\kappa)}\operatorname{cosec}\theta\int_0^\infty f(\xi)\,e^{-\alpha_1\xi}\cos\{\kappa\,(x-\xi\cot\theta)\mp\sigma t\}\,d\xi,\\ v &\approx -\frac{4j^2(2\kappa^2-j^2)}{h^2F'(\kappa)}\operatorname{cosec}\theta\int_0^\infty f(\xi)\,e^{-\alpha_1\xi}\sin\{\kappa\,(x-\xi\cot\theta)\mp\sigma t\}\,d\xi.\end{aligned}\right\}\quad ..(13)$$

In these the negative and positive signs should be applied to each system of waves progressing towards the positive and negative directions of x-axis.

3. Let us suppose that

$$f(\xi)=\text{constant}=c,\quad ....(14)$$

then the surface displacement at any time, say $t=0$, is expressed by

$$\left.\begin{aligned} u &= -\frac{8\beta\, j^2 c}{h^2F'(\kappa)}\left\{\operatorname{cosec}\theta\,\frac{\frac{\alpha_1}{\kappa}\cos\kappa x+\cot\theta\sin\kappa x}{\left(\frac{\alpha_1}{\kappa}\right)^2+\cot^2\theta}\right\},\\ w &= -\frac{4j^2(2\kappa^2-j^2)\,c}{h^2\kappa F'(\kappa)}\left\{\operatorname{cosec}\theta\,\frac{\frac{\alpha_1}{\kappa}\sin\kappa x-\cot\theta\cos\kappa x}{\left(\frac{\alpha_1}{\kappa}\right)^2+\cot^2\theta}\right\}.\end{aligned}\right\}\quad ......(15)$$

The absolute values of $\{\ \}$ for different values of θ in the above equations are given by the lines named $n=1$ in Fig. 1 and Fig. 2 and the lines named $a=0$ in Fig. 3 and Fg. 4.

The fact that the amplitudes of the generated surface waves in an incompressible material are independent of the inclination of the splitting surface is apparently curious.

4. Next, consider that

$$f(\xi)=c^n\,\xi^{n-1},\quad ....(16)$$

then the surface displacement at $t=0$ is written by

$$\left.\begin{aligned} u&=-\frac{8\beta_1 j^2}{h^2F'(\kappa)}\left(\frac{c}{\kappa}\right)^n\left\{\operatorname{cosec}\theta\sin^n\omega\,(\cos\kappa x\cos n\omega+\sin\kappa x\sin n\omega)\right\},\\ w&=-\frac{4j^2\,(2\kappa^2-j^2)}{h^2\,\kappa F'(\kappa)}\left(\frac{c}{\kappa}\right)^n\left\{\operatorname{cosec}\theta\sin^n\omega\,(\sin\kappa x\cos n\omega-\cos\kappa x\sin n\omega)\right\},\end{aligned}\right\} \qquad \text{(17)}$$

where $\tan\omega=\cot\theta\Big/\dfrac{\alpha_1}{\kappa}$.

The absolute values of $\{\ \}$ of the above expressions in the cases $n=1$, 2, 3, 4 are plotted in Fig. 1 and Fig. 2. Fig. 1 is the propagation of the waves in a medium whose Poisson's ratio is $\frac{1}{4}$, while Fig. 2 is that in an incompressible solid body. It will be seen that the amplitude of Rayleigh-waves has the maximum value at $\theta=90°$ and it decreases as the angle θ is diminished. It will also be noted that the decrease of the amplitude with the diminution of the angle θ is conspicuous for the greater values of n.

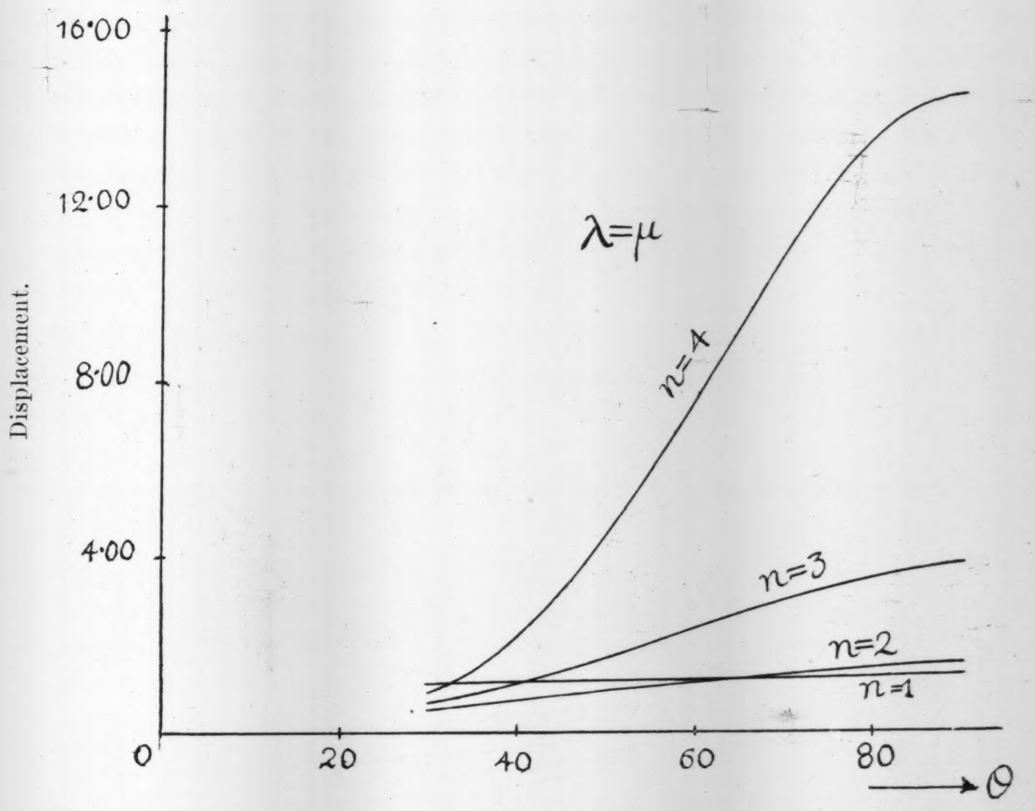

Fig. 1.

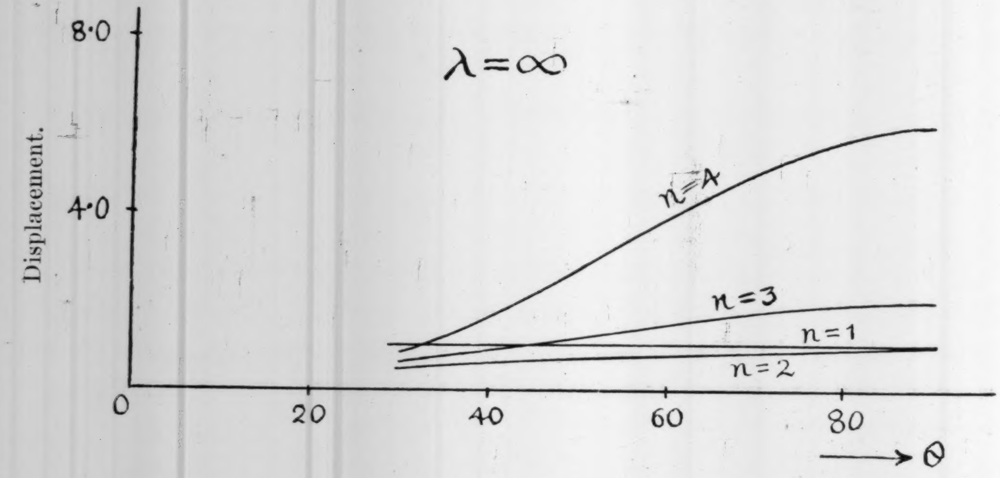

Fig. 2.

5. Now we suppose that

$$f(\xi)=ce^{-a\xi}, \qquad \dots\dots\dots\dots\dots\dots\dots\dots (18)$$

then we find

$$\left.\begin{aligned} u&=-\frac{8\beta_1 j^2 c}{h^2F'(\kappa)}\left\{\operatorname{cosec}\theta\,\frac{\dfrac{\alpha_1+a}{\kappa}\cos\kappa x+\cot\theta\sin\kappa x}{\left(\dfrac{\alpha_1+a}{\kappa}\right)^2+\cot^2\theta}\right\},\\ v&=-\frac{4j^2(2\kappa^2-j^2)c}{h^2\kappa F'(\kappa)}\left\{\operatorname{cosec}\theta\,\frac{\dfrac{\alpha_1+a}{\kappa}\sin\kappa x-\cot\theta\cos\kappa x}{\left(\dfrac{\alpha_1+a}{\kappa}\right)^2+\cot^2\theta}\right\}.\end{aligned}\right\}\dots\dots(19)$$

The absolute values of { } of the above expressions in the cases $a/\kappa=0$,

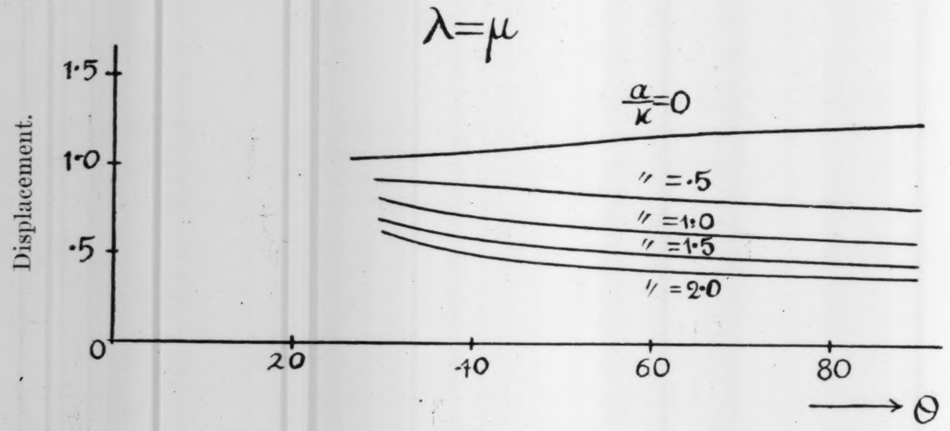

Fig. 3.

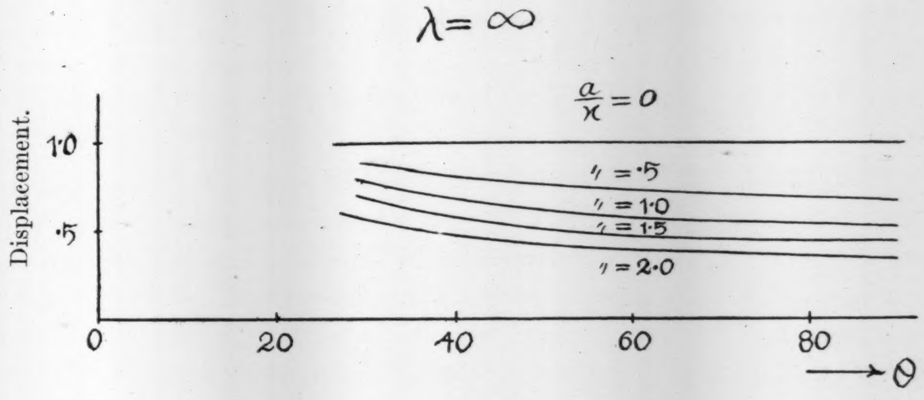

Fig. 4.

0.5, 1.0, 1.5, 2.0 are plotted in Fig. 3 and Fig. 4. Fig. 3 gives us the case $\lambda=\mu$ and Fig. 4 gives us that of $\lambda=\infty$. It will be noticed that the greater the value of a/κ becomes, the more diminishes the amplitude of the resulting surface waves. This can be easily anticipated from the assumed functions of the origin. The more remarkable fact is that, for a large value of a/κ the displacement is diminished as θ is increased, while, for a small value of a/κ, say $a/\kappa=0$, the displacement is enlarged with the increase of θ. This conforms with the result of the preceding section, in which the displacement increases with θ for a greater value of n.

6. If we put

$$\left.\begin{array}{ll} f(\xi)=c, & \xi_1<\xi<\xi_2 \\ f(\xi)=0, & 0<\xi<\xi_1 \text{ and } \xi_2<\xi<\infty \end{array}\right\} \quad \ldots\ldots\ldots\ldots (20)$$

we get without any difficulty the following result:

$$\begin{aligned} u=-\frac{8\beta_1 j^2 c}{h^2F'(\kappa)}\frac{\operatorname{cosec}\theta}{\left(\frac{\alpha_1}{\kappa}\right)^2+\cot^2\theta}\Bigg[&\cos\kappa x\left\{e^{-\alpha_1\xi_2}\left(\cot\theta\sin\overline{\kappa\cot\theta\xi_2}\right.\right. \\ &\left.-\frac{\alpha_1}{\kappa}\cos\overline{\kappa\cot\theta\xi^2}\right) \\ &\left.-e^{-\alpha_1\xi_1}\left(\cot\theta\sin\overline{\kappa\cot\theta\xi_1}-\frac{\alpha_1}{\kappa}\cos\overline{\kappa\cot\theta\xi_1}\right)\right\} \\ -\sin\kappa x&\left\{e^{-\alpha_1\xi_2}\left(\cot\theta\cos\overline{\kappa\cot\theta\xi_2}+\frac{\alpha_1}{\kappa}\sin\overline{\kappa\cot\theta\xi_2}\right)\right. \\ &\left.-e^{-\alpha_1\xi_1}\left(\cot\theta\cos\overline{\kappa\cot\theta\xi_1}+\frac{\alpha_1}{\kappa}\sin\overline{\kappa\cot\theta\xi_1}\right)\right\}\Bigg], \end{aligned}$$

$$w=-\frac{4j^2(2\kappa^2-j^2)\,c}{h^2\kappa F'(\kappa)}\,\frac{\operatorname{cosec}\theta}{\left(\frac{\alpha_1}{\kappa}\right)^2+\cot^2\theta}\left[\sin\kappa x\left\{\begin{matrix}\text{The same expression}\\ \text{as that in the first}\\ \text{bracket of the above}\end{matrix}\right\}\right.$$

$$\left.+\cos\kappa x\left\{\begin{matrix}\text{The same expression}\\ \text{as that in the second}\\ \text{bracket of the above}\end{matrix}\right\}\right] \qquad \ldots\ldots\ldots\ldots\ldots\ldots\ldots\ldots\ldots(21)$$

The numerical computation of the above equations has been omitted in the present paper.

7. If the source is at the depth η from the surface and if

$$f(\xi)=c, \qquad (-\xi_1<\xi<\xi_1, \quad \theta=0). \ldots\ldots\ldots\ldots\ldots(22)$$

then we obtain

$$\left.\begin{aligned} u_0&=\frac{16\beta_1 j^2 c}{h^2 F'(\kappa)}\,e^{-\alpha_1\eta}\cos\kappa x\sin\kappa\xi,\\ v_0&=\frac{8j^2(2\kappa^2-j^2)\,c}{h^2\kappa F'(\kappa)}\,e^{-\alpha_1\eta}\sin\kappa x\sin\kappa\xi.\end{aligned}\right\}\ldots\ldots\ldots\ldots(23)$$

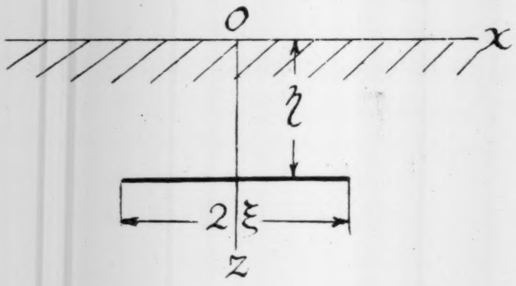

8. When the disturbance is of a sliding type, the method of the analysis is somewhat modified. In this case we should consider the distortional disturbance as an element of the sources. Let the intensity of an element be

$$-ie^{i\sigma t}H_0^{(2)}\{j\sqrt{(x-\xi\cot\theta)^2+(z-\xi)^2}\}\,f(\xi), \quad \ldots\ldots\ldots\ldots(24)$$

where $j^2=\frac{\rho\sigma^2}{\mu}$, then the general distortional waves from the sliding surface

$$z=x\tan\theta, \quad \ldots\ldots\ldots\ldots\ldots\ldots\ldots\ldots(2')$$

are expressed in the forms:

$$2\varpi_0'=\frac{e^{i\sigma t}}{\pi}\int_0^\infty f(\xi)\,d\xi\operatorname{cosec}\theta\int_{-\infty}^{\infty}\frac{e^{\beta(z-\xi)+ik(x-\xi\cot\theta)}}{\beta}\,dk, \ldots\ldots(25)$$

where $\beta^2=k^2-j^2$.

Superposing the effect of the images, we obtain finally

$$\left.\begin{aligned} u_0&=\frac{2e^{i\sigma t}}{\pi j^2}\int_0^\infty f(\xi)\,d\xi\ \mathrm{cosec}\,\theta\int_{-\infty}^\infty \mathrm{sh}\,\beta z\ e^{-\beta\xi+ik(x-\xi\cot\theta)}\,dk,\\ w_0&=-\frac{2ie^{i\sigma t}}{\pi j^2}\int_0^\infty f(\xi)\,d\xi\ \mathrm{cosec}\,\theta\int_{-\infty}^\infty \frac{\mathrm{ch}\,\beta z}{\beta}\,e^{-\beta\xi+ik(x-\xi\cot\theta)}\,k\,dk.\end{aligned}\right\}\ldots\ldots(26)$$

The normal stress at the surface due to this displacement is nil, but the tangential stress is in existence. To cancel the tangential stress, the following surface waves should be superposed:

$$\left.\begin{aligned} u_1&=\frac{2e^{i\sigma t}}{\pi j^2}\int_0^\infty f(\xi)\,d\xi\ \mathrm{cosec}\,\theta\int_{-\infty}^\infty \frac{[(2k^2-j^2)\,e^{-\beta z}-2k^2\,e^{-\alpha z}]\,(2k^2-j^2)}{F(k)}\\ &\qquad\qquad\times e^{-\beta\xi+ik(x-\xi\cot\theta)}\,dk,\\ w_1&=\frac{2ie^{i\sigma t}}{\pi j^2}\int_0^\infty f(\xi)\,d\xi\ \mathrm{cosec}\,\theta\int_0^\infty \frac{[(2k^2-j^2)\,e^{-\beta z}-2\alpha\beta\,e^{-\alpha z}]\,(2k^2-j^2)}{\beta F(k)}\\ &\qquad\qquad\times e^{-\beta\xi+ik(x-\xi\cot\theta)}\,kdk.\end{aligned}\right\}$$

$$\ldots\ldots\ldots\ldots\ldots\ldots(27)$$

The composed waves gives the surface displacement of the type

$$\left.\begin{aligned} u=u_0+u_1&=-\frac{2e^{i\sigma t}}{\pi}\int_0^\infty f(\xi)\,d\xi\ \mathrm{cosec}\,\theta\int_{-\infty}^\infty \frac{(2k^2-j^2)}{F(k)}\,e^{-\beta\xi+ik(x-\xi\cot\theta)}\,dk,\\ w=w_0+w_1&=\frac{4ie^{i\sigma t}}{\pi}\int_0^\infty f(\xi)\,d\xi\ \mathrm{cosec}\,\theta\int_{-\infty}^\infty \frac{\alpha k}{F(k)}\,e^{-\beta\xi+ik(x-\xi\cot\theta)}\,dk.\end{aligned}\right\}(28)$$

Proceeding in the same manner as before, we arrive at

$$\left.\begin{aligned} u&\approx\frac{8e^{i\sigma t}(2\kappa^2-j^2)}{F'(\kappa)}\,\mathrm{cosec}\,\theta\int_0^\infty f(\xi)\,e^{-\beta_1\xi}\sin\kappa\,(x-\xi\cot\theta)\,d\xi,\\ v&\approx-\frac{16ie^{i\sigma t}\,\alpha_1\,\kappa}{F'(\kappa)}\,\mathrm{cosec}\,\theta\int_0^\infty f(\xi)\,e^{-\beta_1\xi}\cos\kappa\,(x-\xi\cot\theta)\,d\xi,\end{aligned}\right\}\ldots\ldots(29)$$

which are, too, of the same forms as those of the splitting origin, except the interchange of α_1 and β_1. Though the compiling of the above equations has been omitted, the generated surface waves will shew the more pronounced characters in the direction of the case $\lambda=\mu$ than that of $\lambda=\infty$ in the splitting disturbances.

II. Three-dimensional Propagation.

9. We shall take the free surface of a semi-infinite solid to be $z=0$, and its positive sense downwards. Suppose that the sheet of the dilatational sources lies in a straight line in a three-dimensional space. Then the element of the sheet is expressed by

$$\frac{e^{i\sigma t}\, e^{-ih\sqrt{R^2+z^2}}}{\sqrt{R^2+z^2}}, \quad \dots\dots\dots\dots\dots\dots\dots\dots (30)$$

where $R^2=r^2+(\xi\cot\theta)^2-2r\xi\cot\theta\cos\omega$.

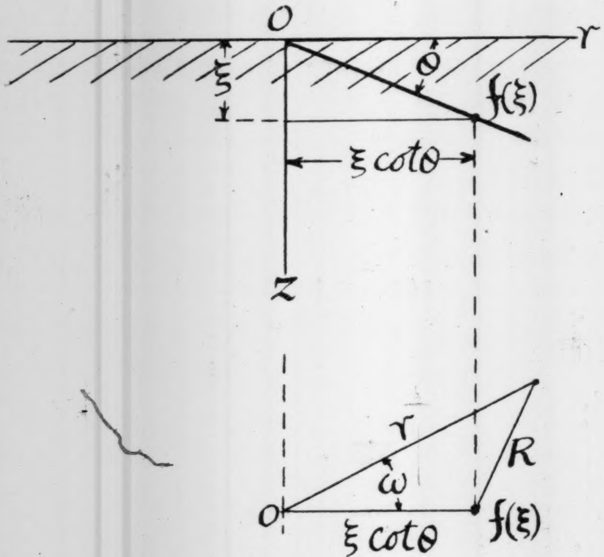

Now by means of Lamb's formula:[3)]

$$\frac{e^{-ih\sqrt{R^2+z^2}}}{\sqrt{R^2+z^2}}=\int_0^\infty \frac{e^{-\alpha z}}{\alpha} J_0(kR)\, kdk, \quad \dots\dots\dots\dots\dots\dots (31)$$

we get the total dilatational waves from the splitting sources in the form:

$$\Delta_0'=e^{i\sigma t}\int_0^\infty f(\xi)\, d\xi \operatorname{cosec}\theta \int_0^\infty \frac{e^{\alpha(z-\xi)}\, J_0(kR)\, kdk}{\alpha}, \quad \dots\dots\dots (32)$$

Adding the effect of the image to (32), we get

$$\Delta_0=\Delta_0'+\Delta_0''=2e^{i\sigma t}\int_0^\infty f(\xi)\, d\xi \operatorname{cosec}\theta \int_0^\infty \frac{\operatorname{ch}\alpha z\, e^{-\alpha\xi}\, J_0(kR)\, kdk}{\alpha} \dots (33)$$

The corresponding values of the components of the displacement in radial, azimuthal and vertical directions are expressed by

$$\left.\begin{aligned}
u_0&=-\frac{2e^{i\sigma t}}{h^2}\frac{\partial}{\partial r}\int_0^\infty f(\xi)\, d\xi \operatorname{cosec}\theta \int_0^\infty \frac{\operatorname{ch}\alpha z}{\alpha}\, e^{-\alpha\xi} J_0(kR)\, kdk,\\
v_0&=-\frac{2e^{i\sigma t}}{h^2 r}\frac{\partial}{\partial \omega}\int_0^\infty f(\xi)\, d\xi \operatorname{cosec}\theta \int_0^\infty \frac{\operatorname{ch}\alpha z}{\alpha}\, e^{-\alpha\xi} J_0(kR)\, kdk,\\
w_0&=-\frac{2e^{i\sigma t}}{h^2}\frac{\partial}{\partial z}\int_0^\infty f(\xi)\, d\xi \operatorname{cosec}\theta \int_0^\infty \frac{\operatorname{ch}\alpha z}{\alpha}\, e^{-\alpha\xi} J_0(kR)\, kdk.
\end{aligned}\right\} \dots (34)$$

---

3) H. LAMB, *Phil. Trans. Roy. Soc.*, **203** (1904).

The expressions of the superposed waves are given by

$$\left.\begin{aligned} u_1 &= \frac{2e^{i\sigma t}}{h^2}\frac{\partial}{\partial r}\int_0^\infty f(\xi)\,d\xi\,\operatorname{cosec}\theta \\ &\qquad \times\int_0^\infty \frac{(2k^2-j^2-2\alpha\beta)}{\alpha F(k)}(2k^2-j^2)\,e^{-\alpha\xi}J_0(kR)\,kdk, \\ v_1 &= \frac{2e^{i\sigma t}}{h^2 r}\frac{\partial}{\partial\omega}\int_0^\infty f(\xi)\,d\xi\,\operatorname{cosec}\theta \\ &\qquad \times\int_0^\infty \frac{(2k^2-j^2-2\alpha\beta)}{\alpha F(k)}(2k^2-j^2)\,e^{-\alpha\xi}J_0(kR)\,kdk, \\ w_1 &= \frac{2e^{i\sigma t}}{h^2}\int_0^\infty f(\xi)\,d\xi\,\operatorname{cosec}\theta\int_0^\infty \frac{j^2(2k^2-j^2)}{F(k)}e^{-\alpha\xi}J_0(kR)\,kdk. \end{aligned}\right\}\ldots(35)$$

The resultant displacement on $z=0$ is denoted by

$$\left.\begin{aligned} u=u_0+u_1 &= \frac{4e^{i\alpha t}}{h^2}\frac{\partial}{\partial r}\int_0^\infty f(\xi)\,d\xi\,\operatorname{cosec}\theta\int_0^\infty \frac{\beta j^2}{F(k)}e^{-\alpha\xi}J_0(kR)\,kdk, \\ v=v_0+v_1 &= \frac{4e^{i\sigma t}}{h^2 r}\frac{\partial}{\partial\omega}\int_0^\infty f(\xi)\,d\xi\,\operatorname{cosec}\theta\int_0^\infty \frac{\beta j^2}{F(k)}e^{-\alpha\xi}J_0(kR)\,kdk, \\ w=w_0+w_1 &= \frac{2e^{i\sigma t}}{h^2}\int_0^\infty f(\xi)\,d\xi\,\operatorname{cosec}\theta\int_0^\infty \frac{j^2(2k^2-j^2)}{F(k)}e^{-\alpha\xi}J_0(kR)\,kdk. \end{aligned}\right\}\ (36)$$

The method of contour integrations applied on the above integrals gives us

$$\left.\begin{aligned} u &\approx \frac{8\pi e^{i\sigma t}}{h^2}\frac{\partial}{\partial r}\int_0^\infty f(\xi)\,d\xi\,\operatorname{cosec}\theta\,\frac{\beta_1 j^2\kappa}{F'(\kappa)}e^{-\alpha_1\xi}\,Y_0(\kappa R), \\ v &\approx \frac{8\pi e^{i\sigma t}}{h^2 r}\frac{\partial}{\partial\omega}\int_0^\infty f(\xi)\,d\xi\,\operatorname{cosec}\theta\,\frac{\beta_1 j^2\kappa}{F'(\kappa)}e^{-\alpha_1\xi}\,Y_0(\kappa R), \\ w &\approx \frac{4\pi e^{i\sigma t}}{h^2}\int_0^\infty f(\xi)\,d\xi\,\operatorname{cosec}\theta\,\frac{j^2(2\kappa^2-j^2)\kappa}{F'(\kappa)}e^{-\alpha_1\xi}\,Y_0(\kappa R). \end{aligned}\right\}\ldots.(37)$$

Now we know the relation

$$\begin{aligned} Y_0(\kappa R) &= Y_0(\kappa r)\,J_0(\kappa\xi\cot\theta) \\ &\qquad +2\sum_{n=1}^{\infty} Y_n(\kappa r)\,J_n(\kappa\xi\cot\theta)\cos n\omega, \qquad [r>\xi\cot\theta] \end{aligned}$$

where $\ldots\ldots\ldots\ldots\ldots\ldots\ldots\ldots(38)$

$$R=\sqrt{r^2+(\xi\cot\theta)^2-2r\xi\cot\theta\cos\omega}.\ldots\ldots\ldots\ldots\ldots\ldots\ldots(39)$$

Substituting from (38) in (37), we get

$$u=\frac{8\pi e^{i\sigma t}}{h^2}\frac{\beta_1 j^2\kappa}{F'(\kappa)}\operatorname{cosec}\theta\int_0^\infty f(\xi)\,d\xi\,e^{-\alpha_1\xi}\left[\frac{\partial Y_0(\kappa r)}{\partial r}J_0(\kappa\xi\cot\theta)\right.$$
$$\left.+2\sum_{n=1}^{\infty}\frac{\partial Y_n(\kappa r)}{\partial r}J_n(\kappa\xi\cot\theta)\cos n\omega\right],$$
$$v=-\frac{16\pi\, e^{i\sigma t}\,\beta_1\, j^2\kappa}{h^2\, r\, F'(\kappa)}\operatorname{cosec}\theta\int_6^\infty f(\xi)\,d\xi\,e^{-\alpha_1\xi}$$
$$\times\sum_{n=1}^{\infty}nY_n(\kappa r)\,J_n(\kappa\xi\cot\theta)\sin n\omega,$$
$$w=\frac{4\pi e^{i\sigma t}}{h^2}\frac{j^2(2\kappa^2-j^2)\kappa}{F'(\kappa)}\operatorname{cosec}\theta\int_0^\infty f(\xi)\,d\xi\,e^{-\alpha_1\xi}\left[Y_0(\kappa r)\,J_0(\kappa\xi\cot\theta)\right.$$
$$\left.+2\sum_{n=1}^{\infty}Y_n(\kappa r)\,J_n(\kappa\xi\cot\theta)\cos n\omega\right].$$
$$\dots\dots\dots\dots\dots\dots\dots(40)$$

To get the progressive waves, we superpose on the above type of solutions Bessel's function of the first kind, and after the same operation as in the two-dimensional case, we get finally

$$u=\frac{4\pi e^{i\sigma t}}{h^2}\frac{\beta_1 j^2\kappa}{F'(\kappa)}\operatorname{cosec}\theta\int_0^\infty f(\xi)\,d\xi\,e^{-\alpha_1\xi}\left[\frac{\partial H_0^{(2)}(\kappa r)}{\partial r}J_0(\kappa\xi\cot\theta)\right.$$
$$\left.+2\sum_{n=1}^{\infty}\frac{\partial H_0^{(2)}(\kappa r)}{\partial r}J_n(\kappa\xi\cot\theta)\cos n\omega\right],$$
$$v=-\frac{8\pi e^{i\sigma t}}{h^2\, r}\frac{\beta_1 j^2\kappa}{F'(\kappa)}\operatorname{cosec}\theta\int_0^\infty f(\xi)\,d\xi\,e^{-\alpha_1\xi}$$
$$\times\sum_{n=1}^{\infty}nH_n^{(2)}(\kappa r)\,J_n(\kappa\xi\cot\theta)\sin nw,$$
$$w=\frac{2\pi e^{i\sigma t}}{h^2}\frac{j^2(2\kappa^2-j^2)\kappa}{F'(\kappa)}\operatorname{cosec}\theta\int_0^\infty f(\xi)\,d\xi\,e^{-\alpha_1\xi}\left[H_0^{(2)}(\kappa r)\,J_0(\kappa\xi\cot\theta)\right.$$
$$\left.+2\sum_{n=1}^{\infty}H_n^{(2)}(\kappa r)\,J_n(\kappa\xi\cot\theta)\cos n\omega\right].$$
$$\dots\dots\dots\dots\dots\dots\dots(41)$$

These equations give us the excited Rayleigh-waves on a boundary plane of a semi-infinite solid, when the sources are distributed in any assigned manner on a straight line.

10. For an example, suppose that

$$f(\xi)=\text{constant}=c, \quad \dots\dots\dots\dots\dots\dots\dots(42)$$

then the surface displacement is given by

$$u=\frac{4\pi e^{i\sigma t}\beta_1 j^2 c}{h^2 F'(\kappa)}\left[\frac{\operatorname{cosec}\theta}{\sqrt{\left(\frac{\alpha_1}{\kappa}\right)^2+\cot^2\theta}}\left\{\frac{\partial H_0^{(2)}(\kappa r)}{\partial r}\right.\right.$$

$$\left.\left.+2\sum_{n=1}^{\infty}\frac{\partial H_n^{(2)}(\kappa r)}{\partial r}\left(\frac{\sqrt{\left(\frac{\alpha_1}{\kappa}\right)^2+\cot^2\theta}-\frac{\alpha_1}{\kappa}}{\cot\theta}\right)^n\cos n\omega\right\}\right],$$

$$v=-\frac{8\pi e^{i\sigma t}\beta_1 j^2 c}{h^2 rF'(\kappa)}\left[\frac{\operatorname{cosec}\theta}{\sqrt{\left(\frac{\alpha_1}{\kappa}\right)^2+\cot^2\theta}}\right.$$

$$\left.\times\sum_{n=1}^{\infty}nH_n^{(2)}(\kappa r)\left(\frac{\sqrt{\left(\frac{\alpha_1}{\kappa}\right)^2+\cot^2\theta}-\frac{\alpha_1}{\kappa}}{\cot\theta}\right)^n\sin n\omega\right],$$

$$w=\frac{2\pi e^{i\sigma t}j^2(2\kappa^2-j^2)c}{h^2 F'(\kappa)}\left[\frac{\operatorname{cosec}\theta}{\sqrt{\left(\frac{\alpha_1}{\kappa}\right)^2+\cot^2\theta}}\left\{H_0^{(2)}(\kappa r)\right.\right.$$

$$\left.\left.+2\sum_{n=1}^{\infty}H_n^{(2)}(\kappa r)\left.\frac{\sqrt{\left(\frac{\alpha^2}{\kappa}\right)^2+\cot^2\theta}-\frac{\alpha_1}{\kappa}}{\cot\theta}\right)^n\cos n\omega\right\}\right].$$

$$\dots\dots\dots\dots\dots\dots\dots\dots(43)$$

The absolute values of [ ] in the equation of w multiplied by $\sqrt{\frac{\pi\kappa r}{2}}$ for different angles of θ are expressed in Fig. 5 and Fig. 6. In these figures the curves marked $a/\kappa=0$ give the result of the present examples.

11. Next, let us take

$$f(\xi)=ce^{-a\xi},\dots\dots\dots\dots\dots\dots(44)$$

then we obtain

$$w=\frac{2\pi e^{i\sigma t}j^2(2\kappa^2-j^2)\kappa}{h^2 F'(\kappa)}\left[\frac{\operatorname{cosec}\theta}{\sqrt{\left(\frac{\alpha_1+a}{\kappa}\right)^2+\cot^2\theta}}\left\{H_0^{(2)}(\kappa r)\right.\right.$$

$$\left.\left.+2\sum_{n=1}^{\infty}H_n^{(2)}(\kappa r)\left(\frac{\sqrt{\left(\frac{\alpha_1+a}{\kappa}\right)^2+\cot^2\theta}-\frac{\alpha_1}{\kappa}}{\cot\theta}\right)^n\cos n\omega\right\}\right]$$

$$\dots\dots\dots\dots\dots\dots\dots\dots(45)$$

and similar expressions for u and v. The absolute values of [ ] in this equation multiplied by $\sqrt{\frac{\pi\kappa r}{2}}$ for various angles θ are plotted in Fig. 5 and Fig. 6. Fig. 5 gives us the case $\lambda=\mu$ and Fig. 6 gives us that of $\lambda=\infty$. It will be noticed that for a greater values of a/κ the amplitude of the waves takes a smaller value. As already stated, this is self-evident from the nature of the assumed distribution of the sources. A most noteworthy fact is that there is a miximum value of the displacement at a certain angle between 0 and $\pi/2$ for each value of a/κ. It will also be seen that the angle θ which gives the maximum of the displacement changes for different values of a/κ. The maximum of the displacement when $a/\kappa=0$ and $\lambda=\mu$ takes place at $\theta\doteqdot 65°$ and the similar maximum in the case $\lambda=\infty$ occure at $\theta\doteqdot 45°$, while for a larger values of a/κ the position of the maximum shifts more and more in the sense of the smaller angle θ.

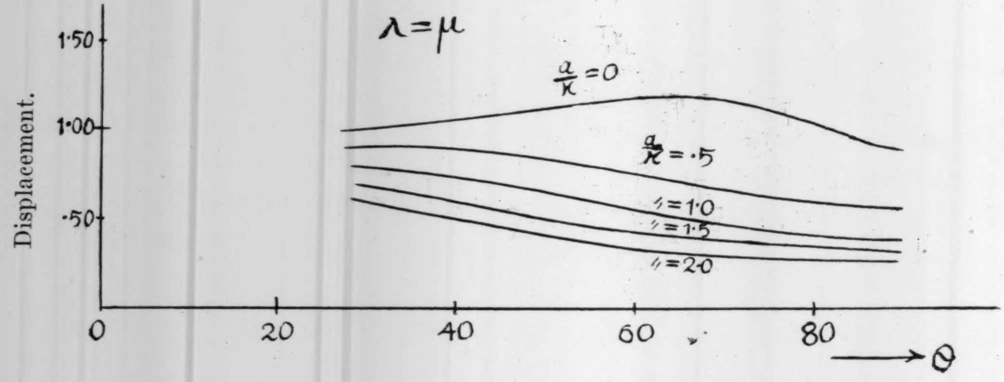

Fig. 5.

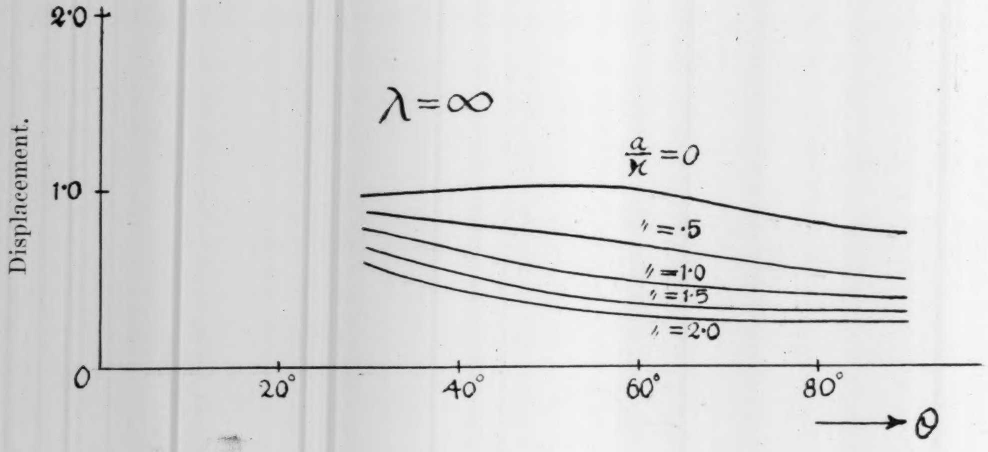

Fig. 6.

12. Let us take

$$f(\xi)=c^m\,\xi^{m-1}, \qquad \ldots\ldots(46)$$

then, by means of the formula

$$\int_0^\infty e^{-\alpha_1\xi}J_n(\kappa\xi\cot\theta)\,\xi^{m-1}\,d\xi$$

$$=\frac{\left(\frac{1}{2}\frac{\kappa\cot\theta}{\alpha_1}\right)^n\Gamma(m+n)}{\alpha_1{}^m\,\Gamma(n+1)}\,F\left(\frac{m+n}{2},\ \frac{m+n+1}{2},\ n+1,\ -\left(\frac{\kappa\cot\theta}{\alpha_1}\right)^2\right),$$

$$[R(\alpha_1\pm i\kappa\cot\theta)>0]$$

$$\ldots\ldots(47)^{4)}$$

where

$$F(\alpha,\beta,\gamma,x)=1+\sum_{s=1}^{\infty}\frac{\alpha(\alpha+1)\ldots(\alpha+s-1)\,\beta(\beta+1)\ldots(\beta+s-1)\,x^s}{s!\,\gamma(\gamma+1)\ldots(\gamma+s-1)},$$

$$\ldots\ldots(48)$$

we find

$$u=\frac{4\pi e^{i\sigma t}\beta_1 j^2\kappa}{h^2F'(\kappa)}\left(\frac{c}{\alpha_1}\right)^m\left(\frac{\kappa\cot\theta}{2\alpha_1}\right)^n\operatorname{cosec}\theta$$

$$\times\left[\frac{\partial H_0^{(2)}(\kappa r)}{\partial r}\,\Gamma(m)\,F\left(\frac{m}{2},\ \frac{m+1}{2},\ n+1,\ -\left(\frac{\kappa\cot\theta}{\alpha_1}\right)^2\right)\right.$$

$$+2\sum_{n=1}^{\infty}\frac{\partial H_n^{(2)}(\kappa r)}{\partial r}\,\frac{\Gamma(m+n)}{\Gamma(n+1)}$$

$$\left.\times F\left(\frac{m+n}{2},\ \frac{m+n+1}{2},\ n+1,\ -\left(\frac{\kappa\cot\theta}{\alpha_1}\right)^2\right)\cos n\omega\right]$$

$$[R(\alpha_1\pm i\kappa\cot\theta)>0]$$

$$\ldots\ldots(49)$$

and similar expressions for v and w.

13. When the sheet of sources forms a plane surface, the problem can be analysed in the same manner. The process is, however, too complex and we will leave the problem to the future occasion.

14. The case where the source of the disturbance is of a sliding type, the direction of the slip being in the sense of the line of the sheet, can be treated first by solving the problem of a point nucleous and then superposing a number of such solutions.

---

4) WATSON, *Theory of Bessel Functions*, (1922), 385.

Let the intensity of an element be

$$\frac{e^{i\sigma t}\,e^{-ij\sqrt{R^2+z^2}}}{\sqrt{R^2+z^2}}f(\xi), \qquad\qquad (50)$$

then the general distortional waves generated from the sliding line

$$z=x\tan\theta, \qquad\qquad (2'')$$

may be expressed by

$$2\varpi_0'=e^{i\sigma t}\int_0^\infty f(\xi)\,d\xi\,\mathrm{cosec}\,\theta\int_0^\infty\frac{e^{\beta(z-\xi)}\,J_0(kR)}{\beta}kdk. \qquad\qquad (51)$$

Superposing the effect of the image, we get

$$\left.\begin{aligned}
u_0&=2\,\frac{e^{i\sigma t}}{j^2}\int_0^\infty f(\xi)\,d\xi\,\mathrm{cosec}\,\theta\cos\omega\int_0^\infty\sin\beta z\,e^{-\beta\xi}\,J_0(kR)\,kdk,\\
v_0&=-2\,\frac{e^{i\sigma t}}{j^2}\int_0^\infty f(\xi)\,d\xi\,\mathrm{cosec}\,\theta\sin\omega\int_0^\infty\sin\beta z\,e^{-\beta\xi}\,J_0(kR)\,kdk,\\
w_0&=-2\,\frac{e^{i\sigma t}}{j^2}\int_0^\infty f(\xi)\,d\xi\,\mathrm{cosec}\,\theta\cos\omega\int_0^\infty\frac{\mathrm{ch}\,\beta z}{\beta}\,e^{-\beta\xi}\,\frac{\partial J_0(kR)}{\partial r}\,kdk.
\end{aligned}\right\}\qquad (52)$$

Adding to these displacement some free displacement $(u_1,\ v_1,\ w_1)$ accumulated on the surface of the solid to annul the surface stress, we find

$$\left.\begin{aligned}
u&=u_0+u_1=-2e^{i\sigma t}\int_0^\infty f(\xi)\,d\xi\,\mathrm{cosec}\,\theta\cos\omega\int_0^\infty\frac{(2k^2-j^2)}{F(k)}\,e^{-\beta\xi}\,J_0(kR)\,kdk,\\
v&=v_0+v_1=2e^{i\sigma t}\int_0^\infty f(\xi)\,d\xi\,\mathrm{cosec}\,\theta\sin\omega\int_0^\infty\frac{(2k^2-j^2)}{F(k)}\,e^{-\beta\xi}\,J_0(kR)\,kdk,\\
w&=w_0+w_1=4e^{i\sigma t}\int_0^\infty f(\xi)\,d\xi\,\mathrm{cosec}\,\theta\cos\omega\int_0^\infty\frac{\alpha}{F(k)}\,e^{-\beta\xi}\,\frac{\partial J_0(kR)}{\partial r}\,kdk,
\end{aligned}\right\}$$

$$\qquad\qquad (53)$$

at the surface $z=0$.

Proceeding in the same manner as before, we get finally

$$u=\frac{2\pi e^{i\sigma t}(2\kappa^2-j^2)\,\kappa}{F'(\kappa)}\,\mathrm{cosec}\,\theta\int_0^\infty f(\xi)\,d\xi\,e^{-\beta_1\xi}\Big[H_0^{(2)}(\kappa r)\,J_0(\kappa\xi\cot\theta)\cos\omega$$

$$+2\sum_{n=1}^{\infty}H_n^{(2)}(\kappa r)\,J_n(\kappa\xi\cot\theta)\cos n\omega\cos\omega\Big],$$

$$v=-\frac{2\pi e_{i\sigma t}(2\kappa^2-j^2)\,\kappa}{F'(\kappa)}\,\mathrm{cosec}\,\theta\int_0^\infty f(\xi)\,d\xi\,e^{-\beta_1\xi}\Big[H_0^{(2)}(\kappa r)\,J_0(\kappa\xi\cot\theta)\sin\omega$$

$$+2\sum_{n=1}^{\infty} H_n^{(2)}(\kappa r)\, J_n(\kappa\xi\cot\theta)\cos n\omega\sin\omega\Big],$$

$$w=-\frac{4\pi e^{i\sigma t}\,\alpha_1\kappa}{F'(\kappa)}\operatorname{cosec}\theta\int_0^{\infty} f(\xi)\,d\xi\, e^{-\beta_1\xi}\Big[\frac{\partial H_0^{(2)}(\kappa r)}{\partial r}\, J_0(\kappa\xi\cot\theta)\cos\omega$$

$$+2\sum_{n=1}^{\infty}\frac{\partial H_0^{(2)}(\kappa r)}{\partial r}\, J_n(\kappa\xi\cot\theta)\cos n\omega\cos\omega\Big]. \qquad \ldots\ldots\ldots\ldots\ldots\ldots\ldots\ldots (54)$$

These integrals can be evaluated in a very simple manner.

15. Thus, in the case

$$f(\xi)=\text{constant}=c, \qquad \ldots\ldots\ldots\ldots\ldots\ldots\ldots (55)$$

the results of evaluation are of the forms:

$$u=\frac{2\pi e^{i\sigma t}(2\kappa^2-j^2)\,c}{F'(\kappa)}\,\frac{\operatorname{cosec}\theta}{\sqrt{\left(\frac{\beta_1}{\kappa}\right)^2+\cot^2\theta}}\Bigg\{H_0^{(2)}(\kappa r)\cos\omega$$

$$+2\sum_{n=1}^{\infty} H_n^{(2)}(\kappa r)\left(\frac{\sqrt{\left(\frac{\beta_1}{\kappa}\right)^2+\cot^2\theta}-\frac{\beta_1}{\kappa}}{\cot\theta}\right)^n\cos n\omega\cos\omega\Bigg\}.$$

$$v=-\frac{2\pi e^{i\sigma t}(2\kappa^2-j^2)\,c}{F'(\kappa)}\,\frac{\operatorname{cosec}\theta}{\sqrt{\left(\frac{\beta_1}{\kappa}\right)^2+\cot^2\theta}}\Bigg\{H_0^{(2)}(\kappa r)\sin\omega$$

$$+2\sum_{n=1}^{\infty} H_n^{(2)}(nr)\left(\frac{\sqrt{\left(\frac{\beta_1}{\kappa}\right)^2+\cot^2\theta}-\frac{\beta_1}{\kappa}}{\cot\theta}\right)^n\cos\omega\sin\omega\Bigg\},$$

$$w=-\frac{4\pi\, e^{i\sigma t}\,\alpha_1\, c}{F'(\kappa)}\,\frac{\operatorname{cosec}\theta}{\sqrt{\left(\frac{\beta_1}{\kappa}\right)^2+\cot^2\theta}}\Bigg\{\frac{\partial H_0^{(2)}(\kappa r)}{\partial r}\cos\omega$$

$$+2\sum_{n=1}^{\infty}\frac{\partial H_n^{(2)}(\kappa r)}{\partial r}\left(\frac{\sqrt{\left(\frac{\beta_1}{\kappa}\right)^2+\cot^2\theta}-\frac{\beta_1}{\kappa}}{\cot\theta}\right)^n\cos n\omega\cos\omega\Bigg\}. \qquad \ldots\ldots\ldots\ldots\ldots\ldots\ldots\ldots (56)$$

From these it may be concluded that Rayleigh-waves propagated from a sliding source of the present type have not the component which is symmetrical about a vertical line $r=0$, but they manifest the nature of the polarity with respect to the azimuthal angle ω.

Concluding Remarks.

16. We may now review some results of this investigation from the general consideration. Although the sliding or splitting sources are of sheets of nuclei, yet we may believe that the theory is some guidance for the acknowledgment of the generation of Rayleigh-waves from a sliding or a splitting origin.

The principal results obtained in this paper are enumerated as follows:

1. Generated surface waves are bestowed with more energy in a compressible solid than in an incompressible solid.
2. In a two-dimensional motion, the amplitude of the surface waves generated from a line source of increasing intensity downwards reaches its maximum value at the upright position of the line of the source.
3. When the intensity of the element of the source is constant at any depth on the line of source, the displacement of the surface waves is constant for any angle of inclination of the above line.
4. When the intensity of the line source decreases with the depth, the amplitude takes its maximum value at a certain angle θ between 0 and $\pi/2$.
5. The angle θ of the maximum displacement in the above example changes with the rate of the decrease of the intensity in the downward direction.
6. In a three-dimensional motion, there is a certain angle θ corresponding to the maximum displacement even in the case of the constant intensity of the elementary portion of the source for all depths.
7. In spite of the existence of the component of displacement which is symmetrical about a vertical line in the case of the splitting sources of any inclination, there is no such component in the case of the sliding source.

In conclusion I am much indebted to Mr. G. Nishimura for his laborious assistance in all the numerical calculations and the preparation of this paper.

22. 内部の層源によるレーレー波の生成

地震研究所　妹　澤　克　惟

この論文は半無限體の內部の斷層面が辷る場合や切離される場合に出るレーレー波を研究する事を目的としたものである。內部に幾何學的の點があつて之れから出る波動を研究する方が寧ろ學理的であり又普遍性もある筈であるが、多くの地震學者があまり之を認めて呉れぬ樣に思はれたから、態々この論文を書いた次第である。

研究の方法は點源を種々組合せて層面を作り、これから出る彈性波が細長い切れ目から出る波動と結果に於て一致する樣に工夫をした。

研究の主な結果を拔萃すれば、

1. 固體が非變容性の時よりも變容性がある時の方が餘計に表面波の勢力を與へる。
2. 層の中の蓄積力が地下に進む程大きいものでは層面が垂直の時に表面波に一番大なる勢力を與へる。
3. 非變容性固體中にある層面の中の蓄積力が深さに無關係の時は、表面波の振幅は層の傾斜に無關係となる。
4. 層面の中の蓄積力が下程小になる場合に層面の傾斜の零度と 90 度との中間に極大表面波を與へる角度がある。
5. この角度は層の深さに從ひ蓄積力が減少する割合によつて異つて居る。
6. 三次元の場合には非變容性固體中にある層の中の蓄積力が深さに無關係の時でも層面の或角度の傾が極大表面波を與へる。
7. 層面が切離される時は、層面の如何なる傾斜を持つ場合でも表面波が垂直線に對して對稱をなす成分が存在するが、層が辷る場合には決して斯る成分が現はれる樣な事がない。

23. *Propagation of Love-waves on a Spherical Surface and Allied Problems.*

By **Katsutada SEZAWA,**

Earthquake Research Institute.

(Received Sept. 20, 1929.)

1. Quite recently Dr. H. Nakano[1] gave a problem of Love-waves in cylindrical coordinates and pointed out that there is a clear distinction between cylindrical Rayleigh-waves and cylindrical Love-waves. The problem has also attracted my attention since the occasion[2] of studying the propagation of Rayleigh-waves having azimuthal distribution, because of the fact that the second constituent of the general expressions of the displacement obtained at that time, namely (u_2, v_2, w_2), both in two-dimensions and on a spherical surface had no any significance on Rayleigh-waves but the forms of u_2, v_2, w_2 resembled those of the distortional waves.

As highly appreciated by European seismologists,[3] Love-waves are much important, indeed, on the problem of the surface waves which are propagated to very long distance. From this consideration I have taken the case of Love-waves on a spherical surface and for the point very near the epicentre I have taken into account of the depth of the origin. The azimuthal distribution is not, of course, to be taken uniform.

2. We shall take the origin of the disturbance to be at the portion of the axis, $\theta=0$, of the spherical coordinates, and suppose that the waves are transmitted in the direction of the colatitude. The radius of the free surface is to be a, while the thickness of the surface layer is to be taken $a-b$. Let u_2, v_2, w_2 be radial, colatitudinal and azimuthal components of the displacement which are of no use on the problem of Rayleigh-waves, then we have from my preceding paper[4] that

---

[1] H. NAKANO, "Love-wave in Cylindrical Coordinates," *Geophys. Mag.*, 8 (1929).
Added Nov. 1929.—I regret that I have been informed of Dr. NAKANO's death on Oct. 3, 1929. He is one of the mathematical seismologists to whom I have paid many respects. I have never expected that this paper would become my condolence on his death.

[2] K. SEZAWA, "Propagation of Rayleigh-waves having a Certain Azimuthal Distribution of Displacements," *Proc. Imp. Acad.*, 4 (1928), No. 6, 267; and also "Further Studies on Rayleigh-waves having Some Azimuthal Distribution," *Bull. Earthq. Res. Inst.*, 6 (1929), 1.

[3] B. GUTENBERG, H. JEFFREYS and similar eminent seismologists.

$$u_2=0,$$

$$v_2=\frac{m}{n(n+1)}C_{mn}\frac{J_{n+\frac{1}{2}}(kr)}{\sqrt{r}}\left\{\frac{P_n^m(\cos\theta)}{\sin\theta}+\alpha_n^m\frac{Q_n^m(\cos\theta)}{\sin\theta}\right\}\begin{Bmatrix}\cos\\ \sin\end{Bmatrix}m\phi\, e^{i\sigma t},$$

$$w_2=-\frac{1}{n(n+1)}C_{mn}\frac{J_{n+\frac{1}{2}}(kr)}{\sqrt{r}}\left\{\frac{dP_n^m(\cos\theta)}{d\theta}+\alpha_n^m\frac{dQ_n^m(\cos\theta)}{d\theta}\right\}\begin{Bmatrix}\sin\\ -\cos\end{Bmatrix}m\phi\, e^{i\sigma t},$$

$$\qquad\qquad\qquad\qquad\qquad\qquad\qquad\qquad\qquad\qquad\qquad\qquad\qquad\qquad\qquad\qquad\cdots\cdots\cdots\cdots\cdots(1)$$

where $k^2=\rho\sigma^2/\mu$, in which ρ is the density and μ is the modulus of the rigidity. α_n^m is a number, whose value is constant for a given n and m and which is to be so adjusted that $P_n^m(\cos\theta)$ and $Q_n^m(\cos\theta)$ may have enveloping curves in common, excepting near the antipode and the origin. We take that the above expression (1) applies to the inner core of the sphere. For the outer layer we may write the expressions of the displacement without any difficulty such that

$$u_2'=0,$$

$$v_2'=\frac{m}{n(n+1)}\left\{A_{mn}\frac{J_{n+\frac{1}{2}}(k'r)}{\sqrt{r}}+B_{mn}\frac{Y_{n+\frac{1}{2}}(k'r)}{\sqrt{r}}\right\}\left\{\frac{P_n^m(\cos\theta)}{\sin\theta}\right.$$

$$\left.+\alpha_n^m\frac{Q_n^m(\cos\theta)}{\sin\theta}\right\}\begin{Bmatrix}\cos\\ \sin\end{Bmatrix}m\phi\, e^{i\sigma t},$$

$$w_2'=-\frac{1}{n(n+1)}\left\{A_{mn}\frac{J_{n+\frac{1}{2}}(k'r)}{\sqrt{r}}+B_{mn}\frac{Y_{n+\frac{1}{2}}(k'r)}{\sqrt{r}}\right\}\left\{\frac{dP_n^m(\cos\theta)}{d\theta}\right.$$

$$\left.+\alpha_n^m\frac{dQ_n^m(\cos\theta)}{d\theta}\right\}\begin{Bmatrix}\sin\\ -\cos\end{Bmatrix}m\phi\, e^{i\sigma t},$$

$$\qquad\qquad\qquad\qquad\qquad\qquad\qquad\qquad\qquad\qquad\qquad\qquad\qquad\qquad\qquad\cdots\cdots\cdots\cdots\cdots\cdots\cdots(2)$$

where $k'^2=\rho'\sigma^2/\mu'$, in which ρ', μ' are the density and the rigidity of the outer medium. When $\mu'/\rho'<\mu/\rho$, we find at the vicinity of $b<r<a$,

$$\frac{n+\frac{1}{2}}{kr}\,(=\cosh\tau)>1,\qquad \frac{n+\frac{1}{2}}{k'r}\,(=\cos\tau')<1.\ \cdots\cdots\cdots\cdots(3)$$

In applying the formulae (1) and (2), we should exclude the epicentral and the antipodal regions from the consideration because of the divergence of Q_n^m-functions at such regions.

As the boundary conditions, we should put

---

[4] K. SEZAWA, *Bull. Earthq. Res. Inst.*, **6** (1929), 14.

$$\frac{\partial}{\partial r}\frac{v'}{r}=\frac{\partial}{\partial r}\frac{w'}{r}=0, \qquad [r=a] \dots\dots\dots\dots\dots\dots (4)$$

$$\left.\begin{aligned} \mu'\frac{\partial}{\partial r}\frac{v'}{r}&=\mu\frac{\partial}{\partial r}\frac{v}{r},\\ \mu'\frac{\partial}{\partial r}\frac{w'}{r}&=\mu\frac{\partial}{\partial r}\frac{w}{r},\\ v'&=v,\\ w'&=w. \end{aligned}\right\} \quad [r=b] \dots\dots\dots\dots\dots\dots (5)$$

From (4) and (5), we obtain the equation to determine the velocity of propagation as in the following form:

$$\begin{vmatrix} \dfrac{\partial}{\partial a}\dfrac{J_{n+\frac{1}{2}}(k'a)}{a^{\frac{3}{2}}}, & \dfrac{\partial}{\partial a}\dfrac{Y_{n+\frac{1}{2}}(k'a)}{a^{\frac{3}{2}}}, & 0 \\ \dfrac{\mu'}{\mu}\dfrac{\partial}{\partial b}\dfrac{J_{n+\frac{1}{2}}(k'b)}{b^{\frac{3}{2}}}, & \dfrac{\mu'}{\mu}\dfrac{\partial}{\partial b}\dfrac{Y_{n+\frac{1}{2}}(k'b)}{b^{\frac{3}{2}}}, & \dfrac{\partial}{\partial b}\dfrac{J_{n+\frac{1}{2}}(kb)}{b^{\frac{3}{2}}} \\ J_{n+\frac{1}{2}}(k'b), & Y_{n+\frac{1}{2}}(k'b), & J_{n+\frac{1}{2}}(kb) \end{vmatrix}=0. \dots\dots (6)$$

To solve this equation, we take the asymptotic expansion due to P. Debye, namely

$$J_p(x)=-\frac{i}{2\pi}\,e^{x(\tau\operatorname{ch}\tau-\operatorname{sh}\tau)}\sum_{n=0}^{n=m}(-1)^n B_n(\tau)\frac{\Gamma\left(n+\frac{1}{2}\right)}{\left(\frac{x}{2}\operatorname{sh}\tau\right)^{n+\frac{1}{2}}},$$

(m: finite limiting value.)

$$\dots\dots\dots\dots\dots\dots\dots\dots\dots\dots\dots (7)$$

where $\operatorname{ch}\tau>1$ and

$$B_0(\tau)=1, \quad B_1(\tau)=\frac{1}{8}-\frac{5}{24}\operatorname{cth}^2\tau, \quad B_2(\tau)=\frac{3}{128}-\frac{7}{576}\operatorname{cth}^2\tau+\frac{385}{3456}\operatorname{cth}^4\tau,$$

$$\dots\dots\dots\dots\dots\dots\dots\dots\dots\dots\dots\dots\dots\dots\dots\dots\dots\dots,$$

$$\dots\dots\dots\dots\dots\dots (8)$$

while

$$J_p(x)=\frac{1}{\pi}\sum_{n=0}^{n=m}A_n(\tau)\frac{\Gamma\left(n+\frac{1}{2}\right)}{\left(\frac{x}{2}\sin\tau\right)^{n+\frac{1}{2}}}\cos\left\{x(\sin\tau-\tau\cos\tau)-(2n+1)\frac{\pi}{4}\right\},$$

$$Y_p(x)=\frac{1}{\pi}\sum_{n=0}^{n=m}A_n(\tau)\frac{\Gamma\left(n+\frac{1}{2}\right)}{\left(\frac{x}{2}\sin\tau\right)^{n+\frac{1}{2}}}\sin\left\{x(\sin\tau-\tau\cos\tau)-(2n+1)\frac{\pi}{4}\right\}. \qquad \dots\dots(9)$$

where $\cos\tau<1$ and

$$\left.\begin{array}{l}A_0=1, \quad A_1=\frac{1}{8}+\frac{4}{24}\cot^2\tau, \; A_2=\frac{3}{128}+\frac{7}{576}\cot^2\tau+\frac{385}{3456}\cot^4\tau, \\ \dots\dots\dots\dots\dots\dots\dots\dots\dots\dots\end{array}\right\}\dots(10)$$

Taking each first term of these asymptotic expansions, we get

$$\frac{\mu' k'(\sin\tau'-\tau'\cos\tau')}{\mu k(\tau\operatorname{ch}\tau-\operatorname{sh}\tau)}=\cot k'\{a(\sin\tau_1'-\tau_1'\cos\tau_1')-b(\sin\tau'-\tau'\cos\tau')\}, \qquad \dots\dots(11)$$

where

$$\cosh\tau=\frac{n+\frac{1}{2}}{kb}, \qquad \cos\tau'=\frac{n+\frac{1}{2}}{k'b}, \qquad \cos\tau_1'=\frac{n+\frac{1}{2}}{k'a}, \dots(12)$$

in which $2\pi/k$ is the wave length of Love-waves.

When the radius of the sphere is very large compared with the thickness of the surface layer, we may put

$$\sin\tau_1'\longrightarrow\sin\tau', \dots\dots(13)$$

so that we obtain in place of (11)

$$\frac{\mu' k'(\sin\tau'-\tau'\cot\tau')}{\mu k(\tau\operatorname{ch}\tau-\operatorname{sh}\tau)}=\cot\eta k'(\sin\tau'-\tau'\cos\tau'). \dots\dots(14)$$

This expression is quite equivalent to Love's formula[5] to determine the velocity of the propagation of the long waves of the plane type, since the exponents in the expressions of displacements (v_2, w_2) and (v_3, w_3) in the present case are

$$rk(\tau\operatorname{ch}\tau-\operatorname{sh}\tau); \quad rk'(\sin\tau'-\tau'\cos\tau') \dots\dots(15)$$

respectively, which may be taken as the exponents of the factor defining the vertical variation of the displacements in the ordinary Love-waves.

The velocity of the propagation, thus, ranges between those of both distortional waves peculiar to the upper and inner medium. The expressions of the displacements are given (1) and (2).

---

[5] Cf. LOVE, *Some Problems of Geodynamics* (1911), 162.

From the expressions of (1), (2), (14), we may easily arrive at the conclusion that, besides the ordinary transverse component of the displacement, Love-waves having azimuthal distribution on a spherical surface have large co-latitudinal component of displacement, and that this component cannot disappear as the waves proceed towards the equatorial circle. It appears that even at the equatorial circle such long Love-waves as affected by the curvature of the earth have the longitudinal and transverse components of comparable magnitudes. The vertical component is not existent as at the plane surface.

3. Though in the preceding section we have studied the propagation of Love-waves on a spherical surface, the vibrations at the epicentral and antipodal regions have been excluded. To get the solutions of the problems at these regions, we should take the case of a plane surface and suppose that the waves are causd by the disturbance at a certain point in the solid body. Hence we will treat of a simplest case where Love-waves are excited due to the oscillations of a point in the interior of the solid body. In this section we shall study the excitation of Love-waves due to a disturbing origin at the bottom medium.

We shall take the boundary surface between the upper layer and the bottom medium to be $z=0$ and also that the positive sense is directed downwards. When the axis of each element of a multiplet is vertical, the primary waves generated from this multiplet can be easily written by

$$2\varpi_z = e^{i\sigma t}\sum_{p=0}^{p=2m}\frac{(-1)^p}{m!}\left[l_p\frac{\partial}{\partial x}+m_p\frac{\partial}{\partial y}\right]^m\frac{\partial^n}{\partial z^n}f(x,y)\,ds_1^m\,ds_2^n, \quad \ldots\ldots(16)$$

in which $f(x,y)$ is the mean strength of the source at the point (x, y), $2m$ is the number of the sides of the equiangular polygon made of the horizontal elements of the multiplet, l_p, m_p are the direction-cosines of the angular point p of the equiangular polygon, and n is the degree of the vertical elements. ds_1 and ds_2 are the radial distance of the equiangular point and the vertical length of the multiplet. The sign of the strength of each source at the equiangular point of the polygon changes alternately.

If the source is of a simple-harmonic type, we may write

$$f(x,y) = \frac{e^{-ij\sqrt{r^2+(z-\xi)^2}}}{\sqrt{r^2+(z-\xi)^2}}, \quad \ldots\ldots\ldots\ldots\ldots\ldots\ldots(17)$$

where ξ is the depth of the origin below the surface $z=0$ and $j^2=\rho\sigma^2/\mu$. Now by means of the formula

$$\frac{e^{-ij\sqrt{r^2+(z-\xi)^2}}}{\sqrt{r^2+(z-\xi)^2}}=\int_0^\infty \frac{e^{-\beta(\xi-z)}}{\beta}J_0(kr)\,kdk, \qquad \left[\begin{array}{l}\beta^2=k^2-j^2,\\ j^2=\dfrac{\rho\sigma^2}{\sigma},\end{array}\right] \quad \ldots\ldots(18)$$

and omitting the constant factor $e^{i\sigma t}ds_1{}^m ds_2{}^m$, we get $[0<z<\xi]$

$$2\varpi_z=\frac{2(-1)^m}{m!}\left(1-\cos^2\frac{\pi}{m}\right)\cos m\omega\int_0^\infty e^{-\beta(\xi-z)}J_m(kr)\,\beta^{n-1}k^{m+1}\,dk, \quad [m>2] \quad \ldots\ldots\ldots\ldots\ldots\ldots\ldots\ldots(19)$$

with the exceptions that

$$2\varpi_z=\int_0^\infty e^{-\beta(\xi-z)}J_0(kr)\,\beta^{n-1}\,kdk, \qquad [m=0]\ldots\ldots(20)$$

$$2\varpi_z=-2\cos\omega\int_0^\infty e^{-\beta(\xi-z)}J_0(kr)\,\beta^{n-1}\,k^2dk. \qquad [m=1]\ldots\ldots(21)$$

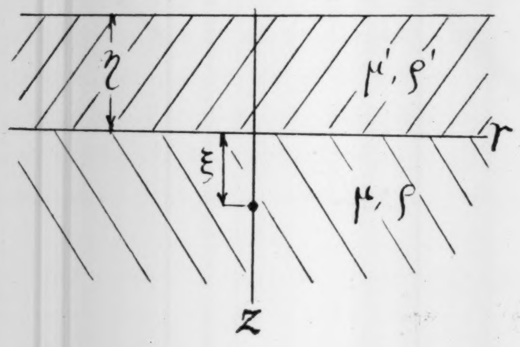

These rotations ϖ_z are always accompanied by the corresponding ϖ_r and ϖ_ω, as the displacements of the material point necessitate some relations among these rotations. The relations are as in the forms:

$$2\varpi_r=\frac{1}{r}\frac{\partial w}{\partial z}-\frac{\partial v}{\partial z}, \quad 2\varpi_\omega=\frac{\partial u}{\partial z}-\frac{\partial w}{\partial r}, \quad 2\varpi_z=\frac{1}{r}\left(\frac{\partial(rv)}{\partial r}-\frac{\partial u}{\partial\theta}\right), \quad \ldots(22)$$

where u, v, w are the radial, azimuthal, vertical components of displacement. We can, thus, write down the expressions:[6]

$$2\varpi_r=\frac{2(-1)^m}{m!}\left(1-\cos^2\frac{\pi}{m}\right)\cos m\omega \times\int_0^\infty e^{-\beta(\xi-z)}\frac{\partial J_m(kr)}{\partial r}\beta^n k^{m-1}dk, \qquad [m>2]\ldots(23)$$

$$2\varpi_r=\int_0^\infty e^{-\beta(\xi-z)}\frac{\partial J_0(kr)}{\partial r}\beta^n k^{-1}dk, \qquad [m=0]\ldots(24)$$

---

[6] Here use has been made of the result of my calculation on Rayleigh-waves, *Bull. Earthq. Res. Inst.*, **6** (1929), 4–5.

$$2\varpi_r = -2\cos\omega\int_0^\infty e^{-\beta(\xi-z)}\frac{\partial J_0(kr)}{\partial r}\beta^n\,dk, \qquad [m=1]\ldots\ldots(25)$$

and

$$\begin{aligned}2\varpi_\omega &= -\frac{2(-1)^m}{m!}\left(1-\cos^2\frac{\pi}{m}\right)m\sin\omega\\ &\qquad\times\int_0^\infty e^{-\beta(\xi-z)}\frac{J_m(kr)}{r}\beta^n k^{m-1}dk, \qquad [m>2]\ \ldots\ldots(26)\end{aligned}$$

$$2\varpi_\omega = 0, \qquad [m=0]\ldots\ldots(27)$$

$$2\varpi_\omega = 2\sin\omega\int_0^\infty e^{-\beta(\xi-z)}\frac{J_1(kr)}{r}\beta^n k dk. \qquad [m=1]\ldots\ldots(28)$$

The expressions of displacement corresponding to these ϖ_z, ϖ_r, ϖ_ω can be written by

$$\left.\begin{aligned}u &= -\frac{2(-1)^m}{m!}\left(1-\cos^2\frac{\pi}{m}\right)m\sin m\omega\int_0^\infty e^{-\beta(\xi-z)}\frac{J_m(kr)}{r}\beta^{n-1}k^{m-1}\,dk,\\ v &= -\frac{2(-1)^m}{m!}\left(1-\cos^2\frac{\pi}{m}\right)\cos m\omega\int_0^\infty e^{-\beta(\xi-z)}\frac{\partial J_m(kr)}{\partial r}\beta^{n-1}k^{m-1}\,dk,\\ w &= 0,\end{aligned}\right\}[m>2]$$

$$\ldots\ldots\ldots\ldots\ldots\ldots\ldots\ldots(29)$$

$$\left.\begin{aligned}u &= 0,\\ v &= -\int_0^\infty e^{-\beta(\xi-z)}\frac{\partial J_0(kr)}{\partial r}\beta^{n-1}k^{-1}\,dk,\\ w &= 0,\end{aligned}\right\}[m=0]\ldots\ldots\ldots\ldots(30)$$

$$\left.\begin{aligned}u &= 2\sin\omega\int_0^\infty e^{-\beta(\xi-z)}\frac{J_1(kr)}{r}\beta^{n-1}\,dk,\\ v &= 2\cos\omega\int_0^\infty e^{-\beta(\xi-z)}\frac{\partial J_1(kr)}{\partial r}\beta^{n-1}\,dk,\\ w &= 0.\end{aligned}\right\}[m=1]\ldots\ldots\ldots\ldots(31)$$

The reflected waves at the surface $z=0$ can be denoted by considering the image point $(r=0,\ z=-\xi)$ in the forms:

$$\left.\begin{aligned}2\varpi_z' &= \frac{2(-1)^m}{m!}\left(1-\cos^2\frac{\pi}{m}\right)\cos m\omega\\ &\qquad\times\int_0^\infty A_m\,e^{-\beta(\xi+z)}J_m(kr)\,\beta^{n-1}k^{m+1}\,dk,\\ 2\varpi_r' &= -\frac{2(-1)^m}{m!}\left(1-\cos^2\frac{\pi}{m}\right)\cos m\omega\\ &\qquad\times\int_0^\infty A_m\,e^{-\beta(\xi+z)}\frac{\partial J_m(kr)}{\partial r}\beta^n k^{m-1}\,dk,\end{aligned}\right|$$

$$\left.\begin{aligned}
2\varpi_\omega' &= \frac{2(-1)^m}{m!}\left(1-\cos^2\frac{\pi}{m}\right) m \sin m\omega \\
&\qquad \times \int_0^\infty A_m\, e^{-\beta(\xi+z)} \frac{J_m(kr)}{r}\, \beta^n k^{m-1}\, dk, \\
u' &= -\frac{2(-1)^m}{m!}\left(1-\cos^2\frac{\pi}{m}\right) m \sin m\omega \\
&\qquad \times \int_0^\infty A_m\, e^{-\beta(\xi+z)} \frac{J_m(kr)}{r}\, \beta^{n-1} k^{m-1}\, dk, \\
v' &= -\frac{2(-n)^m}{m!}\left(1-\cos^2\frac{\pi}{m}\right) \cos m\omega \\
&\qquad \times \int_0^\infty A_m\, e^{-\beta(\xi+z)} \frac{\partial J_m(kr)}{\partial r}\, \beta^{n-1} k^{m-1}\, dk, \\
w' &= 0,
\end{aligned}\right\}[m>2]\,..\,(32)$$

where A_m is an unknown factor to be determined presently. The special cases of $m=0$ and $m=1$ can be written down similarly at once.

In the stratum of the upper layer the waves are reflected multiply and in effect they may be imagined to be equivalent to the stationary surface waves, the expressions of them being written by

$$\left.\begin{aligned}
2\varpi_z'' &= \frac{2(-1)^m}{m!}\left(1-\cos^2\frac{\pi}{m}\right) \cos m\omega \\
&\qquad \times \int_0^\infty (B_m \cos\beta' z + C_m \sin\beta' z)\, e^{-\beta\xi} J_m(kr)\, \beta^{n-1} k^{m+1} dk, \\
2\varpi_r'' &= -\frac{2(-1)^m}{m!}\left(1-\cos^2\frac{\pi}{m}\right) \cos m\omega \\
&\qquad \times \int_0^\infty (B_m \sin\beta' z - C_m \cos\beta' z)\, e^{-\beta\xi} \frac{\partial J_m(kr)}{\partial r}\, \beta^n k^{m-1}\, dk, \\
2\varpi_\omega'' &= \frac{2(-1)^m}{m!}\left(1-\cos^2\frac{\pi}{m}\right) m \sin m\omega \\
&\qquad \times \int_0^\infty (B_m \sin\beta' z - C_m \cos\beta' z)\, e^{-\beta\xi} \frac{J_m(kr)}{r}\, \beta^n k^{m-1}\, dk, \\
u'' &= -\frac{2(-1)^m}{m!}\left(1-\cos^2\frac{\pi}{m}\right) m \sin m\omega \\
&\qquad \times \int_0^\infty (B_m \cos\beta' z + C_m \sin\beta' z)\, e^{-\beta\xi} \frac{J_m(kr)}{r}\, \beta^{n-1} k^{m-1}\, dk, \\
v'' &= -\frac{2(-1)^m}{m!}\left(1-\cos^2\frac{\pi}{m}\right) \cos m\omega
\end{aligned}\right\}[m>2]\,(33)$$

$$\left.\begin{aligned}&\times\int_0^\infty (B_m \cos \beta' z + C_m \sin \beta' z)\, \epsilon^{-\beta\xi} \frac{\partial J_m(kr)}{\partial r} \beta^{n-1} k^{m-1}\, dk,\\ w''&=0.\end{aligned}\right\}$$

The special cases of $m=0$ and $m=1$ can be obtained in a similar manner. In the equations (33), it should be remembered that

$$\beta'^2 = j'^2 - k^2, \qquad j'^2 = \frac{\rho' \sigma^2}{\mu'}, \quad \ldots\ldots\ldots\ldots\ldots\ldots (34)$$

where μ', ρ' are the rigidity and the density of the upper layer.

Now we have the boundary conditions:

$$\left.\begin{aligned}u+u'&=u'',\\ v+v'&=v'',\\ \mu\frac{\partial}{\partial z}(v+v')+\mu'&\frac{\partial}{\partial z}v'',\\ \mu\frac{\partial}{\partial z}(u+u')=\mu'&\frac{\partial}{\partial z}u'',\end{aligned}\right\}[z=0] \quad \ldots\ldots\ldots\ldots\ldots (35)$$

$$\frac{\partial v''}{\partial z}=0, \qquad \frac{\partial u''}{\partial z}=0, \qquad [z=-\eta] \ldots\ldots\ldots\ldots\ldots (36)$$

where η is the thickness of the layer.

Substituting from (29), (32), (33) in (35) and (36), we get

$$\left.\begin{aligned}(1+A_m)&=B_m,\\ \mu\beta(1-A_m)&=\mu'\beta' C_m,\\ B_m \cos\beta'\eta + C_m &\sin\beta'\eta = 0,\end{aligned}\right\} \ldots\ldots\ldots\ldots\ldots\ldots (37)$$

from which we find

$$\left.\begin{aligned}A_m&=\frac{\dfrac{\mu\beta}{\mu'\beta'}\tan\beta'\eta+1}{\dfrac{\mu\beta}{\mu'\beta'}\tan\beta'\eta-1},\\ B_m&=\frac{2\dfrac{\mu\beta}{\mu'\beta'}\tan\beta'\eta}{\dfrac{\mu\beta}{\mu'\beta'}\tan\beta'\eta-1},\\ C_m&=\frac{-2\dfrac{\mu\beta}{\mu'\beta'}}{\dfrac{\mu\beta}{\mu'\beta'}\tan\beta'\eta-1}.\end{aligned}\right\} \ldots\ldots\ldots\ldots\ldots\ldots (38)$$

The reflected waves in the lower medium is therefore given by

$$\left.\begin{aligned}
u' &= -\frac{2(-1)^m}{m!}\left(1-\cos^2\frac{\pi}{m}\right) m \sin m\omega \\
&\quad\times\int_0^\infty \frac{\left(\frac{\mu\beta}{\mu'\beta'}\tan\beta'\eta+1\right)}{\left(\frac{\mu\beta}{\mu'\beta'}\tan\beta'\eta-1\right)} e^{-\beta(\xi+z)}\frac{J_m(kr)}{r}\beta^{n-1}k^{m-1}\,dk, \\
v' &= -\frac{2(-1)^m}{m!}\left(1-\cos^2\frac{\pi}{m}\right)\cos m\omega \\
&\quad\times\int_0^\infty \frac{\left(\frac{\mu\beta}{\mu'\beta'}\tan\beta'\eta+1\right)}{\left(\frac{\mu\beta}{\mu'\beta'}\tan\beta'\eta-1\right)} e^{-\beta(\xi+z)}\frac{\partial J_m(kr)}{\partial r}\beta^{n-1}k^{m-1}\,dk, \\
w' &= 0,
\end{aligned}\right\}[m>2] \ldots (39)$$

$$\left.\begin{aligned}
u' &= 0, \\
v' &= -\int_0^\infty \frac{\left(\frac{\mu\beta}{\mu'\beta'}\tan\beta'\eta+1\right)}{\left(\frac{\mu\beta}{\mu'\beta'}\tan\beta'\eta-1\right)} e^{-\beta(\xi+z)}\frac{\partial J_0(kr)}{\partial r}\beta^{n-1}k^{-1}\,dk, \\
w' &= 0,
\end{aligned}\right\}[m=0] \ldots (40)$$

$$\left.\begin{aligned}
u' &= 2\sin\omega\int_0^\infty \frac{\left(\frac{\mu\beta}{\mu'\beta'}\tan\beta'\eta+1\right)}{\left(\frac{\mu\beta}{\mu'\beta'}\tan\beta'\eta-1\right)} e^{-\beta(\xi+1)}\frac{J_1(kr)}{r}\beta^{n-1}\,dk, \\
v' &= 2\cos\omega\int_0^\infty \frac{\left(\frac{\mu\beta}{\mu'\beta'}\tan\beta'\eta+1\right)}{\left(\frac{\mu\beta}{\mu'\beta'}\tan\beta'\eta-1\right)} e^{-\beta(\xi+z)}\frac{\partial J_1(kr)}{\partial r}\beta^{n-1}\,dk, \\
w' &= 0.
\end{aligned}\right\}[m=1] \ldots (41)$$

Again, the displacement at the surface layer can be expressed in the forms:

$$\begin{aligned}
u'' &= -\frac{4(-1)^m}{m!}\left(1-\cos^2\frac{\pi}{m}\right) m \sin m\omega \\
&\quad\times\int_0^\infty \frac{\sin\beta'(\eta-z)}{\left(\sin\beta'\eta-\frac{\mu\beta}{\mu'\beta'}\cos\beta'\eta\right)} e^{-\beta\xi}\frac{J_m(kr)}{r}\beta^{n-1}k^{m-1}\,dk,
\end{aligned}$$

$$\left.\begin{aligned}
v'' &= -\frac{4(-1)^m}{m\,!}\left(1-\cos^2\frac{\pi}{m}\right)\cos m\omega \\
&\quad+\int_0^\infty \frac{\sin\beta'(\eta-z)}{\left(\sin\beta'\eta-\dfrac{\mu\beta}{\mu'\beta'}\cos\beta'\eta\right)}\,e^{-\beta\xi}\frac{\partial J_m(kr)}{\partial r}\beta^{n-1}k^{m-1}dk,\\
w'' &= 0,
\end{aligned}\right\}[m>2]\,..\,(42)$$

$$\left.\begin{aligned}
u'' &= 0,\\
v'' &= -2\int_0^\infty \frac{\sin\beta'(\eta-z)}{\left(\sin\beta'\eta-\dfrac{\mu\beta}{\mu'\beta'}\cos\beta'\eta\right)}\,e^{-\beta\xi}\frac{J_0(kr)}{r}\,\beta^{n-1}k^{-1}\,dk,\\
w'' &= 0,
\end{aligned}\right\}[m=0]\,..\,(43)$$

$$\left.\begin{aligned}
u'' &= 4\sin\omega\int_0^\infty \frac{\sin\beta'(\eta-z)}{\left(\sin\beta'\eta-\dfrac{\mu\beta}{\mu'\beta'}\cos\beta'\eta\right)}\,e^{-\beta\xi}\frac{\partial J_1(kr)}{\partial r}\beta^{n-1}dk,\\
v'' &= 4\cos\omega\int_0^\infty \frac{\sin\beta'(\eta-z)}{\left(\sin\beta'\eta-\dfrac{\mu\beta}{\mu'\beta'}\cos\beta'\eta\right)}\,e^{-\beta\xi}\frac{J_1(kr)}{r}\,\beta^{n-1}\,dk,\\
w'' &= 0.
\end{aligned}\right\}[m=1]\,..\,(44)$$

To evaluate the integrals in the above expressions, we should apply the formula:

$$J_m(kr)=\frac{2}{\pi}\int_0^\infty \sin\left(kr\,\mathrm{ch}\,f-\frac{m\pi}{2}\right)\cos mf\,df. \quad \ldots\ldots\ldots\ldots(45)$$

The final results of the evaluation of the surface displacement are written by

$$\begin{aligned}
u'' &= \frac{8\pi(-1)^m}{m\,!}\left(1-\cos^2\frac{\pi}{m}\right)m\sin m\omega\,\frac{\sin\beta_1'\eta}{F'(\kappa)}\,e^{-\beta_1\xi}\,\beta_1^{n-1}\,\kappa^{m-1}\,\frac{Y_m(\kappa r)}{r}\\
&\qquad\qquad\qquad +\text{asymptotically vanishing terms,}\\
v'' &= \frac{8\pi(-1)^m}{m\,!}\left(1-\cos^2\frac{\pi}{m}\right)\cos m\omega\,\frac{\sin\beta_1'\eta}{F'(\kappa)}\,e^{-\beta_1\xi}\,\beta_1^{n-1}\,\kappa^{m-1}\,\frac{\partial Y_m(\kappa r)}{\partial r}\\
&\qquad\qquad\qquad +\text{asymptotically vanishing terms,}\\
w'' &= 0.
\end{aligned}$$

$$[m>2]$$

$$\ldots\ldots\ldots\ldots\ldots\ldots\ldots\ldots\ldots\ldots(46)$$

In the above expressions κ is the real, positive root of

$$F(k)=\sin\beta'\eta-\frac{\mu\beta}{\mu'\beta'}\cos\beta'\eta=0, \qquad \text{.................} (47)$$

where $\beta'=\sqrt{j'^2-k^2}$ and $\beta=\sqrt{k^2-j^2}$; while β_1 and β_1' are the values of β and β' corresponding to κ.

The special cases of $m=0$ and 1 can be at once written down by putting m equal to 0 and 1 respectively and afterwards replacing $(1-\cos^2\pi/m)$ by ½ and unity in each case.

As in the case of Rayleigh-waves, the propagated Love-waves can be expressed by

$$\left.\begin{aligned}
u''&\approx\frac{4\pi(-1)^m}{m!}\left(1-\cos^2\frac{\pi}{m}\right)m\sin m\omega\,\frac{\sin\beta_1'\eta}{F'(\kappa)}\\
&\qquad\times e^{-\beta_1\xi}\,\beta_1^{n-1}\,\kappa^{m-1}\,\frac{H_m^{(2)}(\kappa r)}{r}\,e^{i\sigma t},\\
v''&\approx\frac{4\pi(-1)^m}{m!}\left(1-\cos^2\frac{\pi}{m}\right)\cos m\omega\,\frac{\sin\beta_1'\eta}{F'(\kappa)}\\
&\qquad\times e^{-\beta_1\xi}\,\beta_1^{n-1}\,\kappa^{m-1}\,\frac{\partial H_m^{(2)}(\kappa r)}{\partial r}\,e^{i\sigma t},\\
w''&=0.
\end{aligned}\right\}[m>2]\,..\,(48)$$

$$\left.\begin{aligned}
u''&=0,\\
v''&\approx 2\pi\frac{\sin\beta_1'\eta}{F'(\kappa)}\,e^{-\beta_1\xi}\,\beta_1^{n-1}\,\kappa^{-1}\,\frac{\partial H_0(\kappa r)}{\partial r}\,e^{i\sigma t},\\
w''&=0.
\end{aligned}\right\}[m=0]\,..\,(49)$$

$$\left.\begin{aligned}
u''&\approx-\frac{4\pi\sin\omega\sin\beta_1'\eta}{F'(\kappa)}\,e^{-\beta_1\xi}\,\beta_1^{n-1}\,\frac{H_1(\kappa r)}{r}\,e^{i\sigma t},\\
v''&\approx-\frac{4\pi\cos\omega\sin\beta_1'\eta}{F'(\kappa)}\,e^{-\beta_1\xi}\,\beta_1^{n-1}\,\frac{\partial H_1(\kappa r)}{\partial r}\,e^{i\sigma t},\\
w''&=0.
\end{aligned}\right\}[m=1]\,..\,(50)$$

It is important to notice that $F(\kappa)=0$ is the equation to determine the velocity of Love-waves and hence the excited surface waves are transmitted with such a velocity. As this velocity depends on the wave-length, the dispersion of waves is quite possible. Again, in all cases the vertical component of the displacement does not appear, while the displacement component in the direction of the propagation of the waves is consistent in the neighbourhood of the epicentre. This component, however, quickly disappears as the distance from the epicentre is increased. The fact, that the surface displacement decreases at the rate of $e^{-\beta_1\xi}$ as the depth of the origin is increased, is not without significance in the sense that the transverse surface waves have a large amplitude compared with that of Rayleigh-waves whose amplitudes are propotional to $e^{-\alpha_1\xi}$.

4. We now proceed to the case where the origin of the disturbance is situated at a point in the upper layer.

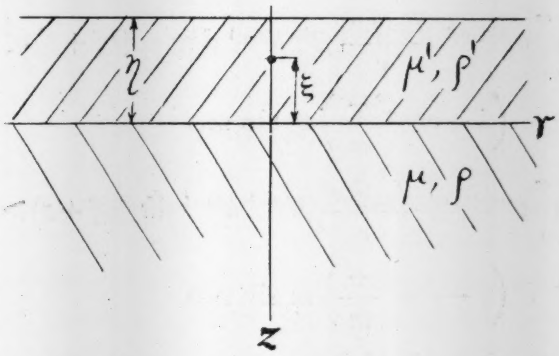

If the source is of a simple harmonic type, we write

$$f(x, y)=\frac{c^{-ij'\sqrt{r2+(z+\xi)2}}}{\sqrt{r^2+(z+\xi)^2}}, \qquad \dots\dots\dots\dots\dots\dots (51)$$

so that the original disturbance is written by

$$\left.\begin{aligned} 2\varpi_z&=\frac{2(-1)^{m+n}}{m!}\,i^n\left(1-\cos^2\frac{\pi}{m}\right)\cos m\omega\\ &\qquad\times\int_0^\infty e^{-i\beta'(z+\xi)}J_m(kr)\,\beta'^{n-1}k^{m+1}\,dk, \qquad [(\xi+z)>0]\\ &=\frac{2(-1)^{m+n}}{m!}\,i^n\left(1-\cos^2\frac{\pi}{m}\right)\cos m\omega\\ &\qquad\times\int_0^\infty e^{i\beta'(z+\xi)}J_m(kr)\,\beta'^{n-1}k^{m+1}\,dk, \qquad [(\xi+z)<0] \end{aligned}\right\}[m>2]\,..\,(52)$$

in which $e^{i\sigma t}\,ds_1^m\,ds_2^n$ is omitted as in the preceding case.

The corresponding values of ϖ_r, ϖ_ω, u, v, w are denoted by

$$\left.\begin{aligned} 2\varpi_r&=-2(-1)^{m+n}\,i^{n+1}\left(1-\cos^2\frac{2\pi}{m}\right)\cos m\omega\\ &\qquad\times\int_0^\infty e^{-i\beta'(z+\xi)}\frac{\partial J_m(kr)}{\partial r}\,\beta'^n k^{m-1}\,dk, \qquad [(\xi+z)>0]\\ &=2(-1)^{m+n}\,i^{n+1}\left(1-\cos^2\frac{\pi}{m}\right)\cos m\omega\\ &\qquad\times\int_0^\infty e^{i\beta'(z+\xi)}\frac{\partial J_m(kr)}{\partial r}\,\beta'^n k^{m-1}\,dk, \qquad [(\xi+z)<0] \end{aligned}\right\}[m>2]\,..\,(53)$$

$$\left.\begin{aligned}
2\varpi_\omega &= 2(-1)^{m+n}\, i^{n+1}\left(1-\cos^2\frac{\pi}{m}\right) m \sin m\omega \\
&\qquad \times\int_0^\infty e^{-i\beta'(z+\xi)}\,\frac{J_m(kr)}{r}\,\beta'^n\, k^{m-1}\, dk, \quad [(\xi+z)>0] \\
&= -2(-1)^{m+n}\, i^{n+1}\left(1-\cos^2\frac{\pi}{m}\right) m \sin m\omega \\
&\qquad \times\int_0^\infty e^{i\beta'(z+\xi)}\,\frac{J_m(kr)}{r}\,\beta'^n\, k^{m-1}\, dk, \quad [(\xi+z)<0]
\end{aligned}\right\}[m>2]\,..\,(54)$$

$$\left.\begin{aligned}
u &= -2(-1)^{m+n}\, i^{n}\left(1-\cos^2\frac{\pi}{m}\right) m \sin m\omega \\
&\qquad \times\int_0^\infty e^{-i\beta'(z+\xi)}\,\frac{J_m(kr)}{r}\,\beta'^{n-1}\, k^{m-1}\, dk, [(\xi+z)>0] \\
&= -2(-1)^{m+n}\, i^{n}\left(1-\cos^2\frac{\pi}{m}\right) m \sin m\omega \\
&\qquad \times\int_0^\infty e^{i\beta'(z+\xi}\,\frac{J_m(kr)}{r}\,\beta'^{n-1}\, k^{m-1}\, dk, \quad [(\xi+z)<0]
\end{aligned}\right\}[m>2]\,..\,(55)$$

$$\left.\begin{aligned}
v &= -2(-1)^{m+n}\, i^{n}\left(1-\cos^2\frac{\pi}{m}\right) \cos m\omega \\
&\qquad \times\int_0^\infty e^{-i\beta'(z+\xi)}\,\frac{\partial J_m(kr)}{\partial r}\,\beta'^{n-1} k^{m-1} dk, \quad [(\xi+z)>0] \\
&= -2(-1)^{m+n}\, i^{n}\left(1-\cos^2\frac{\pi}{m}\right) \cos m\omega \\
&\qquad \times\int_0^\infty e^{i\beta'(z+\xi)}\,\frac{\partial J_m(kr)}{\partial r}\,\beta'^{n-1} k^{m-1} dk, \quad [(\xi+z)<0]
\end{aligned}\right\}[m>2]\,..\,(56)$$

$$w=0.$$

The case of $m=0$ and 1 can be obtained by putting m equal to 0 and 1 respectively and afterwards replacing $(1-\cos^2\pi/m)$ by ½ and unity in each case.

The stationary oscillations of the layer may be expressed in the forms:

$$\left.\begin{aligned}
2\varpi_z' &= 2(-1)^{m}\, i^{n+1}\left(1-\cos^2\frac{\pi}{m}\right) \cos m\omega \\
&\qquad \times\int_0^\infty (A_m\, e^{i\beta' z}+B_m\, e^{-i\beta' z})\, J_m(kr)\, \beta'^{n-1}\, k^{m+1}\, dk, \\
2\varpi_r' &= 2(-1)^{m}\, i^{n+1}\left(1-\cos^2\frac{\pi}{m}\right) \cos m\omega \\
&\qquad \times\int_0^\infty (A_m\, e^{i\beta' z}-B_m\, e^{-i\beta' z})\, \frac{\partial J_m(kr)}{\partial r}\, \beta'^{n}\, k^{m-1}\, dk,
\end{aligned}\right.$$

$$\left.\begin{aligned}
2\varpi_{\omega}' &= -2(-1)^m\, i^{n+1}\left(1-\cos^2\frac{\pi}{m}\right) m \sin m\omega \\
&\qquad \times \int_0^{\infty} (A_m\, e^{i\beta' z} - B_m\, e^{-i\beta' z})\, \frac{J_m(kr)}{r}\, \beta'^n\, k^{m-1}\, dk, \\
u' &= -2(-1)^m\, i^{n}\left(1-\cos^2\frac{\pi}{m}\right) m \sin m\omega \\
&\qquad \times \int_0^{\infty} (A_m\, e^{i\beta' z} + B_m\, e^{-i\beta' z})\, \frac{J_m(kr)}{r}\, \beta'^{n-1}\, k^{m-1}\, dk, \\
v' &= -2(-1)^m\, i^{n}\left(1-\cos^2\frac{\pi}{m}\right) \cos m\omega \\
&\qquad \times \int_0^{\infty} (A_m\, e^{i\beta' z} + B_m\, e^{-i\beta' z})\, \frac{\partial J_m(kr)}{\partial r}\, \beta'^{n-1}\, k^{m-1}\, dk, \\
w' &= 0,
\end{aligned}\right\} \begin{matrix}[z<0]\\ [m>2]\end{matrix} \cdot\cdot (57)$$

and similar expressions for the case $m=0$ and $m=1$.

The bottom medium should make some oscillations in accordance with the disturbances in the superficial layer. The expressions of the motion of the bottom layer are thus given by

$$\left.\begin{aligned}
2\varpi_z'' &= 2(-1)^m\, i^{n+1}\left(1-\cos^2\frac{\pi}{m}\right) \cos m\omega \\
&\qquad \times \int_0^{\infty} C_m\, e^{-\beta z}\, J_m(kr)\, \beta'^{n-1}\, k^{m+1}\, dk, \\
2\varpi_r'' &= 2(-1)^m\, i^{n+1}\left(1-\cos^2\frac{\pi}{m}\right) \cos m\omega \\
&\qquad \times \int_0^{\infty} C_m\, e^{-\beta z}\, \frac{\partial J_m(kr)}{\partial r}\, \beta'^{n}\, k^{m-1}\, dk, \\
2\varpi_{\omega}'' &= 2(-1)^m\, i^{n+1}\left(1-\cos^2\frac{\pi}{m}\right) m \sin m\omega \\
&\qquad \times \int_0^{\infty} C_m\, e^{-\beta z}\, \frac{J_m(kr)}{r}\, \beta'^{n}\, k^{m-1}\, dk, \\
u'' &= -2(-1)^m\, i^{n}\left(1-\cos^2\frac{\pi}{m}\right) m \sin m\omega \\
&\qquad \times \int_0^{\infty} C_m\, e^{-\beta z}\, \frac{J_m(kr)}{r}\, \beta'^{n-1}\, k^{m-1}\, dk, \\
v'' &= -2(-1)^m\, i^{n}\left(1-\cos^2\frac{\pi}{m}\right) \cos m\omega
\end{aligned}\right\} \begin{matrix}[z<0]\\ [m>2]\end{matrix} \cdot\cdot (58)$$

$$\left.\begin{aligned} &\qquad\times\int_0^\infty C_m\, e^{-\beta z}\,\frac{\partial J_m(kr)}{\partial r}\,\beta'^{n-1}\,k^{m-1}\,dk,\\ &w''=0,\end{aligned}\right\}$$

together with similar expressions for the cases $m=0$ and $m=1$.

At the boundary $z=0$, we should have

$$\left.\begin{aligned} &u+u'=u'', && v+v'=v'',\\ &\mu'\frac{\partial}{\partial z}(v+v')=\mu\frac{\partial}{\partial z}v'', && \mu'\frac{\partial}{\partial z}(u+u')=\mu\frac{\partial}{\partial z}u''.\end{aligned}\right\}\cdots\cdots\cdots(59)$$

At the free surface $z=-\eta$,

$$\frac{\partial}{\partial z}(v+v')=0,\qquad \frac{\partial}{\partial z}(u+u')=0,\cdots\cdots\cdots\cdots\cdots\cdots(60)$$

Substituting from (52), (53), (54), (55), (56), (57), (58) in (59), (60), we get

$$\left.\begin{aligned} &(-1)^n e^{-i\beta'\xi}+A_m+B_m=C_m,\\ &\mu'\beta'[(-1)^{n+1}\,i\,e^{-i\beta'\xi}+i(A_m-B_m)]=-\mu\beta C_m,\\ &(-1)^n e^{i\beta'(\xi-\eta)}+A_m\,e^{-i\beta'\eta}-B_m\,e^{i\beta'\eta}=0,\end{aligned}\right\}\cdots\cdots\cdots\cdots(61)$$

from which we obtain

$$\left.\begin{aligned} A_m&=-(-1)^n\frac{\left\{e^{i\beta'(\xi-\eta)}+e^{-i\beta'(\xi-\eta)}\right\}\left(1-i\dfrac{\mu'\beta'}{\mu\beta}\right)}{\left(1+i\dfrac{\mu'\beta'}{\mu\beta}\right)e^{i\beta'\eta}+\left(1-i\dfrac{\mu'\beta'}{\mu\beta}\right)e^{-i\beta'\eta}},\\ B_m&=(-1)^n\frac{\left(1+i\dfrac{\mu'\beta'}{\mu\beta}\right)e^{i\beta'(\xi-\eta)}-\left(1-i\dfrac{\mu'\beta'}{\mu\beta}\right)e^{-i\beta'(\xi+\eta)}}{\left(1+i\dfrac{\mu'\beta'}{\mu\beta}\right)e^{i\beta'\eta}+\left(1-i\dfrac{\mu'\beta'}{\mu\beta}\right)e^{-i\beta'\eta}}.\end{aligned}\right\}\cdots\cdots(62)$$

The displacements at the free surface are now written in the following forms:

$$\left.\begin{aligned} u=&-4(-1)^{m+n}\,i^{n+1}\left(1-\cos^2\frac{\pi}{m}\right)m\sin m\omega\\ &\times\int_0^\infty\frac{\left(\cos\beta'\xi+\dfrac{\mu\beta}{\mu'\beta'}\sin\beta'\xi\right)}{\sin\beta'\eta-\dfrac{\mu\beta}{\mu'\beta'}\cos\beta'\eta}\,\frac{J_m(kr)}{r}\,\beta'^{n-1}\,k^{m-1}\,dk,\end{aligned}\right.$$

$$\left.\begin{aligned} v=&-4(-1)^{m+n}\, i^{n+1}\left(1-\cos^2\frac{\pi}{m}\right)\cos m\omega \\ &\times\int_0^\infty \frac{\left(\cos\beta'\xi+\dfrac{\mu\beta}{\mu'\beta'}\sin\beta'\xi\right)}{\sin\beta'\eta-\dfrac{\mu\beta}{\mu'\beta'}\cos\beta'\eta}\,\frac{\partial J_m(kr)}{\partial r}\,\beta'^{n-1}\,k^{m-1}\,dk. \\ &\qquad\qquad\qquad\qquad [m>2,\ z=-\eta] \end{aligned}\right\}\ldots\ldots(63)$$

Integrating these in the same manner as that of the preceding section, we get finally

$$\begin{aligned} u\approx\, & 8\pi(-1)^{m+n}\, i^{n+1}\left(1-\cos^2\frac{\pi}{m}\right) m\sin m\omega \\ &\qquad\times\frac{\cos\beta_1'\xi+\dfrac{\mu\beta_1}{\mu'\beta_1'}\sin\beta_1'\xi}{F'(\kappa)}\,\beta_1'^{\,n-1}\,\kappa^{m-1}\,\frac{H_m^{(2)}(\kappa r)}{r} \\ v\approx\, & 8\pi(-1)^{m+n}\, i^{n+1}\left(1-\cos^2\frac{\pi}{m}\right)\cos m\omega \\ &\qquad\times\frac{\cos\beta_1'\xi+\dfrac{\mu\beta_1}{\mu'\beta_1'}\sin\beta_1'\xi}{F'(\kappa)}\,\beta_1'^{\,n-1}\,\kappa^{m-1}\,\frac{\partial H_m^{(2)}(\kappa r)}{\partial r} \\ w=\, & 0. \qquad\qquad\qquad\qquad [m>2,\ z=-\eta] \end{aligned}$$

$$\ldots\ldots\ldots\ldots\ldots\ldots\ldots\ldots\ldots\ldots(64)$$

In the above expressions κ is the real and positive root of

$$F(k)=\sin\beta'\eta-\frac{\mu\beta}{\mu'\beta'}\cos\beta\eta=0,\ldots\ldots\ldots\ldots\ldots\ldots(65)$$

where $\beta'=\sqrt{j'^2-k^2}$ and $\beta=\sqrt{k^2-j^2}$, while β_1 and β_1' are the values of β and β' corresponding to κ.

The special cases of $m=0$ and $m=1$ can be obtained by the same operations as before.

It is worth noticing that in this case the surface displacement does not decrease even if the depth of the origin is increased, but the displacement varies as certain harmonic functions of the depth. The other natures are quite similar to those of the preceding case where the origin of the disturbance is resident at the bottom medium.

5. We have now arrived at the results which have some importance on the practical seismology. We may enumerate them in the following conclusive forms:

1. Long Love-waves having azimuthal distribution on a spherical surface have the large colatitudinal component of displacement, besides the ordinary azimuthal component, and this colatitudinal component cannot disappear even at the equatorial circle.

2. The vertical component is not existent from the start.

3. The velocity of the propagation of Love-waves on a spherical surface is approximately equal to that on a plane surface, even though the waves are relatively long.

4. The dispersion of Love-waves is possible also on a spherical surface.

5. The growth of Love-waves towards the antipode is also possible.

6. The azimuthal variation of displacement of Love-waves is maintained towards the antipode.

7. In considering the neighbourhood of the origin, the longitudinal component of displacement of the short waves becomes quiescent as the waves are propagated towards infinity. When the waves are generated from an internal source, the displacement at the free surface conspires with the modes of the oscillations at the origin.

8. In this case the azimuthal variation of the azimuthal displacement at the surface conforms for all radial distances with the type of the oscillations of the internal source.

9. When the source is resident at the bottom medium, the amplitude of the surface waves decreases with the depth of the source in the bottom medium at the rate of $e^{-\beta_1\xi}$. It is interesting to compare this with the case of Rayleigh-waves in which the amplitude of the waves is proportional to $e^{-\alpha_1\xi}(\alpha_1>\beta_1)$.

10. When the source is situated at the superficial layer, the amplitude of the surface waves varies as some harmonic functions of ξ.

In conclusion I have to express my sincerest thank to Mr. G. Nishimura who has assisted me in preparing this paper.

---

23. 球面上に於けるラブ波の傳播とこれに關聯する一二の問題

地震研究所 妹 澤 克 惟

ラブ波の問題は數學的には餘り簡單過ぎて興味が薄く、又地體構造の上からは常に表面層が必要な爲めに人爲的の嫌ひがある。しかし其結果が驗震上の事實に極めてよく符合する爲、歐洲の地震學者に可なり信頼され且つ種々の場合に應用されて居る。殊に地球を一周しても勢力を失はぬ樣な

ラブ型の長波は地球內部の構造を究める爲めに尊重され過ぎる傾向がある。しかしながら球面上を傳播するラブ波の問題は未だ解かれずに殘されて居る。殊に其が方向性を持つ場合は猶更省みられぬ樣である。私は此等の場合を力學的に研究し、尙震源に極く近い場所では一般解法が反て不正確になる爲に別に考へ、且つ震源の位置も考慮に入れて算出して見た。

地震學的に重要な結果を摘錄して見ると、

1. 方向性を有するラブ波は球面上で進行方向の變位を持ち、震波赤道に到つても其變位を消滅させる事が出來ぬ。
2. 地表に直角な變位は絕對に存在することがない。
3. 波長が相當長い場合でも球面上でのラブ波の速度は平面上の場合と大した變りがない。
4. 球面上でもラブ波の分散が可能な事は勿論とする。
5. 球體の對蹠點に進むに從つて變位が再び增大する事も當然な事ながら認められる。
6. ラブ波の方向性は對蹠點に到る迄保持される。
7. 震源附近を考へて見る時、地表上の變位が內部の震源の型と或程度迄一致する。
8. 橫變位の方向性のみはすべての距離に於て內部の震源の型と一致する。
9. 震源が下層の媒體中にある時は表面波の振幅は $e^{-\beta_1\xi}$ に比例して少くなる。レーレー波の $e^{-\alpha_1\xi}$ に比較して面白い對照を造る。
10. 震源が上層中にある時は震源の深さの影響は全く別の形式となる。

24. *Observation on the Time Variation of the Second Space Derivatives of the Gravitational Potential. (Part I).*

By **Chûji TSUBOI,**

Earthquake Research Institute.

(Received Sept. 20, 1929.)

1. The gravitational state at a definite point on the earth does not remain absolutely constant with time. The intensity and direction of gravity are subject to periodic disturbances of astronomical origin. These effects are mainly due to the attractions of the moon, the sun and of the tide of sea-water produced by them. Schweydar[1] made detailed investigations on these phenomena and detected experimentally the existence of these effects. We must notice further that the main part of the gravitational state at a point on the earth depends on the subterranean mass distribution in its neighbourhood which is not absolutely immobile at all from geophysical point of view. It will thus easily be accepted that if there are some such changes in the subterranean mass distribution at all, they will produce no less influences on the gravitational state at the neighbouring fields of the displaced mass. A few workers[2] already reported that they observed some secular changes in the intensity of gravity which they believed to be due to this latter cause. Some others,[3] however, did not accept these results as undoubtful and regarded these variations rather as due to some residual instrumental errors happened in the respective measurements of these workers. Whichever opinion may be justified in each respective case, it is of great

---

[1] W. SCHWEYDAR, *Veröfftl. d. kön. preuss. geodät. Inst.*, **54** (1912).
„ *ibid.*, **59** (1914).
„ *ibid.* (Neue Folge), **38** (1921).

[2] F. W. PFAFF, *ZS. deut. geol. Ges.*, **51** (1899), 125.
„ *Geogr. Jahresber.*, **15** (1903),.
S. G. BURRAD, *Phil. Trans. Roy Soc.*, **205** (1906), 289.
O. FISHER, *Amer. Journ. Sci.*, **21** (1906), 216.
K. R. KOCH, *Ann. d. Phys.*, **15** (1904), 146.
A. BORN, *Isostasie und Schweremessung*, Berlin (1923), 49.

[3] F. R. HELMERT, *Enz. d. math. Wiss.*, Bd. VI, 1 B., Heft 2 (1910), 177.
O. HECHER and O. MEISSER, *Handb. d. phys. und tech. Mech.*, Bd. II (1928), 174.

importance to make further investigations into these lines and to decide whether or not such secular changes in gravitational states is actually taking place.

The present writer[4] has recently come across with an interesting fact that the gravitationally anomalous regions in this country are also the regions most frequented by earthquakes. This fact suggests that the geological movements taking place at present in a certain region are closely correlated to the special state of the gravitational fields in its environs. If it be allowed further that the geological and volcanic activities are connected with some macroscopic changes in the subterranean mass distribution of any mode, some changes in the gravitational state on the earth must be correspondingly expected especially in earthquake and volcanic regions as their surface manifestation. If there is such a phenomenon at all, this must be especially prevalent in this country in which the crustal strain in much concentrated.

Considering in this way, it seems probable to the writer that the gravitational state *is* actually subject to secular changes and that the only reason why this has not yet been established is that no observation has ever been made from the stand point developed in the above.

The continuous or at least successive observations on any of the quantities relating to the gravitational potential must be made for the object of obtaining some clue to the changes in the subterranean mass distribution. The observations of the intensity of gravity as well as the direction of gravity with respect to the reference ellipsoid may be ones of the methods which will meet this object. Small changes in these quantities are, however, generally hard to be observed. On the other hand, the second space derivatives of the gravitational potential can be determined with considerable accuracy. We can make comparatively easily an accurate continuous measurement of the latter quantities and detect changes in them if any. For these reasons, the continuous observations of the second space derivatives of the gravitational potential will match best for our present purpose. For a time since, the present writer has been engaged in the continuous observation of the second space derivatives with a specially deviced instrument. This instrument is nothing but an extremely sensitive torsion balance fixed in a definite azimuth. The observation was commenced only in the beginning of this year (1929), and the period of observation is not yet long enough for the writer to get some definite conclusions with regard to his primary object. Yet it seems worth while to describe the results of the observations

---

4) C. TSUBOI, *Proc. Imp. Acad.*, 5 (1929), 326.

so far obtained because they will not only serve as an introductory report of the further investigations but will also suggest many interesting problems regarding the short period fluctuations in the value of the gravitational potential.

It is a great pleasure for the writer to record his appreciation of the helpful suggestions of Professor Torahiko Terada in this work.

2. The instrument used in the present observation is a modification of a torsion balance of which the theory of action was originally developed by Eötvös. It consists essentially of a horizontal beam suspended at its middle point from above by a fine fibre. The horizontal beam is loaded at its both extremities by equal spherical masses. The equilibrium of the hanging system will be attained when the torsional moment acting on the beam due to the slight curvature of the gravitational equipotential surface just balances with the restitutive force due to the rigidity of the fibre towards its untwisted position. Let ξ η ζ be three co-ordinate axes taken northwards, eastwards and downwards respectively. Let further V be the gravitational potential, τ the torsional constant of the fibre, θ its angular deviation from the untwisted position, K the moment of inertia of the beam, α the angle between the northward direction and the beam measured from the northward direction clockwise as seen from above. The conditions of equilibrium of the balance is expressed by,

$$\tau\theta = K\left(\frac{\partial^2 V}{\partial\eta^2} - \frac{\partial^2 V}{\partial\xi^2}\right)\sin 2\alpha + 2K\frac{\partial^2 V}{\partial\xi\,\partial\eta}\cos 2\alpha \ldots\ldots\ldots\ldots (1)$$

Suppose some changes happen in the form of the equipotential surface and what is the same thing in either or both of the values of $\left(\frac{\partial^2 V}{\partial\eta^2} - \frac{\partial^2 V}{\partial\xi^2}\right)$ and $\frac{\partial^2 V}{\partial\xi\,\partial\eta}$. In response to them, the corresponding change must take place in the value of θ. Thus we have,

$$\tau\Delta\theta = K\sin 2\alpha\,\Delta\left(\frac{\partial^2 V}{\partial\eta^2} - \frac{\partial^2 V}{\partial\xi^2}\right) + 2K\cos 2\alpha\,\Delta\frac{\partial^2 V}{\partial\xi\,\partial\eta}$$
$$+ 2K\cos 2\alpha\left(\frac{\partial^2 V}{\partial\eta^2} - \frac{\partial^2 V}{\partial\xi^2}\right)\Delta\alpha - 4K\sin 2\alpha\frac{\partial^2 V}{\partial\xi\,\partial\eta}\Delta\alpha, \ldots\ldots (2)$$

and since
$$\Delta\theta = \Delta\alpha, \ldots\ldots\ldots\ldots\ldots\ldots\ldots\ldots\ldots\ldots (3)$$

$$\left\{\tau - 2K\left(\frac{\partial^2 V}{\partial\eta^2} - \frac{\partial^2 V}{\partial\xi^2}\right)\cos 2\alpha + 4K\frac{\partial^2 V}{\partial\xi\,\partial\eta}\sin 2\alpha\right\}\Delta\theta$$
$$= K\sin 2\alpha\,\Delta\left(\frac{\partial^2 V}{\partial\eta^2} - \frac{\partial^2 V}{\partial\xi^2}\right) + 2K\cos 2\alpha\,\Delta\frac{\partial^2 V}{\partial\xi\,\partial\eta} \ldots\ldots\ldots (4)$$

$2K\left(\frac{\partial^2 V}{\partial\eta^2}-\frac{\partial^2 V}{\partial\xi^2}\right)\cos 2\alpha$ and $4K\frac{\partial^2 V}{\partial\xi\,\partial\eta}\sin 2\alpha$ are negligible small against τ, therefore we have at last,

$$\Delta\theta=\frac{K}{\tau}\sin 2\alpha\Delta\left(\frac{\partial^2 V}{\partial\eta^2}-\frac{\partial^2 V}{\partial\xi^2}\right)+\frac{2K}{\tau}\cos 2\alpha\Delta\frac{\partial^2 V}{\partial\xi\,\partial\eta}\dots\dots\dots\dots(5)$$

The equilibrium position of the hanging system is recorded by the ordinary lamp and mirror method on a photographic paper wound round on a revolving circular drum. If the distance between the mirror attached to the horizontal beam and the photographic paper is D and an angular deflection $\Delta\theta$ of the mirror causes a linear deflection Δn of the image of the light source on the recording paper, then

$$\frac{\Delta n}{2D}=\Delta\theta.\dots\dots\dots\dots\dots\dots\dots\dots\dots(6)$$

Substituting (6) in (5), we have,

$$\begin{aligned}\Delta n&=\frac{2DK}{\tau}\sin 2\alpha\Delta\left(\frac{\partial^2 V}{\partial\eta^2}-\frac{\partial^2 V}{\partial\xi^2}\right)+\frac{4DK}{\tau}\cos 2\alpha\Delta\frac{\partial^2 V}{\partial\xi\,\partial\eta}\\&=A\Delta\left(\frac{\partial^2 V}{\partial\eta^2}-\frac{\partial^2 V}{\partial\xi^2}\right)+B\Delta\frac{\partial^2 V}{\partial\xi\,\partial\eta}\end{aligned}$$

for a given value of α, where A and B are geometrical constants. If $\alpha=0$, then

$$\Delta n=B\Delta\frac{\partial^2 \mathrm{V}}{\partial\xi\,\partial\eta},$$

and if $\alpha=\pi/4$, then

$$\Delta n=A\Delta\left(\frac{\partial^2 V}{\partial\eta^2}-\frac{\partial^2 V}{\partial\xi^2}\right).$$

We can thus determine the change in $\frac{\partial^2 V}{\partial\xi\,\partial\eta}$ and $\left(\frac{\partial^2 V}{\partial\eta^2}-\frac{\partial^2 V}{\partial\xi^2}\right)$ separately by means of two instruments set in two different azimuths making an angle of $\pi/4$ with each other.

3. It is of great importance in this observation to secure the constancy of the instrumental constants as accurately as possible. The variation in the instrumental constants will produce the deviation of the records masking the true change in the gravitational fields which it is our primary object to observe. Of all the available materials to be used in these lines, the material of vitreous silica gives the most satisfactory results.[5] The expansion coefficient of this material is extraordinarily small. This material is further

---

[5] C. TSUBOI, *Proc. Imp. Acad.*, **4** (1928), 300.

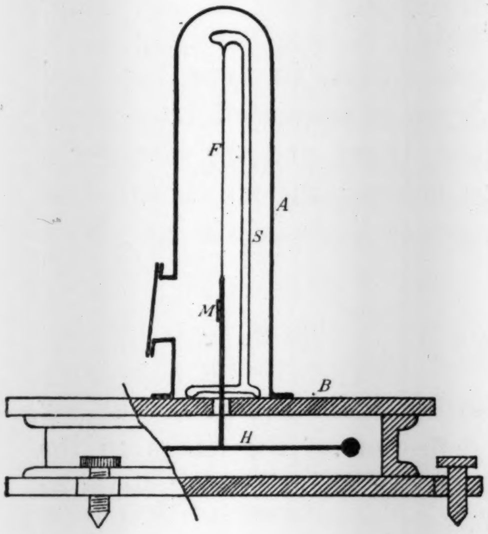

Fig. 1 a.

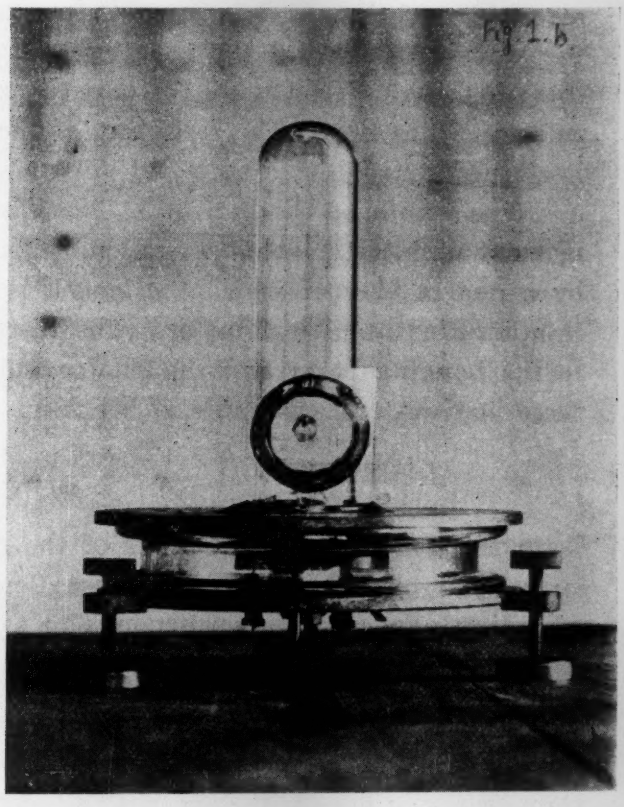

Fig. 1 b.

practically free from elastic hysterisis and can be drawn into an extremely fine fibre, its tenacity being sufficiently large for many purposes. The whole instrument used in this observation was therefore constructed of vitreous silica. Not only the torsional fibre but also the horizontal beam and the frame from which the suspension is to be hung were made of this material. The lower end of the suspension fibre is directly fused to the horizontal beam avoiding the use of any kind of the binding material. So is the upper end of the fibre to the instrumental frame. This is a very significant characteristic of this instrument. Binding materials often cause disturbances in the equilibrium position of the balance in an irregular manner. The working part of the instrument is mounted in a protection case in such a manner as is shown in Fig. 1.

The frame of the instruments is fastened to the brass plate B. The hanging beam H can revolve through full azimuth of 2π, and it reaches at its equilibrium position by itself without any external adjustment. Then the cover glass A is fixed to the plate B in such a position that the opening in A will come just in front of the reflecting surface of the mirror M attached to the hanging system. After this was done, the plate B to which the working part and the cover glass are now fixed is rotated until the direction of the beam takes the desired azimuthal angle with respect to the reference direction. The recording of the equilibrium position of the beam is effected by ordinary lamp and mirror method.

The length of the horizontal beam is about 13 cm., its mass 2 gr., and moment of intertia about 45 gr. cm.^{2} This beam is suspended from above by a quartz fibre of which the length is about 12 cm. and the diameter a few hundredths of millimeter. The distance between the mirror attached to the hanging beam and the photographic paper is about 100 cm. With these instrumental constants, it becomes,

$$\varDelta n = 8\times 10^{+9}\left[\varDelta\left(\frac{\partial^2 V}{\partial \eta^2}-\frac{\partial^2 V}{\partial \xi^2}\right)\sin 2\alpha + \varDelta\,\frac{\partial^2 V}{\partial \xi\,\partial \eta}\cos 2\alpha\right].$$

With this sensitivity, the change of the quantity in the square bracket by an amount of 1.25×10^{-10} will cause 1 cm. deflection of the image on the recording paper. This corresponds to a sensitivity about twenty times as much as the ordinary portable torsion balance.

4. The rigidity μ of the suspension fibre inevitably is affected by its temperature. The equilibrium position of the beam which depends on the rigidity of the fibre will thus be affected by temperature change. We have,

$$\frac{\varDelta\mu}{\mu}+\frac{\varDelta\theta}{\theta}=0$$

On the other hand,

$$\begin{aligned}
\mu_t &= \mu_{15}\{1+1{\cdot}2\times 10^{-4}(t-15)\},\\
\mu_0 &= \mu_{15}\{1-1{\cdot}2\times 10^{-4}\times 15\},\\
\mu_{30} &= \mu_{15}\{1+1{\cdot}2\times 10^{-4}\times 15\},\\
\mu_{30}-\mu_0 &= 3{\cdot}6\times 10^{-3}\mu_{15},\\
\mu &= 3\times 10^{11},\\
\frac{\varDelta\mu}{\mu} &= 1{\cdot}2\times 14^{-14}.
\end{aligned}$$

Therefore,

$$\frac{\varDelta\vartheta}{\theta}=-1{\cdot}2\times 10^{-14}.$$

We see therefore that even a temperature change of 30°C produces only a negligible effect on the equilibrium position of the beam.

The air inside of the vessel is not entirely free from convection and in fact the position of the image taken on the recording paper shows fluctuations within a small range, but this produces no serious objection in the present observation. It is true that defective construction of the torsion balance often causes some irregular fluctuations of the equilibrium position of the balance. Before beginning the observation, we must check the reliability of the records taken by this instrument. For this purpose, two instruments of similar dimension were placed side by side in the same azimuthal direction with respect to the reference direction. The simultaneous records of their equilibrium position were taken and compared. They are shown in Fig. 2 in Pl. XXXII. We see a close resemblance in the two records. Not only they resemble to each other in their general appearances but also in almost every details of minute fluctuations. Thus it is proved that the instruments were recording faithfully what was intended to be recorded without sensibly disturbed by external conditions.

5. We see, in the records of Fig. 2, daily variations of the equilibrium position of the images. They are no doubt due to the gravitational attraction of men who come in the building of our Institute every morning and go out every evening. This was ascertained as in Sundays and National Horidays when few workers come to the Institute, the equilibrium position remains fairly constant all day long. We see further minute fluctuations appearing simultaneously in both of the curves of Fig. 2, almost in the same form. Minute fluctuations in the day time may be explained as due to some external mass displacements, but we see also similar fluctuations even in the midnight. The origin of these disturbances is not yet certain.

6. The equilibrium position of the balance may obviously affected by the gravitational attraction of the underground water. Not so far from the Institute, there is a pond in the compound of our University. The instruments are almost just at the same level as the surface of the water of the pond. This was ascertained by means of precise levellings. A rain will raise the level of the pond as well as of the general underground water. This produces some deformation of the gravitational equipotential surface in the neighbourhood of the instrument. According to calculations, the effect of the rise of the level of the pond alone is very small, the rise of the level of the pond by 1 cm. producing a change $+5.5180\times10^{-12}$ on the term $\left(\frac{\partial^2 V}{\partial\eta^2}-\frac{\partial^2 V}{\partial\xi^2}\right)$ and -3.6469×10^{-12} on the term $\frac{\partial^2 V}{\partial\xi\,\partial\eta}$ of the observing point. The level of the pond may, however, be regarded as an indication of the level of the underground water, thus it may be expected that a correlation may be found in

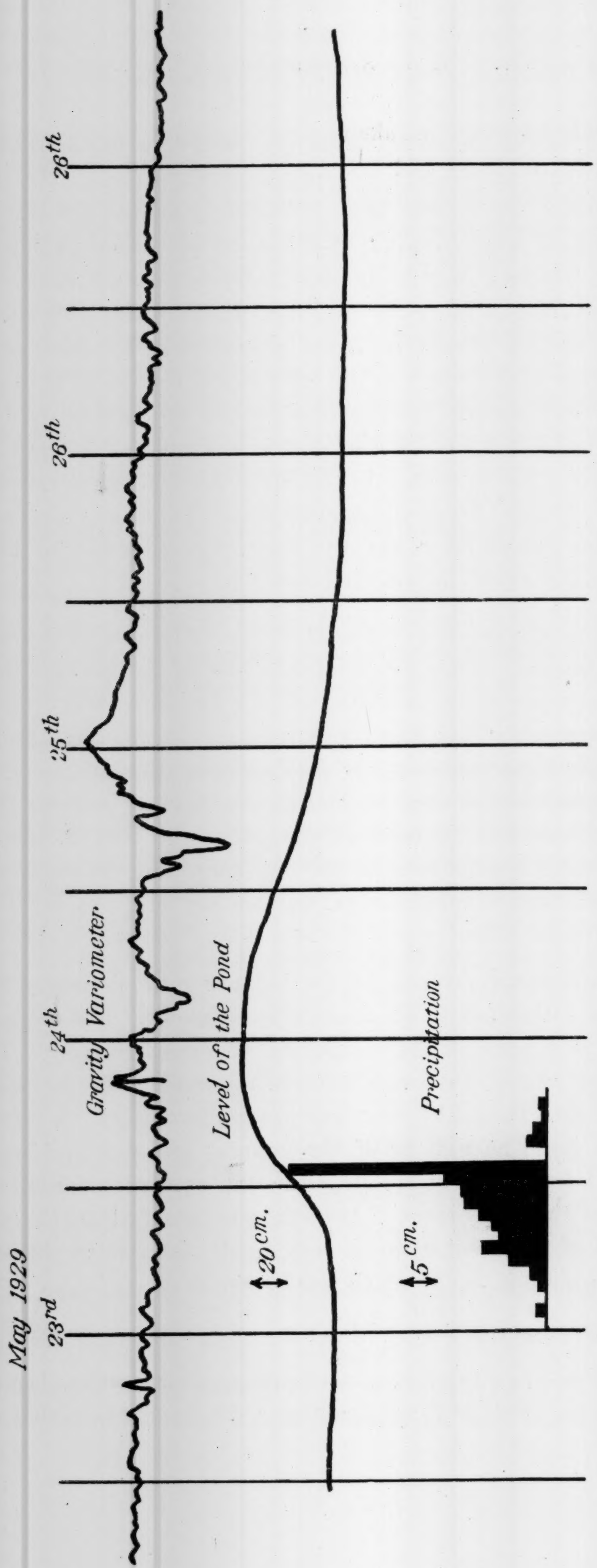
May 1929
23rd
24th
25th
26th
26th
Gravity Variometer
Level of the Pond
Precipitation
20 cm.
5 cm.

Fig. 3.

the level of the pond and the deviation of the equilibrium position of the records. This was actually the case. As a conspicuous example of this relation, a part of the records taken is reproduced in Fig. 3, with the height of the level of the pond and the hourly precipitations for comparison. It rained very hardly on May 23rd, 1929. The total precipitation was measured no less than 119.5 mm. including the maximum hourly precipitation of 35.5 mm.[6] With some lag of time from the rainfall, the level of the pond reached at its maximum. The equilibrium position of the balance began to fluctuate at about this time, continuing further about one day and a half. This is evidently due to general change in the condition of underground water.

7. In Fig. 4 is reproduced a part of the records obtained by this instrument. Through the period of observation, the equilibrium position of the balance was not fairly stationary. The effects of the underground water and others being taken out, we see still other slow variations remaining. They show no apparent correlation with meteorological and other common phenomena. It will need a fairly long continuous observation to find out the origin of these variations and to appreciate their full significances. The present paper must be regarded only as an introductory note for the further investigations.

(*To be continued.*)

---

24. 重力ポテンシャルの空間二次微分係數の時間的變動に就いて

地震研究所　坪井忠二

重力野の狀況が、殊に我が國の樣な不安定な所では、永年變化をなすのではないであらうかと云ふ事を確める爲に始めた實測である。觀測に用ひた器械は重力偏差計の原理によつたもので、全部熔融シリカで製作した。精度は、普通の可搬重力偏差計の約 20 倍程のものである。先づ此の器械が信用すべき記錄を與へると云ふ事を確めた後、連續觀測を始めた。始めたのは今年一月であるから、未だ何等の結論は得られてゐない。只其の間に降雨による地下水の影響が重力野にも及ぶ事を確めた。又夜半にも短週期の重力野の變動が現れる事がある。地下水の影響と認められるものを除いても、かなり長い時間に亘る重力野の變動が見られる。之は何に原因するのかは今の所解つて居ない。

---

[6] These data were given by Professor Takematsu Okada of the Central Meteorological Observatory, to whom the writer wishes to tender his sincere thanks.

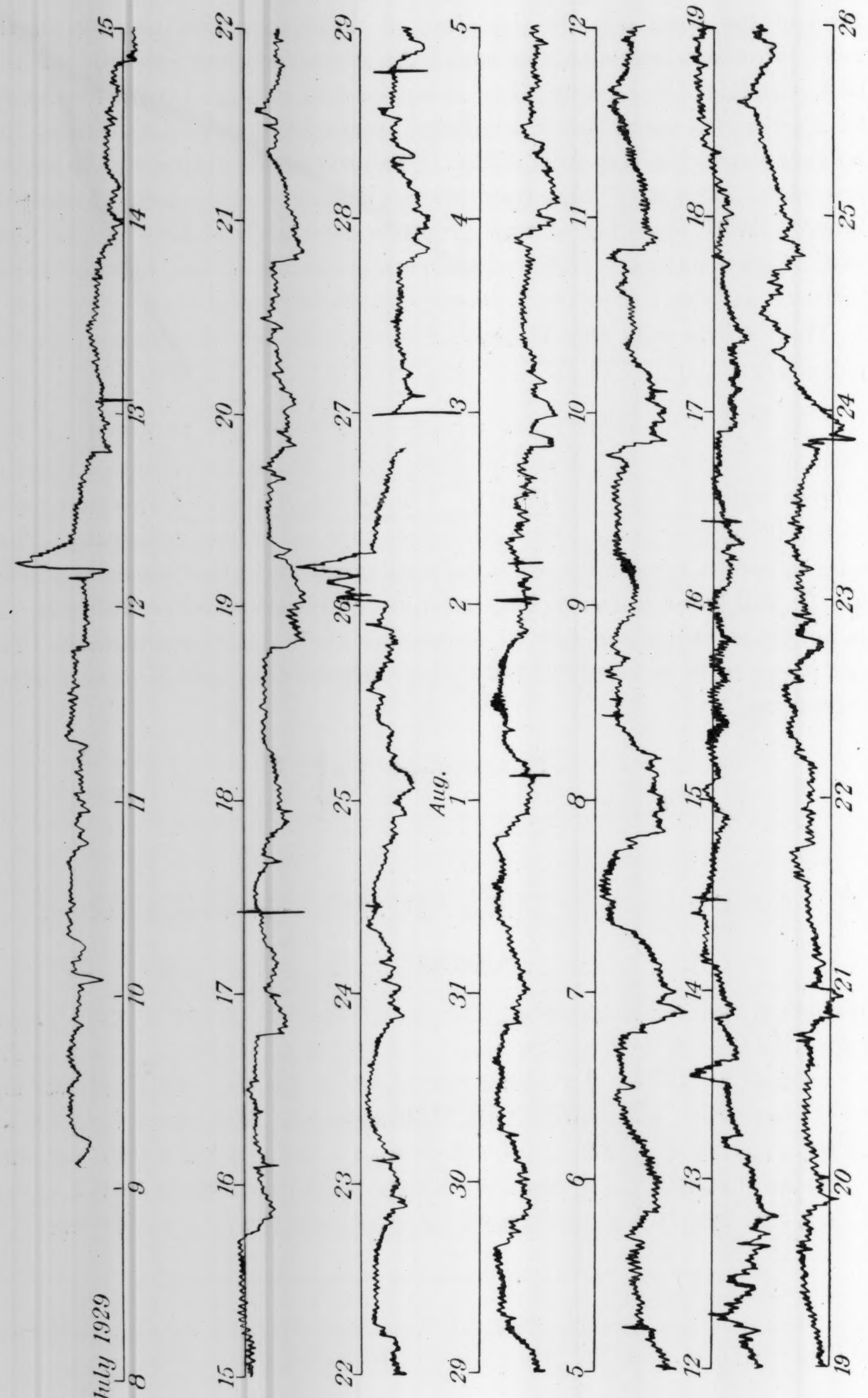
July 1929
8
9
10
11
12
13
14
15
15
16
17
18
19
20
21
22
22
23
24
25
26
27
28
29
29
30
31
Aug.
1
2
3
4
5
5
6
7
8
9
10
11
12
12
13
14
15
16
17
18
19
19
20
21
22
23
24
25
26

Fig. 4.

[C. Tsuboi.]

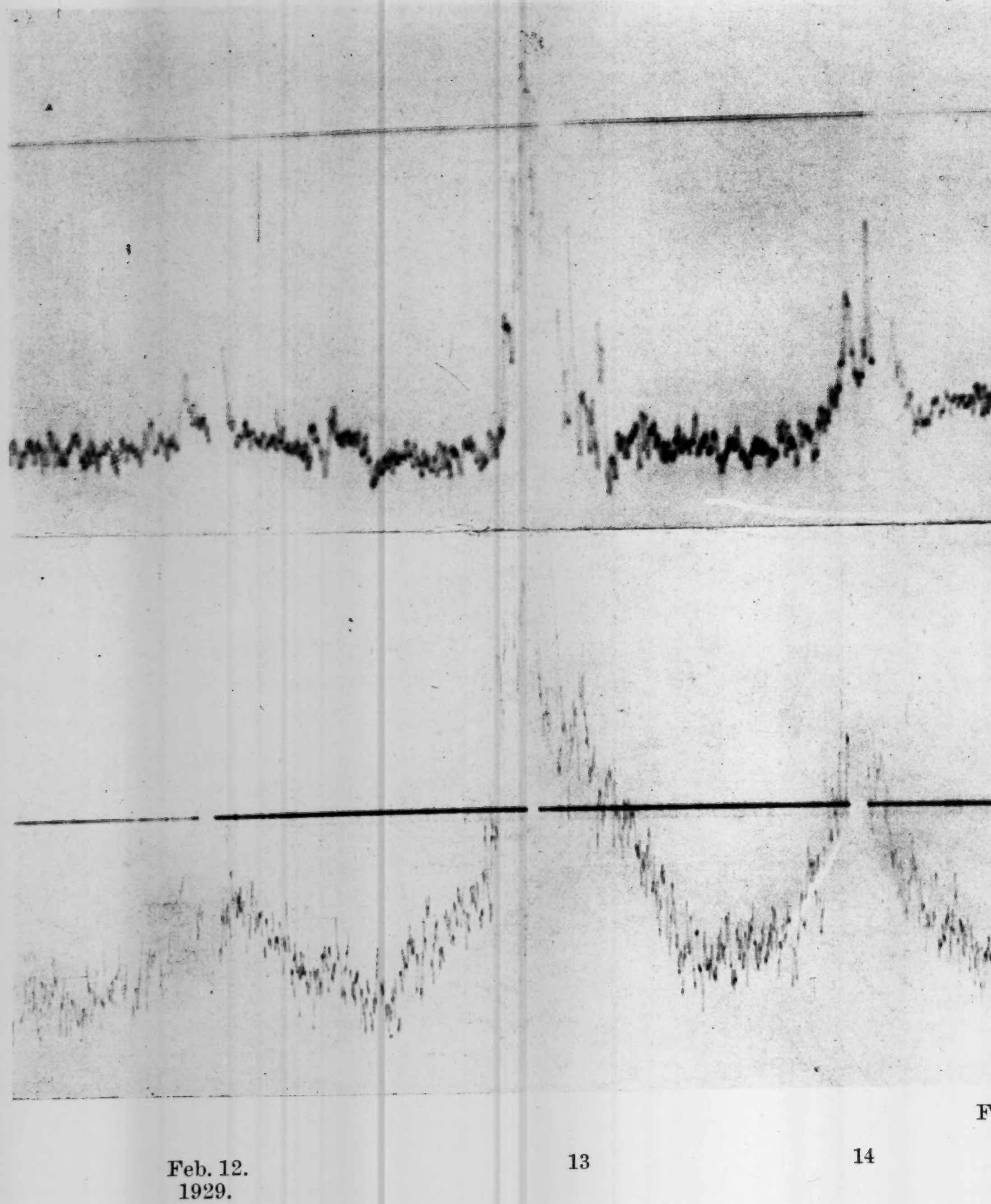

（震研彙報、第七號、圖版、坪井）

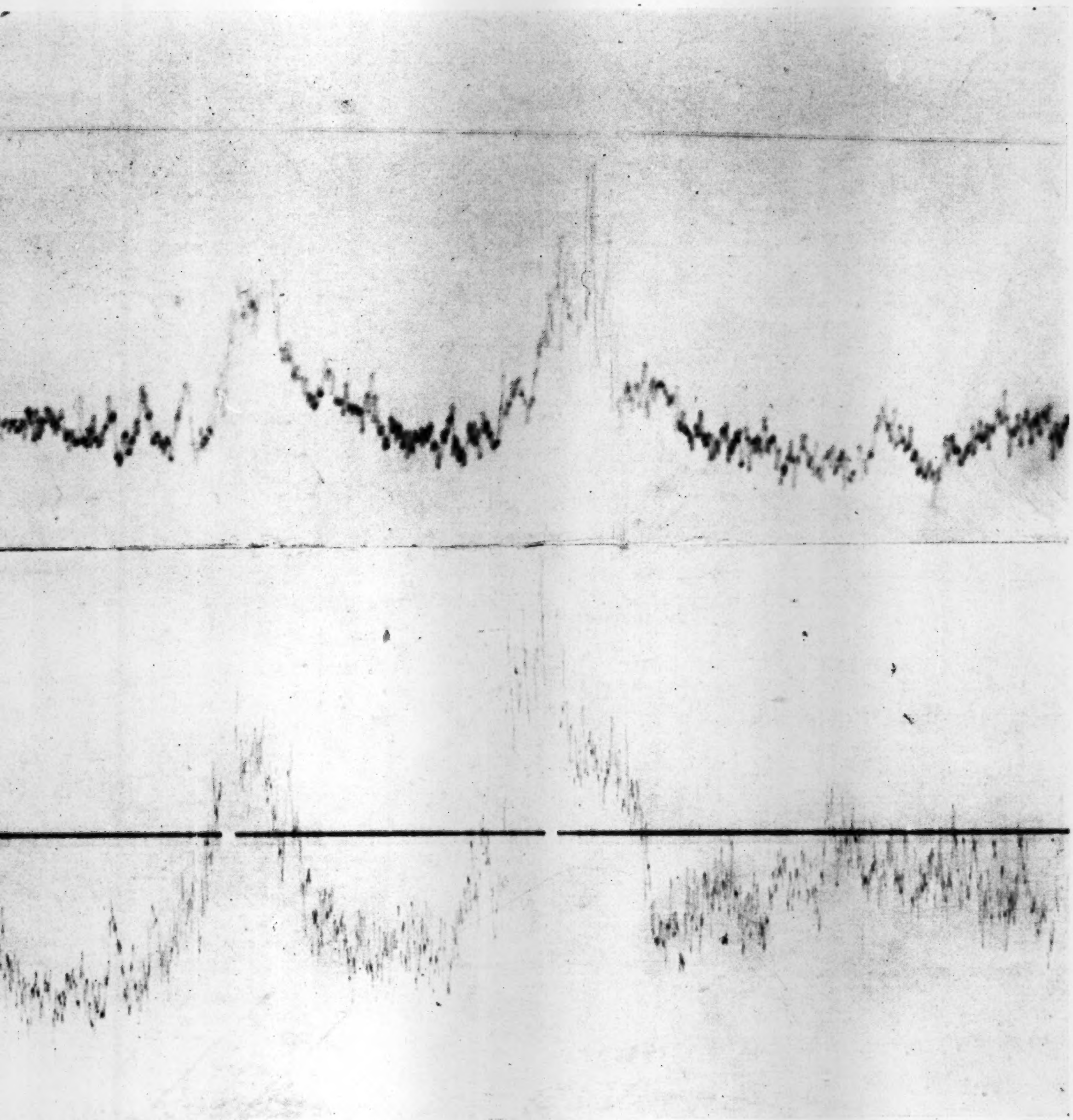

Fig. 2.

25. *On the Nature of Earthquakes Studied by Means of the Seismic Wave Analyser.**

By **Kyoji SUYEHIRO,**

Earthquake Research Institute.

(Read Oct. 16, 1928.—Received Sept. 20, 1929.)

It is not seldom taken, even in these days of the development of the seismology, that seismic waves start from a very narrow region, if not a single point, of the earth crust. From the inference that the tremendous energy of an earthquake cannot be given out from a very limited region, one might be convinced of the incorrectness of such a view. This may partly be attributed to the inadequacy of detecting successive fresh waves, even if exist, out of an ordinary seismogram, since their presence is masked by the trail of the pioneering shock. The writer's seismic wave analyser which works under the principle of selective resonance seems to be competent for the study of the nature of an earthquake in this connection.

From the observations made with this instrument the present writer found that, (1) the district where our laboratory stands had a natural frequency of vibration of 0.3 sec., (2) whenever a near earthquake in which, as a rule, quick vibrations are predominant was recorded by the analyser, the pendulum having the natural period of oscillation of 0.3 sec. oscillated most forcibly. These facts together with the construction of the instrument were reported in this Bulletin[1]

From the record given by this instrument the number of shocks in an earthquake can be detected, except when the shocks emanate simultaneously from a narrow region or continuously one after another from an extended region. This analysis cannot be made out of an ordinary seismograph for the reason described above.

Since the completion of the instrument 16 earthquakes were successfully recorded, which had the epicentre lying within a distance of 100 km. from our laboratory and were of the intensity of 4 and above (according to the Rossi-Forel scale). It is to be regretted that the construction of the instrument does not admit to record a feeble earthquake. The number of groups

---

* An outline of this paper was published in *Proc. Imp. Acad.*, **4** (1928), 2.

1) K. SUYEHIRO, *Bull. Earthq. Res. Inst.*, **1** (1926), 59–64.

TABLE.

No.	Date	Groups of waves	Epicentre	Distance between alleged epicentres	Focal depth	Remark
1	April 18, 1926	5	(o) Kawawa	—	(o) 25 km.	See Fig. 1.
2 (Deep origin)	April 27, 1926	1	(o) Tokyo Bay	—	(o) 55 „	See Fig. 2.
3	Jan. 9, 1927	2	(F) Akabane (o) Urawa	15 km.	(F) 35 „ (o) 30 „	One group was conspicous and the other very feeble
4 (D.o.)	Feb. 25, 1927	5	(F) (o) Anegasaki	0 „	(F) (o) 60 „	
5	May 20, 1927	4	(F) (o) Titibu	0 „	(F) 45 „ (o) 35 „	(M)
6 (D.o.)	May 26, 1927	5	(F) (o) Nagareyama	0 „	(F) 75 „ (o) 70 „	
7	Aug. 7, 1927	11	(F) Off the Tiba Coast (o) Inbanuma	20 „	(F) 55 „ (o) 40 „	
8	Aug. 8, 1927	3	(F) Yokosuka (o) Yokohama	20 „	(F) 45 „ (o) 50 „	
9	Sept. 5, 1927	8	(F) (o) Kakioka	0 „	(F) 45 „ (o) 50 „	(M)
10	Sept. 6, 1927	3	(F) (o) Mt. Tanzawa	0 „	(F) (o) 45 „	
11	Sept. 7, 1927	6	(F) Kawagoe (o) Suikaido	45 „	(F) 30 „ (o) 40 „	
12	Sept. 13, 1927	5	(F) Kitaura (o) Namekawa	25 „	(F) 35 „ (o) 30 „	See Fig. 3.
13 (D.o.)	Oct. 25, 1927	1	(F) Futu (o) Off the Kisarazu Coast	15 „	(F) (o) 55 „	See Fig. 4. Three minor groups followed
14	Sept. 7, 1927	4	(F) Suikaido (o) Sekiyado	20 „	(F) 40 „ (o) 20 „	
15 (D.o.)	Sept. 18, 1927	1	(F) Atuki (o) Ofuna	20 „	(F) 80 „ (o) 85 „	See Fig. 5.
16 (D.o.)	Dec. 31, 1927	2	(F) (o) Noda	0 „	(F) (o) 95 „	(M)

of seismic waves, which may possibly be the number of the shocks (revealed by the 0.3 sec. pendulum), together with the spicentres and the focal depths found from ordinary seismogram are given in the table; needless to say, the latters refer to the pioneer shocks.

In this table the epicentres and focal depths marked (F) were estimated from the ratio of the durations of the preliminary tremor observed at four different stations favourably situated, and those marked (o) estimated from the same durations observed at three stations applying Omori's constant (7.42 km/sec.). With regard to the source of informations, those marked (M) were taken from the observations of the Meteorological Observatory, and the rest from those of this Institute.

The epicentres given by (F.) are shown in the accompanying map (Fig. 6), classifying the focal depths into two kinds, one of which had the depth more than 50 km and the other less than that. This classification is not quite arbitrary; according to the investigations by Wadati,[2] a discontinuity of the earth crust known under the name of A. Mohorovičić seems to exist in our island at a depth of 45 km. or so.

From the table it will be seen that the earthquakes of shallow origin (<50 km.), except only No. 3, showed a number of groups of waves (see Figs. 1, 3), while most of those of deep origin (>50 km.) had only one or two groups (see Figs. 2, 4, 5). These facts seem to suggest that the nature of the breakdown of the earth crust varies in different strata; in the upper stratum where the rock is probably brittle, the breakdown starts one after another or simultaneously at different spots, while in the lower stratum where the rock is possibly plastic, the breakdown occurs all at once on a limited region. Although the writer does not dare to push the inference unreasonably so far as to apply the result of an ordinary engineering strength test[3] directly to the breakdown of the earth crust, yet the fact that generally the breakdown of the granite proceeds gradually while that of basaltic rocks occurs suddenly, may be suggestive in this connection.

It is worthy of notice that in computing the focal depth and also in estimating the position of the epicentre of deep earthquakes either method (F) or (o) gives practically the same value, while those of some shallow earthquakes the waves of which are composed of several groups give irreconcilable values according to the different methods of computation (refer to Nos. 7, 11, etc. in the table). This seems to suggest that the breakdown of the crust near to the earth's surface does not occur all at once on a narrow region, but probably takes place at different spots either simultaneously or succeessively, and accordingly there is every possibility that those shocks which are taken as the initial wave at different stations are not necessarily of one and the same origin.

---

[2] K. WADATI, *J. Met. Soc. Jap.*, [ii], **3** (1926), 8.

[3] An experiment on the strength of stones carried out by Prof. K. YUASA at the writer's request, the result of which will be reported elsewhere.

On the other hand, in the case of those waves starting simultaneously at different spots only those originating nearest are observed at the stations closest to them respectively. Thus the depth and the epicentre estimated as if the wave originates at a single point are rather misleading, and consequently a full consideration of the extent of the origin is quite necessary in estimating them.

The only way of finding the extent of the origin is to draw the exact isochronous lines of earthquakes. Thus, apart from the importance for other purposes, an exact chronography seems to be urgent for finding the correct informations of an earthquake.

In concluding this paper the writer wishes to thank Mr. W. Inoue and Mr. R. Takahasi for their trouble taken in computing the informations given in the table.

25. 振動分解器による地震の性質の研究

地震研究所　末廣恭二

（昭和三年十月十六日發表　昭和四年十月二九日受理）

今日でも尙地震波は地殼の一點から起る樣に考へらるゝ事が稀れではないが、是れは普通の地震計の記象は、最初に起つた振動を明示し得るのみに止まり、夫れのみに就き硏究を爲す習慣があるから、自然前記の樣に考へられる事が無理ではないと思はれる、著者は振動分解器の記錄により、地震波の群を觀測して、次の事柄を示してゐる。

（１） 地震波は普通一個所から起るものではない事。

（２） 隨て所謂震央は、觀測をなす地點により、異なる位置を取り得る可能性ある事。

（３） 著者の觀測の範圍では、深い地震と淺い地震とは、地震群の數に差異ある事實。

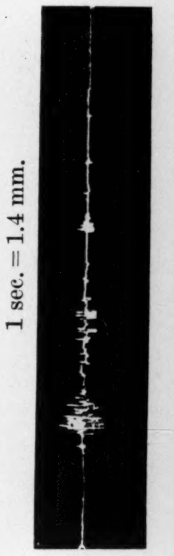

Fig. 1.

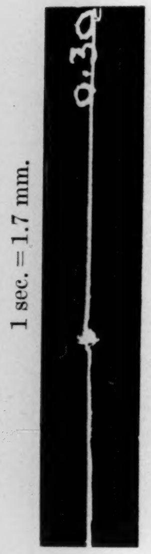

Fig. 2.

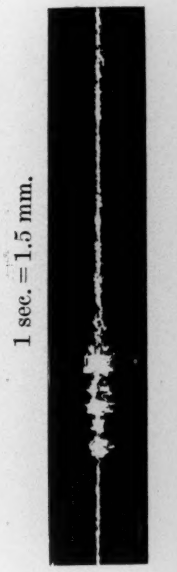

Fig. 3.

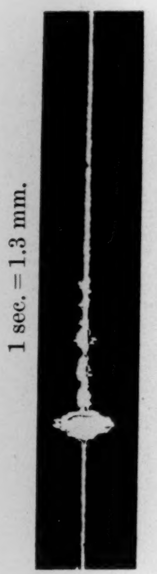

Fig. 4.

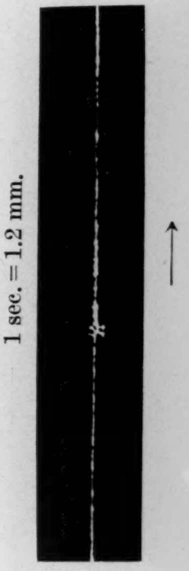

Fig. 5.

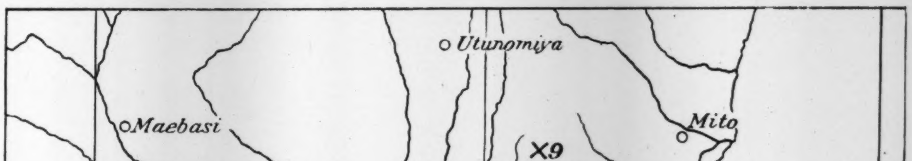
Utunomiya
Maebasi
Mito
9
Tukuba
Kumagai
14
12
Titibu
5
16
6
11
3
Tokyo
Tyōsi
Mitaka
7
1
2
10
Tanzawa
4
Yokohama
15
Kamakura
8
13
Yokosuka
Kiyosumi
Misaki
Numazu
Mera
● Depth > 50 km.
× " < "

Fig. 6.

（震研彙報、第七號、圖版、末廣）

26. 水成岩層の地震波傳播に及ぼす影響

地震研究所
今村明恒
岸上冬彦
小平孝雄

（昭和四年四月十六日發表—昭和四年九月九日受理）

地震の震原位置を求める方法に關して、走時曲線を畫き地震波の傳播狀態を調べて震原を推定するものや、初動の方向によるもの等がある。現今多く用ひられてゐる初期微動繼續時間に或る係數を乘じて震原距離を求める方法、又は等發震時線を畫いて共極限の中心を震央とするもの等は前述の走時曲線の應用と見做される。

走時曲線を畫くには、觀測所が適當な位置•間隔に置かれることと、時の測定が正確なことを要する。時の測定は、天文臺から發する無線電信の報時によつて時差の知れてゐるクロノメートルを用ひて時刻の合圖を行ひ、地震計の記錄裝置は一様な速度で動けば十分である。併し實際には此等の條件を充すことは相當困難なことである。唯前に述べた初期微動繼續時間を用ひる方法では、以上の條件を考慮しないでもよい場合がある。即ち距離の餘り遠くない地震ならば初期微動繼續時間は比較的に短いので、現在の記錄裝置でも時計の良否等は殆ど之に影響しない。

本研究所は理學部地震學教室と協力して、關東地方に東京•三鷹•鎌倉•三崎•秩父•清澄•筑波•東金の八個所に觀測所を設け、地方測候所のつくつてゐる觀測網の內部に細目の網を張つて共不足を補ひ、特に此地方の地震について調査してゐるが、震原位置を求めるには、主として、此初期微動繼續時間を用ひてゐる。

初期微動繼續時間 t と震原距離 d との關係を大森博士[1]は

$$d=kt \quad \dots\dots\dots\dots\dots\dots \quad (1)$$

と置き、$d<1000$ km の場合には $k=7{\cdot}42$ とされた。但し、d は km, t は秒で測る。（以後の記述に於ても、長さは 1 km、時間は 1 秒を以て單位とする。）即ち

$$d=7{\cdot}42\,t$$

となる。一般に之を大森公式といひ、我が國では廣く用ひられてゐる。地震波の傳はる

---

[1] 大森房吉　震災豫防調査會報告 **88** (1919), 1.

土地が等質・等方性を有する彈性體ならば、v_1, v_2 を夫々縱波及び橫波の速度とすれば

$$k=\frac{v_1 \cdot v_2}{v_1-v_2} \quad \dots\dots\dots\dots\dots\dots\dots\dots (2)$$

である。大森博士は k の値を求めるに、淺間火山や臺灣の嘉義の地震等、震央の明かなものに就いてその t と震央から觀測所までの距離を測つて、(1) 式を用ひられたのである。故に大森公式によつて震原を求める方法はその深さに關しては不十分である。近頃多數の學者によつて地球の上層程地震波の速度は小さいことが知られたが、震原の深さに比して觀測所が遠いときは地震波傳播に對し上層の影響は殆ど無いから、此の樣な場合には震央の位置を求めるに大森公式を用ひても大した誤には陷らない。併し、現今の如く觀測所間の距離が短くなつたときに、その附近に起つた地震について前記の k の値を應用することは不適當である。

k の値を調べ直すについて、先づ簡單に一つの地震の各觀測所からの震原距離は其初期微動繼續時間に比例すると假定することにあるが、之によつて震原の位置は定まるのである。其方法は、二觀測所のみに就いて考へれば、其等の震原距離が初期微動繼續時間 t に比例すると假定されてゐるのであるから、震原は二觀測所間の距離を各々の t の比に內分・外分する二點を過るアポロニウスの圓周の上にある。他の觀測所についても同樣に圓を畫き其等の圓の共通弦の交點を震央とする。之を立體的に考へるときは、前述の圓を球に置換へればよろしい。斯くして得た幾つかの球の交點が震央の位置と地表からの震原の深さを與へる。球の交點は球が三個あれば決定するが其球を三個畫く爲には觀測所は四個無ければならない。そこで以上の方法を批評すれば、此は k を既知の常數とするものよりは合理的であるが、作圖に手數が掛り、又四觀測所の觀測結果を用ふるときは球を三個畫くことが出來て震原は一點に定まり幾何學的には無難であるけれども物理學的には多少の誤差を含む筈である。觀測所の數が增すと物理學的には誤差の少かるべき結果を得るが、幾何學的には複雜になつて却つて震原を定めることが困難になる。此の樣に此の方法は實際に應用すると多少の缺點はあるが震原の深さを考慮に入れた點が採るべき所である。

關東地方の地震を前に述べた方法で求め、それから k の値を計算して見ると、多くの場合大森公式で與へられたよりも大きく出て來るが、然し乍ら他の少數の淺い地震では其が却て小さく出て來た。即ち k は常數ではなく、地表近くでは小さく、下に行く程大きいことを示す。又最近、著者の一人が和歌山市附近に發生する極めて局部的

な地震を調査した結果、k は 3·0 と求められた。此の地方の地質は結晶片岩と古世代輝綠凝灰岩であるが、長岡博士[2]は岩石の彈性に關する研究に於て土佐の輝綠凝灰岩につき

$$v_1=4\cdot 63\ \mathrm{km/sec},\ \ v_2=1\cdot 80\ \mathrm{km/sec},$$

といふ結果を得られてゐる。土佐と紀伊とでは岩石の產地は違ふが地質學的に同一系統に屬するもので、その物理的性質も大差はないと考へられるのであるが、之から (2) 式によつて k を求めると 2·95 となつて地震計測の結果とよく合ふ。地震計測から許りでなく、沖積層中の火藥爆發・重錘の落下による實驗でも、又長岡博士の實驗せられた新成岩の中に於ても k は 2 といふ小さい値を示す事からも地表近くでは k の小さいことは明瞭である。

彈性論によれば

$$v_1=\sqrt{\frac{E}{\rho}\cdot\frac{1-\sigma}{(1+\sigma)(1-2\sigma)}},\quad v_2=\sqrt{\frac{E}{\rho}\cdot\frac{1}{2(1+\sigma)}}\ \cdots\cdots\cdots\cdots(3)$$

であるから地震波の速度はヤングの彈性率 E, 密度 ρ, ポアソンの比 σ によつて決まる。然るに長岡[3]・日下部[4]兩博士の實驗的研究によると岩石では彈性波の速度は密度の差よりも彈性の差によつて餘計に影響される。若し σ が知れゝば、(3) 式によつて v_1 と v_2 の比が定まる。そして此の比と k とが判れば v_1, v_2 の各〻の値が求められる。地殼に於ては $\sigma=0\cdot 25$ と假定すれば實際と大差のないことが旣に知られてゐるから、此の値を採れば

$$v_1/v_2=\sqrt{3}\ \cdots\cdots\cdots\cdots\cdots\cdots\cdots\cdots\cdots(4)$$

となる。(2)式で示されてゐる通り、k と v_1, v_2 とは比例するから、深い地震では k が大きく、淺い地震では k が小さいことは、地震波の速度が地表から下に行く程大きいことを意味する。この速度が次第に大きくなることは走時曲線の研究からも知られてゐることである。

松澤助教授[5]の最近の研究の結果によれば、地殼は三つの地震波の速度の異つた層から成立つてゐる。其等の岩石層につき、地表からの深さ、二種の地震波の速度は次の表で示す。

---

[2] 長岡半太郎　震災豫防調査會歐文報告 **4** (1900), 47.
[3] 日下部四郎太　震災豫防調査會歐文報告 **22** B (1906), 27.
[4] 長岡半太郎　震災豫防調査會歐文報告 **4** (1900), 47.
[5] 松澤武雄　地震研究所彙報 **6** (1929), 117.

花崗岩層	底面 20 km	$v_1=5{\cdot}0$ km/sec	$v_2=3{\cdot}15$ km/sec
鹽基性岩層	20—50	6·1	3·7
過鹽基性岩層	50 以上	7·5	4·45

併し前述の k が地表近くに於て小さいことは、上記松澤助教授の研究範圍を超越して居るのである。

著者等の研究は地震波傳播狀態につき、地表に於ける水成岩層の存在を無視することなく、今一歩實際の狀態に近づかんとするものである。此爲に松澤助教授の研究に成れる上記の三段層を其儘應用し、但最上層を少しく變更して次の様にした。

上部　厚さ h km.　k は未知數

下部　厚さ $(20-h)$ km.　松澤助教授の第一層即ち

$$v_1=5{\cdot}0,\ v_2=3{\cdot}15,\ k=8{\cdot}51$$

今上記第一層上部の h と k との價を推定する爲に、昭和二年中に關東地方に起つた東京の有感地震を採つた。其總數は 65 回であるが、震原が觀測網の中にあるもの 21 回を用ひた。觀測網の外にあると、位置の決定が不正確になるからである。此 21 回の地震は我々の觀測所の中四個所以上で觀測されたものであるが、完全を期する爲に接した地方測候所に於ける觀測結果をも借りることにした。本文に收めたものは氣象要覽から拔萃したものである。

此の材料の中、幸にも第一表の十月二十四日 (No. 14) の地震の様に二觀測所の t の値の近いものが二組あり、又三月十六日 (No. 2) の地震の様に三觀測所の t が殆ど等しいものがあつた。此様な場合には震央の位置は其れだけの材料により容易に決定される。何となれば我々は k を變數と考へてゐるから是迄震原決定に用ひられた多くの方法は成立たなくなるが、それにも拘らず t の値の略ぼ相等しきものは震原から略ぼ等距離にありと假定し得られるからである。例へば No. 14 に於て t の値は東京と鎌倉と相等しく三崎と秩父とが略ぼ相等しいから、此二組即ち四點の觀測から先づ震央が決定せられる。即ち震央距離 Δ の値として東京・鎌倉共に 32·5 km.、三崎 51 km.、清澄 81·5 km.、秩父 52·5 km. を得る。次に最初の二點の t が Δ の値に比較して頗る小さく僅に 6·5 s. なることは震原が頗る淺きことを意味するので、k の第一近似値として $32{\cdot}5/6{\cdot}5=5{\cdot}0$ が得られる。又後の三點の t と Δ との値からして、震原の位置は我々の假定した上部層と下部層との境界に近きことを思はしめる。何となれば三點の觀測を組合せた t の差を以て Δ の差を除するとき其値は 8·6 となり、松澤第一層

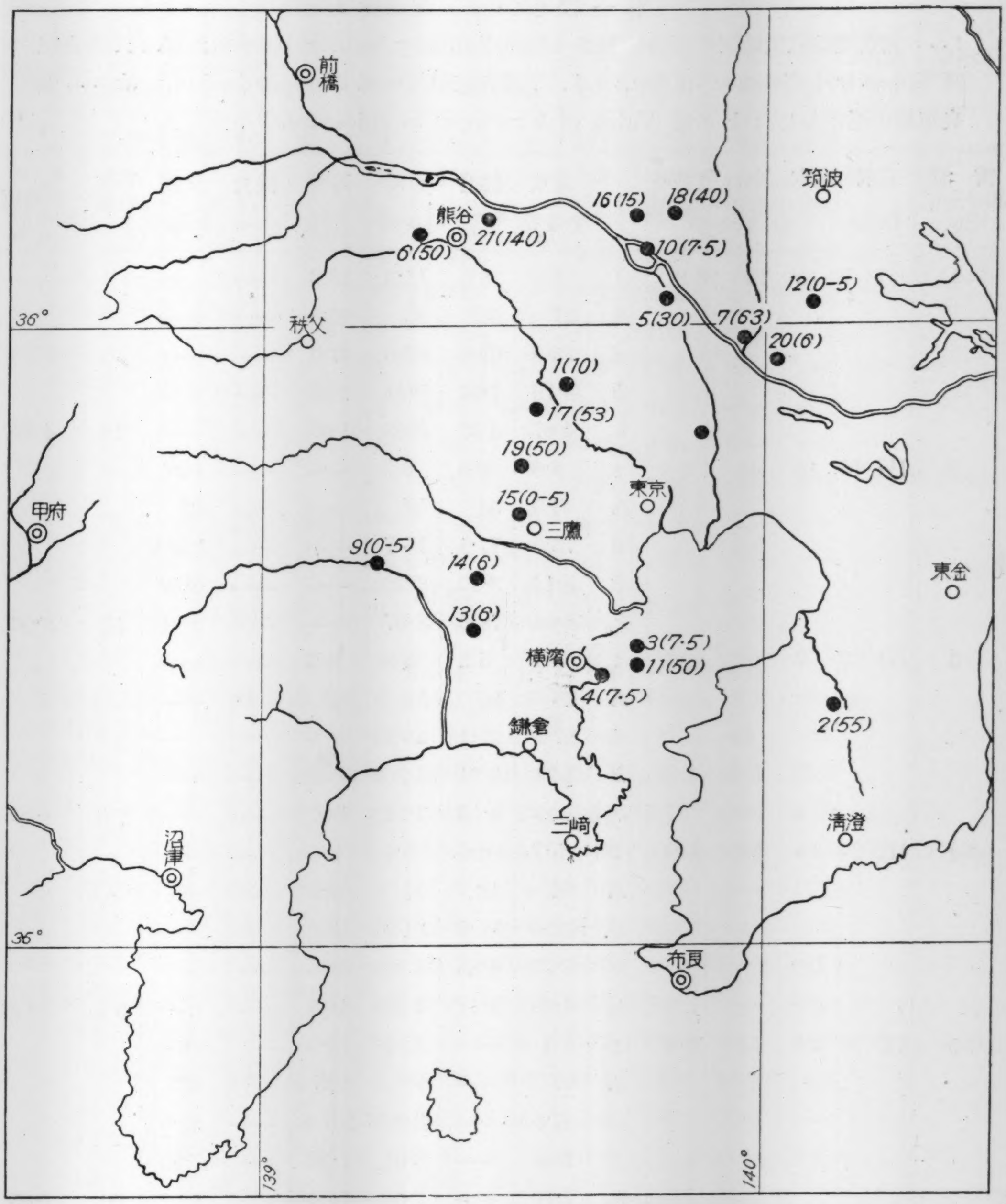
前橋
熊谷
21(140)
6(50)
16(15)
18(40)
10(7·5)
筑波
12(0-5)
5(30)
7(63)
20(6)
36°
秩父
1(10)
17(53)
19(50)
東京
15(0-5)
三鷹
甲府
9(0-5)
14(6)
13(6)
東金
3(7·5)
11(50)
横濱
4(7·5)
2(55)
鎌倉
三崎
清澄
沼津
36°
布良
139°
140°

第一圖 Fig. 1.

地震の分布圖 Map showing the distribution of epicentres.

● 震央 Epicentre. ○ 地震観測所 Seismological station. ◎ 地方測候所 Local meteorological station.

括弧内の數字は震原の深さ (km.) を示す Figure in bracket indicates focal depth in km.

第一表（其の一） TABLE I.

t . . . 初期微動繼續時間（秒） Duration of preliminary tremors in sec.; Δ . . . 震央距離 Epicentral distance in km.; d . . . 震原距離 Focal distance in km.; k_0 . . . 震央距離の更正をした k の値 Value of k reduced to epicentre.

番號 Earthq. No.	月日 Date	東京に於ける發震時 Commencement at Tokyo		東京 Tokyo	鎌倉 Kamakura	三崎 Misaki	清澄 Kiyosumi	秩父 Titibu	筑波 Tukuba	震原の深さ f	k_0 の平均値 Mean value of k_0
1	I 9	18ʰ 18ᵐ 16·8ˢ	t	5·0	9·5	11·3	13·2	——	——		
			Δ	27	66	83	96·5	——	——		
			d	28·8	66·8	83·6	97·0	——	——		
			k	5·76	7·04	7·41	7·35	——	——		
			k_0	4·67	4·92	5·08	4·90	——	——	10	4·89
2	III 16	16 46 0·3	t	9·0	9·5	9·2	——	——	12·4		
			Δ	48·5	54	52	——	——	91		
			d	73·3	77·1	75·7	——	——	106·3		
			k	8·14	8·10	8·22	——	——	8·59		
			k_0	8·01	7·95	8·07	——	——	8·21	55	8·06
3	III 19	8 0 58·5	t	5·1	5·2	6·8	8·5	——	——		
			Δ	26	26	38	51	——	——		
			d	27·1	27·1	38·7	51·5	——	——		
			k	5·31	5·31	5·70	6·06	——	——		
			k_0	4·13	4·13	4·12	4·09	——	——	7·5	4·12
4	III 24	20 13 32·1	t	5·7	4·0	5·4	8·5	——	——		
			Δ	32	18	31	52·5	——	——		
			d	32·9	19·5	31·9	53·0	——	——		
			k	5·77	4·88	5·91	6·25	——	——		
			k_0	4·25	4·12	4·38	4·19	——	——	5·5	4·29
5	IV 26	22 11 38·0	t	6·4	——	12·8	13·5	——	6·0		
			Δ	37	——	98	103	——	32		
			d	47·6	——	102·5	107·3	——	43·9		
			k	7·45	——	8·01	7·96	——	7·32		
			k_0	7·10	——	7·08	7·00	——	7·02	30	7·05
6	V 20	4 18 18·0	t*	9·4	13·2	14·2	17·0	——	10·8		
			Δ	63	95	113	134	——	72		
			d	80·4	107·4	123·6	143·0	——	87·7		
			k	8·55	8·15	8·70	8·41	——	8·12		
			k_0	8·31	7·74	8·08	7·63	——	7·94	50	7·95

* 前橋 $t=7{\cdot}4$, $k_0=8{\cdot}01$. 熊谷 $t=6{\cdot}3$, $k_0=7{\cdot}97$.

第一表（其の二） Table I. (continued.)

番號 Earthq. No.	月日 Date	東京に於ける發震時 Commencement at Tokyo				東京 Tokyo	鎌倉 Kama-kura	三崎 Misaki	清澄 Kiyo-sumi	秩父 Titibn	筑波 Tukuba	震原の深さ f	k_0 の平均値 Mean value of k_0
7	V 30	21	10	59·1	t	8·5	—	12·6	12·5	—	8·0		
					Δ	35	—	95	93	—	28		
					d	72·1	—	114·0	112·3	—	68·9		
					k	8·48	—	9·04	8·98	—	8·62		
					k_0	8·40	—	8·68	8·61	—	8·58	63	8·57
8	VI 10	9	46	43·8	t	5·5	—	10·2	10·4	—	7·2		
					Δ	16	—	76	78	—	46		
					d	43·1	—	85·9	87·7	—	61·0		
					k	7·85	—	8·41	8·44	—	8·48		
					k_0	7·61	—	7·93	7·94	—	8·10	40	7·89
9	IX 6	7	39	43·5	t**	9·5	8·3	10·4	14·5	8·7	—		
					Δ	49·5	42·5	61	97	43·5	—		
					d	49·5—49·7	42·5—42·8	61—61·1	97—97	43·5—43·8	—		
					k	5·22—5·24	5·13—5·15	5·87—5·88	6·69—6·69	5.00—5·04	—	0—5	—
10	IX 7	19	33	35·7	t	7·1	12·7	14·5	15·8	9·1	6·0		
					Δ	46	92	108	113	62	33		
					d	46·6	92·3	108·3	113·3	62·5	33·8		
					k	6·55	7·25	7·48	7·18	6·86	5·63		
					k_0	4·54	4·44	4·42	4·21	4·42	4·15	7.5	4·36
11	IX16	23	05	21·1	t	7·3	7·0	7·6	8·5	—	12·0		
					Δ	29·5	23·8	33·0	48·8	—	91·0		
					d	58·1	55·4	59·9	69·9	—	103·8		
					k	7·95	7·91	7·90	8·21	—	8·65		
					k_0	7·79	7·80	7·73	8·00	—	8·26	50	7·96
12	X 7	23	26	31·2	t	8·8	16·2	18·4	16·4	16·0	4·8		
					Δ	47·5	94	106	97	90·5	19·0		
					d	47·5—47·5	94—94·1	106—106	97—97	90·5—90·6	19·0—19·7		
					k	5·40—5·42	5·80—5·81	5·77—5·77	5·91—5·91	5·65—5·66	3·96—4·10	0—5	—
13	X14	19	7	23·9	t	6·8	4·7	7·1	—	9·8	—		
					Δ	38·2	23·5	42·8	—	61·5	—		
					d	38·6	24·2	43·2	—	61·7	—		
					k	5·68	5·15	6·09	—	6·30	—		
					k_0	4·06	4·06	4·26	—	4·05	—	6	4·11

** 甲府 $t=11·0$, $k_0=5·64-5·65$. 横濱 $t=8·6$, $k_0=4·77-4·84$.

第一表（其の三） Table I. (continued.)

番號 Earthq. No.	月日 Date	東京に於ける發震時 Commencement at Tokyo				東京 Tokyo	鎌倉 Kamakura	三崎 Misaki	清澄 Kiyosumi	秩父 Titibu	筑波 Tukuba	震原の深さ f	k_0の平均値 Mean value of k_0
14	X 24	5	19	57·5	t	6·5	6·5	8·2	11·8	8·5	—		
					Δ	32·5	32·5	51	81·5	52·5	—		
					d	33·0	33·0	51·2	81·6	52·9	—		
					k	5·08	5·08	6·25	6·91	6·21	—		
					k_0	3·72	3·72	4·20	4·24	4·15	—	6	4·01
15	XI 4	2	23	56·2	t	5·4	—	11·8	14·6	9·7	—		
					Δ	23	—	60·5	83·5	50	—		
					d	23—23·6	—	60·5—60·6	83·5—83·5	50—50·2	—		
					k	4·26—4·37	—	5·12—5·14	5·71—5·71	5·15—5·18	—	0—5	—
16	X 7	7	38	11·4	t	7·8	12·4	—	15·2	8·9	6·0		
					Δ	52·5	97·5	—	119·0	62·0	33·2		
					d	54·6	98·6	—	119·9	63·8	36·4		
					k	7·00	7·95	—	7·88	7·16	6·07		
					k_0	5·86	5·91	—	5·67	5·74	5·34	15	5·70
17	XI 23	23	44	56·2	t	7·5	9·6	11·3	—	8·5	—		
					Δ	27	61	79	—	43	—		
					d	59·5	80·8	95·1	—	68·2	—		
					k	7·94	8·43	8·43	—	8·01	—		
					k_0	7·83	8·25	8·12	—	7·86	—	53	8·02
18	XI 30	7	47	0·2	t	8·2	—	14·2	14·7	—	6·0		
					Δ	53	—	116	117	—	26·5		
					d	66·4	—	122·7	123·6	—	48·0		
					k	8·10	—	8·64	8·40	—	8·00		
					k_0	7·74	—	7·86	7·64	—	7·73	40	7·74
19	XII 14	23	03	0·6	t	6·7	8·1	10·0	12·2	8·0	—		
					Δ	24	50	69	89·5	44	—		
					d	55·5	70·7	85·2	102·5	66·6	—		
					k	8·30	8·71	8·52	8·49	8·33	—		
					k_0	8·15	8·48	8·24	8·03	8·13	—	50	8·21

第一表（其の四） Table I. (continued.)

番號 Earthq. No.	月日 Date	東京に於ける發震時 Commencement at Tokyo		東京 Tokyo	鎌倉 Kama-kura	三崎 Misaki	清澄 Kiyo-sumi	秩父 Titibu	筑波 Tukuba	震原の深さ f	k_0の平均値 Mean value of k_0
20	XII 19	17 44 45·9	t	6·3	12·4	14·0	——	——	6·0		
			Δ	35	83	94	——	——	30		
			d	35·5	83·2	94·1	——	——	30·6		
			k	5·64	6·71	6·73	——	——	5·10		
			k_0	4·10	4·13	4·08	——	——	3·78	6	4·02
21	XII 31	14 51 6·0	t*	16·2	16·9	17·5	18·7	14·9	16·0		
			Δ	60·0	92	112·5	129	38·5	59		
			d	152·3	167·5	179·6	190·4	145·2	151·9		
			k	9·41	9·91	10·26	10.18	9·76	9·49		
			k_0	9·33	9·83	10·10	10·03	9·70	9·42	140	9·72

に於ける k の値に大體に於て一致する。即ち觀測された波動は下部層を水平に通過して上部層へ屈折して來たものと見做し得られるのである。然るときは

$$h\cos\theta=\left(t-\frac{\Delta}{8\cdot51}\right)k \quad \ldots\ldots\ldots\ldots\ldots\ldots\ldots (5)$$

なる關係から $t-\dfrac{\Delta}{8\cdot51}$ の値が後の三點に就いて夫々 2·21, 2·22, 2·32 秒となり平均値として 2·3 秒を得る。但し上式に於ける θ は $\sin\theta=\dfrac{k}{8\cdot51}$ に適する値であつて下部層を水平に傳播した波動が上部層へ屈折するときの屈折角である。其故に上に得た 2·3 秒は h なる厚さの上部層を假想位相が垂直線と θ 角をなして進行するに要する時間であつて $\sin\theta=5\cdot0/8\cdot51$ から $\theta=36°$, $\cos\theta=0\cdot81$ が出て來る。故に(5)式により $h=9\cdot5$ km. となる。此計算に於て震原を上下部の境界に近いものと假定したが、若し震原が境界よりも少しく下方にあるときは近似計算に大した影響を與へないことが明かであるけれどもそれが上部の方にあるときは $k=8\cdot51$ と 5·0 との相違によりて誤差の大なるべきことを思はしめるが、然しながら實際には上部層の k の値 5.0 といふものは平均の値であつて、我々が最後に到達した樣に境界面に接近した部分は 8·51 に近く、地表に近づくに從ひ恐らくは 2·0 位の値にまで減ずるものであらう。其故震原を境界面近くに取ることは第一近似計算に於て左までの支障となるものではない。No. 5 は t の値略ぼ相等しき二組の觀測値があるので此點に於て No. 14

---

* 熊谷 $t=14\cdot5$, $k_0=9\cdot66$.

と同種類であるが、震原は松澤助教授の第一•二層境界に近いことが直ちに出て來る。

以上の近似計算に於て先づ水成岩層の厚さは約 10 km. でその k の値は 5·2 と推定された。此の結果を用ひて第二圖の樣な地殼構造を假定して、種々の深さに起る地震の v_1, v_2 の走時を計算した。

計算を簡單にする爲に一つの層の中では速度は一樣であると假定した。第三圖の如く二層あつて、中間層内の震原から發した波動が一度下の層に入り後再び屈折によつて地表に現はれる場合には走時 T 及び震央距離 Δ を求める式は

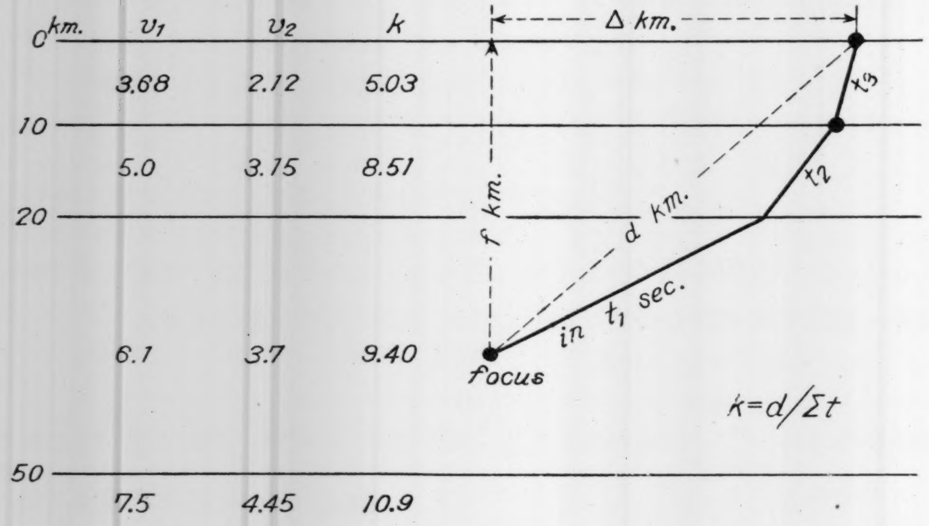
0 km.
v_1
v_2
k
3.68
2.12
5.03
10
5.0
3.15
8.51
20
6.1
3.7
9.40
50
7.5
4.45
10.9
Δ km.
f km.
d km.
in t_1 sec.
t_2
t_3
focus
$k=d/\Sigma t$

第 二 圖 Fig. 2.

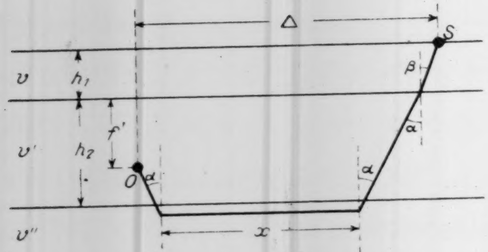
Δ
S
v
v'
v''
h_1
h_2
f'
O
α
β
x

第 三 圖 Fig. 3.
$[v<v'<v'']$
O 震原 focus.
S 觀測所 station.

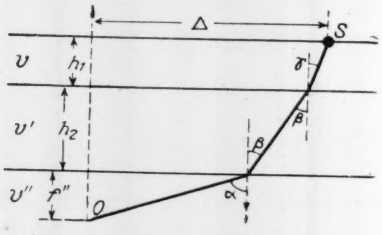
Δ
S
v
v'
v''
h_1
h_2
f''
O
α
β
γ

第 四 圖 Fig. 4.
$[v<v'<v'']$
O 震原 focus.
S 觀測所 station.

$$\left.\begin{aligned} &T=\frac{h_1}{v\cos\beta}+\frac{2h_2-f'}{v'\cos\alpha}+\frac{x}{v''},\\ &\Delta=h_1\tan\beta+(2h_2-f')\tan\alpha+x,\\ \text{但し}\quad &\sin\alpha=\frac{v'}{v''},\quad \sin\beta=\frac{v}{v'}\sin\alpha=\frac{v}{v''}. \end{aligned}\right\}\cdots\cdots\cdots\cdots(6)$$

第四圖の如く震原から觀測所まで順次の屈折によつて到達する波には次の式を用ひた。

$$\left.\begin{aligned} &T=\frac{f''}{v''\cos\alpha}+\frac{h_2}{v'\cos\beta}+\frac{h_1}{v\cos\gamma},\\ &\Delta=f''\tan\alpha+h_2\tan\beta+h_1\tan\gamma,\\ \text{但し}\quad &\frac{v}{v'}=\frac{\sin\gamma}{\sin\beta},\quad \frac{v}{v''}=\frac{\sin\beta}{\sin\alpha}. \end{aligned}\right\}\cdots\cdots\cdots\cdots(7)$$

以上の式を應用して計算した結果、T と Δ との關係が判り、走時曲線が書ける、そこで v_1 と v_2 とについて走時曲線を書き、その走時の差を求める。即ち

$$t=T(v_2)-T(v_1)\cdots\cdots\cdots\cdots\cdots\cdots\cdots\cdots\cdots\cdots(8)$$

但し t は初期微動繼續時間、$T(v_1)$, $T(v_2)$ は夫々縱波・横波の走時である。此處に得た t を (1) 式に入れて k を求めた。即ち波の屈折を無視して震原から觀測所に直線

第二表 k の値 TABLE II. Values of k.

Δ f	0	10	20	30	40	50	60	70	80	90	100	110	120	130	140	150
7·5	4·47	4·70	5·48	6·02	6·25	6·60	6·91	7·10	7·23	7·26	7·45	7·59	7·73	7·82	7·92	8·01
10	5·03	5·16	5·79	6·28	6·64	6·91	7·11	7·28	7·30	7·47	7·64	7·75	7·89	7·98	8·06	8·11
15	5·76	6·01	6·26	6·46	6·68	6·79	7·11	7·27	7·45	7·63	7·76	7·91	8·00	8·06	8·16	8·22
20	6·31	6·40	6·58	6·75	6·97	7·21	7·41	7·60	7·75	7·86	7·99	8·07	8·15	8·25	8·30	8·36
30	7·18	7·18	7·29	7·44	7·58	7·68	7·76	7·85	7·95	8·03	8·16	8·20	8·25	8·34	8·38	8·40
40	7·64	7·78	7·85	7·93	7·97	8·01	8·01	8·05	8·13	8·21	8·29	8·36	8·43	8·50	8·41	8·45
50	7·93	8·03	8·04	8·10	8·10	8·14	8·14	8·20	8·26	8·30	8·41	8·51	8·55	8·70	8·80	8·88
60	8·31	8·35	8·38	8·39	8·39	8·40	8·48	8·53	8·55	8·65	8·76	8·82	8·94	9·02	9·08	9·15
70	8·62	8·62	8·62	8·65	8·67	8·69	8·70	8·69	8·77	8·78	8·85	8·94	9·01	9·10	9·15	9·20
80	8·84	8·86	8·86	8·85	8·86	8·90	8·94	9·01	9·05	9·09	9·09	9·10	9·10	9·14	9·16	9·24
90	9·04	9·05	9·11	9·13	9·11	9·11	9·19	9·19	9·19	9·22	9·28	9·30	9·31	9·31	9·33	9·41
100	9·20	9·22	9·24	9·24	9·25	9·27	9·26	9·26	9·27	9·28	9·31	9·35	9·35	9·36	9·40	9·50

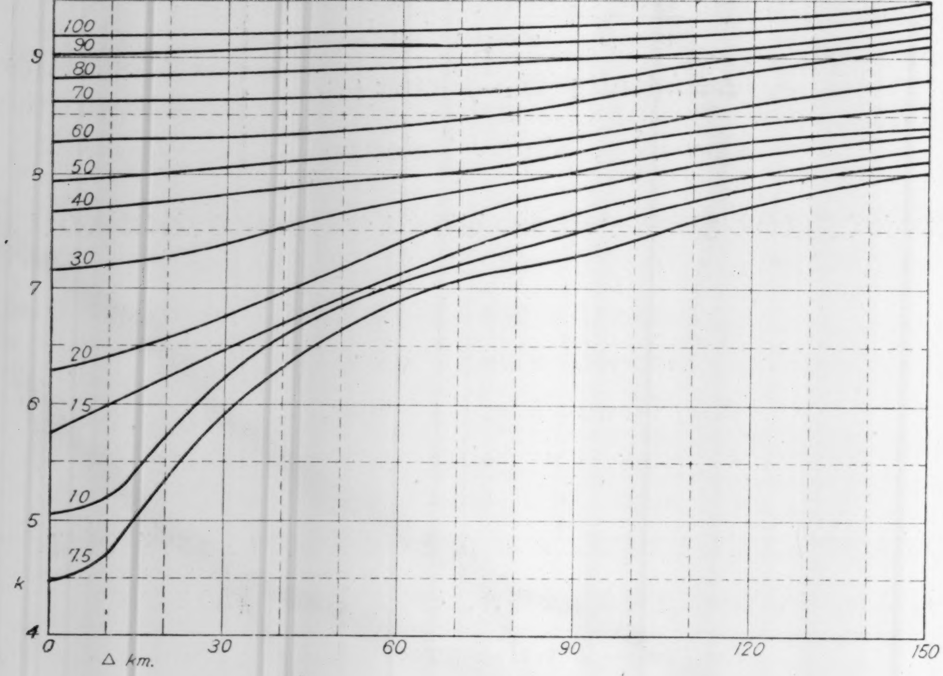

第五圖 Fig. 5.

$f=7{\cdot}5, 10, \ldots, 100$ に於ける Δ-k 圖

Δ-k curve for $f=7{\cdot}5, 10, \ldots, 100$.

的に傳播したと假定した見掛上の k の値を出した。其の k の値は震原の深さ f 及び震央距離 Δ との函數である。（第二表、第五圖、第六圖）但し以上の計算では t は縱波•横波の各〻の最初に到着したものの走時の差と假定した。

震央の近くでは k の値に對する深さの影響が相當に大きいが、Δ が大きくなると深さによる影響は小さくなる。多くの地震では k を 7·4 としては小さ過ぎる。寧ろ 8 附近の値を用ふべきである。

地表から 10 km. までの層に於て k を 5·2 としたのでは 21 回の殘餘の地震に於て正確に合はない場合も生ずるので逐次近似法によつて k と層の厚さ h とに修正を加へたが、斯くして最後に得た結果は挿入の圖及び表に示した樣に、水成岩層の厚さ h は 10·0 km. その k の値は 5·03 となつたのである。

併し地震によつては其震原の深さが 10 km. よりも淺いと考へられるものがあつてそれには 10 km. を更に二つに分けて 7·5 km. の深さまでは $k=4{\cdot}47$、その下 10 km. までは $k=8{\cdot}04$ とすれば更に實際に近づく樣である。7·5 km. の深さまでも詳しく調べれば細かに分けられるのであらうが、$k=4{\cdot}47$ は其部分の平均値と考へればよい。九

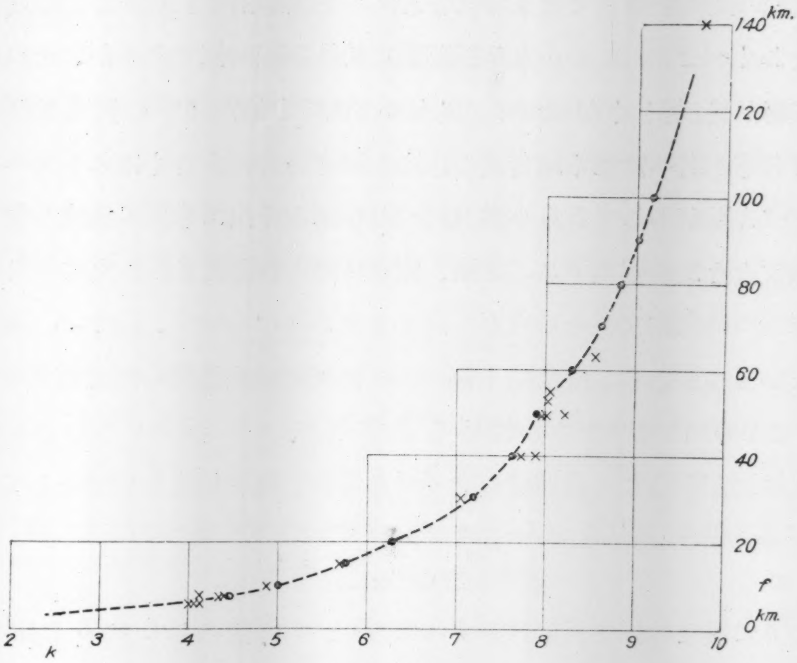

第六圖 Fig. 6.

$\Delta=0$ に於ける f-k 圖
f-k curve for $\Delta=0$.

● **計算値** deduced from the assumption.
× **觀測値** ,, observations.

月六日 (No. 9)、十月七日 (No. 12)、十一月四日 (No. 15) の地震は深さが 7·5km. よりも淺く出て來るので深さを 0 km. と 5 km. の二つの場合について計算した。多分この中間の値をとるであらうが、震原が此樣に淺いとすると現在の觀測所間の距離では此以上論ずることは出來ない。

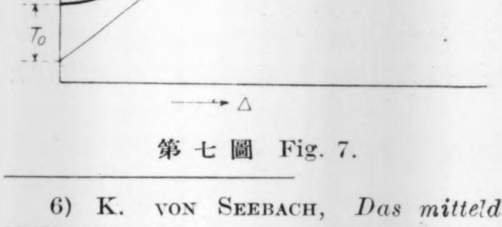

第七圖 Fig. 7.

是まで地震の震原を決定するに當つて、地表近くに發達した水成岩の存在を無視したものが多い。例へばフォン・ゼーバッハ[6]の方法卽ち走時曲線を合理的に（雙曲線として）延長して $\Delta=0$ の線と交はる點と、走時曲線の直線部の切線と $\Delta=0$ と交はる點との時間差（第七圖の T_0）をとり、之を以て地震波が震原から震央に達する時間と考へ、その時間に $\overline{P}$、P 或は $\overline{S}-\overline{P}$

---

6) K. von Seebach, *Das mitteldeutsche Erdbeben vom 6. März 1872* (Leipzig, 1873), 132—175.

など對應位相の速度を乘じて震原の深さとする方法等がそれである。此曲線の決定に特に重きをおくべきは Δ の小なる觀測點に於ける觀測値であるが、それには上層水成岩層の影響が益〻著しくなるから、以上の方法で求めた T_0 の値は頗る不純なものである。著者等が考へた如く地震波の速度が深さと共に大きくなると考へると、方法にも訂正すべき點があるであらうが、假令 T_0 が正しく出て來ても速度の値の取樣によりても亦相當大きな差が生ずる。近頃、國富技師[7] の發表された大正十二年九月一日の關東大地震の研究論文にその震原の深さを求めるについて、「PS-Δ 圖表より求むる方法」といふのがある。此は第七圖の T に初期微動繼續時間を適用せられたものであつて、$\Delta=0$ に於ける t の値を t_0 と書くと、$t_0=3{\cdot}0$ sec であるといふ。此 t_0 につきても疑問があることは前述の通りであるが、假りに之を正確として置く。次に

$$f=\frac{v_1{\cdot}v_2}{v_1-v_2}t_0=kt_0 \quad \dots\dots\dots\dots\dots\dots (9)$$

なる式によりて震原の深さ f を計算するに方り、k の値として 9·46 を採用されたが、著者等の本研究の結果を應用して見ると地表から 10 km. までは $k=5{\cdot}03$ であるからその間の走時は約2秒、殘餘の1秒間では $k=8{\cdot}51$ をとれば地震波は約 8·5 km. 進行したことになる。即ち深さは約 18·5 km. となつて、$k=9{\cdot}46$ としたときは深さ 28km. であるから 10 km. 程淺く出る。勿論國富技師の採用せられた震央の位置についても意見の相違がある。曾つて著者の一人[8] が論じた通り夫の大正十二年九月一日の關東大地震は多元性震原の地震と見做すべきものであつて、東京觀測に於ては第一元が相模灣の中央部に起りそれよりも急激な第二元（東京觀測にて第一元後3秒目に現れてゐるけれども震原地方から西或は北西方にある觀測點にてはこれが第一元と同時か、少くも、もつと接近して現はれた筈である）が小田原附近に起つたと考へられるから、國富技師の採られた震央は此第二元と見れば差支ないのである。但し我々の推定につき自ら不滿足を感ずることは、問題の震央が我々のとつた舞臺の一隅に偏在してゐることである。併し同じ一隅に偏在して居る秩父に於ても特別な異常を見出さないから小田原方面に對する應用も左程不當なものではあるまいと信ずる。

水成岩層の有無を無視しても影響の少ない丹後地方では、那須理學士[9] の研究によ

---

[7] 國富信一「關東大地震の驗震學的考察」驗震時報 **3** (1929), 211—242.

[8] 今村明恒 帝國學士院記事 **2** (1926), 401.

[9] 那須信治 地震研究所彙報 **6** (1929), 245.

ると、震原の深さは大體 15 km. 內外であるが之に相當する k の値は 8·4 である。k が此様に大きな値をもつといふのは土地の地質構造によるのであるから、本問題の如き研究は各地で別々に調査しなくてはならないことであらう。

著者等の研究は近距離地震の觀測結果を基礎にした近似計算の第一段で、未だ不十分なものであるが、地震計測、特に觀測網が更に細目となり、又時刻の測定が進歩すると共に調査は精細となり得べきものであらう。

---

26. *The Effect of Superficial Sedimentary Layers upon the Transmission of Seismic Waves.*

By **Akitune IMAMURA, Fuyuhiko KISHINOUYE**
and **Takao KODAIRA,**
Earthquake Research Institute.

Since k in Omori's empirical formula $d=kt$ may be made to assume the physical meaning $k=v_1.v_2/(v_1-v_2)$, where d is the distance of the seismic focus from a station, t the duration of the preliminary tremors at the said station, and v_1 and v_2 the respective transit velocities of the dilatational and distortional waves, it will be seen that the factor is by no means a constant, but must vary with v_1 and v_2, and must therefore be some function of the focal depth f, say, and the epicentral distance $\triangle$. For near distances, Omori deduced for it the value 7.42, but evidence is not wanting that in the younger geological formations it may take as low a value as 2, or even 1.5. For the local shocks so frequent in the Kii district, one of us obtained the value 3.0. Consequently, in determining the seismic focus by t obtained at four or more stations with the assumption of wave transmission along a single straight line with k as constant, inaccuracies in the results will be inevitable. Similarly, the usual method of estimating focal depths by the time-distance curve of $\overline{P}$, P or $\overline{S}-\overline{P}$ must also be subject to several errors when the presence of a superficial sedimentary layer has been ignored.

This note is an attempt to give the results of our studies made upon introducing into seismometry the conception of a surface layer overlying the granitic one. Out of the 65 moderate shocks that shook the Kwantô district during 1927, we selected 21 as having given fair registers of the initial phase as well as the phase which is assumed to have been transmitted along its entire path as a distortional wave. (Table I.)

According to Prof. Matuzawa the crust in the Kwantô district may be regarded as consisting of three consecutive layers, viz., the granitic layer ($v_1=5.0$, $v_2=3.15$, depth of the lower boundary = 20 km.), the basic layer ($v_1=6.1$, $v_2=3.7$, depth of the lower boundary = 50 km.) and the ultra-basic layer ($v_1=7.5$, $v_2=4.45$) (Fig. 2). Our calculation started by assuming the existence of such substrata, the next process being to evaluate the thickness h and the value k of the surface layer conforming to the results of observations of these 21 shocks.

Fortunately, our observations included a few shocks, the value of t in each of which were nearly equal to one another for two pairs of stations as in No. 14, or to each other for three stations as in No. 2, so that the epicentre could be accurately determined. Further study of the data given by these shocks enabled us to infer that h and k in this case must be about 10 km. and 5.2 km./sec., respectively. For instance, take No. 14 (see Fig. 1 and Table I); Δ for Tokyo or Kamakura (= 32.5 km.) divided by t (= 6.5 sec.) gives $k=5.0$. The data for Misaki ($\Delta=51$ km.), Kiyosumi ($\Delta=81.5$ km.) and Titibu ($\Delta=52.5$ km.) suggest that the seismic focus must be situated near the boundary of the surface layer and Matsuzawa's first layer, and then refracted into the surface layer towards the above-mentioned three stations. Now we have the following relation

$$h\cos\theta=(t-\Delta/8.51)\,k,$$

where θ is the angle of refraction, and t the difference of times of transmission of the two phases in the surface layer. For those three stations, the values of $t-\Delta/8.51$ come out as 2.21, 2.22 and 2.32 sec. respectively. We have already found that the value of k for the surface layer is about 5.0, therefore we have $\sin\theta=5.0/8.51$, and $\cos\theta=0.81$. Accordingly,

$$h=2.3\times 0.81\ k=9.5\text{ km.}$$

Now adopting this result, the paths of the dilatational and distortional waves, and consequently the apparent mean values of k, i.e. d/t (Fig. 2), were computed for various values of f and Δ (see also Fig. 3 and 4), the results obtained after successive approximations being as shown in Table II or Fig. 5.

The next step was to find the epicentres and focal depth of every earthquake such that the mutual relation between k, f and Δ thus deduced from actual observations should approach as near as possible the calculated values (Table II). As, however, a slight discrepancy had been noticed in the f-k curves for $\Delta=0$ of the surface layer, and the curves for the two systems compared again. After successive approximations the two curves coincided (Fig. 6). The values of h and k of the surface layer thus far obtained were 10.0 km. and 5.03 km./sec. respectively.

There is, however, the possibility of earthquakes originating at depths less than 10 km., so it was thought advisable to subdivide the surface layer into two parts, the result giving $h=7.5$ km., $k=4.47$ km./sec. for the upper part and $h=2.5$ km., $k=8.04$ km./sec. for the lower. The final results will be found in Table I and Fig. 1.

As has been stated, there is a method of estimating focal depths by the time-distance curve of the different phases of earthquake motion, usually ignoring the presence of a superficial sedimentary layer. The method of K. von Seebach consists of determining, first, the time T_0 required by the phase $\overline{\mathrm{P}}$ for transmission from the focus to the epicentre by means of simply producing that part of the curve determined from the observations at some distant stations (Fig. 7), and secondly, the depth as the product of T_0 thus worked out and the transit velocity of that phase v_1. On applying this method in the case when the seismic area is overlaid by sedimentary layers of different physical characters, errors arising from ignoring those layers must much be introduced in the determination of the values of T_0 and v_1.

27.　地震波によりて誘起せられたる土地の固有振動に就いて

地震研究所　今　村　明　恒

（昭和四年九月十七日發表—昭和四年九月二十日受理）

我々が平常地震計を以て記錄しつゝある地震記象の中には、震原から傳はつて來た地震波の外に、此地震波の爲めに誘起せられた其土地の固有振動をも含んで居るであらう。筆者は此兩者の分析を試むべく心掛けて居たが、玆に其一二の結果を述べることにする。

第一圖は東京市麴町區に於て建築中の帝國議會議事堂振動驗測の際に得た結果の一を示すものであつて、議院事務所前とあるは永田町通りに近く、路面と同じ水準の庭面に長さ一米程の棒杭を十本程打込み、地面上に露出した一尺程の部分をセメントして地震計の臺となし、之を以て地震觀測點となしたものである。次に貴族院階下とあるは、前記觀測點から北へ二百十米の距離にある基礎臺盤であつて、此上に構造物の鋼柱が据附けられてあるのである。此礎盤は十二本の打杭の上に建てられた面積16·1×11·6平方尺厚さ4·3尺程のコンクリート造の臺であつて、上面は路面下凡そ五米の處にあるけれども、周圍と接續せる部分の重心は更に其の下にあるものと見做し得られる。本圖の記象は大正十四年十一月六日三時十三分頃霞ヶ浦附近に起つた地震に由るものであつて、器械は今村式五十倍簡單微動計（器械の諸常數は本彙報第一號に載せてある）を用ひたのである（以下特に註を加へない限り、器械は同型と承知せられたし）。兩者の比較に於て、著しき相違は事務所前に於て得た記象が複雜な形式を有することである。更に之を詳細に調べると、0·2–0·4秒の週期の微細な波動が稍大きな、さうして比較的に緩かな波動の上に重なつて見えることである。試みに此等の微細な波動を全部除いたと假定するとき、兩所の記象は大體に於て相一致することになる。

以上の結果によりて見るとき、事務所前記象の上に現はれた0·2–0·4秒週期の微細な波動は局部に於て誘起せられた固有振動の出現と見て差支ないであらう。勿論貴族院階下に於て得られた記象の中にも、震原から擴がつて來た地震波の外に、此處で誘

起せられた別種の固有振動を含んで居るであらうが、此は今回の實驗に於ては分析し得られないものである。

斯くして我々は先づ地面に接した薄皮の部分の固有振動を分析し得たと見做し得られるのであるが、之れが如何なる方法に於て誘起せられたかに就いては今日的確な判斷を下すに困難を感ずる。然しながら此事實は我々の地震計測設備につき大切な暗示を與へるものと思ふ。卽ち純粹な地震波を觀測せんとならば、成るべく斯様な土地固有振動の障害から免れる様にすることである。但し此事は地震波によりて誘起せられる土地の固有振動の觀測が無益であるといふ意味ではない。實際此種の振動は人體或は築造物に與ふる影響の重要な部分、少くも一部分を占めて居るのであらうから、地震計測學上から見ても、將た應用地震學の立場から見ても、決して輕視すべきものではないのである。

次に本年六月三日六時三十四分頃東海道志摩沖に起つた地震に由る各地固有振動實測の結果を述べることにする。此地震は地下凡そ三百粁の深さに起つたもの、卽ち deep-seated earthquake なることが、本問題の研究資料として最も適當なる所以である。斯様な地震は人體へ感覺を與へる區域が不規則な分布をなすことからして、石川氏によりては異常震域の地震とも呼ばれ、又 *P* 波が比較的に大なるが爲めに、大森博士により初期微動なしの地震とも呼ばれたことがあつた。本地震に就いても第二圖に示された通り、*P* 波が *S* 波よりも却つて大なることが見られるであらう。又相互に四粁しか離れて居ない和歌山縣鹽津と日方とに於て得た地震記象について、一は人身に感じない緩漫な大搖れからのみに由つて成立つて居るに、他は小刻みの急振動(週期 0·55 秒)が加はつて居るが爲めに、可なり著しく人體に感じたのである。

現時南海道地震研究の爲めに我々の私設觀測所の網は、其小規模の一眼として和歌浦、紀三井寺、日方、鹽津の一組があり、大規模の一眼として、以上の一組の外に、同縣下田邊、淡路福良、德島縣下富岡がある。以上の觀測點中日方を除くの外は、地震計が何れも堅い岩盤の上に据附けてあるので、本文記載地震の記象は全く同様の性質を示して居る。其故に此處には其代表的のものとして鹽津の記象を擧げることにしたのである。

鹽津を代表記象として選んだ理由は、日方との距離が僅に四粁なること、日方町の地盤は表面を土砂の層にて被はれて居るけれども、基底の岩盤は鹽津と共通なものであつて古生層に屬する輝緑凝灰岩なることにある。隨つて此基底盤まで擴がつて來た

地震波は兩方に共通であつて、而も其性質が極めて單純なことは鹽津記象に見る通りである。此爲めに日方記象に就て其土地に於て誘起せられた固有振動を析出することが極めて容易となるのである。

前に述べた通り、震原は深かつた。さうして紀州の觀測點に於て得られた初期微動繼續時間は紀三井寺 39·9 秒、日方及び鹽津共に 39·5 秒、田邊 39·0 秒などであるから、震波が震原から直線的に觀測點へ擴がつて來たとしても、射出角は四十五度程度である。隨つて實際に於ては地面に對して垂直に近く射出したものであらう。これが即ち本問題の研究資料として大切な性質なのである。

遺憾なことには日方の地震計だけが異式であつたことである。即ち此處には大森今村式簡單微動計（常數は本彙報第一卷にあり）即ち大森式簡單微動計改良型を用ひたのであつた。但し此器械は振子の自己振動の週期が比較的に小さい（今村式の半分凡そ4秒）ことを除いては其外に取立てゝ斷る程の相違もない、其故に日方記象から例の 0·55 秒週期の二次的微動を逐出した場合に於ける殘餘の記象と鹽津記象とを比較するときには、以上の相違を念頭に置いて之を見る必要がある。

日方記象について基調の緩い波動の上に重なつて居る 0·55 秒週期の二次的波動は之を更に細に調べると次の二通の特徴を有することが氣附かれる。

(i)　それが第一位相 P 波の上には著しく現はれて居るけれども、第二位相 S 波の上には殆んど現はれて居ないこと。

(ii)　P 波上に重なれる急波動の大さは、それに對應せる基調波の大さに從つて略ぼ其れに比例して變ること。

以上によりて我々が推定し得ることは、基調波によりて誘起せられた土地の固有振動は、日方町の敷地を被覆せる土砂層に於て、地表と底基岩盤との間を往復する振動ならんと考へられることである。換言すれば、基底盤まで進行して來た彈性的平面波が、柔軟なる表面土砂層に進入した後、此土砂層の上下兩境界面の間を反射往復することが、即ち此處に誘起せられた固有振動を形成したのではあるまいか。果して然らば此振動週期 0·55 秒と、其進行速度とによりて、層の厚さを計測することも可能となる譯である。

問題の地震は同時に我々の關東地方小觀測網に於ても觀測せられた。此處でも基調の地動は緩かであり、震原距離も紀州方面に於けると大差なく、唯僅に遠いと思はれるだけであるから（初動繼續時間、東京 41·6 秒、清澄 41·7 秒、秩父 42·7 秒等）、若

し土地の固有振動が出現するならば、日方と鹽津とに於けると類似の記象が得られる筈である。但し實際に於てはそれ程著しくはなかつたけれども、猶ほ次に記す様な二次的振動を認めることが出來た。

觀測點 Station	地質 Formation	二次的振動の週期（秒） Period of secondary vibrations (in sec)		
清澄 Kiyosumi	第三紀層 Tertiary	0·64	—	—
秩父 Titibu	第三紀層上の土砂層 Tertiary overlaid with sand	0·6	—	0·22
鎌倉 Kamakura	同上 Ditto	0·6	—	—
東金 Tôgane	洪積層 Diluvium	0·6	0·35–0·44	0·25
東京 Tokyo	同上 Ditto	0·7	0·5	0·2–0·3

上の表に於ける觀測點の土地構造と二次的振動の週期とを比較すると、其處に兩者の間に密接な關係がある樣に思はれる。第一に清澄記象からして第三紀層に屬するものとして 0·64 秒を取るべく、秩父や鎌倉の記象も此推定に有利なるのみならず、總てに殘りなく、此週期のものが現はれて居ることも、此ことの確實性を增すものであらう。次に 0·2–0·3 秒週期のものが表面の土砂層に屬するものならんとのことも疑なかるべく、最後に 0·4 秒內外のものは洪積層に屬するものとして取殘される譯である。

以上の推定に於て、若し誤謬がなかつたならば、其れを各層に於ける波動進行の速さに結附けて、各層の厚さを計算することが出來るであらう。但し此は後日の研究に讓ることにする。

27. *On the earth-vibrations induced in some localities at the arrival of seismic waves.*

By **Akitune IMAMURA.**

Seismograms may involve, besides seismic waves propagated from the focus to our stations, earth-vibrations induced there by means of the seismic waves thus arrived. The present note contains some analytical study concerning such earth-vibrations.

Fig. 1 shows seismograms due to the earthquake, which occurred on Nov. 6,1925, near Kasumigaura and was registered at diluvial ground in Tokyo, B and D with an Imamura tromometer ($V=50$, $T_0=7$ sec.) installed at the ground level upon a concrete block of 3 × 3 × 1 ft. size, and A and C with another similar instrument set up on a rigid pedestal of 16.1 × 11.6 × 4.3 ft. size. The pedestal is situated about 210 m. apart from the first station, with its upper level lower than the ground-level by 4.9 m. The difference of the earth-movements indicated by the seismograms obtained at these two stations reveals that there were induced in the thin surface layer of the place small earth-vibrations of a period ranging from 0.2 to 0.4 sec.

Fig. 2 is a reproduction of the seismograms due to the deep-seated earthquake (depth about 300 km.), which occurred on June 3,1929, at 6h 34m off the coast of Sima Province. It was registered with instruments essentially of the same type as above and installed at Siotu and Hikata in Kii Province, the mutual distance between the two stations being only 4 km. The ground of Siotu is Palaeozoic diabase tuff in formation, whereas that of Hitaka is of the same formation covered with soil of certain depth. It will be noticed that the *P* phase is much bigger than the *S* phase—a characteristic special to earthquakes of such a depth. The duration of the *P* phase at both stations come out as 39.5 sec.

Special interest of the observation of such earthquake at a distance as in the present case is due to the facts that the seismic waves emerge almost at right angles to the earth's surface, and consist for the most part of slow undulations almost free from vibrations of quick period (see the Siotu register). In fact, both seismograms are similar to each other, except that the Hikata register involves in addition a series of secondary vibrations of a constant period of about 0.55 sec. These secondary vibrations are present only in the *P* phase, and are approximately proportional to the magnitude of the fundamental waves accompanying them. This would suggest that they are earth-movements induced in the superficial soil layer possibly as plane elastic waves making reflection at the upper and lower boundaries of the layer.

Exmination of the seismograms due to the same earthquake and obtained at our seismological stations in the Kwanto district has brought out as the periods of similarly induced earth-vibrations the following values (see also Table in the text in Japanese):

For superficial soil layer	....	0.2–0.3 sec.,
„ Diluvium „	....	0.4–0.5 sec.,
„ Tertiary „	....	0.6–0.7 sec.

If such a method of estimation be legitimate, then the thickness of the different layers may be worked out.

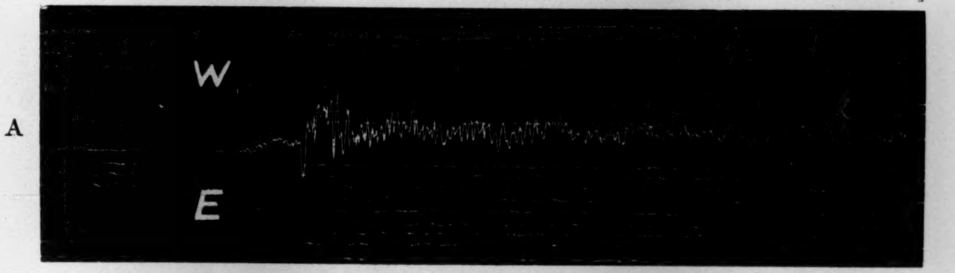

貴族院礎盤上 東西動 Pedestal: E-W component.

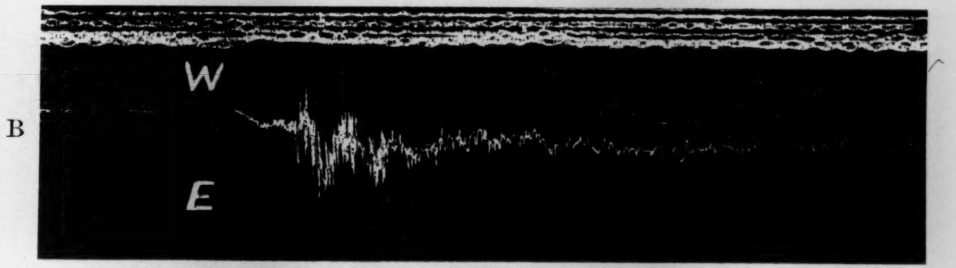

事務所前 東西動 Ground: E-W component.

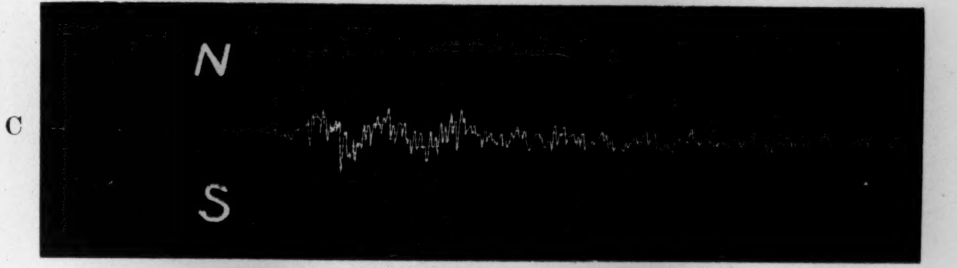

貴族院礎盤上 南北動 Pedestal: N-S component.

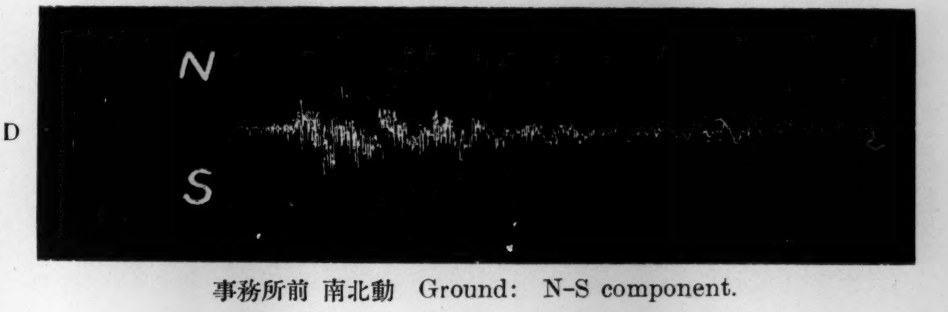

事務所前 南北動 Ground: N-S component.

第 一 圖 大正十四年十一月六日霞浦地震記象

Fig. 1. Seisgrams due to the Kasumigaura earthquake of Nov. 6, 1925, at 3 h 43 m. ($V=50$, $T_0=7$ sec., time scale 58 mm./min.)

（震研彙報第七號、圖版、今村）

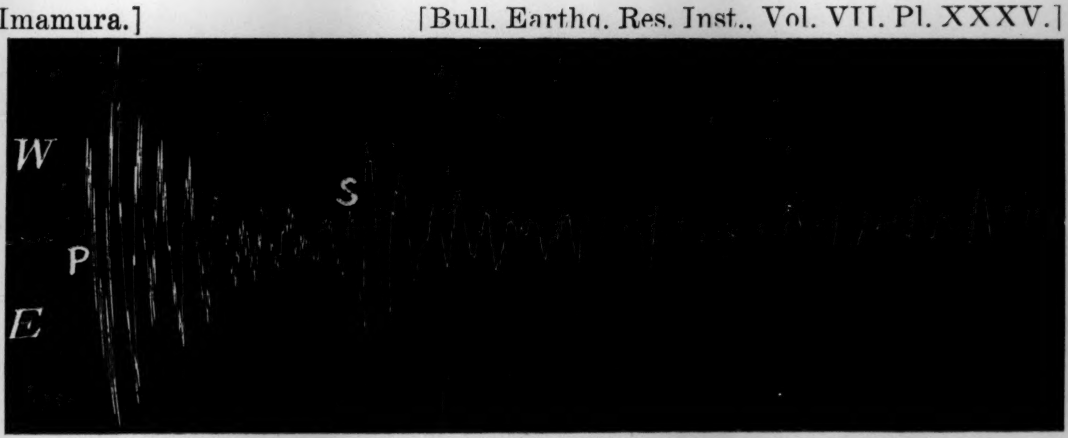

A. Hikata register: E-W component. Time scale=46 mm./min.

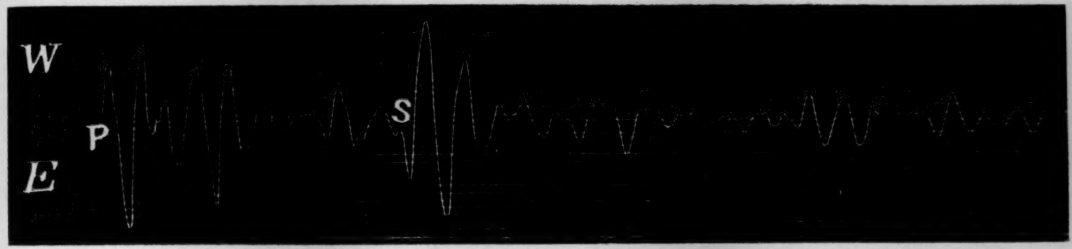

B. Siotu register: E-W component. Time scale=53 mm./min.

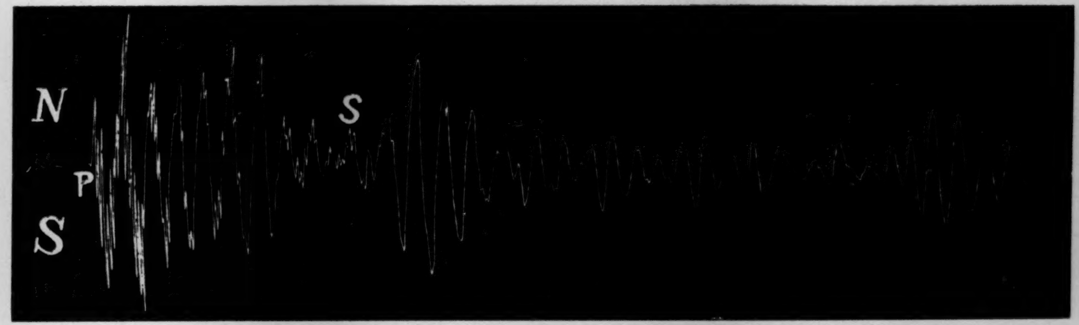

C. Hikata register: N-S component. Time scale=46 mm./min.

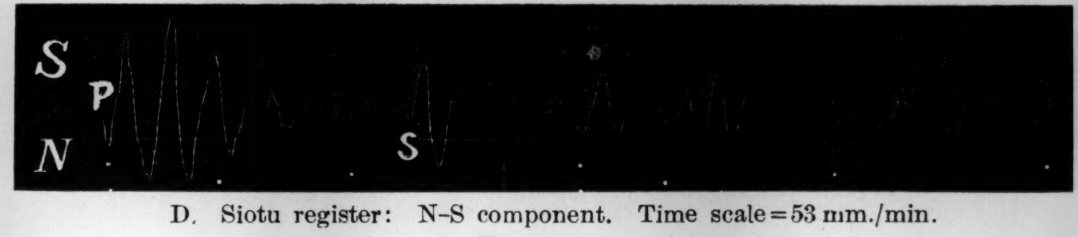

D. Siotu register: N-S component. Time scale=53 mm./min.

第二圖 昭和四年六月三日地震記象

Fig. 2. Seismograms due to the deep-seated earthquake of June 3, 1929.

28. 關東地方改測水準測量結果に就ての研究

武藤勝彦
熱海景良

（昭和三年四月二十四日及び五月二十二日發表—昭和四年九月十九日受理）

其一　水準測量の結果に現はれたる地殼運動の特性

土地の表面が地震や火山の爆發に際し又經年的に其高さを變化する事はよく知られて居る事實である。而して陸地測量部が從來實施した水準線改測作業に於いても之等の變化は明かに報告されて居る。

然るに之等地表の變化の有する一種の特性に關しては從來明確に之を指摘した報告は殆どない樣である。

關東地震後陸地測量部は關東を含む廣汎なる地域に亘つて水準線の改測を實施した、而して斯る廣範圍に亘る水準線の改測は筆者の知れる範圍に於いては未だ其類を見ざるものである。之に關しての詳細は陸地測量部より報告されてあるから此處には省略することとするが此結果が地球物理學、地質學等に關與する諸學者の研究に資する點は蓋し少くないものがあらう筆者等は此の測量結果より從來研究されて居らなかつた樣に見える地殼表面の垂直變動に於ける特性を調べて見た。以下此の調査結果の概要を記るす。

精密水準線に現はれた地塊運動

地表面が舊水準測量施行後ある垂直變位を受けたとすれば其狀態は各水準點の新舊標高差に現はれて來なければならない。即新舊測量結果を比較することに依つて地表の垂直變化は之を明かにすることを得る筈である。

附圖第一は水準原點を不動と假定し新結果より舊結果を引き去りて得たる各水準點標高の變動量に依りて作製せるもので横軸に水準線、縱軸に垂直變動量を示したものである。水準線に於ける隣接標石間の距離は約二粁で圖に於ては之を五粍とした。附

圖を見て直ちに感ずる點は水準線の某區間毎に各水準點の變動量を示す點が夫々傾斜を有する一直線上に殆んど配列して居ることである。

此の事は地殼表面が明かに多くの地塊に分裂し各地塊が夫々獨自の運動をして居る事を示すものであつて決して地表面は完全彈性體の表面に於けるが如き變動を示さざる事を明かにするものである。

次に圖上に於て認め得る著しき點は區域によりて該直線の長さが大略同じ様に見へる事である。勿論本附圖に現した如き水準線の長さが直ちに地塊そのものの幅員を示すものとは考へられないが試みに主要なる線に就てその長さを測定して見れば次表の如くである。但し表に於ける長さの單位は隣接水準點間の距離二粁である。

1. 甲府附近より高崎、今市、水戸を經て佐原附近に至る。

飯沼村――富士見村	23
富士見村――和田村	22
和田村――追分	24
追分――高崎	26
高崎――東村	24
東村――日光	26
日光――水戸	47
水戸――土浦	24
土浦――大倉村	26

2. 佐原附近より勝浦を經て津田沼に至る。

大倉村――成東	37
成東――八積村	14
八積村――勝浦	18
湊村――舘野村	22
舘野村――湊町	18
湊町――楢葉村	14
楢葉村――津田沼町	20

3. 川崎より熱海に至る線。

川崎――戸塚	11
戸塚――吾妻村	17
吾妻村――熱海	14

4. 中央線

甲府――笹子	13
笹子――梁川村	13

梁川村——小原町	11
小原町——八王子	9
八王子——高井戸	15

本表には主要なる地塊に就てのみ記載したのであるが尙大地塊中に小地塊を就中變動の大なる地方に於て之を認むる事が出來る。

附圖第五中水準線上に於ける黑點は主要なる地塊の境界線卽ち地塊の構造線の位置を示すものである。

相模及房總半島に於ける地塊運動

附圖第一により精密水準線上に於ける地塊構造線の位置は明かに之を知る事を得る。然れども精密水準測量の結果のみを以てしては水準環線內に包容する地域の變化狀況を知ることは出來ない。從て構造線が如何なる方面に走つて居るかは單に推定に止る譯である。此水準線內部に於ける地塊運動の狀況も適當な密度に配布された新舊高程差を示す點が在れば勿論明かにし得る筈である。幸に相模及房總半島の激震地一帶に亘つて地震後三等三角測量を施行したので是等の地方に於ては各三角點の標高變化が知られて居る。尤も其精度は精密水準測量の如く良好ではないが地表變位の大勢を知るには充分である。そこで此三角水準網を使用して此地方の地塊運動を調査して見た。尙三角點の密度は一方里に二點程度である。調査の方法は次の如くである。

1. 二十萬分一三角點配置圖に各點の垂直變動量を記入する（附圖第二参照）
2. 次に此上に大體 *SW–NE* 及 *SE–NW* 方向に線を引く此線の方向は小川博士の報告に依る地震構造線を參考とし大體之に平行及直角としたものである（附圖第二参照）
3. 各線に就て其線上及附近の三角點を使用し横軸に三角點間の距離、縦軸に垂直變動量を取り各線の高程變動曲線を作る（附圖第三参照）
4. 隣接高程變動曲線上類似せる傾斜變換點に同一符號を附ける（附圖第三参照）
5. 變動曲線上の記號を之に相當する平面圖上の位置に記入し記號群の表はす點の配列に依り是を含む平均の方向線を描畫する（附圖第四参照）

附圖第五中相模地方及房總半島に於ける實線は上記の方向によりて得たものであつて水準線上に現はれた構造線の位置とよく一致することが認められる又中野—五日市、志村—扇町屋線は大正十四年施行した三角點間の二等水準測量の結果より精密水準線に於けると同樣の操作により得た線である。此等以外の線は精密水準測量の結果

より想像して引きたる線である。各地塊上に示した矢記號は其地塊の下方に傾斜せる方向を示し數値は傾斜の秒數を示す。但し之等方向並變動量は圖上に於て求めたものであつて大略の形勢を示すに過ぎない。

各地塊上の矢を見て特に注意を牽くことは相模地方に於て沼津—八王子線を境として其兩側に於て著しく變動量を異にし且其東側に於けるものゝ方向が反時計式に回轉して居る點及房總半島に於て北條附近より八幡附近に到る縱斷線を境として大體兩側に折れた如き結果を示して居る點である。

隣接地塊構造線間の距離は相模地方に於ては次表に示す如きものであつて約七粁を單位とし其二倍、三倍と云ふ樣な値を持つて居る樣に思はれる。

線號	線名	距離（粁單位）
1	戸塚—府中	14
2	茅ヶ崎—八王子	14
3	吾妻村—水原	14
4	湯原—新倉	12
5	三島—笹子	
6	沼津—八王子	13
7	愛鷹山—上ノ原	12·5
8	富士山—猿橋	
9	湯原—下諏訪	7
10	早川—甲運村	7
11	酒田—笹子	
12	戸塚—秦野	13
13	鶴見—高旗山	9·5
14	大井—川尻	14·5
15	中野—五日市	12
16	志村—扇町屋	

房總半島に於ては構造線は相模地方の如く規則正しくはない。精密水準線に現はれた構造線間の距離が中央線に於ては同じ樣な値を持ち房總半島に於ては餘り統一のない數値を示して居つたがそれは此附圖に示してある地塊で明かになつた樣に思はれる。又甲府附近から高崎、日光を經て佐原附近に至る長い水準線に於ては各地塊上に於ける水準線の長さが大概同じ樣な値を持つて居る點よりして此地方に於ける地塊は相模地方に於ける樣に規則正しく形造られて居るのではないかと思はれる。

附圖第五上に於て東京の上に引いてある線は東京市街水準測量の結果より得たものであつて其詳細は後の報告で述べることにする。

自山梨縣甲府市　至群馬縣高崎市

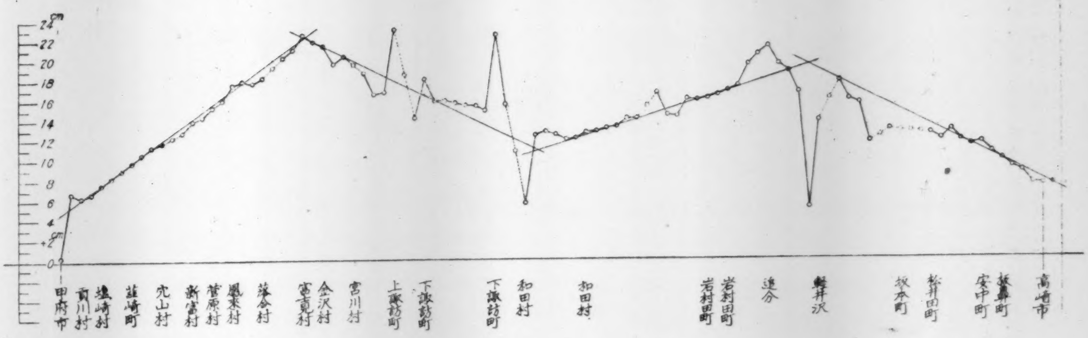

附圖第一ノ(一)

自群馬縣高崎市　至栃木縣宇都宮市

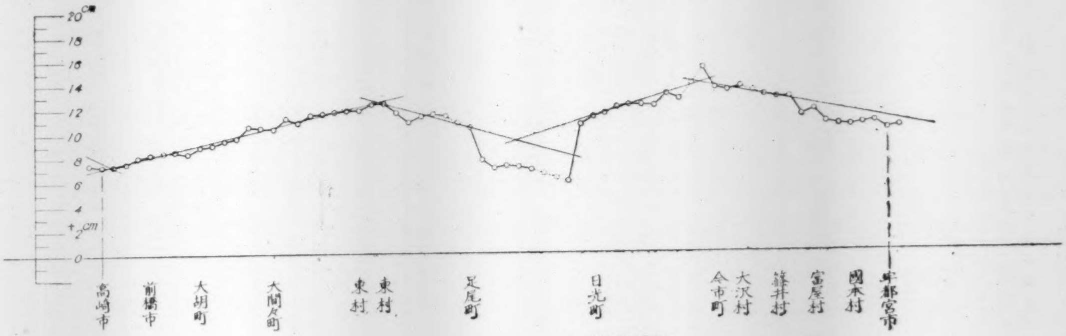

附圖第一ノ(二)

自栃木縣宇都宮市　至千葉縣佐原町

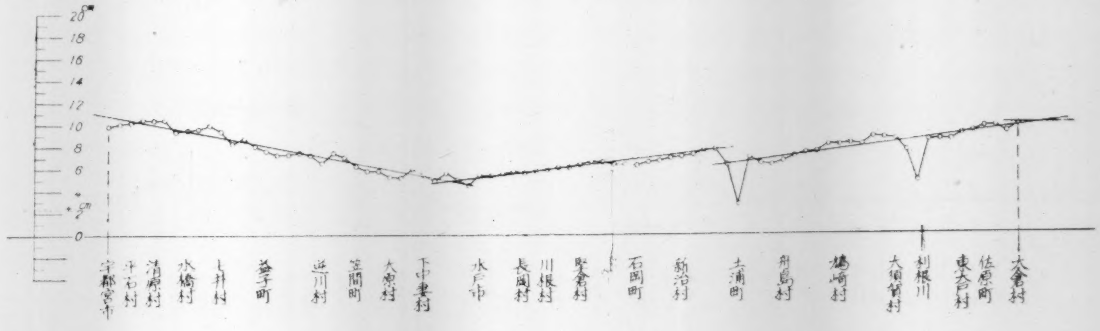

附圖第一ノ(三)

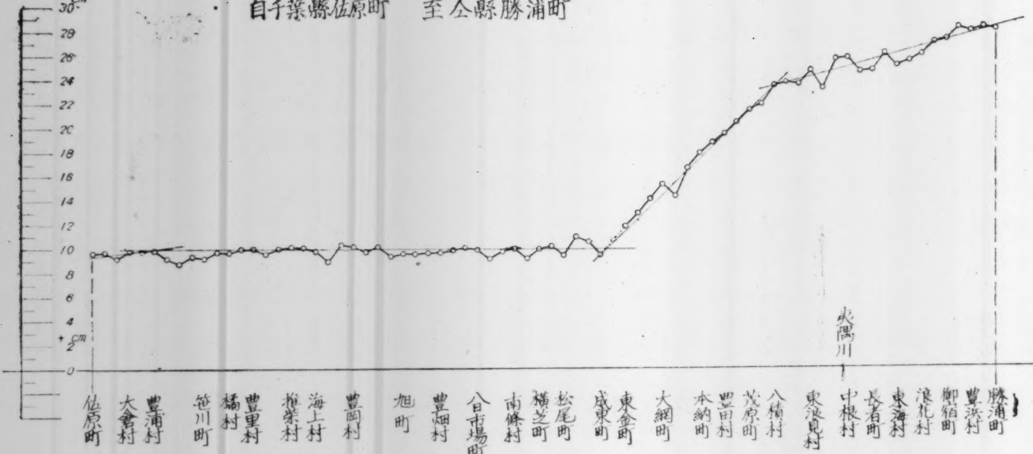

自千葉縣佐原町 至仝縣勝浦町

附圖第一ノ(四)

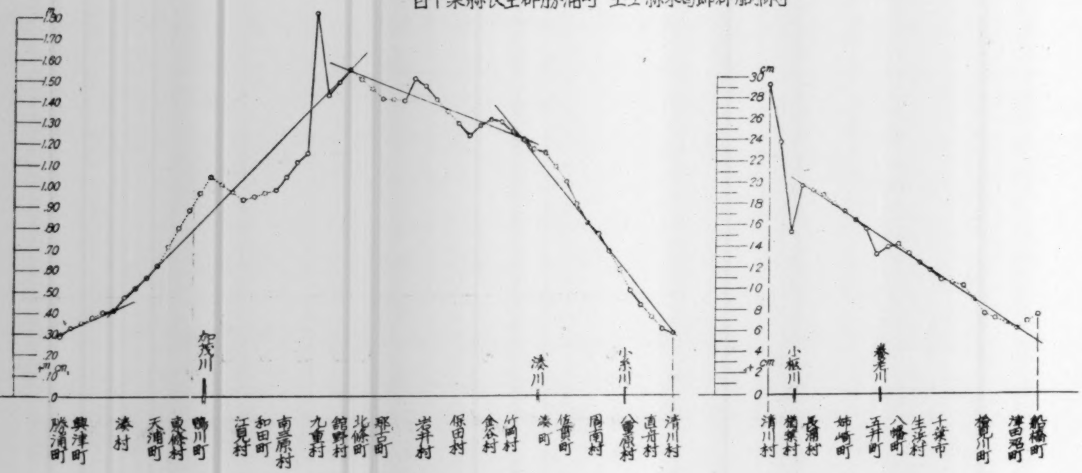

自千葉縣長生郡勝浦町 至仝縣東葛飾郡船橋町

附圖第一ノ(五)

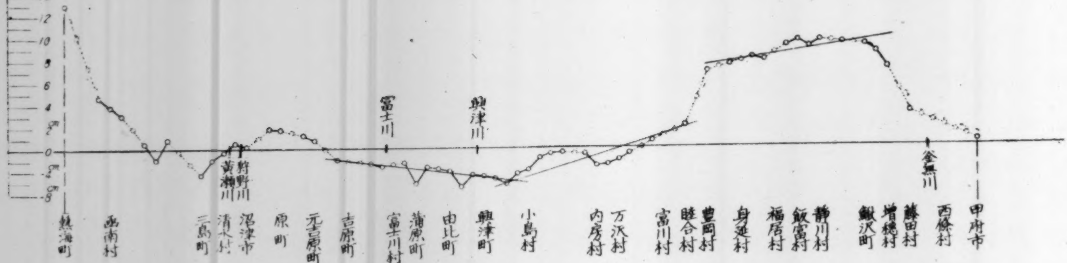

自靜岡縣田方郡熱海町 至山梨縣甲府市

附圖第一ノ(六)

自東京市芝區高輪町　至靜岡縣田方郡熱海町

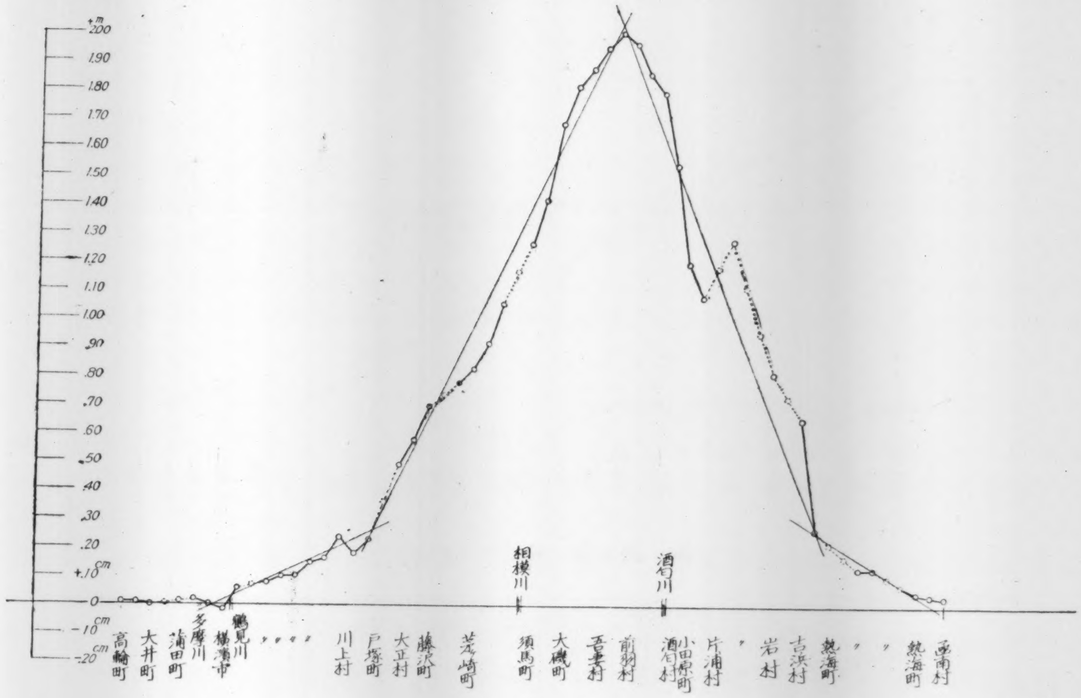

附圖第一ノ（七）

自山梨縣甲府市　至東京府豊多摩郡代々幡町

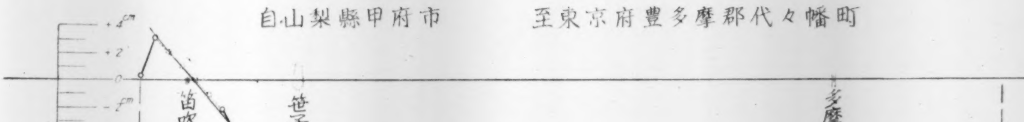

附圖第一ノ（八）

自群馬縣高崎市　至東京府北豊島郡板橋町

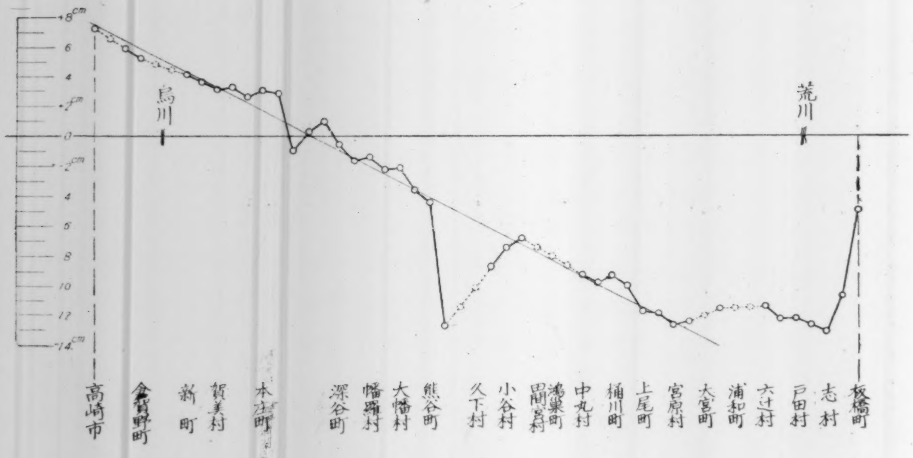

附圖第一ノ(九)

自栃木縣宇都宮市　至東京府南足立郡千住町

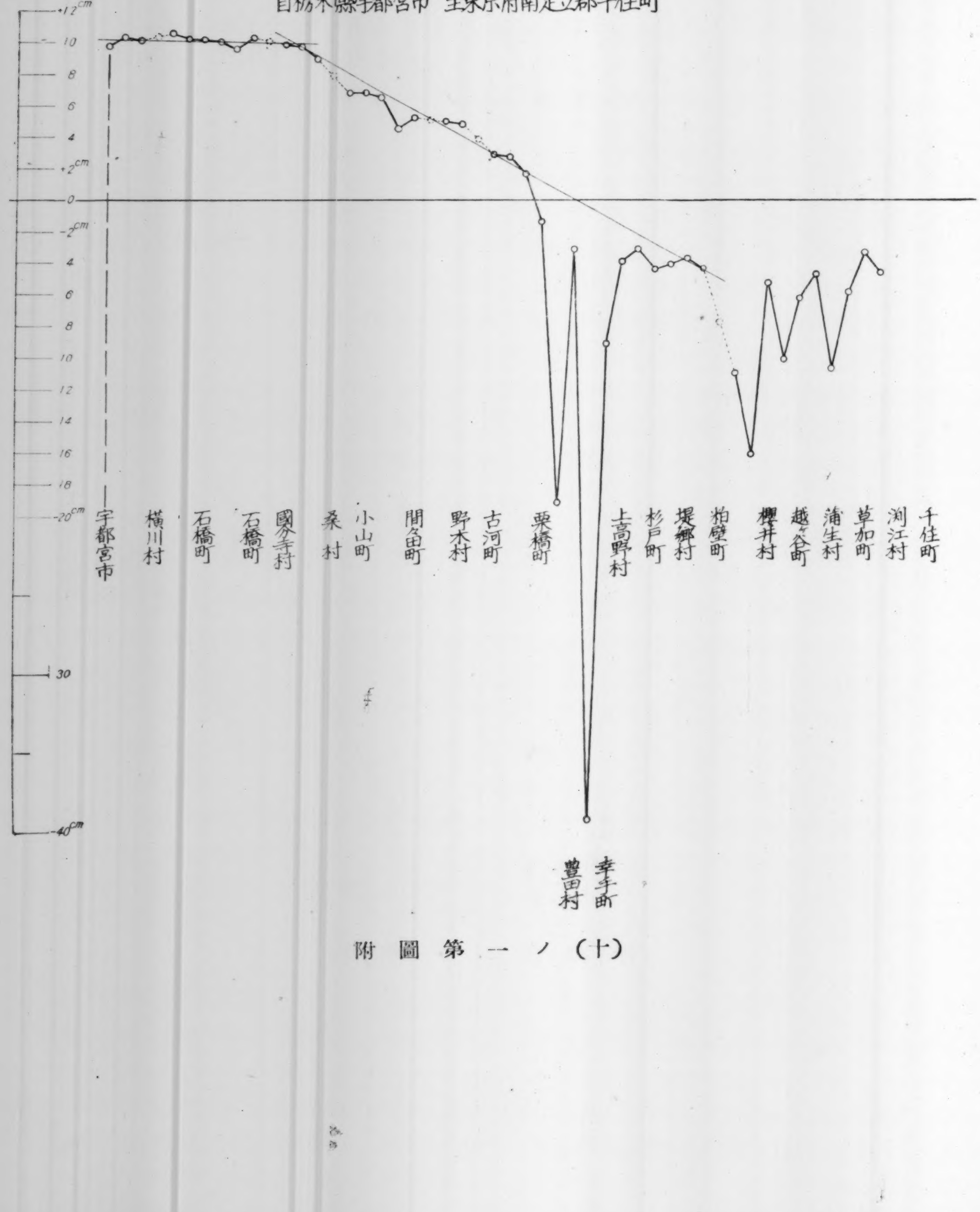

附圖第一ノ(十)

自千葉縣東葛飾郡船橋町　至仝縣香取郡佐原町

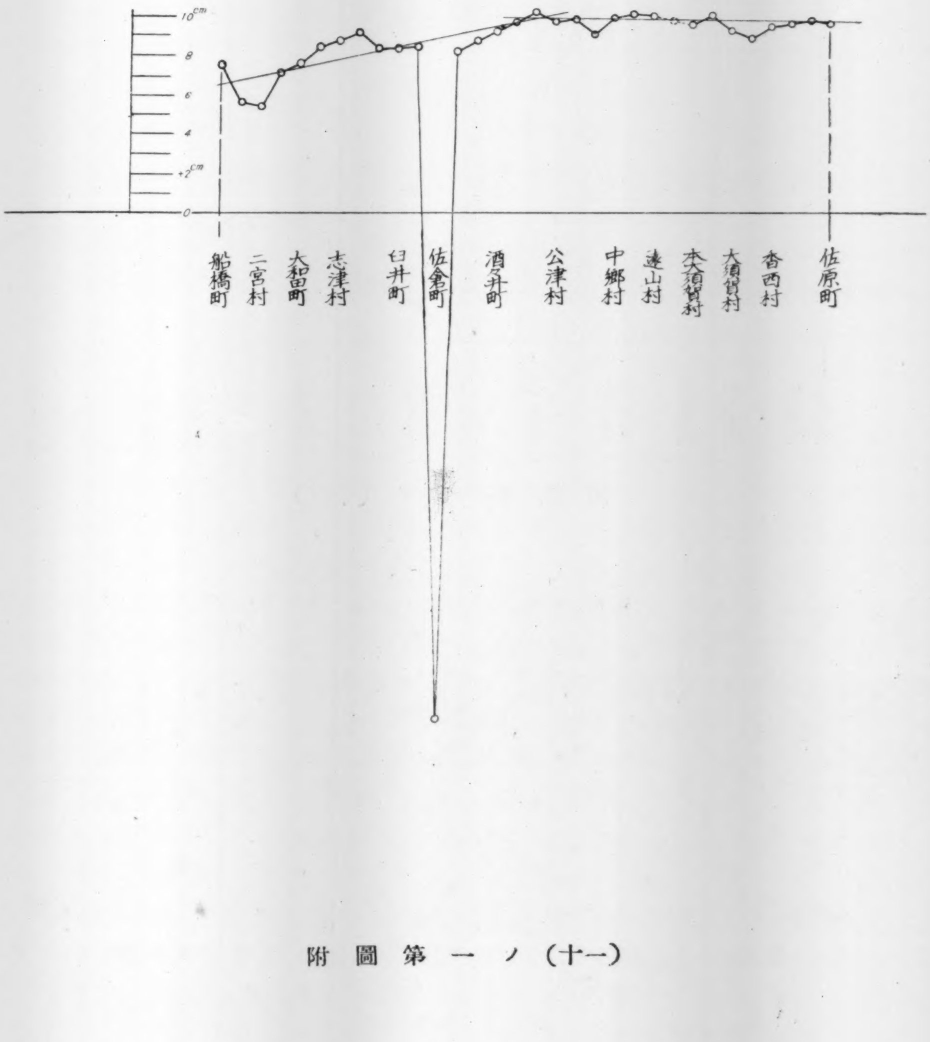

附圖第一ノ（十一）

自神奈川縣足柄下郡土肥村　至靜岡縣賀茂郡下田町

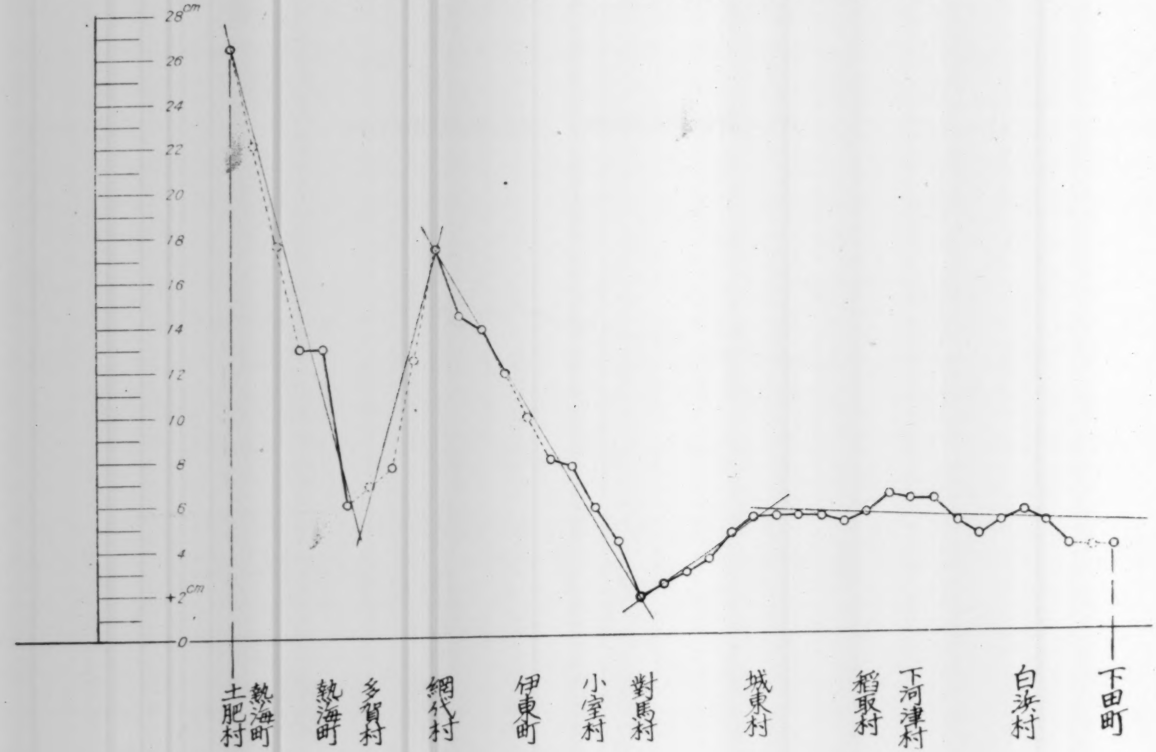

附圖第一ノ(十二)

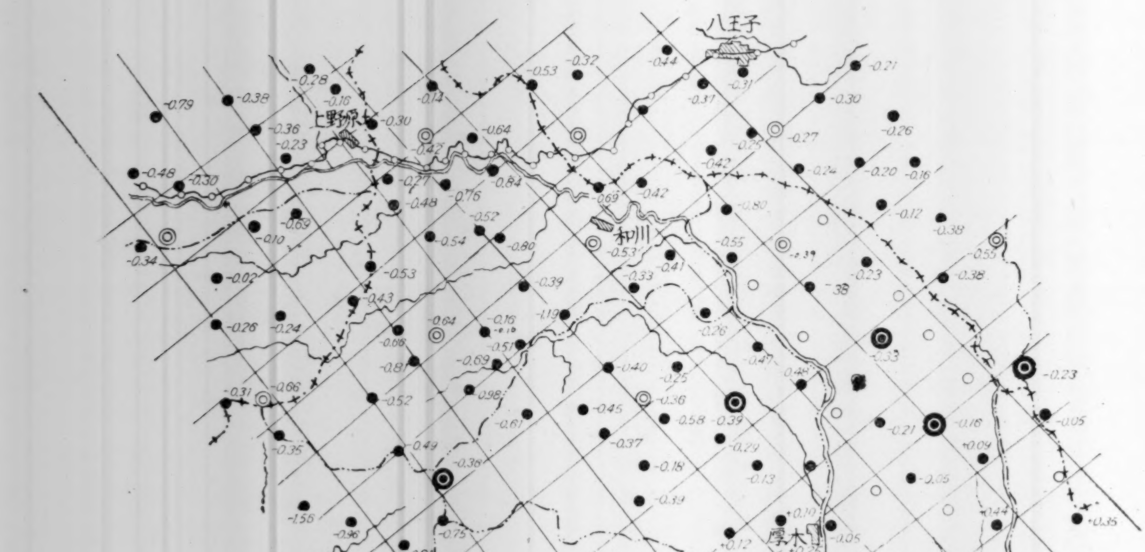
八王子
上野原
和川
厚木

附圖第二

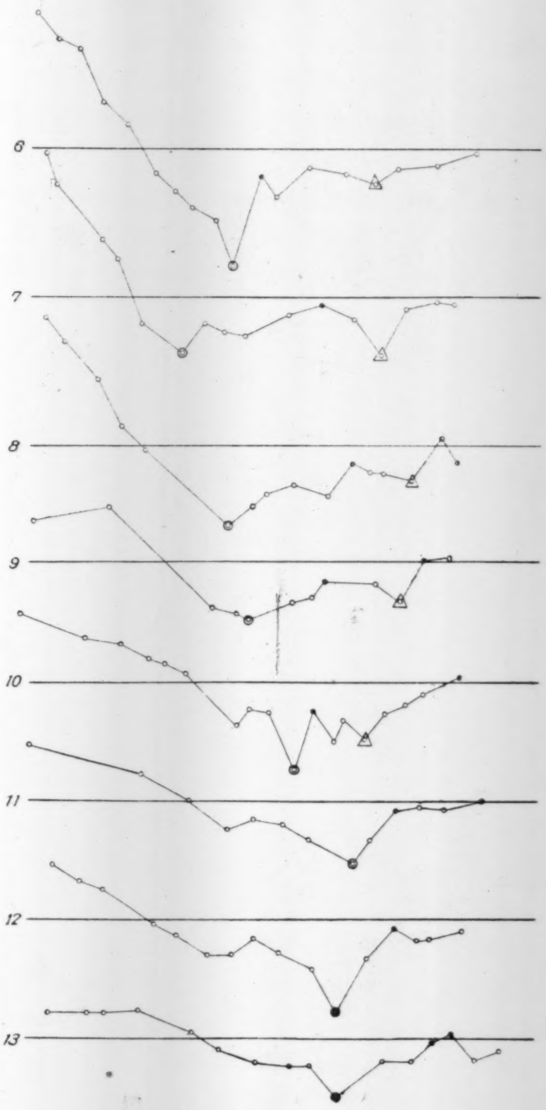

附圖第三

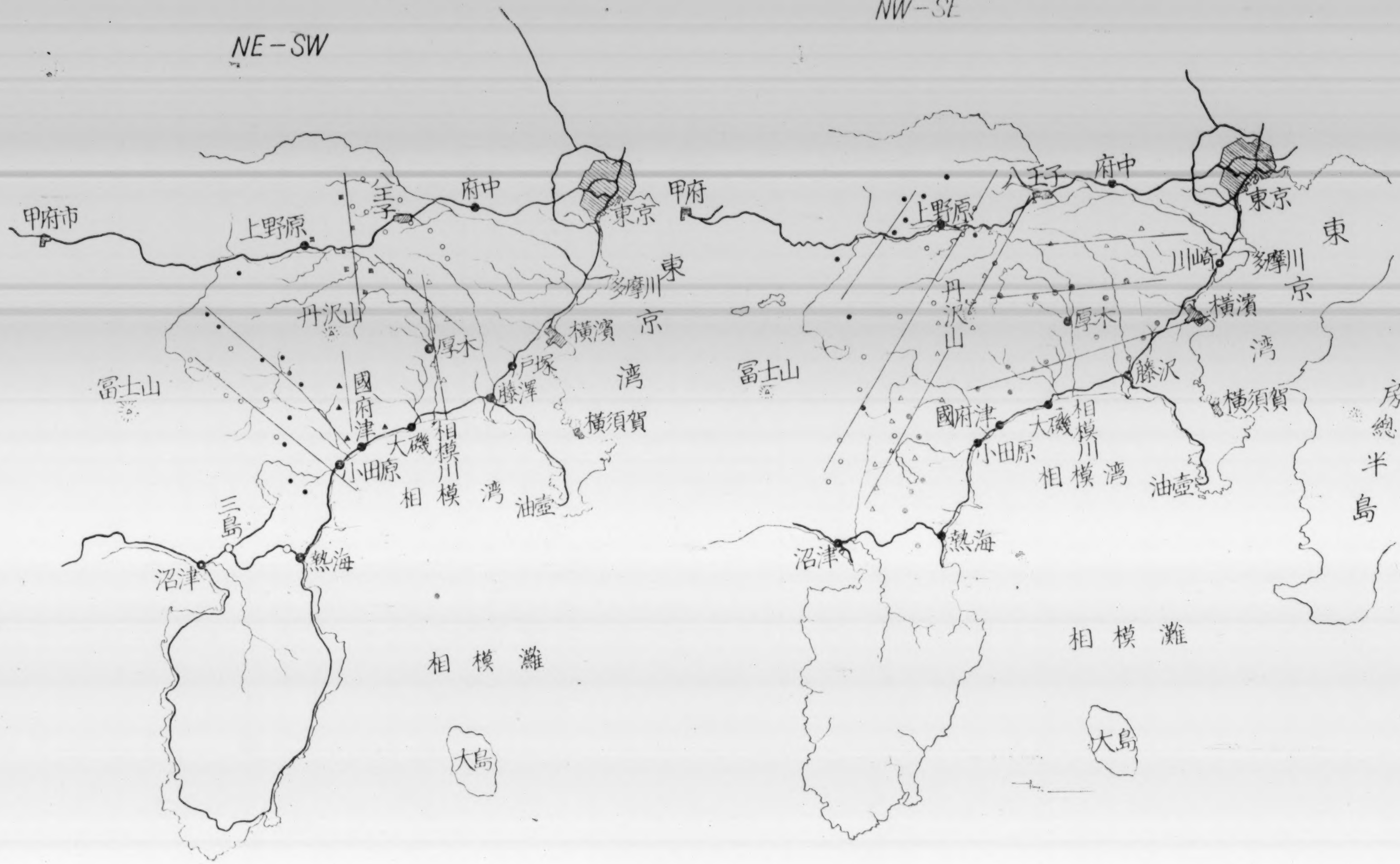
NE-SW
甲府市
上野原
八王子
府中
東京
東京灣
多摩川
丹沢山
厚木
戸塚
横濱
冨士山
國府津
藤澤
横須賀
大磯
相模川
小田原
相模灣
油壺
三島
沼津
熱海
相模灘
大島
NW-SE
甲府
上野原
八王子
府中
東京
東京灣
川崎
多摩川
丹沢山
厚木
横濱
冨士山
藤沢
横須賀
房總半島
國府津
大磯
相模川
小田原
相模灣
油壺
沼津
熱海
相模灘
大島

附圖第四ノ(一)

2

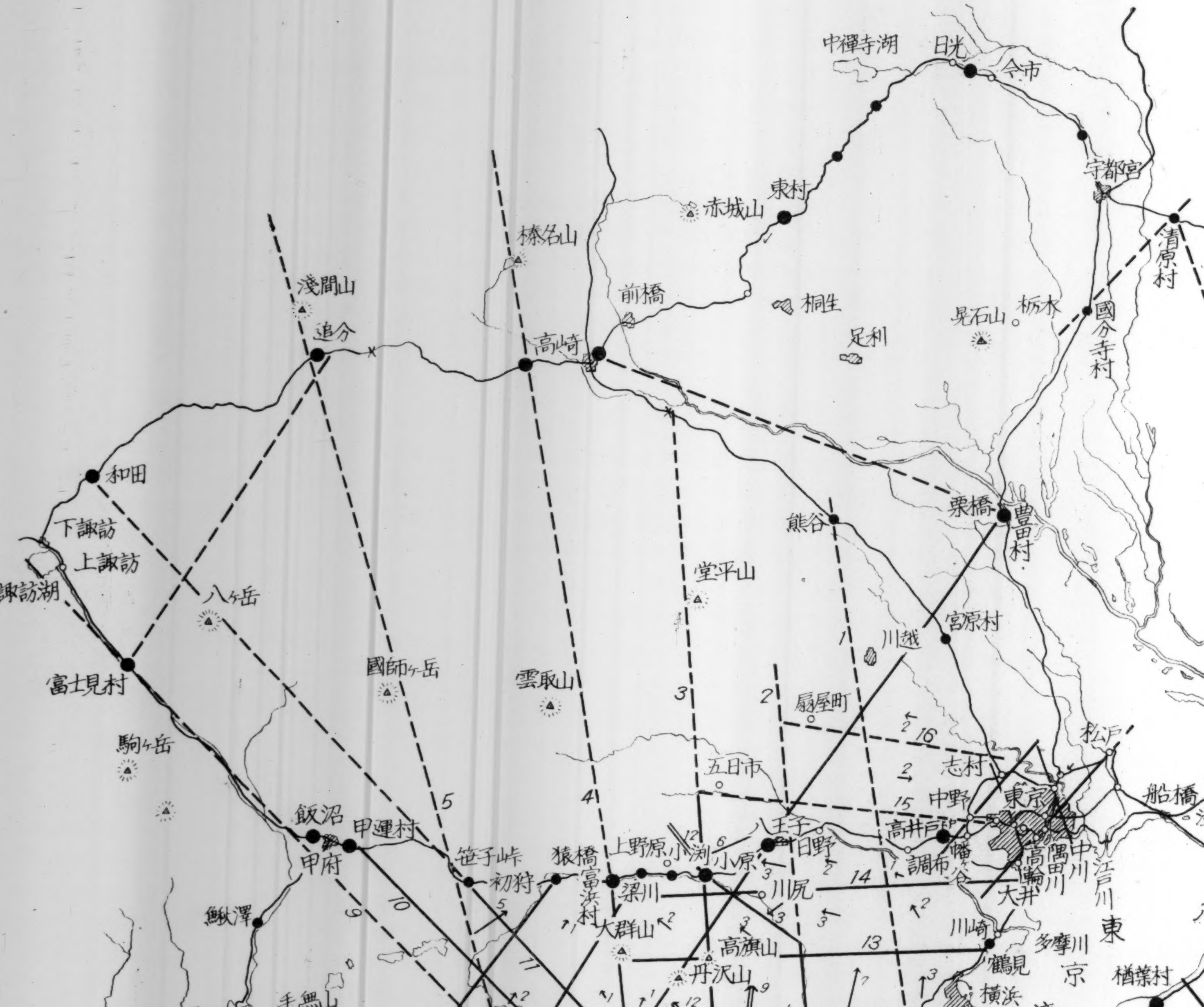
中禪寺湖
日光
今市
宇都宮
清原村
東村
赤城山
榛名山
淺間山
前橋
桐生
足利
晃石山
栃木
國分寺村
追分
高崎
和田
下諏訪
上諏訪
諏訪湖
八ヶ岳
富士見村
熊谷
栗橋
豊田村
堂平山
宮原村
川越
國師ヶ岳
雲取山
扇屋町
駒ヶ岳
五日市
志村
松戸
東京
船橋
飯沼
甲運村
甲府
笹子峠
初狩
猿橋
富浜村
上野原
梁川
小渕
小原
八王子
日野
高井戸
中野
幡ヶ谷
調布
高輪
隅田川
中川
江戸川
大井
川尻
大群山
高旗山
丹沢山
川崎
鶴見
多摩川
東
京
湾
楢葉村
鰍澤
毛無山
富士山
秦野
横浜
戸塚
藤沢
豊岡
淺間山
吾妻村
茅ヶ崎
相模川
横須賀
鹿野山
小田原
早川
湊
宍原
愛鷹山
相模湾
油壺
三島
湯河原
熱海
沼津
松長
平井
狩野川
但沼
富士川
興津
静岡
八東村
豊田村
北條
館野
房大山
伊東
相模灘
藤枝
万城山
駿河湾
大井川
大島
下田
1
2
3
4
5
6
7
8
9
10
11
12
13
14
15
16

（震研彙報第七號、圖版、武藤、熱海）

附　圖　第　五

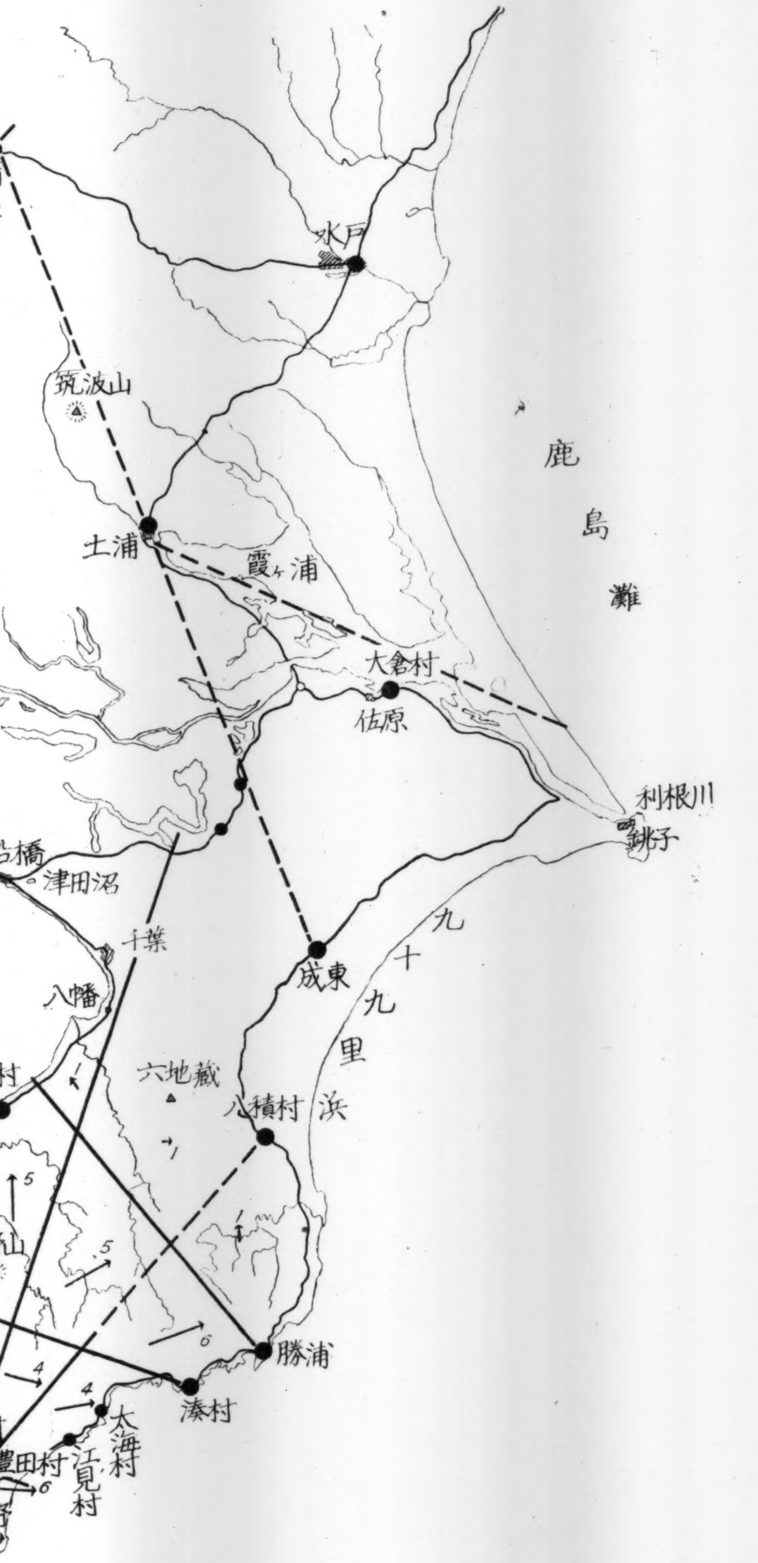
水戸
筑波山
鹿島灘
土浦
霞ヶ浦
大倉村
佐原
利根川
銚子
橋
津田沼
千葉
成東
八幡
九十九里浜
村
六地蔵
八積村
山
5
1
1
5
1
6
4
4
勝浦
湊村
太海村
豊田村
江見村
6

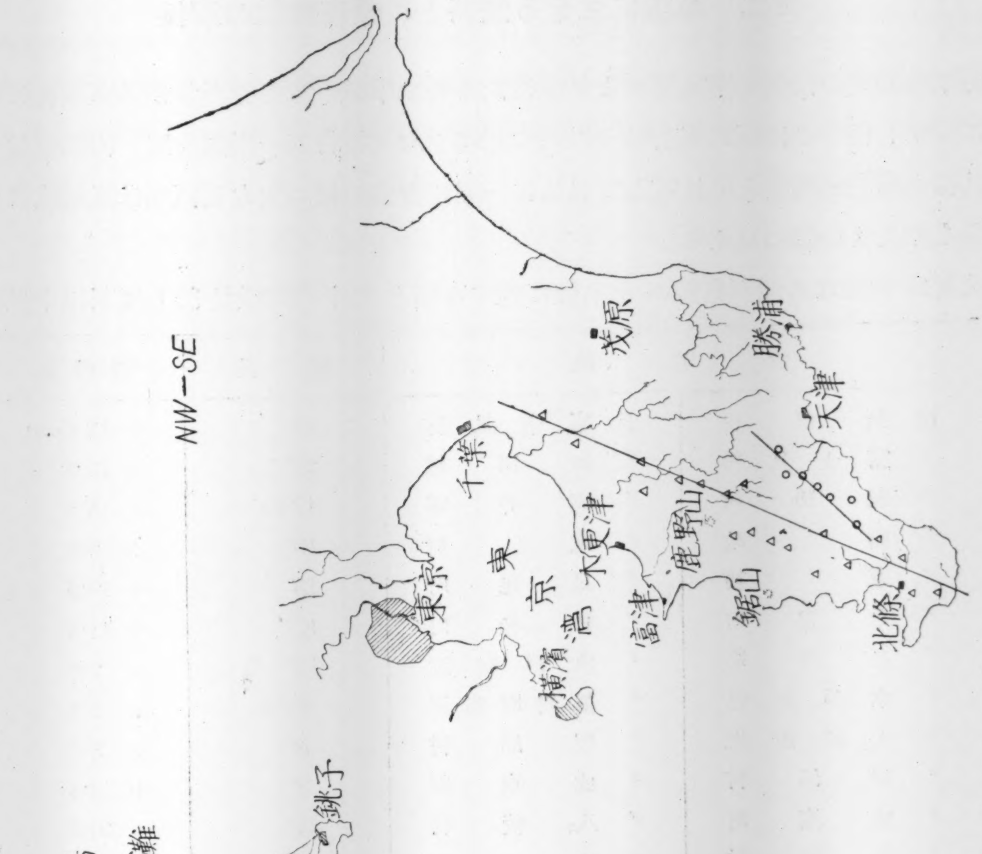
NE-SW
NW-SE
鹿島灘
利根川
銚子
九十九里浜
船橋
江戸川
隅田川
東京
横濱
東京灣
千葉
木更津
佐貫
保田
北條
鴨川
天津
勝浦
東京
千葉
東京灣
横濱
木更津
富津
鹿野山
鋸山
北條
天津
勝浦
茂原

附圖第四ノ（三）

其二 地塊に生ぜる傾斜と其垂直變位の關係

關東地震後の復舊水準測量により求めたる各水準線の垂直變動量が某區間每に略直線にて示し得る事は既に報告其一に於て記述した（報告其一附圖參照）尙此直線の傾と其線の垂直變動量とを比較して見るに一般に直線の傾の大なる區間は隆起或は低下の量も亦大きい樣に見える。

次表は主要なる傾斜直線の水平線に對する傾と其中等變動量即ち傾斜線中點の變

水準線		傾角	變動量
自 飯沼村	至 富士見村	36°	+ 13·8 cm
〃 富士見村	〃 和田村	26°	+ 16·6
〃 和田村	〃 輕井澤	17°30′	+ 15·2
〃 高崎	〃 東村	13°	+ 9·8
〃 東村	〃 足尾町	15°	+ 10·8
〃 足尾町	〃 日光町	17°	+ 11·4
〃 日光町	〃 水戶附近	11°	+ 9·2
〃 水戶附近	〃 眞鍋町附近	6°30′	+ 6·3
〃 土浦附近	〃 豐浦村	8°	+ 8·2
〃 豐浦村	〃 成東町	0°	+ 9·8
〃 成東町	〃 八積村	45°	+ 16·5
〃 八積村	〃 勝浦町	15°	+ 25·7
〃 湊村	〃 館野村	79°	+ 97·5
〃 湊町	〃 清川村	81°	+ 75·1
〃 長浦	〃 津田沼	34°	+ 13·0
〃 宇都宮	〃 國分寺村	1°30′	+ 10·0
〃 國分寺村	〃 幸松村	29°	+ 2·8
〃 甲府	〃 笹子村	50°	− 4·2
〃 笹子村	〃 梁川村	70°	− 29·4
〃 小原町	〃 八王子	66°	− 37·8
〃 八王子	〃 高井戶村	58°	− 16·9
〃 輕井澤	〃 宮原村	28°	+ 3·4
〃 川崎市	〃 戶塚町	67°	+ 13·0
〃 戶塚町	〃 吾妻村	84°30′	+114·5
〃 吾妻村	〃 熱海町	86°	+114·5
〃 豐田村	〃 湊町	65°	+140·0
〃 船橋	〃 公津村	12°	+ 8·3
〃 公津村	〃 佐原	2°	+ 9·8

動量とを示したものである。但し表中の變動量は原點の眞高が舊測量當時以來變化せざりしものと假定して求めたるものにして其正負の値は夫々此假定の下に於ける隆起及び低下を示すものである。傾斜直線の傾角は横軸上五「ミリメートル」を隣接標石間の距離二「キロメートル」とし縦軸上一「ミリメートル」を垂直變動量の二「ミリメートル」とし描いた圖形の上で測定したものであつて勿論直角より小さい方の角をとつた。

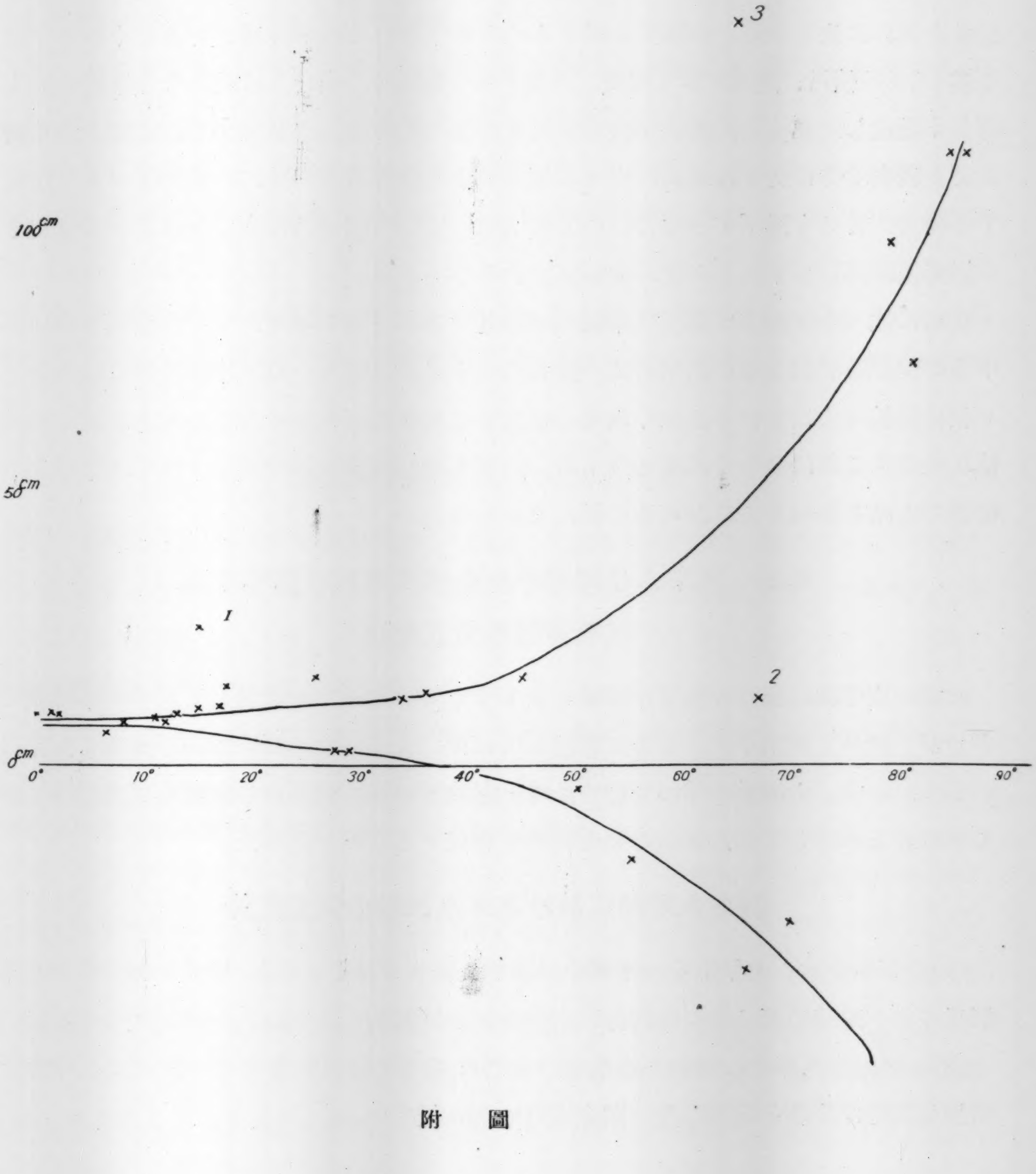

附　圖

附圖は横軸に傾角縱軸に垂直變動量をとり前表を圖示せるものである。圖上各點の位置を見るに一對の殆ど對稱曲線上に配列されて居るそして對稱軸の縱座標は約八「センチメートル」である。此處に示せる變動量は前に述べた如く原點の高さが新舊同一のものとして求めた。實際は原點は舊測量時に比して約九「センチメートル」低下した事が油壺驗潮記錄等より明かになつた。

圖上各點の變動量に此原點の低下による改正を施す時は曲線の對稱軸は横軸に殆ど一致する從つて對稱軸の上下にある曲線は夫々隆起及び低下した地塊に於ける中等變動量と其れに生じた傾との關係を示すものと考へられる圖中曲線より著しく外れて居る點 1.（八積村、勝浦）2.（川崎、戸塚）3.（豐田村、湊町）は孰れも水準線の最も著しく隆起した部分の周邊及中央部に屬するものである。之を要するに此圖上の事實により關東地方に於ては地塊に生ぜる傾と其中等變動量との間には或關係があり隆起する場合に於ても低下する場合に於ても地塊に生じた傾が同程度ならば其中等變動量の絕對值は同程度であると言ふ事が云はれそうである。

此處に述べた變動量は總て水準線の變動量である。もし地塊に生じた傾斜方向と其中央の變動量を知る事が出來れば一層面白いと思ふ、而し一般水準線に於てはもとより相摸房總地方に於けるが如く地塊の狀態が或程度迄明らかになつた地方に於ても其值を決定する事は恐らく出來そうもない、然し現在程度の結果よりするも水準原點の變動の大略を推知する事は可能の樣に思はれる。

其三　東京より興津甲府を經て東京に閉塞する水準環線の垂直變動

標題の水準線は關東大地震の影響を最も多く蒙つた地方を通過して居る水準線路であるが、此れを明治十六、七年に設置して以來、大地震迄の間に改測を實施した記錄があつたので、大地震に伴つて起つた地形變動との間に何等かの關係を見出し得るかも知れぬと注意して見た所次の如き現象を發見することが出來た。

關東大震前に於ける本水準線の測量記錄

(1) 明治十六、七年東京水準網中の高輪九號より發し、興津、甲府を經て東京水準網幡谷交十四號に至る間に四粁毎に水準點を設置觀測した閉塞差一糎五粍である。

(2) 同二十八年右の線の各水準點の中間に均等に卽二粁置きに一點づゝ水準點を增加し同時に全線を改測した、閉塞差は一糎五粍である。

(3) 同三十六年甲府日野間約九十八粁の改測を行つた、其理由は判然しないが二十八年測定の結果、此附近が舊成果と著しく相違せるに注意したからであらう、改測の結果明治二十八年の値との閉塞差は三粍である。

變動量の求め方

(1) 水準點を横軸上に明治十六、七年の測定値に對する同二十八年の値の増減を縦軸に取り各點を連結すると *A* 線が得られた。梯尺は水準點間隔四粁を一糎とし變動量は實際量を表はしてゐる。(別圖第一第二)

(2) 又甲府日野間の明治三十六年改測値を明治二十八年の測定値に比較すると *B* 線を以つて示すやうになる。(梯尺前者に同じ)(別圖第二)

(3) 次に別圖第一、第二に於ける *C* 線は明治二十八年（甲府日野間は明治三十六年）の値と大震後の測定値を比較したもので變動量の梯尺は別圖第一は二分の一とし其內小田原附近變動大なりし地域は二十分の一とした又別圖第二に於ては實際量を與へ特に小淵村の地域のみは二分の一とした、何れも圖示一覽の便宜からそうしたに過ぎない。以上の *A. B. C* 三線に於て零線上「+」は土地の隆起を「−」は沈下を意味する。

變動量曲線に表はれたる現象

(1) 別圖第二に於て甲府日野間の *A* 線と *B* 線を比較するに明治二十八年測定に於て最も沈下甚しかつた笹子峠附近は明治三十六年迄に反對運動を起して隆起して笹子峠は恰も其頂點にあり他の部分に於ては沈下大なりし程隆起も亦大であつて曲線の傾斜變換點は共に一致してゐるのを見る。

(2) 此地域の *C* 線を見るに明治三十六年迄に隆起した一帶は大震に於て甚しく沈下し線中沈下の甚しかつた小淵村附近は *B* 線の頂點とは一致しないが *A* 線の傾斜の變つた頂上卽小淵村に於て一致して居るのを見る。

(3) 東海道方面に於ても右に似た關係が存在する、卽大震に於て隆起の特に著しかつた戸塚熱海の一帶を見るにこれは明治十六、七年から明治二十八年の間に於て隆起しないで却つて微小ながら沈下したことが分る又隆起の最大なりし吾妻村附近は沈下も亦最大で他の部分に於ても變動の大小は各點に於て略一致してゐる。

(4) 全線を通じ大震後に測定した結果に基く變動量曲線が土地の地塊的傾斜運動を示してゐることは報文其一で示した。そして今大震に直接關係のない以前の測定に

より得た *A* と *B* 線のみに就て土地の變動狀態を見ると矢張同樣なる傾斜運動をしたものと認められ其傾斜變換點を求めると別圖第三に水準線上 × ⊗ 印を以て示す諸點（調布、小淵村、富濱村、初狩村、笹子峠、甲運村、鰍澤、豐岡村、宍原、但沼、

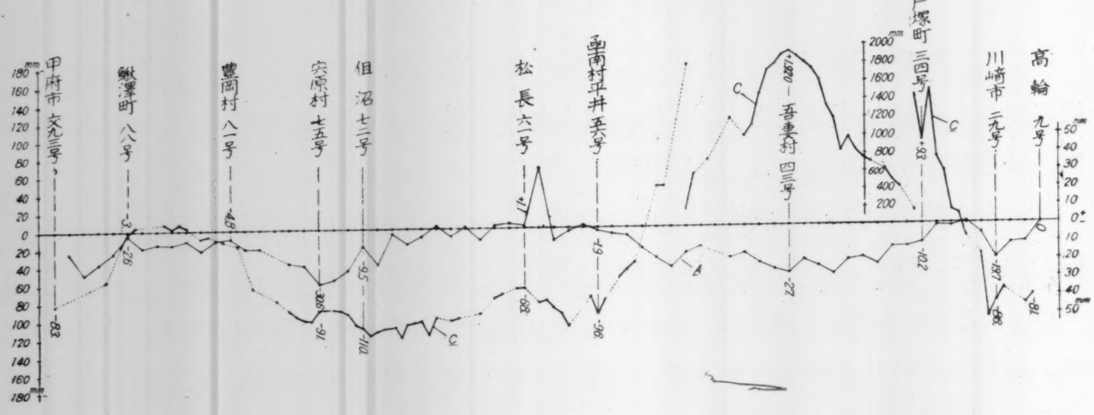

別　圖　第　一

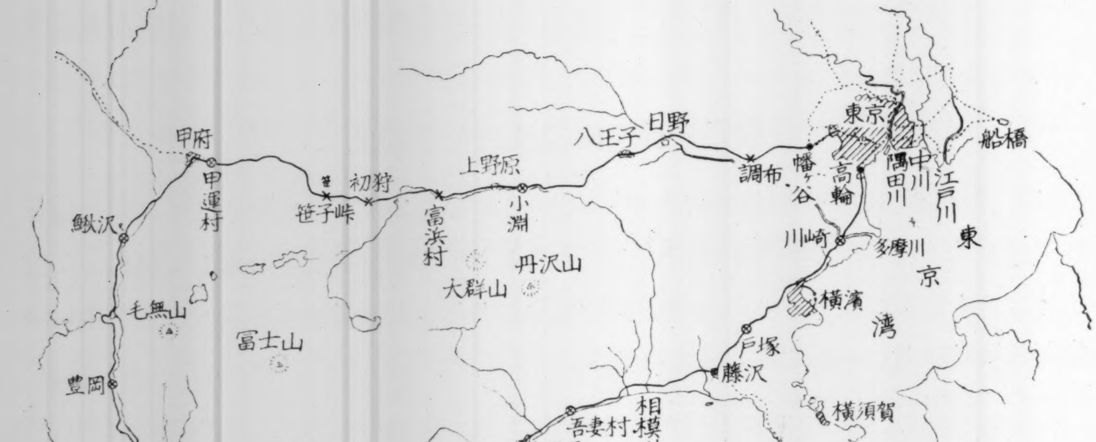
甲府
甲運村
鰍沢
笹子峠
初狩
上野原
小淵
富浜村
八王子
日野
調布
幡ヶ谷
高輪
東京
隅田川
中川
江戸川
船橋
川崎
多摩川
横濱
東京湾
戸塚
藤沢
横須賀
相模川
相模湾
吾妻村
小田原
丹沢山
大群山
冨士山
毛無山
豊岡
愛鷹山
宍原
但沼
興津
静岡
冨士川
沼津
松長
狩野川
平井
熱海
万城山
相模灘

別　圖　第　三

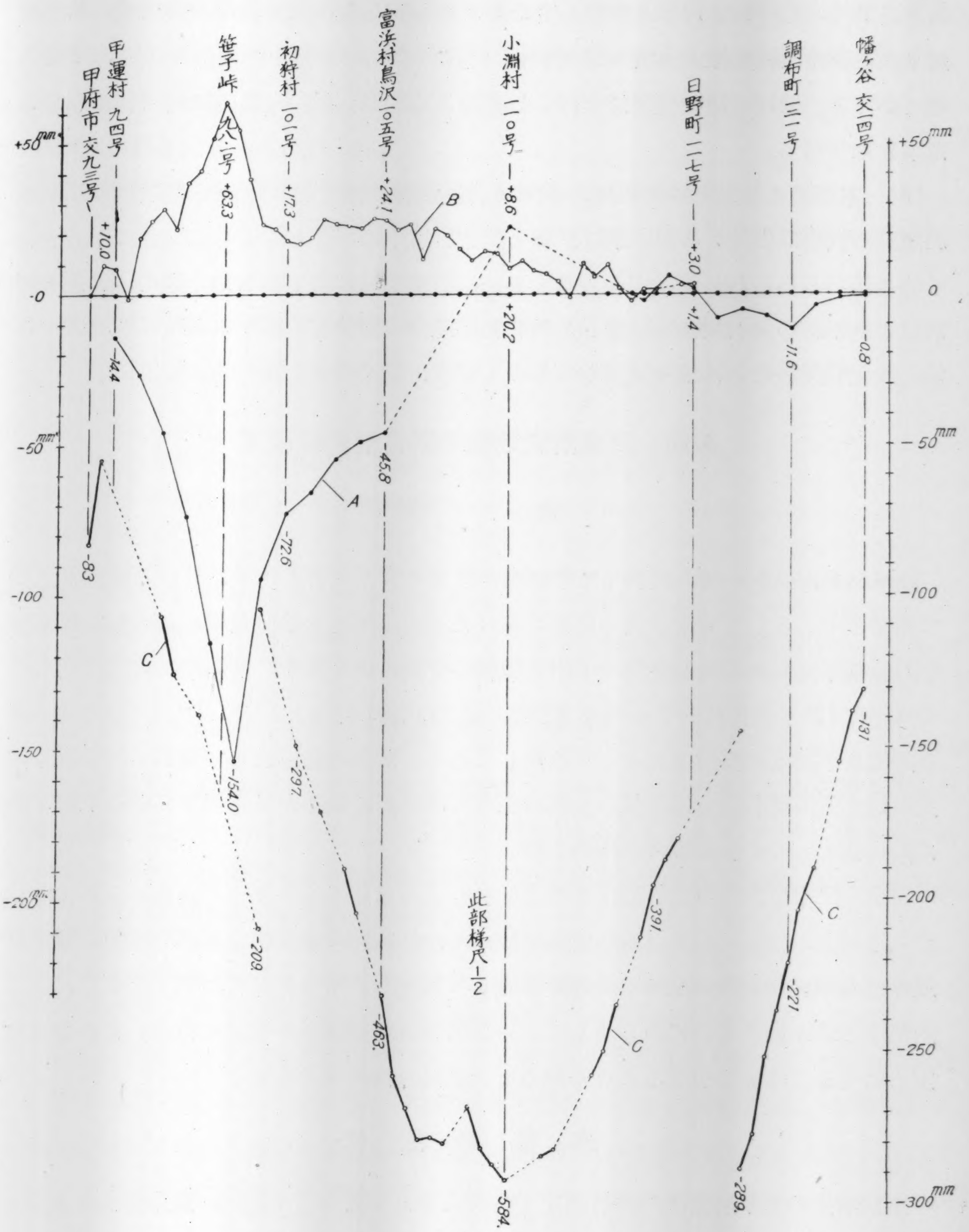
甲府市 交九三号
甲運村 九四号
笹子峠 九八・一号
初狩村 一〇一号
富浜村鳥沢 一〇五号
小淵村 一一〇号
日野町 一一七号
調布町 一二一号
幡ヶ谷 交一四号
+10.0
+63.3
+17.3
+24.1
+8.6
+3.0
+20.2
+1.4
-14.4
-11.6
-0.8
-83
-72.6
-45.8
-154.0
-297
-209.
-463.
-584.
-391
-221
-289.
-131
A
B
C
此部梯尺 1/2
+50 mm
-0
-50 mm
-100
-150
-200 mm
0
-250
-300 mm

別圖第二

松長、平井、吾妻村、戸塚、川崎）であるが此等の點の內大震後の測定結果に基く變動量曲線の傾斜變換點と一致するものは⊗印であつて全體中の大部分を占めてゐることが分る、卽地塊傾斜運動は大震前相當なる時期から同一地塊上に於て行はれてゐた事を知り得る。

(5) 東海道に於ても甲州街道に於ても大震前後の測量結果に於て見る所の反對傾斜運動の發起部と見える線は東は戸塚と調布、府中の中間を過ぎる樣で西は平井及笹子峠の線であるこれを延長すると報文其一の附圖第五に於て見る如く東の線は熊谷に於ける水準線の傾斜變換點に達し又西の線は追分の變換點に達する此等は報文其一に示した大變動線と共に地塊運動なるもの丶規模に就て暗示を與へるのである。

其四　東京附近地盤の垂直變動に就て

緒言

陸地測量部は其の構內に在る水準原點の設置に當り此れが將來に於ける變動を慮つて原點を中心として東京及其の周圍に殊に密集せる精密水準測量網を編成し、爾來一年乃至數年毎に其の改測を行つて附近地盤の變動に就き調査し其結果に就ては明治三十六年に『濃尾震災に對する同地方地盤の垂直變動の附錄』として、又大正四年に『東京周圍水準網改測の結果』として發表してゐる、而其の結論として述ぶる所は東京附近の如き新地層若しくは柔軟の土地に在りては地震の結果たると否とに關せず經年的に漸次低下しつ丶ある事實を指摘した。

大正十二年關東大地震の結果同地方を含む廣汎なる地域に亙つて實施せられたる精密水準測量の結果に就き原點の變動を知らんが爲め特に東京附近局部の地盤の運動に就きて大地震前後改測記錄の全部を綜合して精査した所是に其の地盤運動は單に經年的沈下と云ふ如きものにあらずして、系統的地塊傾斜運動が明瞭に行はれ是れが大地震と密接なる關係を有することを知ることが出來た次第である。

測定の歷史

東京附近の水準測量は內務省測定（明治六年より同十二年迄）の靈岸島水位を零として明治十六年隅田川以西の地域に二十六個の水準點を設置したのが最初である、此の際の測定は二人の測量掛を同一水準線を往復測量せしめて其の中數を採用した。

明治二十五年此の水準線を隅田川以東の地域に千住から松戸、市川を經て兩國に閉

塞する様に擴張し、(水準點の間隔は約二粁) 次いで明治二十九年頃原點の値を靈岸島水位から導いて決定し此の水準網と連絡し、爾後此の原點を測定の基と爲して來た，

大正七年には新に隅田川、靈岸島より船橋に至る水準線を増設し且船橋、松戸迄の既設水準網を完成するに至つた。

此の水準線建設後今日に至る迄に改測した回數は次の十回である。

1. 自明治二十五年 二 月　至同　年四月
2. 〃同 二十七年 一 月　〃同　年四月
3. 〃同 二十八年十二月　〃同 二十九年 三 月
4. 〃同 三十二年 一 月　〃同　年四月
5. 〃同 三十五年 三 月　〃同　年四月
6. 〃同 四十二年十二月　〃同 四十三年 三 月
7. 〃大正 三 年四月　〃同　年七月
8. 〃同 七 年九月　〃同　年十二月
9. 〃同 十二 年十月　〃同 十三 年二月
10. 〃同 十四 年十一月　〃同 十五 年四月

測定使用器械

此れに使用した器械及標尺は大正七年迄は「カール、バンベルヒ」會社製で大正十四年以降は「カール、ツアイス」會社製平面鏡付水準儀と「インバール」帶付精密標尺であつて震災直後は大正十二年から同十三年に至る間は兩者を混用した、此等水準儀の測定の精度は殆ど差がないと認められる。

變動量

東京水準網に含まれた水準點の明治二十五年に於ける測定値を基として順次前後兩測量間の差を求めたるに別表第一の如き結果を得た、表中「逐次變動量」の欄に於て測定年次の下にある數字は其前の測定値に比して其の年測定値の異動を示すもので「+」は隆起「−」は沈下を意味する。

變動量に關する考察

一、 狹小な地域に存在する多數の水準點を繰返し測量した結果は土地の變動傾向

を知る條件として充分であると思はれるから此れを便宜上概して東西の次の四個の區間に分ち各測定年次毎に其前回との變動量を圖示すると別圖第一（イ、ロ、ハ、ニ）の如くになる。

イ、中野——板橋——千住——松戸——市川
ロ、中野——四谷——神田——兩國橋——市川
ハ、靈岸島——船橋
二、幡谷——世田谷——大崎——芝——靈岸島——馬喰町

圖は横方向に水準點を、縱方向に前回の測定値を零線とした次回の測定値差を示してゐる。

二、變動曲線に表れた傾向

圖に於て變動量の最も甚しい地域は隅田川以東中川に至る間で三三七七號（龜戸）の如きは明治二十五年から現在迄に七十糎（原點の沈下量を加ふれば七十八糎强）の沈降を來し變動量の小なる區域は隅田川以西の地域であり概して隆起と沈下を交錯して行つてゐる。

變動量曲線によるに更に次の如き事實を知り得る（別圖第一）

1. 某部分に含まれた水準點若干は同一傾斜線内に含まれること。
2. 傾斜の變換點は各測定次略共通である。
3. 變動する傾斜の方向は年次に依り傾向の異なる場合がある。

三、變動線

此等變動の折點を平面圖上に移し毎測定毎に同一傾斜變動の傾向を有する地域を分つ如く變換點を連ぬる線を引き之れを大震の前後に纒めて見た大震以前のものを示すと別圖第二の如くで

1. 板橋——四谷見附——品川沖
2. 三河島村——兩國驛東——深川
3. 草加——奥戸——松江
4. 大崎——兩國橋東——松戸町

等の線が得られ右の内最も著明に表はれたのは第四の線である、圖には其線の位置及其現はれた測定年次を記入した、關東大地震に依る變動は前記四線と一致して表れた外に此の附近は三等三角高程測量をも併せ實施したので三角點高程變動量をも併せ考察し更に別圖第三に示す如く

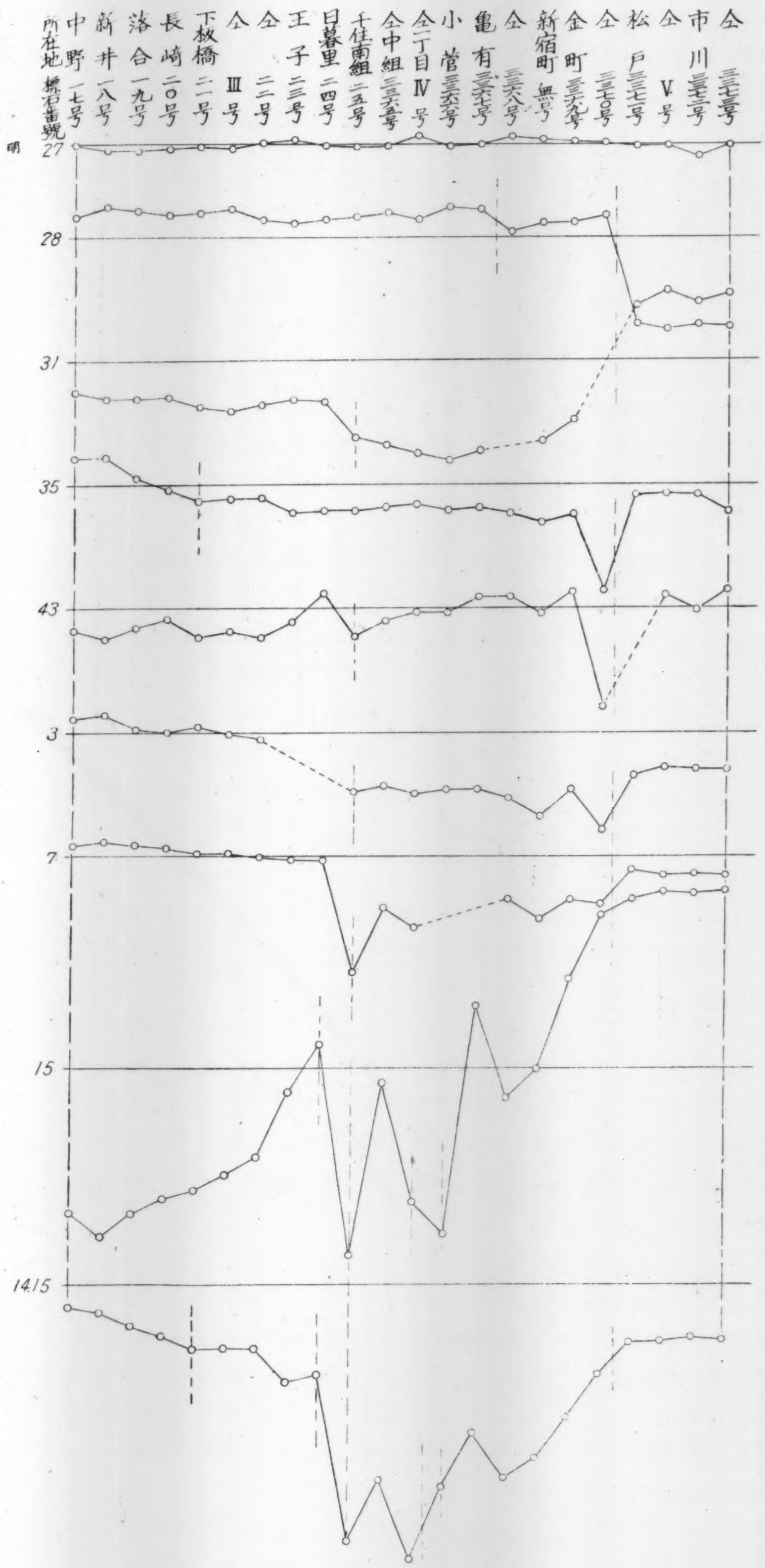

別圖第一ノ(イ)

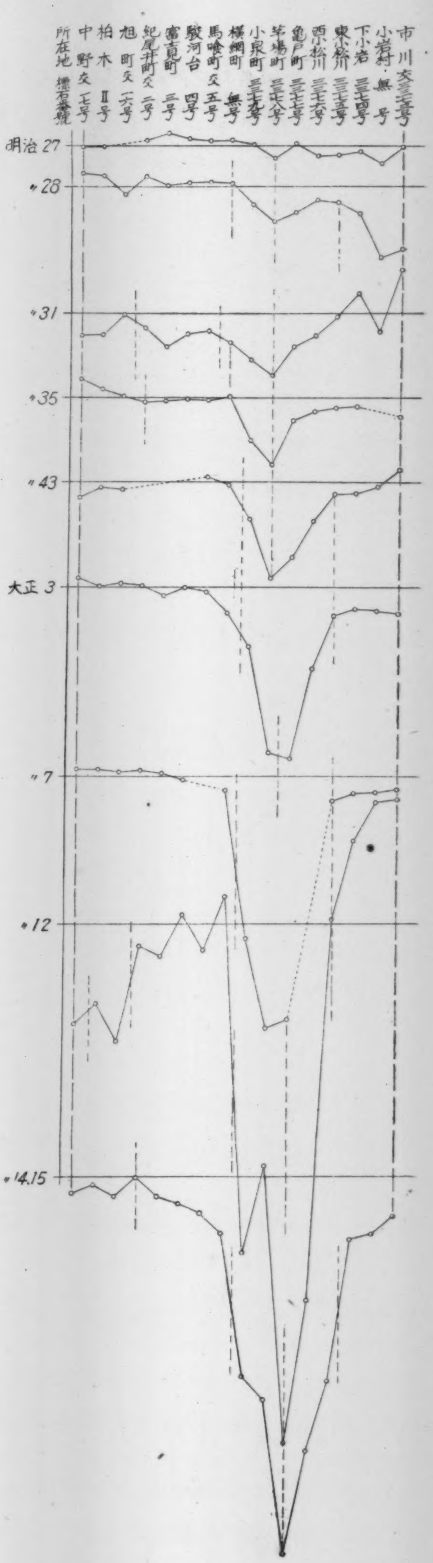

別圖第一ノ(ロ)

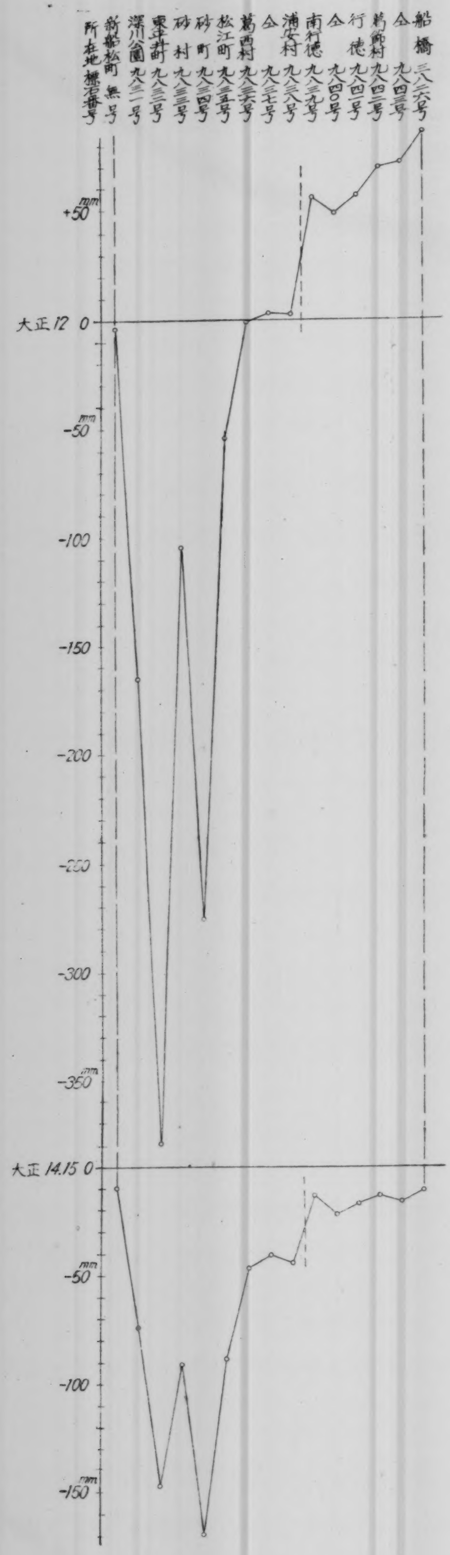

別圖第一ノ（ハ）

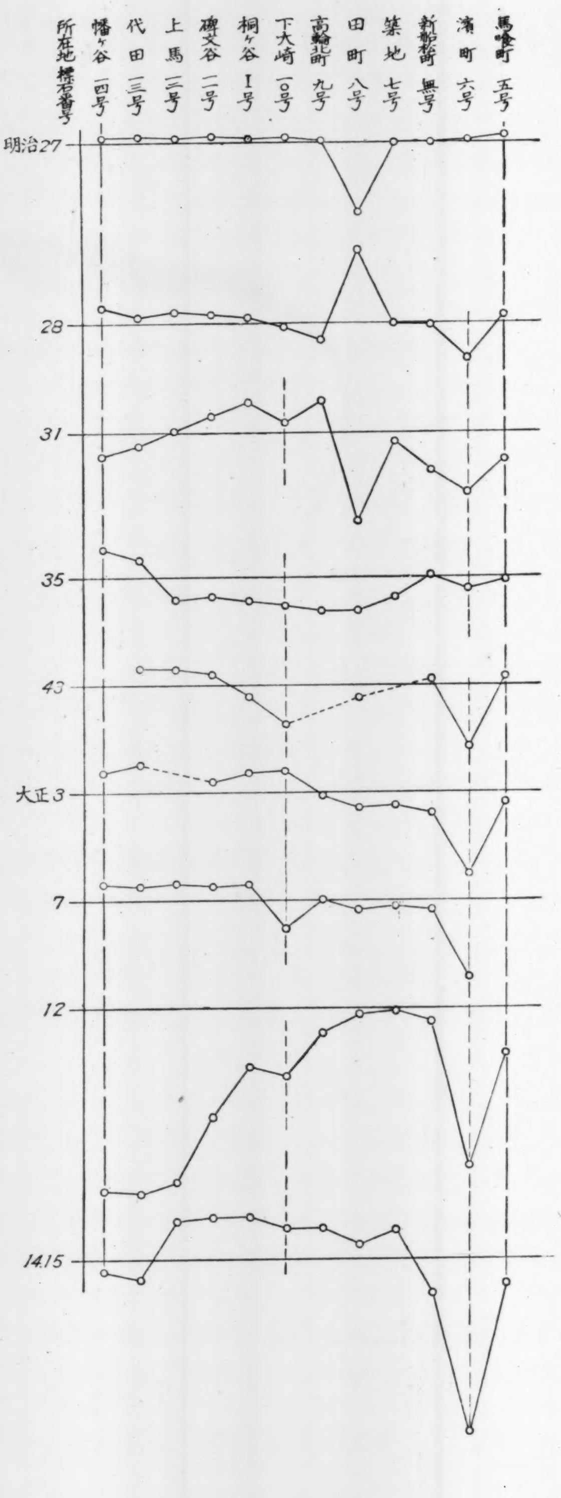

別圖第一ノ（ニ）

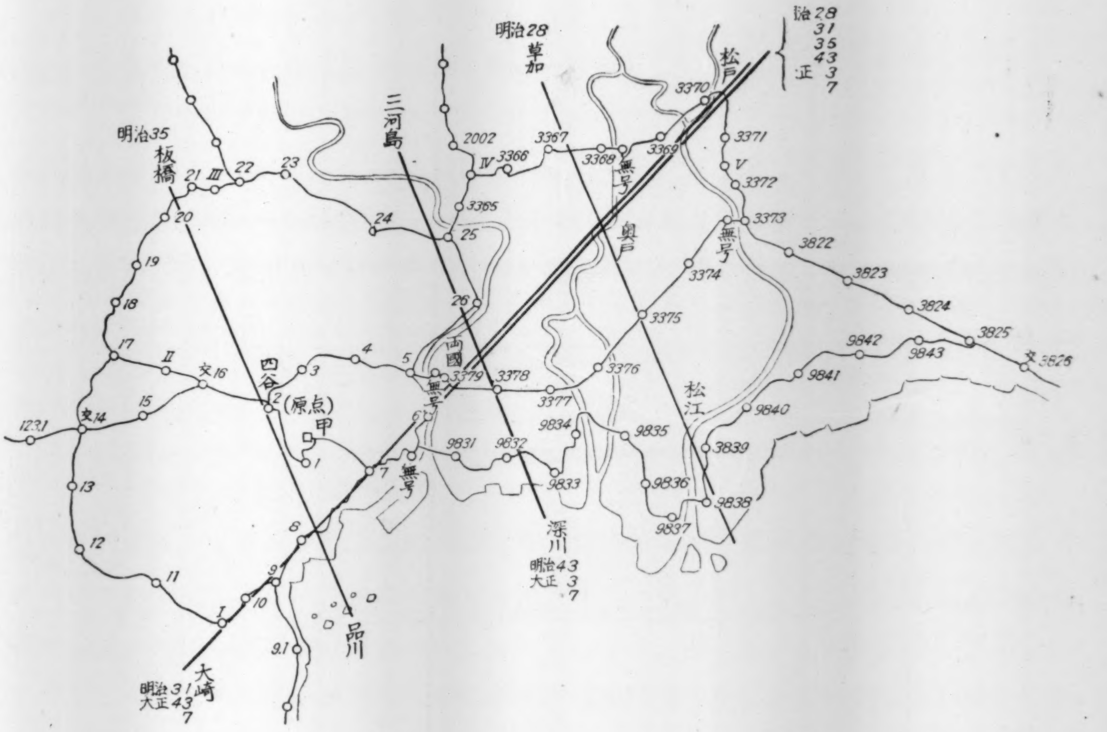
明治35
板橋
三河島
明治28
草加
松戸
明治28 31 35 43 大正3 7
四谷
(原点)
甲
両國
無号
奥戸
松江
深川
明治43 大正3 7
品川
大崎
明治31 大正43 7
文16
文14
文3826
3370
3371
3372
3373
3822
3823
3824
3825
3367
3368
3369
3366
3365
2002
3374
3375
3376
3377
3378
3379
9831
9832
9833
9834
9835
9836
9837
9838
9839
9840
9841
9842
9843
123.1
9.1

別 圖 第 二

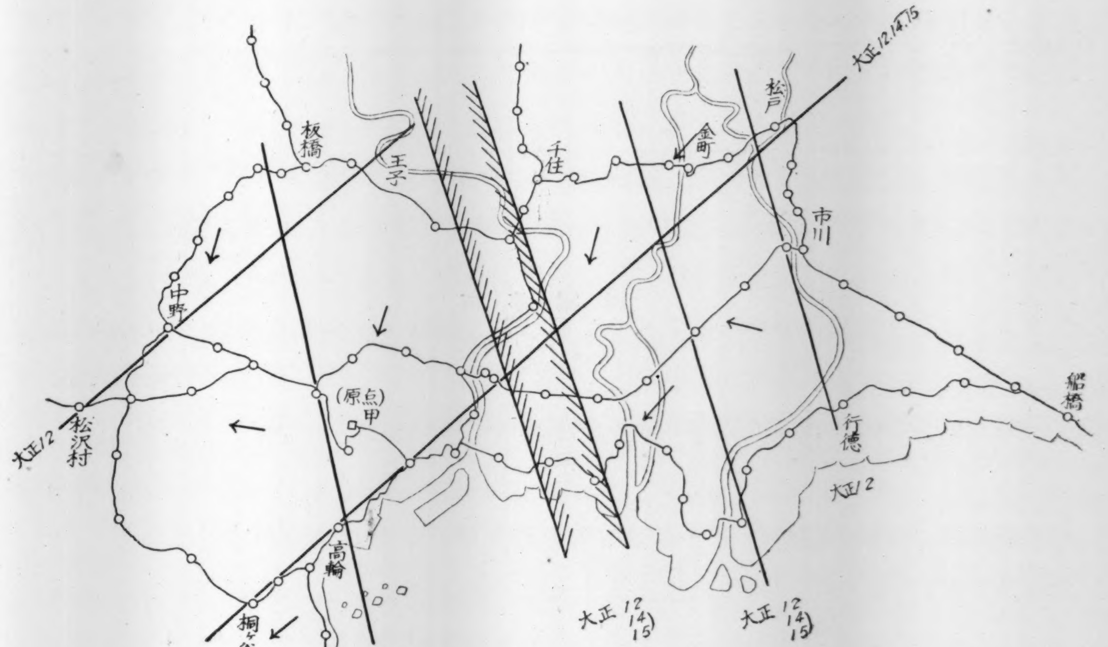
大正12.14.15
板橋
王子
千住
金町
松戸
市川
中野
(原点)
甲
松沢村
大正12
行徳
船橋
大正12
高輪
桐ヶ谷
大正12
大正12 14 15
大正12 14 15

別 圖 第 三

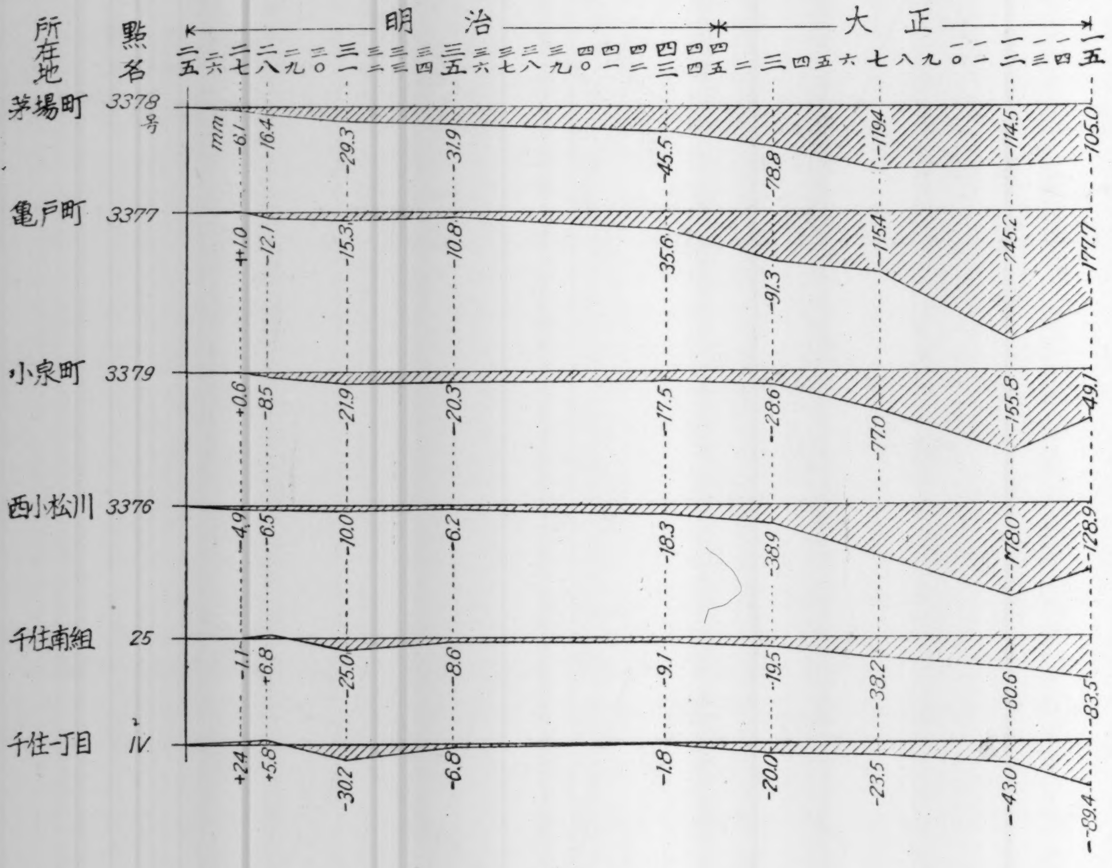
所在地
點名
明治
大正
二五 二六 二七 二八 二九 三〇 三一 三二 三三 三四 三五 三六 三七 三八 三九 四〇 四一 四二 四三 四四 四五 二 三 四 五 六 七 八 九 一〇 一一 一二 一三 一四 一五
茅場町 3378号
mm
-6.1 -16.4 -29.3 -31.9 -45.5 -78.8 -119.4 -114.5 -105.0
亀戸町 3377
+1.0 -12.1 -15.3 -10.8 -35.6 -91.3 -115.4 -245.2 -177.7
小泉町 3379
+0.6 -8.5 -21.9 -20.3 -17.5 -28.6 -77.0 -155.8 -49.1
西小松川 3376
-4.9 -6.5 -10.0 -6.2 -18.3 -38.9 -178.0 -128.9
千住南組 25
-1.1 +6.8 -25.0 -8.6 -9.1 -19.5 -38.2 -60.6 -83.5
千住一丁目 IV
+2.4 +5.8 -30.2 -6.8 -1.8 -20.0 -23.5 -43.0 -89.4

別圖第四

5. 王子——中野——松澤村——菅生
6. 松戸——兩國橋——桐ケ谷——住吉
7. 金町ノ東——行德

の諸線を得た、一般に大震に依る線は其以前のものに比し著しく表れて居るが此等の線の中で三河島村——兩國橋東——深川線（線と云ふよりも帶と云ふ方が適當の樣に思はれるから圖には暈影で示した）は特に明瞭に現はれてゐる、又大震後の變動線に圍まれた地域上に示した矢は其の傾斜の方向を示し大さを示しては居ない。

結論

一、變動量の最も大なる水準點三三七八、三三七七、三三七六、三三七九、二五、四、各號に就いて年次を横方向に各測定年次に於ける値と前回測定値との差を縱方向に取つて各測定年次間に於ける變動量を推定すると明治四十三年以降關東大震迄に其變動が逐次何れも旺盛の度を加へてゐたことが分る、卽大震の震源は遠き相模南方にあつたと云ふも其の準備運動の一部は東京附近に於ても十二、三年前より行はれてゐたと見ることが出來る。

二、大震前に於て地震變動の特徵とも云ふべきは大崎——兩國南——松戸線が著明に表れてゐたことで、彼の明治二十七年東京地震に於て此の線の活動を見るけれども、三河島村——深川線の判然と表れてなかつたことは著目すべき點で地盤の變動が土地の硬軟地質の新舊にのみ支配されないことを立證するものである。

三、大正十二年の大震に於ては東京水準網は全體として西南に向つて傾き然も變動量の最も大きく表れた三河島村——兩國——深川線を界として其の量に大差がある、又大正十四、十五年の測定に依れば隅田川以西が稍復舊運動の傾向ありしに反し同川以東の各地は其沈下を更に繼續してゐるよりして別々の地塊運動をなしてゐることを明らかにしてゐる。

此の三河島——兩國——深川の地帶の陷沒は土地の軟弱なるに基因する疑が掛けられるが

イ、復興局建築部發表の東京地質調査報告に依ると此の地帶の地質は沖積層下約三十米にして第三紀層に達し標石の沈下量五十乃至七八十粍を其の重量（花崗石及此れを取圍むコンクリート塊）に依る軟土中の沈降と見るのは困難であること。

ロ、同樣な地質の地盤上に在る他の水準點にして沈下量の小なるものがある。特

に兩國橋の東側にある無號水準點の如きは其の變動全く隅田川以西の地域のものと同樣で同一期間に三糎の沈下ありしに過ぎない卽此の標石より以東に變動線のあることが知れる。

ハ、 此線は安政二年、明治二十七年東京地震の震央帶として認められてゐる。

其他此の附近を古くより測量せる者の記憶によると土地表面と標石との關係が特に標石のみ沈下せる樣子なしとの事で上述の地帶に一斷層が存在して大震に前後して大なる活動を爲したものと認めるものである。

28. An Investigation into the Results of the New and Old Measurements of the Levelling Net in the Kwanto District.

By

Katuhiko MUTO and Keiryo ATUMI,

The Land Survey Department of the Army.

After the great earthquake of 1923, the Land Survey Department executed remeasurement of the Kwanto levelling net.

By comparing this new result to the old one, the authors investigated the tilting of the land blocks in way of the leveling routes.

The principal results obtained may be summarized as follows:—

1. When the land upheaved or depressed, the crustal surface splits into a mosaic of blocks; it appears that the surface crust is not perfectly elastic.
2. The distance between each tectonic line is generally equal.
3. The block which suffered a large vertical displacement generally made a large tilting.
4. In Tokyo-Okitu-Kohu levelling circuit, the same blocks were active through both periods before and after the earthquake, but the sense of tilting before the earthquake was opposite to that after it.
5. On the approach of the earthquake, the tilting movement of certain blocks in Tokyo was accelerated considerably.

別表第一

所在	標石番號	逐次變動量									大正十四五年測定値
		明 27	28	31	35	43	大 3	7	12	14.15	
測量部內	甲	—	—	—	+0.2	—	+0.2	—	—	—	23.1320
葵町	1	+0.6	-3.7	+2.9		-14.1	-0.2	-5.1	-15.2	-4.5	9.7066
紀尾井町	交 2	+2.6	+5.1	-6.6	-2.0	—	+0.5	+2.9	-10.9	-0.4	30.9964
富士見町	3	+5.8	+0.8	-15.5	-1.3	—	-4.2	+1.3	-15.3	-9.0	17.9496
駿河臺	4	+3.4	+2.0	-9.6	-0.6	—	-0.2	-1.7	+4.1	-12.3	16.5739
馬喰町	交 5	+2.2	+2.2	-7.9	-1.0	+2.4	-2.6	—	-12.5	-16.8	4.2551
濱町	6	+0.9	-9.7	-16.9	-3.1	-17.2	-22.6	-21.4	-44.0	-48.0	1.8366
新船松町	交 無號	—	-0.7	-10.9	+0.5	+1.4	-5.8	-2.4	-3.5	-9.6	2.5352
築地	交 7	+0.2	+0.1	-2.6	-5.6	—	-3.4	-1.5	-0.9	-1.8	2.1238
田町	8	-19.2	+20.5	-24.7	-9.2	-3.7	-4.0	-2.6	-1.4	+4.1	5.0600
高輪北町	9	+0.6	-4.5	+8.6	-9.6	—	-0.5	+0.2	-6.6	+8.9	6.1839
下大崎	10	+1.6	-1.0	+2.7	-7.6	-11.1	+5.8	-7.3	-19.4	+8.8	7.4158
桐ケ谷	I	+1.1	+1.6	+8.1	-6.5	-3.1	+5.4	+4.4	-16.3	+11.9	23.7684
碑文谷	11	+1.7	+2.4	+4.7	-5.1	+2.9	+3.0	+3.9	-30.4	+11.6	29.9169
上馬	12	+1.1	+3.2	+1.3	-6.2	+4.5	—	+4.4	-48.6	+10.9	40.2465
代田	13	+1.9	+2.0	-3.6	+4.7	+4.9	+7.8	+3.8	-51.7	+5.7	33.6144
幡ケ谷	交 14	+1.5	+4.4	-6.5	+7.5	—	+5.5	+4.7	-51.1	+3.2	40.5532
〃	15	+1.0	+4.6	-8.9	+3.9	—	-3.6	+0.5	-45.1	-0.6	38.8281
旭町	交 16	—	-3.7	-0.6	+0.4	-3.3	+1.8	+2.1	-55.3	-9.0	34.6938
中野	交 17	-0.7	+6.6	-10.1	+8.5	-7.1	+4.5	+3.7	-47.0	-7.5	37.8961
柏木	II	+0.6	+5.3	-9.9	+3.9	-2.4	+0.3	+3.3	-37.8	-3.8	36.1843
新井	18	-3.1	+9.5	-12.2	+8.7	-9.9	+5.5	+4.7	-54.4	-9.1	37.4455
落合	19	-3.4	+8.4	-12.2	+1.9	-6.4	+0.9	+3.7	-47.1	-13.5	35.9951
長崎	20	-1.7	+7.2	-11.9	-1.9	-3.9	—	+2.6	-42.3	-17.0	35.7071
下板橋	21	-1.1	+7.8	-14.9	-5.4	-9.3	+1.9	+0.6	-39.6	-21.2	32.2326
〃	III	-1.5	+9.0	-16.6	-4.9	-7.6	-0.9	+0.7	-34.3	-20.9	31.1768
〃	交 22	+0.1	+5.4	-14.4	-4.5	-9.3	-2.4	-0.4	-28.9	-21.0	29.2759
王子	23	+1.4	+4.2	-12.7	-9.2	-4.5	—	-1.5	-7.3	-31.7	16.3469
日暮里	24	-0.6	+5.8	-13.2	-8.7	+4.7	—	-1.9	+7.8	-29.4	9.6418
千住南組	交 25	-1.1	+6.8	-25.0	-8.6	-9.1	-19.5	-38.2	-60.6	-83.5	2.2529
聖天町	26	+0.2	+3.5	-14.6	-4.7	-6.4	-18.5	-19.6	-22.6	-57.3	3.4189
千住中組	3365	-0.7	-7.9	-27.7	-7.3	-4.7	-17.6	-17.1	-4.3	-63.7	2.6612
千住一丁目	交 IV	+2.4	+5.8	-30.2	-6.8	-1.8	-20.0	-23.5	-43.0	-89.4	2.3911
小菅	3366	-0.6	+9.3	-32.2	-8.4	-1.6	-18.5	—	-53.3	-65.9	1.8155
龜有	3367	-0.1	+8.8	-29.4	-7.7	+3.3	-18.5	—	+20.7	-48.3	2.3790
〃	3368	+2.2	+1.7	—	-9.3	+3.4	-21.2	-14.4	-9.1	-63.3	2.0507
新宿町	無號	+1.2	+4.3	-26.2	-12.2	-1.9	-27.6	-20.4	-0.5	-56.6	3.4915
金町	3369	+0.7	+4.9	-19.2	-9.9	+5.1	-18.5	-14.6	+29.5	-43.4	2.2906
〃	3370	+0.2	+7.0	—	-34.9	-32.1	-31.8	-16.0	+50.2	-29.1	7.0439
〃	無號		-2.6								
松戶	3371	-0.9	-28.4	+17.8	-3.7		-14.1	-4.6	+55.8	-18.9	26.2287
〃	V	-0.9	-30.1	+22.1	-3.2	+4.0	-11.8	-6.4	+58.1	-18.1	16.0823
市川	交 3372	-4.4	-28.4	+18.6	-3.8	-0.9	-12.1	-5.9	+57.3	-17.1	23.1173
〃	交 3373	-0.7	-29.4	+21.1	-8.8	+5.8	-12.4	-6.3	+58.9	-18.3	3.9971
小岩村	無號	-8.4	-33.1	-8.6	—	-2.2	-11.6	-7.9	+57.6	-26.9	3.5482
下小岩	3374	-2.7	-12.6	+9.6	-4.2	-5.1	-10.4	-8.0	+39.3	-29.2	2.0722
東小松川	3375	-4.4	-7.6	-1.7	-4.5	-5.4	-13.5	-11.8	+2.1	-96.5	1.2877
西小松川	3376	-4.9	-6.5	-10.0	-6.2	-18.3	-38.9	—	-178.0	-128.9	0.6871
龜戶町	3377	+1.0	-12.1	-15.3	-10.0	-35.6	-91.3	-115.4	-245.2	-177.7	1.6711
茅場町	3378	-6.1	-16.4	-29.3	-31.9	-45.5	-78.8	-119.4	-114.5	-105.0	0.9432
小泉町	3379	+0.6	-8.5	-21.9	-20.3	-17.5	-28.6	-77.0	-155.8	-94.1	1.1776
横網町	無號	+2.5	+1.8	-13.6	+0.4	-1.6	-12.6	-6.6	+13.4	-26.3	1.8241
深川公園	9831								-165.5	-74.3	1.3283
東平井町	9832								-379.5	-147.6	0.8350
砂村	9833								-104.6	-91.3	0.9303
砂町	9834								-275.9	-170.0	0.1339
松江町	9835								-54.1	-88.9	2.5138
葛西村	9836								+0.9	-47.1	1.7273
〃	9837								+3.1	-41.0	1.8742
浦安村	9838								+1.8	-44.5	2.1282
南行德	9839								+55.5	-13.6	2.2497
〃	9840								+48.5	-22.3	2.3992
行德	9841								+56.3	-17.4	2.6674
葛飾村	9842								+69.6	-13.6	1.5654
〃	9843								+72.0	-13.3	1.8937
船橋	交 3826							-30.8	+86.3	-11.0	4.2916

29. 地形から地殼の移動從て地殼に働く歪力を判斷することの可能度に就いて

地震研究所 藤原咲平
高山威雄

（昭和四年七月九日發表—昭和四年九月十八日受理）

1. 緒　言　波の立つて居る水面や渦卷の起つて居る水面を寫眞に撮つて見るに固より瞬間寫眞で有つて面の運動其者が寫されて居ない場合でも、是れは波是は渦卷と判斷し得る場合が多い、例へば水面に浮ぶ泡の模様とか水面の高低の情況とかに於て、波には波形、渦卷には渦卷形が現はれ是に依りて其れが波であるか渦卷で有るかが知れる。更に進んで波がどちらからどちらに進むか等迄も、時に依つては知り得る。

併しながら水面に高低を起こさない程度の渦卷では、例令水面にアルミニュームの粉を置いたにしても露出時間が短かい場合は其寫眞が只雜然たる點群を示す丈で渦卷に見へない事もある。

或は又水面に在る渦卷の模様に似せて粘土を用いて高低の模様を作り之を寫眞に撮れば、是は明に動いて居ないものなるに關はらず、形は水の渦卷と區別の出來ない様なものとなる。

依りて所謂渦卷形が與へられたとしても、夫れが渦卷を表はすと直に斷定は出來ない。又同時に見掛上渦卷模様が無いからと云ふ理由で渦卷が存在しないと斷定する事も不可能である。尤も既に渦卷形が有る以上何か此形を起し易い素因が存した事は考へ得る、粘土に渦卷形を作るにしても、種々方法は有るが一の廻轉を與へる事が一番容易であるから、他の原因に比して此容易な方法が確率の一番多いものである事は考へ得る。

故に地表に渦卷型地形を發見しても直ちに是を以て渦卷の存在を主張する事は出來ないが、確率的に見て何等か之に寄與すべき手段が過去に有つたか又は現に起りつゝあるかを想像する手がゝりとはなる。

水の渦卷に於て數枚の連續寫眞を作り、是等相互の形の差を比較して其運動を定める事が出來る、尤も此數枚の寫眞から定めた運動は極めて斷片的で有つて迚も渦卷の

廻轉などを見得ない、角度にすれば僅かに一度の何分の一位にしか當らない場合も有る。只是丈では矢張り全體の運動は定められない。併し前の場合の瞬間撮影による形が渦巻らしい多大の確率を示し尙其上に短時間の運動では有るが總て瞬間撮影の暗示する運動と Conformal で有るならば吾々は其各自には不完全なる二材料から、可成確信的に渦巻の存在を斷定し得る。

今迄自分等の取り來つた方針は正に上述の如きもので、吾々が一生かゝつて見る所でも地形の變化の速さから見れば全く瞬間的で有る、卽地質學及地形學は共に單に瞬間撮影を行うて居るに過ぎない。此瞬間撮影の効果は固より偉大では有るが、是を活かし更に有力とするには數枚の活動寫眞式撮影法によりて、其極微運動を實證し、依つて其運動の實在方向等を確定しなければいけない。

此方法に依りて既に著者等は大正十二年九月一日の關東大地震に關する地形等と其變化に就て陸地測量部の實測の結果とを對照して相模灣をめぐる地渦の存在と、是に隨伴する諸現象とを說明した。1) 本篇に於ては更に丹後地震其他を材料として研究を進める事にする。

2. 裂罅 先に著者等はまた昭和二年三月七日北丹後地震に際して起つた雁行的斷層線に沿ふ地表模樣より見て、此如き模樣を生じ得る力の中確率の多かるべきものを指摘した。卽郷村斷層は其北西側から南東又は南に東に向ふ水平壓力が加はり斷層面に沿ふて壓縮性剪斷裂罅が生じたものであらう、又山田斷層に沿ふては其れに直角な向きの壓縮內力が働き衝上斷層の露頭に於て表層の撓曲性裂罅を示したものであろうと云ふ事を推定した。2) 是等は前述ぶる所の所謂瞬間現象に屬するもので、從て余等の主張も只一種の蓋然性を有すると云ふ以上には斷定し得ないもので有つた。

然るに陸地測量部の數回に渡る實測の結果に依れば、3) 山田斷層の南方石川村に於ては北西への移動があり山田斷層の北側に在る磯砂山及下岡卽郷村斷層線の西に於ては南南東への移動があり、結局上下山田村附近の斷層を起したる力は壓縮性內力であつた事が明になり、余等の推論した結果を裏書きした。又郷村斷層の東吉澤に於ての移動は北より東へ方位を取りて 317°11′ に於て 1米10で卽北西に向ひ、斷層の西の下岡に於ては 154°48′ に向ひ 1米25の移動が有つた。是に依れば兩者の方向の相違は

---

1) 藤原、高山「關東大地震の機巧」氣象集誌昭和四年第二號；本所彙報 **6** (1929), 149.

2) 藤原高山 驗震時報第三卷第一號 125.

3) 陸地測量部丹後地方震災地復舊二等三角測量記事（昭和四年五月）附圖

180° に近く是に及ばざる事 17°37′ である。故に此兩地點より計算した辷性歪は斷層線に沿ふて約六粁に對する。

$$1{\cdot}25+1{\cdot}10\cos 17^\circ 37'=2{\cdot}30\ \mathrm{m}$$

即毎粁 0·36 米となる。尤も斷層線の直上での辷りは遙に是より大なるもので有るべきで又事實も其通りで有つた。[4]

又壓縮性歪は

$$1{\cdot}10\sin 17^\circ 37'=0{\cdot}34\ \mathrm{m}$$

即六粁に對する 0·34 米、毎粁 0·05 米となつた。

以上に見るに單に地表に生じたる裂罅の形より推定した歪の性質及方向が大體實際の歪の性質を示して大差なき事が判つた。是に依ると過去に起つた斷層で、其時の歪力の測定のないもので其雁行性が分れば其歪力も解る事となる。

尙此場合云ひ得る事は、パテ又は粘土等の如き模型に依る實驗も定性的には地形に現はれる殆んど比較にならぬ程度の大規模の現象に可成り良き類似を示し得ると云ふ事である。

3. 海岸地形　自分等は先きに北太平洋運動の一の事實として日本東北地方東海岸にある渦卷の鎖と同日本海沿岸にある島根半島以北能登半島迄の渦卷狀連鎖とを指示した。東海岸のものはもし收歛性とすれば時計的即正の廻轉方向となり、岬は金華山、小名濱等に於けるが如く南に出て西に灣入する傾向を持つ。日本海岸のものも渦卷としての向きは同じで、岬が北東に突出し東に灣入を持つ。併し是等の形式も緒言に於て述べた如く瞬間撮影に過ぎないので、運動なり歪力なりに對しては只蓋然的に云ひ得るに過ぎない。渦が收歛性ならば前記の廻轉方向であるがもし事實は發散性であるとすれば廻轉方向は逆即反時計的となる。是等の疑問は尙未解決のものであつたが、偶相模灘大地震に關連しての測量の結果から見ると相模灣は沈下收歛性の正渦を示し、其周圍には其逆流による負渦が伴ふて居る。是で見ると恐らく小名濱灣松島外灣に於ける渦卷も亦正の收歛性渦卷なるが如く想像し得るが、果して然りとすれば先に提唱した北太平洋の一般運動と全く階調的である。併し此相模灘の渦卷が小名濱金華山に連る鎖の一員であるや否やに就ては尙不明の點がある爲に、絕對的の斷定は出來ない。

北丹後地震に關した陸地測量部の測量結果を寺田博士及宮部氏が解析を施したもの

---

4) 國富 驗震時報第三卷第一號：渡邊、佐藤 地質調査所報告第百號：今村 本所彙報 **4** (1928).

に見るに若狹灣に沿ふて正負の廻轉區域が交互して居る。而して大體は發散區域であるから地形に現はるゝ所は廻轉を海から岬端上陸して陸に向ふ樣に取ればよい。依りて時計的廻轉に在りては岬の根から岬端に追跡すれば其れが反時計的廻轉を示せばよい。北に突出した岬は西から南へと曲がるべきである。又反時計的廻轉に在りては見かけは時計的となり北に出た岬は東へ次に南へと曲がればよい。是を實地の地形に就て調べて見るに先づ若狹灣西岸を見るに栗田灣附近に著しい渦卷形を見る。寺田博士宮部學士の解析に依れば此附近は測量の結果は反時計的廻轉であるから北に出た栗田半島は見かけ上は時計的に東へ次に南へと廻轉すべきであつて事實正に斯の如くである。又東岸を見るに久須夜ケ岳は見かけ上の反時計的卽實際の時計的廻轉を示して居るが丁度三角點の位置である爲に其廻轉を決定し得ない依つて其西の大島其北の西浦半島を見るに地形上前者は見かけ上の時計的、後者は反時計的で卽實際は反時計的及時計的の廻轉を示す。而して寺田博士等に從へば此地形よりの推定と全然合一した實測を與へて居る。

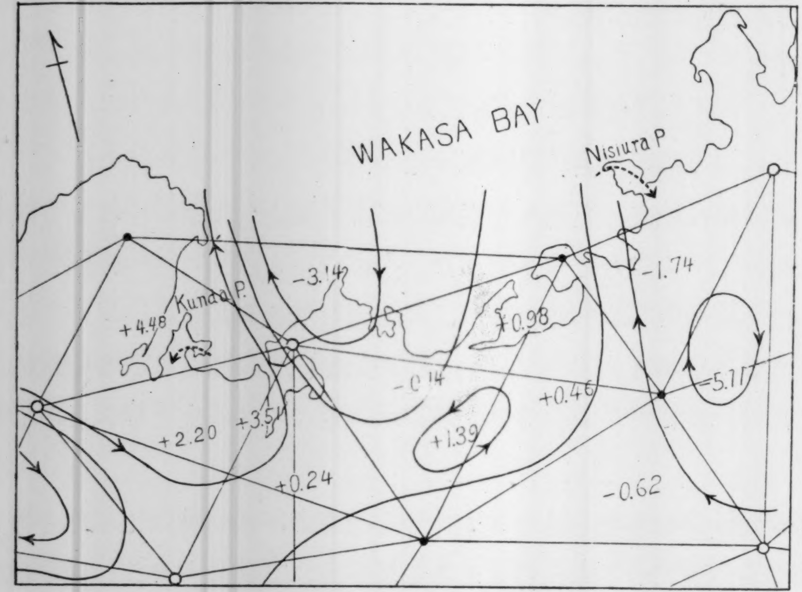

第一圖　若狹灣附近地渦の圖

Fig. 1. Earth Vortices by the Wakasa Bay.

其他此附近には小規模の廻轉形地形が多いが其れ等は更に細分されたる測量の結果と比較さるべきもので、其曉には恐らく上述の推論と階調的結果を與へるであらう。

4. 他の實例 上述の樣に吾々の提唱した方法が幸にも多少は役立つ樣子であるから思ひ切つて之を他に應用して見る。先づ氣の付くのは駿河灣の沿岸である。其西岸

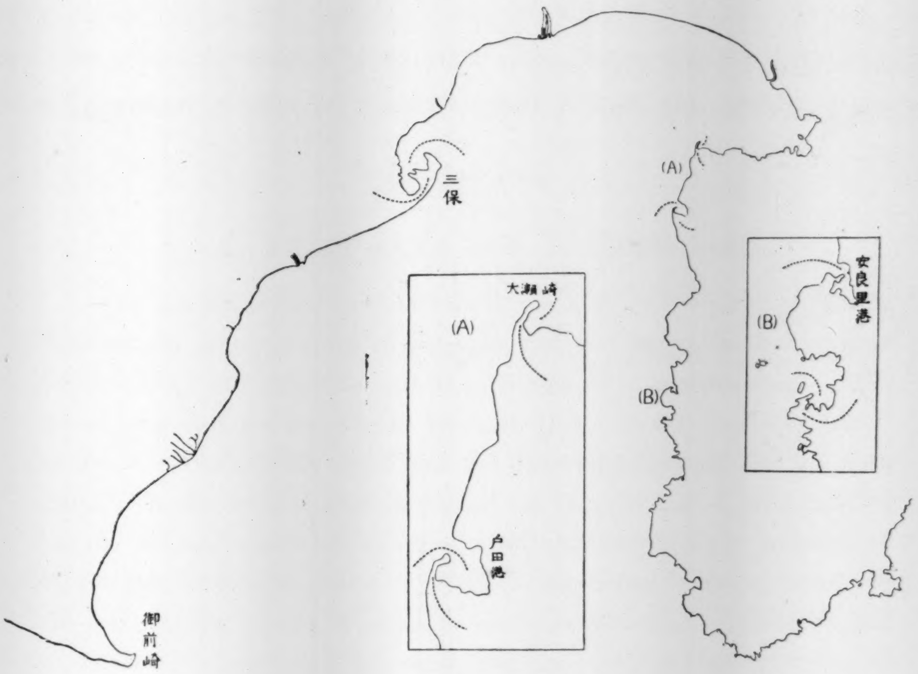

第二圖 駿河灣附近地渦の圖

Fig. 2. Earth Vortices by the Suruga Bay.

に於ては御前崎及三保半島等があり共に先端は北に向ふ。即もし收斂性なれば負、發散性なれば正の廻轉である。又其東海岸を見るに大瀬崎、戸田灣、兩岸の岬角及安良里灣西岸の岬角等に於て總て北に曲り甚しきは更に東に曲る傾向を示す。即もし收斂性となれば正の廻轉である。かく西岸に相對した渦卷の鎖を生ずるものを只一現象として取扱はんとするにはどうしても駿河灣底の地殼の移動を考へなければいけない。假りに外洋から陸を目がけて押し込んで居るものとすれば收斂で有つて其東側には正西側には負の渦卷を作るべきである。又もし灣底が外洋に吸ひ出されて居るものと考へれば、發散性であり、東側は負、西側は正の渦卷をなすべきである。而して此兩方共が實際の岬の形と一致して居る故に、此處では其何れであるかを定める事は出來ない。只此場合はもし發散性ならば沈降を伴ひ、收斂ならば、少なく共海岸に於ては隆起を起すべき樣に考へられる。而して此邊が多くは隆起海岸の特長を示す事から見れば駿河灣底に於ては外洋から押し込む地殼の流れが有ると云ふ結論となる。

第二の例としては土佐の西部の半島である其兩側には共に渦卷の列を伴ひ、而かも對岸九州に於ても又土佐灣の東岸に於ても渦卷形は共に著しくない。依りて考ふるに此場合は陸地が海に相對的に南又は北に移動した爲に起つたものと考へるを便とす

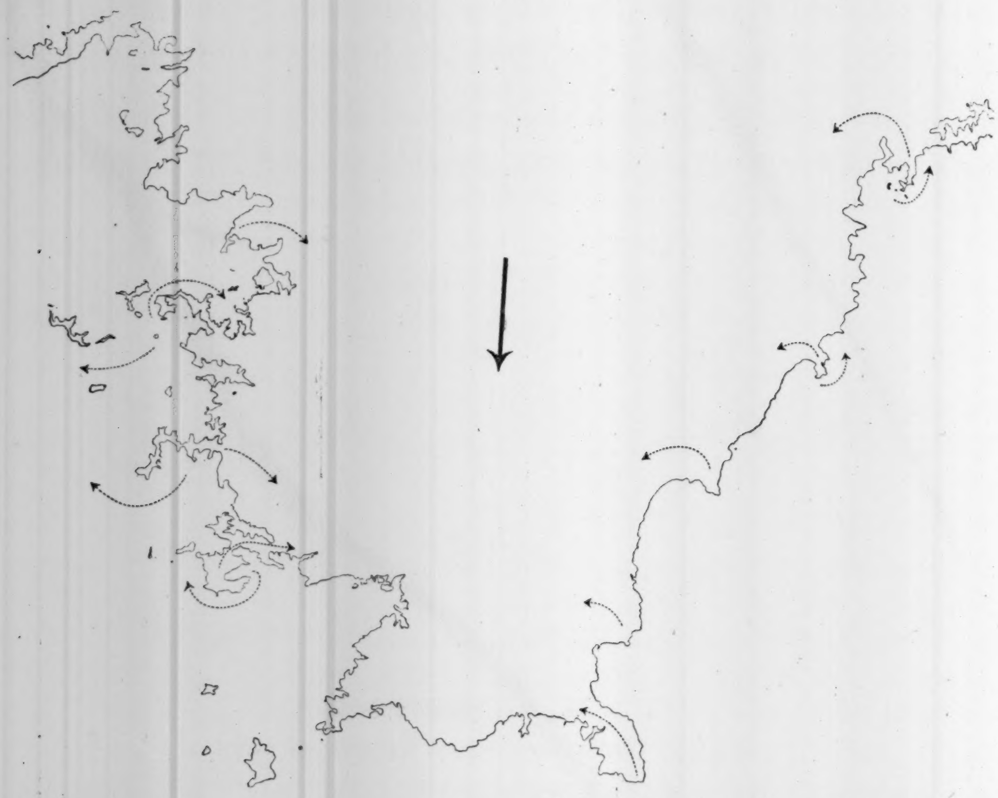

第三圖　土佐南西部地渦の圖
Fig. 3. Earth Vortices in the south western part of Sikoku.

る。偖其向きは半島の東側の渦巻きは收斂とすれば正、發散とすれば負で有る。又其西岸に於けるものは之と反する。此海岸の地形から見れば此海岸は沈水海岸で有る。故に發散と想定すれば東側が負西側が正でなければならない，此爲には陸は海に對して南に移動して居るもので有る。最近江原氏の研究[5]によれば此邊一帶に陸地は北北西より南南東に移動する傾向の下に在りと云ふ、然らば．今海岸地形よりの推論は亦地質學的推論の結果と一致した事となる。

6. 結　論　要するに渦卷的地形及雁行的裂罅は共に地殼に加はる歪力の中立性又は廻轉性の歪力の存在を指示するに效果あり又パテ粘土等に依る模型實驗の結果も亦相當實際に近似せる結果を示す事を知り得る。

---

[5] 江原（印刷未了）

29. *On the Possibility of finding Stresses acting on and Displacements of the Earthcrust from its surface form.*

(ABSTRACT)

By **S. FUJIWHARA** and **T. TAKAYAMA.**

The authors formerly established the law governing the relation between the sense of rotation or shear and that of produced vortex or echelon crack in connection with the divergence or convergence.[6] They already applied the law to the analysis of the Great Japanese Earthquake on Sept. 1, 1923, and found the close agreement of the law with facts.[7] In the present note they point out that the law is quite fulfilled by the echelon cracks of Gō-mura fault produced on the occasion of Tango-Earthquake on March 7, 1927.[8] In virtue of the present law the sence of the echelon suggests to us the existence of compressive and anticlockwise shear along the fault, and the recent actual surveying of the district by the Land Survey Department of Japan[9] proved that this is just the case.

Moreover they draw attention to the vortical form of peninsula along the coast of Wakasa Bay. Since the Bay, as a whole, belongs to diverging area, the sense of rotation, according to the present law, must be that which can be traced from the end of the cape to the neck of peninsula. (Fig. 1.) Hence Kunda Peninsula must be a vortex of counterclock rotation, and Nisiura Peninsula that of clockwise rotation. After the analysis by Prof. T. Terada and Mr. N. Miyabe[10] of the results of the actual surveying of the district by the Land Survey Department,[11] it was proved that the actual senses of rotation are just as inferred above.

From these it seems like that the mere form of land and sea can, to some extent, indicate the stress acting on or the displacement of the crust. So the authors point out more examples of the vortical form of coast lines and in one of them is obtained a good concordance of the sense of stress inferred from their point of view with that from geological point of view by Dr. Ehara[12] on the south western part of Sikoku.

Literatures.

6) S. FUJIWHARA, "On the Echelon Structure of Japanese Volcanic

Ranges and its Significance from the Vortical Point of View,'' *Gerlands Beitr. z. Geophys.*, **16** (1927), also see Fujiwhara Tortional Form on the Face of the Earth: Nagaoka Anniversary Vol. (1925), 337.
7) S. Fujiwhara, T. Takayama, ''On the Mechanism of the Great Sagami Bay Earthquake on Sept. 1, 1923,'' *Bull. Earthq. Res. Inst.*, **6** (1929), 149.
8) N. Yamasaki, F. Tada, ''The Oku-Tango Earthquake of 1927,'' *Bull. Earthq. Res. Inst.*, **4** (1928), 159.
9) Land Survey Dept, ''Map showing the Horizontal Displacements of the Primary Secondary Triangulation Points. observed after the Earthquake of March 7, 1927, in Tango Districts'' *Bull. Earthq. Res. Inst.*, **7** (1929), Pl. VI.
10) T. Terada, N. Miyabe, ''Deformation of the Earth Crust in Kwansai Districts and its Relation to the Orographic Feature,'' *Bull. Earthq. Res. Inst.*, **7** (1929), 223.
11) Land Survey Dept., ''Map showing the Horizontal Displacement of the Primary Trigonometrical Points in Tango Districts,'' *Bull. Earthq. Res. Inst.*, **7** (1929), Pl. VII.
12) Lectured but not yet printed.

30.　川の流路の變遷によつて知り得たる伊賀國島ヶ原地塊の運動

地震研究所　多田文男

（昭和三年十一月二十日發表—昭和四年九月二十日受理）

緒言

一地塊が垂直運動を受けた時は、その運動以前より此地塊を貫流して居た川はこの變動に整調して、その流路の垂直的の變遷を起す事が常である。從つて川の流路の垂直的の變遷を研ぶれば、その川の流域地方の受けた垂直運動の性質並にその量を決定し得るのである。

かゝる目的の爲に地形學者と地質學者とによつて、古くより用ゐられて來た方法は、河畔に發達して居る河成段丘の分布を研べて、それによつて、その川の舊流路を知る方法であつて最も確實な方法である。されど本邦の如き垂直運動の激しくて、狹く且深き流路を有して居る多くの川に於ては、河成段丘の廣く保存せらるゝ事が稀にて、從がつて段丘のみによつてその川の舊流路を求むる事が困難な場合が多い。玆に於て筆者は川の縱斷面に見らるゝ遷急點の諸性質を利用して、此川の流路の變遷を知る方法を考へた。

本文のIに於てはその方法に就いて記し、IIに於てはその一つの試みとして木津川が笠置山地塊の一部島ヶ原地塊を貫流する地域に於て、如何なる流路の變遷を行つたかを研べ、併せて之によつて島ヶ原地塊の運動の一性質を推定して見た。

I

1. 遷急點の形成

グレードに達せる川の縱斷面曲線の形は多くの要素に司配さるゝ爲、簡單なる數式を以つて書き表はすを得ないが、實地に於て、多くの川に就いて研究せられた所によれば、拋物線とも云はれ、双曲線とも云はれ、又指數曲線であるとも云はれて居る。その何れにするも、これは傾斜に遷急點を有せざる凹曲線をなして居るのである。

グレードの狀態にある川の河床の一點を界として、次に擧ぐる如き地殼の垂直運動

第一表

	下流	遷急點	上流
1	緩		緩
	+ 大	+ 小	0
	+	0	−
	+ 大	+ 中	+ 小
	+ 大	+ 小	−
	+	− 小	− 大
	0	− 小	− 大
	− 小	− 中	− 大
2	急		急
	+ 小	+ 中	+ 大
	0	+ 小	+ 大
	−	+ 小	+ 大
	−	0	+
	− 大	− 小	+
	− 大	− 小	0
	− 大	− 中	− 小
5	不動		緩
	+ 等	+ 等	+ 小
	+ 等	+ 等	0
	+ 等	+ 等	−
	0	0	−
	− 等	− 等	− 大
6	海底	河口	上流
		+ 等	+ 等
		+ 大	+ 小
		+ 小	+ 大

	下流	遷急點	上流
3	急		緩
	+ 中	+ 大	+ 小
	+ 等	+ 大	+ 等
	+ 小	+ 大	+ 中
	+ 小	+ 大	0
	+ 小	+ 大	−
	0	+ 大	+ 小
	0	+	0
	0	+	−
	−	+ 大	+ 小
	−	+	0
	− 小	+	− 大
	− 等	+	− 等
	− 大	+	− 小
	− 小	0	− 大
	− 等	0	− 等
	− 大	0	− 小
	− 中	− 小	− 大
	− 大	− 小	− 中
	− 等	− 小	− 等
4	急		不動
	+ 小	+ 等	+ 等
	0	+ 等	+ 等
	−	+ 等	+ 等
	−	0	0
	− 大	− 等	− 等

+ 上昇　　− 沈降　　0 不動
大、中、小、等　　上昇或は沈降の比較的の量

が行はれて、その點に於て上流の縦斷面曲線と下流の縦斷面曲線とがカスプを造る時にはその點に傾斜の遷急點が形造られる。

1. 此點より上流の傾斜が舊よりも緩となり、下流の其も亦舊より緩となり、而も

上流の緩になり方が下流の緩になり方よりも大にして、その結果として下流の傾斜が上流の其よりも急傾斜となりし場合。

2. 此點より上流の傾斜も下流の傾斜も、舊より急となり、而もその結果として下流の傾斜が上流の傾斜より急となりし場合。

3. 此點より上流の傾斜が舊より緩となり、下流の傾斜が舊より急となりし場合。

4. 此點より上流の傾斜は舊流路の傾斜の其と同じであるが下流の傾斜が急となりし場合。

5. 此點より下流の傾斜は舊と同じであるが上流の傾斜が舊より緩となりし場合。

かくの如き遷急點の形造らるゝ垂直運動の種類は第一表に揭げた如くである。此表に於ては +、0、− を以つて夫々隆起せるか、不動なりしか、沈降せるかをあらはし、大、中、小、を以つて夫々上流、遷急點、下流に於ける比較的の垂直運動量を表はし、更に緩、不動、急を以つて夫々、傾斜がこの運動の爲に緩になれるか、不動なりしか或は急になれるかを示して居る。

一般に遷急點の形造らるゝ部分は點に非ずして帶であるが、幅廣き帶をなす時は運動が撓曲の形となつて現はれる事が多く、幅狹き帶をなす時は運動が斷層の形となつて現はれるのが常である。

海底の傾斜は川の下流の傾斜よりも急な事が一般であるから、河口地方に隆起の行はれた場合には舊下流と延長河との間に傾斜の遷急點を見るのが常である。而してその隆起の形態として第一表 6 に擧ぐる三種の場合を考うる事が出來る。

2. 遷急點の後退

第一項に述べた如き垂直運動があつて、川のグレードの狀態が破れたる時は、川はその變動に整調して再びグレードに達せんとし、或は侵蝕力の衰退を起して河床を堆積物によつて高め、或は侵蝕力の回春を起して河床を下刻する。此運動の結果として形造られた遷急點は、侵蝕の衰えたる時は下流に移り、侵蝕力の回春せる時は上流に後退するのである。

川の下刻力は主に水の衝突力と削磨力と運搬力と水によつて運ばれた砂礫の衝突力と削磨力との函數であつてその關係は簡單でないが、大略平均水深 R と平均流速と平衡時の流速との差 V の二乘との積に比例して居る。よつて垂直運動の結果として形造られた遷急點の移動は此點以下の RV^2 の變化によつて決定せられる。

遷急點以下の流速 V の變化に就いて云へば、之は此點より上流の傾斜の變化による

流速の變化量の此點以下の新傾斜面に對する分量 V' と、此點以下の傾斜が變化せる爲のみによつて起つた此點以下の流速の變化量 A' との和に關係して居る。

第一表 2. 3, 4, 6 に示したる如き垂直運動があつて遷急點が形造られ、この點より下流の傾斜が急となれる時は A' は正となり、その量は傾斜が急になる程大である。逆に第一表 1 に示したる如き垂直運動があつて、下流の傾斜が緩となれば、A' は負となり、その量は傾斜の緩になる程小となる。

次に第一表 2 或は 6 の 3 に示したる如き垂直運動があつて、遷急點より上流の傾斜が急となれば V' が正となり、その急になり方が著しければその量は大となる。逆に第一表 1, 3, 5 或は 6 の 2 に示したる如き垂直運動があつて、上流の傾斜が緩となれば、V' は負となり、その緩になり方が著しければその量は小となる。

A' と V' との和が正なる範圍に於ては、遷急點以下の流速は運動前の夫よりも大となり、侵蝕力が回春し、その爲に遷急點は上流に後退してゆくのであり、その速さは $A'+V'$ の大さ言換うれば流速の變化量に比例して居る。然るに A' と V' との和が負なる範圍に於ては侵蝕力が衰へて堆積作用が起り、その爲に遷急點は下流に移り、暫時にして砂礫に埋もれて消失するのである。

故に第一表 1, 5 に示したる如き垂直運動のありし時は、常に $A'+V'<0$ であつて、遷急點は常に下流に移るのであり、第一表 3 或は 6 の 2 に示したる如き垂直運動のありし時は遷急點は $A'+V'>0$ なる範圍に於て上流に後退し、$A'+V'<0$ なる範圍に於て下流に移るのである。第一表 2, 4 或は 6 の 1, 3 に示したる如き垂直運動の起りし時は常に $A'+V'>0$ であつて遷急點は上流に移るのである。

以上述べたる何れかの垂直運動によつて、遷急點が形造られ、それが上流に退いて行くものとして、その速さに就いて考察して見やう。前に下刻力は主として RV^2 に比例すると述べたが、河水はメアンダーをなして流路をかへ側侵蝕の爲にもその勢力を用ゐるを以つて下刻力は主として水量 M と V^2 との積に比例するとしてもよいのである。MV はその川の流量であつて、之は雨量の略々等しい地域に於てはその點迄の流域面積に比例するを以て上流に行くに從ひ減少する。次に V の變化 $V'+A'$ は、遷急點を形造つた運動による傾斜の變化が同一であり、水深は一般に上流程小なるを以つて、遷急點が上流に移るに從つて小となる。故に遷急點下の MV^2 の變化量は點が上流に行く程小となり、從つて遷急點の後退する速さが遲くなるのである。

一つの川に於て流量の大いなる川を本流とし、流量の小なる川を支流と定義すれば、

同樣の理由によつて、本流にある遷急點の退き方は、支流にある其よりも速かである。

又遷急點の後退する速さは、河床を造る岩石の性質にも關係して居るのであつて、河床が侵蝕され易い岩石によつて造られて居る時は、然らざる時よりも、速やかに後退するものである。

かくの如くして、遷急點は次第に上流に移り、遂に遷急點以上の傾斜と、以下の傾斜とが等しくなりし時に甫めて消失する。第一表 6 に示したる如き垂直運動によつて形造られた遷急點は、その下流の傾斜が一般に大に非るを以て、後退する事僅かにしてその上流の傾斜と同じとなり消失するのである。

3. 遷急點の二次的形成

グレードの狀態にある川に於て、傾斜を急にするが如き傾斜運動の行はれた時は、上昇側より下降側に流るゝ川にあつては侵蝕力が回春して河床の下刻が行はれる。その下刻の量は隆起の方向に流るゝ川に於て最も大きく、此方向より遠ざかるに從つて小となり、遂に此方向と直角に流るゝ川に於て 0 となる。從つて本流に沿うて急傾斜となる運動のありし時は、これに直角に交はる支流には垂直運動の二次的の結果として新に遷急點が形造られるのである。

又河床が侵蝕に對する抵抗の度を異にする岩石より成る場合にも、二次的の遷急點が形造られる。卽ち上流が下流よりも侵蝕され易き岩石より成るものとし、何等かの垂直運動があつて、侵蝕力の回春が起りたりとすれば、上流の岩石中に於ける下刻作用は下流の岩石中の其よりも速かであり、從つて上流は下流より速かに緩となり、兩岩石の境界に遷急點が形造られるのである。之に對して、川の上流が下流よりも侵蝕され難き岩石よりなる時は上流にては下刻が遲く、下流にては下刻が速かである爲第一圖に示すが如き遷急點が形造られる。

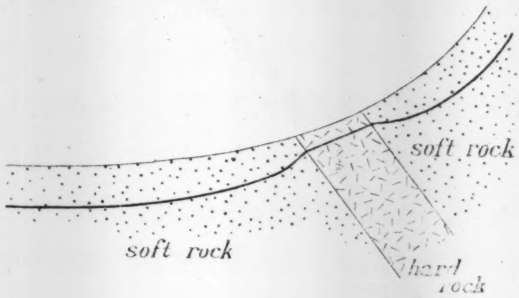

Fig. 1.

そして此等の遷急點は夫夫兩岩石の境界に沿うて移動し上流も下流もグレードに達するに及んで消滅する。一般に河床は硬軟の岩石の互層によつて造られて居るのであつて、グレードに近き縱斷面にもかゝる小遷急點が連なつて居るのが常である。

遷急點の形造られ方には以上述べたる如き垂直運動の直接、間接の結果として形造

られたものゝ外に海蝕作用、氷河作用、氣候の變化による侵蝕の回春作用、海水面の變化による侵蝕力の回春作用、川の蛇行による侵蝕作用、川の爭奪による侵蝕の回春作用火山作用等の結果として形造られたものもあるが、此等に就いては內、外の地形學者[1]によつて說かれて居るので、玆には省略した。

河成段丘の上に集まる水は段丘崖を下つて、その下の川に注ぐのであり、段丘面と段丘崖との境界は支流の傾斜の遷急點に他ならないのであり、段丘面は遷急點より上流の回春の未だ及ばざる河床と同意義を有する。

4. 垂直運動の性質竝びに量

一地塊の受けた垂直運動の性質竝に量を知る爲には先づ此地域をその運動の軸に沿うて貫流する川をとり、その川の縱斷面曲線を畫いて、その中に見らるゝ遷急點を求める。そしてその遷急點より上流の縱斷面曲線を下流に延長して、その延長せる部分が上流の曲線と連なつて拋物線狀の一凹曲線をなすやうにすれば、此曲線が此川の舊き流路を示すのである。此遷急點が第三項に於て述べたる如き垂直運動の二次的の結果として形造られたものに非る事を吟味し、第一表に示せる如き地殼運動の結果として形造られたものと確定する事を得た時は、此川の舊流路の形によつて、此地方に行はれた垂直運動の性質竝に量を知り得るのである。

されど上流の縱斷面曲線を長距離に渉つて誤なく延長する事は困難であり、又延長する途中に於て局部的の垂直運動の挾まれた懼れも多く、本流の縱斷面と遷急點とのみによつて舊流路を復舊する事は危險である。

玆に於て此川の支流の縱斷面曲線を畫き、その中にある遷急點を求め、この點より上流の縱斷面曲線を延長して、その延長部が上流部と連續して一凹曲線狀をなす樣にすれば、この延長部が此支流の舊流路である。更に本流と支流との合流點に於けるこの假定せる支流の舊流路の高さを求める、支流に於て認めらるゝ遷急點が此支流の中に於て形造られたるものに非ずして本流に於て第一表に示したる如き運動によつて形造られたものにて、それが後退して支流の此場所に來たりしものと確め得た時は、此

---

1) L. SIEGERT, "Zur Theorie der Talbildung" *Monatsber. d. D. geol. Ges. Berlin.* (1910), 1–30.

R. DIETRICH, "Entstehung und Umbildung von Flussterrassen" *Geol. Rundschau,* **2** (1911), 445–454.

R. SOKOL, "Die Flussterrassen." *Geol. Rundschau,* **12** (1921), 193–228.

辻村太郎「信州伊那の山間盆地と段丘竝に天龍峽の峽谷」地質學雜誌 **26** (1919), 214–220, 249–266, 346–359, 383–393, 433–446.

辻村太郎 「日本地形誌」(東京 1929), 123–131.

高さが支流の遷急點が本流とこの支流との合流點にありし當時の位置を示して居るのである。(第二圖參照)

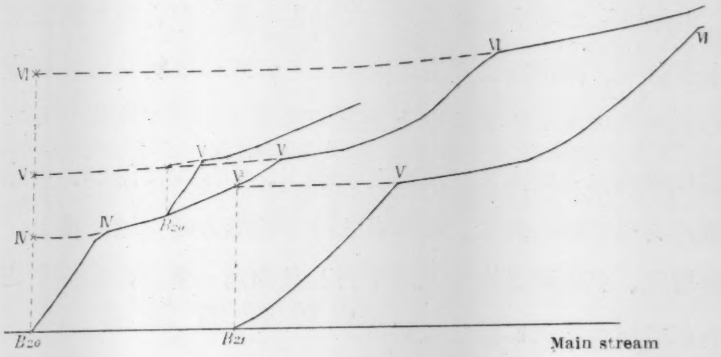

Fig. 2.

支流に存する遷急點の後退する速さが本流の其より遲き事は第二項に於て述べた如くである。故に本支流の合流點より、支流の遷急點に至る距離はその合流點より本流の遷急點に至る距離より短く、從つて支流の遷急點を利用して本流の舊流路の高さを知る事は本流の遷急點を利用せる場合よりも誤に陷る懼れが少いのである。

支流の流路の長き場合は更に此支流のその又支流の縱斷面をとつてその遷急點を求め、前述の如く支流とその又支流との合流點に於ける舊河床の高さを求め、更にかゝる點を連ねて支流の舊流路を求める。かくして曲線を長く延長する時に陷ゐる誤を防ぎ、又途中に行はれたる局部的の垂直運動の性質を知つて、その影響を取り去る事に努めて舊河道を復舊せしめるのである。

本流の河畔に發達して居る河成段丘の、段丘面と段丘崖との境界は、之を縱斷面曲線の傾斜の遷急點と見るのである。

かくの如くして、各支流の本流との合流點に於ける本流の舊河床の高さを知り、其各點を連ねて本流の舊流路を想定し得るのである　かくの如くして舊流路を知り更にこの舊流路と現流路との高さの差を知つて此地方の受けた垂直運動の性質竝にその量を決定し得るのである。

II

5. 島ケ原地塊の位置

島ケ原地塊は笠置山地塊の一部であつて、その東北部を占め、その南竝びに北を斷層によつて限られた地塊である。

辻村助教授[2]の所謂春日山斷層は大和國櫻井町の西方に起つて、奈良市、木津町を經て京都市附近に至る迄略ゝ南北に連なり、その斷層崖を西に向けて居る。此斷層崖

---

2) 辻村太郎「斷層谷の性質竝びに日本島一部の地形學的斷層構造」地理學評論 **2**(1926), 270.

の西側は陷落して大和盆地竝びに京都盆地となり、東側は隆起して高原性の山地となつて居る。

此斷層崖の中央部に當たつて鷲峯山斷層崖と島ケ原斷層崖と上野斷層崖との三斷層崖があり、西南西より東北東に走り、互に雁行して西微南より東微北に連なつて、この高原性山地を甲賀高原と笠置山地塊との二地塊に分つて居る。その南の地塊たる笠置山地塊はその南及び東南を初瀨川、宇陀川に沿ひ、東南側に凸面を向けた弧狀斷層群によつて限られて、その東北の宇陀地方の山地に接し、東北を花の木斷層崖、我山斷層崖、名張斷層崖等互に平行し且西南一東北の走向をとつた齟齬斷層崖によつて限られて伊賀盆地に接して居る。

笠置山地塊は斯の如く四方を斷層崖によつて圍まれ、縱邊、横邊共に 29 粁餘の長さを有した略ゝ四角形の地塊であつて、高度は南側の斷層崖に接した所で高く 800m を超え、北側の島ケ原斷層崖に接せる所にて低く 200 m 以下となつて居る。

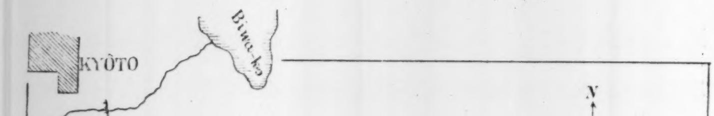
Biwa-ko
KYÔTO
N
KÔGA BLOCK
Kasuga-yama Fault
Kizu-gawa
Shubusen Fault
Shimagahara Fault
Ueno Fault
SHIMAGAHARA BLOCK
Ueno
Nabari-gawa
Hananoki Fault
Nara
KASAGI-YAMA BLOCK
Hase-gawa
Sakurai

Fig. 3. Map showing the major tectonic features of the Kasagi-yama block.

今茲にその運動の狀態を述べんとする島ケ原地塊は笠置山地塊の東北部を占むる一小地塊であつて、その西北を島ケ原斷層崖と上野斷層崖とによつて限られて甲賀高原の地塊に接し、その東南を花ノ木斷層崖によつて限られて南の地塊に接して居る。そして東側は上野陷落地帶に落ちて居るが、西はそのまゝ、地形的不連續なく、笠置山地塊に遷移して居る。此地塊は略ゝ長方形をなし、長軸の長さは 10 km 餘あり、短軸の長さは 5 km 餘である。そして平均の高さはその南部

花ノ木斷層崖に接する所に於て最も高く 360 m を超え、北部島ケ原斷層崖下にて低く 200 m に足らず、此地塊が一つ傾斜地塊の如く見える。

木津川は伊賀伊勢二國の國境なる布引山地にその源を發して、伊賀盆地を灌漑し、上野町の西北方に於て柘植川を合はせ、これより甲賀高原の地塊と島ケ原地塊との間の斷層角窪地を西流して今山に至り、此處に於て南方より來たる名張川の水を併せて更に西に流れて木津町の北方に達して居る。名張川は高見山山地の水を集めて北流して名張町に至り、これより島ケ原地塊を南より北に峽谷をなして横ぎり、今山に於て木津川と合する。

6. 斷層崖の性質

島ケ原地塊の運動の性質を論ずるに先んじて、この地塊の構造竝びに地質に就いて見る事とする。島ケ原斷層は笠置山の西方和束村附近に起つて *S* 80° *W* より *N* 80° *E* に走り、笠置、大河原を經て、島ケ原、新居に至り、之より走向を次第に北に向けて比曾河内に至る迄連なり、東南側に凸面を向けた弧狀斷層であつて、その崖面を南或は南東に向けて居る。その延長は 25 km に及び、その落差は地層の變位より見て 300 m を超ゆるものの如くである。

上野斷層は島ケ原、新居に於て、島ケ原斷層の西にエシエロン狀に連なつて *S* 80° *W* より *N* 80° *E* に走り、佐那具に至り、それより南に凸弧を向けて北に向う迄約 9km の間連なり、東南側に斷層崖を向けて居る。斷層の落差は之を盆地層の變位より見て 250 m 以上と推定せられる。

花ノ木斷層は上野町の西南、花ノ木村北山より起つて、*N* 60° *E* より *S* 60° *W* に走り、法花、白樫を經て更に西南に延びる斷層であつて、西南側に斷層崖を向け、その落差は北東部に於て最も大きく 100 m 以上に達するが西に行くに從つて、次第にその量を減じ遂に撓曲に遷移して居る。最も明瞭なる斷層崖を示す部分のみをとつても、その長さは 5 km を超えて居る。

此等三本の主要斷層崖によつて圍まれた島ケ原地塊を造る地質に就いては北條理學士[3] の精細なる調査がある。此地方の地質は三大別して、古期地層と盆地層と洪積層及び沖積層とにする事が出來る。古期岩石とは此地域の基底をなすものであつて、古生層の諸岩石と花崗岩とより成つて居る。盆地層と茲に名付くる地層は粘土層と凝灰質頁岩及び花崗質砂岩の互層と礫岩及び砂岩の互層とより成つて居り、その中には岩

---

3) 北條敬太郎「三重縣上野町附近粘土調査報文」工業原料用鑛物調査報告 **78** (1925).

木或は淡水棲の貝類の化石を挾んでゐる。

此地層は內陸盆地に於て、古期岩石の略々平坦なる侵蝕面の上に堆積せるものにて、その堆積時代は北條理學士は之を第三紀とされて居るが中村教授[4]が他地方に於て洪積紀舊期とせられて居るものと同時代らしい。その層厚は厚くなく、現今にては後に起りし垂直運動による侵蝕の回春作用によつて削剝せられて、山頂部或は斷層崖下に殘つて居るのみである。

洪積層竝びに沖積層は砂と礫とより成り、之は谷の底を埋めて薄く堆積して居るのみにて、その層厚は數mを出でない。

盆地層は一般には水平に近き傾斜を有して居り、緩漫なる波狀の皺曲をなして居るのみであるが、斷層崖下に於ては變位が著しく急傾斜をなして居る。例せば上野斷層崖下の三田村大谷に於ては、斷層崖より100m餘の幅の範圍に於て盆地層が南に40°以上の急傾斜をなして居り、花ノ木斷層崖下の法花、北山に於ても斷層崖下100m餘の範圍に於て25°以上の急傾斜をなして居る。此事實は盆地層の堆積せる後に斷層運動があつて、その爲に地層が曳づり作用を受けし事を示して居る。

第四圖は北條理學士によつて造られた地質圖の抄圖である。何れの斷層崖下に於ても斷層崖を界として隆起部は花崗岩によつて占められ、沈降部は南に傾斜せる盆地層によつて蔽はれて居る。

尙此兩岩石の境界を見るに、山脚の部に於ては、南に出て居り、谷の部に於ては北に入込んで居る。之は斷層面が北に傾斜して居る事を暗示して居る。此事實と地層に曳きづりのある事とによつて推せば、此等三本の斷層は何れも逆斷層であるらしい。

7. 木津川流路の變遷

島ヶ原地塊の地塊運動の性質を硏べる爲に、此地塊の長軸の方向と短軸の方向とに沿うて行はれたる垂直運動を硏べる事とし、あたかも木津川が長軸に平行して此地塊の北部を流れ名張川が短軸に平行して此地塊の西部を横斷して居るので、此二川の垂直的の流路の變遷を求めて見た。

木津川の縱斷面には海拔70mのW_1地點と、海拔100mのW_2地點と、海拔120mのW_3地點と、更に海拔130mのW_3'地點とに於て著しき傾斜の遷急點が認められる。此等の遷急點が第一項に述べた如き運動の何れかによつて形造られ、そ

---

4) Shintaro NAKAMURA, 'Guide-Book Excursion D,' *Pan-Pacific Science Congress* (Tokyo, 1926), 1–10.

れが第二項に述べたる如く上流に移つて、現在の位置に達せしものと考へれば、その遷急點より上流の縱斷面曲線を延長すれば、此延長せる部分が木津川の舊き流路を示すのである。されど第四項に述べたる如く之を 30 km 餘の長き間誤りなく延長する事は困難であり、又途中に於て局部的の垂直運動の挾まれたる懼れも多い。

玆に於て木津川の支流の縱斷面曲線を畫き、その中にある遷急點を求め、この點より上流の縱斷面曲線を延長して、延長部分が上流部と連續して一種の凹曲線になるようにし、本流とその支流との合流點に於けるその曲線の高さを求めた。此高さは支流の遷急點が合流點にありし當時の位置を示すものにて、本流の舊河床の高さを示して居る。此場合本流の河畔に發達して居る河成段丘の段丘面と段丘崖との境界は之を縱斷面の傾斜の遷急點と見た。かくの如くして各支流の合流點に於ける木津川の舊河床の高さを知り、共各點を連ねて本流の舊き流路を想定し得たのである。

第五圖は上野町より大河原に至る間にある木津川の本流と支流とにある遷急點の位置を示してゐるが、大いなる支流には五個以上の遷急點が存して居る。

第二表には上野町より木津町に至る間の木津川の支流にある遷急點が各々本流とその支流との合流點にありし當時の高さ卽ち舊河床の高さを記入してある。

第六圖は木津川本流の縱斷面曲線にて、それに上述の如き方法を以て求め得た各支流の合流點に於ける舊河床の高さを記入してある。相隣る各群の諸點を連ねた曲線が木津川の舊流路を示すのである。

第一群の諸點を連ねた曲線は木津川本流の W_2 より W_1 に至る現河床の横斷面曲線と連續せる凹曲線の上に載つて居る。W_1 以下の現河床は現在の侵蝕期の流路を示し、W_2 より W_1 に至る間の現河床と第一群の諸點とを結んで得た舊流路とは、前輪廻卽ち第一期侵蝕期の河床を示して居る。同様に第二群の諸點を結べば W_3' より W_2 に至る現河床の曲線の延長上に來り、第二期の侵蝕期當時の流路を示す。第三群、第四群、第五群、第六群の諸點を連ねた曲線も同様に夫々第三期、第四期、第五期、第六期の侵蝕期當時の舊流路を示して居る。此等の曲線は上位のもの程、緩傾斜をなして居るが、木津町附近に於てはそれが略々平行して居り、その各曲線間の高さの差は第三表の如くである。

大いなる支流と本流との合流點には此等の點より更に高く第七、第八、第九、第十の各侵蝕期に相當する舊河床を示す點がある。その高さの概數は第二表に示した。

かくの如くして木津川の最近六期の侵蝕期に於ける流路を推定し、更に古き數期の

Table III.

侵蝕期	現－I	I－II	II－III	III－IV	IV－V	V－VI
高度の差	15 m	20 m	20 m	20 m	30 m	50 m

侵蝕期の存せし事を知り、その高さを知り得たのである。

如何なる運動が行はれて、かゝる遷急點が形造られたかを知る爲に第一項に掲げた遷急點の形造らるゝ諸原因に就いて吟味して見た。

第六圖によつて各侵蝕期の流路を見るに何れも一凹曲線をなし、その中に傾斜の遷急點を認むる事を得ない。此事實は木津川が島ケ原地塊を流るゝ間に於ては新に遷急點の形造らるゝ如き垂直運動の行はれざりし事、即ち全地域が一様に動きし事を意味し、現在此地域に認めらるゝ遷急點は木津町より下流に於て形造られそれが後退し來れる事を示して居るのである。

第六圖に依れば、第六期侵蝕期に於ける木津川の流路は極めて緩漫にて上野町より木津町に至る迄 35 km の間に於て 15 m の落差を有するのみである。此より新しき侵蝕期の流路は新しきもの程急である 之は木津川が第六期に於て略グレードの狀態にあり、その後は未だグレードに達せざる事を示して居るのである。

此二つの事實により、此地域に於ては各侵蝕期の終りに行はれた垂直運動に際して傾斜を急にするが如き、或は緩にするが如き傾斜運動の伴はれざりし事を知り得るのである。

よつて、上野町より、木津町に至る地域が等量に隆起し、下流が上流より少く隆起せるか、不動なりしか、或は沈降せしかによつて遷急點が形造られたものにて、而もかゝる運動が數回繰返されて、以上述べたる如く一つの川に數個の遷急點が形成されたのである,

山頂部が侵蝕され易き盆地層よりなり、山麓部が侵蝕され難き古期岩石よりなる島ケ原地塊に於て、侵蝕力の回春が行はれた事故、當然第三項に述べし如く、地層の境界に沿うて垂直運動の二次的の結果なる遷急點が存す可き筈である。

第四圖に川を入れ、それに遷急點の位置を印づけて見ると、第四群以下の遷急點は花崗岩地域にあり、第五群. 第六群の遷急點は古期岩石と盆地層との境界近くに存して居る。一回の隆起運動によつて起つた一回の侵蝕力の回春によつて形造られた一つの遷急點が、地質の境界に來て二つとなり、第五群、第六群の遷急點となつたものと

も考へられるが、境界線の上にある遷急點のなき事と花崗岩のみよりなる地域にも盆地層のみよりなる地域にも兩群の遷急點の見出さるる所より見て、二回の回春によつて此二群の遷急點が形造られたものと推定せられる。

要するに木津川流路の變遷は垂直運動特に上野町木津町間が一地塊として各部等量に隆起せし爲に起されたものである。而も此運動は間歇的にて、激しき地殼運動の時代と比較的に緩漫なる地殼運動の時代とが交互に存在せしものゝ如くである。島ヶ原地塊の隆起量は第三表に高度の差として記載せし數と同量である。

此等より見て島ヶ原地塊は東西軸に沿うては傾動せず常に各部等量の隆起を繰返せし事を知るのである。

8. 名張川流路の變遷

第七項と同樣の方法を以て名張川の名張町より下流の流路の變遷を研べて見た。第五圖には名張町より名張川と木津川との合流點に至る間の此川の本流と支流とにある遷急點が印されて居り、第四表には名張川の各支流にある遷急點が夫夫本流とその支流との合流點にありし當時の高さ卽ち舊河床の高さが記入されてある。此等はその高さによつて大別して九群とする事が出來る。

第七圖は名張川本流の縱斷面曲線であつて、それに各支流の合流點の位置と、その點に於ける舊河床の高さとが記されて居る。各群の舊河床を連ねたものが名張川本流の舊流路を示すのである。

名張川に於て海拔 90 m の地點にある遷急點 V_2 より下流の現流路が木津川の第一期侵蝕期に於ける流路に相當し、これより高く存する舊流路は夫夫木津川の第二期、第三期、第四期、第五期、第六期、第七期等の侵蝕期に相當する流路を示して居る。

此等の各侵蝕期を示す曲線の高さの差は木津川の各期の流路の高さの差と略等しい。卽ち名張川に於ても木津川に於て見たると同じく最近六期の侵蝕期に於ける流路の位置を推定し、更に之より古き侵蝕期の存在せる事を知るのである。

かゝる流路の變遷を起さしめた原因に就いて木津川に於けると同樣の方法を以て吟味せる結果、名張川流路の變遷は此地域が一つの地塊として等量に且間歇的に數回隆起せる爲めに行はれた事が知られる。而して各期の隆起量は木津川の夫と略ゝ同量であつた。

此より推して島ヶ原地塊はその西部名張川の横斷する邊りに於ては、その短軸卽ち西北より東南に走る軸に沿うては、少くも第六期以後に於ては傾動せず、常に等量の

隆起を繰返せるものの如くである。

9. 花の木斷層崖南部地方の川の流路變遷

木津川の支流 C_2, C_3 等の諸川と名張川の支流 D_4, D_5 等の諸川とは花の木斷層崖の南部地方を灌漑して居る。此等の川の流路の變遷を研べて見た。

第五圖には此等の諸川にある遷急點の位置が記されて居る。此地方は海拔 200 m以下の平夷なる邱稜地であつて、その山頂部には平坦面が殘つて居る。此平坦面と谷頭との境が木津川と名張川とに於ける第六期の遷急點に相當して居る遷急點であり、更に谷の中には之より低く、木津川、名張川の第四群、第五群の遷急點に相當する遷急點が認められる。此地域には名張川との流域に見らるゝ如き高位置の遷急點は認められない、

第六期の侵蝕期を示す平坦面の高さは此地方の南部なる古山村竝に西部なる名張川流域に於ては高くして 200 m を超ゆるが、北東部に行くに從ひ低くなり、花の木斷層崖に接する所にては 180 m 以下となつて居り、下流なる島ケ原地塊に見らるゝ夫よりも低い。

これによつて推せば、此地方に於ては第六期に於て島ケ原地塊と連續せる侵蝕面が形成せられたのであるが花の木斷層が更に運動を續けたる爲に此面が陷落して居るのである。而して此面の高さより云ひても花の木斷層の落差は東部で大で、西するに從ひ小となり遂に名張川が之を橫ぎる邊りにては零となつて居る事が知られる。

10. 島ケ原地塊の運動

伊賀川と名張川と更に花の木斷層崖の南部地方の川の流路の變遷によつて島ケ原地塊の運動を推察して見る。

第四圖、第五圖に於て見たるが如く、第六期の侵蝕期に於ける木津川と名張川と竝に花の木斷層崖南部の諸川との流路は極めて緩漫なる傾斜を有して居り、木津川の例によれば上野町より木津町に至る間 35 km の間に於て 15 m の高度の差を見るのみで、淀川の下流地方の傾斜と略ゝ等しい。之は第六期の侵蝕期の靜止時代が永くして、川が緩傾斜の流路となり、その河畔には一部は侵蝕作用の爲に、一部は堆積作用の爲に廣き冲積平野の形造られし事を意味して居るのである。此靜止時代の後に島ケ原地塊に於ては六回の間歇的隆起が行はれたが、その隆起量は木津川の流域竝に名張川流

域に於ては同性質、等量であつたのである。

島ヶ原地塊には第六期の侵蝕面の上に更に海抜 240—250 m、海抜 270—280 m の箇所に第七期、第八期の侵蝕面を示す平坦面竝にこゝを流るゝ木津川の縦斷面にはその界を示す遷急點が存して居る。然るに花の木斷層崖の南部にては山頂が第六期の侵蝕面であつて、此より高き侵蝕面は見出されない。又第六期の侵蝕面の高さが花の木斷層崖下に於て最も低くなり居る事は第五項に述べた如くである。

これより見て、花の木斷層崖は第八期の侵蝕期以前に形造られたのであるが、それが第六期以後迄變位を續けたものである。

要するに島ヶ原地塊はその長軸の方向卽ち東西の方向には第八期侵蝕期以後常に等量の間歇的隆起を繰返して來たのであり、短軸の方向則ち南北の方向にては、西部名張川流域にては東西の方向にて見たると同様の運動をなして來たのであつたが、東部地方上野盆地に接する所にては第八期の侵蝕期より第六期以後迄その南の地塊と隆起量を異にし、その二地塊の間に花の木斷層崖を成長せしめたのである。

---

30. Recent Deformation of the Shimagahara Land Block in Prov. Iga as determined by Tracing the Vertical Change of River Courses.

By **Fumio TADA.**

The longitudinal profile of a river has been regarded as a curve which resembles a hyperbola or exponential curve, tangent to the base level. A continuous profile of a graded river like this will break and tend to make a cusped point, if such kind of deformation as to make the gradient of the lower course from a point in it steeper than that of the upper one, do occur. There are vertical movements as shown in Table I, **1–5**, by which cusped points will necessarily be formed.

If a change in the relative position of the shoreline, due to upheaval of land or lowering of sea level (Table I, **6**) takes place, the river extends her course on the new coastal plain, and a cusped point is formed just at the former strand line; for the slope of the submarine platform is generally steeper than that of the lower course of the river.

If a cusped point is formed by the vertical movement as shown in Table I, **1** or **5**, the slope of the lower course from that point becomes too gentle to carry the whole loads; the cusped point will be buried sooner or later by the consequent aggradation.

If on the other hand, the interrupting movement as shown in Table I, **2**, **3**, **4**, **6** takes place, the velocity of water current accelerates and erosive power revives; degradation thenceforth will continue until graded condition is again attained. The cusped point, therefore, begins to retreat upstream.

The rate of its retreat depends on the character of the bed rock; it goes up faster in the region of soft rock, slower in the region of hard rock. On the other hand, it depends upon the product of the amount of water discharge and the difference of water velocities in the upper and lower course from the cusped point. The amount of water discharge under normal conditions decreases constantly headwards, as it is proportional to the drainage area; while the difference of water velocities in the upper and lower course from the cusped point decreases as the point retreats upstream, for the depth of water decreases correspondingly with the distance from the river mouth and the declivity of river course under the cusped point remains unchanged. So the rate of retreat of a cusped point decreases upstream.

For the same reason, the cusped point in the main stream goes up more rapidly than those in her tributaries.

By utilizing these characteristics of a cusped point in the longitudinal profile of a river, restoration of her ancient course is possible, provided the interruption is due to crustal movements as shown in Table I. Namely the downward extension of the longitudinal profile of upper course from the cusped point may be considered as the course of the former cycle of erosion. But it is not easy to extend the curve to a long distance without error and to detect minor deformations which might have localized in the way of extension.

Now, the longitudinal profiles of tributaries and the cusped points in them become useful. Extends the curves of upper courses from the cusped points in tributaries down-stream, as to represent the former courses of tributaries; then we get heights of confluences of tributaries and main stream in the former cycle (Fig. 2). A curve tracing these assumed confluences may be regarded as the former course of the main stream. Moreover, as the distances from the confluences to the cusped points in tributaries are shorter than that in the main stream, we have the advantage of restoring the former course more correctly than by the method of only taking the cusped point in the main stream.

In this paper the author tried to trace, after the method as stated above, the vertical change of previous courses of the Kizu-gawa and of the Nabari-gawa, both draining the Shimagahara land block in the central Kinki district (Fig. 3 and Fig. 4).

Fig. 5 shows the positions of the cusped points in the longitudinal profiles of the two main rivers and their tributaries. Table II and Table IV indicate the heights of the respective confluences of the former cycles in the Kizu-gawa and the Nabari-gawa, which were determined by the method above described.

Fig. 6 and Fig. 7 show the longitudinal profiles of these two rivers in the present and the former cycles of erosion. The intermittent upheaval of the Shimagahara land block in the recent geological time is known in detail by tracing the vertical change of these curves.

TABLE I.

	Lower Course	Cusped point	Upper course
1. Vertical movements which make the gradient of the lower course gentle and that of the upper course more gentle.	+ a	+ b	0
	+	0	−
	+ a	+ b	+ c
	+ a	+ b	−
	+	− b	− a
	0	− b	− a
	− c	− b	− a
2. Vertical movements which make the gradient of the upper course steep and that of the lower steeper.	+ c	+ b	+ a
	0	+ b	+ a
	−	+ b	+ a
	−	0	+
	− a	− b	+
	− a	− b	0
	− a	− b	− c
3. Vertical movements which make the gradient of the upper course gentle and that of the lower steep.	+ b	+ a	+ c
	+ b	+ a	+ b
	+ c	+ a	+ b
	+ b	+ a	0
	+ b	+ a	−
	0	+ a	+ b
	0	+	0
	0	+	−
	−	+ a	+ b
	−	+	0
	− b	+	− a
	− a	+	− a
	− a	+	− b
	− b	0	− a
	− a	0	− a
	− a	0	− b
	− b	− c	− a
	− a	− c	− b
	− a	− b	− a
4. Vertical movements which make the gradient of the upper course gentle while that of the lower remains unchanged.	+ b	+ a	+ a
	0	+ a	+ a
	−	+ a	+ a
	−	0	0
	− a	− b	− b
5. Vertical movements which make the gradient of the lower course steep while that of the upper remains unchanged.	+ a	+ a	+ b
	+ a	+ a	0
	+ a	+ a	−
	0	0	−
	− b	− b	− a
6. Change in relative position of shoreline, due to upheaval of land or lowering of sea level.		+ a	+ a
		+ a	+ b
		+ b	+ a

+ Upheaval of land, − subsidence of land, 0 stationary, a, b, c, amounts of vertical deformation, a>b>c.

Table II.

Position \ Cycle	Heights of the river beds in the former cycles of erosion at the confluences of the Kizu-gawa and its tributaries												
	Present	I	II	III	IV	V	VI	VI′	VII	VIII	IX	X	XI	XII
B_1	29^{m}	45^{m}	70—75^{m}	90-100^{m}	115—125^{m}	140—150^{m}	—	—	—	—	—	—	—	—
B_2	30	45	70	90—95	110	—	—	—	—	—	—	—	—	—
Kaseyama	36	50	—	—	—	—	—	—	—	—	—	—	—	—
Hokkezino	36	50	—	—	—	—	—	—	—	—	—	—	—	—
B_3	37	50—55	65—70	90	—	—	190^{m}	—	—	—	—	—	—	—
B_4	38	50—55	70	90	120	140—150	190—200	220^{m}	240^{m}	—	—	—	—	—
B_5	40	55	70—80	85—90	110—120	140—150	190—200	—	—	—	—	—	—	—
B_6	42	55	—	95	—	135—140	190	—	240—25	—	—	—	—	—
B_7	45	60	80	95—100	110—120	145—155	—	—	—	—	—	—	—	—
B_8	47	60	—	—	110	140—150	—	—	—	—	—	—	—	—
B_9	49	60—65	80	—	110—120	—	190—195	—	—	—	—	—	—	—
B_{10}	50	60—65	80—85	90	115—120	155	190	220	250	290—305^{m}	335—340^{m}	350^{m}	420^{m}	—
B_{11}	50	60—65	80—85	—	—	—	190	210	245—250	265—270	—	—	430	490^{m}
A_5	52	60—65	75	—	120	155	190	—	—	290	330	360—370	—	—
A_6	53	60—65	85	100	120	—	185—190	—	—	—	—	—	—	—
B_{12}	54	60—65	85-90	—	—	150	185—190	—	—	—	—	—	—	—
B_{13}	55	—	—	—	—	150—155	185—190	—	—	—	—	—	—	—
A_7	55	60—70	—	—	115	—	—	—	—	—	—	—	—	—

(to be continued.)

TABLE II. (continued.)

Cycle / Position	Heights of the river beds in the former cycles of erosion at the confluences of the Kizu-gawa and its tributaries.						
	Present	I	II	III	IV	V	VI
B_{14}	56^{m}	——	——	——	——	——	185 – 190^{m}
Kitaôgawara	57	60—70^{m}	——	——	——	——	190
A_8	58	——	90^{m}	——	——	——	——
B_{26}	60	——	——	——	——	160^{m}	190
B_{17}	60	——	——	——	——	165	195
W_1	70	cusped pt.	——	——	——	——	——
A_9	——	75	——	——	130^{m}	150	190—195
A_{10}	——	80	100	115 – 120^{m}	——	——	190—200
B_{18}	——	81	——	115—120	130	——	——
P_9	——	81	——	——	——	160	——
B_{19}	——	81	——	115	130	175	190—195
Okuda	——	——	——	——	——	175	——
B_{20}	——	99	110	——	140	165	200
A_{11}	——	100	——	120	135	——	——
P_3	——	100	——	120	——	——	——
B_{21}	——	100	——	120	140	175	200—210
W_2	——	102	cusped pt.	——	——	——	——
A_{12}	——	102	——	120	145	——	——
A_{13}	——	——	104	——	——	——	190—200
A_{14}	——	——	105	125	145	——	——
A	——	——	115	130	140	——	200
W_3	——	——	(cusped pt.)	——	——	——	——
B_{23}	——	——	122	——	140	160	205
A_{16}	——	——	123	——	135	——	200
B_{24}	——	——	123	——	135	160	198
P	——	——	124	——	——	——	198
A_{18}	——	——	126	——	138	160	200
W_3'	——	——	130	cusped pt.	——	——	205
Higasimura	——	——	——	130	140	165	——
Ueno	——	——	——	132	140	165	——
Kigosi	——	——	——	134	143	——	——
Uwatoko	——	——	——	140	150	——	——

TABLE IV.

Cycle / Position	Heights of the river beds in the former cycles of erosion at the confluences of the Nabari-gawa and its tributaries.								
	I	II	III	IV	V	VI	VI′	VII	VIII
V_2	90^{m}	cusped pt.	—	—	—	—	—	—	—
D_1	—	92^{m}	—	135^{m}	160^{m}	190^{m}	210^{m}	—	—
M_1	—	93	—	—	—	195	—	—	—
N_0	—	95	—	—	—	200	210	—	—
N_1	—	96	—	—	—	190	210	—	—
N_1'	—	97	—	—	160—165	190	—	240^{m}	—
N_2	—	98	—	—	—	—	—	230	—
M_1'	—	100	—	—	155—160	190	—	—	270^{m}
N_3	—	102	—	—	—	—	—	240	280
N_4	—	102	—	—	—	—	—	240	—
Q_8	—	102	—	—	—	—	—	—	270—280
N_5	—	104	—	—	160	190—200	—	—	270
N_6	—	105	—	—	160	—	—	230	—
M_2	—	106	—	—	—	190	—	—	280
N_7	—	108	—	—	165	—	—	240	—
M_3	—	110	—	—	—	200	—	—	280
Momokano	—	—	—	—	—	—	—	—	280
N_8	—	112	—	—	170	200	—	225	280
N_9	—	112	—	—	—	195	210	—	280
Q_2	—	—	—	—	—	—	—	—	280
Q_3	—	—	—	—	—	—	—	240	280
N_{10}	—	114	—	135	175	—	215	—	—
M_4	—	114	—	—	175	200	—	—	—
N_{11}	—	114	—	—	180	—	215	—	280
Q_4	—	—	—	—	—	—	—	—	275
D_2	—	115	—	—	170—175	200	—	—	—
D_3	—	118	—	—	—	200	—	—	280
Q_5	—	—	—	—	—	—	—	—	280
M_5	—	119	—	—	170	195	—	—	—
M_6	—	120	—	—	—	200	—	—	—
N_{12}	—	121	—	—	—	190	220	—	—
M_7	—	122	—	—	165	200	—	—	—
P_{20}	—	—	—	—	—	—	—	260	—

(to be continued.)

TABLE IV. (continued.)

Cycle Position	Heights of the river beds in the former cycles of erosion at the confluences of the Nabari-gawa and its tributaries.								
	I	II	III	IV	V	VI	VI'	VII	VIII
D_4	—	127^{m}	—	—	170^{m}	—	215^{m}	—	—
D_4'	—	128	—	140^{m}	165	195	—	—	—
N_{13}	—	—	—	—	170	198	—	260^{m}	—
D_4''	—	130	—	140	165	—	—	—	—
V_3	—	130	cusped pt.	—	—	—	—	—	—
$N_{13'}$	—	—	132	140	170	195	220	—	—
Osogase	—	—	132	—	—	—	—	—	—
N_{13}''	—	—	132	—	170	—	—	—	—
N_{14}	—	—	132	—	170	200	—	260	—
N_{15}	—	—	132	—	170	200	—	—	—
P_3	—	—	134	—	—	190	—	—	—
Nakamine	—	—	—	—	—	200	—	250	—
D_5	—	—	135	—	170	200	—	—	—
N_{16}	—	—	137	—	170	195	—	—	—
P_1	—	—	—	—	—	—	220	—	—
D_6	—	—	140	—	170	195	—	—	—
Q_1	—	—	—	—	—	—	—	—	270^{m}
P_2	—	—	—	—	—	—	220	—	—
N_{17}	—	—	141	—	—	200	—	—	—
N_{18}	—	—	142	—	180	210	—	—	—
P_4	—	—	—	—	—	—	—	—	275
D_7	—	—	145	—	—	195	215	—	—
Katsura	—	—	—	—	—	—	—	—	270
M_8	—	—	147	—	175	200	—	—	—
D_9	—	—	148	—	—	195	—	—	—
M_9	—	—	—	—	—	205	—	240	—
D_8	—	—	152	—	—	200	—	240	—
M_{10}	—	—	155	—	—	200	220	—	—
P_6	—	—	—	—	—	—	220	—	—
N_{20}	—	—	155	—	—	—	—	—	—
P_7	—	—	—	—	—	—	—	240	280

(to be continued.)

TABLE IV. (continued.)

Cycle / Position	Heights of the river beds in the former cycles of erosion at the confluences of the Nabari-gawa and its tributaries.								
	I	II	III	IV	V	VI	VI′	VII	VIII
N_{21}	—	—	157^{m}	—	—	200^{m}	—	—	—
N_{22}	—	—	158	—	—	200	225^{m}	—	280^{m}
M_{11}	—	—	158	—	—	195	—	—	—
N_{23}	—	—	160	—	—	200	225	—	280
N. Kuzuo	—	—	162	—	—	—	220	—	280
Kuzuo	—	—	—	—	—	210	—	—	—
Ieno	—	—	165	cusped pt.	$170-180^{\mathrm{m}}$	200	—	—	—
Komohara	—	—	—	170	170−180	190	—	—	—
E_1	—	—	—	172	180	—	225	—	—
R_2	—	—	—	—	180	—	—	—	—
Kuramoti	—	—	—	—	190	—	—	240^{m}	—
E_{13}	—	—	—	—	—	—	—	240	—

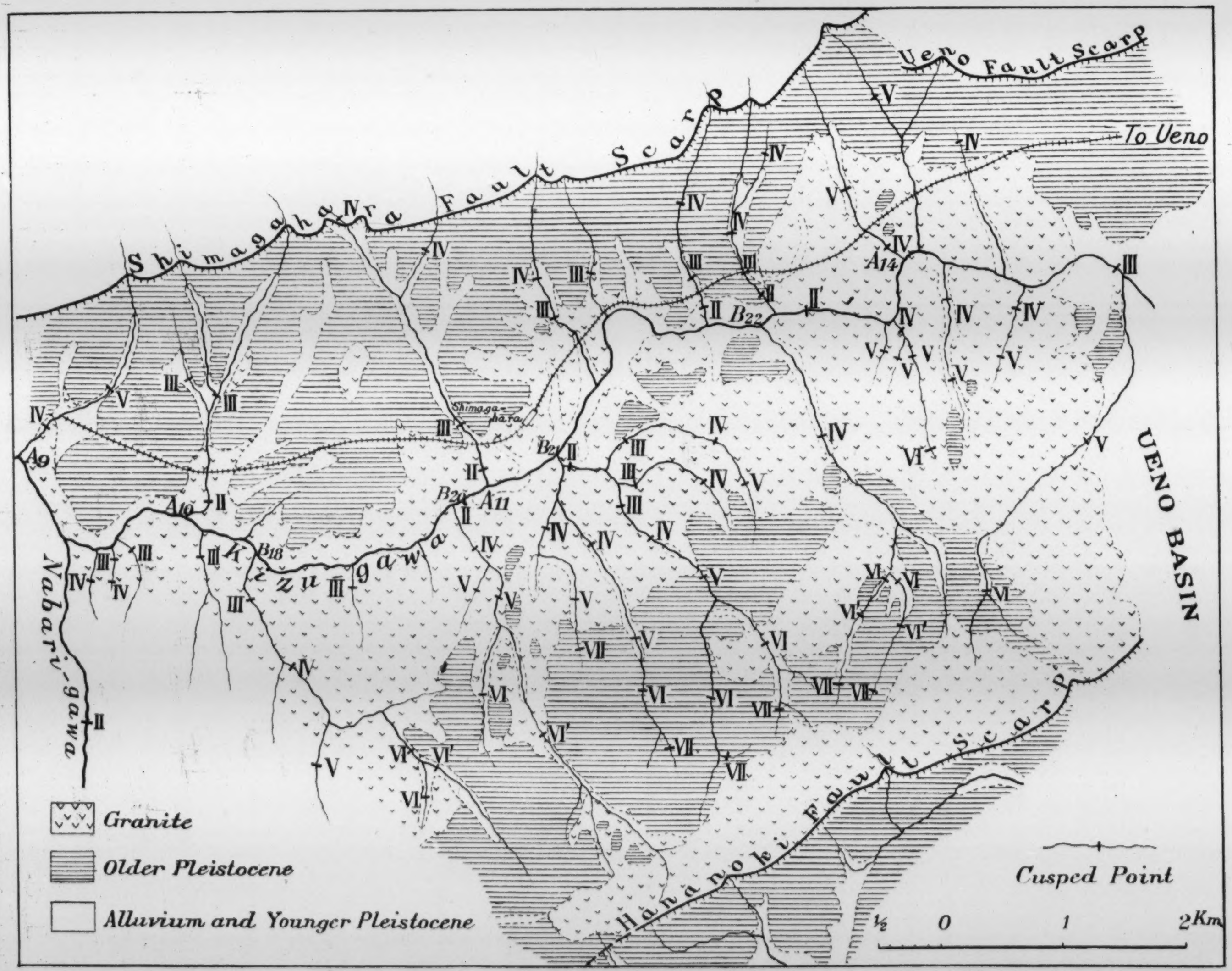
Shimagahara Fault Scarp
Ueno Fault Scarp
Hananoki Fault Scarp
To Ueno
UENO BASIN
Shimagahara
Kizu-gawa
Nabari-gawa
A9
A10
A11
A14
B18
B20
B21
B22
Granite
Older Pleistocene
Alluvium and Younger Pleistocene
Cusped Point
½ 0 1 2Km

Fig. 4. Geological map of the Shimagahara block, showing the relation between geologic structure and cusped points in the longitudinal profiles of two rivers Kizu-gawa and Nabari-gawa.

（震研彙報、第七號、圖版、多田）

（震研彙報、第七號、圖版、多田）

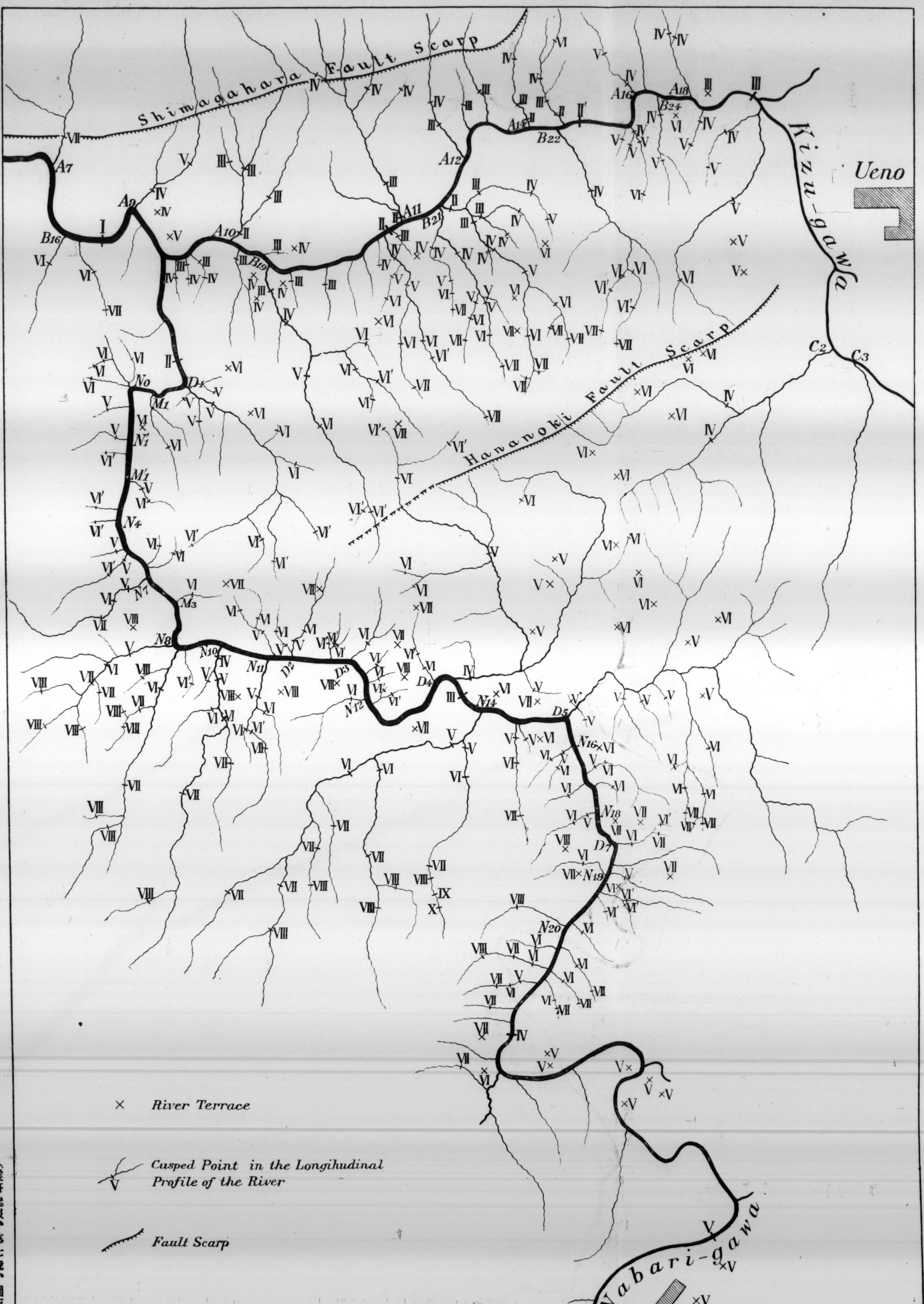
Shimagahara Fault Scarp
Hananoki Fault Scarp
Kizu-gawa
Nabari-gawa
Ueno
Nabari
A7
A9
A10
A11
A12
A14
A16
A18
B16
B19
B21
B22
B24
C2
C3
D1
D2
D3
D4
D5
D7
M1
M'1
M3
N0
N1
N4
N7
N8
N10
N11
N12
N14
N16
N18
N19
N20
× River Terrace
Cusped Point in the Longihudinal Profile of the River
Fault Scarp
½ 0 1 2 3 4Km.

Fig. 5. Map showing distribution of cusped points in the longitudinal profiles of the Kizu-gawa and the Nabari-gawa in the Shimagahara block.

(震研彙報、第七號、圖版、多田)

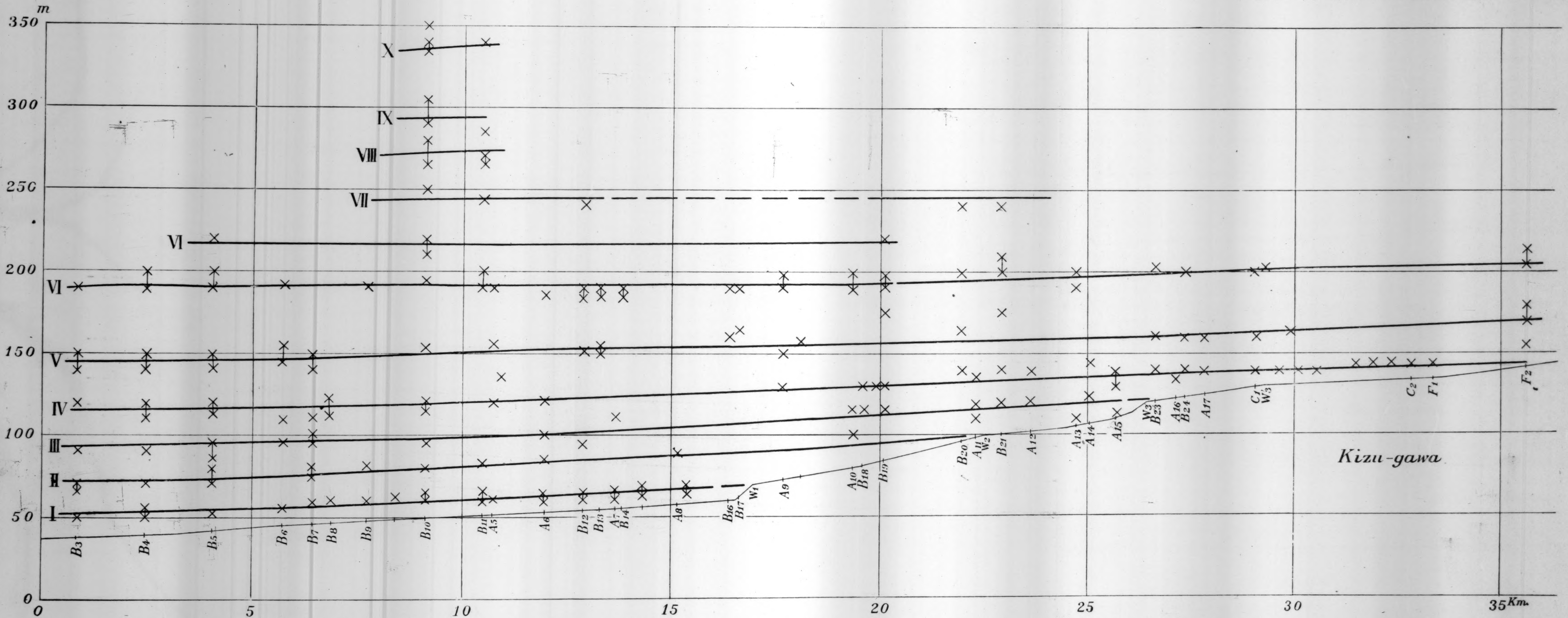

Fig. 6. Longitudinal profile of the Kizu-gawa. Cross points show the former river beds at the confluences of the main stream and its tributaries, thick lines connecting these cross points show the river courses in the former cycles of erosion.

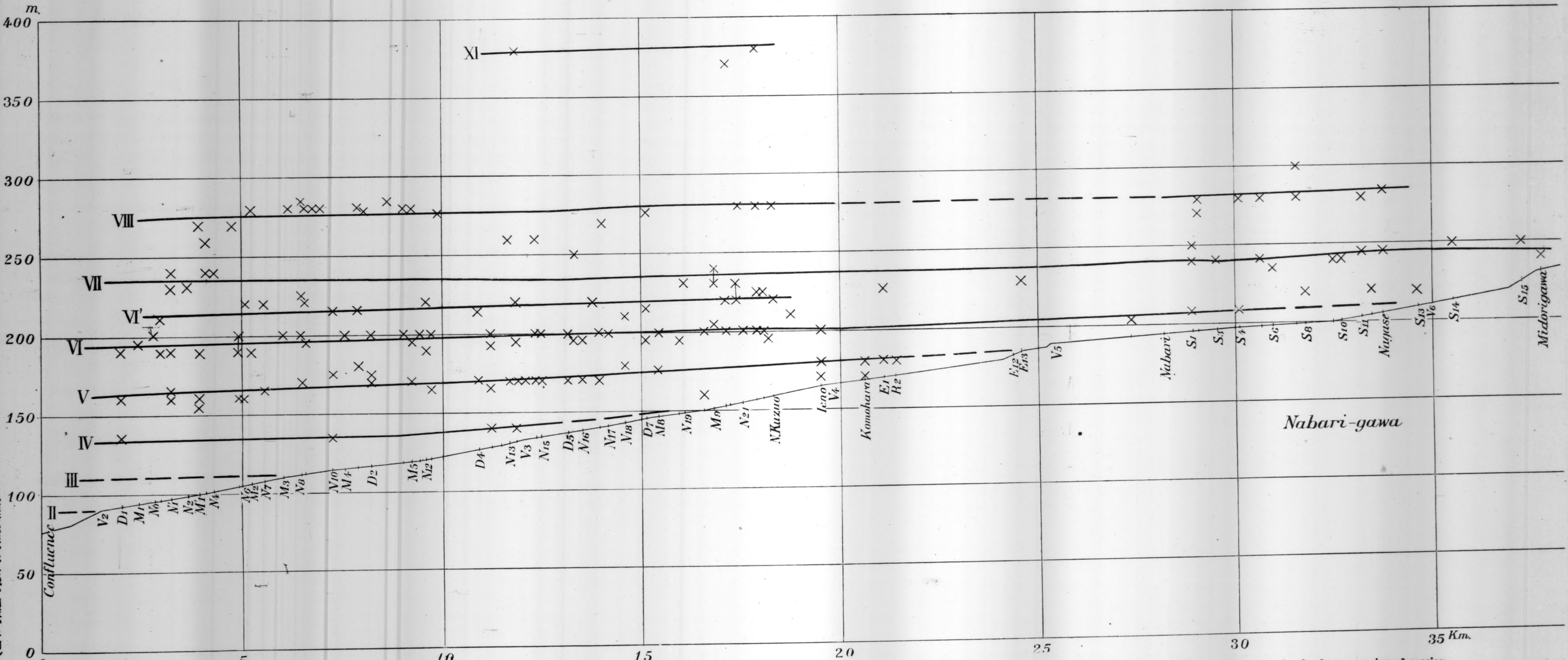

Fig. 7. Longitudinal profile of the Nabari gawa. Cross points show the former river beds at the confluences of the main stream and its tributaries, thick lines connecting these cross points show the river courses in the former cycles of erosion.

（震研彙報、第七號、圖版、多田）

31. 昭和四年一月二日の日本海海水面の異常

山口生知

(昭和四年九月十七日發表―昭和四年九月二十日受理)

昭和四年一月二日午前七時頃新潟縣西頸城郡市振村及親不知附近に非常なる大津浪(約10米と稱せらる)があつて汽車は不通となり人家は押し流されたといふ新聞の報道があつた。著者は大正十二年の關東大地震以來寺田博士と共に太平洋岸に於ては三崎の油壺九州の細島北海道の花咲の三箇所に就いて又日本海方面に於ては能登の輪島に就いて平均海水面の變化に關し研究中であつてその變化を支配する最も主なる原因は低氣壓の影響であるといふことが明白となつた。その報告は既に寺田博士及山口生知の名にて「帝國學士院紀事昭和三年十月第四卷第八號」續いて「地震研究所彙報第七號第一冊昭和四年六月」にて發表した。而して低氣壓の海水面に及ぼす機巧に關する物理學的說明は未だ詳解されてゐない。そこで假令時間は數時間の短時間にしても0米程の大津浪があつたとすれば月々の平均海水面の上に換算しても數糎の膨脹となる。而してその前々日より前日にかけて深度の742粍程度の低氣壓が日本海を通過してをる故にこの一つの事實を捕へて詳細に研究したならば何か物理學的說明の爲の手掛りを得られやうと考へた。

幸に寺田博士の御薦めにより地震研究所よりその調査の爲山形縣酒田より新潟縣富山縣の海岸を經て福井縣敦賀に至る調査出張を命ぜられた。卽酒田、新潟、新港町(伏木)福井縣九頭龍川河口の三國港及敦賀の各內務省土木出張所に參りて自記檢潮曲線又は定時觀測の量水標の寫しを頂戴し又は當時海水面異常の實況につき知れるだけ詳しく各土木出張所長その他の人々のお話を聞いた。又一方新潟、伏木、敦賀の各測候所長をも訪ねて當時の氣象狀態を伺つた。それから又津浪の被害の最も著しかつた市振村及親不知附近は特に詳しく踏査して被害の跡の狀況を目擊した。

研究の方法

先づ各地の檢潮曲線又は定時觀測の値を採つて北方酒田より地理的位置の順序に並べ時刻を合せ尺度を同じうして畫いた曲線群が第一圖である。この圖中下方の二曲線は敦賀港及福井縣杉津に於ける夫々の時刻に對する波浪の振幅を表はす。

第一圖を見れば各地の最高潮が何時頃であるかといふことの大體は分るが尙この中

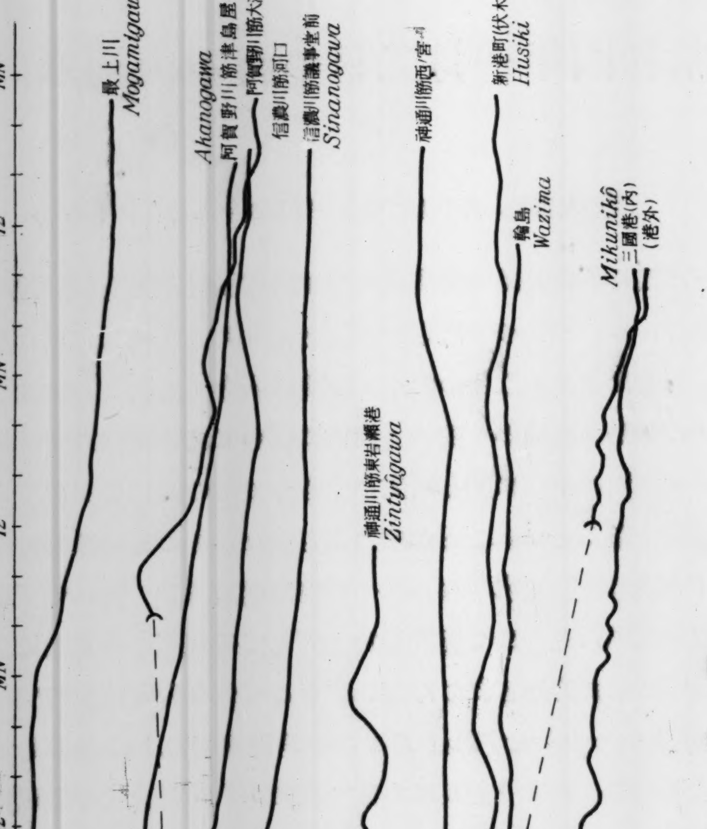
最上川
Mogamigawa
Akanogawa
阿賀野川筋津島屋
阿賀野川筋大浜
信濃川筋河口
信濃川筋議事堂前
Sinanogawa
神通川筋西ノ宮
神通川筋東岩瀬港
Zintûgawa
新港町(伏木)
Husiki
輪島
Wazima
Mikunikô
三國港(內)
(港外)
928
1Dec. 31st
1929
Jan. 1st
2nd
3rd
4th
MN
12
Sea Level
L cm
80
40
0
120
100
60

Fig. 1a. 第一圖 a.

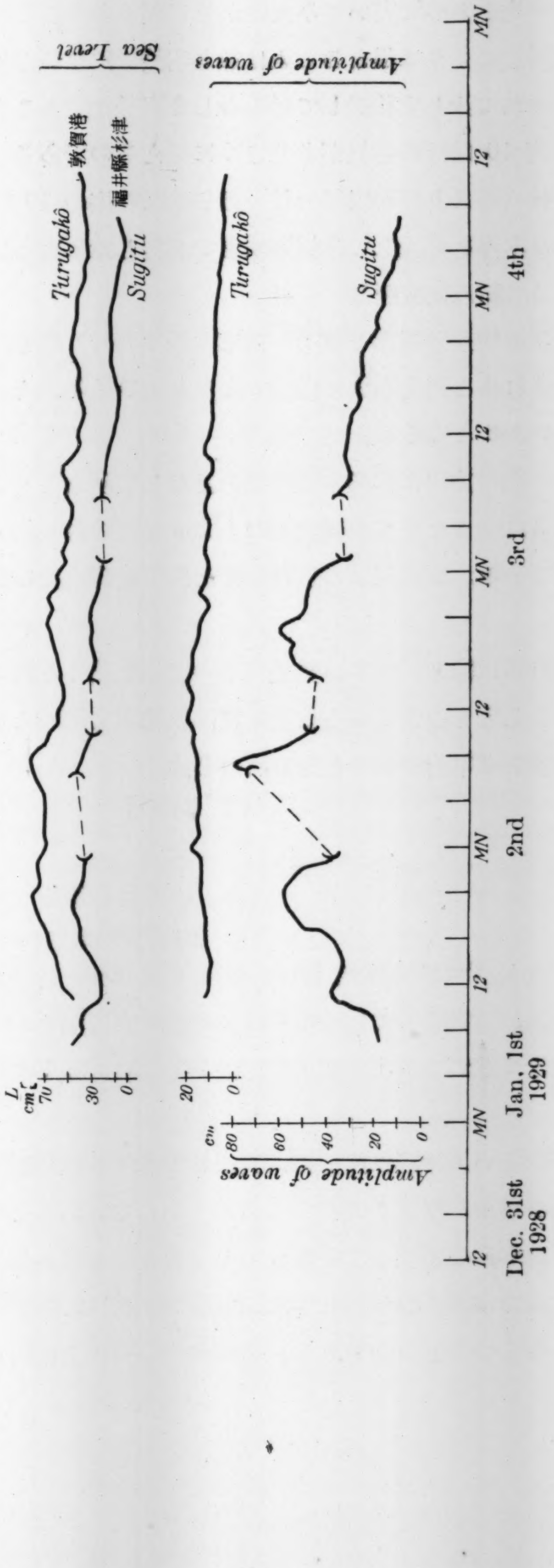
Sea Level
Amplitude of waves
Turugahô
敦賀港
Sugitu
福井縣杉津
Turugahô
Sugitu
L cm
70
30
0
20
0
cm
80
60
40
20
0
Amplitude of waves
12
MN
12
MN
12
MN
12
MN
12
MN
12
MN
Dec. 31st 1928
Jan. 1st 1929
2nd
3rd
4th

Fig. 1b. 第一圖 b.

には小週期の變化が重なつて入つて居て少しく明瞭を缺くから各々3時間だけ重ね掛けた所の6時間毎の平均をとつて畫いてみたのが第二圖である。この圖を見ると海水面の最高位の時刻が場所によりて異なることは餘り明瞭ではないが最南方の敦賀より北東方に進行するにつれて少し宛移動して居るらしき形勢を窺ふことが出來る。而して敦賀と酒田とでは約 10 時間の差異がありさうに見えるのである。故に之を昭和三年十二月三十一日午後六時より昭和四年一月一日午前四時迄の 10 時間に佐渡沖にあつた低氣壓の中心が日本海を通過して津輕海峽まで進行した事實と比較すると次のようなことが想像される（第五圖參照）。

それは前論文（地震研究所彙報第七號第一冊昭和四年六月）にも書いてあるやうに日本海に低氣壓が表はれると對島海峽を通つて海水を吸ひ込み、その爲に日本海全體の水位が高まつたといふことである。

次に長波が日本海の縱の方向に傳播する時間を計算してみると（方法は後に在る）敦賀より酒田まで約3時間となりて曲線記錄の上より見積られる約 10 時間の遲れを說明するには不適當である。故に長波の進行速度を以て最高水位の進みを說明することは困難である。

別問題ではあるが敦賀、輪島、伏木、神通川等の記錄を見ると約12時間若くは 18 時間の週期の副振動らしきものが見ゆる故之を朝鮮及樺太を兩端とする日本海の靜振の週期と見なして海圖より平均の深さを求め次の公式

$$T=\frac{2l}{\sqrt{gh_m}} \qquad \text{但} \begin{cases} T \ \text{は週期} \\ l \ \text{は長さ} \\ h_m \ \text{は平均の深さ} \\ g \ \text{は重力の加速度} \end{cases}$$

を用ゐて計算を試みると $T=11$ 時間を得た。茲に l は 2300 粁 h_m は 1340 米と見積つた。一言 h_m の求め方を謝つて置くならば日本海の表面積を 140 の小矩形に等分してその各の矩形を截口とする水柱の深さを見積りその深さの 140 個の平均をとつて之を h_m とした。

上に求めた 11 時間といふ週期は諸曲線に表はれて居る所の週期と略一致する。之は主なるものは半日の潮汐を意味するのであるかも知れないが又その半日の潮汐や颱風の爲に惹起されて日本海を全體とする靜振が起つたものと考ふることも出來ようかと思ふ。尤も實際には日本海の心中にあつた低氣壓は丁度 12 時間にして日本海を通過し終り津輕海峽まで去つてをるのである。兎に角此の波は上述四ケ所に明白なる記

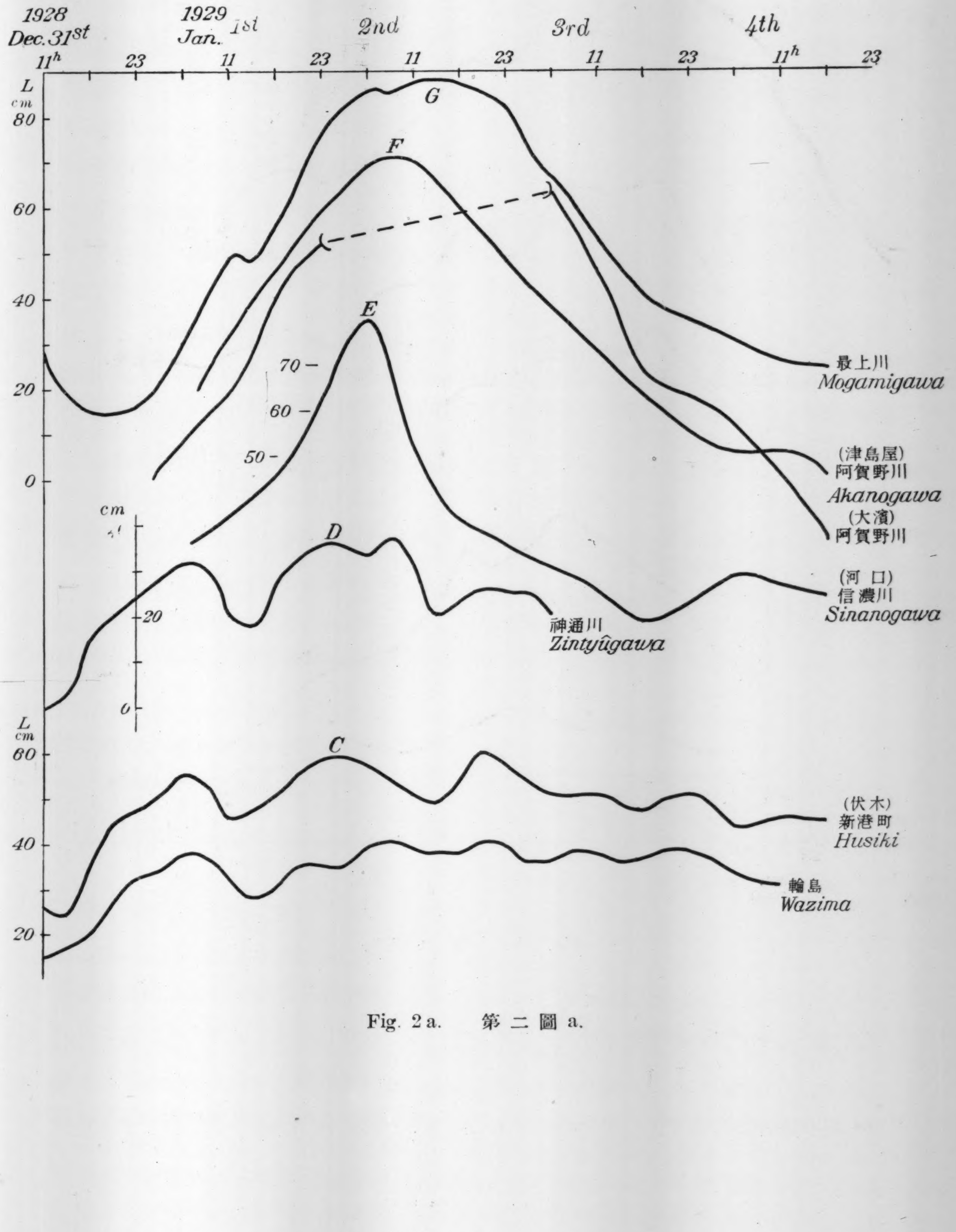
1928
Dec. 31st
1929
Jan. 1st
2nd
3rd
4th
11h
23
11
23
11
23
11
23
11h
23
L
cm
80
60
40
20
0
G
F
E
70
60
50
cm
20
0
D
最上川
Mogamigawa
(津島屋)
阿賀野川
Akanogawa
(大濱)
阿賀野川
(河口)
信濃川
Sinanogawa
神通川
Zintyûgawa
L
cm
60
40
20
C
(伏木)
新港町
Husiki
輪島
Wazima

Fig. 2a. 第二圖 a.

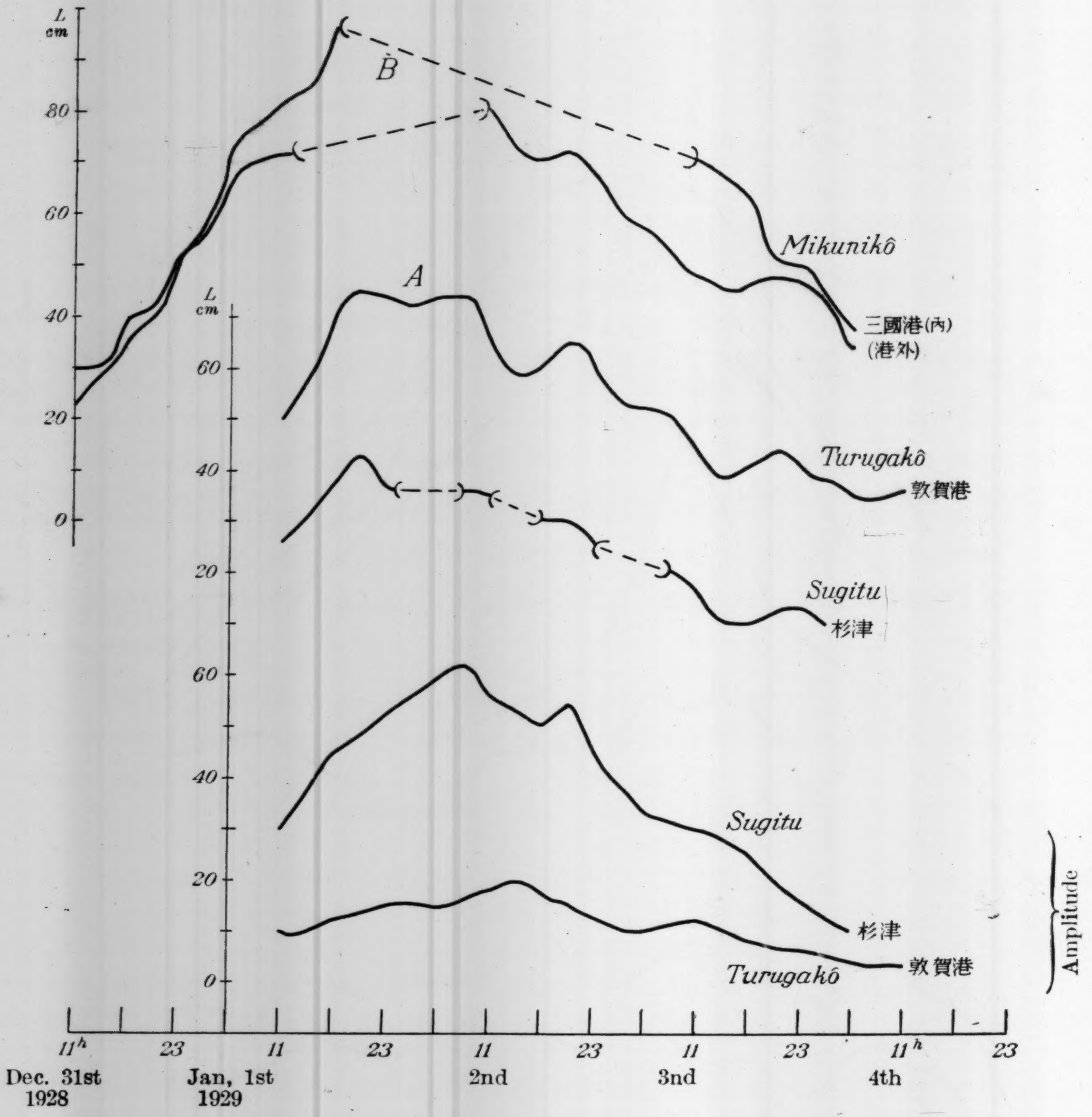
L cm
80
60
40
20
0
B
A
Mikunikô
三國港(内)
(港外)
L cm
60
40
20
Turugakô
敦賀港
Sugitu
杉津
60
40
20
0
Sugitu
杉津
Turugakô
敦賀港
Amplitude
11h
23
11
23
11
23
11
23
11h
23
Dec. 31st 1928
Jan, 1st 1929
2nd
3nd
4th

Fig. 2 b. 第二圖 b.

錄を止め又最上川の線にもその形勢を窺ふことが出來る。他の信濃川、阿賀野川等の曲線は遺憾ながら自記曲線にあらずして定時觀測の値を以て書きたるものなれば之を認むることが出來ない。次に參考の爲に滿洲沿岸及び日本沿岸を兩端とする日本海の横の靜振を考へ前と全く同樣の方法にてその週期を計算してみると

$$T=3{\cdot}8 \text{ 時間}$$

を得る。この場合には $l=900$粁、$h_m=1800$ 米と見積つた

この 3·8時間といふ週期に相當するものは何處の檢潮記錄にも見當らないから恐らくかかる振動は起らないものと思はれる。强いて之を求むるならば三國港の曲線に於て一月一日午前五時以前に約6時間の週期の振動が表はれてをる。併し之は上述の縱方向の振動の倍振動に相當するものと見做した方が穩當であらう。

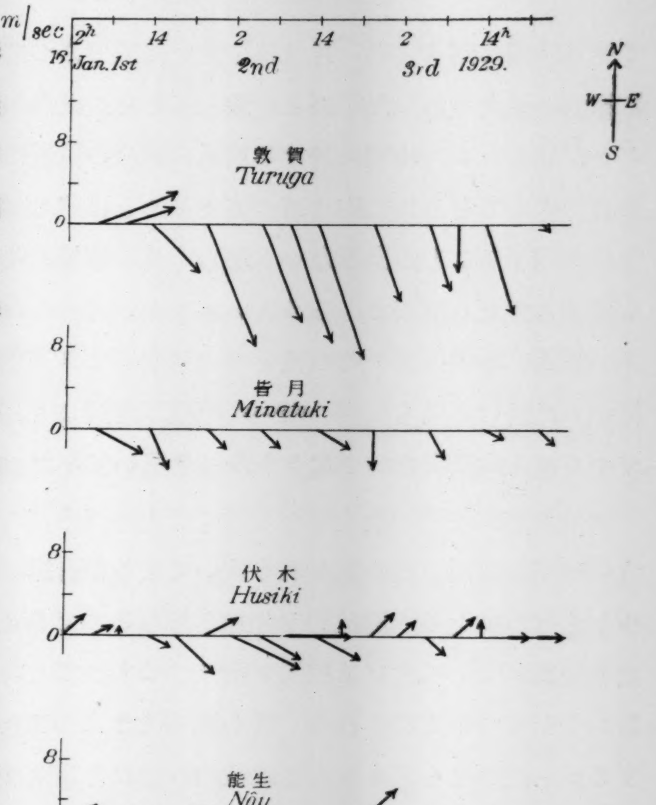

Fig. 3. 第三圖

福井縣杉津及敦賀に於ける波浪の振幅の時間に對する變化を海水面變化と照し合せて見るとその有樣が兩者大方一致してをる。即平均水位の高い時には波の振幅も大にしてそれ等の最大なる値をとつ

て居る時刻は兩者共略一月二日午前七時頃であつて問題の市振村及親不知附近に於ける津浪の最大であつた時刻と一致してをる。此れから水面の上昇が波浪に關係のあることが分る。この時刻に於ける颱風の中心の位置は既に日本海を通過し北海道花咲の沖まで進んでをる故に海水面の高まることは單なる靜力學的の氣壓の影響とのみ考へては說明することが出來ない。恐らく風の影響及その爲に起る波浪の影響が海水面を支配する主なる原因であらうといふことが考へられるのである。そこで敦賀、皆月、伏木、新潟、相川の五ケ所の風を中央氣象臺より寫させて頂き又能生町（親不知に最も近い）に於ける風も出張の際同地築港事務所より伺つてあつたから之等を第三圖に示すやうに4時間置きの**ヴエクトル**圖を畫いてみた。

水位並びに波浪の最大になる前には大略西南西の風が强く吹き丁度波浪や水位の最大の時刻には西北西の風が强く吹いてをるが海岸に於ける風力最大の時刻は之よりも少しく遲れてをる。卽位相の相違を認むるのであるが之は恐らく日本海の沖の方では最初强風が吹いて大なる波浪を造りつつあつても海岸の方は地勢の關係上左程强風でなかつたものかと思はれる。併し風の吹き立つてから波の起るまでは相當の時間を要するから之等をも考ふるときは位相の遲れを說明することは困難になる。又前述の長週期の振動を風の變化より說明してみようとした。卽風の變化は太平洋方面に副低氣壓があることに相當するものと考へて水位及風の變化の週期の關係を比較硏究してみたが甘く說明することが出來なかつた。

以上書き並べた樣に平均水面と風との關係は非常に複雜してをるから風の直接の影響とのみ考へたのでは海水面の變化を充分に說明することが困難となつた。

それ故に前にも述べたやうに低氣壓が海水面を高める機巧としては之に伴ふ土用波式の波浪の影響であるといふことが今回の調査によりていよいよ確らしくなつた。卽海水面の上り下りを論ずるには低氣壓に伴ふ波浪といふことが一つの大切な因子であるといふことが分つた。勿論表面波が水量を運搬して海岸の水位を高めることも考へなければならない（寺田寅彥及山口生知、大正十五年　日本天文學及地球物理學輯報第四卷第一號參照）。

尙この考を確める目的と今一つには特別に親不知、市振村附近のみが津浪の大きかつたのは如何なる理由かを調へる爲に敦賀より酒田まで海岸線に沿ふて之に直角なる鉛直斷面圖を海岸より 18 粁沖まで畫いてみたそれが第四圖である。敦賀より伏木まで能登半島沿岸を傳つて 80 粁每に一ツ宛の斷面圖を畫き伏木より直江津を過ぎ石地

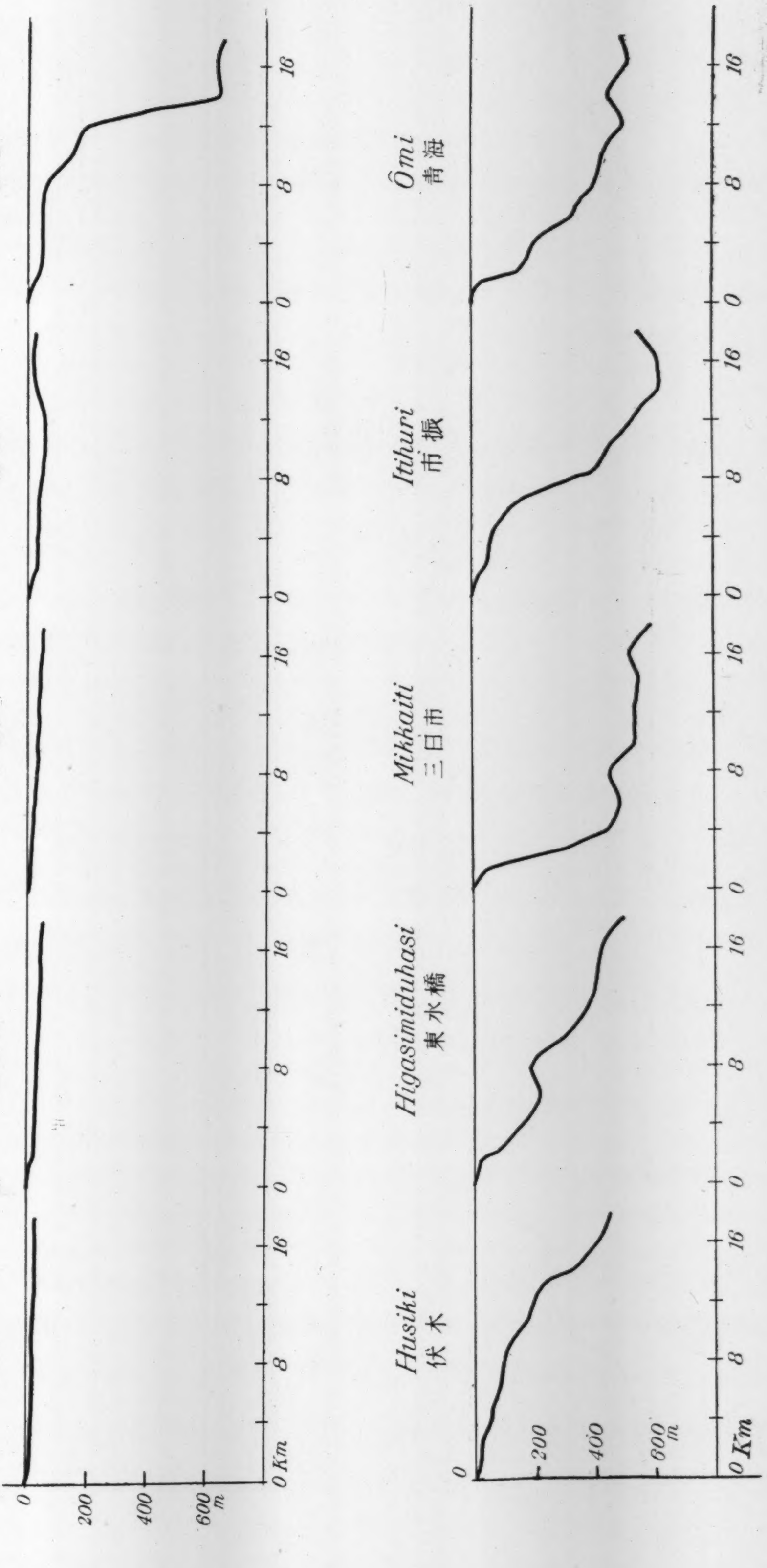
Turuga 敦賀
Mikunikô 三國港
Imahama 今濱
Wazima 輪島
Nanao 七尾
0
200
400
600 m
0 Km
8
16
0
8
16
0
8
16
0
8
16
0
8
16
Husiki 伏木
Higasimiduhasi 東水橋
Mikkaiti 三日市
Ithuri 市振
Ômi 青海
0
200
400
600 m
0 Km
8
16
0
8
16
0
8
16
0
8
16
0
8
16

Fig. 4 a. 第四圖 a.

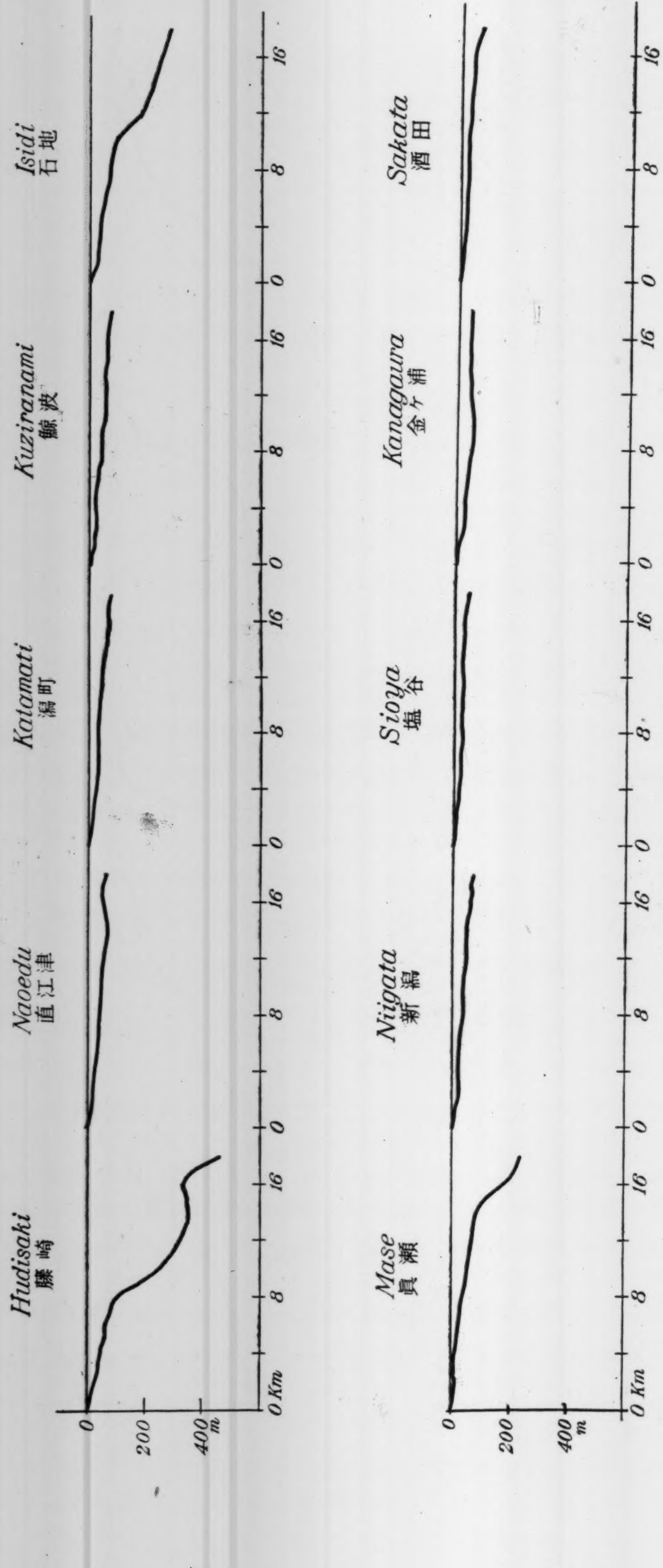
Hudisaki
藤崎
Naoedu
直江津
Katamati
潟町
Kuziranami
鯨波
Isidi
石地
Mase
眞瀬
Niigata
新潟
Sioya
塩谷
Kanagaura
金ケ浦
Sakata
酒田
0
200
400 m
0 Km
8
16
0
8
16
0
8
16
0
8
16
0
8
16

Fig. 4 b. 第四圖 b.

までは特別に 20 粁毎に畫き石地より新潟までは 30 粁毎に又新潟より酒田までは 40 粁毎（最後のみは 50 粁）に鉛直斷面圖を畫いたのである。

之を一見して直ぐに氣の付くことは伏木より藤崎までは他の何れの場所とも桁數を異にして海岸より直に非常に深くなつて居るといふことである。この爲に日本海の沖合より能登半島と佐渡が島との間を通つて押し寄せたと考へられる波浪が親不知、市振村附近では途中少しも勢力を消耗することなく岸まで進んで來た長波と表面波とが二つ重なつて海岸まで打ち上げ反射の理によつて一層高められ又地上の障碍物や摩擦の爲に海水が未だ戻らない中に次の波が打ち上げるといふ具合にして遂に 10 米といふ大きな津浪を起したものと考へられるのである。檢潮曲線に表はれた波浪の振幅だけで 80 糎あり表面波に至つては約 8 米から 10 米に達したといふ人々の話であつた。新潟に於ける波浪の高さに就いては同所測候所長佐々木氏は 9 米と目測され又同所土木出張所主任技師坂田氏は約 6 米と目測された。

而して七尾、伏木邊が同樣に深いにもかかはらず大津浪のなかつた理由は能登半島の蔭に當つてをるといふことと今一つは波の進行の方向がこの附近の海岸線に斜であつた爲と考へられる。親不知附近の現狀を踏査して漁夫等より直接聞いた話を綜合すればこの邊にては寧ろ能登半島を斜後にして海岸線に直角よりも少しく傾ける方向に進んで來た形勢がある。兎に角波が海岸に斜に打ち寄せたといふことについては市振村の津浪被害狀況を視察して面白い事實を發見したのである。それは外波川といふ川幅僅かに 10 米を過ぎない小川の左岸に在つた三軒の家は右岸に建ち並んでをる多くの家よりも約 2 米も高いかと思はるるにかかはらず破損がひどいのでその土地の者に聞いてみると津浪は川の左岸の方向より襲つて來たとの話であつた。卽波の進行の方向は岸に向ふ分方向の外に岸に平行なる分方向も有してをつたことが想像される。

結　　論

低氣壓の中心の進行狀態は第五圖に示す通りであつて中心が日本海に在る間は海岸に於ける風浪は割合に靜かで水位も次第に高まりつつあつたが最大値には達して居ない。低氣壓が北海道方面に去つた後に於て風浪大となり海面は益々高まり又大津浪が起きてをる。卽日本海の特徵として低氣壓の通過に對し海水面の上昇も風浪の起るのも可なり長い時間の位相の遲れがあることが分つた。

神通川附近では平均海水面は左程高まらずして大津浪が襲來して居るが之に反して新潟、酒田等に於ては平均海水面は他の何れの場所よりも著しく高まつてをるにもか

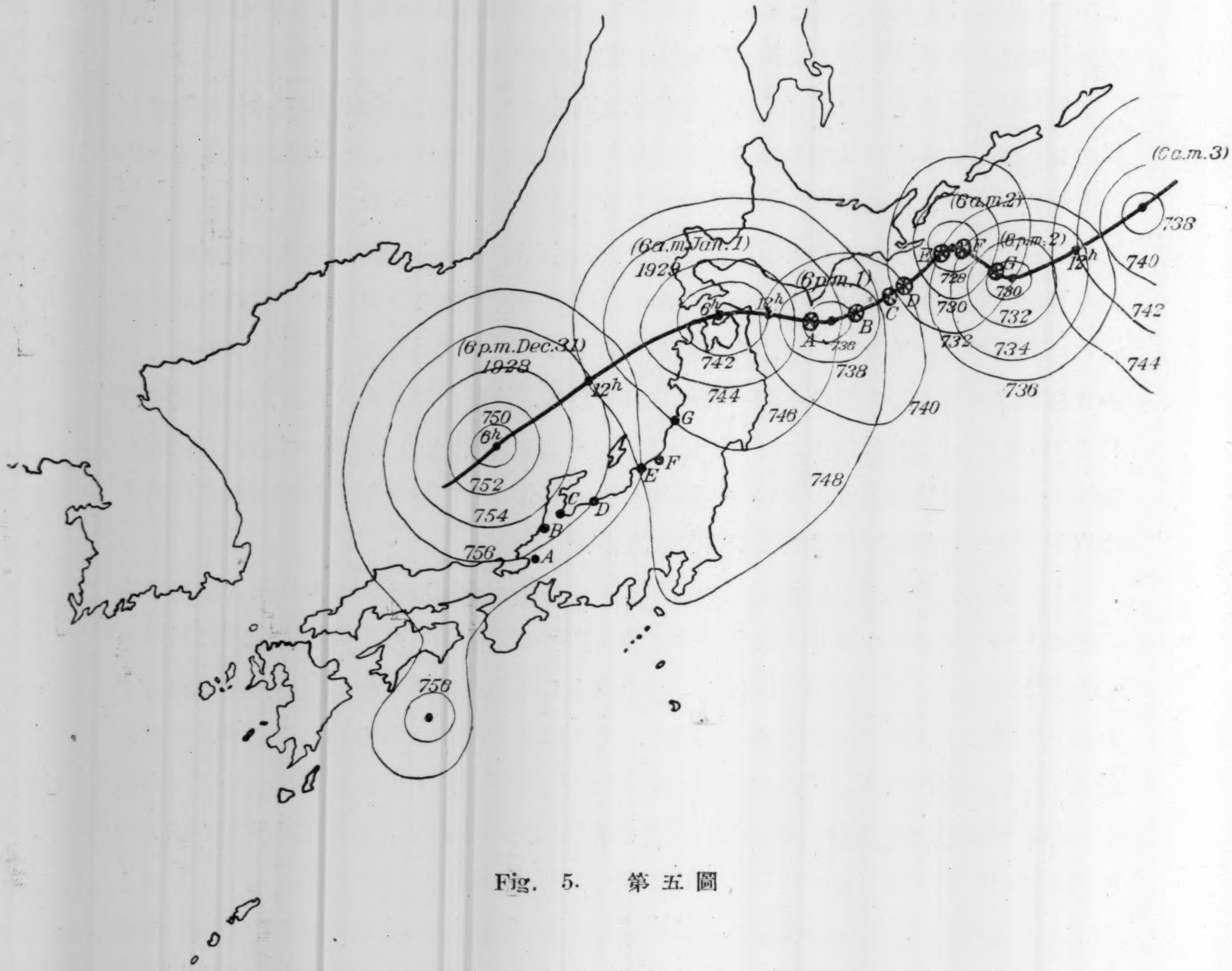
(6 a.m. 3)
738
(6 a.m. 2)
(6 p.m. 2)
740
742
744
12h
728
730
732
734
736
(6 p.m. 1)
A
B
C
D
E
F
G
736
738
740
(6 a.m. Jan. 1)
1929
6h
12h
742
744
746
748
(6 p.m. Dec. 31)
1928
12h
750
6h
752
754
756
A
B
C
D
E
F
G
756

Fig. 5. 第五圖

かはらず津浪の襲來は殆んどなかつたのである。之は卽土用浪が押し寄せたときに神通川附近は海岸より急に深く、而も新潟、酒田等の海岸に比すれば深さの程度を異にしてをる爲勢力の衰滅せざる波が陸地に打ち上げられ前に述べたやうな具合にして大津浪の被害を及ぼしたものと考へらる。卽局部的の津浪が起きたものであるからそこより少しく離れた場所の平均海水面は左程高まらなくともよいこととなる。而るに、新潟、酒田の如き海岸は遠淺であるから波浪が押し寄せた場合に淺海底の摩擦の爲に波浪は前方に倒潰して水の移動を生じ、しかも海底の逆流は妨げられる爲に徐々に水面が高まりその間に波浪の勢力は長い距離の間淺海底の抵抗の爲に衰滅して親不知附近の如き大津浪を起さなかつたのであらう。

以上の考察により日本海輪島附近の海水面變化の原因は氣壓の靜力學的影響や風の直接の影響のみを考へたのでは不充分であつて寧ろ低氣壓に伴ふ所の波浪の影響がその主なるものであるといふことが明瞭となつたのである。勿論波浪の影響を以て低氣壓の海水面に及ぼす影響を悉く説明し得るや否やは尙問題となる處である。

終りに臨み始めより終りまで常住に寺田博士の御懇篤なる御指導の下に本研究を遂行することの出來たことを玆に深く感謝する次第である。

それから又內務省新潟土木出張所長　青山氏同所主任技師坂田氏、最上川改修事務所主任技師坂上氏、伏木港修築事務所主任技師大島氏、敦賀港修築事務所主任技師千田氏、福井縣土木課長青木氏等の各位より貴重なる檢潮曲線の寫しを頂戴し又種々なる便宜を與へ下さつたことに對して深謝の意を表し度いと思ふ。又上記の方々に御紹介下さつた內務省土木試驗所の物部所長及び靑木技師に對しても感謝の意を表し度い。

又新潟測候所長佐々木氏、伏木測候所長若崎氏、福井測候所敦賀出張所の一宮氏より種々有益なる御話を承つたので玆に厚く感謝の意を表する。尙上記測候所長宛御紹介頂きました藤原博士に對しても深く御禮を申し上げ度いと思ふ。

---

31. *Abnormal Rise of Sea Level in the Japan Sea Coast, on Jan. 2, 1929.*

By **S. YAMAGUTI.**

In a previous paper,[1] the report was given of the results of the investigation regarding the conspicuous effect of cyclone upon the sea level. The physical meaning of the relation found was, however not yet elucidated, though some dynamical effects of waves due to the cyclonic winds have been suggested.

On Jan. 2, 1929, a train of abnormally high waves, 10 metres in height, probably generated by the cyclone which was then passing over the Japan Sea, swept and wrought much havoc on the shore near

---

[1] T. TERADA and S. YAMAGUTI, *Proc. Imp. Acad.*, 4 (1928), No. 8; S. YAMAGUTI, *Bull. E. R. I.*, 7 (1929), Part. 1.

Oyasirazu, in Etigo. It was considered that, we may be able to find a clue for explaining the mechanism as to the effect of cyclone upon sea level, if we investigate the details of the phenomena connected with these destructive sea waves.

The mareographic records of various stations along the Japanese coast of the Japan Sea, kindly placed at my disposal by the Authorities of different Divisions of the Public Works, Home Department, were taken as the material of the investigation. The sea levels of these stations, also the amplitudes of waves in the case of Turuga and Sugitu, in Etizen, were plotted in the same scale against the time as abscissa, as shown in Fig. 1. Next, to eliminate the irregular fluctuation of shorter periods, the mean of the sea level, also of the amplitudes of waves for the last mentioned two stations for successive intervals of 6 hours, overlapping by 3 hours, were taken and plotted as before as shown in Fig. 2.

The data for the winds at Turuga, in Etizen; Minatuki and Husiki, in Noto; Aikawa, in Sado; and Niigata, were taken from the original register of the Central Meteorological Observatory. The data for the wind at Nôu, in Etigo, which is the nearest to the station in question, Oyasirazu, were furnished by the Harbour-construction Office of that place. The vector diagrams for these data were plotted on the time axes, as shown in Fig. 3.

We can see from Fig. 2 and Fig. 3, that the time for the maximum amplitude of waves coincides with maximum of mean sea level, and that the change of sea level cannot be explained well with the direct influence of winds. Therefore, we may infer that the main effect of cyclone upon sea level is to be considered as some effect of waves due to the cyclonic winds.

To test this idea, we constructed the profile curves of the sea bed in a number of vertical sections, (Fig. 4) perpenducular to the coast line, up to 18 km. from the coast. About 20 such sections were taken along the coast extending from Turuga, in Etizen, to Sakata, in Uzen.

Looking at Fig. 4, we can see at first glance that the sea bed near Oyasirazu is of a remarkably steep slope and the depth of the coast is of a higher order of magnitude than those off Niigata and Sakata. Therefore, it is considered that the less damped waves, advancing through the space between the Sado Island and the Noto Peninsula, have arrived at the coast in question and enhanced by a partial reflection, have wrought a great damage. On the other hand, the energy of waves which have attacked the seashores in the vicinities of Niigata and Sakata has been greatly damped by the friction of the shallow sea bottom in travelling a long distance before reaching the shore, and consequently the waves in these parts of the coast have not given much damage, except that the general sea level was raised about one metre, whereas the rise of the mean sea level near Oyasirazu was not so conspicuous.

Thus, it will be seen that the effect of waves due to the cyclonic winds must be considered as one of the important factors governing the variation of the sea level. The cyclonic effects investigated in the previous reports seem, therefore, to be intimately connected with this effect of waves, though it is not clear whether the latter effect covers the entire amount of the former effects.

32. 自働車、汽車の振動測定を目的とする加速度計

（第一部） 水平動測定

地震研究所 { 石本巳四雄
高橋龍太郎

（昭和四年九月十七日發表—昭和四年九月二十日受理）

1. 緒言

自働車、汽車等の交通機關において其の運轉中の車體振動狀況、或は車の進行狀態等は、運轉の巧拙、車體の構造、發動機の狀態、路面又は軌道面の良否に密接な關係を持つ事は明かな事である。其れ故此等運動の精密測定は以上の交通機關の進步改良及び路面又は軌道の良否の判定に役立つ事が多い。然も其の振動の測定は、加速度を目的とする事が最も重要であり、意味あるものとなる事は當然の事である。

加速度計には種々の原理に基いて設計製作されたものが數種あるが、其の中或るものは最大加速度を測定するものであつて、振動の周期、形式迄も知る事は出來ない。記錄式の加速度計であつても其の中には一箇所に据付け、例へば地震動の加速度を測定する目的のものもあつて、自働車、汽車等に搭載して疾行しつゝ其の振動を記錄し滿足の結果を與へるものは殆ど無い。

本論文に記載した加速度計は、土木試驗所の依賴によつて設計製作したものであつて、自動車、汽車等に搭載して、車體の水平加速度を記錄せしめる目的のものである。其故に (1) 形狀が小さくて、自動車の坐席の如き狹隘なる場所にも載せられる事、(2) 取扱が簡單で、何等調整も要しない事、(3) 構造が頑丈で、激しい振動に堪えうる事、等の條件を充す樣に設計製作したものである。

2. 原理

加速度計には種々の原理に基くものがあるが、其等については著者の一人の論文[1]

---

[1] M. Ishimoto, *Bull. Earthq. Res. Inst.*, **3** (1927), 87.

中に詳しいから此處には省略する。本論文の加速度計も矢張上記の原理の一つに基いたもので、其の使用の目的に最も便宜と思はれる振動系の原理に基準するものである。今此の如き自己振動の周期を有する加速度計の理論を簡單に說明し、振動系が加速度計として働く場合に滿足すべき條件を求めて見やう。

今第一圖の如き振動系を考へ、

ξ　重錘 M の空間に對する坐標

x　枠 F の空間に對する坐標

$y=\xi-x$　重錘 M の枠 F に對する坐標

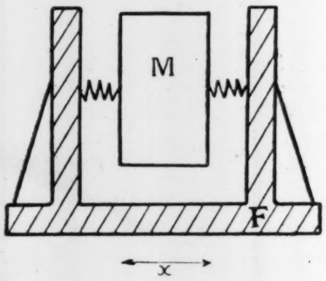

第一圖

とする時は、重錘 M の運動の式は

$$M\ddot{\xi}+2\varepsilon(\dot{\xi}-\dot{x})+k(\xi-x)=0,$$

又は

$$M\ddot{y}+2\varepsilon\dot{y}+ky=-M\ddot{x}$$

となる。今

$$2\varepsilon/M=2\lambda,$$

$$k/M=n^2,$$

$$\ddot{x}=-F\sin pt$$

と置く時は

$$y=e^{-\lambda t}[C_1\sin\gamma t+C_2\cos\gamma t]\quad+\frac{F}{\sqrt{(n^2-p^2)^2+4\lambda^2p^2}}\sin(pt-\delta)$$

となる。但し

$$\gamma=\sqrt{n^2-\lambda^2},$$

$$\delta=\tan^{-1}\frac{2\lambda p}{n^2-p^2},$$

C_1, C_2 任意常數

若し重錘の減衰のない場合の固有振動周期が、測らんとする振動の周期よりも非常に短い時卽ち $n>>p$, ならば

$$y=\frac{F}{n^2}\sin pt+e^{-\lambda t}[C_1\sin\gamma t+C_2\cos\gamma l]$$

となり、若し此の運動系が相當の減衰度を有す場合においては、固有振動である第二

項は速かに減衰して了ふから、結局重錘の器械に對する動きは測らんとする加速度と同じ形となり、之に依つて加速度が求められる事となる。然し乍ら此の場合、器械の不減衰の場合の固有振動周期を T_0 とすると

$$n=\frac{2\pi}{T_0}$$

であつて T_0 の小さい程 y は固有振動周期 T_0 の自乘と比例して小さくなるから、此の重錘の動き y を記録するには大きな倍率の擴大裝置を要する事となる。此の如く、重錘の固有振動周期を測らんとする振動周期に比して非常に短くし、高倍率の擴大裝置を使用する事によつて加速度計が實現されるのであるが、實際の振動は複雜で可成りの短周期の振動も含んでゐるのであるから重錘の固有振動を此に對して無限に少さくする事は不可能となる。又假令實現し得たとしても倍率を非常に大きくしなければならぬから、此の問題でも行詰るのである。固有振動の周期が測らんとする振動の周期より左程大きくない場合には、强制振動の項の係數は

$$A=\frac{F}{\sqrt{(n^2-p^2)^2+4\lambda^2p^2}}$$

となる。今

$$\lambda/n=S$$

と置くと $p/n=T_0/T$ であるから

$$A=\frac{1}{\sqrt{\left(1-\frac{T_0^2}{T^2}\right)^2+4S^2\frac{T_0^2}{T^2}}}\cdot\frac{1}{n^2}$$

となり T/T_0 と S との値によつて n^2f は第二圖の如き値を取る。從つて減衰係數を適當に取れば $T>3T_0$ の範圍に對して略均一の感度となり、T が夫より小さくなるに從つて感度が落ちて $T=0$ に於て感度は零となる。

周期的の振動に於ては、加速度は $4\pi^2a/T^2$ で與へられるのであるから此の量は T が小となれば非常に大となる、それ故若し加速度計の感度が $T=0$ に至るまで均一であるとすれば、斯樣な加速度計に依つて得られる記錄には、短周期のものゝみが著しく表れ、周期の長い加速度は殆ど隱されて了ふのである。又減衰率が零の場合に於いては $T=T_0$ の所で感度が無限大となり、記錄には T_0 の周期のものゝみ異狀に擴大される事も事實である。然し乍ら此樣な短周期の加速度は吾々が力として感ずる性

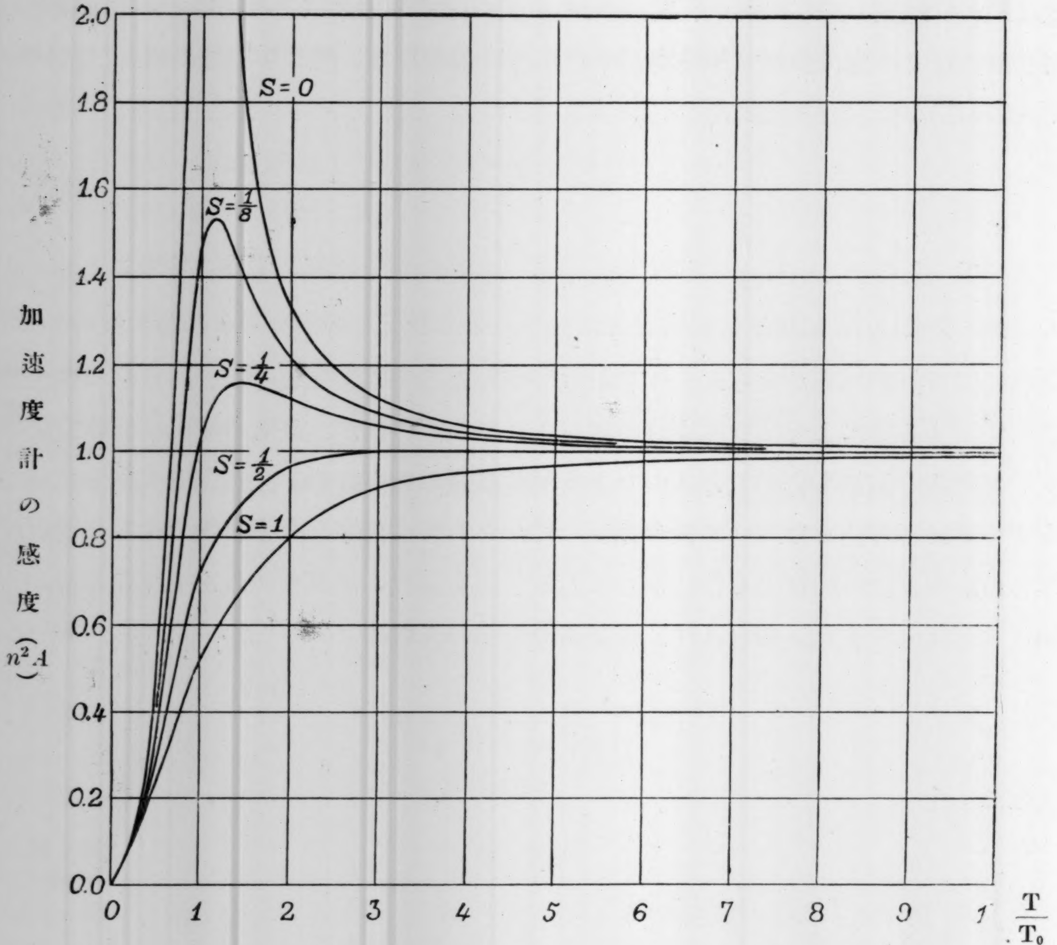

第 二 圖

質のものではないのであつて、吾人は此を一種の振動又は衝撃として取扱はなければならない。なほ材料の强弱を論ずる場合においても、此等の振動は周期が小であると云ふ理由の下に其の變位の割に非常に大なる加速度を與へるには相違ないが、之を長週期の、變位の大なる振動と、加速度が等しいからと言つて、同等に取扱ふ事は出來ない性質のものである。以上の如き理由により工學上の立場においては加速度計の周期、減衰率を適當に選んで、必要以下の周期に對し、感度を急激に低下せしむる方法を採用する事が望ましい事である。

尙ほ一方に於て測らんとする加速度と重錘の動きとの間の位相差 δ を考ふるに

$$\delta=\tan^{-1}\frac{2\lambda p}{n^2-p^2}=\tan^{-1}2S\frac{T_0/T}{1-\left(\frac{T_0}{T}\right)^2}$$

であつて S と T との値によつて第三圖に示すが如き變化を爲すのである。之によつて觀るに S の大きい場合程、又 T の小さい程位相差は大となる。

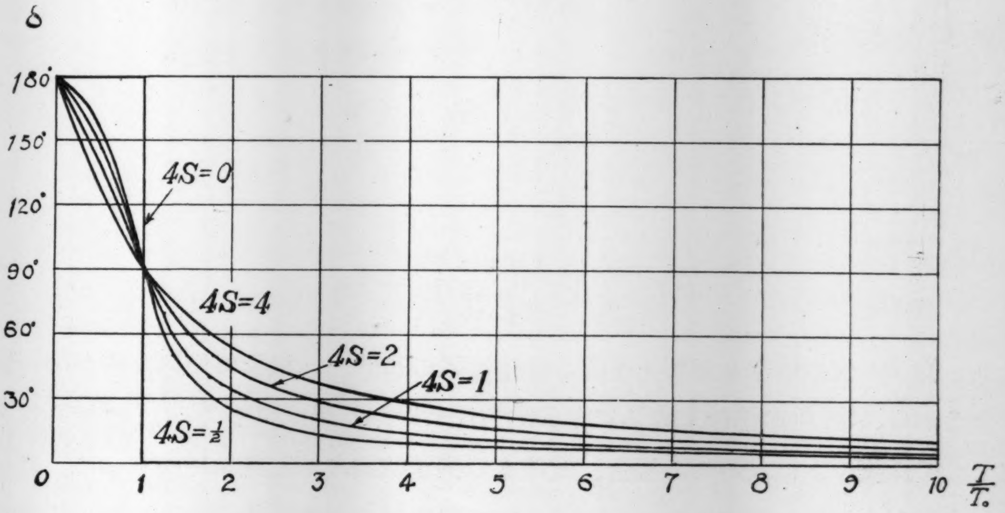

第三圖

即ち S が小さい場合は位相差の方は都合よきも感度の方に於て不都合を來し、S が大きければ感度の方は都合がよいが、位相差の方で不都合となる。

T/T_0 の小さい所を論ずる場合には何れか一方を犧牲にする事を要する。其の何れを捨て、何れを取るかは目的に追從するのである。然し乍ら實際上加速度計に自己振動が減衰されずに存在して居る時は、波形を崩す上に、記錄に決定的の打擊を與へるものである故、位相差の方を捨てゝも減衰度を適當にして感度を都合よくする事に努力しなくてはならない。兎もあれ T の比較的大な所においては位相の差は殆ど問題とならない。

3. 設計

前項に於て述べた如く、減衰係數が適當である場合においては、固有振動の數倍より長い周期の振動に對して、殆んど均一の感度を有し忠實に實際の振動を記錄するものゝ實現は可能である。從つて固有振動周期の小なる程忠實に記錄する範圍は擴大される。但し其と共に設計の困難も擴大されるのである。實際上餘り短い周期まで均一の感度にて忠實に記錄するときは加速度といふものゝ性質上、却つて適當でない場合が屢々存在する。此處に記載する加速度計の目的にあつては 0·1 sec. 程度の振動まで

を忠實に記錄すれば充分であると云ふ理由から設計に當つて先づ第一に固有振動の周期を 0·03 sec. と定めた。

次に重力の加速度 g に相當する加度速が記象紙上に 1 cm. の振れとして表れる爲の倍率 K を求めるに

$$K\frac{g}{n^2}=1\text{ cm.}$$

即ち

$$K=\frac{n^2}{g}=\frac{1}{g}\left(\frac{2\pi}{T_0}\right)^2=45$$

となり、約 50 倍の倍率を必要とする。此の器械の目的上、取扱に便利な事が第一條件であるから、50 倍の倍率を得るに光學的方法を用ふる事は出來ない。機械的擴大法によつて煤紙の上に書かせる場合、幾段もの機械的擴大法を重ね用ゆる事は、自働車の如き激しき振動を爲すものに於ては、徒に振動部分が多くなるのみにて、折角得られたる記錄が正しいものでなく何の振動を記したものであるか頗る疑しい事となる。故に此處に述べる加速度計に於ては機械的一段擴大法を採用して、各部の連結方法、記錄針の形狀等に特に留意して、此等の部分の振動を極力却除する樣に努めたのである。記錄針の形狀を後項に述べる如きものと爲した理由は、普通地震計等に用ひらるゝ型式のものにては、上下動によつて針先が飛上り確實に振動を記錄する事が期し難いからである，

但し此樣の形にしたる爲に針先に於ける摩擦が多少大となる事は止むを得ない。針先に於ける摩擦の大いさを調べる爲に著者等は次の如き實驗を爲した。即ち加速度計の廻轉軸 a（後出第八圖參照）と重錘 M とを連る棒 l を取はづし、加速度計を針が下向になる樣の向に垂直に立て、針に振子運動をなさしめ、其運動をドラム D の上に書かしめた。針先がドラムに觸れる狀態を水平に置かれた場合と同一になる樣注意した事は勿論である。但し針に振子運動を爲さしめる爲に小重錘を針の中途に附加した。但し記錄針が垂直即ち重力の方向と一致してゐる故此の小重錘は針先の摩擦の大きさには影響しない。

摩擦の力は常に一定の大きさで、速度を減じる方向に働くから、針の運動の式は

$$I\frac{d^2\theta}{dt^2}\pm fL+mgl\,\theta=0.$$

但し	I	記錄針及小重錘の慣性能率
	L	記錄針の長さ
	l	記錄針及小重錘系の重心迄の距離
	m	記錄針及小重錘系の重量.

$$\frac{d^2\theta}{dt^2}\pm\frac{fL}{mk^2}+\frac{gl}{k^2}\theta=0.$$

但し　$I=mk^2$

$$\theta=A\sin\sqrt{\frac{gl}{k^2}}\,t\pm\frac{fL}{mgl}.$$

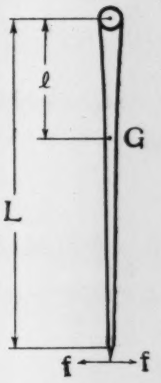

第四圖

卽此振動は振動の向に依つて零點の動く場合であつて、共の振幅は一定量宛減ずるのである(第五圖)。今記象紙上の偏れを δ とすると

$$\delta=L\theta=AL\sin\sqrt{\frac{gl}{k^2}}\,t\pm\frac{fL^2}{mgl}.$$

從つて順次極大振幅の値は

$$\delta_0=AL,$$

$$\delta_1=AL-\frac{2fL^2}{mgl},$$

$$\delta_2=AL-\frac{4fL^2}{mgl},$$

$$\delta_{2n}=AL-\frac{4nfL^2}{mgl},$$

$$f=\frac{mgl}{4nL^2}(\delta_0-\delta_{2n}).$$

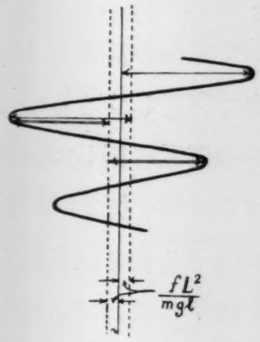

第五圖

此式の $m\,l\,L$ 等に夫々其値を入れて得た f の値は 50·2 dyne となる。故に倍率 50 の場合においても重錘の質量が 15 kg あれば $\frac{g}{100}$ 程度の小加速度に對しても何等の影響を持たぬ事となる。

次に記錄針の慣性能率の影響を考へて見やう。本加速度計の針は第六圖の如き形であるが今之を三角形であると考へ、且全體が同じ厚さであると考へる。此の樣にして計算した針の慣性能率は實際のものより大きくなる。針の慣性能率 I は

$$I=m_1\left(\frac{c^2}{4}+\frac{d^2}{3}+e^2\right)+\frac{m_2}{6}(a^2+b^2).$$

但し m_1, m_2 は夫々平衡錘及記錄計の質量。之に實際の値を入れる時は

$$I=178\ \mathrm{C.G.S.}$$

となる。今重錘 M と針とを連る棒 l が針と接する所と、針の廻轉軸との距離を r とすると

$$I\omega<<Mvr\ \ (v=r\omega).$$

$$\therefore\ \ \frac{I}{r^2}<<M$$

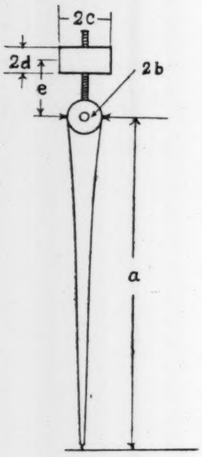

第六圖

でなければならない。r は 0·36 cm. であるから $I/r^2=1363$ gr. となる。即此の針の慣性能率の影響が省略しうる爲には M は少くとも此の十倍以上の 15 kg. の質量を要するのである。

從つて重錘の質量を 15 kg 以上に取れば先づ針の慣性能率の爲の影響、針先の摩擦の影響は省略しうるものと見做して差支ない。

重錘の運動に對して振動力を與ふるものとしては、前論文に記載した樣に重錘の兩面にゴムの輪を置き其の彈性を利用する型式を採用した。ゴム輪を用ひる理由は、此が後に述べる如き減衰作用を與へるのに同時に役立つからである。今此のゴム輪の大きさを求めるに、ゴムのヤング率を E、厚さを H、內徑及外徑を夫々 d 及 D とすれば

$$T_0=2\pi\sqrt{\frac{MH}{2EA}}$$

但し $A=\frac{\pi}{4}(D^2-d^2),$

而て $T_0=0\cdot03$ sec.,

$E=2\cdot1\times10^7$ dyne/cm^2,

$M=15\times10^3$ gr.

であるから

$$\frac{H}{D^2-d^2}=0\cdot0484$$

となる。從つて此樣な値になる H, D, d の組合せならば何でも宜しい筈であるが、使

用上ゴム輪の幅と厚さとは略同じ位でなければならないし、H, D, d 等を非常に大きくしても、又小さくしても不便であつて、其の程よい所は自然と限られる。實際に當つては $D=14{\cdot}5$ cm. $H=2$ cm. $d=13{\cdot}5$ cm. のものを用ひる事にした。之の値では $H/D^2-d^2=0{\cdot}0485$ となる。

次に減衰裝置であるが油を用ひたるものは器械使用上不適當である。この器械に於いてはゴム輪と重錘との間の空隙內の空氣を重錘を支ふる壁體に穿つた細孔を通じて出入せしめ、減衰を惹起さしめる役目をさせる事とした。今第七圖に於て

r	細孔の半徑
l	細孔の長さ
A	空隙の切斷面積
P	空隙內の壓力
Π	外氣の壓力
v	空隙の體積
x	重錘の坐標

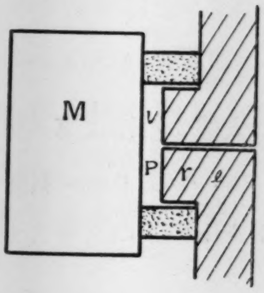

第七圖

とする時は

$$A\,dx=\frac{v}{\gamma P}\,dP+\frac{P^2-\Pi^2}{P}\,\frac{r^4}{16\pi\eta l}\,dt,$$

今 $\dfrac{r^4}{16\pi\eta l}=B$, $P\approx\Pi$ と置けば

$$2\gamma B\,(P-\Pi)=\gamma A\,\frac{dx}{dt}+\frac{v}{P}\,\frac{dP}{dt},$$

今若し A を大きく v を極小さく取る時は、空氣を不可壓縮流體と考へて差支へなく從つて減衰せしめる爲めに働く力は $A(P-\Pi)$ であり、

$$2\gamma B\,(P-\Pi)=\gamma A\,\frac{dx}{dt}$$

であると見ても先づ差支ない。故に

$$\begin{aligned}A\,(P-\Pi)&=\frac{A^2}{2B}\,\frac{dx}{dt}\\&=\frac{8\pi\eta l}{r^4}\,A^2\,\frac{dx}{dt},\end{aligned}$$

従つて

$$2\varepsilon=8\pi\eta l A^2/r^4,$$

$$\lambda=\frac{4\pi\eta l A^2}{Mr^4}$$

となる。前項に於て述べた如き減衰係數を得る爲には　$S=\frac{\lambda}{n^2}=\frac{\lambda T_0^2}{4\pi^2}=\frac{1}{2}$　から $\lambda=1{\cdot}37\times10^2$ 附近である事を要する。之によつて細孔の直徑を算出するに $\eta=1{\cdot}8\times10^{-4}$, M, A は前述の如き値として $r^4/l=1{\cdot}925\times10^{-5}$. となり, $l=1$ cm. とすると $2r=0{\cdot}13$ cm. となる。

4. 製作

機械の大體の構造は第八圖及第九圖（圖版 XLI）に於て見らるゝ通り重錘 M は直徑 17 cm. 厚さ 6 cm. 質量 15·2 kg. あつて、b_1, b_2, b_3, b_4 なる兩壁 W_1 W_2 を連結する四本のボルトの上の二本より吊されてゐて水平の方向に振動しうる。壁 W_1 W_2 は厚さ 4 cm. あり、且外面に三角形のリム二本を有してゐて、重錘 M に g の加速度が働いた場合にも 1 μ 以下の偏れしか起さぬ様に設計されてゐる。W_1 W_2 と重錘との間には蛇の目形のゴムパツキング P_1 P_2 が夾まれてゐる。此のゴムパツキングの厚さは 2 cm. 內徑及外徑は夫ゝ 13·0 cm. 及 14·5 cm であつて、E は $2{\cdot}1\times10^7$ C.G.S であるから 15·2 kg の重錘に對して 0·03 sec. の周期を與へる。後部の壁 W_2 には直徑 1 mm. の細孔が穿れ、ゴムパツキングに依つて圍まれた W_2 と M との間の空隙 v 內

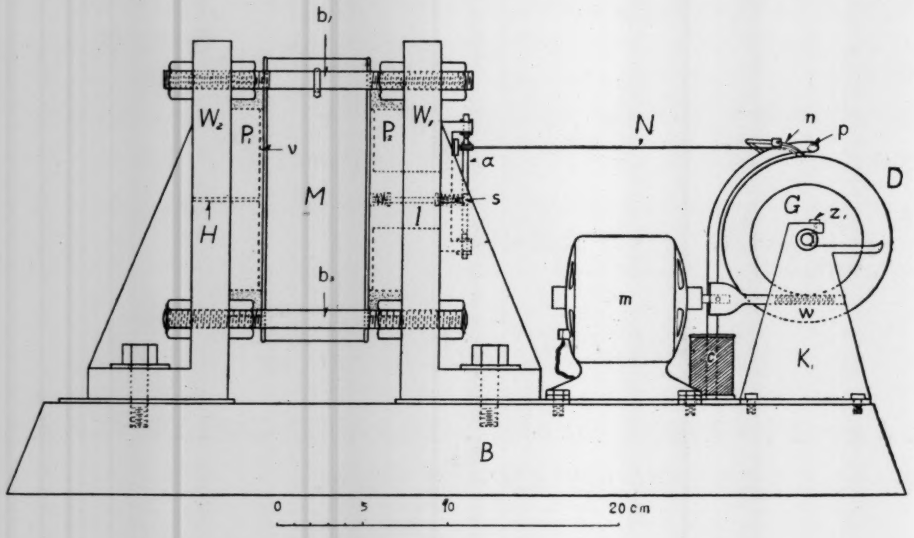

第　八　圖

の空氣の出入によつて制動作用を得る様になつてゐる。v の空隙は W_2 の一部をなす圓板によつて狹められ約 0·05 cm. の厚さになつて居る。

重錘 M の運動は、小棒 l によつて直接小金屬片 s に傳へられ、a 軸の廻轉運動に變ぜられるから同軸に附せる記錄針 N の廻轉を起すのである。l の兩端は尖端を爲しその兩端にあるバネに據つて夫れ夫れ M 及 s にある凹皿中に、押付けられてゐる。l の先端と a 軸の中心との距離は 0·36 cm. 記錄針の長さは 18 cm. であるから、此處で重錘の運動は 50 倍に擴大される事となる。記錄針 N は根元に於て幅 1 cm. 厚 0·05 cm. 先端より 1 cm. の所にて幅 0·2 cm. 厚 0·02 cm. あり全部鋼板にて作られてゐる。其の先端は特に注意して磨き上げ、燒入を施してある。此の針は彈力を以て輕くドラム D に押付けられてある。ドラム D は直徑 10 cm. 幅 10 cm. にして 0·8 cm. の心棒を有し 0·4 cm. の步みを以て軸受 K_1 K_2 內に廻軸しつゝ橫に移動する。ドラム D はピン Z_1 Z_2 を K_1 K_2 より拔き取る事によつて齒車 G を心棒にはめたまゝ軸受から取はづし得る樣になつてゐる。ドラムを廻轉せしむる動力としては 1/30 H.P. 6 volt の直流電動機 m を用ひ、其の廻轉は 150 齒の芋蟲車 W, G に依つてドラムに傳へられる。電動機の廻轉は電流の加減によりドラム上一秒間 0·5 cm.—5 cm. の任意の記錄速度を得る事が出來る。

尙ほ時刻を入れる爲に別に小針 n を附けコイル c によつて勵磁される極片 p によつて吸上げられる樣になつて居る。n の畫く線は、同時に又 N の畫く曲線の零線としても役立つのである。

機械全體は幅 32 cm. 長さ 55 cm. の臺 B の上に取附けられ、箱詰容積は 32 cm. × 55 cm. × 28 cm. 總質量 60·6 kg. である。

5. 實驗室內試驗

此樣にして作られた加速度計の感度と特性とを調べる爲に三種の試驗を行つた。

先づ第一に滑車に通じた絲の一端を加速度計の重錘 M に結び、他端に重量をかけ、重錘 M に靜力學的の水平力を加へて、其に依つて生ずる加速度計の偏れを測定した。其の結果は第十圖の樣になる。此に依つて見ると加速度計の偏れは加へた重量と略ゝ比例する事が分る。此の圖から加速度計の感度を算出すると g の加速度に相應して 0·9 cm. の偏れを與へる事になる。只た負荷が大きくなると感度が大きくなる傾向のあるのは、ゴムパツキングの幅が厚さに比して少しく小さい爲に、變位の大きい時に

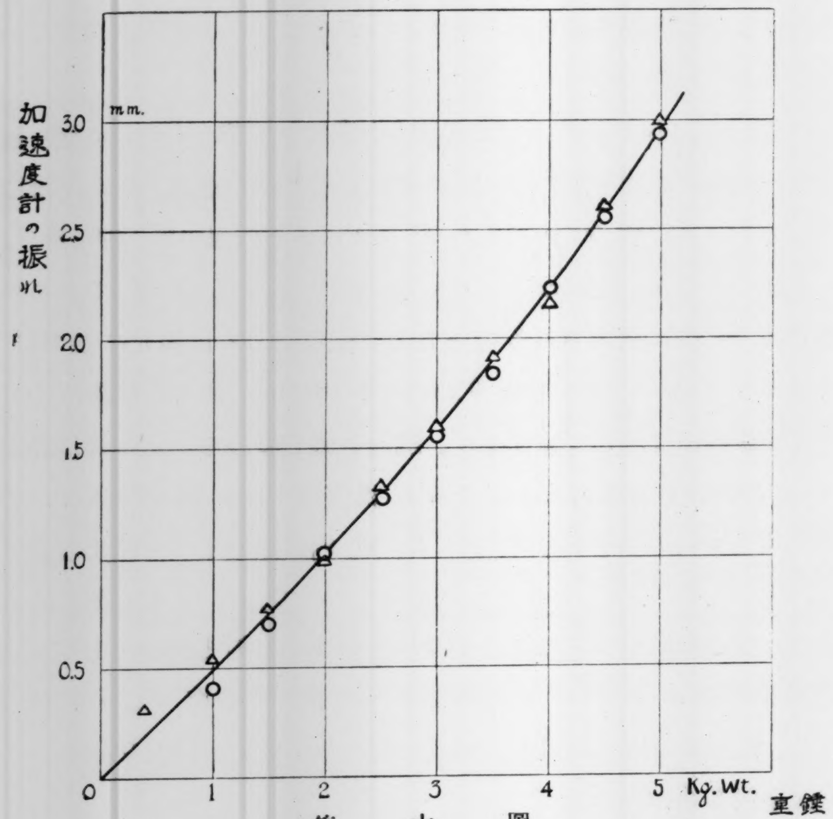
加速度計の振れ
mm.
3.0
2.5
2.0
1.5
1.0
0.5
0
1
2
3
4
5
Kg. Wt.
重錘

第十圖

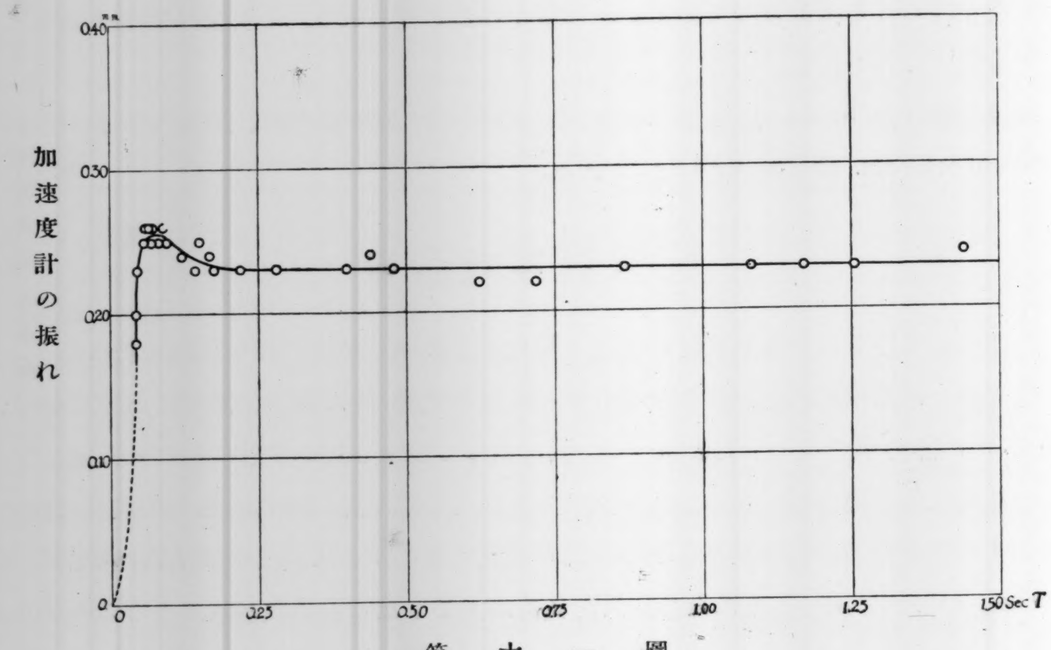
mm.
0.40
0.30
0.20
0.10
0
加速度計の振れ
0
0.25
0.50
0.75
1.00
1.25
1.50 Sec T

第十一圖

はゴムパツキングの變形が單純な壓縮のみではなくて、撓曲が入る爲に恰も彈性率が減少したのと同じ事になつて、感度が增大するのであると思はれる。

第二の試驗は絲ゴムを束ねたものの一端を重錘に連結し、他端を直流電動機の軸に偏心的に連結して、色々の周期に於て一定振幅の正弦波形の水平力が重錘に加る樣にした。此の試驗に依つて得られたものが第十一圖である。此を觀るに 0·1 秒以上の周期に對しては略均等の感度を得てゐる。T が零になるに從つて感度の低下する事は自然であり、又左樣でなくてはならぬ事は前項に於て詳細に說明した通りである。0·075 sec の邊にて感度の少しく上昇するものは、其邊に存在して居る絲ゴムの固有振動が影響して居る爲であらう。

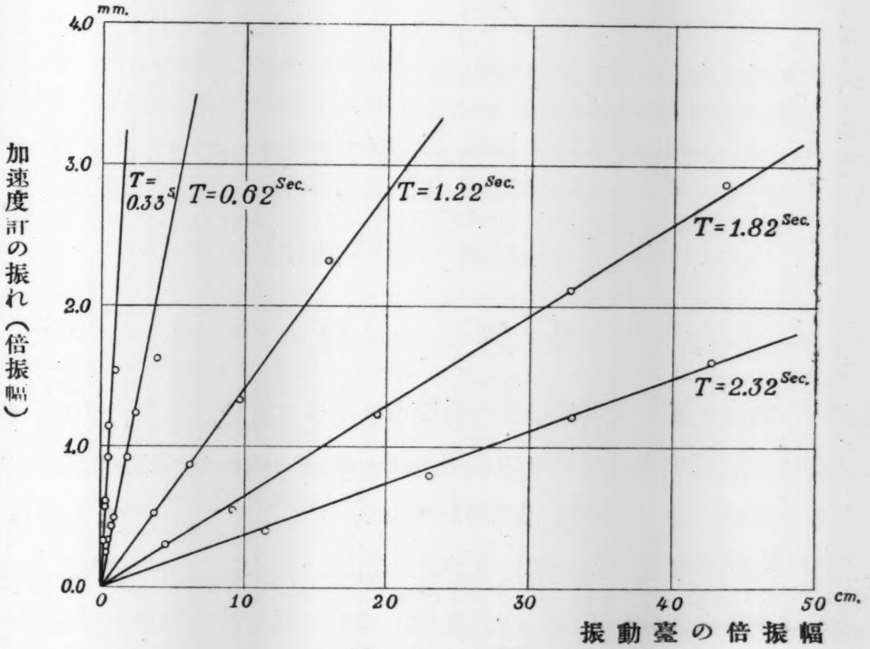

第十二圖

第三の試驗は器械を色々の一定周期を持つた振動臺に乘せて、色々の振幅にて振つたのである。振動臺の振幅は縮少裝置によつて加速度計のドラムの上に同時に記錄しうる樣にした。此の試驗によつて得られたものが第十二圖である。此の圖によつて見るに加速度計の偏れは振動臺の振幅と略〻比例する事が判る。

第十二圖より振動振幅一定にて周期のみ變る場合の加速度計の偏れを求むる時は第十三圖の樣になる。此の直線は加速度計の偏れが外運動の周期の自乘に反比例して變化する事實を示すものであつて、理論上の値に全く從ふものである。

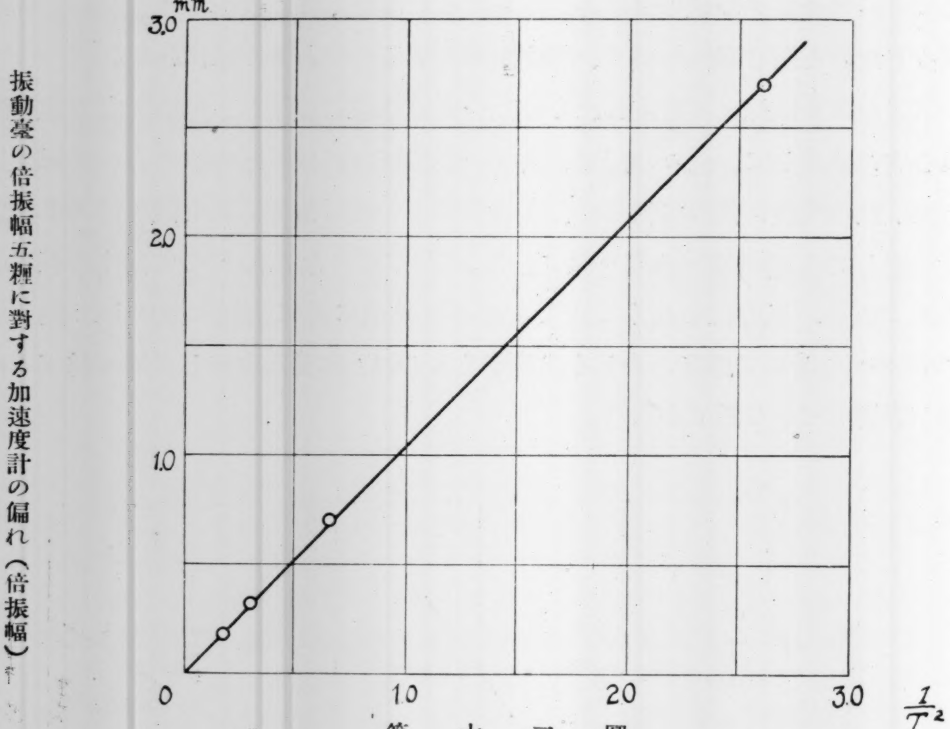

第十三圖

6. 試驗

本加速度計の製作中屢〻土木試驗所の自働車を用ひて實地試驗を行つた。此等の試驗に於ては器械は運轉手席後部の坐席の床上に、前後方向の加速度を記錄する向に乘せたのである。道路、速力、車體、運轉狀態等の如何によつて、如何なる記錄を爲し、如何なる周期の加速度を生ずるか等の詳細なる追求は土木試驗所の研究發表に俟つ事として此處には本加速度計によつて得られた記錄の一部を載せ簡單なる說明を附するに止めて置く。

第十四圖（圖版 XLI）は東京帝大正門前より出發して一高前の東片町のアスファルト道を白山上に至る間の記錄の一部である。圖の細い振動は發動機其他車體の振動であつて、此等振動の平均線が畫く大きな波が、發車、停車、急停車等による加速度である。初めの部分に極規則正しい振動が現れてゐるのは發動機の振動であつて、此時車は未だ進行を初めて居なかつたのである。車は Buick 4 氣筒、1924 年型である。

第十五圖（圖版 **XLII**）は一高前より白山上に至り、上富士前に出、それより肴町を經て大學前に至る間に得た記錄である。車は Buick 1927 年型 6 氣筒である。前の車

の場合と比較して異る所が甚だ多い。途中振動の激しき所は電車軌道に敷いた花剛岩の敷石上を走つた時である。終より四行目の中程は停車の時制動機を用ひた場合であり、終りより三行目は發車の場合で、此の車が發車の時、加速度が幾度にも分れてつく癖のあるのを明瞭に表してゐる。

第十六圖(圖版 XLII)は矢張同じ車にて得たる記錄で、上半は大學構內を走らせた場合、下半は地震研究所前より一高前に至る間の記錄である。此の記錄に於ても、此の車の發車の時に急に進出する癖が表れてゐる。時標は 5 秒每に記入れたものである。

---

32. Construction d'un accéléromètre-enregisteur dans le but de mesurer les mouvements des automobiles, des trains, etc.

par

Mishio ISHIMOTO et Rûtarô TAKAHASI

Un accéléromètre comportant deux bourrelets de caoutchouc est construit dans les conditions suivantes:

1 masse du poids	15,2 kg.
2 période propre	0,03 s.
3 amplification du déplacement de la masse de l'apparail	50
4 amortissement	amortisseur à air
5 sensibilité	1 cm. correspond à g.

Les étalonnages de l'appareil sont exécutés dans des conditions statiques et dynamiques: et les résultats obtenus coïncident bien avec les valeurs théoriques. Dans des enregistrements obtenus sur une automobile, on distingue d'une part les vibrations caractéristiques de la voiture, d'autre part les conditions superficielles de la route.

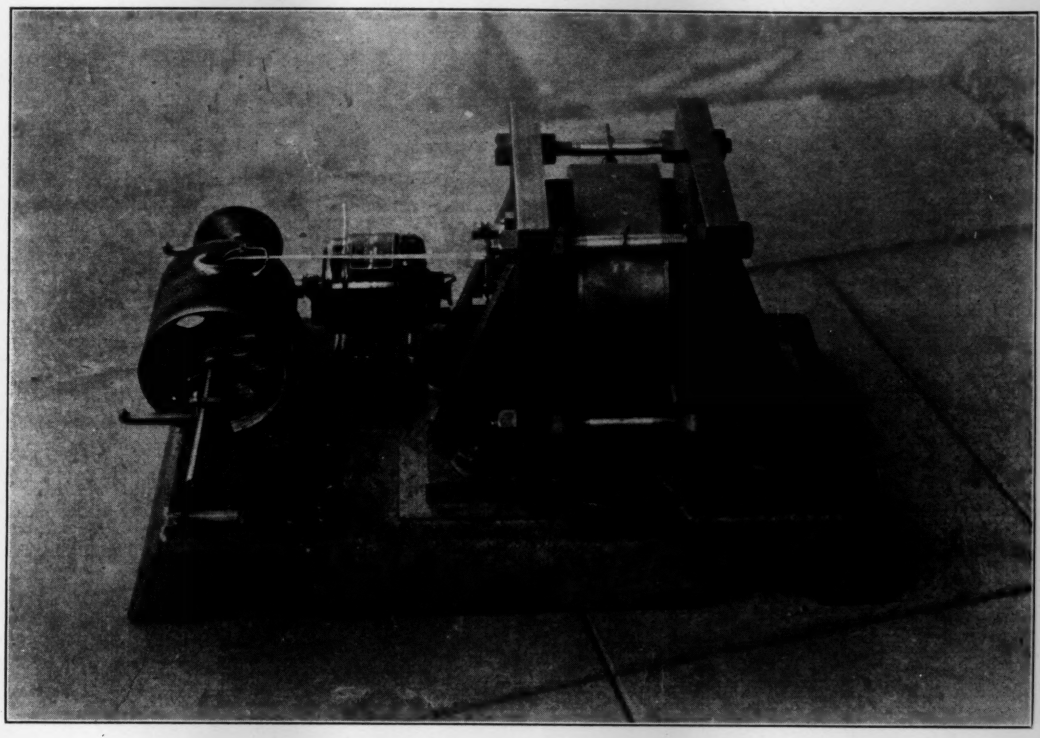

第 九 圖

（震研彙報第七號、圖版、石本、高橋）

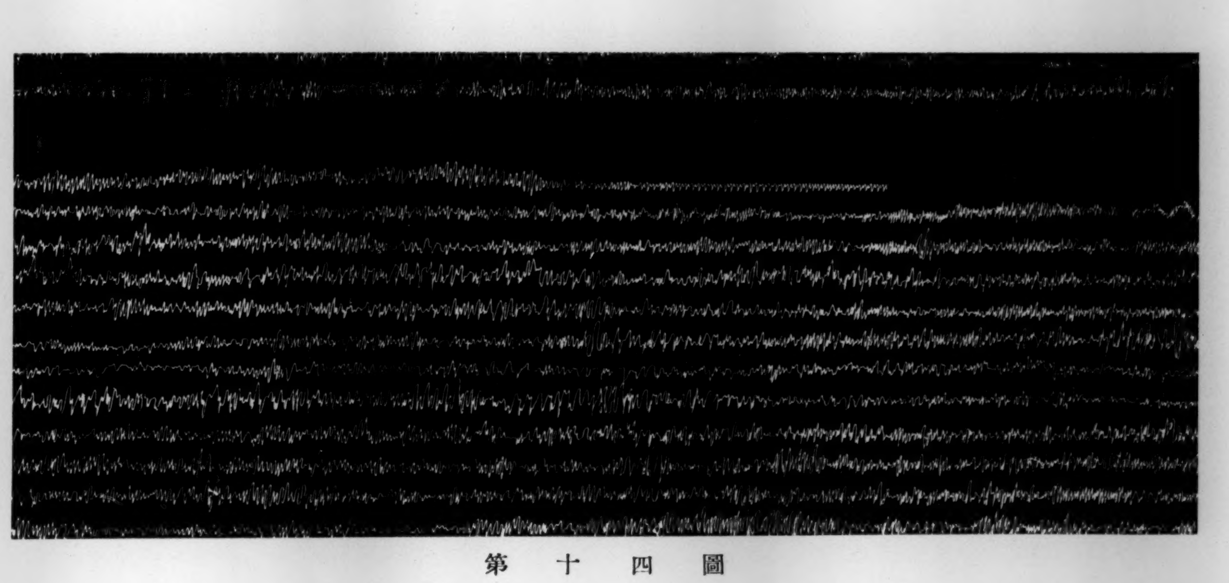

第 十 四 圖

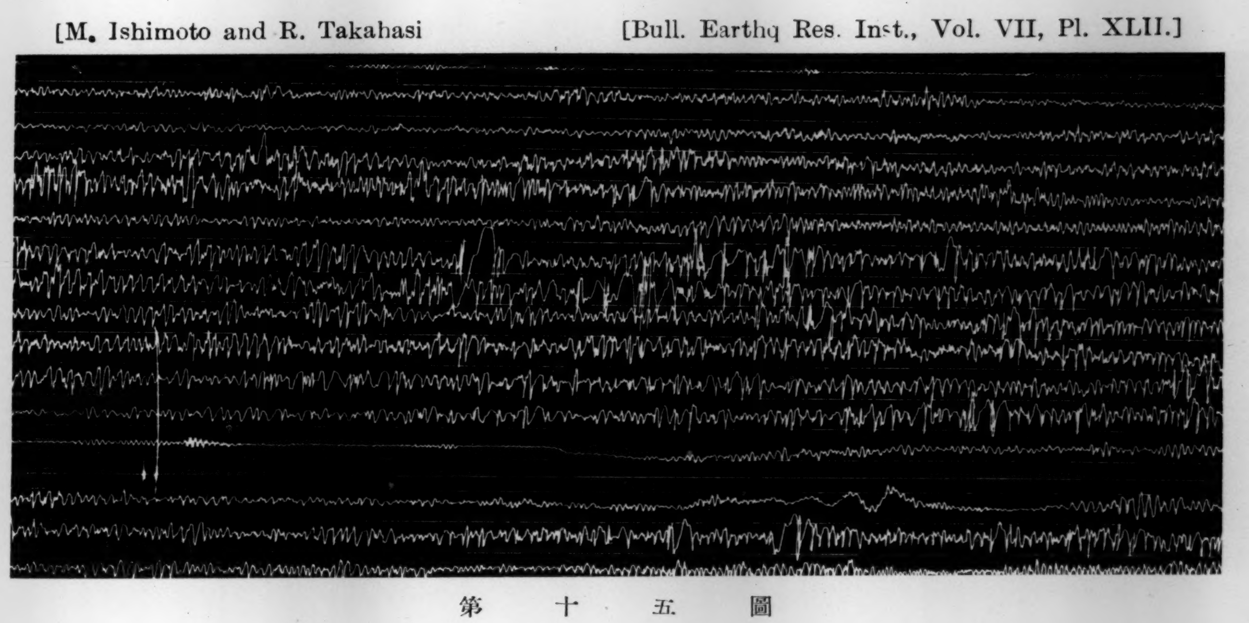

第　十　五　圖

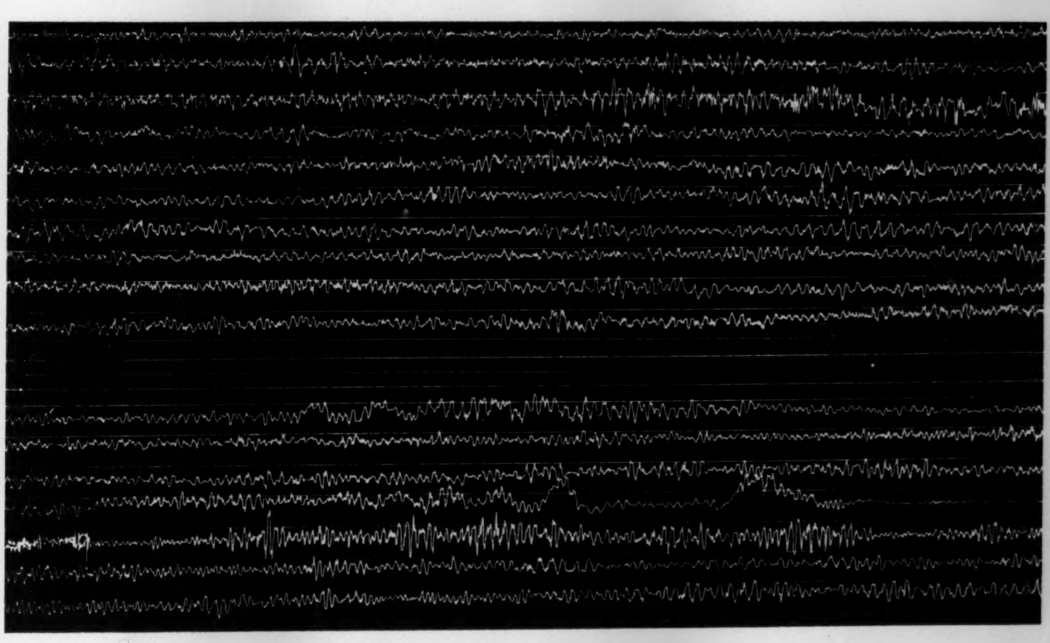

第　十　六　圖

33. 丹後震災地一等水準測量第三回及第四回檢測成果比較要圖[1]

陸地測量部

丹後震災地に於て前回と同一經路に就き更に第四回の一等水準測量を行ひたるにより、其成果を第三回の成果と比較し別紙要圖に圖示して參考に供す。

第三回並第四回檢測作業の期間次の如し。

第三回： 昭和三年三月三日より四月十日迄

第四回： 昭和四年八月七日より十月十日迄

---

33. Comparison of the Results of the Third and Fourth Precise Levellings in the Region Disturbed by the Tango Earthquake.

By **Eikitu Isii**, Major General,

The Land Survey Department.

The precise levelling in the Tango District was resumed for the fourth time along the same route as in the previous surveys. The result of comparison of the data of the third and fourth levellings is summarized in the synoptic map reproduced in the annexed Plate (Pl. XLIII).

The time and duration of the field work for the two levellings are as follows:

The third levelling: March 3—April 10, 1928.

The fourth levelling: August 7—October 10, 1929.

---

[1] 此測量と連關し、本所に於て震災地域の垂直運動の研究を遂行せんとするに當り、岩波茂雄氏の有力なる援助によりて多大の便宜を得たり。此機會を利用して玆に同氏の好意を深謝す。

地震研究所長

說　　　明

一、曲線は第四回觀測値を第三回觀測値に比較せる變動量を示せるものなり

二、變動量の基準は京都府中郡口大野村所在一等水準點第一二三二號を不動と見做したるものなり

三、第三回觀測日——昭和三年——三月三日——四月十日
第四回觀測日——昭和四年——八月七日——十月十日

Explanation.

1. The curves give relative vertical displacements obtained by comparing the results of the fourth levelling with those of the third.
2. B. M. No. 1232 at Kutiôno is assumed fixed in the above comparison.
3. The time and duration of the field work for the two levellings are as follows:

The third levelling: March 3—April 10, 1928.
The fourth levelling: August 7—October 10, 1929.

[Land Survey Dept.]

Camparison of the Results of the Third and Fourth Precise Levellings on the Region Disturbed by the Tango Earthquake.

[Bull. Earthq., Res. Inst., Vol. VII, Pl. XLIII.]

丹後震災地一等水準測量第三回及第四回檢測成果比較要圖

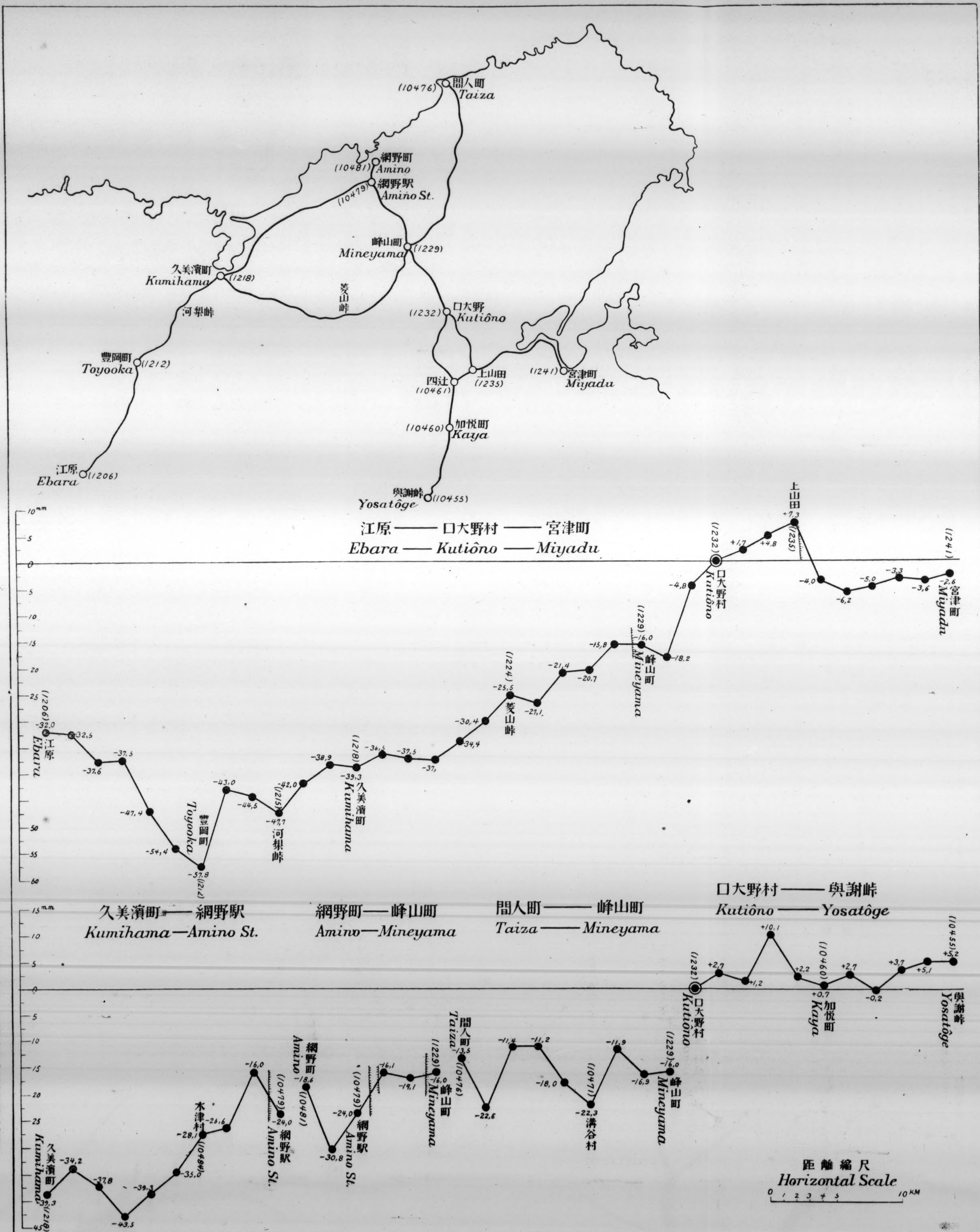

（震研彙報、第七號、圖版、陸地測量部）

——所　報——

○談話會記事

第四拾壹回談話會　（昭和四年九月十七日）

1. 昭和四年一月二日日本海海水面の異狀	囑託	山口生知
1. 大正十二年の關東大地震に伴へる斷層系に就て——非局部大地震々原の多元性	所員	今村明恒
1. 地震波に由りて誘起せられたる土地の固有振動に就て	所員	今村明恒
1. 土佐に於ける急性的地形變動の特徵に就て	所員	今村明恒
1. サンフランシスコ地震と丹後地震との比較	所員	長岡半太郎
1. 潛伏火山 (Latent Volcano) の假說	所員	長岡半太郎
1. 自動車汽車の振動測定な目的とする加速度計	所員 所員	石本巳四雄 高橋龍太郎

第四拾貳回談話會　（昭和四年十月十五日）

1. 日本に於ける重力殘餘の分布と地震の中心の分布との關係に就て	所員	坪井忠二
1. 重力狀況の變動に就て（第三報）（地下水による變化）	所員	坪井忠二
1. 櫻島の地形變化	所員 所員	寺田寅彦 宮部直巳
1. 石油の生成と火山作用	所員	寺田寅彦
1. 海流と海水面との關係	囑託	山口生知
1. 關東地震に於ける三角點の變位に就きて	所員	長岡半太郎
1. 關東地震に伴ひし相模灣底起伏の容積に就き	所員 所員	長岡半太郎 白井俊明

第四拾參回談和會　（昭和四年十一月十九日）

1. 駒ヶ岳噴出物の溫度に就て	所員 所員	坪井誠太郎 津屋弘逵
1. 我國に於ける半島頸部の特異性に就て		武藤陸地測量師
1. 本年七月四日紀伊强震の發生前の地塊傾斜と發生機構とに就て	所員 囑託	今村明恒 小平孝雄
1. 地震波によつて土地の固有振動が誘起される可能度に就て	所員	妹澤克惟
1. 所謂地塊運動の可能度に就て（第一報）	所員 所員	妹澤克惟 西村源六郎

1. カリフォルニアに於ける地殼の變形に就て	所員	宮部直巳
1. 紀伊半島の地形構造	所員	多田文男
1. 日本海溝其他に就き	所員 所員	長岡半太郎 白井俊明

○ 出張

昭和四年十月七日時報受信器修理のため神奈川縣下へ出張	理學士	波江野清藏
昭和四年十月九日時報受信器修理のため千葉縣下へ出張	理學士	波江野清藏
昭和四年十月十日學術上取調のため岩手縣下へ出張	所員	坪井忠二

東京帝國大學

地震研究所彙報

第七號

昭和四年

BULLETIN

OF THE

EARTHQUAKE RESEARCH INSTITUTE

TOKYO IMPERIAL UNIVERSITY

Vol. VII.

1929.

目次

第七號

第一册（昭和四年六月）

頁

1. 内部歪核による半無限固體の表面傾斜（英文） 妹澤克惟 1
2. 水中衝撃による淺海波の生成（英文）…… 妹澤克惟 15
3. 内部にある多重原によるレーレー波の生成（英文）…………………… 妹澤克惟・西村源六郎 41
4. 砂層の崩壞に關する實驗（第三報）（英文）‥ 寺田寅彦・宮部直巳 65
5. 油壺灣内の海水の副振動に因る地殼の傾斜運動（英文）…………………… 高橋龍太郎 95
6. 水準測量に依りて見出されたる地塊運動に就いて（英文）…………………… 坪井忠二 103
7. 低氣壓の海水面に及ぼす影響に就いて（英文） 山口生知 115
8. 丹後地震の餘震調査報告（第二報）（邦文）‥ 那須信治 133
9. 地表面の高さ及び地變の量（邦文）……… 井上宇胤 153
10. 平常時における一建築物の振動測定（佛文）‥ 石本巳四雄・高橋龍太郎 175
11. 丹後震災地一二等三角點移動檢測成果第二報告（邦文）…………………… 陸地測量部 185
12. 丹後地方震災地復舊一等三角測量記事（邦文） 陸地測量部 187

第二册（昭和四年九月）

13. 任意の衝撃によつて起る週期的レーレー波

（英文）………… 妹澤克惟 193
14. 火山の形（英文）………… 寺田寅彥 207
15. 關西地方の地殼變形並に現在地形との關係（英文）………… 寺田寅彥・宮部直巳 223
16. 地震動の前驅部分に就て（英文）………… 松澤武雄・山田國親・鈴木武夫 241
17. 太平洋に於ける激震帶の移動（獨文）………… 宮部直巳 261
18. 神津島火山（英文）………… 津屋弘逵 269
19. 茅ヶ岳火山（英文）………… 市來政兼 335
20. 丹後地方震災地復舊二等三角測量記事（邦文） 陸地測量部 381

第三册（昭和四年十二月）

21. 固體のダイレテーションとロテーションとに無關係な變位に就いて（英文）………… 妹澤克惟・西村源六郎 389
22. 內部の層原によるとレーレー波の生成（英文） 妹澤克惟 417
23. 球面上に於けるラブ波の傳播とこれに關聯する一二の問題（英文）………… 妹澤克惟 437
24. 重力ポテンシャルの空間二次微分係數の時間的變動に就いて（英文）………… 坪井忠二 457
25. 振動分解器による地震の性質の研究（英文） 末廣恭二 467
26. 水成岩層の地震波傳播に及ぼす影響（邦文）…… 今村明恒・岸上冬彥・小平孝雄 471
27. 地震波によりて誘起せられたる土地の固有振動に就いて（邦文）………… 今村明恒 489
28. 關東地方改測水準測量結果に就ての研究（邦文）………… 武藤勝彥・熱海景良 495
29. 地形から地殼の移動從て地殼に働く歪力を判斷することの可能度に就いて（邦文）…… 藤原咲平・高山威雄 623

30. 川の流路の變遷によつて知り得たる伊賀國島ヶ原地塊の運動(邦文)………………… 多田文男 531

31. 昭和四年一月二日の日本海海水面の異常(邦文)………………………………… 山口生知 555

32. 自動車、汽車の振動測定を目的とする加速度計（第一部、水平動測定）（邦文）……… 石本巳四雄・高橋龍太郎 571

33. 丹後震災地一等水準測量第三回及第四回檢測成果比較要圖（邦文）………………… 陸地測量部 587

Contents.

Vol. VII.

Part 1.—June, 1929.

Page

1. K. Sezawa, The Tilting of the Surface of a Semi-infinite Solid due to Internal Nuclei of Strain. (in English) 1
2. K. Sezawa, Formation of Shallow-water Waves due to Subaqueous Shocks. (in English) 15
3. K. Sezawa, and G. Nishimura, Generation of Rayleigh-waves from an Internal Source of Multiplet-type. (in English) 41
4. T. Terada and N. Miyabe, Experimental Investigation of the Deformation of Sand Mass. Part III. (in English).... 65
5. R. Takahasi, Tilting Motion of the Earth Crust Caused by Secondary Undulations of Tides in a Bay. (in English) .. 95
6. Ch. Tsuboi, Block Movements as Revealed by Means of Precise Levellings in Some Earthquake Districts of Japan. (in English) 103
7. S. Yamaguti, On the Effect of Cyclones upon Sea Level. (in English) 115
8. N. Nasu, Further Study of the Aftershocks of the Tango Earthquake. (in Japanese) 133
9. W. Inouye, Statistical Regularities regarding the Altitudes of Mountain Ranges and the Amounts of Dislocations of the Earth's Surface. (in Japanese) 153
10. M. Ishimoto et R. Takahasi, Mesures des Mouvements d'un

bâtiment dans des conditions tranquilles. (en Français) .. 175

11. H. Omura, Horizontal Displacements of the Primary and Secondary Triangulation Points, observed after the Earthquake of March 7, 1927, in Tango Districts. The Second Report. (in Japanese) 185

12. Land Survey Department, Revision of the Primary Trigonometrical Survey in Tango Earthquake Districts. (in Japanese) 187

Part 2.—September, 1929.

13. K. Sezawa, Periodic Rayleigh-waves caused by an Arbitrary Disturbance. (in English) 193

14. T. Terada, On the Form of Valcanoes. (in English) 207

15. T. Terada and N. Miyabe, Deformation of the Earth Crust in Kwansai Districts and its Relation to the Orographic Feature. (in English) 223

16. T. Matuzawa, K. Yamada and T. Suzuki, On the Forerunners of Earthquake Motions. (The Second Paper). (in English) 241

17. N. Miyabe, Die Schwankungen der makroseismischen Tätigkeitszonen um den pazifischen Ozean. (in deutsch) 261

18. H. Tsuya, Volcanoes of Kozu-shima. (in English) 269

19. M. Ichiki, Volcano Kayagatake. (in English) 335

20. Land Survey Department, Revision of the Secondary Trigonometrical Survey in the Tango District. (in Japanese) .. 381

Part 3.—December, 1929.

21. K. Sezawa and G. Nishimura, The Displacement independent

of the Dilatation and the Rotation in a Solid Body. (in English) 389

22. K. Sezawa, Generation of Rayleigh-waves from a Sheet of Internal Sources. (in English) 417

23. K. Sezawa, Propagation of Love-waves on a Spherical Surface and Allied Problems. (in English) 437

24. Ch. Tsuboi, Observation on the Time Variation of the Second Space Derivatives of the Gravitational Potential. (Part 1). (in English) 457

25. K. Suyehiro, On the Nature of Earthquakes Studied by Means of the Seismic Wave Analyser. (in English) 467

26. A. Imamura, F. Kishinouye and T. Kodaira, The Effect of Superficial Sedimentary Layers upon the Transmission of Seismic Waves. (in Japanese) 471

27. A. Imamura, On the Earth-vibrations induced in Some Localities at the Arrival of Seismic Waves. (in Japanese) 489

28. K. Muto and K. Atumi, An Investigation into the Results of the New and Old Measurements of the Levelling Net in the Kwanto District. (in Japanese) 495

29. S. Fujiwhara and T. Takayama, On the Possibility of finding Stresses acting on and Displacements of the Earth-crust from its Surface Form. (in Japanese) 623

30. F. Tada, Recent Deformation of the Shimagahara Land Block in Prov. Iga as determined by Tracting the Vertical Change of River Courses. (in Japanese) 531

31. S. Yamaguti, Abnormal Rise of Sea Level in the Japan Sea Coast, on Jan. 2, 1929 555

32. M. Ishimoto et R. Takahasi, Construction d'un accelerometre enregisteur dans le but de mesurer les mouvements des automobiles, des trains, etc. (in Japanese) 571

33. Isii, Comparison of the Results of the Third and Fourth

Precise Levellings in the Region Disturbed by the Tango Earthquake. (in Japanese) 587

第七號索引

頁
熱海景良、武藤勝彥; 武藤勝彥、熱海景良參照
藤原咲平、高山威雄 (29) 地形から地殼の移動從て地殼に働く歪力を判斷することの可能度に就いて ······················ 623
市來政兼 (19) 茅ヶ岳火山 (英文) ······················ 335
今村明恒 (27) 地震波によりて誘起せられたる土地の固有振動に就いて (邦文) ······················ 489
今村明恒、岸上冬彥、小平孝雄 (26) 水成岩層の地震波傳播に及ぼす影響 (邦文) ······················ 471
井上宇胤 (9) 地表面の高さ及び地變の量 (邦文) ······················ 153
石本巳四雄、高橋龍太郎 (10) 平常時における一建築物の振動測定 (佛文) ······················ 175
石本巳四雄、高橋龍太郎 (32) 自動車、汽車の振動測定を目的とする加速度部 (第一部 水平動測定) (邦文) ······················ 571
岸上冬彥、今村明恒、小平孝雄; 今村明恒、岸上冬彥、小平孝雄參照
小平孝雄、今村明恒、岸上冬彥; 今村明恒、岸上冬彥、小平孝雄參照
松澤武雄、山田國親、鈴木武夫 (16) 地震動の前驅部分に就いて (英文) ······················ 241
宮部直巳 (17) 太平洋に於ける激震帶の移動 (獨文) ······················ 261
宮部直巳、寺田寅彥; 寺田寅彥, 宮部直巳參照
武藤勝彥、熱海景良 (28) 關東地方改測水準測量結果に就ての研究 (邦文) ······················ 495
那須信治 (8) 丹後地震の餘震調査報告 (第二報) (邦文) ······················ 133
西村源六郎、妹澤克惟; 妹澤克惟、西村源六郎參照
妹澤克惟 (1) 內部歪核による半無限固體の表面傾斜 (英文) ······················ 1
妹澤克惟 (2) 水中衝擊による淺海波の生成 (英文) ······················ 15
妹澤克惟 (13) 任意の衝擊によつて起る週期的レーレー波 (英文) ······················ 193
妹澤克惟 (22) 內部の層原によるレーレー波の生成 (英文) ······················ 417

妹澤克惟 (23) 球面上に於けるラブ波の傳播とこれに關聯する一二の問題（英文）……………………… 437

妹澤克惟、西村源六郎 (3) 内部にある多重原によるレーレー波の生成（英文）……………………… 41

妹澤克惟、西村源六郎 (21) 固體のダイレテーションとロテーションとに無關係な變位に就いて（英文）……………… 389

末廣恭二 (25) 振動分解器による地震の性質の研究（英文）…… 467

鈴木武夫、松澤武雄、山田國親；松澤武雄、山田國親、鈴木武夫參照 ……………………………

多田文男 (30) 川の流路の變遷によて知り得たる伊賀國島ヶ原地塊の運動（邦文）……………………… 531

高橋龍太郎 (5) 油壺灣内の海水の副振動に因る地殼の傾斜運動（英文）……………………………… 95

高橋龍太郎、石本巳四雄；石本巳四雄、高橋龍太郎參照

高山威雄、藤原咲平；藤原咲平、高山威雄參照

寺田寅彦 (14) 火山の形（英文）……………………… 207

寺田寅彦、宮部直巳 (4) 砂層の崩壞に關する實驗（第三報）（英文）……………………………… 65

寺田寅彦、宮部直巳 (15) 關西地方の地殼變形並に現在地形との關係（英文）……………………… 223

坪井忠二 (6) 水準測量に依りて見出されたる地塊運動に就いて（英文）……………………………… 103

坪井忠二 (24) 重力ポテンシャルの空間二次微分係數の時間的變動に就いて（英文）……………………… 457

津屋弘逵 (18) 神津島火山（英文）………………… 269

山田國親、松澤武雄、鈴木武夫；松澤武雄、山田國親、鈴木武夫參照

山口生知 (7) 低氣壓の海水面に及ぼす影響に就いて（英文）…… 115

山口生知 (31) 昭和四年一月二日の日本海海水面の異常（邦文）‥ 555

陸地測量部 (11) 丹後震災地一二等三角點移動檢測成果第二報告

（邦文）……………………………………………… 185

陸地測量部　(12) 丹後地方震災地復舊一等三角測量記事（邦文）‥ 187

陸地測量部　(20) 丹後地方震災地復舊二等三角測量記事（邦文）‥ 381

陸地測量部　(33) 丹後震災地一二等水準測量第三回及第四回檢測成果比較要圖（邦文）…………………………… 587

Index to Vol. VII.

Page

Atumi, K. and Muto, K., *See* Muto, K. and Atumi, K.

Fujiwhara S. and Takayama, T. (29) On the Possibility of finding Stresses acting on and Displacements of the Earthcrust from its Surface Form. (in Japanese) 335

Ichiki, M. (19) Volcano Kayagatake. (in English) 335

Imamura, A. (27) On the Earth-vibrations induced in Some Localities at the Arrival of Seismic Waves. (in Japanese) 489

Imamura, A. Kishinouye F. and Kodaira, T., (26) The Effect of Superficial Sedimentary Layers upon the Transmission of Seismic Waves. (in Japanese)......................... 471

Inouye, W. (9) Statistical Regularities regarding the Altitudes of Mountain Ranges and the Amounts of Dislocations of the Earth's Surface. (in Japanese) 153

Ishimoto, M. et Takahasi, R. (10) Mesures des mouvements d'un bâtiment dans des conditions tranquilles. (en français) 175

Ishimoto, M. et Takahasi, R., (32) Construction d'un accéléromètre-enregisteur dans le but de mesurer les mouvements des automobiles, des trains, etc. (in Japanese) 571

Isii, E, (33) Comparison of the Result of the Third and Fourth Precise Levellings in the Region Disturbed by the Tango Earthquake. (in Japanese) 587

Kishinouye, F., Imamura, A. and Kodaira, T., *See* Imamura, A., Kishinouye, F. and Kodaira, T.

Kodaira, T., Imamura, A. and Kishinouye, F., *See* Imamura, A., Kishinouye, F. and Kodaira, T.

Land Survey Department, (12) Revision of the Primary Trigonometrical Survey in Tango Earthquake Districts. (in Japanese). 187

Land Survey Department, (20) Revision of the Secondary Trigonometrical Survey in the Tango District. (in Japanese).. 381

Matuzawa, T., Yamada, K. and Suzuki, T. (16) On the Forerunners of Earthquake-motions (The Second Paper). (in English) 241

Miyabe, N. (17) Die Schwankungen der makroseismischen Tätigkeitszonen um den pazifischen Ozean. (in deutsch) .. 261

Miyabe, N. and Terada, T., *See* Terada, T. and Miyabe, N.

Muto, K. and Atumi, K, (28) An Investigation into the Results of the New and Old Measurements of the Levelling Net in the Kwanto District. (in Japanese) 495

Nasu, N. (8) Further Study of the Aftershocks of the Tango Earthquake. (in Japanese) 133

Nishimura, G. and Sezawa, K., *See* Sezawa, K. and Nishimura, G.

Omura, H. (11) Horizontal Displacements of the Primary and Secondary Triangulation Points, observed after the Earthquake of March 7, 1927, in Tango Districts. (The Second Report.) (in Japanese) 185

Sezawa, K. (1) The Tilting of the Surface of a Semi-infinite Solid due to Internal Nuclei of Strain. (in English) 1

Sezawa, K. (2) Formation of Shallow-water Waves due to Subaqueous Shocks. (in English) 15

Sezawa, K. (13) Periodic Rayleigh-waves caused by an Arbitrary Disturbance. (in English) 193

Sezawa, K, (22) Generation of Rayleigh-waves from a Sheet of Internal Sources. (in English) 417

Sezawa, K, (23) Propagation of Love-waves on a Spherical Surface and Allied Problems. (in English) 437

Sezawa K. and Nishimura, G. (3) Generation of Rayleigh-waves from an Internal Source of Multiplet-type. (in English) 41

Sezawa, K. and Nishimura, G, (21) The Displacement independent of the Dilatation and the Rotation in a Solid Body. (in English) 389

SUYEHIRO, K, (25) On the Nature of Earthquakes Studied by Means of the Seismic Wave Analyser. (in English) 467

SUZUKI, T., MATUZAWA, T. and YAMADA, K., *See* MATUZAWA, T., YAMADA, K. and SUZUKI, T.

TADA, F, (30) Recent Deformation of the Shimagahara Land Block in Prov. Iga as determined by Tracing the Vertical Change of River Courses. (in Japanese) 531

TAKAHASI, R, (5) Tilting Motion of the Earth Crust caused by Secondary Undulations of Tides in a Bay. (in English) .. 95

TAKAHASI, R. and ISHIMOTO, M., *See* ISHIMOTO, M. and TAKAHASI, R.

TAKAYAMA, T. and FUJIWHARA, S., *See* FUJIWHARA, S. and TAKAYAMA, T.

TERADA, T, (14) On the Form of Volcanoes. (in English) 207

TERADA T. and MIYABE, N, (4) Experimental Investigation of the Deformation of Sand Mass. Part III. (in English) .. 65

TERADA, T. and MIYABE, N, (15) Deformation of the Earth Crust in Kwansai Districts and its Relation to the Orographic Feature. (in English) 223

TSUBOI, Ch., (6) Block Movements as Revealed by Means of Precise Levellings in Some Earthquake Districts of Japan. (in English) 103

TSUBOI, Ch., (24) Observation on the Time Variation of the Second Space Derivatives of the Gravitational Potential. (Part I). (in English) 457

TSUYA, H, (18) Volcanoes of Kôzu-shima. (in English) 269

YAMADA, K., MATUZAWA, T. and SUZUKI, T., *See* MATUZAWA, T., YAMADA, K. and SUZUKI, T.

YAMAGUTI, S, (7) On the Effect of Cyclones upon Sea Level. (in English) 115

Yamaguti, S, (31) Abnormal Rise of Sea Level in the Japan Sea Coast, on Jan. 2, 1929. (in Japanese) 555

昭和四年十二月二十八日印刷
昭和四年十二月三十日發行

編纂兼發行者　東京帝國大學地震研究所

東京市神田區美土代町二丁目一番地
印刷者　島連太郎

東京市神田區美土代町二丁目一番地
印刷所　三秀舍

東京市神田區南神保町十六番地
賣捌所　岩波書店

Sold by
Iwanami Shoten,
Minamizinbôtyô, Kanda, Tôkyô.
Price of this copy: 2·40 Yen (Postage exclusive).

BULLETIN OF

THE EARTHQUAKE RESEARCH INSTITUTE

TOKYO IMPERIAL UNIVERSITY

Vol. VII, Part 3. December, 1929.

Contents.

Papers and Reports.

Page

21. K. Sezawa and G. Nishimura, The Displacement independent of the Dilatation and the Rotation in a Solid Body. (in English)............................ 389

22. K. Sezawa, Generation of Rayleigh-waves from a Sheet of Internal Sources. (in English)............................ 417

23. K. Sezawa, Propagation of Love-waves on a Spherical Surface and Allied Problems. (in English)............................ 437

24. C. Tsuboi, Observation on the Time Variation of the Second Space Derivatives of the Gravitational Potential. (Part 1). (in English)............................ 457

25. K. Suyehiro, On the Nature of Earthquakes Studied by Means of the Seismic Wave Analyser. (in English)............................ 467

26. A. Imamura, F. Kishinouye and T. Kodaira, The Effect of Superficial Sedimentary Layers upon the Transmission of Seismic Waves. (in Japanese).......... 471

27. A. Imamura, On the Earth-vibrations Induced in some Localities at the Arrival of Seismic Waves. (in Japanese)............................ 489

28. K. Muto and K. Atumi, An Investigation into the Results of the New and Old Measurements of the Levelling Net in the Kwanto District. (in Japanese).... 495

29. S. Fujiwhara and T. Takayama, On the Possibility of finding Stresses acting on and Displacements of the Earthcrust from its Surface Form. (in Japanese) .. 523

30. F. Tada, Recent Deformation of the Shimagahara Land Block in Prov. Iga as determined by Tracing the Vertical Change of River Courses. (in Japanese) ·· 531

31. S. Yamaguti, Abnormal Rise of Sea Level in the Japan Sea Coast, on Jan. 2, 1929. (in Japanese)............................ 555

32. M. Ishimoto et R. Takahasi, Construction d'un accelerometre-enregisteur dans le but de mesurer les mouvements des automobiles, des trains, etc.(in Japanese) 571

33. E. Isii, Comparison of the Results of the Third and Fourth Precise Levellings in the Region Disturbed by the Tango Earthquake. (in Japanese)............... 587

Institute Notes.

(For the papers written in Japanese or in occidental languages, the abstracts are given in occidental languages or in Japanese respectively.)